colloques et séminaires

GÉODYNAMIQUE ANDINE
ANDEAN GEODYNAMICS
GEODINÁMICA ANDINA

Résumés étendus
Extended abstracts
Resúmenes expandidos

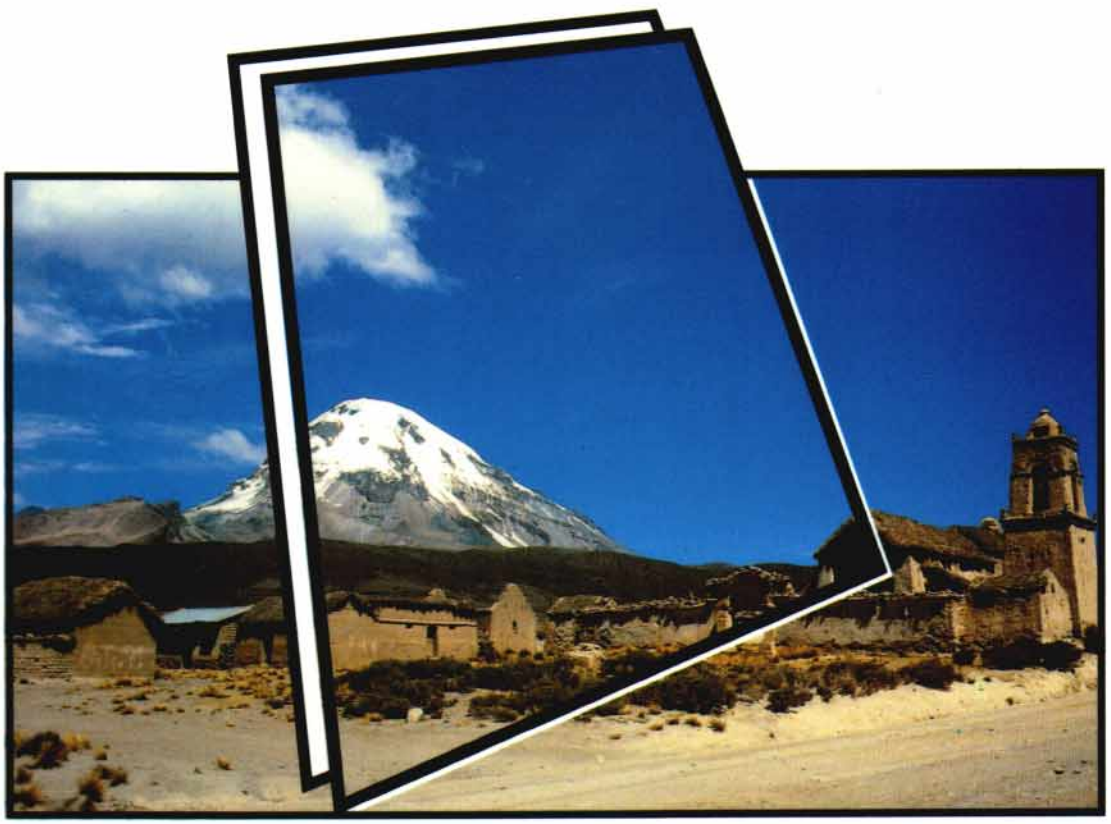

Symposium International
ORSTOM / Université d'Oxford
Oxford (Angleterre), 21 au 23 septembre 1993

ORSTOM Editions

SECOND SYMPOSIUM INTERNATIONAL
GÉODYNAMIQUE ANDINE

ISAG 93

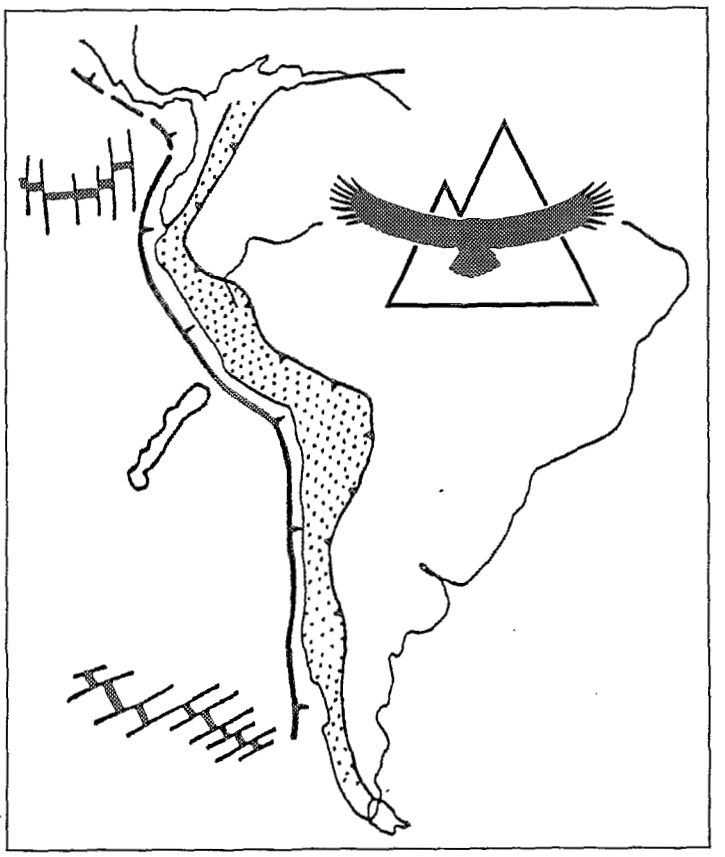

Oxford (Angleterre), 21 - 23 septembre 1993

Résumés étendus - Extended abstracts - Resúmenes expandidos

ORGANISATEURS — ORGANIZERS — ORGANIZADORES

ORSTOM
L'INSTITUT FRANÇAIS DE RECHERCHE SCIENTIFIQUE
POUR LE DÉVELOPPEMENT EN COOPÉRATION
PARIS, FRANCE

UNIVERSITY OF OXFORD
UNITED KINGDOM

Éditions de l'ORSTOM
L'INSTITUT FRANÇAIS DE RECHERCHE SCIENTIFIQUE POUR LE DÉVELOPPEMENT EN COOPÉRATION
Collection **COLLOQUES et SÉMINAIRES**
PARIS 1993

COMITÉ SCIENTIFIQUE ET D'ORGANISATION
SCIENTIFIC AND ORGANIZING COMMITTEE
COMITÉ CIENTÍFICO Y ORGAGANIZADOR

John F. DEWEY (Department of Earth Sciences, University of Oxford)
Catherine DORBATH (ORSTOM UR1E et CNRS URA 1353, EOPG Strasbourg)
Simon H. LAMB (Department of Earth Sciences, University of Oxford)
Stephen MOORBATH (Department of Earth Sciences, University of Oxford)
Thierry SEMPERE (ORSTOM UR1H et Dépt. Géologie Sédimentaire, Univ. Paris 6)
Pierre SOLER (ORSTOM UR1H et CNRS URA 736, Univ. Paris 6)

Le Comité Scientifique et d'Organisation remercie tout particulièrement Mmes Marie Agnès BRAY (Direction de l'Information Scientifique et Technique - ORSTOM), Annie ELKORD (Commission Scientifique de Géologie-Géophysique - ORSTOM), Cecilia GONZALEZ (Mission ORSTOM en Bolivie) et Sally J. THOMPSON (Department of Earth Sciences, University of Oxford) pour leur appui dans la préparation du Symposium.

APPUI FINANCIER
FUNDING
APOYO FINANCIERO

L'organisation de l'ISAG 93 et les aides aux voyages pour un certain nombre de collègues latino-américains ont été rendues possible grâce au soutien financier de l'ORSTOM (Direction de l'Information Scientifique et Technique, Département Terre-Océan-Atmosphère, Commission Scientifique de Géologie-Géophysique), de la Commission des Communautés Européennes (DG XII G4 - Coopération Scientifique Internationale), du Ministère Français des Affaires Etrangères (Ambassade de France au Chili), du Bristish Council (Ambassade Britannique au Venezuela) et du PICG 345 "Andean Lithospheric Evolution" (UNESCO).

ISSN : 0767-2896
ISBN : 2-7099-1154-X

SOMMAIRE / SUMMARY / SUMARIO

STRUCTURE DE LA LITHOSPHERE ANDINE
ANDEAN LITHOSPHERIC STRUCTURE
ESTRUCTURA DE LA LITOSFERA ANDINA

SISMOLOGIE / SISMOTECTONIQUE / NÉOTECTONIQUE
SEISMOLOGY / SEISMOTECTONICS / NEOTECTONICS
SISMOLOGIA / SISMOTECTONICA / NEOTECTONICA

TECTONIQUE
TECTONICS
TECTONICA

BASSINS
BASINS
CUENCAS

MAGMATISME ANDIN
ANDEAN MAGMATISM
MAGMATISMO ANDINO

GITES MINÉRAUX
ORE DEPOSITS
YACIMIENTOS MINERALES

EVOLUTION PRÉ-ANDINE
PRE-ANDEAN EVOLUTION
EVOLUCION PRE-ANDINA

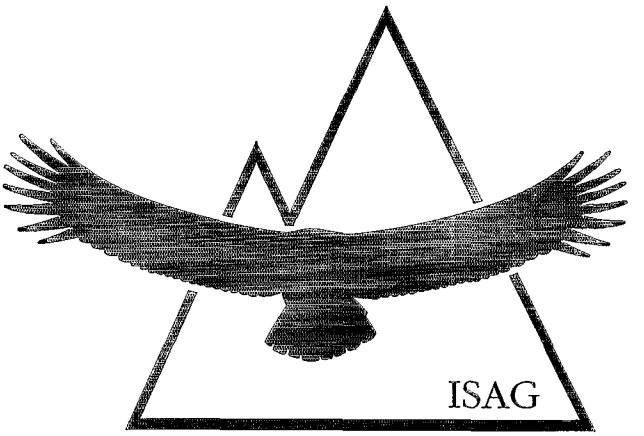
ISAG

STRUCTURE DE LA LITHOSPHERE ANDINE
ANDEAN LITHOSPHERIC STRUCTURE
ESTRUCTURA DE LA LITOSFERA ANDINA

Pb ISOTOPES REVEAL BASEMENT DOMAINS OF THE ALTIPLANO, CENTRAL ANDES.

Susan J. AITCHESON (1), Russell S. HARMON (2), Stephen MOORBATH (1), Albrecht SCHNEIDER (3), Pierre SOLER(4), Eduardo SORIA-ESCALANTE. (1), George STEELE (5), Ian SWAINBANK (2), and Gerhard WÖRNER (6).

(1) Earth Sciences Dept., University of Oxford, Parks Rd., Oxford, OX1 3PR, U.K.
(2) NIGL, Kingsley Dunham Centre, Keyworth, Nottingham, NG12 5GG, U.K.
(3) Proyecto de Cooperación Geológica Alemania-Bolivia (BGR - GEOBOL), casilla 2729, La Paz - Bolivia.
(4) ORSTOM, UR1H, 213 rue Lafayette, 75480 Paris cedex 10, France.
(5) Dept. of Geology & Petroleum Geology, University of Aberdeen, Meston Building, Kings College, Aberdeen AB9 2UE, U.K.
(6) Inst. für Geowissenschaften, Universität Mainz, Obere Zahlbacher Straße 63, D-6500, Mainz, Germany.

RESUMEN: Datos isotópicos de Pb en mineralización y rocas volcánicas del Altiplano permiten definir tres dominios de basamento diferentes: Altiplano Norte, Altiplano Sur y Cordillera Oriental. Los dominios del Altiplano Norte y Sur se encuentran conectados mediante una zona de transición localizada en la Serranía Intersalar, mientras que el límite con el dominio de la Cordillera Oriental parece ser abrupto. Existe una buena correlación entre los dominios isotópicos definidos y estructuras evidentes en mapas gravimétricos publicados.

KEY WORDS: Altiplano, Andes, Ores, Pb-isotopes, Structure, Volcanics

INTRODUCTION

Almost all of the Pb in hydrothermal ore deposits of the Central Andes must have been scavenged directly from the crust with which the ore-forming fluids came in contact since such fluids are initially Pb-poor and their circulation is restricted to the shallow upper crust where open fractures can occur. In addition, quantitative geochemical modelling (Aitcheson and Forrest, 1993) suggests that over three quarters of the Pb in the volcanic rocks of the Central Andes is derived directly from the crust which was in contact with the magmas through crustal contamination processes. When there is such a large proportion of crustal Pb present in ore deposits and volcanic rocks the Pb isotopic composition of these materials can also be regarded as a crude average

for the composition of the crust through which the magmas or fluids passed. Where large regional differences in crustal Pb isotopic composition exist and basement exposures are scarce or absent, as in the Altiplano region of the Central Andes, ore deposits and volcanic rocks are powerful tools for mapping out the different crustal isotopic domains. Such maps can in turn provide insights into the gross crustal structure of the region.

RESULTS FROM THE CENTRAL ANDES

Central Andean igneous rocks and Pb ores of Miocene-Recent age from 16-23°S have a similar and wide range of Pb isotopic compositions ($^{206}Pb/^{204}Pb$=17.3-19.0, $^{207}Pb/^{204}Pb$=15.51-15.85, $^{208}Pb/^{204}Pb$=37.4-39.4) which are interpreted to reflect the isotopic character of the local basement. The data map out several distinct crustal domains which are otherwise hidden by superficial deposits (Fig. 1):

(1) N. Altiplano domain

This domain occupies the northern Altiplano from the volcanic front to Lago Poopo and extends as far south as the Salar de Uyuni at 19.5°S. It is characterized by relatively unradiogenic Pb, i.e. low values of $^{206}Pb/^{204}Pb$ (<18.3) , $^{207}Pb/^{204}Pb$ (<15.619) and $^{208}Pb/^{204}Pb$ (<38.5). This domain may be an extension of the Proterozoic Arequipa Massif of Peru, which is also characterized by relatively unradiogenic Pb isotopic compositions.

(2) E. Cordillera domain

This domain has more radiogenic Pb, i.e. higher values of the Pb isotope ratios ($^{206}Pb/^{204}Pb$ >18.6, $^{207}Pb/^{204}Pb$ >15.64 and $^{208}Pb/^{204}Pb$ >38.9), and extends eastwards from L. Poopo into the E. Cordillera. At L. Poopo this domain is separated from the N. Altiplano domain to the west by a sharp N-S-trending boundary (probably a major fault) which appears to be offset south of L. Poopo ("B" in Fig. 1). At L. Titicaca the two domains appear to be separated by the NW-SE-trending Copacabana Fault Zone.

(3) S. Altiplano domain

This domain occupies the southern half of the Altiplano and is isotopically similar to the E. Cordillera domain, except for its slightly lower $^{208}Pb/^{204}Pb$ ratios (38.5-38.9). The boundary between the N. Altiplano and S. Altiplano domains is a broad transition zone (TZ, Fig. 1) between 19.5°S and 21°S where both (radiogenic and unradiogenic) types of crust are present. This transition zone might represent a single south-dipping thrust zone (Wörner et al., 1992) or a more complex zone in which the two types of crust are tectonically-interleaved.

The boundaries of the three main isotopic domains correspond to important tectonic boundaries inferred by previous workers. Some of the features of the isotopic maps also have an expression in the Bouguer gravity map of the region (Cady, 1992); for example, there is a change from NW-SE trending gravity anomalies in the N. Altiplano to NNE-SSW-trending gravity anomalies in the S. Altiplano, which presumably reflects the different orientations of basement structures in the two areas, while smaller-scale Pb isotopic anomalies such as "A" in Figure 1 seem to correspond to small gravity anomalies.

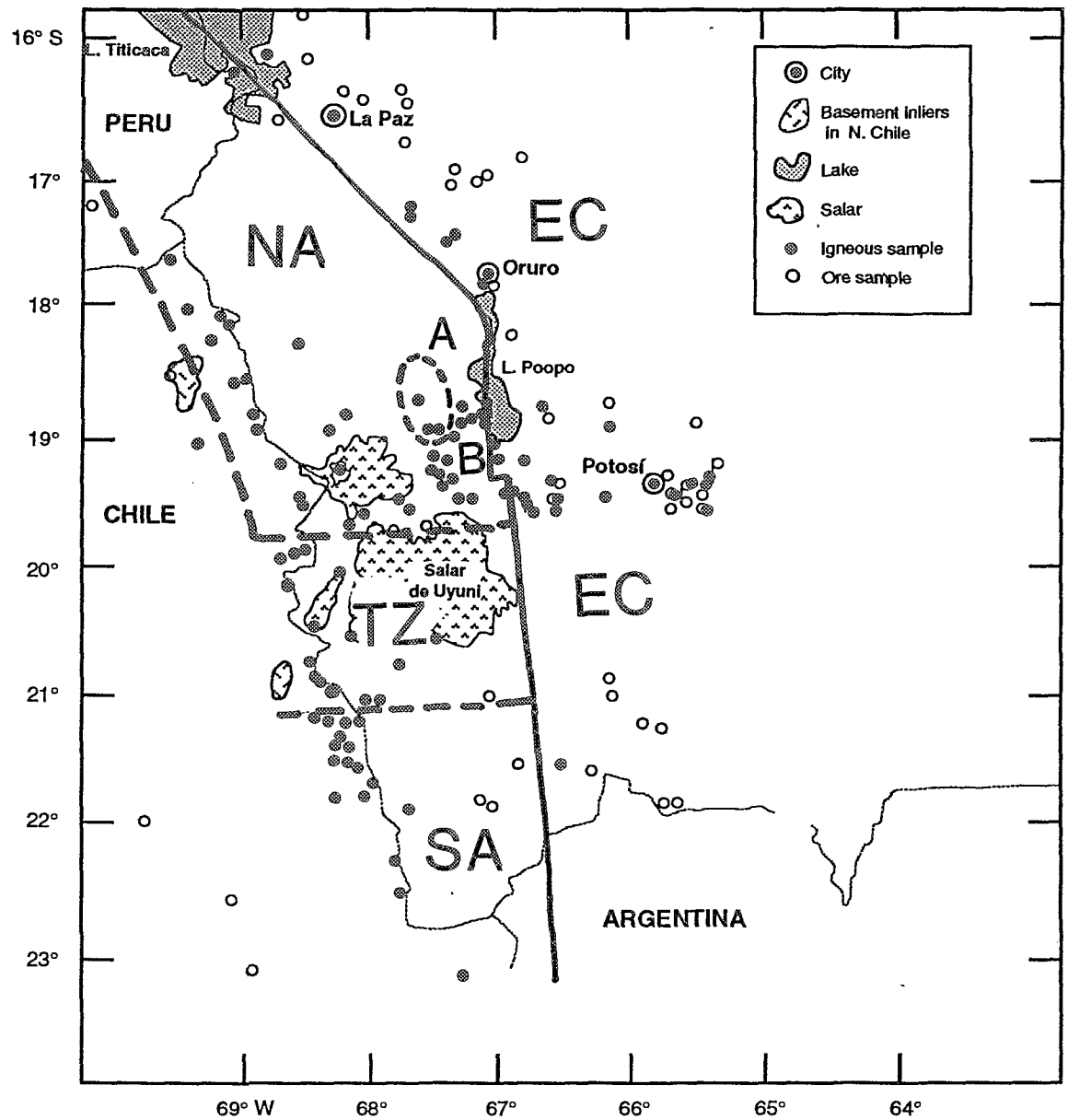

Figure 1: Principal crustal domains of the Altiplano (Bolivia and N. Chile), inferred from Pb isotopic data from ore deposits and volcanic rocks (data from this work, Davidson & de Silva (1992), Wörner et al. (1992), McFarlane et al. (1990) & references therein, and Harmon et al. (1984)). NA = Northern Altiplano domain, SA = Southern Altiplano domain, EC = Eastern Cordillera domain, TZ = Transition Zone between N. & S. Altiplano domains. "A" is a Pb isotope anomaly which corresponds to a small gravity anomaly. "B" is an apparent offset of a domain boundary, perhaps by faulting.

CONCLUSIONS

(1) Pb isotope data from ores and volcanic rocks in the Altiplano region define three distinct basement domains corresponding to the N. Altiplano, S. Altiplano and E. Cordillera.

(2) The data indicate that the boundary between the northern and southern Altiplano domains is a broad transition zone situated in the Salar de Uyuni area, but the boundary between the E. Cordillera and the Altiplano domains appears to be very abrupt.

(3) Most of the isotopic domain boundaries correspond to major tectonic boundaries inferred by previous workers and some also find expression in published gravity maps of the region. Pb isotope data from volcanic rocks and ores thus seem to be an excellent remote sensing tool for mapping large-scale crustal structure in poorly exposed areas.

REFERENCES

Aitcheson, S.J. and Forrest, A.H.F., 1993, Quantification of the crustal contribution during assimilation with fractional cystallization (AFC). Submitted to *Journal of Petrology.*

Cady, J., 1992. Simple Bouguer Gravity Anomaly Map of the Altiplano and Cordillera Occidental, Bolivia. In: *US Geological Survey Bulletin 1975: Geology and Mineral Resources of the Altiplano and Cordillera Occidental, Bolivia*, Plate 4.

Davidson, J. & de Silva, S.L., 1992, Volcanic rocks from the Bolivian Altiplano: insights into crustal structure, contamination, and magma genesis. *Geology*, **20**, 1127-1130.

Harmon, R.S., Barreiro, B., Moorbath, S., Hoefs, J., Francis, P.W., Thorpe, R.S., Déruelle, R.S., McHugh, J. & Viglino, J.A., 1984, Regional O-, Sr- and Pb-isotopic relationships in late Cenozoic calc-alkaline lavas of the Andean Cordillera. *Journal of the Geological Society, London*, **141**, 803-822.

McFarlane, A.W., Marcet, P., LeHuray, A.P. & Petersen, U, 1990, Lead isotope provinces of the Central Andes inferred from ores and crustal rocks. *Economic Geology*, **85**, 1857-1880.

Wörner, G., Moorbath, S. and Harmon, R.S., 1992, Andean Cenozoic volcanic centres reflect basement isotopic domains. *Geology*, **20**, 1103-1106.

A SEISMIC STUDY OF THE ALTIPLANO AND THE EASTERN CORDILLERA IN NORTHERN BOLIVIA: NEW CONSTRAINTS ON A LITHOSPHERIC MODEL

Catherine DORBATH [1,2], Michel GRANET [2], Georges POUPINET [3], Claude MARTINEZ [4]

(1) ORSTOM, 213 rue La Fayette, 75480 PARIS Cedex 10, FRANCE.
(2) EOPG, 5 rue René Descartes, 67084 STRASBOURG Cedex, FRANCE.
(3) LGIT IRIGM, BP 53X, 38041 GRENOBLE Cedex, FRANCE.
(4) Laboratoire de Géologie des Bassins, 34095 MONTPELLIER Cedex, FRANCE.

RESUME: Un profil de 34 stations sismologiques du réseau Lithoscope a été maintenu durant 4 mois en Bolivie, coupant l'Altiplano et la Cordillère Orientale depuis l'arc volcanique jusqu'à la zone sub-andine. Les téléséismes et les séismes locaux enregistrés ont été inversés séparément afin d'étudier la structure de la lithosphère et la géométrie de la subduction. Dans la région étudiée, qui correspond à la virgation des Andes, la zone de faille de la Cordillera Real controle les changements de structure très marqués jusque dans le manteau supérieur.

KEY WORDS: Andean Lithosphere, Altiplano, Tomography.

INTRODUCTION

The most significant geomorphological unit of the Central Andes is the Altiplano: it is, after Tibet, the largest high plateau in the world. The knowledge of its lithospheric structure is essential to the understanding of the mountain building in the Central Andes, which is undoubtedly a very complex process. Seismic tomography has proved to be a powerful tool in studying velocity structures, especially in active regions. In order to improve our knowledge of the deep structure beneath the Central Andes, we performed a seismic field experiment in northern Bolivia in 1989-1990. Thirtyfour vertical short period seismic stations of the French "Lithoscope" network were installed during a period of 4 months along a 320 km long profile, from the Volcanic Arc to the sub-Andean zone, crossing the Altiplano and the Eastern Cordillera in a direction approximately perpendicular to the main structural trend of the Andean chain. Among the 500 recorded earthquakes, we inverted separately the phases generated by 57 teleseismic events and 64 local events to study the lithospheric structures and the geometry of the subducted Nazca plate.

STRUCTURAL SETTING

Figure 1

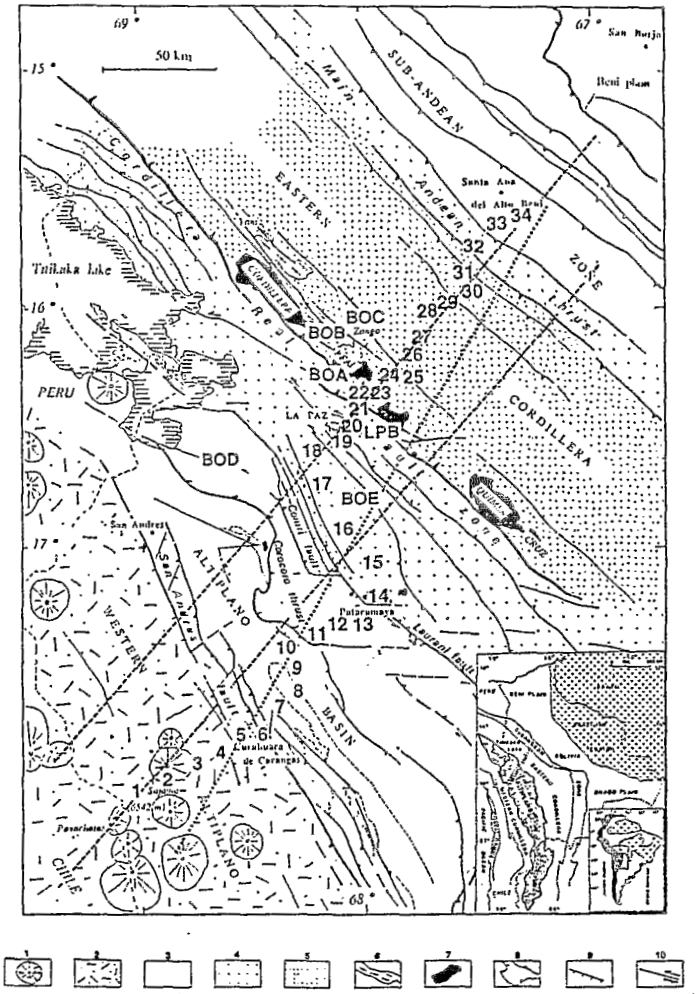

The geological setting of the region under study, after Martinez (Dorbath et al.,1993), is presented on Figure 1. The bold numbers show the location of the temporary seismic stations, the permanent Bolivian stations are represented by their code names. The dotted line shows the location of the cross-section through the teleseismic inversion model presented on Figure 2a. The dashed lines show the locations of the northern and southern cross-sections through the local earthquake inversion model presented on Figure 2b.

The insert shows the morphostructural zoning of the Central Andes. From the Pacific Ocean to the Brazilian craton (area marked with crosses), the main units are: the coastal range, the axial valley, the Western Cordillera, the Altiplano-Puna region (shaded area), the Eastern Cordillera and the sub-Andean zone. Crossing the Altiplano and the Eastern Cordillera, between 15° and 18° S and 67° and 69°W, the dotted line represents the approximate location of the seismic study described in this paper. The rectangle in the insert shows the location of the Central Andes in South America.

The numbers of the legend refer to the different geological and tectonical units:
1: Quaternary volcanoes. 2: Cenozoic volcano-sedimentary cover. 3: Meso-Cenozoic Altiplano Basin and Paleozoic-Mesozoic Cenozoic sub-Andes. 4: Siluro-Devonian borders of the Eastern Cordillera. 5: Ordovician axial zone of the Eastern Cordillera 6: Hercynian plutons. 7: Andean plutons. 8: Thrust fault. 9: Normal fault. 10: Strike-slip fault.

DATA PROCESSING

Teleseismic Tomography (TT): The data set contains 595 observations, nearly equally divided into P and PKP-phases. Relative residuals have been computed taking as a reference the station 10 which is situated in the central part of the Altiplano far from any major structural change. These residuals have a maximum amplitude reaching 3 s for P-phases and they show a strong azimuthal dependence. A noticeable sudden increase is observed, clearly associated with the fault system bordering the Eastern Cordillera to the west, the Cordillera Real fault system (CRFZ). The technique used here to invert the relative residuals follows the method developped by Aki et al. (1977), and involves the partition of the volume under investigation into layers, which are themselves divided into blocks. The starting P-velocity model is a smoothed version of velocity models obtained by previous geophysical studies. Several tests have been performed to check the reliability of this inversion: change of the geometry of the blocks, checkerboard resolution test... The final reduction of the variance obtained is 72%.

Local Earthquake Tomography (LET): As a first step, we computed the location of events reporting more than 15 arrival times with a minimum of 2 S-waves. We then kept only the events that met restrictive criteria insuring a high quality of their location. The complete data set includes about 1600 arrival times consisting of 1200 P and 400 S arrivals. Most of the local events we located are related to the subduction zone. The seismicity defines, between 90 km and 225 km, a part of the slab deeping to the NNE with a low angle of about 30°. The plot of mean P-residuals along the profile shows a pattern similar to the teleseismic profile; particularly, a jump of 1 s is observed when crossing the CFRZ. The tomographic inversion used is that developped by Thurber (1983) for the iterative simultaneous inversion of P-wave arrival times data for a 3D velocity structure and hypocentral parameters, adapted by Eberhart-Phillips (1986) to include S-wave data. The parametrization of the region under study is achieved by assigning velocity values at fixed points on a 3D grid.The same initial velocity model was used as for TT. The possibility offered by LET to get velocity structures and not simply perturbations of velocity as with TT is very useful in order to improve the knowledge of geological units; it also will help to estimate the Moho depth. The stability of the solution has been tested by the usual methods. The reduction of the variance is 87% for P-waves.

RESULTS

The results of the two tomographic studies are presented for P-waves on Figure 2a and b as vertical cross sections (see Fig.1 for their respective positions). They present consistent results, moreover they show a close correlation with the geological and tectonical units. For the two data set, the figures show a similar simple model consisting of two well contrasted blocks separated by a discontinuity sub-vertical or slightly dipping to south-west, which at the surface coincides with the CRFZ. The Altiplano is characterised by low velocities in the crust; the origin of velocity perturbations in the upper-crust is reasonably accounted for by the depth variations of the sedimentary fill, with a maximum thickness of 12 to 20 km under the Altiplano Basin. The spatial consistency between the main fault systems and velocity changes is very precise, particularly on Fig. 2b: the two fault zones bordering the Altiplano Basin, San Andres (SA) and Coniri-Laurani (CL) faults, enclose the well marked slow anomaly connected with this basin. The velocity perturbations in the lower crust interpreted as variations of the Moho depth, as well as the geometry of the iso-velocity lines obtained by LET, show a Moho depth wich decreases from about 60 km below the Altiplano to 50 km below the Eastern Cordillera. The absence of low velocity anomaly below the crust does not support hypothesis of magma accretion at the bottom of the crust under the Altiplano. The high velocity zone under the Eastern Cordillera extends down to 120 km on Fig. 2a, to the bottom of the model on Fig. 2b; we interpret this zone as the Brazilian craton. The representation of the underthrusting of this craton is somewhat different on the teleseismic and local earthquake studies. Nonetheless, both results are not consistent with a thin-skinn underthrusting as proposed in previous models. In the region under study, corresponding to the change of trend of the Central Andes, the western limit of the underthrusting of the craton is clearly the CRFZ, which is interpreted as an old suture zone.

Figure 2

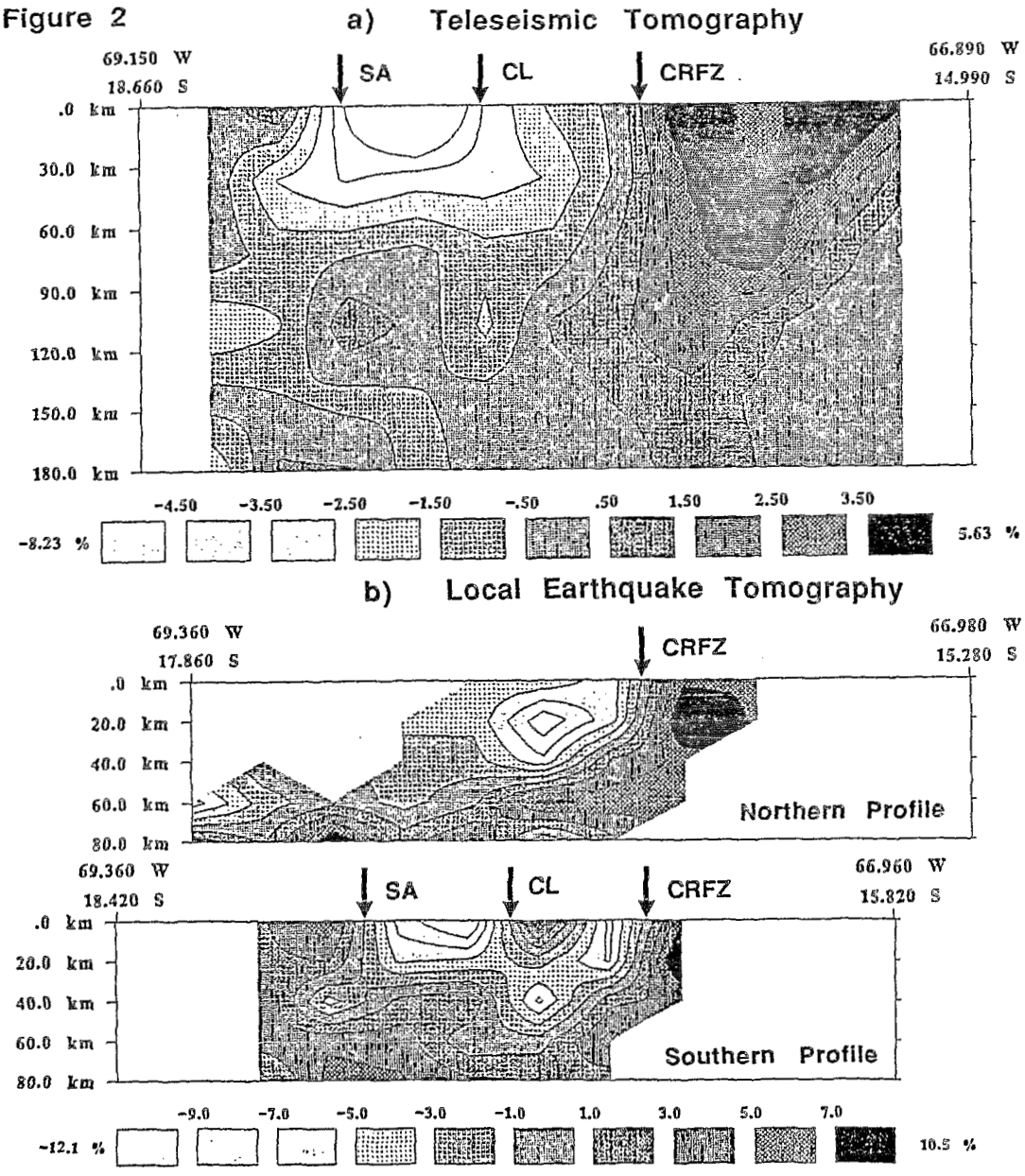

REFERENCES

AKI, K., CHRISTOFFERSSON, A. and HUSEBYE, 1977, Determination of the three-dimensional seismic structure of the lithosphere, J. Geophys. Res., 82, 277-296.

DORBATH, C., GRANET, M., POUPINET, G. and MARTINEZ, C., 1993, A teleseismic study of the Altiplano and the Eastern Cordillera in northern Bolivia: new constraints on a lithospheric model, J. Geophys. Res., to be published.

DORBATH, C. and GRANET, M., 1993, Local Earthquake Tomography of the Altiplano and the Eastern Cordillera in northern Bolivia, J. Geophys. Res., submitted.

EBERHART-PHILLIPS, D., 1986, Three-dimensional velocity structure in Northern California Coast Ranges from inversion of local earthquake arrival times, Bull. Seism. Am., 76, 1025-1052.

THURBER, C.H., 1983, Earthquake locations and three-dimensional crustal structure in the Coyote Lake area, central California, J. Geophys. Res., 88, 8226,8236.

THE INTERDISCIPLINARY RESEARCH PROGRAM "DEFORMATION PROCESSES IN THE ANDES", CONCEPTION AND GOALS

Peter GIESE

Institut für Geologie, Geophysik und Geoinformatik, Freie Universität Berlin, Malteserstraße 74 - 100, W-1000 Berlin 46

RESUMEN: El programa de investigación intradisciplinario "Procesos de Deformación en los Andes" ha sido instalado recientemente en Berlín y Potsdam con el apoyo de la Comunidad Alemana de Investigaciones Científicas (DFG). Se llevarán a cabo investigaciones geofísicas, geológicas, geodestas y petrológicas en los Andes Centrales a fin de resolver los problemas claves de la evolución tectónica andina con respecto a la estructura y la reología de la litósfera, la distribución de las tensiones en tiempo y espacio, el transporte del calor, la evolución de cuencas, la isostasía y el consuo de energía durante el proceso orogénico.

KEYWORDS: Central Andes, deformation processes, interdisciplinary research group Berlin and Potsdam SFB 267

INTRODUCTION

An interdisciplinary research program "Deformation Processes in the Andes" (SFB 267) has been established at the Freie Universität Berlin, the Technische Universität Berlin and the new GeoForschungsZentrum Potsdam, which is funded by the German Research Society (DFG). The results and experiences of the previous project "Mobility of Active Continental margins" which was active in the Central Andes from 1984 to 1990 have been used to design this new project, which is planned to run for about 10 years. The Central Andean segment between 20° and 26°S has been chosen for this program because the orogenic deformation processes are distinctly expressed just along this section. The main and outstanding features on this geotraverse can be outlined as follows:

- a convergence rate of about 10 cm/y and high strain rates,
- a vertical uplift rate of about 1mm/y,
- an extreme crustal thickness up to 60-70 km, caused by magmatic underplating and crustal stacking,
  zones with extremely high electrical conductivity in various tectonic zones and depths ranges,
- high seismicity in shallow, intermediate and large depth ranges,
- recent and subrecent volcanic activity,
- a well developed forearc, magmatic arc and back-arc,
- four magmatic arcs which have been evolved succesively by eastwards migrating from Jurassic to recent time,
- variations of the stress regime during the Andean period causing extensional and compressional deformations.

GOALS OF THE PROJECT

Geophysical, geodetic, geological und petrological studies will be carried along the Central Andean traverse aiming to tackle some of the key problems:

- the structure of the lithosphere and its rheological state and behaviour,
- the interaction between upper and lower plate,
- the distribution of the stress field and strain in time and space,
- the tectonic and petrological evolution of the upper plate under varying conditions of convergence,
- the geothermal field and heat transfer,
- the evolution of intramontanous basins and isostasy,
- energy consumption during the orogenic processes.

A number of various field projects are under preparation for the first three-year period 1993 - 1995. The main activities will be focussed in the magmatic arc of the Western Cordillera because this zone is seen as key region for the problems of stress transfer from the upper- /lower plate system of the forearc into the strongly deformed back-arc region.

In order to investigate the seismic structure of the magmatic arc and its relations to the adjacent zones a network of seismic refraction profiles are designed in the Western Cordillera. Further 20 mobile seismological stations will be set up in this region under operation for about 3 - 4 month aiming to record and investigate shallow and intermediate earthquakes. The study of seismicity, the determination of focal mechanism and tomographic investigations should reveal the deeper structures and behaviour of a recent magmatic arc. Magnetotelluric deep sounding measurements will contribute additional information. Detailed gravimetric measurements will be carried out aiming to study the deeper structure of intramontanous basins.

The measurements on the GPS-profile ANSA transversing the Central Andes and being under execution since 1989 will be continued. This study will be remarkably extended within an international co-operation with a profile running along the Pacific coast in N-S direction.

Special geological and petrological investigations are planned in the old and modern magmatic arcs aiming to reveal the complicated tectonic development of a magmatic arc system. Neotectonic studies are designed aiming to investigate the recent stress and strain field.

Such a project can be only realised by a close cooperation with geoscientific institutions in Argentina, Bolivia and Chile. In the past a successful cooperation has been devoloped which should be intensified and extended.

STRUCTURE OF THE COLLABORATIVE RESEARCH CENTER " DEFORMATION PROCESSES IN THE CENTRAL ANDES"

1. Deformation and stress field:
   Neotectonic studies, recent kinematics by GPS measurements, modelling of the recent stress and strain field.
2. Rheological stratification at a convergent plate boundary:
   Rock behaviour under high temperature and pressure condition derived from lab and field measurements, temperature field, heat transfer mechanism, rheology and fracturing of the Andean crust. Application of GIS.
3. Crustal evolution controlled by varying convergence boundary conditions:
   Structure of magmatic arcs by geological and geophysical studies, magmagenesis and crustal evolution, crustal shortening in the back-arc region.
4. Evolution of sedimentary basins and isostasy:
   Evolution of basins in various crustal environments,
   Balancing studies of erosional and sedimentary processes, isostatic studies.

ANOMALOUS UPPER MANTLE BENEATH THE CENTRAL ANDES. ISOSTASY AND ANDEAN UPLIFT.

Antonio Introcaso+

+ Facultad de Ciencias Exactas,Ingeniería y Agrimensura (U.N.Rosario)
Avenida Pellegrini N° 250 - 2000 ROARIO (Santa Fe) - ARGENTINA

Resúmen: Tres modelos corticales con manto superior "normal" y anómalo en dos secciones gravimétricas (22° S y 25° S) de los Andes Centrales, fueron comparados. Se analiza la elección de uno u otro para evaluar tanto el equilibrio isostático como el levantamiento andino.

Key Words: Central Andes, anomalous mantle, isostasy, andean uplift.

Introduction:

It have been pointed out that below the Central Andes it could exist : (1) significant heating on the lithospheric mantle (Froideveaux - Isacks, 1984; Introcaso - Pacino, 1988; Introcaso, 1988) and (2) cooling produced by the Nazca Plate subduction beneath the continental lithosphere (Grow - Bowin, 1975; Introcaso - Pacino, 1988). We analize two effects : the one on the gravity and the one on the Andean uplift. Both of them would produce density anomalies from (1) and (2). From (1), we would have lesser gravity and uplift ϵ_{c_i}; from (2), it would be high gravity and subsidence ϵ_{e_i}. Our study involves two gravity sections located on 22° and 25° South latitude, with Bouguer anomalies of more than — 400 mGal.

Isostatic compensation. Uplift mechanisms.

In order to analize the relationship between the upper mantle masses anomalies, the isostatic equilibrium and the Andean elevation, we study the compensation by calculating isostatic anomalies in three levels : (a) at the maximun crustal depth, with compensating root $(\Delta R_i)_a = 6.675\ h_t$, where h_t is the topographic elevation. In this case we assume the Bouguer anomaly $(AB)_a$ as totally originated by the crustal root; (b) at 140 km deep, at the bottom of the thermal lithosphere. So, the thickness of the crustal root $(\Delta R_i)_b$ would be diminished in 8.25 ϵ_{c_i} respect to $(\Delta R_i)_a$ and the Bouguer anomaly $(AB)_b$ would involve the thermal root and the crustal thickness, now diminished; (c) at 400 km deep (involving the subducted Nazca Plate). In this case, according

to our model, the oceanic plate effect would demand to diminish the crustal thickness defined in (a) in 8.25 ($\varepsilon_{c_i} - \varepsilon_{e_i}$). So, the Bouguer anomaly $(AB)_c$ would be compensed by the following effects : modificated crustal root, thermal root and subducted Nazca Plate. We must note that ε_{c_i} and ε_{e_i} effects, if they exist toghether, could be partially cancelled.

The three models present perfect masses balance, but at different depths. Because of this, the addition of the gravimetric effects that originates the compensating masses, is different in each one of them. Nevertheless, by comparing (a) and (b), for example, we show that these differences are not significant. In fact, if we think that the real model is (b), but we do not know the masses distribution below the sea level, it is usual to work with a classical model (like (a)) to evaluate isostasy. The gravity results show that, in general terms, the isostatic equilibrium was reached. In this case, the choice between (a) or (b) models is not critical for evaluating isostasy. But it *is* critical to find out the crustal characteristcs and to explain the Central Andean elevations. So, model (a) explains the uplift by: crustal shortening (S_h) or magmatic crustal addition (M_a), or by a combination of both mechanisms ($S_h + M_a$). In model (b), the isostatic compensation of the Andean masses is reached from a thermal lithospheric root and a crustal thickening produced by S_h or M_a or ($S_h + M_a$). Fig. 1 partially shows one of the two gravity sections analized from (a) and (b) models: the one located on 25° South latitude. Fig. 1 A shows the topographic elevation h_t, the crustal roots $(\Delta R)_a$ and $(\Delta R)_b$ and the thermal root $(\Delta R)_t$. Fig. 1 B shows the Bouguer anomalies $(AB)_a$ and $(AB)_b$. Fig. 1 C shows the isostatic anomalies $(AI)_a$ and $(AI)_b$.

From $(AB)_a$ gravity inversion, we found a maximun crustal root of 32 km, while $(AB)_b$ presents a maximun crustal root of 28 km. This crustal root was obtained from $(AB)_b$ gravity inversion with: $(AB)_b = (AB)_a + C_t$ where C_t is the thermal gravity correction.

We have calculated the isostatic anomalies $(AI)_a$ that correspond to the (a) model, with an isostatic correction $(CI)_a$ obtained from $(\Delta R)_a = 6.675\ h_t$. The isostatic anomalies $(AB)_b$ that correspond to the (b) model were calculated starting from $(\Delta R)_b = 6.675\ h_t - 8.25\ \varepsilon_{c_i}$. Now, the density excess produced by the crustal root diminishes in 5.29 km (= $8.25\ \varepsilon_{c_i}$) so balancing the density deficit originated by the thermal root. So, $(8.25 \times \varepsilon_{c_i}) \times 0.4 = 70.6422 \times 0.03$ or, in other words, the Andean masses are compensated at a depth of 140 km , by means of a combination of the crustal root (now diminished) and the thermal lithospheric root. Then, below h_t we have: $h_t \times \sigma' = (\Delta R)_b \times (\sigma_m - \sigma_c) + (\frac{L}{2} + \varepsilon_{c_i}) \times (\sigma_m - \sigma'_m)$. All densities and thickness of this expression can be found in Fig. 1.

Anyone of the models, (a) or (b) defines the isostatical condition. Nevertheless, the seismic results of the Germany Group (mentioned by Strunk, 1990) point out that the crustal thickness is consistent with the thickness found in (b).

Let's return now to model (c). Here, the Andean masses are balanced from a combination of crustal thickness (S_h or M_a or ($S_h + M_a$), thermal lithospheric root (R_T) and vertical contraction (C_V) related to the subducted Nazca Plate.

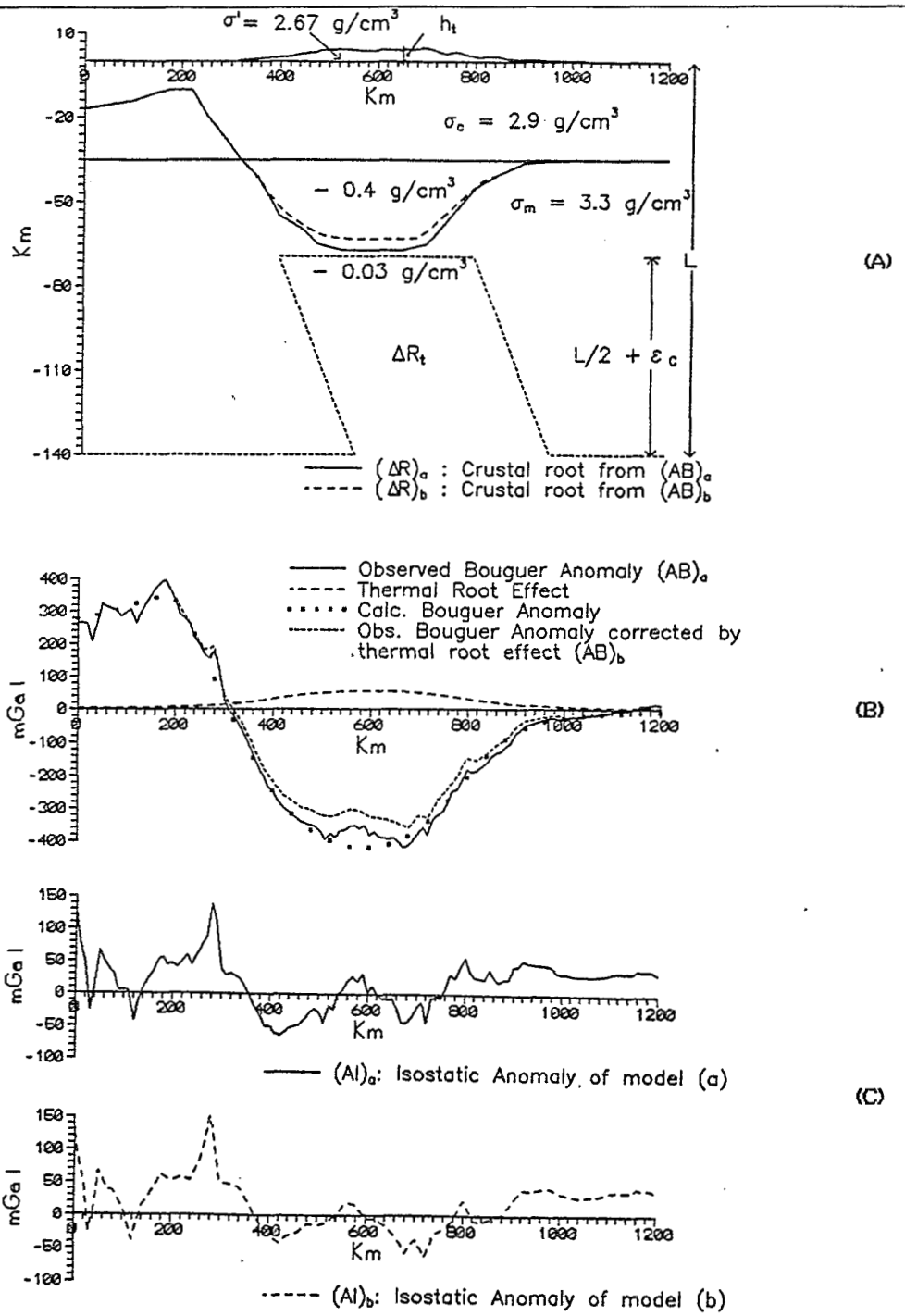

Fig. 1. (A) : Andean crust on 25° South latitude. $(\Delta R)_a$ root corresponds to model (a) with "normal" upper mantle. $(\Delta R)_b$ and $(\Delta R)_t$ roots correspond to model (b) with heating in the lower middle part of the thermal lithosphere. (B) : Observed Bouguer anomaly $(AB)_a$ with maximun amplitude of more than −400 mGal below the andean axis, and Bouguer anomaly $(AB)_b$ corrected by heating effect C_t (maximun C_t values: + 60 mGal). (C) : Isostatic anomalies $(AI)_a$ and $(AI)_b$ calculated from models (a) and (b) respectively.

Conclusions

Different crustal thicknesses from gravimetrical inversions made from $(AB)_a$, $(AB)_b$ or $(AB)_c$ have been found. In particular, we can see this in Fig. 1 for (a) and (b) models. Nevertheless, the isostatic anomalies $(AI)_a$ and $(AI)_b$ are consistent between themselves.

The choice among (a), (b) or (c) defines the posibilities for the different mechanisms to exist. This choice must be done trying to find the model whose crustal thickness could be consistent with the seismic results. In the 25° South latitude section, model (b) is probable.

This work, in its whole version, analizes the posibilities of (a), (b) and (c) models to explain the Central Andes uplift.

Acknowledgements

This work has been supported by the following: "Programa de Fomento a la Investigación Científica y Tecnológica (Universidad Nacional de Rosario) Resol. 239/92; PID-BID N° 214 Resol. 357/92 de CONICET and with the help of Facultad de Ciencias Exactas e Ingeniería (Universidad Nacional de Rosario).

References

Froideveaux, C. and Isacks, B., 1984. The mechanical state of the lithosphere in the Altiplano-Puna segment of the Andes. Earth Planet. Sci. Lett., 71: 305-314.

Grow, J. A. and Bowin, C. O., 1975. Evidence for high-density crust and mantle beneath the Chile trench due to the descending lithosphere. J. Geophys. Res., 80(11): 1449-1458.

Introcaso, A. and Pacino, M. C., 1988. Gravity Andean model associated with subduction near 24°25' South latitude. Rev. Geofis., 44: 29-44.

Isacks, B., 1988. Uplift of the Central Andean Plateau and Bending of the Bolivian Orocline. J. Gephys. Res., 93(B4): 3211-3231.

Strunk, S., 1990. Analyse und Interpretation des Schwerefeldes des aktiven Kontinentalrades der zentral Anden (20°- 26°S). Berliner Geowissenschaftliche Abhandlungen. Freie Universität Berlin : 1-135.

RESISTIVITY CROSS SECTION THROUGH THE SOUTHERN CENTRAL ANDEAN CRUST

Detlef KRÜGER(*) & Gerhard SCHWARZ(*)

(*)Freie Universität Berlin, Fachrichtung Geophysik, Malteserstr. 74 - 100, 1000 Berlin 46, Germany.

RESUMEN: A partir de mediciones magnetotelúricas se determinó a lo largo de un perfil a los 22°S, desde la Costa Pacífica hasta el Chaco, la distribución de resistividades eléctricas hasta 100 km de profundidad. Los resultados están basados en modelados magnetotelúricos bidimensionales, mediante los cuales pudo ser detectada una anomalía de alta conductividad que se extiende bajo la Cordillera Occidental, Altiplano hasta el sector occidental de la Cordillera Oriental.

KEY WORDS: Magnetotellurics - Geomagnetic deep soundings - 2D-modeling - Crustal high conductivity zones - Partial melting

INTRODUCTION

Magnetotelluric (MT) and geomagnetic deep sounding (GDS) experiments were done in the southern Central Andes between the Pacific coast of northern Chile and the Andean lowland plains of southern Bolivia and northwestern Argentina from 1982 to 1989 to investigate the crust and upper mantle structure (e.g., SCHWARZ et al. 1984, 1993, KRÜGER et al. 1990). Cross sections of previous publications are based on one-dimensional models only. Here, two-dimensional electrical resitivity models were constructed to better image conductivity structures. A resistivity cross section at lat 22°S based on 39 sites from the coastline across all morphostructural units up to the foreland region has been derived from three two-dimensional resistivity models using the finite element method.

CROSS SECTIONS OF ELECTRICAL RESISTIVITY

Two-dimensional resistivity models have been obtained by trial-and-error fitting of model data and those measured in the field. Both, MT-data as well as GDS induction vectors were used in modeling. A finite element forward algorithm as described by WANNAMAKER et al. (1986, 1987) was utilized.

Three EW-profiles were chosen for 2D-modeling across the Andes (fig. 1). They are described in detail by KRÜGER (1992, 1993). Due to the strong inductive effect (coast effect) of the Pacific Ocean the model for profile I, which starts at the coast and ends in the Western Cordillera, must include the ocean. The coast effect is caused by the Peru-Chile trench (depth ca. 8000 m), located nearly 100 km away from the coastline. Profile II crosses the Bolivian Altiplano at lat 21° 20' S and has a length of about 150 km. Profile III stretches from the western part of the Eastern Cordillera at about lat 22° 30' S eastwards to the

Andean foreland. It crosses west of Tarija a large scale conductive structure (fig. 1) observed earlier by geomagnetic deep soundings and inferred from 1D-model inversion of magnetotelluric data as well (SCHWARZ et al., 1986).

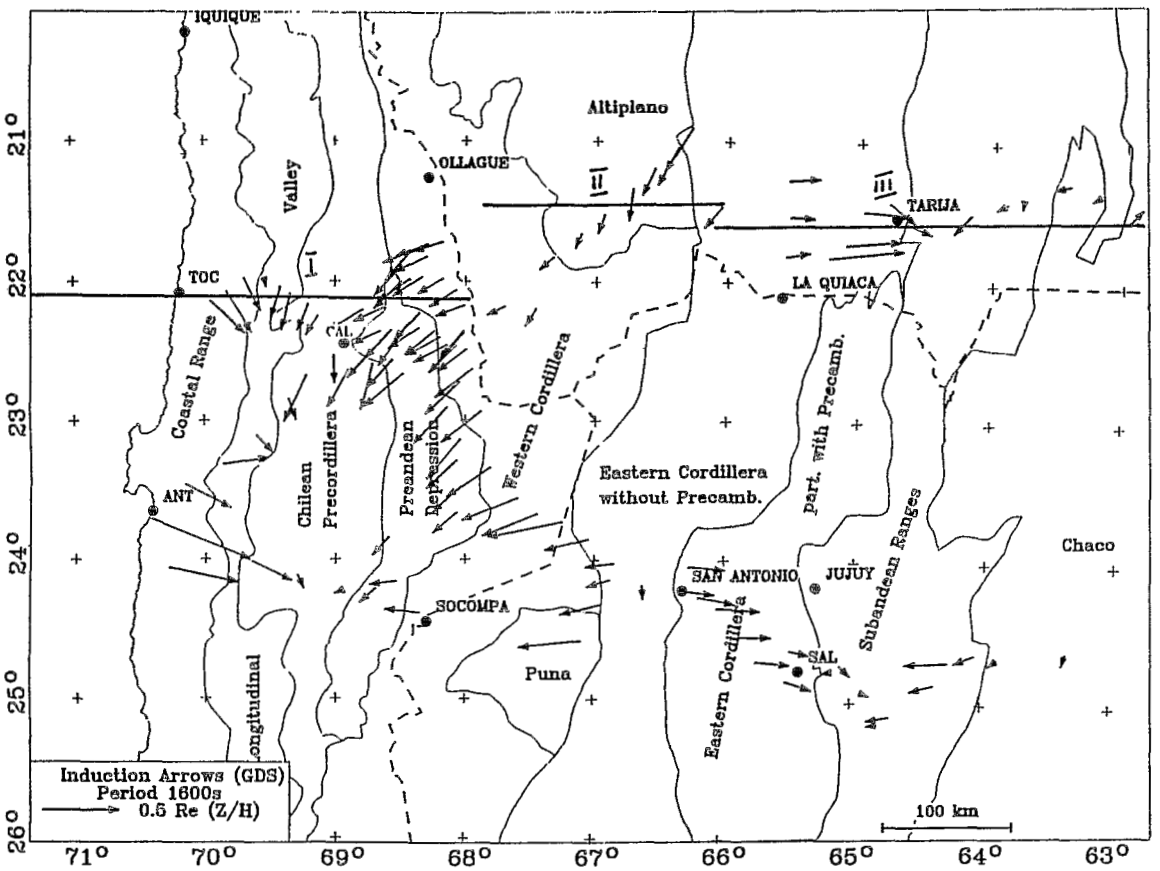

Fig. 1: Induction arrows, pointing away from anomalous high electrical conductivity zones, as results of GDS-data. The profiles, where the two-dimensional model search was carried out, are marked.

CONCLUSIONS

A cross section of the southern Central Andes showing schematically the modelled distribution of the electrical resistivity in the crust is presented in figure 2. The main features described from W to E are:

The crust below the Coastal Cordillera has high resistivities of more than 3000 ohm*m.
In this area the MT-data of E-polarization (parallel to strike of conductive structures) show a good conductor in the upper crust.
The resistivity of the 'normal Andean' upper crust seems to be relatively low, having values of 50 ohm*m $<$ rho $<$ 200 ohm*m.

A high conductivity zone (HCZ) is observed at shallow depth under the Western Codillera with a total conductance (conductivity-thickness product) of more than 25,000 Siemens. Another HCZ is located below the Altiplano with a total conductance of about 15,000 S in the lower crust and uprising from W to E. In

the western part of the Eastern Cordillera the total conductance first increases and then drops abruptly somewhere between La Quiaca and Tarija. The HCZ in the western part may be caused by partial melting in the crust, whereas the eastermost HCZ could be related to tectonic features such as deep rooted thrust levels.

The lowland plains of the Subandean and the Chaco are characterized by a low resistive cover. The resistivity of the crust and upper mantle increases from W to E to more than 3000 ohm*m.

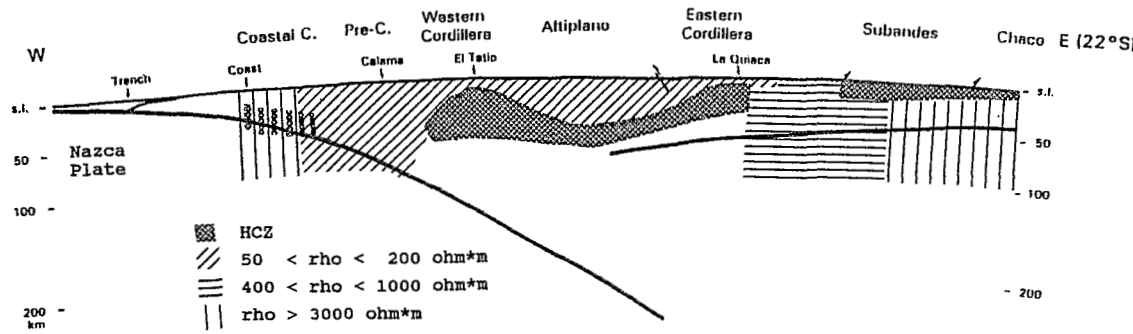

Fig. 2: Cross section (1:1) of the southern Central Andes at lat 22° S showing schematically the observed resistivities at different depth ranges. Most remarkable is a crustal zone of very high electrical conductivity which extends from the W-Cordillera eastwards for about 250 km. Thick lines mark seismological interfaces (WIGGER et al., this vol.).

REFERENCES

KRÜGER, D., MASSOW, W., SCHWARZ, G., 1990, Neues von der Andengeotraverse. In: HAAK V., HOMILIUS, J. (eds), Prot. Koll. Elektromagn. Tiefenforschung, Hornburg, pp 267-278

KRÜGER, D., 1992, 2D-Modellierung auf der Andentraverse. In HAAK V., RODEMANN, H. (eds), Prot. Koll. Elektromagn. Tiefenforschung, Borkheide, pp 243- 260

KRÜGER, D., 1993, Modellierungen zur Struktur elektrisch leitfähiger Zonen in den Zentralen Anden, Berliner geowiss. Abh. (in prep.)

SCHWARZ, G., HAAK, V., MARTINEZ, E., BANNISTER, J., 1984, The electrical conductivity of the Andean crust in northern Chile and southern Bolivia as inferred from magnetotelluric measurments. J. Geophys. 55: 169-178

SCHWARZ, G., MARTINEZ. E., BANNISTER, J., 1986, Untersuchungen zur elektrischen Leitfähigkeit in den Zentralen Anden. Berliner geowiss. Abh. (A) 66: 49-72

SCHWARZ, G., CHONG G., D., KRÜGER, D., MARTINEZ, E. , MASSOW, W., RATH, V., VIRAMONTE, J.G., 1993, Crustal high conductivity zones in the southern Central Andes. In: REUTTER, K.J. SCHEUBER, E., WIGGER, P.J. (eds), Tectonics of the Southern Central Andes, Springer, in press.

WANNAMAKER, P.E., STODT, J.A., RIJO, L., 1986, Two-dimensional topographic responses in magnetotellurics modelled using finite elements, Geophysics, 51, 2131-2144.

WANNAMAKER, P.E., STODT, J.A., RIJO, L., 1987, A stable finite element solution for two-dimensional magnetotelluric modelling, Geophys. J. R. Astron. Soc., 88, 277-296.

HAS DELAMINATION OF THE LOWER LITHOSPHERE OF THE CENTRAL ANDES OCCURRED?

Barbara Moths Sheffels

Department of Earth and Planetary Sciences
Harvard University
20 Oxford St.
Cambridge, MA 02138

RESUMEN La cantidad del acortamiento cortical en los Andes centrales y la evidencia parA la delaminación (o subducción intracontinental) en otros cinturones de montañas indican que la delaminacion puede ser un proceso importante en el desarollo de los Andes. Las estimaciones del acortamiento definen la deformación de la litosfera inferior, y sugieren la cantidad de la corteza y del manto superior que peude ser involucrado en la delaminación. Se considera la evidencia termica, gravimetrica, estructural, y sismologica para la delaminación. Una comparison de los Andes con otros lugares donde la delaminación esta propuesta ayuda en definir el proceso en los Andes y en general.

KEY WORDS: delamination, convective instability, crustal shortening, central Andes, Bolivia

INTRODUCTION

Crustal shortening has played a key role in the formation of mountain belts around the world, ancient and modern, in a variety of tectonic settings. The corresponding shortening within the lower crust and mantle lithosphere has led to various hypotheses concerning the fate of those regions of the continental lithosphere, including subduction, delamination, or convective instability. The central Andes provide a unique opportunity, since they are young and actively forming, to examine the deformation of the entire continental lithosphere, and to assess spatial and temporal variations in the shortening of the lower lithosphere, and its possible loss to the asthenosphere.

This paper will use surface structural data from the Bolivian Andes to place constraints on the deformation of the lower lithosphere, consider some implications of the insights provided by these constraints, and summarize the evidence for and against the process of delamination in the Andes, both from the Andes and in comparison with other mountain belts. The term "delamination" is used in a general sense, to indicate a final geometry that results from loss of the lower continental lithosphere to the asthenosphere, but is not meant to differentiate between specific processes, e.g. the delamination of Bird (1978; Bird and Baumgardner, 1981) or the convective instability of England and Houseman (1988, 1989).

GEOLOGIC SETTING

The central Andes are the site of the earth's second largest plateau and some of the thickest crust on the earth, making them a unique site on the earth today. While these attributes invite comparison to the Himalaya and Tibet, the Andes have formed in response to subduction of oceanic lithosphere only. We currently understand the formation of the high elevations and thickened crust as primarily the result of crustal shortening, the product of deformation in fold and thrust belts extending across the Altiplano, Cordillera Oriental and Sub-Andes (Roeder, 1988; Isacks, 1988; Sempere et al., 1988; Sheffels, 1988; Hérail et al., 1990, Baby et al., 1992).

IMPLICATIONS OF SHORTENING ESTIMATES AND INITIAL GEOMETRIES FOR LITHOSPHERIC DEFORMATION

The amount of crustal shortening documented in the central Andes can be used to constrain the deformation of the lower lithosphere for various initial crustal and lithospheric thicknesses. A range of shortening estimates has been determined from balanced cross sections spanning the Bolivian Cordillera Oriental and Sub-andes at approximately 18°S (Sheffels, 1988), where shortening is plausibly a maximum in the central Andes. A lower bound of 210 kilometers is based on a set of restrictive assumptions for the cross section interpretations; relaxation of individual assumptions yields larger estimates of 325 and a maximum of 670 kilometers. Shortening estimates derived independently (Lyon-Caen et al., 1985; Isacks, 1988; Baby et al., 1992) lie in the range of 300-350 kilometers.

Lithospheric roots corresponding to the various estimates of shortening can be calculated, and demonstrate a sizable space problem. Initial thicknesses of 40 kilometers for the crust and 100 kilometers for the lithosphere (including the crust) and plane strain deformation are assumed initially. Initial crustal thickness is based on paleogeographic evidence and the tectonic history of the region. Substantial thickening of the mantle lithosphere results for each estimate of shortening, even the minimum case; the three estimates given above correspond to 23, 31, or 48 percent shortening. The geometry of the deformation is not addressed. Crustal material contributes to the thickened root if the cross sectional area resulting from a given estimate of shortening and initial crustal thickness exceeds the present-day crustal cross sectional area. The critical values of shortening are as follows: crustal subduction is required if the amount of shortening is greater than 315 kilometers, assuming the crust was initially 40 kilometers thick. If the crust was initially 45 kilometers thick, the necessary amount of shortening decreases to 215 kilometers; if initially 35 kilometers thick, crust will be subducted if shortening exceeds 445 kilometers. If the lithosphere is initially thinned beneath the future mountain belt, but is 140 kilometers thick elsewhere (Isacks, 1988), roots of the same size or larger are formed as when the lithosphere is initially uniformly 100 kilometers thick. A lower limit on initial thinning is determined: to produce a uniform layer of continental mantle 60 kilometers thick today, an average initial thickness of the entire lithosphere of 80 kilometers is required.

HAS DELAMINATION OCCURRED?

In other mountain belts, crustal subduction and loss of the thickened lithosphere are suggested by similar constant area arguments and by independent evidence for a thinned lithosphere. Indications that the asthenosphere has replaced the mantle lithosphere beneath substantially shortened mountain belts, have led to hypotheses of convective instability (Houseman et al., 1981; England and Houseman, 1989), or delamination (Bird, 1978, Bird and Baumgardner, 1981), as mechanisms to remove the thickened lithosphere due to gravitational instability. Theoretical considerations suggest that the instability can develop as quickly as 10 Ma after shortening commences (Houseman et al., 1981), and that a critical amount of shortening is required (England and Houseman, 1989). The involvement of the lower crust is dependent on the initial thicknesses assumed and on the behavior of the mantle lithosphere. Others have argued (Kincaid and Silver, 1993) or demonstrated (the Alps, Fleitout and Froidevaux, 1982) that the thickened lithosphere has not been lost beneath shortened mountain belts. In light of these diverse observations from other mountain belts and the constraints imposed by the surface structural data in the Andes, it is instructive to consider whether delamination has occurred in the central Andes.

Several lines of evidence are available to assess whether delamination has occurred in the central Andes, an argument that has been proposed for the region as a whole or with reference to specific regions (Froidevaux and Isacks, 1984; Sheffels, 1988, 1993; Isacks, 1988; Whitman et al., 1992; Kay and Kay, 1993). Heat flow data that indicate that the Cordillera Oriental and eastern Altiplano are unusually hot (Henry and Pollack, 1988) can be interpreted to indicate that asthenosphere has replaced lithosphere in those regions, although this interpretation is a non-unique one. Gravity data suggest that the lithosphere has elastic strength throughout the Sub-andes (Lyon-Caen et al., 1985), which can be interpreted as a lateral limit on the width of a region of delamination; where the lithosphere no longer behaves elastically, it has delaminated. The geoid anomaly, a high of 25 m (Froidevaux and Isacks, 1984), suggests a thermal component (Isacks, 1988) to the high elevations observed, which could be supplied by replacement of lithosphere by asthenosphere. Seismicity patterns are also suggestive: deep earthquakes (~650 kilometers) may be related to the subduction of the lower lithosphere, tensional earthquakes within the slab at intermediate depths may reflect bending of the slab resulting from deformation by the lithospheric root, and low levels of crustal seismicity may reflect a higher geotherm. Attenuation is described as high in the Altiplano region (James, 1971), although Whitman et al. (1992) restrict high attenuation regions to the active magmatic arc and the southern central Andes, arguing against delamination beneath the Bolivian Andes. The distribution and magnitude of normal faulting does not seem to be related to delamination in either of the ways that extensional processes in the Basin and Range (Sonder et al., 1987) or the Himalaya seem to be (England and Houseman, 1989). While the extension documented in the Andes could be related to delamination, such scenarios are not the simplest explanation. Some of the normal faulting, within the portion of the mountain belt containing the Altiplano, can be shown to be secondary faulting, accommodating tear faulting in thrust systems or steps in strike-slip faults; this interpretation may be the simplest, but additional data are needed. In any case, the absence of extension is not conclusive evidence that delamination has not occurred.

In summary, a definitive case for or against delamination can not be made. In addition to satisfying all of the available data, conclusions regarding delamination in the central Andes must integrate additional factors. For example, the "normal" effects of a subduction zone with an active magmatic arc on geotherms and convection must be considered. Also, the magnitude of shortening affecting the lithosphere suggests that three-dimensional deformation may be important: where shortening is a maximum, the deformation of the continental lithosphere may control the dip of the subducting oceanic slab, rather than vice versa; tectonic style is not determined by slab dip. Furthermore, along-strike flow may result from the convergence; the two-dimensional space problem may be resolved either by moving material down (delamination) or laterally out of the cross section, a possible explanation for the geometry of the Nazca slab. Note that the causal ordering follows from the surface constraints. Finally, comparison with other mountain belts is used to clarify the controls on the delamination process in continental lithosphere.

CONCLUSIONS

Well-constrained surface data from the Bolivian Andes allow the determination of bounds on amounts of lower crustal and upper mantle shortening, and therefore on amounts of subduction or delamination that may have occurred, for a range of initial thicknesses. Crustal subduction is not required for the most plausible estimates of shortening and initial crustal thickness. One implication of the magnitude of shortening is that the shortening may have driven the along-strike variation in the dip of the Nazca slab observed today. Although similar to the Himalaya, a mountain range produced by continental collision, the central Andes have formed in a non-collisional setting. Delamination is suggested by analogy with other mountain belts. Theoretical considerations suggest that sufficient time has passed since the onset of shortening for a convective instability to develop. While atttenuation data suggest that delamination has not occurred in this region, heat flow, gravity, and seismicity data are permissive evidence for delamination.

REFERENCES

Baby, Patrice, Hérail, G., Salinas, R. and Sempere, T., 1992, Geometry and kinematic evolution of passive roof duplexes deduced from cross section balancing: example from the foreland thrust system of the southern Bolivian Subandean Zone: Tectonics, v. 11, p. 523-536.

Bird, P., 1978, Initiation of intracontinental subduction in the Himalaya, Jour. Geophys. Res., 83, 4975-4987.

Bird, P. and J. Baumgardner, 1981, Steady propagation of delamination events, Jour. Geophys. Res., 86, 4891-4903.

England, P. and G.Houseman, 1988, The mechanics of the Tibetan Plateau, Phil. Trans. Roy. Soc. London A, 326, 301-320.

England, P. and G.Houseman, 1989, Extension during continental convergence, with application to the Tibetan Plateau, Jour. Geophys. Res., 94, 17,561-17,579.

Fleitout, L. and C.Froidevaux, 1982, Tectonics and topography for a lithosphere containing density heterogeneities, Tectonics, 1, 21-56.

Froidevaux, C. and B.L.Isacks, 1984, The mechanical state of the lithosphere in the Altiplano-Puna segment of the Andes, Earth Planet. Sci. Lett., 71, 305-314.

Henry, S.G. and H.N.Pollack, 1988, Terrestrial Heat Flow above the Andean Subduction Zone in Bolivia and Peru, Jour. Geophys. Res., 93, 15,153-15,162.

Hérail, G., Baby, P., López, M., Oller, J., López, O., Salinas, R., Sempere, T., Beccar, G. and Toledo, H., 1990, Structure and kinematic evolution of the Subandean thrust system of Bolivia (abs.): Symp. Int. "Géodynamique Andine" 1990, edited by the Institut Francais de Recherche Scientifique pour le Développement en Coopération, p. 179-182, Colloques et Séminaires, Paris.

Houseman, G., D.McKenzie and P.Molnar, 1981, Convective instability of a thickened boundary layer and its relevance for the thermal evolution of continental convergent belts, Jour. Geophys. Res., 86, 6115-6132.

Isacks, B.L., 1988, Uplift of the Central Andean Plateau and bending of the Bolivian Orocline: Journal of Geophysical Research, 93, p. 3211-3231.

James, D.E., 1971, Andean crustal and upper mantle structure, Jour. Geophys. Res., 76, 3246-3271.

Kay, R.W. and S.M.Kay, 1993, Delamination and delamination magmatism, Tectonophysics, 219, 177-189.

Kincaid, C. and P.G.Silver, 1993, Convection and viscous shear heating in the upper mantle (abs.), EOS, Trans. AGU, 74, 209.

Lyon-Caen, H., P. Molnar, and G. Suárez, 1985, Gravity anomalies and flexure of the Brazilian shield beneath the Bolivian Andes, Earth and Planet.Sci. Lett., 75, 81-92.

Roeder, D., 1988, Andean-age structure of Eastern Cordillera (Province of La Paz, Bolivia): Tectonics, 7, p. 23-39.

Sempere, T., G.Hérail, J.Oller, and P.Baby, 1988, Los aspectos estructurales y sedimentarios del oroclino boliviano, Proceedings, Congreso Geológico Chileno, 5th, Santiago de Chile, 1, A127-A142..

Sheffels, B.M., 1988, Structural constraints on crustal shortening in the Bolivian Andes [Ph.D. thesis]: Massachusetts Institute of Technology, Cambridge, MA, 170 p.

Sheffels, B.M., 1993, Constraints on intracontinental subduction in the central Andes (abs.), EOS, Trans. AGU, 74, 311.

Sonder, L.J., P.C.England, B.P.Wernicke, and R.L.Christiansen, 1987, A physical model for Cenozoic extension of western North America, in Continental Extensional Tectonics, M.P. Coward, J.F.Dewey, and P.L.Hancock, eds., Geol. Soc. London Spec. Pub., No. 28, 187-201.

Whitman, D., B.L.Isacks, J.Chatelain, J. Chiu, and A. Perez, 1992, Attenuation of hisgh-frequency seismic waves beneath the central Andean plateau, Jour. Geophys. Res, 97, 19,929-19947.

GEOELECTROMAGNETIC STUDIES IN THE CENTRAL SOUTHERN ANDES REGION

Miguel MUÑOZ

Departamento de Geofísica, Universidad de Chile, Casilla 2777, Santiago, Chile.

RESUMEN: Se exponen resultados de estudios magnetotelúricos y magnetovariacionales realizados en zonas de Argentina y Chile adyacentes a los Andes, y que han significado una contribución para la individuación de capas conductoras en la corteza y el manto, como también para la discusión de los efectos de distorsión en las curvas de resistividad aparente y del nivel hipotético de la conductósfera.

KEY WORDS: Argentina; Chile; Magnetotellurics; Asthenosphere; Conductosphere; Geothermal Fields.

INTRODUCTION

The magnetotelluric method was introduced in South America by H.G. Fournier, and many preliminary results are contained in his *Rapport de mission* (Fournier, 1981). Here a review of studies carried out in the central-southern Andes region in Argentina during the past years is presented, as well as results of magnetotelluric (MT) soundings done between the Coastal Range and the Andean volcanic zone in the area of southern Chile. The areas discussed in this contribution lie between latitudes 26°S and 39°S.

Modelling programs by Kisak and Silvester (1975) and Wannamaker et al. (1987) were used in these studies.

SANTIAGO DEL ESTERO-TUCUMAN GEOTHERMAL AREA

This area in NW Argentina is centered at about 26°S; 67°30'W in the back arc region. 2 D modelling of six MT soundings shows a zone of high conductance (2500-27000 Siemens) from 0 to 75 Km depth. This zone is limited at the south of the area (27°S) by structures of great resistivities (3000 - 20000 ohmm) where seismic activity -absent in the high conductance zone- reinitiates with foci at intermediate depths. Many hot springs are known in

the zone of high conductance, and temperature gradients in water wells are generally of about 100°C/Km.

Modelling of this zone has shown that 3 D distorting effects -which in some situations can be stronger in the E-polarization mode- are acting in some of the MT soundings (Muñoz et al., 1992).

AREA AT 33°S LATITUDE IN ARGENTINA

Near the Andes Cordillera -at longitude 69°W- MT soundings indicate conductive layers at depths of about 16 Km, 34 Km and 80 Km. Towards the south direction the depth of the second conductive layer is shallower (heat flow is here possibly higher). At 64°W longitude only two conductive layers are encountered: one at 40 Km and another at more than 200 Km depth, and both descending in the east direction (Borzotta et al., 1993).

PETEROA ACTIVE VOLCANO AREA (ANDES CORDILLERA, ARGENTINA).

Four MT soundings in an extension of 40 Km at latitude 35°30'S show a monocline conductive layer crossing the crust in the EW direction. At the West end the top level of this layer is at 32 Km depth, and its thickness is of about 12 Km. Under the East extreme of the profile the top of this layer is at only 5 Km depth; its thickness is of about 6.5 Km. Hot sulphurate water springs are found in the centre of the MT sounding profile. Magnetovariational sounding results suggest a conductive zone in the crust, possibly under the Atuel Valley, 25 Km at the NE of the MT profile (Fournier et al., 1993).

AREA BETWEEN THE PACIFIC OCEAN AND VILLARRICA VOLCANO (39°25'S; 71°57'W) - CHILE

1D models give a conductive layer for three sounding sites in the zone of Villarrica active volcano. This conductive layer lies in the depth range between about 40 to 100 Km. Resistivity of this layer is between 20 to 80 ohmm. In the boundary at 500 Km depth -which may be the conductosphere top level- the 1 D modelling gives a resistivity of 2 ohmm which manifests the procedure of tying in of the distorted curve to the geomagnetic global value (Muñoz et al., 1990a).

These results contrast wih 2D models which consider the effects due to heterogeneities in the crust and upper mantle structure from the Pacific Ocean to the volcanic zone in the Andes. In order to construct a more reliable model of the earth's structure of continental Chile at latitude 39°S, a scheme including oceanic structures has been assumed and subjected to nearly 80 model parameter variations (Muñoz et al., 1990b, 1992). The conductive layer under the ocean has been characterized by resistivity values of about 0.1-100 ohmm with its upper level at a depth of nearly 45 Km. Coast effect and diversity of oceanic mantle clearly changes the resistivity pattern under the continental area. Under the area of Villarrica volcano and to the east (Andes Cordillera and Argentina) a resistive lower crust has to be considered; in the eastern region the transition to the upper mantle is also characterized by a high resistivity. The source of magma of Villarrica volcano seems to be

concentrated at depths between 70 and 80 Km but there is not a simple connection with an 'asthenospheic layer' in the upper mantle. The case may be that the asthenosphere in the transition zone of the continent is subjected to cooling by the subsiding oceanic lithosphere. The hypothetical resistivity scheme also gives a conductive layer (200 ohmm) of variable thickness (10-15 Km) which ascends from the Pacific Ocean (30 Km top level) to the Andean Range (25 Km top level) and penetrates into the back arc region in Argentina.

The scatter of data does not allow a reliable determination of the upper level of the conductosphere, but different resistivity values in the range of 20-0.1 ohmm strongly control the coast effect over a large period range.

Hypothetical magma chambers in the crust have not been individuated under the zone of Villarrica volcano. 2D model tests carried out for this area have shown that, besides the quality of data, the discovery of magma chambers by using the MT method may depend on the topography of the region, the type of magma and the extended resistivity distribution pattern. During the *10th Workshop on Electromagnetic Induction in the Earth* (Ensenada, México, 1990), George Keller presented serious objections to such an enterprise, but Mark Berdichevsky objected that one of his colleagues have already done it. Who stands to reason? This is a question difficult to answer, as follows from the literature concerning this problem (e.g., Newman et al., 1985; Sibett, 1988)

CONCLUSIONS

Magnetotelluric studies in the central-southern Andes region are giving important results concerning the thermo-electrical structure of the crust and upper mantle in the arc-trench and back arc regions. These results should be useful for studying the volcanic and geodynamic processes, and for the assessment of geothermal fields in view of energy applications.

REFERENCES

BORZOTTA, E., FOURNIER, H.G., MAMANI, M. and MAIDANA, A., 1993. *Work-in-progress.*

FOURNIER, H.G., 1981. Rapport de Mission en Argentine. Centre de Recherches Géophysiques. Laboratoire de Géomagnetisme, Paris.

FOURNIER, H.G., MAMANI, A., MUÑOZ, M., MAIDANA, A., ROKITYANSKY, I., BORZOTTA, E., CASTIGLIONE, B. and VENENCIA, J., 1993. *Work-in-progress.*

KISAK, E. and SILVESTER, P., 1975. Comp. Phys. Communic., **10**, 421-433.

MUÑOZ, M., FOURNIER, H., MAMANI, M. , FEBRER, J., BORZOTTA, E. and MAIDANA, A., 1990a. Phys. Earth Planet. Int., **60**, 195-211.

MUÑOZ, M., MAMANI, M., FOURNIER, H., BORZOTTA, E., MOYANO, C. and MAIDANA, A., 1990b. Distortion of tensor magnetotelluric apparent resistivities caused by large heterogeneities in the crust and upper mantle at latitude 39°S in Chile. 10th Workshop on Electromagnetic Induction in the Earth. Abstracts (5.3), Ensenada, México.

MUÑOZ, M.A., FOURNIER, H.G., MAMANI, M. and BORZOTTA, E., 1992. In: Electromagnetic Results in Active Orogenic Zones (Editor: A. Adám); Special Issue Acta Geod. Geoph. Mont. Hung., **27**, 65-86

NEWMAN, G.A., WANNAMAKER, P.E. and HOHMANN, G.W., 1985. Geophysics, **50**, 1136-1143

SIBETT, B.S., 1988. Earth-Sciences Rev., **25**, 291-309

WANNAMAKER, P.E., STODT, J. and RIJO, L., 1987. PW2D-Finite element program for solution of magnetotelluric responses of two-dimensional earth resistivity structure. Earth Science Laboratory, University of Utah Research Institute, Publ. ESL-158

THE ANDEAN ELEVATION AT 39º SOUTH LATITUDE FROM GRAVITY DATA

María Cristina Pacino

Instituto de Física Rosario (IFIR)
Av. Pellegrini 250
(2000) Rosario - ARGENTINA

RESUMEN: Se presenta aquí una sección gravimétrica transcontinental E-W en 39º de latitud Sur analizándose, además de los clásicos modelos corticales, posibles mecanismos de compensación isostática y evaluando el acortamiento compresivo que habría contribuído decisivamente al levantamiento Andino.

KEY WORDS: gravity - geodinamics - isostasy - shortenings

INTRODUCTION

The analyzed section is refered to a previous study at these latitudes (Diez Rodriguez and Introcaso, 1986), incorporating gravity anomalies both in the Pacific and Atlantic ocean sectors and altimetric satellital data(Fig.1)

It was prepared with data from the Instituto Geográfico Militar Argentino and the Universidad de Chile, in the continental sector, while at sea, batimetric data from the satellital file of the Instituto Antártico Argentino and Free Air anomalies from Bowin et al (1981) were used. With these data Bouguer anomalies were also calculated by replacing the sea water ($\sigma a = 1.03$ g/cm^3) by materials of density $\sigma = 2.9$ g/cm^3, (the assumed continental crustal density according to Pacino and Introcaso, 1988; Introcaso and Pacino, 1989; ...).

The profile, which exceeds 2000 Km. length, shows minimum Bouguer anomalies of about -90 mGal in coincidence with the largest Andean altitudes, while maximum values of +230 mGal are located offshore, in the Pacific Ocean (Fig.1).

GEOLOGICAL SETTING

This section crosses, in its continental itinerary, important geological provinces in Chile and Argentina: Cordillera de la Costa, Valle Central Chileno, Cordillera de los Andes, Cuenca Neuquina, northwestern section of the

cuenca de Colorado, Cuenca Interserrana Bonaerense and Southern border of Tandilia.

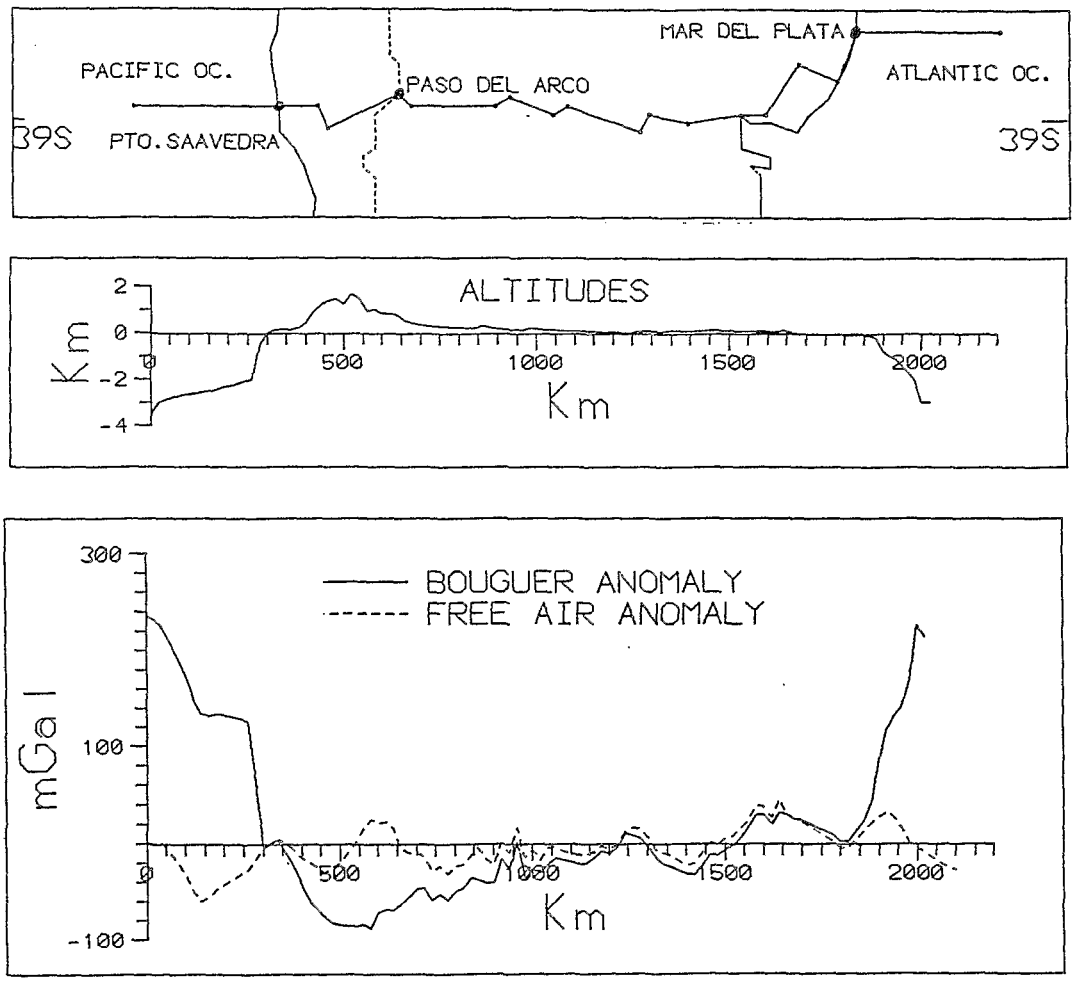

Fig.1: Location of the section. Altitudes, Free Air and Bouguer anomalies profile.

ISOSTATIC BEHAVIOUR

The isostatic balance for the section was analyzed in two ways: (a) by means of a thickened crust in the Airy concept and (b), by means of both, a thickened crust and a thermal root in the upper mantle, according to Pratt's hypothesis.

The results indicate that the studied section essentialy responds to an Airy's isostatic model, with little possitive and negative anomalies which, in a great part, could be justified locally taking into account inhomogeneities in the upper crust in the different crossed geological provinces. The model with a lithospheric thermal root gives no more than 20 mGal in its maximum and it has a short longitudinal extention, but it must be taken into account attending to the important manifestations of active volcanism southwards 33º South latitude and the heat flow expressions detected (Muñoz et al, 1990).

GRAVITY MODELS

It has been analyzed the possible gravimetric influence from the subducted plate, a wedge of asthenospheric materials between the Nazca and Southamerican plates, two "roots" in the intermediate and lower crust in the continental sector and "antiroots" in the lower crust in both oceans. In this way, a simple one layer crustal model shows maximum depth for the continental crust of about 43Km. This value could vary in no more than 10% incorporating the other gravity effects refered. For that, and as a simplification, a one layer crustal model is shown in Fig. 2 together with its gravity response and the observed gravity data. Once again, and according to the results obtained in previous studies for different Andean sections (Introcaso and Pacino, 1988; Pacino and Introcaso, 1989), it was proved that the observed Bouguer anomaly is mainly controlled by the M discontinuity and the subcrustal gravimetric effects are either rather smaller than was supposed or they cancel each other out.

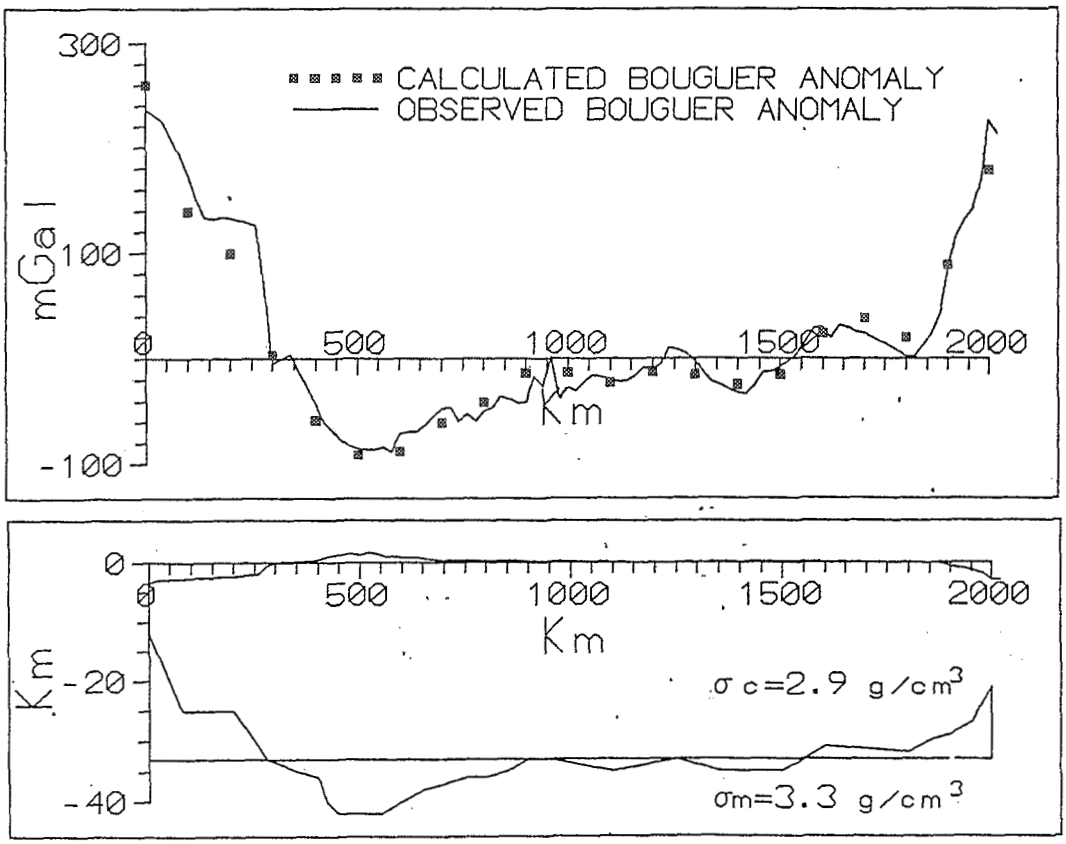

Fig.2: One layer crustal model and its gravity response.

SHORTENINGS

Values of compressive shortening were also calculated from the topographic areas above the sea level, and the areas of crustal roots beneath the assumed "normal" crustal thickness

obtained from the different models.

Following Isacks (1988) and assumming isostatic equilibrium, the shortening value found is 66 Km. By the other side, considering the "roots" from the inversion of gravity data and according to Introcaso et al (1992), the shortening value reaches 72 Km.

CONCLUSIONS

From gravity data, the maximum thickness for the continental crust at 39º South latitude was located beneath the Andean axes, at 43 Km. depth, while the minimum thickness for the ocean crust at that latitude, with 12 Km. depth, would be located 300 Km. offshore, in the Pacific Ocean.

A preliminar isostatic analysis would indicate that the section essentially responds to an Airy's isostatic model showing, as a whole, a reasonable isostatic equilibrium.

The calculated shortening values for all the crustal models are in the order of 70 Km.

ACKNOWLEDGEMENTS

This work was partially supported by CONICET - Argentina (Grant: PID 3-09330088) and by Facultad de Ciencias Exactas, Ingeniería y Agrimensura (U.N.R.) (Res: 239/92).

REFERENCES

BOWIN, C., WARSI, W. AND MILLIGAN,J., 1981, Free Air Gravity Anomaly Atlas of the World. WoodsHole Oceanographic Institution, 38 pp.

DIEZ RODRIGUEZ, A. AND INTROCASO, A., 1986, Perfil transcontinental sudamericano en el paralelo 39º S. Geoacta, 13 (2): 179 - 201.

INTROCASO, A. AND PACINO, M. C., 1988, Gravity Andean model associated with subduction near 24º 25' Soth latitude. Rev. Geofís., 44: 29 - 44.

INTROCASO, A., PACINO, M. C. AND FRAGA, H., 1992, Gravity, isostasy and Andean crustal shortening between latitudes 30º and 35º S. Tectonophysics, 204: 31 - 48.

ISACKS, B., 1988, Uplift of the Central Andean Plateau and Bending of the Bolivian Orocline. J. Geophys. Res., 93 (B4): 3211 - 3231.

MUÑOZ, M., FOURNIER, H., MAMANI, M., FEBRER, J., BORZOTTA, E. AND MAIDANA, A., 1990, A comparative study of results obtained in magnetotelluric deep soundings in Villarrica active volcano zone (Chile) with gravity investigations, distribution of earthquake foci, heat flow empirical relationships, isotopic geochemistry Sr/ Sr and SB systematics. Physics of the Earth and Planetary Interiors, 60: 195 - 211.

PACINO, M. C. AND INTROCASO, A., 1989, Modelo gravimétrico sobre el sistema de subducción Placa de Nazca - Placa Sudamericana en la latitud 33º Sur. V Congreso Geológico Chileno. Actas II: F77 - F90.

CRUSTAL THICKENING IN THE CENTRAL ANDES - RESULTS FROM SEISMIC REFRACTION AND CRUSTAL BALANCING

Michael SCHMITZ*, Peter GIESE* and Peter WIGGER*

* Institut für Geologie, Geophysik und Geoinformatik, FR Geophysik, Freie Universität Berlin, Malteserstraße 74-100, W-1000 Berlin 46

RESUMEN: Las estructuras tectónicas de sobrecorrimiento y el espesor actual de la corteza derivados de los resultados de sísmica de refracción han sido modelados por medio de un balanceo tectónico con un acortamiento cortical de 320 km desde el Cretasico superior con un espesor inicial de 35 km. El volumen de la corteza inferior en el antearco y debajo del arco magmático, aproximadamente el 20% del volumen cortical actual, no puede ser explicado por este acortamiento. La litósfera subcortical debe haber sufrido un acortamiento en el mismo rango que exige un transporte de material hacia el manto más profundo.

KEY WORDS: Central Andes; crustal balancing; seismic refraction; crustal doubling.

INTRODUCTION

The Central Andes are part of the convergence system between the oceanic Nazca plate and the South American plate. Elevations of about 7000 m above sea level in the central parts of the mountain belt are observed where the crustal thickness reaches about 70 km. The importance of tectonic shortening for the thickening of the Central Andean crust has been emphasized by various authors (Suárez et al. 1983; Allmendinger 1986; Reutter et al. 1988; Roeder 1988; Sheffels 1990).

Within the frame of the research group "Mobility of Active Continental Margins", new data on the crustal thickness and the velocity structure of the Central Andean crust on a transect at 21°S, derived from seismic refraction observations, allow to derive a model which combines data from cross-section balancing with seismic refraction data. Calculations about the portion, that contributes tectonic shortening to the thickening of the Andes, are presented.

METHOD

Based on the velocity structure and crustal volume of the Andean crust derived from seismic refraction experiments, the amount of thickening caused by tectonic shortening could be determined. The crustal development was modelled with the program TRUSTBELT II (Linsser 1991), and a regional isostatic compensation following Airy's principles (Buness 1991) was applied to allow the application of cross-section balancing on a crustal scale, here called "crustal balancing" (figure 1). In a forward modelling procedure detachment horizons and thrusts have been changed iteratively until satisfying the observed crustal structures from seismic refraction observations. Further geophysical data were used as boundary conditions and the derived structure was checked by raytracing and gravimetric model calculations.

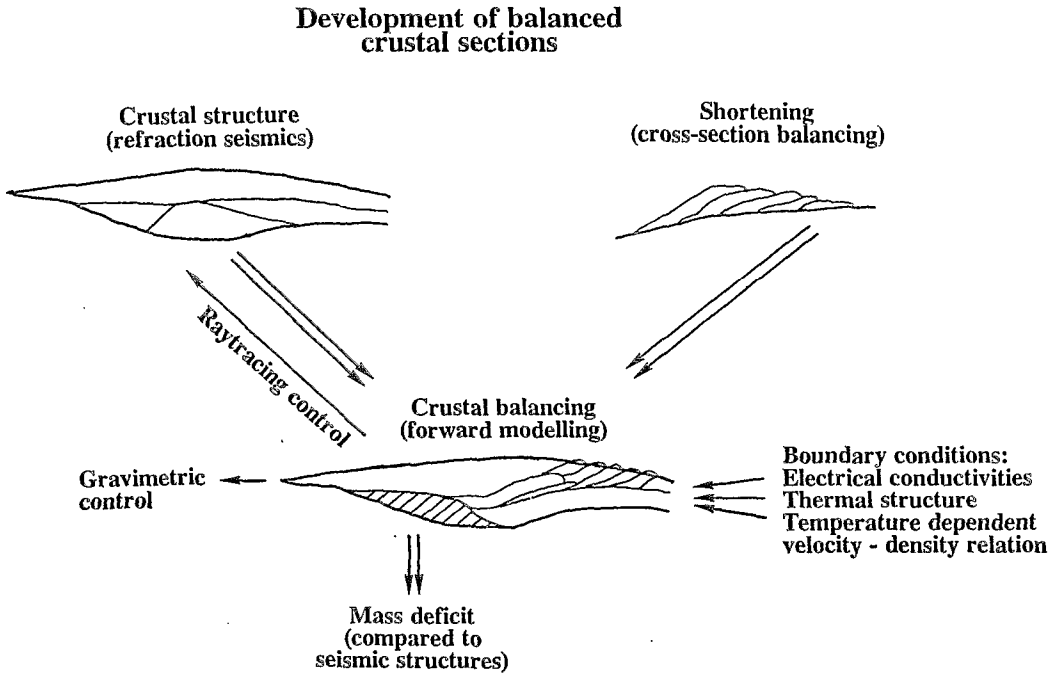

Figure 1. Development of the balanced crustal section from the crustal structure (derived from seismic refraction) and shortening from cross-section balancing.

The aim of the study was to develop an areal balanced model that should be able to explain the velocity model and the seismic discontinuities at 21°S. The program THRUSTBELT II does not allow the modelling of different rheological characteristics of the distinct crustal units. As the program only permits faults with the same vergency, no backthrusts were introduced exept in the forearc, using a "pin-line" on the Altiplano.

GROSS CRUSTAL STRUCTURE FROM SEISMIC REFRACTION

The velocity structure was derived by observations of 4 shotpoints along a profile at 21°S with corresponding N-S profiles in the Coastal Cordillera and in the Precordillera (position map see Wigger et al., this volume). A clear discontinuity at 40 km depth in the Coastal Cordillera is interpreted as Moho of the subducted Nazca plate (Wigger et al. 1993). The continental crust in the forearc has a high average velocity of 6.5 km/s in the Coastal Cordillera, descending to 6.2 km/s in the Precordillera. A division into a high velocity upper and middle crust, dipping from 20 km depth in the coastal region to about 35 km depth beneath the Precordillera, and a deeper crust mainly represented by low velocity zones (LVZ) can be done. Strong absorption of the seismic waves in the Western Cordillera and the Altiplano area leads to a comparable low average velocity (about 6.0 km/s) down to 70 km, but a Moho is not observed. In the backarc, the Moho dips down from 40 km below the Subandean Ranges to about 70 km at the eastern margin of the Altiplano. In the Chaco the velocities increase slightly from 6.1 km/s at 10 km depth to 6.2 km/s at 30 km depth and a 10 km thick high velocity lower crust is observed. Further west, in the Eastern Cordillera, high velocity material (6.8 km/s) at 20-25 km depth is underlain by a broad LVZ down to the crustal base (see Wigger et al., this volume).

INITIAL MODEL AND APPLIED SHORTENING VALUES

A simple layered crust with a 10 km thick lower crust, 15 km middle crust, 5 km (Pre-)Cambrian to Ordovician rocks and a varying thickness up to 10 km of Silurian to Cenocoic sediments is taken for the initial model. Thus, the initial crustal thickness varies between 40 km in the Andean foreland and 30 km in

the Eastern Cordillera, where Cretaceous rifting took place (Marquillas & Salfity 1988). The starting point for the calculation of the modelled shortening is the onset of the strong compressional phases at Upper Cretaceous at 90 Ma (Scheuber et al. 1993).

Cross-section balancing was done for different profiles in the Central Andean backarc and the derived shortening values vary between 210 and 230 km for the Eastern Cordillera and Subandean Ranges (Roeder 1988; Sheffels 1990) at about 18°S and 140 km for the Subandean Ranges and a transition zone (Kley & Reinhardt 1993) at 21°S. In the area of the Altiplano and the recent magmatic arc the determination of tectonic shortening is somewhat more difficult because of the young sedimentary and volcanic cover. Shortening values of 55 km (Baby et al. 1990a) and 42 km (Baby et al. 1990b) for the Altiplano are reported. In the forearc region shortening is most evident in the Precordillera (Chong & Reutter 1985).

An amount of 320 km is taken for the shortening between the trench and the Andean foreland since Upper Cretaceous (Schmitz 1993), modelled mainly for two tectonic phases, the Incaic Phase in the Altiplano/Eastern Cordillera area and the Quechua Phase in the Subandean Ranges. The detachments are located at the base of the younger sediments, on top of the middle crust and at the base of the lower crust.

CRUSTAL DOUBLING IN THE BACKARC

A crustal thickening from 40 km in the Subandean Ranges to about 70 km in the Eastern Cordillera is observed, representing a crustal doubling in the backarc. Material with high seismic velocities (6.8 km/s) was found in 20 to 25 km depth in the Eastern Cordillera. This can be explained by lower crustal material detached from the crustal base and overthrusted to the east (figure 2). The modelled structures of the Subandean fold- and thrust belt are in good coincidence with balanced cross-sections (Kley & Reinhardt 1993). Zones of high electrical conductivities might have acted as detachments.

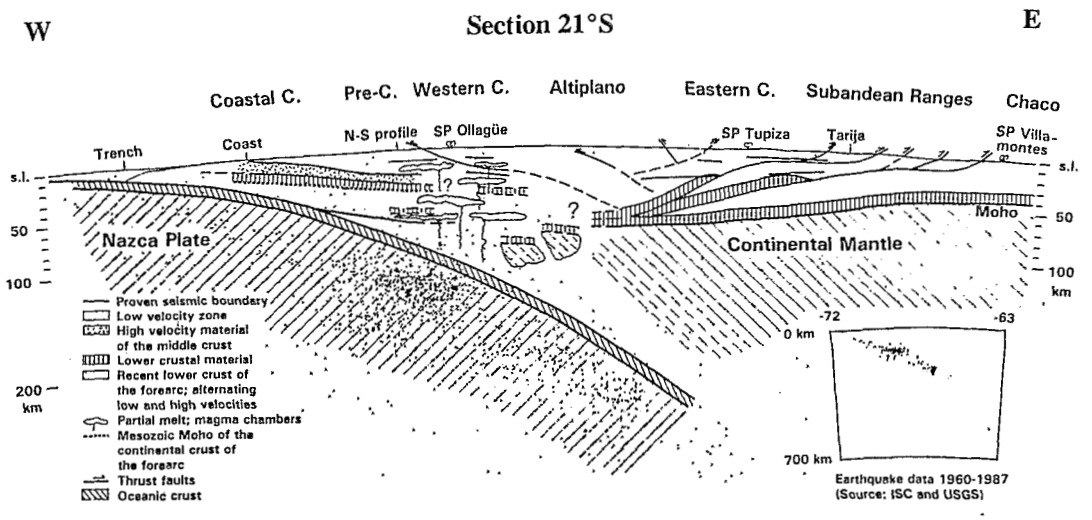

Figure 2. Interpretative cross-section at 21°S with main seismic boundaries and the tectonic structure. The position of the Nazca plate is from Cahill & Isacks (1992).

CONCLUSIONS

Combining seismic refraction data and a cross section balancing method, new aspects on the development of the Central Andes were derived. The crustal thickening in the backarc was modelled as a crustal doubling with an overthrust of the Andean crust over its foreland (figure 2). For the arc- and forearc-region no crustal thickening could be derived which is originated by crustal shortening.

The lower crust of the forearc as well as of the magmatic arc region, which represents together about 20% of the crustal volume under study, cannot be modelled by the assumed shortening of 320 km. Other sources must be taken in account to explain these crustal parts. Tectonically eroded and later underplated material from the continental margin could fill a part of the lower crust of the westerly forearc area. Further east, transformed mantle or magmatic addition could have thickened the crust.

The lithospheric mantle must have undergone the same shortening as the crust. Thus a convergence between the oceanic lithosphere and the continental mantle is evident in the area of the recent magmatic arc. In consequence, mantle material must be transported into the asthenosphere below the magmatic arc.

REFERENCES

Allmendinger RW 1986 Tectonic development, southeastern border of the Puna Plateau, northwestern Argentine Andes. Geol Soc Am Bull, 97: 1070-1082.

Baby P, Sempéré T, Oller J, Barrios L, Hérail G & Marocco R 1990a Un bassin en compression d'àge oligo-miocène dans le sud de l'Altiplano bolivien. C R Acad Sci Paris, 311 (Sér II): 341-347.

Baby P, Sempéré T, Oller J, Blanco J, Zubieta D & Hérail G 1990b Evidence for mayor shortening on the eastern edge of the Bolivian Altiplano: The Calazaya nappe. In: Inst Franc Rech Scient Devel, Colloques er Séminaires, Symp Int "Géodyn Andine", Rés Comm: 163-166, Grenoble.

Buness H 1991 Isostatic compensation of balanced cross sections. In: Giese P , Roeder D & Nicolich R (eds) Joint interpretation of geophysical and geological data applied to lithospheric studies: 181-188, Kluwer, Dordrecht.

Cahill T & Isacks BL 1992 Seismicity and Shape of the Subducted Nazca Plate. J Geophys Res, 97 (B12): 17503-17529.

Chong DG & Reutter K-J 1985 Fenómenos de tectónica compresiva en las Sierras de Varas y de Argomedo, Precordillera Chilena, en el ambito del paralelo 25° sur. IV Congr Geol Chileno, Antofagasta, Actas 2: 2/219-2/238.

Kley J & Reinhardt M 1993 Geothermal and tectonic evolution of the Eastern Cordillera and the Subandean Ranges of southern Bolivia. In: Reutter K-J, Scheuber E & Wigger P (eds) Tectonics of the southern Central Andes: 155-170, Springer, Berlin Heidelberg New York.

Linsser H 1991 Enhanced interpretation of crustal sections with.the Thrustbelt Program. In: Giese P et al. (eds) Joint interpretation of geophysical and geological data applied to lithospheric studies: 165-179, Kluwer, Dordrecht.

Marquillas R & Salfity JA 1988 Tectonic framework and correlations of the Cretaceous-Eocene Salta Group, Argentina. In: Bahlburg H, Breitkreuz C & Giese P (eds) The Southern Central Andes: 119-138, Springer, Berlin Heidelberg New York.

Reutter K-J, Giese P, Götze H-J, Scheuber E, Schwab K, Schwarz G & Wigger P 1988 Structures and crustal development of the Central Andes between 21° and 25°S. In: Bahlburg H, Breitkreuz C & Giese P (eds) The Southern Central Andes - Lecture Notes in Earth Sciences, 17: 231-261, Springer, Berlin Heidelberg New York.

Roeder D 1988 Andean-age structure of Eastern Cordillera (La Paz, Bolivia). Tectonics, 7 (1): 23-39.

Schmitz M 1993 Kollisionsstrukturen in den Zentralen Anden: Ergebnisse refraktionsseismischer Messungen und Modellierung krustaler Deformationen. Dissertation, Freie Universität Berlin.

Schwarz G, Chong DG, Krüger D, Martínez E, Massow W, Rath V & Viramonte J 1993 Crustal high conductivity zones in the Central Andes. In: Reutter K-J, Scheuber E & Wigger P (eds) Tectonics of the southern Central Andes: 49-68, Springer, Berlin Heidelberg New York.

Sheffels BM 1990 Lower bound on the amount of crustal shortening in the central Bolivian Andes. Geology, 18: 812-815.

Suárez G, Molnar P & Burchfiel BC 1983 Seismicity, fault plane solution, depth of faulting and active tectonics of the Andes of Peru, Ecuador and S-Colombia. J Geophys Res, 88 (B12): 10403-10428.

Wigger P, Giese P & Schmitz M 1993 Main crustal anomalies of the Central Andean lithosphere. This vol.

Wigger P, Schmitz M, Araneda M, Asch G, Baldzuhn S, Giese P, Heinsohn W-D, Martínez E, Ricaldi E, Röwer P & Viramonte J 1993 Variation in the crustal structure of the southern Central Andes deduced from seismic refraction investigations. In: Reutter K-J, Scheuber E & Wigger P (eds) Tectonics of the Southern Central Andes: 23-48, Springer, Berlin Heidelberg New York.

THE EVOLUTION OF DEFORMATION AND TOPOGRAPHY OF THE CENTRAL ANDES

Shimon Wdowinski

Geological Survey of Israel, 30 Malkhe Israel st., Jerusalem 95501, Israel

RESUMEN: La deformación y topografía de los Ande Centrales fueron investigados usando un modelo visco-plástico depende de la temperatura de la placa Sud Americana. El modelo predica la topografía solamente en los casos que toman en cuenta que la region bajo del Altiplano se debilita con la temperatura .

Extended Abstract

The central Andean topography is characterized by a wide elevated plateau flanked in the west by a steep slope that descends into the deep Chilean Trench and in the east by a gentle slope that subsides gradually toward the Brazilian Shield. The low elevated trench topography is dynamically supported, whereas the high Andean mountain topography is mostly isostatically supported by a thick crust. The last mountain building phase, which thickened the crust and formed the present-day Andes, began 26 m.y. ago, in the Late Oligocene, with the increase of the convergence rate between the Nazca and the South American plates. The time evolution of the Andean deformation and topography is investigated by applying a temperature dependent visco-plastic flow model of continental lithosphere to the South American plate.

The model predicts the observed present day topography profile across the Central Andes, from the trench across the high Altiplano plateau to the Brazilian Shield (Figure 1). Numerical results, combined with observations of the spatial and temporal distribution of igneous activity in the Central Andes, lead to the conclusion that the Altiplano

developed and extended to its present width of 400 km as a result of thermal weakening of the lithosphere since Late Oligocene until present. The model also predicts the observed eastward migration of the locus of the Andean crustal deformation with time (Figure 2). At early stages of the deformation, both the crustal and mantle locus of deformation lie in the thermally weak region, which results in crustal thickening in this finite region. At later stages, as the crust thickens, it induces buoyancy forces of larger magnitude, which resist crustal thickening beyond 65 km, and as a result the locus of crustal deformation migrates eastward. The detachment of the crustal locus of deformation from that of the mantle can explain the observed change in deformation pattern from thick-skinned tectonism during early stages of the deformation to thin-skinned tectonism during the more recent stages.

Figures

Fig. 1. A comparison between the characteristic observed topographic profile (shaded) and calculated topographic profiles. (a) Evolution of a thermally perturbed lithosphere that initially has a 35 km thick uniform crust. (b) Evolution of a thermally perturbed lithosphere that initially has 50 km thick crust above the wedge tip (300-400 km from the trench). (c) Evolution of a lithosphere with initially thick crust (same as in b) without thermal perturbation.

Fig. 2. Calculated topography, crustal structure, normal strain rate, and shear strain rate during the initial and final stages of the Central Andes mountain building phase. The locus of compressional deformation of the mantle lithosphere is localized near the wedge tip at all time steps. However, the compressional deformation of the crust diffuses with time and its locus migrates inland and is accompanied by a significant shear component concentrated in the weak lower crust.

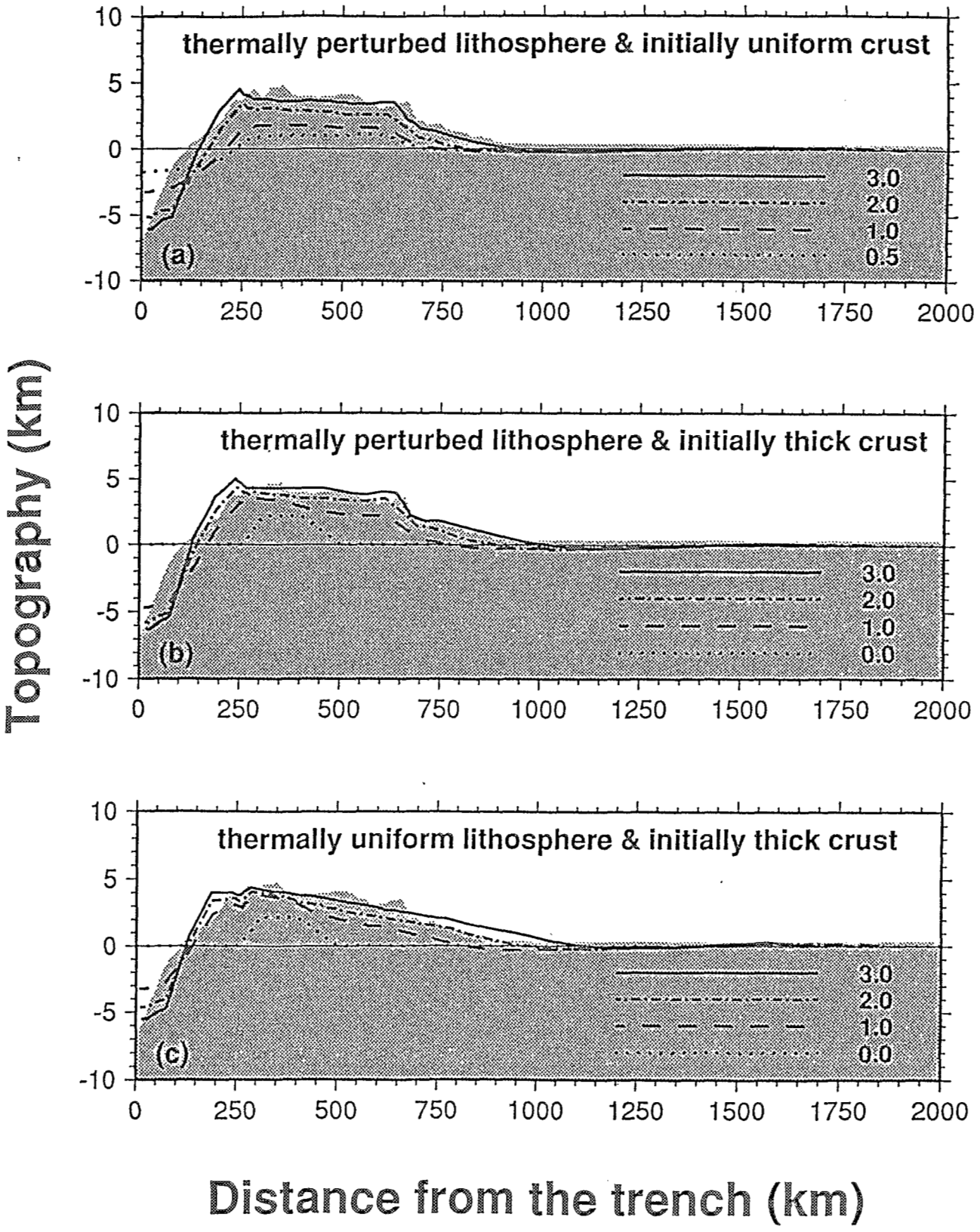
thermally perturbed lithosphere & initially uniform crust
(a)
3.0
2.0
1.0
0.5
thermally perturbed lithosphere & initially thick crust
(b)
3.0
2.0
1.0
0.0
thermally uniform lithosphere & initially thick crust
(c)
3.0
2.0
1.0
0.0
10
5
0
-5
-10
0
250
500
750
1000
1250
1500
1750
2000
Topography (km)
Distance from the trench (km)

Fig. 1

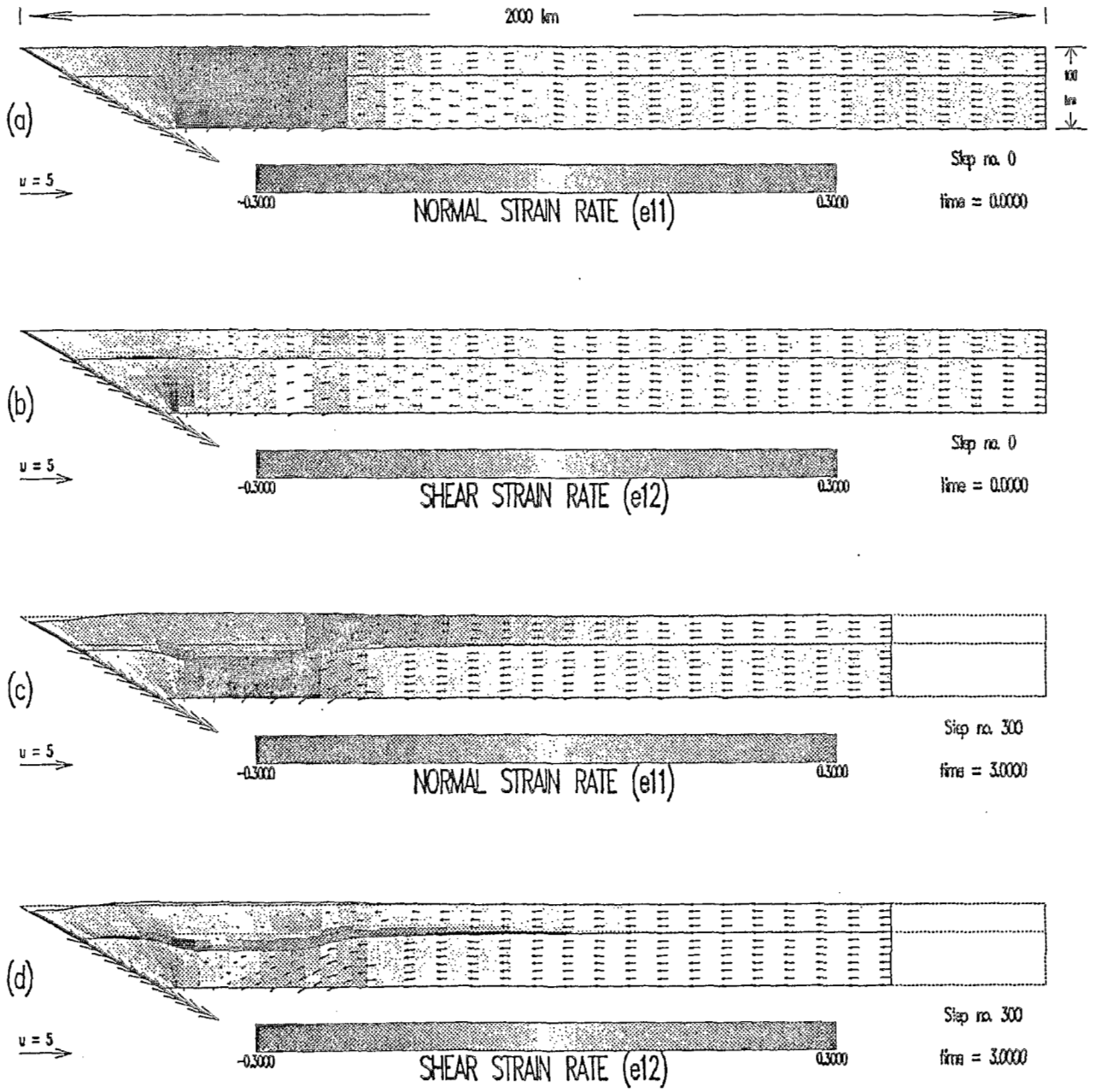
2000 km
100 km
(a)
u = 5
-0.3000
NORMAL STRAIN RATE (e11)
0.3000
Step no. 0
time = 0.0000
(b)
u = 5
-0.3000
SHEAR STRAIN RATE (e12)
0.3000
Step no. 0
time = 0.0000
(c)
u = 5
-0.3000
NORMAL STRAIN RATE (e11)
0.3000
Step no. 300
time = 3.0000
(d)
u = 5
-0.3000
SHEAR STRAIN RATE (e12)
0.3000
Step no. 300
time = 3.0000

Fig. 2

Lithospheric Structure and Along-Strike Segmentation of the Central Andean Plateau, 17 -29°S

D. Whitman, B. L. Isacks, and S. Mahlburg Kay

Department of Geological Sciences & Institute for the Study of the Continents
Snee Hall, Cornell University; Ithaca, NY 14853

RESUMEN: Los datos geofísicos y geoquímicos indican que cerca del paralelo 23° S, el espesor del plateau de los Andes Centrales decrece hacia el sur a lo largo de su rumbo. Mientras una litósfera gruesa subyace el Altiplano y las Sierras Subandinas, una delgada lo hace bajo la Puna y el Sistema de Santa Bárbara. La diferencia en el estilo tectónico de estos dos segmentos puede atribuirse al cambio a lo largo del rumbo del espesor litosférico.

KEY WORDS: Altiplano, Puna, lithosphere, flexure, seismic attenuation, back-arc volcanism

INTRODUCTION:

The central Andean Plateau is a 300 km wide, nearly 4 km high plateau which is situated above a 30°E dipping segment of the subducted Nazca plate. Major along-strike variations in upper mantle structure are demonstrated by systematic changes in the topography, the upper mantle seismic Q structure, the lithospheric flexural rigidity, and the distribution and chemistry of back-arc lavas. South of 23° S, the upper mantle becomes hotter, and the lithosphere becomes thinner and weaker. This change in lithospheric thickness coincides with lateral variations in the tectonic style and timing of deformation in two distinct physiographic segments of the plateau and its adjacent foreland thrust belt to the east: the Bolivian Altiplano and Subandean ranges in the north and the Argentine Puna and Santa Barbara system in the south (see also Allmendinger et al., this volume). We conclude that lateral variations in lithospheric thickness and rheology play an important role in this segmentation.

SEISMIC WAVE ATTENUATION

One of the most sensitive indicators of variations in lithospheric structure and the thermal structure of the upper mantle is the efficiency of regional high frequency P and S wave propagation. In a recent study, Whitman et al. (1992) show that the upper mantle seismic attenuation (Q) structure varies along-strike beneath the plateau and foreland with generally low attenuation (high Q) beneath the Altiplano segment, and high attenuation (low Q) beneath the Puna segment (Fig. 1). Digital seismograms collected during deployment of the portable PANDA network near Jujuy, Argentina (24°S, 65°W) on the eastern margin of the Puna exhibit striking azimuthal variations in frequency content. Ray paths from intermediate depth earthquakes located north and northwest of the network transmit seismic waves with a higher frequency content than ray paths from earthquakes at similar depths and distances but located west and southwest of the network. In the foreland, Sn phases from crustal earthquakes in the Subandean ranges to the north propagate efficiently to the network, while Sn is not observed from shallow earthquakes at similar distances to the south.

This data when combined with previously reported observations of shear wave propagation at La Paz, Bolivia (17°S, 68°W) on the eastern side of the Altiplano (Chinn et al., 1980) define a generally low Q region in the upper mantle beneath the plateau which varies in width along strike (Fig. 1). In the Altiplano, the low-Q is confined to areas of active volcanism in the Western Cordillera, but beneath the Puna, the low Q zone spans the whole width of the plateau and is present beneath the Santa Barbara ranges to the east.

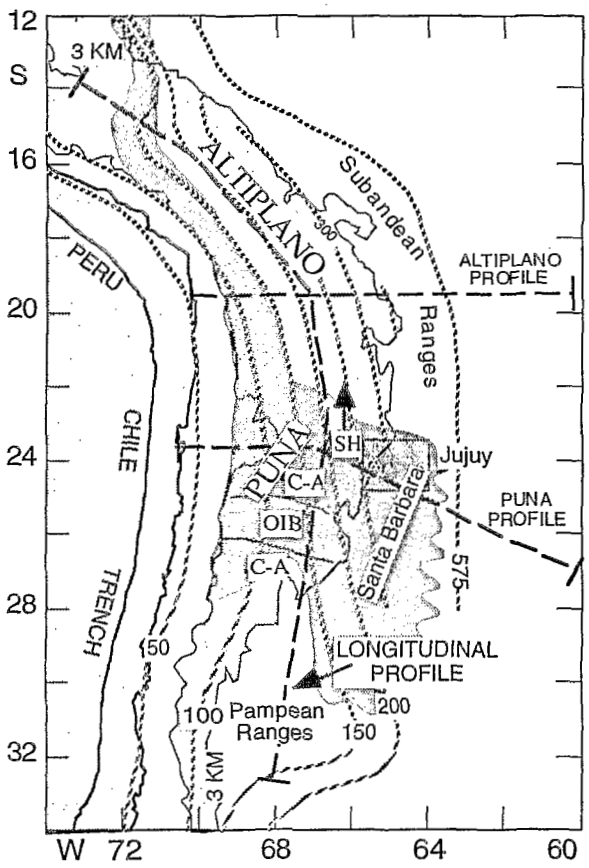

Fig 1. Map showing regions of high seismic wave attenuation (dark, shaded region) inferred to lie between the subducting Nazca plate and the overriding South American plate (after Whitman et al, 1992) and along strike variations in back arc lava composition (after Kay and Kay, 1993). SH: shoshonitic; C-A: calc-alkaline; OIB: ocean island basalt-like lavas. Also shown is depth to the Wadati-Benioff zone (50 km contours after Cahill and Isacks, 1992) and regions with average elevation over 3 km.

MAGMATISM

The southward increase in upper mantle seismic attenuation beneath the plateau is reflected in the distribution of young back-arc mafic (< 60% SiO_2) flows. In the Altiplano and northern Puna, back-arc mafic centers are composed of shoshonitic lavas indicative of small degree melts of enriched mantle lithosphere. From 24°S to 27°S, back-arc mafic centers progressively increase in volume and change in composition from shoshonitic, to calc-alkaline, to OIB (intraplate)-like, to calc-alkaline lavas. (Fig. 1; SH, C-A, and OIB). The change from shoshonitic to OIB-type is consistent with a progressive increase in mantle melting percentage and a decrease in enriched lithospheric component. The largest centers with the highest melting percentages lie above a seismic gap in the subducted Nazca plate and probably reflect anomalously high temperatures in the mantle wedge. These results are consistent with a general north to south decrease in lithospheric thickness and an increase in mantle wedge temperature.

The temporal and spatial distribution of ignimbrites on the plateau suggests that the present day lithospheric thickness of the plateau has evolved since mid-Miocene. Ignimbrites erupted in the Altiplano and northern Puna ceased in mid to late Miocene while those erupted further south in the active Central Volcanic Zone are recent. If the large-scale crustal melting associated with these ignimbrites is due to anomalously thinned lithosphere, then since mid-Miocene, the lithosphere beneath the Altiplano and northern Puna has thickened, whereas the lithosphere of the southern Puna has thinned.

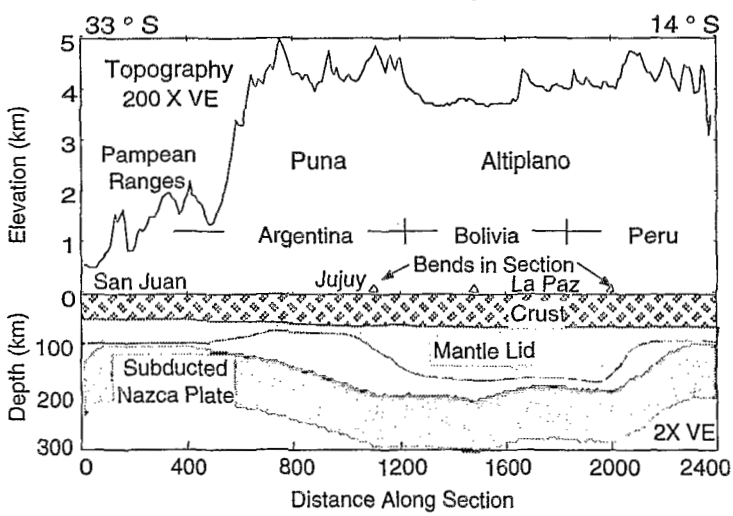

Fig 2. Longitudinal cross section through the central Andes. Location of section is shown in Figure 1. Top shows averaged topography projected into a along a 50 km wide swath along line of section. Bottom shows inferred crust and upper mantle structure along section. Thickness of mantle lid is inferred from the patterns of upper mantle seismic wave attenuation (Chinn et al., 1980; Whitman et al., 1992). Top of the subducted Nazca plate along the section is 15 km above the projected WBZ contours of Cahill and Isacks (1992).

ISOSTASY OF THE PLATEAU AND FLEXURE OF THE FORELAND LITHOSPHERE

The mode of isostatic compensation changes along-strike beneath the plateau. Near 22°S, the average elevation of the plateau increases abruptly from 3.8 km in the Altiplano to around 4.4 km in the Puna (Figs. 2 and 4), and is a consequence of a thinned lithosphere beneath the Puna. Assuming typical thermal parameters for the lithosphere, the increase in elevation in the Puna can be explained by a decrease in lithospheric thickness of 50 - 100 km, depending on whether the thin Puna lithosphere reflects a long standing difference from that of the Altiplano, or is due to a fairly recent (0-10 Ma) rapid removal or delamination of lithospheric material beneath the Puna. The elevation of the Altiplano is compensated primarily by crustal thickening, whereas the Puna is supported by both a crustal root and a thermal mantle root.

In southern Bolivia, the eastern margin of the Andes is compensated regionally due to flexural support of the foreland lithosphere. This is reflected in a high-low isostatic residual anomaly pair which tracks the location of the eastward verging Principal Frontal Thrust in the Eastern Cordillera of Bolivia (Fig 3, top). The 50 mGal high (Fig 3, ECH) is caused by a combination of high density basement rocks in the hanging wall of the thrust and local undercompensation of the topography. To the east, the -75 mGal low (Fig. 3, SAL) is coincident with the Subandean fold-thrust belt and foreland basin, and is due to a combination of low density sedimentary rocks in the foreland basin and the locally overcompensated crust of the downflexed foreland lithosphere. Forward modeling of this gravity profile (Lyon-Caen et al., 1985) indicates that the foreland lithosphere behaves as an elastic plate with thickness of 25-70 km ($D = 10^{23}$-$2 \cdot 10^{24}$ Nm) which has been underthrust beneath Subandean belt and Eastern Cordillera by at least 150 km.

Farther south, the isostatic residual across the eastern margin of the Puna and the Santa Barbara ranges is much smaller than that across the Subandean belt (Fig. 3 bottom). At the latitude of Jujuy, Argentina, modeling of the gravity anomaly and a Moho profile determined from an inversion of seismic traveltime residuals indicates that the effective elastic thickness of the lithosphere is only 6-12 km ($D = 10^{21}$-10^{22} Nm) (Whitman, in prep). This supports the model of a thinner and, hence, less rigid lithosphere beneath the foreland of NW Argentina.

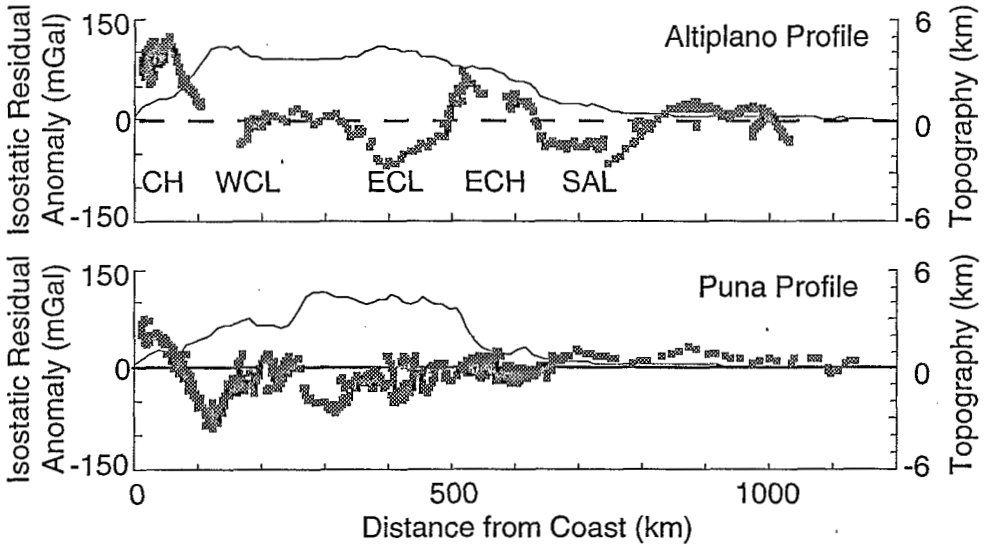

Fig 3. Profiles across the Altiplano and Puna segments of the central Andes showing averaged topography and point values of the isostatic residual gravity anomaly projected into section along a 100 km wide swath. Location of profiles is shown in Figure 1. The profiles were constructed to be approximately perpendicular to regional trends in the gravity anomalies. The isostatic residual was computed by subtracting a calculated isostatic regional and a degree 10 free air regional from the observed Bouguer anomaly. The observed Bouguer anomaly is from Götze et al. (1990) and older DMA sources. The isostatic regional was calculated at station level by assuming local Airy compensation, a zero elevation crustal thickness of 35 km, a topographic density of 2.67 gm/cc, and a density contrast at the crust-mantle boundary of 0.35 gm/cc. CH: coastal high; WCL: Western Cordillera low; ECL: Eastern Cordillera low; ECH: Eastern Cordillera high; SAL: Subandean low.

TECTONIC IMPLICATIONS

The lateral segmentation in upper mantle structure is coincident with changes in the physiography and tectonic style of the plateau. The Altiplano and Puna segments of the plateau exhibit different elevation distributions (Fig. 4). Elevations in the Altiplano are concentrated near 3.8 km, the height of the main Altiplano basin. This relatively narrow elevation distribution reflects cut and fill processes in the Altiplano basin and the lack of compressional deformation in the Altiplano and Eastern Cordillera of Bolivia since Late Miocene (Isacks, 1988; Gubbels et al., 1993). In the Puna, elevations are more evenly distributed about the mean, a consequence of the greater local relief and a longer duration of compressional deformation in the Puna than in the Altiplano (see Allmendinger et al., this volume). This longer history of compression in the Puna may be a direct consequence of thinner, weaker lithosphere.

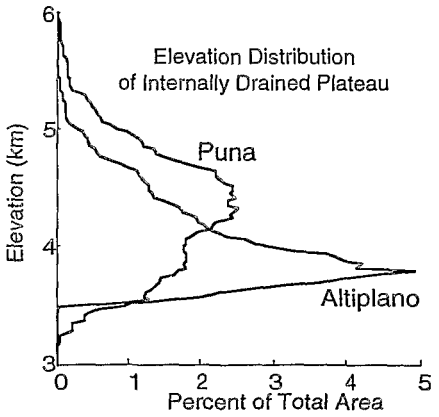

Fig 4. Differential hypsometric curves comparing the elevation distribution of the Altiplano and Puna segments of the central Andean plateau. Elevation distribution was calculated from topography contained within internally drained regions of the plateau only.

The foreland tectonic style changes from thin skinned deformation in the Bolivian Subandes to thick skinned, basement involved deformation in the Santa Barbara ranges of northwest Argentina. We suggest the following explanation connecting the lateral changes in upper mantle structure with those expressed at the surface. The strong, thick lithosphere beneath the Bolivian foreland has allowed the Brazilian shield to be underthrust beneath the plateau margin as a coherent unit, with deformation confined to the overlying Paleozoic sedimentary wedge. A thinner weaker lithosphere beneath the Santa Barbara system of NW Argentina has lead to diffuse basement involved shortening within the crust. Since much of the shortening within the foreland is accommodated within the basement, the NW Argentine foreland has not been extensively underthrust beneath the Puna. The tectonic style of the Puna segment is similar to the thick skinned tectonics of the Pampean ranges farther south. The similarities in tectonic style in these two segments reflect similarities in lithospheric thickness and the consequent overall rheology of the plate, with the lower Pampean elevations resulting from thermal coupling between South American and subducted Nazca plates (Fig. 2)

The along-strike lithospheric segmentation of the central Andean plateau and its adjacent foreland may be due to one or a combination of the following scenarios. The change in lithospheric thickness may predate the main stage of Andean uplift, or preexisting lithospheric properties of the two segments may have at least influenced a later change in the thickness. The change in lithospheric thickness may be due to a larger amount of shortening across the mountain belt in the north with the underthrust Brazilian shield accounting for the thick lithosphere beneath the Altiplano. Finally, the lateral change in lithospheric thickness may be due to a relatively recent removal or delamination of lithosphere beneath the Puna, possibly related to the southward flattening of the subducted Nazca plate.

REFERENCES

CAHILL, T., AND B. L. ISACKS, 1992, Seismicity and shape of the subducted Nazca plate, *J. Geophys. Res., 97,* 17503-17529.

CHINN, D.S., B. ISACKS, M. BARAZANGI, 1980, High-frequency seismic wave propagation in western South America along the continental margin, in the Nazca plate and across the Altiplano. *Geophys. J. R. Astron. Soc., 60,* 209-244.

GÖTZE, H.-J., B. LAHMEYER, S. SCHMIDT, S. STRUNK, M. ARANEDA, 1990, Central Andes Gravity Data Base., *EOS, 71,* 401-407.

GUBBELS, T.L., B.L ISACKS, E. FARRAR, 1993, High-level surfaces, plateau uplift, and foreland development, Bolivian Central Andes, *Geology (in press).*

ISACKS, B.L., 1988, Uplift of the central Andean plateau and bending of the Bolivian orocline, *J. Geophys. Res., 93,* 3211-3231.

KAY, R.W, S.M. KAY, 1993, Delamination and delamination magmatism,*Tectonophysics, 219,* 177-189.

LYON-CAEN, H., P. MOLNAR, G. SUÁREZ, 1985, Gravity anomalies and flexure of the Brazilian Shield beneath the Bolivian Andes, *Earth and Planet. Sci. Let., 75,* 81-92, 1985.

WHITMAN, D., B.L. ISACKS, J-L CHATELAIN, J-M CHIU, A. PEREZ, 1992, Attenuation of High-Frequency Seismic Waves Beneath the Central Andean Plateau, *J. Geophys. Res., 97,* 19929-19947.

MAIN CRUSTAL ANOMALIES OF THE CENTRAL ANDEAN LITHOSPHERE

Peter J. WIGGER*, Peter GIESE* and Michael SCHMITZ*

* Institut für Geologie, Geophysik und Geoinformatik, FR Geophysik, Freie Universität Berlin, Malteserstraße 74-100, W-1000 Berlin 46

RESUMEN: Basadas en observaciones geofísicas obtenidas en la década de los 80 se derivan nuevas informaciones sobre la estructura de la corteza andina. Se revisa la estructura casi simétrica de la corteza con un espesor de alrededor de 70 km en la zona del arco magmático, disminuyendo hacia el antearco y el trasarco. Mientras hay un doblamiento cortical en el trasarco, la corteza continental en el antearco está compuesta por una corteza continental delgada con una zona de "mezcla" inferior. Resulta una estructura asimétrica con un antearco "delgado" y un trasarco grueso. El arco magmático actua como amortiguador ductil entre los dos bloques más rígidos.

KEY WORDS: Central Andes; geophysical anomalies; crustal thickening; asymmetric crustal structure.

INTRODUCTION

Within the frame of the research group "Mobility of Active Continental Margins" at the Freie Universität and Technische Universität of Berlin, geological and geophysical investigations were carried out between 20° and 26°S. Geophysical anomalies not only give knowledge about the lithospheric structure but they also allow to make statements about the dynamic and evolution of the Andean orogene. Across a traverse through the Central Andes a set of geophysical data is available (figure 1.) which allows, together with tectonic and petrological observations, conclusions about the geodynamic processes in the convergence system of the oceanic Nazca plate and the continental South American plate.

THE DATA

In the 80th a considerable amount of geophysical data has been measured in the Central Andes. Seismic refraction lines cover all morphostructural units from the coast to the Andean foreland with a total length of the recording lines of more than 4000 km (Wigger et al. 1993). Magnetotelluric measurements were focussed on two profiles between 21° and 22°S and at 24°S, crossing the Andes in their whole width (Schwarz et al. 1993; figure 1.). The net of gravimetric datapoints covers a great part of the area between 20° and 26°S with varying distances between the recording sites (Götze et al. 1993).

THE CRUSTAL STRUCTURE

The Moho-discontinuity, at 40 km depth in the foreland, can be followed in the seismic observations down to about 70 km depth at the eastern border of the Altiplano (figure 2.). Here, in the backarc region, the

crustal thickening is interpreted as crustal doubling by stacking of different crustal units. The corresponding shortening is documented in the sedimentary cover of the Subandean Ranges by tectonic shortening of 140 km (Kley & Reinhardt 1993). High velocity zones at 20-25 km depth beneath the Eastern Cordillera are interpreted as oversthrusted lower crustal material to the east (Schmitz et al, this volume), corresponding to an A-subduction of the foreland-crust beneath the Andes.

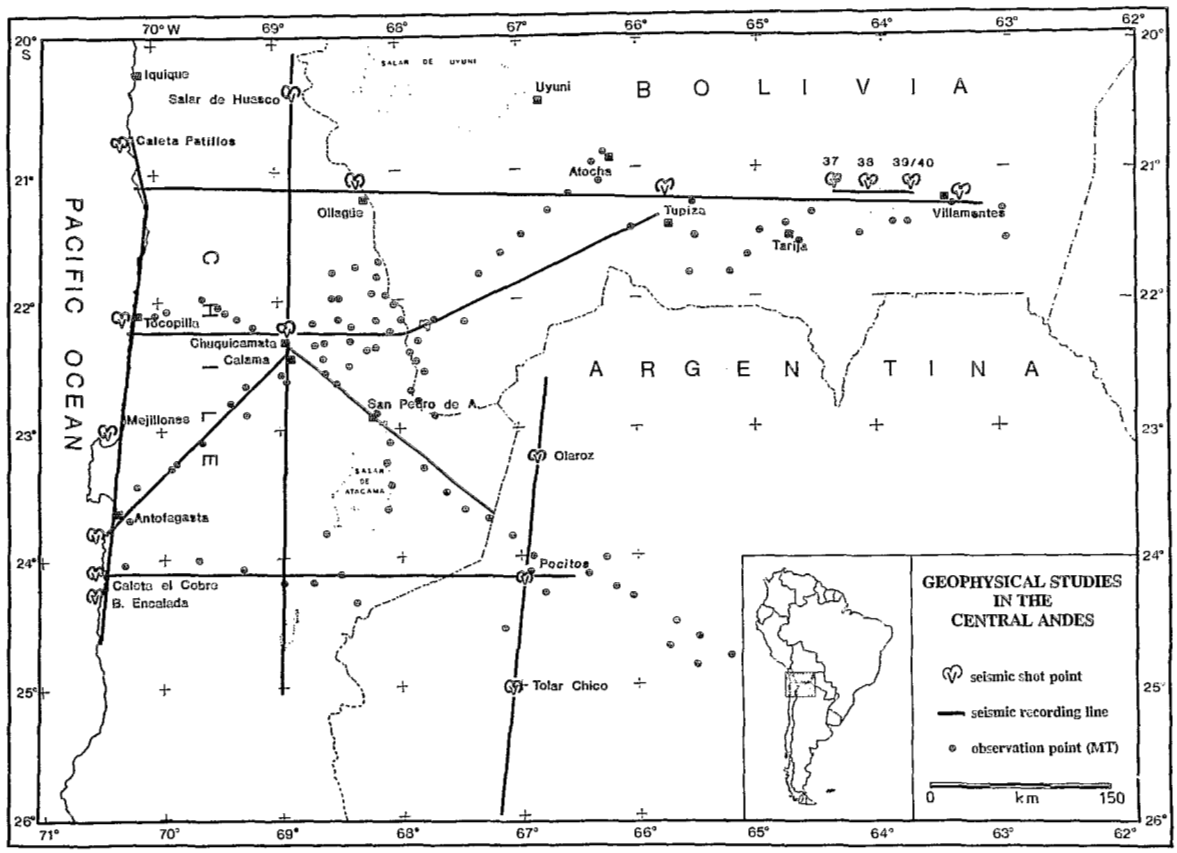

Figure 1. Map with the position of the seismic refraction lines and magnetotelluric (MT) recording sites (Schwarz et al. 1993). A gravimetric survey (Götze et al. 1993) covers almost the whole displayed area.

Beneath the Western Cordillera and the Altiplano no clear crust/mantle boundary can be detected from the seismic results, but intracrustal discontinuities are indicated. Based on the existence of a Bouguer anomaly of less than -400 mGal (Götze et al. 1993) about 70 km of material with crustal densities must be assumed. Zones of high electrical conductivity (HCZ) are observed at varying depths east of the magmatic arc, rising towards the surface in the Eastern Cordillera (Schwarz et al. 1993). In the Western Cordillera, the actual magmatic arc, the HCZ beginning at 10-15 km depth corresponds with low velocity zones (LVZ) in the same position.

A different structure is observed in the forearc. Here, high velocities (7.0-7.2 km/s) are observed at 20 km depth beneath the Coastal Cordillera, dipping to the east to about 35 km depth in the Precordillera. The deeper crust of the forearc is characterized by LVZs with an average velocity of 6.6 to 6.2 km/s down to 40 km depth beneath the Coastal Cordillera and 60-70 km depth beneath the Precordillera. The 40 km discontinuity beneath the Coastal Cordillera is interpreted as oceanic Moho. Its continuation to the east is not exactly known. Thus the forearc crust can be devided into a normal to thinned continental crust in the upper part and and a lower part, consisting of a mixture of material characterized by lower, but also relatively high seismic velocities. A high in the residual anomaly in the Precordillera south of Calama is interpreted by an intracrustal inhomogenity at 15-20 km depth.

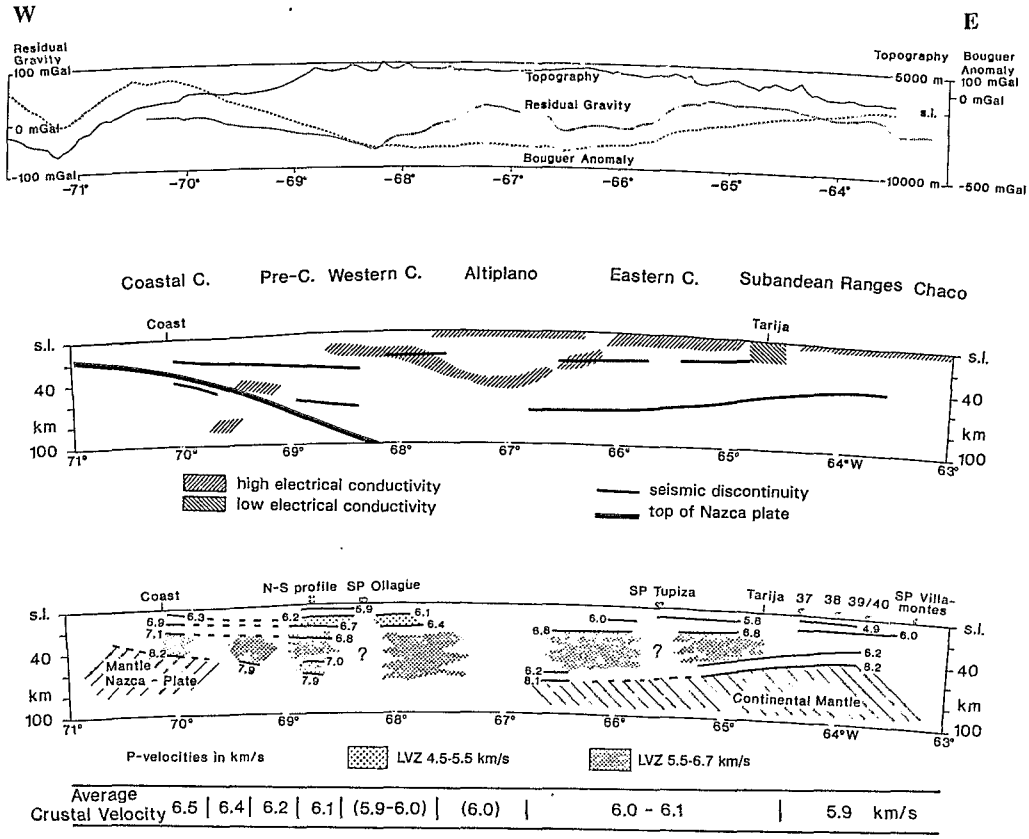

Figure 2. Above: Bouguer anomaly and residual gravity at 21°S (Götze et al. 1993). The topography is given for comparation. *Center*: Electrical conductivities between 21° and 22°S derived from magnetotelluric measurements (Schwarz et al. 1993). *Below*: Seismic discontinuities and P-wave velocities at 21°S in the parts which are proven by vertices (Wigger et al. 1993; Schmitz 1993). The average crustal velocities are given *below*.

CONCLUSIONS

The most outstanding anomaly of the Central Andes is the extreme thickening of the crust to about 70 km beneath the Western Cordillera and the Altiplano area derived from seismic and gravimetric data. Up to now, the thickening of the Andean crust was seen as a more or less symmetric phenomenon, but this picture must be revised. A pronounced asymmetric feature results from the interpretation of the existing geophysical data. Genetic aspects of the andine upper plate point to a "thinned" forearc crust and a tectonically thickened backarc crust.

The Andean crust shows a pronounced rheological structuration in vertical as well as horizontal direction. In the forearc, a normal to thinned continental crust is underlain by a pile of material, that possibly contents a thickened oceanic crust or remnants of that, continental material tectonically eroded from the continental margin and underplated in the forearc region, or remnants of the former continental mantle. From rheological point of view the upper plate shows a rigid behaviour whereas the lower part is probably ductile. The descending plate again shows a rigid behaviour.

The crust of the magmatic arc and the Altiplano is thickened, undifferentiated, without a clear Moho and it has relatively low average velocities and a spectacular high electrical conductivity anomaly (>10.000-20.000 Siemens) in 10-20 km depth (Schwarz et al. 1993) which must be characterized as "world

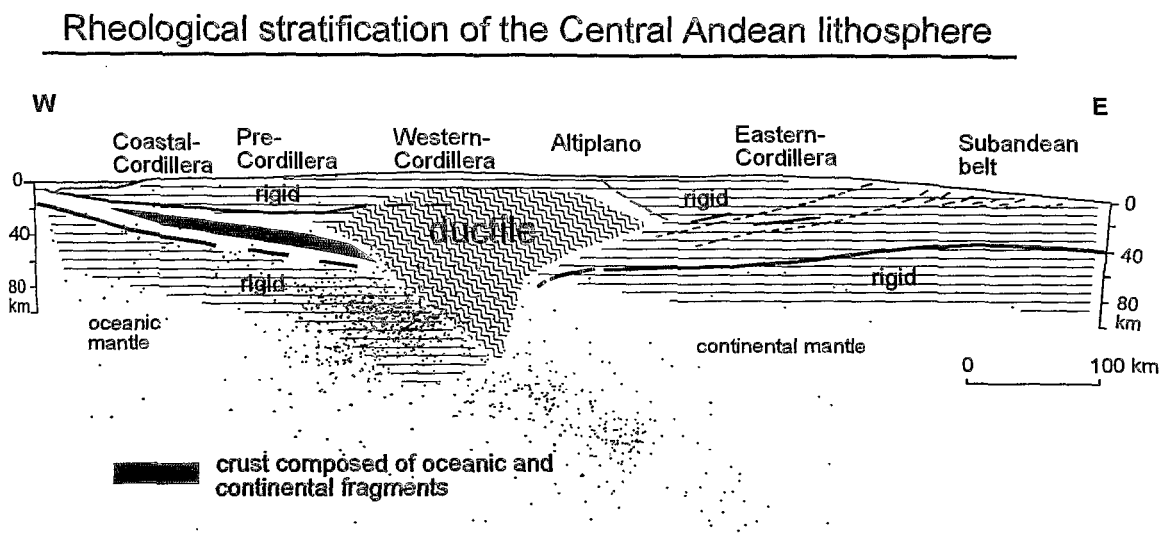

Figure 3. Rheological stratification of the Central Andean lithosphere. Hypocentral data are taken from ICS, USGS and PDE.

anomaly". Such extreme values of electrical conductivity can be explained only by fluids and/or partial melted zones. This crustal segment acts like a ductile buffer between forearc and backarc.

In the Eastern Cordillera and Subandean region of the backarc the crust is thickened with the development of a fold- and thrust belt. As the average crustal velocities increase again to the east, this crustal segment again is assumed to be rigid, but the distribution of high electrical conductivity areas in the sedimentary cover in the Subandean Belt and parts of the middle and lower crust of the backarc are ductile. In this sense the downgoing HCZ under the Eastern Cordillera - Altiplano border could indicate a deep reaching sole thrust.

REFERENCES

Götze H-J, Lahmeyer B, Schmidt S & Strunk S 1993 The lithospheric structure of the Central Andes (20°-26°S) as inferred from interpretation of regional gravity. In: Reutter K-J, Scheuber E & Wigger P (eds) Tectonics of the southern Central Andes: 7-22, Springer, Berlin Heidelberg New York.

Kley J & Reinhardt M 1993 Geothermal and tectonic evolution of the Eastern Cordillera and the Subandean Ranges of southern Bolivia. In: Reutter K-J, Scheuber E & Wigger P (eds) Tectonics of the southern Central Andes: 155-170, Springer, Berlin Heidelberg New York.

Schmitz M 1993 Kollisionsstrukturen in den Zentralen Anden: Ergebnisse refraktionsseismischer Messungen und Modellierung krustaler Deformationen. Dissertation, Freie Universität Berlin.

Schmitz M, Giese P & Wigger P 1993 Crustal thickening in the Central Andes - results from seismic refraction and crustal balancing. This volume.

Schwarz G, Chong DG, Krüger D, Martínez E, Massow W, Rath V & Viramonte J 1993 Crustal high conductivity zones in the Central Andes. In: Reutter K-J, Scheuber E & Wigger P (eds) Tectonics of the southern Central Andes: 49-68, Springer, Berlin Heidelberg New York.

Wigger P, Schmitz M, Araneda M, Asch G, Baldzuhn S, Giese P, Heinsohn W-D, Martínez E, Ricaldi E, Röwer P & Viramonte J 1993 Variation in the crustal structure of the southern Central Andes deduced from seismic refraction investigations. In: Reutter K-J, Scheuber E & Wigger P (eds) Tectonics of the Southern Central Andes: 23-48, Springer, Berlin Heidelberg New York.

SISMOLOGIE / SISMOTECTONIQUE / NÉOTECTONIQUE
SEISMOLOGY / SEISMOTECTONICS / NEOTECTONICS
SISMOLOGIA / SISMOTECTONICA / NEOTECTONICA

TRENCH INVESTIGATION ACROSS THE OCA-ANCON FAULT SYSTEM, NORTHWESTERN VENEZUELA

Franck A. AUDEMARD M.

Venezuelan Foundation for Seismological Research (FUNVISIS)
Apartado Postal 76880, Caracas 1070-A, Venezuela

RESUMEN: Dos trincheras de exploración paleosismológica ejecutadas sobre las fallas de Oca y Ancón, evidenciadas por microescarpes afectando rampas detríticas cuaternarias de las llanuras costeras de Buchivacoa, al Este de Maracaibo, confirmaron la actividad cuaternaria en transcurrencia dextral de éstas y permitieron estimar respectivamente sismos máximos probables de magnitud 7.4 y 7.5 con periodos de retorno de 4300 y 1900 años.

KEY WORDS: Neotectonics, Paleoseismology, Seismic Hazard Evaluation, Trenching.

INTRODUCTION

The Oca-Ancon fault system is a major east-west, right-lateral strike-slip tectonic feature of northern South America which trace extends eastward from the Colombian atlantic-coast, near Santa Marta, to the town of Puerto Cabello located on the caribbean coast of Venezuela, across the Goajira Peninsula, the outlet of Lake Maracaibo, the coastal plains of Buchivacoa (northwestern Falcon State) and the central Falcon range (Fig. 1). This system truncates the north ends of the Santa Marta block and Perija Range. The Oca-Ancon system converges with the Bocono-San Sebastian-El Pilar system on the Aroa - Golfo Triste depression.

Spectacular diagnostic geomorphic features of Quaternary activity have been reported along this tectonic system since the late forties. VOORWIJK (1948) photointerpreted pluri-kilometric fault scarplets related to both Oca and Ancon faults in the Quaternary alluvial plains of Buchivacoa, some fifty Kilometers East of Maracaibo. Few years later, MILLER (1960) observed displacement of Holocene beach strandlines in Sinamaica, slightly North of The city of Maracaibo. This second site was trenched by CLUFF & HANSEN (1969) who could put in evidence the Quaternary activity of the Oca fault but they only could establish the occurrence of the latest seismic event on that segment of the system which has happened in the last 2700 years.

Despite all these evidences, many authors in recent times have seismically underestimated this fault system and they have occasionally considered it inactive. On the contrary, other authors have overestimated its lateral displacement to fit Caribbean Geodynamics models. In fact, Oligocene rocks outcropping along the axis of the Falcon anticlinorium on both sides of the fault system leads to estimates of apparent dextral displacement of 30±3 Km (SOULAS,1987; AUDEMARD,1991). Moreover, JANSSEN (1979) has proposed no more than 50 Km of post-Middle Cretaceous apparent right-lateral displacement along this system based on the apparent offset of the Cogollo Group isopach map from northern Lake Maracaibo and TSCHANZ *et al.* (1974) have estimated 65 Km of apparent right-lateral offset measured on Mesozoic metamorphic rocks. This estimates do not fit in many Geodynamics

models where large transcurrent movements are required along the southern boundary of the Caribbean plate.

Still more amazing is the fact that very few authors have mapped thoroughly the fault trace farther East of Maracaibo since the fifties (JAECKLI & ERDMAN,1952; MENDEZ & GUEVARA,1969; SOULAS,1987; AUDEMARD,1991 and AUDEMARD *et al.*,1992) where profuse geophysical and geological information has been collected by oil companies. In fact, this fault system has been very frequently skechted across the Falcon anticlinorium following diverse positions and trends in order to connect the known western segment of the fault (westward of Maracaibo) with the Bocono-San Sebastian-El Pilar fault system (AUDEMARD*et al., op. cit.*)

GEOLOGICAL SETTING

In the western coastal plains of Falcon State and East of Maracaibo, the Oca-Ancon fault system is farely simple as it is composed by two sub-parallel fault strands: the Oca and Ancon faults (Fig.1). Their traces are defined by pluri-kilometric scarplets in Quaternary alluvial ramps that were reported by VOORWIJK (1948). These scarplets of the Oca and Ancon faults have been smoothed and they are 0.3m and 1.2m in height respectively. Both scarplets face each other and they limit a large area of probable present subsidence because large swamps are present, rivers become meandering and drainage flow is erratic. I believe that the western portion of this area is an active pull-apart basin located in the right-stepover between the dextral Oca and Ancon faults which seems to be corroborated by seismic profiles (AUDEMARD,*op. cit.*).

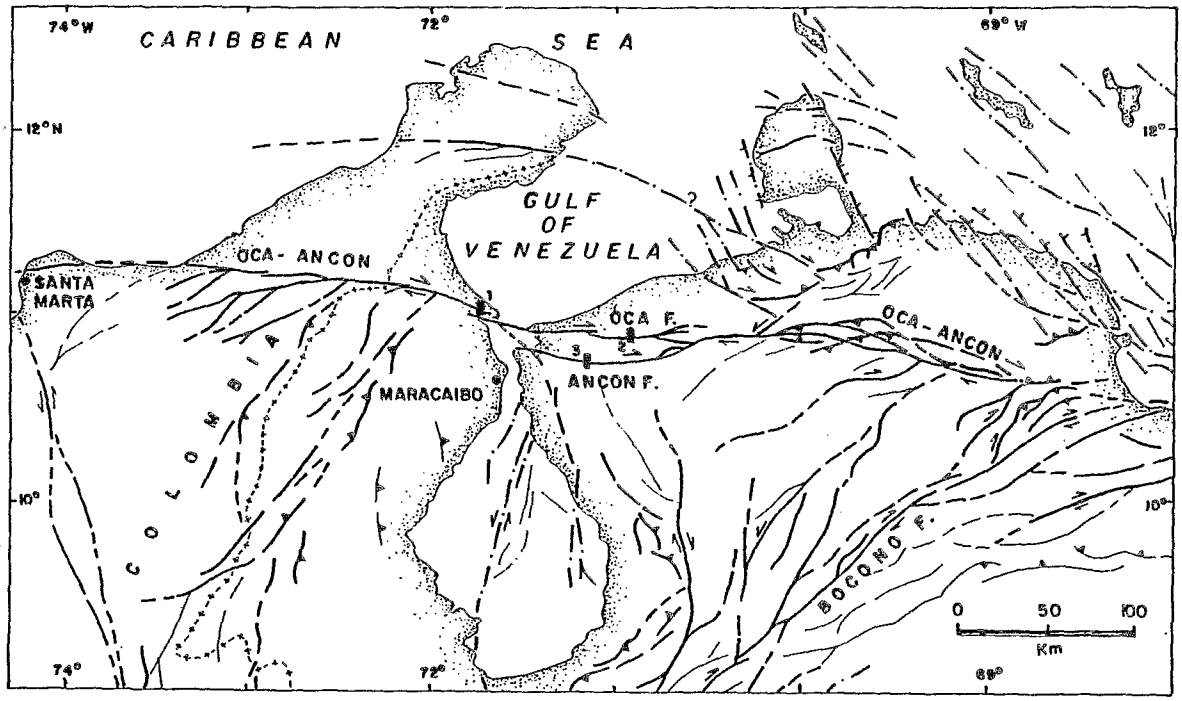

Figure 1.- Netectonic map of northwestern Venezuela and northern Colombia. The most relevant tectonic feature of the region is the WNW-ESE right-lateral strike-slip Oca-Ancon fault system. Small boxes identify trench sites :1- CLUFF & HANSEN (1969); 2 and 3- AUDEMARD (1991). Map sources: MILLER (1960); TSCHANZ*et al.* (1969); SOULAS (1985,1987) ; AUDEMARD (1991) and AUDEMARD*et al.* (1992).

This segment of the system was chosen for trenching among others because of technical facilities and favorable geological conditions, and mainly because the simplest segment, the one West of Maracaibo, had already been trenched in the most favorable site (1 in Fig. 1 ; site described by MILLER (1960) and excavated by CLUFF & JANSEN (1969)) which proved to be poorly satisfactory as trench excavation could not go beyond 2.5 m in depth due to shallowness of water table and unconsolidation of loose sands of Holocene beach strandlines. In consequence, two trenches had to be excavated (a trench per fault strand) in order to evaluate the seismic potential of the system (2 and 3 in Fig. 1).

TRENCH DESCRIPTION AND OBSERVATIONS

Each of both trench sites were located on those scarplets previously mentioned (2 and 3 in Fig.1) and trenches were excavated by bulldozer down to 7 or 8 m in depth . Width of trenches decreased from 8 m at the top to 4 m at the bottom and length varied between 80 and 85 m. Therefore, removal of some 2.500 to 3.000 cubic meters of material per trench was required.

Both faults were clearly observed in trench walls cutting the whole sedimentary sequence, except the present soil horizon. Slickensides were measured on both fault planes. The Oca fault is dextral with a relevant north-side-up reverse component. It is composed of a single, subvertical, north dipping fault plane. On the other hand, the Ancon fault is pure right-lateral strike-slip with an apparent south-side-up component of slip. The Ancon fault is also subvertical and it presents a broader deformation zone where conjugated minor faults accomodate mass volume problems. Striations observed on both fault planes are in agreement with sedimentary layer throws measured on the trench walls and with geomorphic features (scarplets).

PALEOSEISMIC INTERPRETATION

Trench geological observations combined with radicarbon dates of several samples collected from selected stratigraphic horizons outcropping in the trenches allowed us to make paleoseismic reconstructions of the Oca-Ancon fault system and to estimate its seismic potential (AUDEMARD,1991).

The following conclusions can be drawn from this paleoseismic research :

- Three surface rupture events have occurred along the Oca fault, dated 7755±320, 6240±390 and 1945±630 years BP.
- One surface rupture event has happened within the past 3125±185 years BP on the Ancon fault.
- The Holocene slip rate of the fault system is about 2 mm/a.
- Any of both Oca and Ancon faults can generate a maximum probable earthquake of magnitude 7.4 to 7.5. Recurrence of such events on the Ancon fault is close to 1900 years while it is about as twice as long on the Oca fault (4300 years)

REFERENCES

AUDEMARD, F. A. (1991) Actividad cuaternaria y caracterización sismogénica de las fallas de Lagarto y Rio Seco. Afinamiento de las características sismogénicas del sistema de fallas de Oca-Ancón y Urumaco. *Unpubl. Co. Rpt., Maraven S.A., Caracas;* 91pp.

AUDEMARD, F. A.; SINGER, A.; BELTRAN, C.; RODRIGUEZ, J.A.; LUGO, M.; CHACIN,C.; ADRIANZA, A.; MENDOZA, J. & RAMOS, C. (1992) Actividad tectónica cuaternaria y características sismogénicas de los sistema de falla de Oca-Ancón (tramo oriental), de la Península de Paraguaná y región de Coro y de la costa nororiental de Falcón. *Unpubl. Co. Rpt., Intevep S.A., Los Teques;* 2 Vol., 245pp.

CLUFF, L. & HANSEN, W. (1969) Seimicity and Seismic Geology of Northwestern Venezuela. *EPC-70480-I Unpubl. Co. Rpt., Maraven S.A., Caracas;* 2 Vol.

JAECKLI, R. & ERDMAN, D. (1952) Geological compilation report Central and West Falcon. *EPC-1272 Unpubl. Co. Rpt., Shell de Venezuela .*

JANSSEN, F. (1979) Structural style of Northwestern Venezuela . *EPC-6270 Unpubl. Co. Rpt., Maraven S.A., Caracas;* 61pp.

MENDEZ, J. & GUEVARA, E. (1969) Geological compilation map of N.W. Venezuela, Guajira and Aruba (1:250.000). *Unpubl. Co. Rpt., Maraven S.A., Caracas.*
MILLER, J. (1960) Directrices tectónicas en la Sierra de Perija y partes adyacentes de Venezuela y Colombia. *III Cong. Geol. Venezolano, Caracas;* 2: 685-718.
SOULAS, J-P. (1985) Neotectónica y tectónica activa en Venezuela y regiones vecinas. *VI Cong. Geol. Venezolano, Caracas;* 10: 6639-6656.
SOULAS, J-P. (1987) Actividad cuaternaria y características sismogénicas del sistema de fallas de Oca-Ancón y de las fallas de Lagarto, Urumaco, Rio Seco y Pedregal. Afinamiento de las características sismogénicas de las fallas de Mene Grande y Valera. *Unpubl. Co. Rpt., Maraven S.A., Caracas;* 69pp.
TSCHANZ, C. ; JIMENO, A. & CRUZ, B. (1969) Mapa geológico de reconocimiento de la Sierra Nevada de Santa Marta (1:200.000) *Ingeominas, Bogota.*
TSCHANZ, C. ; MARTIN, R.; CRUZ, B.; MEHNERT, H. & CEBULA, G. (1974) Geologic evolution of the Sierra Nevada de Santa Marta, northeastern Colombia. *Geol. Soc. Am. Bull.,* 85: 273-284.
VOORWIJK, G. (1948) Recent faulting in the Buchivacoa-Miranda plains. *EPC-852 Unpubl. Co. Rpt., Maraven S.A., Caracas;* 6pp.

CRUSTAL MOVEMENTS IN CHILE: THE 1985 EARTHQUAKE

Sergio E. BARRIENTOS

Dept. of Geophysics, University of Chile, Casilla 2777, Santiago, Chile
E-mail: sbarrien@cec.uchile.cl

Resumen: Hundimientos y levantamientos co- y post-sísmicos de la costa de Chile han sido evidentes a través del tiempo. Se presenta el caso del terremoto de 1985 ($M_W = 8.0$) en Chile central para el cual se cuenta con datos de nivelación, gravedad y registros inéditos de dos limnígrafos en el lago Rapel, situado sobre la zona de ruptura del terremoto de 1985. Estos muestran una inclinación post-sísmica de gran amplitud (6 μradianes) con duración cercana a un año. Esta señal se interpreta como creep post-sísmico en la continuación de la ruptura cosísmica sobrepuesta a una relajación visco-elástica regional.

Key Words: Crustal movements, fault creep, postseismic relaxation.

Introduction

Historical records of large earthquakes for the past 400 yr along the central Chile portion of the convergence zone between Nazca and SouthAmerican plates indicate an almost periodic earthquake sequence with a recurrence interval of 82±6 yr (*Nishenko*, 1985). The March 3, 1985 $M_S = 7.8$ central Chile earthquake is the last event in this sequence. Aftershock studies, body-wave modeling, surface wave and strong ground motion analysis, gravimetric observations and geodetic estimates revealed a rupture region approximately 160 km long in a north-south orientation (*Christensen* and *Ruff, 1986*; *Korrat* and *Madariaga*, 1986; *Comte et al.*, 1986; *Houston* and *Kanamori*, 1987; *Barrientos*, 1988; *Choy* and *Dewey*, 1988). A first order leveling line, repeatedly surveyed in 1981 and four months after the earthquake, evidenced 0.5 m of uplift near the coastal city of San Antonio and a 10-cm subsidence about 60 km inland (*IGM*, 1985). Between these two points, to the south, lies Rapel lake, a body of water artificially dammed to generate hydroelectric power (Fig. 1).

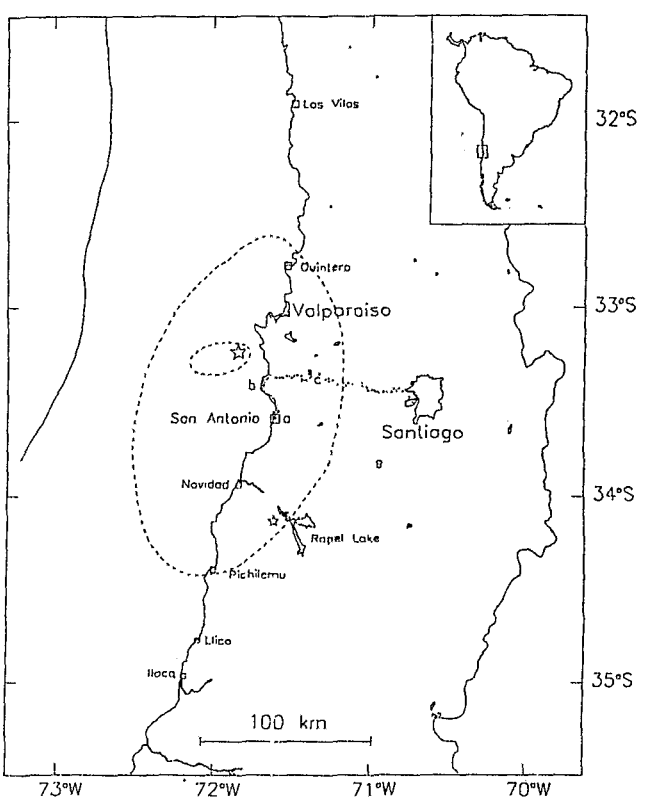

Fig. 1. Location of the foreshock and aftershock areas (small and large dashed ellipse) in reference to Rapel lake. Gages are located on its western and southeastern ends. Leveling line (dots) runs from San Antonio to Santiago.

Two limnigraphs, separated by 20 km, have been recording continuously for more than 10 years the water level of Rapel lake providing a measure of tilt of the lake basin. Gravity data along the leveling line in addition to sea level measurements at a tide gage in Valparaíso complement the information.

Data

The water level of the Rapel lake is recorded by two Stevens A35 limnigraphs. The mechanical principle of operation of these instruments is based on a floating device which transfer water level variations to a recording stylus through a float pulley. A clock connected by suitable gearing, provides the appropriate speed to the drum. From the analog records the daily average is computed by averaging twenty four hourly samples. Figure 2 shows the water level variation at the dam as a function of time. Extreme variations of the lake level reach 6 m, with spectral peaks at periods of one yr, six months and one week (related to seasonal river flow) generated by rain and snow melt, and periodic energy demands. The regional tilt of the lake basin due to deformation associated with the 1985 event can be extracted by directly differencing the records of the two limnigraphs (Fig. 3).

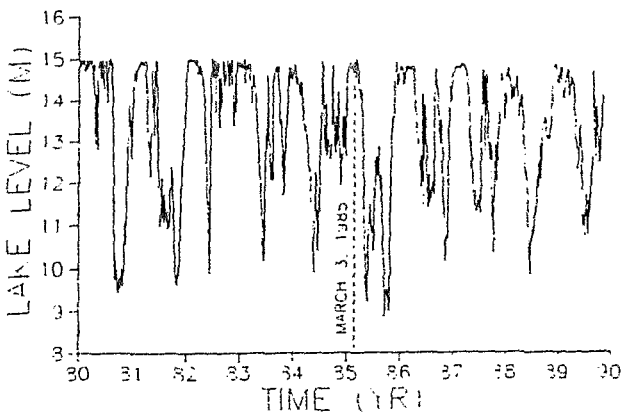

Fig. 2. Water level fluctuations at the western end of Rapel lake. Values beyond the arbitrary height of 15 are not allowed to prevent dam overflow. A one-year cycle dominates the signal.

The time dependent tilt shows several characteristics: a) a steady oscilation around the zero baseline with typical excursions of about 3 cm, which also correspond to typical standard deviations of the daily averages, b) at the time of the earthquake no change was observed, therefore the lake is located in a null coseismic tilt region, c) a progressively larger tilt is developed gradually as a function of time right after the earthquake. It takes between 8 and 12 months to complete, reaching an amplitude of about 12 cm, d) a long term slowly decaying signal which oscilates with a one-year period.

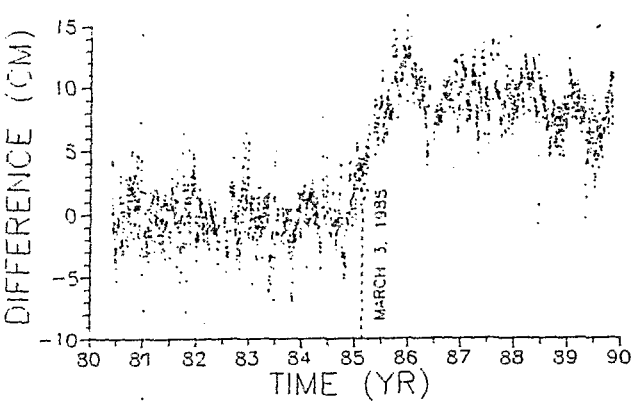

Fig. 3. Daily differences of water level at the two limnigraphs. The three segments of the signal (pre-earthquake, one-year post-earthquake and long post-seismic decay) are discussed in the text.

Analysis

Due to comparable high rates of deformation, the first part of the anomalous signal, which departs significantly from zero and extends for one year after the occurrence of the main event, is modeled as fault creep along the down-dip extension of the coseismic rupture. The second part, which corresponds to the slowly decaying signal, will be modeled independently because it shows a different time scale behavior. Fault creep has been used by *Kasahara* (1975) to explain postseismic deformation associated with the 1973 Nemuro-Oki earthquake along leveling lines and tide gages records. *Savage* and *Plafker* (1991) and *Brown et al.* (1977) offer the same mechanism to model postseismic elevation changes in relation to the 1964 Alaska earthquake.

The vertical displacement $u_z(x, L)$ at a point x on the free surface of a half-space due to an inclined dislocation of width L reaching the surface is (*Barrientos et al.*, 1992):

$$u_z(x,L) = \frac{\Delta s}{\pi} sin\phi[(\pi/2 - \phi) - \frac{Lxsin\phi}{D^2} + tan^{-1}(\frac{L - xcos\phi}{xsin\phi})]$$

where Δs is the amount of fault slip, $D^2 = L^2 - 2Lxcos\phi + x^2$ and ϕ is the dip angle. A more general expression for a buried fault of width $W = L_1 - L_0$ would be $u_z(x, W) = u_z(x, L_1) - u_z(x, L_0)$. The time dependence is incorporated through $L_1(t) = vt$. This is a down-dip expanding rupture with velocity of propagation v of the front L_1. The inputs to the fault model are dip angle, velocity and starting point of the propagating pulse. Dip angle and starting point of creep along the fault are determined by the dip angle and down-dip extension of the coseismic fault. Fig. 4 shows the expected low-pass filtered (30 days) observed vertical movement and that expected due to a down-dip propagating rupture with a velocity of 25 km/yr. The model reproduces amplitude of tilt as well as its time dependence.

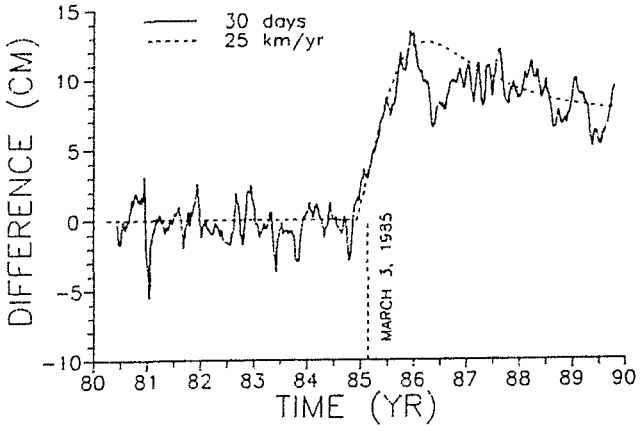

Fig. 4. Expected tilt change produced by the propagating rupture (dashed line) superimposed on the 30-day filtered observations. The model implies a rupture propagation of 25 km/yr.

Coseismic vertical changes established by repeated surveys of the leveling line that extends inland from the coastal city of San Antonio to Casablanca (point labeled *c* on Fig 1.) are shown in Fig. 5. On the same plot, the difference of three gravity surveys are superimposed; these gravity observations were surveyed in 1983, 1985 (three months after the earthquake) and in 1990. The coseismic stage (85-83), shown by long dashed lines, has been scaled such that the amplitudes are coincident with the values observed along the leveling line. The scaling factor turns out to be very close to the inverse of the Free Air Correction.

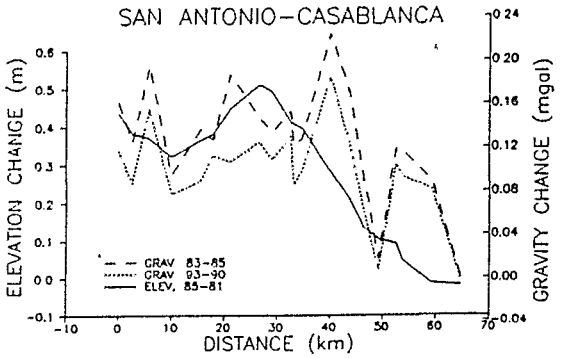

Fig. 5. Observed elevation change based on the leveling line (solid trace) and gravity observations. The gravity co-seismic period (long dashed trace, 85-83) has been scaled to agree with the leveling line. A longer period, 91-83 (small dashed trace) indicates that the region has subsided at a later stage.

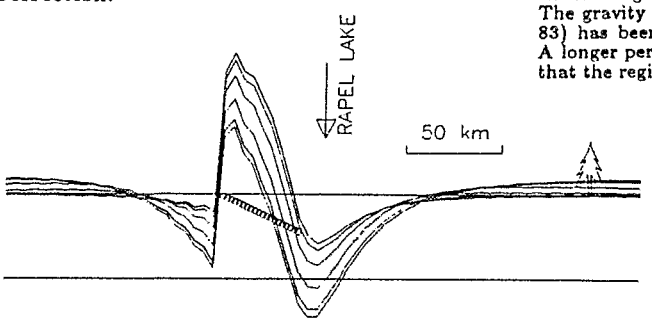

Fig. 6. Visco-elastic response of a layer over a halfspace. The coseismically uplifted region gradually subsides with time.

Even though departures of the gravity derived height changes with respect to those directly observed are important, there is a systematic decrement of the gravity derived height observed in the 90-83 period. This means that the coseismically uplifted region is subsiding in a post-earthquake stage.

To explain the observed differences between the two postseismic gravity surveys in combination with the later part of the observed tilt signal of the lake, a viscoelastic relaxation model is proposed. The procedure used to model the viscoelastic response is a semi-analytical formalism, which can be applied to any two-dimensional dipping fault, based on propagator matrices which allows for variable slip faults embedded in vertically heterogeneous media (*Barrientos*, 1993). Qualitative preliminary results agree with the observed tilt decrement as a function of time (Fig. 6).

Conclusions

Continuous measurements of tilt for ten years at Rapel Lake, located above the rupture region of the 1985 Central Chile earthquake, indicate a lack of coseismic movement. A progressively larger tilt is developed gradually as a function of time immediately after the earthquake. This cumulative tilt takes between 8 and 12 months to complete, reaching an amplitude of approximately 12 cm which is equivalent to 6 μradians considering a baseline of 20 km. After reaching the maximum value, a long term slowly decaying signal is observed. The two parts of the signal are interpreted, due to their different time scales, as the effect of distinct origin. The accelerated part is explained as fault creep on the down-dip extension of the ruptured region and the slowly decaying signal is modeled as the result of viscoelastic adjustments. For a 20° dipping fault a creep velocity of 25 km/yr best fit the observations.

Acknowledgements. This work would have not been possible without the limnigraph data provided by Empresa Nacional de Electricidad. I would like to thank Edgar Kausel for fruitful exchange of ideas and Manuel Araneda for making available the gravity observations along the leveling line. This work has been partially funded by Fondo Nacional de Ciencia y Tecnología (FONDECYT).

References

Barrientos, S. E. 1988, Slip distribution of the 1985 Central Chile earthquake, *Tectonophysics, 145*, 225-241.

Barrientos, S. E., G. Plafker and E. Lorca, 1992, Postseismic coastal uplift in Southern Chile, *Geophys. Res. Lett., 19*, 701, 704.

Barrientos, S. E. Large earthquakes and volcanic eruptions, submitted to *Pure Appl. Geophys.*

Brown, L. R., R. Reilinger, S. R. Holdhal and E. I Balazs, 1989, Postseismic crustal uplift near Anchorage, Alaska, *J. Geophys. Res., 82* 3369-3378.

Chistensen, D. G., and L. J. Ruff, 1986, Rupture process of the March 3, 1985 Chilean earthquake, *Geophys. Res. Lett., 13*, 721-724.

Comte, D., A. Eisenberg, E. Lorca, M. Pardo, L. Ponce, R., Saragoni, S. K. Singh and G. Suárez, 1986, The great 1985 Central Chile earthquake: A repeat of previous great earthquakes in the region?, *Science, 233*, 449-453.

Choy, G., and J. Dewey, 1988, Rupture process of an extended sequence: Teleseismic analysis of the Chilean earthquake of March 3, 1985, *J. Geophys. Res., 93* 1103-1118.

Houston, H. and H. Kanamori, 1987, Source spectra of great earthquakes: Teleseismic constraints on rupture and strong motion, *Bull. Seism. Soc. Am., 76*, 19-42.

IGM (Instituto Geográfico Militar), 1985, El terremoto del 3 de marzo de 1985 y las deformaciones de la corteza, *Terra Australis, 28*, 7-12.

Kasahara, K., 1975, Aseismic faulting following the 1973 Nemuro-Oki earthquake, Hokkaido, Japan (a possibility), *Pure Appl. Gephys., 113*, 127-139.

Korrat, I. and R. Madariaga, 1986, Rupture of the Valparaíso (Chile) gap from 1971 to 1985, in *Earthquake Source Mechanics*, ed. S. Das, J. Boatwright and C. H. Scholz, AGU, Washington, D.C., 247-258.

Nishenko, S. P., 1985, Seismic potential for large and great interplate earthquakes along the Chilean and southern Peruvian margins of SouthAmerica: a quantitative reapprisal, *J. Geophys. Res., 90*, 3589-3615.

Savage, J. C. and G. Plafker, 1991, Tide gage measurements of uplift along the south coast of Alaska, *J. Geophys. Res. 96*, 4325-4335.

VARIATIONS IN THE RUPTURE MODE OF LARGE EARTHQUAKES ALONG THE SOUTH AMERICAN SUBDUCTION ZONE

Susan L. BECK

Southern Arizona Seismic Observatory and Department of Geosciences, University of Arizona, Tucson, AZ 85721, U.S.A.

RESUMEN: Hemos analizado ondas telesísmicas P y S para la mayoría de los terremotos de gran magnitud en la zona de subducción Sudamericana, y hemos encontrado grandes variaciones, tanto espaciales como temporales, en la liberación de momento sísmico. En regiones con una o varias asperezas, la mayor parte de los terremotos se inician en o cerca de la aspereza dominante. El tipo de segmentación definida por los terremotos en el presente siglo, parece ser inconsistente con la secuencia anterior dada por los eventos en las fronteras de las placas a lo largo de la zone de subducción Sudamericana.

Key Words: South American subduction earthquakes, source parameters

INTRODUCTION

During the last decade our understanding of the rupture process of large subduction zone earthquakes has improved dramatically. Recently, many studies have identified temporal and spatial heterogeneity associated with the rupture process of underthrusting subduction zone events using teleseismic body waves. These studies have shown that the seismic moment release is not uniformly distributed but is concentrated in small regions or patches on the fault area. These patches of relatively high moment release and hence high slip are interpreted as asperities (Lay et al., 1982). Detailed waveform studies of earthquakes that occurred since 1963 provide us with a first-order asperity map for part of the South American subduction zone. In order to expand our understanding of the earthquake occurrence along this subduction zone, we have extended our study to include the largest historic earthquakes.

Although plate boundary segments fail repeatedly in large earthquakes, the seismic moment and recurrence interval for these major plate boundary events often vary dramatically. Study of different earthquakes over a long time interval is essential for a thorough understanding of the earthquake phenomenon. Restricting our analysis to recent earthquakes (events in the last 30 years) can lead to erroneous or misleading results for some regions. Thus, detailed analyses of earlier historic earthquakes are critical. For nearly 80 years a large number of seismographs have been recording at stations around the world. Analyzing data from historic earthquakes can yield valuable information about the earthquake occurrence. For events between 1920 and 1963 we have collected and analyzed teleseismic waveform data to determine source parameters. In addition, we have compiled information about tsunamis and intensities for events extending back approximately 400 years (Silgado, 1985; Hatori, 1968, 1981). The historic earthquake record for the South American subduction zone clearly indicates that characteristic earthquakes do not occur, but rather we see large variations in the earthquake rupture mode and segmentation between successive earthquake sequences.

COLOMBIA-ECUADOR SUBDUCTION ZONE

Two different modes of rupture have occurred along the subduction zone segment off the coast of Colombia-Ecuador (Kanamori and McNally, 1982). In 1906 a great earthquake (M_w=8.8) ruptured a 500 km segment of the plate boundary. This same segment subsequently ruptured in three smaller earthquakes, from south to north, in 1942 (M_s = 7.9), 1958 (M_w = 7.7), and 1979 (M_w = 8.2). It has been 50 years since the 1942 earthquake, longer than the 36-year interval between 1906 and 1942; hence, it is important to evaluate the 1942 earthquake. We analyzed long-period teleseismic *P* and *PP* phases to determine the size, source duration and rupture complexity for the May 14, 1942, Ecuador earthquake. The *P*-wave first motions and body wave modeling of the 1942 earthquake indicate an underthrusting mechanism consistent with the focal mechanism determined for the 1979 Colombia earthquake. The source time function deconvolved from body waves indicate a simple pulse of moment release with a duration of ~25 sec and a depth extent of 0-30 km. The 1942 earthquake failed as a single-asperity event with the moment release concentrated near the epicenter. Estimating the spatial extent of the main moment release using the source duration and a rupture velocity of 2-2.5 km/sec suggests that most of the moment release occurred on a small part of the fault area and in a region with very few aftershocks. The 1942 event is larger than the adjacent 1958 event, although both earthquakes initiated rupture at the dominant asperity and had similar numbers of aftershocks with $m_b > 5.5$ (Mendoza and Dewey, 1984). In contrast, the 1979 earthquake had a much longer source duration, initiated rupture ~60 km from the dominant asperity and had few aftershocks with $m_b > 5.5$ (Beck and Ruff, 1984). The historic earthquake record suggests that a large tsunami-generating event has not occurred prior to 1906 for at least 300 years. Large variations occur in the rupture characteristics of the individual earthquakes (1942, 1958, and 1979) as well as between successive earthquake cycles along the Colombia-Ecuador subduction zone.

CENTRAL PERU SUBDUCTION ZONE

The great earthquakes of Oct. 17, 1966 (M_w=8.1), May 24, 1940 (M_w=7.9), Oct. 3, 1974 (M_w=8.1) and August 24, 1942 (M_s~8.2) ruptured adjacent segments along the Peru trench. With the exception of a 80-100 km gap between 1974 and 1942 rupture zones, where the Nazca ridge intersects the trench, the entire segment between 10°S and 16°S has failed in magnitude 8 earthquakes this century. The 1966 and 1940 earthquakes failed as single asperity earthquakes with the dominant asperity near the hypocenter (Beck and Ruff, 1989). In contrast, the 1974 event had a bilateral rupture and failed with two asperities, the largest occurring 80 km south of the hypocenter (Beck and Ruff, 1989). The asperities are concentrated on a small part of the aftershock area (Dewey and Spence, 1979). The 1942 earthquake failed with 2 to 3 pulses of moment release, but we cannot spatially locate the moment release. The historic earthquake record suggests significant variations in the earthquake size during the last 400 years. Previous events in 1687 and 1746 were much larger than the earthquakes this century (Beck and Nishenko, 1990). The intensity and tsunami data indicate that the 1687 event ruptured not only the 1974 segment but the gap between the 1974 and 1942 events. The 1746 earthquake appears to have ruptured both the 1966 and 1940 segments.

CENTRAL CHILE SUBDUCTION ZONE

Four large historic earthquakes have occurred along the central Chilean subduction zone. From north to south, these events occurred on November 11, 1922 (M_s~8.3), April 6, 1943 (M_s~7.9), December 1, 1928 (M_s~8.0) and January 25, 1939 (M_s~8). We have evaluated source parameters for these events using long-period *P* and *SH* waveforms, *P*-wave first motions, intensities, and tsunami heights. We find that the 1922, 1928 and 1943 events are consistent with underthrusting of the Nazca Plate beneath the South American plate. All four events were well recorded in Europe at station DBN. A comparison of the source time functions determined using the *P* waves recorded at DBN indicates that the 1922 event was

approximately 4 times larger than the 1943 event and approximately 6 times larger than the 1928 event. The 1922 and 1943 events produced tsunamis in Japan of 65 and 10 cm, respectively. In contrast, no far-field tsunami was reported in Japan for the 1928 event.

A moment tensor inversion using long-period *P* and *SH* waveforms for the 1928 earthquake yields a range in acceptable focal mechanisms, all of which are predominantly thrust events. The source time function for the 1928 earthquake has one main pulse of moment release with a duration of approximately 24 sec. The reported location of the maximum intensities and aftershocks for the 1928 earthquake are south of the main shock epicenter, suggesting a rupture to the south. The source duration suggests that most of the moment release occurred between the epicenter and approximately 80 km to the south. The 1943 earthquake also has a simple source time function with a duration of 24 sec; however, the rupture direction is unclear. In contrast, the *P*-wave for the 1922 earthquake recorded at DBN indicates that this earthquake has a complex source time function with three pulses of seismic moment release and a total duration of at least 70 sec. The complexity of the 1922 earthquake suggests it failed in a multiple-asperity rupture, indicating that this segment could rupture in several smaller adjacent events rather than one 1922-type earthquake.

The most damaging earthquake along the coast of southern Chile this century occurred on January 25, 1939. The 1939 earthquake caused 28,000 deaths and did extensive damage to the city of Chillan (Campos and Kausel, 1990). The 1939 event occurred just to the south of the 1928 earthquake. Although similar in size, the 1939 earthquake was much more damaging than the 1928 earthquake. Analysis of both these large subduction zone earthquakes indicates that they have different focal mechanisms.

We analyzed *P* and *S* waveforms to determine the type of faulting and source parameters for the 1939 earthquake. A comparison of waveforms recorded at the same station for the 1939 earthquake and underthrusting earthquakes in 1928 and 1943 along the Chile subduction zone confirms that the 1939 earthquake is not an underthrusting event. The *P*, *SV* and *SH* first motions, the amplitude ratio of the *SH* to *SV*, and modelling of *P* waveforms indicate an oblique normal focal mechanism. The high intensities, lack of a tsunami, and inland location associated with the 1939 event are all consistent with an intraplate event within the down-going slab. Thus, large, intermediate-depth, intraplate earthquakes represent a significant seismic hazard along the coast of Chile.

The 1928 earthquake ruptured southward with most of the seismic moment release occurring 60-80 km south of the 1928 epicenter but still north of the 1939 region. In light of this information the underthrusting plate interface segment (updip of the 1939 event) between 36°S and 37.5°S needs to be re-evaluated. This segment failed in 1835, 1751, and 1657 with large tsunami-generating earthquakes. Although we know very little about these previous events, the large tsunamis and intensity patterns suggest that they were underthrusting earthquakes and not intraplate earthquakes similar to the 1939 event. If the 1939 event is indeed not an underthrusting earthquake, then this segment has not failed for 157 years and may be a "seismic gap".

CONCLUSIONS

Much of the South American subduction zone has failed in magnitude 8 or larger earthquakes this century. The rupture characteristics of these individual earthquakes have varied greatly. The regions of high moment release and hence large displacement are concentrated on small patches of the fault area as defined by the aftershock area. Both single- and multiple-asperity ruptures occur and most earthquakes initiated at or near the dominant asperity. We do not understand what these seismically determined asperities represent physically because, in general, they do not correspond to any observable geometric features associated with the subduction zone. The South American subduction zone does not fail in characteristic earthquakes. The segmentation defined by the earthquakes this century appears inconsistent with the previous sequence of plate boundary events. Along segments of the Colombia-Ecuador, central Peru, and Chile subduction zones, the earthquake rupture mode varies between successive earthquake sequences.

REFERENCES

Beck, S. and L. Ruff, 1984. The rupture process of the great 1979 Colombia earthquake: Evidence for the asperity model, *J. Geophys. Res.*, 89: 9281-9291.

Beck, S. and L. Ruff, 1989. Great earthquakes and subduction along the Peru trench, *Physic Earth and Plant. Inter.*, 57: 199-224.

Beck, S. and S. Nishenko, 1990. Variations in the mode of great earthquake rupture along the central Peru subduction zone, *Geophys. Res. Let.*, 17: 1969-1972.

Campos, J. and E. Kausel, 1990. The large 1939 intraplate earthquake of southern Chile, *Seism. Res. Letters*, 61: 43.

Dewey, J. W., and W. Spence, 1979. Seismic gaps and source zones of recent large earthquakes in coastal Peru, *Pageoph.*, 117: 1148-1171.

Hatori, T., 1968. Study on distant tsunamis along the coast of Japan. part 2, tsunamis of South American origin, *Bull. Earthquake Res.*, Inst. Univ. Tokyo, 46: 345-359.

Hatori, T., 1981. Colombia-Peru tsunamis observed along the coast of Japan, 1960-1979, *Bull. Earthquake Res.*, Inst. Univ. Tokyo, 56: 535-546.

Kanamori, H., and K. C. McNally, 1982. Variable rupture mode of the subduction zone along the Ecuador-Colombia Coast, *Bull. Seismol. Soc. Am.*, 72: 1241-1253.

Lay, T., H. Kanamori, and L. Ruff, 1982. The asperity model and the nature of large subduction zone earthquakes, *Earthquake Predict. Res.*, 1: 3-71.

Mendoza, C., and J. Dewey, 1984. Seismicity associated with the great Colombia-Ecuador earthquakes of 1942, 1958, and 1979: Implications for barrier models of earthquake rupture, *Bull. Seismol. Soc. Am.*, 74: 577-593.

Silgado, E., 1985. Destructive earthquakes of South America 1530-1894, 10, Ceresis, Center of Regional Seismology for South America, 315 pp.

SEISMOGENIC SOURCES AND REGIONAL TECTONIC STRESSES IN THE SUBANDEAN ZONE OF MAJOR SEISMIC HAZARD OF ARGENTINA.

Juan C. CASTANO [1] and Mario A. ARAUJO [1]

(1) Instituto Nacional de Prevención Sísmica - INPRES
Roger Balet 47 Norte
5400 - San Juan
Argentina.

RESUMEN: Se analizan las fuentes sismogénicas y su relación con los esfuerzos tectónicos regionales en la zona centro-oeste de la Argentina, desde los 66º W hasta el límite con Chile y desde los 28º S hasta los 33º S, que corresponde al área de mayor peligro sísmico de este país. Es ésta una de las zonas andinas donde la Placa de Nazca subduce en forma horizontal debajo de la Placa Sudamericana. En dicha zona se grafican los mecanismos focales de buena resolución, correspondientes a sismos superficiales modelados con ondas internas, observándose que todos son de tipo compresivo. Tambíen se muestran las fallas activas, predominantemente inversas, así como los principales terremotos históricos asociados a ellas.
Los ejes de presión de los eventos considerados varían su orientación azimutal, entre 65º y 115º, lo que corresponde a un esfuerzo tectónico regional promedio de este-oeste, coincidente con la orientación general del fallamiento.

KEY WORDS: Seismogenic sources, tectonic stresses, focal mechanisms.

INTRODUCTION

The central west part of Argentina is the region with major seismic hazard of this country. Evidences of such hazard are given by historical destructive earthquakes and active faulting. Four historical earthquakes arises over the rest, due to their particular characteristics: (a) the March 20, 1861 earthquake which destroyed the old city of Mendoza, killing 6,000 people over a population of 18,000; (b) the October 27, 1894 earthquake with estimated magnitude Ms $\geq$ 7.5, was felt in an area of more tham three million square kilometers and produced extensive liquefaction; (c) the January 15, 1944 earthquake which produced heavy damage to the city of San Juan, killing 10,000 people over a population of 90,000, and (d) the November 23, 1977 earthquake (Ms = 7,4) that killed 65 people in the small city of Caucete and,as it happen with the 1894 earthquake, produced extensive liquefaction in the same area.

In this region, the main populated centers at risk are the cities of Mendoza and San Juan, with 700,000 and 350,000 inhabitants respectively, and also the cultivated areas and the basic infraestructure, mainly irrigation channels and roads.

Active faults, with observed surface displacements during Holocene time, are present all over the region, some of them bordering or even crossing through the populated areas.

REGIONAL SEISMOTECTONIC SETTING

The region under study is located in a tectonic setting resulting from the ongoing subduction of the Nazca plate eastward beneath the South American plate. This process has created such major structural features as the complex of faulted, folded and uplifted basement rocks called the

Andes and the linear zone of volcanoes occurring within much of the Andes. These features continue to the east with the Precordillera and, finally, the Pampean Ranges .
The major tectonic changes along the east side of the Andes are related to the change in orientation of the subducted Nazca plate as it passes east of the axis of the Andes. It changes dip between 28° S and 33° S to a near horizontal orientation (figure 1), and then rapidly resumes a steep eastward dip. The region overlying the sub- horizontal Nazca plate also demarks a gap in the volcanic chain.

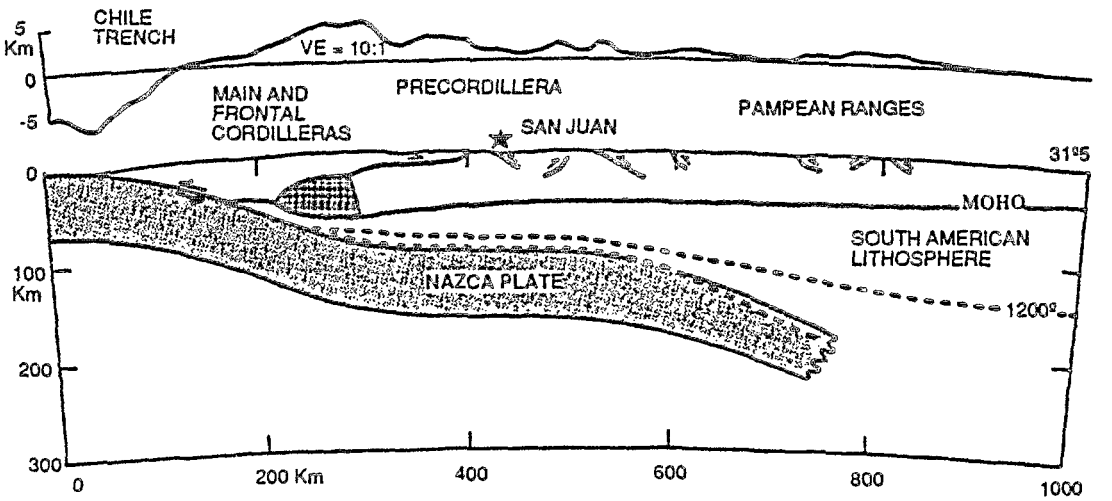

Figure 1: Vertical cross section in the area under study.

In brief, the regional geologic and tectonic setting of this region is characterized by east-west compression. The South American plate is actively deformed along its broad western margin, resulting in active geologic structures, some of which are seismic sources in and around the area under study, mainly thrust faults with generally north-south trending.

SEISMOGENIC SOURCES

Based upon geologic and seismologic studies undertaken in the region, two types of seismogenic sources were identified: (1) active faults and (2) seismic volumes.

Active faults were considered of great importance to this investigacion for two primary reasons: (a) they have been and probably will be sources of damaging earthquakes, and (2) they are potential sources of surface rupture. To study them, the methodology used involved the following steps: literature review, aerial reconnaissance using low sun angle techniques, ground reconnaissance, topographic profiling and trenching. As a result of this study fifteen active faults or fault systems were located and characterized (figure 2), some of them directly related with the historical destructive earthquakes described in the Introduction.

The most important volume of seismic activity affecting this region is the Benioff zone, with an average depth of 100 Km. The April 14, 1927 earthquake, with magnitude Ms = 7.1 and depth H = 110 Km, which produced damages to Mendoza city (Argentina) and Santiago (Chile), is a sample of the potentiality of this seismic source.

FOCAL MECHANISMS

The state of tectonic stresses resulting from the analysis of observables evidences was confirmed by fault plane solutions of the earthquakes which occurred in the region. Eigth seismic events were studied. Only very reliable solutions were considered, which were obtained mainly by modeling body waves of earthquakes with magnitude $m_b \geq 5.3$

These solutions, which are presented in figured 2, show that the pressure axis of all the events have a variable azimuthal orientation betwen 65° and 115°. This result could be interpreted as an average regional tectonic stress regime directed east to west (90°), coinciding with the

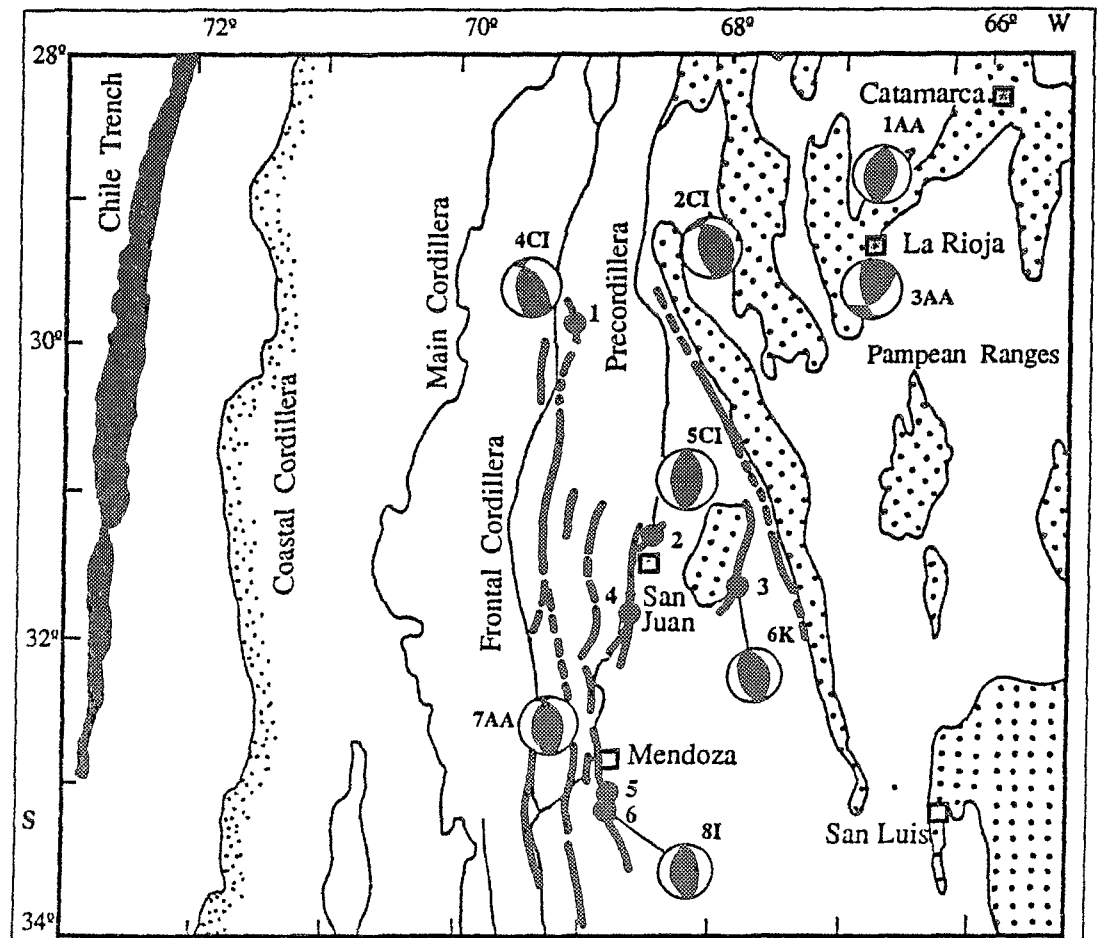

REFERENCES

EARTHQUAKES WITH FOCAL MECHANISM

Number N(i)		Date	Origen Time, UT
1	AA	04-02-83	05 58
2	CI	11-13-65	17 59
3	AA	12-24-79	00 13
4	CI	05-18-63	05 53
5	CI	09-26-72	21 05
6	K	11-23-77	09 26
7	AA	04-25-67	10 36
8	I	01-26-85	03 07

AA : Assumpcào, Araujo; 1993
CI : Chinn, Isacks; 1983
K : Kadinsky-Cade; 1985
I : INPRES, 1985

HISTORICAL EARTHQUAKES

Number N	Date	Magitud Ms
1	10-27-1894	7.5
2	01-15-1944	7.4
3	11-23-1977	7.4
4	06-11-1952	7.0
5	03-20-1861	7.0
6	01-26-1985	6.0

Active Fault

Figure 2: Active faults, historical earthquakes and focal mechanisms.

general orientation of fault movement, with localized deformations from this average in certain areas, due to concentrated local stresses.

CONCLUSIONS

The main characteristics of the clear evidences of active faulting observed in the subandean zone of major seismic hazard of Argentina, agree with the results obtained from the analysis of focal mechanisms of important earthquakes which occurred in the region.

This is in accordance with the tectonic setting of this particular portion of the Andes, where the ongoing subduction of the Nazca plate eastward beneath the South American plate, with near horizontal orientation, gives place to an east-west compression frame, where important intraplate earthquakes occur and where no volcanic activity is present.

REFERENCES

Araujo, M. 1985. Estudio de sismos en el noroeste argentino mediante mecanismo de foco y modelado de ondas de cuerpo. M. Sc. thesis, UNAM, México, D.F., 1-101.

Assumpsào, M. and Araujo, M., 1993. Effect of the Altiplano - Puna Plateau in the regional interplate stresses. Accepted for publication in Tectonophysics.

Castano, J. and Zamarbide, J.L., 1992. A seismic risk reduction program for Mendoza city, Argentina. Proceedings of the XWCEE. Balkema, Rotterdam. 5953-5958.

Castano, J., 1993. La verdadera dimensión del problema sísmico en la provincia de San Juan. Publicación Técnica Nº 18, INPRES, 1- 47.

Chinn, D. and Isacks, B., 1983. Accurate source depths and focal mechanisms of shallow earthquakes in western South America and in the New Hebrides Island Arc. Tectonics, 2, Nº 6, 529.

Kadinsky-Cade, K.,1985. Seismotectonics of the Chile margin and the 1977 Caucete earthquake of western Argentina. Ph. D. thesis, Cornell University. Ithaca, N. Y. , 1-253.

INPRES, 1977. El terremoto de San Juan del 23 de noviembre de 1977. Informe preliminar. INPRES, Argentina, 1-102.

INPRES, 1982. Seismic microzonation of Tulum Valley-San Juan province, Argentina. Executive Summary. INPRES, Argentina, 12 chapters.

INPRES, 1985. El terremoto de Mendoza del 26 de enero de 1985. Informe general. INPRES, Argentina, 1-137.

INPRES, 1989. Seismic microzonation of Gran Mendoza-Argentina. Executive Summary. Inpress, 13 chapters.

Smalley, R. and Isacks, B., 1987. A hight resolution local network study of the Nazca plate Wadati-Benioff zone under western Argentina. J.G.R., 92,13,903.

Zamarbide, J.L. and Castano, J.C., 1993. Analysis of the January 26th, 1985, Mendoza (Argentina) earthquake effects and of their possible correlation with the recorded accelerograms and soil conditions. Tectonophysics, 218, 221-235.

MORPHOLOGY OF THE NORTHERN CHILE SUBDUCTION USING LOCAL DATA

Diana COMTE[1,2] and Gerardo SUAREZ[1]

(1)UACPyP, Instituto de Geofísica, UNAM, Mexico DF, 04510, Mexico
(2)Depto. de Geología y Geofísica, U. de Chile, Casilla 2777, Santiago, Chile

RESUMEN: La subducción en el norte de Chile es analizada con sismos locales obtenidos en dos experimentos realizados en torno a Iquique-1991 (21°S) y Antofagasta-1988 (24°S). La inversión simultánea de hipocentros y estructura permitió obtener modelos bi-dimensionales de la litósfera oceánica, del manto superior y de la corteza continental en ambas regiones. Los mecanismos focales obtenidos permitieron estudiar el contacto sismogénico interplaca y la distribución de esfuerzos intraplaca, que sugiere una zona sísmica doble a 100 km de profundidad con esfuerzos compresionales más profundos que los tensionales.

KEY WORDS: Subduction, northern Chile, seismogenic interplate contact, inverted double seismic zone.

INTRODUCTION

Considering that northern Chile is one of the more active seismic zones of the circum Pacific belt, and that the last great event occurred there at the end of the last century (1877,M_W=8.7), two local microearthquake field experiments were carried out in the northern Chile seismic gap. The first experiment was located in the southern edge of the estimated 1877 rupture zone in 1988 near Antofagasta, and the second one was located in the middle of that rupture zone in 1991, near Iquique (Fig. 1). About 200 reliable microearthquakes were located in each experiment, and they were the data base for the simultaneous 2-D inversion of hypocenters and velocity structure of the oceanic and continental lithosphere, and the upper-mantle in both regions. With the resulting 2D velocity model, the morphology of the subduction was better defined around the Iquique and Antofagasta regions. The analysis of the local event focal mechanisms allows us to study the seismogenic interplate contact zone, and the distribution of stresses in the down-going part of the slab which shows an inverted double seismic zone.

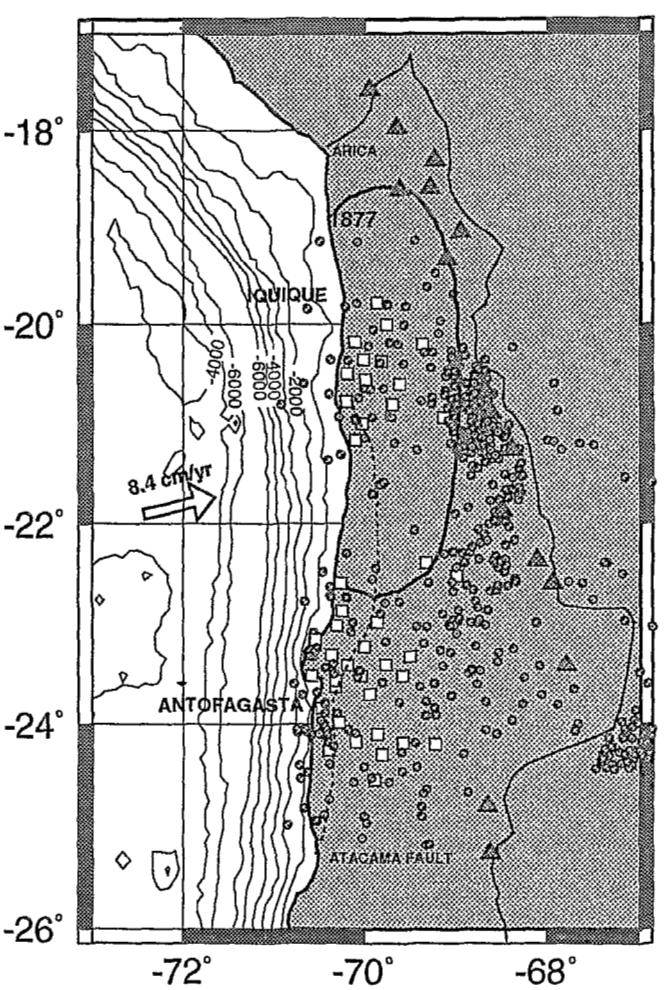

Figure 1.- Distribution of seismic stations (squares) and events (circles). Black triangles represent the active volcanoes. The open-ellipse shows the 1877 estimated rupture area.

TWO-DIMENSIONAL, P-WAVE VELOCITY STRUCTURE

The set of arrival times recorded by the two local microseismic experiments performed in northern Chile are used to simultaneously determine the hypocentral locations and the local seismic velocity structure around the Iquique and Antofagasta regions. A detailed description of the inversion is found in Comte et al. [1993]. The northern Chile margin is parametrized in metablocks, where the size of the blocks is governed by the ability of the data to resolve the structures. The initial velocity models were obtained from the refraction profiles perfomed in northern Chile by Wigger et al. [1991; 1993]. P-wave velocities of the upper-mantle below the continental lithosphere were not well resolved. However, they converged consistently to about 8.4 ± 0.2 km/s in both experiments (Fig. 2). The P-wave velocity of the continental lithospheric metablocks are in good agreement with that determined by the refraction studies. The inversion of the data collected near Iquique shows an average P-wave velocity of 8.1 ± 0.1 km/s within the slab. It was not possible to resolve more details in the oceanic lithosphere near Iquique, mainly because the majority of the events occurred at a depth of about 100 km. Near Antofagasta there is evidence in the slab of subducted oceanic crust with a thickness of approximately 10 km, with a P-wave velocity of 7.4±0.1 km/s, which is observed down to a depth of about 60 km. The subducted oceanic crust overlies an oceanic upper-mantle with a P-wave velocity of 7.8±0.1 km/s. The thickness and the velocity of the subcrustal zone indicates that it is made up of untransformed basaltic oceanic crust subducted with the underlying lithospheric mantle, and that the transformation of basalt to eclogite does not take place in the subducting slab at least down to depths of about 60 km. In the Antofagasta experiment, a low-velocity zone under the continental lithosphere was also observed. This low-velocity zone and the subducted oceanic crust agree with the low-velocity layer observed in seismic refraction studies..

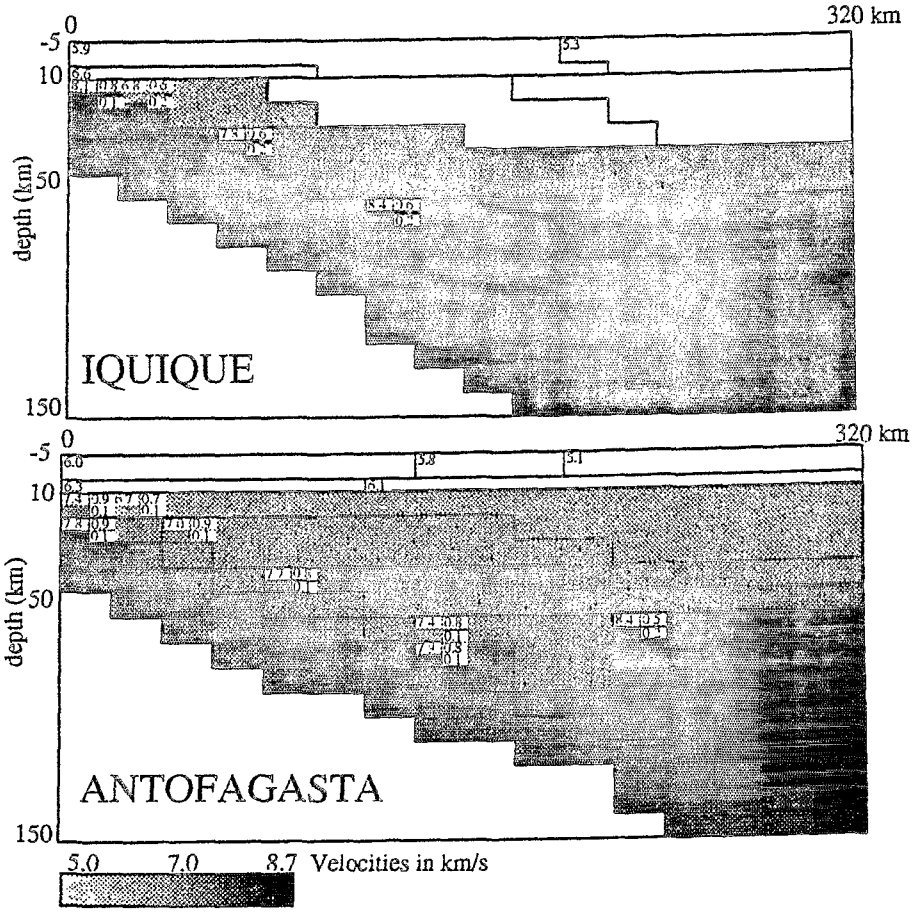

Figure 2.- 2D P-wave velocity model obtained for Iquique and Antofagasta. The first two layers were not included in the inversion. The white metablocks are unresolved by the inversion. In the left-upper corner of each metablock, the velocity (km/s), the resolution and the values error in km/s (below the resolution) are presented. In Antofagasta a low-velocity layer in the upper part of the slab is interpreted as oceanic crust.

SEISMOGENIC INTERPLATE CONTACT

The seismically coupled zone is the depth range of the plate interface that is capable of producing large underthrusting earthquakes [Tichelaar and Ruff, 1991]. However, the determination of that depth is difficult in northern Chile because of the lack of geodetic measures of coseismic ruptures. Tichelaar and Ruff [1991] studied the Chilean subduction zone using thrust earthquakes with magnitudes greater than 6.0 recorded teleseismically. Comte and Suárez [1993] discuss the difficulties involved in measuring the depth of the seismogenic interplate contact, and the different values obtained from teleseismic recording earthquakes in comparison with those obtained with locally-recorded data using permanent and temporary networks in Chile. We observed that the depth of the seismogenic coupling extends to approximately 50 km along northern and central Chile without showing appreciable variations along strike, and the landward extent of the coupled zone has a width of about 40 to 60 km. There is also a change from high-angle reverse faulting to down-dip tensional events. This could be an alternative method to determine the maximum depth of the seismogenic coupling. The mechanical idea is that near and below the interplate surface, where unstable sliding occurs, the subducted slab is under compression. The compressive regime causes not only thrusting along the plate interface, but also intraplate, reverse faulting events within the slab. At a certain depth, the slab becomes completely decoupled from the upper plate and begins to sink due to its negative bouyancy. Thus, the transition from compressive to tensional behavior would reflect the mechanical conditions in the shallow part of the subducted slab and may help to map indirectly the depth of the seismogenic coupling. In the three regions, where a good local data exists to control this change, Iquique, Antofagasta and central Chile, this transitional depth lies consistently at a depth of about 70 km.

AN INVERTED DOUBLE SEISMIC ZONE IN NORTHERN CHILE

The epicentral distribution of the seismicity observed in Iquique during 1991 is similar to that observed in Antofagasta in 1988, in the sense that the seismic activity is mainly concentrated to the east, in the downgoing slab. A nucleation of intraplate events is observed in both experiments at about 100 km depth, the focal mechanisms of the nucleations show that these intraplate events present a variety of tensional and reverse faulting events. The down-dip tensional events are shallower than the compressional micro-earthquakes, suggesting a double-planed seismic zone in northern Chile (Fig. 3).

The Iquique intraplate nucleation shows that the tensional events ranges from 88 to 108 km depth, and the compressional events show depths varying from 106 to 126 km. In the case of Antofagasta, the tensional events have depths from 80 to 108 km, and the compressional ones are located between 104 to 122 km depths. The error in depth for these events is estimated to be about 3 km for both experiments, therefore, instead of the two sheets of tensional and compressional events are very close in depth, the lower errors obtained from 2-D velocity model resulting from the inversion, permits us to conclude that there is a double seismic zone in northern Chile with the polarity inverted relative to that observed in other subduction zones in the world, such as those found in the Aleutians, Tonga and Honshu.

The only intermediate-depth earthquakes reported teleseismically which shows a compressional mechanism in northern Chile, is the reverse faulting earthquake occurred on January 17, 1977 [Araujo and Suárez, 1993]. The focal depth of this event is 152 km, and clearly is located beneath the sheet of tensional events which lie at an average depth of 110 km. Kono et al. [1985] also identified this earthquake as an intermediate-depth event and suggested the presence of a double seismic zone. However, due to their lack of good hypocentral depth control, they incorrectly assumed that the sheet of down-dip tensional events was beneath this reverse-faulting earthquake as in other subduction zones of the western Pacific.

Engdahl and Scholtz [1977] explained the presence of double-planed seismic zones as a result from the flexure suffered by the subducted slab as it unbends beneath the shallow interplate contact. This hypothesis does not explain our observations because the polarity of the expected stress sheets would be opposite to what is observed in northern Chile. Araujo and Suárez [1993] suggested that the presence of this anomalous double-planed seismic zone is the result of the sudden downward flexure of the slab where a drastic change in the radius of curvature of the downgoing plate occurs. However, we observed the double seismic zone in northern Chile in two regions with different dipping. The dip angle observed around Iquique is about 30°, and around Antofagasta is about 20°, therefore the northern Chile double-seismic zone probably is not controlled by the geometry of the slab.

The question arises: Why is there an inverted double seismic zone in northern Chile, and why it is mainly observed with local data? The double seismic zone in northern Chile is observed beneath the volcanic Andean belt in the Iquique and Antofagasta regions. Therefore, it is probably associated with the process involved with the generation of magmas and the production of arc volcanos. Recently, Kirby and Hacker [1993] present new evidence suggesting a phenomenon associated with the earthquakes that occur at depth of 90-150 km in the subducting lithosphere. In summary, they argue that the oceanic plates has a laminated

structure, with a thin crust on the top composed by basaltic minerals, and a thicker mantle of peridotite minerals beneath. The subducting crust is densified to eclogite due to the pressurization during the plate descent. However, the peridotite in the upper mantle does not change because it is stable to greater pressures. Their numerical results suggest that this volume change produces a surface stretching deformation in the transformed crustal layer and a smaller compressional deformation near the top of the underlying mantle. This explain apparently the inverted double seismic zone observed in northern Chile, and also the fact that it is observed mainly with events of smaller magnitude.

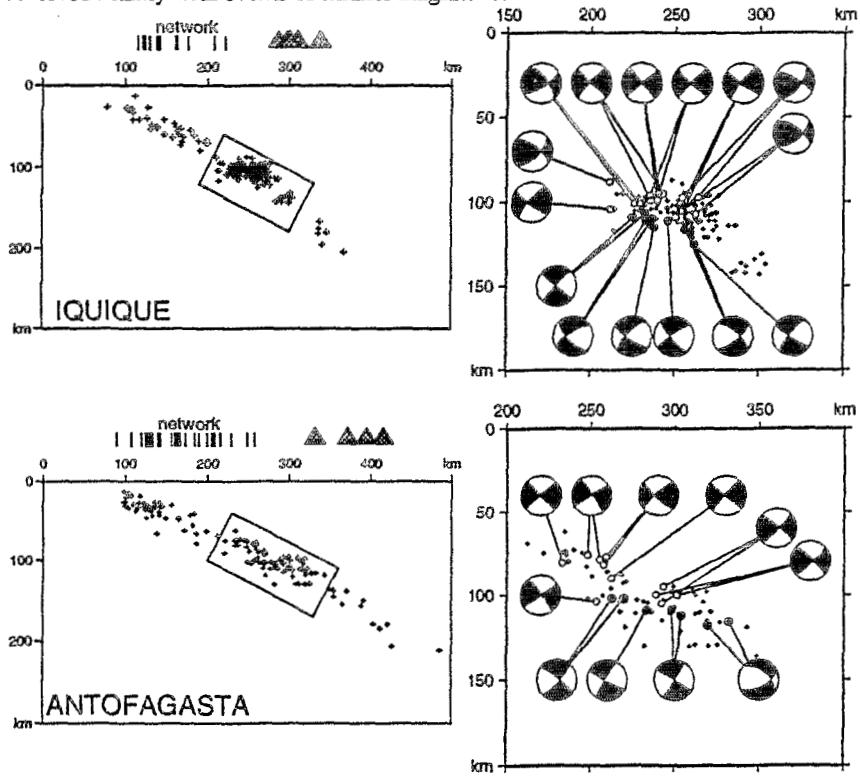

Figure 3.- Cross-sections along the N77°E directions in Iquique and Antofagasta regions. The focal mechanisms solutions of the events that are within the boxes are projected on a side-looking, lower hemispheric projection where dark quadrants indicate compression and the white ones dilations.

REFERENCES

Araujo, M. and G. Suárez. Detailed geometry and state of stress of the subducted Nazca plate beneath central Chile and Argentina: Evidence from teleseismic focal depth determinations. Accepted in *Geophys. J. Int.*

Comte, D., G. Suárez and S. Roecker. Two-dimensional P-wave velocity structure of the subducting Nazca plate in northern Chile using locally recorded earthquakes. Submitted to *Geophys. J. Int.*

Engdahl, E. R. and C. H. Scholtz. A double Benioff zone beneath the central Aleutians and unbending of the lithosphere. *Geophys. Res. Lett.*, **4**, 473-476, 1977.

Kirby, S. and B. Hacker. Earthquakes at the deep roots of arc volcanos. *EOS*, **76**, 70.1993

Kono, M., Y. Takahasho and Y. Fukao. Earthquakes in the subducting slab beneath northern Chile?. *Tectonophys.*, **112**, 211-225, 1985.

Suárez, G. and D. Comte. Comment on "Seismic coupling along the Chilean subduction zone" by B. W. Tichelaar and L. R. Ruff. *J. Geophys. Res.*, 1993. in press.

Tichelaar, B. W. and L. R. Ruff. Seismic coupling along the Chilean subduction zone. *J. Geophys. Res.*, **96**, 11,997-12,022, 1991.

Wigger, P., M. Araneda, G. Ash, P. Giese, W. Heinsohn, P. Rower, M. Scmitz and J. Viramonte. The crustal structure along the central Andean transect derived from seismic refraction investigations. *AGU*, 13-19, 1991.

Wigger, P., M. Scmitz, M. Araneda, G. Ash, S. Baldzuhn, P. Giese, W. Heinsohn, E. Martinez, E. Ricaldi, P. Rower, and J. Viramonte. Variaton of the crustal structure of the southern central Andes deduced from seismic refraction investigations. In Tectonics of southern central Andes. In prep., 1993.

THE ANDEAN SUBDUCTION ZONE BETWEEN 22°S AND 25°S (NORTHERN CHILE): PRECISE GEOMETRY AND STATE OF STRESS

Bertrand DELOUIS[(1)], Armando CISTERNAS[(1)], Louis DORBATH[(1)(2)]
Luis RIVERA[(1)] and Edgar KAUSEL[(3)]

(1) Institut de Physique du Globe, 5 rue René Descartes, 67084 Strasbourg Cedex, France
(2) ORSTOM, 213 rue Lafayette, 75480 Paris Cedex 10, France.
(3) Dpto de Geologia y Geofisica, Universidad de Chile, Casilla 2777 Santiago, Chile

RESUME : Un an d'enregistrement microsismique au Nord-Chili a permis de mieux préciser la géométrie de la subduction andine entre 22°S et 25°S et d' analyser l'évolution du régime de contraintes à profondeur superficielle et intermédiaire. L'interface entre les deux plaques en contact est sismiquement couplé jusqu'à la profondeur de 50 km. La relation entre cette profondeur critique et le champ de contraintes est discutée.

KEY WORDS : Subduction geometry, Stress field, Faulting, Seismic coupling.

INTRODUCTION

A permanent telemetric seismological network has been installed in june 1990 in the surrounding of the Antofagasta city and the Mejillones peninsula (northern Chile), in the geografical place of what can be considered the southern end of the great 1877 earthquake rupture zone. The operating of the network gives the opportunity to improve the knowledge of the present state of the subduction zone and to study the temporal evolution of the seismic activity in the area where the rupture of a great earthquake may initiate in the near future. The present work describes results obtained from the analysis of about one year (june 1990 - august 1991) of locally recorded microseismicity. As a first objective, more precision about the geometry of the Wadati-Benioff Zone is looked for. Then, the characteristics of the stress field and its variations along the subducting slab are investigated. Special attention is given to the caracterisation of the transition between underthrusting at the plate interface and the deeper intra-slab faulting.

METHOD AND DATA PROCESSING

The hypocenters are located with the HYPOINVERSE program (Klein, 1978). The crustal velocity structure is represented by a model of flat homogeneous layers based on seismic refraction profiles (Schmitz, 1991). The average crustal velocity for P wave is 6.6 km/s and the depth of the Moho is set to 48 km. The mantle velocity is taken to be 7.9 km/s. Travel times are corrected for the elevation of the stations. The Vp/Vs ratio was determinated from Wadati plots. So as to minimize the effect of dependance of the final hypocentral solution with the initial (trial) solution, each earthquake is localised with different trial depths. Trial depth is varied from 1 to 280 km with a 10 km increment. We retain as the "best" solution the one combining low RMS and the higher possible number of P and S arrivals taken into account. In order to avoid bad quality and poorly constrained hypocenters we submitted the hypocentral determinations to a sorting based on the following criteria: RMS inferior or equal to 0.25, total number time arrivals (P and S) taken into account greater or equal to 7, number of S-phases superior or equal to 2, computed horizontal and vertical errors inferior or equal to 5 km. Using the selection criteria indicated above, and restricting the latitude to the 22°20'S to 24°40'S interval, we obtained 412 hypocenters over the period june 1990 - august 1991. We present the distribution of the epicenters in Figure 1 and an EW cross-section in Figure 2.

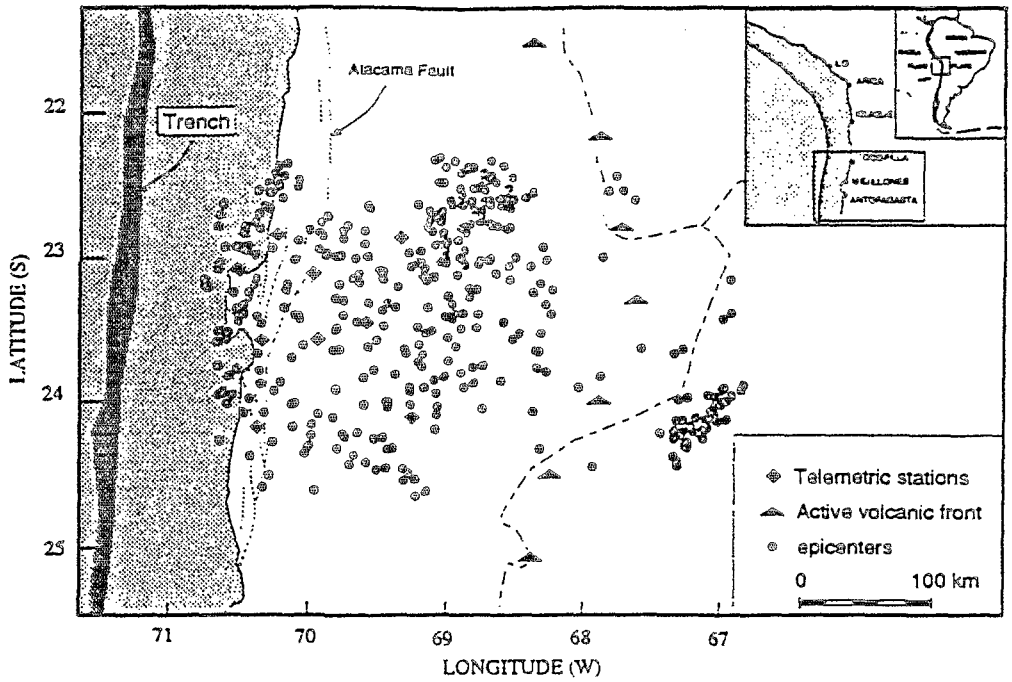

Figure 1. Epicentral map of the 412 selected earthquakes locally recorded during the period june 1990 - august 1991. The selection criteria is detailed in the text.

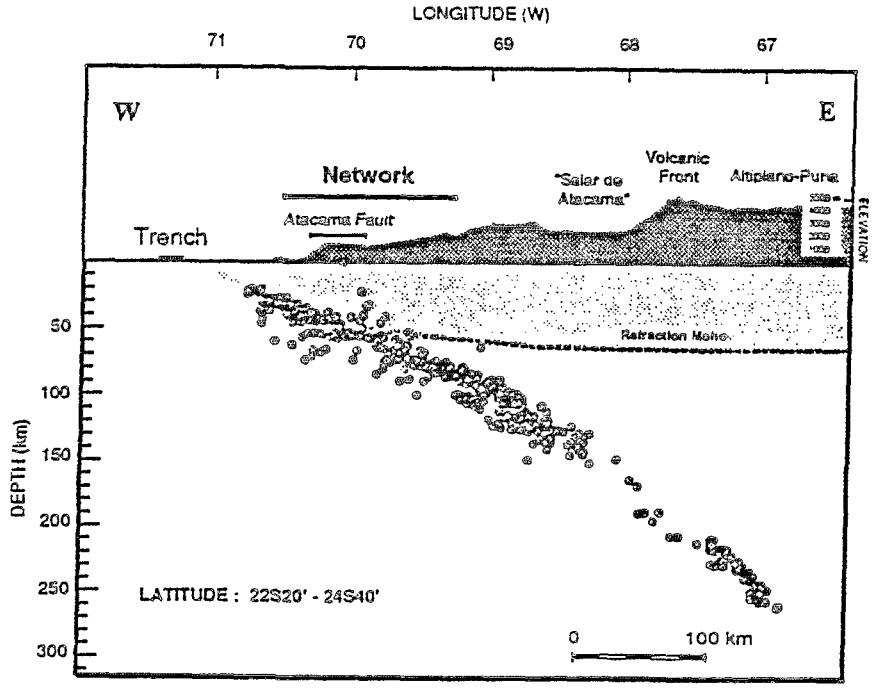

Figure 2. E-W cross section showing the hypocentral location of the 412 selected earthquakes locally recorded. The topografic profil in dark gray is taken at latitude 23°S15'. The refraction Moho is from Schmitz (interpreted seismic profil at latitude 24°S15', 1991). The shaded area above the Moho (light gray) and its prolongation towards the trench represent the continental crust.

In order to specify the stress field and the geometrical characteristics of the faulting along the subducted slab, we used an algorithm which provides simultaneous inversion of the orientation and shape of the stress tensor and of individual focal mechanisms for a population of earthquakes (Rivera and Cisternas, 1990). The method assumes that the stress tensor is locally homogeneous over the area of study. The avantage of the method is that we obtain the stress tensor not from previously and individually determined focal mechanisms which contain a certain degree of arbitrary choice, but rather from the original data of first motion polarities. The best way to detect variations in the stress regime in the Wadati-Benioff Zone is to define a sliding window along the slab. We limited our investigation to the upper part of the slab (longitude>69°, depth<100 km). Deeper earthquakes are too distant from the local network to permit a good enough constrain of their focal mechanisms. So as to rely on the most trustworthy data, we tested the stability of the hypocentral locations and the focal mechanisms with different velocity models.

RESULTS

Almost all earthquakes are located along a narrow tongue of concentrated sismicity related to the subduction of the Nazca plate, i.e. defining a sharp Wadati-Benioff Zone (WBZ, see Figure 2). The upper limit of the WBZ is particulary well defined. The WBZ dips with an angle of 17°-18° up to about 100 km depth. The deeper part of the slab dips more steeply but we observe a systematic displacement of our hypocenters in the downward-westward direction relative to the world wide recorded teleseismic events below 100 km depth (Cahill and Isacks, 1992). Lareral heterogeneities, in particular the slab/mantle velocity contrast, not taken into account in the velocity model, may explain such discrepancy (McLaren and Frohlich, 1985). A seismically quasi-quiescent zone is observed below 150 km depth, under the volcanic arc. Deeper events occur mainly in a clustered form at 200-260 km depth. Synthetics tests proved that the quiescent zone cannot be an artificial gap produced by the location process and that the sharp definition of the deep cluster is not an artificial concentration of hypocenters. The intermediate depth quiescent zone is a characteristic feature of the WBZ along southern Peru and northern Chile. A strong concentration of intra-slab seismicity is generally observed updip of the quiescent zone and is possibly related to the effective deshydratation of the oceanic crust and to the phase transformation from basalt to eclogite. Those mechanims are supposed to activate faulting (Liu, 1983; Haak and Giese, 1986). The onset of the quiescent zone may correspond to the limit beyond which those mechanisms end, and/or may be related to the proximity of the asthenospheric wedge below the volcanic front.

The inversion of the stress tensor and the focal mechanisms for different depth range along the WBZ give very coherent results. From 20 km to 50 km depth we observe only underthrusting earthquakes with a north-south nodal plane dipping sligthly towards the East (Figure 3). Although the rupture and the seismic moment release of great interplate earthquakes may extend further down, those underthrusting microearthquakes indicate that the seismogenic part of the interface ends at 50 km depth. Downdip, intra-slab normal faulting prevails. Normal faulting, rather heterogeneous first, becomes very homogeneous at about 80-100 km depth (Figure 3). It is then characterized by a vertical or east steep dipping nodal plane of NNW to NW orientation.

Over the full range of depth investigated (20-100 km) the stress field is characterized by a minimum principal stress σ_3 oriented in the mean azimut 070°. The intermediate principal stress σ_2 is horizontal and strikes in the azimut 335°. Below 50 km depth, where normal faulting plus a few strike-slip faulting occur (Figure 3), the stress regime is extensional and σ_3, which is low dipping, can be related to the slab pull force. Above 50 km depth, where underthrusting occur, the dip angle of σ_3 is loosely constrained and may vary from 35° to 70°. Underthrusting focal mechanisms can be so well explained by a σ_3 low dipping or by a σ_3 steep dipping. Two different scheme may be proposed as possible interpretations for the evolution of the stress regime along the WBZ, depending on the dip angle of σ_3 in the underthrusting zone.

If σ_3 is steep dipping (70°), then σ_1 dips only slightly (20°) in the azimut 255°. Then, the stress regime is compressional at the locked plate interface, as it is generally assumed, and the compression expresses the convergence between the two plates (azimut 075° or 255°). In that case, the stress field would invert abruptly at the depth of 50 km.

Conversely, if σ_3 has a much greater horizontal component, dipping only 35° in the azimut 075°, we have an alternative scheme in which the slab pull force acts also at superficial depth in the locked segment of the slab, beeing possibly the dominant force there. This alternative is supported by the occurrence of tensional earthquakes beneath the underthrusting interface (Malgrange and Madariaga, 1983, Comte et al., 1992, NEIC). In the present study, one tensional event has been located 100 km east of the trench, 15-20 km beneath the coupled interface. Thus, the transition between interplate underthrusung and intraplate normal faulting would not necessarily suppose a drastic change in the stress regime, but would essentially reflect the change in the mechanical behaviour of the interface which would undergo a unstable-stable slip transition

Some deep crustal seismic activity (20-50 km depth, see Figure 2) is observed locally at the deep root of the Atacama Fault. The pertubation of the thermal structure of the lower continental crust related to the proximity of the cold slab could explain the occurrence of seismic rupture at such depth.

The lower limit of the coupled-seismogenic part of the plate interface has been located precisely at 50 km depth. The transition from underthrusting at the plate interface and intra-plate normal faulting takes place over a very short distance along the slab. Strike-slip faulting occurs in between (Figure 3), immediately downdip of the coupled zone and may indicate that the slab, once unlocked from the overriding plate, undergoes some left lateral motion in response to the obliquity of the convergence. The coupled-uncoupled transition occurs approximatively at the depth where the WBZ and the Moho seem to diverge (Figure 3), suggering that a relation exists between seismic-coupling and the presence of continental crust at the plate interface.

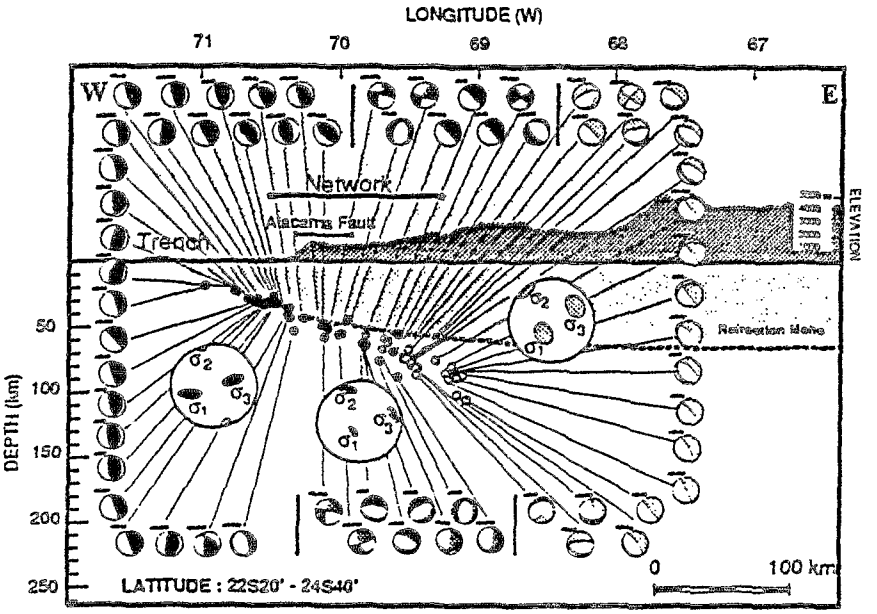

Figure 3. Focal mechanisms and the stress field along the Wadati-Benioff Zone (WBZ) up to 100 km depth. The WBZ has been divided into three consecutive segments corresponding to different depth ranges (dark gray, medium gray and light gray). In each segment the focal mechanisms and the stress tensor have been inverted from the first motion polarities using the Rivera-Cisternas algorithm (1990). Focal mechanisms are represented on the lower hemisphere equal area projection and the shaded areas are the compressional quadrants.

REFERENCES

Cahill T. and Isacks B. L., 1992 - Seismicity and shape of the subducted Nazca plate. - *J. Geophys. Res.*, 97, 17503-17529.

Comte D., Pardo M., Dorbath L., Dorbath C., Haessler H., Rivera L., Cisternas A. and Ponce L., 1992. - Seismogenic interplate contact zone and crustal seismicity around Antofagasta, northern Chile, using local data. - *submitted.*

Haak V. and Giese P., 1986. - Subduction induced petrological processes as inferred from magnetotelluric, seismological and seismic observations in N-Chile and S-Bolivia. - *Berliner Geowiss. Abh.*, (A), 66, 231-246; Berlin.

Klein F. W., 1978. - Hypocenter location program HYPOINVERSE, *U.S. Geol. Surv., Open File Rep.*, 78-694.

Liu L-g, 1983. - Phase transformations, earthquakes and the descending lithosphere. - Phys. Earth Plan. Int., 32, 226-240.

Malgrange M. and Madariaga R., 1983. - Complex distribution of large thrust and normal fault earthquakes in the chilean subduction zone. - *Geophys. J. R. Astr. Soc.*, 73, 489-505.

McLaren J.P. and Frohlich C., 1985. - Model calculations of regional network locations for earthquakes in subduction zones. - *Bull. Seismol. Soc. Am.*, 75(2), 397-413.

Rivera L. and Cisternas A., 1990. - Stress tensor and fault plane solutions for a population of earthquakes. - *Bull. Seismol. Soc. Am.*, 80(3), 600-614.

Schmitz M., 1991. - *Pers. comm.*

CENOZOIC KINEMATICS OF THE ANDES - STRAIN PARTITIONING AND DISPLACEMENT

J.F. Dewey and S.H. Lamb

Department of Earth Sciences, University of Oxford, Parks Road, Oxford OX1 3PR, UK

KEY WORDS: slip vector, strain, displacement, rotation, partitioning

A particular problem of contractional continental plate boundary zones is the way in which the rate and direction of slip between adjacent plates is converted into strain, displacement and rotation within the zone. Few continental plate boundary zones experience purely orthogonal shortening; most have a substantial strike-parallel displacement component leading to transpression within the zone. The oblique plate slip vector causing transpression may be decomposed into an orthogonal coaxial contractional component and a strike-parallel non-coaxial single shear component. How these components are expressed, in space and time, in continental plate boundary zones determines the structure style of the zone. The two possible end members are complete partitioning into a single thrust and a single strike-slip fault versus homogeneous oblique penetrative incremental and finite shortening parallel into the plate convergence vector. We know of no plate boundary zone in which either of these end members is perfectly achieved; most obliquely convergent zones exhibit partitioning into orthogonal, strike slip and plate slip vector parallel components of strain and displacement from the regional to the outcrop scale.

In the Andean plate boundary zone, approximately 90 mma^{-1} of plate convergence is absorbed. The pattern of active tectonics shows great variation in the way in which the plate slip vector is partitioned into displacement and strain and the ways in which compatibility between and within different segments is solved. Along any Andean traverse, the sum of relative velocities between points must equal the relative plate motion. We have developed a kinematic synthesis of displacement and strain partitioning in the Andes from 47°S to 5°N relevant for the last 5 ma based upon: 1) relative plate motion deduced from oceanic circuits giving a roughly constant azimuth between 075 and 080; 2) moment tensor solutions for over 120 crustal earthquakes since 1960; 3) structural studies of deformed Plio-Pleistocene rocks; 4) topographic/geomorphic studies; 5) palaeomagnetic data and 6) geodetic data. We recognize four neotectonic zones, with subzones and boundary transfer zones, that are partitioned in different ways. These zones are not coincident with the 'classic' zones defined by the presence or absence of a volcanic chain or differences in finite displacements and strains and tectonic form; the long term segmentation and finite evolution of the Andes may not occur in constantly-defined segments in space and time. In segment 1 (47° - 39°S), the slip vector is partitioned into roughly orthogonal Benioff Zone slip with large magnitude/large-slip-surface earthquakes and both distributed dextral shear giving clockwise rotations of up to 50° and dextral slip in the curved Liquine-Ofqui Fault System giving 5° - 10° of anticlockwise forearc rotation. In segment 2 (39° - 20°S), the slip vector is partitioned into Benioff Zone slip roughly parallel with the slip vector, Andean crustal shortening and a very small component of dextral slip. Between 39° and 34°S, a cross-strike dextral transfer, which deflects the Chile Trench and the volcanic arc, absorbs the shortening contrast between segments 1 and 2. In segment 3 (20° - 6°S), the slip vector is partitioned into roughly orthogonal Benioff Zone slip, crustal shortening trench-parallel faulting and NE-SW extension. Compatibility between segments 2 and 3 is maintained by the sinistral ESE-trending Cochabamba shear zone and N-trending dextral faults. In segment 4 (6°S to 5°N), the slip vector is partitioned into roughly orthogonal Benioff Zone slip and dextral strike-slip faulting in the fore-arc and volcanic chain.

NEOTECTONIC OF SUBANDES/BRAZILIAN CRATON BOUNDARIES: DATA FROM THE MARAÑON AND BENI BASINS

Jean François DUMONT[1]

(1) ORSTOM and URA D.1369 CNRS, LGDI, Bt 509, Univ. Paris Sud, 91405, ORSAY,. France.

RESUME: L'étude néotectonique des deux bassins de l'avant pays andin montre que la partie distale (coté craton) est déformée par la réactivation des structures du soubassement, alors que la partie proximale subit l'influence des structures andines. On en conclut à la priorité des structures anciennes réactivées sur les structures subandines nouvelles, et à une explication aux anomalies de direction de contrainte observées à la limite entre craton et zone subandine au nord du Pérou.

KEY WORDS: Neotectonics, Subsidence, Foreland basins, Subandes, Peru, Bolivia.

INTRODUCTION

The neotectonic relations between the Andes and the Brazilian craton are poorly documented. The usual model emphasized the subsidence of the foreland basins, which is only true in the case of very large areas and long periods of time. At the scale of the Andean range, the geometry of the subducted oceanic slab is related to the location of subsiding basins over normal Beniof zones, and non-subsiding forelands over flat slab segments (Jordan *et al.* 1983). At a regional scale, subduction in foredeep depends, on the andean side, on the structure of the foothills Piedmont, and on the craton side on reactivated structures in the basement of the basin. The aim of the paper is to focus on the last points, using data from the two main subsiding basins of the Andes, the Marañón basin at the north and the Beni Basin at the South.

GEOLOGICAL SETTING AND STUDY METHODS

The Subandean basins constitute a transition zone between the Brazilian shield to the east and the Subandean Thrust and Fold Belt (Mégard 1984) to the west. They are characterized by extensive floodplains with highly unstable large rivers (Marañón, Ucayali, Beni and Mamore rivers). Neotectonics is studied using geomorphology of the fluvial network, successive shifting of rivers and asymmetrical patterns (Dumont, in press,b), as well as geometric pattern of lakes (Dumont, in press,a). When available, data from surface landforms are combined with structural data from the basement (Laurent and Pardo 1975; Laurent 1985; Sempere 1990) and neotectonic and sismotectonic data from the surrounding regions (Assumpçáo and Suarez 1988; Assumpçáo 1992).

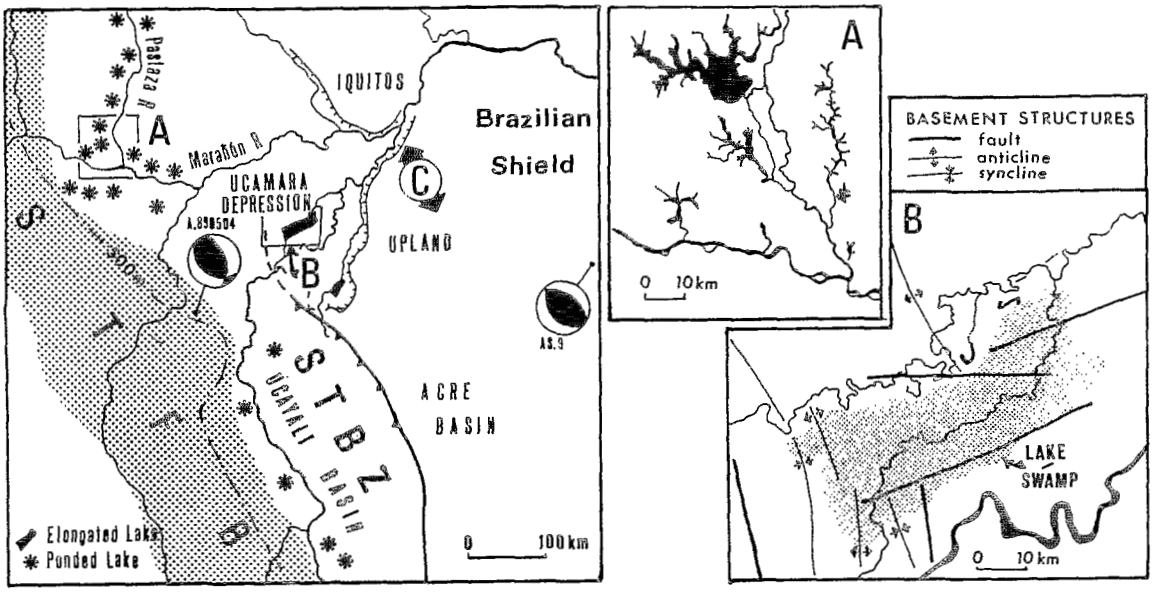

Fig.1. Left: Structural scheme of Peruvian subandes and Brazilian craton border. Right: A: ria lakes; B: elongated lakes. See location on the left figure.

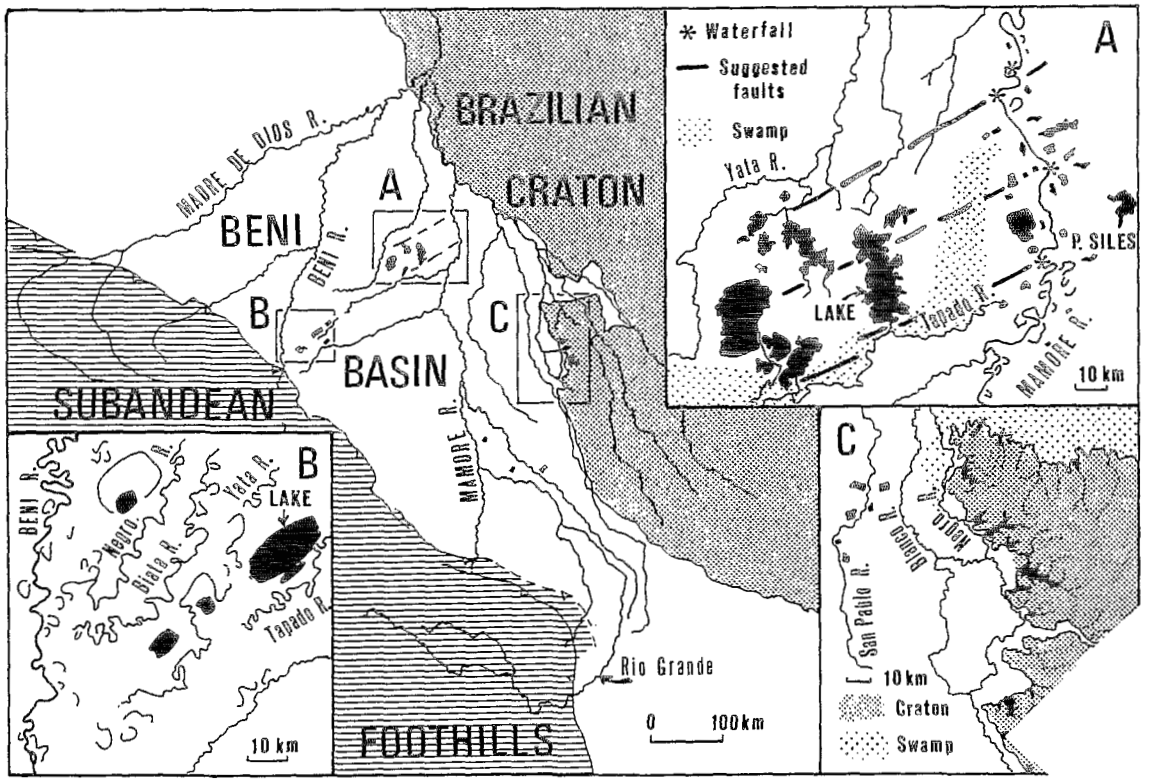

Fig.2. Center: Structural scheme of the Beni Basin and borders, from Sempere (1990), simplified and complemented. A: ria lakes (tilted); B: rectangular lakes; C: ria lakes.

THE MARAÑON BASIN

The basin extends over about 375 km WE and 475 km NW-SE. It comprises two parts (Fig.1): the North-trending Pastaza Depression to the north (Laurent and Pardo, 1975) and the triangle shaped Ucayali-Marañón (shortly Ucamara) Depression to the south. Clusters of ria lakes in the lower Pastaza and west Marañón Basin (Fig. 1,A), (Dumont, in press,a) near the foothills border fit with the structural axis of the basin (Sanz 1974; Laurent and Pardo 1975). In the Ucamara Depression we observe NE trending elongated lakes (Dumont, in press,a), which are parallel with the successive positions of the Ucayali River (Dumont, in press,b). This direction is related to the "en échelon" system of the Marañón Fault Zone, reported for the late Paleozoic by Laurent (1985). The main direction of the lakes is interpreted as the surface expression of tension stress, superimposed over reactivated basement structures (Fig. 1,B), (Dumont and Garcia 1991, Dumont, in press,a). This is compatible with faults observed in the Quaternary deposits of the craton border (Fig.1C; Dumont *et al.* 1988). This direction is parallel to P-axis orientation of focal mechanisms observed on both sides of the depression (stereograms on fig. 1, from: Assumpçáo 1992, and: Assumpçáo and Suarez 1988). P-axis orientation in, and around the depression is about 40 degrees away from the usual (WE) P-axis orientation at the Subandes-Craton border (Assumpçáo 1992).

THE BENI BASIN

The Beni Basin is the southern drainage area from the Andean-Amazonian fluvial network. The flat lowlands are about 800 km NS, broader to the north (500 km) than to the south (150 km) (Fig. 2), which fronts the apex of the Bolivian orocline (Sempere 1990).

The Northwestern part of the basin is characterized by the extensive floodplain of the Beni River. The western part of the floodplain, close to the Piedmont of the foothills, expresses active subsidence, evidenced by the flooding of forested areas (Dumont *et al.* 1991,b), and the formation of large lakes of black water, invaded by sedimentary deltas from the silty white water of the Beni River.

River shifting is obvious in several parts of the basin. In the central part, successive stages of river shifting of the Beni River (Tapado, Yata, Biata and Negro rivers) are evidenced by underfit rivers. This shows a counterclockwise displacement of the Beni River from a Northeast trend up to the present Northern direction (Fig. 2,B). The shifting of the Rio Grande towards the west (counter clockwise) may be correlated to that of the Beni River. Numerous ria lakes on the craton border (Fig.2,C) characterize the former floodplain aggradation of the Rio Grande River in this area. Similar trends of river shifting all over the basin possibly resulted due to the onset of a thrusting event along the subandean border of the Beni basin.

The eastern part of the Beni Basin is characterized by a basement structure control (Allenby 1988). There, the present Beni River valley appears to be structurally controlled (Dumont *et al.* 1991,b). North of Puerto Siles (Fig.2,A), a cluster of more or less rounded ria lakes occurs far away from the influence of sediment charged rivers. The Mamore River has a reduced sinuosity across the cluster area, along reaches limited by rapids. This is interpreted as changes of the slope induced by neotectonic deformations (Schumm 1986). Outcrops of hard rocks generating the rapids suggest the effect of block tectonics (Allenby 1988), and tilting, which has resulted in a flooded topography and ria lakes.

CONCLUSION

Distal, or craton side, areas of foreland basins are characterized by block tectonics which generate subsidence (Ucamara Depression), tilting or uplift (Beni Basin) along

reactivated basement structures. Most of these structures are rapported to faults of pre-cretaceous age. On the other side, regional subsidence occurs in the proximal areas of the basin, in front of the foothills Piedmont.

It is suggested here that reactivated basement structures may explain the local deviation of sismotectonic constraints at the basin-craton boundaries.

Differences in the style of neotectonics between the proximal and distal parts of foreland basins suggest that in a specific region the reactivation of old basement structures predate the onset of Andean structures. This conclusion may help to understand how the reactivated basement structures may influence the development of Andean foreland structures, and specially the observed anomalies.

REFERENCES

ALLENBY, R.J., 1988. Origin of rectangular and aligned lakes in the Beni Basin of Bolivia. *Tectonophysics*, 145:1-20.

ASSUMPÇAO, M., 1992. The regional intraplate stress field in South America. *J.G.R.*,Vol.97,N.B8,11889-11903.

ASSUMPÇAO, M. and SUAREZ, G., 1988. Source mechanisms of moderate size earthquakes and stress orientation in mid-plate South America. *Geophysical Journal*, v.92, p.253-267.

DUMONT,J.F., (in press,a). Lake patterns as related to neotectonics in subsiding basins: the example of the Ucamara Depression, Peru. *Tectonophysics*.

DUMONT, J.F., (in press,b). The Upper Amazon Rivers. in: Engineering Problems Associated with the Natural Variability of Large Alluvial Rivers, Schumm and Winkley ed., *Pub. of the Americain Society of Civil Engineers*.

DUMONT,J.F., LAMOTTE,S. and FOURNIER,M., 1988. Neotectonica del Arco de Iquitos (Jenaro Herrera, Perú). *Bol. Soc. Geol. del Perú*, 77: 7-17.

DUMONT,J.F., and GARCIA, F.,1991. Active subsidence controlled by basement structures in the Maráñón Basin of northeastern Peru. Land Subsidence, Proceeding of the Fourth International Symposium on Land Subsidence, *International Association of Hydrological Sciences*, N.200, p.343-350.

DUMONT, J. F., DEZA, E. and GARCIA, F., 1991,a. Morphostructural provinces and neotectonics in Amazonian lowlands of Peru. *Journal of South American Earth Sciences* v.4, N.4, p.287-295.

DUMONT,J.F., HERAIL,G. and GUYOT,J.L., 1991,b. Subsidencia, inestabilidad fluvial y reparticiones de los placeres distales de oro. El caso del Rio Beni (Bolivia). *Symp. Int. sur les Gis. Al. d'or*, La Paz. abstract 43-46.

JORDAN,T.E., ISACHS,B.L., ALLMENDINGER,R.W., BREWER,J.A., RAMOS, V.A., and ANDO,C.J., 1983. Andean tectonic related to geometry of subducted Nazca plate. *Geol. Soc. America Bulletin*, v.94:341-361.

LAURENT, H., 1985. El pre-Cretáceo en el Oriente peruano, su distribución y sus rasgos estructurales. *Boletín de la Sociedad Geológica del Perú*, v.74, p.33-59.

LAURENT, H., and PARDO, A., 1975. Ensayo de interpretación del basamento del Nororiente Peruano. *Boletín de la Sociedad Geológica del Perú*, v.45, p.25-48.

MEGARD, F., 1984. The Andean orogenic period and its major structures in central and northern Peru. *J. Geol. Soc. London*, vol. 141: 893-900.

SANZ,V.P., 1974. Geología preliminar del río Tigre-Corrientes en el Nororiente peruano. *Boletín de la Sociedad Geológica del Perú*, v.44, p.106-127.

SCHUMM,S., 1986. Alluvial river response to active tectonics. Studies in Geophysics, Active Tectonics, *National Academy press*, Washington D.C., p.80-94.

SEMPERE,T., 1990. Cuadros estratigráficos de Bolivia: propuestas nuevas. *Revista tecnica YPFB*, 11(2-3):215-227.

QUANTITATIVE ANALYSIS OF ASYMMETRICAL FLUVIAL PATTERN TO STUDY ACTIVE DEFORMATIONS IN SUBANDES BASINS

Jean François DUMONT[1][2], Catherine MERING[1][3] Jean François PARROT[1][3] et Hind TAUD[3].

(1) ORSTOM, 213 rue la Fayette, 75480 Paris, Cedex 10.
(2) URA D.1369 CNRS, LGDI, Univ. Paris Sud, Bt 509, 91405 ORSAY.
(3) Laboratoire de Géologie-Géomorphologie Structurale et Télédétection, Dpt Géotectonique, Univ. Paris VI, 4 Place Jussieu, 75230 Paris.

RESUME: Les plaines alluviales dissymétriques metent en évidence la déformation de la surface d'un bassin. Le cas du bas Ucayali est abordé ici à partir de l'analyse quantitative de forme réalisée sur une images SPOT.

KEY WORDS: Fluvial pattern, foreland basins, Ucayali River, Remote sensing, Quantitative analysis.

INTRODUCTION

Neotectonic analysis of alluvial floodplain may be done using two types of fluvial patterns: sinuosity, which changes is related to longitudinal slope variations (Schumm 1986), and asymmetrical floodplain related to lateral tilting (Von Bandat 1964). The case of asymmetrical fluvial patterns from the lower Ucayali River (East Marañón Basin) has been previously described (Dumont et al., 1988; Dumont in press). We present here new developments from this case, in the aim to provide a method for the analysis of short term fluvial response to active deformation.

GEOLOGICAL SETTING

The Marañón and Ucayali rivers cross the Marañón foredeep basin, and join at the eastern border of the basin, in a triangle shaped graben edged by the uplands of the Brazilian Craton. The existence of the graben is documented by recurrent normal faulting in the upland (Dumont et al., 1988). In the graben the Ucayali River has an asymmetrical floodplain. The recent evolution of the Ucayali River is also clearly asymmetric: meanders are simple on the upland side (Fig.1,R) and compound on the floodplain one (Fig.1, L1 and L2 successively). Meander development is clearly related to the trend of the river and the local direction of the upland border (Fig.1, A and B respectively). The channel of the Ucayali River is limited on the upland side by the cohesive silts and clay of the Pebas formation which crop out below the erodible Pleistocene deposits, whereas banks on the floodplain side are made of non consolidated and easily erodible silts and fine sands of late Holocene age.

GENERAL STUDY METHODS

Asymmetrical floodplain is the most classical criterion of the effect of lateral tilting over a valley, evidenced early from aerial photography (Von Bandat 1962). The river channel tends to migrate down the slope of the tilt, abandoning meander loops on the upper side of the floodplain, which are all concave toward the migrating direction of the river. According to the Van Bandat criterion, the observation of tectonic activity is only possible if the process of lateral sliding of the meandering river is effective during a relatively long time, and over a floodplain three or four time wider than the amplitude of the river sinuosity.

It may be inferred from the continuity of the phenomenon that at any time during the period of lateral migration the effect of tectonics over the river behavior is active. So that, it should be possible to get evidence for tectonic activity investigating short time parameters of the floodplain morphology.

We provide here an example from the Ucayali River, on the eastern border of the Marañón Basin. Short time evolution of meanders is studied using the ridge and swale pattern, which is closely related to the recent development of meanders. We have developed a quantitative approach using SPOT image analysis.

EXTRACTION OF RIDGE AND SWALE PATTERN BY IMAGE ANALYSIS

Our objective here is to delimit shape entities that are thematically significant, that is to say the ridge and swale pattern of alluvial floodplain, from the initial SPOT XS scene. The pattern is evidenced by morphological and botanical contrast between the swampy grassland in the swales and the forested ridges. In order to extract these forms, widely-known techniques of multispectral classification is of no use since these objects have no characteristic spectral signature when they have a specific sub-circular shape. On Grey level images such as any of the XS channel (here XS3), one can visually perceive these objects as very thin sub-circular lines of light tone. The scope here is to filter these lines and to obtain a final binary image containing only the specified objects. Many criteria may be used for image analysis: the specific tone of the line (lighter tan the neighborhood), their thickness (one pixel wide) and their shape (subcircular). Experiments have shown that on square grids such as that of satellite images, well-known gradient techniques based on convolution with numerical masks leads to enhance rectilinear shapes and break curvilinear ones. Moreover they transform all contrast lines into very thick ones (Pratt 1978). We prefer here to employ nonlinear methods (Serra 1986). We first transform the initial digital grid into an hexagonal one which respects isotropy and where the euclidian distance between the pixels can be assimilated to the digital grid.

From the grey-tone image on the hexagonal grid (Fig.2A) one first filter thin and light lines by a *Top Hat* Transformation with a linear structuring element of given direction among the six possible ones of the grid (Meyer 1978). The resulting Grey tone image has a narrow histogram, but the lines of the image have the higher values which allows to obtain a pertinent binary image by threshold of the grey-tone function. This binary image contains small lines with wrong directions and disconnected to the desired ones. The "cleaning up" of the binary image is done by a *thinning* followed by a *geodesic reconstruction*: The thinning eliminates groups of pixels having a given configuration inside an elementary hexagon (it may be three pixels on a line or one isolated pixel on the center) and the geodesic reconstruction restores the initial connected components which have not totally disappeared with the previous thinning. At the opposite, lines can be connected along a given direction with a *closing* or a *thickening* Transformation with a linear structuring element, which both fill up the holes inside the hexagon according to the specific direction. This type of sequences enables to clean up the initial binary image and to preserve the "good" lines. Finally, in order to submit to geometric description one pixel-width structure,

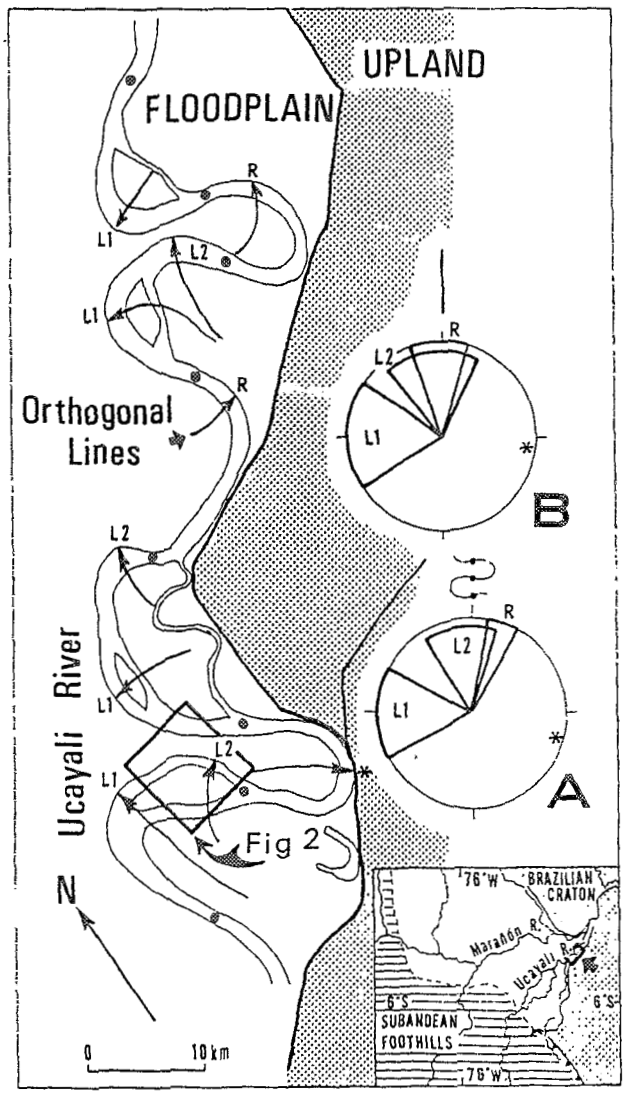

Fig. 1

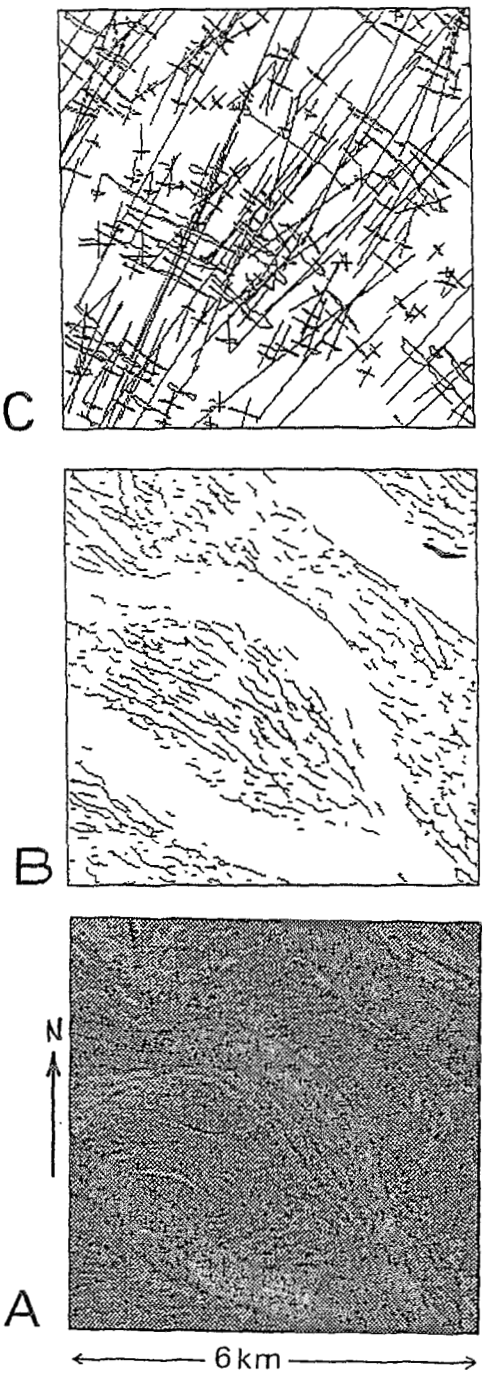

Fig.2 A

Fig. 1. Lower reach of the Ucayali River near Jenaro Herrera. "Orthogonal lines" are the longer lines orthogonal to the ridge and swale pattern. See commentary in text.

Fig.2. See commentary in text

we have computed a *skeleton by thinning* (Lantuejoul 1980) which preserves the connectivity of the initial set (Fig.2B).

SETTING STRUCTURAL PARAMETERS

In order to make quantitative description of the structural features previously detected, specific parameters are computed using the Adonis method (Parrot and Taud 1992): each curve is individualized and approximated by a circular arc which is called reference circle (RC). A set of parameters defined by the curve and its reference circle enables the characterization of the structures. These parameters mainly concern the position of the center and the value of radius of RC, the number of pixels belonging to the curve, the direction of the normal to the chord, and different coefficients (chord, intersections, symetry, etc...). Sorting of these parameters get evidence of different families among the structures encountered.

Fig.2C shows the individualized structures, their chords, and the normal to the chord which passes through the center of the reference circle. According to the radius of the curves, the relative position of reference circle and the direction of orthogonal lines we can characterize the evolution of meanders and obtain quantitative evidence for asymmetrical patterns using automatic analyze.

CONCLUSION

Semi circular patterns derived from active and abandoned meandering rivers cover extended areas of foreland basins. Quantitative image analysis appears to be very effective for quick analysis of large portions of river. Here, we apply the method to asymmetrical pattern, but others fluvial patterns which are related to neotectonics, like sinuosity and river bed width can also be analyzed.

REFERENCES

DUMONT,J.F.,LAMOTTE,S.,and FOURNIER,M.,1988. Neotectonica del Arco de Iquitos (Jenaro Herrera, Perú). *Bol. Soc. Geol. del Perú*, 77: 7-17.

DUMONT, J.F., The Upper Amazon River System. (*sous presse in*: Engineering Problems Associated with the Natural Variability of Large Alluvial Rivers, *Schumm and Winkley ed., Pub. of the Americain Society of Civil Engineers*)

LANTUEJOUL,C., 1980. Squeletonization in quantitative metallography. *Issues of Digital Image Processing, (ed. by R.M.Haralick and J.C.Simon)*, p:107-135, Sijthoff and Noordhoff, The Netherland.

MEYER,F., 1978. Contrast feature extraction. *Special Issue of Practical Metallography*, N 8:374-380.

PARROT,J.F. and TAUD,H., 1992. Detection and classification of circular structures on SPOT images. *IEEE Trans. Geosc. and Remote Sensing*. Vol.30,n 5:996-1005.

PRATT,W., 1978. Digital Image Processing. *Wiley ans Sons, New York*, 750pp.

SCHUMM,S., 1986. Alluvial river response to active tectonics. *Studies in Geophysics, Active Tectonics, National Academy press, Washington D.C.*, p.80-94.

SERRA,J.,1986. Image Analysis and Mathematical Mophology, Theorical Advances. *Academic Press, London*, 628p.

VON BANDAT, H.F., 1962. Aerogeology. *Gulf, Huston, Texas*, 350p.

LARGE SCALE POLYPHASED SUBMARINE SLOPE FAILURE INDUCED BY SUBSIDENCE ALONG THE NORTHERN PERUVIAN MARGIN

Anne DUPERRET (1), Yves LAGABRIELLE (2), Jacques BOURGOIS (1) and Erwin SUESS (3)

(1) CNRS, URA 1315 and LGTE, Département de Géologie sédimentaire, Univ. Pierre et Marie Curie, Paris, FRANCE
(2) CNRS, URA 1278 "Domaines océaniques", Univ. Bretagne occidentale, Brest, FRANCE
(3) GEOMAR, kiel, GERMANY

RESUME : Une récente compilation de données Seabeam et Hydrosweep, acquises de 5°15'S à 6°10'S le long de la marge nord-péruvienne, a permis la mise en évidence d'un méga glissement sous-marin, se développant en plusieurs étapes. 1) La principale étape du glissement est un "debris-avalanche", dont le matériel s'est accumulé sur la pente inférieure et en partie dans la fosse. 2) la deuxième phase d'instabilité correspond au glissement de deux blocs en voie de détachement. 3) Etant donné que la pente moyenne se bombe le long du plan de glissement d'une faille normale majeure, un méga-glissement de la pente est à prévoir dans un avenir proche.

KEY WORDS : Peru, active margin, submarine slide, debris avalanche, subsidence, subduction erosion.

INTRODUCTION

A morphological analysis realised from the bathymetric compilation of Seabeam and Hydrosweep data acquired along the northern margin of Peru, shows the occurence of polyphased mega-submarine slides. The surveyed area is located offshore Paita from 5°15'S to 6°10'S. At this location, the continental shelf is flat and narrow, the continental slope is steeper than to the south of the margin and the subduction of the Nazca Plate triggers a great seismic activity. Therefore, the area presents a typical profile of East Pacific active margin.

STRUCTURAL SCHEME OF THE CONTINENTAL MARGIN

From the continent to the trench, the continental slope is characterized by three distincts domains:
1) The upper slope, with a continuous slope gradient of 7°, which is incised by deep parallel E-W canyons. 2) The middle slope, which presents curved directions in the central part of the area. 3) The lower slope characterized by a rough topography, which represents a debris-slide deposit (Bourgois *et al.*, 1988).
The main morphological features of the area are three curved scarps respectively named from upslope to the trench : the upper slope scarp (USS), the middle slope scarp (MSS) and the lower slope scarp (LSS).
The USS represents the limit between the upper slope and the middle slope area. It is a curved scarp with an average slope gradient of 25°. As shown by a seismic profile, this scarp corresponds to the emergence of a listric normal fault, dipping seaward (Bourgois *et al.*, 1986, 1988). At the base of the USS, the middle slope shows a dome-shape deformation combined with a structural pattern roughly parallel to the curvature of the USS.
The main structure of the area is the MSS. It extends for 30 km along the middle slope and presents an average slope gradient varying from 10 to 30° over a distance of 1 km. The MSS shows a typical shape of debris-slide breakaway.
The LSS appears as an amphitheater shaped scar along which an entire 500 m height block has glided down.
These three curved scarps results from different stages of polyphased mega-submarine slides.

THE POLYPHASED MEGA-SUBMARINE SLIDE

The main stage of failure of this active margin is characterized by a debris avalanche, which has let on the slope a breakaway named MSS. This feature is regarded as a scar along which an important volume of rocks has slid down towards the trench (Bourgois *et al.*, 1986, Von Huene *et al.*, 1988, Bourgois *et al.*, in press). Sixteen deep-sea dives with the submersible *Nautile* were performed along the MSS, during the NAUTIPERC cruise in 1991. The MSS appears to be composed of a succession of small cliffs exposing dominant mudstones and siltstones bounded by steps covered with recent pelagic sediments. Fresh outcrops are frequent and screes are often observed at the foot of the steepest slopes. Generally, the freshness of the outcrops suggests that rock falls and others gravity flows are still active along the scarp.
Micropaleontological results obtained from samples collected during the dives indicate that the sediments are from Quaternary to Miocene in age. The scarp exposes deep strata of the middle slope thus confirming that this feature can be considered as the scar of a major slide.
The debris slide deposit covers the entire lower slope and in-fills a part of the trench. The deposit is characterized by a succession of isolated blocks without specific trends. The chaotic topography observed at the toe of the continental margin is indicative of a debris-avalanche deposit, which originated most probably from the MSS.
At the base of the MSS, the middle slope is characterized by a flat terrace. As shown by seismic profile, this area presents a chaotic seismic facies. This feature is characteristic of a smooth debris-flow deposit, which could represent the fine grained part of the debris avalanche. These deposits are burying the main slide plane.

The second stage of failure is characterized by two glided blocks. They appear as amphitheater shaped scars, that showing the same trend. The first, occured along the middle slope scarp. The second is one of the major feature of the slope and was named LSS. It is located in the flat area of debris-flow deposit created by the main debris avalanche. Both features are aligned along a N80 direction, roughly parallel to the direction of the subducting Nazca Plate.
These blocks have glided down after the main debris avalanche. They are indicative of a secondary stage of failure probably induced by the debris avalanche. This second stage of slope failure would be less catastrophic than the first one.

The dome-shape deformation of the middle slope is combined with a peculiar structural fabric, characterized by the developement of small ridges and valleys. They are roughly parallell to the curvature of the USS. As shown by this structural pattern, the deformation of the middle slope along the listric normal fault could be always active. The continuation of the deformation could able to produce a second giant submarine slide, which would affect the whole middle slope and which would occur along the seaward dipping normal fault.
The upward progression of slope unstability is actually stopped at the location of the main normal fault of the margin (USS), because the upper slope is incised by deep parallel which doesn't progress downward the USS.

ORIGIN OF SLOPE FAILURE

These giant polyphased submarine slides result from a peculiar state of stress of the continental slope in relation with the subduction of the Nazca Pate. For instance, another similar case of great scale slope failure has been recognized along the northern Chile continental slope, offshore Iquique (Li and Clark, 1991).
Slope unstabilities occur generally within unconsolidated materials and are favoured by a supply of sediments inducing an increase in slope gradient. It is not the case here. Because at this location, the continental margin is characterized by a lack of sedimentary supply coming from the land. Moreover, from the *in situ* observations of the submersible *Nautile* along the MSS, the sediments involved in the slope failure are predominantly consolidated. The initiation of this great-scale slope failure are consequently mostly originated from the subduction of Nazca Plate. Obviously, the great seismic activity observed in this area prepare favorable condition for the slope failure.
In such a context of active margin, several processes are able to produce the slope failure :
The main stage of slope failure is assumed to come from the oversteepening of the slope, which is induced by a roll-over deformation of the middle slope along a seaward dipping listric normal fault (USS) (Bourgois *et al.*, in press). The debris avalanche occured for slope gradient greater than 13° (Duperret *et al.*, 1993).
The deep sea dives realised along the MSS, have revealed the occurence of numerous clams fields and associated biological colonies related to fluid vents. Bourgois *et al.*, (in press) assumed that the fluid vents is the result of the unloading create by the failure of the slope. Such emergences could also be induced by an increase of pore pressure fluids along the subduction plane. They could significantly reduce the shear strenght in the upper plate and generate a sedimentary mobility along a minimum shear zone.

Then, the slope failure occurs within consolidated rocks by an oversteepening of the slope. The high seismicity of the area and the circulation of fluids have probably greatly contributed to initiate the failure.

The debris avalanche deposit covers the entire lower slope and extends to the trench axis. In the trench, the topography of the mass-wasting is smoother than on the lower slope ; but the inner trench wall is completely buried by the debris-avalanche. By comparison with northern and southern undisturbed slope profile of the margin, the area covered by the deposit shows a relative topographic low of about 200 m. The topographic low is partially in-filled by the debris avalanche deposit and it is located just below the three main curved scarps of the slope. Therefore, this feature within the Nazca Plate is probably responsible for the initiation of the detachement faulting and the subsequent polyphased submarine slides. The origin of such a depression must be discussed.
1) It could be explain by a process of subduction erosion along the base of the continental margin. 2) It could also result from a change in the dip angle of the subducting Nazca Plate, which could originate from a change in the Nazca Plate motion. This hypothesis must be correlated with a change of the kinematic organisation of the Nazca Plate versus South American Plate. 3) The occurence of topographic asperities within the subducting plate is able to increase locally the process of subduction erosion (Lallemand *et al.*, 1992). These asperities could be representated by horsts and grabens or by a volcanic seamount.
Now, the respective influence of these various processes needs to be clarified.

REFERENCES

Bourgois J., Pautot G., Bandy W., Boinet T., Chotin P., Huchon P., Mercier de Lepinay B., Monge F., Monlau J., Pelletier B., Sosson M. et Von Huene R., 1986, Régime tectonique de la marge andine convergente du Pérou (Campagne Seaperc du N/O. J. Charcot, Juillet 1986), *C. R. acad. Sc. Paris,* 303, II, n°17, p. 1599-1604.

Bourgois J., Pautot G., Bandy W., Boinet T., Chotin P., Huchon P., Mercier de Lepinay B., Monge F., Monlau J., Pelletier B., Sosson M. et Von Huene R., 1988, Seabeam and seismic reflection of the tectonic regime of the Andean continental margin off Peru (4°S to 10°S)., *Earth plan. Sc. lett.*, 87, pp111-126.

Bourgois J., Lagabrielle Y., De Wever P., Suess E. and the Nautiperc team, Tectonic history of the northern Peru convergent margin during the past 400ka., *Geology.*, in press.

Duperret A., Lagabrielle Y. and Bourgois J., 1993, Résultats des plongées du Nautile sur la marge continentale du Pérou à 5°40'S : étude de la zone d'arrachement d'un méga-glissement sous-marin (campagne Nautiperc,1991), *C. R. acad. Sc. Paris,* 316, II, p. 371-378.

Lallemand S.E., Malavieille J. and Calassou S., 1992, Effects of oceanic ridge subduction on accretionary wedges : experimental modeling and marine observations., *Tectonics*, 11, 6, pp 1301-1313.

Li C. and Clark A.L., 1991, SeaMARC II study of a giant submarine slump on the northern Chile continental slope, *Marine Geotechnology*, vol. 10, pp 257-268.

Von Huene R., Bourgois J., Miller J. and Pautot G., 1989, A large tsunamogenic landslide and debris flow along the Peru trench., *Journ. Geophys. Research,* vol 94, n°B2, pp 1703-1714.

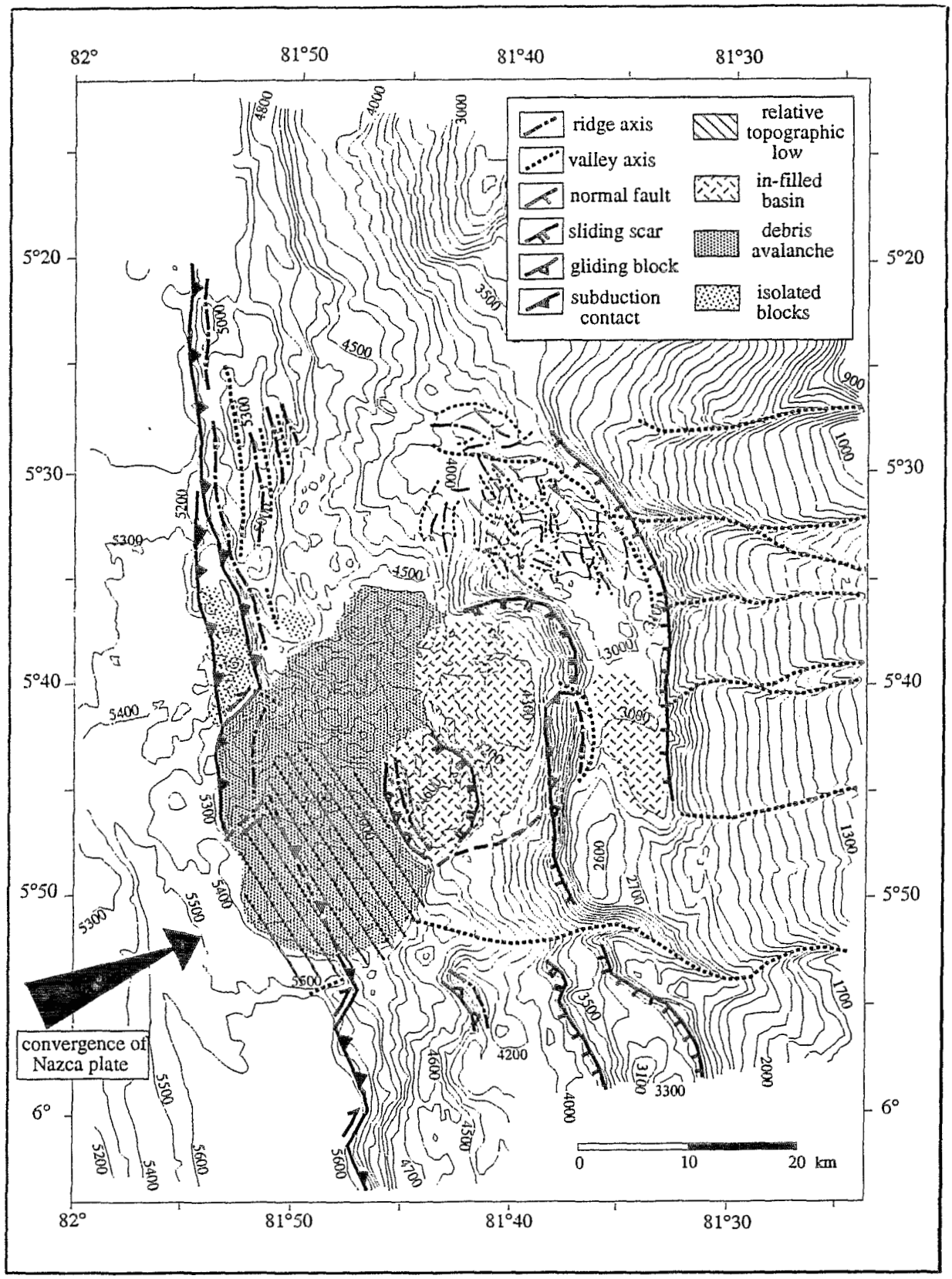
82°
81°50
81°40
81°30
5°20
5°30
5°40
5°50
6°
ridge axis
valley axis
normal fault
sliding scar
gliding block
subduction contact
relative topographic low
in-filled basin
debris avalanche
isolated blocks
convergence of Nazca plate
0
10
20 km

QUATERNARY STATE OF STRESS IN THE NORTHERN ANDES AND THE RESTRAINING BEND MODEL FOR THE ECUADORIAN ANDES

Frédéric EGO (1), Michel SEBRIER (1), Alain LAVENU (2), Hugo YEPEZ (3), Arturo EGUEZ (3)

(1) URA 1369 CNRS, bât 509, Université de Paris Sud, 91405 Orsay cedex, France.
(2) ORSTOM, 213 rue La Fayette, 75480 Paris cedex10, and, LGMBS, UPPA, 64000 Pau, France.
(3) Escuela Politecnica Nacional, Quito, Ecuador.

Résumé : L'inversion des mécanismes au foyer superficiels des Andes septentrionales, et l'analyse néotectonique des Andes d'Equateur, montrent un champ de contrainte homogène (σ_1 ± E-W). Celui-ci induit un mouvement dextre sur les failles N30-35°E et du raccourcissement sur les failles N-S, (relais compressif nord équatorien). Les vitesses de déplacement des failles dextres majeures sont calculées et discutées.

Key Words : Sismotectonics, State of Stress, Quaternary, Andes, Ecuador, Kinematics.

INTRODUCTION

The subduction of the Nazca Plate beneath South America results from a N80°E trending convergence (Fig. 1). This convergence is thus oblique along the N30°E, 1500-km long northern Andes. This obliquity is accommodated in the upper plate by NNE trending, active dextral faults. In Ecuador, two major active strike-slip faults are known. (1) The Pallatanga Fault (PF), that is located in the Cordillera Occidental of southern Ecuador, is well studied (Soulas, 1988; Winter, 1990; Soulas et al., 1991; Winter et al., 1993). (2) The Rio Chingual-la Sofia Fault (CSF), that is located in the Cordillera Real (CR) of northern Ecuador (Soulas et al., 1988; 1991; Tibaldi & Ferrari, 1992), is still poorly known. In addition, several Quaternary, N-S striking folds and reverse faults have been reported in northern Ecuador (Winter, 1990; Ego et al., 1993); They are interpreted as a restraining bend between the PF and the CSF (Ego et al., 1993). In order to address this problem, we have analyzed the stress pattern in northern Andes inverting shallow focal mechanism data. Then, we calculated slip rates on the major strike-slip and reverse faults.

INVERSION OF FOCAL MECHANISMS

In the literature, 113 shallow focal mechanisms, registered by world seismic networks, are available (e.g., Pennington 1981; CMTS by Dziewonski 1981-1992 and USGS catalog 1977-1988). They are mainly distributed along the Andean subduction zone and in the Sub-Andean region; in contrast, few events are located in the Andean mountains. We have defined 8 zones, each one corresponding to a specific structural province. Then, data inversion (same method as Carey-Gailhardis & Mercier, 1987) was performed in each zone in order to calculate its mean state of stress (Fig. 2). The most significant result is that the state of stress is quite homogeneous in northern Andes, σ_1 trending roughly E-W, except nearby the Caribbean.

CSF SLIP RATE DETERMINATION AND IAV SHORTENING ESTIMATE

In order to constrain the CSF slip rate, a detailed fault mapping was performed using LANDSAT imagery coupled with aerial photo analysis and field control. Numerous dextral offsets are seen along the 70 km long, N35°E striking trace of the CSF in Ecuador. The rio Chingual, a major river of the CR, exhibits a dextral offset ranging between 7.5km and 10.5km. Other streams of minor importance show offsets between 50m and 500m. All these offset streams, that are from different ages, allow us to conclude that the fault has been active in a dextral sense for a long time (>1My). These offsets could be used to calculate the slip rate of the fault; however, lacking of precise stream ages, we determined the CSF slip rate using the Soche lava

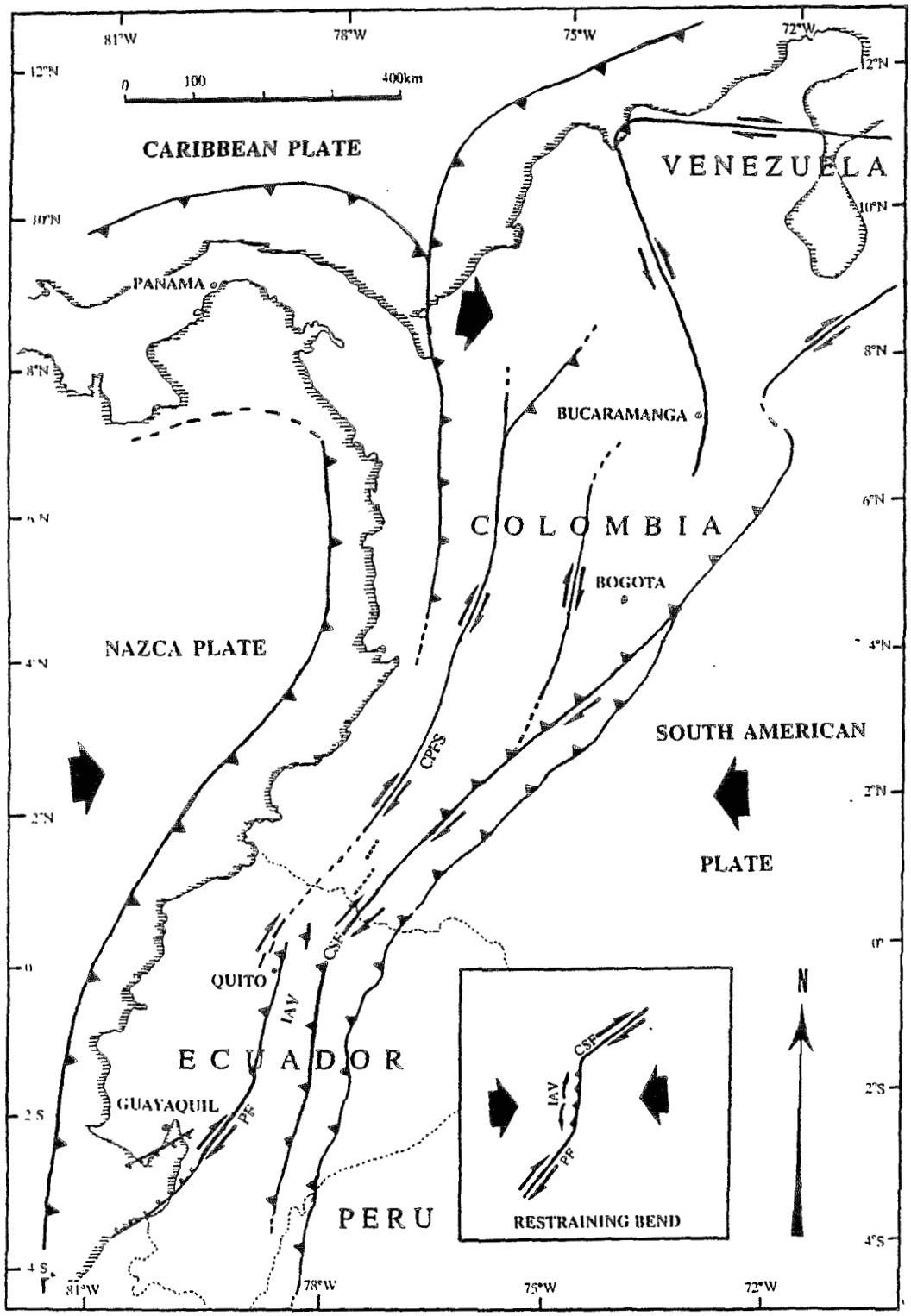

Figure 1: Geodynamic setting and major structures in northern Andes and restraining bend model for the northern Ecuadorian Andes. CSF: Rio Chingual-la Sofia Fault, CPFS: Cauca-Patia Fault System, IAV: Inter-Andean Valley and PF: Pallatanga Fault.

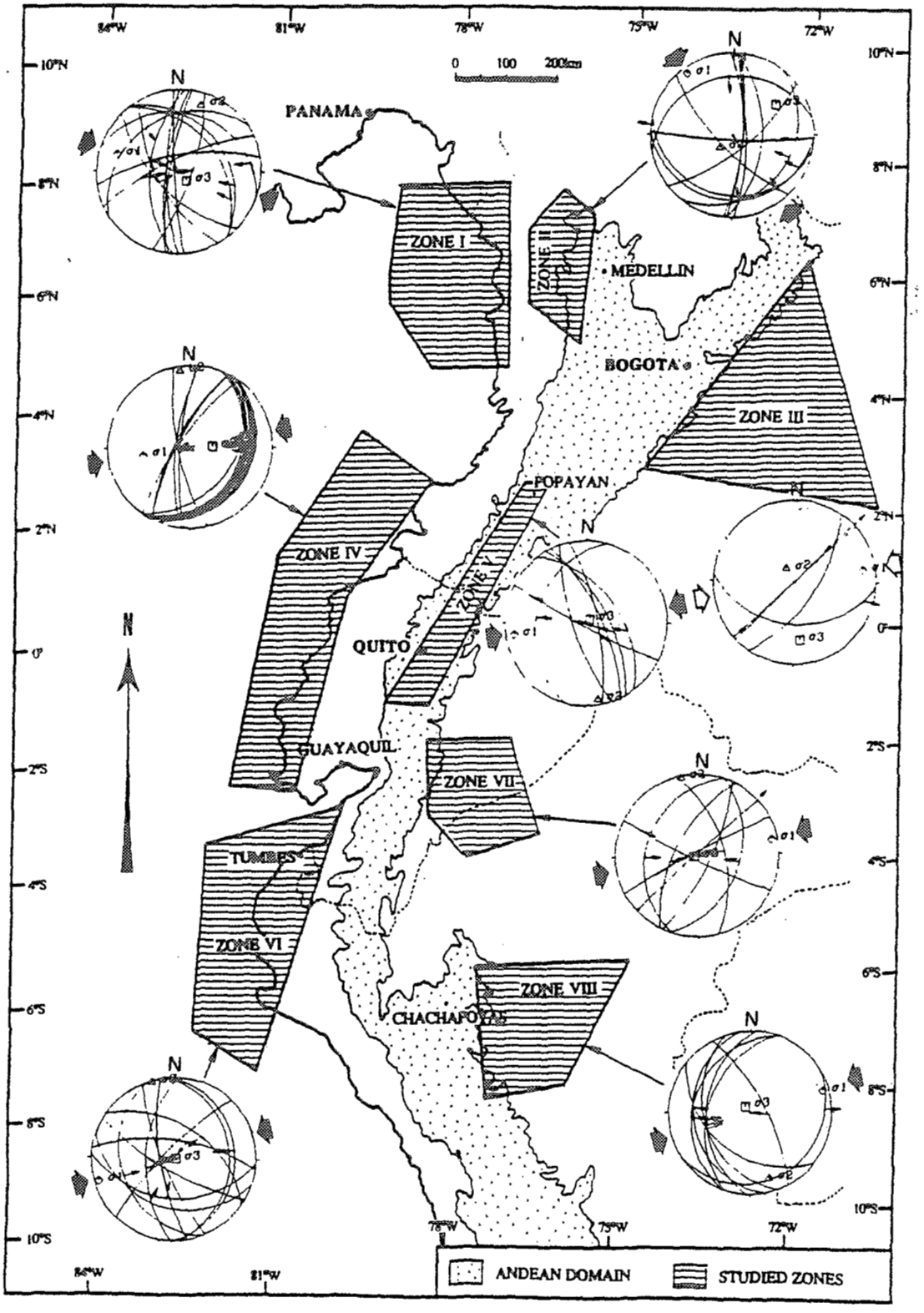

Figure 2: State of stress in northern Andes calculated by inversion from focal solutions. Due to few data, only a test has been performed for zone III. Solid black arrows: σ_1 orientation.

flow dated at 9670 yrBP (Hall & Beate, 1991). Since this lava flow exhibits an offset ranging between 60m and 70m, and assuming a 5% error on the age, the "long term" slip rate is 7 ± 1mm/yr. In contrast, the N30°E trending PF has a slip rate of 4 ± 1mm/yr (Winter (1990; Winter et al 1993). The marked difference in slip rate between PF and CSF suggests a northward increase in dextral slip rate along northern Andes. Assuming that the whole strike-slip motion of the N30°E striking PF is transmitted northward to the N-S striking restraining bend, we can estimate the order of the IAV shortening rate. This simple geometrical pattern yields an E-W shortening of 2 ± 1mm/yr. Conversely, if the whole 7 ± 1mm/yr slip rate of the CSF would be transferred southward to the restraining bend, its shortening rate would be thus 4 ± 1mm/yr. This theoretical calculation shows that there is a difference of 2 mm/yr of E-W shortening between the northern and southern ending points of the Ecuadorian restraining bend.

CONCLUSION

During the Quaternary period, northern Andes are submitted to an homogeneous state of stress. Moreover, the N-S striking Ecuadorian IAV is submitted to an E-W compression and the motion of the two NNE-striking, major dextral fault systems (PF and CSF), located North and South of the IAV, also agree with this regional state of stress. Slip rate calculations on the PF and CSF suggest a northward increase in dextral slip along Ecuadorian Andes. This increase should be the consequence of a northward increase in convergence obliquity. Indeed, the obliquity between the trench normal and the convergence is ±30° in Ecuador (from Guayaquil to Esmeraldas) while it is ±45°E in northernmost Ecuador-southern Colombia (from Esmeraldas to Buenaventura). Taking into account the 78mm/yr convergence rate and the convergence obliquities, there is 39mm/yr of dextral slip, parallel to the trench, to accommodate in Ecuador while this amounts to 60mm/yr in northernmost Ecuador-southern Colombia. In fact, the subduction slip is actually oblique (see zone IV on Fig. 2) and consequently accommodates most of the parallel to the trench component of convergence. A simple calculation shows that the subduction slip accommodates approximately 75-90% of the parallel to the trench component of convergence. The remaining 10-25 % are accommodated by the upper plate dextral faults so that the theoretical dextral slips are: 4-10 mm/yr in Ecuador and 6-13 mm/yr in northernmost Ecuador-southern Colombia, respectively. These theoretical values are of the same order than the PF and CSF calculated slip rates showing that other major dextral faults are unlikely. Finally, the 2 mm/yr excess in shortening rate existing to the North of the restraining bend should correspond to the CFS southward damping on the Reventador reverse fault zone.

REFERENCES

CAREY-GAILHARDIS E. & MERCIER J.L., 1987. A numerical model for determining the state of stress using focal mechanisms of earthquake population: application to Tibetan teleseims and microseismicity of Southern Perou. *Earth Planet. Sci. Lett.*, 82. 165-177.

DZIEWONSKI A.M. et al, from 1981 to 1992. Determination of CMTS in *Phys. Earth. Planet. Int.*

EGO F., SEBRIER M., LAVENU A., EGUEZ A., and YEPES H., 1993. A new geodynamical model for the Northern Ecuadorian Andes. EUG VII, 4-8 April 1993, *Terra abstract* 5 (1): 203.

HALL L.M. & BEATE B.,1991. El volcanismo plio-cuaternario en los Andes del Ecuador. *Estudios de Geografia* Vol 4, 5-17, Quito 1991.

PENNINGTON W.D., 1981. Subduction of the eastern Panama basin and seismotectonics of northwestern south America. *J. Geophy. Res.* , 86, B 11 : 10753-10770.

SOULAS J. P., 1988. Informe de misión en el Ecuador, Proyecto UNDRO-EPN. Programa de prevención y planificación para desastres en el Ecuador y países vecinos. UNDRO, Genève, Suisse, 21p.

SOULAS J. P., EGUEZ A., YEPES H. and PEREZ H., 1991. Tectónica activa y riesgo sismico en los Andes ecuatorianos y el extremo sur de Colombia. *Bol. Geol. Ecuat.* Vol 1, n°1, pp 3-9.

TIBALDI A. & FERRARI L. 1992. Lastest pleistocene-holocene tectonics of the ecuadorian Andes. *Tectonophysics.* 205, pp 109-125.

U.S.G.S., N.E.I.C., 1988. World Data Center_A for Seismology. Listing, 1977 to 1988. U.S. Dept. of the Interior.

WINTER T. 1990. Mécanismes de déformation récentes dans les Andes equatoriennes. *Thèse.* Paris-Sud, Orsay, 205 p.

WINTER T., AVOUAC J. P., and LAVENU A., 1993. Holocene Kinematics of the Pallatanga strike-slip fault (central Ecuador) from topographic measurements of displaced morphological features. *Geophys. J. Inter.* (accepted).

CRUSTAL MICROSEISMICITY IN CENTRAL CHILE: EVIDENCE OF ACTIVE FAULTING?

A. Fuenzalida[1], A. Sandoval, A. Cisternas[1] & L. Dorbath[1,2].

(1) Institut de Physique du Globe de Strasbourg, 5 rue Rene Descartes, 67084 Strasbourg CEDEX, France.
(2) ORSTOM , 213 rue La Fayette, 75480 Paris CEDEX 10, France.

Abstract

Crustal seismicity in Central Chile (32°-34.5°S) has not been studied in detail up to now because it is blurred by the "high noise level" generated by the seismic activity of the subduction. The most important events recorded in the region are directly related to the subduction process, that is they are interplate events. Since these subduction events are the most destructive and strongest ones, seismologists have paid little attention to the crustal seismic activity that reflects the actual deformation to which the overriding border of the South American Plate is being submitted. For example in September 1958 an important but not well known shallow crustal earthquake (m_S=6.8) with epicenter located, in Las Melosas, 50 km to the south-west of Santiago shook the region, causing damages in some nearby villages and being strongly felt in Santiago and Valparaiso. This event was accompanied by surface faulting on the high mountains.

In 1986 a field experiment to record aftershocks of the 1985 Valparaiso earthquake and the microseismicity of the region was carried out from the 20th September to the 5th November, to study in detail the geometry of subduction (Fuenzalida et al, 1992). A group of 14 portable stations was deployed, expanding the permanent network of 10 telemetred stations, mantained by the Seismological Service of the University of Chile. During this time an important number crustal events that evidences active seismic crustal deformation were recorded.

Several clusters were observed in the crust, one 30 km to the west of Santiago and two others toward the Andean cordillera. The activity in the Central valley was rather sparse. Focal mechanism, local tomography and stress analysis are performed to determine the mechanical characteristics of crustal deformation.

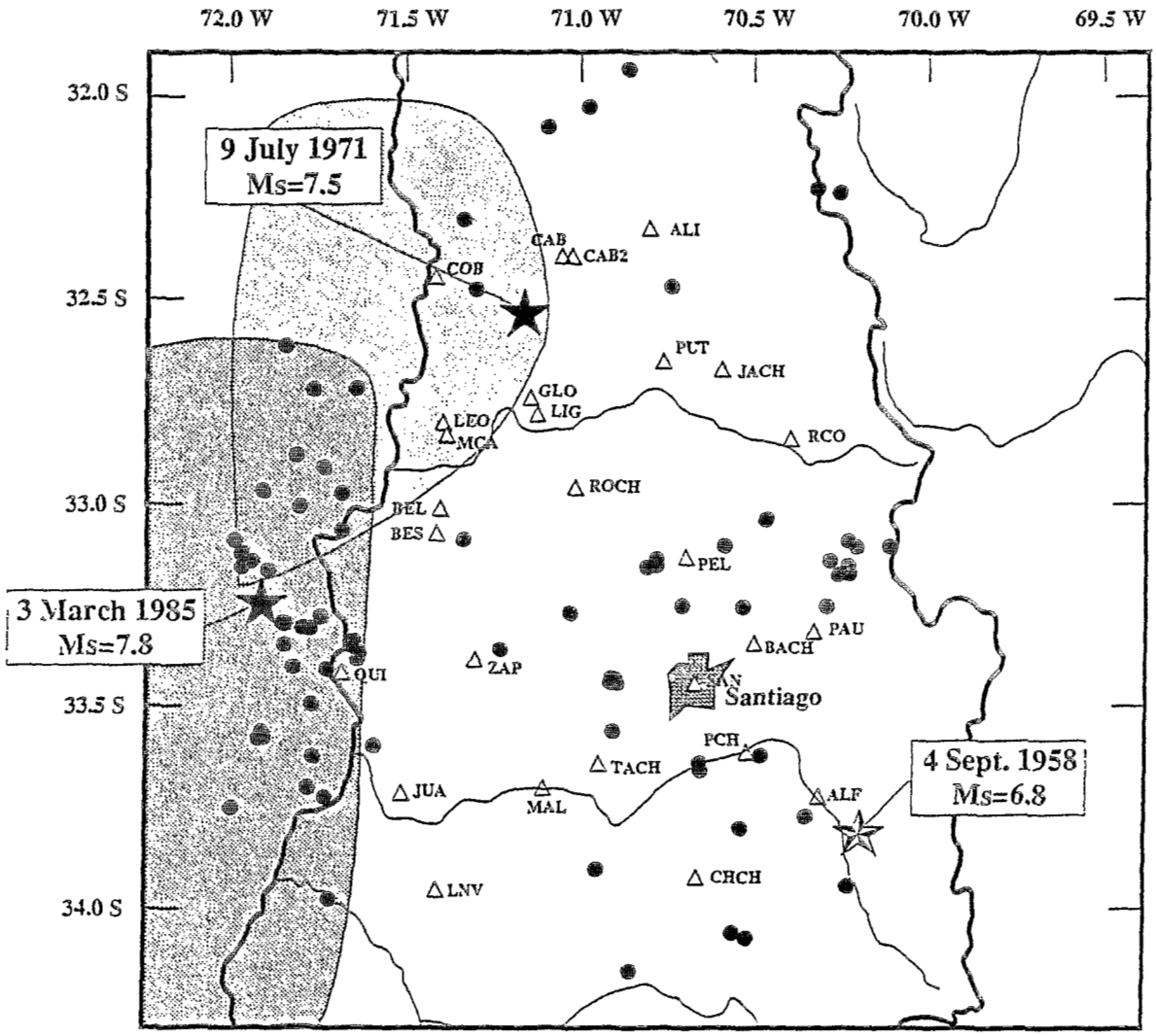

Crustal seismicity (filled circles) for October 1986, all events have depth < 30 km. Triangles represent the network used. The location of the 1958 "Las Melosas" crustal earthquake is shown south-east of Santiago.
The epicenters and aftershock areas of the Valparaiso earthquakes of 1971 and 1985 are also shown.

THE LATE CENOZOIC TECTONO-SEDIMENTARY EVOLUTION OF THE NORTH CHILEAN PACIFIC MARGIN (21°30' - 24°S).

Adrian J. HARTLEY(1) and Elizabeth J. JOLLEY(2)

(1) Department of Geology and Petroleum Geology, Meston Building, King's College, University of Aberdeen, Aberdeen AB9 2UE, U.K.
(2) BP Exploration, Aberdeen.

RESUME: El estudio de la evolucion sedimentologia, geomorfologia y tectonica del Mioceno-Holoceno de la costa norte de Chile entre 21°30' y 24°S ha revelado la siguiente seqeuncia de eventos: 1) Subsidencia y sedimentatcion del mid Mioceno al Pleistoceno, 2) Levantamiento y formacion de terrazas marinas controladas por ascensos eustaticos interglaciones, ascensos tectonico y ascenso controlado por fallamiento asociado a la domacion regional del margen de subduccion.

KEY WORDS: northern Chile, Late Cenozoic, marine terraces, tectonics

INTRODUCTION

The Late Miocene to Recent uplift of the Central Andean Pacific margin of South America is recorded by the development of a number of marine terraces and exposed shallow marine and continental sediments of Miocene to Recent age. However, whilst terrace development has been recognised for some time, correlation along the Pacific margin has proved extremely difficult. Correlation difficulties have arisen because of variations in the ages, numbers and heights of terraces due to a combination of fluctuations in sea-level resulting from the Quaternary glaciation superimposed on areas of differential uplift along the Pacific margin. Here we illustrate how a detailed study of Miocene to Recent sedimentation along the north Chilean coastal margin can help to constrain uplift mechanisms. The understanding of these uplift mechanisms has important implications for the tectonic evolution of the Coastal Cordillera.

PREVIOUS WORK

Previous work on coastal uplift in northern Chile has focussed on marine terrace and beach ridge development across the Mejillones Peninsula (Okada, 1971; Armijo & Thiele, 1990) Descriptions of these uplift related phenomena are restricted to the area around the Mejillones Peninsula and little attention has been paid to uplift related features north and south of the Peninsula. Here we present data on Miocene to Recent shallow marine sedimentation, terrace, beach ridge, alluvial fan and fan delta development along the north Chilean coast between 21°30' and 24°S. These data allow constraints to be placed on the mechanisms of uplift on both local and more regional scales.

MIOCENE-RECENT STRATIGRAPHY

Three Miocene to Recent stratigraphic units can be recognised on the coastal

margin between 21°30' and 24°S overlying the andesitic volcanics of the La Negra Formation, Jurassic granodiorites or Cretaceous sediments: 1) Shallow marine sediments of the 40 m thick La Portada Formation of Mid Miocene-Pliocene age (Herm, 1969; Ferraris & Di Biase, 1978) which crops out over the southern half of the Mejillones Peninsula and extends further southwards to the northern edge of Antofagasta. 2) Pleistocene to Holocene shallow marine and beach sediments of the Mejillones Formation (Ferraris & Di Biase, 1978). The formation is up to 80 m thick and disconformably overlies the La Portada Formation. The Mejillones Formation is exposed over much of the northern part of the Mejillones Peninsula. 3) Pleistocene to Holocene alluvial fan, aeolian, fan delta, beach and shallow marine sediments (up to 50 m thick) which flank the Coastal Cordillera and are equivalent to the Mejillones Formation.

Sedimentology

Detailed sedimentological analysis of these 3 stratigraphic units has led to the following synethesis. Throughout Mid Miocene, Pleistocene and Holocene times virtually continuous shallow marine sedimentation (upper shoreface, shoreface-foreshore trnsition, foreshore and beach) dominated over much of the study area with the exception of 1) a minor interruption in the early Pleistocene indicated by the development of an angular unconformity between the La Portada and Mejillones Formations and 2) localised fault activity during the late Miocene early Pliocene at Caleta Herradura indicated by the development of a minor unconformity restricted to the half-graben. Quaternary alluvial and aeolian sedimentation was restricted to the margins of the basin where sediment was supplied from the Coastal Cordillera and isolated (islands) fault blocks. Areas in the centre of the basin had restricted clastic input during the Pleistocene are characterised by the development of bioclastic limestones with calcareous mudstones and chalks suggesting deposition below fair-weather wave base.

Marine Terraces

Marine terraces (palaeo-clifflines) cut in Miocene-Recent sediments, developed along the coastline of northern Chile in the Holocene (0.5 to 16 m elevation) and Late Pleistocene (16 to 70 m). Up to 6 terrace cutting events are recognised although in a number of places composite terraces are thought to have formed (*i.e.* where 3 or 4 base-level falls are amalgamated to a single cliff line by erosion). A late Pleistocene planation surface and two older planation surfaces are recognised (over 600 m elevation) which are likely to be of Early Pleistocene to Pliocene age. Similar ages for a number of terraces (now at different heights) suggest that terraces were cut by sea-level highstands developed during interglacials. Variations in terrace height are attributed to tectonically-induced tectonic uplift particularly as the highest planation surfaces are associated with active faults.

Regional Uplift

Whilst fault activity and sea-level highstands are responsible for terrace formation, in order to preserve the terraces the study area as a whole must have been uplifted - a feature present along the entire Andean margin. However in the study area, subtle variations in uplift can be determined by examining the present day height above sea-level of the last Pleistocene shoreline deposits exposed in the terraces themselves (as distinct from the shell lags formed on the terraces). The shoreline deposits are older than the oldest terrace dated at 344,000 years (Radtke, 1985) and are therfore likely to be mid to late Pleistocene in age. The deposits can be traced along strike over much of the study area and are considered to represent a single chronostratigraphic event. There is a gradual increase in height of the shoreline from north to south across the study area with the main locus around the Mejillones Peninsula and a gradual decrease to the south.

In addition the distribution of Miocene to Recent marine sediments in Northern Chile follows a similar pattern, with the largest preserved record of marine sediments located adjacent to the Mejillones area and a gradual decrease to the north and south of the peninsula, a feature also also recorded by a narrowing of the coastal plain to the north and south of the Peninsula. These observations imply that there has been a broad updoming of the Coastal Cordillera with the main area of uplift located on the Mejillones Peninsula. A hypothesis supported by recent tide-gauge data which indicate that the area around Antofagasta is in net uplift. Interestingly the present day trace of the Atacama Fault Zone parallels this zone of uplift and basin formation - the fault is at its maximum inland distance at Mejillones but to the north and south the fault trend swings out to sea at Salar Grande in the north and Talatal in the south. This suggests a possible causal relationship between uplift and the trace of the Atacama fault Zone.

Origin of Regional Uplift

Pleistocene to Recent marine terraces have been uplifted along much of the Pacific Margin of South America and as such are almost certainly related to changes in the geodynamics of the subduction zone. The scale and aerial extent of uplift in the study area precludes a fault-related origin, particularly as the scale of fault-related uplift can be identified (*e.g.* on the Mejillones Peninsula). In addition, the regional variation in uplift across the study area suggests that another mechanism of uplift is superimposed on the mechanism responsible for uplift of the entire coastal margin of the Central Andes. Given the proximity to the subduction zone it is likely that any potential mechanism will be relalted to heterogeneities at the subduction zone. The most likely mechanism for this regional uplift is that of aseismic ridge subduction, where subduction of anomalously thick bouyant oceanic crust is thought to induce local uplift of the margin. Examination of bathymetric data for the ocean floor of northern Chile west of the study area reveals the presence of an aseismic ridge which forms a spur to the Iquique Ridge and is located due west of the Mejillones Peninsula. It is possible therefore that the regional uplift of the margin in the study area is related to aseismic ridge subduction concentrated around the Mejillones Peninsula.

The origin of the general uplift of the Pacific Margin of South America is beyond the scope of this paper, however, it is a strong coincidence that the start of uplift of the margin at approximately 21 Ma also conicides closely with the propsed time of shallowing of the subduction zone propsed by Kay *et al.* (1988) for the area between 28 and 33°S.

Origin of the Coastal Scarp

Recently the Coastal Scarp has been intepreted as an extensional fault by Armijo & Thiele (1990). The basis for this observation is the presence of surface fault breaks on the scarp. However, detailed observations from aerial photographs and fieldwork have failed to identify any exposed fault breaks along the scarp with the exception of the Cerro Moreno Fault which has demonstrable left-lateral kinematic indicators and extends for approxiately 35 km. As Armijo & Thiele suggest that the Coastal Scarp fault links to the subduction zone it is somewhat strange that there is no evidence of post-Pleistocene fault breaks along its length or any linear features which could be interpreted as possible palaeo-fault traces given that many faults in the area have been active throughout this time period. Consequently, the Coastal Scarp is interpreted here as a degraded palaeo-cliffline possibly of early Pleistocene or older age.

Conclusions

The Late Cenozoic to Recent tectonic evolution of the Coastal Cordillera of northern Chile records the following series of events:

1) Subsidence and sedimentation in a fault-bounded extensional (half-graben style) shallow marine basin (the La Portada Formation) took place in Late Miocene to Pliocene

times, the presence of localised unconformities testifies to sporadic fault movement. The development of the two oldest planation surfaces on northern and central parts of the Mejillones Peninsula and around the Cerro Moreno Fault is also thought to have taken place at this time.
2) Local tilting resulted in the development of a minor unconformity and continued subsidence and sedimentation in a fault-bounded shallow marine basin during Pleistocene times (Mejillones Formation) with marginal marine, alluvial and aeolian sedimentation along the margin of the basin. Cyclicity deveolped within these alternating continental and marine sediments may reflect mid-Pleistocene glacio-eustatically-induced sea-level fluctuations.
3) Sporadic uplift and development of marine terraces in the form of palaeo-cliffiines (up to a maximum of 6) and basment planation surfaces occurred during the Late Pleistocene and Holocene. Uplift resulted in the exposure of Miocene-Pleistocene marine sediments within the terraces and large scale incision within alluvial fan channels, some of which have followed the same course for over 350,000 years.
4) Terrace formation is related to interglacial sea-level highstands.
5) Terraces of the same age are presently at different heights due to differential uplift caused by fault movement.
6) Uplift of a mid to late Pleistocene shoreline within the study area reveals a regional scale uplift phenomena centered on the Mejillones area which is of too large a scale to be fault-related and of too small a scale to account for the uplift of the entire central Andean margin (represented by uplifted marine terraces noted by other workers). Due to the proximity to the subduction zone (16-30 km below the coastline) uplift is considered to be related to local variations in subduction zone geodynamics. The favoured hypothesis is that of aseismic ridge subduction within the study area.
7) The uplifted area forms a broad, easterly convex zone which parallels the trend of the Atacama Fault Zone, possibly indicating that movement of the Atacama Fault Zone in this area may result from strain partioning between the Coastal Cordillera and the Central Depression (Pampa de Tamarugal) caused by aseismic ridge subduction.
8) The Coastal Scarp is considered to be a Miocene to Pliocene palaeo-cliffline and not a major extensional fault, due primarily to the lack of active faulting along the scarp and the absence of any linear features which could be interpreted as possible palaeo-fault traces.

References

ARMIJO, R & THIELE, R. 1990. Active faulting in northern Chile: ramp stacking and lateral decoupling along a subduction plate boundary?. Earth and Planetary Science Letters, 98, 40-61.
FERRARIS, F. & DI BIASE, F. 1978. Carta Geologica de Chile, Hoja Antofagasta. Instituto de Investigaciones Geologicas de Chile. 48pp.
HERM, D. 1969. Marines Pliozan und Pleistozan in Nord und mittel Chile unter besonderer Berucksichtigung der Entwicklung der Mollusken-Faunen. Zitteliana, 159pp.
KAY, S.M., MAKSAEV, V., MOSCOSO, R., MPODOZIS, C., NACI, C. & GORDILLO, C.E. 1988. Tertiary Andean magmatism in Chile and Argentina between 28°S and 33°S: correlation of magmatic chemistry with a changing Benioff zone. Journal of South American Earth Sciences, 1, 21-38.
OKADA, A. 1971. On the neotectonics of the Atacama Fault Zone region - Preliminary notes on Late Cenozoic faulting and geomorphic development of the Coast Range of northern Chile. Bulletin of the Department of Geography, University of Tokyo, 3, 47-65.
RADTKE, U. 1985. Chronostratigraphie und Neotektonik mariner Terrassen in Nord- und Mittel Chile - erste ergibnisse. Quatro Congresso Geologico Chileno, Antofagaasta, 4, 436-458.

CHILEAN SUBDUCTION SYSTEM: STRUCTURE, TECTONICS, AND RELATED SEISMICITY

Vladimir V. KOSTOGLODOV

Instituto de Geofísica, UNAM, 04510 México D.F., México, (e-mail: vladimir@ollin.igeofcu.unam.mx), also Institute of physics of the Earth, Russian Academy of Sciences, B.Gruzinskaya, 10, D-242, Moscow, Russia.

RESUMEN: El sistema de subducción de América del Sur entre 15°S y 45°S (la costa de Chile) es analizado utilizando datos sísmicos históricos e instrumentales junto con las últimas estimaciones de edad y velocidad de convergencia de la placa Nazca. Se argumenta que la edad de la placa subducente tiene la principal influencia sobre el régimen de subducción (la configuración de superficie sismofocal y también la fuerza de acoplamiento sísmico) en Chile.

KEY WORDS: Subduction, plate coupling, seismicity, seismic slip, slab detachment

INTRODUCTION

The tectonics, seismic regime and structure of subduction systems prevalently depend on the convergence velocity V and age A of descending lithosphere. The main morphologic features of oceanic plate (ridges and fracture zones) involved in subduction process may modify drasticly the "normal" subduction regime and produce noticeable irregularities. The Chilean subduction system merits a special attention for the big variety of A and a presence of subducting Juan Fernandez ridge and a number of fracture zones. The shape of subducting slab in relation with a distribution of quaternary volcanic activity and an orogenic structure of the South America plate provides an insight on the tectonic history of this zone. An important characteristic of present day seismic regime and plate coupling can be obtained from the distribution of seismic energy release rate and seismic slip along the subduction zone. These estimates are based on the study of catalogs of historical earthquakes and the theoretical models of plate coupling. Subduction zone system of the South America between 15° S and 45° S (the coast of Chile) was studied using historical [CERESIS, 1985] and instrumental (NEIC) seismicity data, the last estimates of age and convergence velocity, morphology of subducting Nasca plate, tectonic structure and volcanic activity of overriding South America plate.

Subduction Tectonics and Seismicity

A 3D-image of seismofocal surface of subducting slab was synthesized from filtered NEIC catalog data (Figure 1). Extrapolated strikes of the main fracture zones as well as locations of active volcanoes projected onto that surface revealed a clear segmentation of subducting mode and a linked clustering of active volcanoes confined by the fracture zones.

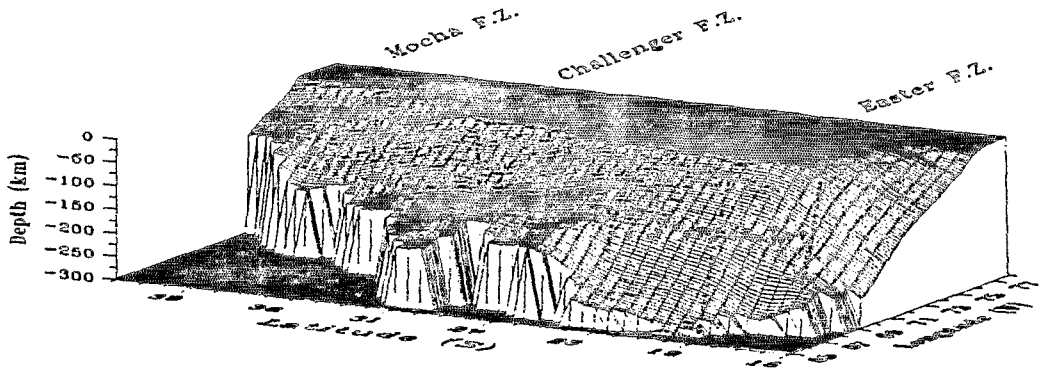

Fig. 1. The shape of Nazca plate subducting under Chile. Dotted lines are the fracture zones and inverted filled triangles are the "roots" of volcanoes (projections of locations of volcanoes onto the surface of the slab).

While the convergence velocity is almost constant (8.1 - 8.4 cm/yr) along the total subduction zone of Chile [DeMets et al., 1990], the age of oceanic lithosphere at the trench varies steadily from 5 m.y. at 45° S to 50 m.y. at 29.9° S, where the Challenger fracture zone intersects the trench (Figure 1,2).

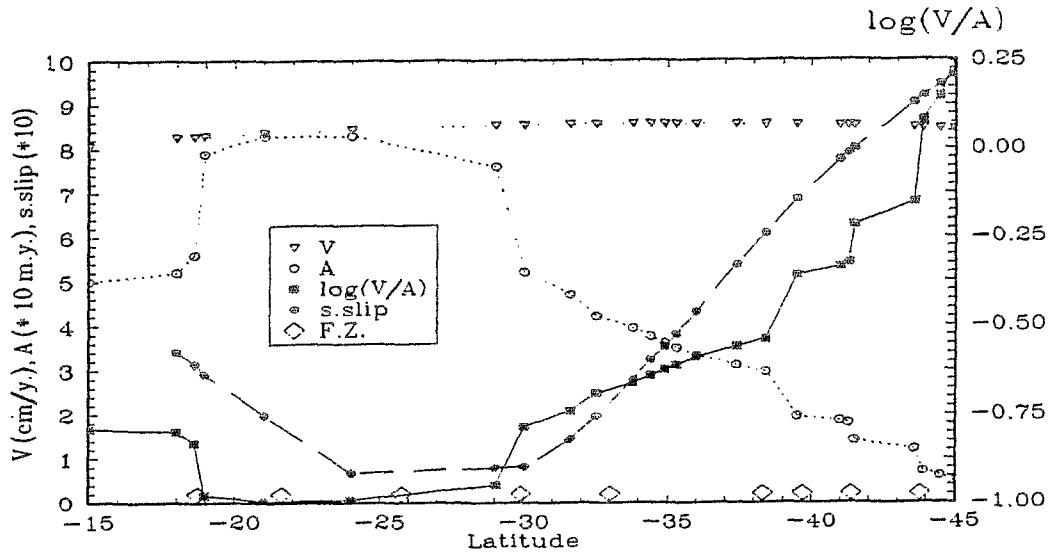

Fig. 2. Variation of age of Nazca plate at the trench, convergence velocity, parameter of coupling (log V/A), and seismic slip along the Chilean trench. Diamonds indicate the intruding points of main fracture zones at the trench.

At this site the age changes drastically up to 75-80 m.y., and drops again to 50 m.y. at the latitude of Easter fracture zone impingement, apr. 19° S [Herron, 1981; Mammerickx et al., 1975; Mayes et al., 1990]. The age of oceanic lithosphere and a state of its buoyancy [Molnar and Atwater, 1978] predominantly control the configuration of subducting slab, the trust and deep seismic regime, the tectonics and volcanism of overriding South-American plate. An important feature of Chilean subduction system is a prominent segment of flattening (apr. 25.5°S-33°S) and ceased volcanic activity (27°S-33°S). Apparently an oblique subduction

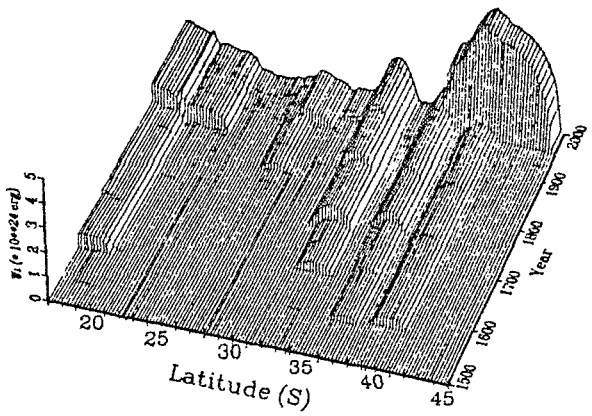

Fig. 3. A three-dimensional Time-Space plot of cumulative seismic energy release along the Chilean subduction zone based on the analysis of catalog of historical events.

of Juan Fernandez ridge [Nur and Ben-Avraham, 1981], and a concept of Gaussian curvature [Cahill and Isacks, 1992] are not convincing as mechanisms of that flattening. An ample distortion of dip and considerable stretching of deep edge of plate is clearly seen between 23°S-26°S, where the buoyancy of plate presumably changes from negative (A > 50 m.y.) to positive. The stretched part of slab conforms adequately to a big gap of deep seismicity (Figure 4).

An analysis of catalog [CERESIS, 1985] of great Chilean thrust earthquakes and the last revisions of a number of historical events [Comte and Pardo, 1991] (Figure 3) enables to estimate a distribution of cumulative seismic energy W, energy release rate W_r, and averaged seismic slip along the Chilean subduction zone (Figure 2). All these properties correlate well with the estimates of coupling between the Nazca and South America plates obtained from the V-model of viscous sedimentary layer interface [Kostoglodov, 1988]. The plate coupling growing up form 29° S to the South agrees with an increase of maximum magnitudes of great historical earthquakes and a rise of W_r. Relatively low values of W_r were obtained for the Northern part of Chile (19°S - 29°S), where the mode of subduction is closer to the "Island arc-type" [Uyeda and Kanamori, 1979]. For the Taltal area (22°S - 25°S) all historical events had magnitudes less than 8.0 (except M_w = 8.0 event, 9 December 1950), nevertheless the seismic coupling here could be of a sufficiently high level to yield earthquakes with a maximum magnitude up to M_w = 8.5.

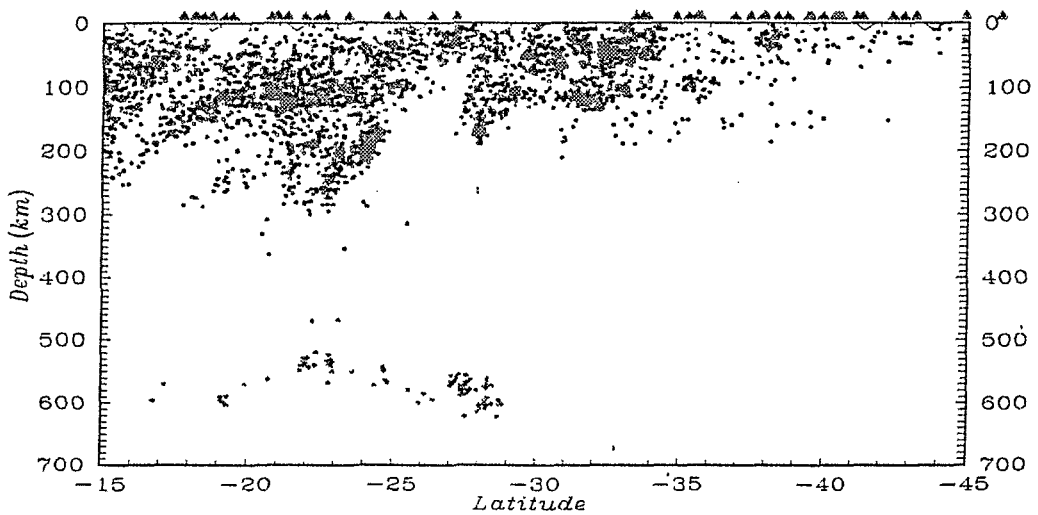

Fig. 4. Vertical projection of seismicity along the Chilean trench. Active volcanoes are shown as filled triangles. The detachment of deeper part of the slab may be to the South of 24°S.

An extended group of deep earthquakes (530-630 km) of Chile matches exactly the higher age zone of Nazca plate (Figure 4). The maximum depths of these events are in agreement with the thermal model of sinking slab with a depressed metastable olivin - shpinel phase transition boundary as a source of deep earthquake faulting [Kostoglodov, 1989]. This denies the hypothesis of Engebretson and Kirby [1992] of probable age discontinuity within the Nazca slab. The deep part of the slab could be fragmentary detached

at its southernmost part, where a marked change in dip and depth is observed (the zone of flattened slab).

The Space-Time plot for the historical catalog shows a probable tendency of North-South migration of strong events (M_w >7.0) with a rate of ≈ 7-8 km/y. which is in agreement with an estimate of Barrientos [1991].

REFERENCES

BARRIENTOS, S, 1991, Large events, seismic gaps, and stress diffusion in Central Chile, *Springer Verlag Vol. on Andean Geodynamics*, (submitted).

CAHILL, T., and **B.L.ISACKS**, 1992, Seismicity and shape of the subducted Nazca plate, *J. Geophys. Res., 97*, 17,503-17,529.

CERESIS, 1985 - Catalog of earthquakes for South America, Hypocenter and intensity data, Chile, Earthquake mitigation program in the Andean region (Project SISRA), Centro Regional de Sismología para América del Sur, Lima 14, Peru, Vol.5.

COMTE, D., and **M.PARDO**, 1991, Reappraisal of great historical earthquakes in the northern Chile and southern Peru seismic gaps, *Natural Hazards, 4*, 23-44.

DEMETS, C., R.G.GORDON, D.F.ARGUS, and **S.STEIN**, 1990, Current plate motions, *Geophys. J. Int., 101*, 425-478.

ENGEBRETSON, D., and **S.KIRBY**, 1992, Deep Nazca slab seismicity: Why is it so anomalous?, AGU 1992 Fall Meeting, *EOS*, 397.

HERRON, E.M., 1981, Chile margin near 38°S: Evidence for a genetic relationship between continental and marine geologic features or a case of curious coincidences?, in *Nazca plate: Crustal formation and Andean convergence, Geol. Soc. Am. Mem., 154*, 755-760.

KOSTOGLODOV, V.V., 1988, Sediment subduction: a probable key for seismicity and tectonics at active plate boundaries, *Geophys. J., 94*, 65-72.

KOSTOGLODOV, V.V., 1989, Maximum seismic depth and phase transition in the lithosphere descending into the mantle."Physics and interior structure of the Earth", (Reports of Soviet geologists on XXVII session of IGC, Washington, 1989), Moscow, Nauka, 52-57.

LOWRIE, A., and **R.HEY**, 1981, Geological and geophysical variations along the western margin of Chile near lat 33° to 36°S and their relation to Nazca plate subduction, in *Nazca plate: Crustal formation and Andean convergence, Geol. Soc. Am. Mem., 154*, edited by L.D.Kulm et al., 741-754.

MAMMERICKX, J., R.N.ANDERSON, H.W.MENARD, and **S.M.SMITH**, 1975, Morphology and tectonic evolution of the East-Central Pacific, *Geol. Sos. Am. Bull., 86*, 111-117.

MAYES, C.L., L.A.LAWVER, and **D.T.SANDWELL**, 1990, Tectonic history and new isochron chart of the South Pacific, *J. Geophys. Res., 95*, 8543-8567.

MOLNAR, P., and **T.ATWATER**, 1978, Interarc spreading and Cordilleran tectonics as alternates related to the age of subducted oceanic lithosphere, *Earth Planet. Sci. Lett., 41*, 330-340.

NUR, A., and **Z.BEN-AVRAHAM**, 1981, Volcanic gaps and the consumption of aseismic ridges in South America, in *Nazca plate: Crustal formation and Andean convergence, Geol. Soc. Am. Mem., 154*, 729-740.

UYEDA, S., and **H.KANAMORI**, 1979, Back-arc opening and the mode of subduction, *J. Geophys. Res., 84*, 1049-1061.

SEISMOTECTONICS OF THE CENTRAL PERUVIAN ANDES FROM PRECISE SEISMOLOGICAL DATA

R. Lindo[1,2], A. Cisternas[1], L. Dorbath[3,1] and C. Dorbath[3,1] and L. Rivera[1]

(1) Institut de Physique du Globe. 5 rue René descartes, 67084 Strasbourg, Cedex. France.
(2) Instituto Geofísico del Peru. Apartado 3747, Lima 100, Peru.
(3) ORSTOM, 213 rue La Fayette, 75480 Paris Cedex 10, France.

KEY WORDS: Central Andes, Seismotectonics, Subhorizontal Subduction, Microseismicity, Tectonics Stress, Local Tomography.

The Andean Cordillera is the result of the convergence between the Nazca and the South American Plates. The Central Peruvian segment is characterized by subhorizontal subduction, absence of recent volcanic activity and subsidence of the coastal region.

High quality seismic data obtained in five field seismic experiments with dense portable networks during the period 1980-86 have been used in order to obtain hypocenters, focal mechanisms, stress shape and orientation, and local tomography. The geometry of subduction, the velocity structure of the crust and upper mantle and the state of stress and deformation in Central Peru are thus determined. In particular, a cross section is made from the coastal area to the subandean region showing a precise picture of the subduction and the subandean crustal seismicity.

Stress tensors are obtained from focal mechanisms (Figure 1), both for the subduction zone under the coast, and for the subandean region. A comparison is made with the focal mechanisms calculated from teleseismic data, and a scale independent behaviour is established. A similar analysis is made for the Cordillera Blanca (North Peru) by using neotectonic and seismic information together. The resulting stress tensor is in a state of extension with a σ_3 axis oriented N60°, namely orthogonal to the trend of the Cordillera. This is consistent with the fact that the main tectonic feature is the outstanding Cordillera Blanca normal fault which strikes along the western margin of the chain.

Tomographic studies from P and S travel times show an uprising of high velocity lower crust material under the coast (Figure 2), a possible explanation for the presence of normal faulting related to bending at the continental shelf. Similar tomography in the subandean region (Figure 3) shows a thickening of the brittle crust due to continental subduction of the Brasilian Shield under the Eastern Cordillera.

Two recent earthquakes (1190, M_S = 6.5 and 1991, M_S = 6.8) in the Moyobamba region of the Subandean region of Norther Peru show thrusting at a low angle that may be continued into visible scarps at the surface, east of the epicenters. This mechanisms are compatible with the compressional stress regime obtained for the Subandean region of Central Peru.

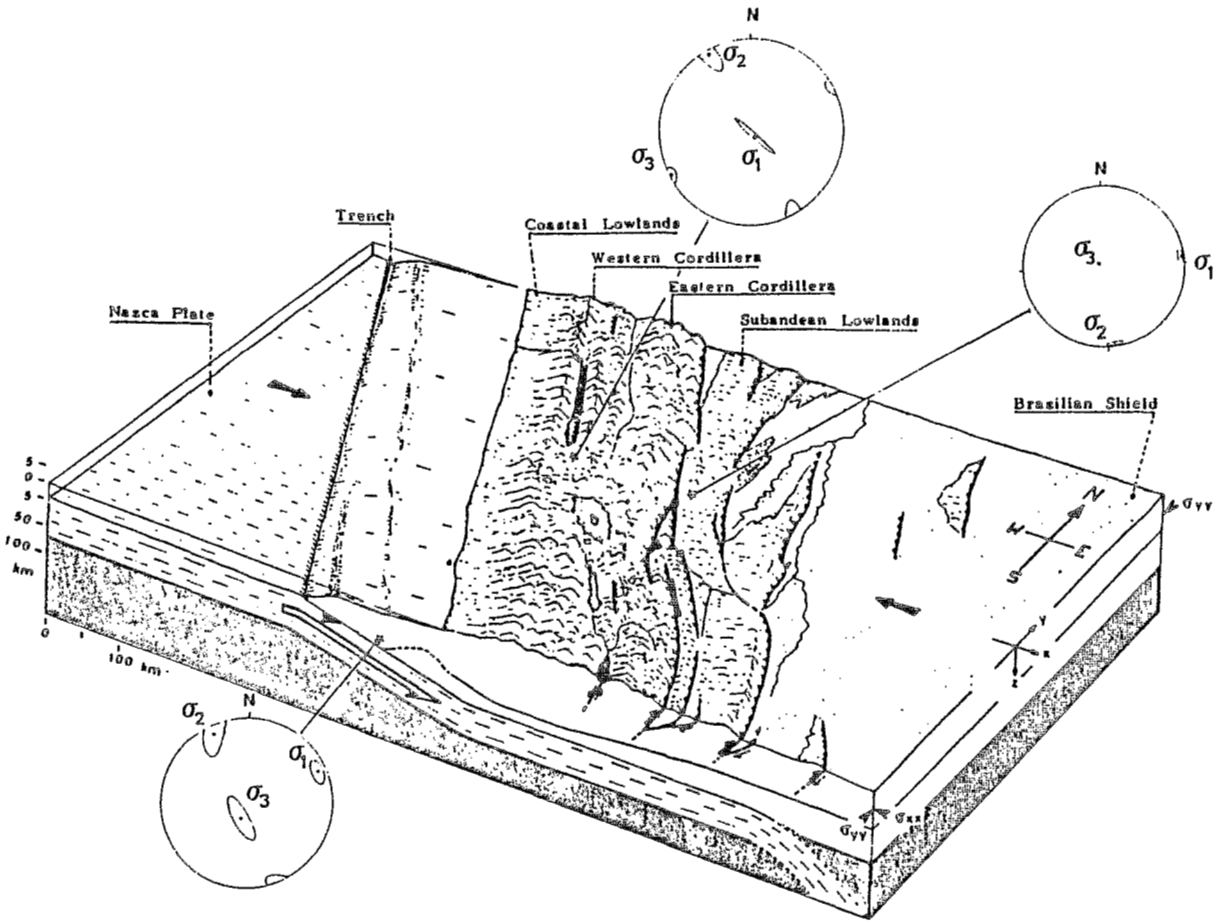

Figure 1: Principal axes of stress in the Coastal Subduction region, and in the Subandean region of Central Peru, and in the Cordillera Blanca, from focal mechanisms of local earthquakes (modified from Sébrier et al., 1988). Representation in the lower hemisphere of a Schmidt equal area projection.

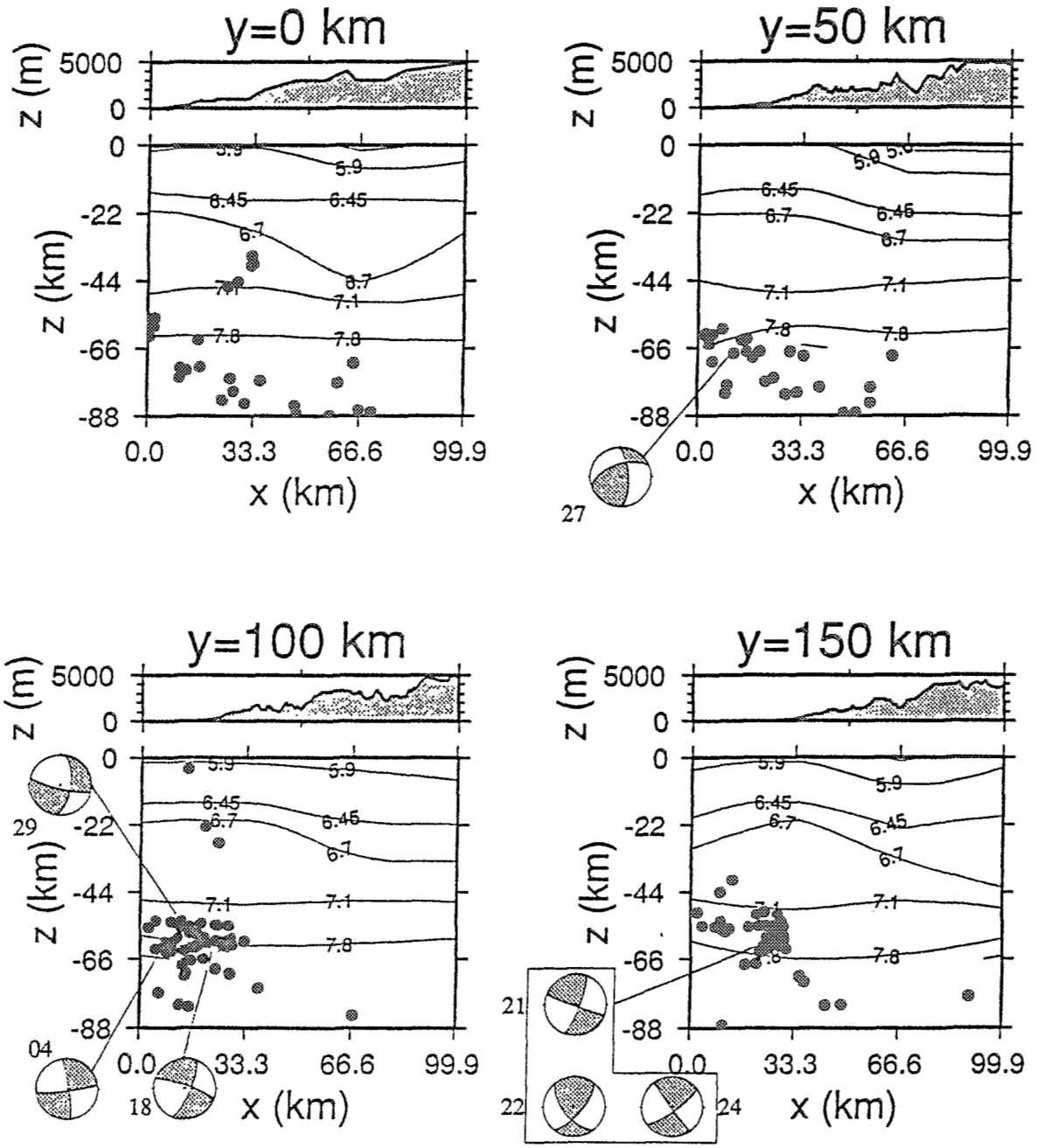

Figure 2: Vertical cross-sections (Azimuth N50°E) of tomography in the Coastal region of Central Peru showing: a) the seismicity within a 50 km wide block. b) focal mechanisms on a backside Schmidt projection. c) the topography. The y-values increase from south to north. The isovelocity line of 6.7 km/sec shows lower crust surrection under the Coastal region.

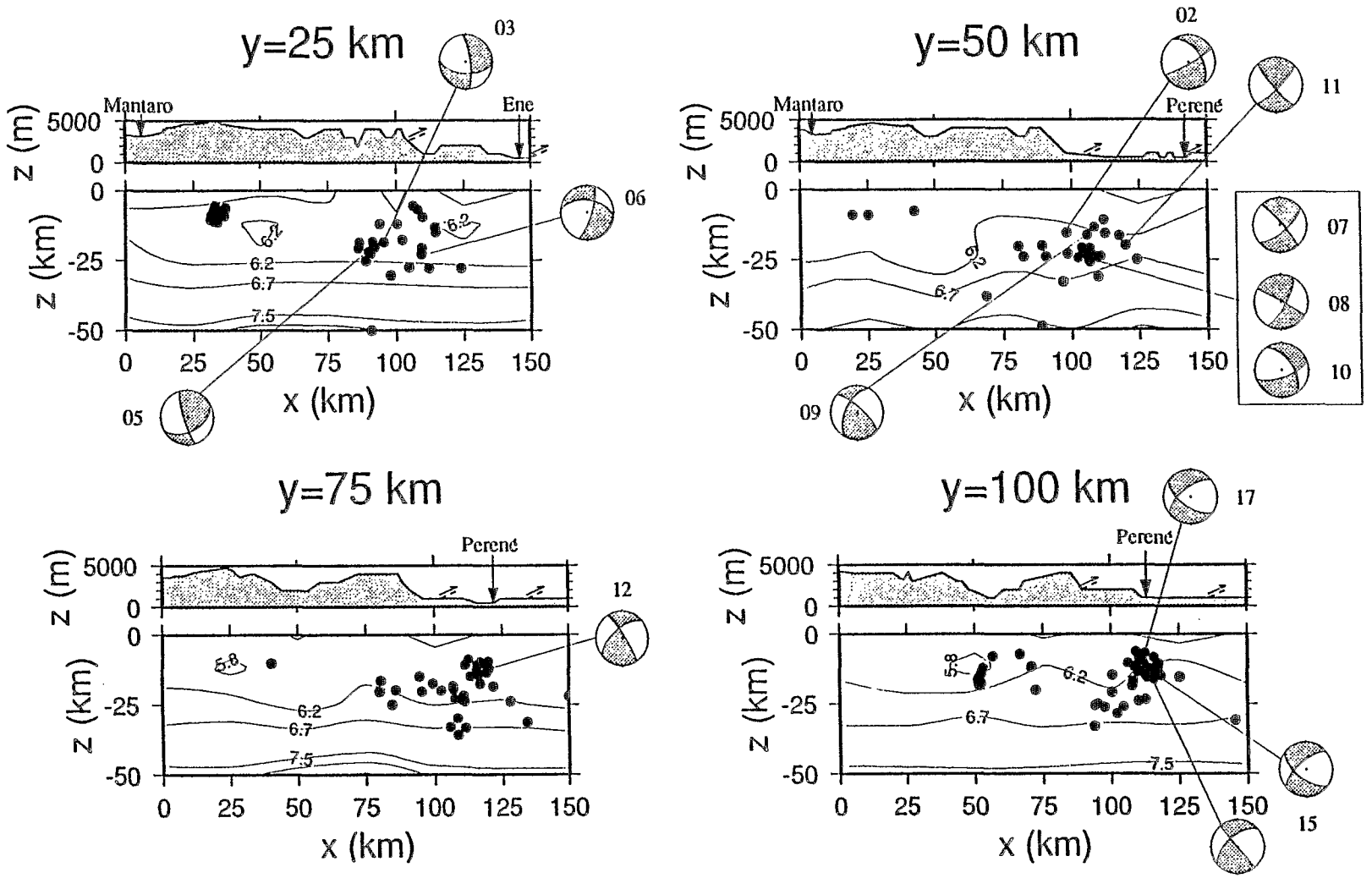

Figure 3: Vertical cross-sections (Azimuth N50°E) of tomography in the Subandean region of Central Peru showing: a) the seismicity within a 25 km wide block. b) focal mechanisms on a backside Schmidt projection. c) the topography, rivers Mantaro, Ene and Perene, and surface trace of thrusts. The y-values increase from south to north. The isovelocity line of 6.2 km/sec shows crustal thickening under the Andes.

COASTAL NEOTECTONICS IN PERU: SUBDUCTION REGIME AND QUATERNARY VERTICAL MOTIONS

José MACHARE[1] & Luc ORTLIEB[2]

[1] Instituto Geofísico del Perú, Apartado 3747, Lima 100, Perú
[2] ORSTOM-Antofagasta, Facultad de Recursos del Mar, Universidad de Antofagasta, Casilla 170, Antofagasta, Chile

RESUMEN: Los desplazamientos verticales que ocurren a lo largo de la costa peruana durante el Cuaternario muestran un patrón complejo en que interactúan la superestructura (subducción bajo la margen andina), las megaestructuras (dorsales asísmicas, estructura cortical del antearco), y las estructuras tectónicas locales. Se analiza la posible influencia de distintos factores geodinámicos en esta zona de subducción sobre la tectonica costera.

KEY WORDS: Neotectonics, vertical movements, subduction, Peru

INTRODUCTION

Neotectonic studies in coastal regions can include precise information on relative and absolute vertical deformation in the course of the last 1-2 my. Marine terraces and Pleistocene shorelines which indicate the former position of a referential horizontal plane (the geoid), at given instants of the past, provide useful data for the reconstruction of both local and regional vertical motions.

For a long time, the Peruvian coast has been recognized as an emergent area (Bosworth, 1922; Steinman, 1929; Broggi, 1946). Recent extensive work on the Peruvian marine terraces now provides a good overview of their distribution along the 3,000 km long coastal zone and also local detailed studies that include geochronological determinations. This work aims to analyze the Quaternary vertical motions, as deduced from marine terrace data, in the area 4°-19°S, and to investigate relationships that link the local/regional deformation pattern and several parameters of the subduction regime.

TECTONIC SETTING OF THE PRESENT-DAY SUBDUCTION IN PERU.

Subduction of the Nazca Plate beneath the South American Plate.

The contact between the Nazca and South American plates is figured on the ocean floor by the Peru-Chile Trench. The trench is grossly parallel to the Peruvian coast, although the shortest distance between these two features varies from 215 km (Trujillo, 9°S) to 65 km (Cabo Blanco-Talara, 5°S). For the last 10 my, at the latitude of Peru, the mean convergence strike and rate have remained stable around the respective values of N080°E and 10 cm/y (Pardo & Molnar, 1987).

The seismicity in Peru, which helps to document the subduction regime, include three groups of events: a) "interplate" events, directly associated to the subduction process and to the east-dipping Wadati-Benioff zone down to a 300 km depth; b) "intraplate" shallow events (<30 km), related to active faulting of the Andean system: and c) deeply-seated events (down to 700 km) which remain poorly understood. The earthquakes of the first group are by far those which release the greatest amounts of energy and elastic deformation.

Geology and structure of the Peruvian coast

The Peruvian coastal region lies upon the Andean forearc, between the trench and the Western Cordillera. During the Tertiary, several sedimentary basins developed on a basement formed by Precambrian and Paleozoic metamorphic rocks and Mesozoic volcano sedimentary arc terranes (Macharé, 1987). The late Tertiary tectonic activity was characterized by tensional stress with basin subsidence interrupted by short-lived compressive pulses that produced uplift of the basins. In Quaternary times, the continental shelf and the emerged coastal region experienced relatively complex and strong deformation: subsidence in the shelf area and vertical uplift motions along the coast that locally reached amplitudes of several hundred meters (up to 1 km, in either direction). The magmatic arc, located on the Western Cordillera, has been active, during the Quaternary, only south of latitude 15°S.

THE THREE SECTORS OF THE PERUVIAN COAST

The main characteristics of the Pleistocene marine terraces (elevation, chronology, deformations) and their distribution along the Peruvian coast were described in a series of papers and doctoral thesis (Sébrier, 1978; DeVries, 1984, 1986, 1989; Macharé, 1987; Hsu, 1988; Hsu et al., 1989; Ortlieb & Macharé, 1990a; Goy et al., 1992). Synthetic analyses of regional deformation deduced from marine terrace data were recently performed in the southern sector of the Peruvian coast (Ortlieb & Macharé, 1990b; Macharé & Ortlieb, 1991, 1992; Hsu, 1992).

The northern Peruvian coast, between 4° and 6°S, shows evidence of uplift motions with mean rates of the order of 150-200 mm/10^3y. Local tectonic factors, including block tilting, upwarping and faulting activity, account for some variations of this mean regional uplift rate and for the geometric deformation of the northern coast "tablazos". Late Quaternary (=last 125 ky) tectonic activity, characterized by differential uplift of the Illescas faulted block and the northernmost Peruvian coastal region, is evidenced by the attitude of the well-preserved Lobitos tablazo. The steeply dipping faults which deformed the tablazos (with either dip-slip or strike-slip motion) seem to be inherited from Tertiary structures.

The 950-km long central sector of the Peruvian coast (6°-14°S) does not show remnants of Quaternary marine terraces. This particularity may be due either to subsident motions or to a relative stability of the coastal region (lack of net uplift motions)(Sébrier & Macharé, 1980; Ort-

lieb & Macharé, 1990). Quaternary tectonic structures in the central sector consist in normal faults that strike perpendicularly or obliquely to the coastline and which produced only small net displacements.

As mentioned above, the southern Peruvian coast (14°-18°30'S) received much attention in the last few years. It was shown that most of the area has been uplifted at a rather homogeneous rate (80-180 mm/10^3y) during Quaternary times. However, marine terrace data indicate that the area between Lomitas (14.6°) and Lomas (15.3°S) experienced mean uplift rates ranging from 300 to 430 mm/10^3y; during the Late Quaternary, this area was uplifted at a higher rate (400-500 mm/10^3y), whith a maximum rate observed in the surroundings of San Juan Marcona (700 mm/10^3y)(Ortlieb & Macharé, 1990a). The rapid Quaternary uplift motions registered at San Juan Marcona, which are the strongest reported in South-America, were used in distinct attempts of modeling the influence of the Nazca Ridge subduction (Moretti, 1987; Macharé, 1987; Hsu, 1988, 1992; Macharé & Ortlieb, 1992).

SUBDUCTION RELATED PARAMETERS AND VERTICAL DEFORMATION

As observed on most active continental margins, the subduction regime seems to induce regional crustal uplift of the coastal areas lying above the interplate contact. Examples were provided in peri-Pacific regions (Ota, 1986), the Aegean area (Mercier et al., 1979), Indonesia (Pirazzoli, 1991), etc.. However, this empirical relationship has never been plainly explained. It is possible that the heat accompagnying the subduction process plays a role (thermal dilatation), and/or that isostatic mechanisms are involved.

At a regional scale, the uprising sectors of the Peruvian coast may thus be viewed as showing a "normal" tectonic behaviour in the context of subduction below a continental margin, while the subsident (or "stable") sector of central Peru would appear as "anomalous".

Jarrard (1986) tested possible relationships between a series of subduction parameters, among 39 case areas, by using multivariate analysis. Unfortunately he did not include any parameter "uplift rate of the overriding plate", probably because of the paucity of reliable data in most areas.

The close relationship between the subduction of the Nazca Ridge and the strong uplift motions of the Lomitas-Lomas sector was already addressed (if not fully understood). The fact that the highest uplift rates recorded in the north Peruvian coast (Cabo Blanco) are located at the latitude of the Sarmiento Ridge is probably significant. The N055°E trending, and 1600-m high relief of this ridge that is subducting beneath the Cabo Blanco-Paita area is thought to produce a deformation pattern similar to the one described in the area affected by the subduction of the Nazca Ridge.

The distance from the trench axis to the coastline is definitely shorter for the sectors that experienced high uplift rates than for the central coast of Peru. This distance is in the range 65-115 km in northern Peru, 80-180 km in southern Peru, and 135-215 km in the central coast sector. Thus there may be some link between the two parameters, even if the relationship is apparently not direct and proportional.

A coincidence is noted between the loci of the Quaternary marine terraces and the main outcrops of the Cordillera de la Costa basement. This major unit is an Andean-trending forearc structure preserved on the southern and northern coastal sectors, and which is sunk offshore central

Peru, to form the Outer Shelf High. Quaternary vertical motions thus appear in some way related to older deformation patterns.

Finally, at a smaller scale, differences in uplift motions within uprised coastal sectors are probably related to local/regional structures that follow a general N-S trending effective horizontal stress (Mercier et al., 1992).

In conclusion, our analysis suggests that in Peru the type and rate of coastal vertical motions are rather independent from the rate and strike of the convergence, the obliquity of the convergence relative to the coastline, the slab age and the slab dip. On the contrary, some relationship is envisioned with the presence of Precambrian/Paleozoic basement (Cordillera de la Costa), the distance between the trench and the present coastline, the crustal structure and the density distribution in the upper crust. The relationship between vertical Quaternary movements and the seismic activity (magnitude and frequency of the events) still remains poorly understood.

REFERENCES

BOSWORTH, T.O., 1922. *Geology of the Tertiary and Quaternary periods in the northwestern part of Peru.* McMillan Co. 434 p.

BROGGI, J.A., 1946. *Bol. Soc. Geol. Peru*, 19:21-33.

DeVRIES, T.O., 1984. *Bol. Soc. Geol. Peru*, 73: 1-14.

DeVRIES, T.O., 1986. PhD, Ohio State Univ., 108 p.

DeVRIES, T.O., 1989. *J. South-Amer. Earth Sci.*, 1: 121-136.

GOY, J.L., MACHARE, J., ORTLIEB, L., ZAZO, C., 1992. *Quatern. Intern.*, 15/16: 99-112.

HSU, J.T., 1988. PhD, Cornell Univ., 310 p.

HSU, J.T., LEONARD, E.M., & WEHMILLER, J.F., 1989. *Quatern. Sci. Rev.*, 8: 255-262.

HSU, J.T., 1992. *Quatern. Intern.*, 15/16: 87-97

JARRARD, R.D., 1986. *Rev. Geophys.*, 24 (2): 217-248.

MACHARE, J., 1987. Thèse Doct.Sc., Univ.Paris-XI,389 p.

MACHARE, J. & ORTLIEB, L., 1991. VII Congr. Peruano Geol., Abstr. vol., 35-39.

MACHARE, J. & ORTLIEB, L., 1992. *Tectonophysics*, 205:97-108.

MERCIER, J.L., DELIBASSIS, N., GAUTHIER, A., JARRIGE J.J., LEMEILLE, F., PHILIP, H., SEBRIER, M. & SOREL, D., 1979. *Rev. Geol. Dyn. Geogr. Phys.*, 21 (1): 68-92.

MERCIER, J.L., SEBRIER, M., LAVENU, A., CABRERA, J., BELLIER, O., DUMONT, J.F. & MACHARE, J., 1992. *J. Geophys. Res.*, 97 (B8): 11945-11982.

MORETTI, I., 1982. Thèse Doct. Univ., Univ. Paris-XI, 107 p.

ORTLIEB, L. & MACHARE, J., 1990a. *Bol. Soc. Geol. Peru*, 81: 87-106.

ORTLIEB, L. & MACHARE, J., 1990b. Symp. Géodynamique andine, ORSTOM, Abstr. vol., 95-98.

ORTLIEB, L., GHALEB, B., HILLAIRE MARCEL, C., MACHARE, J. & PICHET, P., 1990. VII Congr. Peruano Geol., Abstr. vol., 511-516.

OTA, Y., 1986. *Roy. Soc. New Zealand Bull.*, 24: 357-375.

PARDO, F. & MOLNAR, P., 1987. *Tectonics*, 6 (3): 233-248.

PIRAZZOLI, P., RADTKE, U., HANTORO, W.S., JOUANNIC, C., HOANG, C.T., CAUSSE, C. & BOREL BEST, M., 1991. *Science*, 232: 1834-1836.

SEBRIER, M., 1978. Contrib. Inst. Geofis. Peru, 78-1, 29 p.

SEBRIER, M. & MACHARE, J., 1980. *Bull. Inst. fr. Et. andines*, 9: 5-22.

STEINMAN, G., 1929. Proc. IV Pacific Sci. Congr. (Java), 7 p.

RECENT SEISMICITY ($m_b \geq 5.4$) IN NORTHWESTERN VENEZUELA: REGIONAL TECTONIC IMPLICATIONS

Gustavo MALAVE[1,2] and Gerardo SUAREZ[1]

(1) UACPyP, Instituto de Geofísica, UNAM, Ciudad Universitaria, 04510, México, D.F., México
(2) INTEVEP, S.A. Apartado Postal 76343, Caracas 1070A, Venezuela.

RESUMEN: El análisis de la sismicidad de magnitud moderada ($5.4 \leq m_b \leq 5.9$) ocurrida recientemente en el Occidente de Venezuela, ha permitido determinar los parámetros focales de esos sismos y su relación con la tectónica regional. Los resultados obtenidos muestran que dicha sismicidad está asociada principalmente a los sistemas de fallas secundarios y no a los principales sistemas de fallas de Oca-Ancón y Boconó, los cuales han sido postulados como la antigua y actual frontera entre las placas Caribe y Sur América en esta región.

KEY WORDS: Caribbean, Venezuela, Andes, seismicity, tectonics, inversion.

INTRODUCTION

The border between the Caribbean and South American plates in western Venezuela has been a source of controversy in understanding the tectonics of the Caribbean region. The motion on the southeastern Caribbean plate boundary is accommodated mainly by major right-lateral, strike-slip faults like El Pilar and Morón. Towards the west, the continuation of the plate boundary is not clear. The Boconó fault is a right-lateral, strike-slip fault systems which has been postulated to be the boundary between these two plates in western Venezuela (e. g., Dewey, 1972; Schubert, 1982; Soulas, 1986). Most of the seismotectonic studies in this area are based on the analysis of the microseismicity recorded locally by temporary networks, neotectonic field work, and first-motion focal mechanisms. The occurrence of seismicity of moderate to large magnitude ($M \geq 5.0$) associated with this plate boundary is relatively poor. Furthermore, the low relative velocity between the Caribbean and South American plates implies long recurrence periods for large earthquakes, rendering more difficult the evaluation of the seismic hazard in this zone.

In this study, we analize the seismicity $m_b \geq 5.4$ which has occurred in western Venezuela from 1964 to 1992 (15 earthquakes) in order to correlate it with the active faults in the area. The source parameters were determined by the epicentral relocation and the formal inversion of the long period body waves (Nábelek, 1984) recorded at teleseismic stations. Because of a low signal to noise ratio, some of the events were studied through the waveform inversion of the short period body waves. The results show that only the July 19, 1965 earthquake nucleated on the Boconó fault system. The other earthquakes are apparently associated with secondary fault systems. Another important point of this work was to determine the depth of the earthquakes. Most of the events studied here, in particularly those in the soutwest area of Venezuela, have been reported with a depth of 40 km on average, whereas the maximum depth determined by the inversion is of 27 km. The only exception is the intermediate depth earthquake of November 11, 1968.

TECTONIC SETTING

The main tectonic features of Western Venezuela are associated with the interaction between the Caribbean and South American plates. There are several models that explain the relative motion between the Caribbean and its neighboring plates (Jordan, 1975; Sykes et al., 1982; Stein et al., 1988). In general, those models agree that the Caribbean plate has a low absolute velocity in a hot-spot reference frame, and that it is moving predominantly eastwards with respect to both the North and South American plates (Dewey and Suárez, 1991). The relative motion between the Caribbean and South American plates does not seem to be concentrated along a single fault system. Apparently it is distributed over a wide zone of deformation along the Boconó, Morón, and El Pilar fault systems (e. g., Soulas, 1986).

Slip-rates measured at the Oca-Ancón and Boconó fault systems are lower than the predicted relative velocities between the Caribbean and South American plates. Slip-rates of the Boconó fault, measured from the offset of Pleistocene moraines, range from 0.3 cm/yr to 1.4 cm/yr (e. g., Schubert, 1982; Soulas, 1986), whereas the predicted slip rate ranges from 2 to 4 cm/yr. The last great earthquake (Ms=7.8) along the Boconó fault was on March 26, 1812. Aggarwal et al. (1983) suggested that the present movement observed on the Boconó fault began probably during the Plio-pleistocene. The present rate of motion of the Oca-Ancón fault system is in the range of 2.5 to 4.0 mm/yr. However, it appears that during the last 4 m. yr. the Oca-Ancón fault system was moving faster than it is doing at present (Soulas et al., 1987).

Besides these two major fault systems, there are several faults in western Venezuela that appear to be seismically capable (Soulas, 1986). Some of them have a NE-SW direction, parallel to the Boconó fault (e.g., Caparo, NW Piedemonte, SE Piedemonte) and others have a N-S orientation and splinter off the Boconó fault (e. g., Valera, Humocaro, Icotea). Soulas (1985) suggested that the lower velocity observed on the southwest segment of the Boconó fault takes place because the Caparo fault absorbs a fraction of the right-lateral, strike-slip relative motion between the Caribbean-South American plates.

DISCUSSION OF RESULTS

A summary of the results obtained in this study are shown on Table 1 and Figure 1. The recent shallow seismicity in western Venezuela is apparently associated with the secondary fault systems of the region and not with the main fault systems such as Oca-Ancón or Boconó. Only the July 19, 1965 earthquake (event 1 on Figure 1) appears to take place on the Boconó fault system, indicating a right-lateral, strike-slip focal mechanism. The Caparo fault has been the most active feature in the region during the last three decades. The earthquakes of January 27, 1970, May 5,1979, and July 4, 1982 (events 4, 9, and 11) show a right-lateral, strike-slip-faulting mechanisms and were generated probably on this fault. This assumption agrees with the hypothesis of Soulas (1985) that the Caparo fault plays an important role in absorbing a fraction of the Caribbean-South American relative movement. Other faults that show frequent activity in the zone are SE Piedemonte and Humocaro. The events of March 5, 1975 (6) and December 11, 1977 (8) could be attributed to the SE Piedemonte fault. They both show reverse-faulting focal mechanisms, indicating the presence of E-W horizontal compression, oblique to the Venezuelan Andes. The most recent earthquake of magnitude $m_b \geq 5.4$ in Western Venezuela occurred on August 17, 1991 (16). Both this event and that of April 5, 1975 (7) appear to have nucleated on the Humocaro fault, with a left-lateral, strike-slip-faulting displacement. There was an important seismic secuence in northwestern Venezuela during April-May 1989 (events 14 and 15). Those earthquakes have the peculiarity of being multiple rupture processes that originated long body wave trains and induced intense liquefaction in many of the towns located near the epicentral area (Malavé and Suárez, 1993). These earthquakes were generated probably on a fault system trending in the NW-SE direction, with a right-lateral, strike-slip mechanism. The event of October 20, 1969 (3) apparently occurred on the northern end of the El Tigre fault, showing left-lateral, strike-slip solution. This motion agrees with that postulated by Rod (1956) for that fault. The earthquake of July 18, 1986 (event 12) is a reverse faulting focal mechanism. It is not very clear to which fault it could be related, since the motion observed on faults in this region is right-lateral strike-slip, tensional, or a combination of both. On July 12, 1988 (13) a predominantly tensional event occurred inside Lake Maracaibo. Unfortunately, the epicenter of this earthquake lies in a highly faulted

zone, where it is difficult to correlate it with a specific fault. However, the regional trend in Lake Maracaibo shows several en-echelon, left-lateral strike-slip faults oriented in a N-S direction, and pull-apart basins developing between the faults. We suspect this event beneath Lake Maracaibo was probably associated with one of these pull-apart basins. The event of October 18, 1981 (10) is located near the place where Soulas (1985) has postulated that right-lateral, strike-slip motion on the Boconó fault system changes to reverse faulting. There are several faults in this region showing reverse faulting with an important component of strike-slip motion, in agreement with the focal mechanism of this earthquake. The event of November 17, 1968 (2) is different from all the other mentioned above. All of them are shallow earthquakes, whereas this is an intermediate-depth event (166 km). Its fault plane solution shows the T axis dipping at 44° to the southeast. This event probably occurred within the slab subducted in northern Colombia and Venezuela. In order to compare this event and those of the Bucaramanga nest, 200 km to the south, we modeled the event of August 30, 1973 (5) that occurred in the nest. Both earthquakes show a very similar orientation of the T axes. Finally, examining the direction of principal stresses, the results of this study consistently show horizontal compression in the E-W direction in southwestern Venezuela and in a NW-SE to NNW-SSE direction in northwestern Venezuela.

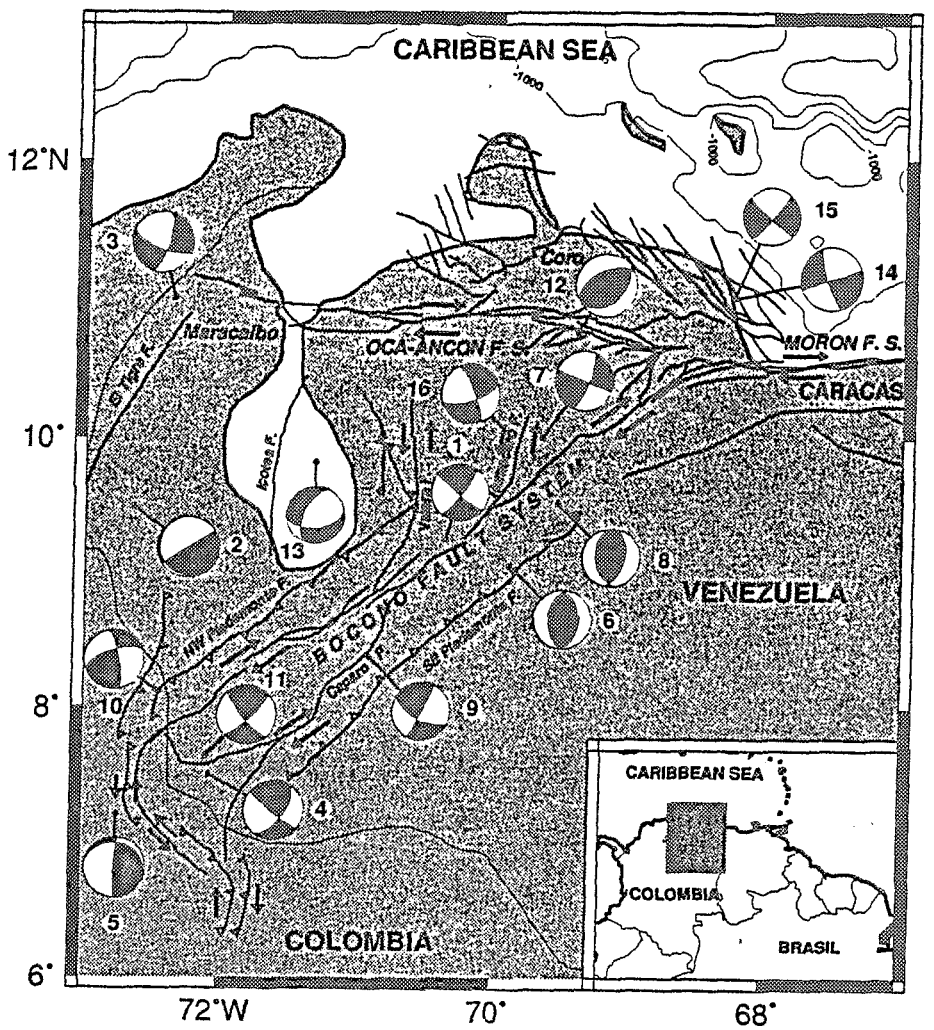

Figure 1. Fault mechanisms determined in this study for earthquakes $m_b \geq 5.4$ occurred in Western Venezuela from 1964 to 1992. The faults are from Soulas, 1986 and Singer et al., 1992. The arrows show the direction of relative motion of the faults. The shadow area in focal mechanisms indicates compressional arrivals. The reference numbers in focal mechanisms are the same on Table 1.

TABLE 1. COMPILATION OF FOCAL MECHANISM SOLUTIONS

Event	Date	Strike°	Dip°	Rake°	Depth(km)	Mo(10^{18}Nm)	Fault
1	650719	38	82	172	14	0.11	Boconó
2	681117	58	90	-82	166	0.81	Subduction
3	691020	16	73	-22	8	0.63	El Tigre
4	700127*	36	61	171	12	-	Caparo
5	730830	183	86	107	175	2.82	Bucaramanga
6	750305	184	47	93	14	0.29	SE Piedemonte
7	750405	21	75	-2	10	0.95	Humocaro
8	771211	173	42	75	8	1.06	SE Piedemonte
9	790505**	28	88	155	16	-	Caparo
10	811018	349	77	28	28	0.82	not known
11	820704*	46	78	166	11	-	Caparo
12	860718	49	41	78	7	0.14	not known
13	880712	83	50	-44	13	0.03	not known
14	890430	162	78	-178	14	3.51	Offshore
15	890504	133	83	-172	12	0.24	Offshore
16	910817	72	69	-169	15	0.12	Humocaro

* Short-period P wave inversion (only waveform), ** Long-period body wave inversion (only waveform)

REFERENCES

AGGARWAL, Y. P., J. P. SOULAS, and D. GARCIA, 1983, Contemporary Tectonics of the Venezuelan Andes and Northern Colombia, X Caribbean Geological Conference, Cartagena, Colombia (abstract).

DEWEY, J., 1972, Seismicity and tectonics of western Venezuela, Bull. Seismol. Soc. Am. 62, 1711-1751.

DEWEY, J. and G. SUAREZ, 1991, Seismotectonics of Middle America, in SLEMMONS, D. B., E. R. ENGDAHL, M. D. ZOBACK, and D. D. BLACKWELL, eds., Neotectonics of North America: Boulder, Colorado, Geological Society of America, Decade Map Volume 1.

JORDAN, T. H., 1975, The present-day motions of the Caribbean plate, J. Geophys. Res, 80, 4433-4439.

MALAVE, G. and G. SUAREZ, 1993, The Boca del Tocuyo earthquake in Northwestern Venezuela: Intense liquefaction induced by a complex rupture process?, Submitted to Bull. Seismol. Soc. Am.

NABELEK, J., 1984, Determination of earthquake source parameters from inversion of body waves, Ph.D. thesis, Massachusetts Institute of Technology, Cambridge, 361 p.

ROD, E., 1956, Strike-slip faults of northern Venezuela, Am. Assoc. Pet. Geol. Bull., 40, 457-476.

SCHUBERT, C., 1982, Neotectonics of Boconó fault, western Venezuela, Tectonophysics 85, 205-220.

SINGER, A., F. AUDEMARD, C. BELTRAN, J. A. RODRIGUEZ, F. De SANTIS, A ADRIANZA, C. CHACIN, M. LUGO, J. MENDOZA, and C. RAMOS, 1992, Actividad tectónica cuaternaria y características sismogénicas de los sistemas de fallas de Oca-Ancón (tramo oriental), de la península de Paraguaná y región de Coro y de la costa nororiental de Falcón, FUNVISIS (unpublished report).

SOULAS, J. P., C. ROJAS, A . SINGER, C. BELTRAN and M. LUGO, 1985, Actividad cuaternaria y características sismogénicas de las fallas de Boconó, Valera, Tuñame, Piñango, Piedemonte, Burro Negro-Mene Grande y otras, FUNVISIS (unpublished report).

SOULAS, J. P., 1986, Neotectónica y tectónica activa en Venezuela y regiones vecinas, Memorias VI Congreso Geológico Venezolano, Caracas, X, 6639-6656.

SOULAS, J. P., C. GIRALDO, D. BONNOT, and M. LUGO, 1987, Actividad cuaternaria y características sismogénicas del sistema de fallas Oca-Ancón y de las fallas de Lagarto, Urumaco, Río Seco y Pedregal, FUNVISIS (unpublished report).

STEIN, S., Ch. DeMETS, R. G. GORDON, J. BRODHOLT, D. ARGUS, J.F. ENGELN, P. LUNDGREN, C., STEIN, D. A WIENS, and D. F. WOODS, 1988, A test of Alternative Caribbean plate Relative Motions Models, J. Geophys. Res., 93, B4, 3041-3050.

SYKES, L., W. R. McCANN, and A. L. KAFKA, 1982, Motion of Caribbean plate during last 7 million years and implications for earlier Cenozoic movements, J. Geophys. Res., 87, B13, 10656-10676.

Neotectonics at Laguna Lejia, Atacama Desert, Northern Chile.

Steve Matthews and Claudio Vita-Finzi.

Department of Geological Sciences, University College London, Gower Street, London, WC1E 6BT.

The location of young faults in the Central Andean Cordillera is often difficult due to the blanket of ignimbrites and other volcanic structures. Alignments of volcanic centres often indicate the presence of large fractures which channel magma in the upper crust. In the area around Toconao, near San Pedro de Atacama, lineaments of this type fall into two groups; N-S alignments which can often be traced for hundreds of kilometres, and NW-SE alignments which may be tens of kilometres long. These lineaments commonly do not correspond to any surface expression of fault movements, and many of them are probably not tectonically active.

A NW-SE lineament joins a series of domes and vents of Cerro Tumisa (approximately 2 m.y.) with a large isolated dome and a basaltic maar eruption. This lineament, the "Tumisa Line", passes under the southern margin of a small salar, or salt lake, known as Laguna Lejia. To the west of the Laguna is a large N-S lineament, the Miscanti Line. This passes through the active Volcan Lascar and a series of elongate dacite domes (5 m.y.) to the north, southwards through Cerro Lejia and Volcan Miscanti.

The southern shore of Laguna Lejia is represented by a lava flow from a nearby volcanic centre. Two distinct raised beaches can be seen on this lava. These are probably due to post-glacial shrinkage of the laguna. Sediments on the southern margin are uplifted and buckled, forming an uneven platform. A section through these consists of interbedded laminated carbonates and coarser lithic-rich siltstones and sandstones. These contain concentrations of thin carbonate tubes, representing

precipitation of carbonate around flamingo feathers which have since decomposed. At least three earthquakes are indicated by recumbent folding and disruption of the beach sediments, followed in each case by a return to laminated carbonate facies. This sequence may represent a gradual upwarping of the southern shore, interrupted by violent resubmergence during earthquakes. It is likely that the Tumisa Line has recently been the locus of earthquake activity since the last glaciation, despite the absence of a fault scarp in the area. In small salars such as Laguna Lejia, it is difficult to distinguish tectonic movements from lake level changes due to climatic effects. It is hoped that a dated section through the sediments will yield information on earthquake frequency and uplift rates.

SOURCE PROCESS AND RUPTURE HISTORY OF THE 3 MARCH 1985 CENTRAL CHILE EARTHQUAKE

Carlos MENDOZA[1], Stephen HARTZELL[2], and Tony MONFRET[3]

(1) U.S. Geological Survey, National Earthquake Information Center, Box 25046, MS 967, Denver Federal Center, Denver, Colorado 80225, USA.
(2) U.S. Geological Survey, Box 25046, MS 966, Denver Federal Center, Denver, Colorado 80225, USA.
(3) Mission ORSTOM, casilla 53390, Correo Central, Santiago 1, CHILE

RÉSUMÉ: Nous avons obtenu par inversion simultanée des données d'accélérométrie, des ondes de volume télésismiques et des ondes de Rayleigh de très longue période, l'histoire du processus à la source du séisme du 3 mars 1985, du Chili central. Cette histoire est aussi confirmée par l'inversion des ondes de volume télésismiques. La modélisation du mécanisme de rupture est donc simple, et ne nécessite pas une composante lente du déplacement pour expliquer l'amplitude observée des ondes de longue période.

KEY WORDS: rupture history, inversion, rise time, seismic moment, source duration.

INTRODUCTION

The use of finite-fault inversion schemes has become relatively common in the study of large earthquake ruptures. They have been applied to near-source strong ground motions and teleseismic body-wave observations to identify the spatial and temporal rupture pattern as a function of position on the fault. To date, seismic data recorded at period longer than 100 sec have not been readily considered in finite-fault studies though they provide information on the overall size and duration of the earthquake.

In this study, we were interested in the large 7.8 Ms Central Chile seismic event of 3 March 1985 . We apply a linear, point -by- point inversion scheme to the long-period Rayleigh waves, in addition to near-source strong motions and teleseismic body-waves, to infer the source properties of the earthquake rupture. For this event, the seismic moment calculated using surface waves and geodetic data are consistently greater than determined using teleseismic body waves. This discrepancy in estimated seismic moment has led some to suggest that the 1985 Chile earthquake involved a slow component of fault slip that radiated little or no body-wave energy. Moreover, the rupture length as the depth extent of faulting are also not well constrained.

Our results indicate however that a single rupture model with a variable dislocation rise time can explain the entire suite of observations well, and it is not necessary to introduce a significant component of slower fault motion to reconcile the long-period Rayleigh-wave amplitudes.

FINITE-FAULT INVERSION

1) Seismic waveform data

Our set of data consist of local strong ground motion records, teleseismic body-wave from the GD-

SN and surface-wave from GEOSCOPE and IDA networks. All the data were corrected for the response of the instrument and bandpass-filtered with a Butterworth filter. The strong motion records were integrated to velocity and filtered from 2.0 to 7.5 sec. Body- and surface-wave records include teleseismic P and SH waveforms filtered at intermediate-periods and very long-period R1, R2 and R3 vertical fondamental Rayleigh wave trains bandpass-filtered from 100 to 350 sec.

2) Method

The procedure requires placing a fault plane in the earthquake source region and subdividing it into a finite number of subfaults. Synthetic Green's functions are then generated for each subfault assuming a dislocation rise time of finite duration and a constant propagation of rupture away from the hypocenter (Hartzell, 1989). Nevertheless, we relax the restriction of a fixed triangular rise time by using a time-window approach that allows multiple consecutive slip intervals that discretize the subfault rise time and rupture time. In this approach, the slip function at any point on the fault is approximated by a discrete number of boxcars of fixed duration and variable amplitude. The inversion then solves for the contribution of slip within each time window thus allowing for a variable subfault rise time and relaxing the constraints of fixed rupture velocity.

Strong-motion and teleseismic body-wave synthetics were calculated using local crustal velocities. Surface-wave synthetics were calculated from the PREM model. Synthetic waveforms were bandpass-filtered in the same way as the data.

Following Choy and Dewey (1988), we identify a realistic fault geometry for the 1985 event: the fault has a srtike of 5° and consists of two separate segments with different dips and rakes. The upper segment has a dip of 15° and a rake of 90° and the lower portion a dip of 30° and a rake of 110°. The two fault segments meet at a depth of 26 km.

3) Teleseismic body-wave analysis

The 1985 Chile earthquake is characterized by a series of multiple events that are well separated in time in the recorded P waveform. Choy and Dewey (1988) identify three distinct P arrivals, including two precursory phases (ms1 and ms2) prior to the main shock (MS).

In this study, we concentrate our analysis on the MS portion of the recorded waveforms to constrain the location and depth of the principal moment release. The nucleation point of this MS event is at a depth of 40 km in the lower segment of the hinged fault (Choy and Dewey, 1988). Slip distribution obtained by inverting the MS teleseismic body waveform show four regions of peak slip on the fault (Fig.1). The corresponding seismic moment is 1.2×10^{28} dyne-cm. This value is computed by summing the individual subfault moments over the entire fault. The most intense moment release occurred in the vicinity of the hypocenter and lesser, but significant, moment release occurred on the southern portion of the fault. Rise times observed for the zones of maximum slip vary between 10-15 sec. The nucleation point of the mainshock MS at a depth of 40 km reaches a depth of about 55 km.

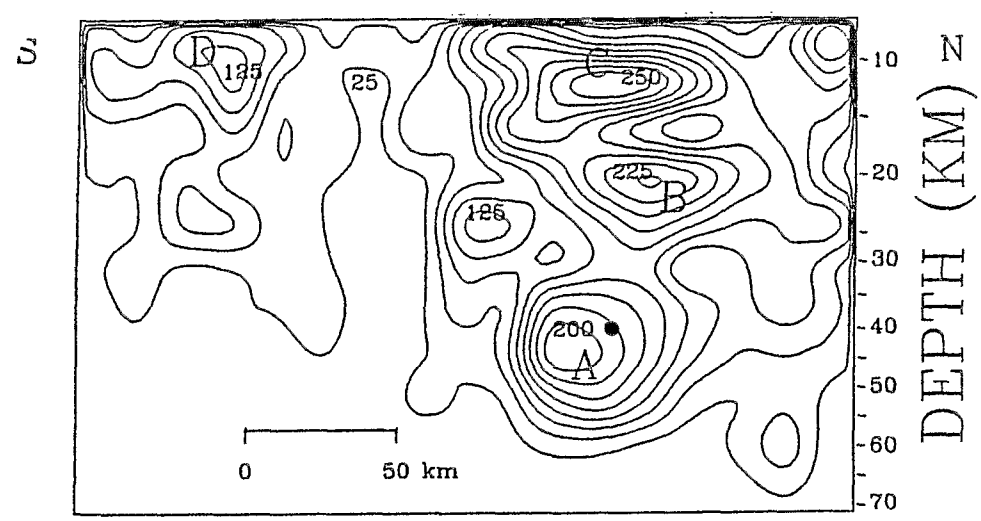

Figure 1. Slip distribution obtained from time-window inversion of the teleseismic body waves using a 1-sec time-window interval. Cumulative slip is contoured at 25-cm intervals and contains all fault displacements occuring within 10 sec after the passage of a rupture front propagating at 3 km/sec away from the hypocenter (filled circle). A, B, C and D mark the areas of maximum slip.

Source durations published for the 1985 Chile earthquake using long-period surface-wave are between 60 and 80 sec. We re-examine the source duration and seismic moment of that event by inverting the full Rayleigh waveforms, using a point-source time-window approach. We find that the majority of the long-period moment release occurs in an interval from 20 to 80 sec following main rupture initiation, consistent with previous surface-wave results. The surface-wave moment in the first 80 sec. is 1.2×10^{28} dyne-cm, consistent with previous estimates and similar to our body-wave moment.

4) Body-wave, surface-wave, and strong-motion analysis

We have performed a simultaneous inversion of the teleseismic body waves, very long-period surface waves, and local strong-motion to further constrain the distribution of mainshock slip on the hinged fault used in the body-wave analysis. Each of the three data sets is weighted appropriately to prevent any one data type to dominate the result. The solution is very similar to that obtained using only body waves (Fig.1) and shows mainly fault motion along the shallow portion of the plate boundary (Fig.2). The mainshock source duration is 68 sec with the principal moment release occurring within a 40-sec time interval beginning about 5 sec after the rupture nucleation. The total seismic moment is 1.5×10^{28} dyne-cm.

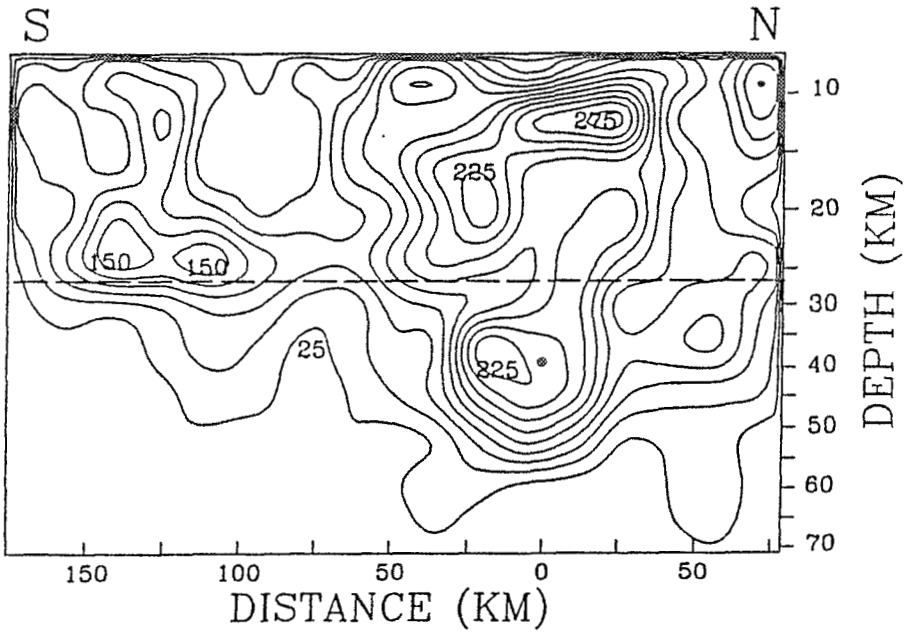

Figure 2. Results of the hinged-fault, time-window inversion of the entire teleseismic, surface-wave, and strong-motion data set. The slip distribution shows cumulative fault slip contoured at 25-cm intervals 10 seconds after the passage of the rupture front propagating at 3 km/sec away from the hypocenter (filled circle). The dashed line marks where the fault dip changes from 15° to 30°.

As we can see in Fig. 2, the majority of the moment released can be attributed to a broad source region in the northen half of the fault which contains two distinct zones of slip spanned between 5 and 55 km depths: one zone of 2.3-m peak, near the rupture nucleation point and another of 2.8-m peak, updip in the more gently-dipping portion of the plate interface (Fig.2). The southern portion of the rupture area includes a narrower region of lesser slip of 1.5-m peak which does not extend deeper than 30 km.

These results indicate that the observed seismic data considered here, which cover a very wide range of frequencies (from 2 to 350 sec), can be explained by a single rupture model. This inferred dislocation model predicts the observed Rayleigh-wave amplitudes quite well and does not require a seperate longer-duration component of fault motion, suggesting that a depth extent of 5-55 km is appropriate for the 1985 Chile earthquake. This depth range is in excellent agreement with the depth extent inferred by Barrientos (1988) from a finite-fault inversion of the post-seismic geodetic measurements. The inferred depth range is also consistent with the long-period surface-wave centroid depths.

CONCLUSIONS

We have examined local strong ground motions and teleseismic body and surface waves recorded for the earthquake using a variable rise-time finite-fault inversion scheme to recover a detailed rupture history of the principal moment release. This data set contains a wide range of frequencies that include periods from about 2 to 350 sec. We assume a hinged fault with two different dips (15° for the shallower portion and 30° for the deeper one) to simulate the landward increase in plate-boundary dip suggested by Choy and Dewey (1988). The inversion yields a rupture model that explains all three data types equally well. The mainshock source duration is 68 sec with the majority of the moment release occurring in the first 45 sec. The total seismic moment is 1.5×10^{28} dyne-cm. The entire rupture area covers a lateral distance of about 200 km.

A variable rise-time inversion using only the teleseismic body-wave data yields a very similar distribution of mainshock slip with a slightly lower seismic moment (1.2×10^{28} dyne-cm); This result indicates that the body-wave data provide a fairly accurate measure of the earthquake rupture history. Thus, a significant downdip component of relatively slow fault motion is not required to fully explain Rayleigh wave data set. The small difference in seismic moment may reflect the band limitation of the body-wave data. The observed rise times are consistent with the dynamic rupture of local asperityies and may indicate a mechanism of earthquake generation characterized by the failure of individual asperities across the fault.

The rate of relative plate convergence in this region (9 cm/yr) would suggest an accumulation of 7.1 meters of tectonic slip in the 78.5 years between the 1906 and 1985 earthquakes. Our inferred maximum slip of 2.8 meters for the 1985 Chile earthquake would indicate that either a significant amount (about 60 percent) of aseismic motion occurs across the entire plate boundary or a future large-slip event has yet to occur in the area.

REFERENCES

BARRIENTOS, S. E., 1988, Slip distribution of the 1985 central Chile earthquake, *Tectonophysics*, **145**, 225-241.

CHOY, G. L. and J. W. DEWEY, 1988, Rupture process of an extended earthquake sequence: teleseismic analysis of the Chilean eartquake of March 3, 1985, *J. Geophys. Res.*, **93**, 1103-1118.

HARTZELL, S. H., 1989, Comparison of seismic waveform inversion results for the rupture history of a finite fault: application to the 1986 North Palm Springs, California, earthquake, *Bull. Seism. Soc. Am.*, **73**, 1553-1583.

The influence of ridge subduction on the geodynamics of the Southern Chile Trench.

Ruth E. Murdie, Peter Styles, Dave Prior, Stephen S. Flint

Dept. Earth Sciences, Brownlow Street, University of Liverpool, Liverpool L18 3BX

Resumen

El Chile Margin Triple Junction es el unico ejemplo actuales de la subducion de un centro de propogacion activo. Datos seimological y gravitional habian usado para investigar el neotectonics de la region. Terremotos de la region no tienen un origen de empujon encambio la majoria son normal. La gravidad exhibe un baja encima de la posicion del centro de propogacion cual desaparecio hacia 3 Ma.

Key words: Chile Margin Triple Junction, Seismicity, Gravity, Slab Window.

Introduction

The Chile Margin triple junction at 46°30'S 75°45'S, is the only current example of the subduction of an active spreading centre beneath a continental plate. This situation has been recognised as having occurred all around the Pacific during the past 200My (Cande & Lewis, Stauder 1973). The main aim of the project is to investigate how the geodynamic processes of plate creation and destruction are modified when a ridge and a trench converge. If the extensional processes associated with seafloor spreading continue after subduction, what are the geological manifestations of this on the upper plate and if at some stage the spreading should cease, how are the differing motions of the Nazca and Antarctic plates accommodated.

Seismological Objectives

The seismicity associated with the normal subduction of the Nazca plate is well known and the shallow seismicity associated with the Chile Ridge spreading axis can be traced into the Trench. However, the seismicity of the area around the Triple Junction is noticably reduced. There is a decrease in the number of events recorded south of the Triple junction in comparison to the north. This has been attributed to the young age, and the shallow and slower subduction of the Antarctic Plate which may be of limited extent in this area (Stauder 1973).

We hope to assess the seismicity of the slab as it enters the trench and from a study of the focal mechanisms distinguish it from transcurrent motions produced by slip on the transform fault. Most of the Taitao Ridge is still exposed and expected to be seismically active. If so, further work could establish whether the Tres Montes and Esmarelda Ridges which are further inland are also still active and may be located by upper plate seismicity.

The detection threshold for teleseismic data from the region is about M=4 and the apparent lack of seismicity may partly reflect this. So a local microseismic network of ten three-component digitally recorded

stations was set up in Region XI of Southern Chile. Data were collected over a four month period.

Gravity Aims

The pre-existing gravity data were mostly marine with very few terrestrial data points. Gravity lows are associated with the trench, Chile Rise and major fracture zones. On land a regional east-west gradient decreases towards the east. Estimates based on the thermal and bathymetric contrasts between differing age oceanic crust across the transform fault suggest that the Taitao Fracture Zone a would give at least a 1 mgal Bouguer anomaly at a depth of 20km and distance from the trench of 50 km. It is hoped that a detailed gravity survey will show the anomalies associated with previously subducted ridge segments and transform faults and their relationship to current volcanism and the predicted slab window.

Several base stations were set up in the area on the mainland from where surveys were conducted over as much of the region as possible. 430 new gravity observations were made.

Seismological Findings

Micro-earthquakes were occurring at a rate of about three a day. The epicentral locations show two linear trends both running WSW-ENE. (fig 1) The more southerly of these lineations lies along the expected location of the Tres Montes Fracture Zone. The more northerly lineation lies along the trend of the Taitao fracture zone indicating that the fracture zones are continuing to be active even though they have entered the subduction zone. It is interesting to note that no activity was recorded from south of the Taitao region confirming that the apparent lack of seismicity associated with the subduction of the Anatarctic Plate from ISC data is in fact real.

It is of note that most of the events recorded display very simple seismic signatures. Most show only P and S-wave phases. The high quality, low-noise, three-component, digital data enables us to use the Gaussian Relative Amplitude Method (GRAM) developed by Rogers and Pearce (1989) to deduce focal mechanisms. Out of the ten focal mechanisms obtained, nine of them showed normal faulting with one strike slip event. There were no thrust mechanisms that are usually associated with subduction zones. This is probably due to the subduction of young crust with a low rigidity. The normal mechanisms are probably a product of the northwards motion of the Chiloe Block in relation to the main continental plate along the Liquini Ofqui Fault.

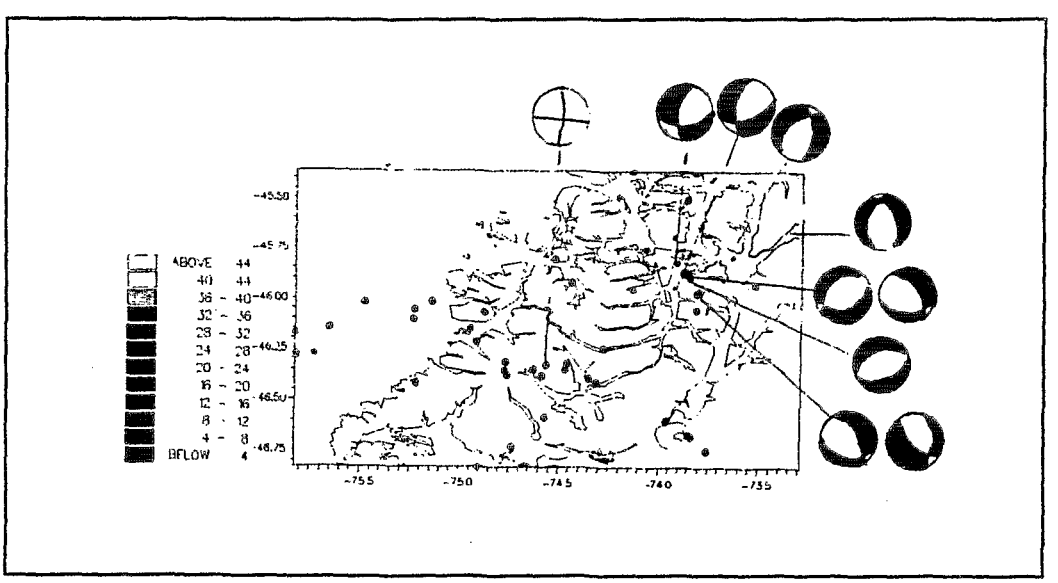

Figure 1 Seismicity and source mechanisms for events detected on the microseismic network from the Taitao region.

Gravity Findings

Figure 2 shows a band-pass filtered Bouguer anomaly map of Region XI. which has had the regional trend removed and then been filtered to remove the high frequency content. . The map shows that the main feature is a Y-shaped, negative anomaly of amplitude -22 mgal which lies along the Golfo Elefantes, crosses perpendicular to the Andes and then strikes eastward for approximately 100 km up the Rio Ibaniez, toward the Argentinian border. The north-south trending arm of the low appears to be related to the Liquiñi Ofqui transcurrent fault which appears to have been produced to accommodate the differential movements between the plates north and south of the Triple Junction. The low along the Ibaniez valley corresponds fairly well to the position of the postulated window in the subducted slab which has opened up due to the differing subduction rates of the Nazca and Antarctic plates as suggested by Ramos and Kay (1992).

The Power spectrum of the Bouger anomaly show linear segments with a slope indicating spectral estimates of the depths to the causative density contrast of about 70km. If we take the angle of subduction to be 15^0, the top of the subducted slab would lie at a depth of 53km. It therefore seems possible that this contrast is related to thermally-derived density differences across the Lithosphere/Asthenosphere boundary at the base of the subducted slab. The gravity anomaly observed is an order of magnitude larger than initial estimates based simply on the effect of a simple subducted ridge. This appears to imply the emplacement of a significant volume of low-density material possibly as an asthenospheric upwelling beneath this region.

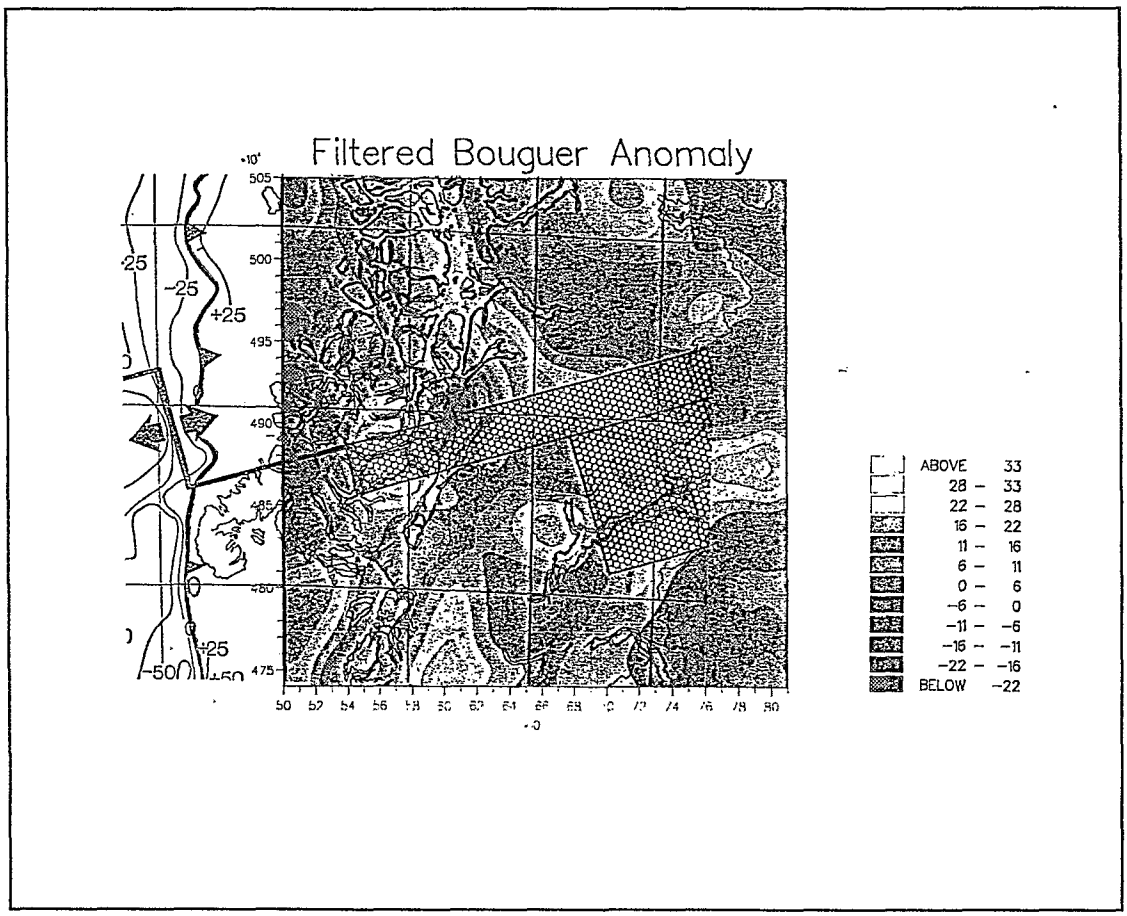

Figure 2 Filtered Bouguer Anomaly map of the Taitao region with the position of the proposed slab window of Ramos and Kay (1992).

Conclusions

This area is definitely shows seismic activity with the majority of events having normal source mechanisms These are probably related to the Liquini Ofqui Fault which is moving the Chiloe Block northwards in relation to the rest of the continent. The gravity data shows the postulated current postion of the Tres Montes Ridge segment and the size of the Bouguer indicates that there has been an injection of a low density material in the region.

References

Cande S.C. & Lewis S. 1988 Investigating the subduction of a spreading centre off southern Chile. Lamont Doherty Geological Yearbook p18-25.

Pearce R.G. & Rogers 1989 Determination of earthquake moment tensors from teleseismic relative amplitude observations. Journal of Geophysical Research 94 p775-786.

Ramos V.A.& Kay S.M. 1992 Southern Patagonian plateau basalts and deformation: backarc testimony of ridge collisiona. Tectonophysics 205 p261-282.

Stauder W. 1973 Mechanism and spatial distribution of Chilean earthquakes with relation to subduction of the oceanic plate. Journal of Geophysical Research 78 p5033-5061

VERTICAL MOTIONS INFERRED FROM PLEISTOCENE SHORELINE ELEVATIONS IN MEJILLONES PENINSULA, NORTHERN CHILE: SOME REASSESSMENTS.

Luc ORTLIEB

ORSTOM-Antofagasta, Facultad de Recursos del Mar, Universidad de Antofagasta, Casilla 170, Antofagasta, Chile

RESUMEN: Los intentos de determinación de la velocidad de levantamiento reciente de la península de Mejillones (costa norte de Chile) produjeron resultados muy diferentes según los autores: de 33,000 a 70 mm/10^3años. Se confirma que, en la parte nor-oriental de la península, los movimientos verticales cuaternarios tuvieron una amplitud total de sólo 220 m y que la tasa de levantamiento ha probablemente ido disminuyendo durante el Pleistoceno, desde ca. 250 hasta 70 mm/10^3años.

KEY WORDS: Neotectonics, vertical movements, Quaternary shorelines, Chile

INTRODUCTION

The 50 x 20 km Mejillones Peninsula (Fig.1) constitutes a salient faulted block that interrupts the N/S-oriented Coastal Escarpment of the northern Chilean coast and disrupts the steep continental margin of the South-American plate, precisely in the area where the Peru-Chile Trench shows its greatest depth (8,060 m). For these morphostructural characteristics and because the Mejillones Peninsula is located at the latitude where some Central Andean structural domains are the most widely developed (Precordillera and "Depresión preandina" with the Salar de Atacama), there is much concern to understand the structure and tectonic evolution of this anomalous block.

The Mejillones Peninsula shows much evidence of Plio-Quaternary deformation: large crustal faults, block tilting, tectonic scarps cutting Quaternary alluvial fans and marine deposits, and deformed abrasion platforms. The preservation of sequences of Pleistocene regressive shorelines (NW, NE and SE sectors of the peninsula) indicates that some steady uplift motions (and not only fault-controlled deformation) also occurred during the Quaternary.

Up to now, strongly discrepant estimates of recent vertical motions have been proposed by investigators who made preliminary field observations and/or geochronological analyses on some of the Pleistocene coastal units of the peninsula. The estimates of mean uplift rates for the late Quaternary (=last 125,000 y) vary by as much as one, or even two, order(s) of magnitude! Such a discrepancy is beyond acceptable

limits for neotectonic studies in a key area like the Mejillones Peninsula.

ESTIMATES OF VERY HIGH LATE QUATERNARY UPLIFT RATES

A few authors estimated mean uplift rates over 2000 mm/10^3y of the peninsula during the late Quaternary. First, Okada (1971) interpreted that, since the last interglacial high seastand, some sectors of the peninsula had been uplifted at a mean rate of 3000 mm/10^3y. Craig (1988) hypothesized that up to 200 m of uplift motions might have occurred since the Holocene sea level maximum (*ca.* 6000 BP), in the area south of the bay of Mejillones; such a motion would imply a mean rate of about 33,000 mm/10^3y in the second half of the Holocene. Lately, Armijo & Thiele (1990) assumed that up to 280 m of uplift was produced since the last interglacial highstand (average rate of 2400 mm/10^3y).

These interpretations are based on unwarranted assumptions, since the last interglacial (or Holocene) deposits were not positively identified. Craig's interpretation was based on radiocarbon results (in the range 38,000-25,000 BP) from shells collected in +200 m-elevated coastal deposits, although ^{14}C results over 25,000 BP should not be trusted without special screening. Okada (1971) and Armijo & Thiele (1990) observed three major sets of marine terraces and abrasion platforms in the peninsula and simply assigned the lowest one (supposed elevation range: +30/+280 m), which included the Mejillones sequence of shorelines, to the last interglacial high seastand. They did not take into account neither the early work of Herm (1969) nor any result of more recent chronostratigraphic studies on the Pleistocene coastal deposits of the area (Radtke, 1985, 1987a, 1987b; Leonard et al., 1987, 1988; Hsu et al., 1989).

CHRONOSTRATIGRAPHIC AND GEOCHRONOLOGICAL AVAILABLE DATA

In a pioneer work on the major sequence of regressive shorelines located south of Mejillones (Fig.3), Herm (1969) interpreted that these conspicuous coastal deposits had been formed during two distinct episodes of high sealevel (Serena I and II) in the Early Pleistocene. Herm (1969) showed that the limit between remnants of the two transgressions was traceable on aerial photographs and was figured by a seacliff at ca.+80/90 m. He also pointed out that the oldest Pleistocene marine features in the area SE of Mejillones were preserved at +220/+200 m.

In the mid-eighties, were performed the first attempts to identify remnants of the last interglacial highstands along the coast of northern Chile. Radtke (1985, 1987a, 1987b) used Th/U and ESR (Electron spin resonance) methods, while Leonard et al. (1987, 1988) and Hsu et al. (1989) developed the first aminostratigraphic studies in northern Chile. Through these dating techniques, the mentioned authors showed that, in Mejillones-El Rincon area (Fig.3), the last interglacial coastal deposits crop out at the top of the modern seacliff, at an elevation below +15 m, and that the local uplift rate was of the order of 70 mm/10^3y for the late Quaternary (Radtke, 1985; Leonard et al., 1988). NE of the bay of Mejillones, the 125 ka shoreline was found at +35 m at Hornitos (Fig.2)(Radtke, 1985), and at +40 m, 20 km N of Hornitos (Leonard & Wehmiller, 1991). These data suggest mean uplift rates of 240-250 mm/10^3y for the narrow coastal plain at the foot of the Coastal Escarpment.

The highest late Quaternary uplift rate determined in the region (500 mm/10^3y), and based on tentative identification of the last

Fig.1.- Location map of the study area.

Fig.2.- Late and (late) Middle Pleistocene shorelines in Hornitos area: the 125 ka and 220 ka shorelines are found at +35 and +50 m.

Fig.3.- The sequence of Middle and Early Pleistocene shorelines preserved in the Mejillones graben. Indicated sets of shorelines might correspond to successive episodes of interglacial high seastands.

interglacial deposits, were found on the northern headlands (Punta Angamos) of Mejillones Peninsula (Leonard et al., 1988).

DISCUSSION AND CONCLUSION

Preliminary observations made in the framework of a program involving detailed mapping and chronostratigraphic analyses of Pleistocene coastal deposits in Mejillones Peninsula (Agreement ORSTOM/Univ. de Chile-Santiago/CSIC-Madrid/GEOTOP-Montréal), lead to the following comments:

- Near El Rincon, the 125 ka and 220 ka shorelines were identified at +15 and +31 m (Radtke, 1985). These two youngest terraces postdate the Mejillones sequence of shorelines.
- The sequence of closely spaced beach ridges preserved on a gently sloping surface, between ca. +200 m and the modern seacliff along the bay of Mejillones (Fig.3), is of Middle-Early (?) Pleistocene age.
- The sequence actually consists in a series of sets of beach ridges (Fig.3) which seem to correspond to successive sedimentation cycles coeval with high seastands. Current studies aim to determine whether each set of shorelines represent eustatically controlled encroachments of the sea (during a series of interstadial and interglacial episodes) in a regime of steady uplift, or if episodic tectonic motions were also involved.
- SE of Mejillones, the Pleistocene marine limit is located at about +200 m at the foot of the Coastal Escarpment, i.e. at the same elevation than the highest regressive shorelines of the sequence. If the oldest of these beach ridges were formed around 1 My ago, the overall mean uplift rate in the area would be about 200 mm/10^3y.
- Vertical motions in the graben of Mejillones probably decreased through time, from about 250 mm/10^3y to 70 mm/10^3y in the Late Quaternary. Morphological characteristics of the shoreline sequence suggest that the apparently steady uplift motions involved deeply seated crustal (thermal?) mechanisms.
- Obviously, the western sector of Mejillones Peninsula was more strongly deformed and experienced higher uplift rates than the Mejillones area. Nevertheless, it still remains to be established whether the highest abrasion surfaces, found between +400 and +600 m, are of Pleistocene age or older.

REFERENCES

ARMIJO, R. & THIELE, R., 1990. *Earth Planet. Sci. Lett.*, 98 : 40-61.
HERM, D., 1969. *Zitteliana* (München), 2, 159 p.
HSU, J.T., LEONARD, E.M., & WEHMILLER, J.F., 1989. *Quatern. Sci. Rev.*, 8: 255-262.
LEONARD, E., MIRECKI, J.R. & WEHMILLER, J.F., 1987. *Geol. Soc. Amer. Abstr. Progr.*, 19 (7): 744.
LEONARD, E., WEHMILLER, J.F. & FERGUSSON, D., 1988. *Comunicaciones*, 39: 21.
LEONARD, E.M., & WEHMILLER, J.F., 1991. *Rev. Geol. Chile*, 18 (1): 81-86.
OKADA, A., 1971. *Bull. Dept. Geogr. Kyoto*, 3: 47-65.
RADTKE, U., 1985. Actas IV Congr. Geol. Chileno (Antofagasta, 1985), 4: 436-457.
RADTKE, U., 1987a. *Berliner geogr. Stud.*, 25: 313-342.
RADTKE, U., 1987b. XII INQUA Congr. (Ottawa), Abstr. v: 247.

GEOPHYSICAL INVESTIGATIONS ALONG THE PERUVIAN CONVERGENT MARGIN

Ingo A. Pecher, Nina Kukowski , Roland von Huene

GEOMAR Forschungszentrum, Universität Kiel, Wischhofstr. 1-3, D-2300 Kiel 14

RÉSUMÉ

La marge continentale de Perou représent un sujet important des études géophysiques chez GEOMAR. Les résultats des interprétations des profiles sismiques réflexion sont présentés en combinaison avec la détermination du flux de chaleur apart de la profondeur du BSR (Bottom Simulating Reflection), des modélisations avec la méthode des éléments finites (FE) pour le flux des fluides et du chaleur, ainsi que des modèles réduits analogiques pour tester les interprétations kinematiques.

KEY WORDS: Peruvian Continental Margin, Reflection Seismics, Heat Flow, Fluid Transport, Finite Element Modelling, Sandbox Experiment

INTRODUCTION

The Peruvian continental margin is the subject of an integrated geophysical investigation at GEOMAR. Results from an interpretation of reflection seismic profiles are presented along with determinations of heat flow from the depth of the Bottom Simulating Reflection (BSR). These results can be used in finite element (FE) modelling of fluid and heat flow. Sandbox modelling is used to test kinematic interpretations.

SEISMIC STUDIES

From 13 reflection seismic profiles in three locations offshore Peru we present results from the southernmost profiles, lines 1017 and 1018, which are located at about 12° S (Fig. 1). These two profiles were acquired by SHELL in 1973 and have been re-processed at GEOMAR. In addition to conventional processing with a post stack time migrated section as output we have applied state of the art pre stack depth migration. The MIGPACK software package which we use for this purpose provides both a depth section and a velocity model. Two major advantages of this technique, which has been described by Diet et al. (1990), are the reduction of smearing effects compared to conventional post stack migration and the

possibility to accomodate in the migration small scale lateral velocity variations. This leads to significant improvements for the imaging of structures in tectonically complex regions.

Fig. 2 presents a tectonic interpretation of line 1017. On the seaward side of this line, the subducted oceanic plate and its cover of sediments can be clearly identified. These sediments are underthrusted and can be followed some 20 km down the subduction zone. Duplex structures are interpreted in the accretionary wedge. A strong BSR marks the lower boundary of the stability zone for methane hydrates. The BSR shows a sharp negative seismic impedance contrast and is most probably caused by free gas beneath the hydrate zone. A major structural element further towards the continent is intensive normal faulting. Stratigraphic correlation of seismic horizons based on borehole information from ODP leg 112 allows a tectonic reconstruction of the Peruvian continental margin at this latitude. An unconformity which can be seen about 60 to 75 km landward from the trench represents a hiatus between late Miocene/early Pliocene during which there was an uplift of the continental plate, presumably caused by the subduction of the Nazca Ridge.

ASSESSMENT OF HEAT FLOW

A temperature gradient can be determined from seismic reflection lines in which a BSR is identified. This method, which has first been presented by Shipley et al. (1979) and Yamano et al. (1982), is based on the assumption that the BSR is located at the lower boundary of the methane hydrate stability zone. Thus, it represents a pressure/temperature point in the phase diagram for methane hydrates. Pre stack depth migration yields both a relatively accurate depth and good velocity information for the sediments above the BSR. Pressure at the BSR can be derived using a velocity/density correlation which is determined from core or logging data. Oceanographic data give access to temperatures at the seafloor. Information about thermal conductivity, which is available from ODP leg 112, then allows an estimation of heat flow values. The major advantage of this indirect method is that heat flow can be determined continuously along the BSR. Therefore, small scale lateral variations, which could indicate fluid venting, can be identified. A general increase in heat flow values towards the continent can be observed in the lower slope portions of both lines 1017 and 1018.

NUMERICAL MODELLING

Fluid and heat transport within the subducition zone off Peru is quantified using 2D coupled finite element modelling. These investigations assume a porous model with Darcian flow. Based on the interpretation of the seismic data, tectonic units have been discretized using unregularly spaced meshes. The physical parameters, which we have systematically varied, are permeability, porosity, thermal conductivity, heat production, and matrix compressibility. Our model calculations show the strong control of the tectonic structure on the fluid flow regime. Convective heat transport dominates only, if permeability exceeds 10^{-14} m^2.

SANDBOX EXPERIMNENT

Sandbox experiments have been conducted at the Laboratory for Structural Geology in Montpellier in April and December 1992 to test the concept of tectonic deformation at this convergent margin. They are based on the assumption that sediments in accretionary margins act as Coulomb material. It was possible with these experiments to model major structural elements and geometrical features at convergent margins and observe, how underplating elevated the front of the "backstop" off Peru. A period of tectonic erosion followed, which is

assumed to have caused the subsidence observed in sediment from ODP cores.

DISCUSSION AND OUTLOOK

Different geophysical methods have been applied to achieve a better understanding of the complex processes which control the tectonic mechanisms in the subduction zone along the Peruvian continental margin. Improved images of tectonic structures clearly show the accretionary prism, the buttress of crystalline rock, against which accreted sediment was stacked, the normal faults from flexing of the continental crust during erosion, and the seismic stratigraphy resulting from uplift and subsidence.

Heat flow derived from the depth of the BSR generally increases towards the contintent, probably due to heat production in the continental crystalline. Friction at the subducted plate, however, could also play a role as another possible heat source. This should be investigated using modelling techniques.

Numerical modelling yields constraints on the thermal state and fluid flow pattern, whereas dynamic evolution and deformation behaviour is tested with sandbox experiments. Interpretations are constrained and greatly improved by integrating these techniques.

Future seismic work will focus on the Chimbote region further north, at about 9° S. We have a relatively dense set of seismic profiles from this area, which provides a three dimensional map of the main tectonic features. Heat flow in 3D will be estimated using the method described above.

It is planned to develop a FE model concept which allows for fluid transport in discrete fractures and for non-linear flow laws. We plan to work on the Chimbote data set for future investigations to get a basis for 3D modelling. We will try to include mechanical deformation in the numerical modelling.

REFERENCES

Diet, J.-P., Audebert, F., 1990: A focus on focusing. Abstract, paper presented at the 52nd EAEG Meeting, 28 May - 1 June 1990 in Copenhagen, Denmark, p. 107-108.

Shipley, T.H., Houston M.H., Buffler, R.T., Shaub, F.J., McMillen, K.J., Ladd, J.W., Worzel, J.L., 1979: Seismic evidence for widespread possible gas hydrate horizons on continental slopes and margins. AAPG Bull., v. 63, no. 12, p. 2204-2213.

Yamano, M., Uyeda, S., Aoki, Y., Shipley, T.H., 1982: Estimates of heat flow derived from gas hydrates. Geology, v. 10, p. 339-343.

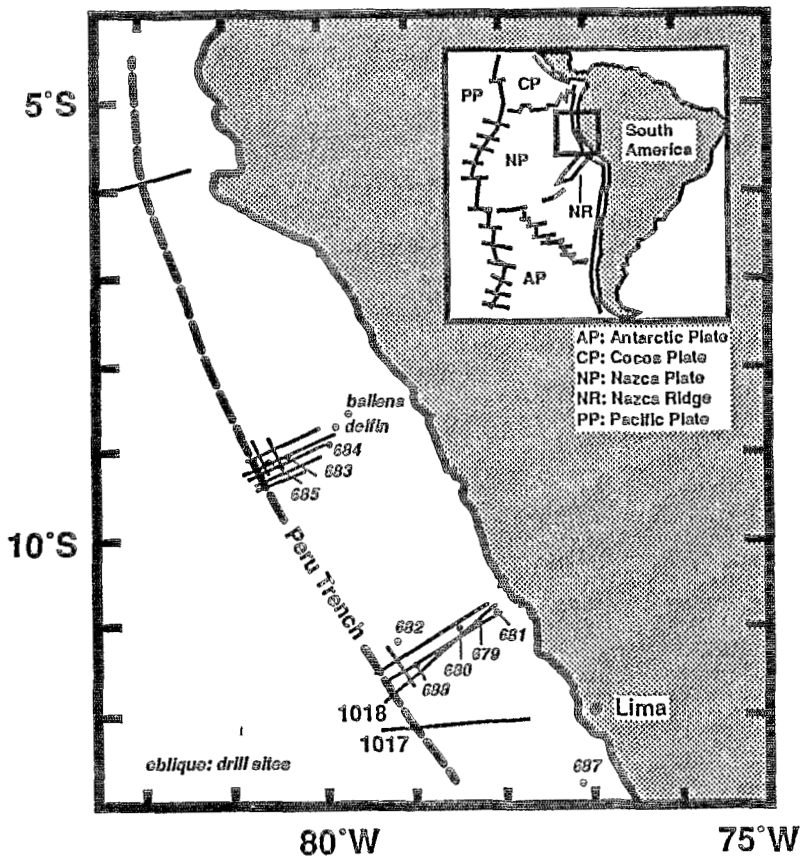

Fig. 1: Seismic lines from offshore Peru which are available at GEOMAR

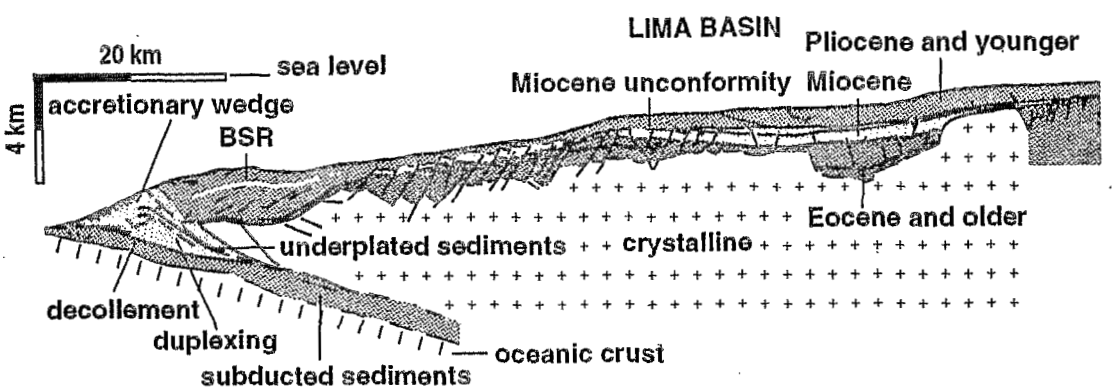

Fig. 2: Tectonic interpretation of line 1017.

THE SEISMIC PERCEPTIBILITY IN DETERMINING SOME FOCAL PARAMETERS OF HISTORICAL EARTHQUAKES IN CHILE

David RAMIREZ L.(1)

(1) Universidad de Santiago de Chile, Facultad de Ciencia, Departamento de Fisica, Casilla 307, Santiago 2. CHILE

RESUMEN : Sobre la base de algunas expresiones obtenidas por diferentes autores y tomando en consideración la ubicación geográfica de Chile, se propone utilizar la distancia de máxima perceptibilidad para estimar el tamaño de los terremoros históricos.

KEY WORDS : Size, Historical, Earthquakes, Regression, Parameters, Perceptibility

INTRODUCTION

In Chile we have had many earthquakes of great magnitude such as M_s = 7.5 to M_s = 8.6. The ones that have happened after the year 1906 have been determined with the use of instruments. For this reason, some of their focal parameters as seismic magnitude, length of rupture, seismic moment, etc. are fairly well estimated.

Although, the earthquakes that have happened before 1906 (or historical) have been estimated through some indirect parameters, that we will call "Macroseismic Parameters". Some of them are, duration of the main earthquakes, distance of maximum perceptibility, duration of aftershocs, etc.

One of the macrosismic parameters most frequently, quoted in the historical documents, it is the distance of maximum perceptibility (L*), which is the distance between, the epicentral zone and the zone where the earthquake was felt by a normal watcher who declares "to have perceived the earthquake".

The reason why this is one of the best registered parameters is due to the geographical shape of the Chilean territory, which is a long and narrow zone located in geogra-

phical North - South direction so that the rupture zones go in the same direction (parallel) to the coast line.

So, the differents isoseismic lines in the graphic of a great isoseismic lines in the graphic of a earthquakes have an elliptical form whose largest diameter is approximately oriented to N.S. direction (See Fig. 1). So it is often probable that the limit of any isoseismal reachs, a city, town or village in our country.

For the earthquakes that have happened after 1906 (contemporany) it has been determined with fair accuracy the area involved by the isoseismal of levels VII and VIII (M.M.), and up although, this has not been possible for the isoseismal of levels IV, III (M.M.) and inferior, because their largest dimension involve as the Pacific Ocean, so the Andean mountains, so that for this levels of seismic intensity the lenght of the major semiaxis, represents with higher precision the level of seismic perceptibility.

GEOLOGICAL SETTING

Richter, (1958) proposed some data that connected the maximum intensity of a seism (I_{max}) to his seismic magnitude (M) and the distance of maximum perceptibility (L^*) starting from this data Ramírez (1988), obtained an empirical relation that linked L^* to M. The same way Barrientos (1980), obtained some relations of attenuation for a group of 73 Chilean earthquakes in which this three parameters connected themselves in a consistent way.

Asuming that for a normal watcher whose level of perceptibility, is equivalent to that of a witness present in a historical earthquakes, the limit of the seismic perceptibility approaches to the extreme value of the isoseismal III (M.M.) Ramírez (1988), it is feasible to deduct from the formula of attenuation, an empirical relation that link L^* and M for big earthquakes with epicenters inferior to 100 (Km) depth.

Also S.K. Singh et al. (1980), obtained some empirical relations that linked the areas delimited by the contours of the isoseimal IV, V, VI to the seismic magnitude of some earthquakes, which occurred in Mexico. As a consequence, it is extremely possible to derive empirical relations between the lenght of the major semiaxis of that areas with the seismic magnitude, so that it will become similar to the situation which occurs presently in Chile.

Finally, it is important to bring out that also Hanks and Johnston (1992) obtained and empirical relations that linked the Kanamori magnitude (M_w), to the area of perceptibility of a seism (A_{perc}) by using data of seisms registered in the region of California (U.S.A.).

On the basis of this antecedents we have selected a group of great Chilean earthquakes after the year 1900 of magnitude M_s 7.0 (Table 1) such that their distance of maximum perceptibility has been determined in a equivalent way of the one registered by a witness present in some historical earthquake. Kausel y Ramirez (1993). Using the methods of regression by minimum squares, starting from the data indicated in Table 1, we can get the following equations of empirical character :

$$\log L^* = 0.23 + 0.35\ M_s \quad (1)$$
$$\log L^* = 0.44 + 0.32\ M_w \quad (2)$$
$$\log L^* = 1.97 + 0.48 \log L \quad (3)$$

The distribution and correlation of the points can be seen in figures 2, 3 y 4 respectively.

TABLE N°1

DATE	LAT.	LONG.	PROF.	M_s	M_w	L(km)	L*(km)
17.08.06	33.0	72.0	25.0F	8.4	8.2	250	1600
11.11.22	28.5	70.0	25.0F	8.4	8.5	390	1500
01.12.28	35.0	72.0	25.0F	8.0	7.6	90	1300
25.01.39	36.3	72.3	---	8.3	---	200	1600
06.04.43	30.8	72.0	---	7.9	8.2	200	1000
02.08.46	26.5	70.5	50.0G	7.9	7.9*	110	950
20.04.49	38.0	73.5	70.0E	7.3	7.3*	---	660
17.12.49	54.0	71.0	---	7.8	7.8*	---	1000
09.12.50	23.5	67.5	100.0F	8.0	---	120	1200
06.05.53	36.5	73.0	60.0F	7.6	7.6*	---	560
29.11.57	21.0	66.0	200	7.8	7.8*	---	800
22.05.60	39.5	74.5	---	8.5	9.4	950	1600
23.02.65	25.7	70.6	36.0I	7.0	7.0*	---	450
28.03.65	32.4	71.1	68.0I	7.1	7.5	80	560
28.12.66	25.5	70.7	23.0I	7.8	7.7	140	800
17.06.71	25.4	69.1	76.0I	7.0	7.0*	40	600
09.07.71	32.5	71.2	40.0I	7.5	7.8	135	750
04.10.83	26.5	70.6	15	7.3	7.3*	100	650
03.03.85	33.1	71.9	17	7.8	8.0	170	1300

* $M_s = M_w$ if $M_s < 8.0$ - Kausel y Ramirez (1993)

CONCLUSIONS

The results indicate that the equation (1) it is the one that shows the better correlation due to the fact that the Richter (M_s) magnitude is proportional to the logarithm of the extent of the seismic waves of intermediate period (10 to 20 sec.), so they are registered with a better "human perceptibility". But the relations (2) and (3) reveal a coefficient of inferior correlation, showing the problem of saturation in the seale of magnitude M_s facing the rupture length (L) and the distance of maximum perceptibility (L^*) facing the magnitude M_w, what is the impossibility of joint the regressions (2) and (3) the earthquake happened in 1960.

This is consistent with the condition that the magnitude Mw is determined in relation to periods higher than 100 (sec.), as by definition M_w is proportional to the logarithm of the seismic moment (M_o) and this is measured in cero frecuency. The length of rupture L shows a similar behaviors to the magnitude M_w in front to Log L^*, as theoretically both parameters appear linked each other, Geller and Kanamori (1977).

Due to that logarithm L^* is proportional to M_s is possible expect that the empiric relation of the form log $L^* = A + B\ M_s$ with $M_s > 8.0$ shows a excellent correlation.

The determination of L^* for a historical earthquakes has to start by an exhaustive test of the historical antecedents available, allowing an estimation of no more than 10% of the measure of L^* of uncertainty.

REFERENCES

BARRIENTOS, P.S., 1980, Regionalización Sísmica de Chile. Tesis para optar al Grado de Magister en Ciencias, Depto. de Geofísica, Fac. de C.F. y M., Univ.Chile. N°total de págs.123.

GELLER, R. and KANAMORI, H., (1977), Magnitudes of great shallow earthquakes from 1904 to 1952. Bull. Seism. Soc. Amer., 67, N°3, 587-598.

HANKS, T.C. and JOHNSTON, A.C. (1992), Common features of the excitation and propagation of stron ground motions for North American earthquakes". Bull.Seism.Soc.Amer. 82, N°1, 1-23.

KAUSEL, E. and RAMIREZ, D. (1993), Relaciones entre parámetros focales y macrosísmicos de grandes terremotos chilenos. Revista Geofísica Instituto Panamericano de Geografía e Historia. Edit. México. (En preparación).

MONGE, J. (1986) (Editor), El sismo del 3 del marzo 1985 - Chile. Editorial Acero, Comercial S.A. Santiago, Chile, 2° Edición, N° total de páginas 264.

RAMIREZ, D. (1988), Estimación de algunos parámetros focales de grandes terremotos históricos chilenos. Tesis de Grado para optar al grado académico de Magister en Ciencias con mención en Geofísica, Fac.de C.F. y M., Univ. de Chile, Chile, 463 pp.

RICHTER, C.F. (1958). Elementary Seismology W.H. Freeman, San Francisco, California, U.S.A. N° total de págs. 768.

SINGH, S.K. et al. (1980), Expected Earthquakes. Magnitude from a Fault. Bull.Seism.Soc.Amer. N° 3, 903-914.

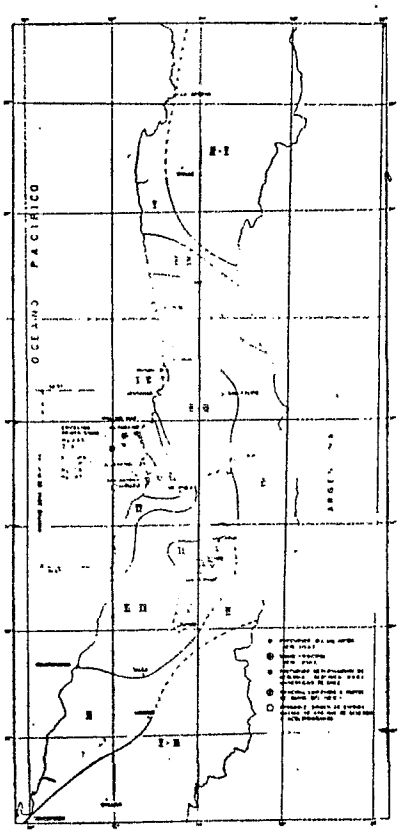

Fig. 1 Isosistas del terremoto de 3 de Marzo de 1985.
Monge, J. (1986) (Editor)

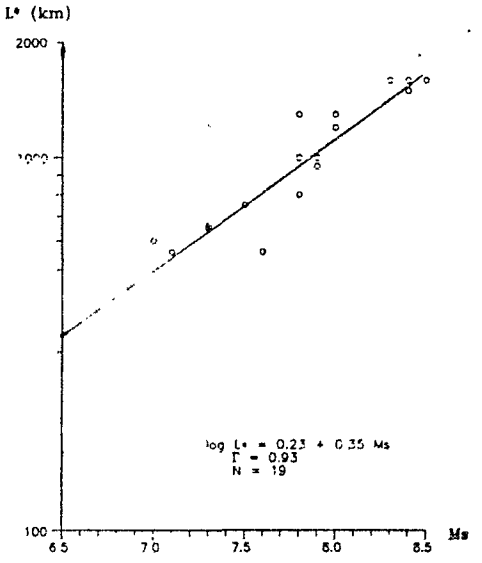

Relacion entre la Distancia de Maxima Perceptibilidad (L*) y la Magnitud Richter (Ms)

FIG. 2

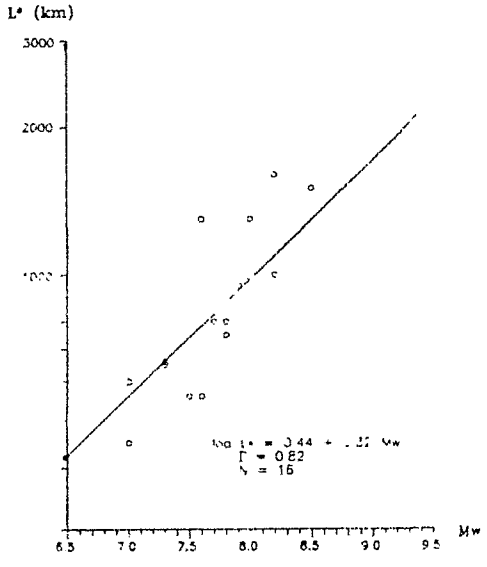

Relacion entre la Distancia de Maxima Perceptibilidad (L*) y la Magnitud Kanamori (Mw)

FIG 3

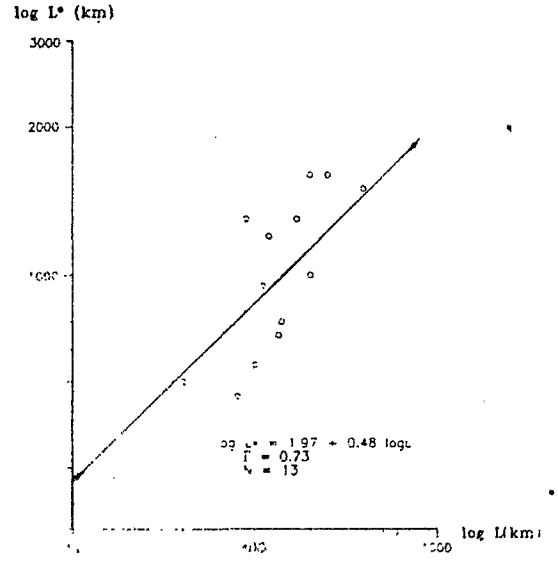

Relacion entre la Distancia de Maxima Perceptibilidad (L*) y la Longitud de Ruptura (L)

FIG. 4

HOW IS ACCOMMODATED THE PARALLEL-TO-THE-TRENCH SLIP COMPONENT IN OBLIQUE CONVERGENT SUBDUCTION: THE ANDEAN CASE

Michel SEBRIER and Olivier BELLIER

URA 1369 CNRS, Géophysique et Géodynamique Interne, bât 509, Université de Paris Sud, F91405 Orsay cedex, France.

Résumé : La composante parallèle à la fosse dans une convergence oblique avec subduction est accommodée par un des déformations décrochantes dans la plaque chevauchante ou par un glissement oblique de la subduction. La comparaison entre les Andes septentrionales et centrales suggère que si la nature de l'avant-arc est océanique, celle-ci favorise une subduction oblique.

Key Words : Sismotectonics, State of Stress, Subduction, Andes, Oblique Convergence.

INTRODUCTION

Studies of subduction zones in oblique convergent settings argued for a simple strain partioning of the convergence vector between a normal-to-the-trench component, that should be accomodated by thrust mechanisms at the subduction contact, and a parallel-to-the-trench component that should be accommodated by major strike-slip fault(s) (Fitch, 1972; Jarrard, 1986). More recently, a careful re-examination of subduction slip vectors at some oblique convergent margins showed that substantial amount of oblique slip may occur at the subduction contact (McCaffrey, 1992). Consequently, the amount of strike-slip deformation should be significantly lower than previously expected what may explain that the measured transcurrent slip is frequently lower than the one theoretically expected from global models. In order to understand how is accommodated the parallel to the trench component of convergence associated with a subduction zone, we compared two different cases along the same convergent margin: northern and central Andes. In fact, this comparison suggests there is a mechanical effect induced by the oceanic or continental nature of the forearc wedge. Indeed, the orientation of convergence, and its rate remains roughly identical from southern Colombia (3°N) to central Peru (12°S). However, three striking differences are observed: the age of the oceanic lithosphere at the trench is younger in northern Andes than in central Andes, the trench orientation is NW in central Peru while it is NNE in northern Andes, and the forearc wedge is made of oceanic material in northern Andes while it is continental in central Andes. In order to compare northern and central Andes, we calculated in both cases the theoretical component of convergence that is parallel to the trench, then the amount of this component which is accommodated by oblique slip at the subduction contact, and consequently the amount of transcurrent slip that has to be accommodated by deformation of the overriding plate. Then, we compared with the observed deformations. This shows that obliquity is predominantly accommodated by oblique subduction slip in northern Andes while it is essentially accommodated by the deformation of the overriding plate in central Peru.

METHOD TO CALCULATE THE AMOUNTS OF TRANSCURRENT SLIP

The subduction of the Nazca Plate beneath South America results from a N80°E±5° trending convergence (Fig. 1) with a rate V_C=80°±5° (DeMets et al., 1990), Along central Peru, the trench is oriented N150°E, i.e., the trench normal T_n is N60°E while along northern Andes, the trench azimuth is between N20° (Ecuador) and N35° (southern Colombia), i.e., T_n is between N110°E and N125°E. Thus, the obliquity angle, α, between the Trench normal and the convergence is 20° in central Peru and -30° to -45° in northern Andes. This allows to calculate the component of convergence, V_p, that is parallel to the trench in both central and northern Andes. From the above definitions:

$$V_p = V_C \sin\alpha \quad (1)$$

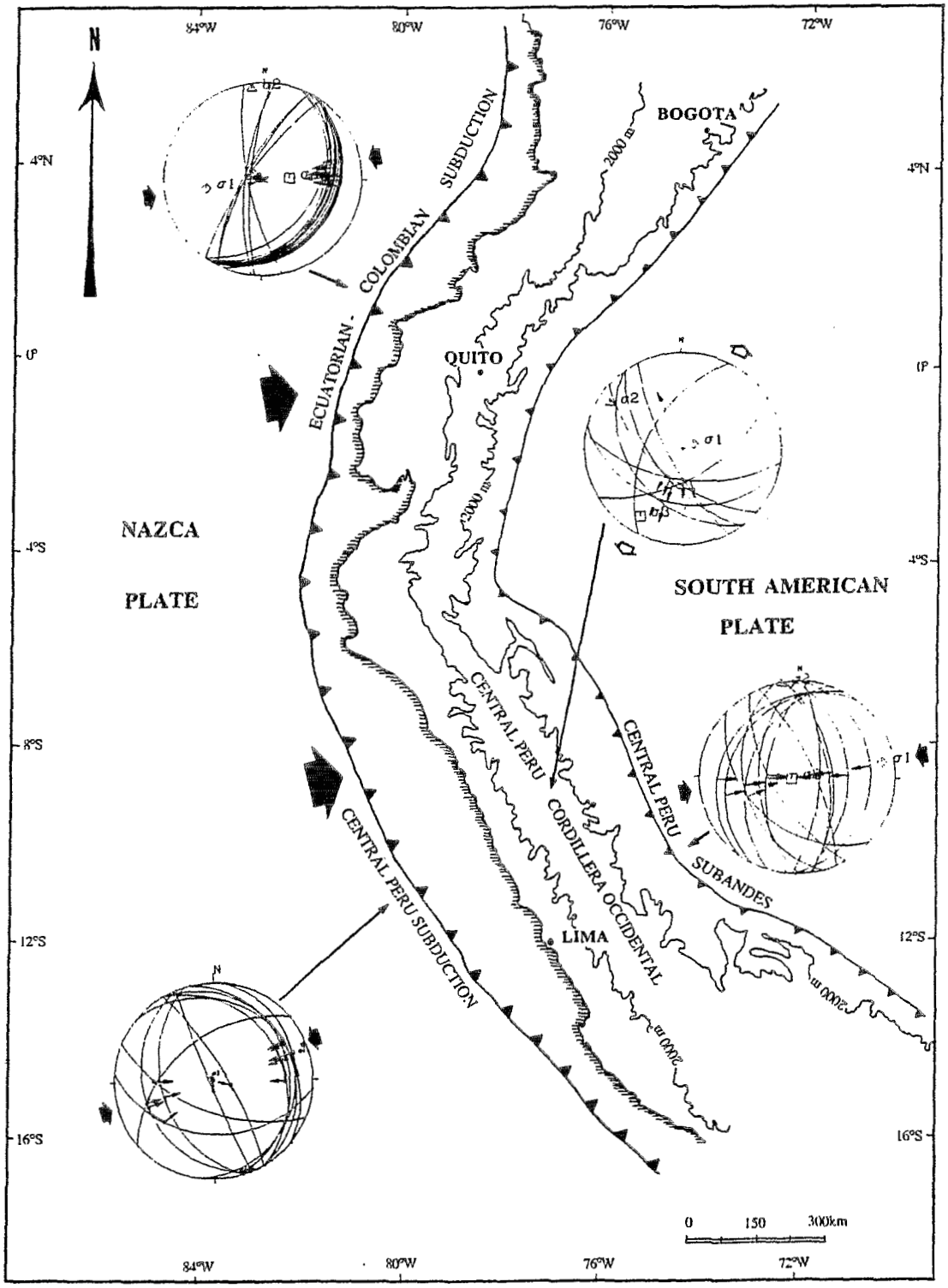

Figure1: State of stress along the northern Andes and central Peru subduction zones and in the Subandes, calcutated from available focal solutions. The state of stress in the central Peru Cordillera Occidental has been performed from field data. Small black convergent arrows: σ1; small white divergent arrows: σ3; large black arrows: N80°E trending convergence of Nazca Plate.

Then, taking V_C=78 mm/a for northern Andes and V_C=80 mm/a for central Peru, we obtain V_P=40 to 60 mm/a of theoretical dextral motion in northern Andes and V_P=27 mm/a of theoretical left-lateral motion in central Peru. This simple calculation shows that the amount of parallel-to-the-trench component of convergence is higher in northern Andes than in central Peru (Dewey and Lamb, 1992). However, this does not indicate how it is accommodated. In order to address this problem, we used the method proposed by McCaffrey (1992) that calculate the amount of transcurrent slip, V_S, that has to be accommodated by the deformation of the overriding plate.

$$V_S=V_C(\sin\alpha-\cos\alpha\tan\beta) \quad (2)$$

with V_C convergence rate, α obliquity angle between the trench normal and the convergence, β angle between the trench normal and the slip azimuth of the subduction.

INVERSION OF SUBDUCTION FOCAL MECHANISMS

In order to determine the mean β angle for both northern Andes and central Peru, we used the available shallow thrust focal mechanisms registered by world seismic networks in those subduction zone areas (e.g., Pennington 1981; CMTS by Dziewonski 1981-1992 and USGS catalog 1977-1988). Then, data inversion (same method as Carey-Gailhardis & Mercier, 1987) was performed in the two zones in order to determine the preferred fault plane for each solution (Fig. 1). The most significant result is that the subduction slip vectors are oblique in northern Andes while they are close to the trench normal in central Peru. This calculation allows to estimate $\beta=8°\pm7°$ for central Peru and $\beta=23°\pm5°$ to $38°\pm5°$ for northern Andes.

TRANSCURRENT SLIP RATES IN THE OVERRIDING PLATE

Knowing the β angle, the amount of transcurrent slip rate, V_S, may be calculated from formula 2 in both northern Andes and central Peru. In northern Andes V_S= 7±3 to 10±4 mm/a of dextral slip (see Ego et al., this volume) while in central Peru V_S=17±10 mm/a of left-lateral slip. Although V_S value is not precisely constrained in central Peru, it suggests that the overriding plate in central Peru has to accommodate a larger amount of transcurrent slip than the overriding plate in northern Andes. Indeed, in northern Andes only 10-25% of V_P is accommodated by strike-slip deformations in the overriding plate while in central Peru, this appears to be at least 26%. However, major strike-slip fault have been reported in northern Andes, conversely some scarce strike-slip faults are only known in the Cordillera Oriental of central Peru

DISCUSSION

In northern Andes, V_P is accommodated by major right-lateral strike-slip faults (see Ego et al., this volume). In central Peru, may be accommodated either by the N-S extension that affects the Cordillera Occidental and the Coastal area or by the strike-slip deformations that prevail in the Cordillera Oriental (Sébrier et al., 1988). Indeed, thrust and reverse faults of the Subandes are nearly purely dip slip and consequently cannot account to accommodate strike-slip deformations (Figure 1). N-S trending extension may be interpreted as resulting from normla to the topography gravitational forces and a left lateral component of strike-slip that would accommodate V_P. However, the rate of extension that is calculated in the Cordillera Blanca (Sébrier et al., 1988) may explain 1.5 mm/a of left-lateral slip. Thus, the strike-slip deformations of the Cordillera Oriental should at least accommodate of the order of 5 mm/a of left-lateral slip. Finally, the striking difference in the obliquity of subduction slips between northern Andes and central Peru might be explained by the difference of nature of the forearc wedge : oceanic in northern Andes and continental in central Peru. This conclusions appears in good agreement with observations performed by Jarrard (1986) that support the fact that the subduction zone where the overriding plate is oceanic seems to have a more oblique slip than the ones where it is continental. This should indicate that the oceanic or continental nature of the overriding plate induces different mechanical behavior.

REFERENCES

DE METS C., R.G. GORDON, D.F. ARGUS, & S. STEIN, 1990, Current plate motions, *Geophys. J. Int.*, 101, 425-478.

DEWEY J.F. & S.H. LAMB, 1992, Active tectonics of the Andes. Tectonophysics, 205, 79-95

CAREY-GAILHARDIS E. & MERCIER J.L., 1987. A numerical model for determining the state of stress using focal mechanisms of earthquake population: application to Tibetan teleseims and microseismicity of Southern Perou. *Earth Planet. Sci. Lett.*, 82, 165-177.
DZIEWONSKI A.M. et al, from 1981 to 1992. Determination of CMTS in *Phys. Earth. Planet. Int.*
EGO F., SEBRIER M., LAVENU A., EGUEZ A., and YEPES H., 1993. A new geodynamical model for the Northern Ecuadorian Andes. EUG VII, 4-8 April 1993,Terra abstract 5 (1): 203.
FITCH T.J., 1972, Plate convergence, trancurrent faults, and internal deformation adjacent to Southeast Asia and Western Pacific. *J. Geophy. Res.* , 77, 4432-4460.
JARRARD R.D., 1986, Relation among subduction parameters. *Rev. of Geophysics and Space Physics*, 24, 217-284.
MC CAFFREY R., 1992, Oblique plate convergence, slip vectors, and forearc deformation. *J. Geophy. Res.*, 97, B 6, 8905-8915.
PENNINGTON W.D., 1981. Subduction of the eastern Panama basin and seismotectonics of northwestern south America. *J. Geophy. Res.* , 86, B 11 : 10753-10770.
SÉBRIER M., J.L. MERCIER, J. MACHARÉ, D. BONNOT, J. CABRERA, AND J.L. BLANC, 1988, The state of stress in an overriding plate situated above a flat slab: the Andes of Central Peru, Tectonics, 7, 895-928.
U.S.G.S., N.E.I.C., 1988, World Data Center for seismology. Listing years 1977 to 1988, U.S. Dept. of the Interior.

TRENCH-PARALLEL MANTLE FLOW BENEATH THE SUBDUCTED NAZCA PLATE

P. G. Silver and R. M. Russo

DTM, Carnegie Institution of Whashington
5241 Broad Branch Rd., N.W., Washington, DC 20015

We examine seismic anisotropy of the Andean subduction zone and NE South America, through shear-wave splitting measurements, in order to characterize mantle flow beneath the subducted Nazca Plate. The shear-wave splitting parameters (fast polarization direction ϕ and delay time δt between the two split shear waves) from two data sets are discussed: splitting from the SKS phases recorded at Andean stations, and S waves originating in the descending slab and recorded at other stations at teleseismic distances. This latter data set primarily samples the region directly below the slab. The SKS data, however, also sample layers above the slab: part of the descending slab itself, the mantle wedge and the subcontinental mantle below the station. It appears as though the dominant contribution, however, is coming from below the slab. The splitting delay times for upgoing S waves from events in the descending slab, which sample these same layers are much too small to account for the SKS splitting parameters.

ϕ and δt provide constraints on the direction of mantle flow and thickness of the flowing layer respectively. Based on reasonably well established relationships between splitting parameters and deformatin characteristics, and assuming that below the Nazca plate there is an asthenospheric shear flow parallel to the absolute plate motion direciton (APM) of the Nazca plate, then we would expect a roughly EW direction for ϕ for nearly al of the west coast of South America. Instead, we find that about half of the available data yield values of ϕ that are locally parallel to the trench. The other half are more nearly trench-normal, most of which are localized in two bands at 14°S and 24°S. The delay times δt vary from about 0.7s (for SKS) to more than 3.0s for the direct S phases. These large values for S are found between latitudes of 15°S and 25°S and constitute the largest S delay times recorded globally thus far.

We propose the following model for our data. We interpret the trench-parallel values of ø as a manifestation of significant trench-parallel flow beneath the Nazca plate with the flowing region having a thickness of order 100 km. We suggest the flow is a direct result of the retrograde motion of the Nazca slab due to compression-driven slab retreat, and represents the transfer of mantle material from the Pacific to the Atlantic basins. The two

zones of trench-normal values of ϕ are coincident with two changes in slab dip: from 'normal' subduction beneath the Altiplano to 'flat' subduction both north and south. We suggest that the trench-normal values of ϕ represent either a modulation in the trench parallel flow, or possibly flow associated with an actual breack in the slab. Finally, we consider the possibility that the existence of Caribbean and Scotia arcs, as well as the Altiplano are direct or indirect manifestations of the trench parallel flow.

TECTONIQUE
TECTONICS
TECTONICA

STRUCTURAL STYLES IN THE SANTIAGO FOLD AND THRUST BELT, PERU :A SALT RELATED OROGENIC BELT

Antenor M. Alemán and Robert Marksteiner
Amoco Production Co
P.O.Box 3092
Houston, TX 77253

RESUMEN

Inestabilidades gravitacionales, inmediatamente después de la depositación de evaporitas, inició los primeros movimientos de sal en la faja plegada del Santiago. Estos movimientos y el desplazamiento lateral de la sal está manifestado en los cambios bruscos de espesores de las secuencias posteriores a la deposición de sal. Este estilo de deformación fué interrumpido durante las fases Quechua de la Orogenia Andina, la cual se caracterizó por deformación de escamas en la cual la sal jugó un papel muy importante como nivel de despegue. Los pliegues y las fallas no tienen una vergencia preferida y la intrusión de diapiros de sal ha dado como resultado la formación de estructuras periclinales. Análisis de huellas de fisión en apatita ha confirmado una edad de 10 Ma para el fallamiento y plegamiento de esta cadena.

GEOLOGICAL SETTING OF THE SUBANDEAN FOLD AND THRUST BELT (SFTB)

The Subandean Fold and Thrust Belt, adjacent to the Marañon Foreland Basin, is a zone of mainly easterly verging steep to shallow reverse faults and asymmetric folds developed from Late Cretaceous (Peruvian phase) to Pliocene (Quechua-3) phases of the Andean Orogeny (Megard, 1984). The evolution of this FTB is linked in space and time to the presence and interaction of the arc-trench system. Along strike variations in the styles of deformation and width, however, are mainly controlled by the facies, anisotropy and thickness of the sedimentary wedge rather than by the angle of subduction (Jordan et al, 1983). Present day tectonic activity in this belt is documented by tilting of fluvial terraces and by a large number of earthquakes (Suarez et al, 1983).

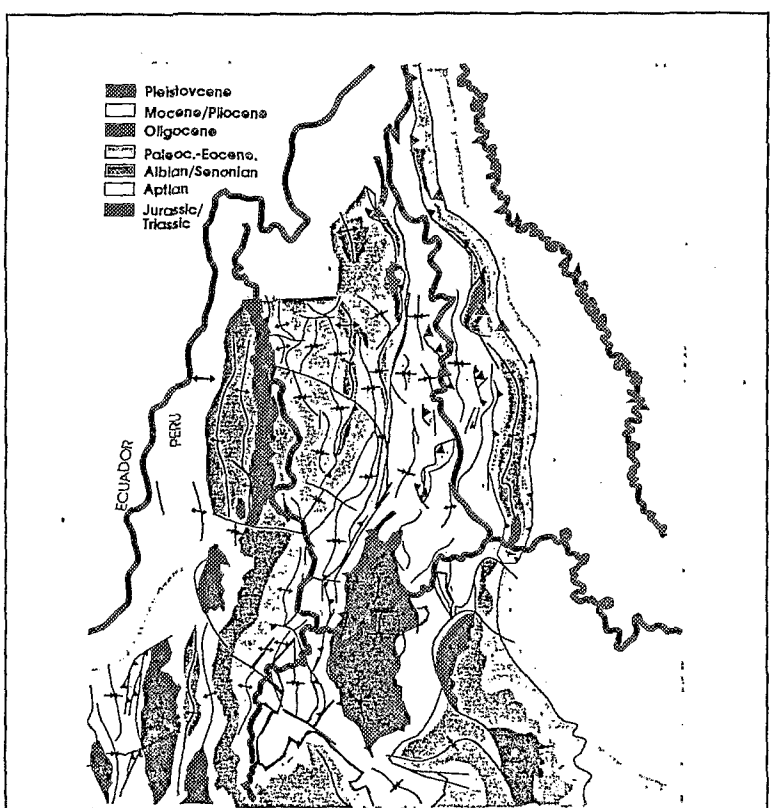

FIG. 1 Geological Map of the Santiago Basin.

The hinterland, known as the Marañon Geanticline (Benavides, 1956), is made up of Precambrian to Late Paleozoic rocks. This structural element was always positive during Cenozoic deformation and often was a submerged high during Mesozoic sedimentation. The SFTB is made up of Mesozoic and Cenozoic clastic and carbonate sequences with folds and faults subparallel to the arc. The Marañon Foreland Basin is a west dipping monocline in which Pre-Cretaceous rocks have been truncated following moderate tilting during the Late Jurassic (Araucanian) movements. This basin consists of up to seven kilometers of Mesozoic and Cenozoic rocks characterized by broad to gentle structures formed during Late Cretaceous to Cenozoic inversion of Jurassic grabens. Intrabasinal highs such as the

Loreto High and the Contamana Hills were active during Cretaceous and Tertiary deposition and are thought to reflect reactivation of pre-existing highs.

SANTIAGO FTB STRATIGRAPHY.

The rocks outcropping in this orogenic belt range in age from Triassic to Pleistocene, and the presence of Paleozoic rocks as old as Ordovician is suspected in this belt in the subsurface as documented in some foreland wells (Fig. 1 and 2). Two distinctive tectono-stratigraphic sequences are present in the Santiago F.T.B. A pre-orogenic sequence, older than Santonian, is represented by the Triassic to Late Jurassic shallow water limestones and bituminous shales of the Pucará Formation (Rodriguez,1982) which are overlain by the red, varicolored sandstones and shales of the Jurassic Sarayaquillo Formation. Cretaceous sedimentation was initiated in the Aptian with the deposition of cross-bedded sandstones of the Cushabatay Formation and , after several transgressive-regressive pulses, terminated with the Senonian (Santonian ?) shales of the Cachiyacu Formation (fig.2).

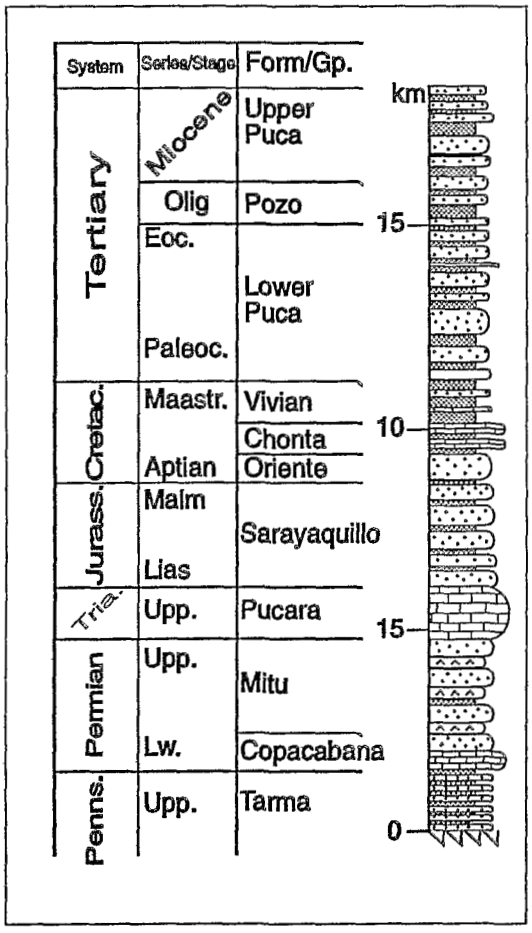

The synorogenic sequence in the Santiago FTB began with the Late Cretaceous molasse sandstones and shales of the Huchpayacu Formation, which have not been differentiated in this belt and are probably included in the Lower Tertiary red sandstones and shales of the Lower Puca Formation (Fig.2). A period of relative tectonic quiescence was recorded during the Oligocene with deposition of marine shales, sandstones and tuffs of the Pozo Formation. A new pulse of molasse deposition was triggered in the Miocene with deposition of the Upper Puca Formation which probably continued throughout the Pliocene and Pleistocene with subtle breaks in sedimentation (Neiva and Corrientes Formation). Different pulses of molasse deposition are correlated to known phases of the Andean Orogeny which involved supracrustal thrusting and uplifting of the hinterland.

AGE AND ROLE OF THE EVAPORITES

Benavides (1968), in his detailed analysis of the Huallaga diapirs, was the first to address the problem of the age of the evaporites in the Sub-Andean Basins of Peru. Because of the poorly defined structural and stratigraphical relationship of the salt source, he concluded that the age of the salt could be either Permian, Triassic and/or Jurassic. However, he did not rule out the possibility of multiple sources for some of the salt domes.

Indeed, the Late Permian red sandstones, shales and conglomerates of the Mitu Group contain significant amounts of gypsum and salt (Newell et al, 1953). The salt in the San Blas dome, in the central Andes, has been assigned to this unit by Benavides (1968). He also described some beds and lenses of gypsum with a maximum thickness of 8 meters in the Mitu Group near to the Pongo the Rentema (about 80 Km west of the Santiago Basin). Further evidence for a Permian and/or Triassic age for the salt is found in the Huallaga Basin where the salt in the Yuramarca dome contains limestones fragments that are interpreted to be from the Triassic/Jurassic Pucara Group. Furthermore, salt flowage in the Pilluana dome has brought up limestones containing *Myophoria pascoensis* of Late Triassic age and an Early Jurassic ammonite *Arietites sp.* (Benavides, 1968).

Rodriguez and Chalco (1975), based on S^{32}/S^{34} ratio in some of the evaporites in the Huallaga Basin, have suggested a Permian age for the salt domes in the Huallaga Basin; unfortunately, they did not

elaborate on their analysis. Therefore, the age of the salt in the Santiago and Huallaga FTB is Early Jurassic or older.

Recently, some wells (Loreto-1), drilled on the Marañon Foreland Basin, cored crystalline anhydrite interbedded with red and varicolored sandstones and limestones in the upper part of the Jurassic/Triassic Pucara Formation. Sabkha type limestones and dolomites are found in the Upper Ucayali Basin while Benavides (1968) has described some massive dolomites and limestones of Triassic age which rest upon gypsum beds that appear to be also of the same age in the Utcubamba valley of northern Peru. He also describes the overlying Middle Jurassic (Bajocian) beds near the Yeso locality which contain anhydrite and gypsum correlateing with the gypsiferous Chambará Formation near Tarma, in central Peru (Megard, 1978). In the central Andes, at Morococha, Benavides (1968) also describes a body of 150 meters thick of anhydrite unit with shale and limestone interbeds interpreted to be Middle Jurassic in age.

The Pucará Group is transitionally overlain by the Sarayaquillo Formation of Middle to Late Jurassic age which, in central Peru near La Merced, contains beds of salt near Cerros de la Sal. North of this locality, the Oxapampa-7-1 well contains 1720 meters of clear to white salt and anhydrite below Cretaceous beds and above rhyolites and conglomerates of the Permian Mitu Group. Benavides (1968) interpreted two of these salt intervals to be Jurassic in age. In northern Peru, in the Utcubamba region, the red beds of the Sarayaquillo Formation contain several beds of gypsum, some reaching several tens of meters in thickness (Benavides, 1968).

Although the cores of most salt diapirs in the Huallaga Basin are surrounded by the Sarayaquillo Formation, the age of the salt is still unknown. According to Benavides(1968) the source was a pre-Late Jurassic unit. Distribution of different thicknesses of salt bearing units along the foreland fold and FTB seems to have played a very important role, not only in the in the structural style but also in variations in the width of the S.A.F.T.B. Distribution of the Late Permian Mitu Group was controlled by the preservation of grabens and half-grabens formed during Late Permian extension (Megard, 1978) which has not been recognized in Ecuador. On other hand, the Triassic/Jurassic Pucara Group continues to the north in Ecuador where it is Known as the Santiago Formation. No evaporites have been described in this unit however. The Pucara Group seems to thin out southward near the Sira Mountains. Finally, the Jurassic Sarayaquillo Formation, which reaches significant thickness in northern Peru and southern Ecuador, contains only thin evaporites in the Cutucu Mountains where it is known as the Chapiza Formation (Tschopp, 1953), also thins out southward and disappears near the Sira Mountains.

STRUCTURAL STYLES OF THE SANTIAGO FTB.

Gravitational instability triggered early salt movement soon after the first evaporite deposition and was manifested by major outward and lateral movement of salt toward the Campanquiz and Huaracayo Ranges. This event is documented by rapid changes in thickness and facies of the post-salt to Pelogene units. Indeed, Late Cretaceous to Paleogene loading by molasse deposition associated with the Peruvian and Incaic phases of the Andean Orogeny in the hinterland have merely enhanced the rate of salt movement, and thus the facies and thickness changes. A pulse of relative tectonic quiescence with little or no salt movement (Pozo Formation deposition) preceded the maximum paroxysm of the Quechua phase (Neogene) of the Andean Orogeny. In the Santiago Basin, this Quechua event has been dated with apatite fission track (AFT) methods and was characterized by thin skinned deformation and the formation of a salt related fold and thrust belt with a relatively moderate amount of shortening.

The Santiago FTB, formed by the complex interaction of gravitational instabilities of salt and compressional forces, is similar to other salt related thrust belts in the world which are characterized by low taper angle (Davis and Engelder, 1985). This orogenic belt consists of a complex in and out-of-sequence fold and thrust belt with low cross-sectional taper angle similar to the Huallaga FTB to the south. The folds are characterized by anticlinal thickening and synclinal thinning of the salt, with faulting dominated by high angle back thrusts and diffuse forward vergent thrusts (Fig.. 3 AND 4). In general, there is a lack of a preferred structural vergence of ramps and folds. Salt domes are often developed near the axis of synclines with common development of rim synclines by either salt withdrawal at the footwall of the listric faults or by normal listric faults formed by reactivation of pre-existing thrust faults. Salt

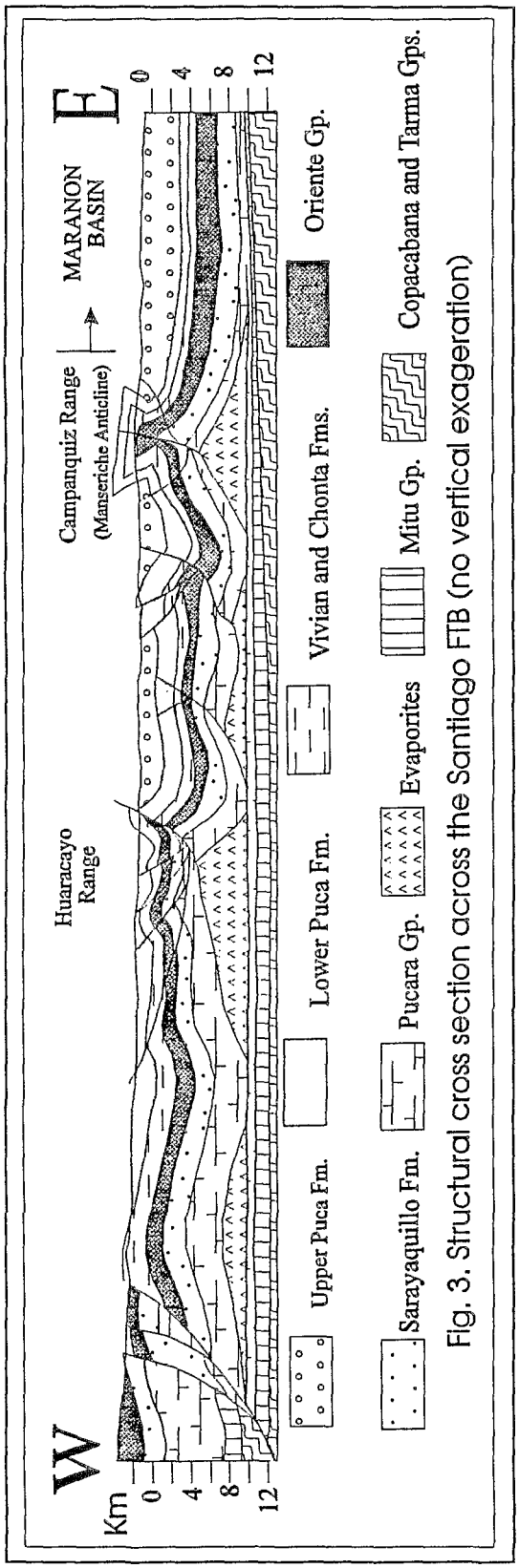

Fig. 3. Structural cross section across the Santiago FTB (no vertical exageration)

piercement accounts for narrow periclinal structures and the enlargement of pre-existing broad synclines. Most of the periclines are pierced by diapiric structures. Significant uplifts of the frontal thrust and in the
adjacent hinterland are related to pronounced salt thickening (Huaracayo and Campamquiz Ranges). The frontal thrust is usually characterized by the development of box-folds, overturned folds, or upright folds above a major salt core. Indeed forward and back thrusting at the mountain front are often propagated in several splays over a paleo high formed by early salt withdrawal.

The main orientation of the folds and thrusts changes from N-NE to NW near the latitude of the Marañon River, similar to changes reported in the Eastern Cordillera (Ham and Herrera, 1963). This oroclinal bending was initiated during Early Creataceous accretion of the Tahuin Terrane to the Peruvian margin and post-Oligocene clockwise and counterclockwise rotations respectively north and south of the Huancabamba deflection (Mitouard et al, 1990, Laj et al, 1992).

EVOLUTIONARY STAGES OF THE SANTIAGO FTB

The Late Jurassic Araucan Orogeny is poorly defined in Peru and Ecuador and is represented in the S.A.F.T.B. by moderate tilting of the Sarayaquillo/Chapiza formations before the deposition of the Aptian Cushabatay/Hollin Formations. Several sismic lines in the area (Touzett and Sanz, 1985) provide strong evidence for at least Early Cretaceous salt withdrawal with coeval growth and variable sedimentation rates throughout the Late Miocene. The structural depression, along the Santiago River, was formed by pervasive thrusting accompanied by salt diapirism.

The evolution of the Santiago Basin seems to have undergone the following structural/ depositional stages since the Mesozoic.

STAGE I.- Once deposition of evaporite bearing units terminated, sedimentation and tectonic movements caused gravitational instabilities and triggered early movement of the evaporites. Evaporite withdrawal took place during the Araucan Orogeny (Late Jurassic) when the evaporites moved laterally and upward into the cores of the Campanquiz and Huaracayo Ranges. Sediment loading at the center of the basin caused the evaporites to move in a double end toothpaste tube fashion. Cretaceous sedimentation was thicker in the center of the basin (Santiago and Neiva Basins s.s.)

than on the flanks (ranges). This pronounced change in thickness was accompanied by significant changes in facies across the belt.

Sediment loading continued throughout the Paleogene with local intrabasinal salt movement within the Santiago depression as illustrated in the Apingrasa Structure in which some sort of growth faulting is recorded (Touzett and Sans, 1985). High rates of sedimentation associated with Late Cretaceous and Paleogene molasse of the Peruvian (Santonian) and Incaic (Middle Eocene) phases of the Andean Orogeny provided the mechanism for evaporite remobilization.

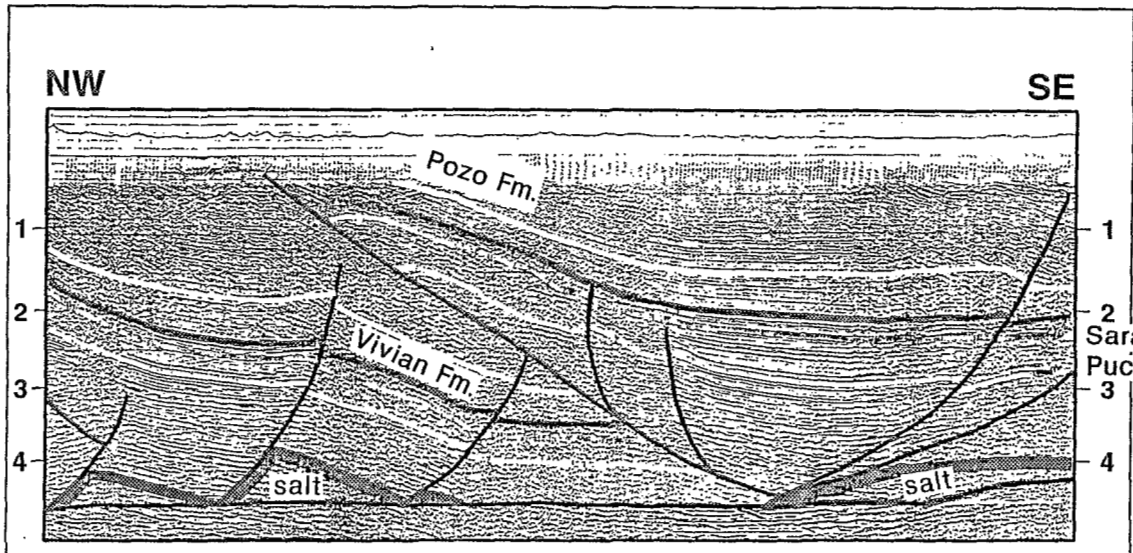

Fig.4

STAGE II.- The Oligocene was a period of tectonic quiescence with little or no salt movement. Sedimentation changed from fluviatile in the Lower Puca Formation to the shallow marine environment in the Pozo Formation (Rodriguez, 1982).

STAGE III.- Reactivation of salt movement during the Early and Middle Miocene was accompanied by a recurrence of the fluviatile Upper Puca Formation. Salt piercement accounted for narrow periclinal anticlines and the enlargement of pre-existing broad synclines.

STAGE IV.- The Late Miocene and Pliocene/Pleistocene movements of the Quechua phase of the Andean Orogeny were the result of horizontal compressional forces which reactived and modified the structural pattern established early in the evolution of the basin. Forward-vergent thrusting was rather diffuse while back thrusts were steeper and more localized. Most of the periclinal anticlines were broken by diapiric structures located above synclinal counterfolds.

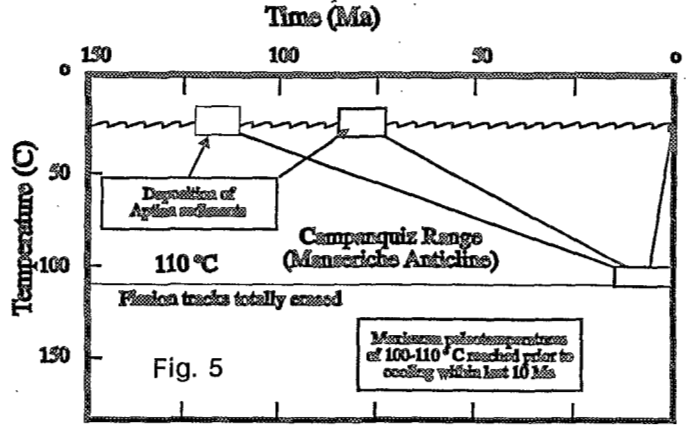

Fig. 5

AFT ANALYSIS

Four outcrop samples of Campanian to Aptian age were analyzed for apatite fission tracks with the purpose of obtaining possible constraints on the thermal history, maximum depth of burial, and timing and rate of uplifts and exhumation (Table I). Two samples were from the Campanquiz Range (sample 1 and 2) and the other two were from the Huaracayo Range (samples 3 and 4). The analyses were conducted by Geotrack International.

The four samples show consistent evidence of elevated temperatures at some time since deposition. Indeed, mean fission track ages are significantly less than the respective Cretaceous stratigraphic ages, and the majority of individual grains give fission track ages which are very much less than the stratigraphic age. Furthermore, measured mean track lengths are all much less than the predicted values of of the mean length (l_p=14.9 μm). This means that the great majority of tracks in these samples are shorter than would be expected if they had formed at the prevailing temperatures in each sample. The shorter tracks were the result of enhanced fission track annealing at elevated paleotemperatures at some time after deposition.

TABLE I. APATITE FISSION TRACK ANALYSIS

Samp.	Formt.	# of grains	Standard track density $x10^6 cm^{-2}$	Fossil track density $x10^5 cm^{-2}$	Induced track density $x10^6 cm^{-2}$	Chi squar prob %	Fiss. track age (Ma)	U cont. ppm	Mean track length (μm)	σ μm
1	Cush.	20	1.221	0.904	2.323	<1	8.4 ± 1.2	25	10.76 ± 1.30	3.89
			(1921)	(52)	(1336)		20.3 ± 10.5*		(9)	
2	Cush.	20	1.221	1.010	2.343	2.2	9.3 ± 1.1	25	13.14 ± 0.54	2.07
			(1921)	(73)	(1693)		13.3 ± 3.6*		(15)	
3	Vivian	11	1.221	3.786	3.422	<1	23.8 ± 2.9	37	13.19 ± 0.03	0.04
			(1921)	(76)	(697)		60.7 ± 43.2*		(2)	
4	Cush.	20	1.221	6.409	4.428	<1	31.1 ± 1.9	48	11.16 ± 0.46	2.39
			(1921)	(363)	(2508)		39.0 ± 22.2*		(27)	

Brackets show number of tracks counted

Standard and induced track densities measured on mica external detectors (g =0.5, and fossil track densities on internal mineral surfaces

* Mean age used where pooled data fail χ^2test at 5%. Errors quoted at ± 1σ

Ages for samples calculated using ζ = 3.527using (Analysis P.O. Sulivan) for dosimeter glass SRM612 (Hurford and Green, 1983).

All four samples show clear evidence of having undergone paleotemperatures in the range of 100° to 110° C reached prior to a Late Tertiary cooling event (within the last 10 Ma). Two samples from the Campanquiz Range (samples 1 and 2) reached a maximum post depositional paleotemperatures during the Neogene heating episode (Fig. 5). However, the two from the western Huaracayo Range (samples 3 and 4) show evidence to have experienced even higher paleo-temperatures at some other time prior to the Neogene (Fig. 6).

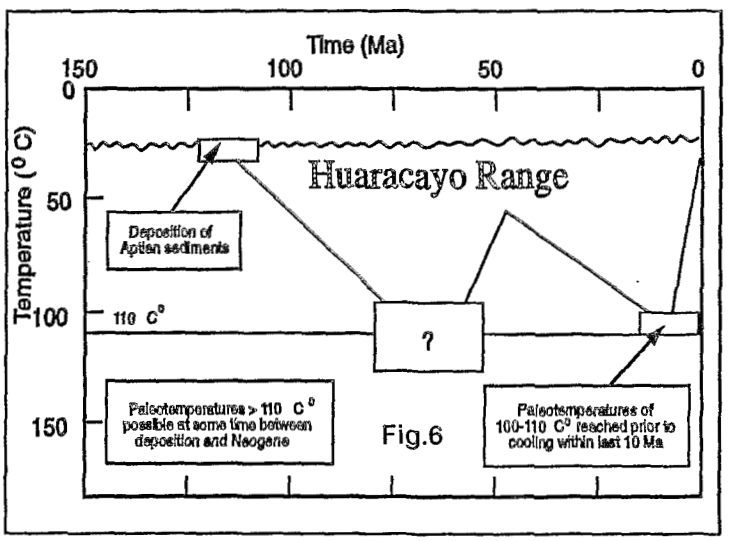

Fig.6

Cooling was rapid with up to 3.5 to 4.5 km of section removed from both areas since cooling begun assuming that the present day gradient is 1.15 °F/100 ft (21°C/km) and the present day surface temperature of 80°F (27 °C) prevailed at the time of uplift. The data do not allow accurate assessment of the active exhumation rate, but a minimum average rate of 350 to 400 m/Ma, is estimated assuming continuous uplift since 10 Ma to the present.

REFERENCES

Benavides, V. (1956) Cretaceous system in northern Peru: Bull. Am. Museun Nat. History, v.108, art.4, p.359-488.

_____ (1968) Saline deposits of South America, in: R. B. Mattox (ed.) "SalineDeposits", Geol. Soc. Amer. Sp. Paper 88, p.249-290.

Davies, D. M., and Engelder, 1985; The role of salt in fold-and-thrust belts, Tectonoph. 119, p. 67-88.

Ham, C. K.; and Herrera, L. Jr.; 1963, Role of the Subandean fault system in tectonics of eastern Peru and Ecuador, in Childs, O., and Beebe, W. (editors) " Backbone of the Americas" Amer. Ass. Petr. Geol. Memoir 2, p.47-61.

Jordan, T. E. ; Isacks, B. L.; Allmendinger, R. W.; Brewer, J. A.; Ramos, V. A.; and Ando, C. J., 1983, Andean tectonics related to the geometry of subducted Nazca Plate: Geol. Soc. Amer. Bull. , v.94, p. 341-361.

Laj, C.; Mittouard, P.; Roperch, P.; Kissel, C.; Mourier, T.; and Mégard, F.; 1993, Paleomagnetic rotations in the coastal areas of Peru and Ecuador: in Kissel, C. and Laj, C. (editors, "Paleomagnetic rotations and Continental Deformation", NATO Series, (in press)

Mégard, F., 1978, Etude géologique des Andes du Pérou Central, Mem. ORSTOM 86, Paris

_____, 1984; The Andean orogenic period and its major structures in central and northern Peru; Jour. Geol. Soc. London, 141, 893-900.

Mitouard, P.; Kissel, C.; and Laj C.; 1990, Post-Oligocene rotation in southern Ecuador and northern Peru and the formation of the Huancabamba deflection in the Andean Cordillera: Earth and Plan. Sc. Let. 98, p. 329-339.

Newell, N. D.; Chronic, J., and Roberts, T. G., 1953, Upper Paleozoic of Peru: Geol. Soc. Amer. Memoir 58, 276 p.

Rodriguez, A., 1982; Exploración por petróleo en la Cuenca Santiago,18 pgs, in: Simposio de Exploración Petrolera en las Cuencas Subandinas de Venezuela, Colombia, Ecuador y Perú; Assoc. Col. de Geol. and Geof., Bogotá, Colombia.

Rodriguez, A.; and Chalco, A.; Cuenca Huallaga, Reseña geológica y posibilidades petrolíferas: Bol. Soc. Geol. del Perú, T. 45, p. 187-212.

Suares, G.; Molnar, P.; and Burchfield, B; 1983, Seismicity,fault plane solutions, depth of faulting and active tectonics of the Andes of Peru, Ecuador and souther Colombia: J. Geoph. Res. 64(1), p. 49-58.

Touzett, P. and Sans, V., 1985; Presente y futuro de la exploración petrolera en las Cuencas Subandinas del Perú: Simposio Bolivariano- Exploración Petrolera en las Cuencas Subandinas, Bol II, Assoc. Col. de Geol. and Geof., Bogotá, Colombia.

Tschopp, H. J., 1953, Oil explorations in the Oriente of Ecuador: Amer. Ass. Petr. Geol. Bull. 37, p. 2303-2347

LATERAL VARIATIONS IN LATE CENOZOIC DEFORMATION, CENTRAL ANDES, 20 – 28°S

R. W. ALLMENDINGER, T. GUBBELS, B. ISACKS, T. CLADOUHOS

Dept. of Geological Sciences & Institute for the Study of the Continents
Snee Hall, Cornell University, Ithaca, NY 14853-1504 USA

RESUMEN:

KEY WORDS: Altiplano, Puna, Neotectonics, paleotectonics, deformation timing

INTRODUCTION

Major changes in the timing and geometry of late Cenozoic Andean structure occur between 23 and 24°S and include: (1) The southward terminus of the Subandean thin-skinned thrust belt occurs at between 23 and 24°S and farther south the foreland is dominated by the thick-skinned, basement-cored blocks of the Sierras Pampeanas. (2) The temporal transition from major thrust faulting to minor normal and strike-slip faulting across the entire plateau region occurs much later in the south (at ~1-4 Ma) than it does in the north (at ~10 Ma). In general, neotectonic activity is much greater in the Puna than it is in the Altiplano. (3) The average topography of the Puna is about 1 km higher, and its internal relief is greater, than that of the Altiplano. (4) Cenozoic sedimentary basins of the Eastern Cordillera-northern Puna are 2-4 km thinner than those of the southern Puna. Major geophysical and petrologic changes between 23 and 24°S — including the southward termination of a high-low paired isostatic residual gravity anomaly, lateral variations in seismic waves attenuation, and primitive mafic magmatism — are described in the accompanying paper by Whitman et al. (this volume). We suggest that these spatial and temporal variations in late Cenozoic structure and volcanism in the Central Andes are probably linked to major, N-S changes in lithospheric structure and thickness. Some of these changes have been associated with changes in angle of subduction (e.g. Jordan et al., 1983) and several are spatially correlated with major paleotectonic features.

FORELAND: SUBANDEAN BELT TO SIERRAS PAMPEANAS

Throughout Bolivia, the thin-skinned Subandean foreland thrust belt bounds the eastern margin of the Andes. The thrust wedge taper varies from about 7° north of Santa Cruz to 2-3° in southern Bolivia. The basal decollement is at ~12 km beneath the Principal Frontal thrust which marks the boundary between the Subandean belt and Eastern Cordillera. Between 23° and 24°, the structure of the foreland changes dramatically. At 24°, Cahill et al. (1992) showed that seismicity in the foreland extends to depths greater than 30 km. This area, known as the Santa Barbara ranges, constitutes the northernmost extent of the Sierras Pampeanas province of thick-skinned basement deformation. Seismicity data throughout the Sierras Pampeanas shows that virtually the entire crust is involved in young deformation (Chinn & Isacks, 1983; Smalley et al., 1993).

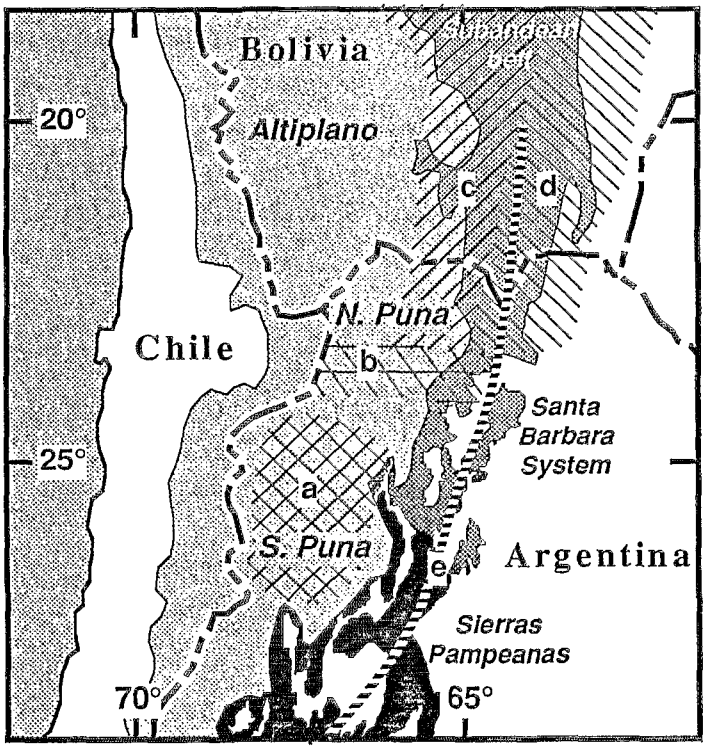

Fig. 1. Regional location map of the Central Andes between 18 and 28° S, showing some of the major lateral changes. (a) region of primitive mafic magmatism in the southern Puna. (b) Approximate boundary between cessation of thrusting at ~10 Ma to the north and 1-2 Ma to the south. (c, d) Positive and negative, respectively, isostatic residual gravity anomalies. (e) Location of longitudinal stratigraphic section shown in Fig. 3.

Shortening in the Subandean belt is probably less than 10 Ma in age (Gubbels et al., in press). Several different areas in the northern Sierras Pampeanas contain evidence for uplift younger than 6 Ma and locally younger than 2-3 Ma ago (Allmendinger et al., 1989; Strecker et al., 1989).

Altiplano-Puna-Eastern Cordillera

The morphology of the Altiplano is dominated by a broad flat basin at an average elevation of about 3.7 km (Isacks, 1988). In contrast, the Argentine Puna has many interior mountain ranges and has an average elevation of just under 4.5 km. The high flat, shallow basins in the vicinity of La Quiaca and Abra Pampa are continuous in northern Argentina but in Bolivia they occur as isolated erosional remnants in the Eastern Cordillera. These basins overlie a regionally extensive unconformity, the San Juan del Oro surface, that truncates compressional structures and is deformed only by small normal and strike-slip faults. Tuffs overlying the unconformity have been dated at 8-9 Ma; they unconformably overlie folded and thrust faulted mid-Miocene strata, locally dated at 12-17 Ma. Deposits near the top of the surface have yielded ages between 2 and 4 Ma. Kinematic analysis of the Miocene deformation near the international border indicates WNW shortening, perpendicular to the strike of the mountain ranges, and vertical extension. The surfaces are deformed by well preserved scarps of younger normal and strike-slip faults which have produced minor, SSE subhorizontal extension and WSW or vertical shortening.

South of 23°S, the southern Puna and Eastern Cordillera display the same relative kinematic

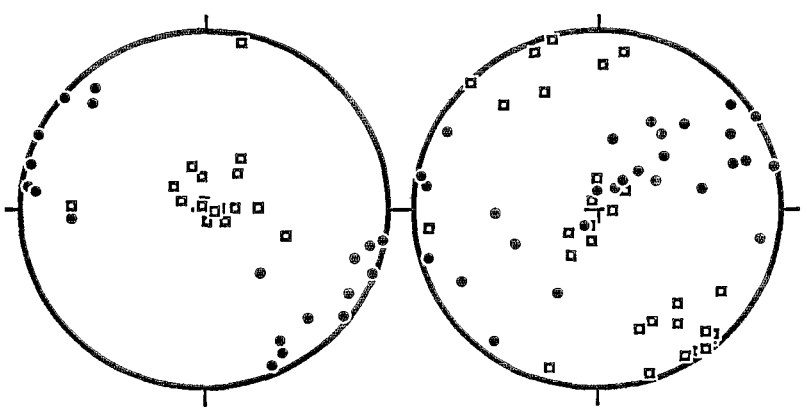

Fig. 2. Lower hemisphere equal area projections summarizing kinematic data from the Puna and southernmost Bolivian Eastern Cordillera. Left: Older deformation (pre-9 Ma in north and pre-1 Ma in the south). Right: Younger deformation. In both, solid dots are shortening and open boxes are extension.

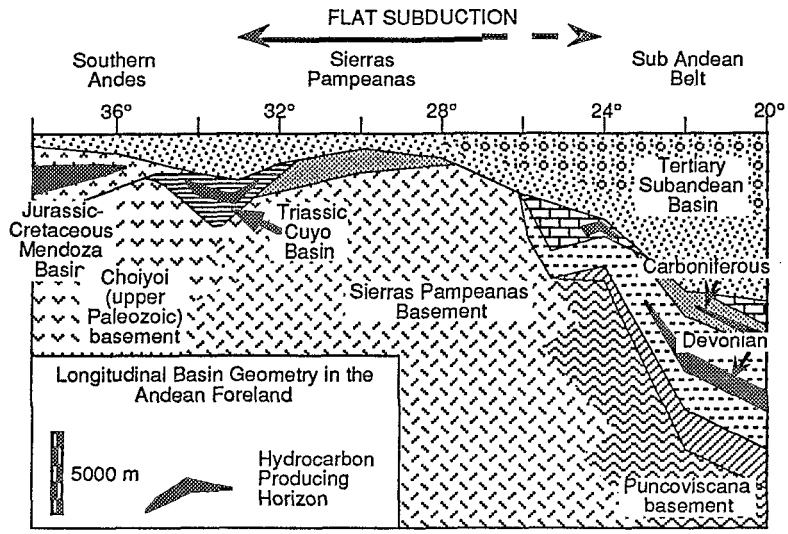

Fig. 3. Longitudinal stratigraphic section which shows the orogen-parallel variation in basin geometry in the Andean foreland. Note that most of the variation is in the pre-Tertiary subcrop and thus pre-dates the Cenozoic Andes.

sequence (Fig. 2) but the transition from older thrust faulting to younger strike-slip and normal faulting occurred as recently as 1 Ma in the Quebrada del Toro and < 4 Ma in the Puna. Younger deformation is probably no older than about 1 Ma and continues today. Tertiary strata in the northern Puna and Eastern Cordillera are generally less than 1 km in thickness. Tertiary strata in the Puna from ~23° southward are much thicker than farther north. Several Neogene basins have more than 2000 m of strata, including the Hombre Muerto region with 5000 m of Miocene rocks (Alonso et al., 1991).

Paleotectonics

Comparison of Cretaceous subcrop and pre-Cretaceous isopach maps with modern geologic maps of the Central Andes clearly shows that the many of the modern tectonic provinces have inherited their location, extent, and even structural geometry from pre-Andean tectonic events (Allmendinger et al., 1983; Gubbels et al., in press). The style of late Cenozoic foreland deformation in Bolivia and Argentina correlates almost exactly with the extent of pre-Andean basins (Fig. 3). The Subandean thin-skinned belt is restricted to the thick previously undeformed Paleozoic basins which mostly pinch out between 23 and 24°S; the basement rocks of the Sierras Pampeanas have been at or near the surface for the last 150 Ma (Jordan et al., 1989). The Bolivian Eastern Cordillera was deformed prior to the Mesozoic and was a relative positive element during the Cretaceous.

Interpretation

We suggest the following scenario to explain the family of changes that occur near 23°S: The entire region shares a similar mid-Miocene structural history. Crustal shortening, oriented WNW-ESE (~120°), was concentrated in the regions of the Altiplano, Eastern Cordillera, and Puna. A major change occurred at about 10 Ma: horizontal shortening in the Altiplano and Eastern Cordillera ceased and shifted eastward into the thick, undeformed, eastward-tapering Paleozoic through Tertiary cover of the Brazilian Shield. Subsequent shortening in the Subandean belt was predisposed to be thin-skinned because of the pre-existing basin geometry; thin-skinned shortening requires underthrusting of cold Brazilian shield lithosphere beneath the orogen north of ~23°. In contrast, shortening in the Puna and Argentine Eastern Cordillera continued to <4 Ma and locally is as young as 1 Ma. Shortening probably remained concentrated in the thermally weakened Puna rather than propagating eastward as a thin-skinned belt because pre-existing basins in the foreland are thin and irregular. Thus, north of 23°S, the Andes have experienced a two phase deformation sequence during the Late Cenozoic with a transition at about 10 Ma (Gubbels et al., in press). The Puna remained in phase 1 until much more recently and only entered phase 2 with the uplifting of the northern Sierras Pampeanas.

Geochemical data, the difference in altitude, seismic wave attenuation, and an inferred change in stress regime all suggest that the lithosphere south of 24°S is substantially thinner than it is to the north; delamination, sub-lithospheric erosion or stoping are the most logical explanations (Whitman et al., 1992;

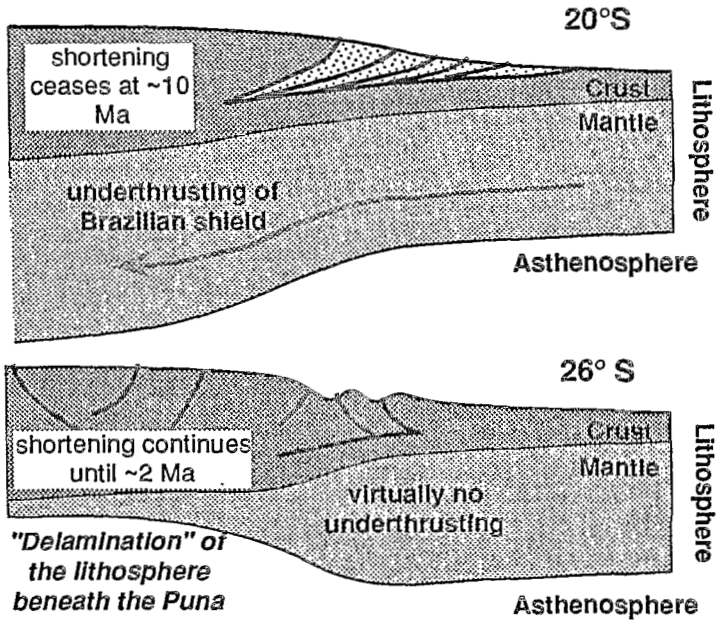

Fig. 4. Schematic, lithospheric-scale cross-sections across the Andes at the latitudes of the Altiplano and the southern Puna. See accompanying abstract by Whitman et al. (this volume) for the discussion of geophysical and geochemical data relating to the same model. Not to scale.

Kay & Kay, 1993). Lithospheric thinning may be due to continued shortening concentrated in the high plateau or more likely to thinning in front of a northward migrating zone of flat subduction.

References

ALLMENDINGER, R. W., RAMOS, V. A., JORDAN, T. E., PALMA, M., AND ISACKS, B. L., 1983, Paleogeography and Andean structural geometry, northwest Argentina: Tectonics, v. 2, p. 1-16.

ALLMENDINGER, R. W., STRECKER, M., EREMCHUK, J. E., AND FRANCIS, P., 1989, Neotectonic deformation of the southern Puna plateau, NW Argentina: Journal of South American Earth Sciences, v. 2, p. 111-130.

ALONSO, R. N., JORDAN, T. E., TABBUTT, K. T., AND VANDERVOORT, D. S., 1991, Giant evaporite belts of the Neogene central Andes: Geology, v. 19, p. 401-404.

CAHILL, T., ISACKS, B. L., WHITMAN, D., CHATELAIN, J.-L., PEREZ, A., AND CHIU, J.-M., 1992, Seismicity and tectonics in Jujuy Province, northwestern Argentina: Tectonics, v. 11, p. 944-959.

CHINN, D. S., AND ISACKS, B. L., 1983, Accurate source depths and focal mechanisms of shallow earthquakes in western South America and in the New Hebrides island arc: Tectonics, v. 2, p. 529-564.

GUBBELS, T. L., ISACKS, B. L., and FARRAR, E., in press, High-level surfaces, plateau uplift, and foreland development, Bolivian Central Andes: Geology.

ISACKS, B. L., 1988, Uplift of the central Andean plateau and bending of the Bolivian orocline: Journal of Geophysical Research, v. 93, p. 3211-3231.

JORDAN, T. E., ISACKS, B. L., ALLMENDINGER, R. W., BREWER, J. A., RAMOS, V. A., AND ANDO, C. J., 1983, Andean tectonics related to geometry of subducted Nazca plate: Geological Society of America Bulletin, v. 94, p. 341-361.

JORDAN, T. E., ZEITLER, P., RAMOS, V., AND GLEADOW, A. J. W., 1989, Thermochronometric data on the development of the basement peneplain in the Sierras Pampeanas, Argentina: Journal of South American Earth Sciences, v. 2, p. 207-222.

KAY, R. W., and KAY, S. M., 1993, Delamination and delamination magmatism: Tectonophysics, v. 219, p. 177-189.

SMALLEY, R., JR., PUJOL, J., REGNIER, M., CHIU, J. M., CHATELAIN, J.-L., ISACKS, B. L., ARAUJO, M., AND PUEBLA, N., 1993, Basement seismicity beneath the Andean Precordillera thin-skinned thrust belt and implications for crustal and lithospheric behavior: Tectonics, v. 12, p. 63-76.

STRECKER, M., CERVENY, P., BLOOM, A. L., AND MALIZZIA, D., 1989, Late Cenozoic tectonism and landscape development in the foreland of the Andes: Northern Sierras Pampeanas (26-28°S), Argentina: Tectonics, v. 8, p. 517-534.

WHITMAN, D., ISACKS, B. L., CHATELAIN, J.-L., CHIU, J.-M., and PEREZ, A., 1992, Attenuation of high frequency seismic waves beneath the central Andean plateau: Journal of Geophysical Research, v. 97, p. 19,929-19,947.

STRUCTURAL SYNTHESIS OF THE BOLIVIAN SUBANDEAN ZONE

Patrice BABY (1), Bertrand GUILLIER (2), Jaime OLLER (3), Gérard HERAIL (4), Genaro MONTEMURRO (3), David ZUBIETTA (3) and Martin SPECHT (5).

(1) ORSTOM, CC 4875, Santa Cruz, Bolivia.
(2) IFEA, CC 4875, Santa Cruz, Bolivia.
(3) YPFB - GXG, CC 1659, Santa Cruz, Bolivia.
(4) ORSTOM, CC 53390, Correo Central, Santiago, Chile.
(5) IFP, Division Géologie-Géochimie - RB10, B.P. 311, 92506 Rueil Malmaison Cedex - France.

RESUME: Une synthèse structurale de la Zone Subandine Bolivienne est présentée à partir de coupes équilibrées et d'une nouvelle méthode d'équilibrage de cartes. On met ainsi en évidence et on quantifie les relations chevauchements-décrochements de part et d'autre du Coude de Santa Cruz.

KEY WORDS: Subandean, Bolivia, balanced cross section, map balancing, wrenching, plate convergence.

INTRODUCTION

The Subandean Zone of Bolivia is a complex foreland fold and thrust belt [Sheffels,1988; Roeder, 1988; Baby et al., 1989, 1992] that forms the eastern edge of the central Andes mountains (fig. 1). In its central part (between 16°S and 18°S), this fold and thrust belt forms a bend (Santa Cruz bend) characterized by important transfer zones. From north to south, the structural geometry as the amount and direction of shortening present important variations.

The purpose of this paper is to present a geometric and kinematic study of this complex foreland fold and thrust belt deduced from cross section and map balancing. The geometry of the entire Bolivian Subandean Zone is analyzed and its deformation quantified.

GEOLOGICAL SETTING

The Bolivian Subandean Zone is bounded at the Cordillera Oriental edge by the Main Frontal Thrust (CFP), whereas the orogenic front developed below the Beni and Chaco plains at the eastern edge. The deformation started in the Late Oligocene and is still developing [Sempere et al., 1990]. The material involved in Subandean thrusting in Bolivia consists of a series from Ordovician to Jurassic and a Late Oligocene to recent continental foredeep fill. This pre-orogenic sedimentary series presents lateral variations of facies and thicknesses which play an important role in controlling the structural geometry. From north to south, three structural zones characterize the Bolivian Subandean fold and thrust belt: the Northern

Subandean Zone NW-SE oriented, the Central Subandean Zone which changes from a NW-SE to a N-S orientation and the Southern Subandean Zone N-S oriented. They are described in the following balanced cross sections.

BALANCED CROSS SECTIONS

Construction of balanced cross sections has been made possible due to surface mapping, reflection seismic data, and drilling information provided by the Bolivian State Oil Company (YPFB).

Northern Subandean Zone - between 13° et 16° S - (Fig. 1A): It is characterized by important thrust sheets (10-20 km) and broad synclines filled by Tertiary sediments (piggy back basins with 6,000 m of synorogenic sediments). The main detachments are located in the Ordovician shales, in the Silurian shales, in the Devonian shales and in the Permian shales. The foredeep has a bottom that slopes at 4°. The maximum amount of shortening is 135 km, i.e. 50%.

Central Subandean Zone - between 16° et 18° S - (Fig. 1B-1C): It is characterized by the Boomerang-Chapare transfer zone which is interpreted as a lateral ramp whose propagation was guided by the northern border of a Paleozoic sedimentary wedge, obliquely oriented vis-à-vis the regional shortening direction [Baby et al., 1993]. This sedimentary wedge consists of a continuous series ranging from Ordovician to Carboniferous thinning northwards lies on the Cambrian-Precambrian Brazilian shield, and unconformably covered by an isopachus series of 500 meters of Mesozoic and more than 1,600 meters of Oligocene to Actual deposits. The major decollement is located in the bottom of the Paleozoic sedimentary wedge. The maximum amount of shortening is 130 km, 45%.

Southern Subandean Zone - between 19° et 22° S - (Fig. 1D): An important east verging thrust (Mandiyuti Thrust) divides the southern Bolivian Subandean Zone into two fold and thrust belts that differ according to their thrust system geometry. The western belt is characterized mainly by fault propagation folds and fault bend folds, whereas the eastern belt is characterized by fault propagation folds and passive roof duplexes [Baby et al., 1992]. The main detachments are located in the Ordovician shales, in the Silurian dark shales, in the early Devonian shales, and in the base and top of the Middle to Late Devonian dark shales. The Silurian-Devonian succession is covered by more than 2000 m of late Paleozoic and Mesozoic sandstones with no potential detachments; in some places it is also covered by several thousand meters of synorogenic Tertiary sedimentary rocks. The foredeep has a bottom that slopes at 2°. Total shortening decreases from 20° S (140 km, i. e. 50%) toward the south (70 km, i. e. 30%, at 22° S).

MAP BALANCING

In order to study the lateral variation in structural geometry, surface data and balanced cross sections were integrated to construct a Lower Oligocene palinspastic map of the entire Bolivian Subandean Zone. This method consists to divide the actual structural map in elements characterized by a direction of shortening and an amount of shortening calculated from cross section balancing. Then, every elements are moved to their pre-andean position. The final palinspastic map (Fig. 2) contributes to the understanding of the kinematics of the bending of the Bolivian Subandean Zone. Wrench components of displacement are shown and quantified in the Northern Subandean Zone (senestral) and in the Southern Subandean Zone (dextral).

CONCLUSION

The Bolivian Subandean Zone developed during the N75° convergence between the Nazca and the South America plates [Isacks, 1988]. In the Northern Subandean Zone, SW-NE

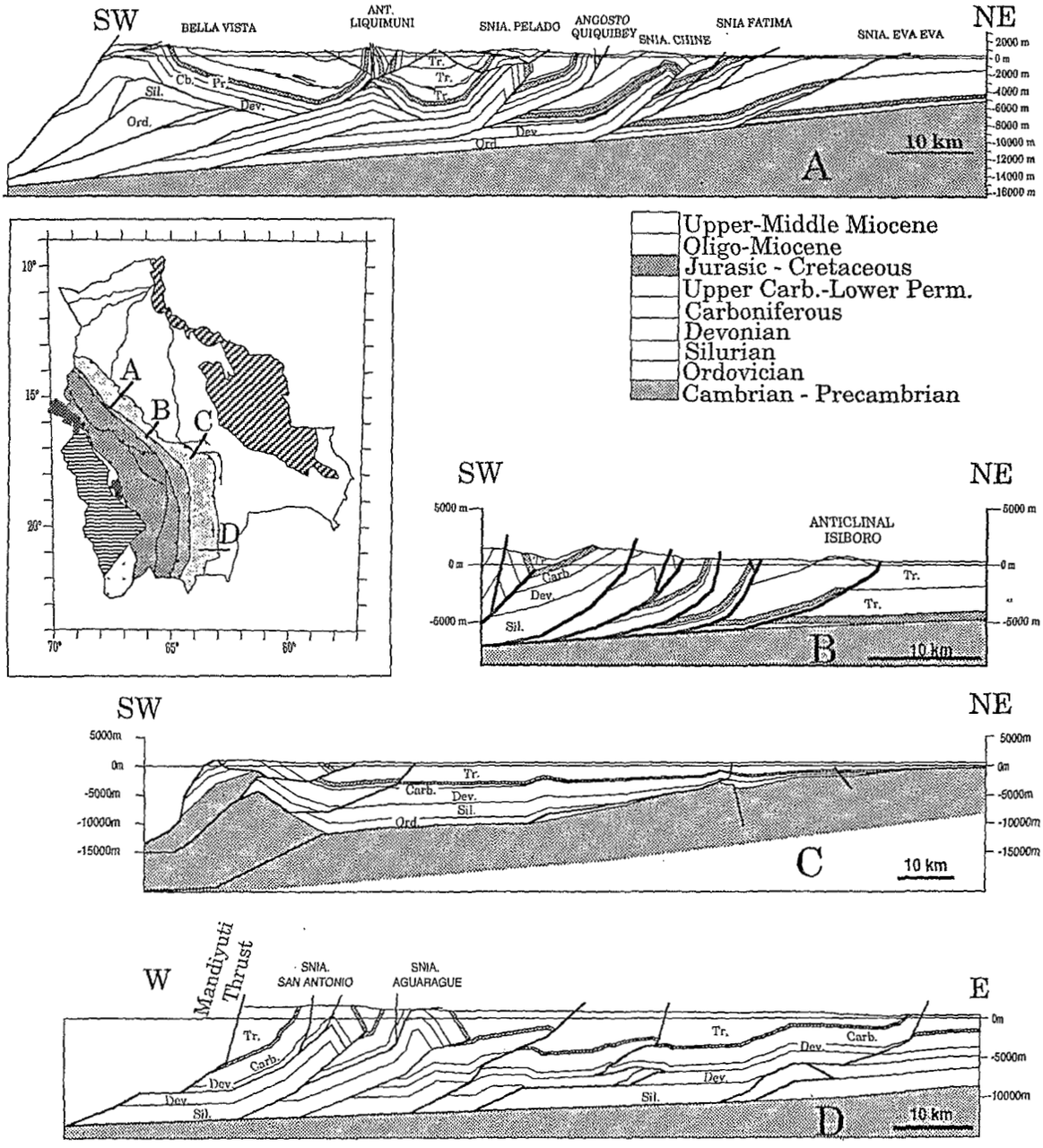

Fig. 1: Balanced cross sections in the Bolivian Subandean Zone

NW-SE senestral wrenching have accommodated the convergence, whereas in the Southern Subandean Zone, it is accommodated by W-E shortening and N-S dextral wrenching. The amount of shortening can reach 140 km and the amount of wrenching 35 km. The structural geometry of the Santa Cruz bend has been controlled by the northern border of the Paleozoic sedimentary wedge.

REFERENCES

Baby, P., G. Hérail, R. Salinas, and T. Sempere, 1992, Geometric and cinematic evolution of passive roof duplexes deduced from cross section balancing: example from the foreland thrust system of the southern Bolivian Subandean zone, *Tectonics*, vol. 11, n° 3, 523-536.

Baby, P., G. Hérail, J.M. López, O. López, J. Oller, J. Pareja, T. Sempere, et D. Tufiño, 1989, Structure de la Zone Subandine de Bolivie: influence de la géométrie des séries sédimentaires antéorogéniques sur la propagation des chevauchements, *C. R. Acad. Sci. Paris, ser. 2,* 309, 1717-1722.

Baby P., Specht M., Oller J., Montemurro G., Coletta B. and Letouzey J., 1993, The Boomerang-Chapare transfer zone (recent oil discovery trend in Bolivia): structural interpretation and experimental approach, publication spéciale Congrés EAPG, Moscou, mai 1992, IFP édition, (in press).

Isacks, B.L., 1988, Uplift of the Central Andean Plateau and bending of the Bolivian Orocline, *Journ. Geoph. Res., v. 93, n° B4, 3211-3231.*

Roeder, D., 1988, Andean-age structure of Eastern Cordillera (Province of La Paz, Bolivia), *Tectonics, 5*, 23-39.

Sempere, T., G. Hérail, J. Oller and M.G. Bonhomme, 1990, Late Oligocene-early Miocene major tectonic crisis and related basins in Bolivia, *Geology, 18*, 946-949.

Sheffels, B., 1988, Structural constraints on crustal shortening in the Bolivian Andes, Ph.D. Thesis, 170 pp., Mass. Inst. of Technol..

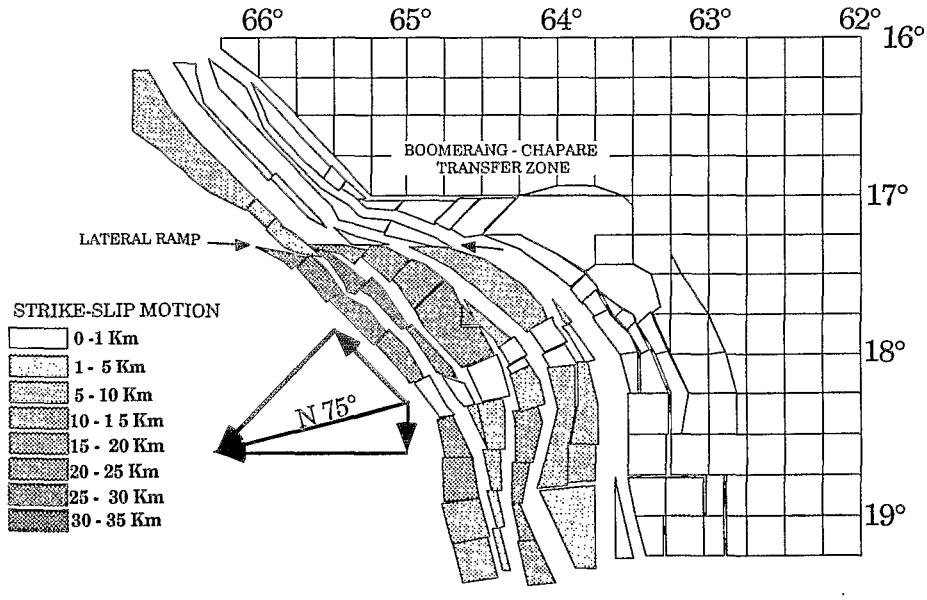

Fig. 2: Final palinspastic map - between 16° and 19° - contributing to understand the kinematics of the bending of the Bolivian Subandean Zone.

STRUCTURAL EVOLUTION OF THE NORTHERN SUB-ANDES OF ECUADOR: THE NAPO UPLIFT

Wilfrido. BALSECA[1], Luca FERRARI[2], Giorgio PASQUARE'[2] and Alessandro TIBALDI[2]

(1)Instituto Ecuatoriano de Electrificacion (INECEL), Division Ingenieria y Geotecnica,
Av. 6 de Diciembre 2275 y Av. Orellana, Casilla 585 - A, Quito, Ecuador
(2)Dipartimento Scienze della Terra, Università di Milano, Via Mangiagalli 34, 20133 Milan, Italy

Resumen

La Zona Subandina ecuatoriana està formada por los dos levantamientos estructurales regionales del Cutucù al Sur y del Napo al Norte, separados entre sì por la depresiòn del Pastaza. La evoluciòn tectonica del Levantamiento del Napo ha sido estudiada por medio de un levantamento geologico regional y estructural a la escala 1: 50.000 integrado por datos de subsuelo proporcionados por Petroecuador e INECEL. El Levantamiento Napo resulta ser formado por una faja de escamas semimetamorficas y cabalgamientos, un combamiento regional afectados por fallas trascurrentes y una flexura. Estas estructuras se han formado en tres etapas pricipales de deformaciòn desde el Cretacico superiòr hasta el presente.

Key Words: Ecuador, sub-Andes, Napo uplift, tectonics, structural evolution

Introduction

The sub-andean zone of Ecuador is a NNE trending deformed belt which connect the higher "Sierra" region to the west with the lowlands of the Amazonian foreland to the east. The sub-andes are formed by two structural highs, known as Cutucù and Napo uplifts, which are separated by the Pastaza depression. The "Sierra" is formed by the parallel ranges of Cordillera Real (CR) and Cordillera Occidental (CO), which are considered allochtonous terranes accreted onto the South American margin during two major tectonic phase in early Creataceous and early Tertiary times respectively (Wallrabe-Adams, 1990). The CR is made of cristalline rocks dating back to Paleozoic and early Mesozoic which undergone several orogenic phases since early Triassic (Baldock, 1982). In early Cretaceous this terrane has been metamorphosed, often dynamically, (Litherland and Aspden, 1992) while during Tertiary has been thrusted onto the Sub-Andean zone with a ESE vergence. (Pasquarè et al., 1990).

In this work we present a new synthesis on the tectonic evolution of the Napo uplift which is the result of six years of stratigraphic and structural studies in the northern sub-Andes of Ecuador. This work is based on an extensive geologic mapping of the whole Napo uplift and parts of the adjoining areas (Balseca and Pasquarè, in press) integrated with subsurface geologic data kindly made available by Petroecuador and INECEL. The new data depict a tectonic evolution characterized by rapid changes in the deformation styles and a strong rigidity of the whole rock masses. The structure of the Napo uplift is more complex than

previously reported, being formed by the justapoxition of embricated thrust slices, strike-slip faults and flexures.

Structural setting

The Napo uplift is a 70km-wide, 150km-long positive structure which has a structural relief of about 1.6 km with respect to the Amazonian foreland. The core of the Napo uplift is made of Jurassic to Cretaceous sedimentary and volcanic rocks (Misahualli, Hollin, Napo and Tena Formations), with a general sub-horizontal attitude and, to the west, by various granitoids of Jurassic age (Abitagua, Cuchilla), emplaced with a NNE trending alignment. All these rocks are cut mainly by NNE to NE trending right-lateral strike-slip faults and, to a lower extent, by NNW-SSE left-lateral faults. The NNE and NE faults show sometimes a vertical component of motion particularly where the two set of faults converge to give rise to restraining bands which contribute to produce the central culmination of the Napo uplift. At a regional scale the maximum elevation of the Napo uplift is located along a NNW-SSE trending axis passing through the Sumaco volcano. The southern sector is characterized by some kilometric folds trending from N-S to NNE.

Toward the west, approaching the CR, the sub-horizontal attitude of the core strata turns to a more complicated arrangement. Jurassic-Cretaceous formations are involved in WNW dipping thrust slices which display a dynamic metamorphism and both ductile and brittle deformations. These rocks are exposed in a NNE trending belt which is cut by NE trending right-lateral strike-slip faults. Blocks of the CR are thrusted along W and WNW dipping reverse and right-lateral reverse faults over the dinamometamorphosed belt producing a relatively lowering of this zone with respect to the CR and the central Napo core. Such a topographic situation has previously suggested the existence of a western flank of a large Napo anticline.

In the northern sector, the limit with the Amazonian foreland is a wide flexure where Cretaceous to Miocene strata dip 50° up to 70° eastwards. This structure is interpreted as the surface manifestation of a blind thrust, which has been encountered at least in one site by an oil well (Rivadeneria and Ramirez, 1985). The flexure is furtherly complicated by several NE trending right-lateral strike-slip faults which coincide with large deformations of its geometry. Southwards, the flexure disappears and the Napo uplift is truncated by a system of NE striking right-lateral strike-slip faults.

Further to the south the Pastaza depression is characterized by N-S trending reverse faults and folds while its limit with the Amazonian plain is an arcuate thrust buried underneath the Plio-Quaternary alluvium.

Age of faulting

Although many tectonic phases can be recognized in the study area, we focussed on the late Cretaceous to Quaternary tectonic history which is responsible for the formation of the Napo uplift. The first pulse in this tectonic cycle evidenced by the erosion of the upper part of the Napo Formation during the Campanian. Among the main structures of the Napo uplift the N-S to NNE-SSW trending reverse faults resulted to be the oldest structures, in agreement with previous works in the CR (Pasquarè et al., 1990). These faults absorbed most of the shortening which accompanied the formation of the dynamometamorphic slice belt. The age of the rocks involved in this belt constrained to the Paleogene the developing of this structure. Later, the N-S to NNE-SSW fault planes were partially rejuvenated with right-lateral reverse motions. The NNW trending left-lateral strike-slip faults are older than the NNE to NE trending right-lateral strike-slip faults because are systematically displaced by the latter but no absolute age is available for the formation of the former. Quaternary alluvial deposits of the Amazonian plain onlap the flexure and are generally undeformed. Nevertheless, they locally show remote-sensed lineaments which may suggest an extension of the transcurrent faulting towards the east. Finally, motions along the NE to NNE trending right-lateral strike-slip faults occurred during the Quaternary as witnessed by morphological neotectonic indicators and seismicity analyses (Tibaldi and Ferrari, 1992).

Tectonic evolution

Field data suggest that the Napo uplift developed during three main stages of deformation since Paleogene times, although the first upraise of the region begun in late Cretaceous. In a first stage, occurred between Paleogene and Miocene, the CR was thrusted toward the ESE onto the western side of the Napo

area producing the dynamometamorphic slice belt. In a second stage, the eastward propagation of deformation produced the regional arching and the flexure which limits the eastern flank of the Napo uplift. During this second stage, N-S to NNE right-lateral reverse faults developed within the dynamometamorphic slice belt, while NNW left-lateral and NE right-lateral faults developed eastwards. We think that this stage could correspond to the Neogene time. During the third stage, in the Quaternary, right-lateral transcurrent motions along NE to NNE trending faults cut the Napo uplift into four main blocks. These blocks were differentially thrusted toward the NE creating in the distortion and the truncation of the flexure.

ACKNOWLEDGMENTS

We thanks Instituto Ecuatoriano de Electrificacion (INECEL) Quito, for the logistical support in the field works and for the continuous sustaining of W.B. throughout the study. We also acknowledge Petroecuador for the kind permission of studying subsurface data.

W.B. and L.F. benefited of a grants of Consorzio Milano Ricerche. A.T. was partially supported by a Ph.D. grant from Ministero Italiano della Pubblica Istruzione.

REFERENCES

Aspden J.A. and Litherland M., 1992. The geology and Mesozoic collisional history of the Cordillera Real, Ecuador. Tectonophysics, 205, 187-204.

Baldock J. W., 1982. Geologia del Ecuador (Boletin de la explicaciòn y mapa geologico de la Republica del Ecuador, escala 1 : 1,000,000). Direcciòn General de Geologia y Minas, Quito, 71 pp.

Balseca W. and Pasquarè G. Regional geologic map of the Napo uplift, northeastern Ecuador. Acta Vulcanologica, in press.

Pasquarè G., Tibaldi A. and Ferrari L., 1990. Relationships between plate convergence and tectonic evolution of the Ecuadorian active Thrust Belt. In: Agusthithis S.S. (Ed.), Critical Aspects of Plate Tectonic Theory, Theophrastus Publications, 365-387.

Rivadeneria M.V. and Ramirez F.H., 1985. La zona subandina amazonica ecuatoriana y sus prospectos hidrocarburiferos. VI° Latinamerican geological congress, Bogotà, Colombia.

Tibaldi A. and Ferrari L., 1992. Latest Pleistocene-Holocene tectonics of the Ecuadorian Andes. Tectonophysics, 205, 109-125.

Wallrabe-Adams H., 1990. Petrology and geotectonic development of the Western Ecuadorian Andes: the Basic Igneous Complex. Tectonophysics, 185, 163-182.

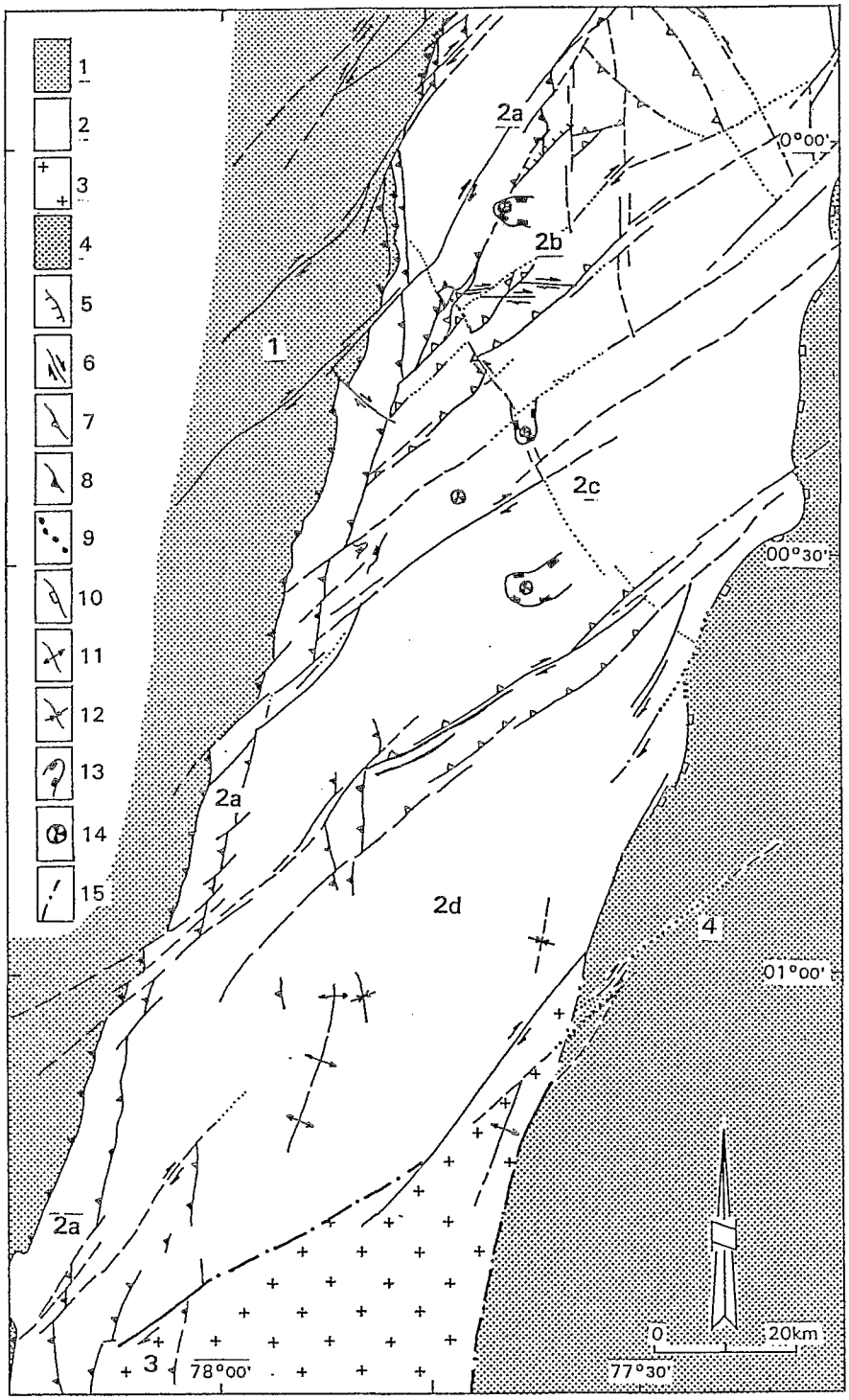

Figure 1. Structural sketch-map of the Napo uplift.

1 = Polimetamorphic rocks of the Cordillera Real. 2 = Napo uplift: a) thrust slice zone; b) zone with strike-slip and reverse faults; c) zone with strike-slip faults; d) zone with strike-slip and folds. 3 = Pastaza depression. 4 = Amazonian foreland. 5 = normal faults. 6 = Strike-slip faults. 7 = reverse faults. 8 = Thrusts. 9 = buried faults. 10 = flexure. 11= anticline fold axis. 12 = sycline fold axis. 13 = volcanic collapse. 14 = volcanic vent. 15 = inferred faults.

TECTONIC CONTROLS ON MESOZOIC ARC MAGMATISM IN NORTH CHILE

Michael BROWN[1], R. David DALLMEYER[2], and John GROCOTT[3]

(1) Department of Geology, University of Maryland at College Park, MD 20742, USA
(2) Department of Geology, University of Georgia, Athens, GA 30602, USA
(3) School of Geological Sciences, Kingston University, Penrhyn Road, Surrey, KT1 2EE, UK

RESUMEN: Complejos plutonicos Jurasicos (*c.* 190 Ma and *c.* 153-138 Ma) se ubican escencialmente al oeste del Sistema de Falla Atacama (SFA), emplazados en el basamento metasedimentario y los complejos plutonicos anteriores. El SFA corresponde a una zona de fractura a escala cortical con una larga y compleja historia de desplazamientos desde el Jurasico-Cretacico (*c.* 158 Ma, *c.* 132-126 Ma) al Reciente. Complejos plutonicos Cretacicos se urbican a lo largo (*c.* 127 Ma) y al este (*c.* 106 Ma) del SFA emplazados en volcanitas andesiticas Cretacicas, ya que durante el Cretacico, el foco de la actividad magmatica migro hacia el este.

KEY WORDS: Ar ages; dip-slip faulting; Mesozoic arc magmatism; strike-slip faulting; syn-kinematic plutonism; transtension.

INTRODUCTION

One perplexing feature of arc systems relates to the relationship between the apparently continuous nature of subduction processes and the episodicity of regional magmatic events. Such episodicity suggests that the rates of tectonic processes must be relatively rapid. Also, the relationship between arc-related strike-slip faults and magmatism is uncertain. Arc-parallel trench-linked strike-slip faulting is common along convergent margins and is particularly important in continental arc systems. As a result, fore-arc slivers typically are stranded between strike-slip faults and trenches. Trench-linked strike-slip faults, in addition to accommodating the horizontal component of oblique subduction, cut and may localize arc intrusions and volcanic rocks. One major question is whether relative thermal 'softening' within an evolving magmatic arc is required for development of strike-slip fault systems or whether development of strike-slip fault systems facilitates the ascent and emplacement of arc-related magma? One aim of our ongoing research in North Chile is to understand better the spatial and temporal development of plutonic complexes and associated tectonic structures within an eroded continental arc system to provide data to evaluate more fully these issues.

GEOLOGICAL SETTING

The major geological features of the western South American continental margin are a manifestation of the longevity of subduction along this regional plate boundary. Evolutionary stages have been influenced by the direction and magnitude of plate convergence vectors. In North Chile, upper Paleozoic back-arc basin and fore-arc sedimentary sequences (including an extensive accretionary prism) formed during rollback of subducting oceanic lithosphere. These successions host a broad Permian-Triassic magmatic arc. The metasedimentary basement/arc complex comprised a country rock terrane for subsequent Lower Jurassic, Upper Jurassic and Lower Cretaceous magmatic arcs which presently are exposed in the Coastal Range. Mesozoic arc complexes are transected by a trench-linked strike-slip fault system: the Atacama Fault System (AFS). The AFS extends for at least 1000 km between La Serena and Iquique within the Coastal Range of North Chile. It has been active from at least the Upper Jurassic, with displacement continuing intermittently into the Upper Miocene. The trend of the system is sub-parallel to the continental margin, but the major faults within it change orientation systematically to define three arcuate segments. We are concerned with the relationship between magma emplacement and fault displacement in the southern part of the AFS between Taltal and Copiapo, which has been referred to as the El Salado segment. Between 25°00'S and 27°30'S, in the El Salado segment of the AFS, steep foliations in ductile simple shear belts have been reworked by brittle fault zones. To the east, inboard of the arc rocks, sedimentary and volcanic rocks of a Mesozoic back-arc basin are exposed. This Mesozoic back-arc basin formed part of a system extending throughout Chile. The major contractional event east of the AFS in North Chile occurred in the late Oligocene - early Miocene when Paleocene and older rocks of the Mesozoic back-arc basin were thrust to the east.

During the Jurassic and early Lower Cretaceous South America appears to have been essentially static, which likely allowed development of the behind-arc basins as a consequence of subduction zone rollback and syn-subduction extension. Plate reconstructions for the Lower Cretaceous suggest that the Aluk plate subducted southeastward at an oblique angle relative to the South American continental margin. This kinematic setting appears to have been maintained until the late Upper Cretaceous, when the Farallon plate was tectonically juxtaposed along the plate boundary of North Chile.

THE CHANARAL REGION (25°00'-27°30'S)

In the Chanaral Region, Upper Paleozoic sedimentary sequences and granites of a broad Permian-Triassic magmatic arc formed the crust into which Lower Jurassic (LJ), Upper Jurassic (UJ) and Lower Cretaceous (LC) magmatic arc rocks were emplaced. Each of these arcs is composed of an expanded range of compositions from gabbro-diorite through tonalite to granodiorite (Brown, 1991). LJ plutonic complexes have equant outcrop patterns and are located west of the AFS, whereas the UJ and LC plutonic complexes are elongate north-south and their emplacement clearly was controlled by the geometry of the Atacama Fault System. Plutonic complexes younger than *c.* 100 Ma are emplaced into the marginal basin behind the arc during structural inversion of the basin and here again plutonic complexes have equant outcrop shapes. Individual plutons within these Mesozoic complexes display field, textural and petrological characteristics which reflect upper crustal levels of magma emplacement and associated rapid post-magmatic cooling. Al-in-hornblende barometry across the UJ and LC arcs on rocks with the appropriate full phase assemblage suggests *c.* 2 kbar load pressure during emplacement of plutonic complexes along the AFS. Several dike swarms were emplaced during the development of the Mesozoic arcs and account for east-west dilation of up to 15%. They show that the arc was extending during emplacement of arc magmas.

Magmatism appears to have been episodic as revealed by peaks in a histogram of number of ages (published, various sources, all methods) *v.* geologic series (*c.* 30 Ma interval), by published U-Pb zircon data, which reflect crystallization ages, and by new $^{40}Ar/^{39}Ar$ hornblende plateau and isotope correlation ages. The rapid cooling implied by a shallow crustal level results in intracrystalline mineral argon systems recording isotopic ages very similar to the time of initial

magma emplacement. Thus our precise $^{40}Ar/^{39}Ar$ dates also reflect crystallization ages. Peaks of activity occurred in the Lower Permian (LP), the Triassic (T), the LJ, the UJ and the LC. Using the $^{40}Ar/^{39}Ar$ method, we have determined precise emplacement ages of individual plutonic complexes both along strike and across strike within each of the Mesozoic arcs. On the west side of the Coastal Range, $^{40}Ar/^{39}Ar$ hornblende isotope correlation ages of *c.* 190 Ma characterize the LJ arc suite along more than 1° of latitude. Ages of 153, 139 and 138 Ma have been determined on hornblende from samples W to E across the UJ arc suite, and ages of *c.* 127 and 106 Ma have been determined on hornblende from localities across the LC suite. These ages indicate that as the locus of magmatic activity stepped successively E, each previous arc cooled. Furthermore, whole rock $^{40}Ar/^{39}Ar$ ages of 156 and 154 Ma from calc-alkaline basaltic andesite dikes indicate emplacement of the earliest magmas of the UJ suite in an extensional environment.

The geochemical features of granitoid (> 63% SiO_2) samples from the LJ, UJ and LC plutonic complexes from the Coastal Range include enrichment in Rb, Th, U and K and depletion in Ba, Ta, Nb, Sr, P and Ti, characteristic features of continental margin granitoids, and relative enrichment in the LREE relative to the HREE. Normalized values for Y of *c.* 5 suggest shallow magma sources. For the expanded range of compositions, K/Rb and Rb/Sr do not change dramatically with increasing SiO_2 until very high SiO_2 contents, features that are consistent with fractional crystallization as the dominant control of the chemical variation. The low on average Ba/La ratios exhibited by the rocks suggest low alkali earths in the source region and argue for limited subduction zone enrichment within the mantle wedge. This is confirmed by low Ba/Nb ratios at low SiO_2 contents.

THE ATACAMA FAULT SYSTEM

In the El Salado segment, the AFS transects intrusive and volcanic rocks of the Upper Jurassic and Lower Cretaceous magmatic arcs. At El Salado, and for 20 km to the S, the AFS contains three principal fault zones where distinct brittle faults have reworked rocks that display an earlier record of penetrative ductile strain. For much of its length, the western fault zone juxtaposes Jurassic diorite/tonalite to the W with Cretaceous tonalite/granodiorite to the E. This brittle fault contact is located within a *c.* 800 m wide ductile shear zone which appears to have initiated during upper amphibolite facies conditions. A variety of kinematic indicators all indicate east-side-down displacement (Brown *et al.*, 1993). Because field relations constrain at least an early Lower Cretaceous age for ductile displacement, the AFS could have initiated within a fault system responsible for Jurassic - Lower Cretaceous subsidence in the Mesozoic marginal basin to the E. Jurassic plutonic rocks exposed west of the main shear zone are cut by small-scale shear zones which again display amphibolite facies mineral assemblages, and which may have formed during the early stages of development of the AFS. The eastern fault zone of the AFS marks a boundary between Cretaceous volcanic rocks and Cretaceous tonalite/granodiorite to the E. Cretaceous plutonic rocks adjacent to the boundary are penetratively ductilely deformed in a 700-1400m wide belt of steep east-dipping mylonites. Kinematic indicators indicate sinistral displacement across the high ductile strain zone (Brown *et al.*, 1993). Field relations suggest Lower Cretaceous movement, and intrusive rocks of the UJ and LC magmatic arcs are elongate parallel to the AFS.

Further W than the main AFS, ductilely-deformed metasedimentary rocks and leucogranites occur at the west margin of the Upper Jurassic plutonic complexes, east of Flamenco. Poorly defined kinematic indicators are consistent with vertical displacement. $^{40}Ar/^{39}Ar$ plateau ages on muscovite of *c.* 159 and 156 Ma suggest that the earliest ductile displacement recorded within the Mesozoic plutonic complexes is of Upper Jurassic age.

Hornblende from two samples of mylonitic diorite from within the western fault of the AFS both display well-defined $^{40}Ar/^{39}Ar$ plateaus and yield isotope correlation ages of *c.* 132-130 Ma, interpreted to date cooling through the appropriate argon closure temperature following deformation under amphibolite facies conditions within the AFS. This provides a minimum age for the down dip component of ductile displacement on the AFS. Hornblende from a foliated mylonitic diorite from within the east fault of the AFS displays a well-defined $^{40}Ar/^{39}Ar$ plateau and yields an isotope correlation age of *c.* 126 Ma, interpreted to date greenschist facies ductile

deformation during strike-slip displacement on the AFS.

The upper amphibolite facies, east-side-down shear zones along the west fault of the AFS are interpreted to have formed in the wall-rocks of Lower Cretaceous intrusions during emplacement. The shear zones dip steeply at the surface but may become low-angle at depth. Ductile deformation was promoted by heat supplied from the arc plutons which were emplaced at dilational jogs in this extensional shear zone system. The east fault of the AFS represents a boundary to the extensional domain. The mylonites were reworked by successively lower temperature, sinistral strike-slip ductile-to-brittle faults.

CONCLUSIONS

Our preliminary $^{40}Ar/^{39}Ar$ data on plutonic complexes suggest that arc magmatism is partly episodic. A significant time gap exists between the Lower Jurassic plutonic complexes and Upper Jurassic plutonic complexes. Smaller, possibly significant time gaps occur within the Upper Jurassic and Lower Cretaceous plutonic complexes.

The Atacama Fault System likely was initiated *c.* 160 m.y. ago and was characterized by extension until *c.* 130 Ma. Since plate kinematic reconstructions suggest south-east directed subduction during this interval, due to the expansion of the Pacific Ocean Basin while South America remained essentially static in a mantle reference frame, it is likely that the AFS represents a transtensional fault during the Upper Jurassic. The outcrop shape of plutonic complexes, spacing of emplacement at *c.* 30 m.y. interval and the plate kinematic framework all indicate that in the interval 190 Ma to 160 Ma subduction zone rollback initiated a transtensional regime which at 160 Ma controlled pluton emplacement. In addressing the question of whether relative thermal 'softening' of an evolving magmatic arc is required for development of a strike-slip fault system or whether the development of a strike-slip fault system facilitates the magmatism associated with the arc, our data suggest that thermal weakening during pluton emplacement at 190 Ma and extensional stresses generated by subduction zone rollback allowed initiation of the AFS at *c.* 160 Ma and subsequent growth of the AFS during the next 30-m.y. period to *c.* 130 Ma. Magmatism and thermal weakening likely precede initiation of arc-parallel fault systems at active continental margins, although in detail each intrusion likely was associated with weakening of the arc that allowed ductile deformation followed by a ductile-brittle transition during cooling. Once established, arc-parallel fault systems at active continental margins may control ascent and emplacement of magma, as evidenced by the UJ and LC plutons.

The $^{40}Ar/^{39}Ar$ results from the Atacama Fault System suggest a polyphase history of ductile displacement. The data suggest a change from down-dip ductile displacement under amphibolite facies conditions to strike-slip ductile displacement under greenschist facies conditions during the interval 130-126 Ma. The transition from down-dip to strike-slip may correspond to a decrease in depth and may reflect exhumation on the evolving fault system. These data permit two interpretations of arc tectonics. Either extension and magma emplacement occured together with sinistral strike-slip on the AFS but partitioned from it in a transtensional regime, or extension associated with emplacement of arc magmas preceded strike-slip displacements on the AFS during the waning stages of arc magmatism. In the second interpretation, cooling due to arc abandonment, rather than exhumation, may have contributed to the ductile-brittle transition.

REFERENCES

BROWN, M., 1991. Relationship between magmatism and tectonics in northern Chile. Geochemical evidence from 25°30'-27°00'S. *6 Congreso Geologico Chileno*, Actas, 1, 631-634.

BROWN, M., DIAZ, F., and GROCOTT, J., 1993. Displacement history of the Atacama Fault System 25°00'S-27°00'S, northern Chile. *Geological Society of America, Bulletin*, **105**, in press.

STRUCTURAL INTERPRETATION OF CEUTA FIELD, LAKE MARACAIBO, VENEZUELA

Emilio BUENO, Alfredo CHIRINOS, Johnny PINTO and José MORENO (*)

(*)Maraven, S.A., Apartado 829 Caracas 1010A, Venezuela

RESUMEN: La interpretación estructural del levantamiento tridimensional del Campo Ceuta , en la Cuenca de Maracaibo, fué realizada considerando los diferentes estilos de deformación a los cuales estuvo expuesta la cuenca desde el Triásico-Jurásico hasta el Neógeno. La deformación tuvo lugar alternando fases tensionales y compresionales.

KEY WORDS: Ceuta Field, Pueblo Viejo Fault, Maracaibo Basin, Structural Inversion

INTRODUCTION

This interpretation, achieved in an interactive workstation, is centered around an area covered by a 3D seismic survey acquired over most of the Ceuta Field, located in the Maracaibo Basin, which is situated between two Andean chains, on the northern edge of the South American Plate.

GEOLOGICAL SETTING

The stratigraphic column shows over a paleozoic basement, the volcano-sedimentary complex of Triassic-Jurassic La Quinta Formation, which fills deep basement depressions, and is uncomformably covered by Cretaceous and Paleocene platform sediments, followed by passive margin Eocene sediments and finally, the continental Neogene embankment.

The structural deformation took place under alternating extensional and compressional tectonics. The major structural features of the field are the Pueblo Viejo and the VLG-3693 faults.
During Eocene and Miocene times, the Ceuta Field was located in a regional high structure, which gradually has been inverted during the Upper Neogene reaching the deep today situation (Roberto, Cramez and Duval, 1993).

The Ceuta Graben
The North-South oriented Pueblo Viejo fault is interpreted as the border fault of a Triassic-Jurassic graben, which western part is situated in the Ceuta Field, in Lake Maracaibo. The eastern border-fault, the Valera Fault, is outcropping in the Trujillo Andes and the Lara-Trujillo Mountains, in the eastern coast of Lake Maracaibo.

Lower Eocene Extensional Deformation
The graben was covered by Cretaceous and Paleocene platform sediments, and was reactivated under extension during Early Eocene times.
During the same time, and due probably to the forebulge originated by the emplacement of the Lara nappes in the northeastern part of the Maracaibo Basin (Rodriguez, Bueno and Ostos, 1993), a series of listric faults were developed.
To the South of the field exists a remanent of a Mesozoic structural high, "the Merida Arch", which is bounded by the big listric VLG-3693 growth-fault, dipping to the North.

Structural Inversion
During Upper Eocene times, and as a result of collision of the Caribbean and the South American Plates, followed by the oblique subduction of the Caribbean crust under the Maracaibo Block (Van der Hilst, Rob and Mann, 1993), the sediments of the Maracaibo Basin were deformed under compression, which gave place to the structural inversion of the Ceuta graben.
The main stress deformation axis was oriented in a NW-SE direction (Willemse, Van de Graaff and Sancevic, 1990).
During this phase, the normal border-faults of the graben were converted in reverse faults, particularly at Eocene levels. Due to the high angle of the Pueblo Viejo fault at Cretaceous and Basement levels, the inversion was of little significance there.
Antithetic faults situated in the East flank of the Pueblo Viejo fault were also converted in reverse faults, giving place to the formation of wedge shaped blocks, which, locally are squeezed up as pop up structures.
Due to its orientation almost parallel to the main deformation stress, the big VLG-3693 fault has not been inverted, excepted in its Northwesten edge, where the Pueblo Viejo fault overprints the VLG-3693 fault.

Strike slip Faulting
This analysis of the Ceuta graben leds to dynamic and cinematic processes, which are different to the traditionally used for the structural interpretation of the area, until now considered as a result of strike slip tectonics only (VST, 1986). The present interpretation considers the strike slip deformation of the Pueblo Viejo fault as an event associated to the structural inversion, and due to block rotations.

Post-Eocene Deformation
An extensional deformation took place in Early Miocene, which was followed during Late Miocene, by a new phase of compressional deformation. This deformation took place during the uplift of the Merida Andes, which also involved the eastern eastern part of the graben, which is now outcropping. During this phase, the Maracaibo Block escaped northward from its Colombian Eastern Cordillera convergence (Pindell, 1993).
The main stress deformation axis had an East-West orientation (Willemse et al. 1990). During this phase occurred also a conjugated shear-fault system, which cut the Ceuta High with 45 degrees angles to the Pueblo Viejo fault.

Hydrocarbon Traps
The tectonic processes were very important for the development of different types of hydrocarbon traps recognised in the Ceuta Field.
Four different kinds of plays can be distinguished, the Miocene-, Upper Eocene-, Lower Eocene- and Cretaceous-plays, which are related to specific deformation phases.
The Miocene plays are related to the entrampment caused by the Pueblo Viejo fault.
The Upper Eocene play consists also in traps developed next to the Pueblo Viejo reverse fault and its antithetic faults.
The Lower Eocene plays are situated against the normal faults oriented NW-SE, and developed during the extensional deformation.
The Cretaceous plays are related to the highs, which existed in the upthrown flank of the Pueblo Viejo fault, during the extensional Lower Eocene deformation phase, assuming a migration previous to the structural inversion.

CONCLUSIONS

Ceuta Field is located in the western half of a graben originated during Triassic-Jurassic times, which after being eroded was covered by Cretaceous and Paleocene platform sediments. During Lower Eocene times the graben was reactivated under extension. During the Upper Eocene, and as a result of subduction of the Caribbean crust under the Maracaibo Block, the sediments were deformed under compression, which gave place to the structural inversion of the graben. Finally, an extensional deformation phase took place during Early Miocene, which was followed by Late Miocene, by a new phase of compressional deformation during the uplift of the Merida Andes.

REFERENCES

PINDELL, JAMES (1993):
Mesozoic-Cenozoic Paleogeographic Evolution of Northern South America.
AAPG/SVG International Congress and Exhibition, Caracas

RODRIGUEZ, J., BUENO, E. and OSTOS, M. (1993):
Tectonic Significance of the Valera Fault Zone, Northwestern Venezuela.
AAPG/SVG International Congress and Exhibition, Caracas

VAN DER HILST, ROB and MANN, PAUL (1993):
Tectonic Implications of Tomographic Images of Subducted Lithosphere beneath Northwestern South America.
AAPG/SVG International Congress and Exhibition, Caracas.

VENEZUELAN STUDY TEAM (VST), (1987):
Integrated Reservoir Study of the Eocene Lower B, Areas 4,5,6
Shell Technical Services BV, The Hague, Internal Document.

WILLEMSEE, E.J.M., VAN DE GRAAFF, W.J.E. and SANCEVIC, Z. (1990):
Characterization of an overpressured, Cretaceous Reservoir, Lake Maracaibo, Venezuela, A.A.P.G. Bull. 74 (1990) 791.

The Liquiñe Ofqui Fault Zone : a major Cenozoic strike slip duplex in the Southern Andes

José CEMBRANO and Francisco HERVE

Departamento de Geología - Universidad de Chile
Casilla 13518 Correo 21, Santiago-CHILE

RESUMEN

La zona de falla Liquiñe-Ofqui (ZFLO) se extiende por casi 1000 kms en los Andes del sur. Rocas deformadas ocurren a lo largo de la ZFLO, que coincide con el eje Mioceno del Batolito Norpatagónico y con cuencas extensionales terciarias. Un movimiento dextral en el rumbo y luego normal, es consistente con la convergencia entre las placas de Nazca y Sudamérica que ha variado de oblicua a casi ortogonal.

KEY WORDS: Southern Andes, strike-slip duplex, Cenozoic.

INTRODUCTION

The overall deformation resulting from converging plates is partitioned into strain, displacement along discrete faults and block rotation (Lamb and Bibby, 1989; Jackson and Molnar, 1990). Attempts to assess the contribution of these three components of deformation along different mountain belts (Dewey and Lamb, 1992) face the problem that short and long-term slip rates, distributed strain, and the amount and sense of block rotation are generally poorly constrained. This is the case in the Chilean Andes, where hundred-kilometer long crustal lineaments, regarded as major long-lived strike-slip fault systems, have been causally linked to the margin parallel component of oblique subduction of the Nazca (Farallon) plate beneath South America (Hervé, M., 1976; Beck, 1988; Pardo Casas and Molnar, 1988).

The most relevant tectonic feature of the southern Chilean Andes, the 1000 km long Liquiñe-Ofqui fault zone (LOFZ) , has been lately the subject of geologic, geochronologic and paleomagnetic research. An updated synthesis of all available relevant information about the LOFZ is given below.

GEOLOGICAL SETTING

Geometry

The Liquiñe-Ofqui fault zone is represented by a series of NNE-trending crustal lineaments, mainly corresponding to aligned glacial valleys and fjords.

Their spatial arrangement as observed in satellite images, aerial photographs and geologic maps (Fuenzalida & Etchart, 1975; Hervé et al., 1979; Thiele et al., 1986) allows the distinction of three categories of lineaments based on length and shape : straight long segments; *en échelon* features; and curved splays.

The main trace of the LOFZ is represented by two NNE-trending straight segments with a left step in between. These two main segments are linked by a series of NE-trending *en échelon* lineaments resulting in an extensional strike-slip duplex geometry (as described in

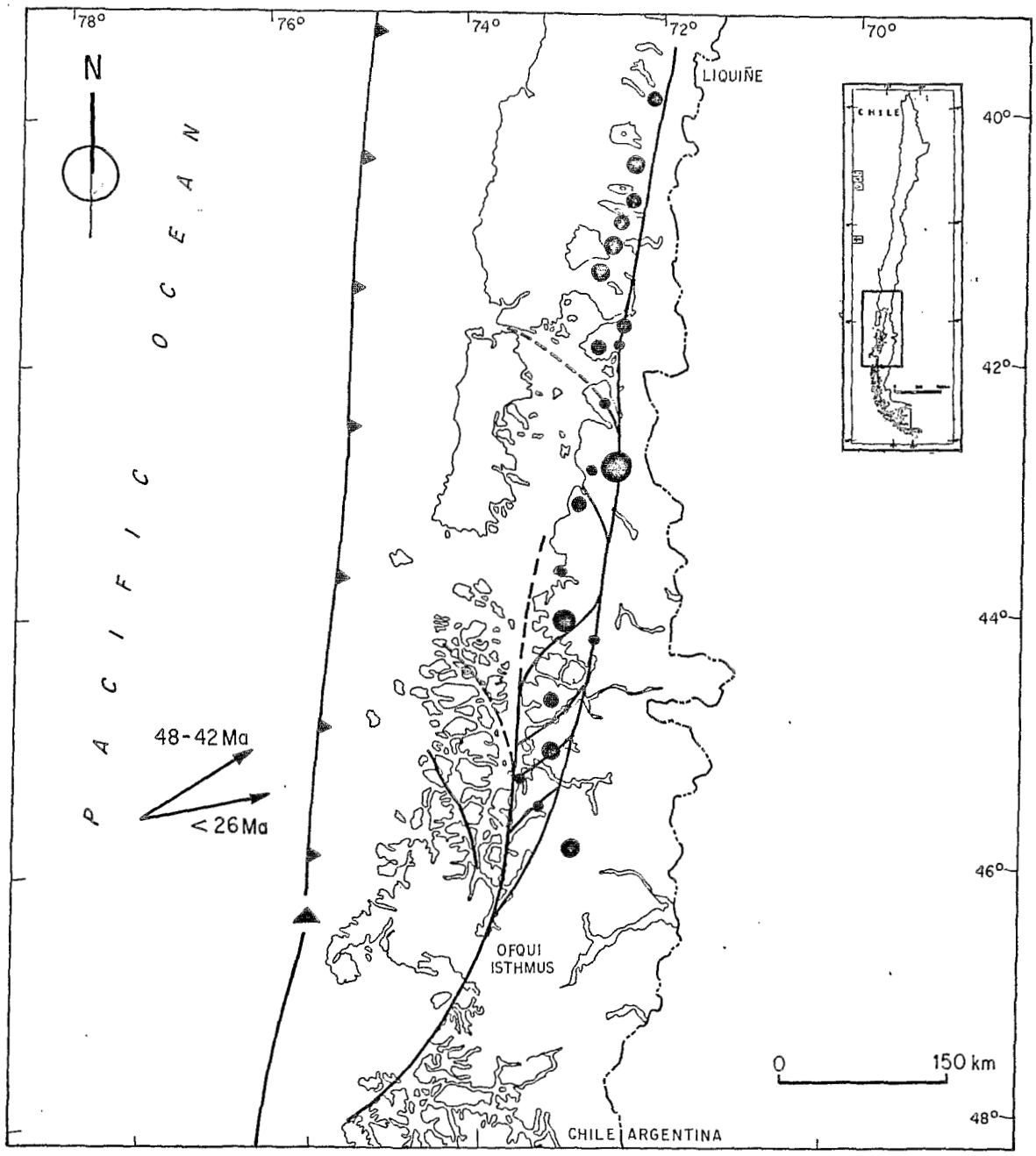

Fig. 1 Sketch map of main lineaments of the LOFZ. Position of the holocene volcanoes (black dots), the trench, the triple point (black triangle) and of the slip directions of the Nazca Plate approximate.

Woodcock and Fisher, 1986). The third important element is a series of NW-trending, concave to the southwest, oceanward splays off the two main segments (Fig. 1).

The LOFZ, along most of its main trace, runs through plutonic rocks of the Meso-Cenozoic North Patagonian batholith, metamorphic rocks of the Paleozoic Accretionary Complex and Cenozoic volcanosedimentary units (Hervé, 1976; Parada et al., 1987; Cembrano, 1992). The Miocene belt of the North Patagonian batholith has a close spatial relationship with the main trace of the LOFZ, as does the holocene southern Andes volcanic chain. It has been suggested that the LOFZ is a deep-seated structure cutting through the lithosphere, favouring magma rising and emplacement. (Parada et al., 1987; Pankhurst et al., 1992).

NS-trending strips of fault rocks, crop out in discrete areas along the LOFZ, between extensive exposures of non-deformed rocks. A steeply-dipping foliation striking NNW characterizes the mylonites. Limited available data on mineral stretching lineations and fault striae are consistent with lateral displacement.

Mid-Tertiary extensional basins (Bartholomew and Tarney, 1986) and holocene volcanoes are spatially compatible with the extensional duplex geometry described.

Paleomagnetism

Paleomagnetic data on rock units adjacent to the LOFZ (García et al., 1988; Cembrano et al., 1992; Rojas et al. in press) have shown a pattern of crustal block rotation consistent with the LOFZ geometry and motion, characterized by small counterclockwise rotations west of the LOFZ and small to moderate clockwise rotations within and to the east of the LOFZ. Beck et al. (in press) propose that the observed pattern is the result of small north-south displacement of blocks along curved splays west of the LOFZ, giving rise to counterclockwise rotation in contrast with distributed dextral shear producing clockwise rotations within and to the east of the LOFZ. Large-scale north-south transport -as found in the US western Cordillera- has not been documented, but available data do not rule out a few hundred km of lateral offset.

Nature and timing of motion

Hervé (1976) proposed that it was a Cenozoic fault zone with both pre-Oligocene dextral and Late Tertiary normal up-on-the-east motions. The main evidence for the early strike-slip component was a steeply-dipping mylonitic foliation along with a conjugate set of NNE-trending dextral and ENE-trending sinistral mesoscopic faults found in a 3km wide NNE - trending belt of fault rocks. The normal, up-on-the-east motion, was interpreted from the fact that deeper crustal levels crop out east of the LOFZ main trace. At 41°S the LOFZ juxtaposes weakly deformed Miocene and Cretaceous plutonic rocks (Drake et al. 1992). At 42°S, NNW striking foliations, subhorizontal mineral lineations and structural asymetries found in both Mio-Pliocene granitoid and their Paleozoic metamorphic wallrocks document a right lateral ductile shear zone of pre-Pliocene age (Cembrano, 1992).

High uplift rates have been calculated for the LOFZ by Thiele et al. (1986) for the last 10 Ma and, up to 9 mm/year, by Hervé and Ota (in press) for the late Holocene, respectively.

CONCLUSIONS

The LOFZ is represented by two major NNE-trending crustal lineaments along which isolated outcrops of ductilely-brittlely deformed rocks occur. Purely geometric considerations of spatially related *en échelon* and curved oceanward features can be assimilated to a strike-slip extensional duplex and associated splays.

Field evidence from within the LOFZ is consistent with a right lateral shear zone with sharp variations in the nature of rock deformation along strike.

The fact that both the Miocene plutonic rock belt and Recent volcanoes spatially coincide with the LOFZ suggests that the structure has exerted control on magma rise and emplacement.

Paleomagnetic data show a pattern of block rotation consistent with the geometry and sense of motion assigned to the LOFZ.

Right lateral followed by normal motion on the LOFZ reflects the Nazca-South America convergence which varied from highly oblique to nearly orthogonal during the Cenozoic.

Acknowledgements

Projects FONDECYT 1931096 (J.C.) and 92/0914 (F.H.) are financing current research on the subject.

REFERENCES

Bartholomew, D.S. and J. Tarney, 1984, Crustal extension in the Southern Andes (45-46°S). In: B.P. Kokelaar and M.F. Howells (Editors), Marginal Basin Geology: Volcanic and Associated Sedimentary and Tectonic Processes in Modern and Ancient Marginal Basins. Geol. Soc. London, Spec. Publ., 16: 195-205.

Beck, M.E. Jr., 1988, Analysis of Late Jurassic-Recent paleomagnetic data for active plate margins of South America. J. of S. Amer. Earth Sci. 1, 39-52.

Beck, M., Cembrano, J., Rojas, C. and F. Hervé, On the significance of curvature in strike-slip fault systems. Geology (in press).

Cembrano, J., 1992, The Liquiñe-Ofqui Fault Zone (LOFZ) in the Province of Palena: field and microstructural evidence of a ductile-brittle dextral shear zone. *Comunicaciones* N° 43, 3-27.

Cembrano, J., Beck., M.E. Jr., Burmester, R.F., Rojas, C., García, A. and F. Hervé, 1992, Paleomagnetism of Lower Cretaceous rocks from east of the Liquiñe-Ofqui fault zone, southern Chile: evidence of small in-situ clockwise rotations. Earth and Planetary Science Letters, 113, 539-551.

Dewey, J.F. and S.H. Lamb, 1992, Active tectonics of the Andes. Tectonophysics, 205, 79-95.

Drake, R., Hervé, F., Munizaga, F. and M. Beck, 1992. Magmatism and the Liquiñe-Ofqui Fault Zone, southern Chile (40°-46° S. Lat.). Comunicaciones N° 42 (Vth International Circumpacific Terrane Conference), 69-74.

Fuenzalida, R. and H. Etchart, 1975, Geología del territorio de Aysén comprendido entre los 43°45' y los 45° latitud Sur. Instituto de Investigaciones Geológicas, Santiago, Chile, 99 pp.

García, A., Beck, Jr. M.E., Burmester, R.F., Hervé, F. and F. Munizaga, 1988, Paleomagnetic reconnaisance of the Región de los Lagos, southern Chile, and its tectonic implications. Revista Geológica de Chile, 15, 13-30.

Hervé, F., Araya, E., Fuenzalida, J.L., et al., 1979, Edades radiométricas y tectónica neógena en el sector costero de Chiloé continental, X Región. In Congr. Geol. Chileno, N°2, Actas vol. 1, p. F1-F18, Arica.

Hervé, F. and Y. Ota. Fast Holocene uplift rates at the Andes of Chiloe, southern Chile. Revista Geológica de Chile (in press).

Hervé, M. 1976, Estudio geológico de la falla Liquiñe-Reloncaví en el área de Liquiñe; antecedentes de un movimiento transcurrente (Provincia de Valdivia). Actas I Congreso Geológico Chileno, B39-B56.

Jackson, J. and P. Molnar, 1990, Active Faulting and Block Rotations in the Western Transverse Ranges, California. Journal of Geophysical Research, vol. 95, N°B13, 22,073-22,087.

Lamb, S.H. and H.M. Bibby, 1989, The last 25 Ma of rotational deformation in part of the New Zealand plate-boundary zone. Journal of Structural Geology, vol. 11, N° 4, 473-492.

Pankhurst, R.J., Hervé, F., Rojas, L. and J. Cembrano, 1992, Magmatism and tectonics in continental Chiloe, Chile (42°-42°30'S). Tectonophysics, 205, 283-294.

Parada, M.A., Godoy, E., Hervé, F. and Thiele, R., 1987, Miocene calc-alkaline plutonism in the chilean southern Andes, Revista Brasileira de Geosciencias 17, 450-455.

Pardo-Casas, F. and P., Molnar, 1988, Relative motion of the Nazca (Farallon) and South American plates since Late Cretaceous times, Tectonics, 6, 233-248.

Rojas, C., Beck, M., Burmester, R., Cembrano, J. and F. Hervé. Paleomagnetism of the Mid-Tertiary Ayacara Formation, southern Chile: counterclockwise rotations in a dextral shear zone. Revista Geológica de Chile (submitted).

Thiele, R., Hervé, F., Parada, M.A. and Godoy, E. 1986, La megafalla Liquiñe-Ofqui en fiordo Reloncaví (41°30'S), Chile, Comunicaciones (Universidad de Chile, Santiago) 37, 31-40.

Woodcock, N.H. and M. Fisher, 1986, Strike-slip duplexes. Journal of Structural Geology, 8, 7, 725-735.

THE MESOZOIC-CENOZOIC EVOLUTION OF THE ECUADORIAN ANDES

Arturo EGUEZ[1] and John A. ASPDEN[2]

[1] Escuela Politécnica Nacional, Casilla 2759, Quito - ECUADOR
[2] Misión Británica, Quito, British Geological Survey, Keyworth, Nottingham NG12 5GG, U.K.

RESUMEN: Los principales eventos en la evolución geodinámica del Ecuador han sido registrados en el Triásico, Jurásico, Cretácico inferior, Campaniano y Eoceno superior-Oligoceno. Estos eventos se han determinado a partir de levantamientos geológicos regionales y la determinación radiométrica de aproximadamente 350 muestras.

KEY WORDS: Ecuador, Andes, Autochthonous/Allochthonous, accretionary prism, geochronological, Mesozoic-Tertiary evolution.

MESOZOIC-CENOZOIC EVOLUTION

Recent studies by various groups, including the publication of ca. 350 radiometric ages, allow a more precise interpretation of the geological evolution of the Ecuadorian Andes.

In the Cordillera Real (Eastern), during the Late Triassic, the semi-pelitic, Loja division sediments were metamorphosed. This event was accompanied by regional, dextral (transpressional) shearing, the emplacement of syn- to late- tectonic, granitoid batholiths (of S- and I-type character) and mafic amphibolite bodies, migmatite formation and, possibly, minor volcanism in the east. Zircon and monazite, U/Pb dates indicate plutonic ages of 228 $\pm$ 1 Ma and 227.6 $\pm$ 3.2 Ma.

In the Middle-Late Jurassic (ca. 190-140 Ma), major, volcano-plutonic activity occurred throughout the sub-Andean zone and in the eastern part of the Cordillera Real, to the north of 2°S. During this period the Zamora, Abitagua, Azafran, Chingual and Rosa Florida batholiths were emplaced and the (?)contemporaneous, volcanic Misahuallí and the volcano- sedimentary Upano sub-divisions were formed.

Following the cessation of this activity, in the Late Jurassic-Early Cretaceous (ca. 140-120 Ma), the Cordillera Real and sub-Andean zone were deformed, uplifted and eroded. Young, K/Ar mineral ages (ca. 135-120 Ma) and a reset, Rb/Sr whole-rock isochron (120 $\pm$ 5 Ma) obtained

from the Jurassic batholiths are interpreted to relate to this event which, within the Cordillera, included an important component of (?)dextral shearing along steep-to-vertical, NNE/SSW-trending zones.

The western structural (?autochthonous) limit of the Cordillera Real is defined by the Baños-Las Aradas fault zone which represents the southern extension of the Romeral fault in Colombia. Westward of this structure, and possibly mainly during Late Jurassic-Cretaceous time, the principle elements of an accretionaly prism complex were assembled. Much of this complex is now buried by Tertiary and Quaternary volcanic deposits but it includes: the east-west trending, metamorphic rocks of El Oro province in the southwest, the Late Jurassic volcanic, oceanic arc sequence of the Alao division and the quartzose/pelitic metasediments of the (?)Lower Jurassic Guamote division in Central Ecuador, and various "basement/metamorphic" windows reported from the Chota valley, in the north, and the Chaucha/Manu areas, in the south.

Detailed mapping in the El Oro Province has established that the accretionary complex contains inclusions of both 'continental' and 'oceanic' affinities. The former include a variably metamorphosed (HT/LP), semi-pelitic sequence, syn-to late-tectonic, S- and I-type character granitoids, migmatites and amphibolites, all of which can be correlated with rocks occurring in the Loja division of the Cordillera Real to the east. It is suggested that the El Oro rocks were tectonically scavenged from the western margin of this Cordillera (or possibly its southern extension into northern Peru-the Olmos Arch) and incorporated into the accretionary prism from ca. 140 Ma onwards, most probably as a result of dextral shearing. High-pressure inclusions (blueschists and eclogites) of oceanic origin were also tectonically emplaced into the accretionary complex. A single K/Ar (phengite) determination for the El Oro Province gave an (?cooling/ emplacement) age of 132 $\pm$ 5 Ma and similar dates, obtained from Colombian blueschists, that are interpreted to represent the northward continuation of the accretionary complex, range from 125 $\pm$ 15 to 120 $\pm$ 5 Ma.

In the Early-Late Cretaceous (ca. 120-85 Ma), in the sub- Andean zone, and probably extending westwards over the Cordillera Real, the epicontinental sandstones, shales and limestones of the Hollin and Napo formations were deposited, with marked unconformity, over eroded, deformed, pre-Cretaceous lithologies. The depositional environments recorded by these sediments and the general absence of plutonism, indicate a period of relative tectonic quiesence. However, volcanic debris was shed into the extensional (?transtensional) Alamor/Lancones basin which was forming above the accretionary complex in southwest Ecuador and northwest Peru. Paleomagnetic data from the Lancones basinal sediments suggest progressive, clockwise (up to 90°) rotation took place during Early-Late Cretaceous time, implying a dextral shear regime, possibly with a limited subduction component. This rotation would also account for the marked east-west structural trend of the accretionary complex in the El Oro Province.

Following the deposition of the Upper Napo formation in the east, a major period of Upper Cretaceous (Campanian, ca. 83-73 Ma) uplift and erosion affected the Cordillera Real and sub-Andean zone. This event coincides with a regional, thermal disturbance (resetting) of the K/Ar mineral ages and the emergence of the Cordillera as a positive topographic feature. During this period plutonic activity was restricted.

In the uppermost Cretaceous-Paleocene (ca. 73-60 Ma) the continental Tena formation was deposited along the eastern margin of the Cordillera Real and the marine Yunguilla formation was laid down in the west, in (?)tensional basins developed on top of the Late Jurassic-Cretaceous accretionary complex. During Early Tertiary time (60-38 Ma) the calc-alkaline, oceanic Macuchi-Sacapalca arc and associated marine sediments developed on top of the oceanic, Early Cretaceous Piñon terrane which was probably located somewhere to the west. To the east in the

sub- Andean zone and Oriente, the widely distributed, continental Tiyuyacu formation was deposited. In the Cordillera Real a number of generally small (undeformed) stocks and plutons were emplaced.

Near to the Oligocene-Eocene boundary (ca. 38-35 Ma) an important change resulted in regional uplift and erosion and probably, the widespread reactivation of older structures. It was possibly at this time that the Early Cretaceous, oceanic Piñón terrane, together with its Upper Cretaceous-Lower Tertiary (pre-Oligocene), marine cover sequence, and the Macuchi-Sacapalca arc were accreted. The Piñón terrane now forms the basement of the Cordillera Occidental (Western) and Coastal Plain and the tectonic contact between this terrane and the western limit of the Late Jurassic-Cretaceous accretionary complex is marked by the Calacali-Pallatanga fault in Ecuador and by the Cauca-Patía fault in Colombia. During the accretion the Cordillera Occidental was deformed and sliced-up by a series of dextral, NNE-SSW trending, horse tail faults that terminated in the Calacali-Pallatanga fault. In the Oligocene (ca. 35-27 Ma) the continental, calc-alkaline Saraguro volcanic arc developed over the Ecuadorian Andes. Dextral, transtensional, intermontane basins were opened between the Cordillera Real and Cordillera Occidental. In the coastal (forearc) region sedimentation changed from marine to continental and in the Oriente (back-arc), the continental Orteguaza formation was deposited.

At ca. 26 Ma there was a major reorientation in the relaitve motions of the oceanic and South American plates. Events relating to this change are not well-documented but in the Cordillera Occidental, Miocene (ca. 20-9 Ma) granitoid batholiths were emplaced and Miocene-Pliocene (ca 20-4 Ma) acid-intermediate, volcanic activity (Pisayambo Group) was widespread.

At ca. 2 Ma the Carnegie ridge came into contact with the active subduction zone. This collision brought about the cessation of volcanic activity to the south of ca. 2°30'S, whereas to the north, large, andesitic, stratiform volcanoes were formed, especially along reactivated, regional structures such as the Baños-Las Aradas and the Calacali-Pallatanga faults. The oblique, NE-SW trending, regional faults, especially in the Cordillera Occidental were also reactivated, movements along which continue until the present-day.

TECTONIC INTERPRETATION OF MESOSCOPIC STRUCTURES IN A HIGH STRAIN SHEAR ZONE OF THE ATACAMA FAULT SYSTEM, COASTAL RANGE, NORTHERN CHILE.

Gabriel GONZÁLEZ(1)

(1) Universidad Católica del Norte Chile, present adress: Freie Universität Berlin, Fachrichtung Geologie, Haus B, Malteser Str. 74-100, D-1000 Berlin 46, Germany

RESUMEN: Se estudia una zona de cizalle ductil pertenciente al Sistema de Falla de Atacama. La zona contiene buenos indicadores cinemáticos mesoscópicos para inferir movimientos transtensionales en el Jurásico-Cretácico inferior. Los desplazamientos son sincinematicos con el emplazamiento de un cuerpo plutónico (Plutón de Cerro Cristales).

KEY WORDS: Kinematic indicators, transtensional strike-slip fault, magmatic arc, Jurassic-Cretaceous boundary.

INTRODUCTION

The Atacama Fault System (AFS) is exposed in the Coastal Range of northern Chile. Its shows fault rocks (mylonites and cataclasites), that are an expression of the paleotectonic movements along of the Coastal Range. The fault rocks are exposed as a N-S trending belt between 22° und 29° S (URIBE & NIEMEYER 1984, SCHEUBER & ANDRIESSEN 1990, BROWN et al. 1991). Radiometric dating of mylonites of the differents segments of the AFS demonstrates that the AFS was active during the Upper Jurasic-early Cretaceous (NARANJO et al. 1984, HERVE 1987, SCHEUBER & ANDRIESSEN 1990). Kinematic reconstructions show that the AFS acted as a zone of sinistral strike-slip faults caused by oblique convergence between the Pacific Aluk Plate and the South American Plate. However, according to preliminary results of structural observations carried out in a ductile shear zone in the AFS between 23°55' and 24°11' S, the AFS displays, in addition, mylonites with kinematic indicators of vertical movements. This shows that the history of the desplacements along the AFS is not yet fully understood.

GEOLOGICAL SETTING

The Coastal Range in the study area is composed mainly of plutonic rocks and andesitic lavas (Formación la Negra, GARCIA 1967). The plutonic rocks consist of gabbros, diorites and granodiorites that have an age range from early Jurassic to early Cretaceous, while the age of the volcanic rocks is confined to the Jurassic. The scarce sedimentary rocks of the area are represented by the Caleta Coloso Formation of early Cretaceous age (GARCIA 1967).

Brittle faults form the boundaries between units corresponding to blocks of differents structural levels. An example is the Caleta Coloso Fault that exhibits, in the western block, plutonics rocks that shows deformational characteristics of a deep level, while lavas and sedimentary rocks are exposed in the eastern block. The rocks of the western blocks are transected by a N-S trendig ductile shear zone, about 400 m wide, that can be followed for 12 km. It forms the western boundary of the Plutón Cerro Cristales (PCC). The rocks on western side of this shear zone are lavas of the La Negra Formation and plutonic rocks of Jurassic age (mainly gabbros and diorites).

The shear zone contains mylonites that were formed and recrystallized under middle to upper amphibolite-facies conditions. The rocks of the PCC of the eastern side of the shear zone display a magmatic flow orientation wich is overprinted by solid-state deformation: The magmatic flow structures are revealed by preferred orientation of plagioclase crystals that have weakly developed core and mantle structures. At the mesoscopic scale, the magmatic flow is expressed by a well developed steeply dipping foliation that is parallel to the mylonitic foliation and the contact between the PCC and the ductile shear zone. This suggests that the emplacement the PCC was synkinematic with the displacement along the shear zone. This means that the AFS in this segment was activity during the development of the magmatic arc of the Jurassic-early Cretaceous.

The mylonitic rocks show granoblastic and lepi-nematoblastic textures suggesting strong recrystallitation that has obliterated the primary tectonic structures. For this reason the sense movement can not be determined using microscopic kinematic indicators. On mesoscopic scale, however, the shear zone contains a variety of kinematic indicators that permit the reconstruction of the displacement history.

MESOSCOPIC KINEMATIC ANALYSIS

The mylonitic rocks show an intense steeply dipping foliation with not only subhorizontal stretching lineations, but also steeply plunging to vertical stretching lineations. The orientation of the lineation changes systematically at a deflection of the shear zone in its southern segment, where the N-S trend of the foliation changes abruptly to an E-W direction. The mylonitic rocks in the northern segment (foliation N-S) have subhorizontal lineations, parallel to the western boundary of the PCC, with a variety of kinematic indicators (asymmetric extensional crenulation cleavage, sigmoidal foliation, asymmetric foliation boudinage) all evidencing sinistral displacement. The mylonites on the southern segments have steeply

plunging lineations toward the PCC, with kinematic indicators (asymmetric extensional crenulation clivage, sheat folds, asymmetric foliation boudinage), which show that the NE-side was displaced downward, correspondingly to the displacement in a normal fault.

In both segments strain markers (chocolate tablet boudinage in basaltic dykes, ptygmatic folds in quarz-feldspar veins) indicate strong shortening perpendicular to the mylonitic foliation. Thus, a deformation in a advanced state with both simple shear and pure shear can be deduced, and a mechanism of sub-simple shear deformation (SIMPSON & DE PAOR in press) is suggested for this shear zone. The asymmetric extensional crenulation cleavage was produced when the principal axes of the strain ellipsoid were almost parallel to the limits of the shear zone.

TECTONIC INTERPRETATION

The shear zone at the western border of the Plutón Cerro Cristales represents a transtensional strike slip fault which was active contemporaneously with the emplacement of the pluton at the Jurassic-Cretaceous boundary (according to radiometric datings by SCHEUBER & ANDRIESSEN 1990). The movements were determined by sinistral slip and additional vertical normal slip in the southern segment, where the shear zone changes its direction. The tectonics which produced the described structures in a deep crustal level caused, at the surface, the opening of a sedimentary basin which gave rise to the clastic sedimentation of the Caleta Coloso Formation (Titonian-Neocomian, GARCIA 1967).

REFERENCES

BROWN, M; DIAZ, F; & GROCOTT, J. (1991). Atacama fault system history of displacement and tectonic significance for the mesozoic-recent evolution of northern Chile. 6 Congreso Geológico Chileno, Actas volumen 1 p. 129-132.

GARCIA, F. (1967). Geología del Norte Grande de Chile. Soc. Geol. de Chile. Simposium sobre geosinclinal andino 1962.

HERVE, M. (1987). Movimiento sinistral en el Cretácico Inferior de la Zona de Falla de Atacama, Chile. Rev. Geol. Chile N° 31, p. 37-42.

NARANJO, J.A; HERVE, F; PRIETO, X. & MUNIZAGA, F. (1984). Actividad mecánica de la Falla de Atacama al este de Chanaral: milonitización y plutonismo. Comunicaciones Univ. Santiago 34. p. 57-66.

SCHEUBER, E. & ANDRIESSEN, A. M. (1990). The kinematic and geodynamic significance of the Atacama fault zone, northern Chile. Journal of Structural Geology, Vol. 12. No.2, p. 243-257.

SYMPSON, C. & DE PAOR, D. (in press) Strain and kinematic analysis in general shear zones.

URIBE, F. & NIEMEYER, H. (1984). Franjas miloníticas en La Cordillera de la Costa de Antofagasta (Cuadrángulo de Cerro Cristales, 24°00'-24°15' S) y la distribución del basamento precámbrico. Rev. Geol. de Chile No 23. p. 87-91.

MESOZOIC EXTENSIONAL AND STRIKE-SLIP FAULT SYSTEMS IN MAGMATIC ARC ROCKS OF THE ANDEAN PLATE BOUNDARY ZONE, NORTHERN CHILE

John GROCOTT[1], Graeme K. TAYLOR[2] and Peter J. TRELOAR[1]

(1) School of Geological Sciences, University of Kingston, Kingston-upon-Thames, Surrey KT1 2EE, U.K.
(2) Department of Geological Sciences, University of Plymouth, Drake Circus, Plymouth, Devon PL4 8AA, U.K.

SUMMARY

Middle Jurassic to Early Cretaceous plutonic rocks were emplaced in an extensional magmatic arc between 25°S and 27°S in the Andean convergent plate boundary zone of northern Chile. Abandonment of the magmatic arc in the Early Cretaceous was accompanied by a change from an extensional to a strike-slip regime in the plate boundary zone. Sinistral strike-slip displacements on the Atacama fault system are part of this regime.

KEY WORDS: Magmatic arc, Mesozoic, Extension, Strike-slip, Atacama, Chile

INTRODUCTION

The mechanisms of magma emplacement in continental magmatic arcs differ according to whether the plate boundary zone is in extension or compression. Studies which attempt to relate displacements in the arc to emplacement mechanisms often focus on displacements associated with emplacement of plutonic igneous rocks. In fact, the ductile and brittle fault systems which accompany magma emplacement are often linked to fault systems affecting the fore-arc, back-arc and the volcanic sequences at higher structural levels within the arc.

In extensional continental magmatic arcs, the arc and back-arc are often thought of as distinct tectonic units. Indeed, the back-arc is typically characaterized by a marine marginal basin, whereas the arc remains at or largely above sea level because of the addition of arc magmas to the crust. This conventional subdivision of tectonic units at convergent plate margins tends to obscure an important unifying aspect of the arc/back-arc couplet, namely the linked fault system responsible for the overall extension of the convergent plate boundary zone.

We have studied deformation and magma emplacement in a Middle Jurassic to Early Cretaceous magmatic arc exposed between 25°S and 27°S in the Coast Ranges of northern Chile. We focus on the displacement history of arc-parallel fault systems, including the Atacama fault system, and point to the likely relationship between fault systems developed in the arc and those in the adjacent back-arc.

DUCTILE EXTENSIONAL DEFORMATION IN THE MAGMATIC ARC

Plutonic rocks now exposed in the Middle Jurassic to Early Cretaceous magmatic arc of northern Chile were emplaced between c.153 Ma and c.126 Ma at high levels in the crust - above the regional ductile-brittle transition. This is known because of the concordance of mineral and whole-rock cooling ages obtained for individual plutons by a range of isotope systems (Brown and others, 1991; 1993). However, ductile deformation is present in the wall rocks of individual intrusions and has been shown by field relations (Brown and others, 1993) and $^{40}Ar/^{39}Ar$ geochronology (Brown and others, 1992) to be related to emplacement of the intrusions. Therefore the magmas must have carried sufficient heat to high structural levels to allow ductile deformation of their wall rocks at temperatures as high as the upper amphibolite facies.

Steeply-dipping, ductile shear zones in the wall rocks of arc plutons are up to 800m wide, exhibit intense mylonitic fabric and contain steeply-plunging stretching fabrics. This implies kilometers of vertical displacement on these shear zones yet there is no evidence for such large changes in structural level across these zones. Therefore the shear zones probably reach a low-angle detachment at shallow depth beneath the plutons. That this is probably an extensional detachment is implied by: (a) passive emplacement mechanisms; (b) general lack of pre-main crystallization fabrics in the intrusions; (c) lack of contractional structures in the arc and (d) emplacement of conjugate dyke swarms indictive of east-west extension throughout the period of pluton emplacement and ductile shear zone formation.

BRITTLE EXTENSIONAL FAULT SYSTEM

Middle Jurassic (post Sinemurian, pre Kimmeridgian) shallow- water limestones (Pan de Azucar Formation) are exposed in the magmatic arc overlain by coarse conglomerates and a very thick sequence of lavas and volcaniclastic sediments (La Negra Formation). Both formations are cut by west-dipping, listric normal faults associated with rollover anticlines. The hangingwall of the faults was displaced to the west and the fault system accommodated east-west extension. Given that the exposed Middle Jurassic plutons were emplaced in an extensional regime also involving east-west extension, and are probably slightly younger than the La Negra Formation, it is likely that the extensional faults in the plutonic and volcanic rocks of the arc belong to the same (linked) fault system.

ATACAMA FAULT SYSTEM

Arc plutons become consistently younger from west to east across the arc towards a major arc-parallel fault system: the Atacama fault system (Brown and others, 1992). The fault system is characterized by sinistral strike-slip displacement, first in the ductile mode and subsequently in the brittle mode. The brittle sinistral strike-slip deformation is associated with intense Cu-Fe mineralization.

Ductile deformation under greenschist facies conditions in the Atacama fault system resulted in the formation of a belt of mylonitic rocks up to 1 km wide characterized by sinistral strike-slip displacements. An $^{40}Ar/^{39}Ar$ isotope correlation age from recrystallized hornblende in the mylonite gives a cooling age of 126 Ma - similar to the cooling age of the intrusion in which the mylonitic rocks were developed. Subsequent sinistral strike-slip deformation is ductile/brittle and later brittle and implies progressively declining temperature during continued displacement. Structures characteristic of the ductile/brittle transition include brittle faults with flexural-slip folds in their sidewalls which could indicate that the tectonic regime is transpressional. Mineralization is associated with the latest, most brittle, displacements.

ROTATION OF THE MAGMATIC ARC

Recent palaeomagnetic work by Taylor and others (1993) has shown that the rocks of the La Negra Formation exhibit a primary remanence indicating a net local block rotation of c.35°, west of the Atacama fault system between 25°S and 27°S. This rotation could be due to a combination of:
(a) rotation on linked extensional faults associated with development of the magmatic arc;
(b) dilation of wedge-shaped plutons;
(c) antithetic rotation in sidewall ripout structures associated with sinistral displacement on the Atacama fault system.

EXTENSIONAL FAULT SYSTEM IN THE BACK-ARC AREA

Recent work by Mpodozis and Allmendinger (1993) has identified major extension on low-angle detachments in the back-arc area. This extensional deformation is between Aptian and Cenomanian in age. The major displacements involved displacement of the hangingwall to the northeast and the development of basin and range-type structures. They also identify an earlier phase of extensional deformation with displacement of the hangingwall to the northwest.

Mpodozis and Allmendinger (1993) propose that northeast extension could be related to sinistral strike-slip on the nearby La Ternera-Domeyko fault system (and on the Atacama fault system) in a transpressional regime. Further, they suggest that northwest extension may be related to an earlier extensional regime in the plate boundary zone. Our work in the magmatic arc relates well to the conclusions of Mpodozis and Allmendinger (1993) and this allows important generalizations to be made about linkage of the arc/back-arc fault systems.

CONCLUSIONS

(1) Emplacement of arc magmas between c.153 Ma and c.126 Ma in the MJ-LC arc was associated with east-west extension. Strike-slip displacements did not occur in the overriding plate at this stage despite the probability that oblique convergence characterized the plate boundary zone at this time. Extension in the arc was likely linked to northwest-southeast extension in the back arc.

(2) Linked extensional fault systems are probably present across both the magmatic arc and the back-arc basin in extensional margins. Emplacement of magmas in the arc counteracts extension so that the arc remains at or above sea level.

(3) Ductile strike-slip displacement on the Atacama fault system was initiated at c.126 Ma. Subsequent transition from ductile to brittle sinistral strike-slip suggests that the arc was abandoned at this time. Initiation of transpression in the margin and migration of magmatic activity to the east is linked to the start of opening of the South Atlantic in the mid-Cretaceous.

(4) A second phase of extensional deformation in the back-arc may be linked with sinistral strike-slip on the La Ternera/ Domeyko and Atacama fault systems.

REFERENCES

Brown, M., Dallmeyer, R.D. Diaz, F. and Grocott, J. 1991. EOS Transactions American Geophysical Union v. 72/17, p. 263.

Brown, M., Diaz, F. and Grocott, J. 1993. Bulletin Geological Society of America v. 105 (In press).

Brown, M., Dallmeyer, R.D. and Grocott, J. 1992. Geological Society of America Annual Meeting (Cincinnati) Program and Abstracts A63-A64.

Mpodozis, C. and Allmendinger, R.W. 1993. Bulletin Geological Society of America v. 105 (In press)

Taylor, G.K., Randall, D., Grocott, J. and Treloar, P.J. 1993. 2nd International Symposium on Andean Geodynamics (Oxford) Program and Abstracts (In press).

THE TUPIZA, NAZARENO AND ESTARCA BASINS (BOLIVIA): STRIKE-SLIP FAULTING AND THRUSTING DURING THE CENOZOIC EVOLUTION OF THE SOUTHERN BRANCH OF THE BOLIVIAN OROCLINE

Gérard HERAIL(1), Jaime OLLER(2), Patrice BABY(3), Javier BLANCO(4), Michel G. BONHOMME(5), and Pierre SOLER(6).

1 - ORSTOM, UR1H, Casilla 53390, Correo Central, Santiago 1, Chile.
2 - PETROLEX, Casilla 3969, Santa Cruz, Bolivia.
3 - ORSTOM-YPFB, Casilla 4775, Santa Cruz, Bolivia.
4 - YPFB, Casilla 1659, Santa Cruz, Bolivia
5 - CNRS URA 69, Université Joseph Fourier, 15 Rue M. Gignoux, 38031 Grenoble, France.
6 - ORSTOM, UR1H, Casilla 9214, La Paz, Bolivia.

RESUME: Des bassins de Tupiza, Estarca et Nazareno (sud de la Bolivie) le plus ancien d'entre eux (celui de Tupiza) s'est ouvert aux environs de 23 Ma sur une zone en décrochement senestre orientée N-S. Ce n'est qu'à partir de 20 Ma environ que l'évolution tectonique et sédimentaire a été controlée par des chevauchements N-S. Ces mouvements se sont fortement ralentis vers 10 Ma permettant le développement de topographies d'aplanissement étendues (Surface San Juan de Oro).

KEY WORDS: Cenozoic basin, thrusting , strike-slip, Bolivia.

INTRODUCTION.

During the Cenozoic, the tectonic structuration of the Bolivian Andes has been adquired through thrusts. This tectonics is responsible for an important amount of shortening (Sempere et al., 1990; Sheffels, 1990). Before these thrustings took place, left-lateral transcurrent deformation is documented in the southern part of the Bolivian Altiplano (Baby et al. 1990) but, generally speaking, it is impossible to analyse with much detail these movements and their chronology. In the Tupiza region the sedimentary rocks and deformational features formed under the influence of changing stress conditions are well exposed and their chronology can be constrained.

REGIONAL SETTING.

The Tupiza basin is 6 to 13 km wide and extends over 80 km in a N-S direction, parallel to the Aiquille-Tupiza Fault, and continues towards the South in Argentina. The bottom of the valley that drains it at present, is located at around 2800 m above sea level and is surrounded by highlands reaching 4000-4200m. These highlands are made of Early to Mid-Ordovician rocks and are cut by remains of well-preserved erosion surfaces (Servant et al., 1989): the Chayanta Surface (above 4000m high) and the San Juan de Oro Surface (≈3500-3800m). On the western side, a highland separates the Tupiza basin from the Estarca basin which extends N-S over 70 km

and is 6 to 12 km wide. Towards the east, another highland separates the Tupiza basin from the Nazareno basin which extends in a N-S direction over 80 km. Towards the south, the Nazareno basin and the Estarca basin gradually lead to flat regions: Chaupi Yacu (3500m) and Livia Pampa (3800m) respectively that correspond to the San Juan de Oro Surface. In contrast, north of the three mentioned basins, San Juan de Oro Surface remnants (Mochara Pampa) are exposed at an altitude of ≈ 3500 m, at 500 m above the bottom of the present valleys.

THE SEDIMENTARY INFILL

The Cenozoic sediments of the Tupiza basin have a continental origin. Conglomeratic facies constitute the bulk of the basin infill with minor sands, clays, sometimes gypsiferous clays, and less commonly carbonate deposits. The sedimentary pile is discordant on the top of the Ordovician, which in turn is composed essentially of black pelites (Cieneguillas Fm and Obispo Fm).

The sedimentary infill starts with the deposition of red breccias (frequently affected by synsedimentary normal faults) composed of Ordovician rock fragments and clays. Locally, in the deepest parts of the basin (Palquiza and Quebrada Catati area) a more complete sequence is preserved which, in addition to the basal breccias, contains around 50 cm thick layers of well-sorted sands with ripples or cross bedded channels. To the top, these sandy sediments change laterally into either scarce lacustrine deposits or into flood plains sediments in a evaporitic environment (greenish, violaceous and sometimes reddish clays whith gypsum veinlets, gypsum and halite layers that can reach 50 cm thick, and scarce beds of limestones with fish-teeth and gasteropods-shells). This formation (Catati Fm) is around 50 m thick.

The Catati Fm is overlaid by a thick accumulation of red, coarse-grained conglomerates (Tupiza Fm - Montaño, 1966) which outstands in the landscape of the basin These matrix-supported conglomerates, organized in fluvial to fluviotorrencial channels with normal graded bedding, are essentially composed of pebbles and boulders of Ordovician rocks, the diameter of which may exceed 50 cm. In addition, they locally contain Cenozoic lava clasts, Mesozoic sandstone and Pucalithus limestone fragments preoceeding from the El Molino Fm (Maastrichtian) which does not crop out in the surrounding area of the basin at present. The matrix is often very abundant and interbedded mudflows are numerous. In the lowest part of the Catati Fm., lava flows crop out (Cerro Bolivar, along the way Tupiza-Mochara, on the foothills from the Cerro Cruz to the Cerro Chaupiloma). Due to their alkaline feature, we assimilate them to the lava flows of the Rondal Fm. (see Soler and Jimenez, this volume). Clasts of these lavas flows are frequent in the conglomerates of the Tupiza Fm, but they are scarce in the brccias of the Catati Fm.

The Nazareno Fm overlies the Tupiza Fm. Generally, a reverse fault juxtaposes both formations; in some spots of the central part of the basin however (Quebrada Catati, Quebrada Checona) the stratigraphic, unconformable contact between them is observed. In the Nazareno basin, the Nazareno Fm starts with a deposit of subangular conglomerate the clasts of which come from the Ordovician (some 10 m thick only) The conglomerates are overlaid by argillaceous and sandy layers interbedded with either conglomerates or dacitic pyroclastics. The same pink-coloured facies with clasts from volcanic origin (dacite) and scarce ash-beds crop out widely in the Tupiza basin. Moreover, the conglomerates of the base of the Nazareno Formation often contain reworked fragments of the underlaying Tupiza Formation sediments.

The sediments of the Estarca basin are contemporaneous with the Nazareno Fm. These conglomerates are made of Ordovician fragments. The basin infill corresponds to only one sedimentary wedge. To the eastern side of the basin the series is thicker (1000 to 1500m) than towards the west, and the alluvial fan conglomeratic facies prevail. These conglomerates come from the east. On the western side of the basin, the sedimentary infill is thinner and overlaps progressively the Ordovician strata. On this side the sediments are formed by Ordovician subangular fragments which were deposited by a sheet flood. These sediments come from the

west. To the center of the Estarca basin both these sediments and those coming from the east are interbedded with flood plain fine-grained deposits.

The Oploca Fm (Montaño, 1966) overlies by progressive unconformity the Nazareno Fm, or by an unconformity the Ordovician basement. The light brown Opoca Fm is composed of fluvial conglomerates containing well rounded pebbles. Sometimes the sandy matrix is very abundant. Volcanic clasts (essentially of dacitic composition) are abundant, and volcanic tuff levels, generally reworked, are exceptionally found. The strata, generally from one to several meters thick, are very continuous. The gradded-bedding is normal. Measurements of paleoflow directions show that these fluvial sediments were transported by streams flowing according to the basin orientation; in contrast, in the older formations, flow directions predominantly went from the edges towards the center of the basin. The transition between the Nazareno Fm and the Oploca Fm does not show a sharp change in the composition of the sediments, only the coarse fraction becomes more abundant.

In the Tupiza Fm, a sample of an alkaline lava flow of the Cerro Bolivar gave a K/Ar whole rock age of 22.7±0.6 Ma. In the Nazareno Fm two biotite K/Ar ages yielded 20.0±0.6 Ma (Cerro Filosola) and 18.0±0.5 Ma (near Catati). Fauna collected in the flood plain sediments of Nazareno basin was assigned to the Friasian (Oiso, 1991) and a armadillo armor discovered near Suipacha (Castellanos, 1925) was attributed to the Late Miocene (Hoffstetter, 1977). In the southern part of the Tupiza basin, an $^{40}Ar/^{39}Ar$ age of 12.79±0.12 Ma has been obtained (Gubbels et al., 1993). A volcanic ash layer interbedded with sediments covering the San Juan de Oro Surface yielded $^{40}Ar/^{39}Ar$ ages of 9.32±0.12 and 8.78±0.17 Ma (Gubbels at al., 1993).

THE DEFORMATION OF THE CENOZOIC SEDIMENTS

The oldest sediments (Catati and Tupiza Fm) are the most intensively deformed. They have been affected by two tectonic events:

a) an early event, characterized by synsedimentary normal faults with relatively small displacements (about 1 m). Metric strike-slips faults, decimetric drag folds and hectometric oblique folds (oriented around N25° to N30°) are present along the Tupiza basin. These tectonic features are compatible with sinestral strike-slip shear process.

b) a late event is characterized by the development of N-S oriented fold with subvertical limbs.These folds are cut by a convergent thrust system. The Tupiza and Catati Fm have been transported to the center of the basin by thrusts with a detachment level in the black Ordovician pelites. Minor thrusts were developed from the gypsum levels of the Catati Fm.

The Nazareno Fm is overthrusted by the Tupiza Fm and its Ordovician basement (Quiriza Fault, Uralica Fault). On both the western and eastern edges of the basin the Cenozoic sedimentary infill is directly overthrusted by the Ordovician; these thrusts are convergent and the dip of these thrusts is gentle (10° to 15° eastward in Quebrada Epicaya for example). The total displacement of this thrusts is unknown.

The Oploca Fm, like the Nazareno Fm, is folded and thrusted but the deformation is less marked than in the Nazareno Fm. Geological mapping shows that the Oploca Fm progressively seals tectonic structures developed in the Nazareno Fm.

After the opening and infilling of these basins the waning of the deformation permits the progressive levelling of the reliefs surrounding these basins (formation of the San Juan de Oro Surface).

CONCLUSIONS

Three groups of tectono-sedimentary events have been recognized in the studied basins:

- the first one corresponds to the deposition of the Catati and Tupiza Fm. These sediments, as well as the alkaline lavas (Rondal Fm) associated with the opening of a transtensional basin, have arised from distributed left lateral shear. This event began before 23 my ago and ended before ≈ 20 my.

- the second one corresponds to the deposition of the Nazareno and Oploca Fm. These sediments were deposited in the basins of Tupiza, Nazareno and Estarca and correspond to different contemporaneous sedimentary wedges associated with N-S trending thrusts. In the Tupiza basin itself, these thrusts cross-cut the structures formed during the opening of the basin, and control the development of younger basins such as the Estarca basin which has been, in turn, transported to the west (piggy-back basin) during the development of the San Vicente Fault. The Oploca Fm was deposited at the end of this tectonic event which began before 20 my and finished after 13 my.

- the third one corresponds to the San Juan de Oro Surface formation which started around 10-9 my and corresponds with a quiescent tectonic period.

REFERENCES

BABY, P., SEMPERE, T., OLLER, J, BARRIOS, L., HERAIL, G., and MAROCCO, R., 1990, Un bassin en compression d'âge Oligo-Miocène dans le sud de l'Altiplano bolivien. *Compt. Rend. Acad. Sci., Paris*, sér. II, v. 311, 341-347.

CASTELLANOS, A., 1925, Un nuevo dasipodino extinguido en la parte meridional de Bolivia. *An. Mus. Nac. Hist. Nat. Buenos Aires*, 33, 255-285.

GUBBELS, T.L., ISACKS, B.L. FARRAR ,E. 1993, High-level surfaces uplift, and foreland development, Bolivian central Andes. Geology, *in press.*

HOFFSTETTER, R., 1977, Un gisement de mammifères Miocènes à Quebrada Honda (Sud Bolivien). *Compt. Rend. Acad. Sci., Paris*, sér. D, v. 284, 1517-1520.

MONTAÑO, D.,1966, Estudio geológico de la región de Tupiza-Estarca-Suipacha. *Thesis Univ. Mayor de San Andres, La Paz*, 76p, unpub.

OISO, Y., 1991, New land mammal locality of Middle miocene (Colloncuran) age from Nazareno, Southern Bolivia. *Rev. Tec. YPFB*, 12 (3-4), 653-672.

SEMPERE, T., HERAIL, G., OLLER, J., and BONHOMME, M., 1990, Late Oligocene-early Miocene major tectonic crisis and related basins in Bolivia, *Geology*, 18, 946-949.

SERVANT, M., SEMPERE, T., ARGOLLO, J., BERNAT, M., FERAUD ,G., and LOBELLO, Ph.,1989, Morphogénèse et soulèvement de la Cordillère Orientale des Andes de Bolivie au Cénozoïque. *Compt. Rend. Acad. Sci.*, Paris., sér. II, t.309, 417-422.

SHEFFELS, B., 1990, Lower bound on the amount of crustal shortening in the central Bolivian Andes, *Geology*, 18, 812-815.

SOLER, P., and JIMENEZ CH., N., 1993, Magmatic constraints upon the evolution of the Bolivian Andes since Late Oligocene times, *this volume.*

THE CRETACEOUS TO EARLY PALEOGENE TECTONIC EVOLUTION OF THE CENTRAL ANDES AND ITS RELATIONS TO GEODYNAMICS.

Etienne JAILLARD [1]

(1) Misión ORSTOM, Rusia y Eloy Alfaro, Apartado postal 17.11.06596, Quito, Ecuador.

RESUMEN : Las fases compresivas y la subsidencia de la margen andina durante el Cretáceo superior-Paleógeno están analisadas en relación con la geodinámica. El regimen compresivo a largo plazo sería controlado por el movimiento hacia la fosa de la placa americana, mientras que las fases compresivas breves coinciden con cambios en la velocidad de convergencia (aceleración). Además períodos de convergencia rápida coinciden con épocas de subsidencia importante.

KEY-WORDS : Late Cretaceous, Paleogene, Andean tectonic phases, Subsidence, Plate Tectonics.

INTRODUCTION

Many classical geodynamic models proposed to explain the origin of the tectonic phases in continental active margin have been elaborated through the observation and comparison of various present-day active margins or through physical modelling. Only few have been elaborated through the study of active margin during long-termed periods. The aim of this paper is to propose some geological constraints and new hypothesis about the origin of the tectonic phases of continental active margins, through the study of the Central Andes from middle Cretaceous up to late Eocene times.

EVOLUTION OF THE CENTRAL ANDES FROM LATE JURASSIC TO EOCENE TIMES.

The Cretaceous evolution of the Central Andes actually began by late Jurassic times. It can be divided into various periods (Jaillard 1993a, Sempéré 1993, and references therein). At this time, the Andean margin comprised a subsident Western trough and an Eastern, less subsident basin, separated by an axial swell.

1. Tithonian-Berriasian (Virú period). During Tithonian times, tectonic, mainly extensional events are coeval with the activity of a volcanic arc along the Peruvian margin, and provoked the sedimentation of widespread clastic deposits, the emergence of part of Southern Peru and the creation of a very subsident sedimentary basin in Northern Peru.

2. Valanginian-Aptian. During early Cretaceous times, east-deriving fluvio-deltaic sandstones were laid down throughout the Central Andean domain. Magmatic and tectonic activities are virtually lacking.

3. Late Aptian-Turonian (Mochica period). During late Aptian times, the Andean margin recorded an extensional tectonic activity, scattered volcanic outflows related to intracontinental tensional regime, and the large-scale on-lap of fluvio-deltaic deposits on the Eastern border of the Andean Basin, due either to eustatic sea-level rise or to tectonic subsidence. The Albian period is marked by a marine transgression that overwhelmed the whole domain, and then by a regression, that culminated in early Cenomanian times with the progradation of eastern deltaic sandstones. The Western part of the margin recorded the intense activity of a volcanic arc, the beginning of magmatic intrusions, and alternating extensional and compressional tectonic deformations. The volcanic activity ceased by late Albian-early Cenomanian times, as the western part of the margin was deformed by a first major compressional phase (Mochica phase). This was probably asso-

ciated with a strong dextral wrenching component, and is recorded by extensional synsedimentary tectonic features in the whole western domain.

During Cenomanian and Turonian times, a major transgression deposited widespread shelf carbonates that recorded the main eustatic discontinuities.

4. Coniacian-early Late Paleocene (Peruvian period). On the whole Andean margin, Coniacian times were marked by the beginning of fine-grained detrital, mainly argillaceous sedimentation, probably related to the erosion of locally tectonized coastal areas. After a period of tectonic quiescence (Santonian-early Campaian), a major compressive phase occurred during late Campanian times. It is responsible for large-scale overthrusts (SW Peru), creation of subsident troughs (Cuzco), marine transgression in the forearc regions (Talara) and deposition of widespread sandstones in the Eastern domain. A new tectonic quiescence occurred during Maastrichtian times, which are characterized by widespread, short-lived marine transgressions. Maastrichtian and Paleocene times were a period of intense and widespread volcanic activity throughout the Central Andean margin.

5. Late Paleocene-Late Eocene (Inca period). From Bolivia to N Peru, widespread unconformities are observed between fine-grained Paleocene and coarse-grained Eocene continental deposits (Inca 1 phase). In the forearc regions, the accretion of the oceanic-floored Peninsula of S Coastal Ecuador was concealed by latest Paleocene unconformable coarse-grained high density turbidites (Benitez et al. 1993). It was followed by the accretion of the Amotape continental Terrane of N Peru (Berrones et al. 1993), concealed by early Eocene coarse-grained conglomerates, and expressed by a sedimentary gap in Coastal Ecuador. Middle Eocene times were a period of extensional subsidence and of eustatic sea-level rise, which provoked the deposition of a shallowing-upward marine sequence. This period ended up by the deposition of polygenic sandstones and conglomerates, interpreted as resulting from the overthrust of the oceanic-floored coast of Ecuador on the continental Andean margin by early Late Eocene times (Benitez et al. 1993).

In summary, compressional deformations of the Andean margin began in Albian times. Discrete tectonic phases occurred during late Albian-early Cenomanian, Coniacian, late Campanian, late Paleocene, earliest Eocene times and middle to late Eocene times, and are separated by quiescence periods.

SUBSIDENCE HISTORY

The Cretaceous-Paleogene subsidence evolution of the Peruvian margin can be divided into four periods.

Between **145 and 130 Ma** (late Jurassic-Berriasian) either uplift (SW Peru), or rapid subsidence occurred. In N Peru, a major extensional tectonic phase was responsible for the creation of the Chicama basin, that controlled the whole Cretaceous subsidence history of this area (fig. 1).

During early Cretaceous times (**130 to 110 Ma**), important thermal subsidence occurred in the newly created basin, whereas the unstretched areas recorded a slow subsidence rate.

From **110 up to 90 Ma** (late Aptian-Turonian), the subsidence rate increased in all the Western Peruvian areas, floored by stretched continental crust. In Eastern Peru, no significant changes are observed.

Between **90-80 and 40-30 Ma** (Senonian-late Paleogene), two situations occurred. In all areas of N Peru, the

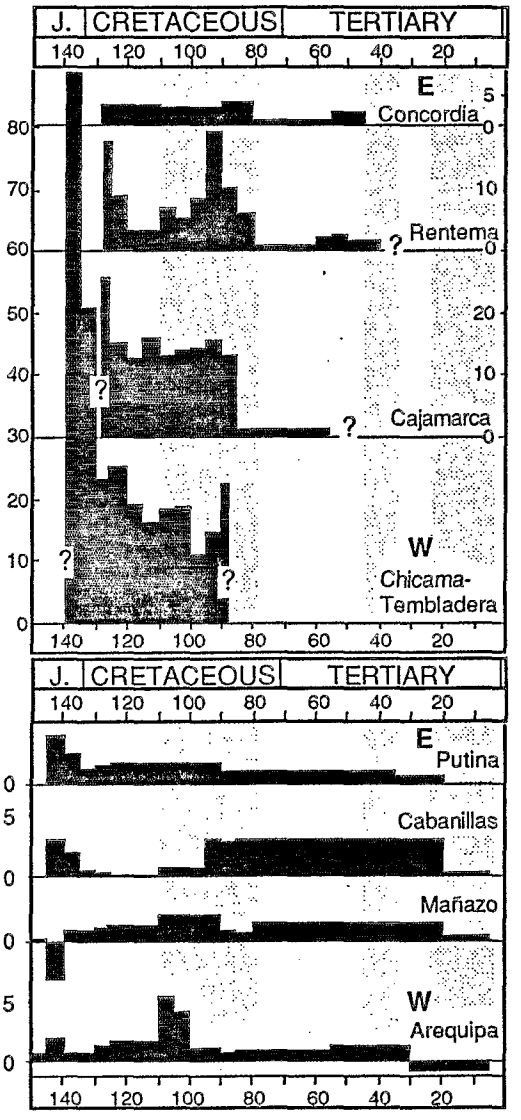

Fig. 1: Average subsidence rates (in cm/Ma) in Northern (above) and Southern Peru (below).

subsidence rate drastically decreased, whereas it remained unchanged or slightly increased in S Peru (fig. 1). In Bolivia, the strong increase of subsidence is interpreted as due to lithospheric flexion related to the incipient Andean shortening (Sempéré 1993).

RELATIONS TO GEODYNAMIC PARAMETERS

Although the geodynamic reconstructions are rather uncertain for the late Cretaceous period, some parameters can be analyzed in relation to the tectonic evolution of the Andean margin.

1. Age of the subducted slab. Classical models assume that the subduction of a young, buoyant oceanic lithosphere induces a the compressional strain in the overriding continental plate (Molnar &, Atwater 1978, Cross & Pilger 1982). After Soler et al. (1989), the rejuvenation of the oceanic plate roughly coincides with the beginning of the compressional period (Albian). However, the late Cretaceous and Paleogene compressional phases occurred during a continuous increase in the age of the slab, fig. 2). Therefore, the age of the slab could contribute to the appearance of a long-termed compressional regime, but cannot account for short-termed compressional tectonic phases.

2. Absolute trenchward movement of the overriding plate. As noted by many authors (e.g. Bourgois & Janjou 1981), the beginning of the westward shift of the South American plate at the equatorial latitudes during Albian times roughly coincides with the beginning of the compressive period in the Andean margin. Thus, this parameter seems to control the long-termed compressive regime of the continental active margin.

3. Collision of continental or oceanic obstacles. Cross & Pilger (1982) proposed that the arrival in the subduction trench of oceanic or continental obstacles (aseismic ridges, sea-mounts, continental microplates), will provoke the blocking of the subduction and the compressive deformation of the continental margin. However, near the Peru-Ecuador border, the accretions of the Amotape continental terrane (earliest Eocene) or the oceanic terranes of Coastal Ecuador (late Paleocene p.p, late Eocene) coincide with compressional phases observed in Bolivia or Southern Peru where no collisions are known to have occurred. Thus, it seems that accretions or collisions of terranes are consequences rather than causes of the compressional phases, and that both accretion-collision and compressional phases are consequences of a same mechanism.

4. Convergence rate. Following Uyeda & Kanamori (1979), Cross & Pilger (1982) or Pardo-Casas & Molnar (1987), a rapid convergence between the oceanic and continental plates provokes a compressional stress in the latter. On the Andean margin, periods of high convergence rates occurred in Albian-Campanian and late Eocene-early Oligocene times, which roughly coincide with tectonic periods (fig. 2). However, the short-lived compressional events seem to concide with changes in the convergence velocity (i.e. acceleration), rather than with the velocity itself. If the reconstruction of Soler & Bonhomme (1990) is correct (fig. 2), such changes occurred in late Aptian (≈ 110 Ma), late Albian-early Cenomanian (≈ 100-95 Ma), late Santonian (≈ 85 Ma), late Campanian (≈ 75 Ma), late Paleocene (≈ 55 Ma) and late Eocene times (≈ 45 Ma). Except for the late Santonian, all these periods coincide with important compressional tectonic Andean phases.

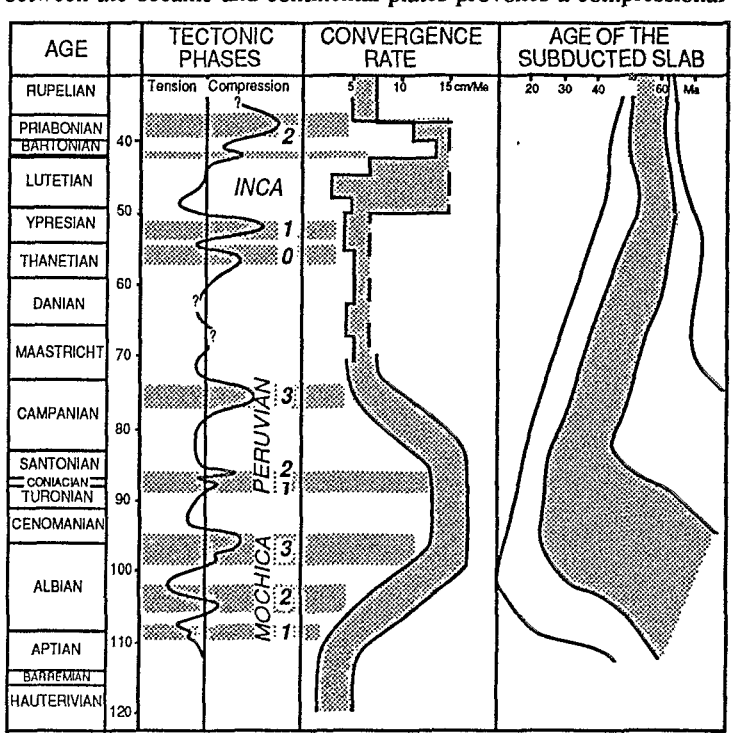

Fig. 2: Relations between tectonic phases and subduction parameters during middle Cretaceous - Paleogene times.

5. Mechanical instabilities at the trench. According to Sébrier & Soler (1991), the late Tertiary Andean compressive phases are due to mechanical instabilities in the sub-

duction zone, that make impossible the retreat of the trench to accomodate the trenchward movement of the continental plate. However, the causes of these instabilities are not clear. Further investigations would be necessary to explore the relations between such instabilities and the convergence pattern.

6. Direction of Convergence. The geometry of the geodynamic reconstruction are too poorly constrained to allow a valuable discussion for the late Cretaceous. The Inca tectonic phases (late Paleocene to late Eocene) coincide with changes in both direction and rate of convergence (Pilger 1984, Pardo-Casas & Molnar 1987), that make difficult to separate the part of each parameter. Whatever the case, a change in the convergence direction, necessarily provokes a change in the normal convergence rate, and, therefore, could have the effects assumed for the convergence acceleration. Moreover, the important changes in the convergence direction from NNE to ENE by late Paleocene-early Eocene times must have induced drastic changes in the subduction geometry. The Ecuadorian margin changed from a mainly transform to a chefly convergent regime, inducing the accretion of neighbouring terranes and the birth of new subduction zones West of them (Benitez et al. 1993). Thus changes in the convergence direction play a part both in the normal convergence rate, and in the regional subduction regimes, that could in turn influence the tectonic regime.

7. Relation convergence rates-subsidence. In Northern Peru, slow convergence correlates with low subsidence rates (130-110 Ma ?, 80-45 Ma). Conversely, the periods of high convergence velocity are coeval with periods of increased subsidence rate (110-80 Ma, and 45-35 Ma ?). This could be explain by an increased tectonic erosion of the deep continental margin (von Huene & Lallemand 1990, von Huene & Scholl 1991). However, this model only account for the subsidence of the external part of the margin, close to the subduction zone, whereas increased subsidence is observed as far as the present-day Eastern Cordillera. In contrast, these observations are consistent with the thermal model of Mitrovica et al. (1989), that assumes that a fast convergence provokes an increase of the subsidence rates in the whole continental margin. The lack of such correlations in S Peru is most probably due to the fact that compressional tectonics began earlier than in N Peru. There, tectonic uplift of the margin by crustal shortening and thickening, and overload tectonic subsidence of the foreland prevailed since Senonian times (Sempéré 1993, Jaillard 1993b).

CONCLUSIONS

According to the study of the Andean continental margin during Cretaceous-Paleogene times, long-termed compression seems to be controlled by the absolute trenchward motion of the overriding plate, and, to a lesser extent, by the young age of the subducted lithosphere. Short-lived compressional phases seem to be mainly linked to acceleration (or deceleration) in the convergence between the oceanic and continental plates, and probably to changes in the convergence direction. Periods of high and low convergence rates seem to coincide with increased and decreased subsidence ratse in the margin, respectively, and appears to be rather independant to compressional-extensional regimes.

REFERENCES

BENITEZ, S. et al., 1993, ISAG 93, Abstract, Oxford.
BERRONES, G., et al., 1993, ISAG 93, Abstract, Oxford.
BOURGOIS, J. & JANJOU, D., 1981, *C. R. Acad. Sci. Paris*, (II), **293**, 859-864, Paris.
CROSS, T.A. & PILGER, R.H., 1982, *Geol. Soc. Am. Bull.*, **93**, 545-562.
JAILLARD, E., 1993a, *in: Cretaceous tectonics in the Andes*, Earth Evol. Sci. ser., Vieweg, Wiesbaden.
JAILLARD, E., 1993b, *Bull. Soc. géol. France*, Paris, in press.
MITROVICA, J.X., BEAUMONT, C. & JARVIS, G.T., 1989, *Tectonics*, **8**, 1079-1094.
MOLNAR, P. & ATWATER, T., 1978, *Earth Planet. Sci. Lett.*, **41**, 330-340, Amsterdam.
PARDO-CASAS, F. & MOLNAR, P., 1987, *Tectonics*, **6**, 233-248.
SÉBRIER, M. & SOLER, P., 1991, *Geol. Soc. Am. Spec. Paper*, **265**, 259-278.
SEMPERE, T., 1993, *in: Cretaceous tectonics in the Andes*, Earth Evol. Sci. ser., Vieweg, Wiesbaden.
SOLER, P. & BONHOMME, M., 1990, *Geol. Soc. Am. Mem.*, **241**, 173-191.
UYEDA, S. & KANAMORI, H., 1979, *J. Geophys. Res.*, **84**, B3, 1049-1061.
von HUENE, R. & LALLEMAND, S., 1990, *Geol. Soc. Am. Bull.*, **102**, 704-720.
von HUENE, R. & SCHOLL, D.W., 1991, *Reviews of Geophysics*, **29**, 279-316.

CENOZOIC EVOLUTION OF THE COCHABAMBA AREA, BOLIVIA

L. Kennan

Department of Earth Sciences, University of Oxford.

Resumen La tectónica Andina en la Cordillera Oriental fué iniciada en el Eoceno, formando una cuenca de antepaís en el éste de la Cordillera y al oeste de la zona Subandina. Esta cuenca fue plegada en el Oligoceno superior. Las fallas transcurrentes y las cuencas de Cochabamba fueron activas desde entonces hasta el Pleistoceno superior, cuando tuvo lugar una transferencia de fallamiento al este.

Keywords: Bolivia Orocline Tectonics Shortening Basins Strike-slip

Introduction

The Cochabamba region lies in the heart of the Bolivian Orocline, the origin of which is still a matter of controversy. Studies in the area have concentrated on two principle problems: 1) identifying the relationship of regional NW-trending folds and faults to mappable unconformities at the base of widespread Cretaceous and Eocene sequences in order to assess the relative importance of Andean (post-Cretaceous) and pre-Andean structures and 2) understanding the relationship of these structures to the prominent ESE trending Cochabamba-Tapacari Lineament System (CTL) and associated basins. These studies are then put in the context of recent models for the development of the Bolivian Andes (Sempere et al., 1990, Isacks, 1988).

Structural mapping was supplemented with sedimentological studies of regionally significant sequences and localised basin fills. A programme of K-Ar dating provided the first reliable dates from many of the basins and associated valley fills. The results suggest the history of tectonism in the Eastern Cordillera is

more complex than recent published models have suggested (Sempere et al., 1990 and Sheffels, 1990).

Regional folding and faulting

The strong NW-SE tectonic grain of the region consists of c.5 km wavelength, mainly upright, folds, locally with a weak slaty axial-planar cleavage. These are transected by steep faults with both reverse and strike-slip displacements. A very angular post-lower Permian, pre-Cretaceous unconformity can be mapped throughout the region. The observed cleavages clearly underlie this unconformity. In addition all observed overturning is a result of reorientation of earlier folds on the limbs of larger-scale post-Cretaceous folds.

In many cases the angularity of the unconformity prevented further folding. Flexural-slip folds locked at limb dips of 50°-60° were prevented form further homogenous flattening because their post-Cretaceous depth of burial was insufficient to cause cleavage formation. Folding of Cretaceous and younger sequences is largely confined to areas where the unconformity is low angle or where competent units are not present.

Present estimates of shortening in the region (Sheffels, 1990) are likely to be overestimates because cross-section restoration failed to take this unconformity into account.

In the core of the Morochata syncline there is a conformable 500 m transition from fine-grained Cretaceous and Palaeocene facies into coarse conglomerates of likely Eocene age. The same transition can be traced throughout the eastern part of the Cordillera as far south as the Camargo syncline, near the Argentinian border. Sedimentological studies indicate the conglomerates were shed from a mountain front not more than 50 kms to the southwest in what is now in the westerm Eastern Cordillera.

West of Cochabamba the structures of the source area consist of broad folds of Devonian sandstones overlain by Mesozoic and Cretaceous strata. These are preserved locally in the footwalls of east verging high angle reverse faults (eg at Sayari). Nowhere are Tertiary strata preserved. East of the Sayari fault the coarse conglomerates can be found lying on a few metres of preserved Cretaceous sandstones and basalt indicating this area was at or near the uplifting mountain front and was eroding, in contrast to the deposition occurring to the east. In the western Subandes a late-Cretaceous to late Oligocene hiatus indicates this foreland basin was relatively narrow.

Between the Eocene and the late-Oligocene deformation advanced eastwards deforming the Eocene foreland basin. This advance can possibly be

linked to the initiation of deposition of the late Oligocene Petaca formation in the Subandes. The low rate of deposition of this formation (<25m/Ma, Sanjinés and Jiménez, 1975) suggests there was not a marked mountain front.

Faulting and basin formation in the CTL

The timing of basin formation and associated faulting in the CTL is key to constructing a kinematic model of the bend region.

The first movements on the prominent ESE fault system possibly coincide with the mountain front advance described above. A series of short wavelength en echelon folds with associated sinistral faults formed during gentle sinistral transpression on the Tapacari fault system. These folds are overlain by the deposits of the Parotani basin, a shallow half-graben formed by transtensive reactivation of the Tapacari fault. Tuffs in the basin have been dated at 20 Ma.

The basin was later subjected to phases of sinistral transpression and transtension, the latter possibly coinciding with the earliest sinistral-normal faulting seen on faults south of the Tunari lineament. Faulting along the Viloma fault clearly predates regional erosion surfaces which were dissected by 500 m by about 7 Ma.

Movements on the Tunari fault, which forms the prominent 2000 m scarp along the north sides of the Cochabamba and Sacaba basins are complex. Displacements on the fault's continuation west of Cochabamba are small, totalling about 5 kms sinistral and 1 km throw down to the south. This pre-dates prominent pediments cut into the scarpline between 3200 and 3800 m. Offsets of regional folds indicate the normal faulting that formed the basins was not accompanied by significant strike-slip.

Conglomerates around the margins of the Sacaba basin onlapped the fault scarps to about 3100 m and pass into fine lacustrine facies in the centre of the basin. Tuffs and fossils indicate an age of 2.2 Ma for these sediments suggesting the Sacaba basin started to form in the late Miocene and that transpressional folding and faulting in the basin is very young. Younger fault movements, forming prominent fresh faceted spurs, dropped the floor of the Cochabamba basin at least 500 m in the Pleistocene resulting in the dissection of the Sacaba basin and the accumulation of a thick Quaternary fill in the Cochabamba basin which is not yet dissected.

Although the area is moderately seismically active there are almost no post-glacial fault breaks. Very young sinistral breaks have been identified along the

line of the NW-trending Colomi fault to the east. If motion on this fault is as much as 5mm/yr then the CTL west of the Colomi fault would become inactive. Partitioning of strike-slip between the narrow northern and wide southern Subandes and of strike-slip and extension required to maintain compatibility between the two diverging thrust belts could be taken up entirely within the Subandes.

Conclusions

1) Pre-Cretaceous deformation is more important than thought in the Cochabamba region. There is still a marked deficit between observable shortening and that required by models explaining crustal thickening and orocline formation purely in terms of shortening.

2) A proto-Eastern Cordillera and foreland basin developed in the Eocene, coincident with eastward thrusting in Chile, indicating that a double Cordillera structure developed early in the uplift of the Andes.

3) Displacements on the CTL are smaller, and have a longer history, than thought. The principle role was probably the accommodation of arc-tangential extension, with modest sinistral slip. Transpressive and transtensive phases probably represent changes in the balance between tangential and radial stress in the bend reflecting stick/slip propagation in the Subandes. The CTL west of Cochabamba is presently inactive. Significant partitioning of thrusting and strike-slip is now taking place to the east.

References

Isacks, B.L. 1988. Journal of Geophysical Research. 93B. 3211-3231.
Sanjinés, G. and Jiménez, F. 1976. Revista Tecnica de Y.P.F.B. 4. 147-158.
Sempere, Th. et al. 1990. Geology. 18. 946-949.
Sheffels, B.M. 1990. Geology. 18. 812-815.

BASEMENT-INVOLVED THRUSTING IN THE EASTERN CORDILLERA-SUBANDEAN TRANSITION ZONE, SOUTHERN BOLIVIA: EVIDENCE FROM CROSS-SECTION BALANCING AND GRAVIMETRIC DATA

Jonas KLEY(1) and Alfredo H. GANGUI(1)

(1) Institut für Geologie, Geophysik und Geoinformatik, Freie Universität Berlin, Malteserstr. 74-100, W-1000 Berlin 46, Germany

RESUMEN

Mediante la utilización de perfiles balanceados junto con modelado gravimétrico bidimensional se interpreta la existencia de "basamento cristalino" involucrado en los corrimientos que constituyen la zona de transición entre la Cordillera Oriental y las Sierras Subandinas del Sur de Bolivia, lo que permite acotar el acortamiento producido en las Sierras Subandinas y sector oriental de la Cordillera Oriental a unos 140 km.

KEY WORDS: Southern Bolivia, Crustal shortening, Balanced cross-sections, Gravimetrical data

INTRODUCTION

The exceptionally thick continental crust of the central Andes was initially believed to have been built mainly by addition of mantle-derived magmas from the subduction zone (e.g.James, 1971). Meanwhile, tectonic shortening is envisaged as the main process responsable for crustal thickening, probably with some minor magmatic contribution. Estimates of shortening during the Andean orogeny have been published by a number of authors (e.g. Allmendinger et al. 1983, Roeder 1988; Baby et al. 1989). However, attention has so far mainly focussed on the external part of the thrust belt at the eastern slope of the Andes (the Subandean Ranges). This contribution deals with a cross-section at 21°15 S which includes the internal belt (the eastern part of the Eastern Cordillera) where basement becomes involved into thrusting. Especially, gravimetrical data are shown to constrain the structural interpretation and, consequently, shortening values.

GEOLOGICAL SETTING

In southern Bolivia north of 21°45 S, the Eastern Andean thrust belt can be subdivided into three strike-parallel belts. These are, from east to west: (1) The Subandean Ranges, which form a classical thrust belt. Its basal décollement is not located at the top of crystalline basement, but lies within the sedimentary cover in a Silurian shale unit. Outcropping rocks range from Devonian to Neogene in age. Andean-age shortening which started in the late Miocene is on the order of 80-100 km. (2) A tightly folded and thrust transition zone, made up mainly of Silurian and Devonian rocks. No units younger than Triassic are preserved. (3) The Eastern Cordillera proper, with Ordovician to Precambrian rocks surfacing in a large

anticlinorium. Cretaceous sediments unconformably overlying the folded and foliated Ordovician document a pre-Cretaceous orogenic event.

GRAVIMETRIC DATA

Gravimetric data measured by the Bolivian Instituto Geográfico Militar (IGM 1974) were tied to the IGSN 71 point in La Paz, Bolivia (Strunk 1990). Correction for topographic effects was based on the digital elevation model of Isacks (1988) and detailed topographic maps of the IGM, using the algorithm by Ehrismann & Lettau (1971). In calculating the Bouguer anomaly, a reduction density of 2.67 g/cm^3 was used with sea level as reference datum. For the 2D gravimetric modeling we used an interactive computer program based on the algorithm by Won & Bevis (1987) developed by the gravity working group at the FU Berlin.

BALANCED CROSS-SECTION AND GRAVIMETRIC INTERPRETATION

The thin-skinned tectonic style of the Subandean Ranges is evidenced by the existence of a gently west-dipping "regional" which can be traced from the foreland throughout the Subandean Ranges up to the westernmost ocurrences of Neogene strata. In the transition zone, the elevations of stratigraphic horizons in the synclines again define a subhorizontal regional level, thus suggesting the existence of a shallow décollement at the base of the structures. This surface, however, is raised by almost 10 km relative to the basal décollement of the Subandean Ranges. On the other hand, the undeformed sub-décollement section (the "basement") of the Subandean Ranges from which the post-Ordovician sedimentary cover has been sheared off and thrust eastward must extend westward under the whole of the transition zone, as can be estimated from the shortening documented in the Subandean Ranges. The space between this "bottom" and the basal décollement of the transition zone might be filled by a thick thrust sheet involving the basement (Ordovician to Precambrian) or, alternatively, by imbrications of the same Silurian to Neogene sequence that builds up the Subandean Ranges. Cross-sections based on either assumption give shortening values about twice as high in the latter case (>300 km vs. ca. 140 km).
Gravimetric data in the Subandean Ranges show several small highs and lows which correlate with Paleozoic sediments in the cores of fold-thrust structures and the thick low-density Neogene sediments of their backlimbs, respectively (Fig. 1). In contrast, the transition zone coincides with a marked gravity high of longer wavelength. In the Bouguer residual gravity field, this feature stands out as a positive anomaly of more than +10 mGal. Hence, the latter of the two structural models considered above which predicts an accumulation of low-density sedimentary rocks in the subsurface of the transition zone can be discarded. "Basement" rocks appear to be present in buried thrust sheets immediately west of the western limit of the Subanden Ranges, although the easternmost outcrops of these rocks lie some 50 km further west. Detailed modelling of the gravity curve furthermore suggests that the basement of the transition zone is lithologically quite different from the basement exposed in the Eastern Cordillera farther west and south (Puncoviscana Fm. in northwestern Argentina), and possibly comprises intermediate to basic crystalline rocks. We can only speculate on the exact nature and origin of these rocks, which could be more basic equivalents of the mid-Cambrian Cañaní granitoids of northwestern Argentina but which might as well be much younger. (The latest magmatic events of the region are the effusion of the Mesozoic Entre Ríos Basalt of uncertain age and the intrusion of a granitoid pluton in the Eastern Cordillera close to the Argentine border at the (?) Jurassic-Cretaceous boundary).

Fig. 1: Above: 2D-Gravity model of a cross-section through the Subandean Ranges, Transition Zone and eastern margin of the Eastern Cordillera at 21°15 S. Numbers are densities in g/cm^3. Boundary between 2.99 and 3.16 corresponds to Moho as derived from refraction seismic data (Baldzuhn 1993).
Below: Balanced cross-section. Surface geology of the Subandean Ranges according to unpublished data from YPFB. Deep imbricates of the transition zone are shown with a thick Lower Palaeozoic sedimentary sequence as would be estimated from surface geology, but should contain high density material according to gravity data.

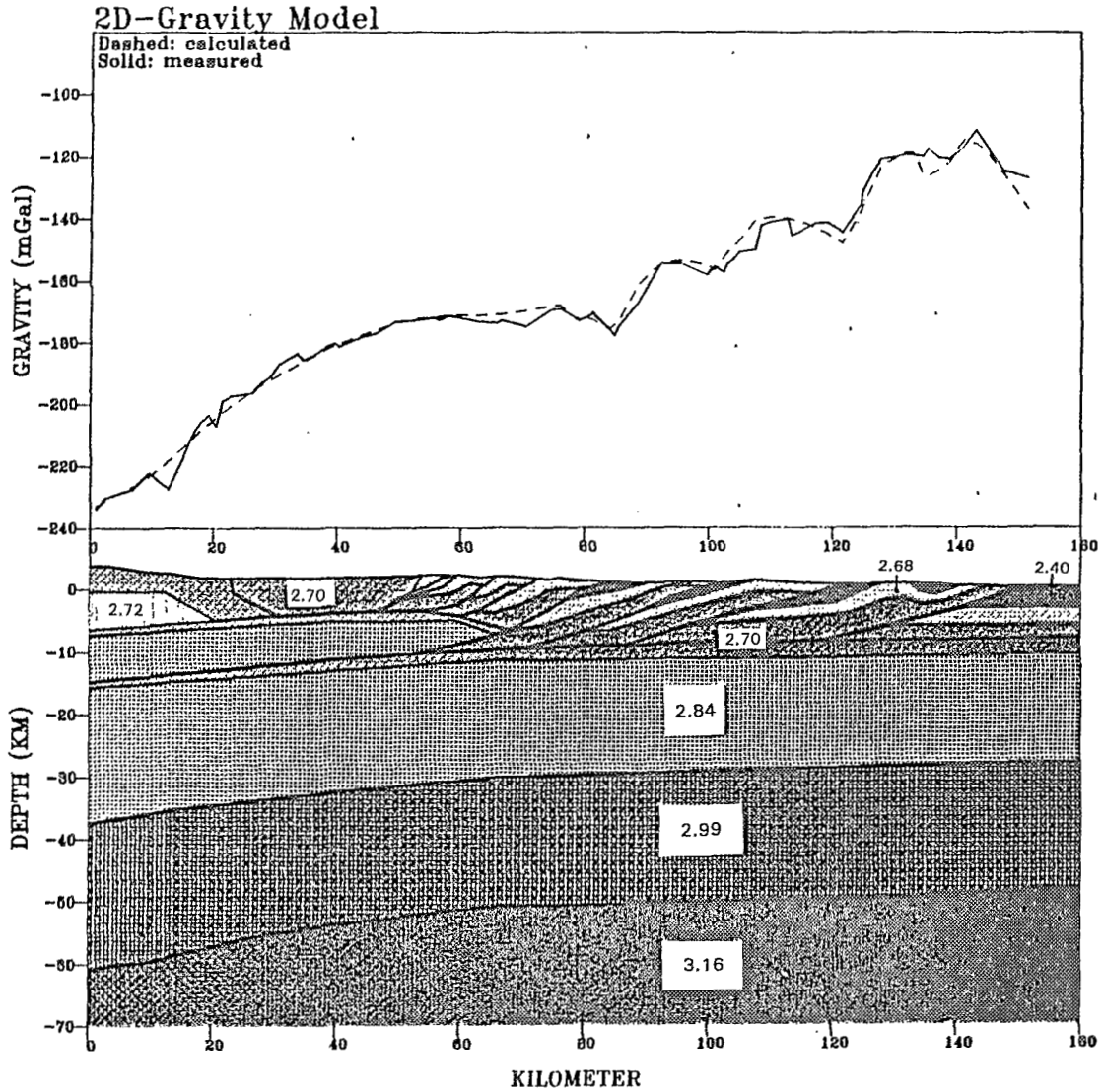
2D-Gravity Model
Dashed: calculated
Solid: measured
GRAVITY (mGal)
DEPTH (KM)
KILOMETER
2.72
2.70
2.68
2.40
2.70
2.84
2.99
3.16

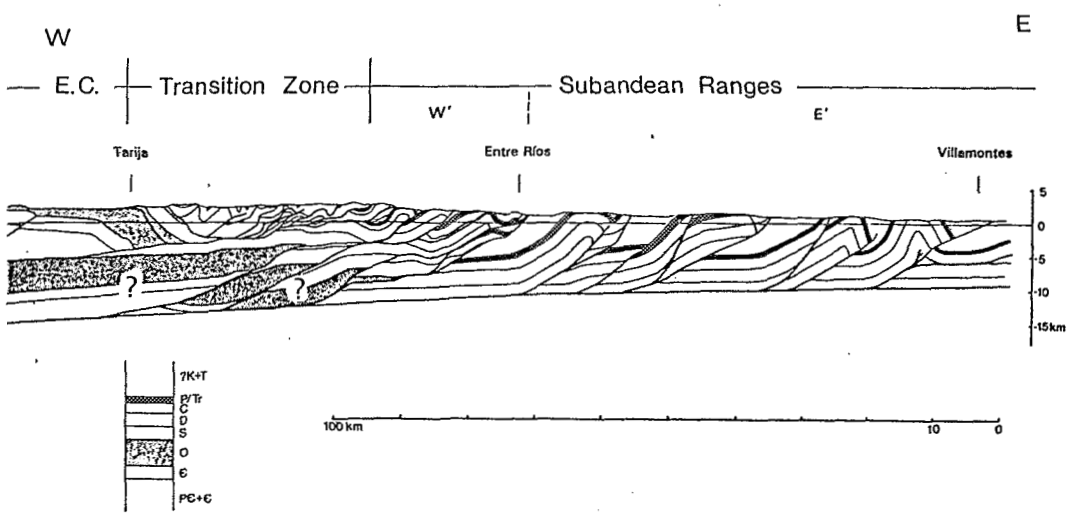
W
E
E.C.
Transition Zone
Subandean Ranges
W'
E'
Tarija
Entre Ríos
Villamontes
?
?
5
0
-5
-10
-15km
7K+T
P/Tr
C
D
S
O
Є
PC+C
100 km
10
0

CONCLUSIONS

Gravimetrical data demonstrate that basement rocks become involved into thrusting immediately west of the Subandean Ranges. This limits the shortening value that can be deduced from balanced sections for the region from the undeformed foreland to the eastern part of the Eastern Cordillera to about 140 km. As these account for only about half of the shortening required to thicken the Andean crust to its present state, considerable shortening should have occured in areas farther west where extensive thrusting is often not evident at first sight. Besides the southern Altiplano., for which substantial shortening has been described (Baby et al. 1990), these regions may include the western part of the eastern Cordillera as well as areas which are now covered by Neogene to Recent volcanics.

REFERENCES

ALLMENDINGER, R.W., RAMOS, V.A., JORDAN, T. E., PALMA, M. & ISACKS, B.L. (1983): Paleogeography and Andean structural geometry, Northwest Argentina.- Tectonics, 2 (1), 1-16.

BABY, P., HERAIL, G., LOPEZ, J.M., OLLER, J., PAREJA, J., SEMPERE, T. & TUFIÑO D (1989): Structure de la Zone Subandine de Bolivie: influence de la géométrie des séries sédimentaires antéorogéniques sur la propagation des chevauchements.- C. R. Acad. Sci. Paris, **309**, Série II: 1717-1722

BABY, P., T. SEMPERE, J. OLLER, L. BARRIOS, G. HERAIL, R. MAROCCO (1990): Un bassin en compression d'âge oligo-miocène dans le sud de l'Altiplano bolivien.-C.R. Acad. Sci. Paris, **311**, Série II: 341-347.

BALDZUHN, S. (1993): Tiefenseismische Untersuchungen in der Ostkordillere und im Subandin Südboliviens. Diplomarbeit FU Berlin, unpublished.

EHRISMANN, W. & LETTAU, O (1971): Topographische Reduktion von Scweremessungen in der näheren und weiteren Stationsumgebung mit Digitalrechnern.- Arch. Met. Geoph. Biokl., Ser. A, 20, 383-396.

Instituto Geográfico Militar (IGM) de Bolivia (1974): Mediciones gravimétricas en Bolivia.- Departamento Geofísico, 165 p., La Paz, Bolivia.

ISACKS, B.L. (1988): Uplift of the Central Andean Plateau and Bending of the Bolivian Orocline.- J. Geophys. Res., **93** (B4), 3211-3231.

JAMES, D.E. (1971): Plate Tectonic Model for the Evolution of the Central Andes.- Geological Society of America Bulletin, **82**, 3325-3346.

ROEDER, D.(1988): Andean-age structure of Eastern Cordillera (Province of La Paz, Bolivia).-Tectonics, 7 (1), 23-39.

STRUNK, S. (1990): Analyse und Interpretation des Schwerefeldes des aktiven Kontinentalrandes der zentralen Anden (20°-26°S).-Berl. geowiss. Abh., (B), **17**, 1-135.

WON, I.J. & BEVIS, M. (1987): Computing the gravitational and magnetic anomalies due to a polygon: algorithms and FORTRAN subroutines.- Geophysics, **52** (2), 232-238.

TECTONIC EVOLUTION OF THE CENTRAL ANDES SINCE THE CRETACEOUS

Simon LAMB, Lorcan KENNAN, Leonore HOKE

Department of Earth Sciences, Parks Road, Oxford, OX1 3PR, UK.

RESUMEN

Los Andes Centrales de Bolivia y Norte de Chile forman parte de un límite de placas entre Sudamérica continental y la placa subductante de Nazca. Desde el Cretácico, esta región ha sido solevantada hasta formar la parte más ancha de los Andes. La deformación ha sido contínua durante este período, aunque su localización ha cambiado marcadamente. Se incluye un esquema de la evolución terciaria de los Andes de Bolivia, basada en un estudio de las secuencias sedimentarias cretácicas y terciarias, y en datos paleomagnéticos

KEY WORDS: Central Andes, tectonic evolution, palaeomagnetism.

INTRODUCTION

The Central Andes of Bolivia and northern Chile form part of the plate-boundary zone between the continental South American and subducting oceanic Nazca plates. Since the Cretaceous, this region has been uplifted to form the widest part of the Andes, reaching an average elevation of ca. 4000m in a region 700 km wide. Though deformation has occurred throughout this period, its locus has changed markedly. The following description briefly outlines the Cretaceous and Tertiary evolution of the Bolivian Andes, based on extensive field work, K-Ar dating (Kennan et al. in preparation) and palaeomagnetic studies, as well as information from unpublished oil company reports and seismic sections. The Central Andes is viewed as a continuously growing mountain belt, rather than the product of discrete tectonic events.

PRE-CRETACEOUS AND CRETACEOUS DEFORMATION

There is a marked angular unconformity at the base of the Cretaceous. Open to tight folding, with limb dips up to 50°, a weak axial planar cleavage and extensive quartz veining are found in Palaeozoic flysch deposits beneath the Cretaceous throughout the Cordillera Oriental which are truncated by basal Cretaceous conglomerates. At least 5 km of pre-Cretaceous rocks were stripped off by erosion prior to Cretaceous deposition. In places the pre-Cretaceous deformation appears to have influenced the style and orientation of Tertiary structures.

Thin Cretaceous sequences (usually <1 km) of lacustrine and possibly marine deposits are preserved throughout the Bolivian Andes, and demonstrate that most of the present region of the Andes was at or near sea level at that time. Local mafic volcanism, including pillow lavas, suggest a small amount of extension concomitant with subsidence of the Cretaceous basin. Interestingly, the depocentre of the Cretaceous basin coincides with the region of most intense pre-Cretaceous shortening. The active plate margin at this time was a relatively narrow zone much further west, with a wide back arc region of slow subsidence and limited extension several hundred kilometres wide.

EARLY TERTIARY DEFORMATION

Cretaceous sandstones, often containing fossilised dinosaur tracks, pass conformably into thick red-bed sequences. For instance, in the Camargo area of southern Bolivia, this transition can be traced along strike for over a hundred kilometres and is perfectly conformable. The basal part of the red-bed sequence consists of red siltstones with thin medium sandstone interbeds. However, within 150 m stratigraphically of the base of the sequence, conglomerates and thick coarse sandstones are well developed.

In both the Altiplano region and Cordillera Oriental, the basal few hundred metres of the Tertiary red-bed sequence shows a large dispersion in sediment transport directions, but then these become essentially unidirectional further up the sequence. This is interpreted as a transition from a highly meandering fluvial environment in a region of low topographic gradient, to a more uniform flow regime down a steeper gradient, representing the onset of deformation in this part of the Andes in the earliest Tertiary.

The uplifting regions can be defined with some precision from the pattern of sediment transport directions. The centre of the Cretaceous basin was inverted, so that the deepest part formed a narrow uplifting region in the earliest Tertiary, which shed sediment both to the east and west. This proto-cordillera developed as a narrow isolated range in what is today the western part of the Cordillera Oriental, separated from the active arc by a region several hundred kilometres wide. The intervening region formed a large intermontane basin which is now preserved in the Altiplano region of the Bolivian Andes, where up to 5 km of Early Tertiary continental sediments were deposited.

MIDDLE AND LATE TERTIARY DEFORMATION

Underformed Early Miocene ignimbrites show that north of the latitude 22°S, significant shortening deformation in northern Chile ceased in the Middle Tertiary. Deposition also continued in the Altiplano basin to the east, which received sediment both from the west and east. The distribution of Oligo-Miocene sedimentary sequences in the Bolivian Cordillera Oriental show that many local structural basins formed at this time, which locally sit with angular unconformity on older sequences. Shortening here also extended much further east than in the Early Tertiary. However, the nature of the eastern front of the Andes is not understood, but there is no evidence for a region of intense Middle Tertiary shortening similar to the present SubAndean zone. However, sedimentation in the SubAndean zone suggests a foreland basin began to form at this time. Shortening throughout the Cordillera Oriental was accommodated by km to 10's km scale folding and relatively high angle reverse faulting, with changes in vergence. No evidence for nappe-style deformation has been observed in the Cordillera Oriental. The best estimate of Tertiary crustal shortening comes from crustal thickness balancing, as much of the structure in the Cordillera Oriental is pre-Cretaceous in age.

In the Late Miocene, during a period of a few million years, the Altiplano basin started to shorten internally. Essentially undeformed Late Miocene to Pliocene sedimentary basins, which are found throughout the Cordillera Oriental, suggest that shortening in the Cordillera Oriental, except for local conjugate strike-slip deformation, effectively ceased. However, in the Pliocene, the locus of deformation again shifted to the frontal parts of the Andes in the east, in what is today the Subandean zone. This forms an active thin-skinned fold and thrust belt which has accommodated ca. 100 km of shortening. Also, no evidence for either active normal faulting or significant Plio-Pleistocene extension has been observed in the Bolivian Altiplano.

The present drainage pattern in the Cordillera Oriental, including deep valleys with a vertical relief reaching several kilometres, is the product of erosion during the last 3 Ma. Prior to that, the topography in the Cordillera Oriental was relatively subdued with the development of regional peneplains.

TECTONIC ROTATIONS

Deformation since the middle Miocene (ca. 15 Ma) has been responsible for substantial rotations about a vertical axis in the Central Andes, relative to the South American plate. Palaeomagnetic work has defined three principal zones which can be characterised by particular rotations about a vertical axis.

In the north, the Bolivian Andes is characterised by small anticlockwise rotations between 0 and 10°, observed in Cretaceous to Late Miocene sediments and volcanics, right across the width of the Andes. Further south, a zone can be defined, also extending right across the Andes, in which clockwise rotations between 0 and 10° are typical, observed in Cretaceous to Early Miocene sediments. And even further south, there is a zone, which again extends right across the width of the Andes, characterised by clockwise rotations between 20° and 30°, observed in Cretaceous to Late Miocene sediments and volcanics. These three principal zones can be ascribed to along strike gradients in the shortening in the Subandean zone, which has resulted in 'bending' of almost the entire width of the Central Andes since the Late Miocene.

In the Cochabamba area, in a region ca. 100 km by 100 km, local clockwise rotations, between 20° and 30°, have been detected in Cretaceous sediments, within the general area of anticlockwise rotations. These are related to block rotation accommodated by sinistral strike-slip on ESE-trending faults, active in the Miocene-Pliocene and accommodating the divergence in shortening round the pronounced bend in the Bolivian Andes. In addition, a local zone of large anticlockwise rotations, up to ca. 50°, is found in Middle Miocene rocks at the southern end of Lake Titicaca. This may be related to along strike sinistral shear in the northern Altiplano, which is partly accommodating the component of plate motion parallel to the trend of the Andes. In general, zones of tectonic rotation can be correlated with the general structural trend. However, regions of anomalous strike orientation, for instance in the Otavi syncline near Potosi, are not always associated with significant Cenozoic tectonic rotation and probably reflect the reactivation of pre-Cretaceous trends which differ from prevailing Andean trends.

NEOGENE TO PRESENT TECTONIC EVOLUTION AND STRESS FIELD IN ECUADOR

Alain LAVENU (1), Frédéric EGO (2), Christophe NOBLET (3), Thierry WINTER (4)

(1) ORSTOM, 213 rue La Fayette, 75480 Paris cedex 10, France and Laboratoire de Géodynamique et Modélisation des Bassins Sédimentaires, UPPA, Avenue de l'Université, 64000 Pau, France.
(2) Laboratoire de Géologie Dynamique Interne, URA CNRS, Géophysique et Géodynamique Interne, Université de Paris-Sud, Centre d'Orsay, Bat. 509, 91405 Orsay cedex, France.
(3) BHP Minerals, 550 California street, San Francisco, California 94104-1020, USA.
(4) Laboratoire de Tectonique et Mécanique de la Lithosphère, IPGP, 4 place Jussieu, 75252 Paris cedex 05, France.

Résumé : L'analyse de la microtectonique, celle des déformations synsédimentaires et celle de la morphologie des bassins néogènes et quaternaires de la zone intracordillèraine des Andes d'Equateur montrent une persistence de la tectonique compressive NNE-SSW à E-W du Miocène inférieur à l'Actuel. Des modifications locales du champ de contrainte peuvent être dues à des contitions particulières.

Key Words : Synsedimentary deformations, stress, Neogene, Andes, Ecuador.

INTRODUCTION

Strong continental sedimentation had developed during the Neogene (Bristow, 1973; Baldock, 1982), in basins formed along major crustal faults in the Ecuadorian Andes. This concerns particularly the basins of Cuenca, Giron, Nabon, Loja, Malacatos and Zumba, in south Ecuador and the Interandean Depression (IAD) with the Quaternary basins of Quito and Latacunga-Ambato in central and northern Ecuador (Figure).These basins are located between the Eastern Cordillera composed essentially of Paleozoic and Mesozoic rocks and the Western Cordillera represented by a series of Cretaceous (and some Cenozoic) volcanic rocks. In southern Ecuador, the Neogene basins are limited by two families of N-S and NE-SW trending faults. In central Ecuador, the Interandean Depression is characterized by an uppermost Pliocene – Quaternary basin, developed alongside great regional N-S faults.

STRATIGRAPHY

In south Ecuador, the Tertiary rocks can be regionally grouped into three superposed lithostratigraphic units (Noblet et al., 1988).

- a lower, essentially volcanic unit (U1, Saraguro Fm.) which comprises the substratum of the basins, and consists of intermediate and acidic lava and pyroclastic deposits (35.3 to 26.8 Ma; 1000 m thick).

- an intermediate sedimentary unit (U2) corresponding to most of the infill. This unit lies in discordance with unit U1 and correspond to the Neogene infill of the basins (22 to 8 Ma; 1500 to 4000 m thick). The unit can be divided into two megasequences: M1 and M2.

-an upper volcano-sedimentary unit (U3, Llacao and Tarqui Fm.) which disconformably overlies the previous units.

The IAD infilling consist of Pliocene to Recent volcaniclastic continental, fluviatile and lacustrine sediments. In recent studies we have shown that these deposits consist of four distinct sedimentological units (Lavenu et al., 1992).

- The oldest unit, U1, is essentially composed of lahars, pyroclastic levels, interstratified andesitic flows (400 m thick; 1.4 to 1.8 Ma).

- Unit U2 forms a progressive unconformity over the previous unit (fluvial and lacustrine deposits, 50 to 80 m thick).

These two units represent the Latacunga Formation.

- Unit U3 lies unconformably over the previous units (Chalupas Fm.; 1.2 Ma; >50 m thick).

- Unit U4 is composed of recent pyroclastic tuffs (Cangagua Formation).

NEOGENE SOUTH ECUADORIAN BASINS

Synsedimentary folding deformations affected the basin sediments (Lavenu and Noblet, 1989).

The M1 megasequence deposits (lower Miocene) display sedimentary wedges which indicate the presence of a normal component in the N20-N40°E faults during sedimentation. An additional folding deformation corresponds to a NNE-SSW shortening direction, perpendicular to the NW-SE tensional direction. This tensional deformation characterizes the basin's opening.

In megasequence M2 a synsedimentary folding deformation with a N60°E trending shortening direction affects the lower to middle Miocene deposits. The development of these folds is kinematically compatible with a right-lateral component of the movement along the N20°E faults.

The upper levels of the megasequence M2 (upper Miocene) show a series of progressive unconformities related to synsedimentary N-S folding with a mean E-W trending shortening.

A microtectonic study evidences an ongoing compressive stress regime during at least the Miocene period.

Lower sediments (M1) and substratum (U1) of the basins display a first direction of the major stress component $\sigma 1$ during lower Miocene, between N23°E and N64°E. Then, in the deposits of middle to upper Miocene (M2) and substratum, the direction of major stress component $\sigma 1$ is between N71°E to N107°E. A relative chronology of the striations is coherent with a NE-SW compression followed by an E-W compression.

PLIOCENE-QUATERNARY INTERANDEAN BASINS

The IAD is characterized by a large late Pliocene - Quaternary basin situated between N-S reverse basement faults.The formation of the IAD probably began in the Upper Miocene. An E-W shortening drives the reverse faults since upper Pliocene.The shortening became more pronounced during and after deposition of unit U1 (Latacunga Fm.). Analysis of folds and flexures demonstrates that at least between 1.7 and 1.2 Ma, the southern part of the IAD was subject to major shortening along an E-W direction. This deformation began while U1 sediments were being deposited, and continued and intensified during the deposition of U2. The morphology (deviation of rivers, landslides etc...) reveals the continuation of the shortening during the recent Quaternary. The seismicity and focus mechanisms highlight the present-day persistence of the E-W shortening. All of these arguments are in favor of a "push-down" basin interpretation.

CONCLUSION

From a sequential analysis of infill deposits in the South Ecuadorian basins, a phase of deepening of the lower Miocene basins, followed by infilling in the middle to upper Miocene has evidenced. Synsedimentary deformations affected the entire Miocene. They reveal a normal component on N20°E-N40°E trending faults during M1 and compressive tectonics during M2. Shortening directions deduced from fold axes of synsedimentary folds

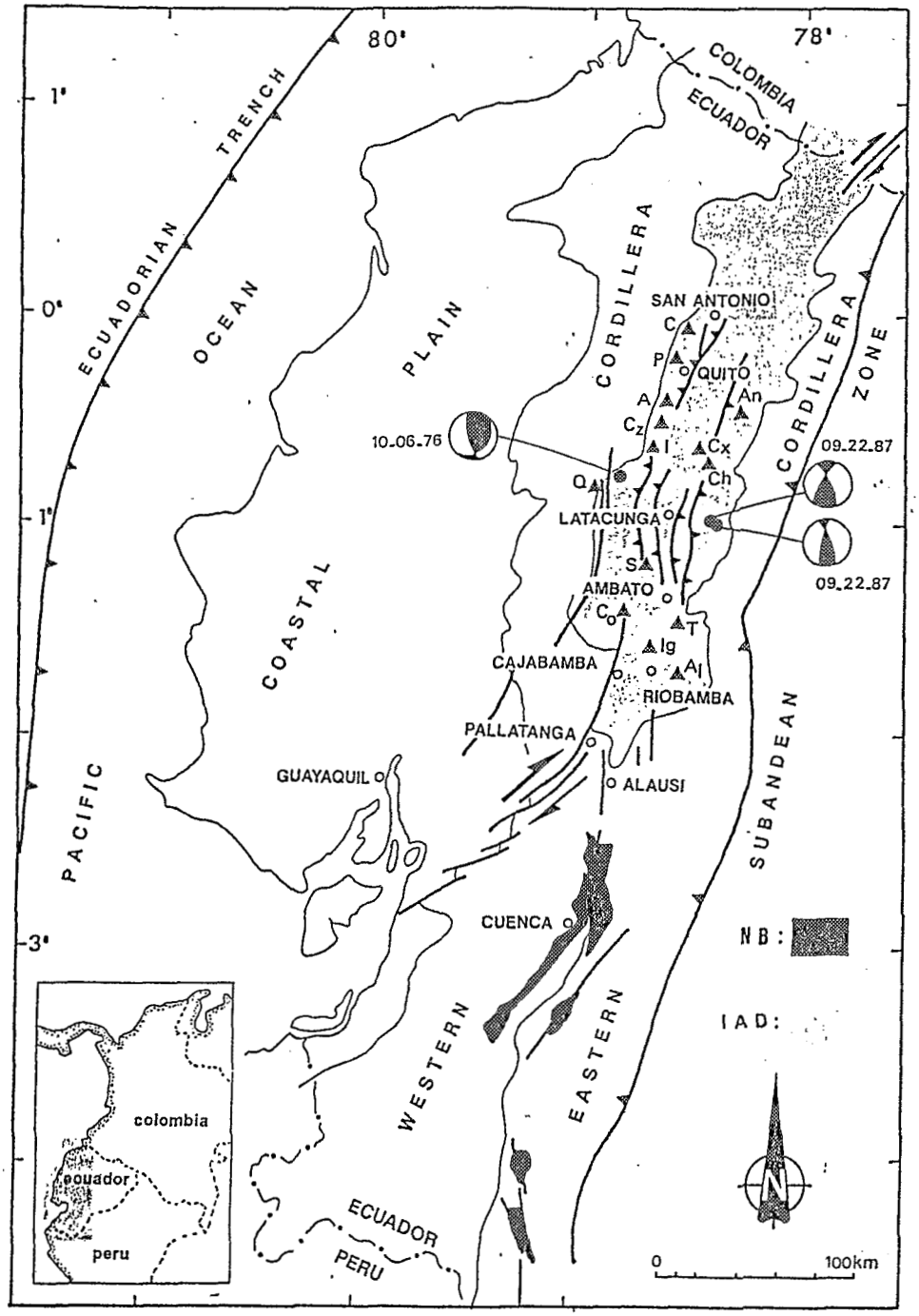

Figure: Schematic tectonic map of the mean recent and active faults. Location of the Neogene basins.

IAD: Interandean Depression; NB: Neogene basins; Black triangles, volcanoes: A= Atacazo, Al= Altar, C= Casitagua, Co= Chimborazo, Cx= Cotopaxi, Cz= Corazon, I= Iliniza, Ig= Igualata, Q= Quilotoa, P= Pichincha, S= Sagoatoa, T= Tungurahua. Focal mechanism solutions of three shallow-focus (>30 km) earthquakes (lower hemisphere projection). P axis in white quadrant. At the present time Andes of central Ecuador are affected by an E-W trending shortening.

vary between N60°E at the base of M2 to N80°E-N130°E at the top of M2. Microtectonic analysis has evidenced a state of compressive stress with σ1 following a NNE-SSW direction in the lower Miocene. The lower Miocene deepening is the consequence of right-lateral strike-slip movements along N-S faults and right-lateral-normal movements along N20°E-N40°E faults. The stress field in the middle and upper Miocene is characterized by a major stress σ1 approximately E-W. Results of the microtectonic analysis, the sedimentological study and the analysis of synsedimentary deformations, suggest that the basin infilling is due to movements with a strong reverse component along N-S and N20°E faults.

The E-W shortening observed in the IAD is kinematically compatible with the present right-lateral kinematics (with a slight reverse component) of the Pallatanga Fault (Winter and Lavenu, 1989; Winter et al., in press). It is also compatible with the pull-apart basin interpretation given for the Gulf of Guayaquil and related to right-lateral movements since the Miocene along the D-G M fault.

The central part of the Ecuadorian IAD between Quito and Ambato is characterized by structures (folds, flexures, reverse faults) which are due to E-W shortening.

To the south of this area, active Quaternary structures have reverse-right strike slip movements, of NE-SW direction which are also due to the E-W compression (Pallatanga Fault).

To the north of this area, in the south of Colombia, a system of active NE-SW right-lateral faults is also due to E-W compression.

The behavior of the Quito-Ambato zone can be illustrated as a compressive N-S relay in a system of large right strike-slip structures.

So, sedimentological, synsedimentary folding deformation and microtectonic analyses show a persistent and continuous compressional stress regime in the Interandean basins of Ecuador, from Miocene times to Present-day.

REFERENCES

BALDOCK J.W. 1982. Geology of Ecuador: Explanary Bulletin of the National Geological Map of the Republic of Ecuador. Esc. 1:1 000 000, Min. Rec. Nat. Energ., Quito, 70 p.

BRISTOW C.R. 1973. Guide to the geology of the Cuenca Basin, southern Ecuador. Ecuadorian Geological and Geophysical Society, 54 p.

LAVENU A. and NOBLET C. 1989. Synsedimentary tectonic control of Andean Intermontane strike-slip basins of South Ecuador (South America). International Symposium on Intermontane Basins: Geology and Resources: 306-317, Chiang Mai, Thailand.

LAVENU A., NOBLET C., BONHOMME M.G., EGUEZ A., DUGAS F., and VIVIER G. 1992 New K/Ar age dates of Neogene and Quaternary volcanic rocks from the Ecuadorian Andes : Implications for the relationships between sedimentation, volcanism, and tectonics. J. of S. Amer. Earth Sci., 5, 3/4 : 309-320.

NOBLET Ch., LAVENU A. and SCHNEIDER F. 1988. Etude géodynamique d'un bassin intramontagneux tertiaire sur décrochements dans les Andes du sud de l'Equateur: l'exemple du bassin de Cuenca. Géodynamique, 3, (1-2): 117-138.

WINTER T., AVOUAC J.P., and LAVENU A. 1993. Holocene kinematics of the Pallatanga strike-slip fault (Central Ecuador) from topographic measurements of displaced morphological features. Geophys. J. Intern. (in press).

WINTER Th. and LAVENU A. 1989b. Morphological and microtectonic evidence for a major active right lateral strike-slip fault across central Ecuador (South America).Annales Tectonicae, III, 2: 123-139.

THE GEOTECTONIC EVOLUTION OF ECUADOR IN THE PHANEROZOIC

Martin LITHERLAND[1], John A ASPDEN[1] and Arturo EGUEZ[2]

1. International Division, British Geological Survey, Keyworth, Nottingham, NG12 5GG, UK.
2. Dept de Geologia, Escuela Politecnica Nacional, Apartado 17-1-2759, Quito Ecuador

RESUMEN: Durante el Cretacico se acrecionaron terrenos continentales paleozoicos y terrenos oceanicos jurasicos y cretacicos. Estructuras mas tardes, relacionados al levantiamento de los Andes, puede relacionarse a la reactivacion de las fallas de acrecion.

KEY WORDS: Ecuador, terrane, accretion

INTRODUCTION

Studies of the metamorphic rocks of the Ecuadorian Andes by the British Geological Mission and CODIGEM (ex-INEMIN) (Aspden and Litherland, 1982), and the subsequent preparation of national geologic and tectono-metallogenic maps in collaboration with Quito Polytechnic, has led to a new interpretation of the geotectonic evolution of Ecuador involving terrane accretion followed by normal "Andean" subduction.

TERRANES (Fig. 1)

1 *The Amazonic craton,* underlying the eastern lowlands of Ecuador, comprises Precambrian metamorphic rocks overlain or intruded by essentially unmetamorphosed Phanerozoic units. Whilst the Precambrian rocks may have resulted from Proterozoic collisions, during the Phanerozoic the craton acted as a stable block at the margin of Gondwana.

2 *The Loja terrane* occurs as two Andean-trending tectonic units within the Cordillera Real. Rocks comprise low- to medium-grade semipelitic schists and paragneisses, all of presumed Palaeozoic depositional age, associated with amphibolites and foliated, migmatitic and mylonitic S-type granites of the Tres Lagunas

suite dated by U-Pb at 228 + 3 Ma: regarded as the metamorphic age.

3 *The Amotape and Chaucha terranes* contain semipelitic metamorphic rocks, of Palaeozoic depositional age, amphibolites, and foliated S-type granites dated by U-Pb at 228 + 1 (the metamorphic age): a lithological association practically identical to the Loja terrane (above). The rocks of the Amatope terrane trend E-W in Ecuador; those of the Chaucha terrane are largely buried, but small windows and float indications in the south around Chaucha and tectonic lenses in the Pujili ophiolite further north suggest its extension as basement to the Inter-Andean valley.

4 *The Salado and Alao terranes* of the Cordillera Real comprise Jurassic greenstones of basalt to andesite in composition, with associated greenschists, pelitic schists and metagreywackes. Geochemistry indicates the Alao volcanics to be typical of oceanic island arc basalts, but those of Salado show more crustal contamination. The latter are also associated with Jurassic calc-alkaline plutons, the Abitagua-Zamora chain, parallel to a similar, but undeformed, magmatic arc along the adjacent western margin of the Amazonic craton.

5 *The Pinon terrane* comprises Cretaceous oceanic crust overlain by Cenozoic forearc basins. *The Pinon-Macuchi terrane* is overlain by the Palaeocene-Eocene Macuchi island arc of calc-alkaline affinity (Bourgois et al, 1990).

TERRANE BOUNDARIES (Fig. 1)

1 *The Cosanga fault* separates undeformed rocks of the stable Amazonic craton in the east from deformed and metamorphosed Triassic-to-Cretaceous rocks in the west. In particular it separates the undeformed Late-Triassic Piuntza volcano-sedimentary unit from S-type granites and migmatites of the same age in the Cordillera Real.

2 *The Banos fault zone* is a regional, Andean-trending, dextral shear zone affecting the Jurassic rocks of the Alao terrane.

3 *The Peltetec fault zone* is marked by an ophiolitic melange with Middle/Upper Jurassic palynoflora in the sedimentary phase.

4 *The Raspas fault zone* comprises serpentinites, eclogites, blueschists, greenschists and pelitic schists. It is parallel with the dextral shearing event associated with the production of the 228 Ma S-type granites in the adjacent Amotape and Chaucha terranes. A K-Ar date gave a Lower Cretaceous age (Feininger and Silberman, 1982).

5 *Both the Pujili and Guayaquil fault zones* contain ultramafic and mafic rocks regarded as derived from the lower portions of the Cretaceous Pinon oceanic crust.

TERRANE ACCRETION

1 The Palaeozoic sediments of the Loja, Amotape and Chaucha

terranes were sheared, metamorphosed and intruded by S-type granites at around 228 Ma, possibly related to proto-Tethyian rifting or collision.

2 In the early Cretaceous the Amatope and Chaucha terranes were accreted from the SW along with the Jurassic Alao island arc; the Loja terrane may be para-autochthonous. Over the Cordillera Real, this collision resulted in strike-slip and nappe tectonics and regional metamorphism.

3 The Pinon-Macuchi terrane may have been juxtaposed in Late Cretaceous times, but was finally accreted towards the end of the Eocene judging from the presence of reworked continental material in Eocene formations.

TERRANE BOUNDARY REACTIVATION

In the Oligocene the formation and consequent subduction of the Nazca plate produced a continental volcanic arc, with intermontane basins, bounded by a coastal forearc and an Amazonic backarc basin. Major Andean uplift occurred in the Pliocene and many of the accompanying compressive and extensional faults can be identified as reactivated terrane boundaries, in particular the Cosanga, Peltetec, Pujili and Guayaquil faults. Opening up of the Pujili and Peltetec faults to form the Inter-Andean "graben" may have produced the conduits for the double chain of Plio-quaternary volcanoes (Litherland and Aspden, 1992).

REFERENCES

ASPDEN, J.A. and LITHERLAND, M. 1992. The geology and Mesozoic collisional history of the Cordillera Real, Ecuador. In: R.A. Oliver, N. Vatin-Perignon and G. Laubacher (Editors), Andean Geodynamics, Tectonophysics, 205, 187-204.

BOURGOIS, J., EGUEZ, A., BUTTERLIN, J. and DE WEVER, P. 1990. Evolution geodynamique de la Cordillere Occidental des Andes d'Equateur: la decouverte de la formacion eocene d'Apagua. C. R. Acad. Sci. Paris, t. 311, Serie II, p. 173-180.

FEININGER,T. and SILBERMAN, M.L. 1982. K-Ar geochronology of basement rocks on the northern flanks of the Huancabamba Deflection, Ecuador. USGS Open File Report, No 82-206.

LITHERLAND, M. and ASPDEN, J. A. 1992. Terrane-boundary reactivation: A control on the evolution of the Northern Andes. Journal of South American Earth Science, 5, 71-76.

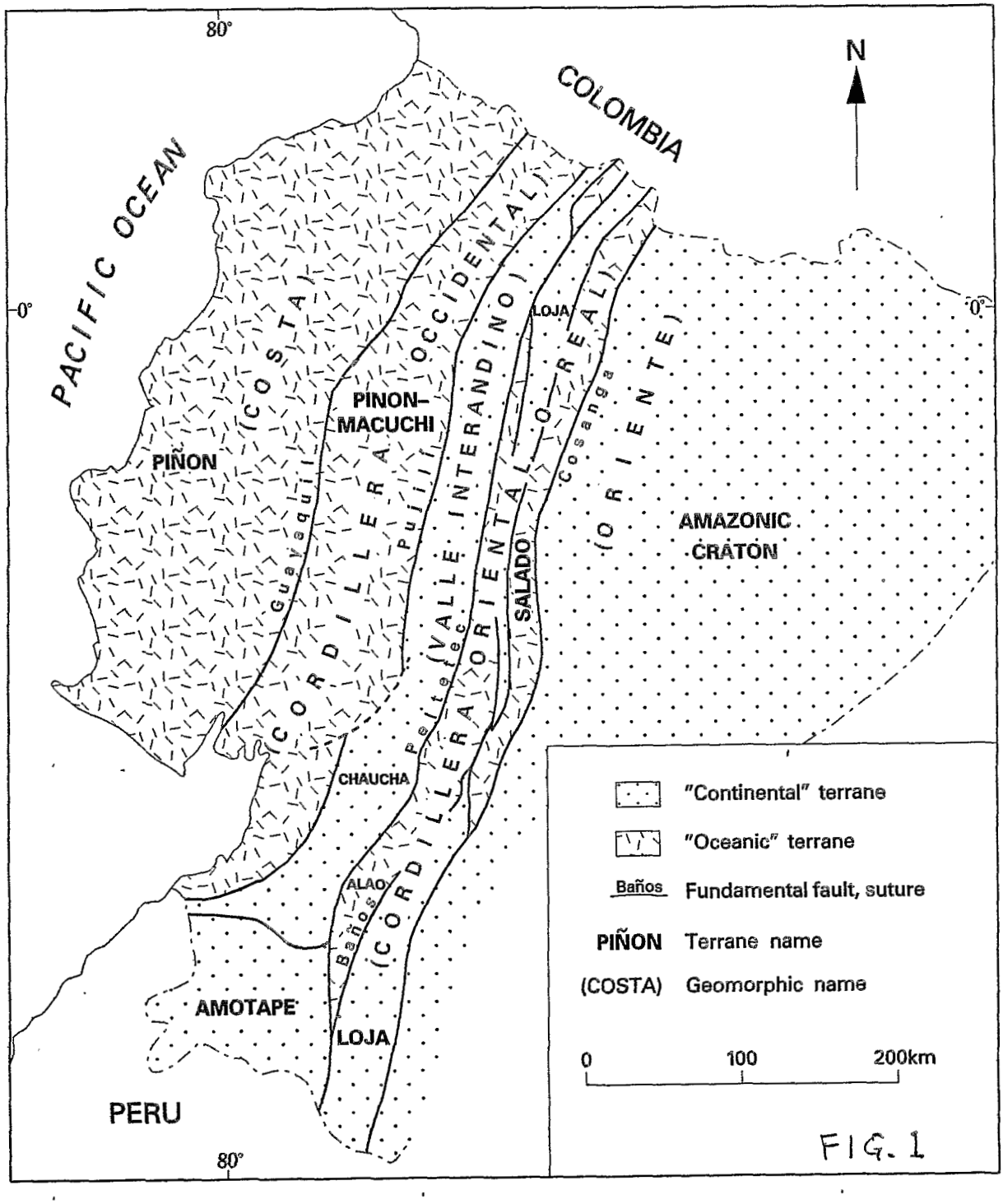
80°
N
COLOMBIA
PACIFIC OCEAN
0°
0°
LOJA
PINON–
MACUCHI
PIÑON
(COSTA)
Guayaquil
CORDILLERA OCCIDENTAL
Pujilí
Pallatanga
VALLE INTERANDINO
SALADO
CORDILLERA ORIENTAL
REAL
(ORIENTE)
AMAZONIC
CRATON
CHAUCHA
Peltetec
ALAO
Baños
AMOTAPE
LOJA
PERU
80°
"Continental" terrane
"Oceanic" terrane
Baños Fundamental fault, suture
PIÑON Terrane name
(COSTA) Geomorphic name
0 100 200km

FIG. 1

CENOZOIC TECTONICS AND PALEOMAGNETISM WEST OF ROMERAL FAULT ZONE, COLOMBIAN ANDES

William D. MACDONALD (1), Juan J. ESTRADA (1,2), Gloria M. SIERRA (1,3), and Humberto GONZALEZ (2)

(1) Dept. of Geological Sciences, State University of New York, Binghamton, New York, USA, 13902-6000
(2) Instituto de Investigaciones en Geociencias, Mineria y Quimica (INGEOMINAS), Apartado Aereo 65160, Medellin, Colombia
(3) Universidad EAFIT, Apartado Aereo 3300, Medellin, Colombia

RESUMEN: Se reportan resultados paleomagneticos en intrusivos subvolcanicos del Cenozoico Tardio y en sedimentos asociados localizados ambos a lo largo de la zona de falla de Romeral. Los cuerpos intrusivos muestran dos tipos de rotacion, al rededor de ejes horizontales perpendiculares a la falla y al rededor de ejes verticales. Los sedimentos sugieren leves rotaciones al rededor de ejes verticales. Ambos grupos de rocas han sido afectados por movimientos laterales tanto sinistrales como dextrales aunque este ultimo ha dominado en el tiempo.

KEY WORDS: Paleomagnetism, Late Cenozoic, Andes, Colombia, Romeral, tectonic rotation.

INTRODUCTION

The Romeral fault zone (Grosse, 1926) is one of the major fault zones of the northern Andes. It bounds the Cauca depression on the east for hundreds of kilometers between the Central and Western Cordillera of Colombia. Long thought to be a right-lateral fault zone (Campbell, 1974), this fault has been shown by seismic studies (Hutchings et al, 1981) to have left-lateral recent movements. A paleomagnetic study of late Cenozoic (approximately 8 Ma) silicic hypabyssal intrusives revealed an interesting but enigmatic dispersal pattern of the paleomagnetic vectors into vertical planes (MacDonald, 1980) of N40W trend. The present study extends the paleomagnetic sampling both geographically, to approximately 100 km further south, and geologically to younger stratified units, in the Irra pull-apart basin west of Manizales.

PALEOMAGNETIC RESULTS AND TECTONIC SIGNIFICANCE

1. Late Cenozoic intrusive rocks. Paleomagnetic studies of approximately 14 sites from the region south of the earlier study show dispersal patterns similar to those obtained previously, except that the trend is N-S instead of N40W. Eigenvalue analysis shows the planes of dispersal to be nearly vertical. These trends are recognized now as being parallel to the trend of the Romeral fault system adjacent to the east. Dispersal within individual bodies is relatively minor, but large relative rotations about horizontal axes have occurred between bodies. These rotation axes are perpendicular to the Romeral fault zone.Two episodes of rotation can be inferred from these patterns. An earlier period of non-coherent rotations of individual bodies about horizontal axes of E-W trend was followed by a period of rotations in which both fault zone and adjacent rocks were rotated, presumably as vertical panels, about vertical axes during bending or kinking of the fault zone.

2. Late Cenozoic strata of the Irra basin. Sediments of the Irra basin near the south limit of the sampled hypabyssal rocks are latest Cenozoic, approximately coeval with the Combia Formation. These strata are folded and thrust with NE structural trends. Sediments, volcaniclastic rocks, and ashflows have paleomagnetic declinations dominantly N10E to N20E. For 16 sites investigated, normal and reverse polarities are approximately equal suggesting primary remanence is preserved. The clockwise sense of

rotation is consistent with right-lateral slip on the marginal faults of the Irra basin. However, compressional patterns are consistent with left-lateral shear across this right-stepping offset.

CONCLUSIONS

These paleomagnetic results indicate multi-modal rotational histories for both the sedimentary and intrusive rocks of the Cauca depression in this region of the Romeral fault. Among the most important conclusions are the following:

1. The rotation of the massive intrusives about horizontal axes perpendicular to the Romeral fault system suggests a kind of mechanical behavior in fault zones not observed previously. It should be looked for in other strike-slip fault zones.

2. The structural evidence for the Irra basin indicate reversals of the sense of slip along the Romeral system. The pull-apart formed in right-lateral shear, and the folding and thrusting in left lateral shear. The timing of the paleomagnetically indicated rotations is tentatively placed as pre-folding.

REFERENCES

Campbell, C.J., 1974, Colombian Andes, in A.M. Spencer, editor, Mesozoic-Cenozoic orogenic belts: Geol. Soc. London, Special Publication 4, p. 705-724.
Grosse, E., 1926, Estudio Geologico del Terciario Carbonifero de Antioquia: D. Reimer, Berlin, 361 p.
Hutchings, L., Turcotte, T., McBride, J., and Ochoa, H., 1981, Microseismicity along and near the Dolores shear zone in Antioquia, Colombia: Revista, Centro Interamericano de Fotointerpretacion, Bogota, v. 6, p. 243-256.
MacDonald, W.D., 1980, Anomalous paleomagnetic directions in Late Tertiary andesitic intrusions of the Cauca depression, Colombian Andes: Tectonophysics, v. 68, p. 339-348.

IDENTIFICATION OF FAULTS ON MONTAINOUS AREAS BY ANALYSIS OF SPOT IMAGES. APPLICATION TO THE EXTRACTION OF STRIKE FAULTS FROM A SUB-SCENE OF SOUTHERN PERU

Catherine MERING(1) (2) and Jean CHOROWICZ(2)

(1) Laboratoire d'Informatique Appliquée, ORSTOM, 72 Rte d'Aulnay, 93143 Bondy Cedex France
(2) Université Pierre et Marie Curie, Paris VI, Dpt de Géotectonique, 4 place Jussieu, 75252, Paris Cedex 05 France Fax: 33(1)44275085

RESUME: L'exploitation des images satellites à haute résolution en vue d'identifier les structures géologiques se fait généralement par photo-interprétation. Les nouveaux développements de l'analyse d'image numérique ouvrent la voie à une photo-interprétation assistée par ordinateur qui permet d'améliorer la mise en évidence des traits structuraux, ainsi que leur extraction. Nous montrons ici un exemple de mise en évidence et d'extraction de failles perceptibles sur une scène de SPOT Panchromatique sur les Andes Centrales (région d'Arequipa, au Sud du Pérou).

KEY-WORDS: image analysis, remote sensing, recognition of faults, structural map.

INTRODUCTION

One of the objectives of remote sensing on the Earth is to enable the survey and mapping of objects on the ground surface. The maps obtained from remotely sensed images can be exploited in various ways like traditional cartography does. Being indeed numerical images, they can easily be combined to any kind of geocoded data inside a Geographic Information System: an example would be the combination of structural maps and observed geocoded epicentres for seismic prevision. On these images, geological structures have no specific reflectance but they have a specific morphology. That is why methods of classification on multispectral data are of no use to map them. On images produced by passive sensors as the ones of SPOT, forms are detected thanks to the cast shadow resulting from grazing illumination on the relief. In the following example, we try to show how these images can be processed with the methods and algorithms of Image Analysis to identify structures, and more generally to demonstrate the feasibility of a "computer aided photo-interpretation". We had recourse here to binary or grey tone *morphological* and *geodesic* transformations (Serra, 1986), the last ones having the property to preserve the contours of the structures. All the Morphological Transformations have been processed without any modification of the original square digital grid. The algorithms have been adapted to the case where the volume of data is very high: indeed, a Panchromatic Spot scene has 42 millions of pixels We have therefore performed iterative computation, in which only the strip of pixels having the required width according to the size of the structuring element involved in the transformation, is stored at each step.

MAPPING OF FAULTS IN MONTAINOUS AREAS

In order to illustrate the method, we have made the choice of a scene upon Central Andes because, although the whole region is highly affected by eruptions and earthquakes (Dorbath, 90), there is no exhaustive mapping of the faults. We attempt here to map strike faults, easily perceptible on SPOT images. Strike faults can be described as dark and sub-rectilinear lines with specific orientation. A large part of normal or reverse faults correspond on the field to abrupt scarps which have to be associated to the fault throw. The darkness and the thickness of the lines interpreted as faults depends on the geomorphology of the scarps but also on the conditions of the viewing. On Figure 1 (corresponding to a square of size 10km on the ground) which is a partial view on the zone of Arequipa (South of Peru) taken in July, the deduction of the structures by extraction of continuous dark lines seems easy to be done by simple photo-interpretation. Nevertheless we try to learn how to extract them by image analysis, our middle-date scope being to find available automatic sequences of treatments and to reproduce them on the scenes collected above the whole target (southern Peru, northern Chile). The darkness, the shape, and the size of the objects may be pertinent criteria to extract faults or elements of faults; on the image other elements are both linear and dark: the darker and the thicker ones are

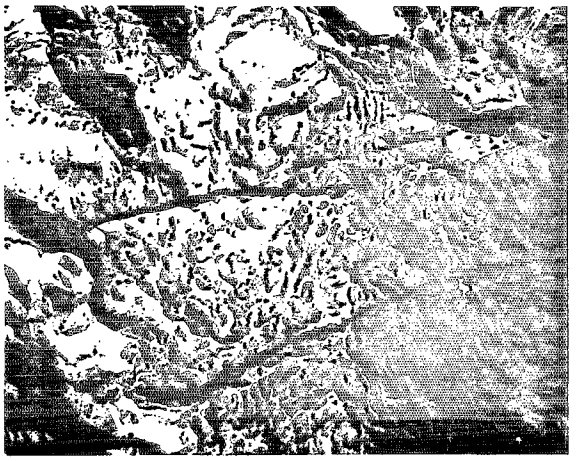

Figure 1

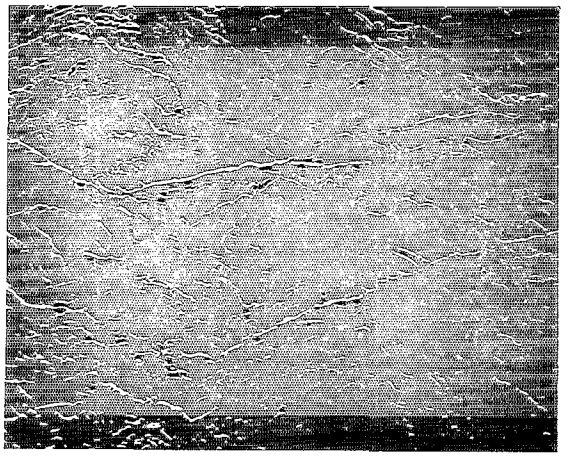

Figure 2

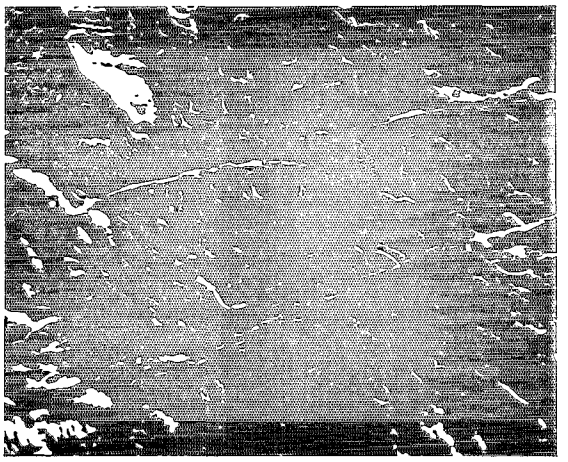

Figure 3

Figure 4

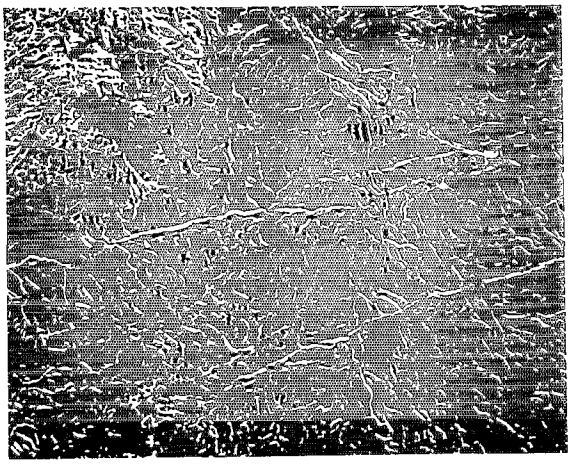

Figure 5

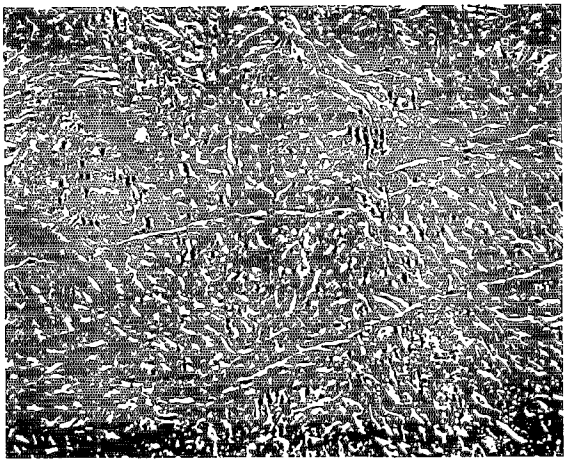

Figure 6

actually ravines inside versants in the shadow (see for example north-west of the image). The widely-known technique of numerical convolutions with *gradient masks* (Pratt, 1978) enhances the contrasts in a given direction: in the present case, the drawback of such a technique is that both dark and light lines are enhanced on the resulting image (see Fig 2 which is the north-south gradient-image). Our strategy was then to apply Morphological Transformations on grey tone function having the property to filter the darker objects from the image. By thresholding the resulting function, we should retain two types of binary images: "maximal images" are the ones where the significative entities are connected, regardless to the presence of other entities, when "minimal images" would be those where only the significative entities are present, even if disconnected. Theoretically, a Geodesic Dilation of a minimal image into a maximal one should provide a good solution to our problem.

We first apply on the original image a *h-minima* filter (Beucher, 1987) that does not take into account any morphological criterion, but selects only dark objects having a given contrast with the neighborhood (Fig. 3): all types of dark components have then been selected such as large spots or thin lines; the faults are of course comprised into the resulting binary image (Fig. 4) and their shapes are well preserved. But one has to find then the way of suppressing undesired large or small black spots. A *size distribution analysis* has to be done to find whether faults have a specific size or not on the h-minima thresholded function. The robustness of the method has to be tested on a large sample of scenes upon the target.

Other transformations called *Top Hat* (because they allow the selection of objects according to their tone, local contrast and thickness) are experimented. We applied here a *Top Hat* from *Morphological Closing* (Fig. 5) and a *Top Hat from Geodesic Closing* (Fig 6) to select dark lines On the first image (Fig. 5), the contours of the faults are better preserved for they are actually dark and continous entities when Top Hat from Geodesic Closing filter (Fig. 6) selects the darker even disconnected elements (Grimaud, 1991).

One solution for finding a minimal image was to process a stepwise "cleaning up" of the binary image from the morphological Top Hat:

-smallest disconnected entities have been eliminated by a *Reconstruction* following a binary *Erosion* (Fig. 7).

-entities the direction of which are whether different than the one of the faults (ie roughly East-West) have been eliminated by the following way: a local multidirectional Gradient filter produces an image of codes of the associated direction of the highest local gradient (ie 8 directions on the square grid); we have selected the pixels having the same code than the one of both faults (Fig 8). Then a *Geodesic Dilation* of the result into the "cleaned" Top hat image is performed (Fig 9). The remaing big entities on north-west of the image are very close one to another: they are ravines inside abrupt versants; they have been eliminated by the application of a mask obtained by a Morphological Closing of size 5 on the resulting image "cleaned up" with a *Geodesic Reconstruction* (Fig.10) This "minimal image" is then reconstructed into a low thresholding of the original Top Hat (Fig 11). On the resulting image (Fig 12) the faults have not been completely connected and their shape is not as well preserved as on a h-min filtered image (see Fig 4) Moreover all entities other than faults have not been eliminated. We think these last ones could be elimined by regional directional operators (Kurdy, 1990) or by further quantitative description of the structures.

CONCLUSIONS

Various experiments of image analysis and morphological transformatons have been made upon a SPOT image of Central Andes in order to extract strike faults. On this example we show how satellite images may be filtered until specified structures are identified. Plans of transformations to be tested on the scenes of the whole region were also described. The kind of computer aided photo-interpretation can be easily tested and reproduced. Furthermore, the results can directly be exploited in order to perform quantitative analysis on the structures or to be inserted into a Geographical Information System..

REFERENCES

(Beucher, 1987) S.Beucher, J.M. Blosseville, M. Bilodeau, F. Lenoir, S. Espie. *Titan: système de mesure du trafic par analyse d'images.* Rapport commun INRETS/CMM. Note interne CMM: N.46/87/MM.Oct.1987.

[Dorbath, 90] L. Dorbath, A. Cisternas and C. Dorbath. *Assessment of the size of large and great historical earthquakes in Peru* Bull. of Seism. Soc. of America, Vol 80, N°3, 1990, pp551-576,

(Grimaud, 1991) M. Grimaud. *La Géodesie numérique en morphologie mathematique. Application à la détéction automatique de microcalcification en mammographie numérique.* These Ecole des Mines de Paris..Décembre 1991.

(Kurdy, 1990) B. Kurdy. *Transformations mophologiques directionnelles et adaptatives: Application aux sciences des matériaux.* Thèse Ecole des Mines de Paris. Septembre. 1990.

(Serra, 1986) J. .Serra. *Image Analysis and Mathematical Morphology. Vol.2. Theoretical advances.* Academic Press. London. 1986.411p.

Figure 7

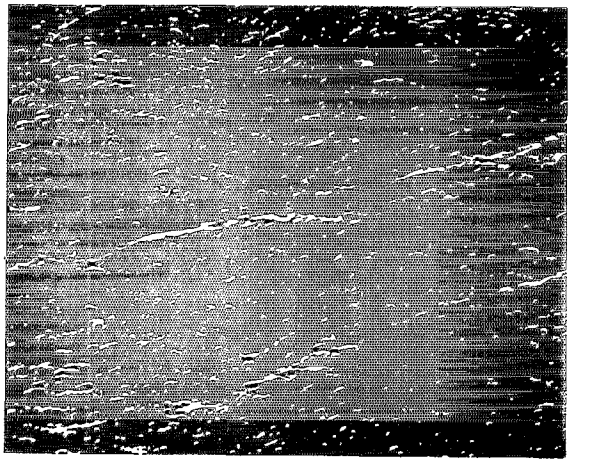

Figure 8

Figure 9

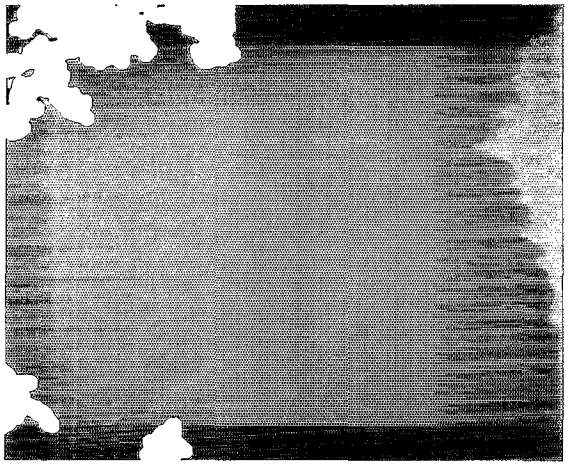

Figure 10

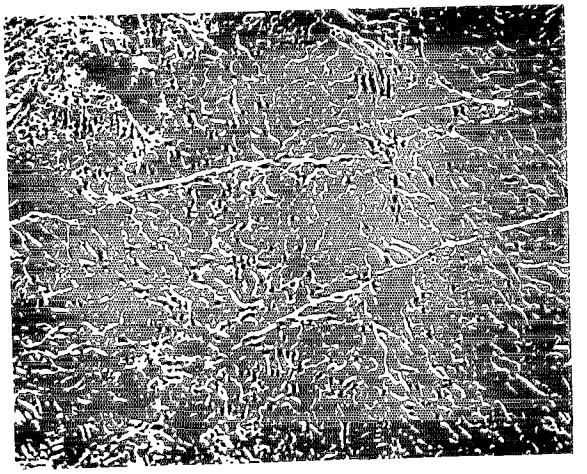

Figure 11

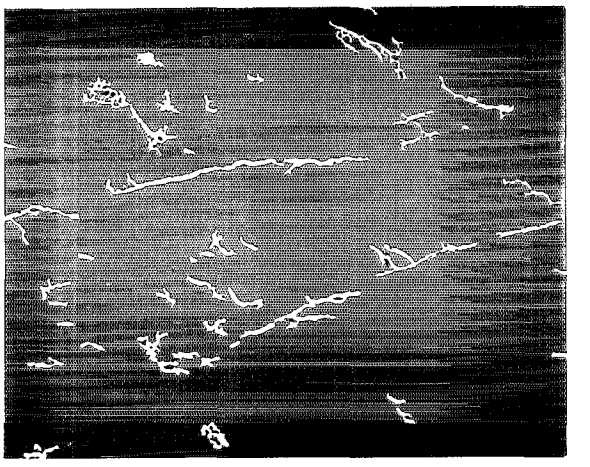

Figure 12

EOCENE LEFT LATERAL STRIKE SLIP FAULTING AND CLOCKWISE BLOCK ROTATIONS IN THE CORDILLERA DE DOMEYKO, WEST OF SALAR DE ATACAMA, NORTHERN CHILE

Constantino MPODOZIS[1], Nicolás MARINOVIC[1], Ingrid SMOJE[1]

(1) Servicio Nacional de Geología y Minería, Avda. Santa María 0104, Santiago, Chile

RESUMEN: La Cordillera de Domeyko, al oeste de Salar de Atacama, en el norte de Chile, constituye parte de un orógeno transcurrente, originado en el Eoceno, por movimientos de rumbo sinistrales a lo largo del Sistema de Fallas de Domeyko. En el segmento comprendido entre el Salar de Punta Negra, al sur y Sierra de Limón Verde, al norte, el movimiento hacia el norte de la Cordillera de Domeyko fue bloqueado por la presencia de una mole rígida (Sierra Limón Verde); y transferido hacia el este por rotaciones de bloques en sentido horario, en dirección a la la cuenca cretácica de Purilactis (proto salar de Atacama), la más occidental de las cuencas de rift cretácicas del noroeste de Argentina y norte de Chile. La inusual combinación de rotaciones horarias acompañando a movimientos transcurrentes sinistrales se debería a que el sistema transcurrente sinistral estuvo limitado al norte por una mole rígida y a al este, por una cara libre: la cuenca de Purilactis.

Key Words: Northern Chile, Domeyko Fault System, Eocene, Clockwise block rotations

INTRODUCTION

Cordillera de Domeyko and its northern prolongation, Sierra de Moreno, extends for more than 800 km (21-28°S) in Northern Chile (Figure 1) separating the Central Depression, to the west, from a series of closed basins (Salar de Atacama, Punta Negra, Pedernales etc) located along the foothills of the western Cordillera, that is capped by the volcanic centers of the modern volcanic arc of the Central Andes. The narrow (60 km wide) range, reaches altitudes well above 4000 m and is composed mainly of Late Paleozoic volcanic and plutonic complexes (Boric et al, 1990. Mpodozis and Ramos, 1990; Reutter, et al., 1991). Cordillera de Domeyko is a transcurrent orogen formed during Eocene left-lateral strike-slip motion, but also recording late increments of oligocene (right lateral) and even quaternary (normal) faulting activity. The strike slip Domeyko fault system (Maksaev, 1990), is closely related with the northern Chile porphyry copper deposits, most of which were emplaced along strike slip faults along the axis of the Cordillera de Domeyko in the Eocene or Oligocene. Although the Cordillera de Domeyko is dominated by strike slip deformation, the structural grain and the geometry of related structures show important variations along strike. The segment west of Salar de Atacama, between 22°30'-25°S (Sierra Limón Verde to Salar de Punta Negra) exhibits an unusual structural geometry compatible with left lateral strike slip deformation accompanied by clockwise block rotations

STRATIGRAPHY

The Cordillera de Domeyko, between Salar de Punta Negra and Sierra Limón Verde is composed mainly by Late Paleozoic magmatic complexes including a suite of basalts to andesites interbedded with lacustrine sediments of late Carboniferous-Early Permian age (Breitkreutz et al, 1992), extensive outcrops of high silica rhyolites and granitoid plutonic centers, some of which are the eroded roots of large collapse calderas (Sierra Mariposas caldera, Davidson et al, 1985). K-Ar, Rb/Sr and U-Pb (zircon) ages fall in the range between 300-200 Ma (Mpodozis et al, 1993). To the west there are large exposures of late Triassic to early Cretaceous marine carbonates, terrestrial red beds and volcanics of the northern Chile mesozoic back-arc basin, covered by volcanics of the paleocene Cinchado formation and related shallow level intrusives (K-Ar ages ≈70-50 Ma, Figure 1). A major structural discontinuity (Sierra de Varas Fault) and a large shear lens (Ringenbach et al., 1992) straddles the contact with the basement core of Cordillera de Domeyko. To the east

of the range, the Paleozoic is also in fault contact with the up to 5 km thick red bed sequence of the Cretaceous to Eocene Purilactis Group, the infill of a large rift basin formed over the present site of modern Salar de Atacama (Macellari et al., 1991) and connected, to the east, with the Salta Group rift basins of northwestern Argentina (Grier et al., 1992). The tectonic contact between the Cordillera de Domeyko and the Purilactis basin sediments has been recently interpreted as a reactivated, down to the east, listric normal growth fault, developed, in the Cretaceous, along the western edge of the Purilactis rift basin (Macellari et al., 1991; Hartley et al., 1992)

STRUCTURE

Figure 1 is a structural sketch of the segment of the Cordillera de Domeyko between Salar de Punta Negra and Sierra Limón Verde. A close inspection of the geological map reveals that in this region: (1) none of the faults of the Domeyko fault system seems to continue north of Sierra Limón Verde; (2) Salar de Punta Negra, at the southern end of the segment, is a Tertiary extensional basin limited at its southern side by a NNW trending normal fault; (3) the Cordillera de Domeyko itself is formed by a series of discrete basement blocks separated by small, interior-drained, basins (Salar de Los Morros, Verónica Elvira... Figure 1); (4) the northwestern faces of the rhomboidal southern blocks (Imilac, San Carlos) are bounded by high angle reverse faults; (5) the northernmost blocks (Quimal, Los Morros, Mariposas) are limited to the west, by left lateral, subcircular to NE oriented, strike slip faults while to the east , they are thrusted over the Purilactis basin sediments; (6) Deformation in the Purilactis sediments is specially strong in front of the basement blocks where the red beds show isoclinal to chevron folds with subvertical axis; (7) Purilactis outcrops away from the basement blocks show no evidences of pervasive deformation.

Sense of asymmetry of large scale "sidewall ripouts" (Swanson, 1989) and displacement of geological contacts indicates left lateral shear along most of the major fault traces. The change from sandstones to coarse grained sediments in the Purilactis basin dated at 44 to 40 Ma (tuffs at the base of the conglomeratic part of the Purilactis Group, Ramírez and Gardeweg, 1982, Hammerschmidt et al.. 1992) and the 45-42 Ma K-Ar ages of the bimodal, syntectonic intrusives and domes of the Cerro Casado complex in the Quimal block indicate a middle to late Eocene age for the beginning of strike slip deformation. A similar age for the onset of the deformation (42 Ma) has been documented further south, in the El Salvador-Potrerillos region (26-27° S, Tomlimson et al., 1993). Oligocene porphyry coppers (Figure 1) were emplaced afterwards along some of major fault strands in the Oligocene, but the tectonic regime seems to have been dominated by dextral shear (at least in the 34-41 Ma Chuquicamata porphyry system, Maksaev, 1990)

DISCUSSION

This special structural association can be described as a strike slip structural province bounded to the north by a rigid butress (Sierra Limón Verde) and, to the east, by a free face: the Cretaceous-Eocene Purilactis basin. This interpretation is similar to the theoretical model recently presented by Beck et al. (1993). In the Eocene, passive northward displacement of the Domeyko range formed an extensional basin (Salar de Punta Negra) at the trailing edge of the displaced block. As northward motion was obstructed by the Limon Verde butress, the displacement could have been transfer to the east towards the Purilactis basin. To overcome the butress, displacement transfer in the Quimal block occurred by a combination of tectonic escape associated with extension (to the west) and compressive deformation and thrusting of the basement block to the east, over the sedimentary fill of the Purilactis basin. In the Mariposas block (Figure 1) deformation seems to have occurred by clockwise rotation along a subvertical axis of a basement sliver bounded by subcircular faults that may correspond to be the reactivated ring fractures of an old, Late Paleozoic, caldera. In this segment of the Cordillera de Domeyko, at least, 30 to 40 km of eocene northward displacement could have been compensated by 10-20% widening of the original surface area of the range.

Critical to this interpretation is the assumption that Sierra Limón Verde behaves a "rigid" butress that prevented northward displacement of the Domeyko block. In fact, as we already stated, none of the major fault traces seems to displace any of the Limón Verde plutonic units. The "West Fissure" fault system of Chuquicamata (Maksaev, 1990) show no obvious connections with the faults to the south. Structurally, Sierra Limón Verde is a huge, northward plunging half dome, cored by late Carboniferous granitoids and metamorphics of early Paleozoic or even Precambrian age; synmagmatic and mylonitic foliations show that the granitoid are deep seated plutons. Jurassic limestones, dipping away from the plutonic core, surround Sierra Limón Verde along its western, northern and eastern margins.

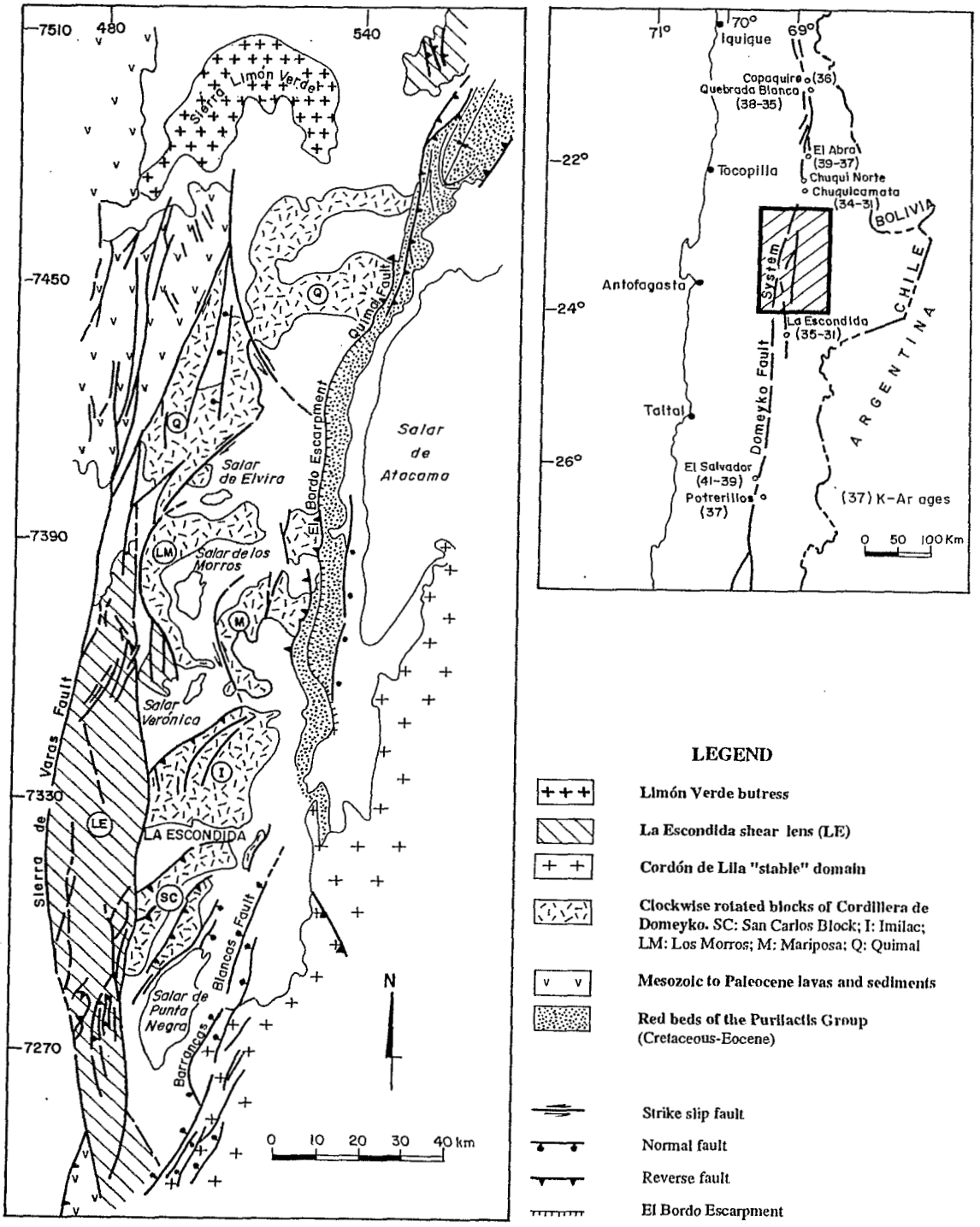

Figure 1: Structural domains and mayor faults of the Cordillera de Domeyko, west of Salar de Atacama, northern Chile.

TECTONIC IMPLICATIONS

Large scale left lateral Eocene strike slip faulting contradicts the Early Tertiary plate reconstructions (Pardo Casas and Molnar, 1987) indicating that during the Eocene deformation along the Chilean active margin should have a significative component of dextral shear If the plate reconstructions for the period are correct, and if he Arica elbow is an ancient feature of the margin, the presence of such a sharp bend in the coastline could effectively prevent,t any kind of northward transport of the coastal sliver (see Beck, 1987). In such an scenario characterized by a locked (and cold) forearc block, it is may be possible to envisage a mechanism to transfer the strain induced by right lateral oblique convergence to the hot and ductile lower crust behind the eocene magmatic front. Northward flow of ductile lower crustal material could result in limited amounts of passive transport of the brittle upper crust, accompanied, at least in the area to the west of Salar de Atacama, by clockwise block rotations.

Acknowledgements; This work is part of a project supported by the Servicio Nacional de Geología y Minería and CODELCO-Chile. This is a contribution to IGCP project.345 (Andean Lithospheric Evolution)

REFERENCES

BECK M. E., Jr., 1987, Tectonic rotations on the leading edge of South America: The Bolivian orocline revisited: Geology, v. 15, p. 806-808.
BECK, M. E, CEMBRANO, J., ROJAS, C., HERVE, F. 1993, On the significance of curvature in strike slip fault systems: G.eology (in press)
BORIC R.; DIAZ, F.; MAKSAEV, V, 1990, Geología y yacimientos metalíferos de la Región de Antofagasta: Servicio Nacional de Geología y Minería, Boletín 40, p. 1-246, Santiago.
BREITKREUTZ, C.; HELMDACH, F. F.; KOHRING, R.; MOSBRUGER, V., 1992, Late Carboniferous Intra-arc sediments in the North Chilean Andes: Stratigraphy, Paleogeography and Paleoclimate : Facies, v. 26, p. 67-80.
DAVIDSON, J., RAMIREZ, C. F., BROOK, M., PANKHURST, R. 1985, Calderas del Paleozoico superior-Triásico inferior y mineralización asociada Comunicaciones, v 35, p 53-57, Santiago
HAMMERSCHMIDT K., DOBEL, R., FRIEDRICHSEN H., 1992, Implication of 40Ar/39Ar dating or Tertiary volcanics rocks from the north-Chilean Precordillera.: Tectonophysics, v. 202, p. 55-81.
GRIER, M., E., SALFITY, J. A., ALLMENDINGER, R. W., 1992 Andean reactivation of the Cretaceous Salta rift basins, northwestern Argentina: Journal of South American Earth Sciences, v 4 (4), p. 31-372.
HARTLEY, A. J., FLINT, S., TURNER, P., JOLLEY E. J., 1992, Tectonic controls on the development of a semi-arid, aluvial basin as reflected in the stratigraphy of the Purilactis Group (Upper Cretaceous-Eocene) northern Chile: Journal of South American Earth Sciences, v. 5(3/4), p. 275-296.
MACELLARI C. E., SU, M. J., TOWSEND, F. , 1991, Structure and seismic stratigraphy of the Atacama Basin, Northern Chile: Cogreso Geológico Chileno N°6, Actas, v. 1, p. 133-137, Viña del M.ar.
MAKSAEV, V, 1990, Metallogeny, geological evolution, and thermochronology of the chilean Andes between latitudes 21° and 26° south, and the origin of major porphyry copper deposits: Phd Thesis, Dalhousie University, p. 1-554, Halifax, Nova Scotia, Canada,
MPODOZIS, C., RAMOS, V. A., 1990, The Andes of Chile and Argentina: Circum Pacific Council for Energy and Mineral resources,Earth Science Series, v. 11, p. 59-90.
MPODOZIS, C., MARINOVIC, N., SMOJE, I, CUITIÑO, L. 1993 Estudio geológico-Estructural de la Cordillera de Domeyko entre Sierra Limón Verde y Sierra region de Antoagasta. Servicio nacional de Geología y Minería-Codelco Chile (unpblished report), p. 1-231, Santiago
PARDO CASAS, F., MOLNAR P., 1987, Relative motion of the Nazca (Farallon) and South American plates since Late Cretaceous time: Tectonics, v. 6, p. 233-248.
RAMIREZ, C. F.; GARDEWEG, M., 1982, Hoja Toconao, Región de Antofagasta: Servicio Nacional de Geología y Minería, Carta Geológica de Chile(1:250.000) 58, p. 1-121, Santiago.
REUTTER, K. J.; SCHEUBER, E.; HELMCKE, D., 1991, Structural evidence of orogen-parallel strike slip displacements in the Precordillera of northern Chile: Geologische Rundschau, v. 80(1), p. 135-153.
RINGEBACH J. C.; PINET N.; DELTEIL J.; STEPHAN, J. F., 1992, Analyse des structures engendrées en régime décrochant par le séisme de Nueva Ecija du 16 Julliet 1990, Luzon, Phillipines: Bulletin Societé Géologique de France, v. 163, p. 109-123.
SWAMSON, M.,T.,1989,Sidewall ripouts in strike slip faults: Journal of Strucural Geology, v 11(8), p 933-948s
TOMLIMSON, A. J; MPODOZIS, C., CORNEJO, P; RAMIREZ, C. F., 1993 Structural geology of the Sierra Castillo-Agua Amarga fault sytem, Precordillera of Chile, El Salvador-Potrerillos (this symposium).

OBDUCTION EVIDENCE ON THE BOLIVAR ULTRAMAFIC COMPLEX, SOUTH-WESTERN COLOMBIA

Alvaro NIVIA G. (1)

(1) INGEOMINAS - Regional Pacífico, Apartado Aerèo 9724, Cali, Colombia.

RESUMEN: Asociado a un complejo de rocas ultramáficas y máficas, deformadas, anfibolitizadas y localmente migmatizadas ocurren tanto diques pegmatíticos que cortan a través de éste, como un depósito de magnesita criptocristalina. Estos rasgos se interpretan como producto del transporte de fluidos derivados de la base de un bloque de litósfera oceánica durante su obducción sobre la margen continental de Sur América.

KEY WORDS: ultramafic rocks, pegmatitic dykes, magnesite, obduction, plateau basalt province.

INTRODUCTION

Geological and geophysical studies show that the Northern Andes are made of two lithospheric Cretaceous provinces of different affinities: continental to the east and oceanic (the Oceanic Western Lithospheric Province - OWLP) to the west. The boundary is marked by the Cauca-Almaguer Fault (also called Romeral Fault and Dolores-Guayaquil Megashear) that parallels the western flank of the Central Cordillera from the Gulf of Guayaquil, through Ecuador and Colombia, to the Caribbean sea. To the east of the fault, calculated values of both gravimetric anomalies and seismic velocities (Case *et al.* 1971, 1973; Meyer *et al.* 1977; Ocola *et al.* 1977) suggest a crust composed of sialic materials (M=40-50 Km; Case *et al.* 1984). To the west the Andes are made of high density, high velocity materials, commonly interpreted as oceanic crust (M=25-30 Km; Case *et al.* 1984). The Pre-Cenozoic rocks of the eastern province consist on Precambrian and Paleozoic igneous and metamorphic rocks intruded by Mesozoic granitoid plutons, whereas the OWLP is made of Mesozoic (not older than Lower Cretaceous) basic volcanic rocks, associated with ultramafic complexes and marine sedimentary strata. Interpretations of the evolution of the lithosphere in Colombia (Barrero 1979; Bourgois *et al.* 1982; McCourt *et al.* 1984; Aspden & McCourt 1986) consider that the OWLP was accreted to the northern margin of the South American continent during the Late Cretaceous.

Associated with the OWLP, within a belt situated some 20-30 Km to the west of the Cauca-Almaguer Fault, are found several bodies of ultramafic rocks, the best known of which is the Upper Cretaceous Bolivar Ultramafic Complex (BUC). This complex is a) the host rock of a stockwork deposit of cryptocrystalline magnesite, b) cut by a suite of mafic pegmatitic dykes and c) exhibits local zones of strong pervasive deformation and amphibolitization. It is proposed that these three features are related with the suture event of the two provinces during which the the leading edge of the OWLP was obducted on top of the Cretaceous continental margin of South America.

GEOLOGICAL SETTING

The Upper Cretaceous BUC outcrops on the eastern flank of the Western Cordillera of the Andes in southwestern Colombia. To the east and north it is covered by the recent deposits of the Cauca River. To te west the Roldanillo fault marks its contact with the Volcanic Formation a thick sequence of Cretaceous tholeiitic basalts and dolerites. Based on similarities in the geochemical characteristics between fine grained isotropic gabbros from the BUC and tholeiites from the Volcanic Formation the two units have been interpreted as comagmatic (Nivia 1987), the former representing the products accumulated on the magmatic chambers where the latter evolved. The chemistry of tholeiites from the Volcanic Formation include low LIL-element abundances (Zr/Nb =8 to 17) and flat to enriched REE patterns (Ce_N/Yb_N = 0.9 to 3.5) that allow positive comparisons with thick oceanic crust typical of Iceland or with plateau basalt provinces such as those of the Nauru Basin or the Caribbean (Millward *et al.* 1984; Nivia 1987). These suspected materials of the WOLP might represent fragments of the Caribbean Plate stripped off during its emplacement between North and South America.

Three different horizons are present in the BUC: a lower one of intercalated bands of serpentinized dunites, lherzolites, olivine websterites and olivine gabbronorites; and intermediate horizon of banded (cumulus) gabbronorites and an upper one of isotropic gabbronorites. Replacement of pre-existing pyroxenes by uralite, cummingtonite and hornblende is conspicuous on the gabbro layers. On outcrop, these same horizons show strong pervasive foliation parallel to the cumulus banding and local development of migmatitic textures with clear intrusive relationships between coarse grained leucogabbros cutting through fine grained, often cumulitic, melagabros.

The BUC is cut by a suite of dykes, 50 cm thick on the average, that consist mainly on very coarse grained hornblende, plagioclase and quartz crystals. The composition of the dykes seems to vary according to their level of intrusion. The lower parts of the complex are cut by plagioclase-hornblende dykes whereas in the upper parts the dykes are rich in plagioclase, quartz, muscovite and sericite. The presence of dumortierite associated with the latter phases is also reported.

Serpentinites of the lower horizon form the host rock of a stockwork deposit of cryptocrystalline magnesite veins that are 5 cm thick on the average. Opal veins deposited after the magnesite ones occur in the upper levels of the deposit.

The facts previously presented can be interpreted in terms of an obduction event during which the leading edge of the Caribbean plateau was overthrust on the continental margin of northern South America. The lack of the tectonic harzburguite on the BUC and on other ultramafic complexes placed in similar structural situation might indicate that the decoupling of this piece of oceanic lithosphere was produced at the level of the petrological Moho. During this processes the geotherm of the lithosphere that carried the obduction shifted to a region of higher temperature distilling the H_2O, CO_2 and boron contained in the terrigenous and calcareous sediments found in the continental lithosphere's upper part. The transportation of these fluids through the overthrusted block might then have cause both local fusion (by lowering of the solidus) leading to the formation of migmatites and amphibolitization of gabbros. Also, the products of the reaction between these fluids and the liquids produced by local fusion might have crystallized at fractures leading to the formation of the pegmatite dykes that cut the BUC. On the other hand, the mechanism of forming the magnesite deposits associated with ultrmafic rocks is commonly believed to involve altering serpentine by CO_2-rich waters, produced by steam distillation at depth. This mechanism agreed with the obduction model proposed and allowed to postulate a genetical model for the formation of the Bolivar magnesite deposit. In addition, the world's most important deposits of this type, located on a discontinuos belt through former Yugoslavia, Albania and Greece (particularly those of the Chalkidiki Peninsula in Greece; Dabitzias 1980) have similar characteristics to those of the Bolivar deposit. These characteristics suggest that these deposits formed as the result of obduction processes during the closure of Neo-Tethys.

CONCLUSIONS

The BUC was probably formed by crystallization in the magmatic chamber where the Volcanic Formation tholeiites (documented as formed on a oceanic plateau basalt province) evolved. During the collision of this plateau against the proto-South American continent its leading edge was obducted on top of the continental margin. During this process, connate waters contained on terrigenous and calcareous sediments that laid on top of the continetal platform were expelled as well as B and CO_2. The introduction of H_2O to the base of the obducted lithosphere (probably hot) and the heat generated by friction during thrusting of the oceanic plateau helped in the production of fluids that filled the open cracks where crystalized as pegmatitic dykes. The action of hydrothermal CO_2-rich waters on serpentinites formed by alteration of basal dunites of the CUB, produced Mg-enriched solutions that precipitated as veins close to the surface when the total pressure change from lithospheric to hydrospheric or whenever the craks caused by tectonism produced pressure drops.

REFERENCES

APSDEN, J. & McCOURT, W.J. 1986. Mesozoic oceanic terrane in the central Andes of Colombia. *Geology*, **14**, 415-418.

BARRERO, D. 1979. Geology of the central Western Cordillera, west of Buga and Roldanillo, Colombia. *Publicaciones Geologicas Especiales del INGEOMINAS*, **4**, 75p.

BOURGOIS, J., CALLE, B., TOURMON, J. & TOUSSAINT, J.F. 1982. The Andean ophiolitic megastructure on the Buga-Buenaventura transverse (Western Cordillera-Valle Colombia). *Tectonophysics*, **82**, 207-229.

CASE, J.E., BARNES, J., PARIS, G., GONZALES, I.H. & VINA, A. 1973. Trans-Andean geophysical profile, Southern Colombia. *Geological Society of America Bulletin*, **84**, 2895-2904.

CASE, J.E. , DURAN, S.L.G., LOPEZ, A. & MOORE, W.R. 1971. Tectonic investigations on Western Colombia and Eastern Panama. *Geological Society of America Bulletin*, **82**, 2685-2712.

CASE, J.E, HOLCOMBE, T.L. & MARTIN, R.G. 1984. Map of geological provinces in the Caribbean region. In BONINI, R.B., HARGRAVES, R.B. & SHAGAN, R. (Eds) The Caribbean - South American plate boundary and regional tectonics. *Geological Society of America Memoir*, **162**, 1-30.

DABITZIAS, S.G. 1980. Petrology and genesis of the Vavdos criptocrystalline magnesite deposits, Chalkidiki Peninsula, Northern Greece, *Economic Geology*. **75/8**, 1132-1151.

MEYER, R.P., MOONEY, W.D., HALES, A.L. HELSLEY, A.L., WOOLARD, G.P., HUSSONG, D.M. & RAMIREZ, J.E. 1977. Refraction observation across a leading edge, Malpelo Island to the Colombian Cordillera Occidental. In RAMIREZ, J.E. & ALDRICH, L.T. (Eds.) *The Ocean-Continent Transition in SW-Colombia*. Instituto Geofísico - Universidad Javeriana, Bogotá. 83-105.

MILLWARD, D., MARRINER, G. & SAUNDERS, A.D. 1984. Cretaceous tholeiitic volcanic rocks from the Western Cordillera of Colombia. *Journal of the Geological Society, London*, **141**, 847-860.

NIVIA, A. 1987. *Geochemistry and origin of the Amaime and Volcanic Sequences, Sothwestern Colombia.* (unpubl. M.Phil. thesis) University of Leicester, Leicester, U.K. 163p.

OCOLA, L.C., ALDRICH, L.T., GETTRUST, J.F., MEYER, R.P. & RAMIREZ, J.E. 1977. Project Nariño I: Crustal structure under southern Colombian - Northern Ecuador Andes from seismic refraction data. In RAMIREZ, J.E. & ALDRICH, L.T. (Eds.) *The Ocean-Continent Transition in SW-Colombia*. Instituto Geofísico - Universidad Javeriana, Bogotá. 47-70.

TIME CONSTRAINTS OF THE ANDEAN DEFORMATION ALONG THE CENTRAL ANDES OF ARGENTINA AND CHILE (32°-33°S LATITUDE)

Victor A. RAMOS (*) and José M. CORTES (*)

(*) Departamento de Ciencias Geológicas, Universidad de Buenos Aires, Ciudad Universitaria, (1428) Buenos Aires, Argentina

RESUMEN: Las restricciones temporales en el desarrollo de la faja plegada y corrida de la Cordillera Principal, el levantamiento y la deformación de la Cordillera Frontal, así como el de la Precordillera, cuando se comparan con sus depósitos sinorogénicos, indican que el período principal de acortamiento orogénico de los Andes Centrales a estas latitudes abarca desde el Mioceno inferior (circa 22 Ma) al reciente.

KEY WORDS: Central Andes, Tectonics, Synorogenic deposits, Tertiary, Quaternary.

INTRODUCTION

The analysis of the synorogenic deposits in a corridor from the Pacific coast to the Mendoza city shows a series of broken foreland basins that indicate a continuous shifting of the orogenic fronts. New radiometric ages of the volcanic arc rocks and the interfingered tuffs of the synorogenic deposits portrayed a main Late Cenozoic episode of deformation as responsible for the crustal shortening and uplift of the Principal Cordillera, the Frontal Cordillera, and the Precordillera.

GEOLOGICAL SETTING

At these latitudes, the Andes are composed by a series of parallel cordilleras separated by Tertiary synorogenic deposits. The rocks involved in the deformation of the different cordilleras are mainly Mesozoic in the Principal Cordillera, Late Paleozoic to Triassic in the Frontal Cordillera, and Early Paleozoic in the Precordillera. This distribution is the result of two facts: 1) a series of distinct detachment levels that from west to east correspond to Late Jurassic gypsum, Late Carboniferous shales, and Early Ordovician marls; 2) The amalgamation of different Paleozoic terranes which produced major crustal boundaries.

THE SYNOROGENIC DEPOSITS

The synorogenic deposits are distributed east of the Aconcagua fold-and-thrust

belt, the Uspallata valley, and the foothills of Mendoza-Sierra de Las Peñas (see figure 1).

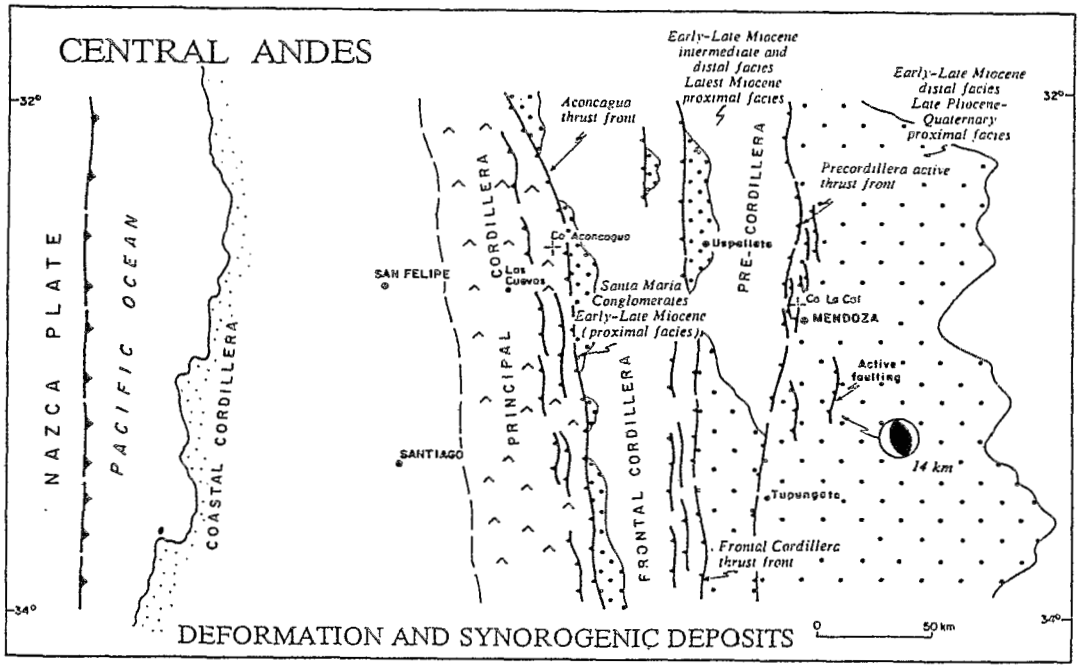

Figure 1: Main thrust fronts with distribution of proximal to distal synorogenic deposits, Central Andes of Argentina and Chile (modified from Ramos, 1988).

a) The Aconcagua fold-and-thrust belt

The volcanic arc rocks in the western side of this region show in the Chilean side, a major angular unconformity where 20.4/16.6 Ma old rocks (Rivano et al., 1990) of the Farellones Formation overly older volcanic sequences. These ages together with the cooling age of post-tectonic granitoids in the Argentine side (Ramos and Cingolani, 1989) of 21.6 Ma indicate the beginning of the shortening at approximately 22 Ma at these latitudes. The migration of the volcanic activity from the Chilean side to the Aconcagua area as a result of the beginning of the shallowing of the subduction zone (Jordan et al., 1983), produced an angular unconformity between volcanic rocks of 15.8/8.9 Ma and different sedimentary and volcaniclastic Mesozoic deposits (Ramos et al., 1991).

At the same time that the fold-and-thrust belt was deformed, a series of synorogenic deposits were accumulating east of the Aconcagua area. The westernmost proximal facies of the Santa María Conglomerates, with boulders up to one cubic meter show a coarsening upwards sequence. The basal beds are mainly composed by Mesozoic limestones and sandstones clasts with some interfingered tuffs, while towards the top volcanic andesitic breccias and pyroclastic flows are dominant. The younger ages of this sequence indicate active sedimentation up to 8.1 Ma (Ramos et al., 1990) while towards the west the arc activity was ceasing due to the shallowing of the subduction zone (Kay et al., 1987).

b) The Uspallata valley

The Frontal Cordillera at these latitudes has been uplifted almost as a single block during Late Miocene times, by a series of imbricated thrusts that bound to the west the Uspallata valley (Cortés, 1993). As a result of that, an extensive Early Miocene peneplain has been uplifted up to 6,000 meters a.s.l.

The synorogenic deposits between the Frontal Cordillera and the Precordillera

record two unconformably overlying sequences. The oldest one can be correlated with the Mariño Formation (Cortés, 1993), and has been deposited prior to 11.4 Ma. The sedimentary facies indicates distal to intermediate fluvial deposits for the Miocene. The youngest one includes proximal facies of Late Miocene to Pliocene age, and has been erroneously correlated with the Late Pliocene Mogotes Formation.

c) Precordillera foothills

The thrust front of Precordillera is at present the most active seismotectonic zone of the Andes at these latitudes. Focal mechanisms of intraplate earthquakes indicate crustal shortening at 14 km depth (Triep, 1987). The east-verging thrust front affects Latest Tertiary, Pleistocene, and Holocene deposits. Quaternary terraces are tightly folded and blind thrusts (Bettini, 1981) developed within the Cenozoic cover are doming the present surface.

The synorogenic deposits display three major angular unconformities; one between the Mariño Formation and previous Early Tertiary-Late Cretaceous sag deposits; other between the Mogotes Formation (3.8 to 1.2 Ma, Yrigoyen, 1993) and older Miocene units, and the third between latest Pliocene and Pleistocene deposits.

This Late Pliocene-Early Pleistocene deformation was also responsible for the final uplift of the Sierra de San Luis (Costa, 1992) the westernmost Sierras Pampeanas at these latitudes.

CONCLUSIONS

The new data constrain the main period of shortening of the Andes between the base of the Early Miocene (approx. 22 Ma) and the Present. Although there is a shifting of the thrust front to the east associated with the migration of the magmatic activity, related to the shallowing of the subduction zone, this activity was episodic and discontinuous as recorded by the synorogenic deposits.

This shortening could be linked to an increase of the convergent rate as previously proposed by several authors (Pilger, 1984; Ramos, 1988). This increase was due to the break-up of the Farellones plate and the formation of the Nazca and Cocos plates around 25 millon years ago.

ACKNOWLEDGEMENTS

The authors wish to acknowledge the funding from projects UBACYT-Ex 066 and PID CONICET/93.

REFERENCES

BETTINI, F.H., 1981. Nuevos conceptos tectónicos del centro y borde occidental de la Cuenca Cuyana. Asociación Geológica Argentina, Revista 35(4): 579-580, Buenos Aires.

CORTÉS, J.M., 1993. El frente de corrimiento de la Cordillera Frontal y el extremo sur del valle de Uspallata, Mendoza. XII° Congreso Geológico Argentino, Actas (in press).

COSTA, C.H., 1992. Neotectónica del sur de la Sierra de San Luis. Universidad Nacional de San Luis, Tesis Doctoral (unpublished), 1-390, San Luis.

JORDAN, T.E., B. ISACKS, V.A. RAMOS and R.W. ALLMENDINGER, 1983. Mountain building in the Central Andes. Episodes, 1983(3): 20-26, Ottawa.

KAY, S.M., V. MAKSAEV, R. MOSCOSO, C, MPODOZIS and C. NASI, 1987. Probing the evolving Andean lithosphere: Mid-late Tertiary magmatism in Chile (29° -30°30'S) over the modern zone of subhorizontal subduction. Journal Geophysical Research, 92(B7): 6173-6189.

PILGER, R.H., 1984. Cenozoic plate kinematics, subduction and magmatism: South American Andes. Journal geological Society of London 141: 793-802.

RAMOS, V.A, 1988. The Tectonics of the Central Andes; 30° to 33°S latitude. In Processes in Continental Lithospheric Deformation, S.Clark y D. Burchfiel (eds.), Geological Society America, Special Paper 218: 31-54.

RAMOS, V.A. and C. CINGOLANI, 1989. La Granodiorita Matienzo: intrusivo mioceno de la Alta Cordillera de Mendoza. Asociación Geológica Argentina, Revista 43(3): 404-408, Buenos Aires.

RAMOS, V.A., D. PÉREZ and M.B. AGUIRRE-URRETA, 1990. Geología del Filo de Zurbriggen, Aconcagua, Mendoza. XI° Congreso Geológico Argentino, Actas II: 361-364, San Juan.

RAMOS, V.A., F. MUNIZAGA and S.M. KAY, 1991. El magmatismo cenozoico a los 33°S de latitud: geocronología y relaciones tectónicas. VI° Congreso Geológico Chileno, Actas I: 892-896, Santiago.

RIVANO, S., E. GODOY, M. VERGARA and R. VILLARROEL, 1990. Redefinición de la Formación Farellones en la Cordillera de Los Andes de Chile Central (32°-34°S). Revista Geológica de Chile 17(2): 205-214, Santiago.

TRIEP, E.G., 1987. La falla activada durante el sismo principal de Mendoza de 1985 e implicancias tectónicas. X° Congreso Geológico Argentino, Actas I: 199-202, Tucumán.

YRIGOYEN, M.R., 1993. Los depósitos sinorogénicos terciarios. En Geología y Recursos Naturales de la provincia de Mendoza. XII° Congreso Geológico Argentino, Relatorio (in press), Buenos Aires.

THE "WEST FISSURE" AND THE PRECORDILLERAN FAULT SYSTEM OF NORTHERN CHILE

Klaus-J. REUTTER[1], Guillermo CHONG[2], and Ekkehard SCHEUBER[3]

(1) and (3) Freie Universität Berlin, Fachrichtung Geologie, Haus B, Malteser Str. 74-100, D-1000 Berlin 46, Germany; (2) Universidad Católica del Norte, Departamento de Ciencias Geológicas, Casilla 1280, Antofagasta, Chile

RESUMEN

La Falla Oeste, o West Fissure, de la mina de cobre de Chuquicamata muestra en sus rocas de falla estructuras de desplazamiento transcurrente sinistral N-S. Lo cual es opuesto a los desplazamientos dextrales comprobados en otras fallas N-S de la Precordillera del Norte Chileno. De esta forma existen evidencias de una inversión de los movimientos transcurrentes en el Oligoceno.

KEY WORDS: Magmatic arc, strike-slip faults, porphyry copper deposits, tectonic inversion

INTRODUCTION

The Chilean Precordillera, situated between the Longitudinal Valley and the Western Cordillera of northern Chile, was the site of the Andean magmatic arc from the late Cretaceous to the early Oligocene. During the Late Eocene Incaic Phase, the basement with its sedimentary and volcanic cover was folded to elongate, mostly N-S-trending anticlines, and dextral strike-slip faults developed parallel or at low angles to the fold structures (Reutter et al. 1991: Precordilleran Fault System). Orogen-normal shortening and dextral orogen-parallel strike-slip movements are considered as magmatic arc tectonics under the influence of oblique subduction (Scheuber and Reutter 1992). The Precordilleran Fault System is related to the development of the great porphyry copper deposits of that region. The West Fissure which is an essential branch of the Precordilleran Fault System runs, in N-S direction, through the Chuquicamata open pit (68°54' W; 22°16' S). A detailed study of this main fault and other accompanying faults in Chuqicamata and its surroundings (Fig. 1) shows that the kinematics along the West Fissure differ from those of most parts of the Precordilleran Fault System.

GEOLOGICAL SETTING

The exposures of the open pit of Chuquicamata (1.8 km E-W, >4 km N-S) exhibit an abundance of vertical faults belonging to different directional groups. More than 90% of the striae developed on the fault surfaces are horizontal, thus showing that wrench tectonics determined the kinematics. The West Fissure is the most important fault of the Chuquicamata mine, as it separates a western non mineralized granodiorite of ~36 Ma from the mineralized eastern block consisting of Paleozoic granite intruded by porphyries of 32-30 Ma and their alteration products (Maksaev et al. 1988, Maksaev 1990). It can be traced as a continuous structure >100 km to the N and about 20 km to the S. A black argillitic fault gouge up to 2,5 m thick demonstrates that this fault absorbed the maximum of the tectonic energy. Evidently, the throw along the West Fissure is younger than the mineralization and, therefore, it is discussed whether the original westward extension of the mineralization was displaced to the N by dextral slip or to the S by sinistral slip.

As structures indicating dextral slip are frequent in the Precordillera (Reutter et al. 1991), the same sense of displacement was assumed for the West Fissure. The fault pattern of Chuquicamata (Fig. 1) shows several faults entering the the West Fissure from the left at angles of ~15° (e.g. Falla San Lorenzo, F. Chucos, F. Zaragoza) and ~75° (e.g. F. El Negro, F. Balmaceda, F. Estanques Blancos). This asymmetric distribution could be interpreted as a set of Riedel shears accompanying the the West Fissure as the master fault of the system, although the evident dextral displacements along the supposed R' had to be explained by secondary effects. Nevertheless, dextral shear is also suggested by fold structures with a wavelength of ~5 km and NW-SE trending axes which are cut by the West Fissure about 15 km to the N of Chuquicamata.

Because of the arid climatic conditions, the argillitic fault gouge of the West Fissure is well preserved in the pit and shows internal meso- and microstructures which are quite similar to those of coherent cataclastic rocks and mylonites. Especially S-C-fabrics, ecc-fabrics, δ-clasts and σ-clasts could be recognized and their asymmetry, as well as that of folded s-planes, could be used for determining the sense of shear. It turned out that all these structures uniformly indicated sinistral strike-slip, i.e. a displacement contrary to what had been expected. The detection of similar structures in other ~N-S-striking faults of the Chuquimatamata mine, such as F. Americana, F. C-2, F. Chucos, and F. Mesabi, coroborated these results.

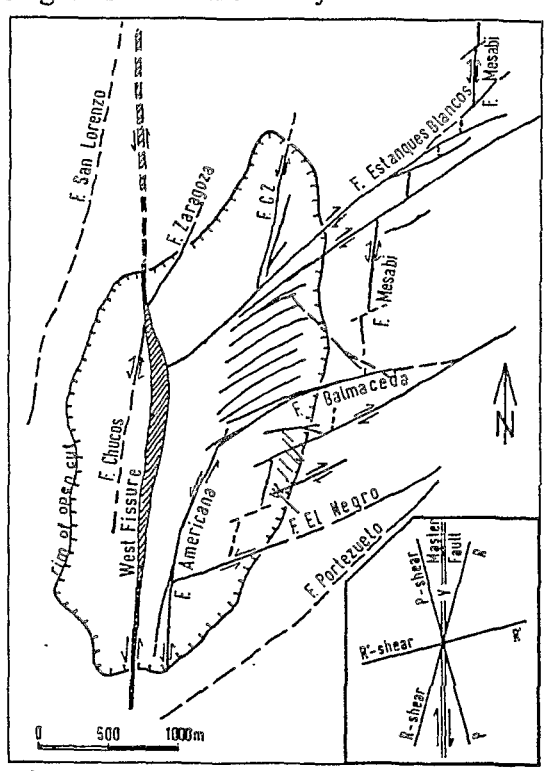

Fig. 1. The secondary faults in the Chuquicamata copper mine apparently form a set of Riedel shears related to a dextral master fault (Reutter et al. 1991, with modifications). However, the shear directions established, as indicated by arrows (dextral, sinistral, and dextral overprinted by sinistral), reveal that such a simple model is not applicable.

These last two faults, however, display not only structures due to sinistral horizontal shear, but also others formed by dextral shear. This is especially true for the Mesabi Fault to the N of the Chuquicamarta mine. There, it follows a band of sediments (Jurassic?) which were rotated in a vertical position during Late Eocene folding of the Precordillera. Dextral shear movement parallel to the strike of these sediments is indicated by vertical folds and mesoscopic S-C- and ecc-fabrics. Evidence of dextral N-S-directed shear also comes from the 36-Ma-old Granodiorita Fortuna at the western side of the Chuquicamata mine. In severals places it is pervaded by N-S-striking and vertically dipping mylonitic bands (Fig. 1), whose age, determined by Maksaev (1990), is slightly younger than that of the intrusion. Dynamic recrystallisation of feldspars in the mylonites indicates temperatures of up to ~500°C during deformation.

CONCLUSIONS

These examples of orogen-parallel dextral shear in the surroundings of the West Fissure of Chuquicamata agree with the observations made in many places of the North Chilean Precordillera between 21° and 25° S (e.g. Sierra de Moreno, Cordillera de Domeyko, and western scarp of the Salar de Atacama). Asymmetric fault arrays and Z-shaped vertical folds in upfolded sediments revealed a uniform dextral sense of shear along parallel faults of the Precordilleran Fault System, while stratigraphic discontinuities across major faults suggested lateral throw possibly in the order of tens of km (Reutter et al. 1991). So, probably, also the West Fissure was generated as a dextral strike-slip fault.

The sinistral shear movement along the the West Fissure and parallel faults in the Chuquicamata mine must be explained by an inversion of the sense of shear when the dextral transpression tectonics had come to an end. Evidence for this chronological sequence comes from the following observations:

- The West Fissure fault rocks, which display the structures of sinistral strike slip, formed at very low temperatures close to the surface. The ductile dextral shear deformation of the mylonites, however, was produced at a depth of >2 km. Thus, an event of uplift and erosion separated the two developments.
- Sinistral movements along the West Fissure are younger than the mineralization of the Chuquicamata deposit and the porphyric intrusions, dated to 32 Ma (Maksaev 1990).

This rises the question if mineralization occurred still during dextral shear or contemporaneously with sinistral shear. In the El Abra copper ore deposit, situated at the eastern side of the West Fissure about 40 km to the N of Chuquicamata, mineralization took place in a complex of granodioritic intrusives 39-32 Ma old (Maksaev 1990), and, as evidendenced by the orientation of joints, faults and veins, under a regime of NE-SW extension which is compatible with sinistral shear in the nearby West Fissure. The maximum of mineralized quartz veins in the Chuquicamata mine also corresponds to NE-SW extension, but other veins which indicate NW-SE and E-W-extensions suggest that mineralization in Chuquicamata took place more or less at the time of the inversion of the shear movement, probably under reduced E-W compression, as testified by a few normal faults (Fig.2).

From a general point of view it can be concluded that the structures connected with the Precordilleran Fault System and the West Fissure reflect, first, strong dextral transpression related to the Incaic Phase, which may have lasted from 38 Ma to <36 Ma. Intrusive activity was at a maximum at this time but continued until 32 Ma. Then, a sinstral transtensive stress regime was established, perhaps as a consequence of reduced convergence rates during the

Oligocene (Pardo-Casas and Molnar 1987) which may have allowed relaxation. The sinistral shear stress at this time is not in accordance with the convergence obliqueness deduced by these authors. It may have been generated by a clockwise rotation of the southern Central Andes, as proposed by Armijo and Thiele (1990) for sinstral shear along the Atacama Fault of the Coastal Cordillera during the Quaternary.

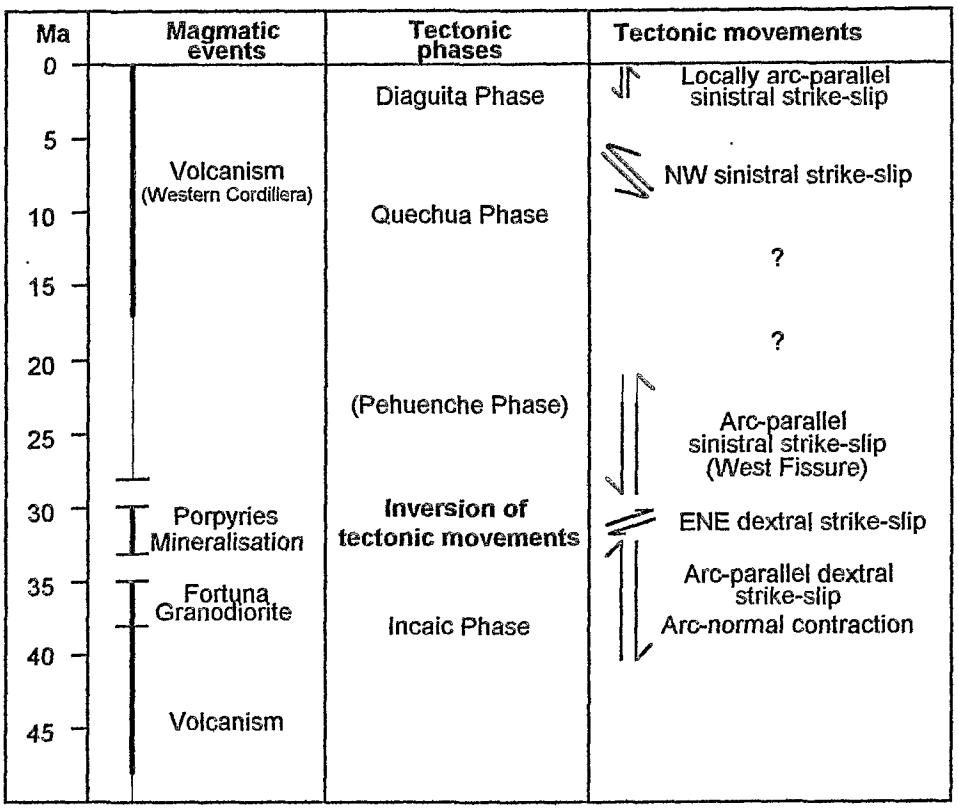

Fig. 2: Sketch of the tectonic development of the Chilean Precordillera near Chuquicamata.

REFERNCES

Armijo, R. and Thiele, R. (1990) Active faulting in northern Chile: ramp stacking and lateral decoupling along a subduction plate boundary. Earth Planet Sci Lett 98: 40-61.

Maksaev, V. (1990) Metallogeny, geological evolution, and thermochronology of the Chilean Andes between latitudes 21° and 26° South, and the origin of major porphyry copper deposits. PhD Thesis Dalhousie University Halifax Canada, 554 p.

Maksaev, V.; Boric, R.; Zentilli, M. and Reynolds, P.H. (1988) Metallogenetic implications of K-Ar, 40Ar-39Ar, and fission track dates of mineralized areas in the Andes of northern Chile.- 5 Congr Geol Chileno Actas 1: B65-B86.

Pardo-Casas, F. and Molnar, P. (1987) Relative motion of the Nazca (Farallon) and South American plates since late Cretaceous time.- Tectonics 6: 233-248.

Reutter, K.-J., Scheuber, E and Helmcke, D. (1991) Structural evidence of orogen-parallel strike slip displacements in the Precordillera of Northern Chile.- Geol Rdsch 80: 135-153.

Scheuber, E. and Reutter, K.-J. (1992) Magmatic arc tectonics in the Central Andes between 21° and 25° S.- Tectonophysics 205: 127-140.

A PALEOMAGNETIC STUDY OF THE ALTIPLANO

Pierrick Roperch(1), Michel Fornari(2) and Gérard Hérail(3)

(1) ORSTOM et Laboratoire de Géophysique, Campus de Beaulieu, 35042 Rennes, Cedex
(2) ORSTOM, C.P. 8714, La Paz, Bolivia
(3) ORSTOM, Casilla 53390, Correo Central, Santiago 1, Chile

RÉSUMÉ: Les résultats paléomagnétiques disponibles pour le Mésozoique et le Cénozoique indiquent des rotations antihoraires au Pérou et horaire au Nord Chili. Cette étude présente des résultats obtenus sur l'Altiplano bolivien (1) dans une séquence volcanique miocene du sud-Lipez, (2) dans des sédiments tertiaires de la formation Tiwanaku et Kollu Kollu à l'ouest de LaPaz et (3) dans les formations permo-carbonifère au niveau du lac Titicaca.

KEY WORDS: Palaeomagnetism, Tectonic Rotation, Bolivian Altiplano, Orocline

INTRODUCTION

Previous paleomagnetic results (Heki et al., 1983, Kono et al., 1985, Macedo et al., 1992, Roperch and Carlier, 1992) from Mesozoic rocks from coastal Peru and northern Chile have suggested that the present shape of the Andean chain is the result of oroclinal bending. A model of in situ block rotations associated to oblique convergence is an alternative interpretation of the paleomagnetic data (Beck, 1988; Dewey and Lamb, 1990).
In order to better understand the pattern of tectonic rotations observed in the Central Andes, we have undertaken a paleomagnetic study of the Bolivian Altiplano. The structure of the Altiplano is complex with fold-thrust belts and wrench-fault zones (Sempéré et al, 1990). Thus, the paleomagnetic sampling was made in several structural zones. Miocene volcanics and sediments were sampled in the southern part of the Lipez basin. A paleomagnetic sampling was undertaken in Eocene red sandstones from the Camargo syncline. The Oligo-Miocene Tiwanaku red beds formation was sampled south-west of La Paz and four sites were drilled in the Miocene sediments of Kollu-Kollu formation. Finally we will present preliminary results obtained in Permian-Carboniferous rocks (Copacabana limestone and Permian red-beds) which outcrop near the Lake Titicaca.

PALEOMAGNETIC RESULTS

About 80 sites were sampled in Bolivia. At each site about 10 cores were collected with a portable gasoline core drill. The magnetization of all samples from volcanic units was measured with a spinner magnetometer while a cryogenic magnetometer was used for most sedimentary units. The characteristic remanent magnetizations were determined after stepwise (10 to 15 steps) progressive thermal or alternating field demagnetizations.
The results will be presented for each region shown on Figure 1.

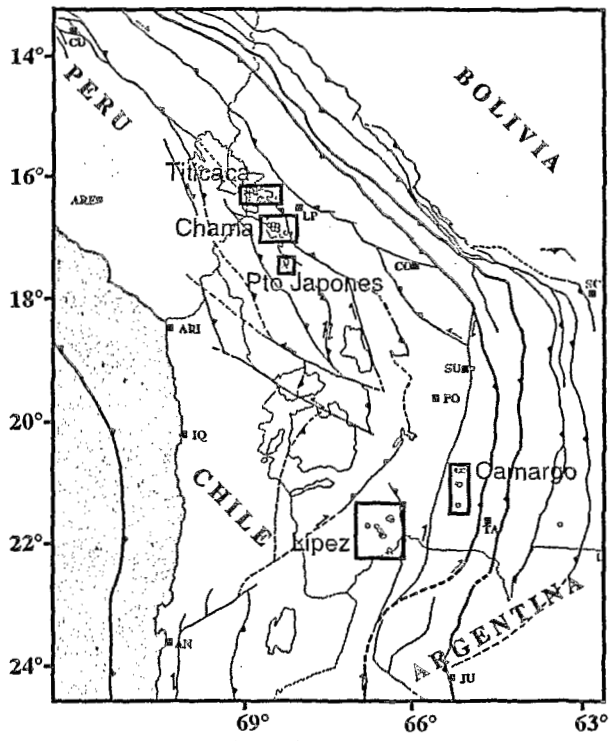

Figure 1: Paleomagnetic sampling map in Bolivia (structural sketch from Sempere et al., 1990)

A) Lipez

Thirty two sites were sampled in tertiary units south of the locality of San Pablo de Lipez. Out of these 32 sites, 16 sites correspond to the Miocene Rondal volcanics dated by K-Ar to about 20 Ma (Bonhomme, unpublished results).

The characteristic magnetizations were easily identified in the Rondal formation (Figure 2a). Directions of reversed polarity (positive inclination, south-west declination) are found at 13 sites and a normal polarity is observed at two sites. An intermediate direction is observed at one site and is rejected from the mean calculation. The mean direction (Declination=219°; Inclination= 38°, $\alpha 95$=11°) is rotated about 40° clockwise from the expected direction.

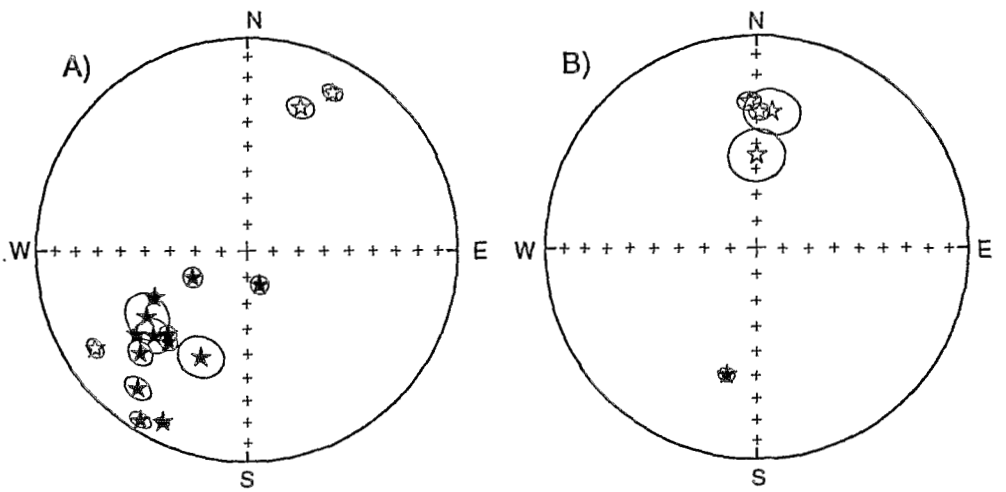

Figure 2: Equal area projection of mean-site paleomagnetic results with associated angle of confidence at 95% for the Lipez area. (A) Miocene Rondal volcanics, (B) sediments. Open symbols correspond to negative inclinations and solid symbols to positive inclinations. All data are tilt-corrected.

Results from sediments are only available at 5 sites located north of the Guadalupe area where the volcanics were sampled. The declinations in the sedimentary sites are not deflected clockwise as it was observed in the volcanics. The structural and stratigraphic relations between the Guadalupe and San Pablo areas which are 20 km apart still need to be clarified for an accurate interpretation of the discrepancy between the two sets of paleomagnetic data in south-west Bolivia.

B) Camargo syncline
Eight sites (85 samples) were drilled in the Eocene red sandstones. A complex remanent magnetization is observed possibly due to several phases of diagenetic formation of hematite. Thus, no characteristic mean paleomagnetic result is available for this area.

C) Pto. Japones and Chama
Four sites (44 samples) were sampled in the Kollu Kollu formation in the area of Pto Japones and 13 sites (148 samples) were obtained in red beds from the Tiwanaku and Coniri formations. Normal and reversed magnetizations are found after thermal demagnetization (Figure 3a,b). The mean-site paleomagnetic directions observed at both localities (Pto Japones, 3 sites: D=162°, I=21°, $\alpha 95$=5°) (Chama, 9 sites: D= 167°, I=34°, $\alpha 95$=13°) are not statistically different. Thus a mean direction can be computed from all sites (12 sites: D=166°, I= 30°, $\alpha 95$=10°).

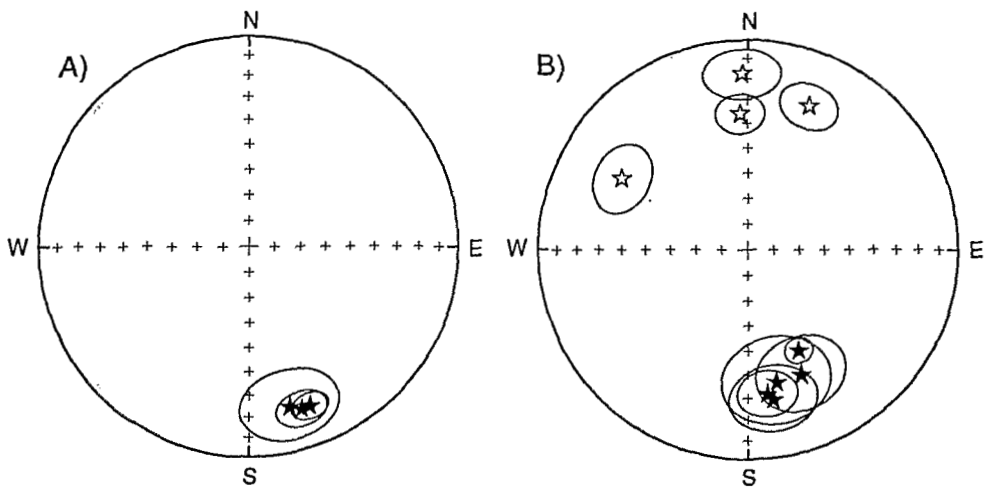

Figure 3: Equal area projection of mean-site paleomagnetic results with associated angle of confidence at 95% for (A) Miocene sediments from Pto Japones locality, (B) Oligo-Miocene red beds of the Tiwanaku formation (Chama locality). Same conventions as in Figure 2

D) Lake Titicaca

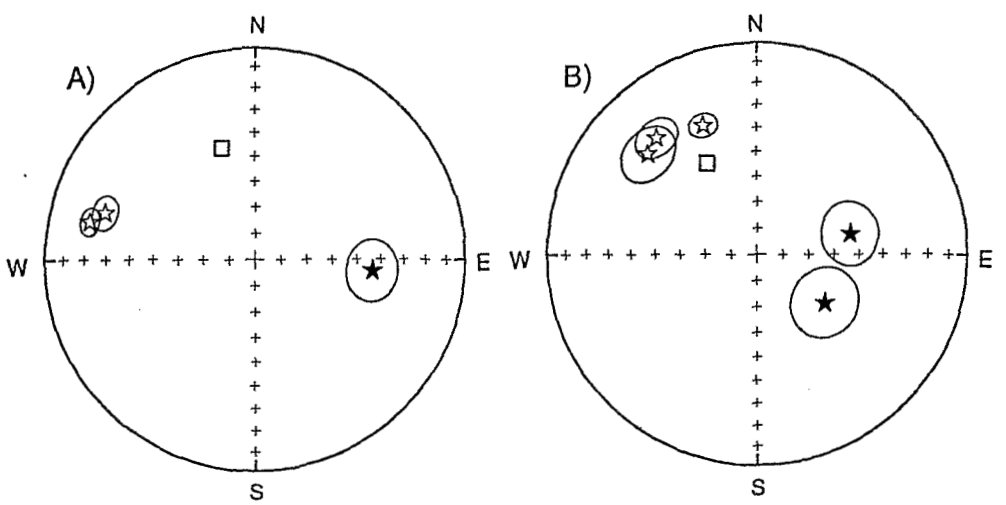

Figure 4: Equal area projection of mean-site paleomagnetic results with associated angle of confidence at 95% for the Titicaca area (A) Upper permian red-beds, (B) Copacabana limestone. The square corresponds to the expected paleomagnetic direction for stable South-America at about 250Ma (A) and 310Ma (B). Same conventions as in Figure 2.

Three sites (41 samples) were sampled in the Permian units near the Tiquina straits and 6 sites (59 samples) were taken in the Copacabana limestone. A soft component of magnetization removed by alternating field demagnetization is often found in the limestone making difficult an accurate determination of the primary magnetization. However the between-site scattering decreases after bedding correction suggesting a primary origin for the magnetization. Normal and reversed magnetizations are found that suggest that the copacabana limestones were deposited before the long-reversed Kiaman superchron and that the permian red-beds postdates the end of the Kiaman. The large counterclockwise deviation of the declinations observed for the Permian sites is not clearly documented by the other Carboniferous sites. The Permian sites are located nearby a major fault and the recorded counterclockwise rotation suggests a sinistral motion along that fault.

DISCUSSION

Few paleomagnetic data from Bolivia have been published. The most significant data are those reported by Mc Fadden (1990). Our result from the Rondal volcanics and the clockwise rotation of about 18° reported from a middle Miocene section at quebrada Honda (McFadden, 1990) demonstrate the existence of clockwise block rotations in southern Bolivia, possibly associated to dextral faults.
In northern Bolivia, the deviation of the mean declination in a late Oligocene-early Miocene section in the eastern Cordillera (Salla locality, McFadden, 1990) is only of -7°. In contrast, our mean result from the Oligocene-Miocene red beds from the Altiplano indicates a deviation of -14°. This result is not different from those reported for tertiary units in Peru, the Ocros dyke swarm (Heki et al., 1985) and the Lima area (Macedo et al., 1992). Although the amount of tectonic rotations is dependent of local structures and a mean paleomagnetic result obtained from several sites in different structural blocks does not imply that the whole area is rotated by the mean paleomagnetically derived rotation, the apparent coherence in the mean paleomagnetic declinations from Lima to La Paz is striking.

In conclusion, the paleomagnetic results obtained during this study confirm the existence of relative rotations between the northern and southern structural blocks that composed the Altiplano.

REFERENCES

BECK, M.E., 1988, Analysis of late-Jurassic-recent paleomagnetic data from active plate margins of South America, *J. S. Amer. Earth Sci.,1*, 39-52.
DEWEY, J.F. and S.H. LAMB, 1990, Andean displacement and strain partitioning of the Nazca-South America slip vector during the last 5 Ma., in *"Colloques et Séminaires" Symposium International : Géodynamique Andine*, ORSTOM ed., p77.
HEKI, K., Y. HAMANO, and M. KONO, 1985, Paleomagnetism of the neogene Ocros dike swarm, the Peruvian Andes: implication for the Bolivian orocline, *Geophys. J. R. astr. soc., 80*, 527-534.
KONO, M., K. HEKI, and Y. HAMANO, 1985. Paleomagnetic study of the central Andes: Counterclockwise rotation of the Peruvian block, *J. Geodyn., 2*, 193-209.
MACEDO-SANCHEZ, O., J. SURMONT, C. KISSEL, and C. LAJ, 1992, New temporal constraints on the rotation of the Peruvian Central Andes obtained from paleomagnetism, Geophys. Res. Lett., 19, 1875-1879.
MCFADDEN, B.J., 1990, Paleomagnetism of late cenozoic Andean basins and comments on the Bolivian orocline hypothesis, in *"Colloques et Séminaires" Symposium International : Géodynamique Andine*, ORSTOM ed., p57-60.
ROPERCH, P., and G. CARLIER, 1992, Paleomagnetism of mesozoic rocks from the Central Andes of Southern Peru: Importance of rotations in the development of the Bolivian orocline, *J. Geophys. Res., 97*, 17,233-17,249.
SEMPÉRÉ, T., G. HÉRAIL, J. OLLER, P. BABY, L. BARRIOS, and R. MAROCCO, 1990, The Altiplano: A province of intermontane foreland basins related to crustal shortening in the Bolivian orocline, in *"Colloques et Séminaires" Symposium International : Géodynamique Andine*, ORSTOM ed., p.167-170, 1990.

ANDEAN GEODYNAMIC SETTING AND ARCHITECTURE OF THE CALINGASTA-IGLESIA INTERMONTANE VALLEY (31°-31° 40' S), ARGENTINA

Eduardo A. ROSSELLO (1) and Oscar R. LOPEZ-GAMUNDI (2)

(1) CONICET - Departamento de Ciencias Geológicas, Universidad de Buenos Aires, 1428 - Buenos Aires, Argentina.
(2) TEXACO Inc., Frontier Exploration Department, Bellaire, 77401-2324, Texas, USA.

RESUMEN: El extremo austral del Valle intermontano Calingasta-Iglesia está caracterizado por una tectónica andina (Plio-Pleistocena) compresiva con una componente transcurrente dextral subordinada En esta latitud (aproximadamente 31° S), la Precordillera se superpone por retrocabalgamiento al relleno de edad triásica y neógena del Valle Calingasta-Iglesia, contrastando con el menor acortamiento expresado en el extremo septentrional del mismo valle.

KEY WORDS: Andean geodynamics, Calingasta-Iglesia Valley, ramp basin, western Argentina

The Calingasta-Iglesia Valley (**CIV**) is a N-S trending intermontane depression between the Frontal Cordillera (Paleozoic marine rocks and Permo-Triassic volcanics and associated granitoids) and the Precordillera (Paleozoic to Triassic clastic sediments and metasediments) morphostructural provinces. The **CIV** fill is mainly constituted by a Neogene sedimentary pile deposited in a foreland setting during crustal shortening and uplift of the Frontal Cordillera and the Precordillera. The preserved section, characterized by non-marine, often tuffaceous, clastic deposits, locally exceeds 4 km of thickness. The Miocene to Quaternary sediments, along with Triassic fluvial and lacustrine deposits, are extensively exposed on the western flank of the Precordillera.

In the southern part of the **CIV,** at the latitude of Calingasta (31° 30' S), excellent exposures show folds and westward-verging thrusts. Detailed structural field observations, coupled with evidence from seismic information, indicate that the eastern margin of the valley was subjected to compression by the end of the Tertiary and Quaternary. Kinematic indicators suggest a tectonic transport vector towards N 80° E. Eastward-verging backthrusts on the western flank of the Precordillera imparts a ramp basin configuration,with a subordinate right lateral component, to the **CIV.**

Contrastingly, a recent model for the northern segment of the **CIV,** at the latitud of Iglesia (30° 20' S), suggests a piggyback basin passively transported above a horizontal decollement (Beer *et al.*, 1990). This change of tectonic style may be tentatively related to depth variations in the Benioff zone (*cf.* Isacks,

1988) or shortening contrast due to cross-strike dextral transfer (Dewey & Lamb, 1992).

REFERENCES

Beer, J. A., R. W. Allmendinger, D. E. Figueroa & T. E. Jordan, 1990. Seismic stratigraphy of a Neogene piggyback basin, Argentina. Am. Assoc. Petrol. Geol., Bull. 74 (8),1183-1202.
Dewey, J. F. & S. H. Lamb, 1992. Active tectonics of the Andes. Tectonophysics, 205, 79-95.
Isacks, B. J., 1988. Uplift of the Central Andean Plateau and bending of the Bolivian Orocline. J. Geophys. Res., 93, 3211-3231.

STRUCTURAL ANALYSIS OF THE EASTERN BORDER OF CORDILLERA ORIENTAL BETWEEN 24 50 AND 26° 50 SOUTH LATITUD-ARGENTINA

José SOSA GOMEZ (1) and Ricardo GOMEZ OMIL (2)

(1) CONICET UNT M. Lillo 205 4000 Tucumán Argentina
(2) Pluspetrol S.A. La Rioja 301 1214 Bs. As. Argentina

Resumen:

Se analiza la geometría estructural en la faja del antepaís andino sobre el frente E de Cordillera Oriental (FECO),allí se observa un cambio del estilo en sentido N-S coincidiendo con alteraciones en la paleogeografía del antepaís.Se determinan dos eventos importantes en la compresión con reactivación de fallas normales del graben Cretácico.

Key Words: Andine compression, Thrust front, Cordillera Oriental

Introduction

In this paper we summarized several observations about the Andean tertiary deformation in the fold thrust belt between 24°50 and 26°50. The work is focused on the activity of the compressive front of the eastern border of the Cordillera Oriental (FECO) in a region of Hydrocarbon interest.

The Cordillera Oriental, is a region characterized by relatively steep faults, with antagonic vergences of the fault planes.

North of the Juramento river are exposed Paleozoic and Cenozoic rocks units in the mountain nucleous,south of them, are only Precambrian. As yet this work give a coherent solutions in the styl and structural geometry, there are still many unanswered questions, in our oppinion treatment of the following questions are still needed: 1- Influence of basement foliation, 2-vertical uplift vs. lateral desplacement, 3-timing of evolution. The present geometry is the product of several events or phases of development during the Neogene.

Stratigraphy

Rock units exposed in the studied area range from the Precambrian to the Cenozoic. Older rock units built the nucleous from the uplifted blocks at the mountain front.

Precambrian. These units are exposed in the nucleous of the Metán and Cumbres Calchaquíes ranges. They are monotonous lithologies from marine sequences, dominated by alternating shale and sandstone in lower metamorphic and twofold phases.

Cambrian Meson Group overlay in angular unconformity the Precambrian, consists in pink quartzite, or bedded sandstone and less conglomerate this units are only exposed in the Mojotoro ranges.Skolithos is the

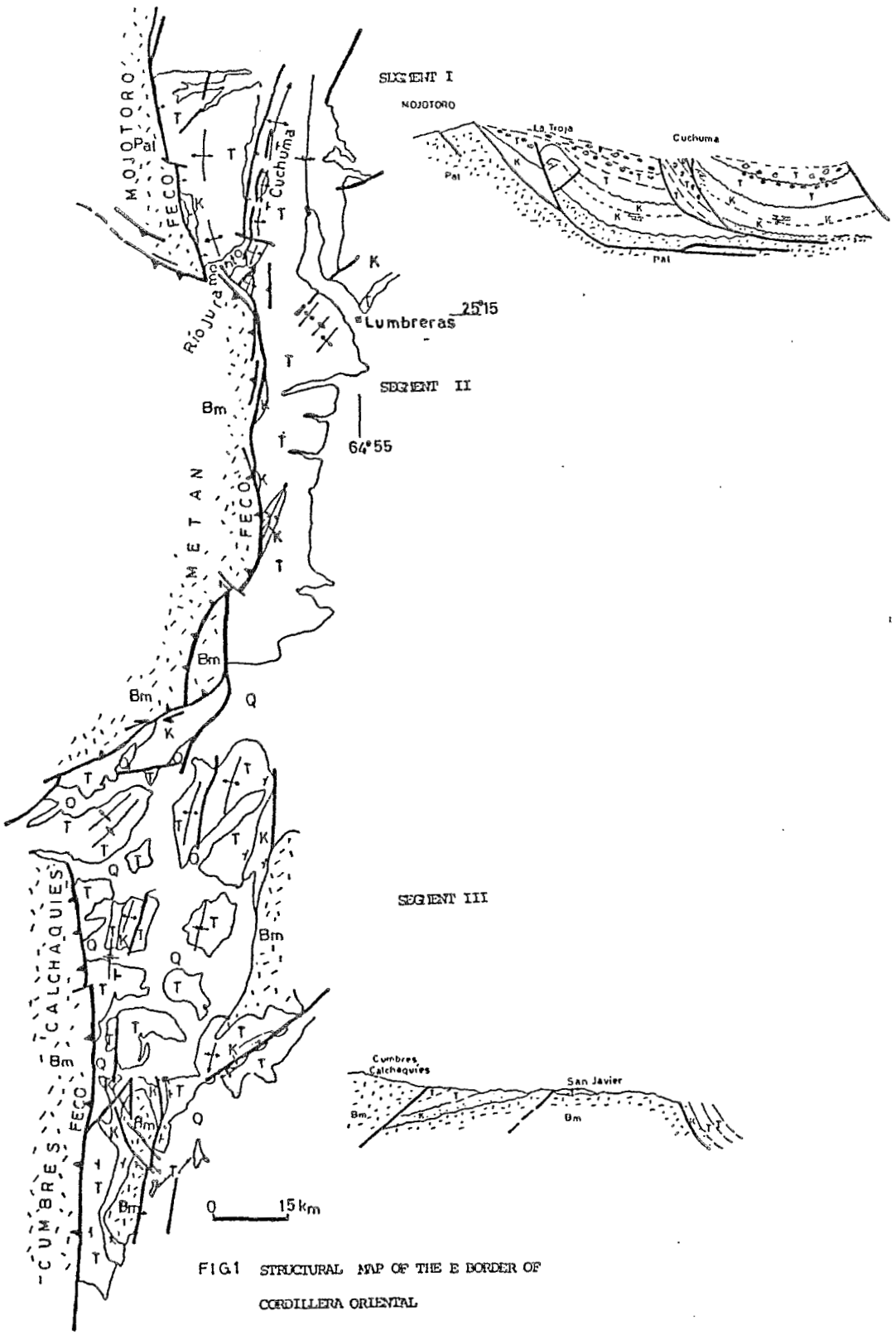

FIG.1 STRUCTURAL MAP OF THE E BORDER OF CORDILLERA ORIENTAL

Bm Basement-Pal Paleozoic-K Cretaceous
T Tertiary

common bioturbation.

Ordovician rock overlay in angular unconformity the Precambrian and conformable the Meson Group, consists in fossilifcrous siltston whith trilobites and brachiopods.

Cretaceous-Eocene;Salta Group.The Balbuena reds beds with calcareous intercalations outcrops direct at the principal front.From the Santa Bárbara upper red beds only the Lumbrera Fm was found in the core of the Cuchuma anticline, consisting mainly of a succession of red mudstones with layer of nodular gypsum, a basal contact is not observed. Depositional environment was characterized as shallow lakes.

The Mio-Pliocene Oran Group is a synorogenic continental sequence divided into five formations. The lower Río Seco Fm, overlays in angular unconformity the Lumbreras Fm. It consists of reddish fine grained sandstones thick-cross bedded.The features define an eolian environment. The Anta Fm consists of lacustrine strata, lithologiclly is composed by red and green mud-siltstone, on the top interbeded with nodular gypsum of considerable lateral continuity. The Jesús María Fm comprises fine-medium grained sandstones lenticulary stratified with intercalations of brown shales exhibiting parallel lamination. The Río Guanaco Fm is basically a polimictic conglomerate, supported in a calcareous matrix with well clasts ephericity.Thickness is greater in the synclines (structural controlled subsidence). The Piquete Fm overlay unconformable the Río Guanaco Fm, consists in conglomerates and breccias with large clasts poorly consolidate, distal intercalations of lenticular sandstones.As the distance from the front is greater, the angular unconformity is less important.

Structure

Eastward of the (FECO), a large and irregular fold fault belt was built due to an effort of the Cenozoic compression, the structural geometry is variable along the N-S trend.

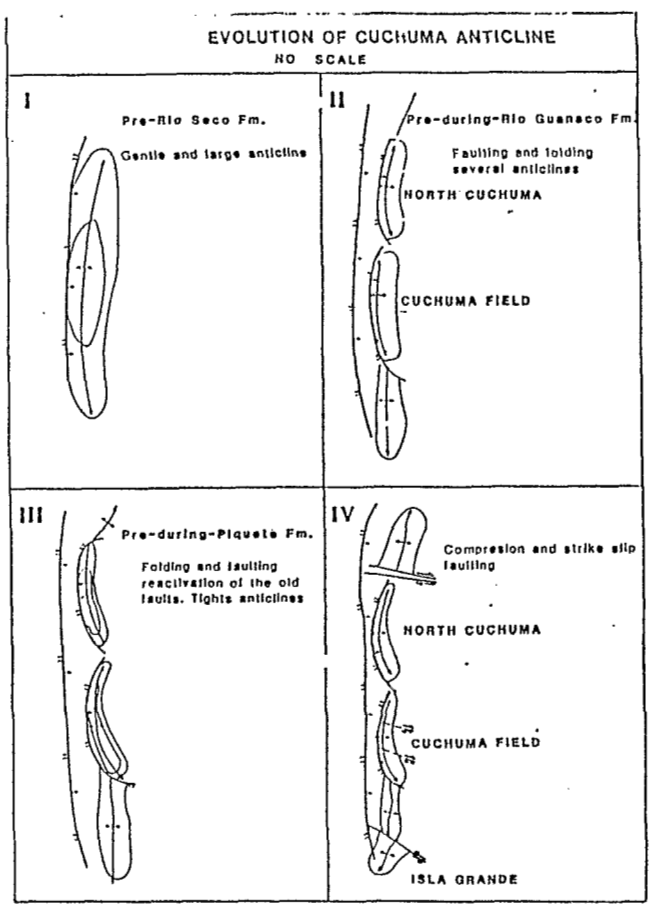

FIG 2

Fig.1 shows the geological features, by wich the FECO is divided into three segments. In the first segment, the frontal ramp of the Mojotoro sheet is W-vergent as the other eastward fault planes in the Tertiary-Cretaceous cover. One of the exhumated fault plane created the Cuchuma anticline; at the W limb of Cuchuma, a blindthrust built "La Troja" anticline. In this segment all fault planes may be defined as backthrust . Two angular unconformities are observed here; Fm Lumbrera-Río Seco and Fm Guanaco -Piquete; the first represent an older compressive event with the beginning of the inversion of the Cretaceous graben, the evolution of folds and faults is progesive as is interpreted in the fig.2.

The step into the south segment is coincident with a lateral ramp probably asociated with the Lineamiento del Toro (Mon, 1979; Sosa Gómez 1984) it is a left strike-slip fault with a reversal componcnt whose hangingwall lies at the S. Lateral desplacing is 8 km, similar in magnitude as in the Quebrada del Toro K.Schwab (pers.commun.)

The Metan sheet shows a progressive migration of the thrust front eastward; the older sequences in the block are Precambric. It is the eastern most migrates sheet in the FECO overthrusted folds structures near the front ramp fig. 1. As we can deduce from the position of the folds axis trend, the compression axis in this segment has changed from NW-SE at the earlier deformation to W-E in the latest. Thrust planes direct an the thrust front are cover by a variable thickness of conglomerate.

The souther most segment is the Cumbres Calchaquíes sheet, the transition between them and Metan is also a lateral ramp with right strike-slip an reversal component wich hanginwall lie at the N; NE- trending folds has alredy developed. The uplifted sheet exhumated Precambric sequences, with E-vergent fault plane. The folds train ends at S at a transverse structure "Lineamiento de Tucumán" (Mon 1979). At this front the conglomeratic sequences are not developad as the other two; the contact between Eocene-Miocene is an erosive unconformity.

Two schematic cross sections show the strong structural differences between the N and S sections (fig.1).

Conclusions

The tectonic activity of the FECO is heterogeneous and not fully understood; more detailled studies are necessary. The assumption generaly admited is that the shortening in this area began in the Pliocene-Pleistocen, but the angular unconformity (Fm Lumbrera-Río Seco), suggest a compressive event in the Upper Eocene-Lower Miocen, at least in the N segment.

The development of the Cuchuma anticline and the progressive migration of the Metán sheet reveal polystage events in the compressive regimen. The sedimentation of younger conglomerate sequences at the E border of the FECO are even indicators for a repeat activity of the thrust front.

Recent movements of the FECO are expressed in reversal faults that cut off the conglomerate sequences.

References

MON, R. 1979 Esquema tectónico de los Andes del Norte Argentino. Rev Asoc. Geol. Arg. XXXIV (1):53-60.

SOSA GOMEZ, J. 1984. Investigación de fotolineamientos sobre imágenes LANDSAT en Las Sierras de San Antonio de Los Cobres, Crestón de la Aguada y los Nevados del Chañi. IX Congr. Geol. Arg. IV 95-103.

VERGANI, G. STARCK, D. 1989. Aspectos estructurales del valle de Lerma, al S de la ciudad de Salta. Boletín de Inf. Petroleras. pg. 2-9

COMPARATIVE EVOLUTION OF THE EASTERN CORDILLERA (COLOMBIA) AND THE ANDES OF MERIDA (VENEZUELA) SINCE MIOCENE

Jean-Pierre SOULAS

. Laboratoire Tectonique et Mécanique de la Lithosphère, Institut de Physique du Globe, Paris.
. Correspondance to : J.P. SOULAS, 18, allée des Mésanges-33120 Arcachon-France. tel.: (33)56830529 , (33)57522021

RESUMEN : La historia orogénica de los Andes de Venezuela y de la Cordillera Oriental de Colombia empieza en el Mioceno inferior. Después de este período de inicio común, las dos cordilleras evolucionaron separadamente hasta principios del Cuaternario, cuando adquieren el funcionamiento de conjunto actualmente vigente.

KEY WORDS : Venezuela, Colombia, Neogene, Quaternary, Tectonic evolution.

The Andes Cordillera of Merida forms, over about 450 km long and 100 km wide, a double-sided buckling structure oriented NE-SW. This structure seems to be rootless. Both of its sides are overthrusting extended lowlands in the NW and SE directions, respectively. Both vaults are separated by a strike-slip fault system (Bocono faults), which is running from one end of the chain to the other. The double-sided buckling structure is symetrical, or not, whether the strike-slip fault system lies along the chain axis, or not.

This mountain belt was generated by the convergence between the Lake of Maracaibo block and the South American shield. This convergence is lasting through the times since Miocene until now, with variable rates and directions . Since early quaternary times the convergence is oblique and one can observe that it is accomodated by the major sub parallel fault systems. The right-lateral component is parallel to the chain axis and is essentially absorbed by the central strike-slip system. The perpendicular component results in overthrusts oriented outward with respect to the chain axis. Such a mechanism implies that the overthrusts extends below the chain like surfaces of décollement, below which both convergent crustal blocks are slipped and quizzed. Moreover this mechanism implies that the main strike-slip fault system is a weak fault. This interpretation is in good agreement with the observed directions of maximum horizontal stress, closely perpendicular to the chain axis.

The Oriental Cordillera of Colombia looks more or less like a triangle extended NNE-SSW, 800 km long, and at most 240 km wide at its northern end. With respect to the classical andean system, which can be followed from the center of Peru, it represents an additional cordillera. These two mountain systems are separated by the depression of the Magdalena river, except at the southern end of the Oriental Cordillera, where both mountain belts join together. When sufficiently wide the Oriental Cordillera of Colombia looks like a locally highly broken highland. It is presently colliding obliquely with the South American shield. The angle between the chain axis and the direction of convergence is

very small southward and opens gradually northward. The most active deformations are concentrated eastward within a 20 to 60 km wide band. Two sub-regions with different tectonic mechanisms and separated by a transition zone must be considered in this strip band.

In the southern sub-region, over about 350 km, the convergence is accomodated by several subparallel systems similar to the Andes of Merida. Some faults are pure thrust. Others form a system of large en-echelon right-lateral strike- slip faults cutting obliquely through the southern part of the chain, from its western flank to the South, to its eastern flank to the North.

The transition zone is centered on Villavicencio. Here, thrust faults are not always parallel to the chain axis, right-lateral strike slip faults smoothly vanish northeastwards and the frontal underthrusting becomes more and more oblique. Finally, in the northern region, strike-slip faults become minor over the last 250 km and the underthrusting of the shield is accomodated with a large dextral component.

It must be noticed that the underthrusting of the shield is more important northeastward. This explains both the widening of the cordillera and a larger internal shortening, which partly takes place on the great reverse faults by which the cordillera is overthrusting the depression of the Magdalena river.

The active front of the Oriental Cordillera of Colombia is connected with the Venezuelan Andes through an extremely complexe deformed zone, oriented NW-SE, about 50 km wide, which is located at the border of both countries. Since early Quaternary both systems have the same pole of rotation and form the main limit between the Caribbean and South American plates.

Both cordilleras started their orogenic history simultaneously, in early Miocene, when the Venezuelan Andes began to be very progressively uplifted, with reverse faulting of its northwestward flank and intense continental flexuration outward from the chain. Meanwhile, the Oriental Cordillera of Colombia also began to be uplifted with almost the same tectonic features as the Venezuelan Andes : continental flexuration and intense reverse faulting.The orogenic initiation of both cordilleras could be the consequence of the collision of the Arc of Panama against the Occidental front of the South American continent.

Nevertheless, between this common early start and the Quaternary times, these two cordilleras develop themselves in different ways. In fact, the collision is already acting in Colombia in the middle Miocene (starting at the upper part of the lower Miocene ?), although probably following rates and directions different to the present ones. In the meantime, the convergence remains nearly perpendicular to the Venezuelan Andes except in Pliocene times when its orientation is such that the central strike-slip system becomes left lateral, opposite to the actual one.

PALAEOMAGNETIC STUDIES OF FAULT BLOCK ROTATIONS IN RELATION TO TRANSTENSION ON THE ATACAMA FAULT SYSTEM AND GRANITE EMPLACEMENT

Graeme K. Taylor(1), Darren Randall(1), John Grocott(2) and Peter J. Treloar(2)

(1) Department of Geological Sciences, University of Plymouth, Drake Circus, Plymouth, Devon PL4 8AA U.K.
(2) School of Geological Sciences, University of Kingston, Kingston Upon Thames, Surrey KT1 2EE U.K.

RESUMEN :

Los resultados palaeomagntic de rocas del Formación La Negra de la Cordillera de la Costa, entre 26° y 27° S, presenta dirección rotaciones horarias 35°. Esta rotacion son probalemente un resultado de moveimientos rotacionales in situ de bloque, esta resultado rotacion compuesta Juarsico y Cretacico.

KEY WORDS : Palaeomagnetism Jurassic Rotation Atacama Chile

INTRODUCTION

Palaeomagnetic studies of Jurassic and Cretaceous volcanic, sedimentary and intrusive units of the Coastal Cordillera of northern Chile have revealed the widespread occurrence of clockwise crustal block rotation. In contrast to this similar aged units in northernmost Chile, southern Peru and Bolivia have undergone anticlockwise rotation. These rotations have been viewed as being complimentary to one another and interpreted in terms of oroclinal bending (Kono et al., 1985), differential shortening across the arc induced by the pre-existing shape of the Pacific margin of South America (Isacks, 1988) or systematic regional shear of the forearc region (e.g. Beck, 1988). Fundamental to these models is the kinematic control of strike-slip fault systems on fault block rotation. This study aims to integrate the palaeomagnetic determination of the magnitude of fault block rotations with the detailed structural analysis of the kinematics of the block bounding faults in relation to transtension on the Atacama Fault System and the emplacement of plutonic complexes within the arc.

GEOLOGICAL SETTING

The area studied lies between 26 and 27° S and to the east of the Upper Palaeozoic Chañaral Melange (Bell 1987) and is bounded by the El Salado segment of the Atacama Fault System. The structurally highest unit is the Le Negra Formation thought to be of Upper Sinemurian to Lower Bajocian or Kimmeridgean in age and which is underlain by the Pan de Azucar formation of Hettangian-Sinemurian age (Naranjo 1978). These are separated from the basement and cut by, brittle, listric, left normal faults linked to the sinistral strike-slip faults of the Atacama Fault System. These units are intruded by Jurassic (c. 153 Ma) and Cretaceous (c. 127 Ma) wedge shaped plutons which are elongate parallel to the arc and young systematically to the east. These plutons are in turn cut by a series of dyke swarms which account for up to a further 15% East-West dilation of the area and which also systematically young to the east.

Over 80 palaeomagnetic sampling sites have been collected from the andesitic flows, tuffs and sandstones of the Le Negra formation and from dyke swarms which have yielded reliable Ar-Ar ages of 154Ma and 126Ma which intrude the plutons and from an undated, as of yet, but apparently younger third swarm which cuts the fault system itself. A total of 12 sites from the Le Negra formation have currently been studied. These yield a characteristic remanence which passes both a reversal and fold test which coupled with the remanence being found in a variety of lithologies clearly indicates the primary nature of the remanence. The mean direction (declination = 47.2, inclination -41.3, $k = 15.0$, $\alpha 95 = 4.2$ from 43 samples) indicates that the area has suffered a clockwise rotation of some 35° but no latitudinal transport, which is consistent with previous results from the Coastal Cordillera. At least part of this rotation is believed to be linked to and contemporaneous with the emplacement of the wedge shaped plutons., in particular the Cretaceous, 127 Ma, Las Tazas pluton whose outcrop and structure indicate that some 15-20° rotation of the area took place at this time.

CONCLUSIONS

The Le Negra formation exhibits a primary Jurassic palaeomagnetic remanence which indicates a net local block rotation of some 35°. At this time it is believed that this rotation is compound and comprises at least two separate age components. The palaeomagnetic analysis of the dated dyke swarms will reveal the timing and extent of rotation associated with the evolution of the fault system itself and will help to differentiate between progressive and punctuated fault block rotation. The study as a whole will better constrain the kinematic evolution of the arc itself and delineate the effects of back-arc basin development.

REFERENCES

Bell, C. M. 1987. The origin of the Upper Palaeozoic Chañaral melange of N. Chile. J. Geol. Soc. Lond., 144, 599-610.

Beck, M. E. 1988. Analysis of Late Jurassic-Recent palaeomagnetic data from active plate margins of South America. J. South American Earth Sciences, 1, pp 39-52.

Kono, M., Heki, K. and Hamano, Y. 1985. Palaeomagnetic study of the central Andes: Counterclockwise rotation of the Peruvian block. J. Geodyn., 2, 193-209.

Isacks, B. L. 1988. Uplift of the central Andean plateau and bending of the Bolivian orocline. J. Geophys. Res., 93, 3211-3231.

Naranjo, J. A. 1978. Zona Interior de la Cordillera de la Costa entre Los 26° y 26°20'. Carta Geologica de Chile, No. 34.

VERGENCE OF THE CORDILLERA OCCIDENTAL, ECUADOR: INSIGHTS FROM THE GUARANDA-RIOBAMBA AND ALOA-S. DOMINGO DE LOS COLORADOS STRUCTURAL TRAVERSES

Alessandro TIBALDI and Luca FERRARI

Dipartimento Scienze della Terra, Via Mangiagalli 34 Milano-20133, Italia

Resumen

Un levantamientos estructural de campo ha permitido reconstruir el estilo de deformaciòn y el sentido de transporto en la parte central de la Cordillera Occidental. A la latitud de Riobamba se encuentran pliegues cierrados hasta "chevron" con immersion constante del piano axial a ONO. Algunos pliegues son cargados con el fianco oriental reverso. Las fallas son inversas con inmersiòn dominante al oeste. A la latitud de Aloa, la deformaciòn principal es de tipo fragil con fallas inversas inclinadas hacia el ONO y algunos pliegues abiertos con eje N-S.

Key Words: tectonics, folds, faults, vergence, Ecuador.

Introduction

The Ecuadorian Andes are formed by the parallel mountain ranges of Cordillera Occidental (CO) and Cordillera Real (CR), separated by the Interandean Valley (IV). The CO is mainly formed by Cretaceous volcanic rocks with island arc affinity (Macuchi Fm.) (Henderson, 1979) covered by discontinuous flysch-like deposits and carbonatic rocks of Cretaceous to Eocene age. The CO is considered an allochtonous terrane accreted onto the South American margin during a major tectonic phase in early Tertiary time (Lebras et al., 1987; Roperch et al., 1987; Wallrabe-Adams, 1990), while during Plio-Quaternary times was affected only by minor tectonic activity (Pasquarè et al., 1990; Ferrari and Tibaldi, 1992).

The suture between the CO island arc and the continental paleomargin represented by the CR is concealed under the Tertiary and Quaternary volcanic and continental deposits of the IV, as confirmed also by geophysical prospecting (Feininger and Seguin, 1983). The geometry of the suture zone fault system has important implications on the deformation models for the IV and for the whole Ecuadorian Andes. Juteau et al. (1977) recognized ophiolitic slices of the CO dipping steeply towards the East and interpreted this setting as resulting from accretion along east-dipping thrust planes. Nevertheless some field inspections in selected areas of the CO (Tibaldi and Ferrari, 1992a), showed that the main faults have a relatively constant NNE-SSW strike and WNW dip.

Here we present structural data collected along two E-W transects crossing the CO at the latitude of Riobamba and S. Domingo de Los Colorados (30 km) which contribute to clarify the vergence problem of the CO, at least in its central part.

Geological and structural setting

The CO, along the studied transects, is made of three main geological units (Fig. 1). The western part of the area is made of andesite rocks belonging to the Cretaceous Macuchi Formation. In the main part of the section are exposed late Cretaceous carbonatic rocks of the Yunguilla Formation which are covered toward the east by pliocenic andesite lava flows.

The Cretaceous andesites show only brittle deformations in the form of closely-spaced fractures along vertical and sub-vertical north striking planes. Reverse faults (pitch between 60° and 90°) are are also present and dip mostly westward at variable angles (10°-80°, dominant 10°-20°). A few E dipping planes are also found with inclination of 10°-15°. The contact between the Macuchi andesites and the marine sediments of the Yunguilla Formation is vertical.

The whole Yunguilla succession is folded with variable intensity and style. Going eastwards along the traverse of Figure 1, the strata are arranged in moderately closed folds with hinge lines striking between NNW and NNE. Reverse faults have a strongly dominant W to WSW dip and their inclination is usually high (60°-70°). About 3 km eastwards of the limit with the Macuchi Fm. the Yunguilla strata depict moderately closed decametric folds. Hinge lines strike N-S with a clear and constant W dip of fold planes. More to the east, along the E-W course of the Ganquis river the Yunguilla Formation is involved in a sequence of large east-vergent folds which culminate with an eastward recumbent fold. All these folds have NNE striking hinge lines. Some west dipping reverse faults also cut this section. Where the Ganquis river course passes to an ESE strike, a large eastward recumbent anticlinal is associated to west dipping reverse faults. From this point up to Mount Cangagua, large moderately closed folds are dominant. Hinge line azimuth is NNE while vergence, when present, is towards ESE. As in other cases, the hinge line of a given fold sometimes changes from a NNE to a NNW direction. Eastwards of Mt. Cancagua, deformation rate increases; large recumbent synclines and anticlines with NNE striking hinge line are followed by densely spaced chevron folds with N-S hinge lines and west dipping axial planes. A reverse fault dips westwards at low angle (5°) with the sense of shear marked by small drag folds with NNW striking hinge lines. Near the contact with the Pliocene andesites, sedimentary rocks are arranged in closely spaced folds with axial planes dipping towards NW. Pliocene andesites show a low grade of deformation. They are cut by small fractures and faults dipping mainly towards NE with inclination angles between 60° and 70°. Slikensides indicate reverse motions with pitches ranging between 80° and 90°.

The Aloa-S. Domingo de los Colorados structural traverse is characterized by brittle deformations interesting mainly the Macuchi Formation. The main structures are represented by west dipping reverse faults with inclination from 45° to 75° (Fig. 2). The general bedding arrangement suggests broad anticlines with N-S to NNE-SSW hinge lines. Nevertheless this section is covered by very dense jungle and, as a consequence, data are less abundant than in the other traverse.

Conclusions

The data collected along the two structural traverses are consistent and show a vergence towards the angular sector comprised between E and ESE. This is expressed by dominant folding with WNW dipping axial planes in the carbonatic rocks. Reverse faults are widespread and represent the only evident deformation in the volcanic units. The dominant westward dipping of the fault planes is consistent with the fold vergence, although a small amount of backthrusts is also present. High angle reverse faults with near vertical motions (fault plane inclination > 50°, pitch > 70°) could indicate the presence of rotated motion planes and therefore a polyphase deformation history with no major changes of motion vectors. As a whole, the southern and more complete traverse is characterized by a gradual changing in the deformative style toward the east, passing from nearly symmetric, moderately closed folds to recumbent and chevron folds with west dipping axial plane. The majority of these deformations should have occurred between Paleocene and Miocene. Pliocene rocks are only cut by fractures and a few NE dipping reverse faults.

If these two traverses are representative of the style and geometry of deformation of the central CO front, they suggest a tectonic transport of this CO segment towards ESE and a WNW dip of the fault system buried under the IV filling. On the other hand another possibility is that this fault system would be vertical, while a ESE dip should be considered unlikely. A high angle WNW dip, as proposed in Baldock (1982, 1985), seems more coherent with the interpretation of the CO structure as due to obduction and is consistent with the hypothesis of Tibaldi and Ferrari (1992b) that the IV could be a basin carried piggyback (passively) on a transpressive thrust complex.

ACKNOWLEDGMENTS

We thanks N. Fusi for field assistence. The research was partially supported by Ph.D. grants from Ministero Italiano della Pubblica Istruzione, by INECEL, Quito and ELC Electroconsult, Milan.

REFERENCES

Baldock J. W., 1982. Geologia del Ecuador (Boletin de la explicaciòn y mapa geologico de la Republica del Ecuador, escala 1 : 1,000,000). Direcciòn General de Geologia y Minas, Quito, 71 pp.

Baldock J. W., 1985. The Northern Andes: a review of the Ecuadorian Pacific Margin. In "The Ocean Basins and Margins", A. E. M. Nairn, F. G. Stelhi and S. Uyeda (eds.), Plenum Press, New York and London, Vol. 7A, (The Pacific Ocean), 181-217.

Feininger T. and Seguin M.K., 1983. Simple Bouguer gravity anomaly field and the inferred crustal structure of continental Ecuador. Geology, 11, 40-44.

Ferrari L. e Tibaldi A., 1992. Recent and active tectonics of the North-eastern Ecuadorian Andes. J. of Geodynamics, 15, 39-48.

Henderson W.G., 1979. Cretaceous to Eocene volcanic arc activity in the Andes of northern Ecuador. J. Geol. Soc., London, 136, 367-378.

Juteau T., Megard F., Raharison L. and Whitechurch H., 1977. Les assemblage ophiolitique de l'occident equatorien: nature petrographique et position structurale. Boll. Soc. Geol. France, t. XIX, n° 5, 1127-1132.

Lebras M., Megard F., Dupuy C. and Dostal J., 1987. Geochemistry and tectonic setting of pre-collision Cretaceous and Paleogene volcanic rocks of Ecuador. Geol. Soc. Am. Bull., 99, 569-578.

Pasquarè G., Tibaldi A. and Ferrari L., 1990. Relationships between plate convergence and tectonic evolution of the Ecuadorian active Thrust Belt. In: Agusthithis S.S. (Ed.), Critical Aspects of Plate Tectonic Theory, Theophrastus Publications, Athens, 365-387.

Roperch P., Megard F., Laj C., Mourier T., Clube T.M. and Noblet C., 1987. Rotated oceanic blocks in western Ecuador. Gophys. Res. Letts., 14, 5, 558-561.

Tibaldi A. and Ferrari L., 1992a. Latest Pleistocene-Holocene tectonics of the Ecuadorian Andes. Tectonophysics, 205, 109-125.

Tibaldi A. e Ferrari L., 1992b. From Pliocene pure shear to Quaternary transpression and transtension in the Interandean Valley, Ecuador. J. of Geodynamics, 15, 59-84.

Wallrabe-Adams H., 1990. Petrology and geotectonic development of the Western Ecuadorian Andes: the Basic Igneous Complex. Tectonophysics, 185, 163-182.

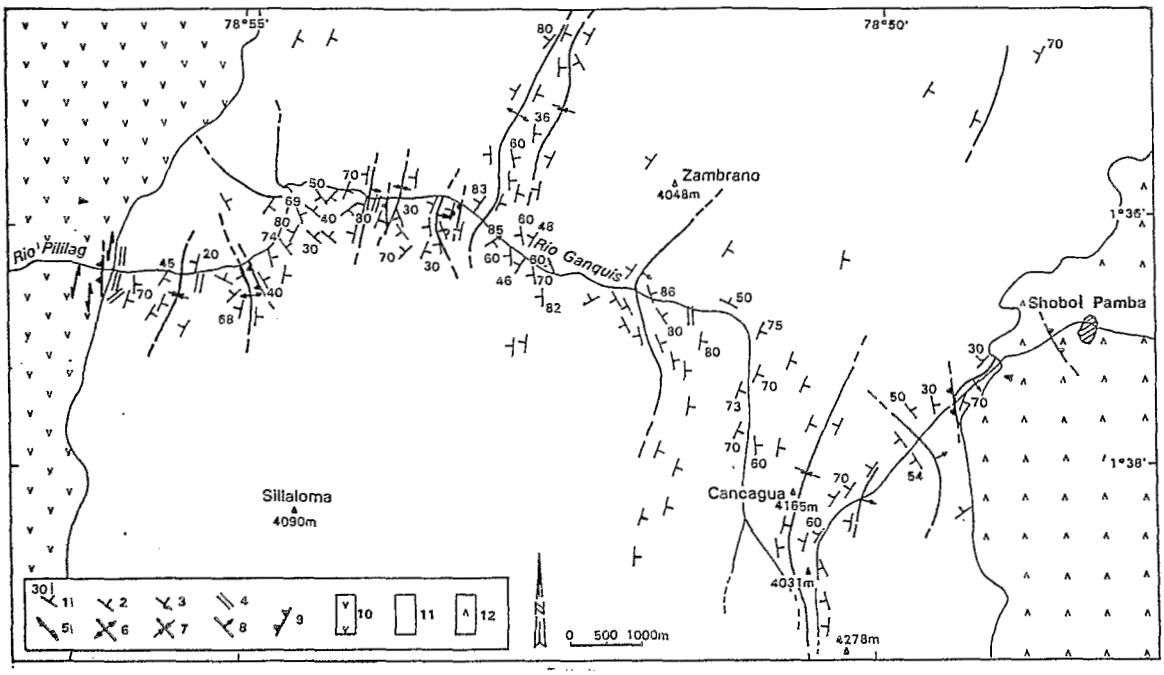

Figure 1. Structural map of the Guaranda - Riobamba traverse. 1 = Bedding attitude (with inclination) measured in the field. 2 = Bedding attitude deduced by aerial photograps. 3 = Recumbent strata. 4 = Vertical strata. 5 = Average direction of fractures. 6 = Anticline axis. 7 = Syncline axis. 8 = Recumbent fold. 9 = Reverse fault. 10 = Cretaceous volcanics (Macuchi Fm.) 11 = Late Cretaceous carbonate rocks (Yunguilla Fm.) 12 = Pliocene andesites.

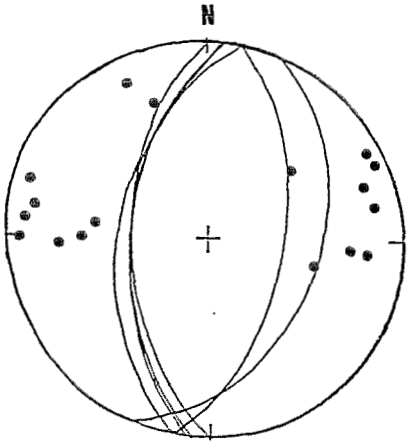

Figure 2. Main structures in the Aloa-S. Domingo de los Colorados traverse. Great circles represent major reverse faults; dots are poles to bedding. Schimdt projection, lower emisphere.

STRUCTURAL GEOLOGY OF THE SIERRA CASTILLO - AGUA AMARGA FAULT SYSTEM, PRECORDILLERA OF CHILE, EL SALVADOR-POTRERILLOS

Andrew J. TOMLINSON[1], Constantino MPODOZIS[1] , Paula C. CORNEJO[1], and Carlos F. RAMIREZ[1]

(1) Servicio Nacional de Geología y Minería, Avda. Santa María 0104, Santiago, Chile

RESUMEN: El sistema de la falla Sierra Castillo - Agua Amarga es parte de un sistema de fallas activas a lo largo del eje del arco magmático Eoceno-Oligoceno inferior, asociado al emplazamiento de pórfidos cupríferos del norte de Chile. Las estructuras y relaciones de edad en las zonas adyacentes al sistema de la falla Sierra Castillo - Agua Amarga indican un régimen transpresivo sinistral regional, durante a lo menos el rango de ~42-39 Ma. El sentido de movimiento sinistral en el margen continental es contradictorio con las reconstrucciones de movimiento de placas en el Eoceno, indicando que habría un error en las reconstrucciones o bien, una mayor complejidad cinemática para la deformación del margen continental.

Key Words: Structure, Northern Chile, Eocene, Copper porphyry, Transpression

INTRODUCTION

The Eocene-Lower Oligocene magmatic belt in northern Chile is anomalous for its numerous and large copper porphyry systems, and is closely associated with the Domeyko fault system, a system of strike-slip and reverse faults in the Chilean Precordillera. Increasingly, studies indicate the Domeyko fault system was active during the life span of the Eocene - Lower Oligocene copper porphyry magmatic arc, having both important strike-slip and shortening deformation associated with it (Maksaev, 1990; Reutter et al., 1991). However, there is still uncertainty concerning the sense of shear of the strike-slip movement, with evidence for both sinistral and dextral shear being found on the master fault system (Maksaev, 1990)

In the El Salvador - Potrerillos area, 26° - 27° S latitude, the Domeyko fault system is represented by the Sierra Castillo and Aqua Amarga faults (Figure 1). Although the timing and kinematics of these faults is poorly constrained, the deformation in their eastern borderland is well constrained and can be related to their movement. First the master fault system is described, and then the deformation in the eastern borderland, which contains in its northern part the Potrerillos fold-and-thrust belt and in its southern part a domain of NW-trending, sinistral strike-slip faults.

SIERRA CASTILLO - AGUA AMARGA FAULT SYSTEM

The Sierra Castillo fault is a subvertical fault, with considerable up-on-the-east throw, juxtaposing Paleozoic batholithic rocks on the east against Jurassic and Cretaceous volcanic sequences on the west (Figure 1). The Agua Amarga fault is a moderately to steeply west dipping fault with considerable up-on-the-west reverse throw, placing the same Jurassic and Cretaceous volcanic formations on the west over Paleocene-Lower Eocene volcanic units on the east. Despite the opposed senses of vertical separation, the Sierra Castillo and Agua Amarga faults are different segments of the same fault. Although separated for 6 kms by a cover of Miocene gravels at the town of Potrerillos, they appear to be contiguous, and each serve as the major

fault in the area separating a Mesozoic platform sequence on the east from a coeval volcanic sequence on the west.

The timing of movement of the Sierra Castillo and Agua Amarga faults are poorly constrained. The Sierra Castillo fault cuts rocks as young as Cretaceous and is overlain by the Miocene Atacama Gravels. However, several faults subparallel to and apparently linked to the Sierra Castillo fault, cut intrusive rocks as young as 40-38 Ma (K-Ar whole rock and biotite ages). Similarly, the Aqua Amarga fault cuts Middle Eocene intrusive rocks (46.6 ± 1.5 and 44.2 ± 1.2 Ma) and is overlain by the Miocene Atacama Gravels.

POTRERILLOS FOLD-AND-THRUST BELT

The Potrerillos fold-and-thrust belt is an approximately 14 km wide and 45 km long (minimum) east-vergent belt (Figure 1) exhibiting two different styles of deformation in its eastern and western parts. The eastern part exhibits thin-skin, ramp-flat style folding and thrusting, and deforms primarily a Mesozoic platform carbonate and clastic sequence. The western part shows thick-skinned folding and thrusting, involving deformation of the underlying Paleozoic batholithic basement. In the southern part of the belt, near Potrerillos, the Lower Tertiary volcanic sequence is also involved in the deformation. A balanced cross section indicates a minimum of ~14.5 kilometers of shortening, or about 45%, across the belt.

Another prominent set of structures in the fold-and-thrust belt is a set of east-west trending subvertical strike-slip faults (Figure 1). The faults are more prevalent in the southern part of the belt, but are distributed throughout. Slickensides exhibit subhorizontal to shallowly plunging stria. The sense of offset of marker beds and sense of shear from secondary fractures on slickenside surfaces (Petit, 1987) indicate the majority of the faults have a dextral sense of slip, but that several faults have subhorizontal sinistral slip. The opposed senses of slip on faults of the same orientation require two kinematically separate deformations. Several of the larger east-west trending dextral faults are seen to be oblique ramps transfering slip between different thrusts. The relations indicate they are kinematically related to movement on the thrusts and on this basis are considered part of the deformation that formed the fold-and-thrust belt. The sinistral faulting probably represents a reactivation of the dextral faults at a younger time.

In the southern part of the fold-and-thrust belt, cross-cutting relations with radiometrically dated units provide tight constraints on the timing of deformation. Thrusts cut a ~42 Ma dacitic pyroclastic breccia unit and are cut by a dike swarm emanating from the 32 Ma Cerro El Hueso porphyry. Furthermore, several relations, including a cleavage which exhibits a textural-metamorphic up-grade towards the Potrerillos Copper Porphyry, indicate the ~39 Ma porphyry is a syntectonic intrusion.

DOMAIN OF NORTHWEST-TRENDING SINISTRAL STRIKE-SLIP FAULTS

To the south and to the east of, but also partially overlapping with, the Potrerillos fold-and-thrust belt, is a domain of northwest-trending subvertical faults (Figure 1). They have a mean strike of N25°-30°W, and have significant vertical and sinistral separations. Several similar faults also occur at the northern end of the Potrerillos fold-and-thrust belt. Stria on slickenside surfaces have subhorizontal to moderate plunges and invariably show sinistral senses of shear from secondary fractures and sinistral offsets on geologic markers. Several of the faults, occurring within the fold-and-thrust belt, also have a second set of steeply plunging, near dip-slip stria. Shear sense indicators indicate a reverse sense of movement on the dip-slip stria set. They are interpreted to indicate that those faults occurring within the fold-and-thrust belt also accommodated some shortening at some stage of their slip history.

The age of movement of the NW-trending faults is well constrained. A group of Eocene rhyolitic domes, porphyries, and dikes, and subvolcanic andesite and dacite porphyries occurs associated with, and follow several of these faults. They are localized along the faults for distances of 25-30 kilometers, at a significant angle to the overall trend of the Eocene-Oligocene magmatic arc. Furthermore, inconsistent cross cutting relations, with both dome rocks being cut by the faults and pyroclastic rocks derived from the domes overlying the faults, indicate the faults were existent and active at the time of emplacement of the domes. K-Ar whole rock ages indicate an ~42 Ma age for one of these rhyolitic domes, and a rhyodacitic dike, intruded along another of these faults, yield a 39.3 Ma. The relations indicate the faults were existent and active by ~42 Ma. One of the sinistral faults cuts the ~39 Ma Potrerillos Copper Porphyry, indicating their activity continued until sometime after ~39 Ma. These cross cutting relations are consistent with the age constraints in the fold-and-thrust belt.

Several of the thrusts, at the south end of the fold-and-thrust belt, terminate at the northern ends of NW-trending sinistral faults (Figure 1). The sinistral sense of displacement on the NW-trending faults is compatible with the sense of the movement on the adjacent thrusts. This, and their similarity in age, indicate the NW-trending faults and thrusts are kinematically related and part of the same deformation.

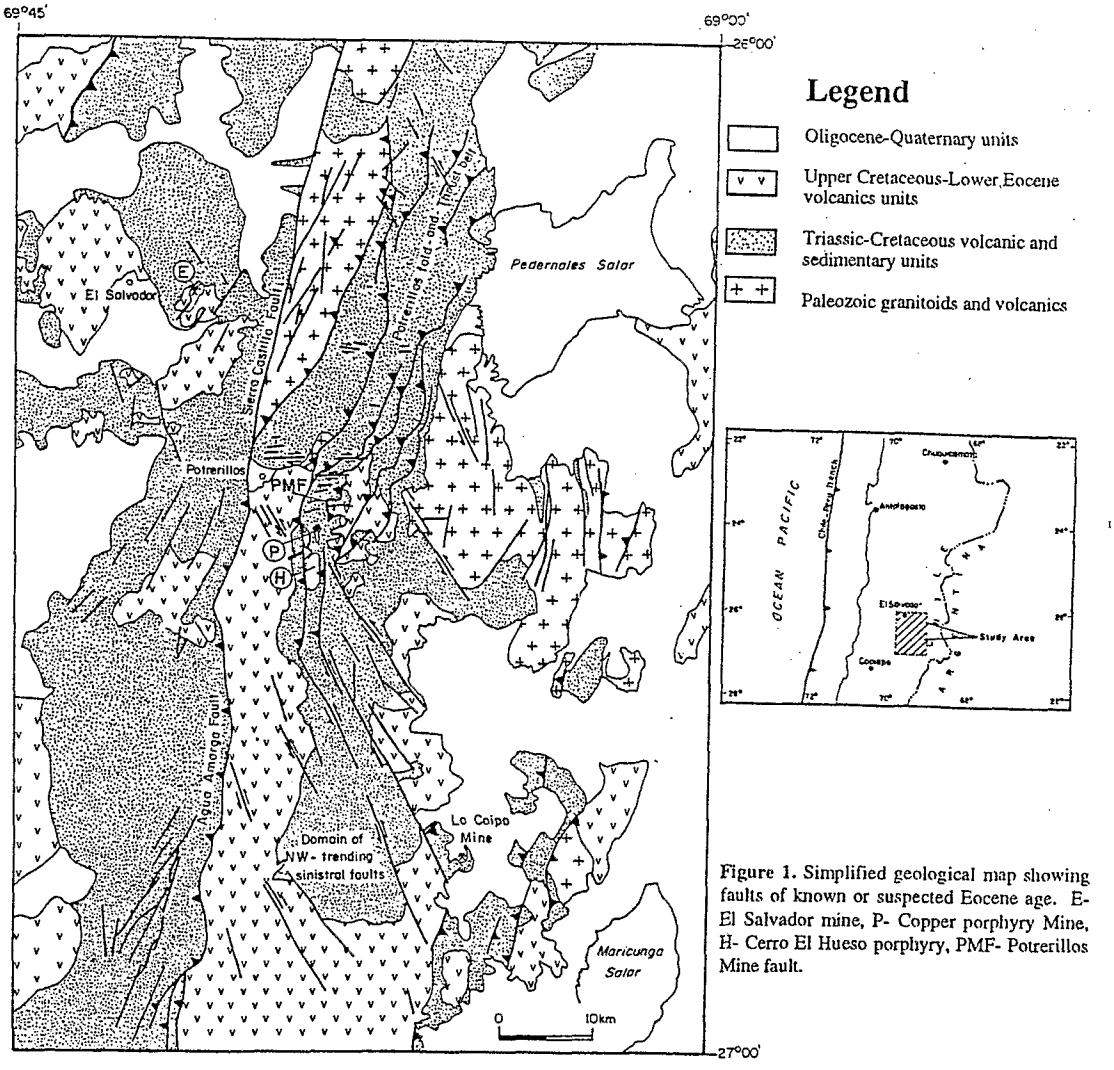

Figure 1. Simplified geological map showing faults of known or suspected Eocene age. E- El Salvador mine, P- Copper porphyry Mine, H- Cerro El Hueso porphyry, PMF- Potrerillos Mine fault.

RELATION OF FAULT SEPARATIONS ON THE SIERRA CASTILLO - AGUA AMARGA SYSTEM WITH DEFORMATION IN THE EASTERN BORDERLAND

The change in the bulk strain pattern, from the fold-and-thrust belt to the domain of sinistral strike-slip faults, is spatially associated with, and compatible with the change in the separation sense on the Sierra Castillo - Agua Amarga system. The horizontal shortening across the Potrerillos fold-and-thrust belt is accommodated by vertical thickening and uplift in its hinterland, adjacent to the Sierra Castillo fault, resulting in uplift on the eastern side of the fault. In contrast, in the domain of NW-trending sinistral faults, there are few folds and thrusts. Most of the strain is accomplished by subhorizontal or oblique sinistral movement on subvertical faults. Since there is negligible horizontal shortening, there is negligible thickening and uplift on the east side of the Agua Amarga fault, thereby more readily allowing the west side to be displaced over the east side. The relations indicate the borderland deformation and movement on the Sierra Castillo and Agua Amarga faults are related and therefore the Sierra Castillo - Agua Amarga system is also Middle-Late Eocene.

REGIONAL SINISTRAL TRANSPRESSION IN THE MIDDLE - LATE EOCENE

Sinistral transpression is indicated by two relations on the regional scale, and two independent observations on the local scale. On the regional scale, since the kinematic and age relations indicate the NW-trending sinistral faults and E-W-trending dextral faults are part of the same deformation, the two sets are interpreted to form a conjugate pair. This interpretation is further supported by the orientation of subvertical

Eocene dikes (~39 Ma), whose mean trend (~N55°W) approximately bisects the dihedral angle between the two fault sets. Latite dikes in the El Salvador Mine (42.0 ± 1.0 Ma K-Ar biotite, recalculated from Gustafson and Hunt, 1975) have the same orientation and are interpreted to have intruded under the same regional stress state.

The asymmetric development and domainal distribution of the conjugate set is interpreted to indicate formation during a noncoaxial strain history (Choukroune et al., 1987; Gapais et al., 1991), as occurs in major strike-slip fault systems. In this regard, the NW-trending sinistral faults are interpreted to be Riedel-shears and the dextral faults conjugate Riedel-shears. The orientation of the shortening direction given by the conjugate set and bisecting dikes, with respect to the Sierra Castillo - Agua Amarga system, indicates a sinistral sense of shear on the master fault system. Furthermore, the high angles of the structures to the master fault indicate regional transpression (Sanderson and Marchini, 1981). Likewise on the regional scale, the orientation of the Potrerillos fold-and-thrust belt indicates NW-SE shortening and implies sinistral displacement on the Sierra Castillo - Agua Amarga system.

Two features, in association with the Potrerillos Mine thrust fault, support the regional relations of sinistral transpression. One is the sense of slip on the fault, determined from the geometric relations of a cleavage with the thrust, giving a sinistral oblique thrust movement. The other is the clockwise sense of cleavage transection of a forced fold in the hangingwall of the fault, indicating sinistral shear.

The above observations indicate regional sinistral transpression with the Sierra Castillo and Agua Amarga faults as the master fault system. The vertical throws on the Sierra Castillo and Agua Amarga faults can be easily accomplished by even small pitches in the slip direction in a system having only 10's of kilometers of strike-slip motion.

Reviewing the timing, the data indicate the deformation started by ~42 Ma, age of the latite dikes at El Salvador and rhyolitic domes occurring along the NW-trending sinistral faults; was ongoing at ~39 Ma, age of the syntectonic Potrerillos Copper Porphyry; and over by 32 Ma, age of the Cerro El Hueso dikes.

PROBLEMS FOR LOWER TERTIARY PLATE TECTONIC FRAMEWORK

The Domeyko fault system has been previously interpreted to be a trench-linked strike-slip fault system (Mpodozis and Ramos, 1990; Maksaev, 1990; Reutter et al., 1991), but a sinistral sense of shear in the Middle - Late Eocene contradictions the plate reconstructions which predict dextral shear in the continental margin (Pilger, 1983, 1984; Pardo-Casas and Molnar, 1987). There are two possible solutions to this problem. One, the deformation in the continental margin is not related to the plate convergence in the simple fashion indicated by the "classic" trench-linked strike-slip fault models. Or two, another, now subducted plate, was converging with the continental margin in a sinistral sense in the Eocene.

Acknowledgements: This work is part of a proyect supported by the Servicio Nacional de Geología y Minería and Codelco Chile

REFERENCES

CHOUKROUNE, P., GAPAIS D., MERLE O., 1987, Shear criteria and structural symmetry: Journal of Structural Geology, v. 9, N° 5/6, p. 525-530.

GAPAIS D., FIQUET G., COBBOLD, P. R., 1991, Slip system domains, 3. New insights in fault kinematics from plane-strain sandbox experiments: Tectonophysics, v. 188, p.143-157.

MAKSAEV, V., 1990, Metallogeny, geological evolution, and thermochronolgy of the Chilean Andes between latitudes 21° and 26° south, and the origin of major porphyry copper deposits: PhD Thesis, p 1-554, Dalhousie University, Halifax, Nova Scotia, Canada.

MPODOZIS, C., ALLMENDINGER, R., JORDAN, T., 1991, La zona del Nevado de Jotabeche y Laguna del Negro Francisco: evolución tectónica y volcánica de la extremidad meridional del Altiplano Chileno: VI Congreso Geológico Chileno, Actas, p.91-95, Viña del Mar.

PARDO-CASAS, F., MOLNAR, P., 1987, Relative motion of the Nazca (Farallon) and South American plates since Late Cretaceous time: Tectonics, v. 6, p. 233-248.

PETIT, J. P., 1987, Criteria for the sense of movement on fault surfaces in brittle rocks: Journal of Structural Geology, v. 9 N° 5/6, p. 597-608.

PILGER, R. H., JR., 1983, Kinematics of the South American subduction zone from global plate reconstructions: American Geophysical Union, Geodynamics Series 9, p.113-125.

PILGER, R. H., JR., 1984, Cenozoic plate kinematics, subduction and magmatism: South American Andes: Journal of the Geological Society of London, v. 141, p. 793-802.

REUTTER, K. J., SCHEUBER, E., HELMCKE, D., 1991, Structural evidence of orogen-parallel strike slip displacements in the Precordillera of northern Chile: Geologische Rundschau, v. 80(1), p. 135-153.

SANDERSON, D. J.; MARCHINI, R. D., 1981, Transpression: Journal of Structural Geology, v. 6 (5), p. 449-458.

A simple shear/ pure shear flexural model of thrust sheet emplacement and foreland basin formation: Application to the Eastern Cordillera and Subandean zone, Central Andes.

Toth J.[1], Yrigoyen M.R.[2], Flint S.S.[1], Kusznir N.J.[1]

1. University of Liverpool, Liverpool, UK.
2. ASTRA Compania Argentina de Petroleo S.A.

A mathematical model has been constructed of the geometric, thermal and flexural isostatic response of the lithosphere to shortening by faulting in the upper crust and plastic distributed deformation in the lower crust and mantle. The model has been applied to late Cenozoic compressional tectonics of the eastern thrust belts of the Central Andes (figure 1) and used to predict foreland basin geometry and stratigraphy. The model predicts the flexural isostatic response to lithosphere shortening, thrust sheet emplacement, sediment loading and erosional unloading. Fault geometry, the amount of compression, detachment depth, the relative lateral position of the pure shear and simple shear and the flexural rigidity of the lithosphere during shortening control the form of the resulting foreland basin and thrust belt topography.

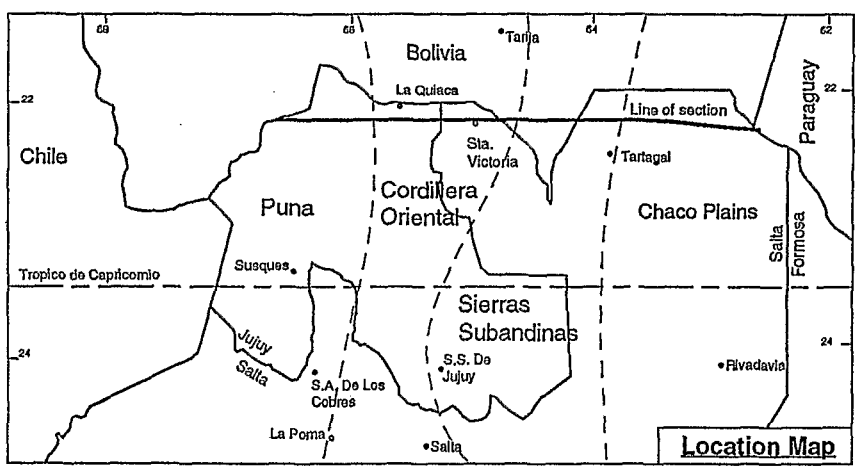

figure 1

Figure 2 shows a model in which three thrust faults, dipping at 35°,detaching at 15km and with 10km, 10km and 8km shortening respectively, are moved in-sequence. The initial thrust produces a flexural foreland basin which is iteratively sediment loaded to base level (figure 2a). The subsequent thrusts incorporate the earlier foreland basins into their thrust sheets (figures 2b,c). The model uses an effective elastic thickness of 5.0km.

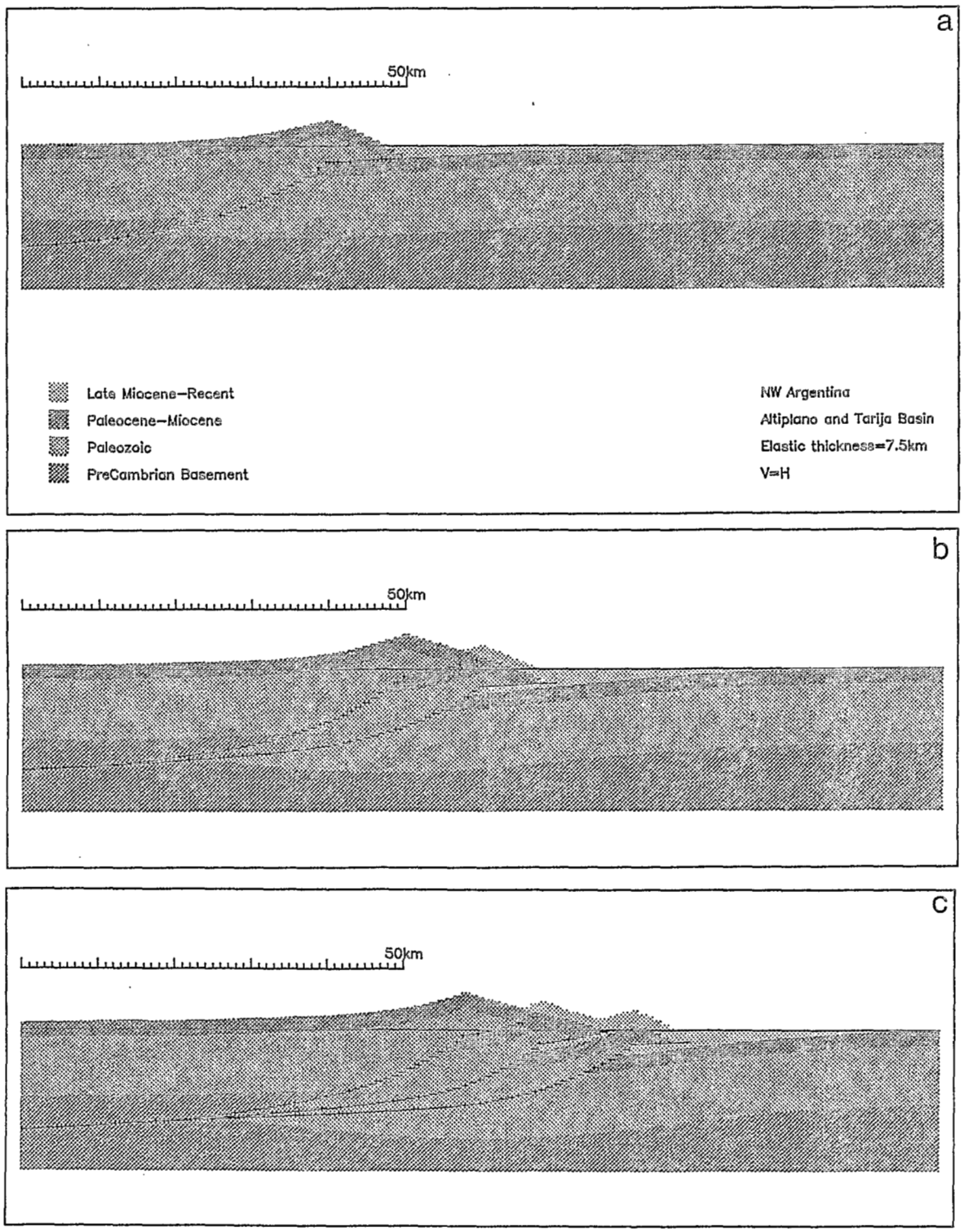
a
50km
Late Miocene–Recent
Paleocene–Miocene
Paleozoic
PreCambrian Basement
NW Argentina
Altiplano and Tarija Basin
Elastic thickness=7.5km
V=H
b
50km
c
50km

figure 2

The Eastern Cordillera and Subandean zones are Late Miocene-Recent thrust belts on the eastern edge of the Puna. Shortening has been estimated by section balancing to be of the order of 100km or more. To the East of the thrust belts the Chaco Plains form an active depositional basin (figure 1). The PreCambrian metamorphic basement across the area dips West beneath the Andes. Unconformably above the basement lies a thick elongate eastwardly tapering wedge of Paleozoic sediments. The Paleozoic thickness increases from 2km beneath the Chaco Plains to 14km at the western boundary of the subandean zone.

Seismic reflection profiles across the Subandean zone show East verging thin skinned thrust faults detaching along horizons within the Paleozoic. The boundary between the Subandean zone and the Eastern Cordillera marks a structural change to deeper fault detachments bringing PreCambrian material to the surface.

In N.W.Argentina the Cretaceous Salta rift basin may be a controlling factor on the evolution of the Andean foreland. Continued postrift thermal subsidence has provided increased sedimentary accommodation space and inversion of the rift structures may control fault positions and geometries.

Using available geological and seismic data to identify fault positions and structural styles the model has been used to predict late Cenozoic crustal evolution, foreland basin stratigraphy and basin geometry along a line of section from the Puna to the Chaco Plains (figure 1). In particular the model allows us to constrain lower crustal structures and fault detachment depths in response to lithosphere shortening. The relative lateral position of the pure shear and simple shear is an important control on crustal thickness and resulting topography.

The initial starting template is shown in figure 3. The progressive formation of

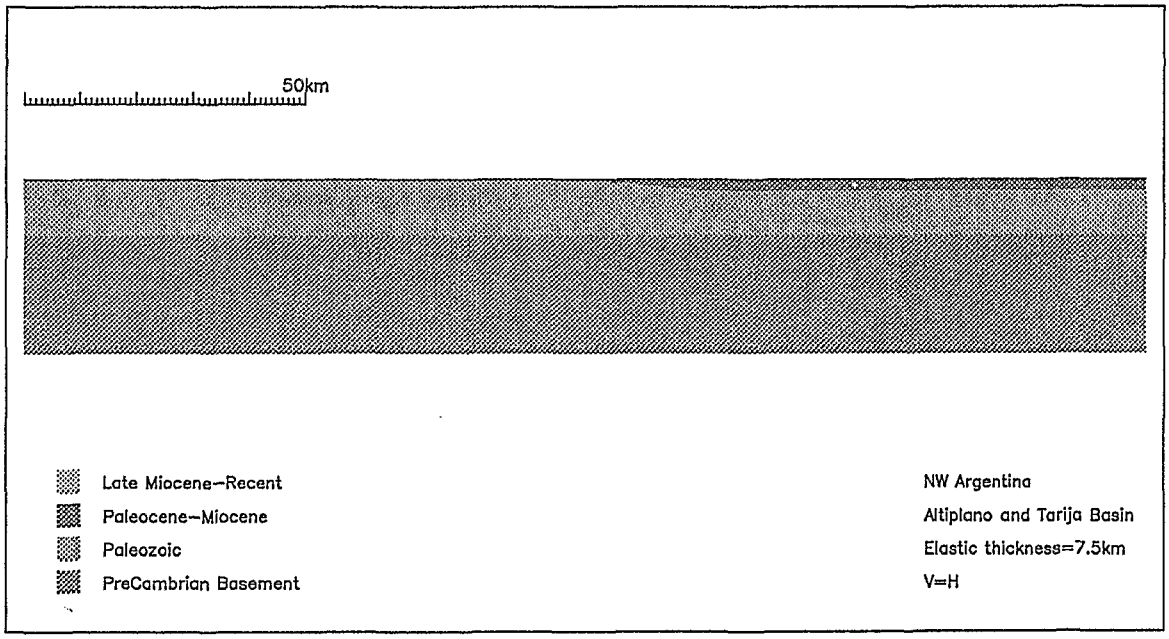

figure 3

thrust belt and foreland basin is show in figure 4. Cumulative total shortening used in the model is 110km. In figure 4a shortening on predominately thick skin thrusts, involving PreCambrian basement, has generated a significant foredeep which has been filled to form a foreland basin of up to 5km depth. In figure 4b the thrust belt propagates on thin skin thrusts detaching within the lower Paleozoic. Figure 4c shows the present day situation from the eastern border of the Eastern Cordillera to the Chaco plains.

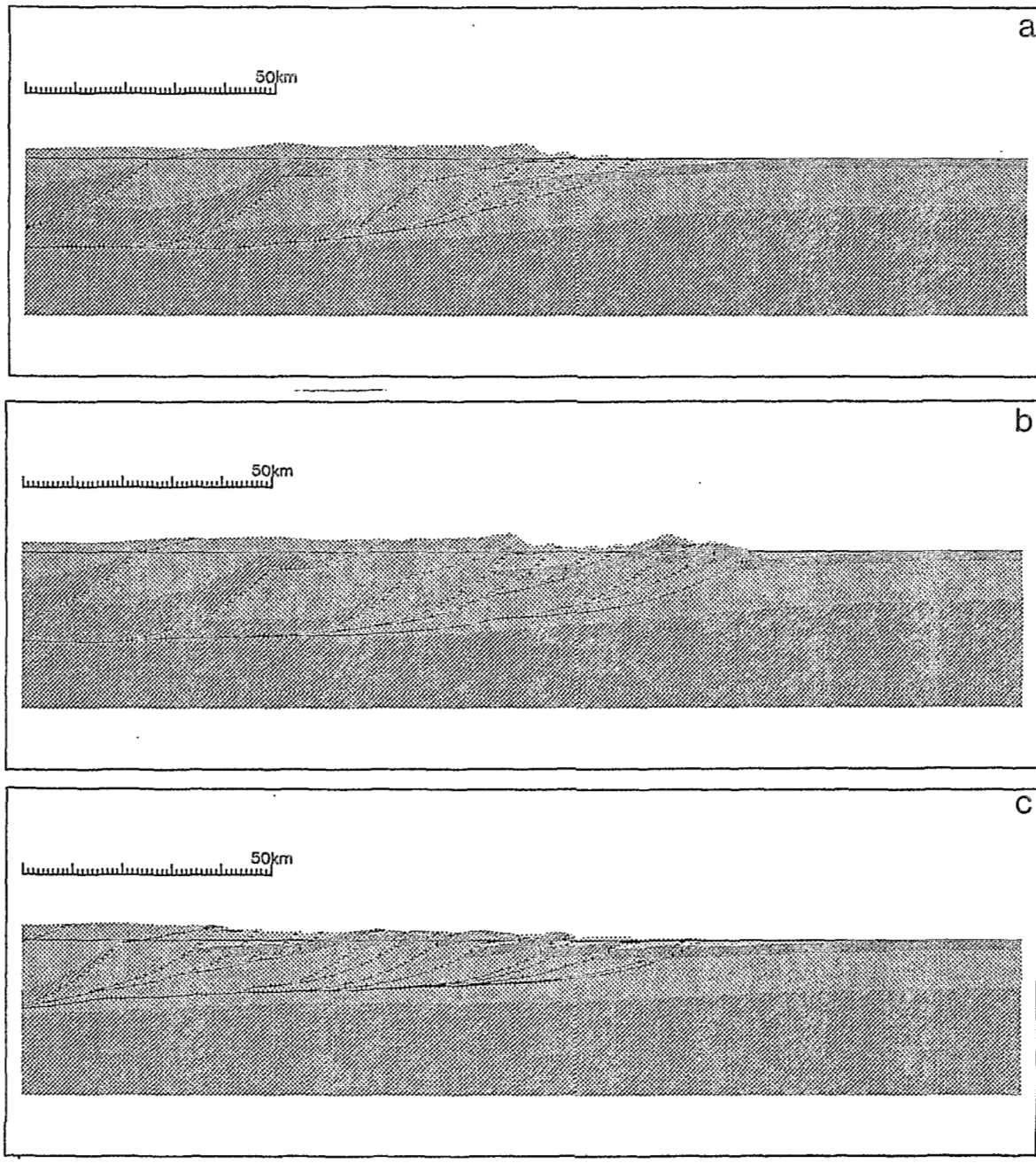

figure 4

NEOGENE DEXTRAL TRANSPRESSION AT THE SOUTHERN EDGE OF THE ALTIPLANO-PUNA (N-W ARGENTINA).

Marc de URREIZTIETA(1), Eduardo A. ROSSELLO(2), Denis GAPAIS(1), Claude Le CORRE(1), and Peter R. COBBOLD(1).

(1) Géosciences Rennes, CNRS, Université de Rennes I, 35042 Rennes Cedex, France.
(2) CONICET and Departamento de Ciencias Geológicas, Universidad de Buenos Aires, Ciudad Universitaria, 1428, Buenos Aires, República Argentina.

RESUME: Le haut-plateau andin (Altiplano-Puna) constitue la manifestation topographique majeure de la chaîne des Andes centrales associée à la convergence Est-Ouest entre la plaque pacifique Nazca et l'Amérique du Sud. Dans le NW de l'Argentine (27°S), la limite Sud-Est de la Puna est une zone de transfert majeure entre deux domaines crustaux, l'un au nord fortement raccourci et épaissi, l'autre au sud plus modérement déformé. L'étude d'un Modèle Numérique de Terrain, d'images satellitaires (SPOT), nos observations de terrain, et l'analyse cinématique des populations de failles, permettent d'interprêter cette zone comme une zone transpressive et dextre, accommodant une augmentation du taux de raccourcissement Est-Ouest, depuis le Sud vers le Nord.

KEY WORDS: Andes, Altiplano-Puna, Transpression, Digital Mapping, Fault kinematics.

INTRODUCTION AND GEOLOGICAL SETTING

The main topographic feature of the Central Andes is the Altiplano-Puna (grey area, Fig.1). In northwestern Argentina (27°S), the Andean cordillera narrows abruptly and the foreland Pampean province contains alternating basins and ranges (black, Fig.1). The transition (stipped area, Fig. 1) coincides with two features (Stelzner, 1923): (1) a change in the dip of the subducting Nazca plate, from about 30° easterly dip below the Puna, to subhorizontal below the Pampean province (Cahill & Isacks,1992), and (2) a disappearance of the Neogene andesitic volcanism (Jordan et al.,1983).

The Pampean Ranges strike subparallel to the chain. The ranges consist of Precambrian to Paleozoic plutonic and metamorphic rocks. Basins are filled with Tertiary to Quaternary continental sediments, deposited on a Pre-Miocene erosion surface often well exposed on the ranges. Basins and ranges are generally bounded by high-angle reverse fault zones of dominantly eastward vergence. Sediments show an overall upward coarsening and increase in thickness from the Miocene to the Pliocene (Malizzia,1988), reflecting an increase in tectonic activity.

This paper presents a structural interpretation of the area using digital mapping, satellite images (SPOT), and a kinematic analysis of fault populations.

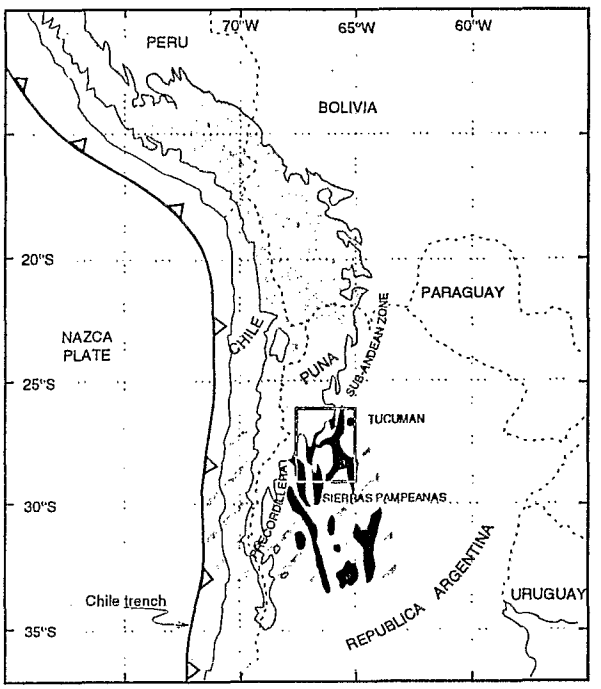

Figure 1.

REGIONAL STRUCTURES

We have produced numerical topographic images of an area covering the northern

Pampean Ranges (Fig.2). From SE to NW, the altitude increases in steps, from the Chaco-Pampean level (230 m) (Fig.2b. SE corner) to the Puna (average altitude >3700 m) (Fig.2b. NW corner). As basins become higher, the sedimentary infill becomes thicker and their surface area decreases. This, we interpret as illustrating an increase of the degree of basin evolution, i.e. an increase in the amount of bulk crustal shortening towards the Altiplano.

Basins and ranges are generally asymmetric, with a spacing of several tens of kilometers.

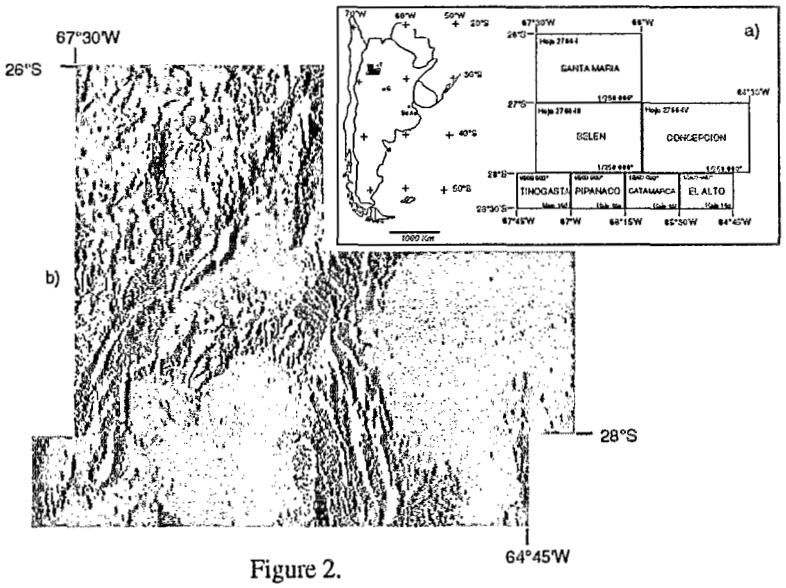

Figure 2.

Unfaulted margins of individual basins are gently dipping and controlled by the pre-Miocene erosion surface; whereas thrusted margins show sharp relief (Fig. 2). More symmetrical depressions, bounded by fault zones of opposite vergence, also occur (Fig. 3).

The overall strike of basins and ranges changes sharply, from a regional NS attitude, to NE-SW orientations within the transition zone between the southern Sierras Pampeanas and the Puna. This zone, previously known as the Tucumán lineament (Mon, 1976), is also marked by (1) en échelon ranges (Figs. 2 and 3), and (2) strong changes in the amount of thrusting along individual basin margins. These features suggest that significant wrenching and block rotations have occurred within this zone.

FAULT KINEMATICS

Striated fault planes were measured at several localities along basin boundaries, within both basement and tertiary sediments (Fig. 4). A statistical analysis of fault populations indicates that (1) the principal direction of bulk shortening is subhorizontal and strikes dominantly EW to ENE-WSW at regional scale, (2) it changes to dominantly NW-SE along the Puna boundary, (3) the principal extension direction is variable, from steeply dipping to subhorizontal, indicating that substantial stretching along strike has locally occurred, and (4) strains are of plane-strain to flattening type. Thus the local kinematics associated with basin development differ significantly from pure thrusting. The principal shortening direction is frequently oblique to basin boundaries (Fig. 4). Hence we infer substantial components of dextral strike-slip along NNE-SSW to NE-SW directions. Conjugate sinistral strike-slip occurred to a lesser extent along NNW-SSE directions.

CONCLUSIONS

For the northern Sierras Pampeanas, we infer substantial dextral wrenching along the southern border of the Puna Plateau during the Neogene. This transpressive basin and range province (the Tucumán Transfer Zone), is interpreted as accommodating a change in the amount of horizontal shortening, between the strongly thickened domain of the Puna to the North and the less deformed Sierras Pampeanas to the South.

REFERENCES

R.W. Allmendinger, 1986, Tectonic development, southeastern border of the Puna Plateau, northwestern Argentina Andes, Geol. Soc. Amer. Bull., 97, 1070-1082.

R.W. Allmendinger, 1989, Neotectonic deformation of the southern Puna Plateau, northwestern Argentina, J. South Amer. Earth Sci., 2, 111-130.

T. Cahill and B.L. Isacks, 1992, Seismicity and shape of the subducted Nazca Plate, Journal of Geophysical Research, 97, 17503-17529.

T.E. Jordan, B.L. Isacks, V. Ramos and R.W. Allmendinger, 1983, Mountain building in the Central Andes, Episodes, 1983, 20-26.
D.C. Malizzia, 1988, Indicadores litológicos de paleoclima en el Neógeno de Sierras Pampeanas, II reunión Argentina de sedimentología., Actas I, 160-164.
R. Mon, 1976, La tectónica del borde oriental de Los Andes en las provincia de Salta, Tucumán y Catamarca, República Argentina, Rev. Assoc. Geol. Argentina, XXXI, 65-72.
A. Stelzner, 1923, Contribuciones a la geología de la República Argentina, con la parte limítrofe de los Andes Chilenos entre los 32 y 33° S, VIII Actas Acad. Nac. Cienc. (Córdoba).

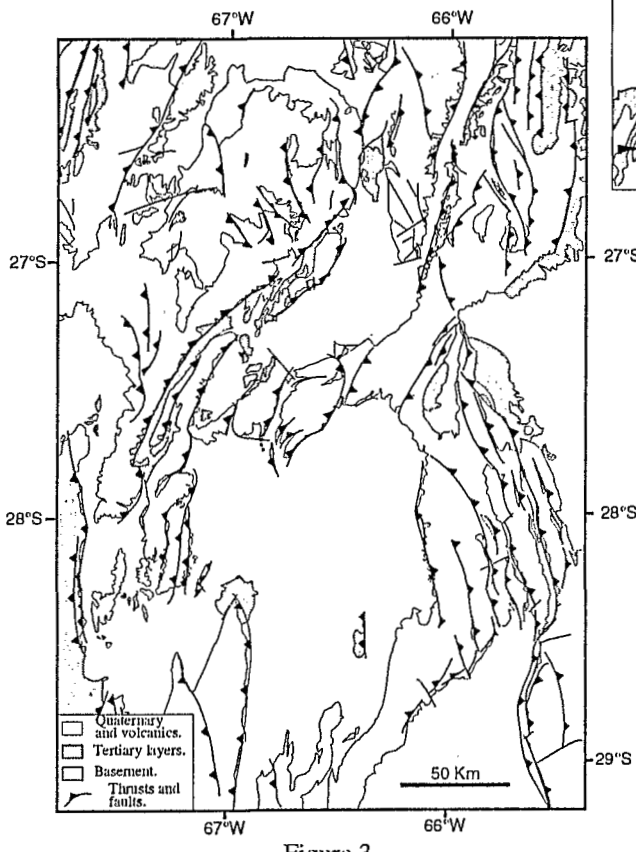

Figure 3.

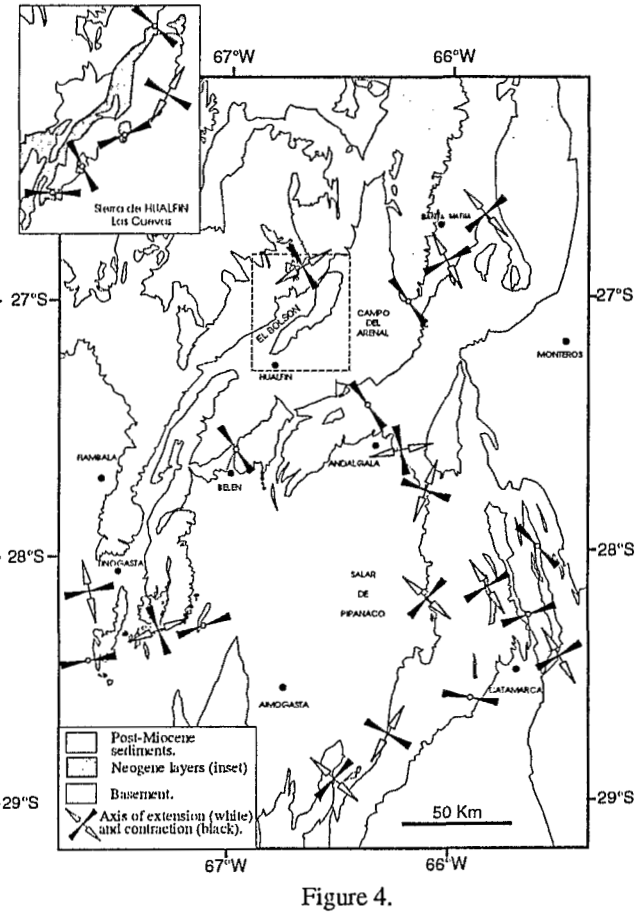

Figure 4.

ANDEAN TECTONICS AND CRUSTAL SHORTENING : THE ANDES OF ACONCAGUA AND THEIR STRUCTURE

Jean-Claude VICENTE(1)

(1) Département de Géotectonique, Université Pierre et Marie Curie, 4, Place Jussieu, 75252 PARIS Cedex 05, France.

RESUMEN: Se enfatiza la notable disimetría del llamado sinclinorium volcanígeno andino, cuya ala oriental cabalgó fuertemente hacia el Este la faja plegada e imbricada externa; mientras el ala occidental descanza tranquilamente sobre el basamento de la Cordillera de la Costa. El equivalente a nivel de zocalo del acortamiento registrado en la cobertura lleva a considerar el total despegue del ala oriental del sinclinorium y admitir la existencia de una zona de sutura crustal mayor profunda hacia al Oeste. Así, regulando las relaciones de convergencia entre ambos basamentos

KEY WORDS: Argentine-Chile Andes, Andean tectonics, Crustal shortening, Intra-plate convergence, Deep-seated structures,Continental accretionary wedges.

A synthesis of the results along a transect through the Andes at the latitude of Aconcagua (32°40' S) shows the following.

If we disregard post-Miocene deformation, essentially responsable for the uplift of the Frontal Cordillera and Precordillera units (the most external part of the chain characterized by a thick-skinned tectonics), it remains that the main andean tectonics for the left set Coastal Cordillera-Principal Cordillera is restricted to the eastern slope of the Main Range (argentinian flank) and concentrated within a narrow thin-skinned easterly tapering fold-and-thrust belt known as the Aconcagua imbricate zone (MPODOZIS & RAMOS 1989).

This zone of imbricate thrusts and related folds has undergone a general detachment above the oxfordian gypsum (Yeso Principal) (VICENTE 1972). It represents the collapse of the previous Mesozoic andean back-arc basin which has been tectonically prograded eastward over the edge of the relatively undeformed craton. It is a typical trailing imbricate fan since the thrust with the maximum eastward slip (Main Andean Overthrust, MAO),is at the back and brings the volcanics of the andean arc over the external zone.This MAO is a typical backarc thrust which marks the basic tectonic boundary between internal (western) and external (eastern) zones in the Andes (VICENTE 1970). The stratigraphic record of deformation within the belt indicates the tectogenesis of this back arc basin occured progressively eastward in 3 successive stages between the Upper Cretaceous and the Lower Miocene. They are namely the classical peruvian (Coniacian-Santonian), incaic (Late Eocene) and pehuenche (Late Oligocene) tectonic events.

The amount of shortening of the detached cover of the Fold and Thrust Belt.is about 75%. Keeping in view a present width of 20 km, this implies at least 50 km of shortening. Obviously, such a shortening within the sedimentary cover must have been balanced by a crustal shortening of the same order at a deeper crustal level located further West.

Westward, the structure of the Mesozoic and Paleogene volcanic series of the andean arc domain shape a huge synclinorium (the Andean Synclinorium) characterized by a remarkable asymmetric pattern contrarily to LEVI and AGUIRRE's (1981) opinion. Dispite its thickness, the eastern limb appears concentrically folded and shows an increase in tightness and asymmetry of folds eastward as we get closer to the MAO indicating a clear vergency to the East. In contrast, the western limb is simply homoclinal resting stratigraphically on the coastal basement. This synclinorium appears as a major structural feature of the Andes since it involves a volcanigenous serie which thickness is close to 20,000 m in the Coast Range (THOMAS 1958) and about 7-8,000 m in the Main Range. This implies a deepening of the basement below the axis of the synclinorium confering to it, in depth, a very likely pinched shape, seeing the general increase of dip of the series with age and the various unconformities separating the formations. The intrinsic asymmetry of the system.explains the hidden behaviour of the insular substratum and suggests a major crustal buckling in shear context.

Considering the western extension of the essentially undeformed basement of the Frontal Cordillera under the imbricate zone, the amount of shortening of this zone and the basic eastward overthrust of the eastern edge of the synclinorium, we are to extend the MAO much further West (practically over the synclinorium axis). That implies a complete regional detachement of the eastern flank of the synclinorium and its draping over the edge of the cratonic foreland. Besides, this is evidenced by the proper geometry of the folded volcanics of the chilean flank of the Main Range. That means the existence at the rear, on a level with the basement, of a major zone of crustal shearing controlling the relationship between the genuine arc basement i.e. the one of the Coast Range and that of the Foreland. In a word, we must accept a major underthrusting of the western edge of the South American craton beneath the Coastal basement. This constitutes a kind of subduction with an east vergency involving andean continental crust (A-subduction type of BALLY 1975, 1981). However, considering the depth reached by the through of the synclinorium, we question if a portion of the necessary 50 km of crustal shortening is not absorbed in some ways by a continuous deformation within the basement.However, according to this model, the Aconcagua fold and thrust belt should represent nothing but the most frontal and surficial bearing of a major structure involving the main eastward overthrust of the coastal basement driving forward, as a scraper, the huge asymmetric volcanogenic andean synclinorium with its frontal imbricate fan of cover wedges. That structural device shows similarities with typical continental accretionary wedge with frontal damping. The andean originality derives from the striking synclinorium and its basal shear zone which acts as a large scraper acting ahead of the coastal basement

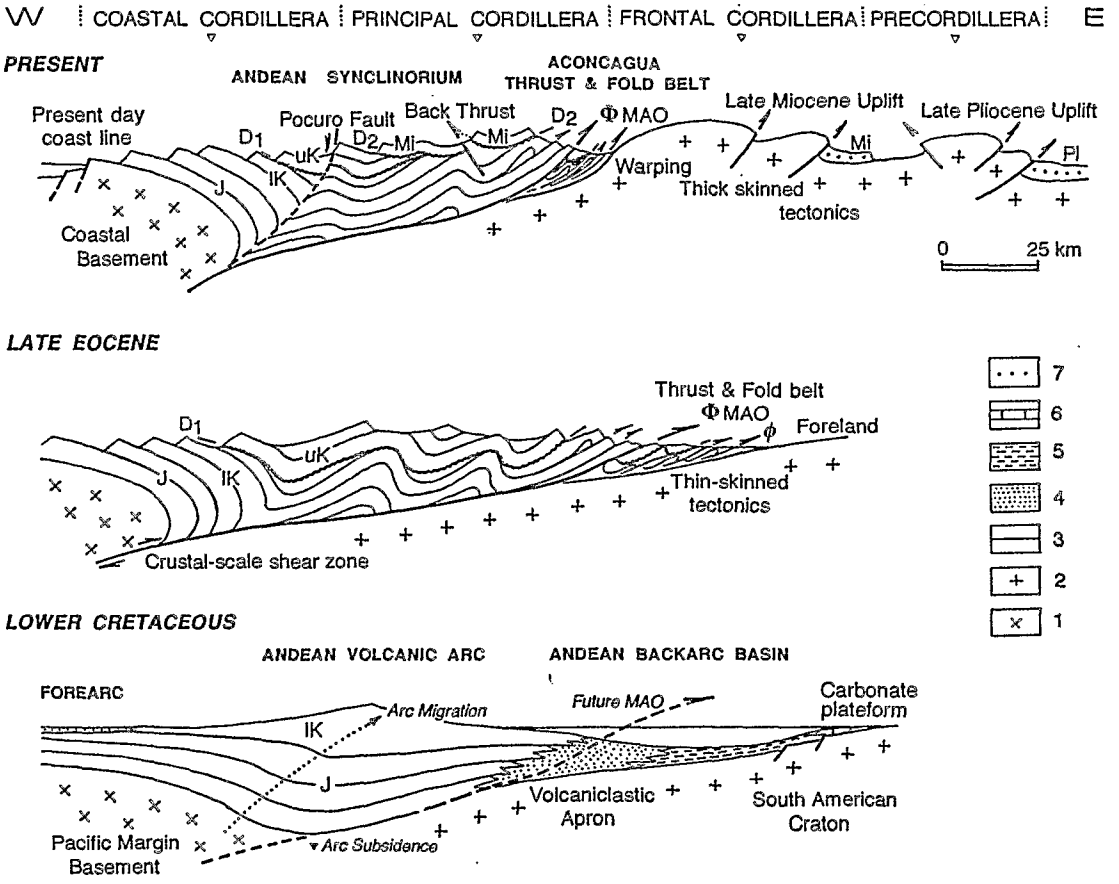

Interpretative palinspatic reconstruction (Lower Cretaceous and Late Eocene) based on a synthetic cross-section (uppermost section ; vertical scale not respected) of the Andes of Aconcagua (32°40' S).

(1) Arc basement (coastal basement) ; (2) Foreland basement (South American craton) ; (3) Arc volcanics ; (4) Volcaniclastics ; (5) Lutites ; (6) Carbonates ; (7) Continental red beds (Foreland molasses) ; J : Jurassic ; lK : Lower Cretaceous ; uK : Upper Cretaceous ; Mi : Miocene ; Pl : Pliocene ; D_1 : Upper Cretaceous unconformity ; D_2 : Lower Miocene unconformity ; Φ : Main Andean Overthrust (MAO).

It appears that the noticeable crustal subsidence related with the arc building occurs at the biginning of the crustal buckling which developed from the Upper Cretaceous under the convergent system and evolved in crustal shearing. The thermal differencies between the crust of the magmatic arc (hot) and that of the foreland (cold) would favour the relative underthrusting of the foreland basement beneath the coastal one and should result into the eastward andean polarity of structures. In addition the uplift of the Frontal Cordillera after the Late Miocene Quechua phase which brought its basement to culminate close to 7,OOO m (C° Mercedario), has produced a significant straightening of the frontal imbricate and a general warping of the eastern part of the synclinorium accompanied by several backthrusts This suggests that the thrusts were previously much more reclined and low-angle.and therefore, that the original system may have been more tangential.

To sum up, the andean tectonics of the Main Cordillera can be viewed as the consequence of a large net crustal convergence between the sialic arc basement of the Pacific Margin and the South American Craton. That implices the existence of a major suture below Central Chile.

Since this structural pattern is also recognized in Peru (VICENTE 1989), we open on a very homogeneous geotectonic model for the Marginal Andes. In this respect, the differential of shortening observed along the strike of the Andes for the Main Range appears to be directly related to the previous width and degree of Mesozoic subsidence of the backarc basin i.e. to the amount of previous stretching and thinning of its continental crust.

At last, we wonder if the significant zone of normal faulting, known as the Pocuro Fault (CARTER & AGUIRRE 1965) which limits to the West the Principal Cordillera and controls the relations with the Central Valley to the South, can be interpreted as the emergence of a late reactivation as listric fault of the earlier crustal shear in the mainly tensional context affecting the chilean margin since Middle Tertiary.

REFRENCES

BALLY,A.W. 1975. Geodynamic scenario for hydrocarbon occurrences. *9th World Petroleum Congress (Tokyo),*.**2,** 33-34.

BALLY 1981, Thoughts on the tectonics of folded belts. In: McCLAY & PRICE (eds.), Thrust and nappe tectonics. *Geol. Soc. London, Special Publ.* **9**, 13-32.

CARTER,W.D. & AGUIRRE,L. 1965. Structural geology of Aconcagua Province and its relationship to the Central Valley Graben, Chile. *Bull. geol.Soc. Am.* **76**,651-664.

LEVI, B. & AGUIRRE, L. 1981. Ensialic spreading-subsidence in the Mesozoic and Paleogene Andes of central Chile. *J. geol. Soc. London.* **138**, 75-81.

MPODOZIS, C. & RAMOS, V. 1989. The Andes of Chile and Argentina. In: ERICKSEN, G.E., CAÑAS PINOCHET, M.T. & REINEMUND, J.A. (eds.),*Geology of the Andes and its relation to hydrocarbon and mineral resources.* Circum-Pacific Council for Energy and Mineral Resources, Earth Science Series. **11**, 59-90.

THOMAS, H. 1958. Geología de la Cordillera de la Costa entre el Valle de la Ligua y la Cuesta de Barriga. *Bol. Inst. Invest. Geol. Chile.***23**, 1-86.

VICENTE, J.C. 1970. Reflexiones sobre la porción meridional del sistema peripacífico oriental. *Conference on solid earth problems (Buenos Aires).* Symposium on the results of upper mantle investigations with special emphasis on Latin America. **37-1**, 162-188.

VICENTE, J.C. 1972. Aperçu sur l'organisation et l'évolution des Andes argentino-chiliennes centrales an parallèle de l'Aconcagua. *24th Intern. Geol. Congr. (Montréal).***3**, 423-436.

VICENTE, J.C. 1989. Early Late Cretaceous overthrusting in the Western Cordillera of southern Peru. In: ERICKSEN, G.E., CAÑAS PINOCHET, M.T. & REINEMUND, J.A. (eds.), *Geology of the Andes and its relation to Hydrocarbon and mineral resources*. Circum-Pacific Council for Energy and Mineral Resources
Earth Science Serie. **11**, 91-11.

BASSINS
BASINS
CUENCAS

STRATIGRAPHIC ANALYSIS OF THE DOMEYKO BASIN, NORTHERN CHILE

John R. ARDILL[1], Guillermo CHONG DIAZ[2] & Stephen S. FLINT[1]

(1) Sequence Stratigraphy Research Group, Department of Earth Sciences, University of Liverpool, Liverpool, England.
(2) Departmento de Geociencias, Universidad de Norte, Casilla 1280, Antofagasta, Chile.

RESUMEN: La cuenca Domeyko de Chile Norte (Triasico a Cretacico) corrientemente parace a habia crecedo dentro un "back-arc" activo medio. La llenar de la cuenca es sastrazido pana muchos distintos secencias de caliya y siiciclasticos que paracen a coutenir una responsia stratigraphic relatido a cambios grandes del nivel del mar velativo. La objeto del esto projecto es a utilizer leceucia stratigrafico resolucion-alto cono un herramienta para intrepetir la cronostratifia de un cuenca back-arc activo.

KEY WORDS: Domeyko Basin, Jurassic, active back-arc, chronostratigraphy, strike-slip.

INTRODUCTION

The Triassic to Cretaceous Domeyko Basin of Northern Chile is currently thought to have formed within an active back-arc setting. Positive inversion has concentrated Triassic to Cretaceous outcrop along the N-S trending Domeyko Mountain Belt, with perpendicular valley incision allowing excellent exposure. The Domeyko Range has long been recognised as one of the world's richest mineral provinces but is otherwise relatively unknown.

The Western Fissure Fault System runs N-S through the Domeyko Range and adds the complexity of bedding parallel strike-slip giving juxtaposition of unrelated, time equivalent strata. Some of the earlier work on this area has overlooked the strike-slip component and considered tectonically emplaced strata as being in stratigraphic succession.

GEOLOGICAL SETTING

The Domeyko Basin is placed within an active back-arc domain because of the distribution of arc related volcanics and high volcanoclastic content. The Jurassic arc trended N-S and was located along the present day position of the Coastal Cordillera. Since Jurassic times the arc has migrated to the east with it's current position on the west side of the Puna (High Andes). Figure 1 shows a generalised Jurassic Palaeogeography with the present day positions of the Jurassic outcrops.

MESOZOIC STRATIGRAPHY

The basin fill is characterised by a variety of carbonate and siliciclastic sequences with interbedded volcanic and volcanoclastic units. Carbonate and clastic sequences contain a well developed palaeontological evolution with 85% of ammonite biochronozones, exceptions being the Kimmeridgian & Tithonian. From initial fieldwork the Jurassic stratigraphy appears to contain marked stratigraphic responses related to major changes of relative sea-level. For example, the Kimmeridgian is represented by a thick sequence of evaporites (800m), hence giving the loss of palaeontological resolution.

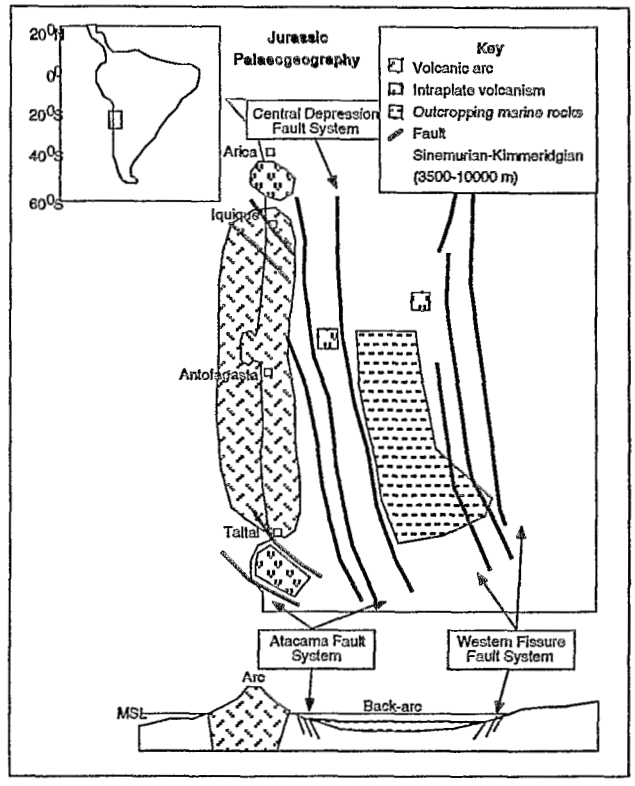

Figure 1: General Jurassic Palaeogeography for Northern Chile.

TECTONICS

Tectonics are still relatively unknown with the possibility of a subduction related strike-slip component active during basin development. This would possibly explain the formation of small isolated areas of very rapid subsidence. Two currently active major fault systems (Atacama Fault System & Western Fissure Fault System) appear to control the Mesozoic outcrop and are thought to represent the original basin bounding fault systems.

CONCLUSIONS

Initial work has laid down a provisional outline for Mesozoic basin evolution with current fieldwork being concentrated on detailed facies analysis. The aim of this project is to use high resolution sequence stratigraphy as a tool to develop a more detailed chronostratigraphic framework for the basin's evolution.

LATE CRETACEOUS TO EOCENE TECTONIC-SEDIMENTARY EVOLUTION OF SOUTHERN COASTAL ECUADOR. GEODYNAMIC IMPLICATIONS.

Stalin BENITEZ [1], Etienne JAILLARD [2], Martha ORDOÑEZ [1], Nelson JIMENEZ [1] and Gerardo BERRONES [1].

(1) Petroproducción, Km 6,5 via a la Costa, casilla 10829, Guayaquil, Ecuador.
(2) Misión ORSTOM, Rusia y Eloy Alfaro, Apartado postal 17.11.06596, Quito, Ecuador.

RESUMEN : La parte Sur de la Costa de Ecuador (Península) experimentó dos fases tectónicas mayores en el Paleoceno superior y Eoceno inferior respectivamente, desconocidas más al Norte (Costa s.s.). La primera corresponde a la colisión de la Péninsula contra la margen continental, mientras que la segunda representaría su acreción con la Costa. Luego, el conjunto cabalga la margen andina en el Eoceno superior. Dichos eventos acrecionarios coinciden con fases tectónicas conocidas en todos los Andes.

KEY-WORDS : Late Cretaceous, Paleogene, Andean margin, Oceanic terranes, Accretion.

INTRODUCTION

Coastal Ecuador is interpreted as an oceanic terrane accreted to the Andean continental margin by Late Cretaceous or Early Tertiary times. This has been confirmed by paleomegnetic studies that evidenced a 70 ° clock-wise rotation of its Northern part (Roperch et al. 1988). As a consequence, the sediments of Coastal Ecuador must have recorded the main geodynamic events occurring along the subduction zone. The sedimentologic and tectonic study of these series has been undertaken, in order to understand the subduction and accretion history of the Andean margin during Late Cretaceous and Paleogene times, and to attempt correlations between the early Andean tectonic phases and the geodynamic processes.

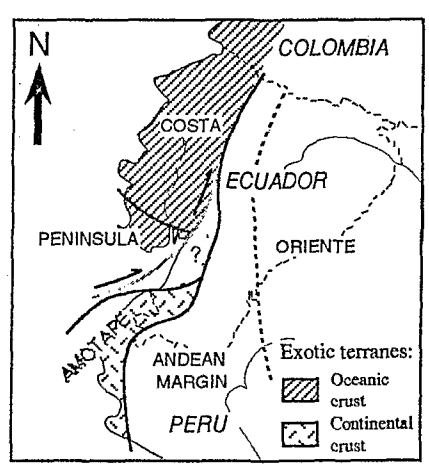

Fig. 1: Location sketch.

GEOLOGICAL SETTING

Southern Coastal Ecuador is usually subdivided into two zones separated by the Chongón-Colonche Fault (C-C Fault), thus considered as a major paleogeographic feature. North of the C-C Fault, the Chongón-Colonche Cordillera (C-C Cordillera) is characterized by the lack of late Paleocene-early Eocene deposits, whereas the Santa Elena Peninsula (Peninsula) is marked by

a thick turbiditic sedimentation of Paleocene age. Coastal Ecuador is considered as having been accreted to the Andean margin by early Tertiary times (Feininger & Bristow 1980).

At the beginning of this century, the discovery of small Oil fields in the SE Peninsula motivated the paleontological study of the Late Cretaceous-Paleogene sediments of Southern coastal Ecuador. These works, combined with the well data obtained in the 30-40s by different Oil Companies, led to the statement of local, often contradictory stratigraphic models. Some stratigraphic synthesis were then attempted (Marchant 1956, Canfield 1966). In the 70s, in the light of the Plate Tectonics concepts, the age contradictions, the scarcity of the outcrops and the tectonic complexity led some authors to interpret this zone as the result of a giant olistostrome of late Eocene age, involving all kind of older rocks (Colman 1970, Bristow & Hoffstetter 1977, Feininger & Bristow 1980). More recently, ecuadorian geologists interpreted these series, again regarded as a normal stratigraphic succession, as a stack of thick turbiditic sequences (Benitez et al. 1986).

SEDIMENTARY AND TECTONIC EVOLUTION OF SOUTHERN COASTAL ECUADOR

Late Cretaceous- Early Late Paleocene. The basement of Coastal Ecuador is made up of early Cretaceous basalts (Piñon Fm), interpreted as an oceanic floor. It is overlain by Cenomanian (?) to Coniacian siliceous shales, pelagic limestones and fine-grained turbiditic grauwackes (≈ 200 m, Calentura Fm, Amoco 1991). These are followed by a thick series of coarse-grained volcaniclastic turbidites of Santonian to Campanian age, that would result from the erosion of an Eastern volcanic arc (≈ 2000 m, Cayo Fm, Benitez 1990-91). These formations crop out in both sides of the C-C Fault. The Cayo Fm grades upward into fine-grained pelagic black shales, cherts and tuffs, with few limestones beds of Maastrichtian to early Thanetian age (≈ 500 m, Guayaquil Fm, Amoco 1991, fig. 2).

South of the C-C Fault, the Santa Elena Fm, dated as Maastrichtian and Paleocene (Jaillard et al. 1992), is stratigraphically equivalent to the Guayaquil Fm (fig. 2). It is affected by roughly E-W trending tight overfolds (fig. 3), associated with penetrative E-W-trending, S-dipping axial plane cleavage, and with numerous shear plane indicating Northward thrust movements. Although no relative chronology has been firmly established, it seems that these structures comprise early 110-trending folds and later N 70-trending ones (fig. 3). The lack of any deformations North of the C-C Fault indicates that the two domains were still far from each other at this time (Jaillard et al. 1992).

The nature of both the basement and the sedimentary cover indicates that Coastal Ecuador was an oceanic basin during this period.

Late Paleocene-Early Eocene. Deposits of late Paleocene age are known only South of the C-C Fault. The deformed Santa Elena Fm is capped by a thick series of coarse-grained high-density turbidites (≈ 1500-2000 m, Azúcar Gp, fig. 2), which contains clasts of Quarz, metamorphic rocks, and of the Santa

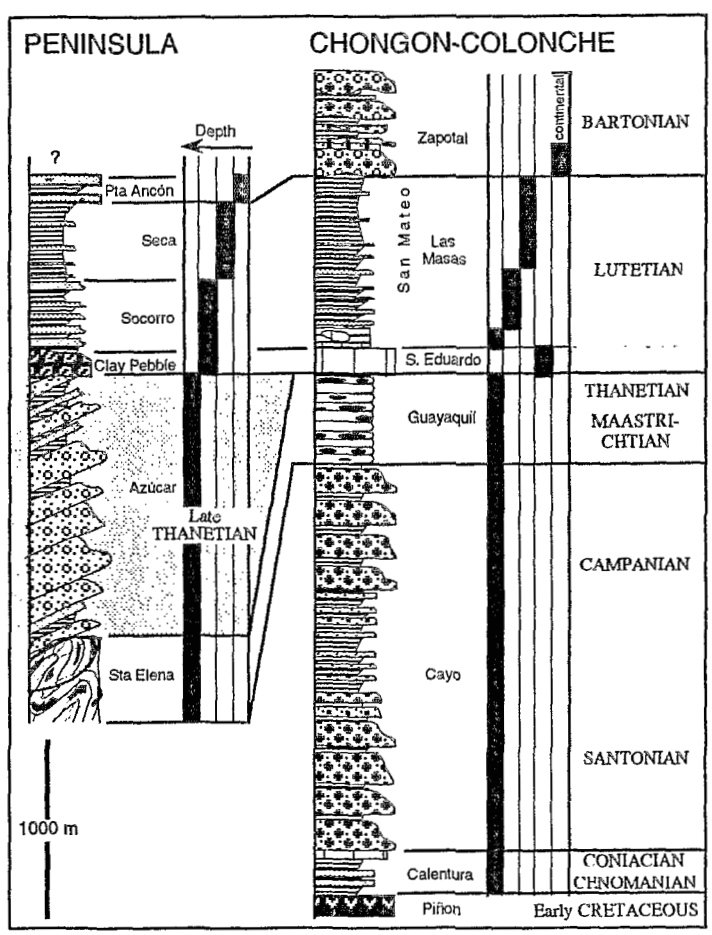

Fig. 2: Stratigraphy of the series of Southern Coastal Ecuador.

Elena and Guayaquil Fms. Part of the deformation thus occurred during Late Paleocene times. The irruption of continent-derived clastic material in the oceanic basin indicates that the Late Paleocene phase is the result of the collision of the Peninsula with the Andean continental margin (Jaillard et al. 1992).

The widespread early Eocene sedimentary gap in Coastal Ecuador is most probably due to a new tectonic phase of latest Paleocene to earliest Eocene age. As a matter of fact, the report of early Eocene fauna (Small 1962) within lignite-bearing sandstones and shales (Atlanta Fm) in wells of the Ancón Oil field (Marchant 1956) suggests that this timespan is a period of erosion and local subaerial deposition. Moreover, the late Paleocene turbidites (Azúcar Gp) are often deformed by N 70-trending tight folds with steep-deeping axial planes, which are unknown in the Eocene deposits. Finally, in the Talara Basin of Northwesternmost Peru, coarse-grained polygenic conglomerates of early Eocene age disconformably overly fine-grained Paleocene marine black-shales. Note that on the Eastern part of the C-C Cordillera, late Paleocene and early Eocene deposits are locally represented by a few meters of transition beds between the Paleocene pelagic cherts (Guayaquil Fm) and the mid-Eocene transgressive limestones.

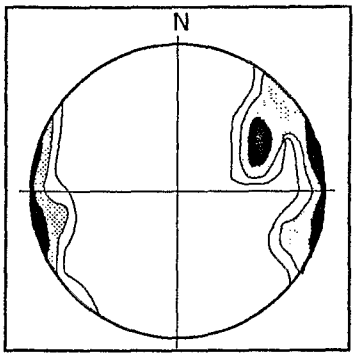

Fig. 3: Fold axis of the early deformations of the Peninsula.

The early Eocene tectonic phase could correspond to the acretion of the Peninsula to the C-C Cordillera, since the subsequent deposits are rather comparable at both side of the C-C Fault (see below).

Lutetian. On the C-C Cordillera and North of it, the Lutetian transgression is diachronous and the erosion of the substratum increases westward. Toward the East, early Lutetian calciturbidites and limestones containing algae and benthic foraminiferas (≈ 100 m, San Eduardo Fm, fig. 2) disconformably overly the paleocene cherts (Guayaquil Fm). Farther West, the transgression is of middle to late Lutetian age, and is associated with a rapid subsidence related to extensional tectonics, that provokes the reworking (Javita Fm) of the early Lutetian and Paleocene sediments, or the deposition of olistolites of Maastrichtian rocks within pelagic limestones and cherts (≈ 200 m, Cerro, lower San Mateo Fms). These unconformably overly the late Cretaceous volcaniclastic turbidites (Cayo Fm). These pelagic deposits are overlain by a shallowing-upward sequence of mud to clastic shelf environment comparable to that of the Peninsula (see below).

South of the C-C Fault, the Lutetian cycle begins with slumped shales and sandstones (0 to ≈ 200 m, Clay Pebble Fm), that express a tectonic activity. The presence of reworked blocks of early Lutetian calciturbidites suggests that the whole area was submitted to extensional tectonic subsidence. Middle to Late Lutetian times are then mainly represented by a shallowing-upward sequence of mud-clastic shelf environment (fig. 2). The lower part (≈ 1000 m, Socorro Fm) is characterized by the abundance of turbidites and slumpings indicating a NW- slope. The upper part (≈ 500 m, Seca Fm) is marked by the increase of the bioturbations and of the carbonate contain, the diversification of the fauna, the vanishing of the tectonic activity and the appearance of tempestites

Bartonian. Along the Southern and Western coast of Southern Coastal Ecuador, the Lutetian cycle is abruptly overlain by coarse-grained sandstones and conglomerates deposited in a shoreline environment, which exhibit a noticeable enrichment in volcanic clasts and plant fragments (≈ 100-400 m, Punta Ancón, upper San Mateo Fms, fig. 2). These deposits presents abundant small-scale, synsedimentary tectonic features. Paleocurrents are roughly perpendicular to the present-day coast (fig. 4), thus suggesting that its morphology was grossly similar to the present-day one, and comprised a central source-area. In the Peninsula, these deposits are mainly made up of shales and sandstones (Punta Ancón Fm), whereas farther North (upper San Mateo Fm, fig. 4), they include thick lenses of coarse-grained conglomerates of alluvial fan type, and abundant blocks suggesting the presence of coastal cliffs. These deposits seem to laterally grade eastward into fluvial conglomerates and coarse-grained fanglomerates nammed upper San Mateo Fm on the Northern part of the C-C Cordillera, and Zapotal Fm on its Southern part and in the Penin-

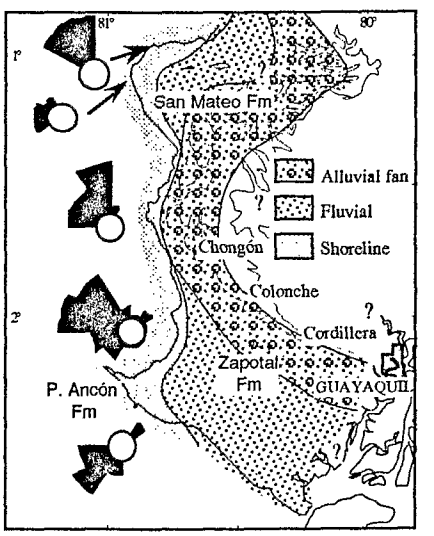

Fig. 4: Paleogeographic interpretation of the Bartonian (and early Priabonian?) deposits of Southern Coastal Ecuador.

sula (fig. 4). The latter undated formation has been ascribed either to the late Eocene (Canfield 1966), or to the late Oligocene (Bristow & Hoffstetter 1977). Though no reliable paleontological data are yet available, our observations support the former hypothesis (fig. 2).

The emergence of the whole Coastal Ecuador by early Late Eocene times, is regarded as the result of its collision or, more likely, its thrusting on the Andean continental margin (Bourgois et al. 1990).

Late Eocene. In the studied area, this time-span seems to be characterized by a widespread sedimentary gap, which will follow up to Late Oligocene, and corresponds to the early Late Eocene major Incaic phase. However, in the Northern part, the upper San Mateo Fm could reach the early Late Eocene (Bristow & Hoffstetter 1977). In the Peninsula, the late Eocene deformation is only marked by gentle folds exhibiting a N-S to NNE-SSW axial plane, associated with reverse faults, that dip gently toward the E or SE.

GEODYNAMIC IMPLICATIONS

The evolution of Coastal Ecuador presents two periods. Late Cretaceous to early Late Paleocene times are characterized by an oceanic basin evolution. The late Late Paleocene-late Eocene time-span is marked by its progressive tectonic accretion to the continental margin. From then on, it constitutes the forearc basins of the Andean margin.

Untill now, Southern Coastal Ecuador have been considered as a single accreted oceanic terrane. The discovery in the Peninsula of two major deformation events unknown North of the C-C Fault, indicates that these areas are characterized by different accretionary histories and constitute two different oceanic terranes.

These early tectonic phases, of Late Paleocene and Early Eocene age, respectively, together with the late Eocene, Incaic phase, are the major deformational events recorded in Coastal Ecuador, and are of decreasing intensity with time. Surprisingly, in spite of its location very close to the subduction zone, Coastal Ecuador did not undergo subsequent important deformations, and virtually all the subsequent tectonic shortening has been accounted for by the more distal continental crust.

The tectonic phases of late Paleocene-earliest Eocene age coincide with a major geodynamic reorganization. Between 56 and 50 Ma, the convergence direction of the paleoPacific plate changed from N or NNE to NE (Pilger 1984, Gordon & Jurdy 1986, Pardo-Casa & Molnar 1987). As a consequence, the formerly mainly dextral transform margin of Ecuador might have changed to a chiefly convergent regime at that time. If so, the oceanic or continental microplates, formerly submitted to a Northward shift along the Andean margin, were successively accreted to the continent, due to this new convergence direction, that must have triggered the formation of a new Ecuadorian subduction system, along the continental margin and the newly accreted terranes.

REFERENCES

AMOCO, 1991, *Internal unpublished Report, Petroecuador* , 2 vol., Guayaquil.
BENITEZ, S. et al., 1986, *Actas IV Cong. Ecuat. Ing. Geol. Min. y Petrol.* , tomo I, 1-24, Quito.
BENITEZ, S., 1990-1991, *Geociencia* , **3**, 7-11; *Geociencia* , **4**, 18-20; & *Geociencia* , **5**, 11-14, Guayaquil.
BOURGOIS, J. et al., 1990, *C. R. Acad. Sci. Paris* , (II), **311**, 173-180.
BRISTOW, C.R. & HOFFSTETTER, R. ,1977, Lexique Intern. Stratigr., CNRS ed., Paris, Va2, 410 p.
CANFIELD, R.W., 1966, *Rep. Minist. Indust. Comer.* , 101 p., Quito.
COLMAN, J.A.R., 1970, *Ecuad. geol Geophys. Soc.* , Quito.
FEININGER, T. & BRISTOW, C.R., 1980, *Geologische Rundschau* , **69**, 849-874, Stuttgart.
GORDON, R.G. & JURDY, D.M., 1986, *J. Geophys. Res.* , **91**, B12, 12,389-12,406.
JAILLARD, E. et al., 1992, ORSTOM-Petroproducción internal Reports, Guayaquil, unpubl..
MARCHANT, S., 1961, *Quat. Jour. geol. Soc.*, **117**, 215-232, London.
PARDO-CASAS, F. & MOLNAR, P., 1987, *Tectonics* , **6**, 233-248.
PILGER, R.H. Jr., 1984, *Journ. geol. Soc. London* , **141**, 793-802.
ROPERCH, P. et al., 1987, *Geophys. Res. Lett.* , **14**, 558-561.
SMALL, J. Jr, 1962, *Ph. D. Thesis, Univ. Colorado* , 185 p., 6 pl. h.t., unpubl..

STRATIGRAPHY OF THE "CELICA-LANCONES BASIN" (SOUTHWESTERN ECUADOR- NORTHWESTERN PERU). TECTONIC IMPLICATIONS.

Gerardo BERRONES [1], Etienne JAILLARD [2], Marta ORDOÑEZ [1], Peter BENGTSON [3], Stalin BENITEZ [1], Nelson JIMENEZ [1] and Italo ZAMBRANO [1].

(1) Petroproducción, Km 6,5 via a la Costa, casilla 10829, Guayaquil, Ecuador.
(2) Misión ORSTOM, Rusia y Eloy Alfaro, Apartado postal 17.11.06596, Quito, Ecuador.
(3) Geologisch-Paläontologisches Institut, Im Neuenheimer Feld 234W, 6900 Heidelberg, Germany.

RESUMEN : En la "Cuenca de Celica-Lancones", se distingue una serie sedimentaria occidental, que constituye la cobertura del Bloque Amotape-Tahuin, y una serie oriental en parte volcánica perteneciendo a la margen andina. Están separadas por una sutura tectónica, que involucra rocas maastrichtianas. Por lo tanto, la colisión del Bloque Amotape-Tahuin con la margen andina ocurrió despues del Maastrichtiano, probablemente en el Eoceno basal.

KEY-WORDS : Late Cretaceous, Paleogene, Andean margin, Terrane, Accretion.

INTRODUCTION

The Andes are classically divided into Central, liminal Andes without accretions nor ophiolites, and Northern and Southern Andes, which underwent obduction and/or accretion of oceanic and/or continental terranes. Moreover, the tectonic rotations are clockwise in the Northern Andes, whereas they are counter-clockwise in the Central Andes (Kissel et al. 1992). Therefore, the Peru-Ecuador border, that roughly coincides with the Northern to Central Andes transition (Mourier 1988), is a key area to understand the tectonic behaviour of the Andean margin and of the allochtonous terranes.

GEOLOGICAL SETTING

The Cretaceous series of the Celica (Southwestern Ecuador) and Lancones (Northern Peru) zones were interpreted as the infilling of a back-arc basin located on the suture of the Amotape-Tahuin Block (ATB), accreted to the Andean margin at the Jurassic-Cretaceous boundary (Mourier 1988, fig. 1). In these interpretations, western facies unconformably overly the Paleo-

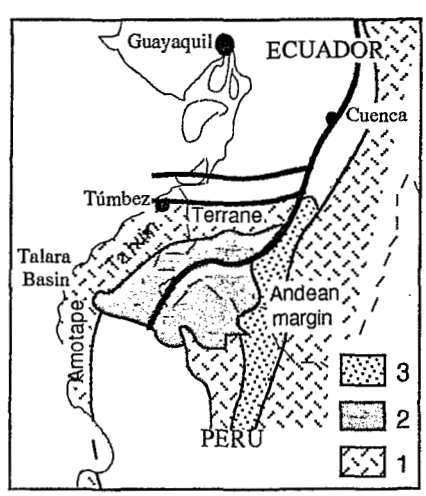

Fig. 1: Location sketch. 1: Paleozoic rocks; 2: Cretaceous "Celica-Lancones Basin"; 3: early Tertiary rocks of the Andean margin.

zoic rocks of the ATB, and laterally grade eastward into volcanic and volcaniclastic deposits, which are separated from the Andean margin by important faults (Kennerley 1973, Morris & Alemán 1975, Bristow & Hoffstetter 1977, Reyes & Caldas 1987, Mourier 1988). Paleomagnetic studies indicate that the ATB underwent a northward drift of hundreds of kilometers and a ≈110° clockwise rotation since the Paleozoic, whereas the Cretaceous rocks of the "Celica-Lancones Basin" recorded a ≈ 60° rotation, without significant migration (Mourier et al. 1988).

New stratigraphic, sedimentologic and structural field data, as well as partial geologic survey in the ecuadorian part of the "Celica-Lancones Basin" led to distinguish two tectonic units, separated by a major tectonic suture. The western series constitutes the stratigraphic cover of the ATB, whereas the eastern one represents the sedimentation of the Andean continental active margin.

STRATIGRAPHY

The Cretaceous-Paleogene sedimentary cover of the Amotape-Tahuin Block.

Disconformably overlying the Paleozoic rocks of the Eastern side of the ATB, is a thick, undated series of deltaic (?) shales and sandstones, overlain by mature, coarse-grained fluvial sandstones. They are correlative with the early Cretaceous Goyllarisquizga Gp of the West-peruvian margin (Benavides 1956, Gigantal Fm of Mourier 1988, Huayllapampa Gp of Myers 1980). A marine transgression then deposited shales, sandstones and limestones, correlative with the late Aptian-earliest Albian transgression of Peru (Inca and Pariahuanca Fms, Benavides 1956, Wilson 1963). They are overlain by black laminated, bituminous limestones, which yielded middle Albian ammonites (Bristow & Hoffstetter 1977), coeval with similar deposits of Peru (Chulec-Pariatambo and Pananga-Muerto Fms, Benavides 1956, Reyes & Caldas 1987).

These are overlain by a thick series of black shales and feldspathic sandstones, interpreted as low density turbidites representing the erosion of a continental cristalline basement with a noticeable volcanic contamination. These are known as the Copa Sombrero Gp in Northwestern Peru, and are dated as Cenomanian (Olsson 1934) to Campanian (Morris & Alemán 1975)(fig. 2). In Ecuador, they are capped by a 100 m-thick conglomerate correlative with the Campanian Tablones Fm of Peru (Reyes & Caldas 1987), and then by black shales, with thin-bedded turbidites intercalations and limestone nodules, dated as Maastrichtian in Peru (Pazul, Monte Grande Fms, Olsson 1934, Reyes & Caldas 1987)(fig. 2).

On the western side of the ATB (Talara Basin), a major transgressive unconformity (Sandino Fm) is overlain by Campanian to Paleocene marine shales (Redondo Fm, Mal Paso Gp, Gonzalez 1976). These are disconformably overlain by coarse-grained, continental, polygenic conglomerates (Mogollón Fm) grading westward into shallow-marine sandstones and shales of early Eocene age (Salina Gp, Gonzalez 1976, Séranne 1987).

The Cretaceous to Paleogene series of the Andean continental margin.

The lowermost unit is a thick series of massive, faulted and altered andesites, ascribed to the **Celica Fm.** Although it is crosscut by granites dated as Aptian (114-111 Ma K-Ar ages, Kennerley 1973), the Celica Fm is thought to correlate with the Albian volcanics of Western Peru (Casma Gp, Myers 1980, Soler 1991).

The Celica Fm is overlain by sandstones and greywackes (≈ 200 m), and then by thick-bedded, coarse-grained volcaniclastic high-density turbidites (≈ 1500-2000 m), with few thin intercalations of lavas and black laminated limestones. We propose to call this unit the **Alamor Group** (fig. 2). A poor microfauna locally indicates a post-Albian, probably Turonian age. Though the basal contact has not been observed, the lack of important deformation and alteration within this unit indicates that the Celica Fm was deformed before its deposition.

The **Naranjo Fm** (≈ 150-200 m) unconformably overlies either the Celica Fm or the Alamor Gp. It begins with transgressive pebbly marls containing Santonian ammonites, followed by coarsening-upward sequences of marls, fossiliferous limestones and grauwackes, of shallow-marine shelf to deltaic environment. Thee upper part of the unit yielded a late Campanian or early Maastrichtian microfauna (fig. 2).

The **Casanga Fm** (≈ 200-400 m) consists of shales, thin-bedded turbiditic grauwackes and nodular limestones of marine shelf environment. It differs from the underlying strata by the presence of coarse-grained conglomeratic lenses and beds, that reflect the progradation of coastal alluvial fans. The Casanga Fm contains a poor late Cretaceous microfauna, and would be mainly of Maastrichtian age (fig. 2).

Locally, it is unconformably overlain by undated, red-coloured, continental shales, siltstones and volcaniclastic beds, which seem to belong to the **Sacapalca Fm**, that crops out farther East. The latter is made up of

thick subaerial andesitic flows with intercalations of fluvial red beds, crosscut by an early Eocene pluton (49 Ma, Kennerley 1973). It is thus probably coeval with the Llama and Porculla volcanics of Northern Peru (Reyes & Caldas 1987, Mourier 1988).

This volcanic series is overlain by the undated **Catamayo Fm.** It comprises regressive sedimentary sequences, grading from coastal-marine shales to fluvial coarse-grained conglomerates (fig. 2). The latter mainly contain clasts of metamorphic rocks, and thus contrast with the underlying, mainly volcaniclastic formations.

Southerly, the Sacapalca Fm is overlain by lacustrine black shales and turbiditic grauwackes, with abundant slumpings and olistolites belonging to the undated **Gonzanamá Fm.** Its relationship with the Catamayo Fm is unknown.

The latter formations are unconformably capped by the probably Oligocene volcanic flows of the Loma Blanca Fm.

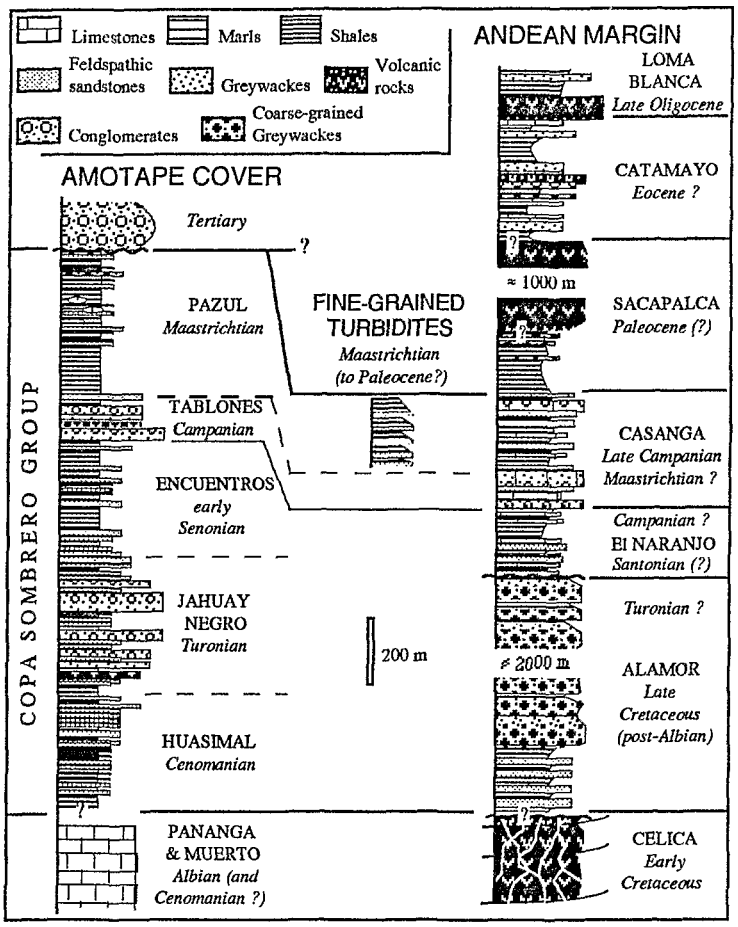

Fig. 2: Stratigraphic sketch of the Celica-Lancones series.

The Maastrichtian slices. The above-described series are separated by a major fault, whithin which are pinched discontinuous slices of black-coloured, thin-bedded turbidites and cherts, which have been locally dated as Maastrichtian (Bristow & Hoffstetter 1977)(fig. 2). These are ususally affected by tight folds associated with well-developped axial plane cleavage.

TECTONIC INTERPRETATIONS

The eastern, Andean series differs from the western, ATB cover, through : (1) the presence of an early Cretaceous volcanic "basement", (2) the dominant volcanic nature of the detritism throughout late Cretaceous and Paleocene (?) times and (3) the presence of a mixed carbonate-detritic shelf during Senonian times. These major differences indicate that they belonged to quite different paleogeographic domains, and that they cannot have deposited in a same "Celica-Lancones Basin" of Cretaceous and Paleocene age.

In spite of still poor stratigraphic data, the eastern series recorded all the major early Andean geodynamic events (Jaillard 1993, fig. 3). The thick andesitic Celica Fm probably represents the products of the Albian subduction-related volcanic arc, which is well known along the Peruvian margin (Casma Gp, Quilmana Fm, Soler 1991). Its deformation before the deposition of the Alamor Gp woulde result from the late Albian-early Cenomanian Mochica compressive phase of Peru (Mégard 1984). The subsequent accumulation of thick, coarse-grained deposits (Alamor Gp) indicates the creation of a subsident trough (fig. 3), possibly related to dextral wrench movements (e.g. Soler 1991). The Coniacian (?) unconformity below the Naranjo Fm is correlative with the early Peruvian phase, defined in Southwestern Peru (Jaillard 1993). The appearance of conglomerates in the Casanga Fm seems to be coeval with the late Campanian major Peruvian phase. The late Maastrichtian or Paleocene regression, the intense volcanic activity of probable Paleocene age (Sacapalca

Fm), and the marine transgression of possible Eocene age (Catamayo Fm) still need stratigraphic confirmations, before to attempt correlations with Andean events known elsewhere. Whichever the case, the Celica series is one of the quite scarce examples of a complete sedimentary series deposited in a forearc setting throughout the whole central Andes.

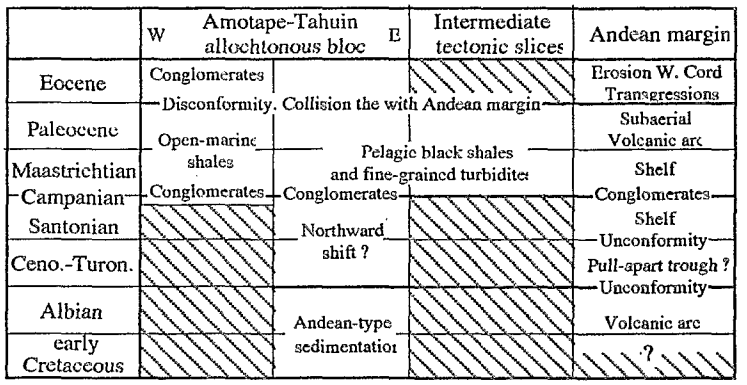

Fig. 3: Tectonic interpretations of the late Cretaceous-Paleogene evolution of the Amotape and Andean series.

The early Cretaceous to Albian facies of the ATB cover are comparable with those of the West- Peruvian margin, and it probably belonged to this latter at this time (fig. 3). Since Cenomanian times onwards, the turbiditic sedimentation on the ATB differs totally from that of the Andean margin. This drastic change could be interpreted as the beginning of the northward migration of the ATB. As a matter of fact, late Cretaceous times are a period of very oblique, northward convergence, which would have induced dextral wrenching along the Andean margin. This could also account for the coeval creation of the Alamor, possibly pull-apart basin (fig. 3).

The presence of Maastrichtian rocks in the suture between the two units demonstrates that these cannot have been emplaced in their present-day location before Maastrichtian times. Therefore, the hypothesis of the latest Jurassic to earliest Cretaceous collision of the ATB must be left out. The age of the accretion of the ATB could be indicated by the irruption of the early Eocene coarse-grained deposits (Mogollón Fm) in the Western side of the ATB (Talara Basin).

CONCLUSIONS

The Celica-Lancones area comprises two distinct late Cretaceous-Paleogene sedimentary series and can no longer be considered as a "Basin" of that age. The western unit represents the cover of the Amotape-Tahuin Block, whereas the eastern one is a well-preserved example of an Andean series in a arc to fore-arc setting. The presence of deformed Maastrichtian slices between both units indicates that the accretion of the Amotape-Tahuin terrane occurred after Maastrichtian times, probably near the Paleocene-Eocene boundary.

REFERENCES

BENAVIDES, V., 1956, *American Museum of Natural History Bulletin*, **108**, 352-494, New York.
BRISTOW, C.R. & HOFFSTETTER, R., 1977, Lexique Intern. Stratig., CNRS ed., **Va2**, 410 p., Paris.
GONZALEZ, G., 1976, Dr Thesis, Univ. San Agustin, 225 p., Arequipa.
JAILLARD, E., 1993, *in : Cretaceous tectonics in the Andes*, Earth Evol. Sci. ser., Vieweg, Wiesbaden.
KENNERLEY, J.B., 1973, London Institute of Geological Sciences, Report **23**, 34 p., London.
KISSEL, C. et al., 1992, *Bull. Soc. géol. France*, **163**, 371-380, Paris.
MORRIS, R.C. & ALEMAN, A.R., 1975, *Bol. Soc. geol. Perú*, **48**, 49-64, Lima
MOURIER, T., 1988, Dr Thesis Sci., Univ. Paris XI, 275 p., Orsay.
MOURIER, T. et al., 1988, *Earth Planet. Sci. lett.*, **88**, 182-192, Amsterdam.
MYERS, J.S., 1980, *Boletín INGEMMET*, **33**, 145 p., Lima.
OLSSON, A.A., 1934, *Bulletin of American Paleontology*, **20**, 104 p., New-York.
REYES, L. & CALDAS, J., 1987, *Bol. Inst. Geol. Min. Met.*, A, **39**, 83 p., Lima.
SÉRANNE, M., 1987, IFEA - Petroperú, unpubl. Report, 73 p., Lima.
SOLER, P., 1991, Dr Thesis Sci., Univ. Paris VI, 950 p., Paris.
WILSON, J.J., 1963, *American Association of Petroleum Geologists Bulletin*, **47**, 1-34, Tulsa.

SEDIMENTATION, PALEOGEOGRAPHY AND TECTONIC OF THE CUZCO AREA BETWEEN KIMMERIDGIAN?-PALEOCENE TIMES : RELATION WITH THE SOUTH PERUVIAN MARGIN

Victor CARLOTTO (1), Etienne JAILLARD (2), Georges MASCLE (3).

(1) Univ. Nac. San Antonio Abad del Cuzco, Av. de la Cultura, Cuzco, Peru.
(2) ORSTOM-UR 1H, 213, Rue La Fayette, 75480 Paris Cedex, France.
(3) Institut Dolomieu, rue M. Gignoux, 38031 Grenoble, France.

RESUMEN

Estudios de sedimentación, paleogeografía y tectónica de rocas del Kimmeridgiano?-Paleoceno de la región de Cusco, muestran que estas se depositaron sobre un umbral que separaba dos cuencas, las que se hallaban en una posición de tras arco distal y que registran eventos tectono-sedimentarios que están en relación con la evolución de la margen sur peruana.

KEY WORDS: sedimentation, paleogeography, tectonic, Kimmeridgian?-Paleocene, Cuzco, Peru.

INTRODUCTION

The tectonic and sedimentary evolution between Kimmeridgian?-Paleocene times of the Cuzco area (South Peru) is divided in 5 stages. The sedimentation developed over the Cuzco-Puno swell which separated the Western trough and the Eastern trough. The formation of the Eastern trough began during Kimmeridgian? times. This region in back-arc basin position recorded the external tectonic evolution of the South Peruvian margin.

GEOLOGICAL SETTING

During Mesozoic times, the Peruvian margin had a contrasted paleogeographic pattern (Jaillard, 1992)(Fig. 1). It can be divided into several NW trending zones, parallel to the subduction trench. In South Peru margin is possible to distinguish from W to E: 1) a narrow Coastal zone, which mainly comprises pre-Cretaceous rocks; 2) a Western subsiding trough which received thick marine sediments (presently Western Cordillera); 3) a positive swell, which received a reduced sedimentation (Cusco-Puno swell), and 4) an Eastern, less subsiding basin filled by mainly continental deposits (presently Eastern Cordillera).

During Kimmeridgian?, Cretaceous and Paleocene times, the sedimentation of the Cuzco area developed over the Cuzco-Puno swell which was emerged before latest Jurassic times.

GEOLOGICAL EVOLUTION (Fig. 2)

1. Kimmeridigian?-Berriasian? (Huambutio Fm).

The Huambutio Fm is composed by alluvial fan conglomerates (Lower Mb), thin marine limestone beds (Middle Mb), and continental sandstone, shales and conglomerates (Upper Mb). This formation is marked by numerous synsedimentary tectonic features which expresses a NW-SE trending extensional regime. During this period, the contrasted paleogeography is an effect of the beginning of the Eastern trough opening. All of this is interpreted as a distal consequence of the Araucan tectonic phase, which can be observed in North Chile and Argentina (Sempere et al. 1988).

In the Western trough developed a marine sedimentation and extensional regime related with the geodynamic events ocurred in the Paleopacific plate. So, the latest Jurassic-lower Neocomien period appears as a transition period between the convergence NNW-SSE Phoenix-South America (Bathonian-Kimmeridgian), and NE-SW (Valangian-Aptian)(Soler, 1991).

2. Neocomian (Huancane Fm).

The Huancane Fm is mainly composed by quartz white sandstones which are deposited in fluvial environments and which proceed from east. The clean neocomian sandstones are good expressed in the whole Peruvian territory (Moulin, 1989). In the Cuzco area, the fluvial sedimentation is mainly controlled by the eustatic sea level fluctuations (Carlotto, 1992). The eastern (Brazilian Shield) origin of the clastics can be interpreted as the result of the incipient rifting of the norther South-Atlantic Ocean (Jaillard, 1992).

The tectonic and magmatic quiescence in the whole Peruvian margin is related to the low convergence rate beetwen Phoenix-South American plates (Soler, 1991).

3. Late Aptian-Turonian (Lower Yuncaypata Gp).

The lower Yuncaypata Gp is characterized by the shallow internal carbonate platform evolution. This one began with a transition of late Aptian-middle Albian sandstones and shales that reached its maximum during the interval upper Albien-Turonian (Yuncaypata limestones). The limestones registered weakly extensive tectonic features.

In the Western trough developed a carbonate platform that is marked by a magmatic activity probably related to an arc (Albien-Cenomanian) and the beginnig of the emplacement of the Coastal Batholith. This period is related to a modification of the subduction, now with a low angle that correspond to a high convergence velocity that makes the oceanic slab become young. All of that, causes extensive and compressives tectonic phases well known in Central and North Peru, (Mochica phases) (Soler, 1991; Jaillard, 1992).

4. Senonian- Maestrichtian (Upper Yuncaypata Gp).

The Upper Yuncaypata Gp is divided in 3 major sedimentary secuences called M1, M2 and M3 (Carlotto, 1992). They are mainly composed by red shales, sandstones and evaporites. This time span corresponds to a global regressive period, which however registers weakly Santonian and middle Campanian transgressions. This regressive episod is related to the successive uplift of the Coastal zone (boundary Turonian-Campanian), followed by the uplift of the SW border (Santonian-Campanian), and later by the uplift of the NE border (Campanian-Maestrichtian) of the Western trough in association with progressive thrusting which develops foreland

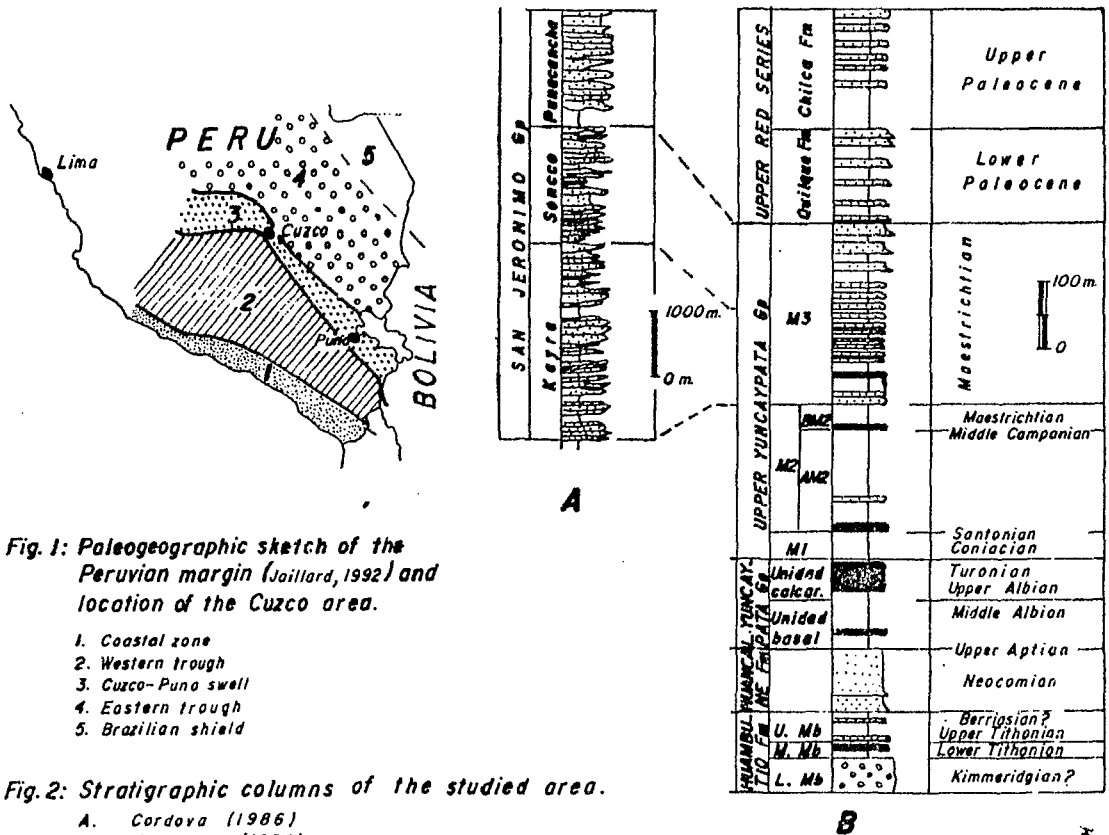

Fig. 1: Paleogeographic sketch of the Peruvian margin (Jaillard, 1992) and location of the Cuzco area.

1. Coastal zone
2. Western trough
3. Cuzco-Puno swell
4. Eastern trough
5. Brazilian shield

Fig. 2: Stratigraphic columns of the studied area.

A. Cordova (1986)
B. Carlotto (1992)

Fig. 3: Schematic sketches of the structural evolution of southern Peru margin.

A. Jurassic-Turonian.
B. Senonian-Maestrichtian.

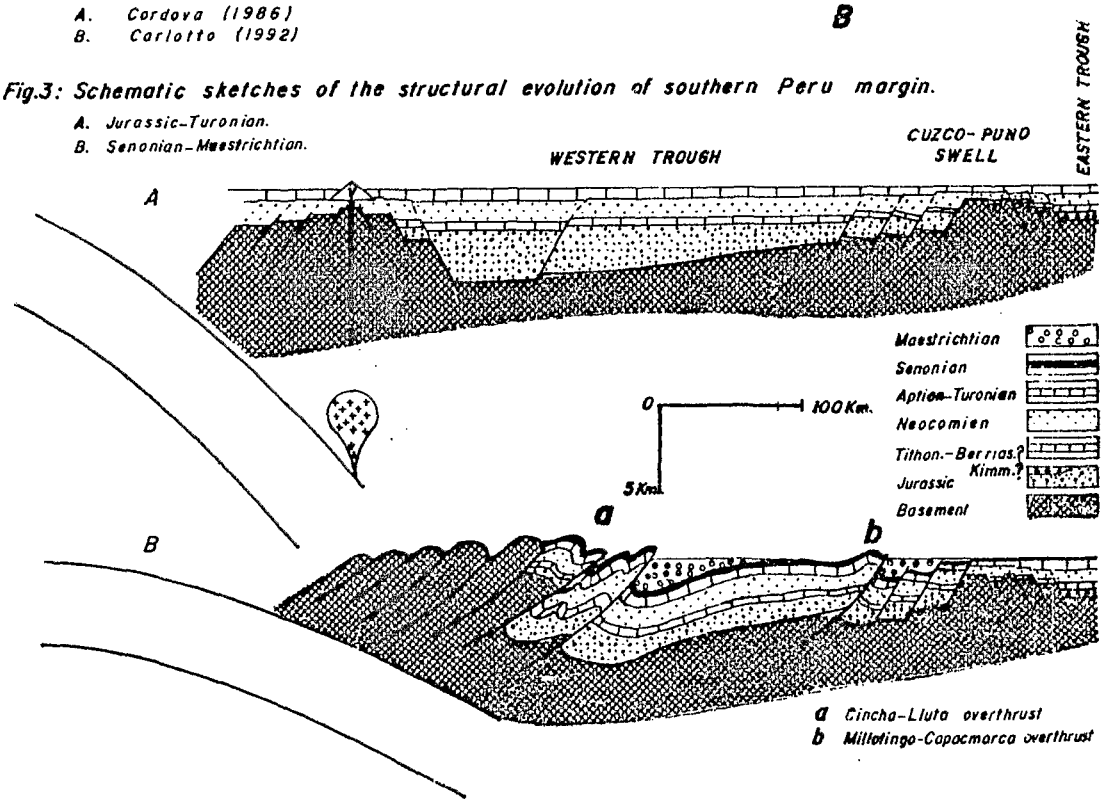

basins (Jaillard, 1992). So, a foreland basin develops during lates Campanian and Maestrichtian San Jeronimo Gp deposition. It was probably located at the boundary between Western trough and Cuzco-Puno swell, and it results the emplacement of the Millotingo-Capacmarca overthrust (Fig. 3). The foreland basin distal part was situated above the Cuzco-Puno swell, corresponding to the sequence M3. After, the San Jeronimo Gp thrust the Cretaceous-Paleocene autochtonous series (Red Beds Nappe).

All these tectonic events except the Red Beds nappe are known as the Peruvian tectonic phase, which is related, first, to a high convergence velocity of the Pacific and South American plates (Coniacian)(Soler, 1991; Jaillard, 1992), and second with the subduction of oceanic obstacle (Mollendo ridge)(Soler et al 1989) that provoked a magmatic gap and a compressive tectonic (progressive migration ot the thrusting toward NE).

5. Paleocene (Upper Red Series).

The Upper Red Series are composed by 2 formations: Quillque and Chilca separated by an unconformity. Each one explains the progradation of the fluvial deposits, the first one from SW origin, the second one from NE origin. Both, probably correspond to the foreland basin evolution.

In the Western trough a volcanic arc activity which began in the Maestrichtian times reached its maximum in the Paleocene times.

CONCLUSIONS

The tectono-sedimentary evolution in the Cuzco area between Kimmeridgian?-Paleocene can be divided in 5 stages grouped in 2 great periods. The first one (Kimeridgian?-Turonian) is mainly a distensive episod. The beginning corresponds to the Eastern trough opening in relation with the Kimmeridgian Araucan tectonic phase. In this moment, there is a change of the Phoenix and South American plates convergence. The ending is characterized by the subduction angle modification for the high convergence velocity of the Pacific and South American plates. The Second one (Coniacian-Paleocene) corresponds to a global regressive episod in association with progressive thrusting that develops the foreland basins. This period is related, first to the Peruvian tectonic phase which begins in the Coastal zone (lowest Coniacian times), and reaches the Cuzco-Puno swell (Maestrichtian). The origin is the high convergence velocity of Pacific and South-American plates and the subduction of oceanic obstacle (Mollendo ridge). Moreover, it is related with the tectonic phases of the boundary Maestrichtian-Paleocene and middle Paleocene.

This sedimentology and stratigraphic study evidence the nappe structure of the San Jeronimo Gp which overlies the Cretaceous-Paleocene autochtonous Cuzco series. Such a nappe is a new evidence of the important shortening ocurred in this part of the Andes.

REFERENCES

CARLOTTO, V. (1992). DEA Univ. Grenoble, 43 p.
CORDOVA, E. (1986). These, Univ. de Pau, 272 p.
JAILLARD, E. (1992).In: J.A. Salfity ed Cretaceous tectonics of the Andes, Earth Evol. Sci. Monog. Ser. Vieweg Publ., Wiesbaden, in press.
MOULIN, N. (1989). These Univ. Montpellier, 287 p.
SEMPERE, T., OLLER, J. & BARRIOS, L. (1988). Actas V Congreso Geológico de Chile, 3: H37-H65, Santiago.
SOLER, P., CARLIER, G. & MAROCCO, R. (1989). Tectonophysics, 163: 13-24.
SOLER E. (1991). These, Univ. Pierre et Marie Curie Paris VI, 845 p.

SUBSIDENCE AND CRUSTAL FLEXURE EVOLUTION OF THE NEOGENE CHACO FORELAND BASIN (BOLIVIA)

Laurent COUDERT[1], Thierry SEMPERE[2],
Michel FRAPPA[1], Claude VIGUIER[1], and Rafael ARIAS[3]

(1) Laboratoire d'Études et de Recherche en Géotechniques et Géophysique Appliquée, 351 Cours de la Libération, 33405 Talence, France.
(2) Orstom (UR 1H), Convention YPFB-ORSTOM, Santa Cruz, Bolivia. Present address: Département de Géologie sédimentaire (LGTE), case 119, Université Paris VI, 75252 Paris cedex 05, France.
(3) YPFB-GXG, cc 1659, Santa Cruz, Bolivia.

RÉSUMÉ: L'évolution de la subsidence dans le bassin du Chaco (Bolivie) est étudiée à l'aide de sismique réflexion, de gravimétrie et de diagraphies différées. Les courbes de subsidence depuis le Miocène supérieur mettent en évidence trois étapes tectoniques avec des taux de subsidence compris entre 0,1 et 0,4 km/Ma. L'application d'un modèle de flexion, avec une rigidité de flexion de 10^{23} N.m et une épaisseur de la croûte de 30-31 km, permet de décrire l'évolution de la géométrie et de la topographie du bassin depuis 10 Ma.

KEY WORDS: Bolivia, foreland basin, crustal flexure, tectonic subsidence, geophysics, model.

INTRODUCTION AND GEOLOGICAL SETTING

During the last decade, important progress has been made in understanding the subsidence mechanisms of foreland basins. Several modelling studies in continental regions have shown that the flexural response to tectonic loading can be represented by an elastic plate overlying a weak fluid (Turcotte and Schubert, 1982; Flemings and Jordan, 1989). The purpose of this paper is to quantitatively estimate the evolution of tectonic subsidence and crustal flexure in the Chaco basin of Bolivia (lat 19°-20°S) through study of geological, seismic reflexion, gravity and log-welling data (mostly unpublished and borrowed from the Bolivian State Oil Company YPFB).

The study was carried out in the Subandean belt of southern Bolivia (Río Grande-Parapetí area; lat 19°-20°S and long 62°-63°S; Fig. 1). The Subandean belt is bounded in the west by the Main Frontal Thrust (CFP, "Cabalgamiento Frontal Principal"), and the Subandean deformation dies out toward the east into the Chaco plain (Hérail et al., 1990; Baby et al., 1992). During the Neogene, the width of the foreland basin has apparently varied from 100 to 120 km in general. The basin is filled by late Oligocene to recent sediments (Sempere et al., 1990) with a maximum thickness of 3000 m in the study àrea. The Tertiary deposits consist of conglomerates, sandstones, siltstones and mudstones, and are subdivided in the Petaca, Yecua, Tariquía, Guandacay and Emborozú formations (see Marshall and Sempere, 1991; Marshall et al., 1993).

RESULTS

Wireline data and cutting descriptions from two wells (further on referred to as well 1 and well 2) were used to build the two corresponding synthetic stratigraphic columns. Structural maps and seismic reflexion lines, in which four Tertiary sequences — bounded by reflectors T_1, T_2, T_3 and T_4 — were selected, were interpreted and correlated with these two logs (Fig. 2). Ages tentatively attributed to these reflectors are respectively: T_4 ≈10 Ma (beginning of local onlap of Neogene deposition), T_3 ≈7.5 Ma (top of Yecua Formation; see Marshall et al., 1993), T_2 ≈4.5 Ma (by interpolation), T_1 ≈1 Ma (major out-of-sequence

reactivation of the CFP system; Sempere, unpublished). Future precisions on the ages of these reflectors may obviously lead to modifications of some of the results presented hereafter.

In order to approach the effects of subsidence, the "back-stripping" method (Steckler and Watts, 1978) was used. The effect of compaction was incorporated for computation of tectonic subsidence. Paleobathymetry and sea-level changes were neglected because the depositional environment remained fluvial.

The porosity of argillaceous sands and mudstones as a function of depth was deduced from sonic tool (BHC) and density tool (FDC) using the matrix parameters and assuming a linear relation between porosity and well logs (Steckler and Watts, 1978).

Three stages were identified (Fig. 3). During stage T_4-T_3 (≈10-≈7.5 Ma), the tectonic subsidence rate was ≈0.4 km/Myr. During stage T_3-T_1 (≈7.5-≈1 Ma), this rate decreased to ≈0.1 km/Myr. Stage T_1-T_0 (from ≈1 Ma to the present) apparently shows an increase in subsidence rate to ≈0.4 km/Myr (Coudert, 1992).

The Bouguer anomaly regularly increases toward the east, i.e. toward the "Alto de Izozog" forebulge (YPFB, unpublished data). In order to understand the distribution of the successive loads on the continental lithosphere, the power spectrum of gravity anomalies (Karner and Watts, 1983) was determined. Discontinuities evidenced through this method are located at the top of and within the basement, i.e. below the base of the sedimentary pile (2-2.2 km-thick). The deepest discontinuity, at 31-32 km, apparently corresponds to the Moho. This crustal thickness is used for estimation of the flexural rigidity, which appears to be $\approx 10^{23}$ N.m (Coudert, 1992).

The evolution of crustal flexure using an elastic model (Turcotte and Schubert, 1982; Flemings and Jordan, 1989) is shown in Fig. 4. The best fit between computational results and seismic and well data is obtained when a flexural parameter (≈horizontal extension of the flexure) of ≈70 km is chosen.

In addition, the position (x_b) and height (w_b) of the forebulge were estimated for each period (Fig. 4). A migration of the forebulge of about 90 km is observed for the last ≈7.5 Myr, which indicates an average migration velocity of ≈9-10 km/Myr.

CONCLUSIONS

Analysis of multiple geophysical data in the late Miocene Chaco continental foreland basin of Bolivia permits to sketch out its evolution and to tentatively describe its successive geometries and topographies since 10 Ma. At least three tectonic stages are identified, which include an interval of relatively low subsidence (≈0.1 km/Myr; ≈7.5-≈1 Ma) intercalated between intervals of higher subsidence (≈0.4 km/Myr). Models used agree with a flexural rigidity of $\approx 10^{23}$ N.m and a crustal thickness of ≈30-31 km.

Acknowledgments

This work was funded by the French Research Administration, the Institut Français de Recherche Scientifique pour le Développement en Coopération (Orstom), and Yacimientos Petrolíferos Fiscales Bolivianos (YPFB). We thank the Gerencia de Exploración of YPFB for granting permission to publish this paper.

REFERENCES

Baby, P., Hérail, G., Salinas, R., and Sempere, T., 1992. Geometry and kinematic evolution of passive roof duplexes deduced from cross-section balancing: Example from the foreland thrust system of the Southern Bolivian Subandean Zone. Tectonics, 11: 523-536.

Coudert, L., 1992. Apports de la sismique et des diagraphies différées à l'étude stratigraphique du bassin du Chaco de Bolivie (Río Grande-Parapetí) — Traitements statistiques et modélisations. Thèse de Doctorat de l'Université de Bordeaux I, 250pp.

Flemings, P.B., and Jordan, T.E., 1989. A synthetic stratigraphic model of foreland basin development. Journal of Geophysical Research, 94: 3851-3866.

Hérail, G., Baby, P., Oller, J., López, M., López, O., Salinas, R., Sempere, T., Beccar, G., and Toledo, H., 1990. Structure and kinematic evolution of the Subandean thrust system of Bolivia. International Symposium on Andean Geodynamics, 1st, Grenoble: 179-182.

Karner, G.D., and Watts, A.B., 1983. Gravity anomalies and flexure of the lithosphere at mountain ranges. Journal of Geophysical Research, 88: 10449-10477.

Marshall, L.G., and Sempere, T., 1991. The Eocene to Pleistocene vertebrates of Bolivia and their stratigraphic context: a review. In: Fósiles y Facies de Bolivia, R. Suárez-Soruco (ed.), Revista Técnica de YPFB, Santa Cruz, 12: 631-652.

Marshall, L.G., Sempere, T., and Gayet, M., 1993. The Petaca (late Oligocene-middle Miocene) and Yecua (late Miocene) formations of the Subandean-Chaco basin, Bolivia, and their tectonic significance. Documents du Laboratoire de géologie de Lyon, 125: in press.

Sempere, T., Hérail, G., Oller, J., and Bonhomme, M. G., 1990. Late Oligocene-early Miocene major tectonic crisis and related basins in Bolivia. Geology, 18: 946-949.

Steckler, M.S., and Watts, A.B., 1978. Subsidence of the Atlantic-type continental margin off New-York. Earth and Planetary Sciences Letters, 41: 1-13.

Turcotte, D.L., and Schubert, G., 1982. Geodynamics: Applications of Continuum Physics to Geological Problems. J. Wiley and Sons, New York, 650 pp.

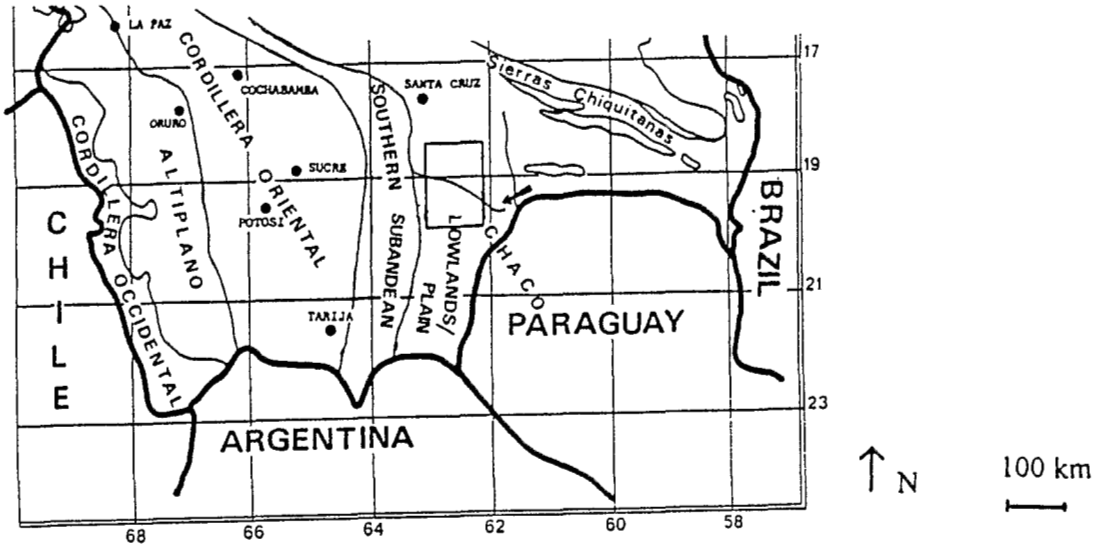

Fig. 1 — Map of southern Bolivia showing location of studied area.

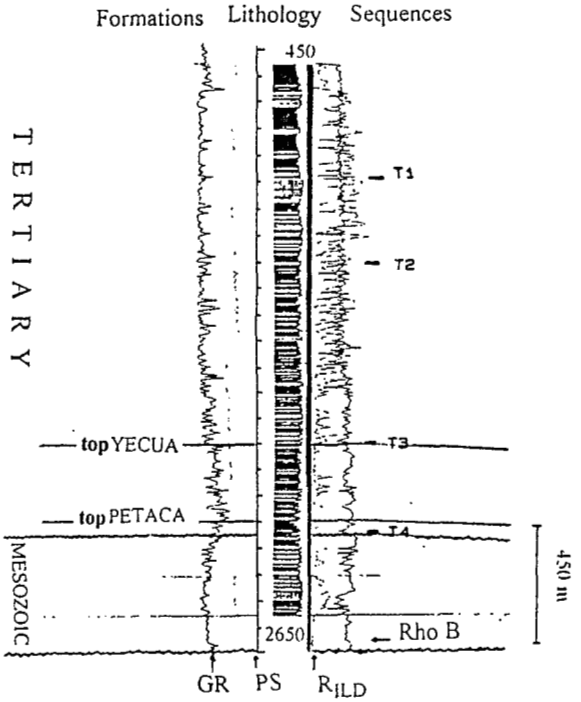

Fig. 2 — Schematic lithology and stratigraphy of well 1, with indication of stratigraphic location of reflectors T_1 through T_4. Wireline logs: GR = gamma ray, PS = spontaneous potential, R_{ILD} = induction resistivity, Rho B = density tool (FDC). Lithology: sandstones are in white; mudstones are in black.

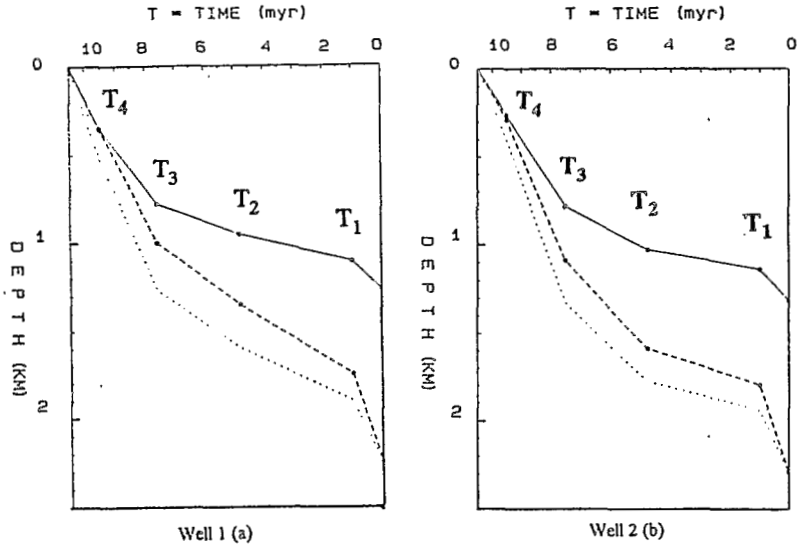

Fig. 3 — Tectonic subsidence curves since 10 Ma for wells 1 and 2. Dashed line: observed subsidence; dotted line: subsidence after decompaction; solid line: computed basement subsidence.

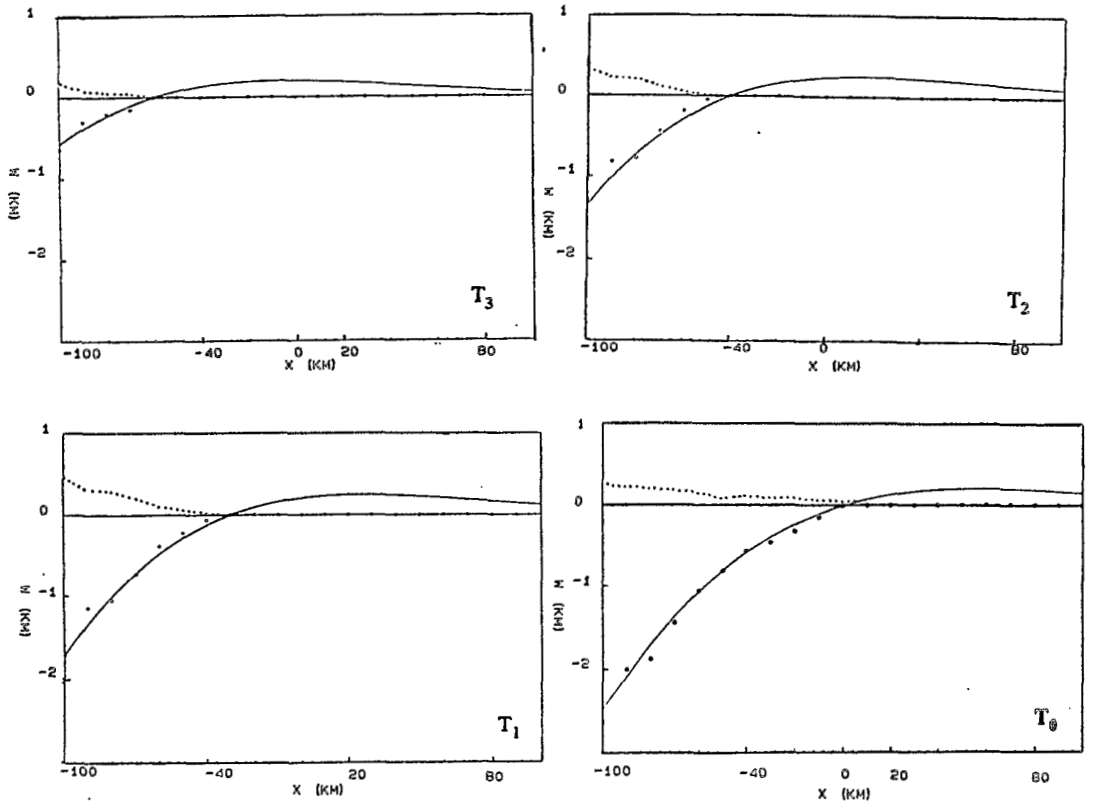

Fig. 4 — Successive depths of the top of the basement at "times" T_3, T_2, T_1, and "T_0" (present). Points: observed seismic data; solid line: computed flexure profile; dotted line: compensated topography.

GEODYNAMICS OF ANDEAN BASINS: AN EXAMPLE FROM THE SALAR DE ATACAMA, BASIN, NORTHERN CHILE

Stephen FLINT[1],
Adrian HARTLEY[2],
Peter TURNER[3], Liz JOLLEY[3]
Guillermo CHONG[4]

1. Department of Earth Sciences, University of Liverpool, P.O. Box 147, Liverpool L69 3BX, U.K.
2. Department of Geology & Petroleum Geology, University of Aberdeen, Aberdeen AB9 2UE, U.K.
3. School of Earth Sciences, University of Birmingham, P.O. Box 363, Birmingham B15 2TT, U.K.
4. Departamento de Geociencias, Uinversidad Catolica del Norte, Antofagasta, Chile

KEY WORDS: Chronostratigraphy, Central Andes, Extensional tectonics, Basin analysis

INTRODUCTION

We describe the history of the Salar de Atacama, a long-lived (Permo-Triassic - Recent) nonmarine basin which, owing to the geodynamic development of the Central Andes, has evolved from a non-arc-related rift basin, through complex "arc-related" stages, to a Miocene-Recent forearc basin. We attempt to demonstrate that sedimentary basins at convergent plate margins preserve the most complete record of the local geodynamic history of the orogen and their analysis is an essential component in studies of crustal evolution. Our database includes over one hundred logged sections (some 20 km of stratigraphy), field maps, and the interpretations of aerial photographs/satellite images and several regional seismic lines across the basin.

GEOLOGICAL SETTING

The Salar de Atacama has a long geological history, from Permo-Triassic to Recent, all of it non-marine. The composite, approximately 10 km of stratigraphy can be divided into five unconformity-bounded megasequences (Fig. 1). These are the Permo-Triassic Peine Formation and equivalents, the latest Cretaceous-Eocene Purilactis Group (Hartley et al., 1992), the Oligocene-earliest Miocene Paciencia Group (Flint, 1985), the early Miocene-Plio-Pleistocene San Bartolo Group/Vilama Formation (Jolley et al., 1990) and the Holocene alluvial fans and saliferous deposits. The major types and periods of faulting and folding within the composite stratigraphy of the Salar de Atacama include:-

1. Permian listric normal faults, striking north-south, downthrowing to the east.
2. Late Cretaceous reactivation of the Permian fault system, resulting in thickening of the Purilactis Group in the hanging walls of these faults.
3. Local intense folding of the Purilactis Group in the northwest of the basin, linked to dextral strike-slip faulting (late Eocene).
4. East to southeast thin-skinned thrusting and related folding in the early Miocene.
5. Neotectonic thrusting of Tertiary strata over Holocene gravels.

Outcrop and particularly seismic reflection data indicate that the dominant control on basin formation and deposition of the bulk of the Salar basin fill was extensional to oblique extensional

faulting. Our seismic stratigraphic analysis indicates 1500 m+ of pre-Purilactis Group sedimentary rocks, characterized by discontinuous reflectors. This earliest basin fill unit shows large thickness variations across the Salar de Atacama area; these variations coincide with the positions of several large faults. Thickening of stratal units towards the faults indicates synsedimentary fault activity, which defined several sub-basins. The Cordon de Lila was a basement high during this time. We think that the whole Permo-Triassic succession represents a major episode of rifting; the internal unconformities interpreted from seismic data and in the limited outcrops are interpreted as the products of discrete extensional faulting events. Our data also indicate that Permo-Triassic extension here did not continue into the Jurassic, as in the case of the Domeyko basin to the west, as no marine strata were deposited. We thus conclude that the El Bordo area represents a Paleozoic basement high, separating the easterly Salar "failed rift" from the western Domeyko basin. The Salar basin thus received some continental detritus during the late Triassic but had probably filled to depositional base level by Jurassic time. A seismic interpretation of lines across the northern Salar basin (Macellari et al. 1991) defined five unconformity-bounded depositional megasequences but the inferred stratigraphy of their units 1 and 2 and ties to western outcrops differ from ours for the Paleozoic through Purilactis Group.

DISCUSSION

We consider that the dominance of extensional tectonics in the Late Paleozoic-early Miocene of the Central Andean belt is due to several causes (Fig. 2):
1) the late Permian hosted the splitting of Pangea, due to thermal doming and rifting (Mpodozis and Kay, 1992). Thus the early Salar basin extension was driven by stretching in a setting with no direct evidence of subduction or volcanic arc activity. Continued extension and thermal subsidence took place through the Triassic and early Jurassic.
2) following middle Cretaceous contraction and uplift of the proto Cordillera de Domeyko (driven by the opening of the South Atlantic ocean), Purilactis Group deposition was controlled by extension, now in a back-arc basin setting. This extension re-used the Permo-Triassic fault systems.
3) extension and oblique slip during Paciencia Group time (Oligocene) was partially controlled by collapse of the Cordillera de Domeyko, which had been uplifted again during late Eocene transpression.

We therefore propose that the Salar de Atacama stratigraphy preserves a series of "basins" which, owing to the longevity of the Andean margin and hemisphere-scale tectonic evolution, have evolved from a continental rift, through a back-arc basin and possible inter-arc stages to a Late Tertiary-Recent forearc basin. Accumulation of the sedimentary succession was mainly due to extensional faulting. Important but short-duration contractional episodes do link to known first order plate margin changes (Fig. 2) but their stratigraphic effect appears to be restricted to uplift/erosion rather than creation of significant flexural subsidence.

REFERENCES

Coira , B., Davidson, J., Mpodozis, C., and Ramos, V., 1982, Tectonic and magmatic evolution of the Andes of northern Argentina and Chile: Earth Science Reviews, v. 18, p. 303-332.

Flint, S., 1985, Alluvial fan and playa sedimentation in an Andean arid, closed basin: the Paciencia Group (mid Tertiary), Antofagasta Province, Chile: Geological Society of London Journal, v. 141, p. 533-546.

Hartley, A.J., Flint, S., Turner, P. and Jolley, E.J., 1992, Tectonic controls on the development of a semi-arid, alluvial basin as reflected in the stratigraphy of the Purilactis Group (Upper Cretaceous-Eocene), northern Chile: Journal of South American Earth Sciences, v. 5, p. 273-294.

Jolley, E.J., Turner, P., Williams, G.D., Hartley, A.J. and Flint, S., 1990, Sedimentological responses of an alluvial system to Neogene thrust tectonics, Atacama desert, northern Chile: Geological Society of London Journal, v. 147, p. 769-784.

Macellari, C.E., Su, M.J. and Townsend, F., 1991, Structure and seismic stratigraphy of the Atacama basin (northern Chile): Actas, VI Congreso Geologico Chileno, Viña del Mar, p. 133-137.

Mpodozis, C. and Kay, S.M. 1992, Late Paleozoic to Triassic evolution of the Gondwana margin: evidence from Chilean frontal cordilleran batholiths (28°S-32°S): Geological Society of America Bulletin, v. 104, p. 999-1014.

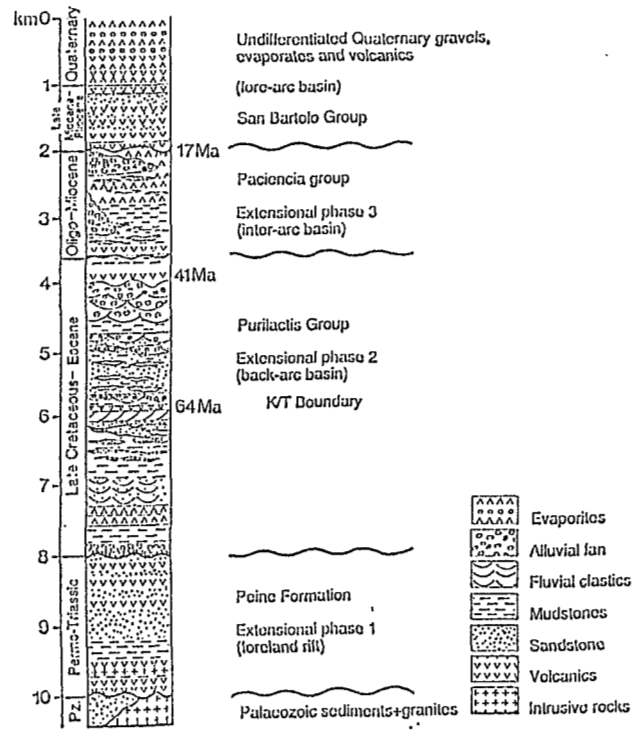

Figure 1: Lithostratigraphy of the Salar de Atacama basin-fill, as exposed on the inverted basin margin and interpreted from seismic data.

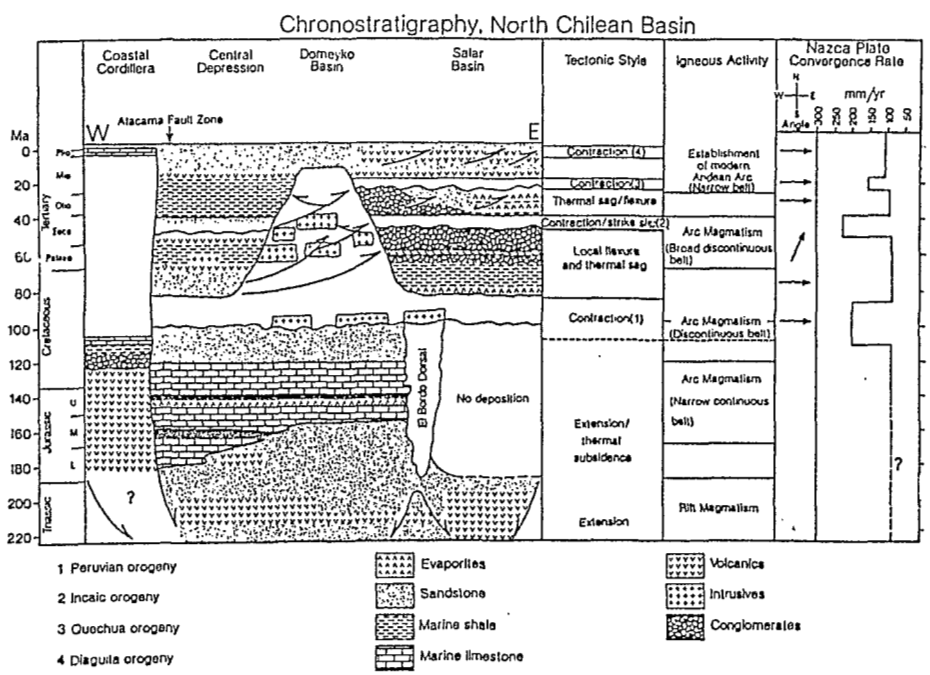

Figure 2: Chronostratigraphic diagram for the Andean forearc, northern Chile, showing all phases of basin filling and inversion. Magmatic and tectonic activity are plotted alongside convergence rate/angle data and show a good correlation between plate dynamics and continental margin evolution.

EVOLUCION DE LA CUENCA CHICAMA (JURASICO SUPERIOR-CRETACEO INFERIOR) ANDES NOR PERUANOS

Javier JACAY[1], Etienne JAILLARD[2]

(1) IFEA casilla 18-1217 Lima-18, Perú
(2) Petroproducción-ORSTOM casilla 10829 Guayaquil, Ecuador

Résumé

Grâce aux observations effectuées dans les aires d'étude, qui ont permis de différencier leurs milieux de dépôt respectifs, on a pu distinguer trois étapes:

a) Individualisation du bassin: elle commence au cours du Tithonique inférieur; les dépôts de la Formation Simbal illustrent les débuts de la formation du bassin jusqu'à la forte subsidence de celui-ci, qui est à l'origine d'un changement important dans les conditions de sédimentation.

b) Remplissage turbiditique (Tithonique supérieur): formé par la Formation Punta Moreno et la Formation Sapotal; ces formations se déposent dans un système d'éventails sous-marins, puis de remplissages de talus.

c) Colmatage (Berriasien): il se produit dans un milieu de plate-forme de faible profonfeur, il est constitué par la Formation Tinajones.

Palabras claves: Cuenca Sedimentaria, Subsidencia, Jurásico Superior, Cretáceo Inferior, Medios Sedimentarios.

Introducción

Al fin del Jurásico, la margen norperuana está dividida en varias zonas paleogeográficas, que son de oeste a este:

- Una Cuenca Occidental (Cobbing et al. 1981) (actual Cordillera Occidental) muy subsidente donde ha sido formada la Cuenca Chicama (Jacay, 1992).
- Un Umbral Axial (Benavides, 1956) (geoanticlinal del Marañón) con sedimentación reducida.

- Una Cuenca Oriental (Pardo y Zúñiga, 1976) (actual zona subandina) poco subsidente, con una sedimentación continental.

Marco Geológico y Evolución Sedimentaria

La sedimentación jurásica de los Andes Norperuanos comprende a la gran plataforma carbonatada del Triásico-Liasico (Grupo Pucará) (Pardo y Sanz, 1979; Prinz, 1985), la serie volcano-sedimentaria del Calloviano-Oxfordiano (Formación Colán) (Pardo y Sanz, 1979) (Mourier, 1988), y la serie volcano-sedimentaria del Tithoniano-Berriasiano (Grupo Chicama) (Jacay, 1992) (Jaillard et Jacay, 1989)

Con datos obtenidos en diferentes lugares se establece una orientación preferencial N-S, para la evolución de la Cuenca Chicama, en la región norte del Perú. Así en el:

TITHONIANO INFERIOR = INDIVIDUALIZION DE LA CUENCA

Durante esta época corresponde a la etapa de individualización de la cuenca, que se inicia con la Formación Simbal (Jacay, 1992) (Jaillard et Jacay, 1989), de carácter clástico-carbonatado.

La Formación Simbal se depositó en un medio de poca profundidad en lagoones protejidos del mar abierto, por cordones litorales. El ambiente abrigado y la circulación restringida del lagoon en esta formación, permite la precipitación de carbonatos, yeso, desarrollo de algas y una fauna de pelecípodos. Hacia la parte superior de la Formación Simbal, la desaparición de los niveles carbonatados y el abrupto aumento de lutitas negras indican una subsidencia de la cuenca, que dará lugar a condiciones batiales, que dominarán en el siguiente ciclo'

TITHONIANO SUPERIOR = RELLENO DE LA CUENCA

Como consecuencia de un evento tectónico importante (Jaillard et al. 1990) una brutal subsidencia da lugar al relleno turbidítico muy rápido de la Cuenca Chicama (Jacay, 1992) (Formación Punta Moreno, Formación Sapotal); se inicia con un potente conglomerado polimíctico basal, en los alrededores de Simbal, sobre estos conglomerados redepositados sobrevienen sedimentos volcanoclásticos correspondientes a la Formación Punta Moreno, con un suministro continuo de material al sistema de abanicos submarinos; la distribución del aporte terrígeno da lugar a la Formación de lóbulos que van progradando hacia el interior de la cuenca.

En el sector de Cascas-Ascope-Compartición, la Formación Punta Moreno representa depósitos de cono submarino proximal, los modos de transporte son mayormente de debris flow, con conglomerados, slumps, etc., en el sector de Simbal las facies se sitúan en la parte proximal del lóbulo de suprafán del abanico medio y hacia el río Santa las facies evidencian medios de abanico inferior (Fig. 1).

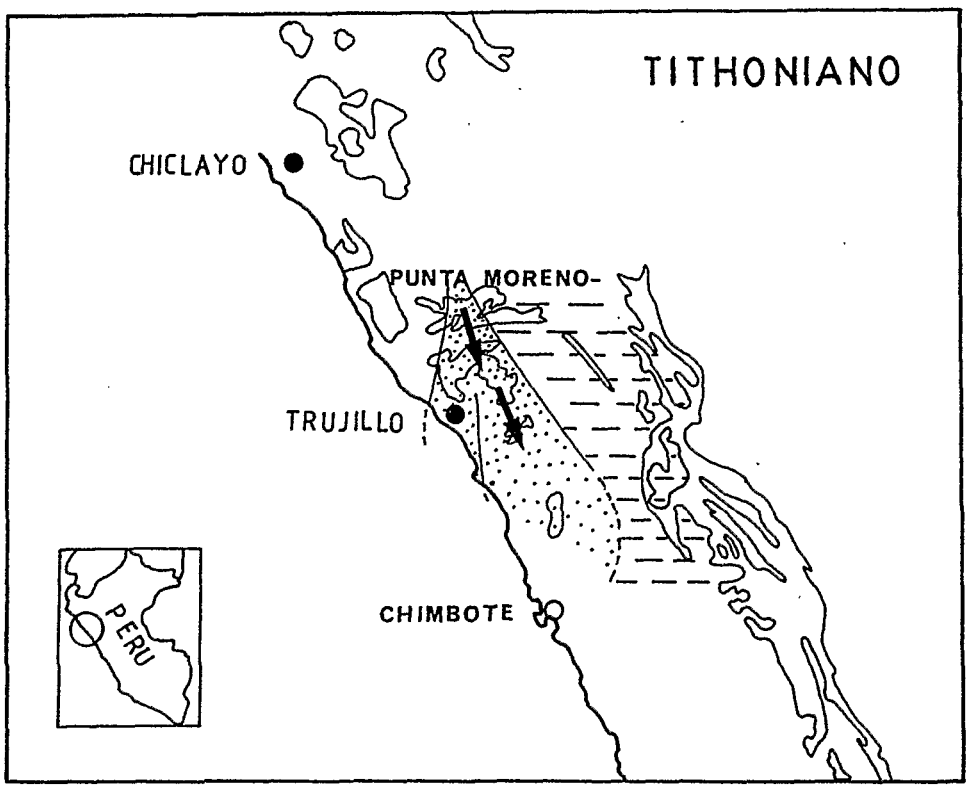

Fig. 1 Mapa paleogeográfico al Tithoniano Superior

Conclusiones

La evolución de la cuenca Chicama corresponde a etapas de formación, relleno y colmatación ocurridos entre el fin del Tithoniano Inferior y el Berriasiano.

La alta subsidencia inicial de la cuenca Chicama expresa un importante adelgazamiento de la corteza continental del noroeste peruano (Jaillard, 1990). La subsidencia térmica posterior controlaría la paleogeografía del Cretáceo.

La cuenca Chicama muestra una evolución tectónicamente móvil, creada por el sistema transformante de la margen peruana hacia el Jurásico Medio Superior (Jaillard et al. 1990).

REFERENCIAS

Benavides, V., 1956 Amer. Mus. Nat. Hist. Bull., New York, 108: 352-494.
Cobbing, J., Pitcher, W. S., Wilson, J., Baldock, J., McCourt, W., Snelling, N. J., 1981 Bol. INGEMMET, D-10, 252 p.
Jacay, J., 1992 Tesis Ing. Geol. UNMSM 160 p.
Jaillard, E., 1990 Symp. Intern. Géodynamique Andine, Grenoble, 269-272.
Jaillard, E., Jacay, J., 1989 C.R.A.S., Paris, (II), 308: 1459-1465.
Jaillard, E., Soler, P., Carlier, G., 1990 Jour. Geol. Soc., London, 147: 1009-1022.
Mourier, T., 1988 Thèse Doc. d'Etat, Univ. Paris Sud, 280 p.
Pardo, A., Zúñiga, F., 1976 2do Cong. Latinoamer. Geología, Caracas 1973, 2: 569-608
Pardo, A., Sanz, V., 1979 Bol. Soc. Geol., Perú, 60: 251-266.
Prinz, P., 1985 Palaeontographica A, 188: 153-197.

REGIONAL DEVELOPMENT OF THE SALTA GROUP FACIES IN THE ARGENTINE PUNA

Rosa A. Marquillas, José A. Salfity and César R. Monaldi

Universidad Nacional de Salta-Conicet
Buenos Aires 177, 4400, Salta, Argentina

ABSTRACT

The influence of the San Pablo high during deposition of the Salta Group in the extreme northwest of Argentina is shown. The synrift deposits (Pirgua Subgroup) and postrift deposits (Balbuena and Santa Bárbara Subgroup) of this Group were laid down during the Cretaceous-Eocene time lapse.

KEY WORDS
Argentina, Cretaceous, Salta Group, Yacoraite, limestones, anoxic environment.

INTRODUCTION

The San Pablo high was a positive element which governed the deposition of the (Cretaceous-Eocene) Salta Group in the northwest corner of Argentina, the south of Bolivia and northeast Chile.
Special attention has been paid to the Balbuena Subgroup, in which the calcareous nature of the Yacoraite Formation facies has made it possible to detect subtle paleogeographic changes and significant regional modifications in the development of these facies.
To this end, a series of cross-sections of the Salta Group in the Argentine Puna (Figure 1) were studied in detail, especially those of the Balbuena Subgroup. These sections are grouped round the southern flank of the San Pablo ridge, which in this region shows a NW-SE strike.

GEOLOGICAL SETTING

The synrift deposits of the Pirgua Subgroup show a typical basal conglomerate facies, such as those of Cuevas and Lipán (Figures 1 and 2), made up of Ordovician basement fragments, both igneous and sedimentary. These conglomerates normally lie on the Ordovician through a primary unconformity relationship. Despite this, in some sections their relationship with the Ordovician is tectonic, through reverse faults which are of medium to high angle on the surface and dip both to the west. Some of these fault must have been the active borders of the synrift grabens in this part of the basin. No intercalations of intrusive rocks were observed in the sections studied.
The postrift deposits of the Balbuena Subgroup overlie both the Pirgua Subgroup, within the synrift troughs, and the San Pablo high, where they rest on the Ordovician basement.
The Santa Bárbara Subgroup is present in almost all sections

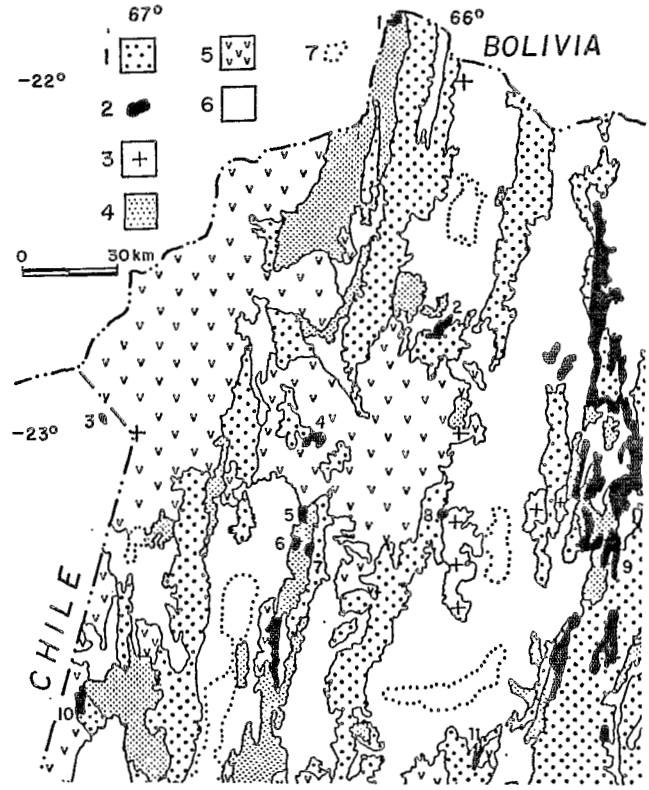

FIGURE 1. Geological map of the North Argentine Puna. 1 Pre-Cretaceous basement, 2 Salta Group, 3 Cretaceous Granitoid, 4 Neogene sediments, 5 Neogene volcanic rocks, 6 Quaternary, 7 Salar. Control points: 1-Chaupiorco, 2-Casa Colorada, 3-Poquis, 4-Coranzuli, 5-Calvario, 6-Lipán, 7-Cuevas, 8-Queñoal, 9-Yacoraite, 10-Huaitiquina, 11- Chirincho.

of the Sey depocenter, although with sandy and even conglomeratic facies. In the Tres Cruces depocenter it contains typical pelitic facies (Figure 2).

BALBUENA SUBGROUP

The lithology of the predominant units found in the Yacoraite Formation in the area of the San Pablo high indicates they were laid down under the depositional conditions found in pelitic and calcareous ooze environments. These sedimentary settings remained in great part below the oxygen exhaustion level, or if they did not arrive at such a situation were favored by euxinic conditions which governed the nature of their facies. However, inundation was not permanent, as the deposits are interbedded with records of rocks from environments of shallower depths and higher energy.
In this proximal basin are the Yacoraite Formation deposits are far from showing the typical high-energy limestone facies -oxygenated, light-colored and having interbedded shallow sequences- seen in other areas of the basin border, such as those surrounding the Salta-Jujuy high.
The main lithologic characteristics of the Balbuena Subgroup -especially those of the Yacoraite Formation- are given below, grouped according to the main facies, and including microscopic examination data.
The Balbuena Subgroup lies on an Ordovician basement in Chaupiorco, Casa Colorada, Coranzuli?, Poquis and Queñoal? (Figures 1 and 3). In some cases it contains the coarsely stratified sandy deposits of the Lecho Formation in its base.

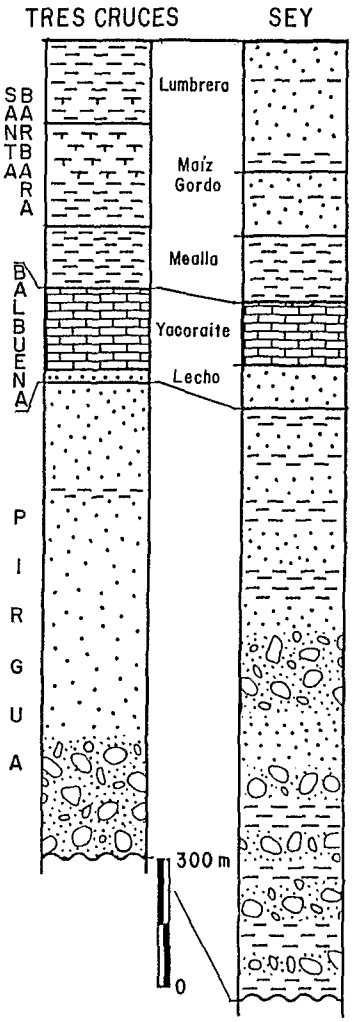

FIGURE 2. Composite stratigraphic columns of the Salta Group in the Tres Cruces and Sey depocenters.

These deposits usually include conglomerates containing quartz fragments, and Ordovician sedimentary and extrusive rock fragments from the Puna.The Lecho Formation facies are generally in keeping with those of the rest of the basin, and point to a distal braided system setting, influenced by eolian processes which created inter-dunes. This setting has been considered that of a prior clastic platform, in relation to the transgressive carbonate depositions of the Yacoraite Formation. When the Lecho Formation is not present as a lithologic unit, the facies in the basal portion of the Yacoraite Formation acquire characteristics similar to it.
The lower section of the Yacoraite Formation contains a stretch of high-energy arenaceous and arenaceous-calcareous rocks which frequently lie directly on the Paleozoic basement. It is formed of fine to medium grained gray, white and green sandstones, containing quartz, potash feldspar, scarce plagioclase, hornblende, zircon, and scattered lithic grains, plus small phosphatic bone fragments. Above this set of sediments lie limestones of medium to high energy characteristics (wackestones, packstones, and grainstones), containing diverse oolites, intraclasts, abundant ostracods, gastropods, fish remains and other bone fragments, and scarce organic matter. Immediately above these lies a low-energy sequence -probably representative of the first regional flooding episode under reducing conditions- made up of greenish gray lime mudstone and green, gray and black shales, containing pyrite and other sulphides, scarce collophane, abundant widespread organic matter -probably vegetable in origin- and scarce gypsum and anhydrite.
The upper section of the Yacoraite Formation shows that the relatively deeper environment, associated with anoxic conditions, continued until the end of deposition. This was only briefly interrupted by several shallowing pulses, combined with terrigenous supplies, the formation of the skeletal and nonskeletal grain limestones, the growth of algal stromatolites, and the intrabasinal fragmentation od sediments through subaerial exposure. These sediments are intercalated by thin isolated tuff and tuffite levels.
Thus, a rhythmic sedimentation of dark pelitic rocks and laminated scarcely bioturbated carbonates characterizes the

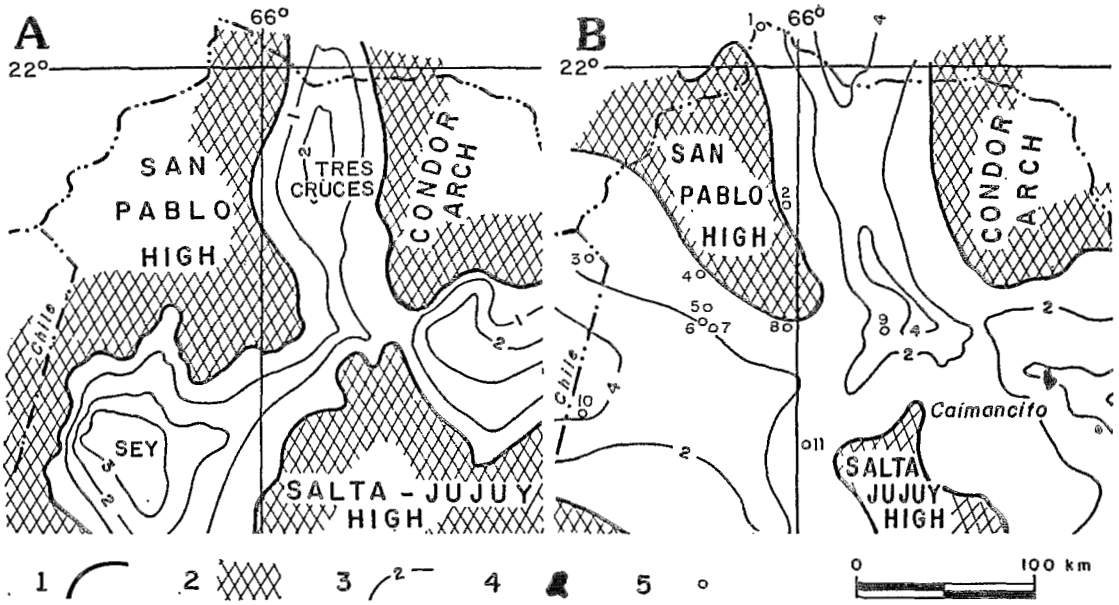

FIGURE 3. Synrift sedimentary filling of the Pirgua Subgroup (A), and postrift sequence of the Balbuena Subgroup (B). 1 Inferred basin edge, 2 Structural high, 3 Isopach line, thickness in km (A) and in hundreds of meters (B), 4 Oil field (Yacoraite Formation as both source and reservoir), 5 Control point (see Figure 1).

greater part of the upper section of the Yacoraite Formation. This section consists of claystone, black shale, stinkstone, dark micrite, dolomicrite, lime mudstone with scarce small terrigenous grains floating in a carbonate-evaporite paste, interlaminated siltstone and very fine calcareous sandstone, wackestone with abundant ostracods, some packstones and grainstones (with collapsed oolites, bivalves, gastropods, and fish and plant fragments), and black stromatolite boundstone. Organic matter is frequently abundant (kerogenes and bitumens),, as are iron sulphides, other unoxidized metallic sulphides, scattered phosphates and phosphatic nodules. On the other hand, evaporites -gypsum and anhydrite- are scarce, as is chert.

CONCLUSIONS

The foregoing confirms that during the Yacoraite Formation deposition there was a region-wide zone, that included the western portion of the Tres Cruces depocenter, the San Pablo high and the northern part of the Sey depocenter, in which the subsident episodes were of sufficient magnitude to effectively govern both the relative deepening of the sedimentary environment and the accumulation of reducing facies, despite deposition taking place in areas of strictly littoral location.

Subsidence during the Yacoraite Formation deposition was steady and of a similar nature both in the depocenters and in the flooded portion of the San Pablo high, only being altered by brief intervals of shallowing.

JURASSIC-EARLY CRETACEOUS FACIES DISTRIBUTION IN THE WESTERN ALTIPLANO (18°-21° 30'S.L). IMPLICATIONS FOR HYDROCARBON EXPLORATION

Nelson MUÑOZ G.[1], *Reynaldo CHARRIER G.*[2]

(1) Empresa Nacional del Petroleo-Chile. Compañia #1085, Piso 12, Santiago, CHILE.
(2) Depto. de Geologia, Univ. de Chile. Casilla #13518, Correo 21, Santiago, CHILE.

ABSTRACT: *Facies analyses of Jurassic-Early Cretaceous sequences suggest an extensive distribution of marine deposits toward the East. This paleogeographic model has implications for hydrocarbon exploration in the Altiplano, since it suggests that the Jurassic-Early Cretaceous backarc basin may be preserved in the subsurface of the western Altiplano.*

KEY WORDS: *Chile, Altiplano, Jurassic, facies, hydrocarbon.*

INTRODUCTION

A system of magmatic arc related backarc basins developed along the western margin of South America was covered by several marine advances during the Jurassic-Early Cretaceous period. Sediments deposited during these events are widely exposed along the Andes and preserved in the subsurface of subandean basin. Sedimentary Jurassic-Early Cretaceous units are of great economic importance as they provide the source and reservoirs for the largest accumulations of hydrocarbons of the western margin of the continent. This composite system of arc and backarc basin remained active until the middle Cretaceous, when a generalized tectonic event inverted of some of these backarc basins [1,5,11].

The remnants of the Jurassic-Early Cretaceous magmatic arc are well exposed for more than 1000 km along the present coastal line. However, the distribution of the backarc basin toward the east between 18° and 21°S latitude has not been studied in detail. In this paper we discuss the probability that, in this area, the backarc basin could have spread eastward and that it may be preserved in the western border of Altiplano. Based on published and unpublished information we discuss the stratigraphy and the paleogeography of the backarc basin along three profiles located at 18°, 20° and 21°30'S latitude (Figs 1,2).

GEOLOGICAL SETTING

In most of the studied sections, it is possible to identify three distinctive major intervals with different facies assemblages: (a) transgressive deposits (basal unit) that indicate the inception of the sea level rise; (b) widespread open marine deposits (middle unit) indicating a stable state of basin subsidence, and (c) regressive sequences that indicate a marine regression due to base level uplift.

18° South Latitude. Jurassic-Early Cretaceous sedimentary deposits are distributed between Arica, in the actual Coastal Range, and the Titicaca Lake in the south-eastern part of Peru. In the Coastal Range

of Arica, thick Pliensbachian to Oxfordian andesitic and basaltic-andesitic unitis are interbedded with detritic and calcareous marine deposits.

Inland from Arica, the Mesozoic sedimentary series begin in the Sinemurian and lie disconformably on an acidic tuff unit. In the upper Azapa Valley, a series of terrigenous clastic and carbonate sedimentary rocks with minor pyroclastic intercalations is exposed. This unit contains marine fauna of Lias to Lower Neocomian age[4].

Farther to the northeast, these facies are replaced by 1,200 m of a monotonously interbedded sandstones and shales, characterized by thinning-upward successions[6,10]. This facies association is interpreted as a turbiditic series.

A regional interpretation of these sequences indicates that in the upper Azapa Valley as well as in Arica the sedimentation took place on a shallow marine shelf. However, progressively deeper facies found to the east indicate that sedimentation took place through gravity flow deposits, suggesting that the deeper part of the Jurassic-Early Cretaceous back-arc basin was located in that direction.

19° South Latitude. In the Coastal Range of Iquique the sedimentation is characterized by shallow marine limestone and shales, interbedded with andesitic pillow lavas[9]. Similarly to the coast near Arica, these sequences represent the interaction of shallow marine conditions with a submerged portion of the volcanic arc.

To the East of Iquique, the Noasa Formation rests unconformably over Paleozoic metamorphic rocks. This formation includes basal conglomerates followed by shales and thin limestone intercalations, with diagnostic Sinemurian ammonites, that indicate the initial transgressive episode. Farther east these facies are replaced by a rhythmic interbedding of siltstones and sandstones that have been interpreted as a turbidite facies[2].

Post-Sinemurian - pre-Calovian sediments are dominated by clastic deposits that reflect the transition towards a fluvio-deltaic environment in this area. However, farther east the facies are correspond to distal deposits characterized by finer grained sediments than their western equvalents[2]. To the east no marine deposits of this age have been reported.

A regional analyses at 19° S latitude indicates that the marine facies are progressively deeper towards the East. However, eastern outcrops are incomplete and do not allow a clear definition of the facies changes during the Sinemurian-Calovian.

21° 30' South Latitude. The Coastal Range of this region was dominated by an almost continuous volcanic activity. The La Negra Formation is formed by up to 2,500 meters of andesitic lavas with at least two marine intercalations of calcareous sandstones and limestones with Sinemurian to Calovian-Oxfordian diagnostic ammonites[7]. To the east, this facies association gives way to exclusively by marine deposits.

To the East in the Cerro Jaspe area, the basal transgressive unit is followed by oolitic limestones and calcareous sandstones and siltstones. Farther east and north, in the Cerro Yocas-Guatacondo area, these calcareous facies associations were replaced during the Sinemurian-Aalenian by terrigenous clastic sequences. These facies associations can also be interpreted as turbidity currents deposits, which resulted from the retrogradation of a deep fan into the deeper part of the backarc basin in this area. Paleocurrent data show that sedimentation took place through flow deposits flushed northward and northeastward. The clastic influence decreases to the south where calcareous sequences dominate [3,8].

These formations represent the major depocentre during the Jurassic-Early Cretaceous in northern Chile. In this area up to 4,500 meters of different facies associations were deposited into the backarc basin. The deeper facies are located toward the east and there is no base to establish the eastern border of the backarc basin in Chilean territory.

CONCLUSIONS

A preliminary paleogeographic interpretation of the Jurassic-Early Cretaceous sequences exposed along the Coastal Range, Precordillera and the western border of Altiplano between 18° and 21° 30', shows a clear west-to-east sediment depth polarity. This polarity varies from shallow water calcareous deposits to the west, to deeper water terrigenous clastic deposits to the east. Pillow lavas interbedded with fossiliferous limestones are located in the present Coastal Range, give way to the east to calcareous marine sequences. Still farther east the facies equivalents are turbidite flow deposits.

The greatest thickness of Jurassic-Early Cretaceous sediments have been reported at 21° 30' south latitude (Cerro Yocas-Guatacondo areas) where up to 4,500 meters are exposed. In this region, the facies distribution suggests that the backarc basin had an extensive marine distribution toward the Altiplano.

This interpretation implies that the Jurassic-Early Cretaceous backarc basin may be preserved in the subsurface of the western Altiplano Basin (Fig.5). Consequently, this region could be considered as a hypothetic hidrocarbon exploration area.

REFERENCES

1.- CHARRIER, R. & N. MUÑOZ, 1992, Jurassic-Cretaceous paleogeographic evolution of the Chilean Andes at 23°-24° S.L. and 34°-35° S.L.: A comparative analysis, in: Tectonics of the Southern Central Andes (Reutter, K.J., Scheuber, E. and Wigger, P., editors), Sringer Verlag, Berlin, Heidelberg, New York, in press.

2.- HARAMBOUR S., 1990, Geología pre-Cenozoica de la Cordillera de los Andes entre las quebradas Aroma y Juan de Morales. I Región, Chile. Thesis, Dep. of Geology, Univ. de Chile, Santiago, 228 p.

3.- LIRA, G., 1989, Geología del area pre-andina de Calama, con énfasis en la estratigrafía y paleogeografía del Mesozoico, 22 a 22° 40' Latitud sur: Región de Antofagasta, Chile. Thesis, Depto. de Geología Univ. de Chile, 211 p., Santiago.

4.- MUÑOZ, N., ELGUETA S. & HARAMBOUR, S., 1988, El sistema Jurásico en el curso superior de la quebrada de Azapa, I Región: Implicancias paleogeográficas. V Congreso Geológico Chileno. Tomo I, A403-415.

5.- MUÑOZ, N., CHARRIER, R. & PICHOWIAK, S., 1989, Cretácico Superior volcánico-sedimentario (Formación Quebrada Mala) en la Región de Antofagasta, Chile, y su significado geotectónico. Contrib. Simposios Cretácico de America Latina, Parte A: Eventos y Registro Sedimentario, Spalletti, L., Edit., Buenos Aires, p. 133-148.

6.- SALINAS, E., 1983, Paleogeografía y Sedimentología de la etapa de individualización de la Cuenca Andina externa (NE de Tacna). Tésis de grado en Bachiller en Ing. Geol., Univ. Nac. de San Agustin de Arequipa, Perú.

7.- SKARMETA, J. & MARINOVIC N., 1981, Hoja Quillagua, Región de Antofagasta: Santiago, Instituto de Investigaciones Geológica, Carta Geológica de Chile, No.51,p. 1-63.

8.- SMOJE, I., 1989, Estratigrafía y fácies del sistema jurásico en la Precordillera, entre las latitudes de Pica y Quillagua. Thesis Dep. Geol. Univ. de Chile.

9.- THOMAS, A., 1970, Cuadrangulos Iquique y Caleta Molle. Carta Geológica de Chile N°21-22. SERNAGEOMIN, Santiago.

10.- WILSON, J. & GARCIA, W. 1963, Geología de los cuadrángulos de Pachia y Palca. Carta Geológica Nacional. Vol II, Hojas 36-V y 36-X, Perú.

11.- VOLKHEIMER W. & MUSACCHIO E. (Eds.) 1981, Cuencas Sedimentarias del Jurasico y Cretacico de America del Sur. Contribucion del comite Sudamericano del Jurasico y Cretacico al II Con. Lat. de Paleontologia, Puerto Alegre, 1981.

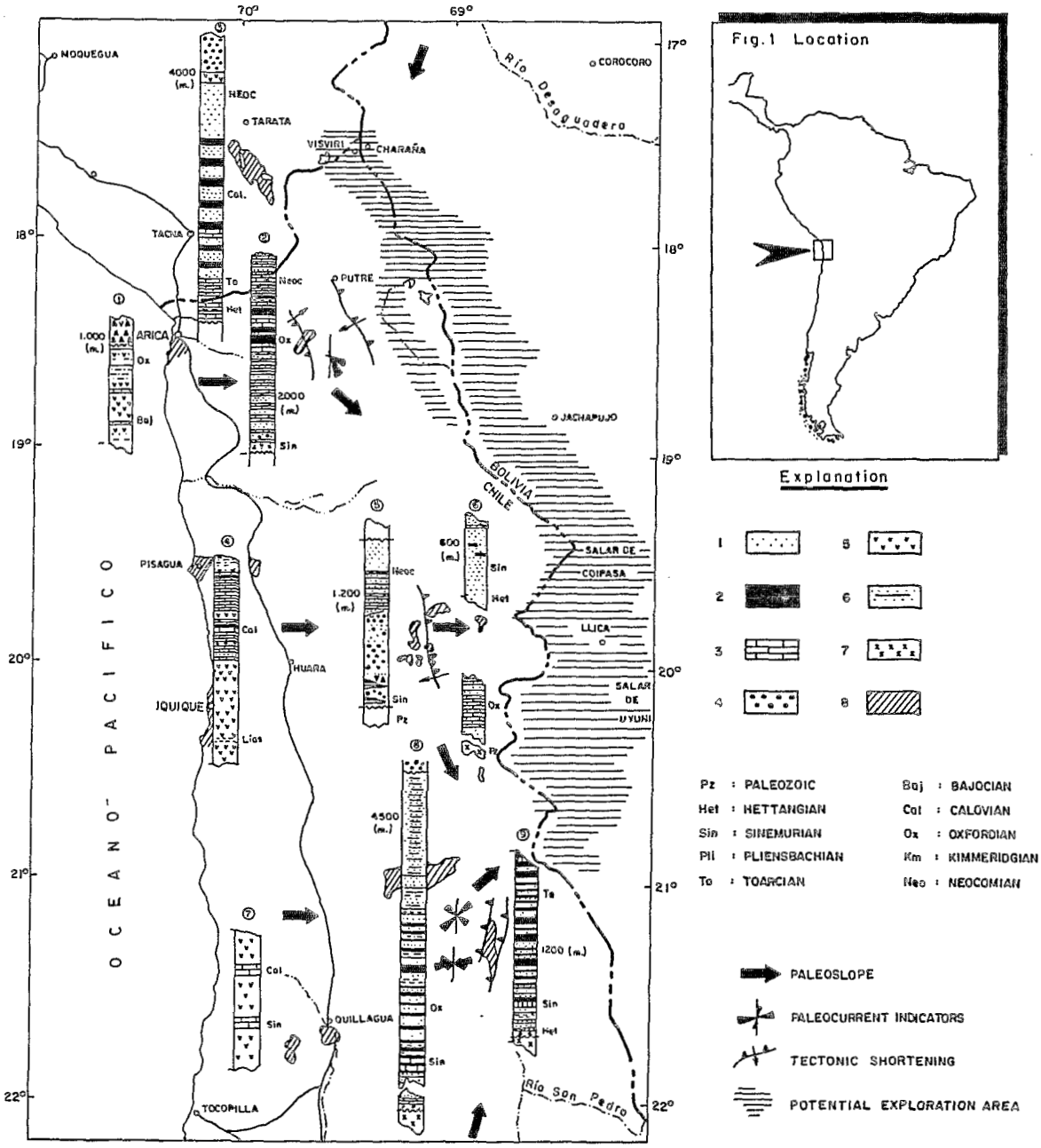

FIG.2 JURASSIC–LOWER CRETACEOUS STRATIGRAPHY. 1.-SANDSTONE ; 2.-BLACK SHALES ; 3.-LIMESTONE ; 4.-CONGLOMERATE 5.-LAVA ; 6.-SILTSTONE ; 7.-BASEMENT ; 8.-OUTCROP.—

TERTIARY STRATIGRAPHY AND STRUCTURE AROUND LAGO GENERAL CARRERA, SOUTHERN CHILE: IMPLICATIONS FOR PLATE MARGIN EVOLUTION.

David J. PRIOR, Stephen FLINT, Fran RAY, Nick PETFORD (1)
Sue AGAR (2)
Peter TURNER (3)
Rita ARQUEROS (4)

(1) Department of Earth Sciences, Liverpool University, L69 3BX, U.K.
(2) Department of Geological Sciences, Northwestern University, Evanston, Illinois, USA.
(3) School of Earth Sciences, Birmingham University, Edgbaston, Birmingham, U.K.
(4) Universidad de Chile, Santiago, Chile

KEY WORDS: Chile Margin Triple Junction, Cosmelli Basin, Tertiary

INTRODUCTION

The Tertiary stratigraphy and structure of southern Chile between 44° S and 47°S is poorly known yet is critical to the understanding of the evolution of the Andean Plate margin in this region, most specifically the evolution of the Chile Triple Junction (Forsythe & Prior, 1992). Field studies carried out in the Cosmelli area ,10km east of Guadal, and in the Cerro Rocosso area, 15km south of Chile Chico, have provided new data relevant to the Tertiary evolution of southern Chile. Here we outline these reconnaissance studies together with some ideas as to their implications for the Tertiary plate dynamics of this region.

GEOLOGICAL WORK

Our studies show that immediately south of Lago General Carrera four distinct lithostratigraphic formations overly the Devisadero Formation (Cretaceous: Niemeyer et al., 1974). The successions at the western and eastern ends of Lago General Carrera are:

West (Cerro Rocosso)	East (Cosmelli)
Galera Fm	*Galera Fm*
Guadal Fm	*Guadal Fm*
San Jose Fm	*San Jose Fm*
Cerro Rocosso Fm	*Divisadero*
Divisadero	

The Galera Fommation contains a Tertiary Fauna (Niemeyer et al., 1974) although this does not discriminate the age within the Tertiary. The age of the San Jose Fomation and the Cerro Rocosso Fomation are not tightly constrained. These are mostly conformable with each other and pass conformably into the Guadal and we postulate that these are Tertiary. The

Cerro Rocosso Formation may be equivalent to the Chile Chico Formation, postulated to be Tertiary by Niemeyer (M. Suarez, pers comm).

The Cerro Rocosso Formation comprises acidic and intermediate volcanics and volcanogenic fluvial/alluvial sediments. This passes upwards, mostly conformably but locally unconformably, into the San Jose Formation; a series of alluvial plain and fluvio-deltaic sediments and intercalated ash deposits Palaeocurrents are to the east corresponding with a change from floodplain sediments in the west to deltaic in the east. The top of the fluvio-deltaic succession is locally marked by a coal shale horizon in the east.

In the Cosmelli area the Guadal Formation overlies the San Jose conformably and comprises estuarine sandstones and marine silts/sands. The lower parts of the Guadal Succession are dominantly open marine and are laterally extensive over a 10km scale. The upper parts show tidal influences and lateral variations in facies on a kilometre scale. The succession contains basaltic sills. In the Cerro Rocosso to the east the San Jose Formation is conformably overlain by at least a kilometre of basaltic lavas. Within the first 100m a there is marine succession which contains identical lithostratigraphic and faunal elements to the Guadal of further west.

The Galera Formation comprises a few km thickness of unfossilifierous, continental, fluvial sandstones and silts with palaeocurrents to the east. The Galera is unconformable upon the Guadal sediments in the west and upon the Guadal equivalent basalts in the east.

The sedimentary succession observed indicates some significant base-level changes, most notably the Guadal marine incursion and the rapid change to continental sedimentation represented by the Galera. There may be base-level changes of similar or greater significance correspondent with fluvial facies changes within the Galera Formation.

The Tertiary is folded and imbricated by a series of N-S striking thrusts and backthrusts. The deformation is active during San-Jose to Upper Guadal/ Lower Galera deposition in the west and may be responsible for the observed base-level changes. In the west deformation continues later into the Galera and suggests that deformation propagated in a west to east direction.

Tertiary alluvial/fluvial sediments north and south of the study area, dated at ~18Ma using mammal bones, are conventionally correlated to the Galera Formation. Identification of earlier alluvial/fluvial systems (San Jose & Cerro Rocosso Formations) lends the possibility of a different correlation. The lithostratigraphy of the dated sections corresponds much more closely to the San Jose/Cerro Rocosso than to the Galera. This new correlation is crucial to a geodynamic understanding of this region.

CONCLUSIONS

The implication is that the Guadal and Galera formations and associated tectonics and magmatism must have developed in the Late Miocene or Pliocene, corresponding to the time period over which the Chile Triple Junction has evolved. The basaltic volcanism has been related to the passage of slab windows corresponding to continued subduction of segments of the Chile Ridge (Ramos & Kay, 1991). The thermal and gravitational anomaly associated with the passage of slab windows may also explain the observed base level changes and tectonic evolution within the Tertiary sediments.

REFERENCES

Forsythe, R.D., & Prior, D.J., 1992, Cenozoic continental geology of South America and its relations to the evolution of the Chile Triple Junction. In Behrmann, Lewis et al., *Proceedings of the Ocean Drilling Program, Initial Reports*, **141**, 23-31.

Niemeyer, H., Skarmeta, J., Fuenzalida, P., Espinosa, W., 1974, Hojas peninsula de Taitao y Puerto Aisen: *Carte Geologica de Chile* No **60-61**.

Ramos, V., & Kay, S.M., 1991, Southern Patagonian plateau basalts and deformation: backarc testimony of ridge collisions. *Tectonophysics*, **205**, 261-282.

THE WESTERN MARGIN OF THE NEUQUEN BASIN (ARGENTINA) IN THE UPPER JURASSIC AND LOWER CRETACEOUS

Ulrich ROSENFELD[1)] & Klaus-Jürgen EPPINGER[2)]

1) Geologisch-Paläontologisches Institut der Universität, Corrensstraße 24, D-4400 Münster/BRD
2) Universidad de Atacama, Dep. de Ing. de Minas, Casilla 240, Copiapó/Chile

RESUMEN: Los sedimentos del Jurásico Superior y Cretácico Inferior (138 - 117 Ma) de la Cuenca Neuquina (Argentina) son origen de un arco magmático en el oeste, una región metamórfica (Macizo Norpatagónico) en el sur y un orógeno de colisión retrabajado en el este. El arco magmático aparece en forma de "transitional arc" y "dissected arc".

KEY WORDS: Upper Jurassic, Lower Cretaceous, sediment provenance, magmatic arc, Neuquen Basin, Argentina

The Neuquén Basin, situated approx. 33° - 40° S and 67° - 71° W, forms the southern part of the Andean Basin. It is bordered in the east by the block of San Rafael and in the south by the North Patagonian Massif. In the west it is limited by a magmatic arc as is suggested by DIGREGORIO & ULIANA (1980) and other authors. In this study type and effectiveness of the magmatic arc from the Late Jurassic up to the Early Cretaceous (138 - 117) are discussed. For this purpuse, modal analyses of sandstones and heavy mineral analyses were carried out. The stratigraphical classification of profiles and samples was based on the sequence stratigraphical investigations by LEGARRETA & GULISANO (1989).

As a result of the modal analyses of sandstones from the southern part of the basin, two different source areas for the sediments could be identified. The influence of a third source area could be detected only by heavy mineral analyses. In general it can be said that sediments originate from both a magmatic source area in the west and a metamorphic area, indicated by the heavy mineral contents of the sediments, in the south or southwest of the Neuquén Basin. The third source area becomes noticeable only for a short time when sediments from the east, derived from a reworked collision orogen, are being transported into the northern Neuquén Basin.

The sequence stratigraphical division of the sequence and facies maps, derived from it, show that the basin was continually subjected to strong, short-termed changes in extension and facies distribution. The reasons for these changes are sea level fluctuations which are connected with and correspond to the global eustatic changes.

By classifying the samples sequence stratigraphically, it was possible to sort and interpret the results of the modal and heavy mineral analyses more accurately. The data clearly indicate that the magmatic source area is a magmatic arc which is bordering the basin in the west and presumably forms a barrier to the Pacific

Ocean open from time to time. Additionally, different levels appear to have been eroded within the magmatic arc: During the Tithonian (138 Ma) the magmatic arc supplies material which corresponds to a transitional arc (sensu DICKINSON 1985). In the further development of the source area -- during the lower and upper Berriasian (130,5 Ma) and the uppermost Berriasian (128 Ma) -- the transported material comes from a dissected arc. This proves that also parts of the plutonic root of the magmatic arc have been eroded. In the lower Valanginian (126 Ma) and upper Hauterivian (117 Ma) the characteristics of the transported sedimentary material can again be related to a transitional arc.

In the east to northeast a reworked collision orogen borders the basin and supplies material into the northern Neuquén Basin for a short time (at 128 Ma). The southwest and south of the basin is limited by a metamorphic highland (North Patagonian Massif) where the supplied material is mixed with detritus from the western magmatic arc.

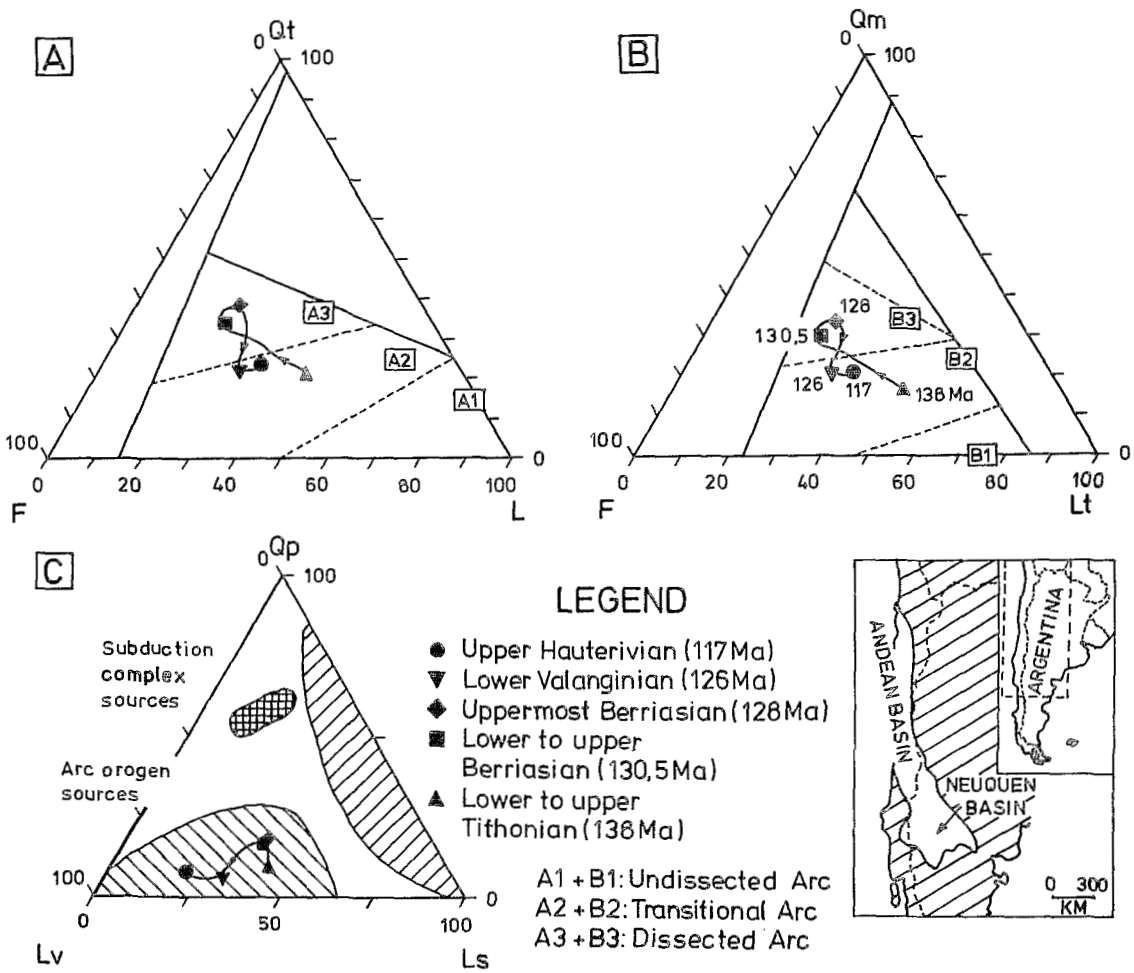

Fig. 1. Variations of provenance of sediments, Neuquen Basin (Argentina). Diagrams after DICKINSON (1985); arithmetic mean of 65 samples

REFERENCES

DICKINSON, W.R.(1985): Interpreting provenance relations from detrital modes of sandstones. -- In: ZUFFA, G. G. (Ed.): Provenance of Arenites: 333 - 361; Dordrecht/Boston/Lancaster (Reidel Publ. Comp.).

DIGREGORIO, J. H. & ULIANA, M. A. (1980): Cuenca Neuquina. -- In: LEANZA, A. F. (Ed.): Geología Regional Argentina: 985 - 1032; Córdoba.

LEGARRETA, L. & GULISANO, C. A. (1989): Analisis estratigrafico secuencial de la Cuenca Neuquina (Triasico Superior - Terciario Inferior). -- In: CHEBLI, G. & SPALLETTI, L. (Ed.): Cuencas Sedimentarias Argentinas: 221 - 243; Tucumán.

MESOZOIC STRATIGRAPHY AND PALEOGEOGRAPHY OF NORTHERN PATAGONIAN CORDILLERA (LAT. 45°-47°S), CHILE.

Manuel SUAREZ[1] and Rita DE LA CRUZ[1]

(1) Avenida Santa María 0104, Correo 9, Santiago, Chile

ABSTRACT: Mid-Upper Jurassic rift-related volcanism in Northern Patagonian Cordillera, between 45°-47° Lat.S, was followed by the development of a Lower Cretaceous marine basin formed by post-rift thermotectonic subsidence. Subaerial volcanism was reinstalled by the mid-Cretaceous. Extensional, strike-slip and contractional tectonics locally ocurred.

KEY WORDS: Patagonian Cordillera, stratigraphy, paleogeography, tectonics.

INTRODUCTION

During the Jurassic-Cretaceous thick volcanic and sedimentary sequences accumulated in northern Patagonian Cordillera (45°-47° L.S), in southern Chile. Recent work identified volcanic and sedimentary facies and environments and a new stratigraphic scheme; this allows paleogeographic and tectonic reconstructions.

GEOLOGICAL SETTING

Six Mesozoic formations (with a seventh of Cretaceous?-Tertiary age) were recognized (Fig.1; Suárez and De La Cruz, 1992). The oldest (Ibañez Formation, Niemeyer et al., 1984), includes a Mid-Upper Jurassic thick acid volcanic unit (calderas) with intercalated sedimentites. This unit was coeval with a widespread rifting episode in Patagonia (see Gust et al., 1985). An intermitent marine transgresion, that left preserved parts of truncated volcanic cones and locally was synchronous with active volcanism, marked the initiation of an Upper Jurassic - Lower Cretaceous widespread marine basin. A deepening - shallowing upward trend can be recognized in the sedimentary infill of it; from base to top the following units were recognised (Suárez and De La Cruz, 1992, in prep.):

. shallow marine limestones, 6-40 m thick (Cotidiano Formation, defined in Argentina, see Ramos, 1981).
. over 100 m thick succession of tuffs (including ignimbrites), tuffaceous sandstones and limestones. Toqui Formation (Suárez and De La Cruz, in prep.),.
. Shelf and prodelta black shales (Katterfeld Formation defined in Argentina, see Ramos, 1981).
. Deltaic (braid-delta) and tidal bioturbated sandstones, prograding to the west overlain by fluvial sandstones (Apeleg Formation, defined in Argentina, see Ramos, 1981).

Subsequently, the products of active subaereal volcanism (calderas) covered the area (Divisadero Formation, see Niemeyer et al., 1984; Suárez and De La Cruz, 1992).

Extensional, strike-slip and locally contractional tectonics affected this rocks. The latter was observed north and south of Lago General Carrera, where post-Lower Miocene thrusts were identified (Suárez and De La Cruz, 1992).

CONCLUSIONS

The Upper Jurassic - Lower Cretaceous marine formations includes relatively shallow marine facies; no important fan-delta system were observed, suggesting the absence of steep margins. Therefore, it is infered that the basin was formed by a widespread post-rift thermotectonic subsidence.

The post-Lower Miocene thrusting may be related to that described in Argenina at latitud 48°S (Ramos, 1989) and formed as a result of the collision of the Chile Ridge with the Chile Trench.

ACKNOWLEDGEMENTS

This work was financed by SERNAGEOMIN, Intendencia XI Region ad FONDECYT N°1930246.

REFERENCES

GUST,D.A.; BIDDLE, K.T.; PHELPS, D.W. and ULIANA, M.A., 1985. Associated Middle to Late Jurassic Volcanism and extension in southern South America. Tectonophysics 166, 223-253.
NIEMEYER, H.; SKARMETA, J.; FUENZALIDA, R.; ESPINOSA, W., 1984. Hojas Península de Taitao y Puerto Aisén, Región de Aisén del Gral. Carlos Ibañez del Campo. Carta Geológica de Chile, N°60-61, SERNAGEOMIN, Santiago, Chile 80pp.
RAMOS, V.A., 1981. Descripción geológca de la Hoja 47ab. "Lago Fontana". Provincia del Chubut. Ser. Geol. Nacional. Ministerio de Economía, Subsecretaría, Boletín N°83, Buenos Aires.
RAMOS, V.A., 1989. Andean foothills structures in northern Magallanes Basin, Argentina. American Assoc. Petrol. Geol. Bull. 73, 887-903.
SUAREZ,M. and DE LA CRUZ, R., 1982. Geología de la parte oriental de las Hojas Puerto Cisnes, Coyhaique, Chile Chico. Unpublished report. Servicio Nacional de Geología y Minería, Chile.

FIG. 1 SCHEMATIC MESOZOIC STRATIGRAPHIC DIAGRAM

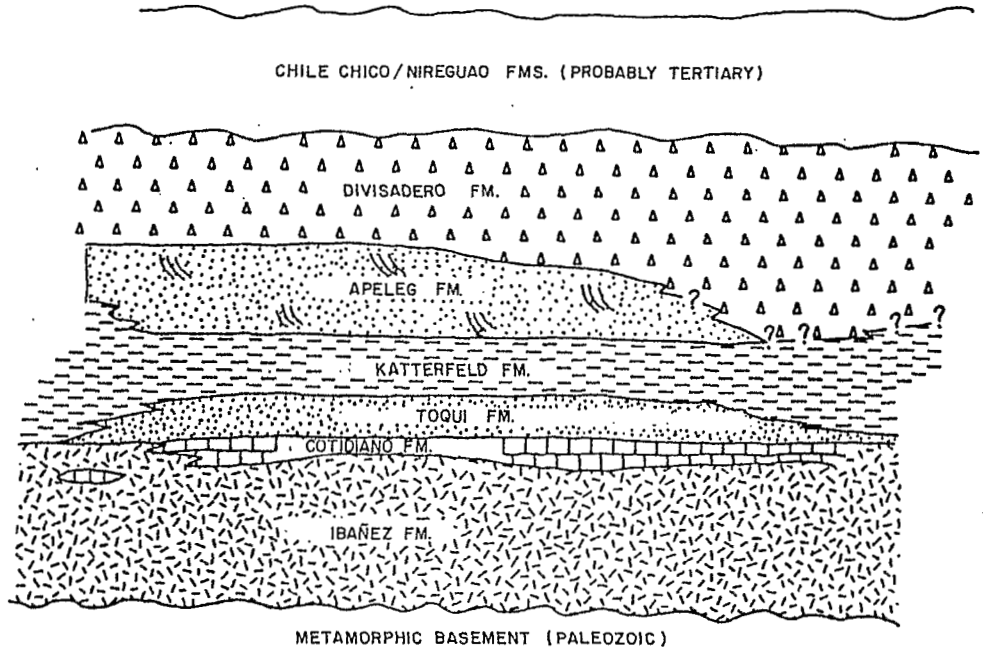

A SHORT-LIVED COMPRESSION RELATED SEDIMENT FILL IN THE ANDEAN INTERMOUNTAIN BASIN OF NABÓN (LATE MIOCENE, SOUTHERN ECUADOR)

Wilfried WINKLER, Arturo EGÜEZ(1), Diane SEWARD, Mary FORD, Friedrich HELLER, Dominik HUNGERBÜHLER & Michael STEINMANN

Department of Earth Sciences, ETH-Zentrum, 8092 Zürich, Switzerland
(1) Department of Geological Sciences, Escuela Politécnica Nacional-Quito, Ecuador

RESUMEN: El relleno volcano-sedimentario de la cuenca del tipo cono aluvial y fluvio-lacustrin fue depositado hace ≈ 8 Ma (dataciones por trazas de fisión y datos paleomagneticos). Las deformaciones sinsedimentarias permiten determinar un regimen compresivo durante el relleno.

KEY WORDS: Ecuador, Miocene, intermountain basin, basin analysis, zircon fission track, paleomagnetics.

INTRODUCTION

The Nabón basin is an elongated NNE-SSW oriented structure of ca. 120 km^2 situated in the Interandean depression south of the town Cuenca. The basin fill (500-600m) consists of volcaniclastic and pyroclastic continental deposits which overlies a volcanic series of mostly ignimbrites. The basin is a part of several Interandean continental basins (Cuenca, Girón, Loja etc.) formed after the Paleocene-Eocene accretion of the Piñon/Macuchi arc terrain and during the Tertiary subduction of the Nazca plate with related volcanic activity and uplift of the Ecuadorian Andes (e.g. Daly, 1989). In southern Ecuador a latest Oligocene to Miocene age of basin opening and filling under compressive strike-slip movements is generally assumed (Noblet et al., 1988, Lavenu et al., 1992). The reconstruction of the sedimentary history and synsedimentary deformation reveals the tectonic evolution of this part of the Andean chain (e.g. Noblet & Marocco, 1989, Lavenu et al., 1990). We present new data from the Nabón basin concerning the age and evolution of the sediment fill and its deformation.

RESULTS

The basin is floored by an ignimbrite series (Saraguro Fm.) dated by zircon fission track at 29-23 Ma. The oldest basin fill deposits (Fig. 1) are composed of reworked tuffs

and alluvial fan system sediments followed by braided river deposits. For a short period the center of the basin was occupied by a lake with high detrital sediment input and few diatomite layers (Letrero Fm.). Afterwards braided river and alluvial fan deposition is generally re-established. The basin fill series is topped discordantly by thick volcanic debris flows and pyroclastics. According to sediment geometries, flow indicators and the presence of reworked metamorphic pebbles characteristic of the eastern Andean cordillera the basin was mainly supplied from the eastern to the northern edge.

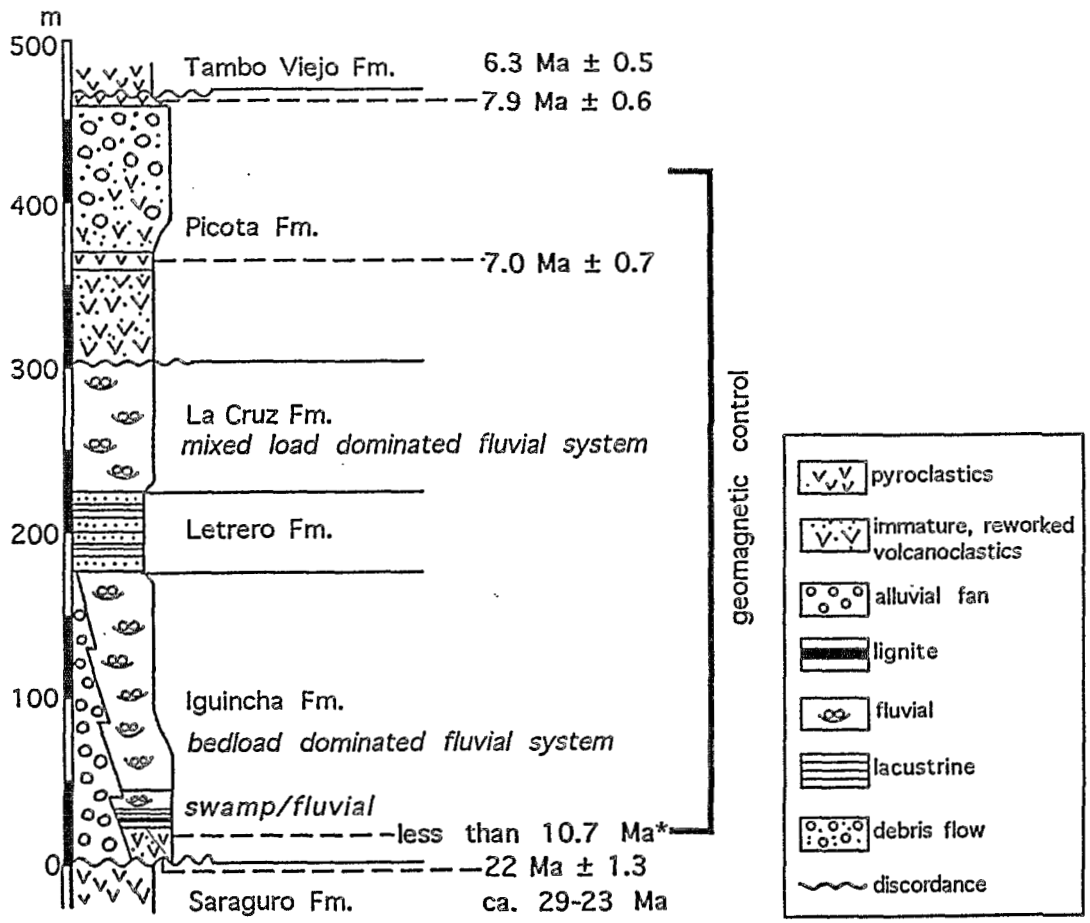

Fig. 1: Simplified stratigraphy and sedimentology of the Nabón basin. Only fission track data from samples without and minor (*) detrital component are shown. Error is ± 1 s.

The zircon fission track ages from two pure ashfall tephra in the upper part of the series range from 7.0 to 7.9 Ma. Many other samples contain some detrital component (see e.g. a 10.7 Ma* mean age at the base of the basin fill in Fig. 1) but there is always a younger mode at 8 Ma. The statistical extraction of the precise eruption ages is in progress. Younger volcanic air-fall deposits considered as Tarqui Fm. (DGGM, 1982) are scarcely preserved and one zircon fission track sample points to an age of 6.3 Ma (our Tambo Viejo Fm. in Fig. 1). Geomagnetic measurements reveal a reversed polarity for most of the basin fill (see Fig. 1) and combined with the fission track data it appears that the sedimentation occurred mainly during the 4r paleomagnetic chron (8.5-7.9 Ma in Cande & Kent, 1992). Tectonic block rotation was only detected in the volcanic basement

(see Fig. 2). Therefore, we observe a long time gap between basement formation and the main basin fill. This time is documented only by very few relic fluvial/alluvial sediments.

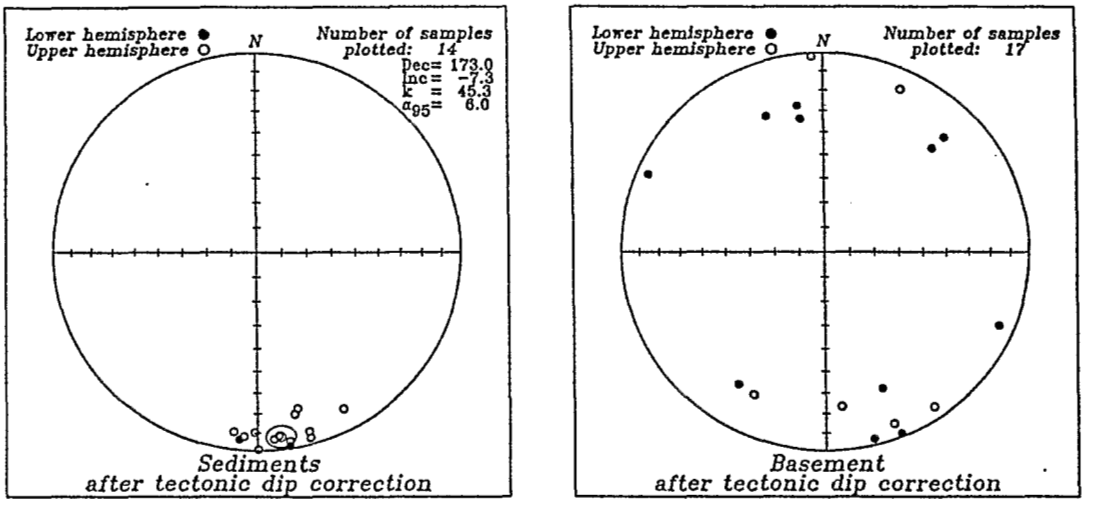

Fig. 2: Geomagnetic measurements obtained from the sediment fill and basement of the Nabón basin (it is to note that the indicated numbers of samples represent numbers of drill sites each one comprising 3-4 measured samples).

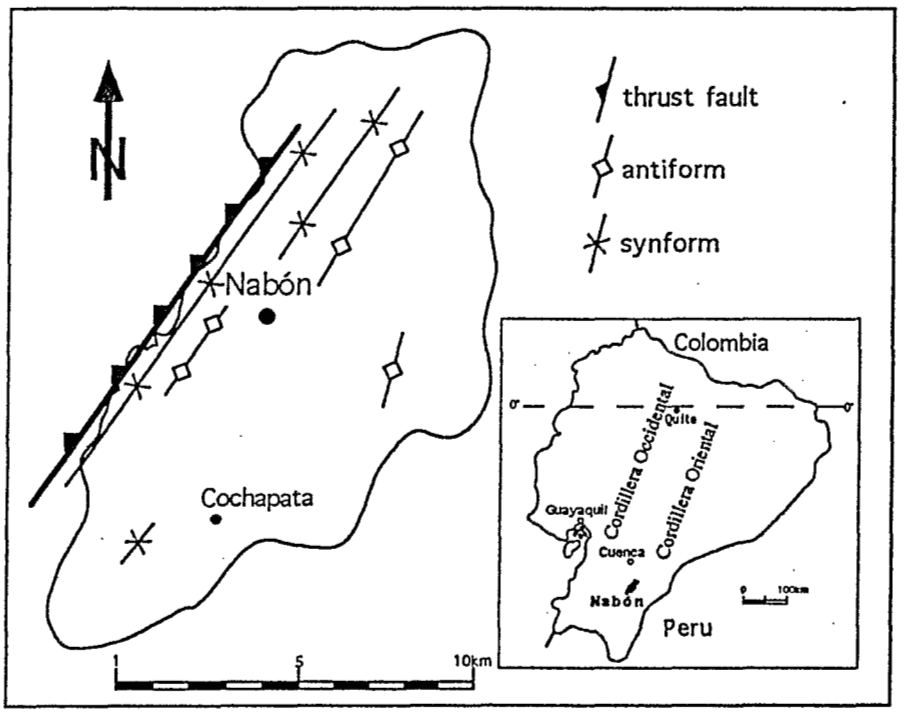

Fig. 3: Sketch of the main synsedimentary tectonic structures affecting the Late Miocene sediment basin fill.

The presence of synsedimentary thrusts along and near the western basin edge, growth folds striking parallel to the basin edge and related, orthogonally oriented normal faults point to a compressive tectonic regime that was active during the time of the main sediment fill (Fig. 3).

CONCLUSIONS

It appears that the tectonic structure hosting the young Nabón basin fill was formed at the transition between Oligocene and Miocene (probably as a part of a larger strike-slip system as proposed for other intermountain basins in southern Ecuador) but at first erosion and by-pass prevailed. Due to later compression (around 8 Ma, Late Miocene) and pronounced alluvial fan sedimentation it was partly closed and general sediment fill was enabled. The unconformable covering of the basin fill series by younger pyroclastics indicates that erosion and by-pass were re-established soon after sedimentation. The time of the observed local compressional regime coincides with the known general Miocene compressive stage (e.g. Lavenu et al., 1992) and the assumed accelerated subduction (Daly, 1989) at the Ecuadorian trench from Middle Miocene to Pliocene.

REFERENCES

Cande, S.C. & Kent, D.V. (1992): A new geomagnetic polarity time scale for the Late Cretaceous and Cenozoic. J. of Geophys. Res. 97 (B10), 13917-13951.

Daly, M.C. (1989): Correlations between Nazca/Farallon plate kinematics and forearc evolution in Ecuador.- Tectonics 8, 769-790.

Dirección General de Geología y Minas (DGGM) (1982): Mapa Geológico Nacional de la República del Ecuador. Escala 1: 1´000.000.

Lavenu, A., Noblet, C. & Winter, Th. (1990): Neogene stress pattern in southern Ecuador, Symp. intern. "Geodynamique Andine", Grenoble, 15-17 May, 1990.- Edition ORSTOM, 211-214.

Lavenu, A., Noblet, C., Bonhomme, M.G., Egüez, A., Dugas, F. & Vivier, G. (1992): New K-Ar age dates of Neogene and Quaternary volcanic rocks from the Ecuadorian Andes: Implications for the relationship between sedimentation, volcanism, tectonics.- J. South. Am. Earth Science, 5, 309-320.

Noblet, C. & Marocco, R. (1989): Lacustrine megaturbidites in an intramontane strike-slip basin: the Miocene Cuenca Basin of South Ecuador.- Inter. Symp. "Intermontane Basins, Chiang Mai, Thailand, 30 Jan.-2 Feb., 1989, 282-293.

Noblet, C., Lavenu, A. & Schneider, F. (1988): Etude géodynamique d'un bassin intramontagneux tertiare sur décrochements dans les Andes du sud de l'Equateur: l'example du bassin de Cuenca.- Géodynamique 3, 117-138.

This work was funded by the Swiss Directorate for Development Cooperation and Humanitarian Aid in Berne and the ETH-Zürich.

MAGMATISME ANDIN
ANDEAN MAGMATISM
MAGMATISMO ANDINO

RECHARGE-ASSIMILATION-FRACTIONATION-TAPPING ("RAFT") PROCESSES AND MAGMA ENRICHMENT IN THE CENTRAL ANDES

Susan J. AITCHESON (1), Alan H. FORREST (2) and Jürgen ENTENMANN (3).

(1) Earth Sciences Dept., University of Oxford, Parks Rd., Oxford, OX1 3PR, U.K.
(2) Dept. of Pure Mathematics & Mathematical Statistics, University of Cambridge, Mill Lane, Cambridge, U.K.
(3) Inst. für Geowissenschaften, Universität Mainz, Obere Zahlbacher Straße 63, D-6500, Mainz, Germany.

RESUMEN: La variación restringida de los enriquecimientos isotópicos y amplia de los enriquecimientos de elementos trazas observados en la ZVC puede ser satisfactoriamente explicada por la contaminación cortical de un magma basáltico empobrecido con la simultánea occurencia de cristalización fraccional y recarga magmática. El aumento exponencial en la concentración de elementos incompatibles en el líquido durante la crystalización fraccionale evita que la composición isotópica tenga mayores cambios. Todos estos enriquecimientos pueden ser explicados con sólo un 15% de contribución cortical al sistema magmático, sin necesidad de invocar una fuente de manto enriquecido.

KEY WORDS: Central Andes; Volcanics; Crustal contamination; Isotopes; Trace elements

INTRODUCTION

Miocene to Recent subduction-related volcanic rocks of the Central Volcanic Zone (CVZ) of the Andes occur in a region of exceptionally (ca 70 km) thick continental crust. In comparison with Andean arc volcanics from areas of thinner (<40km) crust the CVZ lavas have: extremely high abundances of incompatible elements; enriched isotope ratios (e.g. $^{87}Sr/^{86}Sr>0.7055$, $\varepsilon_{Nd} < -2$); and generally more evolved bulk compositions (basaltic andesite to rhyolite, with minor shoshonites in the eastern part of the arc). The genesis of these rocks and, especially, how they acquired their enriched chemical character is central to the following questions:

(I) Is there widespread enrichment of the mantle beneath the Central Andes?

(II) What is the balance in the Central Andes between crustal growth by addition of magma from the mantle and crustal recycling by intracrustal contamination of mantle-derived magmas?

Proposed explanations for the CVZ lava enrichments include: (1) involvement of the magmas with enriched lithospheric mantle (Rogers & Hawkesworth, 1989); (2) enrichment of the mantle source with subducted crustal material (Stern, 1991); and (3) intracrustal contamination of formerly depleted magmas (Wörner et al., 1992). The first two explanations imply widespread mantle enrichment under the CVZ but the third requires no enriched source. The explanations also imply crustal growth which is: almost equal to (explanation 1); a little less than (explanation 2); or substantially less than (explanation 3) the mass of young CVZ igneous rocks.

In this contribution we use new techniques for quantitative geochemical modelling to test the ability of intracrustal contamination to produce the enrichments observed in the CVZ magmas.

CAN INTRACRUSTAL CONTAMINATION EXPLAIN THE ENRICHMENTS?

Although there is ample evidence that *some* intracrustal contamination has affected the CVZ lavas, previous quantitative crustal contamination models have failed to account adequately for the observed enrichments. Simple bulk mixing calculations produce conflicting results for different elements and the *combined* process of assimilation with fractional crystallization (AFC; DePaolo,1981) has been rejected by workers such as Feeley & Davidson (1992), even although the CVZ rocks are highly fractionated, because of the general lack of correlation between isotopic ratios (which change with contamination) and element abundances or ratios (which change mainly by crystal fractionation). Apart from one or two exceptional centres (e.g. Ollague) with clear chemical evidence for the operation of upper crustal AFC processes, the vast majority of CVZ centres have an extremely small range of isotopic compositions coupled with an enormous range of enriched trace element abundances.

New techniques

The new techniques of Aitcheson & Forrest (1993) allow isotopic data from real rocks to be inverted by means of simple equations which are solved to give independent estimates of the relative rates of assimilation, fractional crystallization and magma recharge. These equations also explicitly quantify the crustal component and its dependence on the rate of venting or eruption. The existence of a solution means that all of the isotopic data from the sample being studied can be reconciled by a Recharge-Assimilation-Fractionation-Tapping ("RAFT") process. Having obtained this information, and given reasonable endmember concentrations and bulk distribution coefficients, it is possible to predict the concentrations of any other elements in the liquid (sample) and thus to test (by comparison with the observed sample composition) whether the isotope data and estimates of relative rates of assimilation, fractional crystallization, etc. are also consistent with the trace element data.

Application to the CVZ

We used these new techniques to test the ability of crustal contamination of a typical depleted arc basalt to produce the isotopic and trace element enrichments observed in the northern part of the CVZ. We used a depleted parental magma composition similar to that at Okmok in the Aleutian arc (Nye & Reid, 1986) with ε_{Nd} =+8.5 and $^{87}Sr/^{86}Sr$=0.7033. We estimated the contaminant composition from our analyses of basement rocks and crustal xenoliths from the northern Altiplano of Bolivia and Chile and allowed this composition to vary within reasonable limits to reflect crustal heterogeneity. Bulk distribution coefficients were based on various proportions of the minerals olivine, orthopyroxene, clinopyroxene, amphibole and garnet in the fractionating assemblage, plus published distribution coefficients for the different elements in these minerals with respect to basaltic melts. Note that Sr will behave incompatibly since in general there is no evidence for plagioclase removal from the liquids.

Results

For every sample we have investigated so far it has been possible to reconcile all of the isotopic data by the RAFT process, although the relative rates of assimilation, fractionation and recharge obtained vary slightly

		$\dot{M}_a : \dot{M}_c : \dot{M}_r$	Crust/magma Max.	Min.
VOLCAN PARINACOTA (18°S)				
TIME ↑	Side crater eruption (BA*)	0.17: 1 :0.25	0.20	0.16
	Side crater eruption (BA)	0.15: 1 :0.15	0.15	0.14
	"Healing flow", old crater (BA)	0.15: 1 :0.15	0.16	0.15
	(Cone collapse, sealing, new cone buildup)			
	Andesite from old cone	0.22: 1 :0.40	0.24	0.18
GENERALIZED LEAST-ENRICHED NORTH CVZ COMPOSITION				
	N. CVZ "baseline" compositions	0.15: 1 :0.48	0.17	0.12

Table 1: Examples of results of RAFT calculations for samples from the northern CVZ. $\dot{M}_a$:$\dot{M}_c$:$\dot{M}_r$ are the relative rates of assimilation, fractional crystallization and magma recharge. The crust/primitive magma mass ratio is that for the whole system. The maximum value corresponds to no venting prior to sample formation, while the minimum value is that at maximum venting rate, here assumed to equal the rate of recharge. BA is basaltic andesite, * is sample PAR-11 (see Fig.1).

from sample to sample. Table 1 illustrates some of these results for samples from a single centre (Parinacota, 18°S, N. Chile) and for a generalized least-enriched "baseline" composition for centres along the volcanic front in the northern CVZ. When these results are used to predict the trace element patterns of the samples we find that there is excellent agreement between the calculated and observed patterns, demonstrating that RAFT can also explain the trace element enrichment patterns in the CVZ (e.g. Fig.1). In general even the most extreme enrichments can be achieved with as little as 15% crust in the system. The RAFT equations may also be used to compute how much liquid remained in the system at the time of sample formation. These calculations indicate that, in general, at the time of eruption of the CVZ samples less than 10% of the systems were still liquid; >90% of the system had already crystallized as cumulates which presumably remained hidden in the lower crust.

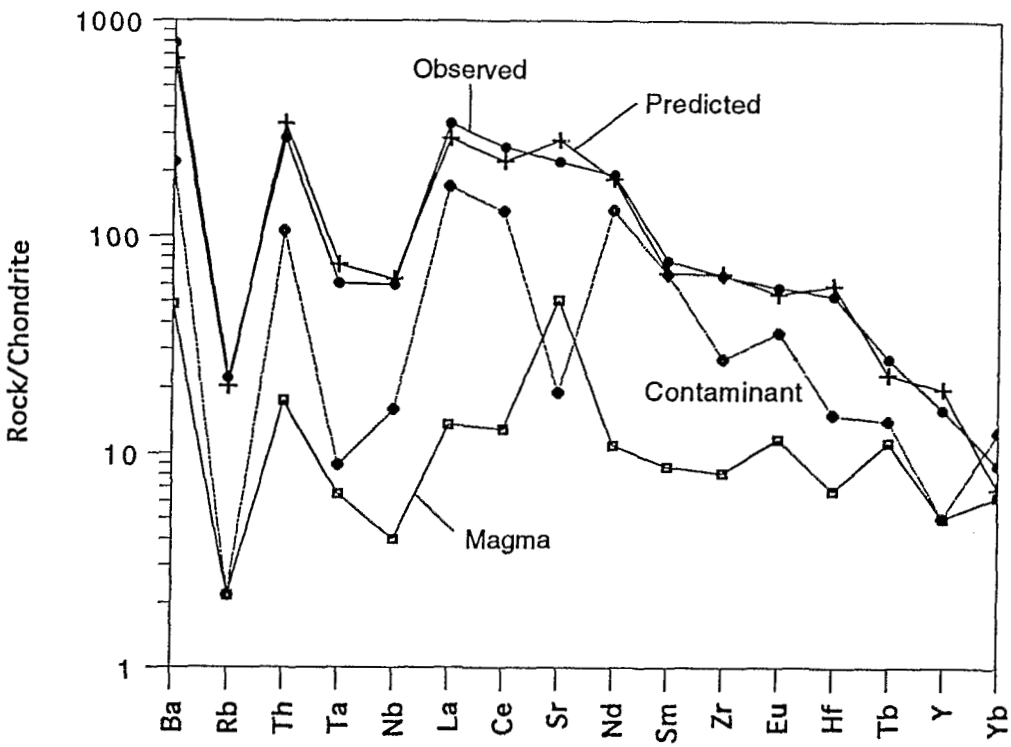

Figure 1: Chondrite-normalized spider diagram illustrating the calculated composition of sample PAR-11, the youngest basaltic andesite erupted at Parinacota, which was computed using the RAFT equations with the end member compositions shown in the figure, the results in Table 1, and assuming a fractionating assemblage of 9% olivine, 63% clinopyroxene, 7% orthopyroxene, 18% amphibole and 3% garnet. The measured composition is also shown for this sample and agrees closely with the computed composition, demonstrating that the RAFT process can explain both the isotopic and trace element enrichments in the sample. Compositions are normalized to the chondrite composition given by Anders & Ebihara (1982).

BUFFERING OF CVZ ISOTOPIC COMPOSITIONS BY THE RAFT PROCESS

The RAFT equations can readily predict the evolution of the isotopic and trace element composition in a magma, given reasonable endmember compositions, bulk distribution coefficients and relative rates of assimilation, fractional crystallization, etc. In the CVZ magmas the incompatible element concentrations

increase exponentially due to crystal fractionation. The isotopic composition of the liquid therefore soon becomes buffered against further change by the high concentration of that element in the liquid. For liquids (such as most CVZ magmas) erupted only after this concentration buffer was in force, a narrow range of enriched isotopic compositions and a wide range of high incompatible element concentrations are inevitable. On a plot of isotopic ratio vs. element concentration the samples will define an elongate field parallel to the concentration axis. Broadly similar end member compositions, fractionating minerals and physical nature of the magmatic plumbing systems will cause liquids to be buffered at about the same isotopic composition. This is presumably why the isotopic compositions of CVZ volcanoes are so similar from centre to centre.

CONCLUSIONS

(1) Crustal contamination of a depleted arc basalt can satisfactorily explain the isotopic and trace element enrichments observed in the CVZ if fractional crystallization and magma recharge were also occurring. There is thus no need to invoke an enriched mantle source for these magmas, although the existence of such a source cannot be excluded.

(2) A restricted range of isotopic compositions occurs together with a wide range of enriched trace element concentrations because crystal fractionation causes incompatible element abundances to rise exponentially in the liquid and this quickly buffers the isotopic composition of the liquid against further change.

(3) Some 85% of the total mass of CVZ igneous rocks, including hidden cumulates, represents new (i.e. mantle-derived) continental crust. The calculations suggest that less than 10% of the magmatic system is visible at the surface. Together this suggests that magmatism has caused an increase in the crustal thickness of about 5 km under the Central Andes.

REFERENCES

Aitcheson, S.J. and Forrest, A.H., 1993, Quantification of the crustal contribution in assimilation with fractional crystallization (AFC). *Journal of Petrology* (submitted).

Anders, E. and Ebihara, M., 1982, Solar-system abundances of the elements. *Geochimica et Cosmochimica Acta*, **46**, 2363-2380.

DePaolo, D.J., 1981, Trace element and isotopic effects of combined wallrock assimilation and fractional crystallization. *Earth and Planetary Science Letters*, **53**, 189-202.

Feeley, T.C. and Davidson, J.P., 1992, Across-strike geochemical variations in Late Cenozoic volcanic rocks from the southern Salar de Uyuni region (20-22°S), Andean Central Volcanic Zone. *Transactions, American Geophysical Union*, **73**, 644.

Nye, C.J. and Reid, M.R., 1986, Geochemistry of primary and least fractionated lavas from Okmok Volcano, Central Aleutians: implications for arc magmagenesis. *Journal of Geophysical Research*, **91**, 10271-10287.

Rogers, G. and Hawkesworth, C.R., 1989, A geochemical traverse across the North Chilean Andes: evidence for crust generation from the mantle wedge. *Journal of the Geological Society, London*, **138**, 237-277.

Stern, C.R., 1991, Role of subduction erosion in the generation of Andean magmas. *Geology*, **19**, 78-81.

Wörner, G., Moorbath, S. and Harmon, R.S., 1992, Andean Cenozoic volcanic centres reflect basement isotopic domains, *Geology*, **20**, 1103-1106.

PLUTONISM AND THE GROWTH OF ANDEAN CRUST AT 9° S FROM 100 TO 3 MA.

M.P. ATHERTON & N. PETFORD

Department of Earth Sciences, University of Liverpool, Liverpool L69 3BX, UK

RESUMEN: Chemical variations into the continent in plutonic rocks, 9° S Peru, do not conform to models involving increasing continental crust components etc. They relate to melting of new basaltic crust at increasing depth into the continent as the thick keel of the Andes evolved over the period 100-5 Ma.

KEY WORDS: Cordillera Blanca Batholith, Coastal Batholith, Transverse Variations, Trondhjemite.

INTRODUCTION

The Andes have been considered to be the archetype of a mountain belt produced by subduction of oceanic crust beneath continental crust. In Peru magmatism is confined to belts parallel to the present trench and coast (Fig. 1) and from 100-3 Ma there was a migration of the plutonic locus with time towards the interior. Such progressions are usually coupled with a change in composition considered to reflect thickening, reworking and uplift, which according to some authors reflects a fundamental plutonic cycle (eg. Pitcher, 1983). Thus the Mesozoic batholiths of western north America show an eastwards change in composition and isotopic signature related to the leading edge of the continental shield. Chemically based models related to island/continental arcs indicate transverse variations in elements and isotopes away from the subduction zone (Saunders et al., 1980). Here we describe the transverse changes in chemistry of the plutonic rocks in the Andes of Peru (9° S) which are not consistent with generalised models but relate to a change in source and depth of melting.

GEOLOGICAL SETTING

The Cordillera Blanca Batholith (CBB) lies 300 km inboard of the Coastal Batholith (CB, Fig. 1) and together they represent almost continuous plutonism over the period 100 to 3 Ma, apart from a gap between 36-13 Ma which is filled by minor intrusions lying between the two batholiths. Here we contrast the two batholiths and relate the differences to the evolution of the Andean margin over the period 100-3 Ma. Aspects of the geological setting are outlined below.

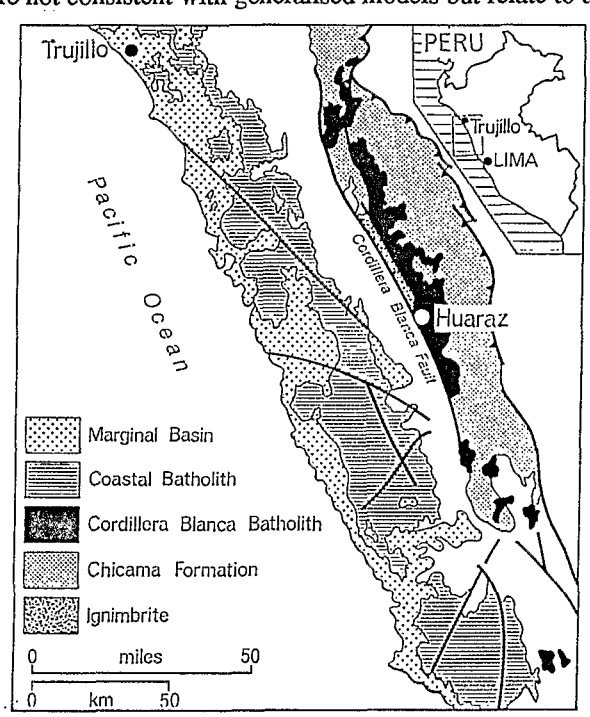

Fig. 1. Simplified map of area north of Lima showing Cordillera Blanca Batholith lying inboard of the Coastal Batholith.

Coastal Batholith	Cordillera Blanca Batholith
Intruded - along continental margin; with Andean trend;	Intruded - over deep crustal keel (60km) with Andean trend;
within Albian marginal basin, + 10km, (entirely volcanogenic); along a major crustal lineament, 1600km long;	within axial zone of Jurassic basin (mainly graphitic shales + sandstones) along major, deep megafault + 400km long
within the extensional lineament, 100-37Ma;	within transtensional strike-slip pull apart, 12-3Ma; Uplift in Miocene.
Uplift in U. Cretaceous and L. Tertiary.	

Specifically, both batholiths were intruded into basinal systems related to continental margin extension which started in the Jurassic at least. Furthermore the crustal source for both magmas was *new basaltic* material, at the bottom of the marginal basin for the CB and at the bottom of the thick (> 60 km) Miocene keel of the Andes for the CBB.

Both batholiths are calc-alkaline with tonalitic rocks dominating the CB and granitic rocks with trondhjemitic character (Atherton & Petford, 1993) dominating the CBB.

The increase in peraluminosity in the CBB is not related to an old crustal component in the source. Indeed there is no old crust beneath this sector of Peru (Atherton & Petford, 1993). Rather it relates to late deformation associated with fluid infiltration and alkali loss (Petford & Atherton, 1992). Variations in composition inboard from the continental lip are shown below.

West Coastal Batholith → Cordillera Blanca Batholith East

Into the continent with increasing distance from present trench
No K/Si, Rb/Si, Th/Si, Ce/Si increase inboard

but increase in Na_2O, Sr, Ta, A/CNK, Ce_N / Yb_N and subtle decrease in CaO, Th, Y, Ce.*

** A/CNK increase relates to late high level deformation and fluid penetration*

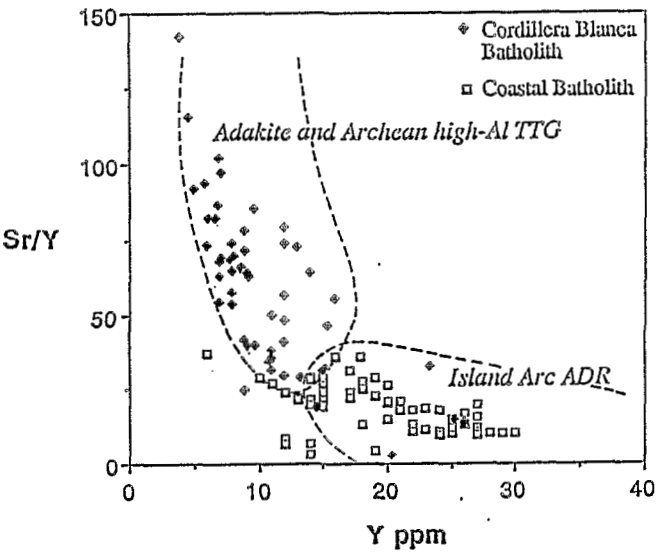

Fig. 2. Plot of Sr/Y vursus Y for rocks of the Cordillera and Coastal Batholiths. Island arc andesite-dacite rhyolite fields and Adakite Archean high-Al tonalite-trondhjemite-granodiorite fields are shown

DISCUSSION: BASALT TO BATHOLITH

Transverse variations at 9° S in Peru do not conform to any of the simple models put forward for continental margins. Rather, compositional variations into the continent relate to shallow melting (< 10 km) of Albian basaltic crust to produce the CB (Atherton, 1990) and deep melting (ca. 50 km) of the newly thickened basaltic keel of the Andes in the Miocene to produce the CBB (Atherton & Petford, 1993). CB magmas are calc-alkali with compositions determined by slab enriched mantle mineralogies with residues of mainly olivine and pyroxene (Fig. 2). In contrast the Na-rich magmas of the CBB are more alkalic and relate to garnet-hornblende residues in the source. They are thus similar to adakite and Archean high Al-TTG (Fig. 2 and Atherton & Petford, 1993). Similar Tertiary Na-rich plutons in Chile suggest that this transverse pattern is not unique to Peru. However, it is clear that this variation will only relate to sectors along the continental margin where the source is basaltic and Precambrian lower crust is absent (see Petford et al., this volume).

REFERENCES

Atherton, M.P., 1990. The Coastal Batholith of Peru:the product of rapid recycling of new crust formed within rifted continental margin. Geol. J. 25, 337-349.

Atherton, M.P. & Petford, N., 1993, Generation of sodium-rich-magmas form newly underplated basaltic crust. Nature, 363, 144-146.

Petford, N. & Atherton., M.P., 1992. Granitoid emplacement and deformation along a major crustal lineament: the Cordillera Blanca, Peru. Tectonophysics, 205, 171-185.

Petford, N, Atherton, M.P. & Halliday, A.N., 1993. Miocene plutonism in N. Peru: Implications for along strike variations in Andean magmatism (this volume).

Pitcher, W.S., 1983.Granite type and tectonic environment. In. Hsui, K. (ed.) Mountain Building Processes. Academic Press, London, 19-40.

Saunders, A.D., Tarney, J. & Weaver, S.D., 1980. Transverse geochemical variations across the Antarctic Peninsula: implications for the genesis of calc-alkaline magmas. Earth. Planet. Sci. Letts. 46, 344-360.

TIN-BEARING GRANITES FROM BOLIVIA: TECTONIC SETTING AND GEOCHEMICAL PARAMETERS

Waldo Arturo AVILA-SALINAS (1)

(1) Academia Nacional de Ciencias de Bolivia-P.O.Box 5829- La Paz

RESUMEN
Se establecen las características geoquímicas de los granitos estannífe-ros bolivianos y se discute su ambiente tectónico.Así, los granitos triá-sicos del norte de la Cordillera Real (La Paz) ostentan una tipología "S-like" y se ubican tanto en el campo de los granitos sincolisionales como en los de arco volcánico.Mientras que los granitoides del sur de la misma cadena montañosa tienen edad Oligocena y se relacionan a un arco magmático vinculado a la subducción temprana de la placa de Nazca.
En contraste, los granitos proterozoicos del Escudo Precámbrico Bolivia-no (Santa Cruz) poseen rasgos del tipo "I" y ambiente intraplacas. Adi-cionalmente,los granitoides alcalinos y sienitas del Complejo alcalino de Velasco conforman plutones anulares de edad Jurásica Superior-Cretácica Inferior y ambiente de rift ensiálico.

KEY WORDS: Bolivia; tin-bearing granites; geochemical parameters.

INTRODUCTION

The petrological and geochemical research of the granitoid rocks is par-tially devoted to establish the sources of the magmas,the depth of its emplacement and the features of their tectonic settings. In this context the tin-bearing granites from Bolivia will be examined in terms of its petrochemical nature and geochemical constraints determined by the usage of certain discriminant diagrams,such as: Rb/ Sr versus DI; Rb (ppm) vs Nb + Y (ppm); Rb-Sr-Ba,etc.
The Bolivian tin-bearing granites correspond to three main magmatic pro-vinces. These are: a) tne Cordillera Real of the eastern Andes (CR); b) the Bolivian Precambrian Shield (PS); and c) the Velasco Alkaline Com-plex (VC).

GEOLOGICAL SETTING

The Cordillera Real is a high mountainous range conformed by Paleozoic sediments that were intruded by six small granitoid batholiths in its axis. Among them,the northern intrusive bodies have been consolidated during the Triassic (230-200 Ma.ca.),whereas the southern plutons were dated by K-Ar in an Upper Oligocene-Lower Miocene range (28-23 Ma.ca.)
The granitoid batholiths of CR are mostly composed by the granite-grano-diorite association with minor quartz-monzonite,tonalite,quartz-diorite, leucogranite and monzogabbro seggregations. These calc-alkaline pluto-nics are commonlly enriched in potassium and they encompassed a wide si-lica range for variable alumina contents.
The geotectonic situation of northern Triassic plutons of CR is still enigmatic but probably is tenously related to a paleo-subduction event rather than rifting (Avila-Salinas,1990). Whilst the southern Oligocene granitoids are linked to the uplift of the Quechua phase.

b) The tin-bearing granitic plutons of the Bolivian Precambrian Shield have been consolidated during the Middle Proterozoic San Ignacio Orogenic Cycle (1400-1280 Ma.ca.),as well as, during the next Sunsas Orogeny (1280-950 Ma.ca.)
The syn-kinematic stannogenic plutons associated to the Pensamiento granitic Complex (Litherland et all,1986) have a scattered distribution. Among them, the Florida granite (1244 Ma.ca.) and the granophyric complexes of Bella Vista and Cerro Grande are peculiar examples. In contrast, the post-kinematic intrusions of significant tin content belong to the "I" type granitoids,such as: the Diamantina and Orobayaya "allochthonous" plutons. Examples of tin-bearing granites related to the Sunsas Orogenic Cycle are provided by the Cerro Talcoso and Casa de Piedra plutons.
The tin content of the Bolivian Precambrian granites ranges from 3 to 15 ppm Sn.
c) The Velasco Alkaline Province (Fletcher and Litherland,1981) consists of a suite of 15 ring-type plutons and associated alkaline volcanics that are mainly composed by granitoid and s yenitic rocks of a Late Jurassic-Lower Cretaceous age (142-120 Ma.ca.). These alkaline plutonics overlie a Proterozoic gneissic basement and their intrusions result from cauldron subsidence of volcanic edifices.
The tin-bearing rocks from the Velasco Complex are aegirine-bearing granites (i.e; Cabeza de Toro and Tirari plutons,with 2-7 ppm Sn), as well as, quartz-syenites,nordmarkites and melasyenite dikes.

PETROCHEMICAL FEATURES
The granitoid rocks of CR are both peraluminous to moderately metaluminous plutonics displaying a characteristic "S-like" signature (Avila-Salinas, 1990),that resulted from fractional crystallization of the magmatic melts originated at the upper mantle,followed by variable assimilation of crustal rocks (such as the tin-bearing Precambrian granites of the Basement). In a such way, the tin-bearing granites of CR exhibit a wide silica range, moderate alumina surplus and MgO and CaO depletions into their most acidic terms (leucogranites).
The Triassic plutons consist predominantly of granites (leucogranites, syenogranites,monzogranites) with lesser granodiorite and tonalite seggregations,while the Oligocene intrusives are mainly composed by granodiorite and quartz-monzonite.
Furthermore, the tin-bearing granitoid rocks of the PS are both syenogranites and/ or monzogranites belonging to an "I" type. Whereas other areas of the Bolivian Shield present certain syn-kinematic "authoctonous" granites associated to granitization or migmatization of the late stages of the San Ignacio Orogeny. These are barren granites (with lack of tin),that are distinguished by a "S" type,with common gneissoid banding,restite minerals and sedimentary xenoliths.
Among the tin-bearing granites of the PS,the composite Orobayaya pluton show an ellipsoidal shape,displaying an external envelope of biotite-bearing monzogranite followed by inner pulses of syenogranite and syenogranite porphyry (in the core).
The Velasco Complex (Santa Cruz department) conform several ring-type plutons,some of them with nepheline syenite in their cores and external rings consisting of pulses of nordmarkite,pulaskite,aegirine-bearing granite, quartz-syenite and biotite-bearing calc-alkaline granite.
A magmatic differentiation process from a parental magma of pulaskitic composition has been invoked for the origin of these alkaline rocks.

The tin content of the VC alkaline granitoids is probably related to fenitization rather than greisenization or albitization of those ring-complexes.

GEOCHEMICAL CONSTRAINTS

The geotectonic settings of the Bolivian tin-bearing granites have been examined in the light of discriminant geochemical diagrams. Thus, the Rb/ Sr versus DI variation diagram was applied for the three magmatic provinces selected here. In this context, the high Rb/ Sr ratios combined with high DI values distinguished the alkaline rocks from VC, and similarly, high values were observed in samples of the Proterozoic granites of the Bolivian Shield. These rocks lie on the field of the "I" type granites. Likewise, the population of granodiorites from the southern CR show features of volcanic arc granitoids. Whilst the Triassic granitoids of the northern CR lie alternatively in the field of the "S" and "I" types, and particularly, on the experimental boundary line established with comparative samples of Malasian tin-bearing granites.

With the usage of the Rb (ppm) versus Nb + Y (ppm) variation diagram several populations of Bolivian granitoids were plotted. Thus, the PS granites and alkaline rocks of VC fall on the field of the within-plate granites (WPG), that are characterized by high Nb and Y contents.

The field of the Volcanic Arc Granites (VAG) is mostly occupied by samples of southern CR and from the Triassic Sorata batholith. Other granitoids of the northern CR lie alternatively, in the area of syn-collisional granites and in the VAG field. Consequently, the enigmatic nature of those "S-like" cordilleran granitoids is still underlined in this diagram. Nevertheless, a plotting of granitoids from CR in the Log CaO% / Na_2O + K_2O % versus SiO_2 % variation diagram emphasizes the increase in arc maturity for samples of southern CR (that are subduction-related rocks), and also for granitoids of Sorata batholith .Assuming the origin of the former as the result of the Nazca plate subduction is inferred, consequently, a paleo-subduction as explanation of the emplacement of the northern Sorata pluton, whose population lies in the same place.

CONCLUSIONS

a) The northern Triassic granitoids of the Cordillera Real of the eastern Andes of Bolivia (which is an important mining district) form part of an enigmatic igneous arc, that is tenously related to a paleo-subduction process (of the PaleoPacific lithospheric plate ?). These rocks have a "S-like" status, considered formerly.

b) The tin-bearing granitoids of the southern CR correspond mostly to "I" type granitoids, consolidated in a volcanic arc linked to the Nazca plate subduction (circa 25 Ma.)

c) The tin-bearing granitoids of the Bolivian Precambrian Shield consist of isolated intrusions within the huge gneissic basement. These rocks have a within-plate setting and "I" type status.

d) The alkaline granitoids and syenitic rocks of the Velasco Complex are classed as "A" type granitoids, resulting from the rift-controlled emplacement of a suite of 15 ring-type plutons of Late Jurassic-Lower Cretaceoua age.

REFERENCES

Avila-Salinas,W; (1990): Tin-bearing granites from the Cordillera Real, Bolivia; A petrological and geochemical review. In:

Kay,S.M and Rapela,C.W; eds: "Plutonism from Antarctica to Alaska". Geological Society of America Special Paper 241; 145-159, Boulder.

Fletcher,C.N.J; and Litherland,M; (1981): The Geology and tectonic setting of the Velasco Alkaline Province, eastern Bolivia. Journal of the Geological Society, v 138 (5);541-548.

Litherland,M; and 15 others;(1986): The Geology and mineral resources of the Bolivian Precambrian Shield. British Geological Survey Overseas Memoir N° 9 ; 1-153.

ULTRAPOTASSIC AND PERALUMINOUS MAGMA MIXING AND ORIGIN OF THE HIGH-K LATITES FROM THE EASTERN CORDILLERA OF SOUTHERN PERU.

Gabriel CARLIER (1-2), Jean-Pierre LORAND (3), Jean-Robert KIENAST (2) & Etienne AUDEBAUD (4)

(1) ORSTOM, TOA, UR 1H, 213 rue La Fayette, 75480 Paris, France.

(2) CNRS, URA 736, Laboratoire de Pétrologie, Université Paris VII, 4 place Jussieu, 75230 Paris, France.

(3) CNRS, URA 736, Laboratoire de Minéralogie du Museum National d'Histoire Naturelle, 61, rue Buffon, 75005 Paris France.

(4) Laboratoire de Pétrologie, Institut Dolomieu, Géologie et Minéralogie, rue Maurice Gignoux, 38031 Grenoble, France.

RESUMEN : Las latitas potásicas neógenas de la Cordillera Oriental del Sur del Peru resultan de la mezcla magmática entre magmas de composiciones riolítica peraluminosa y lamproítica respectivamente. Se presentan argumentos texturales, mineralogícos y geoquímicos que comproban este proceso magmatico.

KEY WORDS : Olivine lamproite, peraluminous monzogranite, high-K latite, magma mixing, Southern Peru.

INTRODUCTION :

During the upper Oligocene and lower Miocene, the Eastern Cordillèra of Southern Peru is the centre of an important magmatic activity characterized by peraluminous monzogranites, shoshonites and banakites [see Clark & al., 1990 and references herein]. In the Nuñoa area, lamprophyres (now classified as high-K latites) have been first reported by Audebaud & Vatin Perignon [1974]. Subsequent K/Ar datations [Bonhomme & al., 1985] indicated that these rocks are contemporaneous with the late Oligocene-lower Miocene peraluminous magmatic intrusions. Based on petrographical, mineralogical, and geochemical data, we demonstrate that the high-K latites are generated by mixing involving peraluminous and lamproitic magmas.

MAGMA MIXING EVIDENCES IN MONZOGRANITES AND HIGH-K LATITES :

The monzogranites contain quartz, oligoclase, sanidine, biotite and cordierite phenocrysts in a fine-grained groundmass made of quartz, oligoclase, biotite, apatite, zircon, sillimanite and secondary muscovite and tourmaline. They also include phlogopite xenocrysts and chromite-olivine-phlogopite-bearing mafic inclusions. The high-K latites are composed of a groundmass made of phlogopite, andesine, sanidine, hypersthene, apatite, ilmenite, graphite and sometimes osumilite microlites and colourless glass. Olivine, phlogopite, biotite, quartz, oligoclase, augite, ilmenite and rare cordierite xenocrysts are also frequent. Millimetric inclusions of chromite-olivine-phlogopite-bearing mafic inclusions have been observed in a single high-K latite.

Xenocrysts in high-K latites systematically are partially resorbed (quartz, phlogopite) or exibit reaction textures (olivine, augite and quartz rimmed by polycristalline orthopyroxene coronas, sieve-textured biotite and mantled oligoclase, granular intergrowths of aluminous spinel, ilmenite, orthopyroxene and osumilite or K feldspar in biotites). All these features are consistent with assimilation of solid crustal material or magma mixing processes. Nevertheless, textural evidences (ellipsoidal shape, finger-like, cuspate margins...) indicate that the olivine-phlogopite-bearing mafic inclusions have been incorporated in a molten state into the magmas now represented by the monzogranites and high-K latites. Then, we conclude that magma mixing is an important process involved in the genesis of the monzogranites and the high-K latites of the Eastern Cordillera of Southern Peru. The xenocrysts of the high-K latites represent the mutual mechanical exchange of phenocrysts crystallized prior the mixing in both magmatic components.

CHEMICAL AND MINERALOGICAL COMPOSITION OF MAGMA COMPONENTS PRIOR THE MIXING :

The absence of chemical disequilibrium evidences in phenocrysts of the monzogranites that contain phlogopite xenocrysts and mafic inclusions, suggests that the mixing process is essentially mechanical (mingling). Moreover, as xenocrysts and inclusions are scarse and do not significatively altered the whole-rock chemistry, the mineralogical and chemical characteristics of the monzogranites may be reasonably considered as representative of one of the magmatic components involved in the mixing process.

The chromite-olivine-phlogopite-bearing mafic inclusions in both monzogranites and high-K latites supply the best evidences for the identification of the other magma components involved in the mixing. Unfortunately, their small size precludes their characterization by classic procedures of whole-rock chemistry. Consequently, only the chemistry of the mineral phases provides informations on the original crystalline characteristics of this component. The crystallization order in these mafic inclusions, prior to mixing, are chromite, olivine, phlogopite and ilmenite. This sequence is unusual in potassic and ultrapotassic rocks and has been only experimentally obtained by Foley (1989) for lamproitic compositions at low oxygen fugacity and low water activity. The high Cr/Cr+Al ratio of the chromite that is liquidus phase implies a low Al content in the coexisting melts. Low oxygen fugacity conditions are supported by very low Fe^{3+} content and probably presence

of Cr^{2+} in chromite and Ti^{3+} in ilmenite whereas the Si-Al tetrahedral deficiency and the high K/Al ratio of the phlogopite phenocrysts are indicative of both low oxygen fugacity and low water activity. All these features are consistent with a lamproitic affinity for the mafic inclusions and then for the mafic magma component involved in the mixing.

All large crystalline phases occurring in the high-K latites define incompatible mineral assemblages (quartz-olivine, aluminous biotite-phlogopite associations) and systematically are in chemical disequilibrium with the groundmass. They represent relicts of phenocrysts that have crystallized either in lamproitic or in peraluminous magmas.

All the high-K latites are ultrapotassic according to the geochemical classification proposed by Foley & al. (1987). On the element-element plots, the high-K latite and monzogranite compositions define systematic straight correlations that when extrapolated towards the mafic compositions lie on the olivine lamproite domain. From these mineralogical and geochemical data, the origin of high-K latite by mixing between peraluminous rhyolitic and olivine lamproitic magmas are deduced.

MAGMA COMPONENT PROPORTIONS INVOLVED IN THE HIGH-K LATITE GENESIS AND TEMPERATURE-PRESURE OF MIXING :

The relative proportions of the two magma components involved in the mixing cannot be accurately estimated in absence of precise chemical composition of these components. Nevertheless, mineral chemistry of high-K latite microphenocrysts and microlites indicates that low oxygen fugacity (Fe^{3+}-free Ti^{3+}-bearing ilmenite, graphite) and low water activity (osumilite) conditions persist in the "new" magma after mixing. Pyroxene and felspar thermometry suggest that microphenocrysts have crystallized at nearly 1000°C. Experimental data on peraluminous and lamproitic compositions suggest that the monzogranitic and lamproitic magmas were at the time of mixing at 800-850°C and 1050-1100°C respectively. The thermal contrast between the two magmas is large (200°C) and would provocate rapid crystallization of the lamproitic component if the peraluminous magma proportion involved in the mixing is high (> 50%). At the contrary, the texture of minerals crystallising during the first stages of the mixing (phlogopite, augite) suggest low thermal contrast. We conclude that the lamproitic component involved in the magma mixing is widely predominating (>50%). Pressure at which the mixing occur is not accurately determinated. Nevertheless, the absence of cordierite and sanidine xenocrysts and the occurrence of osumilite in some high-K latites suggest pressures above 4 kbar and below 11kbar.

CONCLUSION :

The high-K latite of the Eastern Cordillera of southern Peru originated by mixing of lamproitic and peraluminous magmas. Temperature and pressure evaluation suggests that mixing process may operate in the

lower crust. The Peruvian and Bolivian shoshonitic rocks exhibit strong mineralogical and geochemical affinity with the studied high-K latites. Magma mixing process would be an important process generating these rocks.

REFERENCES :

Audebaud E and Vatin-Pérignon N. (1974) The volcanism of the northern part of the Peruvian Altiplano and of the Oriental Cordillera on a traverse Quincemil-Sicuani-Arequipa. International association of volcanology and chemistry of the earth's interior, 34p.

Bonhomme M. G., Audebaud E. and Vivier G. (1985) K-Ar ages of Hercynian and Neogene rocks along an East West cross-section in Southern Peru. Comunicaciones, 35, 27-30.

Clark A. H., Farrar E., Kontak D. J., Landgridge R. J., Arenas M. J., France L. J., McBride S. L., Woodman P. L., Wasteneys H. A., Sandeman H. A. and Archibald D. A. (1990) Geologic and geochronologic constraints on the metallogenic evolution of the Andes of southeastern Peru. Economic Geology, 85, 1520-1583.

Foley S. F. (1989) The genesis of lamproitic magmas in a reduced fluorine-rich mantle. in Ross J., Jaques A. L., Fergusson J., Green D. H. and O'Reilly S. Y. Eds, Proceedings of the fourth international kimberlite conference. Kimberlites and related rocks. Vol 1 : Their composition, occurrence, origin and emplacement. Geological Society of Australia Special Publication, 14, 616-630

Foley S. F., Venturelli G., Green D. H. and Toscani L. (1987) The ultrapotassic rocks : characteristics, classification and constraints for petrogenetic models. Earth-Science Reviews, 24, 81-134.

THE SOUTH-WESTERN MEJILLONES PENINSULA. BASEMENT TERRANE OR DEFORMED HIGH LEVEL MAGMA CHAMBER?

COLIN CLERK[1], HILARY DOWNES[1], and NICK PETFORD[2]

(1)Research School of Geological and Geophysical Sciences, Birkbeck College & University College London, Gower Street, London WC1E 6BT
(2)Department of Earth Sciences, University of Liverpool, Liverpool L69 3BX, UK.

RESUMEN: La parte suroeste de la Peninsula de Mejillones, la que està ubicada al noroeste de Antofagasta en el norte de Chile se ha considerado componerse de gneises atribuìdo al basamento cristalino. Ahora es possible para entender estas rocas como los productos de una recàmara de magma de nivel alto.

KEY WORDS: Chile, Mejillones Peninsula, acid/basic relationships.

INTRODUCTION

The Peninsula de Mejillones is located in Northern Chile (23° - 23° 30' S), immediately to the north west of Antofagasta (Fig. 1). The southwestern part of the peninsula is composed of a suite of deformed gabbroic to dioritic rocks, which are extensively intruded by sheets and veins of acidic and tonalitic composition, as well as basic dykes. These rocks have previously been regarded as basement gneisses (Venegas Carvajal 1979) and have been assigned ages ranging from Palaeozoic (Ferraris and Di Biase 1978) to Pre-Cambrian.(Skarmeta and Suarez 1979; Vengas Carvajal 1979).

FIELD RELATIONS

Recent field work has led to a reinterpretation of these rocks as the remnants of a deformed mid to upper crustal magma chamber. Field observations suggest strongly that the foliated nature of the complex developed from syn-to-post magmatic deformation of co-existing intermediate and acid melts. Evidence for magma mingling include early mafic to intermediate dykes, sheets, and pillows exhibiting crenulate and cauliform margins typical of fluid-fluid contacts. Microdioritic enclaves are abundant, and often show signs of chilling (grain size reduction) at their margins.Texturally the rocks are extremely variable with the dioritic facies showing extensive interaction on all scales with the invading acid melt. In addition to obvious liquid-liquid contacts between veins and host rock, there is local evidence on an outcrop scale of thorough magma mixing, producing a melanogranite/leucodiorite rock. Coarse appinitic pods with skeletal amphibole and plagioclase are also present, suggesting the presence locally of rapid quenching of water rich magmas. These observations are consistant with those reported from well documented examples of mid to upper crustal mixed and magma mingled complexes from the Channel Islands and the Coastal Batholith of Peru (D'Lemos 1993; Bussell 1992).

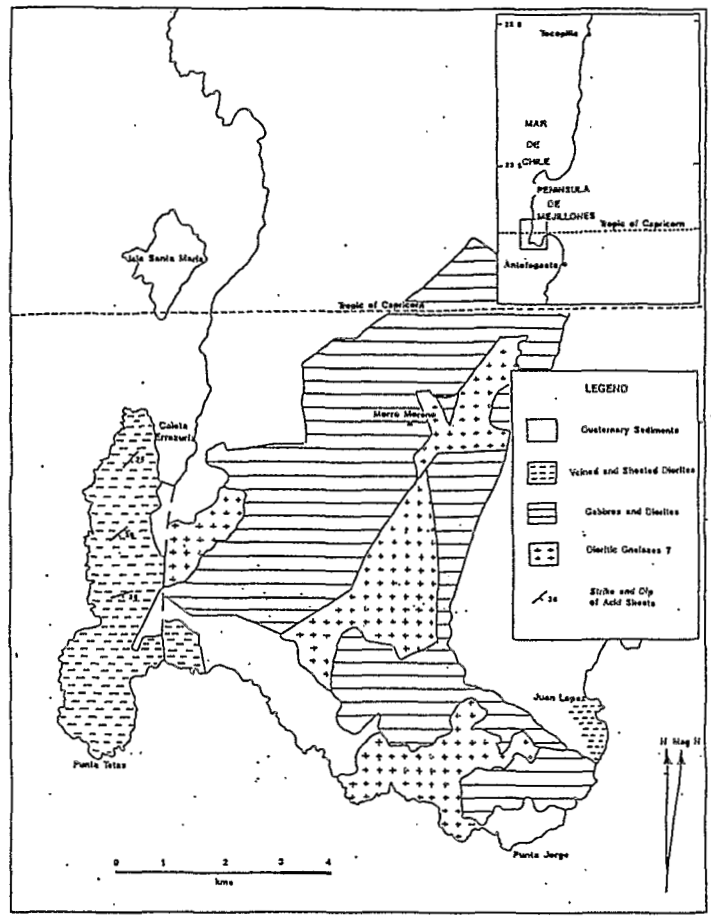

FIG. 1 Simplified Geological Sketch-map of the Southern Mejillones Peninsula, Region 2, Chile
(Modified after Venegas Carvajal 1979)

A pervasive foliation occurs throughout all but the very latest intrusions, although its intensity is variable from place to place, often being concentrated in local intense shear zones. It is however, usually continuous through the host diorites into the invading veins with no apparent change in orientation from one rock type to the other. A later foliation is locally present which cross cuts the earlier one at a high angle, but it is only poorly developed.

The sheeting and veining in the study area is complex. There are several types of veins, including garnetiferous leucogranites, acid pegmatites, aplites, and tonalites, as well as veins of pure quartz. In addition, the geometry of the veins and sheets is very variable. Contacts between the veins and the host rock frequently change in character, from fluid-fluid type contacts to seemingly brittle contacts, along the length of the vein. This is interpreted as being due to variations in the rheological properties of the fluids with varying strain rates, in combination with local variations in the crystal:melt ratio. The most significant intrusions volumetrically are the garnetiferous granites and aplites, which comprise approximately 15% of the entire rock mass of the outcrop. They occur as sheets ranging in thickness from 30 cms to 60 cms, and exhibit an obvious preferred orientation, typically striking at around 160-240° with an average dip of 30° SE.(Fig. 2). A multitude of smaller veins occur, though these appear to have a more random orientation.

Basic dykes have been intruded into the complex, both during, and after deformation. Syntectonic dykes show evidence of shearing, and exhibit the same foliation as the host rocks.

Mechanical interaction between these dykes and the host diorites has led to the formation of basic enclaves. Completely undeformed dykes are also present, which have clearly been intruded into a solid host after deformation had ceased. Typical orientations of the basic dykes are shown on Fig. 2.

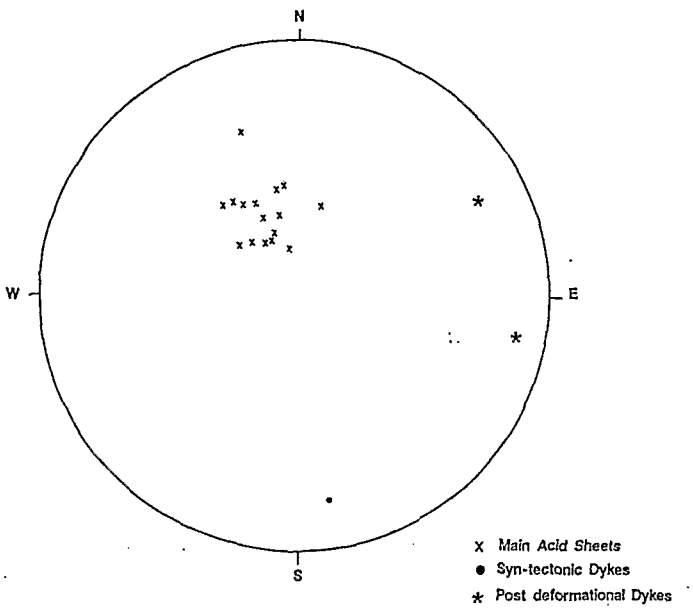

FIG. 2 Stereonet Showing Orientations of Acid Sheets and Basic Dykes

DISCUSSION

On the basis of field relationships it is suggested that the rocks of the southwestern Mejillones Peninsula are the products of a mid to high level magma chamber, and not lower crustal basement migmatites as previously thought. Given this new interpretation, it is possible that these rocks may be 'Andean' and thus of an age significantly younger than previously supposed. These ideas are currently being tested using a combination of radiometric age dating and mineral chemistry.

REFERENCES

D'Lemos, R.S. 1992, Magma-mingling and melt modification between granitic pipes and host diorite, Guernsey, Channel Islands. J.Geolsoc.London. 149, 709-720.

Ferrari, F.& DiBiase,F 1978, Carta Geologica de Chile, Hoja Antofagasta.Instituto de Investigaciones Geologicas No.30

Skarmeta, J.& Suarez, M., 1979 Complejo Granitico - Gabroico Milonitizado de la Peninsula de Mejillones: Nota Preliminar, Segundo Congreso Geologico Chileno

Venegas Carvajal, R. 1979 Rocas Metamorficas y Plutonicas de la Peninsula de Mejillones al Sur de los 23°17' Lat.Sur, y al Oeste de los 70°30' Long, Oeste II Region-Chile Segundo Congreso Geologico Chileno

UPPER CRETACEOUS-LOWER EOCENE POTASSIC VOLCANISM IN AN EXTENSIONAL REGIME IN THE PRECORDILLERA OF COPIAPO, CHILE

Paula C. CORNEJO (1), Constantino MPODOZIS (1), Suzanne M. KAY (2), Andrew J. TOMLINSON (1) and Carlos F. RAMIREZ (1)

(1) Servicio Nacional de Geología y Minería, Casilla 10465, Santiago, Chile.
(2) Department of Geological Sciences, Snee Hall, Cornell University, Ithaca, New York 14853, USA.

RESUMEN: Durante el Cretácico superior al Eoceno inferior (80-55 Ma) se desarrolló, en el norte de Chile (23-28° S), un extenso volcanismo calcoalcalino, potásico, que representa una asociación magmática formada en un régimen tectónico extensional, con posterioridad a la deformación compresiva del Cretácico superior, documentada en la Precordillera de Copiapó.

KEY WORDS: Northern Chile, Lower Tertiary, Synextensional magmatism.

INTRODUCTION

In Northern Chile, occupying large parts of the Central Depression and the andean Precordillera of the Copiapó-Antofagasta Region (23-28° Lat. S) there are extensive exposures of Upper Cretaceous-Lower Eocene volcanic rocks, which were generally interpreted as the relicts of a "Paleogene magmatic arc" (Naranjo y Puig, 1982; Boric et al.,1990). This volcanic association was deposited discordantly over Jurassic - Lower Cretaceous sedimentary and volcanic sequences of extensional intra- and back-arc settings affected by an event of compressive deformation in the Upper Cretaceous (Mpodozis and Ramos, 1990, Mpodozis and Allmendinger, 1992). Recent studies carried out in the Precordillera of Copiapó indicate that this late Cretaceous-Early Eocene event (K-Ar ages between 80 to 52 Ma) is associated with the formation of large collapse calderas in an extensional tectonic setting (Rivera and Mpodozis, 1991).

In this work we discuss the volcanic stratigraphy, geochronology and geochemistry, and the tectonic significance of a part of the volcanic-plutonic complex that is exposed in the region of El Salvador - La Coipa, northeast of Copiapó (Fig. 1).

VOLCANIC STRATIGRAPHY

In the region of El Salvador-La Coipa, the volcanic and intrusive products of this period are represented by two major volcanic cycles that consist of lava flows and explosive pyroclastics deposits of trachybasalt-rhyolite suites, that in some zones, are related to collapse calderas and rhyolitic dome fields, synchronous with more basic volcanic activity. The first cycle corresponds to the Cerro Los Carneros Sequence (80-66 Ma), which is initiated with a section of rhyolitic tuffs (ages K-Ar, 80-70 Ma) intruded by olivine-pyroxene gabbros; continuing, between 70 and 66 Ma, with the effusion of potassic trachybasalts and flow banded, sanidine-biotite trachyandesites, culminating with the eruption of hornblende bearing dacitic pyroclastics (66-63 Ma), intruded by olivine-pyroxene gabbros,

monzodiorites and dacite porphyries (64-60 Ma). The second cycle (Cerro Valiente Volcanic Sequence, 63-55 Ma) ranges from Paleocene to Lower Eocene (63-52 Ma) and includes extensive lava flows of trachybasalt to clinopyroxene (±olivine, biotite) and trachyandesites. During this period, explosive rhyolitic volcanism related to large collapse calderas and extrusive rhyolitic flow-banded domes is associated with extremely welded (reomorphic) ignimbrites and high silica rhyolitic lavas with sanidine and biotite. The distal facies pyroclastics of these domes and calderas interfinger with the trachyandesite and basaltic lavas. The event ends with the intrusion of monzonitic porphyries (55 Ma) and the emission of dacitic lavas, tuffs and hornblende andesites. Collapse and downsag caldera includes the Los Amarillos, El Salvador (60-55 Ma), Sierra San Emilio (62-57 Ma), San Pedro de Cachiyuyo and Sierra Banderita (Fig. 1). The complex of rhyolitic domes includes the Indio Muerto Dome (host rock for the Upper Eocene copper porphyry system of El Salvador) and the flow-banded Potrerillos Dome (60 Ma), formed by glassy rhyolites with sanidine, plagioclase, and scarce biotite.

GEOCHEMISTRY

Both groups include rocks of the high potassium calcalkaline series, although, in the Harker diagrams, potassium and sodium show a large scatter, in spite of the fact that precaution was taken to analyze fresh volcanic and intrusive rocks. Nevertheless, the mineral assemblage of biotite and sanidine, found ubiquitously in the trachyandesites and rhyolites, indicates that effectively the rocks are potassium-rich. The two cycles show similar time-composition trends. The Upper Cretaceous-Paleocene event began with a bimodal association of gabbros and monzogabbros (45-53% SiO_2); trachybasalts and trachyandesites (49-59% SiO_2) associated with high silica rhyolitic tuffs (75-77% SiO_2), followed in later stages, by a large volume of pyroxene-biotite trachyandesites and hornblende dacite tuffs (62-66% SiO_2) filling the initial compositional gap. In the Paleocene-Lower Eocene event a similar trend was found, with large initial volumes of trachybasalts and andesites (50-58 % SiO_2) interstratified with high silica rhyolitic ignimbrites, lavas and domes (70-78 %SiO_2) and late-stage lavas and intrusives of dacitic composition (60-66% SiO_2). Both suites show relatively high contents of Al_2O_3, but the late stage dacites, are enriched in FeO* and TiO_2 and impoverished in MgO and alkalis (tholeithic behavior). The early bimodalism could be explained if the basic rocks have a mantle or lower crustal source, while the rhyolites could have a more significative crustal component. The late dacites could be the result of mixing of crustal and mantle magmatic components and low pressure differentiation-fractionation in high level magma chambers.

DISCUSSION

The Upper Cretaceous - Lower Eocene magmatism already described, represents a large volcanic field (80 km wide) stretching more than 500 km from Copiapó (28°S, Rivera y Mpodozis, 1991) to the Central Depression of the Antofagasta region (23° S, Boric et al., 1990) There, large collapse calderas developed synchronously with volcanic centers erupting extremely fluid trachyitic lavas. The Late Cretaceous - Early Tertiary magmatic successions of northern Chile probably represents a synextensional magmatic suite, similar, in some regards, to the Eocene Basin and Range volcanic province of the western U.S. (Gans et al., 1989), although, in the chilean case, large scale extensional structures controlling the location of the centers have not yet been recognized. Like in the Basin and Range, this episode occurred after a major, Late Cretaceous, crustal thickening contractional deformation episode (Jones et al., 1992) although, in northern Chile, the subsequent extension, doesn't seem to have evolved to the extreme that has been documented for the Basin and Range province.

ACKNOWLEDGEMENTS

This work is part of a proyect supported by the Servicio Nacional de Geología y Minería, Codelco Chile and Fondecyt (Proyect 49/92); and a contribution to Proyect IGCP 345: Andean Lithospheric Evolution.

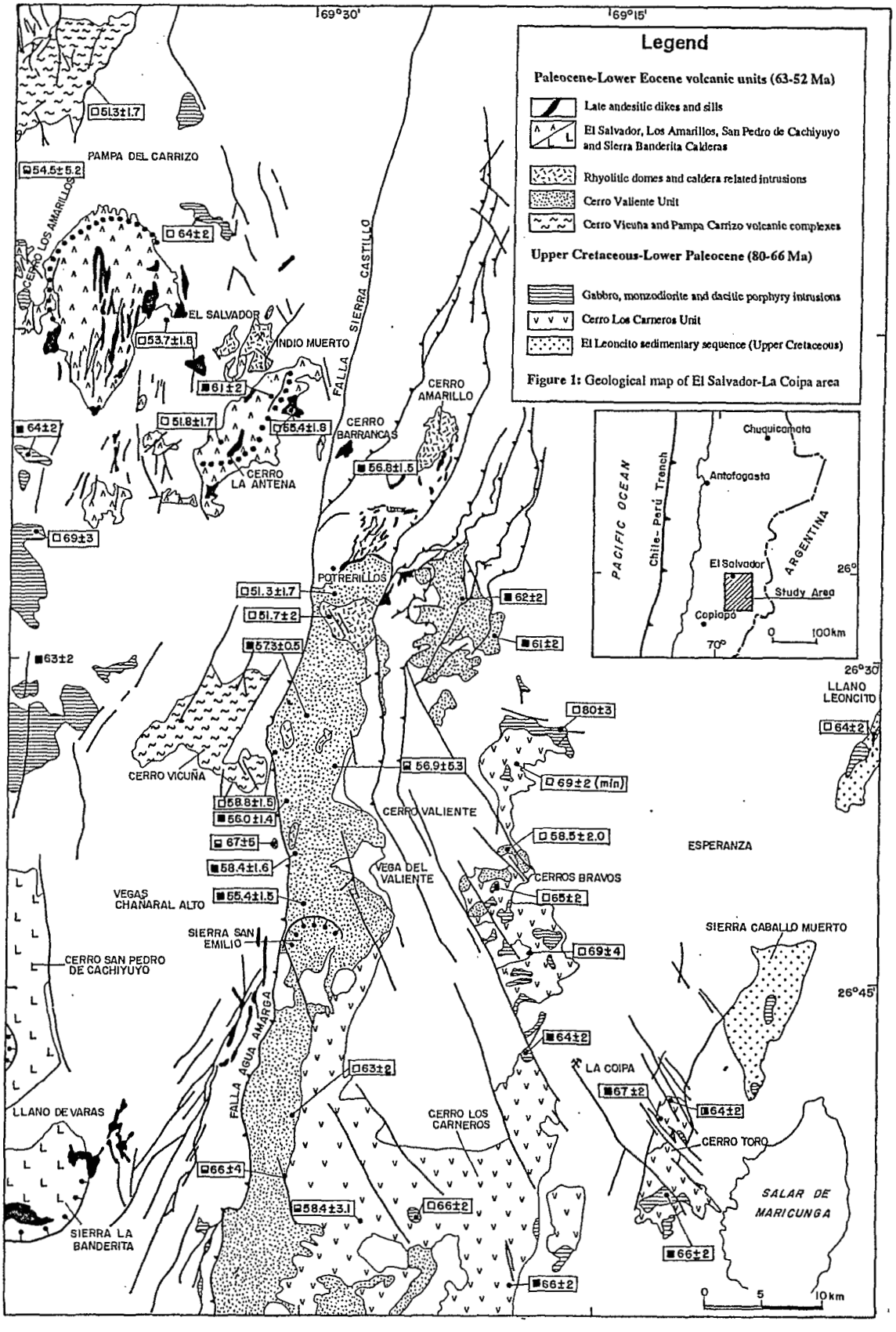
69°30'
69°15'
Legend
Paleocene-Lower Eocene volcanic units (63-52 Ma)
Late andesitic dikes and sills
El Salvador, Los Amarillos, San Pedro de Cachiyuyo and Sierra Banderita Calderas
Rhyolitic domes and caldera related intrusions
Cerro Valiente Unit
Cerro Vicuña and Pampa Carrizo volcanic complexes
Upper Cretaceous-Lower Paleocene (80-66 Ma)
Gabbro, monzodiorite and dacitic porphyry intrusions
Cerro Los Carneros Unit
El Leoncito sedimentary sequence (Upper Cretaceous)
Figure 1: Geological map of El Salvador-La Coipa area
PAMPA DEL CARRIZO
CERRO LOS AMARILLOS
EL SALVADOR
INDIO MUERTO
FALLA SIERRA CASTILLO
CERRO AMARILLO
CERRO BARRANCAS
CERRO LA ANTENA
POTRERILLOS
CERRO VICUÑA
CERRO VALIENTE
VEGA DEL VALIENTE
VEGAS CHANARAL ALTO
SIERRA SAN EMILIO
CERRO SAN PEDRO DE CACHIYUYO
FALLA AGUA AMARGA
LLANO DE VARAS
SIERRA LA BANDERITA
CERRO LOS CARNEROS
CERROS BRAVOS
ESPERANZA
LLANO LEONCITO
SIERRA CABALLO MUERTO
LA COIPA
CERRO TORO
SALAR DE MARICUNGA
26°30'
26°45'
0 5 10km
Chuquicamata
Antofagasta
PACIFIC OCEAN
Chile-Perú Trench
ARGENTINA
El Salvador
Study Area
Copiapo
26°
70°
0 100km

REFERENCES

BORIC, R., DIAZ, F., MAKSAEV, V., 1990, Geología y yacimientos metalíferos de la Región de Antofagasta: Servicio Nacional de Geología y Minería , Boletín N°40, 246 p.

GANS, P.B., MAHOOD, G.A., AND SCHERMER, E., 1989, Synextentional magmatism in the Basin and Range Province; A case study from the eastern Great Basin. Geological Society of America. Special Paper 233.

JONES, C.H., WERNICKE, B.P., FARMER, G.L., WALKER, J.D., COLEMAN, D.S., MCKENNA, L.W., PERRY, F. V., 1992, Variations across and along a mayor continental rift: an interdisciplinary study of the Basin and Range Province, western USA. Tectonophysics, 213:57-96.

MPODOZIS, C., RAMOS, V. A., 1990, The Andes of Chile and Argentina: Circum Pacific Council for Energy and Mineral Resources, Earth Sciences Series, v. 11: 59-90.

NARANJO, J.A., PUIG, A., 1984, Hojas Taltal y Chañaral: Servicio Nacional de Geología y Minería, Carta Geológica de Chile (1:250.000) 140 p.

RIVERA, O., MPODOZIS, C., 1991, Volcanismo explosivo del Terciario inferior en la Precordillera de Copiapó, región de Atacama, Chile: Las Calderas de Lomas Bayas y El Durazno: Congreso Geológico Chileno N° 6 , Actas, p. 213-216, Viña del Mar.

A SIMILAR MAGMA SOURCE FOR IGNIMBRITES AND NON-IGNIMBRITIC LAVAS FROM SOUTH-CENTRAL ANDES.

Bernard DÉRUELLE (1) and Stephen MOORBATH (2)

(1) Laboratoire de Magmatologie et Géochimie Inorganique et Expérimentale, Université Pierre et Marie Curie, 4, Place Jussieu, 75252 Paris Cedex 05, France.
(2) Department of Earth Sciences, University of Oxford, Parks Road, Oxford OX1 3PR, U.K.

RÉSUMÉ. Les ignimbrites contemporaines et avoisinantes des strato-volcans des Andes Centrales du Sud ont des rapports $^{87}Sr/^{86}Sr$ compris entre 0.7062 et 0.7096 semblables à ceux (0.7056 - 0.7089) des laves non-ignimbritiques de ces volcans. La zonation géochimique déjà observée pour les laves non-ignimbritiques, est la même pour les ignimbrites, impliquant bien des sources magmatiques et des processus de genèse communs pour ces deux types de laves.

KEY WORDS : Ignimbrites, Non-ignimbritic lavas, South-Central Andes, $^{87}Sr/^{86}Sr$.

INTRODUCTION

Ten Plio-Quaternary calc-alkaline strato-volcanoes and groups of small volcanoes have been studied in the South Central Andes (SCA), southern part of the Central Volcanic Zone, between latitudes 22°—24°30'S (Déruelle, 1982; Déruelle et al., 1983; Harmon et al., 1984). Field evidence shows that these volcanoes erupted contemporaneously with large ignimbritic lavas. Numerous data on these ignimbrites indicate ages younger than 10.7 Ma (De Silva, 1989a and references therein). Non-ignimbritic lavas were probably produced from mantle-derived magmas subsequently modified by crustal contributions as in the MASH model (Hildreth and Moorbath, 1988). The origin of ignimbrites is still controversial but crustal anatexis is generally invoked to explain the large volumes of ignimbrite erupted (De Silva, 1989b, Francis et al., 1989).

GEOLOGICAL SETTING

Ignimbrites studied here were sampled in adjacent areas around strato-volcanoes and groups of small volcanoes (Fig. 1). They have generally typical ignimbritic texture with Y-shaped shards and abundant glass, and phenocrysts of plagioclase, hornblende, biotite, Fe-Ti oxides, orthopyroxene, K-feldspar, quartz and rare clinopyroxene. Ignimbrites ($58.6<SiO_2$ wt %<73.6) are mostly dacites, rhyolites, and high-silica andesites whilst non-ignimbritic lavas are mostly dacites, andesites and rare rhyolites ($55.2<SiO_2$ wt%<71.2). In SCA, ignimbrite chemical composition (major elements, Rb, Sr, Ba, and transition elements) is similar to that of non-ignimbritic lavas with similar silica content (Déruelle, 1989).

SR-ISOTOPE RESULTS

Sr-isotopes were measured at Oxford on 27 ignimbrites. The ignimbrite Sr-isotope ratios (Fig. 2) range between 0.7062 and 0.7096, similar to that (0.7056—0.7089) of non-ignimbritic lavas (39 samples, Harmon et al., 1984) from the same area. The range of Sierra de Lípez non-ignimbritic lavas (0.7090—0.7149) is clearly distinct from that other volcanoes of SCA. The only analyzed ignimbrite value from Sierra de Lípez (0.7108) falls within this range.

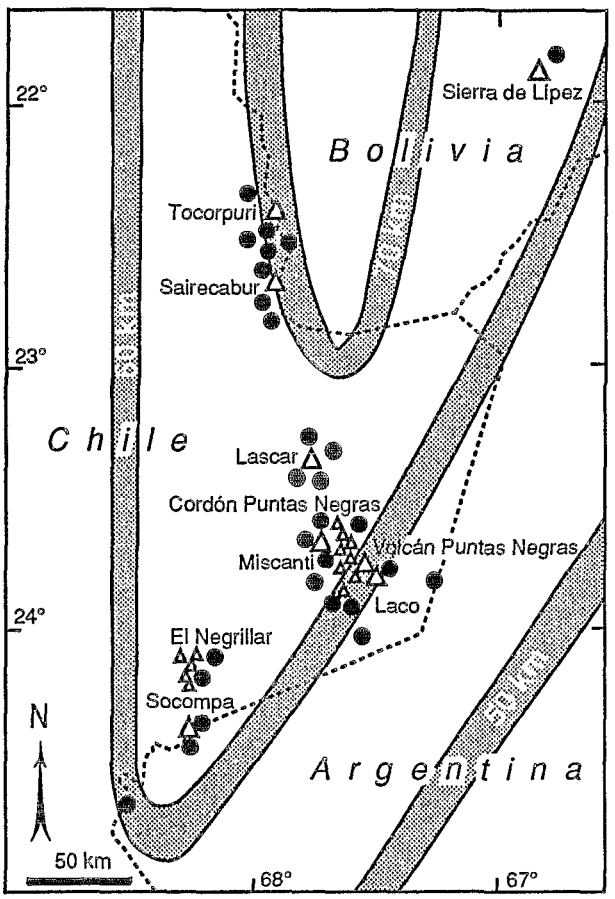

Fig. 1. Localisation of ignimbrites (●) studied in the present work. Thickness of continental crust is after James (1971).

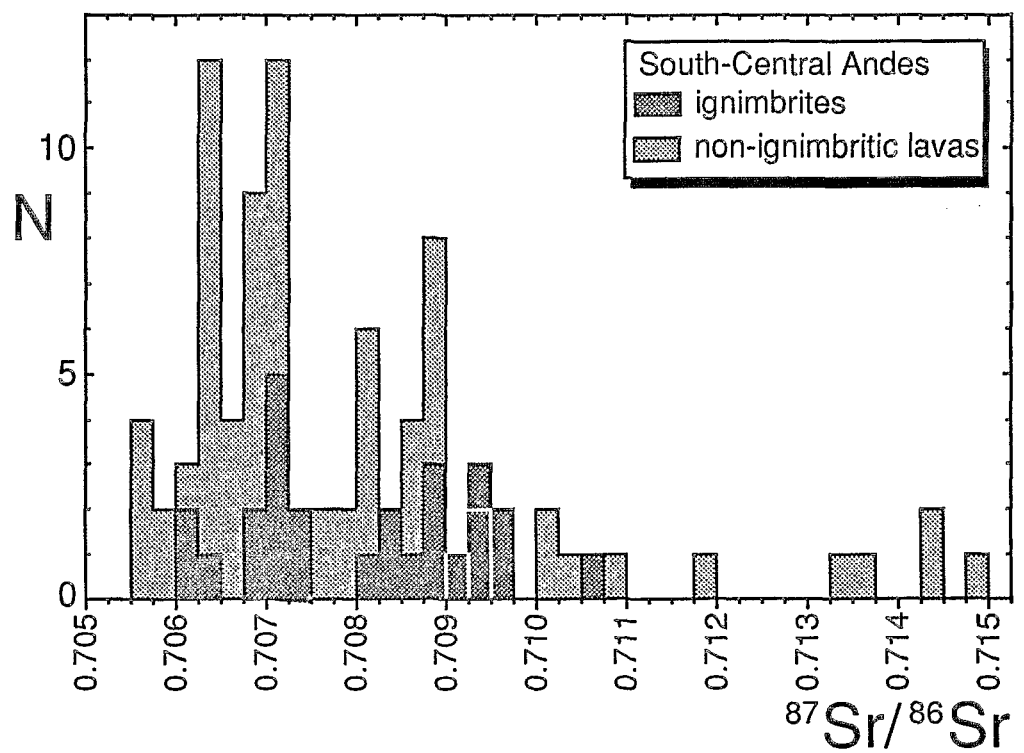

Fig. 2. Histogram of whole-rock $^{87}Sr/^{86}Sr$ ratios for SCA ignimbrites and non-ignimbritic lavas.

DISCUSSION

There is a zonation of Sr-isotope data (Fig. 3) in the five main volcanic areas of the SCA (Sierra de Lípez, Tocorpuri—Sairecabur, Lascar, Miscanti—Cordón Puntas Negras—Volcán Puntas Negras—Laco, and Socompa—El Negrillar). This zonation is neither directly related to crustal thickness nor to depth of

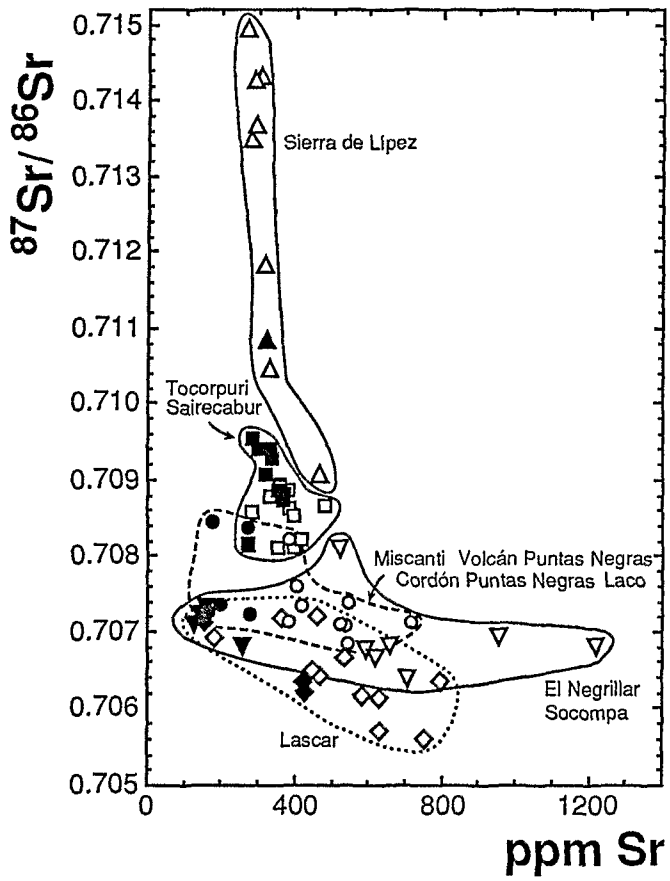

Fig. 3. Sr *vs* $^{87}Sr/^{86}Sr$ plot for SCA ignimbrites (filled symbols, present work) and non-ignimbritic lavas (empty symbols, data after Harmon et al., 1984).

subducted slab (150 km ± 25 km) although geophysical data are imprecise (Fig. 1). There is an overall northwest increase in the ratios. This increase may be related to age and nature of the continental crust, which is Precambrian in Bolivia and Paleozoic in Chile. Similar conclusions have been drawn from isotopic data on non-ignimbritic lavas from the area (17°30'S to 22°S) just to the north of SCA (Wörner et al., 1992). The present work for the first time includes data on ignimbrites.

CONCLUSION

The similarity of Sr-isotope values for ignimbrites and non-ignimbritic lavas from specific volcanic centers of SCA implies a common magmatic source for these two types of lavas. It is concluded that the parental magmas to both ignimbrites and non-ignimbritic lavas resulted from a MASH process between mantle- and crust-derived melts in deep reservoirs at or near the mantle-crust boundary. Further low-pressure crystal fractionation was important during ignimbrite differentiation. The difference between ignimbrites and non-ignimbritic lavas results from the controlling influence of a volatile phase during explosive ignimbritic eruption.

REFERENCES

DÉRUELLE, B., 1982. Petrology of the Plio-Quaternary volcanism of the South-Central Andes. *J. Volcanol. Geothermal Res.* 14, 77-124.

DÉRUELLE, B., 1989. Petrology of ignimbrites of South-Central Andes, *Terra abstracts* 1, 176.

DÉRUELLE, B., HARMON, R.S., and MOORBATH, S., 1983. Combined Sr-O isotope relationships and petrogenesis of Andean volcanics of South America. *Nature* 302, 814-816.

DE SILVA, S.L., 1989a, Geochronology and stratigraphy of the ignimbrites from the 21°30'S to 23°30'S portion of the Central Andes of Northern Chile. *J. Volcanol. Geothermal Res.* 37, 93-131.

DE SILVA, S.L., 1989b, The Altiplano-Puna Volcanic Complex of the Central Andes. *Geology* 127, 1102-106.

FRANCIS, P.W., SPARKS, R.S.J., HAWSKESWORTH, C.J., THORPE, R.S., PYLE, D.M., TAIT, S.R., MANTOVANI, M.S., and McDERMOTT, F., 1989, Petrology and petrogenesis of volcanic rocks of the Cerro Galan Caldera, northwest Argentina. *Geol. Mag.* 126, 515-547.

HARMON, R.S., BARREIRO, B.A., MOORBATH, S., HOEFS, J., FRANCIS, P.W., THORPE, R.S., DÉRUELLE, B., McHUGH, J., and VIGLINO, J.A., 1984. Regional O-, Sr-, and Pb-isotope relationships in late Cenozoic calc-alkaline lavas of the Andean Cordillera. *J. Geol. Soc. London* 141, 803-822.

HILDRETH, W. and MOORBATH, S., 1988. Crustal contributions to arc magmatism in the Andes of Central Chile. *Contrib. Mineral. Petrol.* 98, 455-489.

JAMES, D.E., 1971. Andean crustal and upper mantle structure. J. Geophys. Res. 76, 3246-3271.

WÖRNER, G., MOORBATH, S. and HARMON, R.S., 1992. Andean Cenozoic volcanic centers reflect basement isotopic domains. *Geology* 20, 1103-1106.

PETROGRAPHIC AND GEOCHEMICAL STUDIES OF THE SOUTHWESTERN COLOMBIAN VOLCANOES

Alain DROUX (1), and Michel DELALOYE (1)

(1) Département de Minéralogie, 13 rue des Maraîchers, 1211 Genève 4, Switzerland.

RESUME:
Les volcans actifs plio-quaternaires du sud-ouest de la Colombie sont situés dans la Zone Volcanique Nord (NVZ) des Andes. Ils appartiennent tous à la série calcoalcaline moyennement potassique typique des marges continentales actives. Les laves sont principalement des andésites et des dacites avec des teneurs en silice variant de 53% à 70%. Les analyses pétrographiques et géochimiques montrent que les phénomènes de cristallisation fractionnée, de mélange de magma et de contamination crustale sont impliqués à divers degrés dans la génèse des laves des volcans colombiens.

KEY WORDS: Volcanology, geochemistry, geochronology, Neogene, Colombia.

INTRODUCTION:

This publication is a comparative of petrographical, geochemical and geochronological analysis of six quaternary volcanoes of the Northern Volcanic Zone of southwestern Colombia (0-3°N): Puracé, Doña Juana, Galeras, Azufral, Cumbal and Chiles. The Colombian volcanic arc is the less studied volcanic zone of the Andes despite the fact that some of the volcanoes, which lie in it, are ones of the most actives in the Andes, i.e. Nevado del Ruiz, Puracé and Galeras.

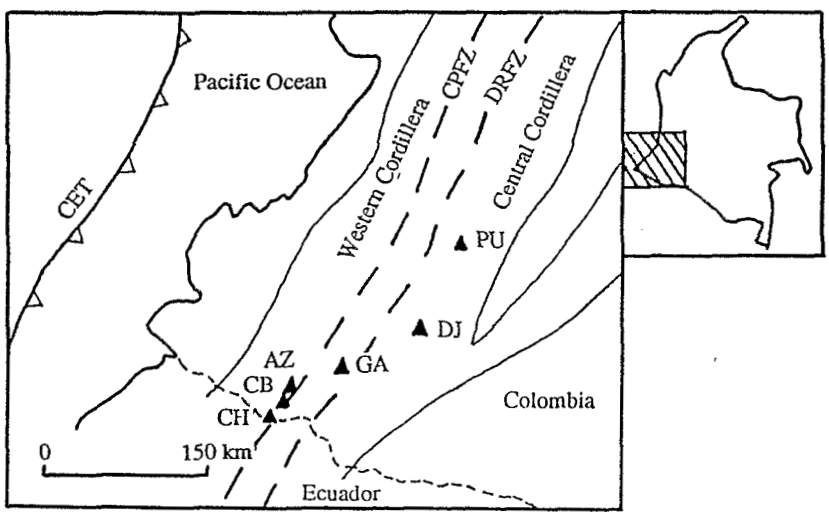

Figure 1: Location map of the studied area. Solid triangles indicate the active volcanoes. PU: Puracé; DJ: Doña Juana; GA: Galeras; AZ :Azufral; CB: Cumbal; CH: Chiles; CPFZ: Cauca-Patía Fault Zone; DRFZ: Dolores-Romeral Fault Zone; CET: Colombia-Ecuador Trench.

GEOLOGICAL SETTING:

The main line of active volcanoes of Colombia strike NNE. It lies about 300 Km east of the Colombia-Ecuador Trench, the underthrusting of the Nazca plate beneath South America. The recent volcanoes are located 150 Km above a Benioff Zone which dips eastward at 25°-30°, as defined by the work of Barazangi and Isacks (1976). The crust is 40 Km in thickness and is younger than Mesozoic in age and it includes a large oceanic component (ocean floor) west of the Dolores-Romeral mega-shear zone in the Western Cordillera of Colombia (Marriner and Millward; 1984). East of this fault zone, in the Central and Eastern cordilleras, the crust is predominantly of pre-Cretaceous igneous and metamorphic rocks type. The Late Pliocene-Holocene volcanoes from the Central and Western cordilleras are situated either on the Cauca-Patía or on the Dolores-Romeral fault systems which represent the main active fault zones of the area. Both systems are sub-parallel, oriented NE-SW, and run over more than 800 Km through Ecuador and Colombia. The volcanoes belong to the medium-potassic calcalkaline serie typical of active continental margins. The lavas are predominantly andesites to dacites with lesser amount of basalts and rhyolites, and range from 53% to 70% SiO2. The andesitic lavas are highly porphyritic with phenocrysts content as high as 25-30%. The groundmass texture is microlitic-intergranular to hyalopilitic in the more siliceous rocks. Phenocrysts include plagioclase, clinopyroxene and orthopyroxene found as groundmass as well. The basalts and basaltic andesites are less porphyritic than the acidic andesites and usually show a well preserved flow structure. The olivine is rare and partially to completely altered or replaced by iddingsite/serpentinite.

CONCLUSIONS:

The nature and the age of the downgoing oceanic plate, the geometry of subduction and the thickness of the continental crust remain nearly constant in the segment studied (Cauca Segment; Pennington, 1981). In contrast, the chemical composition of the continental crust vary greatly from west to east reflecting the chemical variation of the lavas along the same direction.

The petrographic desequilibrium assemblages and the coexistence of normal and reverse zoning in the phenocrysts of plagioclases and pyroxenes, within a single sample, suggest that fractional crystallization surimposed by various stages of magma mixing has occured in the magmatic sequences of each volcano with important differences among them. For the Puracé, the northernmost studied volcano, the K-group elements (K, Ba, Rb, Sr) silica-normallized values are higher than those for the southernmost volcanoes. Rb content decrease twofold from the Puracé (north) to the Cumbal (south), instead the distance to the Trench and the Benioff zone top remain constant. It is important to note that the Puracé shows the lowest K/Rb normallized ratio (near the bulk crust value) and the highest K (fig. 2) and Rb content which is undoubtly due to a high sialic crustal contribution (Hildreth and Moorbath, 1988). Although, the high variability of alkalies and Ba content within nearby southern volcanoes (20-30 Km interval) could also reflect heterogeneous continental crust composition related to the wide zone affected by the tectonic mélange due to both the Cauca-Patía and the Dolores-Romeral fault zones. The Puracé, located 30 Km east of the latter, lie above a quiet homogeneous metamorphic crust.

This northward increase of K-group elements of the calcalkaline lavas is therefore attributed to the High contribution of the siliceous "old crust" (pre-Mesozoic) in the north of the studied area, compared to the younger oceanic basement of the southernmost volcanoes.

The REE patterns show strong relative enrichment in the LREE (fig. 3) and have a high normallized Ce/Yb ratio for the Puracé and Doña Juana volcanoes which are located on the "siliceous" metamorphic crust of the Central Cordillera. The HREE content of mafic to intermediate lavas is nearly constant for all volcanoes, what is expected for calcalkaline suites in active continental margin environment (Gill, 1981).

According to the geochemical data, it can be concluded that the contribution of crustal material is more important in the magmatic processes on the volcanoes located above the sialic crust of the Central Cordillera than those situated above the oceanic crust of the Western Cordillera, west of the Dolores-Romeral fault zone.

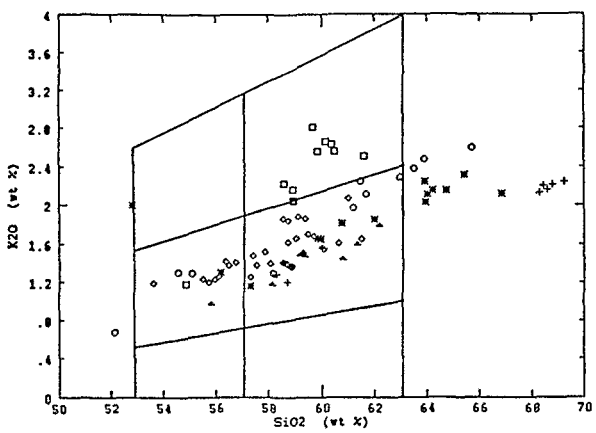

Figure 2: K2O content vs SiO2 of the active southwestern Colombian volcanoes (modified from Gill, 1981).

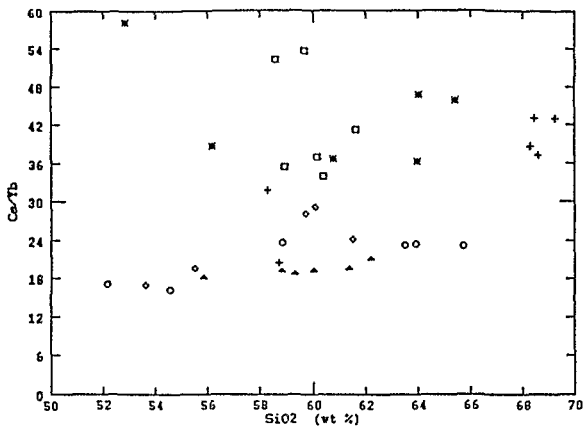

Figure 3: Ce/Yb ratio vs SiO2.

Symbols:
square: Puracé; star: Doña Juana; diamond: Galeras; cross: Azufral; triangle: Cumbal; circle: Chiles.

REFERENCES:

Barazangi, M., Isacks, B.L.: Geology, volume 4, p. 686-692, 1976.
Gill, J.: Springer-Verlag, Berlin Heildelberg New York, 390 p., 1981.
Hildreth, W., Moorbath, S.: Contrib. Mineral. Petrol., volume 98, p.455-489, 1988
Marriner, G.F., Millward, D.: Journal of Geological Society, London, volume 141, p. 473-486, 1984.
Pennington, W.D.: Journal of Geophysical Research, volume 86, NO.B11, p. 10753-10770, 1981.

Petrology, Metamorphic History and Structure of El Oro Ophiolitic Complex, Ecuador

Pablo DUQUE (1)

(1) Departamento de Geología, Escuela Politécnica Nacional, Casilla 17-01-2759, Quito, Ecuador

RESUMEN: El Complejo Ofiolítico El Oro, localizado en la parte SW del Ecuador, está constituido mayormente por rocas metamórficas de alta presión (eclogitas, esquistos pelíticos, esquistos azules, esquistos verdes). Sus condiciones de formación son 9 kb y 465°C. Se formó por procesos asociados con subducción bajo un grueso prisma acrecionario. La trayectoria P-T de subducción fué 45.41°C/kb. Su edad es 132Ma y fué intruido en rocas Jurásicas. Es parte de una extensa zona de melange.

KEY WORDS: Ophiolitic complex, blueschist, eclogite, accretionary prism, melange, P-T subduction path.

INTRODUCTION

The east-west striking rocks of the El Oro province in southwest Ecuador form the northern part of the allochthonous Amotape - Tahuín block (Mégard, 1989). Recent geological mapping of the area (Aspden et al., 1993) interprets these rocks to form part of an accretionary prism complex, which contains elements of both 'continental' and 'oceanic' affinity. The rocks of the latter affinity include the El Oro Ophiolitic complex, which is ca. 45 km long and 5 km wide and is bounded to the north and south by the Palenque - El Guayabo and the Zanjón - Naranjo faults, respectively. The El Oro Ophiolitic complex comprises 3 units: the Raspas, the Panupali and the El Toro. The Raspas unit consists of pelitic schists, blueschists and eclogites, which were the first high-pressure rocks to be reported from the Andes (Duque, 1975, 1979, 1993; Feininger, 1980); the Panupali unit comprises greenschists and the El Toro unit corresponds to a variably serpentinized harzburgites. There are no transitions between eclogite and blueschist and Panupali greenschist. Greenschists within the Raspas unit are scarce and some of them show evidences of retrograde metamorphism. Chemical and mineralogical compositions are typical of subduction zone oceanic settings and can be classified as ophiolitic assemblages.

PETROLOGY

Self consistent results among numerous geothermobarometers applied to different Raspas rocks give a close range of peak metamorphic conditions (fig. 1). The Ellis-Green geothermometer (1979) based on calibrations for the exchange reaction clinopyroxene - garnet was used on rocks of eclogitic affinity. Temperature values were calculated in the range 5 - 15 kb and a best fitted curve was obtained by least - squares regression. The geobarometer plagioclase - clinopyroxene - quartz (Holland, 1980), using an ideal molecular solid solution for plagioclase and pyroxene, was applied on eclogite and the barometer garnet - plagioclase - kyanite - quartz, modified after Ghent et al. (1979), was used on pelitic schist. The best values obtained for the physical conditions of metamorphism in the Raspas unit rocks were 9 ± 0.5 kb at 465 ± 30°C. These results indicate that the high-pressure rocks recrystallized under equilibrium conditions within the Albite - Tremolite P-T field. Furthermore, they suggest that the Panupali greenschists belong to the high - pressure rocks and are products of prograde metamorphism.

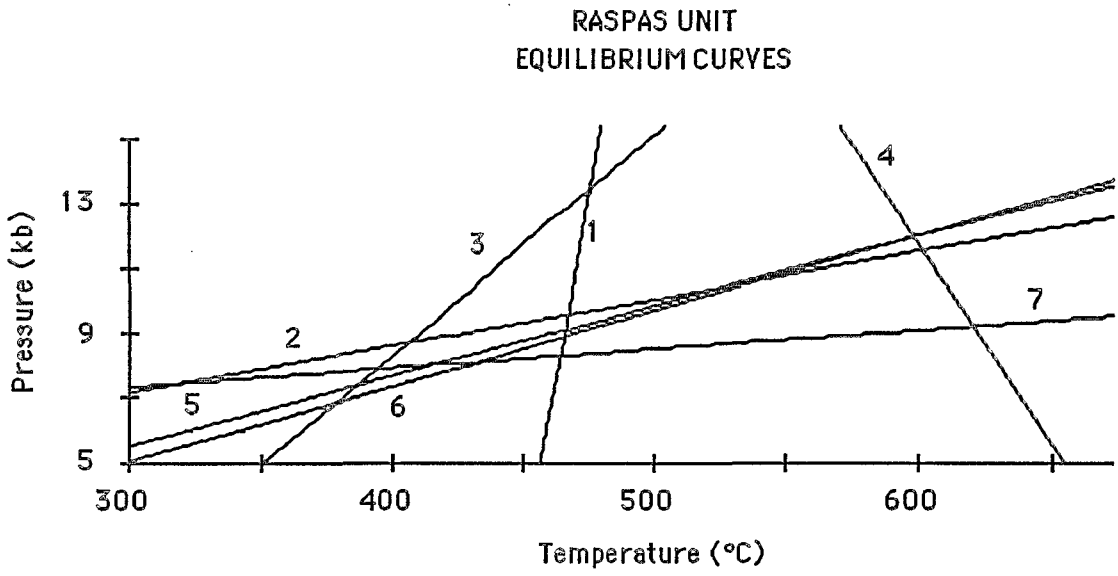

1. Ellis-Green geothermometer
2. calcite = aragonite
3. Lw+Omph=Zo+pa+qz
4. chl+qz=Tc+ky
5. Plg(Ab_{93})=px(Jd_{34})+qz [PD311A1]
6. ga+ky+qz=Plg [PD156A]
7. ga+ru=Ilm+ky+qz

Fig.1: Equilibrium reactions applied in the Raspas unit to obtain its physical conditions of metamorphism (Lw=lawsonite, Omph=omphacite, Zo=zoisite, pa=paragonite, qz= quartz, chl=chlorite, Tc=talc, ky=kyanite, Plg=plagioclase, Ab=albite, ga=garnet, px=pyroxene, Jd=jadeite, ru=rutile, Ilm=ilmenite. PD311A1 and PD156A are samples in which the respective reaction was applied).

Whole-rock XRF analyses of Panupali greenschists and microprobe analyses of major phases in Raspas blueschists and eclogites, when compared by least-squares modeling, prove the bulk-rock chemistry to be essentially the same for all three lithologies. Oxygen fugacity and/or small compositional differences could be major influencing factors in the formation of either one of the rocks under the same metamorphic conditions.

METAMORPHIC HISTORY AND STRUCTURE

It is well established the connection between blueschist facies metamorphism and the low temperature - high pressure conditions encountered in subduction zones. Shreve and Cloos (1986) presented a thermal model in which blueschist facies conditions are encountered by the subduction slab under a thick accretionary prism. However, the return of the rocks to the surface is not well understood.

In order to develop a better understanding of the metamorphic history and of the interactions between tectonic and metamorphic processes, a P - T path of metamorphism was calculated using the analysis of chemical zoning in eclogite garnets. The estimated P-T path is 45.41°C/kb. The zonation scheme (fig. 2) shows that in the recrystallization process, heat was produced during compression, which is characteristic of subduction zones and, in general, of terranes in which cold rocks are emplaced over hot rocks.

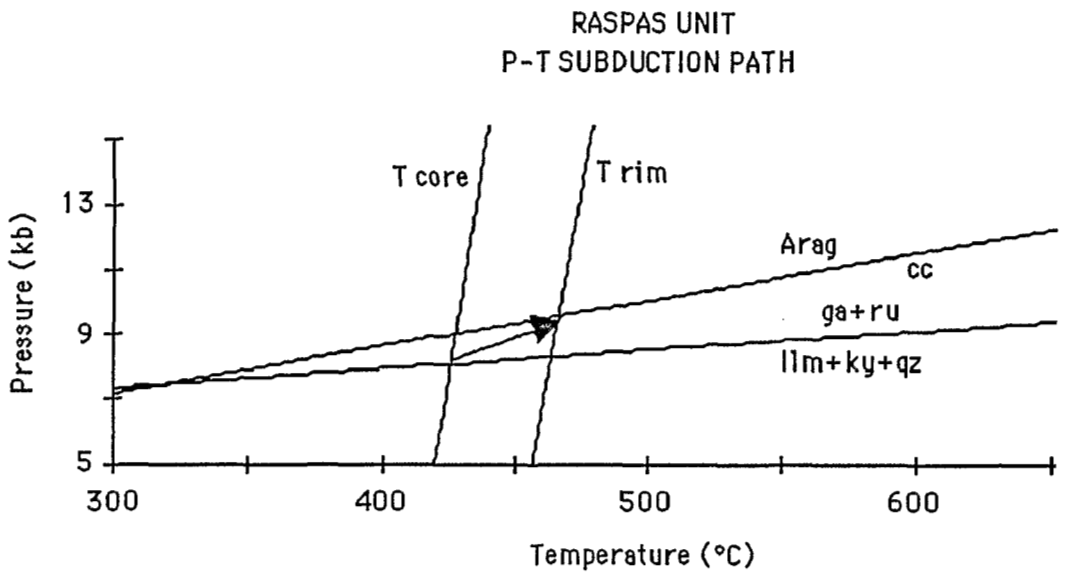

Fig.2: The arrow shows the possible P-T Subduction Path followed during the Raspas Metamorphism.

Duque (1975) estimates an average density of 3.03 gr/cm^3 for the overlaying rocks (mainly amphibolites metamorphosed in the high temperature / low pressure Abukuma type facies series). Using that figure, the formation conditions should be reached at 30 km depth under a thermal gradient of 13.8°C/km. That gradient belongs to a high - pressure facies series.

According to Ernst (1972), there is a secular change of subduction geotherms with time. The geotherms of higher pressure (ca. 12°C/km) correspond to late Cretaceous. If this is true, the Raspas geotherm suggests that the age of 132 ± 5 Ma (Feininger, 1980) is the age of the metamorphic event.

CONCLUSIONS

The high - pressure rocks of El Oro Ophiolitic Complex constitute an allochthonous block that recrystallized under the same metamorphic conditions in an active subduction zone. Upon cessation of the tectonic burial process that created the blueschist facies con-

ditions (subduction), the package was carried upward by the partly serpentinized El Toro unit through the denser and older host rocks. The uplift had to be fast in order to preserve the high - pressure mineral assemblages and could involve complicated processes that occur in accretionary wedges. The age of the uplift could be similar to that of metamorphism. The emplacement of the El Oro Ophiolitic complex produced strong tectonism in the regional rocks that apparently are part of an extensive melange zone which can be traced throughout the Northern Andes (Aspden et al., 1993).

REFERENCES

Aspden, J., Bonilla, W., Duque, P., 1993. Final report of the El Oro Metamorphic Province Subproject. *Unpublished Report*, B.G.S. - CODIGEM, Quito, 115p.

Duque, P., 1975. Petrogénesis de unas rocas metamórficas de alta presión en la Provincia de El Oro. *Unpublished Thesis* , E.P.N., Quito, 66p.

_____, 1979. Rocas metamórficas de alta presión de la Provincia de El Oro, Ecuador. *First Ecuadorian Geological Congress* ,Mem. I, 23-60.

_____, 1992. Condiciones de formación de las rocas metamórficas de alta presión de la Formación Raspas, *Bol. Geol. Ecuat.*, 3, 1, 63-78.

Ellis, D.J. & Green, D.H., 1979. An experimental study of the effect of Ca upon garnet -clinopyroxene Fe-Mg exchange equilibria. *Contrib. Mineral. Petrol.*, 71, 13-22.

Ernst, W.G., 1972. Occurrence and mineralogical evolution of blueschist belts with time. *Amer. Jour. Sci.*, 272, 657-68.

Feininger, T., 1978. Geologic Map of Western El Oro Province, scale 1:50,000., *E.P.N., Quito.*

_____, 1980. Eclogite and related high-pressure regional metamorphic rocks from the Andes of Ecuador. *Jour.Petrol.*, 21, 107-40.

Ghent, E.D, Robbins, D.B. & Stout, M.Z., 1979. Geothermometry, geobarometry, and fluid compositions of metamorphosed calc-silicates and pelites, Mica Creek, British Columbia. *Amer. Mineral.*, 64, 874-85.

Holland, T.J.B., 1980. The reaction albite = jadeite + quartz determined experimentally in the range 600-1200°C. *Amer. Mineral.*, 65, 129-34.

Mégard, F., 1989. The evolution of the Pacific Ocean Margin in South America north of Arica Elbow (18°S), In AVRAHAM, Z. B. (ed.) *The Evolution of the Pacific Ocean Margins, Claredon Press, Oxford*, 208-30.

Shreve, R.L., Cloos, M., 1986. Dynamics of Sediment Subduction, Melange Formation, and Prism Accretion. *Jour. Geophys. Res.*, 91, 10229-45.

MIOCENE VOLCANIC CENTERS IN THE SOUTHERN ALTIPLANO OF BOLIVIA. THE CERRO MOROKHO & CERRO BONETE AREA (SUR LIPEZ).

Michel FORNARI [1,2], Luis POZZO [2], Pierre SOLER [1,2], Laurent BAILLY [3]
Jacques LEROY [3] and Michel G. BONHOMME [4]

(1) ORSTOM, UR1H, CP 9214 La Paz - Bolivia.
(2) Instituto de Investigaciones Geológicas, UMSA, CP 12198, La Paz - Bolivia
(3) Université NANCY I. Laboratoire d'Etude des Systèmes Hydrothermaux BP 239, 54506 Vandoeuvre Cedex - France
(4) Institut Dolomieu et URA CNRS 69, Univbersité Joseph Fourioer, 15 rue Maurice Gignoux, 38031 Grenoble Cedex - France.

RESUMEN: En la terminación SE del Altiplano boliviano (22°S - 67°W), encima de las capas rojas del Oligoceno (Fm. San Vicente), la actividad magmática empieza por un magmatismo básico de afinidad alcalina (andesitas basalticas y micro-gabbros) de edad Oligoceno superior - Mioceno inferior (Fm Rondal). Está seguida por una etapa magmática que genera rocas de composición intermedia a ácida y de afinidad calco-alcalina; se han identificado varios centros volcánicos, entre los cuales los cerros Bonete, Morokho, Lípez (con actividad Mioceno inferior a Medio), y el cerro Panizo (con actividad Mioceno superior a Plioceno). La mayoría de los productos son de composición dacítica, de carácter potásico y peraluminoso (corindon normativo, presencia de granate). Por su posición tras-arco este magmatismo puede representar un equivalente más antiguo de los Frailes y Morococala.

KEY WORDS: Altiplano, Bolivia, Magmatism, Miocene.

INTRODUCTION

In the Southeastern part of the Bolivian Altiplano (25°S-67°W), the deposition of the Oligocene continental red beds (San Vicente Fm.) has been followed by basic magmatic activity which in turn is followed by intermediate to acid magmatism. Several early to mid-Miocene volcanic centers were recognized, e.g. cerro Bonete, cerro Morokho, cerro Lipez (fig.1) whereas a younger center is formed by the cerro Panizo "caldera", a 40 km diameter ignimbritic plateau around a 10-15 km cluster of dacitic lava domes of upper Miocene age (7.87 Ma, $^{40}Ar/^{39}Ar$ date of pumice biotite, 6.1±0.2 Ma K/Ar whole rock date on dacitic lava of the central dome complex, Ort, 1991). Magmatic activity expands to Plio-Quaternary times. In this abstract we report some features of early to mid- Miocene magmatism.

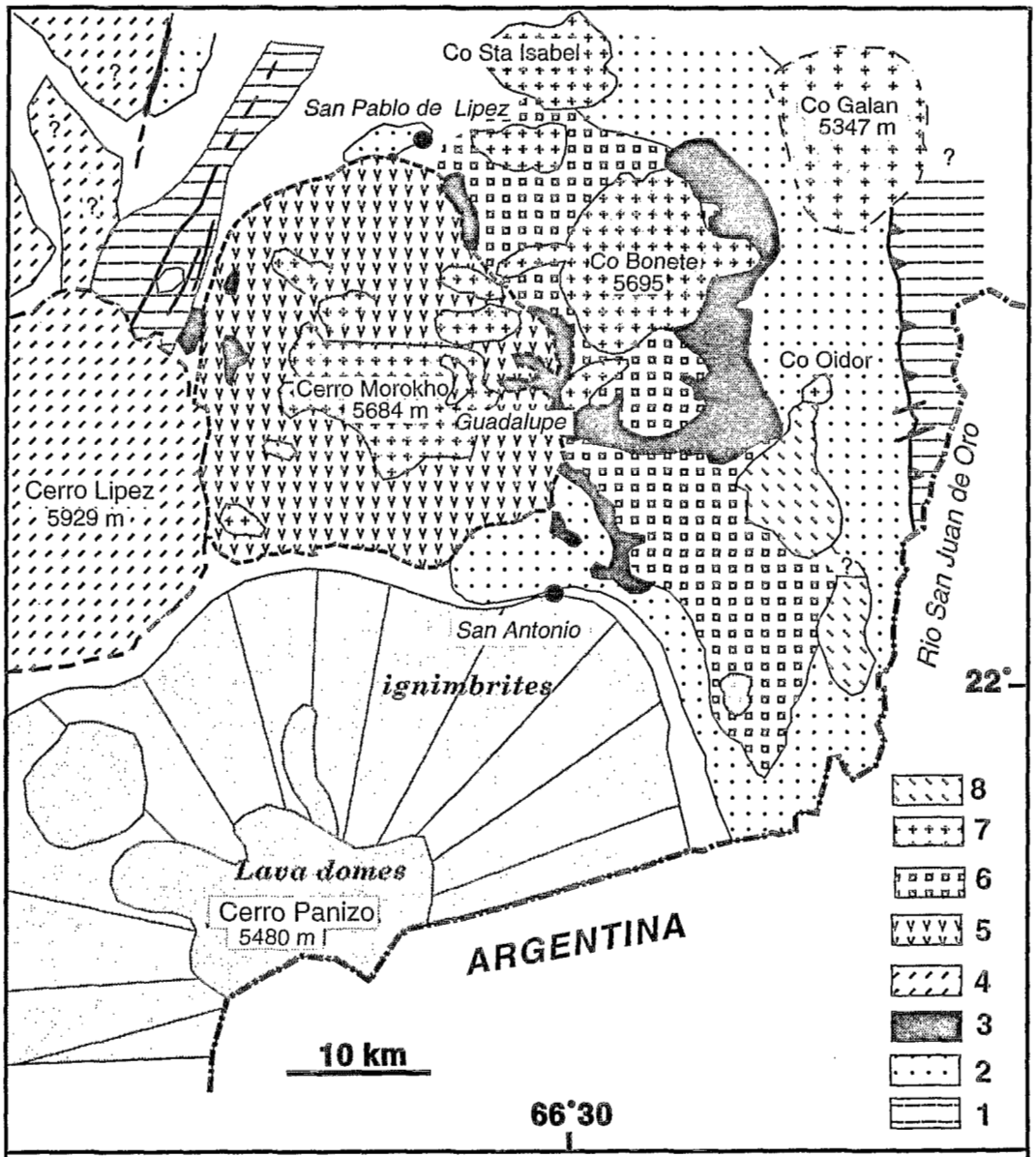

1: Lower Paleozoic shales, 2: Oligocene San Vicente Fm (conglomerates)
3: Rondal Lavas, 4: Co Lipez tuffs and Lavas, 5: Co Morokho tuffs and lavas
6: Co Bonete tuffs and lavas, 7: tuffs and lavas from others volcanics centers
8: Tuffs from undetermined vent (above Bonete tuffs).

Fig. 1: map of the Guadalupe area showing the major volcanic centers.

TABLE 1: K/Ar analytical data and calculated ages, by M. G. Bonhomme, University of Grenoble.

sample #, type of rock	Location	material analysed	K2O (%)	^{40}Ar rad (%)	^{40}Ar rad (nl/g)	Age Ma ± 2 σ
S5, basalt (Rondal)	Qda Herreria	WR	3.72	38.3	2.66	22.1 ± 0.6
S8, ignimbrite	Coripampa	Biotite	8.89	56.7	4.43	15.4 ± 0.5
2210-3, ignimbrite	Coripampa	Biotite	8.89	69.8	4.40	15.3 ± 0.5
S17, ignimbrite	Co Pabellon	Biotite	9.13	71.1	4.39	14.8 ± 0.5

ALKALINE MAGMATISM.

The volcanic activity began with basic magmatic products (mainly basalt-andesitic and micro-gabbroic lava flows, sills, dykes), known as the Rondal Fm. They contains phenocrysts (1-3.5 mm) of forsterite (up to 14%) frequently altered to iddinngsite. Augite phenocrysts (up to 12%) form millimetric automorphic sections and groups of crystals; minor amounts (2.5%) of small corroded orthopyroxenes are present. The matrix contains mainly microlites of plagioclases (An 81-64). Sometimes the dykes contain biotite and amphibole phenocrysts.

The Rondal lavas display high K content (fig. 2) and an alkaline affinity.

A basaltic dyke (sample S5) of the Guadalupe area gave a whole rock K/Ar age of 22.1± 0.6 Ma. Kussmaull et al. (1975) report an age of 23.5 Ma in the same area. Similar lavas in the Tupiza basin (about 60 km ENE of Guadalupe) have been dated at 22.7 ± 0.6 Ma (Hérail et al., this volume).

This magmatism is correlated with the Julaca and Tambillo lavas that form a nearly NS belt of outcrops in the western part of the Altiplano and in the Cordillera Occidental. This magmatism would be related to trans-tensional crustal fractures (see Soler and Jimenez, this volume).

ACID PERALUMINOUS VOLCANISM.

This alkaline episode is followed by a stage of erosion, with a rough paleo-topography which is partially buried by the products of high-K calc- alkaline magmatism. In the studied area, two volcanic centers were investigated (cerros Morokho and Bonete).

The volcanic activity began with an explosive stage represented by voluminous pyroclastics flows and minor ash-fall deposits, sometimes accompanied with their "co-ignimbrite" breccias deposits near the vent. The total thickness of these deposits is about 700 m. The different pyroclastic units defined in the field show variations in thickness, color, abundance and size of pumices and lithoclasts at the scale of the outcrop and in thin section; generally they show low welding grade and the pumices are uncollapsed. They are generally crystal rich (up to 40%), with fragmented and automorphic plagioclases (An40-55), biotite and quartz with minor zircon, apatite, sphene, opaque minerals. Generally they have a dacitic composition (fig 2). Biotite from pumices from the dacitic ignimbritic units from the cerro Bonete gave K-Ar ages around 15 Ma. (table 1).

The main stage of pyroclastic emission is followed by lava domes, flow breccias, and lava flows. This general sketch shows local variations in each centers and in particular pyroclastic flows deposit can be present in the late stages. The rocks are generally similar withstanding they crop out in several stocks and domes; they show a porphyritic texture with plagioclase, biotite and quartz phenocrysts up to 5 mm in length, and in some cases microphenocryst of amphibole. The quartz crystals show rounded and engulfed shapes, plagioclases are zoned (inner part An50-border An30-45) and with thin reaction rims. Minor minerals are apatite, zircon, garnet, rutile and titano-magnetite. The matrix forms about 65% of the rocks; it contains small and generally xenomorphic quartz (50-60%), microlites of automorphic plagioclases, more calcic than the phenocrysts, and very small K feldspar. In spite that they are broadly similar, these rocks present small geochemical differences and represent different magma batches. K/Ar age determinations of these events are in progress.

One characteristic feature of these rocks is their peraluminous nature (presence of garnet, normative corindon (1-3%), high A/KCN ratios - fig 3). Another one is the relatively restricted range of composition (dacitic) of the more voluminous outcrops.

This back arc magmatic activity belongs to a mid-Miocene belt which extends all along the Bolivian Orocline (Soler and Jimenez, this volume) and would represent an older equivalent of the voluminous volcanism of Los Frailes and Morococala.

REFERENCES.

CARLIER G., SOLER P., FORNARI M., & HÉRAIL G., 1992. Orígen y significado tectónico del volcanismo shoshonítico neógeno a cuaternario en los Andes. X Congreso Geol. Boliviano, La Paz. p.173-175.

FORNARI M., HÉRAIL G., POZZO L., & VISCARRA G., 1991. Los yacimientos de oro de los Lipez (Bolivia). Tomo I: Estratigrafía y dinámica de emplazamiento de las rocas volcánicas del area de Guadalupe. Mission ORSTOM Bolivie, La Paz , Rapport n°19, 28p.

HÉRAIL G., OLLER J., BABY P., BLANCO J., BONHOMME M.G., & SOLER P., 1993. The Tupiza, Nazareño, Estarca bassins (Bolivia): strike-slip faulting and thrusting during the Cenozoic evolution of the southern branch of the Bolivian Orocline. This volume.

KUSSMAUL S., JORDAN L., & PLOSKONKA E., 1975. Isotopic age of Tertiary volcanic rocks of SW-Bolivia. Geol Jb, B14, p.111-120.

ORT M. H., 1991. Eruptive dynamics and magmatic processes of the Cerro Panizos, Central Andes, Ph. D. University of California Santa Barbara, 474p.

POZZO I. L., 1991. Geología y características del oro aluvial en ambiente volcánico, región de Guadalupe, Prov. Sud Lipez, Departamento de Potosi. Un método para localizar posibles mineralizaciones primarias. *Thesis UMSA*. La Paz, 92p. unpub.

SOLER P., & JIMENEZ N., 1993. Magmatic constrains upon the evolution of the Bolivian Andes since late Oligocene times. This volume.

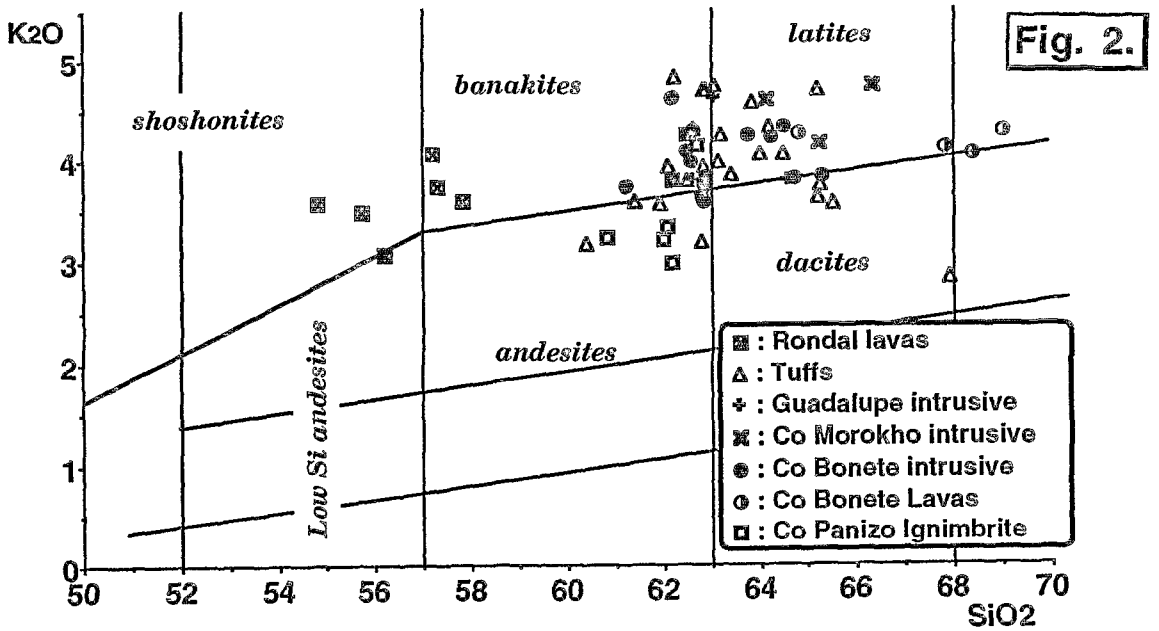

Fig. 2.

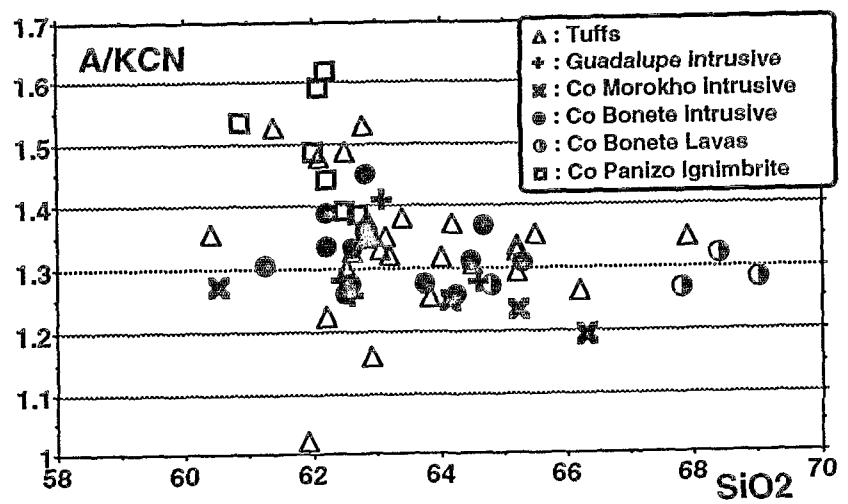

Fig. 3.

BASIC MAGMATISM IN A MID-TERTIARY TRANSTENSIONAL BASIN, ISLA MAGDALENA, AYSEN, CHILE.

F. HERVÉ (1), R.J. PANKHURST (2), M. SUÁREZ (3) and R. DE LA CRUZ (3).

(1) Departamento de Geología, Universidad de Chile, Casilla 13518, Correo 21, Santiago, Chile.
(2) British Antarctic Survey, c/o NERC Isotope Geosciences Laboratory, Keyworth, Nottingham NG12 5GG, U.K.
(3) Servicio Nacional de Geología y Minería, Casilla 14265, Av. Santa Maria 0104, Santiago, Chile.

RESUMEN: El complejo igneo basico de Isla Magdalena, de probable edad Terciario medio, está constuido por metabasaltos, asociados a un enjambre de diques dolerítico y escasos gabros. Los diques se emplazaron en el basamento metamórfico paleozóico y en la serie volcano-sedimentária marina que contiene los basaltos, antes de su litificación. Se sugiere que estos eventos ocurrieren en una cuenca extensional asociada a movimientos de rumbo durante subducción oblícua, la que fue cerrada cuando esta se hizo más ortogonal.

KEY WORDS: Patagonia, Basic volcanism, Tertiary, Strike-slip, Transtension.

INTRODUCTION

Isla Magdalena is an island ca. 50x50 km, in the North Patagonian Andes. It is located immediately west of the main branch of the Liquiñe-Ofqui fault zone, a major coast-parallel strike-slip lineament (Fig.1), north of the Taitao triple junction. It is the site of a basic igneous complex of widespread pillow metabasalts, an associated dolerite dyke swarm, and occasional gabbros. The presence and nature of such rocks is critical to the understanding of the teconic environment.

GEOLOGICAL SETTING AND RESULTS

This complex is developed, at least in part, on older continental crust. The metamorphic basement rocks comprise mica-schists and greenschists, Rb-Sr analyses of which have yield a rough errorchron age of 467±55 Ma. This is significantly older than previous Rb-Sr ages obtained from the accretionary complex in western Aysen, although it is within error of its Devonian age of sedimentation inferred from sparse fossil evidence.

The dolerite dykes that intrude this basement have individual thicknesses of 1-3 m and a strongly preferred NNE-SSW orientation. In some western outcrops the dyke swarm is intensely developed, with intervening schist screens only slightly wider than the dykes themselves. The pillow metabasalts occur within a marine turbidite sequence mainly composed of alternating sandstone-shale horizons, cherts and

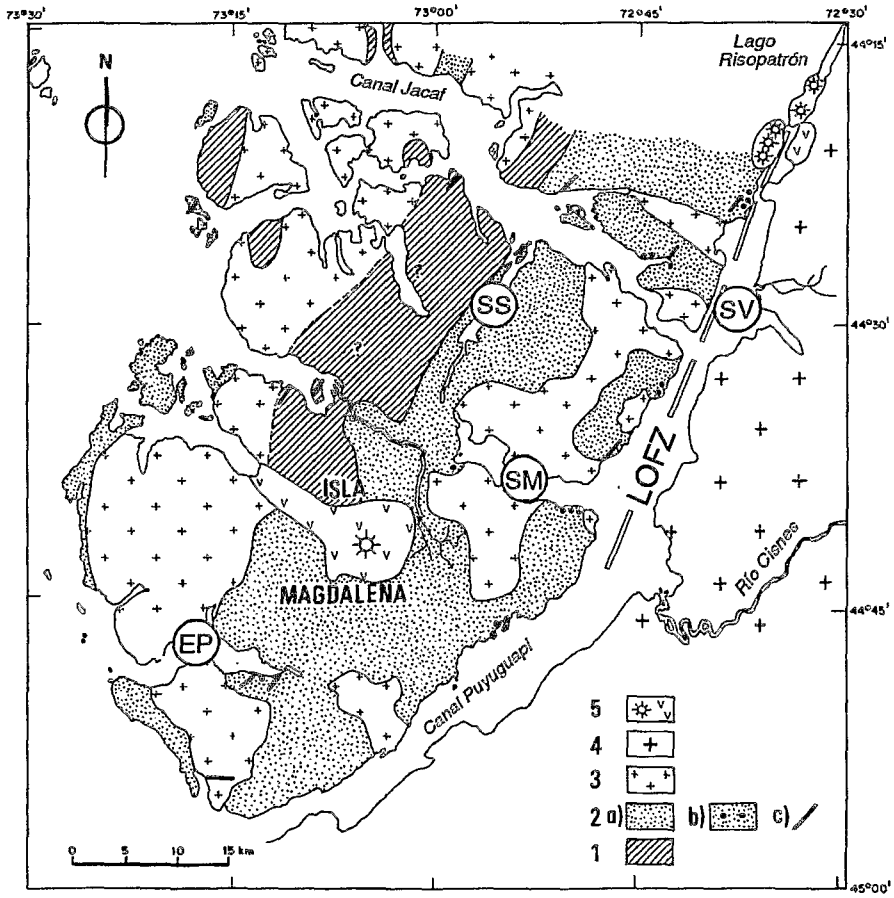

Fig.1: Geological sketch map of Isla Magdalena and surroundings. Legend: LOFZ= Liquiñe-Ofqui fault zone, SS= Seno Soto, SV= Seno Ventisquero, SM= Seno Magdalena, EP= Estero Pangal. Rock-types: 1= metamorphic basement; 2= mid-Tertiary igneous complex; (a)= volcano-sedimentary sequence, (b)= pillow basalts, (c)= dyke swarm locality; 3= Miocene granitoid plutons, 4= Undifferentiated Andean batholith, 5= Pleistocene-Holocene volcanic rocks and volcanoes.

silicic volcanic breccias. This low-grade metasedimentary sequence is also intruded by the dyke swarm; in some cases it can be that emplacement occurred into unlithified, and probably still wet, sediments. Siliceous intrusion into wet sediments also occurred.

Two distinct stages of metamorphism are observable in the pillow metabasalts; an early greenschist facies mineralogy being partially overprinted by a low-grade amphibolite assemblage. Only a faint foliation is developed, indicating a non-compressive environment during metamorphism, which was probably of diastathermal or contact type. Geochemical data suggest primary magmas with mixed within-plate/volcanic arc characteristics. A minimum age for the emplacement and metamorphism of the complex is given by Early Miocene (20 Ma) tonalite-diorite plutons that intrude both the volcano-sedimentary sequence and the basement. Rb-Sr whole-rock analyses of the metabasalts and of the associated slaty metasediments constrain the maximum age to less than 50 Ma, with initial $^{87}Sr/^{86}Sr$ ratios of close to 0.7043 and 0.7049 respectively (Fig. 2).

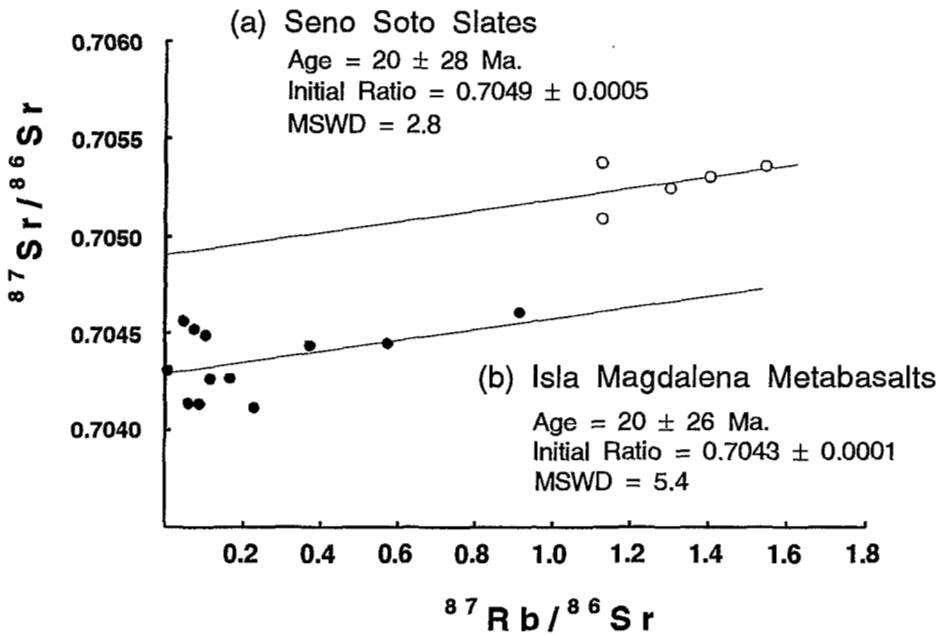

Fig. 2: Rb-Sr whole-rock isochron diagram for slates from the low-grade volcano-sedimentary sequence at Seno Soto (upper line), and for pillow basalts and matrix from the Seno Ventisquero area (lower line).

CONCLUSIONS

The volcano-sedimentary sequence was probably deposited in an extensional basin that formed in association with strike-slip faulting during mid-Tertiary times. NNE-directed oblique subduction at this time (40-25 Ma, Cande et al 1986) could have caused perpendicular extension, allowing ingress of the dykes, which might also have been feeders for the pillow basalts, into the sedimentary basin. When the subduction vector became orthogonal in Miocene times, the basin closed and was deformed under low-grade conditions. This change in the tectonic framework also lead to the subsequent calc-alkaline plutonism of normal Andean type.

Acknowledgements. This work was carried out under Projecto Fondecyt 92-0914 (Chile). M.Beck and R. Drake are thanked for help in part of the fieldwork.

REFERENCE

Cande, S.C. and Leslie, R.B., 1986. Late Cenozoic tectonics of the Southern Chile Trench. *Journal of Geophysical Research*, **91B**, 471-496.

^{3}HE EVIDENCE FOR A WIDE ZONE OF ACTIVE MANTLE MELTING BENEATH THE CENTRAL ANDES.

Leonore Hoke(1), David R. Hilton(2), Simon H. Lamb(1),
Konrad Hammerschmidt(2), Hans Friedrichsen (2)

(1) Department of Earth Sciences, University of Oxford, U.K.;
(2) FR Geochemie, Freie Universität Berlin, Germany.

RESUMEN

Una exploración regional de relaciones $^3He/^4He$ medidas en gases y aguas emitidos en áreas geotermales y aguas minerales de origen volcánico en los Andes Centrales, sugiere la presencia de una zona de fusión activa del manto de 350 km de ancho. La producción de fundidos bajo el arco volcánico probablemente se encuentra controlada por fundentes hídricos por encima de la zona de subducción. Sin embargo, bajo el Altiplano y la Cordillera Oriental, la fusión del manto es probablemente debida al adelgazamiento del manto litoférico acompañado con la resurgencia de astenosfera relativamente caliente.

KEY WORDS: Helium isotopes, Central Andes, geothermal areas, active mantle melting.

INTRODUCTION AND GEOLOGICAL SETTING

We report results of a comprehensive survey of $^3He/^4He$ ratios measured in gasses emitted in volcanic sulfataras, geothermal and mineral water areas of the Central Andes of Northern Chile and Bolivia between the latitudes 16°S and 23°S. Samples were collected from the active volcanic arc (Western Cordillera) and along several west to east transects across the high plateau region (Altiplano) into the Eastern Cordillera. The Andes are at their widest within this area (900km), and are unusual in that the Altiplano is underlain by ~70km of continental crust (Cahill & Isacks, 1992), comparable in thickness only to the Tibetan Plateau.

RESULTS

The highest $^3He/^4He$ ratios (R) are associated with active arc volcanoes along the western side of the Altiplano, and approach ratios found at other convergent margins in the circum - Pacific region. For example, Volcan Isluga and Irruputuncu have R/R_A ratios (R_A = air $^3He/^4He$) of 5.52 and 4.96 respectively. Surprisingly, a significant ^3He component ($R/R_A>1$) is also present in mineral and geothermal fluids sampled in the Altiplano and in the Eastern Cordillera - up to distances ~250km east of the active arc and more than 300km above the subducting slab (Cahill & Isacks, 1992). This wide zone of ^3He anomalies is delineated both to the east and to the west by low $^3He/^4He$ ratios ($\leq 0.1R_A$) typical of radiogenic helium production in the crust. All helium ratios were corrected for any air contamination. Furthermore, consideration of the regional ground water regime shows that the wide zone of elevated

$^3He/^4He$ values is unlikely to be caused by lateral transport of ^3He away from the active volcanic arc. In addition there is no evidence for significant sources of ^3He in the crust.

CONCLUSION

It is concluded, therefore, that the high $^3He/^4He$ ratios reflect degassing of volatiles from mantle derived magmas emplaced over a wide area of crust as a result of mantle melting. The radiogenic $^3He/^4He$ ratios on either side of this zone delineate a 350km wide zone of active mantle melting, where the subducting slab is at depths of 100 to 350km. In the west, underneath the active volcanic arc, mantle melt production is probably largely controlled by hydrous fluxing above the subduction zone. However, further east, underneath the Altiplano and Eastern Cordillera mantle melting may be due to thinning of the lithospheric mantle, concomitant with upwelling of relatively hot asthensphere.

REFERENCES

CAHILL, T., ISACKS, B., 1992: Seismicity and shape of the subducted Nazca Plate. Journal of Geophysical Research, 97, p 17503-17529.
POREDA, R., CRAIG, H., 1989: Helium isotope ratios in circum - Pacific volcanic arcs. Nature, 338, p 473-478,

Remote Sensing contribution on seismotectonic hazard in a volcanic active area (Nevado Sabancaya, southern Peru)

HUAMAN-RODRIGO D.[1,2], CHOROWICZ J.[2], GUILLANDE R.[3], ANTALLACA A.[1], CACERES R.[1] and AGUILAR A.[1]

1: Instituto Geofisico del Perú, P.O. Box 2041, Arequipa, Perú.
2: Laboratoire de Géologie Géomorphologie Structurale et Télédétection, UPMC. 4, Pl. Jussieu, BP. 129, 75252 Paris, France.
3: GéoSciences Consultants. 11-13, rue des Filles du Calvaire, 75003 Paris, France

Resumen

Utilizando imágenes SPOT de 1990, una red de fracturas recientes NE-SW fueron detectadas entre el cráter activo del Sabancaya y el valle del Colca, a lo largo del valle de Sepina. Dos terremotos con carácter destructor, ocurrieron el 23-07-1991 y el 01-02-1992, con epicentros localizados en el área de Sepina, estarían relacionados a dichas fracturas. Un nuevo escenario de amenaza sismotectónica se delinea en el valle de Sepina, cerca del volcán Sabancaya.

Key words: Remote sensing, Spot images, seismotectonic hazard, Sabancaya volcano,Andes south Peru

Introduction

The Nevado Sabancaya Volcano (NSV) is located near the Colca Valley in the department of Arequipa (Fig. 1). After 200 years of repose, this unknown volcano began an intense fumarolic emission in november 1986. Then, a very abrupt phreatomagmatic eruptive phase started on 28 may 1990 and is still continuing with increasing intensity.We have used two methods to monitor the volcanic eruptive process:

- SPOT imagery allowed us to compare different features before and after the eruption — the modifications of the snow cap, changes in the morphological features of the crater, and the occurence of open fractures —;[1, 2 and,3]
- the measurement of the seismic and tremor activities around the volcano.

The Sepina Valley which is a tributary of the Colca Valley is the most important seismotectonic zone in the area.In this zone the fracture network can be observed clearly and the hyposeismic activity can be recorded. Indeed, two relativety destructive earthquakes occured in this valley on 23 july 1991 and 01 february 1992.

Both methods together constitute a major new tool for identifying hazard zones as demonstrated in the Sepina area example which is described in the following sections.

The aim of this study is to develop a methodology using satellite images, field observation and seismological data.in the study of geological hazards It is a project borne out of the scientific cooperation between the Institut of Geophysics, Peru and the Department of Geotectonics, UPMC-France.

Local geologic setting

Spot images analysis enables detailed geological mapping (1/50 000) which clearly highlight lithological and tectonic features; in particular faults and fractures [4 and 6].

Approximatly 80% of the area studied is covered by Mio-Plio-Quaternary volcanic formations which are in angular unconformity on a deformed Mesozoic sedimentary substratum. This volcanism is

characterised by an enormous volume of ignimbrite, andesitic and dacitic lava streams. During the Quaternary stage the andesitic volcanism predominates; it is accumulated in the valley floor and the high plateau (+ 4500 m.). On this plateau there are several volcanic edifices with various sizes and forms.

The Ampato-Sabancaya-Hualcahualca volcanic complex constitutes a main morpho-structural feature in this area by its height (6000 m.).and by the associated natural hazard. Within this complex, the NSV is a recent edifice built by at least 11 efusive stages of lava rocks. The composition of the lava ranges from andesite to dacite which contain 61-63 % of Si O_2. Morphological analysis of streams on SPOT images and from field observations show that the volcano would belong to the Holocene age. In 1750-1784, spanish chronicles served as witnesses to an eruptive activity possibly similar to the ones observed nowadays (vulcanian explosions).

Recent observations indicate that the eruptive activity of the NSV is evolving dangerously; indeed samples from the december 1992 explosion clearly show a high abondance of juvenile products (fresh magma) as compared to the amount collected in october 1990, (comm. J.C.THOURET).

There are numerous fault alignements detected on the images, some of them are obvious, while others are more discrete. One can distinguish 4 directional groups:

- NW-SE, is poorly represented but belongs to the big regional structures;
- E-W, the most visible, is abondant in the Colca Valley, and shows.downthrows in the south compartment;
- N-S, small and discrete;
- NE-SW, thin and faintly visible. They are mainly localised in the Sepina area where the seismic activity is actually registered. This group defines an important tectonic system : the Sepina Tectonic Faults, STF.

SPOT image after eruption

Seven SPOT images of the NSV have been acquired, — two before the start of the eruption (28 may 1990) and five successive scenes later —, in order to monitor the volcanic process and its consequences on the environment. Volcanic hazards maps were established using SPOT data, Digital Terrain Model and field observations [4 and 5].

- Images acquired in july 1990 (1 scene every week for 3 weeks) showed ash falls covering a 60 x 35 km^2. area. Also the icecap was partially melted by the tephras and new fractures appeared. Two small groups of fractures E-W and NE-SW have been clearly located close to the crater.
- Images acquired in september and december 1990 indicate a continuing evolution of the NE-SW fractures which are aligned along the Sepina Valley (on the STF). That of december shows that the summit of the NSV is bordered by semicircular structures on the outer rim of the crater, an observation that would indicate a possible widening of the latter. After the Sepina earthquake of the 01 february 1992 an observation from an aircraft confirmed that the crater had become wider (an increase of 100 m approximately) after a couldron subsidence.

Seismicity activity

Seismic monitoring started in july 1990, one month after the beginning of the eruption of the NSV. Four portable stations were installed at distances of between 10 and 20 km. around the volcano. There were difficulties during data collection because of geographical contraints and technical problems. However, nearly 9000 microseisms were recorded in the Cajamarcana station (from the end july 1990 to march 1992) and, 131 seismic hypocenters were calculated. The seismic activity is superficial (1 to 9 km. deep) and is concentrated between in a zone 5 and 20 km. NE the volcano in the Sepina area.

The eruptive process of the NSV was accompagnied by numerous seismic crisis which are still going on with increasing intensity.

- On 23 july 1991, at 2:45 p.m. local time, a superficial seism (Mb=5.1; depth= 4 km) was felt 7 km south of Maca. Shaking, landslides and numerous fractures NS and NNE-SSW were observed in the Colca Valley. 80 % of Maca and Lari villages were destroyed and 14 people were killed. The worst surface damages are probably the consequence of the rock formation (sandy clays, laminated shales and, alluvial fans interstratified containing saturation levels that could have amplify the seismic waves) and the unstable nature of the houses too.

- The first february 1992, at noon, another seism with the same characteristics (M=4.5) occured in the rural Sepina area. This earthquake was accompagned with 300 aftershocks recorded the same day by the Cajamarcana station. On day 3rd and 5th of february, other strong aftershocks led to strong damages in the Sepina area. In poorly poblated areas, open fractures NE-SW and NNW-SSE several meters long were observed and boulders were displaced. The landslide failures were formed at the downstream part of the Sepina Valley.

New scenery of the volcanic hazard (Fig. 1)

Is the Sepina Valley a highly geologic hazard area?

Beside the hazards directly associated with the eruptive process of the NSV in the Colca region, the Sepina area appears as a highly unstable geodynamic zone as shown by recent tectonic features and seismics events.

Indeed, the location of the epicenters of the two destructive earthquakes (23 july 1991 and 01 february 1992) on each side of the STF is an evidence of a probable tectonic stress accumulation throughout this structure.

Therefore we can consider that the STF is a high seismotectonic hazard zone centered in Sepina area.

Conclusion

This study clearly demonstrates that the combination of SPOT images and seismical data constitute a valuable tool to monitor the seismotectonic hazards.

In the study area, the Sepina Valley, we have identified a high hazard zone connected to the STF. In case of a high magnitude earthquake inside this structure, we predict severe consequences on the STF itself and also whit in the active volcano area or in the lanslides zone located in the Colca and Sepina valleys.

Therefore the 30,000 inhabitants of the Colca Valley are particulary exposed to a these natural phenomena.

Bibliography

[1] Chorowicz J., Deffontaines B., Huaman-Rodrigo D., Guillande R., Leguern F. et Thouret J.C. (1992). *Remote Sens; Environ.* **42**: 43-49

[2] Francis P.W. and Da Silva S. (1989). *Remote Sens. Environ.* **28**: 245-255.

[3] Glaze L.S., Francis P.W., Self S. and Rothery D.A. (1989). *Bull Volcanol.* **51**: 149-160.

[4] Guillande R., Thouret J.C., Huaman-Rodrigo D. et Leguern F. (1992). *Rapport. Min. Env., et CNES, France,* pp. 133.

[5] Huaman-Rodrigo D; et Guillande R., (1990) Symp. Int. Géoddynamique Andine, 15-17 Mai 1990, ORSTOM Ed., pp. 387-389.

[6] Huaman-Rodrigo D., Chorowicz J., Deffontaines B., Guillande R. et Rudant J.P. (1993). In press *Bull. Soc. Géol. de France.*

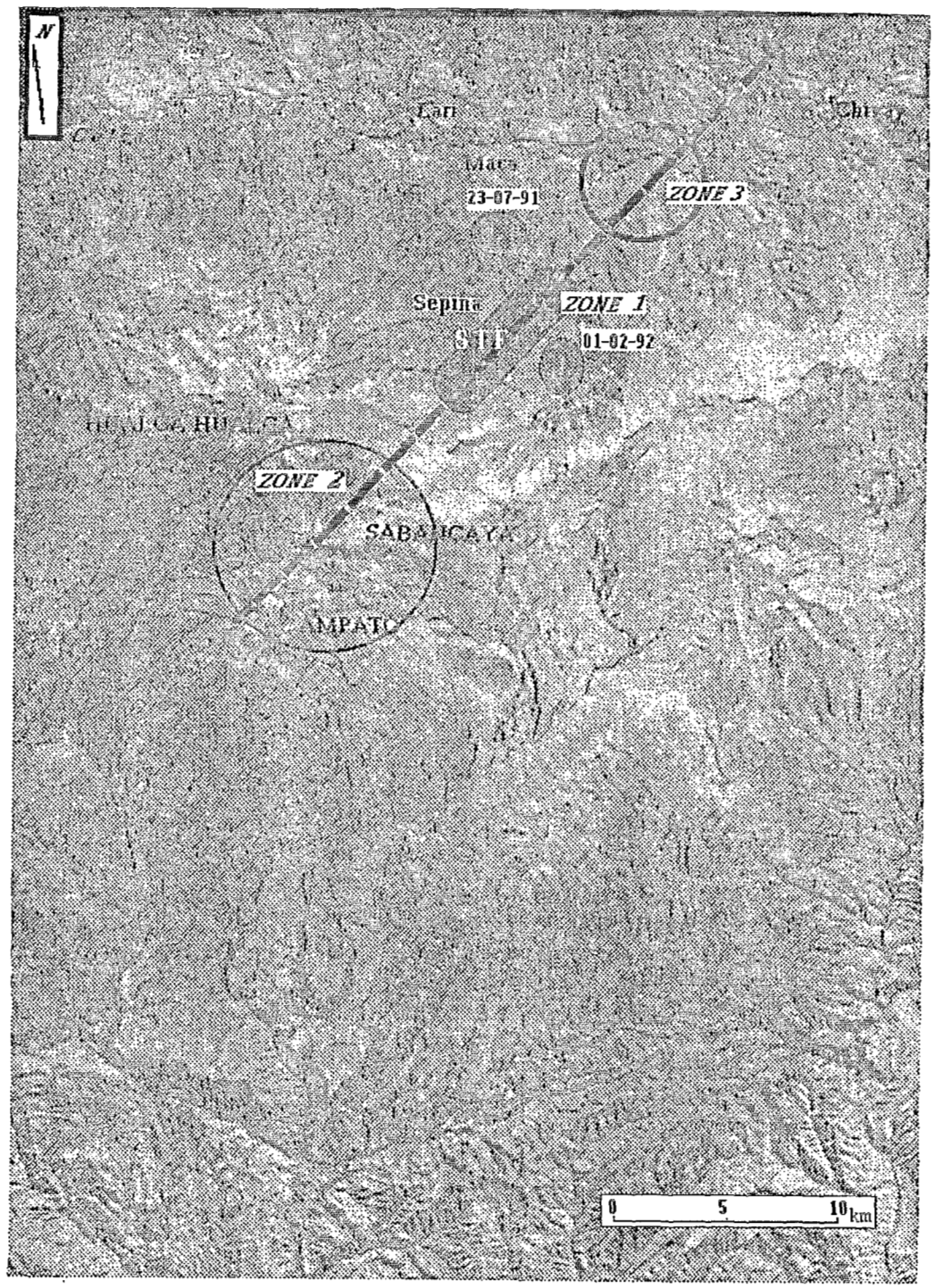

Fig. 1 Sketch of the seismotectonic hazard based on SPOT image.

The STF (zone 1) is a highly unstable geodynamical structure. Both severe earthquakes of 23 july 1991 and 01 february 1992 clearly suggest that a strong seismic event may occur soon along the STF. The 2 and 3 zones could be affected.

MAGMATIC EVOLUTION OF THE BERENGUELA-CHARAÑA REGION NORTHWESTERN ALTIPLANO, BOLIVIA

Néstor JIMENEZ CH.[1], Luis BARRERA I.[1], Oscar FLORES B.[1], José Luis LIZECA B.[1], Fernando MURILLO S.[1], Orlando SANJINES [1], Richard F. HARDYMAN[2], Richard M.TOSDAL[3], Alan R. WALLACE[4]

(1) Servicio Geológico de Bolivia, casilla 2729, La Paz
(2) U.S. Geological Survey, Mackay School Mines, Reno, Nevada 89557
(3) U.S. Geological Survey, 345 Middlefield Road, Menlo Park, California
(4) U.S. Geological Survey, Box 25046 M.S. 905, Denver, Colorado

RESUMEN: El magmatismo cenozoico de la región Berenguela-Charaña se inició en el Oligoceno superior y se prolongó, casi en forma continua, hasta el Cuaternario. Un cambio composicional de los magmas de afinidad alcalina y shoshonítica a calcoalcalina rica en potasio ocurrió en el límite Mioceno inferior y medio.

KEY WORDS: Cenozoic, Altiplano, magmatism, alcaline, calc-alkaline

INTRODUCTION

The Berenguela-Charaña region, located East from tripartite point border of Bolivia, Peru and Chile, was the site for long although intermittent Cenozoic magmatic activity alternating with periods of sedimentation. Conspicuous changes in the magma composition suggest variations in the tectonic regime and thickness of the continental crust throughout Late Cenozoic time. New field investigations, supported by K-Ar data and chemical analyses, carried out as part of an international cooperation program (Jiménez et al., 1993; Wallace et al., 1993), give some insight for the discussion of the magmatic evolution of the Bolivian Altiplano.

GEOLOGICAL SETTING

The oldest rocks outcropping in the area are the Eocene-Oligocene sandstones of the Berenguela Fm (Sirvas, 1964)

deposited over a basement formed by unexposed precambrian rocks and cretaceous sediments (Lehmann, 1978). These sandstones were gently folded by an orogenic phase about 28 Ma (Lavenu et al., 1989). Unconformably to disconformably over them, a thick sequence of sedimentary and volcanic rocks was deposited. This sequence is constituted by basaltic to andesitic lava flows intercalated with violaceous and well stratified arcosic sandstones in the base, and brownish, massive, and unconsolidated siltitic sandstones and conglomerates in the top. Sirvas (1964) and Ferrey (1970) named this sequence either Abaroa Fm or members 1, 2, 3 and 4 of the Mauri Fm. In this work, all these rocks are called Abaroa Fm. Avalaible K-Ar data for this formation range from 25 to 13 Ma (Evernden et al., 1977; Lavenu et al., 1989), but recent field observations and correlations with another areas of the Altiplano (Soler and Jiménez, this volume) constrain the bulk magmatic activity between 25 and 20 Ma. The younger ages seem to be obtained in some of the younger dikes and sills emplaced in the Abaroa Fm.

The name of Mauri Fm is reserved, in this work, for a volcanic and volcaniclastic sequence overlaying both the Berenguela Fm and the Abaroa Fm. It includes tuffaceous sandstones, reworked tuffs, nonwelded ash flow tuffs, debris flows and conglomerates. A tuff from the base of this Formation, disconformably emplaced over the underlaying units, gave an age of 18.3$\pm$0.7 Ma (Jiménez et al., 1993). The tuffs of its upper part were dated at 10.5 and 13.6 Ma (Evernden et al., 1977; Jiménez et al., 1993), On the other hand, many dacitic and rhyolitic intrusive bodies, dated at 10 and 11 Ma (Soria and Terrazas, 1992; Jiménez et al., 1993), were emplaced in all the area. Since the composition of the ash flow tuffs of the Mauri Fm is rhyolitic, a remarkable change of the magma composition occurs during the early Miocene (at 20-18 Ma).

In the Late Miocene and Early Pliocene a chain of volcanoes and a field of domes were built in the area. The Antajavi, Huaricunca and Serkhe volcanic complexes are made of rhyolitic nonwelded tuffs, dacitic to andesitic lava flows and intrusives, and other volcaniclastic deposits. The Antajavi volcano has been dated at 7$\pm$0.3 Ma (Jiménez et al., 1993), and two ages of 5.7$\pm$0.7 Ma were obtained for the Huaricunca and Serkhe volcanoes (Lavenu et al., 1989; Jiménez et al., 1993). The Thola Kkollu dome field is not dated but the chemical composition of its rocks is closely similar to the composition of the rocks of the volcanoes.

A huge volume of pyroclastic volcanism has been emitted during the Late Pliocene in the Berenguela-Charaña region giving rise to extended plateaus in the southern part of the area. First, a rhyolitic, crystal rich, weakly welded ash flow tuff (Pérez Fm of Sirvas, 1964), poured out from an unknown vent. Evernden et al. (1977) dated it in 2 and 3 Ma. Later, lacustrine sediments and a nonwelded, rhyolitic pumice flow of the Quaternary Charaña Fm (Sirvas, 1964) deposited over the nearly horizontal topography formed by the Pérez tuff.

PETROGRAPHIC AND CHEMICAL COMPOSITION

Basalts and andesites of the Abaroa Fm exhibit pilotaxic matrix with microlites of labradorite and small rounded crystals of augite. Occasionally, small crystals of nepheline can be found in the groundmass. The common phenocrysts of these rocks are zoned augite and labradorite +/- olivine. In the more differentiated terms lamprobolite and phlogopite are usual.

Dacitic to andesitic lavas and intrusives of the Medium to Late Miocene are characterized by hornblende, biotite and plagioclase (oligoclase-andesine) phenocrysts. In some of these rocks augite is the principal mafic mineral, but usually it is present in minor proportions. Quartz and sanidine are found in the rhyolites. The matrix can be either glassy or microcristaline.

The weakly welded ash flow tuff of the Pérez Fm, and the nonwelded ash flow tuffs of the Mauri Fm and of the Huaricunca and Serkhe volcanoes exhibit the same mineralogy. All these tuffs are rhyolites with laths of biotite and fragmented phenocrysts of quartz, plagioclase and sanidine scattered in a glassy groundmass with shards and spherolites. Xenoliths of basalts and Precambrian rocks are not uncommon.

The chemical analyses confirm the existence of two groups of magmatic rocks. Basalts and andesites of the Abaroa Formation have contents of SiO_2 ranging between 46 and 56%. Many of these rocks are nepheline-normative and usually they are silica undersaturated. Although some terms can be classified in the shoshonitic series, most of these rocks show alkaline affinities with TiO_2 varying between 0.71 and 1.35%, MgO from 1.90 to 9.90%, and often with $K_2O/Na_2O>1$. Contents of Cu vary between 56 and 285 ppm, Sr between 542 and 2500, Ni from 9 to 71, and Co between 15 and 100 ppm. On the contrary, the felsic rocks of the mid-Miocene to Quaternary exhibit contents of SiO_2 between 58 and 75%. Cu vary between 5 and 67 ppm, Sr between 46 and 1620, Ni from 2 to 31, and Co between 1 and 41 ppm. All these rocks are subalkaline but an increase in the alkalis content is evident in the rocks of the Late Miocene compared with the Medium Miocene ones. Some terms prove to be corindon-normative.

CONCLUSIONS

The magmatism of the Berenguela-Charaña region started in the Late Oligocene with the eruption and intrusion of rocks of alkaline affinities (Abaroa Fm). These rocks can be correlated with another ones known in the central and southern Altiplano (Tambillo lavas, Julaca and Rondal Formations, etc.) which are part of a more or less continuous belt (discussion and references in Soler and Jiménez, this volume). The origin of these rocks is poorly understood yet, but they seem to be generated in the upper mantle without noticeable crustal

contamination, probably during an transtensional period (Soler et al., 1992; Soler and Jiménez, this volume). The magma composition changes to a "normal" high-K calc-alkaline composition of the arc magmas of the Central Volcanic Zone in the Medium Miocene. This compositional change can be interpreted as a result of changes in the tectonic regime and the thickness of the continental crust.

REFERENCES

Evernden, J., Kriz, S., Cherroni, C., 1977, Potassium-Argon ages of some bolivian rocks. Economic Geology, v. 72, 1042-1061.

Ferrey, C.J., 1970, Estudio geológico de la región de la Estación ferroviaria Eduardo Abaroa. Unpublished thesis, Universidad Mayor de San Andrés, La Paz, 70 p.

Jiménez, N., Barrera, L., Flores, O., Lizeca, J.L., Murillo, F., Hardyman, R.F., Tosdal, R.M., Wallace, A.R., 1993, Marco geológico de la región de Berenguela. In Investigación de metales preciosos en los Andes Centrales, final report of Proyecto BID-USGS-GEOBOL, p. 63-74.

Lavenu, A., Bonhomme, M.G., Vatin-Perignon, N., De Pachtere, P., 1989, Neogene magmatism in the bolivian Andes between 16° and 18°S: Stratigraphy and K/Ar geochronology. Journal of South American Earth Sciences, v. 2, n° 1, p. 35-47.

Sirvas, J.F., 1964, Estudio geológico de la región Tambo Mauri-Berenguela, Provincia Pacajes del Departamento de La Paz, República de Bolivia. Unpublished thesis, Universidad Mayor de San Andrés, La Paz, 84 p.

Soler, P. and Jiménez, N., this volume, Magmatic constraints upon the evolution of the Bolivian Andes since Late Oligocene times.

Soler, P., Carlier, G., Fornari, M., Hérail, G., 1992, An alternative model for the origin and the tectonic significance of the Neogene and Quaternary shoshonitic volcanism of the Andes. AGU, Spring Meeting Suppl., 73, 14, p. 341.

Soria, E., Terrazas, R., 1992, La Española prospect. In Geology and Mineral Resources of the Altiplano and Cordillera Occidental, Bolivia, U.S. Geological Survey bulletin 1975, p. 184-187.

Wallace, A.R., Hardyman, R.F., Tosdal, R.M., Jiménez, N., Lizeca, J.L., Murillo, F., 1993, Cenozoic geology and mineral deposits of the Berenguela district, northwestern Bolivia. In Advances related to United States and international mineral resources-developing frameworks and exploration technologies, B.R. Berger and P.S. Detra eds., U.S. Geological Survey Bull. 2039, p.79-86.

ISOTOPIC CONSTRAINTS ON MIOCENE TO RECENT EVOLUTION OF THE CENTRAL ANDEAN LITHOSPHERE OVER THE "FLAT-SLAB"

Suzanne Mahlburg Kay, Jeffrey Abbruzzi, Richard Allmendinger, and Teresa Jordan

Dept. of Geological Sciences, Snee Hall, Cornell University, Ithaca, NY 14853 USA

RESUMEN: Relaciones isotópicas de Pb, Sr y Nd de rocas volcánicas pertenecientes al "flat-slab" son utilizadas como indicadores de cambios litosfericos debido a la horizontalización de la Placa de Nazca. Las relaciones isotópicas reflejan entre otras cosas un engrosamiento cortical de la Cordillera Principal, un basamento no radiogenico de ≈ 1100 Ma en la Precordillera, y la posibilidad de un componente litospherico basal que debe haberse desplazado hacia el este durante la horizontalización en rocas volcánicas de las Sierras Pampeanas.

KEY WORDS: Shallow subduction, arc volcanism, isotope, Miocene to Recent, lithosphere, crust

INTRODUCTION

Pb, Sr and Nd isotopic ratios of Late Oligocene to Pliocene volcanic rocks in the Central Andean "flat-slab" region (28° S to 33° S; Fig. 1) can be used as tracers for crustal and mantle processes occurring above a shallowing subduction zone. These tracers are most powerful when combined with geophysical and geologic data that constrain lithospheric geometries. The purpose here is to integrate Pb, Nd and Sr isotopic constraints (Figs. 2 and 3) on "flat-slab" magma sources into a refined lithospheric model (Fig. 4) for the late Miocene to Recent evolution of the "flat-slab".

LITHOSPHERIC CONSTRAINTS FROM GEOPHYSICAL AND GEOLOGIC DATA

Constraints on the modern lithospheric geometry of the "flat-slab" come from seismic studies (e.g., Smalley and Isacks 1990) that define the shape of the seismic zone and put limits on lithospheric and asthenospheric thicknesses (see Fig. 4). Reconstructions of past lithospheric geometries are based on modern day analogues in the Southern Volcanic Zone (SVZ; Fig. 1) chosen by matching the geologic setting and chemistry of "flat-slab" magmatic rocks with those in the SVZ. Using this method, Kay et al. (1991) concluded that early Miocene "flat-slab" volcanism occurred over a steeply dipping slab like that south of 35° S, that mid Miocene volcanism occurred over a shallower slab like that near 33° S, and that late Miocene volcanism occurred over a shallower slab than exists in the SVZ. These comparisons imply an increase in Main Cordillera crustal thickness from ≈ 40 to 45 km at ≈ 20 Ma to near the poorly constrained modern value of ≈ 65 km at 6 Ma.

Temporal constraints on thickening come from field and seismic data that suggest that 170 to 190 km of early Miocene to Recent crustal (and lithospheric) shortening has occurred in three north-south trending belts (Allmendinger et al. 1990). From west to east, these belts are the Main Cordillera, the Precordillera fold and thrust belt, and the block faulted ranges of the Sierras Pampeanas (Fig. 1). Approximately 100 km of the surface shortening occurred in the Precordillera above a decollement that is now at ≈ 15 km. Another 50 to 60 km took place in the Main Cordillera, and the rest (20 to 30 km) in the Sierras Pampeanas. A combination of radiometric, stratigraphic and paleomagnetic data shows that shortening began at ≈ 20 Ma in the Precordillera, primarily occurred

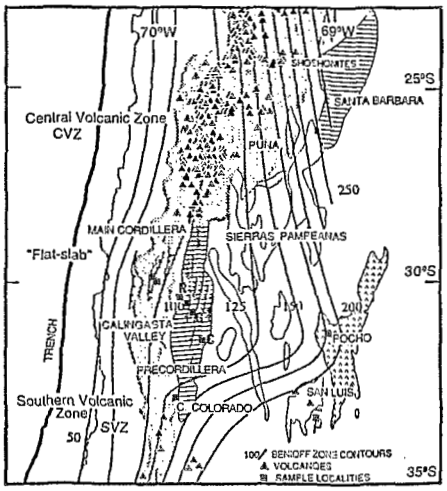

FIGURE 1 - Map of central Andes showing important geologic provinces in the "flat-slab" and adjacent Central and Southern Volcanic Zones. Base map and contours to seismic zone after Isacks (1988).

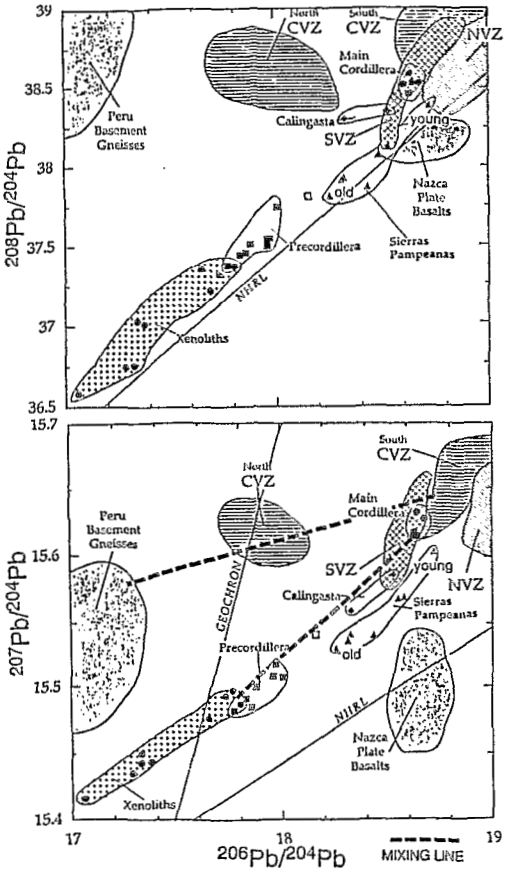

FIGURE 2 - Plots of central Andean Pb isotopic data. Fields for Peruvian, CVZ, CVZ, SVZ and Nazca plate rocks are from Davidson et al. (1988). Points are our unpublished data. NHRL is Northern Hemisphere Reference Line. CVZ mixing model is from Barreiro (1984).

in the early Miocene in the Main Cordillera, and was principally post-late Miocene in age in the Sierras Pampeanas (Allmendinger et al. 1990; Jordon et al. 1993). A temporal correlation between Main Cordilleran and Precordilleran crustal shortening and Main Cordilleran crustal thickening is consistent with crustal thickening primarily resulting from crustal shortening.

CONSTRAINTS ON "FLAT-SLAB" MAGMA SOURCES FROM ISOTOPIC DATA

Main Cordillera - Sr and Nd isotopic ratios in Main Cordilleran arc rocks (basaltic andesite to rhyolite in the early Miocene, hornblende andesite to dacite in the mid Miocene, dacitic ignimbrites in the late Miocene) fall in three age-dependent groups (Fig. 3). All of these samples have lower ϵ Nd and higher Sr ratios than early Miocene back-arc tholeiitic basalt to the east showing that they have an excess radiogenic crustal component that cannot be attributed to an ancient enriched mantle component. A trend of increasing Sr ratios and decreasing ϵ Nd with decreasing age among the arc groups shows that greater amounts of this crustal component were added through time. Given other evidence for a simultaneous increase in crustal thickness, larger amounts of radiogenic crustal contaminant can be explained by augmented interaction of mantle magmas with crust as ascent paths became longer and more difficult.

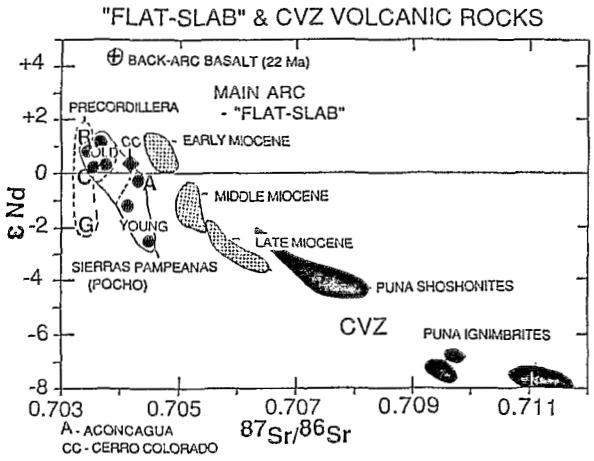

FIGURE 3 - Plot of Nd and Sr isotopic data for "flat-slab" and CVZ volcanic rocks. Main Cordillera data are from Kay et al. (1991). Points are our unpublished data. CVZ data is from the literature and our unpublished data.

An additional contribution to these magmas from a subducted sediment component is suggested by Pb isotopic data. Unlike Nd and Sr isotopic data, Pb isotopic data for Main Cordilleran magmatic rocks fall in a restricted field (Fig. 2). This field, like those of young Andean SVZ and southern CVZ arc rocks (Fig. 2), is within the typical range for arc rocks world-wide. This Pb signature is commonly attributed to the mixing of subducted upper crustal sediments with melts of the mantle wedge above the subducting slab. In the "flat-slab", this interpretation requires a subducted sediment component in the backarc as both backarc and arc rocks have similar Pb signatures. An alternative is that both subducted sediments and in-situ crustal contamination play a role. Either way, Main Cordillera sources have a distinctive Pb signature that is important in interpreting isotopic signatures of Mio-Pliocene Precordillera and Sierra Pampeanas volcanic rocks.

Precordillera - Pb, Sr, and Nd isotopic ratios of mid to late Miocene silicic andesitic and dacitic Calingasta Valley and Precordilleran rocks are unlike those of Main Cordillera rocks (Figs. 2 and 3). In fact, the Pb and Sr ratios in these rocks are the lowest yet reported in Miocene to Recent central and southern Andean rocks. The least radiogenic ratios are from a ≈ 7 Ma sample from the Cerro Blanco-Ullun center in the eastern Precordillera (C in Fig. 1). The overlap of these ratios with those of xenoliths from the unexposed Precambrian basement (discordant zircon fractions from a silicic xenolith give U/Pb age of 1188±123 Ma) shows that these nonradiogenic ratios reflect the basement. Thus, the trend of Precordilleran Pb isotopic ratios in Figure 2 can be explained by mixing basement with an orogenic arc component, just as northern SVZ Pb ratios were explained by mixing Peruvian basement with an orogenic arc component (Barreiro 1984; Fig. 2). In detail, eruption age and location are important in interpreting sources of Precordilleran Miocene magmas as more radiogenic samples are either older or farther west than less radiogenic ones. Calingasta Valley rocks (e.g., C. Colorado) whose isotopic compositions are the most radiogenic are the oldest and closest to the Main Cordillera.

Sierras Pampeanas - Sr, Nd, and Pb isotopic ratios of Mio-Pliocene Pampean volcanic rocks (Pocho and San Luis; Fig. 1) are intermediate between those of Precordillera and Main Cordillera rocks (Fig. 2 and 3). As in Precordilleran lavas, relatively low Pb and Sr isotopic ratios are best interpreted as reflecting continental basement. Relatively more radiogenic Pb and Sr ratios in Pampean than in Precordilleran lavas have three potential explanations: 1). eastern Pampean Precambrian basement is different, 2). Paleozoic magmatism has added an enriched component to the Pampean basement, and 3). Pampean lavas contain a more enriched sub-crustal component.

Further constraints on Pocho isotopic signatures come from the fact that basaltic andesitic to dacitic magmas erupted at ≈ 4 to 5 Ma are more like Main Cordillera rocks, whereas those erupted at ≈ 6 to 7 Ma are more like the Precordillera group. Two factors could be important: 1). crustal thickening leading to increasing amounts of a within-crust radiogenic component (like the Main Cordillera), and 2). increasing amounts of an enriched subcrustal component. An argument against crustal thickening being the only factor is that crustal shortening is minimal in the Sierras Pampeanas. An argument for a subcrustal component consisting of subducted sediment and continental lithosphere removed from the base of the Main Cordillera comes from combining, isotopic, structural and geophysical constraints.

A REFINED MODEL: MIOCENE TO RECENT MAGMATIC SOURCES AND THE LITHOSPHERIC EVOLUTION OF THE "FLAT-SLAB"

Steep Subduction : ≈ 25 to 20 Ma - The early Miocene geometry of the "flat-slab" was grossly like that of the steep subduction zone near 35° S in the modern SVZ. Main Cordilleran arc magmas formed in the usual way - release of fluids from the slab caused melting in the overlying asthenospheric wedge. These melts then passed into the continental lithosphere where they incorporated crustal and mantle material and fractionated at relatively low pressures before erupting. Minor amounts of back-arc olivine tholeiite erupted along a probable active fault zone. Structural and magmatic activity was virtually absent east of the Main Cordillera.

Initial Shallowing : ≈ 20 to 11 Ma - Shallowing of the subduction zone was underway by ≈ 18 to 20 Ma. Geological evidence for this shallowing comes from early Miocene high angle reverse faulting in the Main Cordillera, the early to mid Miocene broadening of the volcanic arc into the Precordillera, and the early Miocene initiation of thrusting and basin formation in the Precordillera. As a result, Main Cordilleran arc magmas began fractionating at greater depths and assimilating more crust as crustal thickness increased in response to crustal shortening. Upper crustal material was transported to deep levels in the Main Cordillera as Precordilleran crust was wedged into the Main Cordillera (Fig. 4). Magmas erupted in the east were more contaminated by Precordilleran-type basement. During this time, lithospheric geometry changed from like that in the SVZ today at ≈ 35° S to like that at 33° S. As a result the space for asthenospheric and lithospheric mantle above the slab decreased ≈ 30% out to 600 km east of the trench (≈ 20% to 800 km).

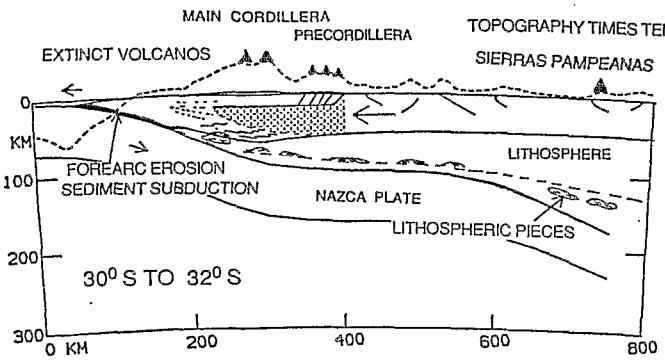

FIGURE 4 - Modern "flat-slab" lithospheric cross-section. Shape of subducting plate, lithospheric thickness, and topography from Smalley and Isacks (1990) and Isacks (1988). Volcano in Sierras Pampeanas represents Pocho volcanic field. Patterned wedge is crust from below decollement in Precordillera that is pushed into Main Cordillera (see Allmendinger et al. 1990).

Main shallowing phase ≈ 10 to 6 Ma - Important changes in "flat-slab" geology occurred between 10 and 5 Ma. Magmatic events included termination of Main Cordilleran andesitic volcanism at ≈ 10 Ma, broadening of the arc across the Precordillera into the Sierras Pampeanas at ≈ 7 Ma, the end of all volcanism in the Main Cordilleran and Precordillera between 7 to 6 Ma, and final Pampean volcanism at Pocho at ≈ 5 Ma. Structural events included important basin formation, thrusting in the Precordillera and uplift of the Sierras Pampeanas.

The dramatic eastward expansion of both magmatic and deformational fronts is taken to signal an important change in slab dip. Given the modern geometry of the seismic zone, the space for asthenospheric and lithospheric mantle above the subduction zone decreased ≈ 60% to a distance of 600 Km east of the trench (≈ 45% to 800 km) after the early Miocene. More than 30% of the continental mantle lithosphere within 600 km of the trench must have been displaced. This calculation is a minimum as it does not allow for lithospheric cooling as the subduction zone shallowed or for lithospheric thickening to accommodate 170 km of crustal shortening in < 600 km. A consequence implied by the section of Smalley and Isacks (1990) is that only crustal lithosphere is now present beneath the Main Cordillera. The proposition here is that continental lithosphere has been removed in pieces that have been carried into the asthenosphere by the mantle flow system circulating above the wedge. Indirect evidence for these lithospheric pieces potentially comes from the geochemistry of the Pocho volcanic rocks in the Sierras Pampeanas.

A consistent interpretation for the crustal component in the Pocho volcanic rocks is that it was, in part, derived from asthenosphere mantle melts that interacted with lithospheric pieces removed from beneath the Main Cordillera (Fig. 4). A temporal increase in this component in Pocho magmas is consistent with continued subduction. A rapid change in subduction zone geometry at ≈ 7 Ma would allow little time for such a component to be incorporated in ≈ 7 Ma Precordillera magmas which have a strong isotopic signature from the local basement.

REFERENCES

ALLMENDINGER, R.W., D. FIGUEROA, D. SNYDER, J. BEER, C. MPODOZIS, B.L. ISACKS, 1990, Foreland shortening and crustal balancing in the Andes at 30° S latitude. Tectonics 9: 789-809.

BARREIRO, B.A., 1984, Lead isotopes and Andean magmagenesis. In Harmon, R.S., Barreiro (eds), Andean Magmatism - Chemical and Isotopic Constraints, Shiva, Bristol, pp. 21-30.

DAVIDSON, J.P., N. MCMILLAN, S. MOORBATH, G. WORNER, R. HARMON, L. LOPEZ-ESCOBAR, 1990, The Nevados de Payachata volcanic region (18° S/69° W, N. Chile) II. Evidence for widespread crustal involvement in Andean magmatism. Contrib. Mineral. Petrol. 105: 412-432.

ISACKS, B.L., 1988, Uplift of the central Andean plateau and bending of the Bolivian orocline. Jour. Geophys. Res. 93: 3211-3231.

JORDAN, T.E., R. ALLMENDINGER, J. DAMANTI, R. DRAKE, 1993, Chronology of motion in a complete thrust belt: the Precordillera, 30-31° S, Andes Mountains. Jour. Geol. 101: 133-156.

KAY, S. MAHLBURG, C. MPODOZIS, V.A. RAMOS, F. MUNIZAGA, 1991, Magma source variations for Tertiary magmatic rocks associated with a shallowing subduction zone and a thickening crust in the Central Andes (28 to 33° S). In Andean Magmatism and its Tectonic Setting. Geol. Soc. Am. Spec. Paper 265: 133-138.

SMALLEY, R.F., Jr., B.L. ISACKS, 1990, Seismotectonics of thin and thick-skinned deformation in the Andean foreland from local network data: Evidence for a seismogenic lower crust. Jour. Geophys. Res. 95: 12487-12498.

GEOLOGY, GEOCHEMISTRY AND RECENT ACTIVITY OF THE HUDSON VOLCANO, SOUTHERN CHILE

Rolf KILIAN [1] Peter IPPACH [2] and Leopoldo LOPEZ-ESCOBAR [3]

1) Institut für Mineralogie, Petrologie and Geochemie, Universität Tübingen, Wilhelmstr. 56, 7400 Tübingen, Germany

2) Institut für Vulkanologie und Petrologie, GEOMAR, Universität Kiel, Wischhofstr. 1-3, 2300 Kiel 14, Germany.

3) Departamento de Geologia, Universidad de Chile, Casilla 13518, Correo 21, Santiago, Chile

RESUMEN

We present first geological and geochemical results of a comprehensive study on Hudson volcano and its Recent activity. An Upper Pleistocene unit form the basis of Hudson volcano. This activity period produced predominantly andesitic pyroclastic flows interbedded with basaltic lava flows forming a caldera like structure. Holocene magmatic activity produced basaltic cones and andesitic to dacitic eruption centers oriented along the main Holocene fracture zones.

Lava flows and pyroclastic products are calcalkaline and range in SiO_2 from 49 to 68 wt.% with medium to high-K character. We distinguish two basalt types. The older, Upper Holocene to Late Pleistocene basalts (type-1), when compared with the younger, Late Holocene to Recent basalts (type-2), have higher X_{Mg} values (50-61), K/Rb (400-520), Ba/La (20-50), and Rb/Cs (60-95) ratios, and lower TiO_2 (›1.5 wt.%), La/Yb (2.3-3.3), Rb/Sr (0.02-0.04) ratios. Type-1 has lower $^{87}Sr/^{86}Sr$ (~0.7036), $^{206}Pb/^{204}Pb$ (~18.48), and higher $^{143}Nd/^{144}Nd$ ratios (~0.51286) than type-2. Late Holocene to Recent basalts of type-2 have lower X_{Mg} values (38-45), K/Rb (320-380), Ba/La (10-17), and Rb/Cs (36-65), but higher La/Yb (3-4), Rb/Sr ratios (0.04-0.06), and TiO_2 (1.6 to 2.3 wt.%) than type-1. The higher Sr, Nd, and Pb isotpic ratios of the type-2 suggest an additional crustal component. Most andesites and dacites originated from the basaltic type-2 by fractional crystallization in a closed system without further crustal contamination.

The youngest activity of Hudson volcano started with a fissure eruption at the 8th of August 1991. These basaltic phase (8/8-10) located at the western caldera rim produced fallout and lava flows. The following paroximal andesitic phase (8/12-15) with eruption centers in the SW part of the glacier filled caldera ejected tephra in a SE-directed plume up to 1000 km SE (Malvinas Islands). Recent gas activity has

apparently increased since August 1991. We observed columns up to 500 m altitude in a crater-like depression around the andesitic eruption centers (8/12-15). Glacier melting by the strong geothermal activity has intensified the mud flow production in the direction to Huemules valley.

KEY WORDS: Southern Andes, Chile, volcanism, volcanic activity, geochemistry, Quaternary.

INTRODUCTION

Active continental margins are characterized by predominantly intermediate to felsic calcalkaline volcanism produced by differentiation and interaction of the mantle-derived basaltic melts with the continental crust. In the Andes basaltic volcanism is restricted to the southern section of the Southandean Volcanic Zone (SVZ). It is controlled by the Liquiñe-Ofqui fault zone (LOFZ) that extends between 39° and 46°S. Hudson volcano is located at its southern end about 300 km NE of the plate triple junction formed by the Nazca, Antarctic and South American plates. The magmatic activity of Hudson volcano is related to the subduction of a Nazca plate segment. The rise of this segment is oriented parallel and in front of the Chile trench. The trench is filled by sediments which were drilled by ODP Leg 141 up to Pliocene formations (BEHRMANN et. al 1992). This implies subduction of young, hot, oceanic crust including sediments. The continental crust is 30 to 35 km in thickness. Plutonic rocks of the Patagonian Batholith and Paleozoic metamorphic rocks form the exposed basement. The latter rocks show a continental isotopic signature (PUNKHURST et al. 1991). Both rock units could have contaminated the primary upper mantle melts of the Hudson volcano by sediments of the subducted slab or/and by intracrustal AFC processes.

GEOLOGY

Geological field work was carried out in the austral summers 89/90, 91/92 and 92/93. Our satellite image investigation on the Hudson basement shows a Holocene fracture framework striking 103°, 125°, and 18-25°. The latter are oriented parallel to the LOFZ. This fracturing was produced by the Recent Chile rise collision with the continental margin. The dikes, eruption centers and cones are located on these lineaments. Andesitic lava flows (each one up to 50 m thickness) and basaltic to andesitic lava flows (each one up to 20 m thickness) form the basal Upper Pleistocene unit of the Hudson. The basic Hudson unit document alternating effusive and highly explosive activity. It is exposed on the North-Western and partly on the Eastern side forming a caldera-like structure. In the Holocene, twelve eruption centers were formed at different locations of the whole volcanic area of about 95 km^2. Basaltic cones and fissures were formed especially on the western and eastern caldera rim. The eruptions centers located in the glaciated Pleistocene caldera were often highly explosive probably due to phreatomagmatic processes forming products of andesitic to dacitic compositions.

GEOCHEMISTRY

Major and trace elements of 70 samples from different volcanic and basement units were obtained by XRF. The trace elements, Cs, Th, U, Ta, Hf, Sc and the REE were determined by INAA from 20 samples. The isotopic ratios of the elements Sr, Nd, and Pb were detected from 11 selected samples (KILIAN & HEGNER 1993).

The effusive and explosive vocanic products are calcalkaline and range in SiO_2 from 49 to 68 wt. % with medium-K to high-K character. Two types of basalts can be distinguished. The older, Upper Holocene to Late Pleistocene basalts (type-1) have higher X_{Mg} values (50-61), K/Rb (400-520), Ba/La (20-50), and Rb/Cs (60-95) ratios, and lower TiO_2 (>1.5 wt.%), Rb (13-20 ppm), La/Yb (2.3-3.3), Rb/Sr (0.02-0.04) ratios than the younger, Late Holocene to Recent basalts (type-2). Type-1 has lower $^{87}Sr/^{86}Sr$ (~0.7036), $^{206}Pb/^{204}Pb$ (~18.48), and higher $^{143}Nd/^{144}Nd$ ratios (~0.51286) than type-2. In comparison with geochemical calculations of BRANDON et al (1989), HAWKESWORTH et al. (1992), and KELLER et al. (1991) trace element pattern for type-1 are consistent with a derivation of a partially melted slab mixed with material from a peridotitic source in the mantle wedge. The isotopic data are consistent with a depleted mantle source contaminated with 1-2 % of old continental crust.

Late Holocene to Recent basalts of type-2 have lower X_{Mg} values (38-45), K/Rb (320-380), Ba/La (10-17), and Rb/Cs (36-65), but higher La/Yb (3-4), Rb/Sr ratios (0.04-0.06), and TiO_2 (1.6 to 2.3 wt.%) than type-1. Higher Sr, Nd and Pb isotopic ratios suggest an additional crustal component as exposed on the surface. Most andesites and dacites originated from the basaltic type-2 by fractional crystallization of plagioclase (An_{90} to An_{35}), olivine (Fo_{90} to Fo_{55}) and augite in a closed system without further crustal contamination as indicated by similar K/Rb, Ba/La, and isotopic data as basalt type-2.

RECENT ACTIVITY

The basaltic eruption phase of 8-9 August 1991 (GVN Bulletin v. 16, no. 7-12) was located at the ice covered (20-30 m thickness) western caldera rim forming an elliptic fissure vent about 2.5 km long, 0.3 km wide, and 0.2 km deep trending N 25°W. Constant fumarolic activity with intense sulfur odor was observed since August 1991. The basaltic eruption phase produced 1.0-1.5 km^3 (DRE) (IPPACH & SCHMINCKE, 1993) of fallout material, lava, and spatter flows. Lava flows extend max. 3.5 km beside the Huemules glacier from the N flank of the fissure vent. Additionally, lava debris flows and aa-like flows were observed at the N flank extending up to 2.5 km from their source. At the western inner caldera rim lava and spatter flows extend down the slope into a 300 m deep depression of the ice covered caldera surface. The inner part of the WNW caldera rim partially collapsed and slid into the caldera. The thickness of the basaltic fallout layers decrease from about 500 cm near the source to 1 cm at a distance of 50 km in direction to the N. The paroximal andesitic eruption phase of 12-15 August 1991 (GVN Bulletin, v. 16, no

7-12) was located in the SW part of the glacier filled caldera. The 17-18 km high eruption column was sheared by strong winds into a norrow SE-directed plume transporting 2.5-3.0 km^3 (DRE) tephra (IPPACH & SCHMINCKE, 1993) to at least 1000 km SE. A large SO_2-rich cloud, ca. 1500 kton of SO_2, circled the south polar region twice in 7 days (DOIRON et al. 1991). In the SW part of the caldera crater-like depressions filled by lakes of 800 and 650 m diameter are indicating the existence of two eruption centers of the andesitic phase. This area of 5 km^2 is surrounded by an intensively cracked glacier.

During the austral summer of 91/92 pyroclastic material was reworked into the lower NW part of the caldera leaving deposits up to 50 m thickness. In the winter of 1992 the pyroclastic material was covered by snow, which is now compacted to 2-3 m thickness. Recent gas emission and increasing geothermic activity is producing a strong melting of the ice in an area of 10 km^2 around the plianian eruption centers. In this zone gas columns from different locations reaching up to 500 m altitude were observed. One phreatic gas eruption (February 1993) produced an ash fan of reworked pumice material 10 km to the E. Consequently, mud flow production is still increasing. In erosional channels of the glacier volcanoclastic material is flowing to the SE of the caldera following the Huemules glacier. This implies a permanent risk for the repopulated Huemules valley.

REFERENCES

BEHRMANN, J., LEWIS, S. D. & MUSGRAVE, R. (1992): Proc. ODP, Init. Repts., **141**: College Station, TX.

DEWEY, J.F. & LAMB, S.H. (1992): Active tectonics of the Andes.- Tectonophysics, **205**: 79-95; Amsterdam.

DOIRON, et al. (1991): Transport of Cerro Hudson SO_2 1991.- Eos, vol. **72**, 45.

GVN BULLETIN (1991): Smithsonian Institute; Bull. GVN, No.7, 9, 10, 11, 12.

IPPACH, P. & KILIAN, R. (1993): Increased gas and mudflow production at Hudson volcano, Southern Chile.- in press.

IPPACH, P. & SCHMINCKE, H.-U. (1993): Volatile buget of the eruption of Mt. Hudson (Chile) in 1993.- in prep.

KILIAN, R. & HEGNER, E. (1993): Pb, Sr, and Nd isotopic ratios of Hudson basalts constraining the Southandean magma genesis.- Geology, in prep.

KILIAN & LOPEZ-ESCOBAR, L. (1991): Petrology of the Southern Southandean Volcanic Zone (41-46°S) with emphasis on Michinmáhuida-Chaitén volcanic complex (43°S).- Zbl. Geol. Paläont., Teil 1, **1991** (6): 1693-1708; Stuttgart.

PUNKHURST, R.J., HERVE, F. ROJAS, L. & CEMBRANO, J. (1992): Magmatism and tectonics in continental Chiloé, Chile (42°-42 30°).- Tectonophysics, **205**: 283-294.

STERN, C.R. (1990): Tephrochronology of southermost Patagonia.- Nat. Geograph. Res., **6**: 110-126.

STERN, C.R. (1991): Mid-Holocene tephra on Tierra del Fuego (54°S) derived from the Hudson volcano (46°S): Evidence for large explosive eruption.- Rev. Geol. Chile, **18** (2): 139-146; Santiago.

PETROLOGY AND GEOCHEMISTRY OF THE TAITAO OPHIOLITE VOLCANIC-PLUTONIC SUITE (CHILE TRIPLE JUNCTION REGION)

José Le Moigne[1], Yves Lagabrielle[1], René Maury[1], Jacques Bourgois[2], Thierry Juteau[1]
1-U.F.R Sciences et Techniques, U.B.O., 6 Av. Le Gorgeu - BP 452, 29275 BREST Cédex - France (Fax 98316620)
2-U.P.M.C., URA n° 1315, 4, place Jussieu, 75252 Paris Cédex 05, France (Fax : 16 (1) 44 27 51 72)

Résumé : Nous présentons les résultats d'une série d'analyses géochimiques conduite sur les principaux termes de l'ophiolite de Taitao. Les arguments de terrain permettent de distinguer deux unités dans l'ensemble volcano-sédimentaire étudié : (1) une unité essentiellement volcanique (OVU) métamorphisée dans le faciès des schistes verts qui pourrait constituer les termes supérieurs de l'ophiolite et (2) une unité volcanique et sédimentaire (CMU) à conglomérats et pyroclastites qui repose en discordance sur le socle métamorphique de la marge du Chili. Les résultats de notre étude pétrographique et géochimique confirment cette distinction et nous amènent à rediscuter l'origine des ophiolites.

KEY WORDS : Taitao ophiolite, Chile Triple Junction, volcanic rocks, geochemistry.

An ophiolitic and an intrusive suites have been discovered recently at 47°S on the Taitao Peninsula, Southern Chile (Forsythe *et al.*, 1986, Mpodozis *et al*, 1985), 50 km southward of the Chile Triple Junction and only 17 km from the Chile trench. The ophiolite and the intrusions have been first considered of Pliocene to Pleistocene age and are supposed to be the result of ridge subduction and collision. Indeed, a portion of the active spreading Chile ridge between the Taitao fault zone and the Tres Montes fault zone collided with the continental margin around 2.5 Ma - 4 Ma (Cande *et al.*, 1987).

The results of a field study conducted in the Taitao Peninsula in 1992 led us to distinguish at least two sequences within the volcano-sedimentary sequence previously interpreted as the stratigraphic cover of the so-called ophiolitic suite (here refered as the Bahia Barrientos Ophiolite, BBO). These two sequences are named the Ophiolite volcanic Unit (OVU) and the Chile Margin Unit (CMU) (Bourgois *et al.*, 1992).

(1) The OVU could represent the upper part of the ophiolite. It consists of a thick volcanic sequence of pillowed and massive lavas showing greenschist facies metamorphic overprint interbedded with marine sedimentary rocks. No microfauna allowing age determination was found in the sediments. This unit has been studied in three separate localities : Rio Oxxean Tres, Estero Lobo and Estero Cono. The corresponding sequences are named respectively : Oxxean Tres, E. Lobo and E. Cono sequences.

(2) The CMU is a thick, vertical, volcano-sedimentary unit. It includes conglomerates and pyroclastic rocks and uncomformably overlies the metamorphic basement of the Chile margin. No pebbles of ophiolitic origin have been found in the coarse detrital levels of this unit. Nannoplankton assemblages give an age ranging from Early Pliocene to Early Pleistocene.

Sixty-one samples of various volcanic rocks from the three distinct volcanic sequences of the OVU and from the CMU have been analyzed for major and trace elements as well as for rare earth elements using unductively coupled plasma emission spectrometry (ICP-ES), except Rb which has been analyzed with flame atomic emission spectrometry. Thirty-one samples have been collected in the Oxxean Tres sequence, nine are from the E. Lobo sequence, five from the E. Cono sequence, and three samples are fresh glass from undetermined origin. Three serpentinized peridotites and eleven gabbroic samples were also analyzed.

The collected volcanics are dominantly pillowed basalts, but massive lavas, dolerites, tuffs, pyroclastic breccias, isolated dikes and other intrusive have also been sampled. The rocks are dominantly

basic lavas (basalts, basaltic andesites and andesites), but three dacitic rocks and one rhyolite are present. SiO_2 content ranges from 46 to 76,8% with LOI (loss of ignition) varying from 1% to 9%. The volcanic sequence of the CMU is characterized by the abundance of pyroclastic facies, the occurrence of fresh glass within pillows and the lack of greenschist facies metamorphic overprint in all the lavas. By contrast, the volcanics of the OVU sequences show frequent greenschist facies metamorphism with crystallization of actinolite, chlorite and the albitization of plagioclase. However, as shown in a SiO_2 *vs* LOI diagram, there is no striking difference in the LOI ranges of both series.

The alkaly contents of the basaltic lavas are often high, higher than expected for typical MORB. The Na_2O+K_2O content varies from 2 to 9 % with the highest values found in basalts and basaltic andesites from E. Cono and E. Lobo sequences. Such variations require special attention to the possible effects of the alteration on the composition of the lavas. But no clear correlations can be established between the LOI and the abundance of major elements, moreover, the highest Na_2O and K_2O values are found in lavas showing low LOI contents suggesting that high alkaly values could be of primary origin. In a simple Na_2O+K_2O *vs* SiO_2 diagram (Fig. 2), two groups of composition can be distinguished : the rocks from the CMU show relatively slight alkaly enrichment for increasing silica contents whereas rocks from the OVU are characterized by high alkaly contents at lower SiO_2 values.

Based on rare earth elements behaviours, different groups can be distinguished among the samples from the OVU. Our preliminary study shows that at least three different groups do exist : a E-MORB group with a La/Nb ratio =1 (Fig. 3), a group with calk-alkaline affinities and a group of intermediate affinity with high SiO_2 and low K_2O contents. The mafic volcanic rocks of the CMU have REE patterns similar to that of slightly enriched MORB. The siliceous rocks of this unit show similar pattern with higher trace elements abundances and Nb, Ti and V negative anomalies probably in relation with fractionation of titanomagnetite and amphiboles.

The plutonic rocks of the Bahia Barrientos Ophiolite include isotropic and cumulate gabbros, gabbro-norites, Fe-Ti gabbros, wherlites and various intrusives such as andesite dikes and silicic anastomozing veinlets. The mineralogy of the gabbros is similar to that of oceanic gabbros (Ol, Pl, Cpx, Opx, Fe-oxides). Primary amphibole was found only in few samples. Some samples contain sulfides. The gabbros have very homogeneous geochemical compositions with silica content varying from 47% to 52,8% and very low K_2O and Na_2O contents.

These preliminary results indicate that the presumed upper volcanic sequence of the BBO, *i.e.* the OVU, is not typical of volcanic sections found at mid-oceanic ridges. Therefore, the Taitao complex cannot be regarded as a section of oceanic lithosphere simply obducted during ridge-trench collision. A more complex scenario is now needed to explain both obduction of ophiolitic rocks and the near trench Pliocene-Pleistocene magmatism registered in the CMU sequence and in the Chaicayan islands region.

Bourgois J., Lagabrielle Y., Maury R., Le Moigne J., Vidal P., Cantagrel J. M. and Urbina O., Geology of the Taitao peninsula (Chile margin triple junction area, 46°-47°S) : Miocene to Pleistocene obduction of the Bahia Barrientos ophiolite, *EOS*, 73, 1992, p. 592.

Cande S. C., Leslie R. B., Parra J. C. and Hobart M., Interaction between the Chile ridge and Chile trench : geophysical and geothermal evidence, *J. Geophys. Res.*, 92, 1987, p. 495-520.

Forsythe R. D., Nelson E. P., Carr M. J., Kaeding M. E., Hervé M., Mpodozis C. M., Soffia M. J. and Harambour S., Pliocene near trench magmatism in southern Chile : a possible manifestation of ridge collision, *Geology*, 14, 1986, p. 23-27.

Mpodozis C. M., Hervé M., Nasi C., Soffia M. J., Forsythe R. D. and Nelson E. P., El magmatismo plioceno de Peninsula Tres Montes y su relacion con la evolucion del punto triple de Chile austral, *Rev. Geol. de Chile*, 25-26, 1985, p. 13-28.

Figure captions :

Fig. 1 - Geological map of the Taitao Peninsula established on our observations.

Fig. 2 - $Na_2O + K_2O$ versus SiO_2 diagram. Dark squares, open squares, dark lozenges and open lozenges are for the Ophiolite Volcanic Unit (OVU). Black triangles are for the gabbroic and serpentinized rocks (BBO). Open triangles are for the lavas of the Chile Margin Unit (CMU).

Fig. 3 - La versus Nb diagram. Same symbols as fig. 2.

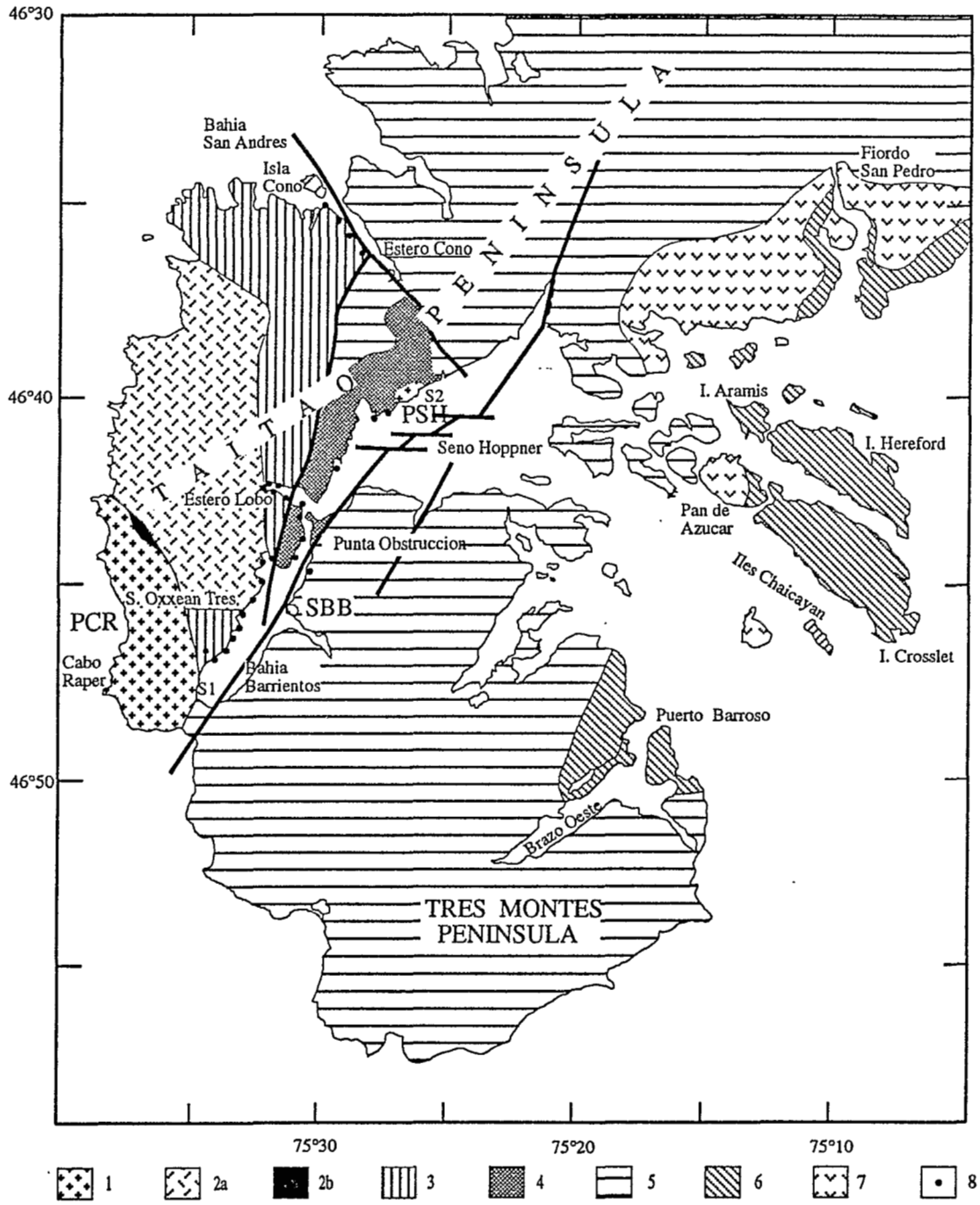

Fig. 1 - Structural diagram of the Taitao Peninsula :

1- Pliocene Taitao intrusive suite (3.2 - 5.5 Ma) ;
2- BBO : Bahia Barrientos Ophiolite suite : 2a- ophiolitic complex ; 2b- serpentine ;
3- associated volcanism OVU;
4- CMU : Chile Margin Unit ;
5- Pre-Jurassic metamorphic basement ;
6- Golfo Tres Montes Unit ;
7- calc-alcalin volcanism (0.8 - 5.3 Ma) ;
8- localisation of analyzed samples ;
F1, F2 : hot springs. CRP : Cabo Raper Pluton. BBS : Bahia Barrientos Stock. SHP : Seno Hoppner Pluton.

Fig. 2

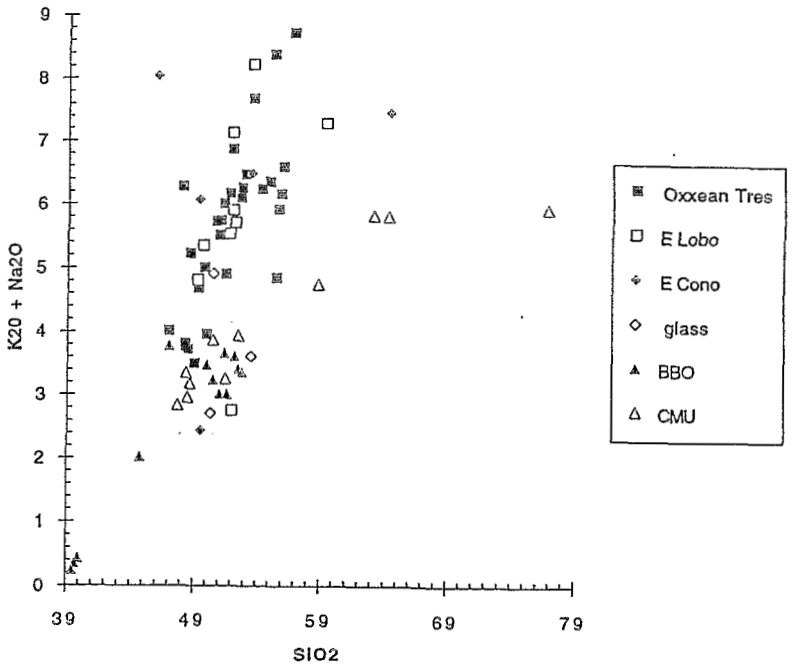
K20 + Na2O
SIO2
0
1
2
3
4
5
6
7
8
9
39
49
59
69
79
Oxxean Tres
E Lobo
E Cono
glass
BBO
CMU

Fig. 3

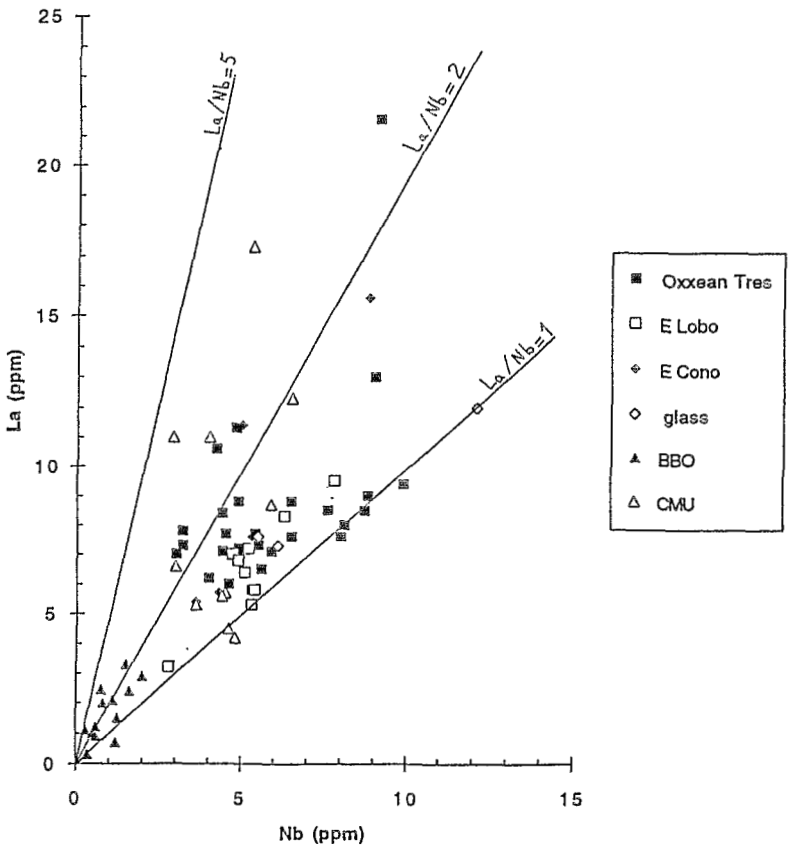
La (ppm)
Nb (ppm)
La/Nb=5
La/Nb=2
La/Nb=1
0
5
10
15
20
25
Oxxean Tres
E Lobo
E Cono
glass
BBO
CMU

PETROGENESIS AND OCCURRENCES OF GABROIC ROCKS IN THE LIMIT EASTERN CORDILLERA-HIGH PLATEAU IN THE ABANCAY DEFLECTION AREA (CURAHUASI -SOUTH PERU)

Rolando LIGARDA C. (1), Gabriel CARLIER. (2) and Víctor CARLOTTO C. (3)

(1) SIMSA, Apartado 10296, Lima 41 - PERU.
(2) ORSTOM, UR 1H,213, Rue la Fayette 75480, Paris cedex 10 - FRANCE.
(3) UNSAAC, Jr Atahuallpa 253, Cusco - PERU.

RESUMEN.- Rocas gabroicas de tipo cumulats que constituyen la cámara magmática en el borde norte del batolito Andahuaylas-Yauri, afloran en la zona de la Deflexión de Abancay, como cabalgamientos plurikilométricos sobre cuarcitas del grupo Yura.

KEY WORDS.- Batholith, Gabbros, Abancay Deflection, Thrust, Curahuasi.

INTRODUCTION

Gabbroic rocks in the Curahuasi zone, north border of Andahuaylas-Yauri batholith, south of E-W striked Abancay Deflection, were described by MAROCCO (1975, 1978), however more detailed investigations about their origin and ocurrences have never been done. In this paper the authors provide information about field relations, petrography, rock and mineral chemistry. The conclusions could have important tectonic implications in setting the Eastern Cordillera-High Plateau limit as well as understanding the Andean shortening.

GENERAL GEOLOGY AND TECTONIC SETTING

Limestones and black shales of lower-middle Permic age (Copacabana Group), continental red beds and andesitic volcanics of upper Permic-Triassic age (Mitu Group) constitute the Paleozoic basament.

During the Mesozoic the basin was divided into two parts with different deposition, separated by E-W faults (Abancay Thrust systems), parallel to the Abancay Deflection (MAROCCO, 1978; LIGARDA et al, 1991). To the south the western basin consists of upper Sinemurian-Bajocian(?) limestones (Lagunillas Group), it follows the deposition of black shales and white quartzites interbedded at the top with limestones of Bathonian-Neocomian age (Yura Group) with more than 900 meters in thickness. This thick sequence, North of the eastern basin, is equivalent to only 15 meters of Neocomian mature sandstones (Huancané Formation), which overlies the volcanics of the Mitu Group (Figs. 1, 2); above the Huancané Formation are red shales and thick evaporitic series with limestones at the top of Aptian-lower Cenomanian age (Yuncaypata Formation).

The tectonic setting was characterized by E-W to WNW-ESE thrust systems, which dip to the south, downdip these faults become listric faults. The Abancay Thrust is the most important structure that puts, the Yura Group and Yuncaypata Formation together; associated with it are E-W isocline foldings in Puente Cunyac. Southward the subhorizontal dipped Curahuasi Thrust sets the gabbroic rocks over Yura Group quartzites, this can be seen in Quebrada Honda (Fig. 3). In the Curahuasi valley small tertiary stock of tonalitic rocks and quaternary shoshonitic volcanics are distributed along the E-W structures; the last one are associated with a distensive reactivation of the faults. Less important NW-SE faults with movement along the strike, associated with microdiorite dykes, are also present.

DISTRIBUTION AND PETROGRAPHY OF GABBROIC ROCKS

In a general way in the north border of the batholith, the Yura Group quartzites are overthrusted by the gabbroic rocks, as a response to the Curahuasi Thrust. Gabbroic rocks constitute in volume the main part of the magmatism, they are dark grey, and have magmatic laminations of cumulat type as a characteristic feature, their age is not well defined, but the authors assume that they intruded during the upper Cretaceous-lower Tertiary.

Modal Analysis using the IUGS diagrams, Pl-Px-Ol and Pl-Px-Hbl (Fig. 4) give three rock families: troctolites, olivine gabbros and hornblende gabbros. The troctolites and olivine gabbros show cumulat textures, with olivine-plagioclase-ortho-clinopiroxene as a prymary paragenesis. The post-cumulat or late magmatic phase consists of brown hornblende-biotite-opaques; the pyroxenes were altered to hornblende and opaques as simplectites. The hornblenda gabbros are dykes, which cut the troctolites and olivine gabbros, they show granular xenomorphic texture, and are made up of plagioclase-brown hornblende-clinopiroxene-opaques; olivine and orthopyroxene can be found occasionally.

MINERALOGY AND MINERAL CHEMISTRY

Minerals of olivine gabbros (samples Cu6, Cu7, Cu9) and troctolites (Cu10), were analized with a Camebax Microsonde (Lab. de Petrologie de l'Ecole Nationale Superieure des Mines de St. Etienne - Paris).

Olivine has a forsterite composition: $65<Fo<74$, with Magnesium content nearly 0.50% (Fig. 5); and contains inclusions of opaque minerals. Plagioclases are the dominant phase and have a subparallel arrangement that indicate the magmatic laminations; the anorthite content average goes from 60 to 74%: Labradorite-bytownite, however the anorthite content can have strong variations, which is typical of adcumulats cristallization. Clinopyroxenes are augite; whereas the orthopyroxenes are associated with both, clinopyroxenes and opaque minerals, and has hiperstene composition: $69<Mg<75$ (Fig. 5). The chemical evolution of these pyroxenes is like that of calc-alkaline plutonic rocks that evolved under high water fugacity (BEST & MERCURY, 1967), the titanium distribution between ortho and clinopyroxene shows that they are in equilibrium, therefore, it is assume that the cristallization temperature was about 1000° C (WELLS 1977). Amphibole cristallize as post-cumulats and has magnesium-hastingsite composition, showing high content of $Mg/Fe+Mg>0.85$ similar to the biotite: $Mg/Fe+mg>0.74$. Magnetite occurs as inclusions in olivine, associated with other ferromagnesian minerals. Illmenite is also present.

ROCK CHEMISTRY

Major-element composition and trace-elements abundances were analized by XRF-Fluorescence (Lab. de Petrologie de Paris VI) in the samples mentioned above. The diagrams A-F-M and $Al2O3$ - $FeO+Fe2O3$ - Mg, show typical calc-alkaline lineal evolution of cumulat rocks;

these gabbros are poors in both, alkalines and incompatible elements (Zr, Rb, Y, Nb, Hf) and are enriched in MgO, CaO, Ni, Co, V (Fig. 6). The comparision of the oxides against the differenciation index DI, with surrounding tonalitic stocks and microdioritic dikes, show that these gabbros are not comagmatic with the last one (LIGARDA, 1989). These chemical data also indicate that the gabbroic rocks are originated from a type I magma (CHAPPELL & WHITE, 1974).

CONCLUSIONS

Based on their mineralogical and petrographic characteristics and chemical data (cumulat rocks); it is belief that these rocks constitute the deepest level of Andahuaylas-Yauri batholith and probably represent the magmatic chamber, that were lifted by a plurikilometric overthrust from south to north (?) caused by thrust systems in the late Cretaceous. Also, these systems controlled the sedimentation in the western and eastern basins in the Jurassic and Cretaceous times, and later, during the andean tectonics, located the western basin over the eastern basin as an allochthonous block.

ACKNOWLEDGEMENTS

The authors wish to thank, H. Poupon for his support; J. Jacay and C. Angeles for their suggestions; C. Loayza, C. Salinas and H. Aspajo for translating the paper.

REFERENCES

BEST, M.G., MERCURY, E.L.P., 1967, Composition and cristallization of mafic minerals in the Guadalupe igneous complex, California. Am. Min. 52, p 436-474

CHAPPELL, B.W. WHITE, A.J.R., 1974, Two contrasting granite types. Pacific Geol. Tokyo 8, p 173-174.

LIGARDA, R., 1989, Estudio geológico del Cuadrángulo de Curahuasi (Dpto. Apurimac) Tesis Ing. Geol. UNSAAC, Cusco. 183 p.

LIGARDA, R. CARLIER, G., CARLOTTO, V., 1991, Estratigrafía del borde Oriental de la Cuenca Mesozoica sur peruana (Sector Curahuasi-Dpto. Apurimac). Res. VII Cong. Peruano Geol., p 633-638.

MAROCCO, R., 1975, Geología de les Cuadrangulos de Andahuaylas, Abancay, Cotabambas. Bol. Ser. Geol. Min. 27, 51 p.

MAROCCO, R., 1975, Estudio Geológico de la Cordillera de Vilcabamba. Inst. Geol. Min. Perú, Lima 22, 51p.

WELLS, P.R.A., 1977, Pyroxene Thermometry in simple and complex systems. Centr. Miner. Petrol. 62, p 129-140.

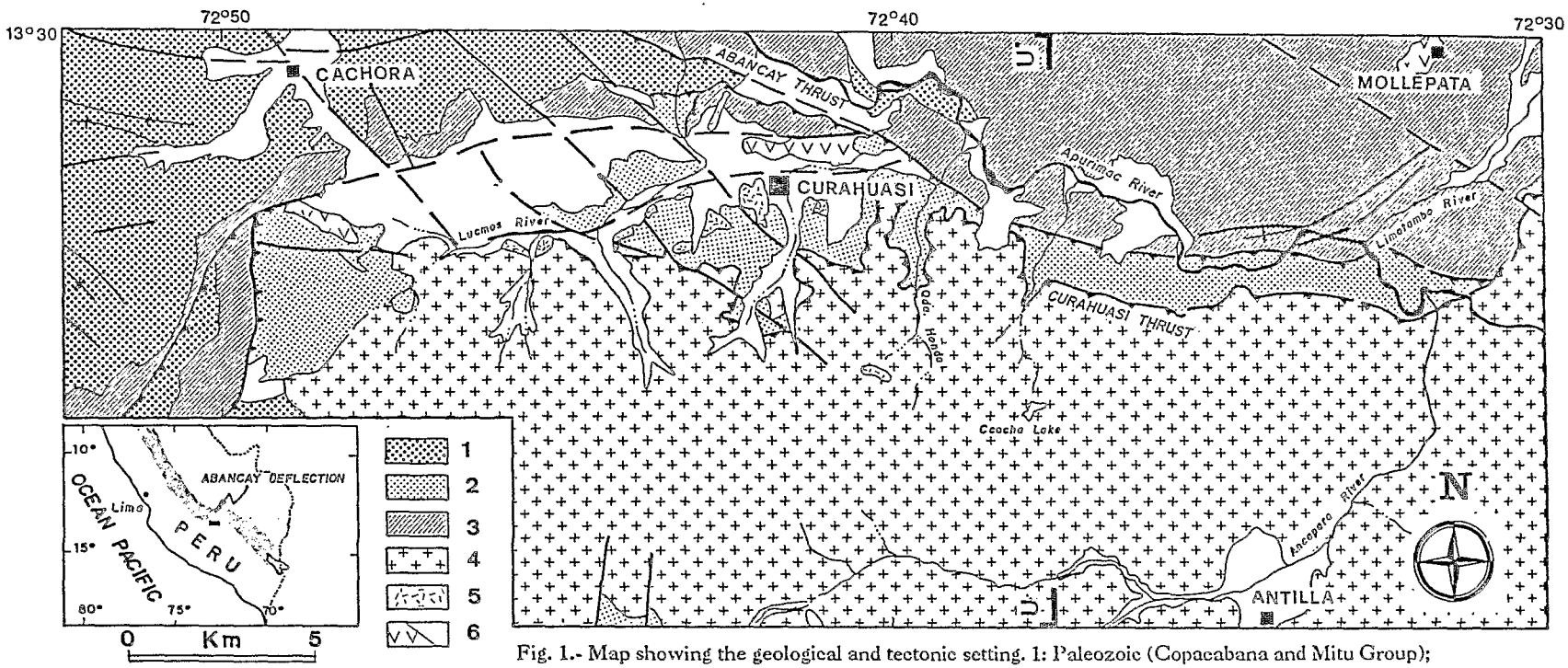

Fig. 1.- Map showing the geological and tectonic setting. 1: Paleozoic (Copacabana and Mitu Group); 2: Western Mesozoic basin (Lagunillas and Yura Group); 3: Eastern Mesozoic basin (Huancané and Yuncaypata Formations); 4: Gabbroic rocks of Andahuaylas-Yauri batholith; 5: Tonalitic stocks; 6: Shoshonitic volcanics/Quaternary deposits.

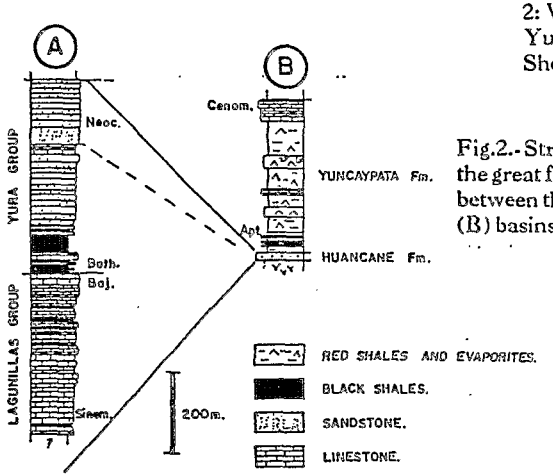

Fig.2.- Stratigraphic sections showing the great facies and thickness changes between the Western (A) and Eastern (B) basins during the Mesozoic times.

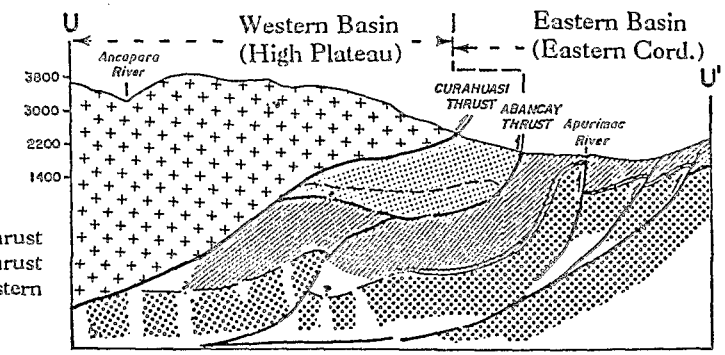

Fig.3.- N-S section showing the thrust systems, which cause the overthrust of the High Plateau against the Eastern Cordillera.

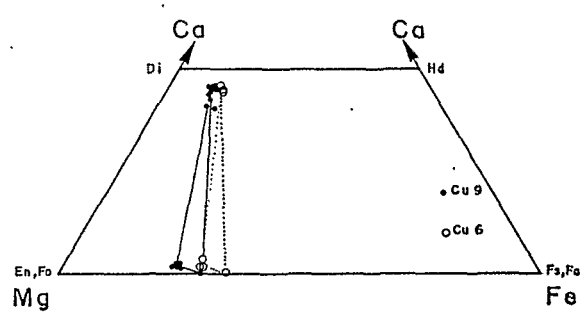

Fig.5.- Ca-Mg-Fe diagram, showing the olivine-ortho-clinopiroxene equilibrium for two gabbroic rocks samples.

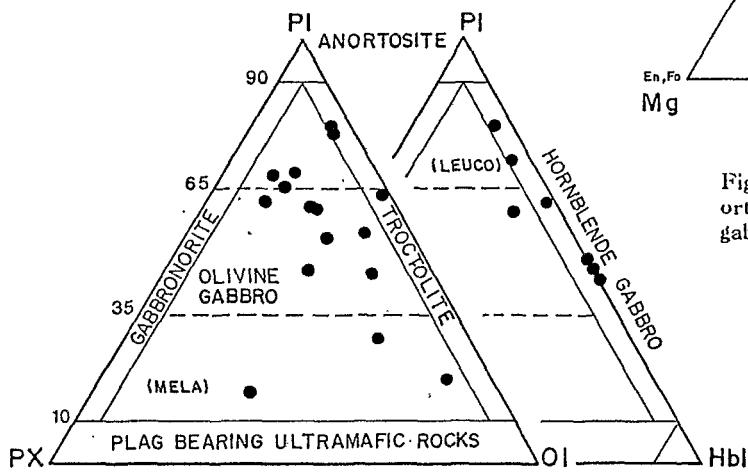

Fig.4.- Modal of gabbroic Rocks using the IUGS diagrams Pl-Px-Ol and Pl-Px-Hbl.

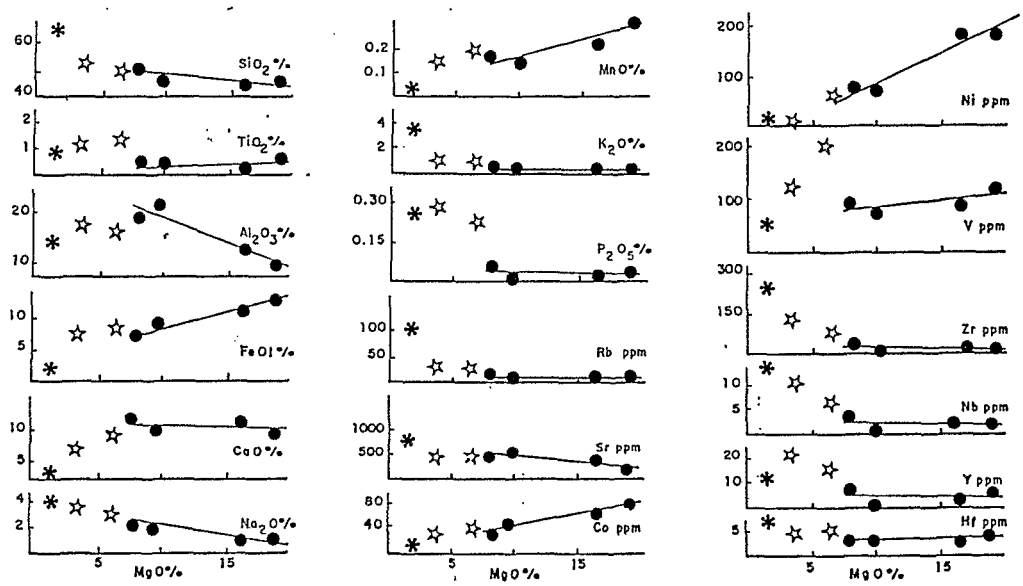

Fig.6.- Harker type diagrams of Curahuasi gabbroic rocks, compared with other magmatic events. circles: gabbroic rocks; stars: microdioritic dikes; asterisces: tonalitic stock.

ARC RELATED IGNEOUS AND METAIGNEOUS ROCKS IN THE COASTAL CORDILLERA OF NORTHERN CHILE: CONTINUOUS REPLACEMENT OF THE CRUST?

F. LUCASSEN (1), G. FRANZ (2) & C.M.R. FOWLER (1)

(1) Geology Department, Royal Holloway, University of London, Egham Hill, Egham, Surrey TW20 0EX, U.K.
(2) TUB, Fachgebiet Petrologie, EB310, Strasse des 17.Juni 135, 1000 Berlin 12, Germany

RESUMEN

Durante la fase jurásica de actividad magmática, la corteza continental pre-andina de la Cordillera de la Costa del norte de Chile (región de Antofagasta) fue reemplazada por rocas intrusivas precoces y sus equivalentes metamórficos, por rocas intrusivas tardías y por rocas volcanicas. El lapso de tiempo de este episodio magmático parece estar restringido a 50 m.a. Terminó alrededor de 150 m.a. y empezó aproximadamente hace unos 200 m.a. Sin embargo, las edades del inicio del magmatismo y del subsequente metamorfismo son imprecisas. Los detalles del marco tectónico y de la evolución de esta adición de magma a gran escala en la corteza no estan aún claros.

Key Words: Arc magmatism, magmatic arc metamorphism, crustal growth by magmatism, tectonic setting of the magmatism

INTRODUCTION

Early intrusive rocks and their metamorphic equivalents, late intrusive rocks, and volcanic rocks replaced the Preandean continental crust during the Jurassic phase of magmatic activity in the Coastal Cordillera of northern Chile, Region Antofagasta. The time span of magmatism seems restricted to 50 Myr. It terminated around 150 Myr and started at +/- 200 Myr). The onset of magmatism and subsequent metamorphism is, however, less certain. The details of the tectonic setting and history of this large scale addition of magma to the crust are not yet clear.

GEOLOGICAL SETTING (Coastal area between 23^{20} - 24^{20}S)

Metaplutonic rocks (metabasites) and plutonic rocks are exposed along the coastline south of Antofagasta and at the southern tip of the Mejillones peninsula. The metabasites constitute low pressure granulites (two pyroxene plagioclase gneisses), relicts of their magmatic protolith and foliated amphibolites derived from the pyroxene gneisses. Layered gabbros (numerous small intrusions) and a quartz diorite pluton (large homogeneous intrusion) intruded into the metamorphic unit. Mafic dyke swarms crosscut the foliation and other textures in the metabasites and the quartz diorite. They were not deformed under ductile conditions. To the south (24^{o}) relicts of volcanic rocks ("Formacion La Negra") are widespread (continental deposits as lava flows). Contacts of the volcanic rocks with their basement are not well known, except in some places, where tectonic and intrusive contacts were observed. Preandean continental crust is not found between south Mejillones and Paposo.(for details: Lucassen & Franz, 1992 and references therein)

METAMORPHISM DURING MAGMATIC ACTIVITY

The recrystallization of the early magmatic rocks under granulite facies temperatures was enhanced by the intrusive magmatic activity. The magmas were essentially dry and the recrystallization occured on the cooling path of the area. No relicts of a prograde temperature path were found for granulite and subsequent amphibolite facies rocks. Temperatures in the pyroxene gneisses (800^{o}C, two pyroxen thermometry) and in the amphibolites (600-700^{o}C, amphibole compositions) are not related to the geographical distribution of the samples (no regional temperature gradient). Quantitative pressure estimations for the formation of the metabasites are not possible because garnet is generally lacking. Considering Mg(Fe+Mg) ratios between 50 and 60 for most samples our suggestion that pressure did not exceed some 5 kbar is "on the safe side". Pressures of $\leq$5 kbar were derived for minerals formed at greenschist facies temperatures by phengite composition and fluid inclusions.

GEOCHEMISTRY

The formation of the pyroxene gneisses from the igneous protolith was isochemical (no dehydration reactions involved), and the compositional changes by the amphibolitization are negligible (major and trace elements including REE, Sr and O isotopes for selected samples). The majority of metabasite samples are typical calcalkaline rocks with SiO_2 contents (48-54 wt%) in the range of the basalt - basaltic andesite transition. The quartz diorite is similar in composition to the rare SiO_2 rich metabasites. The dykes also follow a calcalkaline trend in their element abundances with minor differences compared to the metabasites. The late gabbros show a tholeiitic composition at SiO_2 around 45 wt%. The volcanics are also chemically different from all other (meta)igneous rocks. They are rich in Na, Fe, and HFSE, and low in Al and Ca at a restricted SiO_2 range (mostly between 52 and 55 wt%) compared to the calcalkaline rocks. Even considering a possible influence of alteration on the

mobile elements in the volcanic rocks, they are not related to any other rock unit of the area.
In all rock types including volcanics and gabbros Sr isotope ratios are low (< 0.7040) and REE distribution patterns are flat (La/Yb typically between 2-3 for most samples). We suggest magmas from the upper mantle as the major component in all rocks.

REGIONAL IMPORTANCE OF THE RESULTS

The composition of the crust from a deep section of the arc as outlined above might be representative for the upper 20 km of the present crustal profile in the Coast Range. Geophysical data of the gravity field and the seismic velocities from a north-south profile (20-26°S) in the Coast Range prove the existence of abundant high density mafic rocks (2850-3000 kg m^{-3}) in the upper 5 - 22 km of the crust (Strunk, 1990 and references therein). In E-W direction the high density rocks are restricted to the Coast Range, but they extend over at least 600 km in N-S direction. No major parts of typical continental crust are obvious either in the gravity field or in the distribution of seismic velocities.
A comparision of geochemical data of igneous rocks from the Coastal Cordillera shows striking similarities between data from the literature and our data. The volcanic rocks are not related to any other rock unit on the regional scale.

PROBLEMS

Replacement of the continental crust by prevailing basic intrusions and their metamorphic equivalents at midcrustal levels requires a considerable stretching and thinning of the crust. The intrusion mechanism must have prevented contamination of the basic magmas by a crustal component, and therefore magmatic underplating is preferred. The regional distribution of high density rocks in the upper crust from geophysical data suggest extension normal to the continental margin plate boundary. Typical tectonic settings for large scale plutonism and volcanism are those of continental extension and rifting. Locations with extension normal to the plate boundary at active continental margins are back arc basins (e.g. Aguirre et al., 1989 for the Cretaceous volcanism in the Andes) or the magmatic arc itself (Scheuber&Reutter,1992 for the Jurassic arc of N'Chile). A back arc setting for the Jurassic rocks seems less likely, because there are only minor intercalations of sediments in the volcanic rocks and the volcanic rocks are largely deposited above sea level. Furthermore, we would have to explain where the arc and fore arc region are today. The essential problem is the same for both settings: There is no indication for a widespread distribution or at least important remnants of continental crust in the Coast Range. The complete removal of continental crust by extension of the lithosphere and their replacement by igneous rocks would lead to the special case of continental rifting and spreading caused by extreme thinning of the lithosphere (and crust) in the framework of models considering continuous extension as the only or major tectonic process. Geological settings or chemial compositions of the igneous rocks typical for rift or spreading situations were not found in the area. Recrystallization of the early intrusions , their spatial relationship to the volcanic rocks and the chemical differences between volcanic rocks and the metabasites exclude a contemporaneous

development of the rocks at the same geographical position (thrust tectonics can be excluded). Therefore uplift and erosion of the Coastal Cordillera is required before deposition of the volcanics and before the emplacement of at least some of the late intrusive rocks. The cause and exact timing of this hypothetical event and its relation to the subduction process is yet unclear.
We are working on thermal models of the arc crust with the given data and attempting to obtain age relations of the early history of the Jurassic arc by additional radiometric dating with the aim of testing various hypotheses of the magmatic and tectonic history of the arc crust.

REFERENCES

Aguirre, L., Levi, B. & Nyström, J.O. (1989) The link between metamorphism, volcanism and geotectonic setting during the evolution of the Andes; in: Geological Society Special Publication No.43, pp.223-232

Lucassen, F. & Franz, G. (1992) Generation and metamorphism of new crust in magmatic arcs: a case study from northern Chile, Terra Nova, 4, 41-52.

Strunk, S. (1990) Analyse und Interpretation des Schwerefeldes des aktiven Kontinentalrandes der zentralen Anden (20°-26° S), Berliner Geowissenschaftliche Abhandlungen, Reihe B, Band 17, Berlin 1990

Scheuber, E. & Reutter, K.-J. (1992) Magmatic arc tectonics in the Central Andes between 21° and 25° S, Tectonophysics, 205, 127-140

CRUSTAL GROWTH AND REWORKING ALONG THE ANTARCTIC PENINSULA: AN ISOTOPIC APPROACH

A. J. MILNE[1,2], M. J. HOLE[3] and I.L. MILLAR[4]

1 British Antarctic Survey, High Cross Madingley Road, Cambridge, CB3 0ET
2 Shell International Petroleum, Maatschappij, PO Box 162, 2501 AN 'sGravenhage, The Netherlands.
3. Dept. of Geology and Petroleum Geology, University of Aberdeen, Meston Building, Aberdeen, AB9 2UE.
4. British Antarctic Survey, High Cross Madingley Road, Cambridge, CB3 0ET

RESUMEN

Se Compara las características de isotopes de Nd y las edades modeladas ("model ages") de rocas igneas relacionadas a subducción de la Peninsula Antarctico, a datos publicados de la Cordillera Andina. Se relaciona variaciónes en las edades modeladas, en tiempo y tambien en espacio, a la evolución tectonica de partes diferentes del margin pacifico de Gondwana, anteriormente conjuntadas.

Antarctic Peninsula, subduction-related magmatism, neodymium isotopes, model ages.

Introduction

Continental destructive plate margins are the most important sites of continental crustal growth in the geological record. During subduction-related magmatism, a variety of different geochemical reservoirs may be tapped, and it is generally accepted that subduction-related magmas may contain contributions from depleted mantle, continental crust, variably enriched continental lithospheric mantle, subducted terriginous and pelagic sediments, and the products of slab de-watering. Variable amounts of interaction between the above geochemical reservoirs leads to the geochemical diversity of magmas erupted at active continental margins. However, because some of the above components have similar trace element and isotopic characteristics (e.g. terriginous sediment derived from subduction-related granitoids) determining the contributions from each component may be problematical.

Neodymium isotope systematics, and in particular neodymium 'model ages' have been utilised by a number of workers to give a broad overview of the relative contributions from depleted mantle and crust to magmas during arc evolution, and to separate paeriods of intracrustal re-working from the growth of new crust from the mantle (e.g. DePaolo, 1981; Miller & Harris, 1989).

In this study, we investigate temporal and spatial variations in the Nd-isotope characteristics of arc-related rocks from the Antarctic Peninsula, which was the site of almost 200 Ma of continuous subduction-related magmatism and formed part of the Pacific margin of Gondwana. Previously published geochronological and elemental data along with new isotopic data allow the identification of intrusive rocks which were generated from depleted mantle sources as well as material which clearly represents anatectic melts of pre-existing crustal rocks. The relative contributions of depleted mantle and lithosphere to magmatism can therefore be assessed. We present 83 previously unpublished Nd-isotope analyses supplemented by 50 published analyses of a variety of arc rocks, including pre-subduction gneissose basement, metasedimentary and sedimentary rocks from the accretionary prism complex and back-arc basin and post-subduction alkali basalts. From this data, and by comparison with published analyses for the central Andes, we demonstrate that similar processes of magmagenesis involving similar source compositions (depleted mantle and continental crust), occurred in different parts of the supposedly contiguous Pacific margin of Gondwana but at different times.

Geochronology.

The majority of the exposed geology of the Antarctic Peninsula can be accounted for by processes related to easterly-directed subduction of oceanic crust beneath the peninsula from during the Mesozoic and Cenozoic. Geochronological studies on undeformed granitoids record more than 200 Ma of subduction-related magmatism in parts of the Antarctic Peninsula (Pankhurst, 1982). The oldest reliably dated rocks in the area are mid-Palaeozoic granitoids which have yielded isochrons indicating emplacement at 408 8 Ma (Milne & Millar 1989). Occurrences of migmatitic gneisses do not yield a well-constrained age, but their Sr-isotope characteristics are suggestive of formation at around 600 Ma (Hole et al., 1991). Carboniferous granitoids are also known, and there is some evidence to suggest that subduction may have occurred for at least part of the Palaeozoic (Milne & Millar 1989). However, the most volumetrically important rocks exposed are Late Triassic (c. 214 Ma) to Tertiary (c. 48 Ma) plutonic and extrusive rocks (Pankhurst et al., 1988).

The oldest known sedimentary rocks in the region are the paragneisses of central eastern Graham Land, which were metamorphosed to amphibolite grade during the Carboniferous (Milne & Millar 1989). During the Mesozoic, sedimentation occurred in both fore-arc and back-arc settings as well as in the accretionary prism complex. Accretionary prism metasedimentary rocks of the Trinity Peninsula Group are thought to be Permo-Triassic in age, and back-arc sedimentation in the James Ross Island area was intiated during the Middle-Late Cretaceous.

Nd-isotope systematics of crust and mantle: Model ages

The most commonly used Nd-model age (T_{DMUR}:depleted mantle uniform resevoir) is based on the period of time since the elemental Nd in a sample was last in isotopic equilibrium with an assumed depleted mantle source region. Thus, if the model age of a sample is the same as its stratigraphic age (time of emplacement for granitoids), then it must be have been derived from depleted mantle at that time, whereas a model age that is significantly greater than the stratigraphic age (as is the case for the majority of subduction-related granitoids) implies that intracrustal processes may have been important during the formation of that sample; the greater the discrepancy between the model and stratigraphic ages, the greater the likely importance of intracrustal processes and the longer the 'crustal residence time' of that sample.

It has recently been noted by a number of workers that during the fractional crystallisation of granitic rocks, minor phases such as allanite, zircon and monazite may cause significant fractionation of the REE, often resulting in increasing Sm/Nd ratios with increasing degree of fractionation (e.g. Miller & Harris, 1989; Pimentel & Charnley 1991). This is clearly a major problem in calculating model ages and prevents the projection of $^{143}Nd/^{144}Nd$ ratios beyond the stratigraphic age of the sample. Miller & Harris (1989) circumvented this problem of "resetting" of model ages during magmatic fractionation by calculating the model age of silicic rocks using an assumed average crustal Sm/Nd ratio of 0.19. Here, we have refined this method of back calculation by using the present-day Sm/Nd ratio of acid rocks to calculate the $^{143}Nd/^{144}Nd$ ratio at the time of emplacement (i.e. the initial $^{143}Nd/^{144}Nd$ ratio), and from that point back to the growth line for DMUR, $^{143}Nd/^{144}Nd$ ratios are calculated using the average crustal $^{147}Sm/^{144}Nd$ ratio of 0.12, approximately equivalent to an Sm/Nd ratio of 0.2.

Temporal variations in Nd-isotope geochemistry.

The variation in $^{143}Nd/^{144}Nd$ (expressed as εNd_t) through the Phanerozoic for Graham Land is presented in Fig. 1. Samples from Graham Land define a 'U'-shaped trend between 420 Ma and the present-day. Between 290 and 150 Ma, all samples have εNd_t more negative than -2.0. However, both before and after this period samples have positive εNd_t values and there are clear trends of decreasing εNd_t from 420 Ma to 180 Ma and increasing εNd_t from 180 Ma to the present day. The model age at time of emplacement (MATE) is the difference between calculated two-stage model ages and known stratigraphic age. In Fig. 2. MATE is plotted against stratigraphic age. On this diagram any rock derived soley from depleted mantle will plot on the x-axis, as the effect of mantle evolution through Phanerozoic time is removed. The model age of the Nd in an individual sample at the time of emplacement is the best estimator of the relative contributions from depleted mantle and crust during magmagenesis. A low MATE value indicates limited

involvement of significantly older continental lithosphere during the genesis of an individual sample, whereas a high MATE value gives a minimum model age of the re-worked continental crust.

What is apparent from this study is that the influence of a crustal source-region increased throughout the late Palaeozoic upto a maximum in the Middle Jurassic. It is also clear that the greatest influence from depleted mantle i.e. samples with the youngest model ages (MATE=0.3-0.7 G.y.), occurred during the mid-Palaeozoic and Tertiary, culminating in the eruption of the Late Cenozoic (7-0.1 Ma) post-subduction alkali basalts. Therefore, the most important periods of formation of new crust from depleted mantle were during the late Paleaozoic and Tertiary, whereas during the Late Triassic and Middle Jurassic magmas underwent significant interaction with pre-exisitng crustal sources. These differences appear to be controlled by large-scale tectonic processes. A period of steep slab dips and associated intra-arc extension during the late Creataceous resulted in the generation of granitoids from dominantle deplteds sources, whereas shallower slab-dips in Triassic-Jurassic times resulted in a broad shallow zone of partial melting in the mantle wedge which may may have provided far greater potential for crust-mantle interactions.

Miller & Harris (1989) showed that during the late Palaeozoic, orogenesis in the Central Andes was predominantly by intracrustal re-working. During the Jurassic, a change in tectonic style resulted in the onset of crustal growth before a return to predominantly intracrustal processes in the last 30 Ma. This is illustrated in Fig. 2. Some notable features of this diagram are that both the maximum crustal residence times, and range in residence ages, are broadly similar for the Antarctic Peninsula and Central Andes. A major difference between the two regions is that the maxima of crustal growth and intracrustal reworking appear to have occurred at different times, and so the evolution trends appear to be 'out of phase'.

Clearly, the significant differences in the timing of intracrustal reworking along the Pacific margin of Gondwana, suggests that although the Andes and Graham Land may have been a contiguous arc at that time, tectonic processes were diachronous along its length, and as at the present-day, along-arc variations in the age, thermal structure and angle of dip of the subducting lithospheric slab may show considerable variations along a single continental convergent plate margin. Indeed, Miller & Harris (1989) suggested that crustal growth at continental margins may progessively decelerate during arc evolution. This conclusion is in contrast to the Antarctic Peninsula where crust growth clearly accelerated with arc maturity.

References

DEPAOLO, D. J. 1981. Neodymium isotopes in the Colorado Front Range and crust-mantle evolution in the Proterozoic. *Nature*, **291**, 193-196.

HOLE, M.J., PANKHURST, R.J. & SAUNDERS, A.D., 1991. The geochemical evolution of the Antarctic Peninsula magmatic arc: the importance of mantle-crust interaction during granitoid genesis. *In:* THOMSON M.R.A., CRAME, J.A. & THOMSON J.W. (eds). *The geological evolution of Antarctica.* Cambridge University Press, Cambridge, 369-74.

MILNE A.J. & MILLAR I. L., 1989. The significance of mid-Paleozoic basement in Graham Land, Antarctica, *Journal of the Geological Society, London*, **146**, 207-210, 1989.

MILLER, J. F. & HARRIS, N. B. W., 1989. Evolution of continental crust inthe Central Andes; constraints from Nd isotope systematics. *Geology*, 615-17.

PANKHURST, R. J., 1982. Rb-Sr geochronology of Graham Land, Antarctica. *Journal of the Geological Society, London*, **139**, 701-11.

PANKHURST, R.J., HOLE, M.J. & BROOK, M., 1988. Isotope evidence for the origin of Andean granitoids. *Philosophical Transactions of the Royal Society, Edinburgh: Earth Sciences*, **79**, 123-33.

PIMENTEL, M.M. & CHARNELY, N. 1991 Intracrustal REE fractionation and implications for Sm-Nd model age calculations in late-stage grnaitic rocks: and example from Brazil. *Chemical Geology (Isotope Geoscience Section)*, **86**, 123-138.

Fig.1

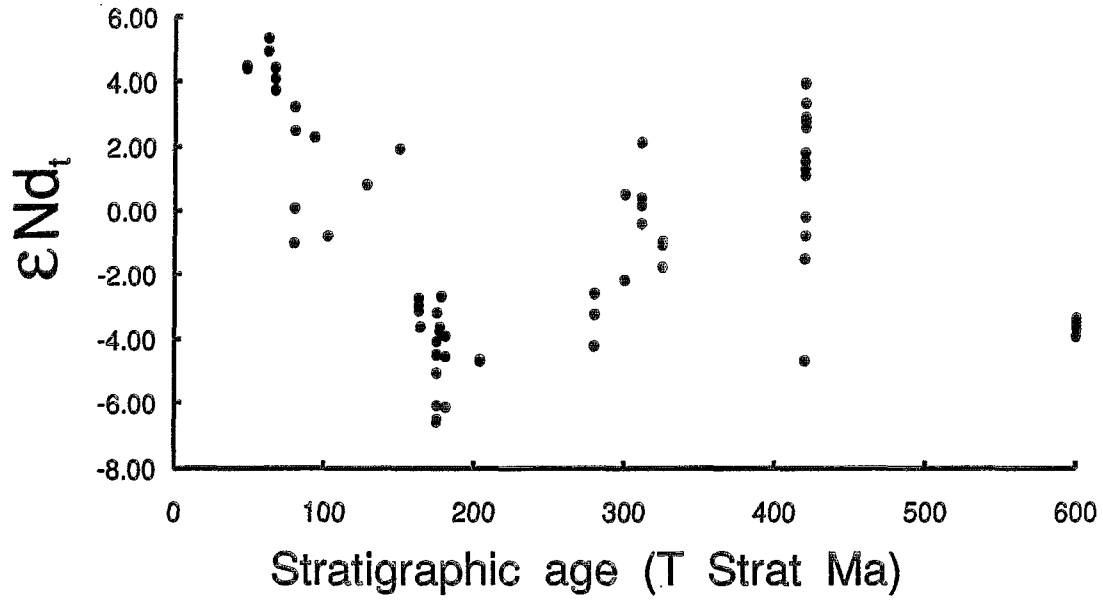
6.00
4.00
2.00
0.00
-2.00
-4.00
-6.00
-8.00
εNd$_t$
0
100
200
300
400
500
600
Stratigraphic age (T Strat Ma)

Fig.2

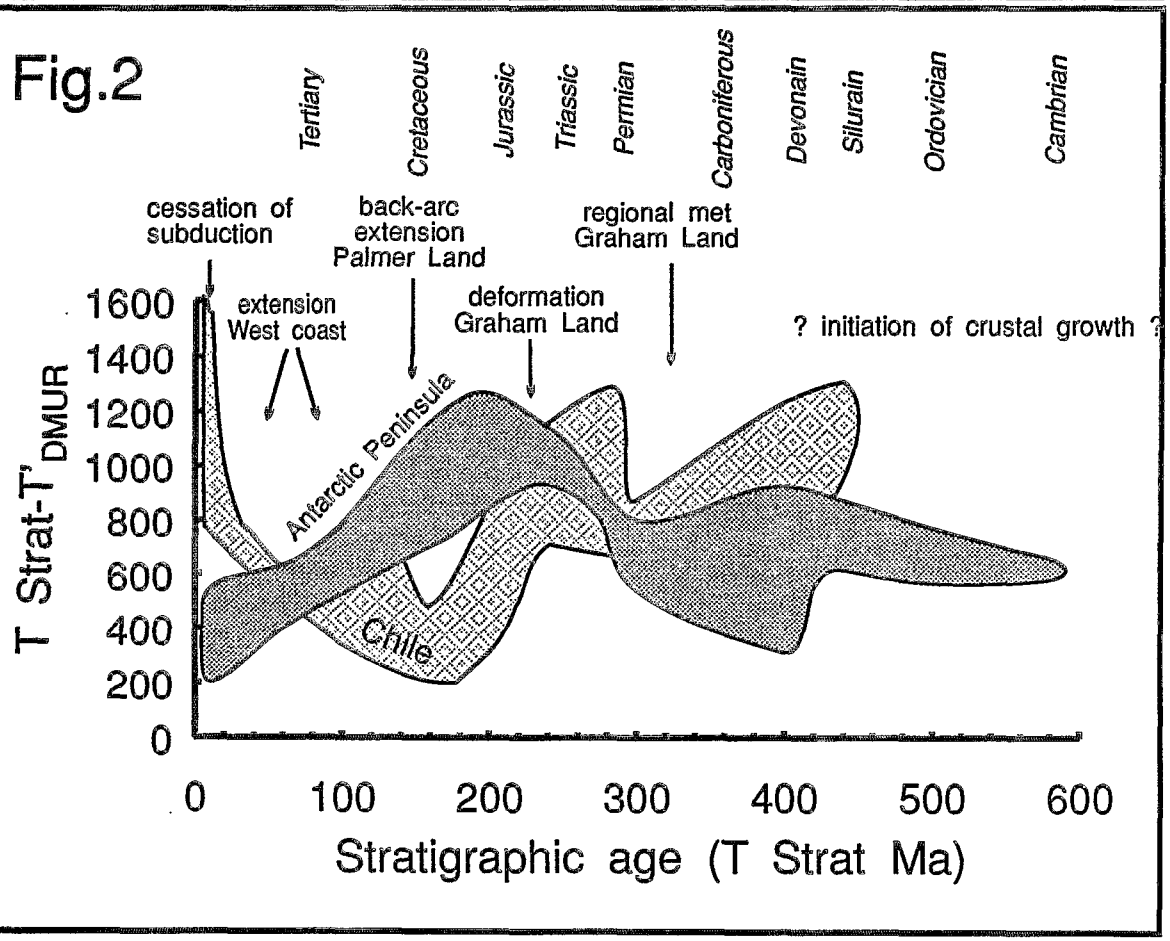
Tertiary
Cretaceous
Jurassic
Triassic
Permian
Carboniferous
Devonain
Silurain
Ordovician
Cambrian
cessation of subduction
back-arc extension Palmer Land
regional met Graham Land
extension West coast
deformation Graham Land
? initiation of crustal growth ?
Antarctic Peninsula
Chile
1600
1400
1200
1000
800
600
400
200
0
T Strat-T'DMUR
0
100
200
300
400
500
600
Stratigraphic age (T Strat Ma)

ADVANCES IN GEOTHERMAL RESEARCH IN CHILE

Miguel MUÑOZ

Departamento de Geofísica, Universidad de Chile, Casilla 2777, Santiago, Chile.

RESUMEN: Los geoindicadores Na, K, Mg and Ca indican un mayor grado de equilibrio fluido-roca en áreas termales del Norte de Chile que en las del Centro-Sur. Por otra parte, se presentan resultados de la producción radiogénica de calor y de la estructura termal en Chile Central, y su relación con la derivación magmática de granitoides.

KEY WORDS: Chile: Mature/Immature Fluids; Heat Production; Thermal Structure of the Crust.

FLUID-ROCK EQUILIBRIUM IN GEOTHERMAL AREAS

Evaluation of fluid-rock equilibrium in 33 geothermal areas and in the Santiago Basin was carried out by means of the relative Na, K, Mg and Ca contents of waters, and following the method established by Giggenbach (1988). In northern Chile only in two of eight geothermal areas fluids have attained a partial or a full equilibrium with both K-Na and K-Mg mineral systems; a partial equilibrium is also indicated for seven of twenty hot springs waters in central-south Chile (Table 1). Other geothermal areas correspond to immature waters which are generally unsuitable for the evaluation of K/Na and K/Mg equilibrium temperature; in these cases also CO_2-fugacities cannot be obtained.

TABLE 1. Full equilibrium or partial equilibrium temperatures in geothermal areas of Chile as indicated by the K/Mg and K/Na geothermometers.

Area	Latitude Longitude	T(K/Mg) (°C)	T(K/Na) (°C)
Northern Chile			
Puchuldiza	19°08'S 68°58'W	135-195	192-235
El Tatio (springs)	22°20'S 68°01'W	145-245	180-250

Area	Latitude Longitude	T(K/Mg) (°C)	T(K/Na) (°C)
El Tatio (wells)	22°20'S 68°01'S	165-285	165-285
Central-South Chile			
Apoquindo	33°25'S 70°25'W	80	140
Baños de Colina	33°48'S 70°00'W	120	180
Baños Morales	33°50'S 70°03'W	100	140
Vegas del Flaco	34°57'S 70°28'S	150	245
San Pedro	35°08'S 70°27'W	195	245
Campanario	35°56'S 70°33'W	125	195
Pemehue	38°03'S 71°44'W	115	180

Correlation between molecular Cl/B ratio and Na-K-Ca temperature (Youngman, 1984) is generally consistent with indications of fluid-rock equilibrium in different aquifers of El Tatio. Isotopic analysis of El Tatio waters and results from magnetotelluric soundings in the area -studies carried out by other workers- have been also used to reexamine the length of fluids circulation path by considering the *transparency* of magma (Lachenbruch and Sass, 1977) through hydrothermal convection; the actual distance travelled by the water may be estimated to be 20 Km, at a rate of about 1.3 Km/year.

Chillán (36°57'S; 71°33'W) and Río Blanco (38°35'S; 71°42'W) plot as immature waters; these are acid sulphate waters characterized by high temperatures at depth (170°C-240°C). In the Santiago Basin -in areas at about 33°20'S; 70°50'W- evaluation of fluid-rock equilibrium indicates that waters are immature; if K/Mg temperatures were still valid, deeper equilibrium temperatures may be of about 80°C.

HEAT PRODUCTION AND THERMAL STRUCTURE OF THE CRUST

The radiogenic surface heat production has been preliminary determined in the three tectonic units of Central Chile (33°S), ranging from the Coastal Range to the Andes Cordillera (Table 2).

TABLE 2. Preliminary thermal parameters in Central Chile batholiths. Q: surface heat flow; N: number of samples for heat production measurements; A_0 : mean surface heat production; A_0*: mean surface heat production of the uneroded crust; D: depth parameter of distribution of radiogenic elements. (Q value in brackets is an assumed value)

	Age (10^6 years)	Q (mWm^{-2})	N	$A_0 \pm \sigma$ ($\mu W m^{-3}$)	A_0* ($\mu W m^{-3}$)	D (Km)
Coastal Batholith	336	(63.0)	7	1.45±0.74	6.56	17.4
Central Batholith	101	78.7	4	1.20±0.62	7.04	26.2
Andean Batholith	41	60.7	6	1.87±0.36	7.16	13.0

Because of the few number of measurements depth parameter D is not well determined. Particularly, low mean radiogenic heat production in the Central Batholith and high measured heat flow allows for a very great value of D. The crustal temperatures of Central Chile were determined by considering the one dimensional heat conduction equation and assuming steady state conditions, and making use of the values given in Table 2. Some of the temperature distributions encountered show the possibility of partial fusion at the Moho level. The highest degree of partial fusion is shown for the Central Batholith; also, preliminary seismic velocity models of this region are showing low velocities in the lower crust, and increasing towards the Andes Cordillera.

It is not possible to fit a trend between SiO_2 contents and surface heat production in the case of Central Chile batholiths. This is similar to what has been observed in data of Sierra Nevada - United States (Tilling et al., 1970). Eastward variations in chemical composition and distribution of rare earth elements indicate that if Central Chile granitoids are derived from magmas of andesitic composition they are also not genetically related to the subducted Nazca plate tholeiitic basalts (López-Escobar, 1974). Similar conclusions have been put forward also for the Sierra Nevada igneous rocks which should envolve derivation from lower crustal and continental upper mantle sources.

The west to east migration of magmatic foci with time and the derivation of granitoids in Central Chile may be related to the change of subduction topology, the rate of tectonic erosion and to the thermal state of the crust. Erosion rates resulting from radiogenic heat production (Table 2) are shown in Table 3, and compared with rates inferred by Scholl et al. (1970) found by considering similar terranes and climates elsewhere in the world and for the last 25 million years -larger denudation rates correspond to glacial periods.

TABLE 3. Erosion rates - Central Chile batholiths.

	(from Heat Production) ($cm/10^3y$)	(from Scholl et al. (1970) ($cm/10^3y$)
Coastal batholith	7.8	1-5
Central batholith	45.9	
Andean batholith	42.7	2-10-80

CONCLUSIONS

Degree of fluid-rock equilibrium is higher for some areas in northern Chile than in the central-south region. In northern Chile, besides the extrusive type of magmatic activity, it is possible to distinguish a developed intrusive type -like in El Tatio- leading to the genesis of larger geothermal areas with fluids circulating through longer horizontal paths in the crust.

In Central Chile (33°S), in zones of the Central and Andean batholiths, the lower crust may be in a state of partial fusion. Distribution of radiogenic elements, changes in the topology of subduction and tectonic erosion rates are important to establish the derivation of granitoids and the geological history of arc magmatism. Thermal stresses due to temperature differences at different levels in the crust from the Coastal Range to the Andes Cordillera may produce seismic activity with foci in the crust.

REFERENCES

GIGGENBACH, W.F., 1988. Geochim. Cosmochim. Acta, **52**:2749-2765.

LACHENBRUCH, A.H. and SASS, J.H., 1977. In: J.G. Heacock (Editor), The Earth's Crust. AGU Geophys. Monogr., **20**: pp. 626-675.

LOPEZ-ESCOBAR, L., 1974. Plutonic and Volcanic Rocks from Central Chile (33°-42°S): Geochemical evidence regarding their petrogenesis. Ph.D Thesis, MIT, 270 pp.

SCHOLL, D.W., CHRISTENSEN, M.N., VON HUENE, R. and MARLOW, M.S., 1970. Geol. Soc. Amer. Bull., **81**, 1339-1360.

TILLING, R.I., GOTTFRIED, D. and DODGE, F.C.W., 1970. Geol. Soc. Amer. Bull., **81**, 1447-1462.

YOUNGMAN, K. J., 1984. Hydrothermal Alteration and Fluid-Rock Interaction in the El Tatio Geothermal Field, Antofagasta Province, Chile. Ms. Sc. Thesis, University of Auckland, 123 pp.

Sr–Nd ISOTOPE COMPOSITIONS OF CRETACEOUS TO MIOCENE VOLCANIC ROCKS IN CENTRAL CHILE: A TREND TOWARDS A MORB SIGNATURE AND A REVERSAL WITH TIME

Jan Olov NYSTRÖM[1], Miguel A. PARADA[2], and Mario VERGARA[2]

[1] Swedish Museum of Natural History, S-10405 Stockholm, Sweden
[2] Departamento de Geología, Universidad de Chile, Casilla 13518, Santiago, Chile

RESUMEN: Las razones isotópicas de Sr–Nd de las rocas volcánicas de la Cordillera de la Costa y de los Andes de Chile central entre 32°30' y 34°30'S muestran una tendencia hacia el campo del MORB desde el Cretácico inferior hasta el límite Oligoceno–Mioceno, y de ahí en adelante un alejamiento hacia los valores del volcanismo Cuaternario, mientras que en el sector entre 26° y 32°30'S el cambio sucede en el Cretácico; en ambos sectores los valores de las rocas volcánicas y plutónicas de la misma edad son similares.

KEY WORDS: Central Chile, volcanic, plutonic, Sr–Nd isotopes, Cretaceous, Tertiary

INTRODUCTION

The studies of Sr–Nd isotope compositions in the Andes of central Chile deal mainly with Quaternary volcanic rocks (e.g. Hildreth & Moorbath, 1988), Tertiary volcanics in the High Andes near the Argentinian border (e.g. Kay et al., 1991) and plutonic rocks (e.g. Brook et al., 1986). Here we present Sr–Nd isotope data for Cretaceous to mid–Miocene lavas from central Chile (46 samples; Fig. 1) with emphasis on the Santiago region (33°30'S), and describe a systematic trend towards and then away from a MORB signature with time.

GEOLOGICAL SETTING

Central Chile between 26° and 34°30'S extends across three tectonic segments: a non–volcanic zone and the end portions of the Central and Southern Volcanic Zones. Within this region Mesozoic volcanic rocks form two parallel longitudinal belts with successively younger units towards a central axis, i.e. a western belt in the Coast Range and an eastern one in the High Andes. The Mesozoic volcanism was mainly of high–K calc–alkaline to shoshonitic character except in the northernmost part of the region where less potassic types dominate (Levi et al., 1988). Oligocene to early Miocene calc-alkaline volcanics of tholeiitic affinity (Abanico Formation), overlain towards the east by mid–Miocene calc–alkaline volcanics (Farellones Formation), occur between the two Mesozoic belts in the south, while similar volcanic units show progressively older ages (up to Late Cretaceous) towards the north, where the Tertiary volcanics are found east of the Mesozoic belts. The Quaternary volcanoes are likewise situated east of (CVZ), or above (SVZ) the eastern belt.

RESULTS

In the southern part of the studied region (32°30' – 34°30'S) the initial $^{87}Sr/^{86}Sr$ ratios of the volcanic rocks decrease and the ε_{Nd} values increase with time from the Early Cretaceous to the Oligocene–Miocene boundary, constituting a trend towards MORB values, regardless of whether the samples come from the Coast Range (Fig. 1A, fields f→ e→ d) or the High Andes (g→ c/e overlap→ d); thereafter the trend reverses with eruption of successively more evolved compositions up to the present (d→ c→ b→ a). The scarce data for granitoids in this area coincide with the results for coeval volcanic rocks (Stern & Puig, 1991; Skewes, 1992). The early Miocene volcanics are slightly more primitive than the mid–Miocene ones (the lower vs. upper Farellones Formation), and the Early Cretaceous lavas in the Coast Range (Lo Prado Formation) at 33°30'S are more primitive than corresponding lavas at 32°40'S. The volcanic rocks analyzed by us from the northern part of the region plot together with granitoids of the same age (mid–Cretaceous; Fig. 1B).

DISCUSSION

A comparison of our and the published Sr–Nd isotope ratios for the region reveals trends towards and then away from MORB with time both in the south (Fig. 1A) and the north (Fig. 1B). However, the reversal took place earlier in the north (during the mid–Cretaceous; unpublished geochemical data suggest a culmination during the Late Cretaceous). The trend towards MORB in Fig. 1A coincides with the shift in geochemistry of the predominant lava types from high–K calc–alkaline/shoshonitic to calc-alkaline with tholeiitic affinity. The subsequent trend away from MORB up to the present is also in agreement with the geochemistry of the lavas. The late Oligocene to early Miocene Abanico Formation represents the point of reversal. This unit, and the younger less primitive Farellones Formation east of it, formed in a caldera–graben setting; the paleo-geothermal gradient was highest during the deposition of the former (Vergara et al., 1993).

An eastward shift of the volcanic front and a change to less primitive compositions occurred also for the late Miocene to Quaternary volcanics between 32–34°S (Stern & Puig, 1991), and north of 32°30'S during the early to late Miocene (Kay et al., 1991). Towards the north rocks of the same age plot further away from the MORB field than in the south (Kay et al., 1991; Skewes et al., 1991); however, differences in longitude might also be a contributing factor. The eastward shift has been explained by a flattening of the subduction angle leading to increased contamination in a thicker crust (Kay et al., 1991), and/or an increase in subduction erosion resulting in a larger contribution of subducted terrigenous sediments in the magmas (Stern, 1991).

The trend towards more primitive compositions from the Cretaceous to the Oligocene might be due to a combination of factors: magma generation in a progressively more depleted mantle, and a decrease in 'fertility' of the lower crust that became more refractive due to successive magmatic events (cf. Parada et al., 1992). This is consistent with upwelling of asthenospheric mantle and an extensional regimen as suggested by Levi et al. (1988) for this region. The rather primitive nature of the Abanico lavas indicates minimal crustal contribution, which is supported by the isotopic uniformity of the samples (Fig. 1A) and very similar values for ignimbrites (not treated here) and intermediate to basic lavas. We suggest therefore that the Abanico rocks formed during en episode of rapid mantle upwelling and crustal thinning.

Acknowledgements. We thank FONDECYT projects 1234 (M.A.P.) and 1223 (M.V.) for economic support.

REFERENCES

Brook, M., Pankhurst, R.J., Shepherd, T.J. & Spiro, B., 1986, Andean geochronology and metallogenesis. Overseas Development Administration, London, Open File Rept., 137 p.

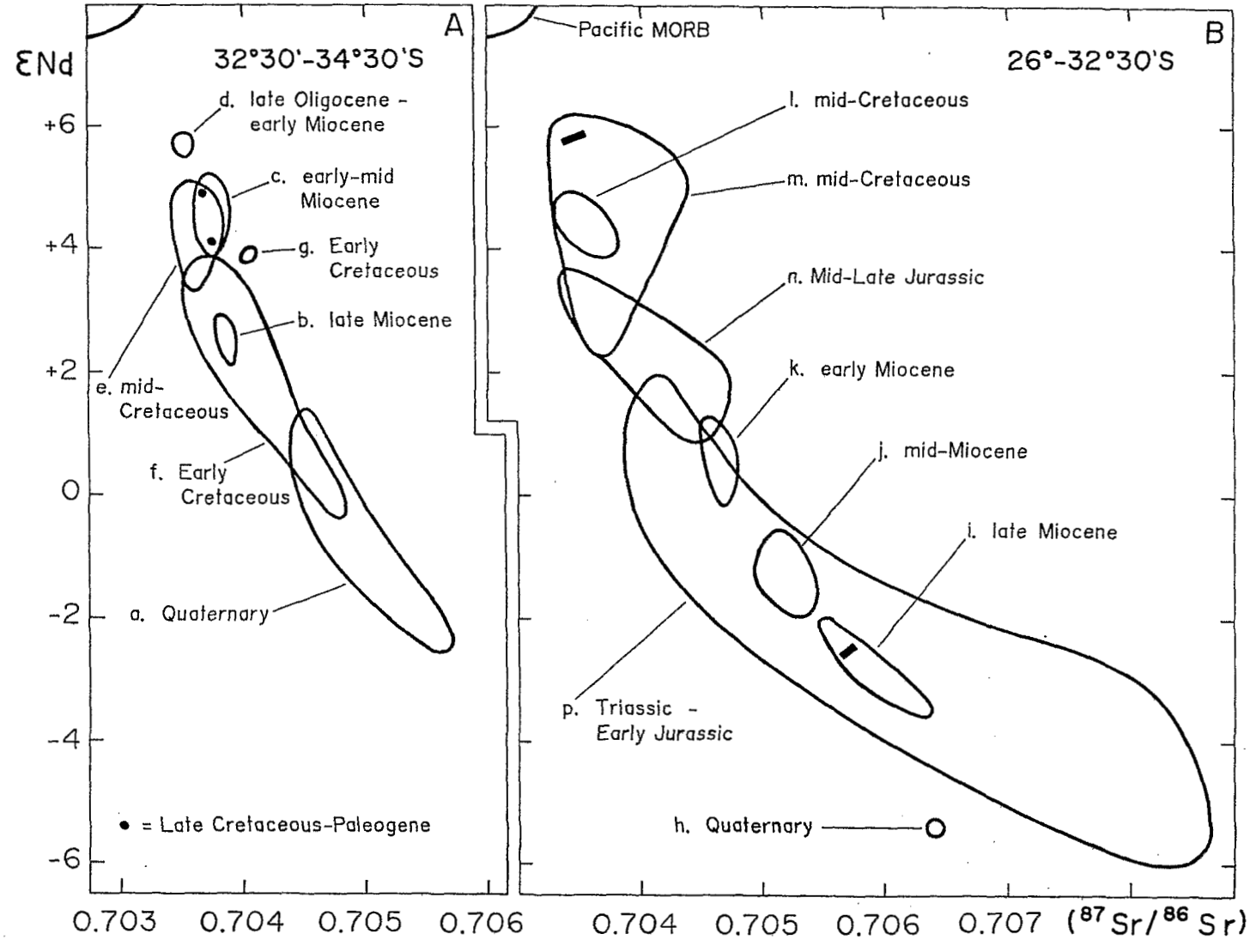
εNd
A
32°30'-34°30'S
d. late Oligocene - early Miocene
c. early-mid Miocene
g. Early Cretaceous
b. late Miocene
e. mid-Cretaceous
f. Early Cretaceous
a. Quaternary
• = Late Cretaceous-Paleogene
+6
+4
+2
0
-2
-4
-6
0.703
0.704
0.705
0.706
Pacific MORB
B
26°-32°30'S
l. mid-Cretaceous
m. mid-Cretaceous
n. Mid-Late Jurassic
k. early Miocene
j. mid-Miocene
i. late Miocene
p. Triassic - Early Jurassic
h. Quaternary
0.704
0.705
0.706
0.707
(87Sr/86Sr)i

Futa, K. & Stern, CR., 1988, Sr and Nd isotopic and trace element compositions of Quaternary volcanic centers of the southern Andes. *Earth Planet Sci. Lett.* **88**, 253–262.

Kay, S.M., Mpodozis, C., Ramos, V.A. & Munizaga, F., 1991, Magma source variations for mid–late Tertiary magmatic rocks associated with a shallowing subduction zone and a thickening crust in the central Andes (28 to 33°S). *In:* Harmon, R.S. & Rapela, C.W. (eds.) *Andean magmatism and its tectonic setting, Geol. Soc. Amer. Spec. Paper* **265**, 113–137.

Hickey, R.L., Frey, F.A., Gerlach, D.C. & López–Escobar, L., 1986, Multiple sources for basaltic arc rocks from the Southern Volcanic Zone of the Andes (34°–41°S): trace element and isotopic evidence for contributions from subducted oceanic crust, mantle, and continental crust. *J. Geophys. Res.* **91**, 5963–5983.

Hildreth, W. & Moorbath, S., 1988, Crustal contributions to arc magmatism in the Andes of central Chile. *Contrib. Mineral. Petrol.* **98**, 455–489.

Levi, B., Nyström, J.O., Thiele, R. & Åberg, G., 1988, Geochemical trends in Mesozoic–Tertiary volcanic rocks from the Andes in central Chile, and tectonic implications. *J. South Amer. Earth Sci.* **1**, 63–74.

Parada, M.A., Nyström, J.O. & Levi, B., 1992, Variaciones en las fuentes magmáticas con el tiempo: evidencias geoquímicas e isotópicas en el plutonismo andino paleozoico y mesozoico. *VIII Congreso Latinoamericano de Geología, Salamanca* **4**, 200–203.

Skewes, A., 1992, Miocene and Pliocene copper–rich breccias from the Andes of Central Chile (32–34°S). Ph. D. Thesis, University of Colorado, 216 p.

Skewes, M.A., Stern, C.R., Holmgren, C., Contreras, A., Godoy, S., Vela, I. & Rivano, S., 1991, Evolución magmática cerca del borde sur del segmento de bajo ángulo de subducción en Chile Central (32–34°S). *VI Congreso geológico chileno*, 146–148 (extended abstract).

Stern, C.R., 1991, Role of subduction erosion in the generation of Andean magmas. *Geology* **19**, 78–81.

Stern, C. & Puig, A., 1991, Geochemical evolution of magmatic rocks in the vicinity of El Teniente copper deposit (34°S), central Chilean Andes. *VI Congreso geológico chileno*, 265–267 (extended abstract).

Vergara, M., Levi, B. & Villarroel, R., 1993, Geothermal–type alteration in a burial metamorphosed volcanic pile, central Chile. *J. metamorphic Geol.* **11** (in press).

Walker, J.A., Moulds, T.N., Zentilli, M. & Feigenson, M.D., 1991, Spatial and temporal variations in volcanics of the Andean Central Volcanic Zone (26–28°S). *In:* Harmon, R.S. & Rapela, C.W. (eds.) *Andean magmatism and its tectonic setting, Geol. Soc. Amer. Spec. Paper* **265**, 139–155.

Fig. 1. Plot of ε_{Nd} versus $^{87}Sr/^{86}Sr$ for Triassic to Quaternary igneous rocks from central Chile showing a trend towards a MORB signature with time, up to the Oligocene–Miocene boundary in the south (= A) and to the Cretaceous in the north (= B); from there on up to the present the compositions became successively less primitive. All the fields except m, n and p in B represent lavas (m–p = granitoids); number of samples within parenthesis; fields without references = this study. Field a = Casimiro, Cerro Alto, Maipo, Marmolejo, Tupungatito (13; Hickey et al., 1986; Futa & Stern, 1988; Hildreth & Moorbath, 1988), b = El Teniente area (2; Stern & Puig, 1991), c = Farellones Formation, the High Andes of Santiago (11), d = Abanico Formation, the Andean foothills of Santiago (4), e = Cerro Morado and Ocoa Members (Veta Negra Formation), profiles in the Coast Range at 33°30' and 32°40'S (15), f = Purehue Member (Veta Negra Fm.) and Lo Prado Formation, the same two profiles as above (8), g = Lo Valdés Formation, the High Andes of Santiago (2), h = Tres Cruces (1; Walker et al., 1991), i = Copiapó, Pircas Negras, Vallecito (4; Kay et al., 1991; Walker et al., 1991), j = Cerro de las Tórtolas, Jotabeche (5; Kay et al., 1991), k = Cerro Pulido, Doña Ana, Infiernillo (5; Kay et al., 1991), l = Bandurrias Group, the Coast Range between 28°30' and 30°15'S (4), m = Inca de Oro, Sierra San Juan (5; Brook et al., 1986), n = Cavilolén, Papudo, Quintero (5; Parada et al., 1992), p = Cerros del Vetado, Chañaral, Guamanga, La Ola, (6; Brook et al., 1986). Late Cretaceous to Paleogene lavas in the High Andes of Santiago plot within the overlap of fields c and e (2 samples = dots). The extreme points of the composite of all fields in A are marked with bars in B.

GEOCHEMICAL CONSTRAINTS ON THE EVOLUTION OF THE SOUTHERN PERUVIAN COASTAL BATHOLITH: TOQUEPALA SEGMENT

Richard A. OLIVER [(1)], Nicole VATIN PERIGNON[(2)], Francine KELLER[(2)] & Guido SALAS[(3)]

(1) Institut Laue-Langevin, B.P.156, Avenue des Martyrs, 38042 Grenoble Cedex, France
(2) Laboratoire de geologie, UA 69 CNRS, Université Joseph Fourier, 15, Rue Maurice Gignoux, 38031 Grenoble Cedex, France.
(3) Universidad nacional San Augustin, Casilla 1203, Arequipa, Peru

RESUME

Key words: Batholith, Toquepala, Ilo, Punta Coles, Yarabamba, Quento, REE

INTRODUCTION

The Coastal Batholith of the Western Cordillera in Peru stretchs for some 1600km along the length of the oceanic trench, and has been extensively studied by a number of workers. The southern part of this magmatic structure has been separated into two segments (Arequipa and Toquepala) which have further been subdivided into a number of super units which were emplaced as discreet magmatic pulses. These segments have been studied by several workers (Moore, 1984; Mukaza, 1986*a*, 1986*b*; Boily et al., 1989). This paper presents new geochemical and isotopic data on intrusives from the Toquepala segment and attempts to distinguish the evolution through time of the different super units involved.

GEOLOGICAL SETTING

Three super units make up the Toquepala segment, Punta Coles, Ilo and Yarabamba. The Punta Coles super unit is patchily exposed as intrusions of gabbroic to dioritic plutons mainly lying along the coast and intruding Jurassic volcanic rocks of the Chocolate and Guaneros formations, and rarely rocks of the Precambrian basement. The Ilo super unit, which consists of plutons ranging in composition from tonalite to granodiorite and even some rare granites, cuts the intrusives of the Punta Coles super unit but generally lies further inland where it cuts the same volcanic formations as before. It is often overlain by sediments from the Moquegua formation and the Toquepala volcanics. The Yarabamba super unit lies much further inland and is generally more evolved than the other two, consisting of plutons of granodiorite to granite which have intruded the earlier intrusives of the Arequipa segment , the Jurassic volcanics as well as the sediments of the Late Jurassic to Early Cretaceous Yura Group.

Within these three super units we present data from the Punta Coles, Ilo, Punta de Bonbon, and El Fiscal plutons in the west and the Coalaque and Quento plutons in the east.

GEOCHEMISTRY

Major and trace and REE element data from the six plutons are presented. Multi-element (Figure 1) and REE (Figure 2.) patterns. The multi-element diagrams show an enrichment in the incompatible LIL elements, typical of calc-alkaline rocks. The chondrite normalised REE patterns show enrichment of the light REE and flattening of the heavy REE with small Eu negative anomalies for the more evolved rocks. The exception to this being the older and more basic Punta Coles unit which shows a marked positive Eu anomaly. The patterns indicate an evolution from the oldest (Punta Coles) to the youngest (Quento).

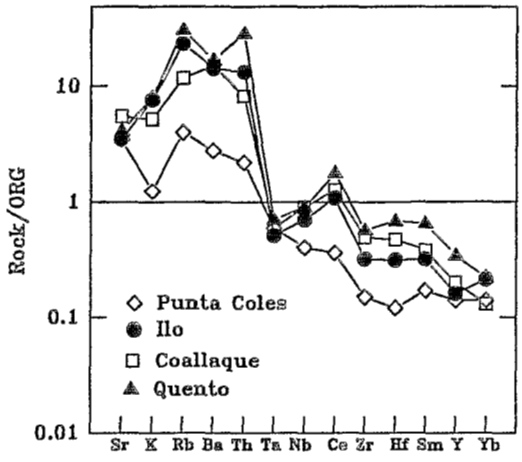

Figure 1. Multi-element diagram of the Toquepala segment.

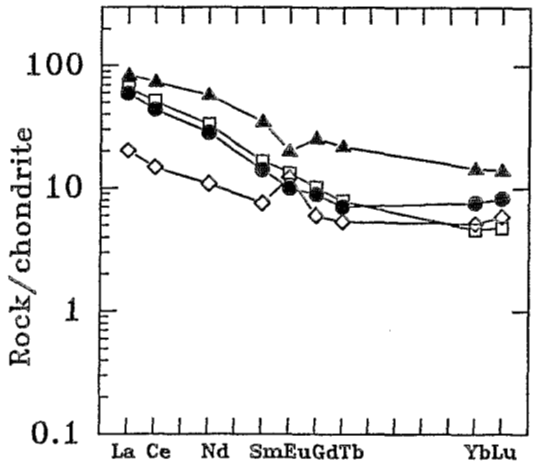

Figure 2. Rare Earth Element patterns for the Toquepala segment

Trace element discriminant diagrams indicate that magmas, from sources close to mantle composition have undergone crystal fractionation with only small amounts of crustal contamination., i.e. Hf/Zr ratios close to mantle values. (Figure 3.)

ISOTOPE GEOCHEMISTRY

Rb/Sr isotope data for the Ilo super unit gives an age of 91.9 ± 9 Ma (Figure 4.). this is somewhat younger than that found by Beckinsale et al., 1985 who give ages of 112 ± 32 Ma. An errorchron of three points for the Quento pluton, the pluton lying the furthest to the east of the investigated plutons, gives an age of 22.8 ±2 Ma (Figure 5.) which classes this pluton, in the Oligocene- Miocene

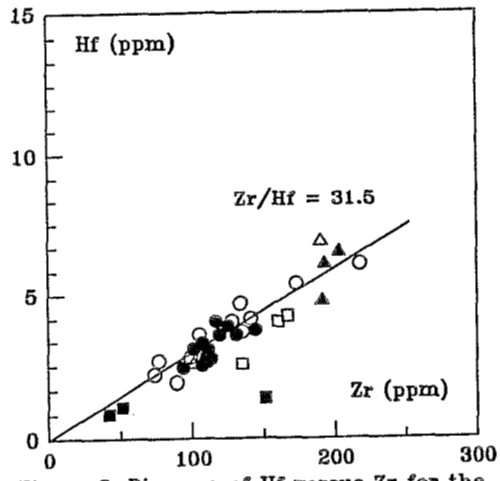

Figure 3. Diagram of Hf versus Zr for the Toquepala segment.

Tacaza group of Sebrier et al.,(1988). $^{87}Sr/^{86}Sr$ ratios are generally more evolved than those reported by Beckinsale et al. (1985) and Boily et al.(1989). Boily et al., (1989) defined three groups for the Arequipa-Toquepala segments from εNdt versus εSrt ratios (Figure 6.).

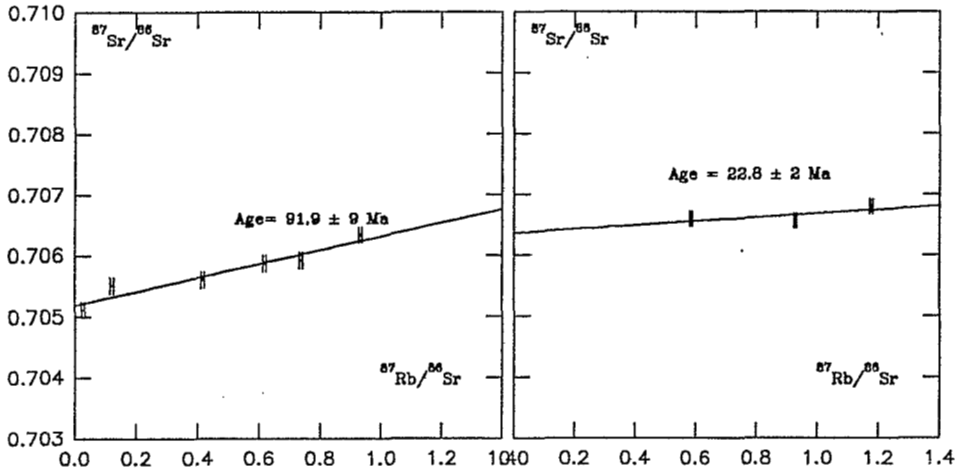

Figure 4. Rb/Sr isochron for the Ilo super unit, Toquepala segment

Figure 5. Rb/Sr errorchron for the Quento pluton,, Toquepala segment

Whilst in general terms the groups occupy roughly the same fields, a major difference occurs with the Punta Coles unit showing a more evolved or contaminated signature in Group 2; Our Group 3 values are from the Quento pluton which could have derived from old, highly enriched mantle or as is more likely, has absorbed deep lying Precambrian crust. Although this must have had a very low Rb/Sr ratio.

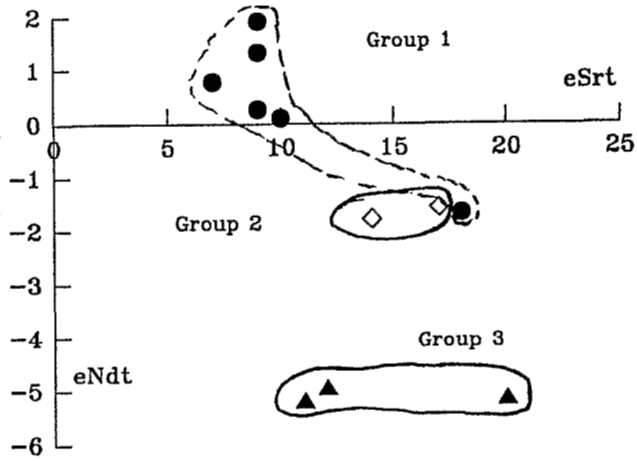

Figure 6. εNdt versus εSrt for the Toquepala segment.

CONCLUSIONS

New geochemical and isotopic data for rocks from the Toquepala segment of the Southern Coastal Batholith, Peru, indicate an evolution through geologic time for the sources of these intrusions. Initial isotopic ratios somewhat higher than previously published data but non the less show the same indications. The Quento pluton outcropping at the head of the Tambo valley appears to be somewhat younger than the rest of the Yarabamba super unit and can be ascribed to the Tacaza group.

REFERENCES:

BECKINSALE R.D.,SANCHEZ-FERNANDEZ A.W.,BROOK M.,COBBING E.J.,TAYLOR W.P. and MOORE N.D., 1985, Rb-Sr whole rock isochron and K-Ar age determinations for the Coastal Batholith of Peru in Magmatism at a Plate Edge, edited by W.S.Pitcher, M.P.ATHERTON, E.J.COBBING and R.D.BECKINSALE, pp 117-202, Blackie, Glasgow 1985.

BOILY M.,BROOKS C. and LUDDEN J.N., Chemical and Isotopic Evolution of the Coastal Batholith of Southern Peru, J. Geophy. Res., Vol 94, No B9, pp 12483-12498

MOORE N.D. 1984, Potassium-Argon ages from the Arequipa Segment of the Coastal batholith of Peru and their correlation with regional tectonic events. J. Geol. Soc. Vol141, 3, pp511-520

MUKAZA S.B. 1986*a*, Common Pb isotopic compositions of the Lima, Arequipa and Toquepala segments in the Coastal batholith, Peru, implications for magma genesis. Geochim. Cosmochim. Acta, Vol 50, pp771-782

MUKAZA S.B. 1986*b*, Zircon U-Pb ages of super units in the Coastal batholith, Peru; implications for magnetic and tectonic processes. Bull; Geol. Soc. Amer , Vol 97, pp241-254

SEBRIER M.,LAVENU A.,FORNARI M. AND SOULAS JP., 1988, Tectonics and uplift in Central Andes (Peru, Bolivia and Northern Chile) from Eocene to present., Geodynamique, Vol 3(1-2), pp 85-106.

A WITHIN-PLATE GEOCHEMICAL SIGNATURE AND CONTINENTAL MARGIN SETTING FOR THE MESOZOIC – CENOZOIC LAVAS OF CENTRAL CHILE

Jorge OYARZUN[1], Beatriz LEVI[2], and Jan Olov NYSTRÖM[3]

(1) Departamento de Minas, Universidad de La Serena, Casilla 554 La Serena, Chile
(2) Department of Geology and Geochemistry, Stockholm University, S-10691 Stockholm, Sweden
(3) Swedish Museum of Natural History, S-10405 Stockholm, Sweden

RESUMEN: A pesar de sus diferencias de edad, ubicación geográfica y condiciones tectónicas inferidas, las lavas Jurásicas a Terciarias de Chile central (210 muestras) presentan patrones químicos similares y característicos para rangos dados de SiO_2–K_2O y tienen una componente común 'within plate'. Las composiciones químicas de estas lavas son consistentes con magmas derivados de la litósfera sub–continental en un margen continental activo.

KEY WORDS: Chile, Andes, Mesozoic-Tertiary, geochemistry, within-plate, continental margin

INTRODUCTION

A predominant part of the stratified sequences in the Chilean Andes is composed of Jurassic to Tertiary volcanic rocks, but relatively little has been published about their geochemistry compared to the much better known Quaternary lavas. In addition, most of the papers on pre–Quaternary volcanic rocks in the Andes treat altered and unaltered samples together or do not mention the problem of alteration. Since the Mesozoic and Tertiary rocks without exception are incipiently to pervasively altered and many elements are mobile during alteration processes, it is important to restrict the sampling to veinlet– and amygdule–free parts of flows with a minimum of alteration (checked with XRD), here referred to as 'unaltered'. Such screening was done in a study of Mesozoic and Tertiary lavas from central Chile (25°30' to 35°S) which showed that shoshonitic and high–K calc–alkaline lavas were common rock types during the Jurassic to Early Cretaceous, and suggested a north–south and east–west pattern of crustal thickness reverse to the present one during that time (Levi et al., 1988).

The purpose of the present study was to determine the chemical variation for the same given rock type (defined by its SiO_2 – K_2O contents according to the diagram of Peccerillo & Taylor, 1976) erupted at different times (Jurassic to Tertiary) in different parts of the ca. 1000 km long segment of central Chile treated by Levi et al. (1988). The samples of these authors were complemented with material from additional profiles, giving a total of 210 analyzed 'unaltered' basalts, basaltic andesites and andesites for this study.

GEOLOGICAL SETTING

The studied segment of the Chilean Andes is characterized by two parallel longitudinal belts of Mesozoic volcanics of successively younger ages towards a central axis that is occupied by a Late Cretaceous to Tertiary volcanic belt. Up to the 'middle' Cretaceous the lavas are intercalated with alternately continental and marine sedimentary rocks, whereas the Late Cretaceous and Tertiary lavas formed in a continental caldera/graben environment (Thiele et al., 1991). The presence of symmetric volcanic belts combined with a lack of geochemical trends expected at an active continental margin (e.g. an increase of K towards the interior of the continent) was interpreted as the result of ensialic spreading-subsidence during volcanism (Levi and Aguirre, 1981; Levi et al., 1988), enhanced by spreading caused by intrusion of granitoids (Drake et al., 1982).

RESULTS

The various populations of lavas at given $SiO_2 - K_2O$ contents (cf. Peccerillo & Taylor, 1976) each have rather uniform chemical compositions, the main exception being the few lavas belonging to the low-K series. The standard deviations for the average compositions are quite small considering that each population is composed of lavas of quite different age and geographic location (see example in Table 1). All the lavas have a common within-plate geochemical signature (i.e. they are enriched in incompatible elements that are

Table 1. Average compositions and standard deviations for 36 samples of calc-alkaline basaltic andesites from six E-W profiles in central Chile (Jurassic: 7 west, 6 east; Early Cretaceous: 1 west, 6 east; Late Cretaceous: 4 west, 4 east; Tertiary: 8). See Levi et al. (1988) for analytical methods.

	Jurassic		Early Cretaceous		Late Cretaceous		Tertiary	
	$\bar{x}$	SD	$\bar{x}$	SD	$\bar{x}$	SD	$\bar{x}$	SD
SiO_2	52.8	1.3	52.8	1.2	52.6	1.3	53.1	1.4
TiO_2	1.60	0.66	1.47	0.49	1.26	0.32	1.21	0.34
Al_2O_3	16.6	2.3	16.4	2.2	17.7	1.5	17.6	1.7
FeO*	9.86	3.15	9.34	2.28	9.30	1.38	8.77	1.21
MnO	0.16	0.04	0.17	0.04	0.22	0.08	0.18	0.04
MgO	3.83	0.69	3.95	1.29	3.39	0.62	3.89	0.96
CaO	8.56	0.75	8.34	0.56	8.01	0.82	7.96	0.83
Na_2O	3.01	0.34	3.59	0.65	3.66	0.38	3.66	0.48
K_2O	1.10	0.37	1.14	0.29	1.26	0.32	1.18	0.21
P_2O_5	0.32	0.15	0.34	0.18	0.28	0.11	0.20	0.12
H_2O^+	1.53	0.56	1.56	0.58	1.65	0.53	1.53	0.52
CO_2	0.16	0.15	0.36	0.29	0.23	0.21	0.30	0.23
Ba	188	59	275	155	366	79	338	69
Ce	42	17	59	19	32	9	37	10
Co	56	28	31	24	36	14	58	26
Cr	31	15	74	102	26	12	52	46
Nb	17	10	12	3	8	3	10	3
Ni	61	83	42	26	18	8	39	23
Rb	21	8	27	11	21	10	21	7
Sm	7.0	3.0	8.3	3.2	4.9	0.9	5.3	1.8
Sr	334	115	473	186	471	77	423	124
V	257	72	264	61	246	49	203	75
Y	43	19	39	20	29	7	26	10
Yb	3.6	1.8	3.5	2.2	2.3	0.5	2.5	1.2
Zr	182	99	210	74	107	26	113	40

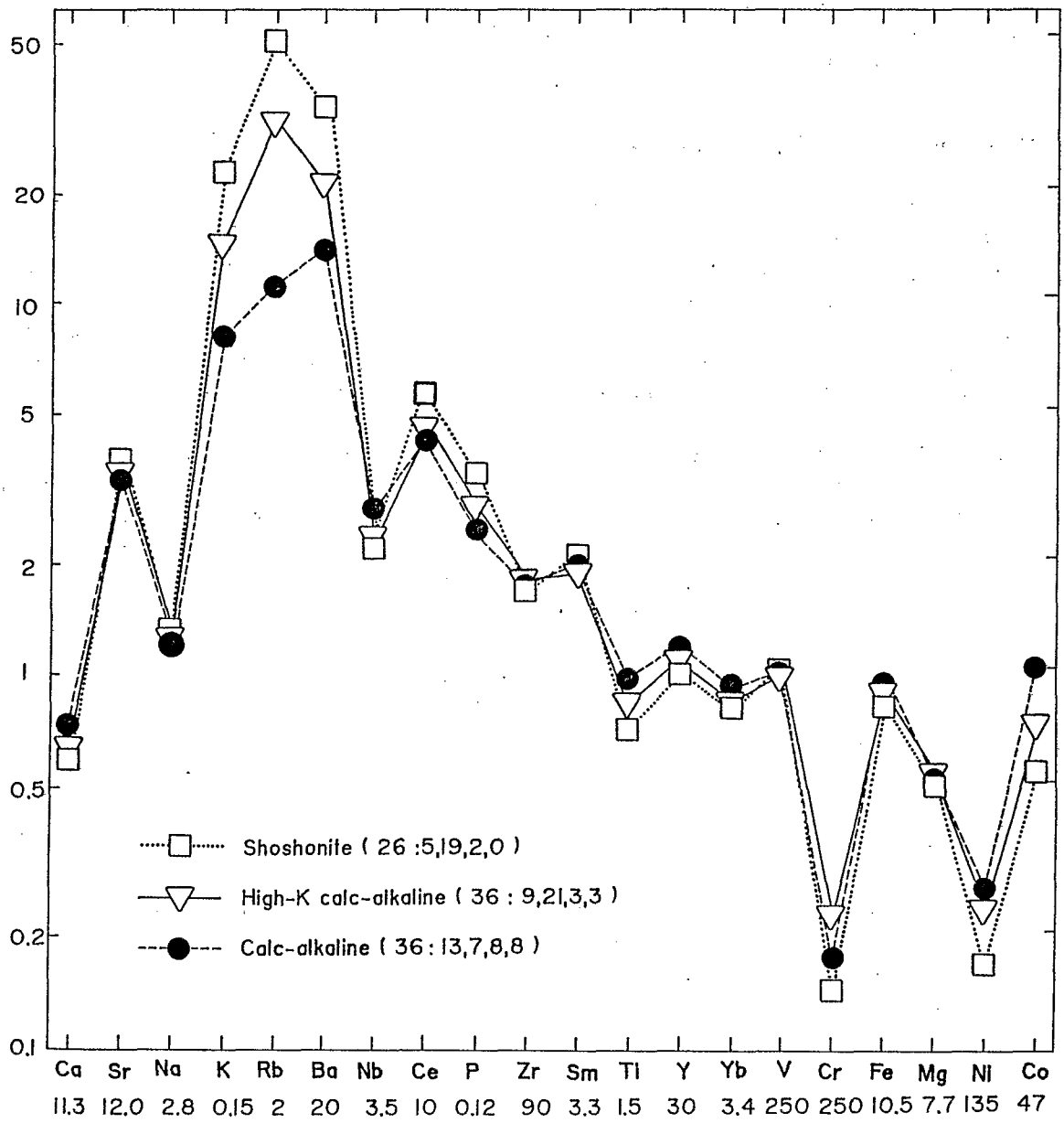

Fig. 1. MORB–normalized multielement diagram for the average compositions of Jurassic to Tertiary basaltic andesites of different K content from central Chile (total number of samples averaged in parenthesis, followed by number of samples within each age group: Jurassic, Early Cretaceous, Late Cretaceous, Tertiary). MORB values from Pearce (1983) except Ca, Na, V, Cr, Fe, Mg, Ni and Co (after Taylor & McLennan, 1985).

known not to be accomodated in the subduction component, with high concentrations of Nb relative to Zr, and of Zr relative to Y and Yb; Pearce, 1983), showing only variations in K, Rb and Ba at constant SiO_2 values and SiO_2–related differences in Cr, Mg and Ni. This signature is illustrated for basaltic andesites of different K–series in Fig. 1.

Discussion and Conclusions

The relatively uniform chemical compositions of each SiO_2–K_2O population of lavas erupted during a time–span of ca. 200 million years in central Chile is remarkable. However, there are some differences related to geographic position and age (e.g. a decrease in Ti with time, and a slight difference between Jurassic to Early Cretaceous and Late Cretaceous to Tertiary lavas; Table 1). Changes in tectonic regime with time in the studied area are reflected in the relative abundance of different rock types rather than their geochemical signature. Shoshonitic rocks, scarce during the Late Cretaceous, appear to be absent during the Tertiary, and high–K calc–alkaline types also become less abundant with time.

A within–plate component, indicating a contribution from incompatible element–enriched upper mantle, has earlier been indicated for some Jurassic to Tertiary lavas in the Chilean Andes (Pearce, 1983). Such component is also seen in the published analyses of Quaternary lavas from the Central and South Volcanic Zones occurring in the investigated area (25°30' to 35°S). This persistent geochemical feature despite considerable differences in age, location, Sr–Nd isotope composition (see Nyström et al., this volume) and inferred tectonic regime is consistent with a simple process of magma generation operating on a similar source material. The within–plate component suggests that the lithospheric plate was a major source for the magma. A geochemical similarity between the lavas studied by us and corresponding SiO_2–K_2O populations of Quaternary lavas in the same segment of the Chilean Andes indicates that this part of the Andean Belt has been an active continental margin since the Jurassic.

References

Drake, R., Vergara, M., Munizaga, F. & Vicente, J.C., 1982, Geochronology of Mesozoic – Cenozoic magmatism in central Chile, lat. 31°–36°S. *Earth–Sci. Rev.* **18**, 353–363.

Levi, B. & Aguirre, L., 1981, Ensialic spreading–subsidence in the Mesozoic and Palaeogene Andes of central Chile. *J. Geol. Soc. London* **138**, 75–81.

Levi, B., Nyström, J.O., Thiele, R. & Åberg, G., 1988, Geochemical trends in Mesozoic–Tertiary volcanic rocks from the Andes in central Chile, and tectonic implications. *J. South Amer. Earth Sci.* **1**, 63–74.

Nyström, J.O., Parada, M.A. & Vergara, M., 1993, Sr–Nd isotopic composition of Cretaceous to Oligocene volcanic rocks in central Chile: a trend towards MORB signature with time. (Extended abstract, this volume).

Pearce, J.A., 1983, Role of the sub–continental lithosphere in magma genesis at active continental margins. *In:* Hawkesworth, C.J. & Norry, M.J. (eds.) *Continental Basalts and Mantle Xenoliths*, 230–249, Shiva, Nantwich, UK.

Peccerillo, A. & Taylor, S.R., 1976, Geochemistry of Eocene calc–alkaline volcanic rocks from the Kastamonu area, northern Turkey. *Contrib. Mineral. Petrol.* **58**, 63–81.

Taylor, S.R. & McLennan, S.M., 1985, *The continental crust: its composition and evolution.* Blackwell Scientific, Oxford, 312 p.

Thiele, R., Beccar, I., Levi, B., Nyström, J.O. & Vergara, M., 1991, Tertiary Andean volcanism in a caldera-graben setting. *Geol. Rundschau* **80**, 179–86.

THE JURASSIC ACIDIC VOLCANISM OF NORTH-EAST PATAGONIA: A SHORT-LIVED EVENT OF DEEP ORIGIN.

R.J. PANKHURST (1) and C.W. RAPELA (2).

(1) British Antarctic Survey, c/o NERC Isotope Geosciences Laboratory, Keyworth, Nottingham NG12 5GG, U.K.
(2) Centro de Investigaciones Geológicas, 644 Calle No. 1, 1900 La Plata, Argentina.

RESUMEN: Se presenta un estudio geocronológico detallado en una de las provincias silícicas mas extensas del mundo. Los resultados condujeron a dos conclusiones principales: (1) Las rocas volcánicas se formaron durante un lapso de tiempo muy corto (3-5Ma) hace 180 Ma atrás, con edades progresivamente más jóvenes hacia el sur. (2) Los magmas se derivaron directa o indirectamente de una fuente isotópicamente uniforme como un manto litosférico enriquecido o una corteza inferior poco evolucionada.

KEY WORDS: Patagonia, Rhyolite volcanism, Jurassic, Geochronology, Sr-isotopes.

INTRODUCTION

The Early Mesozoic rhyolite-ignimbrite association of eastern Patagonia represents one of the most extensive acid volcanic provinces in the world. It has been generally considered that its emplacement was temporally and genetically related to crustal extension throughout the early stages of Gondwana rifting, and its formation has usually been considered to be a result of crustal anatexis associated with increased heat-flow during this period. However, a cogenetic relationship with supposedly contemporaneous volcanic rocks of intermediate composition in western Patagonia would raise the possibility of an origin more closely connected with Pacific margin subduction processes. This work is part of a combined geochemical/geochronological study of the acid magmatism, intended as a basis for more detailed comparison and resolution of this question.

GEOLOGICAL SETTING AND RESULTS

The Jurassic volcanic rocks of Patagonia occur as individual groups of outcrops of distinct lithologies, geographically separated by the basement highs and Cretaceous sedimentary basins (Fig.1). The Marifil Complex is the name give to the most predominantly rhyolitic outcrops that occur around the eastern flank of the North Patagonian Massif. Previous K-Ar ages for these rocks range from 210 to 155 Ma (Late Triassic to Late Jurassic) and have usually been thought to represent long-lived activity. Thirty-nine rocks from four separate areas (mostly lavas/subvolcanic intrusions, cogenetic dykes and ignimbrites) were analysed for major element geochemistry and Rb-Sr geochronology. In terms of normative

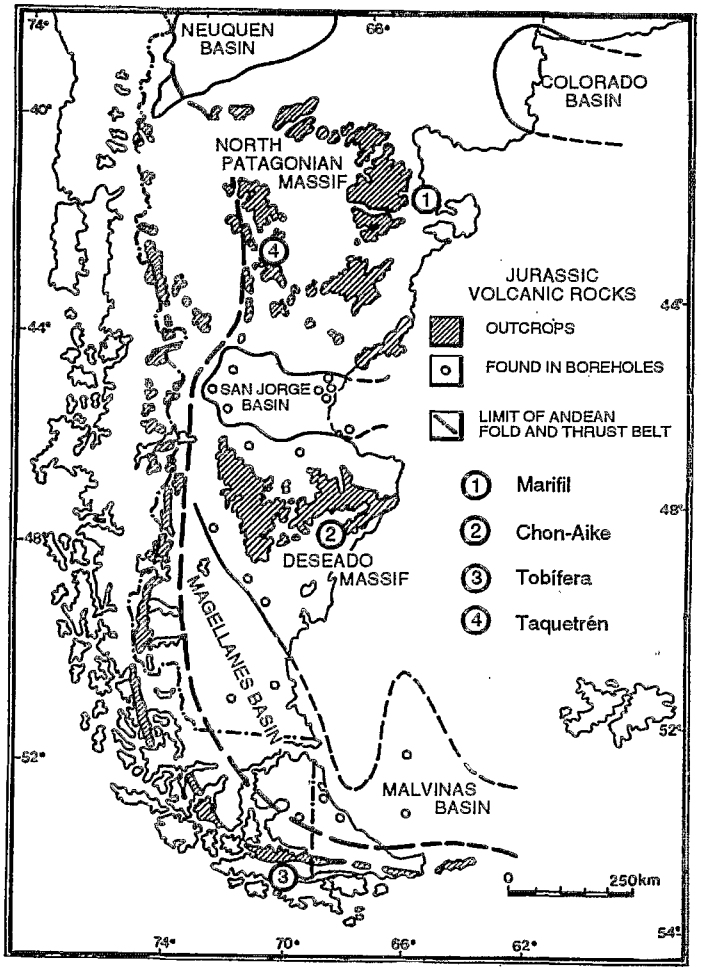

Fig.1: Distribution of the Jurassic volcanic rocks of Patagonia

chemistry, and with the exception of a single basaltic dyke from Dique Ameghino, the samples are all transalkaline rhyolites or trachydacites: in the total alkali-silica diagram, they appear as an extension of the field defined by the more intermediate Taquetrén Formation which occurs to the west. Major element chemistry shows significant differences between the sampled areas. One sample from Peninsula Camarones is peralkaline, the remainder of the lavas spanning the metaluminous-peraluminous boundary: ignimbrites and dykes from Dique Ameghino fall well into the peraluminous field. Most of the data sets define excellent Rb-Sr isochrons (Fig. 2) which are considered to date emplacement. Those from the type section in Arroyo Verde (only four samples, and the only ones not collected as part of the programme) gave 183 $\pm$ 2 Ma, whereas fifteen lava samples from Sierra Negra-Cerros del Ingeniero gave an indistinguishable age of 181 $\pm$ 7 Ma: in fact they fall exactly on the same isochron as the type section which is part of the same general exposure. Lavas and dykes from Peninsula Camarones gave 178 $\pm$ 1 Ma. Only the predominantly ignimbritic section of Dique Ameghino showed scatter beyond that of a true isochron (MSWD= 10.6), probably due to the effects of syn- to late- magmatic fluid interaction: nevertheless, the errorchron obtained of 181 $\pm$ 4 Ma after allowing for the excess scatter is well-defined and compatible with the other results. Initial $^{87}Sr/^{86}Sr$ ratios are surprisingly constant for the four areas (0.7065 $\pm$ 0.0004 to 0.7068 $\pm$ 0.0001).

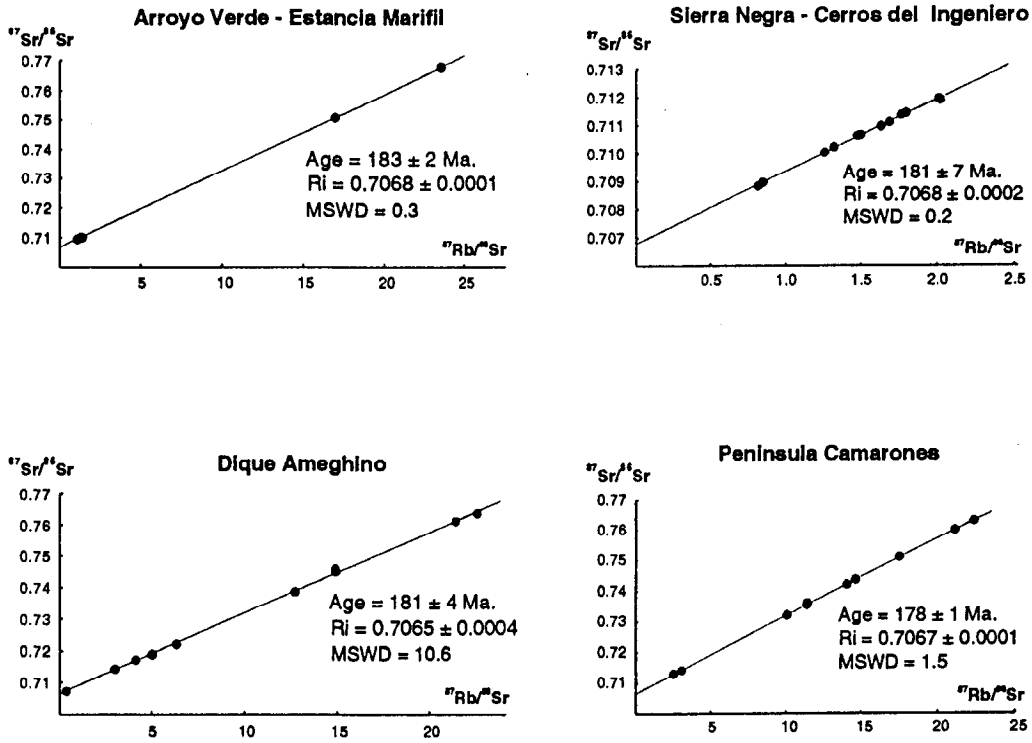

Fig. 2: Rb-Sr whole-rock isochrons for the sampled sections of the Marifil complex.

CONCLUSIONS

These results lead to two major conclusions with regard to this part of the volcanic province. Firstly, the volcanic rocks were formed during a short and well-defined igneous event 180 Ma ago, probably entirely within the Bajocian stage, but possibly including the Aalenian as well. Secondly the parent magmas were not derived by fusion of or even contamination with significantly older upper crustal rocks, but were derived, directly or indirectly, from an isotopically uniform source such as enriched lithospheric upper mantle without the involvement of other materials.

The most probable petrogenetic scenarios are differentiation at depth of less-evolved primary magmas (possibly represented by the andesites of the Taquetrén Formation), or rapid remelting of mafic underplating soon after its generation. Further work is in hand to elucidate these alternatives.

MIOCENE PLUTONISM IN N. PERU: IMPLICATIONS FOR ALONG-STRIKE VARIATIONS IN ANDEAN MAGMATISM (9-22°S).

N. PETFORD[1], M. P. ATHERTON[1], A. N. HALLIDAY[2]

(1) Department of Earth Sciences, University of Liverpool, Liverpool L69 3BX, UK.
(2) Department of Geological Sciences, University of Michigan, Ann Arbor, USA.

RESUMEN: Combined strontium and neodymium isotope data on the Mio-Pliocene Cordillera Blanca batholith (9-11° S) are compared with acid plutonic and volcanic rocks of similar age and composition from the central Andes (16-20° S). The Cordillera Blanca magmas show no evidence of contamination by, or remobilisation of, mature continental basement, contrasting strongly with central Andean volcanics where elevated $Sr_{(i)}$ and negative εNd reflect significant reworking of old continental crust. These contrasting along strike variations relate to horizontal shortening in the central Andes and magmatic underplating in the north.

KEY WORDS: Peru, Cordillera Blanca batholith, Crustal thickening, magmatic underplating.

INTRODUCTION

Unlike the Himalayas, where crustal thickening is the result of continent-continent collision, the mechanism of crustal thickening beneath the central Andes (up to x2 normal thickness) is still a matter of debate, with current opinion divided between tectonic shortening and magmatic underplating. Significantly, the thickness of the continental crust varies along strike of the chain, and is widely believed to correlate with the observed longitudinal variations in the isotopic compositions of Andean magmas (Harmon & Hoefs, 1984).

The Late Miocene-Pliocene Cordillera Blanca batholith and associated acid volcanics are the youngest magmatic rocks in NW Peru, and represent the final stage in the Andean cycle (200-0 Ma) in this region. The batholith lies directly above the thickened continental root of the Andes which in this sector reaches depths of ~ 60 km (James, 1971; Kono et al., 1988). Thus, the batholith magmas were intruded through crust of similar thickness to the Altiplano (CVZ) region further south, where Miocene basic-intermediate rocks with 'enriched' isotopic compositions are believed to result from large scale crustal contamination of mantle-derived magmas (James, 1982; Hawkesworth et al., 1982; Hildreth and Moorbath, 1988). Given the intrusion into similar thickness of continental crust, the Cordillera Blanca batholith may therefore be expected to show evidence for substantial continental crustal involvement in its petrogenesis.

GEOLOGICAL SETTING

The Cordillera Blanca batholith and associated volcanics are situated in the high western Cordillera of Peru between 9 and 11° S where they form a mountain range with an average elevation of over 4000m. The batholith is a linear body over 120 km in length, lying parallel with the main Andean trend in Peru, and is composed mostly of high silica (70-73 wt%) leucogranodiorite, with a subordinate marginal facies of quartz diorite and tonalite. It intrudes a basinal sequence of Jurassic shales, with both magma ascent and emplacement strongly controlled by periods of extension along the NNW/SSE trending Cordillera Blanca fault system. Radiometric dates from the Batholith range from ca. 13.7 to 2.7 Ma, with combined Pb and Ar-Ar ages from the central region of the intrusion giving an emplacement age here of about 6.0 Ma (see Petford & Atherton, 1992).

ISOTOPIC COMPOSITION OF BATHOLITH ROCKS

Sr and Nd isotopic determinations were carried out on fourteen rocks collected along strike of the intrusion. The isotopic compositions of both Nd and Sr show remarkably little scatter, with average εNd values close to bulk earth (-0.7), while $Sr_{(i)}$ varies between 0.7047 and 0.7057 over a range in SiO_2 of 18 wt % and a distance of ca. 60 km. Given the tectonic position of the batholith above thickened continental crust, the isotopic compositions of these rocks are surprisingly primitive, plotting at or close to bulk earth. Taking the batholith data as a whole, the range in isotopic composition of Nd is just over two epsilon neodymium units. Within the marginal facies, the variation is remarkably small, with εNd varying from +0.16 to a maximum of -0.21 over a silica range of 14 wt%. A basaltic andesite dyke that intrudes the Batholith has an εNd value of +3.5, falling broadly within the compositional range of island arc volcanics.

COMPARISON WITH TERTIARY CENTRAL ANDEAN (16-20°S) MAGMAS.

Isotopically, the batholith rocks contrast strongly with Tertiary-Recent rocks that characterise the Altiplano region of southern Peru and northern Chile (ca. 16-20°S). For example, the high silica ($SiO2 > 70\%$) batholith leucogranodiorites have much lower εNd values - ie. they are much more *primitive* - than the majority of *basic* volcanics from the Altiplano region, where εNd values are generally > -4.0 (Rogers & Hawkesworth, 1989; de Silva , 1991). Similarly, the variation in initial Sr ratios for the batholith rocks from 0.7048 to 0.7054 contrasts with Tertiary volcanic and intrusive rocks from the central Andes, where $Sr_{(i)}$ is generally in excess of 0.706 (eg. Hawkesworth et al., 1982).

Figure 2 shows the range in εNd values for the Cordillera Blanca batholith and associated Upper Miocene acid plutonic stocks of central northern Peru, along with acid volcanics of similar age from the central Andes (16-20° S). The most negative εNd values belong to the volcanics extruded through the very thick crust (70 km) beneath the central Andes. εNd of rocks of the Cordillera Blanca batholith and associated Miocene stocks are much more primitive than those further south, in spite of the crust having a similar thickness. Thus, εNd varies from +4 in the batholith to -12 in the central Andean volcanics although the change in crustal thickness is less than 20% between the two sectors.

Increasing $^{87}Sr/^{86}Sr$ ratios in rocks from the central Andes inboard with time (Rogers and Hawkesworth, 1989), combined with a marked increase in Nd model ages with decreasing emplacement age of granitic intrusions over the past 30 Ma have been interpreted as the result of extensive Tertiary crustal reworking (Miller and Harris, 1988). This reworking coincides with extensive crustal thickening and uplift at 12-10 Ma, with crustal thickening thought to be due to tectonic shortening (Isacks, 1988). Intracrustal melting of this tectonically thickened crust has been proposed to explain the elevated $Sr_{(i)}$ and εNd values seen in central Andean acid volcanics (de Silva, 1991).

TECTONIC IMPLICATIONS

Our favoured explanation for the large variation in isotopic composition of magmas intruded and extruded through crust of abnormal thickness along strike above the thickened keel of the Andes is that different source lithologies were melted. Although Miocene crustal thickening and uplift apparently occurred simultaneously in the northern and central Andes (Kono et al., 1988), Sr, Nd (and Pb) isotopic data from the Miocene stocks and Cordillera Blanca batholith show no evidence for melting of old crustal basement, or significant crustal contamination. Recent work (Atherton & Petford, 1993) has shown the Cordillera Blanca batholith rocks to be similar in composition to Na-rich Precambrian trondhjemite-tonalite-dacite (TTD) suites and that they were produced by partial melting of newly underplated basic crust. Sr and Nd isotopic compositions of the Cordillera Blanca rocks support this model, where rapid recycling of *new*, mantle-derived lower crust results in melt compositions that are virtually indistinguishable isotopically from mantle.

Such magmas contrast markedly with melts produced from melting *old* (Precambrian) basement or tectonically thickened continental crust in the manner proposed for the central Andes at 16-20° S. Clearly, isotopic values in magmatic rocks of the Andes depend on the source which, we maintain, was *new crust* in the north and old continental crust in the south. Over thickened crust does not automatically correlate with contamination of mantle-derived magmas.

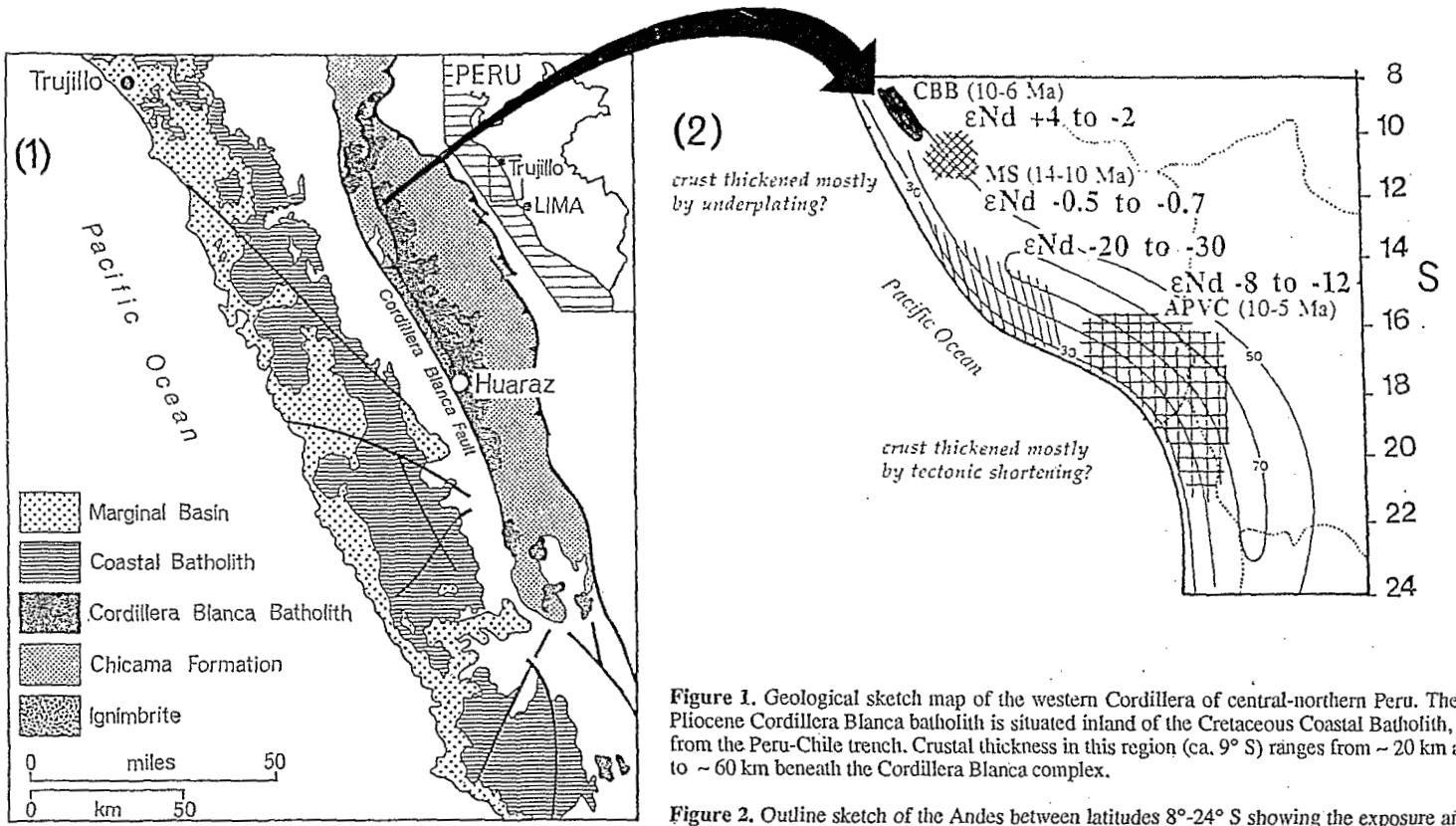

Figure 1. Geological sketch map of the western Cordillera of central-northern Peru. The Miocene-Pliocene Cordillera Blanca batholith is situated inland of the Cretaceous Coastal Batholith, ca 200 km from the Peru-Chile trench. Crustal thickness in this region (ca. 9° S) ranges from ~ 20 km at the coast to ~ 60 km beneath the Cordillera Blanca complex.

Figure 2. Outline sketch of the Andes between latitudes 8°-24° S showing the exposure and range in εNd for selected Upper Miocene plutonic and acid volcanics (ages in brackets). CBB (Cordillera Blanca batholith), MS (Miocene stocks; Soler & Rotach-Toulhoat, 1989), and the Altiplano-Puna volcanic zone (APVC) of the central Andes; de Silva, 1991). The aerial extent of exposed Precambrian basement in southern Peru (hatched) is also shown. Contours show depth to the Moho (James, 1971).

REFERENCES

Atherton, M.P. & Petford, N., 1993, Generation of sodium-rich-magmas form newly underplated basaltic crust. Nature, 363, 144-146.

de Silva, S.L., 1991, Altiplano-Puna volcanic complex of the central Andes. Geology,. 17, 1102-1106.

Hawkesworth, C.J., Hammill, M., Gledhill, A.R., van Calstern, P. & Rogers, G., 1982, Isotope and trace element evidence for late-stage intracrustal melting in the high Andes. Earth and Planet. Sci. Letts. 58, 240-254.

Harmon, R.S. & Hoefs, J., 1984, Oxygen isotope ratios in Late Cenozoic Andean Volcanics. In: Harmon, R.S. & Barrerio, B.A. (eds.). Andean Magmatism: Chemical and Isotopic Constraints. Shiva, Cheshire.

Hildreth, W. & Moorbath, S., 1988, Crustal contributions to arc magmatism in the Andes of central Chile. Contrib. Mineral. Petrol. 98, 45-489.

Issacks, B.L., 1988, Uplift of the central Andean Plateau and bending of the Bolivian Orocline. J. Geophys. Res. 93, 3211-3231.

James, D.E., 1971, Andean crustal and upper mantle structure. J. Geophys. Res. 76, 3246-3271.

Kono, M., Fukao, Y. & Yamamoto, A., 1989, Mountain building in the Central Andes. J. Geophys. Res. 94, 3891-3905.

Miller, J.F. & Harris, N.B.W., 1989, Evolution of continental crust in the central Andes; constraints from Nd isotope systematics. Geology, 17, 615-617.

Petford, N. & Atherton.M.P., 1992, Granitoid emplacement and deformation along a major crustal lineament: the Cordillera Blanca, Peru. Tectonophysics. 205, 171-185.

Rogers, G., & Hawkesworth, C.J., 1989, A geochemical traverse across the North Chilean Andes: evidence for crust generation from the mantle wedge. Earth. Planet. Sci. Lett. 91, 271-285.

Soler, P. & Rotach-Toulhoat, N. 1989, Implications of the time dependent evolution of Pb and Sr isotopic compositions of Cretaceous and Cenozoic granitoids from the coastal region and the lower Pacific slope of the Andes of central Peru. Geol. Soc. Amer. Spec. Pub.

GEOCHEMISTY AND PALAEOMAGNETISM OF IGNEOUS ROCKS FROM THE COSMELLI BASIN, SOUTHERN CHILE

N. PETFORD(1) & P. TURNER(2)

(1) Department of Earth Sciences, University of Liverpool, Liverpool L69 3BX, UK.
(2) School of Earth Sciences, Birmingham University, Birmingham B15, 2TT, UK.

INTRODUCTION

The Cosmelli basin, situated in southern Chile (ca. 46°S) is one of a series of continental Mid-Late Tertiary sedimentary basins that lie inboard of the present day subduction margin. The basin is located above a segment of continental crust that has experienced several ridge subduction events over the last 15 Ma. Subduction of a spreading mid ocean ridge (MOR) beneath continental lithosphere is a rare event and the potential effects of ridge subduction on the overriding continental (South American) plate are still poorly understood.

Recently, Flint et al., (1992) have interpreted the Cosmelli basin as a foreland basin that formed in response to ridge subduction processes. Facies relations within the basin show a sudden marine sediment to continental clastic transition, with intense folding and thrusting of the lower basin fill. Later basin fill material is relatively undeformed, and the overall stress regime during basin initiation and development is considered to be contractional (Flint et al., 1992).

The basin is host to a basic sill complexes and minor intrusives, and palaeomagnetic data implies that as a whole, the basin has suffered some kind of post depositional/intrusive thermal event. The basin also lies within the 'slab window' alkali flood basalt province of Ramos & Kay (1992). Given the proposed relation between ridge subduction, basin formation and magmatism, a study of the igneous rocks may help constrain the origin and thermal evolution of the basin.

IGNEOUS ROCKS

The igneous rocks of the Cosmelli basin range from basic sills to andesitic ignimbrites and dacitic stocks (Fig. 1a and Table 1). The data show some scatter on a silica K2O plot, with rocks ranging from low to high K (Fig. 1a). On Harker plots, the rocks form a fairly coherent group, with MgO, MnO, Fe2O3 and CaO showing a steady decrease with increasing SiO2 (eg. Fig. 1b).

GEOCHEMISTRY

XRF analyses for 9 igneous rocks are given in table 1. In Figure 1c, the dolerite sill SC-13 and a more evolved basaltic andesite (SC-32) are plotted together on a MORB-normalised trace element variation diagram. SC-13 (SiO2 49.1%) is much more primitive than SC-32 (SiO2 54.6), with K, Rb Cr and Ni

approaching MORB values. Although typical of active margin rocks (ie. LIL and HFSE elements are enriched relative to MORB), they lack the distinctive Ta/Nb anomalies characteristic of subduction related magmas (cf. Andean high-Al calc-alkaline-arc basalts). The more basic rocks are similar in some ways to LIL-enriched 'Transitional" alkali plateau basalts from Patagonia (ie. Stern and others, 1990). On a Ba/La v La plot (Fig. 1d) the basic sills lie in a transitional region between island arc (IAB) and ocean island (OIB) basalts.

	SC-7	SC-11	SC-13	SC-16	SC-31	SC-32	SC-37	SC-59	CSM-2
SiO2	54.87	45.61	49.14	60.29	52.49	54.63	65.99	57.20	65.89
Al2O3	14.90	14.99	16.57	19.63	17.02	17.44	16.19	17.45	15.16
TiO2	0.81	1.15	1.25	0.92	1.21	1.16	0.72	1.24	0.73
Fe2O3	7.08	9.34	9.71	6.24	8.97	8.29	4.63	6.44	7.46
MgO	2.71	7.98	8.04	1.30	5.36	4.03	0.55	3.52	1.39
CaO	4.65	10.64	7.84	3.75	8.20	7.25	4.01	5.22	2.93
Na2O	4.51	2.78	4.47	4.43	3.45	3.80	3.76	5.22	3.61
K2O	0.21	0.15	0.17	1.51	1.94	2.05	0.31	1.04	0.33
MnO	0.17	0.15	0.16	0.02	0.16	0.15	0.06	0.08	0.14
P2O5	0.16	0.20	0.20	0.06	0.31	0.44	0.03	0.65	0.03
LOI	9.96	6.98	2.43	1.57	0.58	0.53	3.31	1.61	2.04
Ba	98	151	225	364	616	635	409	466	240
Ce	47	32	18	18	32	66	< 5	67	30
Cr	115	338	222	73	50	32	49	62	65
Cu	20	58	47	8	32	37	29	34	39
F	514	573	482	741	664	786	550	859	546
Ga	17	16	18	19	20	21	15	23	17
Hf	6	6	5	8	6	8	5	7	10
La	11	9	12	7	12	30	< 5	23	10
Mo	1	1	< 1	< 1	< 1	< 1	< 1	< 1	< 1
Nb	3	6	6	4	10	16	5	19	3
Nd	20	13	17	12	16	33	5	31	11
Ni	38	169	97	28	20	12	7	17	6
Pb	7	6	3	7	15	17	9	7	6
Rb	5	3	2	41	61	71	11	11	9
S	93	418	87	55	1234	110	571	463	290
Sc	27	34	30	23	27	20	20	19	11
Sm	6	12	< 2	4	9	7	8	2	14
Sn	2	2	< 2	2	3	< 2	< 2	< 2	2
Sr	271	445	544	433	701	768	317	575	240
Th	7	1	3	4	5	11	3	< 1	5
U	2	2	< 1	< 1	< 1	2	2	< 1	< 1
V	130	224	211	112	209	162	77	123	63
Y	18	18	19	21	25	24	18	18	18
Zn	56	60	59	32	71	65	67	103	74
Zr	128	83	87	127	106	189	124	273	147

Table 1. Major and trace element data for the igneous rocks of the Cosmelli basin

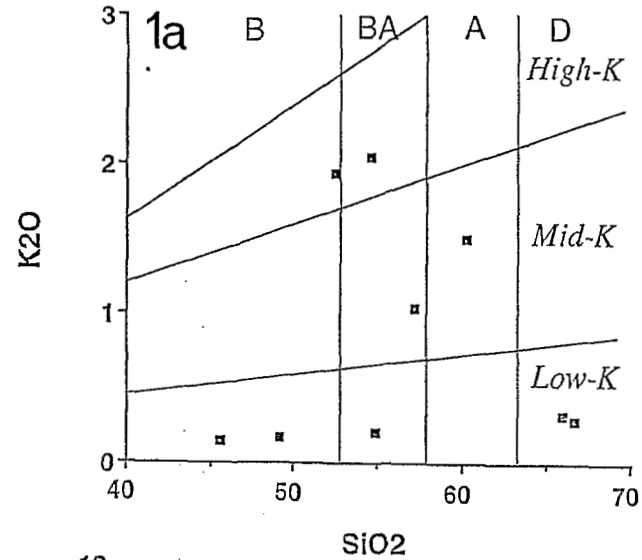

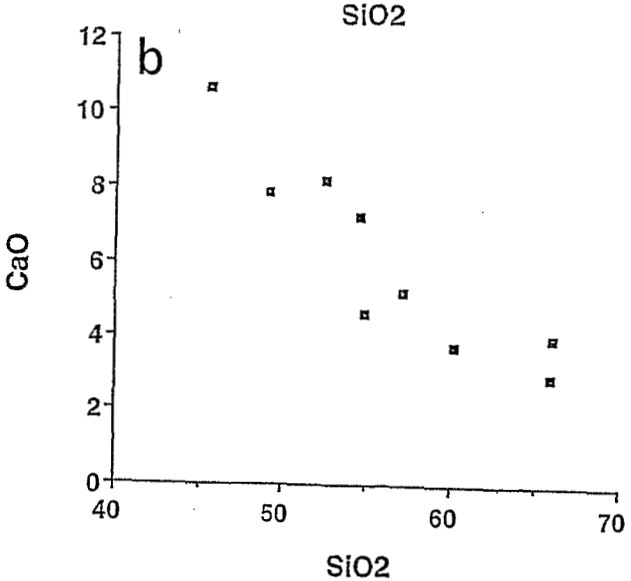

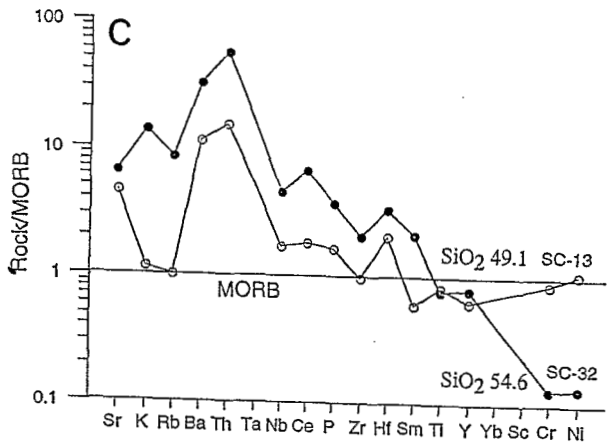

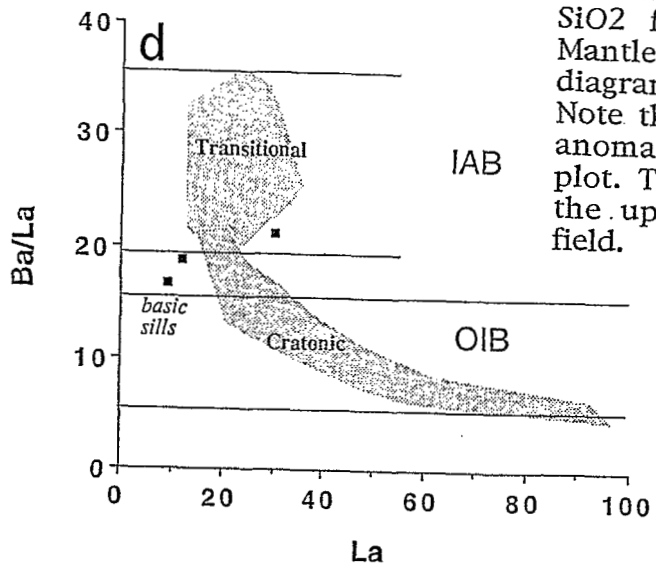

Figure 1a. K2O v SiO2 plot for basin rocks. **1b.** CaO v SiO2 for basin rocks. **1c.** Mantle normalised variation diagram showing basic sills. Note the lack of Ta and Nb anomalies. **1d.** Ba/La v La plot. The basic sills plot in the upper part of the OIB field.

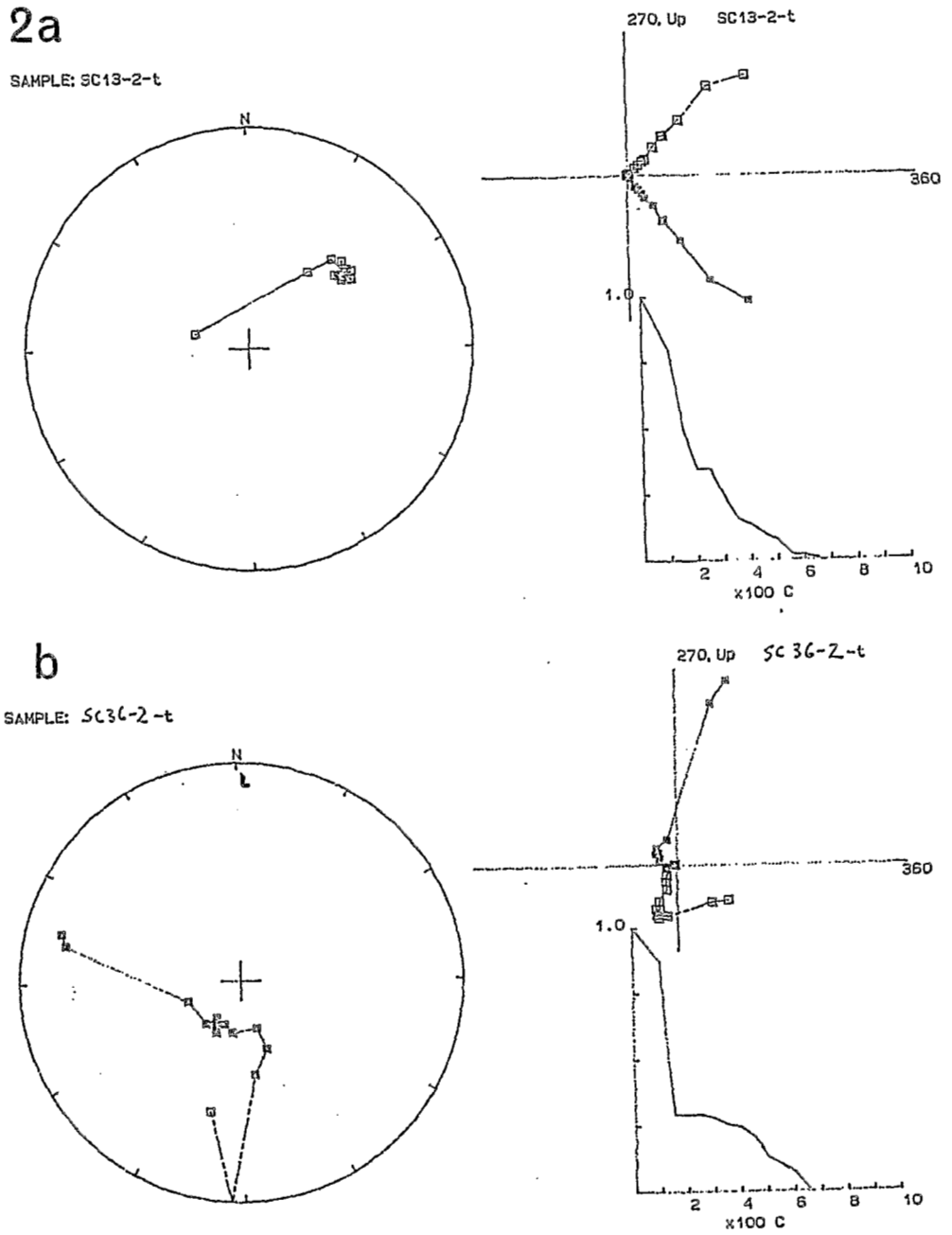

Figure 2a. Steregraphic and thermal demagnetisation plots for the dolerite sill located near the base of the Cosmelli basin. SC-13. **2b.** Same plots for basaltic andesite from higher in the sequence.

PALAEOMAGNETISM

Preliminary palaeomagnetic data for the sedimentary rocks suggest that the primary component is one of reversed polarity. In contrast, the igneous rocks show both reversed and normal polarity. Of particular interest is the dolerite sill sample SC-13 (Fig. 1c), from near the base of the sequence. It is a single vector showing superb demagnetisation characteristics. The rock has a remanence of reversed polarity, and the directions compare most closely with the Tertiary palaeofield before correction for tectonic dip. The basaltic andesite SC-32 from higher up the sequence is shown for comparison (Fig. 2b). One explanation for the normal polarity in the igneous rocks is that the magnetisation was acquired after folding.

DISCUSSION

Consideration of the palaeomagnetic data has led Flint et al., 1992 to conclude that the Cosmelli basin has been thermally overprinted during a normal polarity interval, and that the overprinting was in some way related to igneous activity - possibly coinciding with the extrusion of the voluminous "cratonic" plateau basalts to the east of the basin. Although the chemistry of the basic sills and associated volcanics precludes them from being directly related to the plateau basalts, neither are they classically calc-alkaline. The thermal 'pulse' and the presence of minor intrusives in the basin reflect elevated heat flow in the continental crust at the time of basin formation. The transitional nature of the basic sills is consistent with current models for ridge segment-related magmatism (Ramos & Kay, 1992).

REFERENCES

Flint, S.S., Prior, D.J., Agar, S.M. & Turner, P. 1992. Stratigraphic and structural responses to triple junction subduction, Cosmelli basin, southern Chile. (J. Geol. Soc. London, in review)

Ramos, V.A., & Kay, S.M. 1992. Southern Patagonian plateau basalts and deformation: backarc testimony of ridge collisions. Tectonophysics, 205, 261-282.

Stern, C.R, and others, 1990. Trace element and Sr, Nd,Pb and O isotopic composition of Pliocene and Quaternary alkali basalts of the Patagonian plateau lavas of southernmost Aouth America. Contrib. Miner. Petrol., 104, 294-308.

PRESENT KNOWLEDGE OF THE JURASSIC VOLCANOGENIC FORMATIONS OF THE SOUTHERN COASTAL PERU.

Nathalie ROMEUF (1), Luis AGUIRRE (1), Gabriel CARLIER (2), Pierre SOLER (2), Michel BONHOMME (3), Serge ELMI (4) and Guido SALAS (5).

(1) CNRS, URA 1277, Université d'Aix-Marseille III, Faculté des Sciences et Techniques de St-Jérôme, Laboratoire de Pétrologie Magmatique, 13397 Marseille Cédex 20, France.
(2) ORSTOM, TOA, UR 1H, 213, rue La Fayette, 75480 Paris Cédex 10 and, CNRS, URA 736, Laboratoire de Pétrologie, Université Paris VII, 4, place Jussieu, 75230 Paris, Cédex 05, France.
(3) CNRS, URA 69, Laboratoire"Géodynamique des Chaînes Alpines", Institut Dolomieu, rue Maurice Gignoux, 38031 Grenoble Cédex, France.
(4) CNRS, URA 11, centre des Sciences de la Terre, Université Claude-Bernard, Lyon 1, 27-43, bd du 11 Novembre, 69622 Villeurbanne Cédex, France.
(5) Universidad Nacional San Agustín de Arequipa, Arequipa, Peru.

RESUMEN: Se propone una nueva cronología de las formaciones jurásicas de la costa del Sur del Perú, basada sobre argumentos paleontológicos y geocronológicos, y se presentan observaciones mineralogicas y geoquímicas.

KEY WORDS : Lias, Dogger, low grade metamorphism, calc-alkaline, active continental margin-type setting, Southern Peru.

INTRODUCTION

Jurassic volcano-sedimentary rocks have been recognized in various places of the coastal region of Southern Peru (figure 1A). They have been generally assigned to three main formations. A thick sequence (>3000 m) of volcanic breccias with intercalated rhyolitic to andesitic flows are correlated with the Chocolate Fm defined in the Arequipa area (Jaén & al., 1963; Olchauski, 1980). In this area, an early Sinemurian fauna is present at the top of the Formation (Vargas, 1970, Vicente, 1981). The Chocolate Fm is unconformably overlain by the Bajocian to Oxfordian marine series of Guaneros Fm in the southernmost part of the coastal region (Jaén & al., 1963). Finally, in the northern segment of the area described here, Aalenian to Tithonian marine sediments associated with volcanic material have been regrouped into the Rio Grande Fm (Ruegg, 1956, 1961; Olchauski, 1980).

New stratigraphical, paleontological, and geochronological data from near Nazca, Chala, Ilo and Tacna (figure 1A) have led to a necessary partial or complet redefinition of the jurassic formations exposed in the coastal area of Southern Peru. Moreover, the presence of a low-grade non-deformational metamorphism in all these three formations has been put in evidence. Its characteristics and their consequences on the primary chemistry of the volcanic rocks are also discussed.

THE JURASSIC FORMATIONS OF THE COASTAL AREA OF SOUTHERN PERU

Near Ilo (figure 1B-A), a sequence of conglomerates, volcanic breccias and dacitic to andesitic flows that uncomformably overlain the precambrian basement are intruded by gabbro and diorite rocks dated at 190 Ma and 150 Ma (Mc Bride, 1977; Sánchez, 1983; Mukasa, 1986; Clark & al., 1990) and by granodiorites with a K/Ar, hornblende, age of 205 ± 11 Ma cropping out near Punta de Bombón. This sequence probably represents the lower part of the Chocolate Fm and may be correlated with the lower part of the La Negra Fm of Northern Chile (Muños & al., 1988). Near La Yarada (figure 1B-B), volcanic breccias with intercalated ignimbritic flows of the Chocolate Fm. are unconformably overlain by shales, sandstones

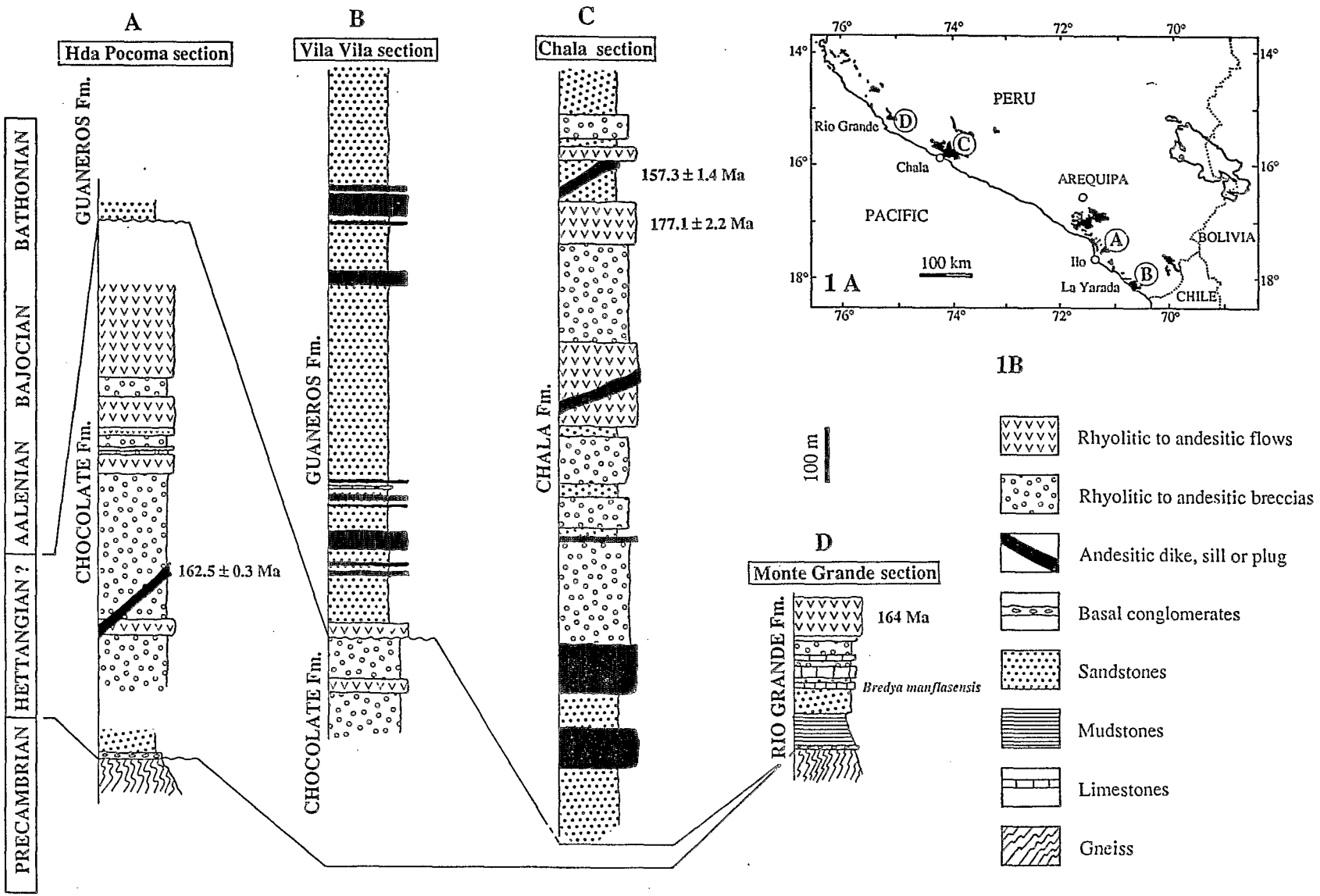

FIGURE 1 : AGE AND PROPOSED CORRELATIONS OF SOUTH PERUVIAN JURASSIC FORMATIONS.

with rare limestone intercalations of the Guaneros Fm. *Leptosphinctidae, Spiroceras sp.* (La Yarada) and *Lilloetia cf. Steinmani Spath* (Ilo) indicate that the base of the Guaneros Fm. is older (upper Bajocian to the upper Bathonian) than previously postulated (Callovian). In the Chala area, a thick sequence of basaltic to ignimbritic flows and dacitic breccias with intercalated red beds (figure 1B-C) was previously assigned to the Chala Fm and correlated with the Chocolate Fm (Olchauski, 1980). Nevertheless, an $^{39-40}Ar$ age of 177 Ma obtained on a basaltic flow from the base of the formation indicate that the Chala Fm should be correlated with the Guaneros Fm and the Rio Grande Fm (figure 1B-D) where occurrence of the Aalenian *Bredya manflasensis* assemblage zone has been reported (Roperch & Carlier, 1992). Various generations of andesitic stocks, sills and dikes crosscut all the Jurassic formations of the coastal range. An $^{39-40}Ar$ age determination performed on dikes from the Ilo and Chala areas (Roperch & Carlier, 1992) indicates magmatic activity contemporaneous with the Middle Jurassic sedimentation. A similar age from an andesitic flow of the Rio Grande area has been reported (Aguirre & Offler, 1985; Aguirre, 1988). Nevertheless, a K/Ar on hornblende of 91.3 ± 9.2 Ma from a dike of Chala area indicates that some of these subvolcanic intrusions can represent the feeding channels of younger volcanic series as the Albian Matalaque Fm or Paleogene Toquepala Fm.

METAMORPHISM

The regional low-grade metamorphism that affects all the volcanogenic formations is marked by the lack of deformation. In the basaltic to rhyolitic flows and basaltic to andesitic subvolcanic intrusions, this metamorphism is characterized (1) by replacement of primary olivine, plagioclase, hornblende, titanomagnetite and groundmass, and (2) by secondary amygdule filling. The metamorphic assemblages consists of various associations of the following minerals : chlorite/smectite, celadonite, albite, K-feldspar, K-rich zeolite ?, sericite, albite, quartz, calcite, epidote, hematite, titanite and rare pumpellyite, prehnite, analcite and actinolite. These assemblages suggest sub-greenschist facies conditions, *i. e.* zeolite to prehnite-pumpellyite facies (T = 150-275° C, P < 3 kbars).

In the other hand, the replacement of primary plagioclase by albite, K-feldspar and K-rich zeolite ?, the secondary filling of amygdules by calcite, quartz, chlorite/smectite and celadonite documente the relatively high mobility of Na, K, Ca, Si, Fe and Mg during the metamorphism.

GEOCHEMISTRY

The Na, K and Si mobility precludes their use to characterize the primary chemistry of the flows and subvolcanic intrusions. Particularly, in some rocks, the very high K_2O content (up to 7.1 wt%) associated with abnormally high Ba (2520 ppm) and Rb (250 ppm) contents results from a secondary enrichment.

The jurassic flows and subvolcanic intrusions show high LILE and LREE contents and characteristically low content of Ti and other HFSE of volcanic rocks associated with convergent plate margins (figures 2 and 3).

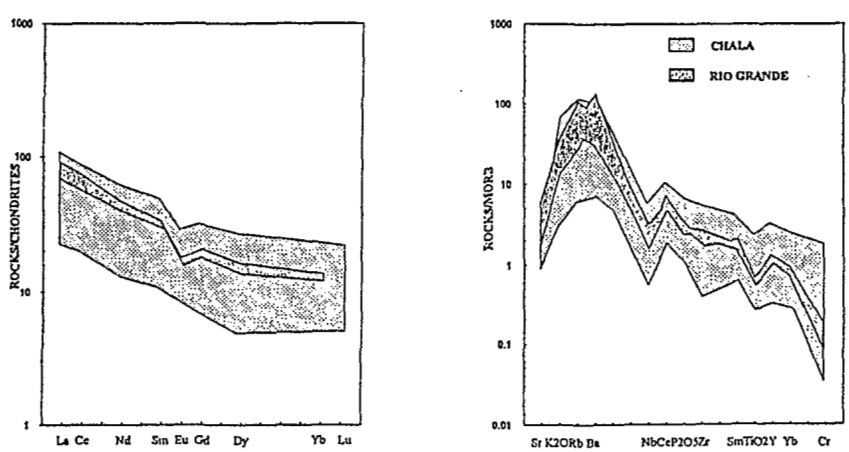

FIGURE 2 : Chondrite-normalized rare earth element diagram (A) and MORB-normalized element abundance diagram (B) of southern peruvian volcanic rocks showing LREE enrichment and typical Ti, Nb, Zr negative anomalies of volcanic rocks associated with convergent plate margins.

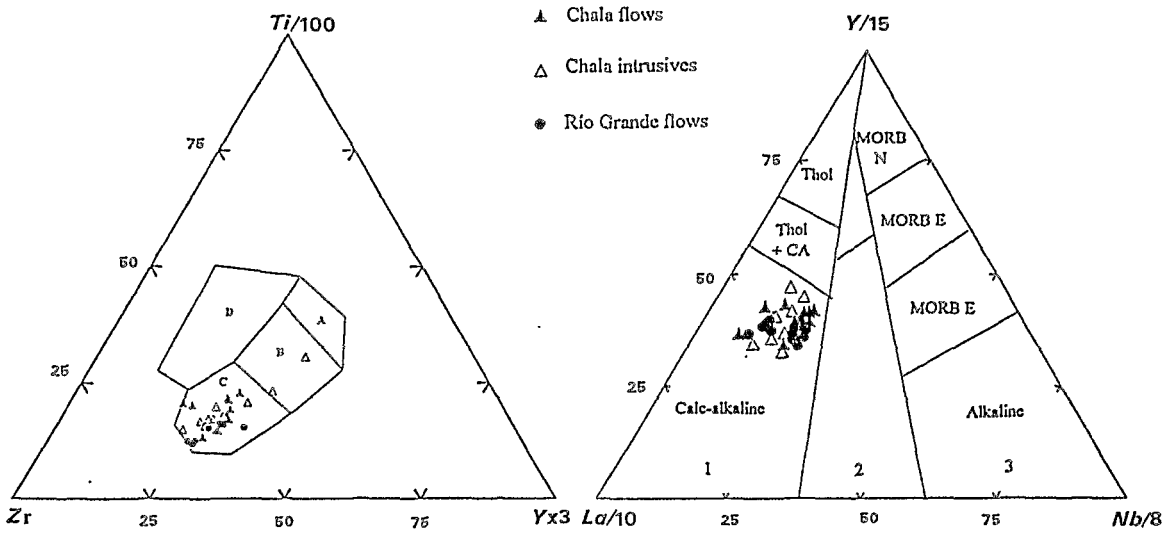

FIGURE 3 : Ti - Zr - Y and Y - La - Nb Plots of southern peruvian volcanic rocks. A is field of low-K tholeiite; B, ocean floor basalt; C, calc-alkali basalt; D, within plate basalt; 1, orogenic domains; 2, late to post orogenic intracontinental domains and 3, anorogenic domains.

REFERENCES

Aguirre, L., 1988, Chemical mobility during low-grade metamorphism of a Jurassic lava flow : Rio Grande Formation, Peru. J. South Amer. Earth Sci., 1, 343-361.

Aguirre, L. and Offler, R., 1985, Burial metamorphism in the western peruvian trough, its relation to Andean magmatism and tectonics. In Magmatism at the Plate Edge, The Peruvian Andes, edited by W.S. Pitcher et al., 59-71, Blackie, Glasgow.

Clark , A.H., Farrar, E., Kontak, D.J., Langridge, R.J., Arenas, M.J., France, L.J., McBride, S.L., Woodmann, P.L., Wasteneys, H.A, Sandeman, H.A. and Archibald, D.A, 1990, Geologic and geochronologic constraints on the metallogenic evolution of the Andes of Southeastern Peru. Econ. Geol., 85, 1520-1583.

Jaén, H., Ortiz, G., and Wilson J.J., 1963, Geología de los cuadrángulos de la Yarada y Tacna, (1/100 000) y geología del cuadrángulo de Huaylillas (1/100 000). Com. de la Carta Geol. Bol. 6, p., Lima, Peru.

McBride, S.L., 1977, A K-Ar study of the Cordillera Real, Bolivia, and its regional setting. Ph.D. thesis, Queen's Univ. of Kingston, Ont., Canada.

Mukasa, S.N., 1986, Zircon U-Pb ages of super-units in the coastal batholith, Peru : Implications for magmatic and tectonic processes. Geol. Soc. Am. Bull., 97, 241-254.

Muños, N., Venegas, R.and Tellez C., 1988, La Formacion La Negra : Nuevos antecedentes estratigraficos en la Cordillera de la Costa de Antofagasta. V Cong. Geol. Chileno, T. 1, A 283-A 311. Santiago, Chile.

Olchauski, E., 1980, Geología de los cuadrángulos de Jaqui, Coracora, Chala y Chaparra (1/100 000). Inst. Geol. Min. y Met. Bol., 34, Lima, Perú.

Roperch, P. and Carlier, G., 1992, Paleomagnetism of Mesozoic Rocks from the Central Andes of Southern Peru : Importance of rotations in the development of the Bolivian Orocline. J. Geophys. Res., 97, 17233-17249.

Ruegg, W., 1956, Geologie zwischen Cañete-San Juan, 13° 00' - 15° 24' Süd Peru. Geol. Rundsch., 45, 775-858.

Ruegg, W., 1961, Hallazgo y posición estratigrafico-tectonico del Titoniano en la costa sur del Perú. Bol. Soc. Geol. Perú, 36, 203-208.

Sánchez, A.W., 1983, Edades K-Ar en rocas intrusivas del area de Ilo, Dpto de Moquegua, Bol. Geol. Soc. Perú, 71, 183-192.

Vargas, L., 1970, Geología del cuadrángulo de Arequipa. Ser. Geol. Min. Bol., 24, 64 p., Lima, Peru.

Vicente, J.C., 1981,Elementos de la estratigrafia mesozoica sur-peruana. In Cuencas sedimentarias del Jurasico y Cretacio de America del Sur, vol. 1, edited by Volkheimer, W. and Musacchio, E.A., 319-351, Buenos Aires.

EVOLUTION OF THE CRUCERO SUPERGROUP, PUNO, SE PERU: AN OLIGOCENE-MIOCENE "COLLISIONAL" MAGMATIC ASSEMBLAGE IN A NON-COLLISIONAL, ARC SETTING

Hamish A. Sandeman[(1)], Alan H. Clark[(1)], Edward Farrar [(1)] and Guido Arroyo [(2)]

(1) Department of Geological Sciences, Queen's University, Kingston, Ontario, Canada. K7L 3N6.
(2) Instituto Peruano de Energía Nuclear, Avenida Canadá 1470, Lima 41, Peru.

Resumen: El Supergrupo Crucero, un ensamblaje de rocas volcánicas diversas de edad Oligoceno-Mioceno, constituye el último período de magmatismo dentro de la sección Peruana del Arco Andino Interno. El supergrupo comprende la asociación típica de orogenias de choque, emplazado durante un episodio breve de extensión cortical en el Oligoceno tardío, seguido por un largo período de compresión oblícua diestra en el Mioceno.

Key Words: Crucero Supergroup, peraluminous, basalt, minette, extrusion tectonics, Bolivian Orocline.

The Crucero Supergroup is a continental assemblage comprising a wide range of crustally-derived peraluminous and mantle-derived mafic volcanic rocks. It is extensively exposed in the Cordillera de Carabaya range of southeastern Peru and represents the most recent magmatism within the Central Andean Inner Arc. The supergroup comprises the 21.2-25.0 Ma Picotani and the 6.5-16.9 Ma Quenamari Groups, each of which consists of numerous, aerially restricted formations. The Picotani Group is a complex assemblage of diverse rock-types, erupted over a brief interval, that show no time-transgressive relationships. The assemblage includes: olivine-plagioclase$\pm$clinopyroxene$\pm$orthopyroxene - phyric and -glomerophyric, high-K, basaltic-to-andesitic lavas of the spatially separate Suratira Formation (22.4-23.6 Ma), Pucalacaya Formation (*ca.* 21.9 Ma) and Cerro Queuta Formation (23.8-25.1 Ma); minette and mixed minette/rhyodacite lava flows of the Lago Perhuacarca Formation (*ca.* 23.9 Ma); biotite$\pm$cordierite - phyric, dacitic-to-rhyodacitic lapilli-tuffs of the Cerro Huancahuancane (23.1-24.4 Ma) and Cerro Sumpiruni Formations (21.2-24.1 Ma); cordierite-biotite - phyric dacitic lavas of the Jama Jama Formation (*ca.* 23.8 Ma); cordierite-biotite - phyric dacitic agglomeratic tuffs of the Pachachaca Formation (23.6-24.4 Ma); and glassy, cordierite-biotite - phyric rhyolitic agglutinates of the Cerro Cancahuine Formation (*ca.* 22.2 Ma). In contrast, the Quenamari Group consists wholly of rhyolitic volcaniclastic rocks, forming a time-transgressive sequence from the muscovite-biotite$\pm$sillimanite - phyric, crystal - lapilli tuffs comprising the Huacchane Formation (16.8-16.9), through the biotite-sillimanite$\pm$muscovite - phyric, vitric - lapilli tuffs of the Quebrada Escalera Formation (16.2-16.4 Ma), to the muscovite-biotite$\pm$andalusite - phyric ash-flow tuffs of the well known Macusani Formation (6.5-10.5 Ma). These two distinct magmatic pulses, constituting a magmatic association typical of collisional orogens, were emplaced in a late Oligocene episode of crustal extension, followed in the Miocene by a prolonged period of oblique, right-lateral compression coeval with antithetic subduction of the Brazilian Shield. We envisage a major petrogenetic role for "extrusion tectonics" during compressional shortening and accentuation of the Bolivian Orocline.

FIELD OBSERVATIONS AND K-Ar DATING OF THE CERRO CHIAR KKOLLU (SOUTHERN ALTIPLANO, BOLIVIA)

Pierre SOLER [1,2], Gabriel CARLIER [1], Michel G. BONHOMME [3], and Michel FORNARI [2]

(1) ORSTOM, UR1H, 213 rue Lafayette, 75480 Paris Cedex 10, France, and CNRS URA 736, Universités Paris 6 et 7, Tour 26, 3ème étage, 4 Place Jussieu, 75005 Paris, France
(2) Mission ORSTOM, Casilla 9214, La Paz, Bolivia
(3) CNRS URA 69, Institut Dolomieu, Université J. Fourier, 15 rue M. Gignoux, 38031 Grenoble Cedex, France

RESUMEN : El cerro Chiar Kkollu, ubicado en el Altiplano Sur de Bolivia, era considerado desde tiempo como un centro volcánico cuaternario alcalino de trás-arco de la Zona Volcánica Central (CVZ) de los Andes. Era el único ejemplo de un volcanismo de tal naturaleza en esta región. Observaciones de terreno y una datación K-Ar sobre roca total muestran que dicho centro es de edad Oligoceno y pertenece a un conjunto de rocas de afinidad alcalina de edad Oligoceno a Mioceno inferior ampliamente distribuidas en el Altiplano boliviano. Los modelos petrogenéticos propuestos anteriormente por diferentes autores en base a las supuestas relaciones entre el Chiar Kkollu y el volcanismo cuaternario de arco y/o de trás-arco de la CVZ no tienen ningun sustento geológico.

KEY WORDS : Bolivia, Oligocene, Alkali basalts, Back-arc

INTRODUCTION

The cerro Chiar Kkollu, in the southern Altiplano of Bolivia, is well known among geoscientists devoted to the recent and present-day volcanic activity of the Central Andes. As a matter of fact, this small volcanic outcrop has long been considered as the unique example of quaternary alkaline back-arc volcanism behind the Central Volcanic Zone in the Bolivian Andes (Thorpe and Francis, 1979; Thorpe et al., 1982), and this "peculiar" volcanic rock has been used by various geochemists (e.g. Thorpe et al., 1984; Rogers, 1985; Rogers and Hawkesworth, 1989; Davidson et al., 1991; Davidson and De Silva, 1992) as a clue for the understanding of the petrogenesis of the modern arc and back-arc magmas of the CVZ.

Our field observations and whole-rock K-Ar dating permit to demonstrate that this apparently peculiar volcanic rock is actually of Oligocene age, and belongs to an alkaline volcanic province of Oligocene-Early Miocene age, which appears to be an important feature of the magmatic and tectonic evolution of the Bolivian orocline.

FIELD, PETROGRAPHIC, AND GEOCHEMICAL OBSERVATIONS

The Cerro Chiar Kkollu (19° 26' S - 67° 23' W - figure) outcrops near Tambo Tambillo along the road between Huari and Salinas de Garci Mendoza in the southern Altiplano of Bolivia. It is an isolated, roughly circular *mesa*, about 800 metres in diameter, surrounded by Plio-Quaternary continental detritics. Topographically this outcrop is rather similar to some of the Quaternary shoshonitic centers known in the same region (e.g. Davidson et al., 1991; Soler et al., 1992, in prep.), which may explain that it has long been considered as Quaternary in age. However, detailed field observations show that small remnants of metamorphosed red pelites are outcropping over the surface of the cerro Chiar Kkollu. These pelites are quite similar to metamorphosed pelites observed

southeastwards at the contact between alkaline basaltic to micro-gabbroic sills and the Oligocene - Early Miocene continental Potoco and Tambillo sedimentary formations. These sills, known as the "Tambillo lavas", outcrop immediatly to the East and Southeast of the cerro Chiar Kollu and dip stoongly (≈ 45°) towards the NE. These field observations suggest that the cerro Chiar Kkollu basalts are not of Quaternary age, and that they rather belong to a folded Late Oligocene - Early Miocene set of alkaline sills.

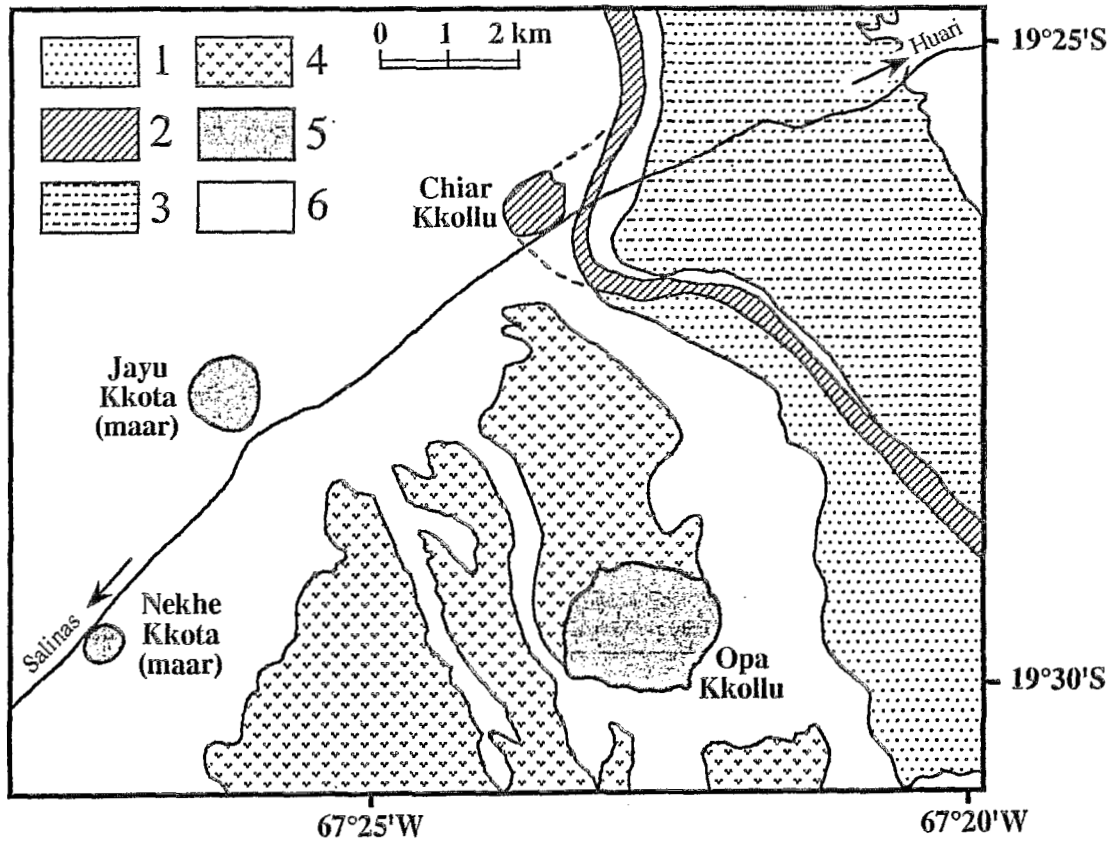

Geological sketchmap of the Cerro Chiar Kkollu area

1 - Eocene-Oligocene Potoco Fm (pelites, red sandstones) ; 2 - Late Oligocene-Early Miocene basalts and micro-gabbros (sills - "Tambillo lavas"); 3 - Early Miocene Tambillo Fm (pelites, red sandstones, conglomerates, tuffs) ; 4 - Late Miocene dacitic ignimbrites; 5 - Quaternary shoshonitic centers; 6 - Plio-quaternary continental detritics.

In addition, as quoted by most authors, the cerro Chiar Kkollu basalts display very peculiar petrographical, chemical and isotopic compositions when compared with basic lavas of the modern arc (CVZ - Thorpe et al., 1984; Rogers, 1985; Davidson et al., 1991; Davidson and De Silva, 1992) and of the back-arc (i.e. shoshonites - Davidson et al., 1991; Davidson and De Silva, 1992; Soler et al., 1992, 1993, in prep.) of the Western Cordillera and the Altiplano of Bolivia. In particular, they are characterized by their very primitive feature, their alkaline affinity, their unradiogenic Sr compositions, and the absence of any crustal xenoliths. It should be noted that quite similar petrographical and geochemical features are observed in the "Tambillo lavas".

K-AR DATING

Sample JAC6 from cerro Chiar Kkollu has been dated by M.G. Bonhomme at the University of Grenoble following the techniques described in Lavenu et al. (1992). The results are given in the table.

Sample	K_2O (%)	^{40}Ar rad (%)	^{40}Ar rad (nl/g)	$^{40}K/^{36}Ar$ (x 1000)	$^{40}Ar/^{36}Ar$	Age (Ma) (± 1σ)
JAC6	1.05	54.2	0.935	218.1	645.3	**27.4 ± 0.8**

This 27.4 ± 0.8 Ma whole-rock age may be slightly older that the actual age of emplacement due to a psssible excess of argon in the abundant clinopyroxenes of these basalts. It confirms however the interpretation proposed on the basis of field observations. This age is slightly older than ages previouly obtained on the Tambillo lavas (22.6 Ma recalculated with new constants Ma; K-Ar age on plagioclase; Evernden et al., 1977; 19.6 ± 2,5 to 23.5 ± 2.6 - IGE-JICA, 1986).

This age fits also with ages obtained on the Rondal Fm (Kussmaul et al., 1975; Fornari et al., this volume), the alkaline basic volcanism of the Tupiza basin (Hérail et al., this volume), and the Abaroa Fm. of the northwestern Altiplano (Lavenu et al., 1989; Jimenez et al., this volume).

Thus the cerro Chiar Kkollu basalts belong to the Late Oligocene - Early Miocene volcanic episode of alkaline affinity known all over the Bolivian Altiplano (Soler and Jimenez, this volume). They probably derived from the subcontinental lithospheric mantle during a trans-tensional tectonic episode (Soler and Jimenez, this volume) and their composition cannot be used as a clue to model the compositions of the subduction-related, asthenosphere-derived magmas of the modern arc (CVZ) as proposed by several authors (e.g. Thorpe et al., 1984; Rogers, 1985; Rogers and Hawkesworth, 1989; Davidson et al., 1991; Davidson and De Silva, 1992). However their compositions may be used to constrain the petrogenetic models for the back-arc, lithosphere-derived shoshonitic and peralkaline volcanism of the Bolivian Andes (Soler and Jimenez, this volume).

REFERENCES

DAVIDSON, J.P. & DE SILVA, S.L., 1992 - Volcanic rocks from the Bolivian Altiplano: insights into crustal structure, contamination, and magma genesis in the central Andes. Geology, 20, p. 1127-130.

DAVIDSON, J.P., DE SILVA, S.L., ESCOBAR, A., FEELEY, T. & BOHRSON, W. 1991 - Evaluation of magma sources for central Andean volcanics. 6to Congreso Geológico Chileno, Resumenes Expandidos, p. 347-349.

EVERNDEN, J. F., KRIZ, S. J., & CHERRONI M., C., 1977 - Potassium-Argon ages of some Bolivian rocks. Economic Geology, 72, p. 1042-1061.

FORNARI, N., HÉRAIL, G., POZZO, L., & VISCARRA, G., 1991 - Los yacimientos de oro de los Lipez (Bolivia). Tomo I: Estratigrafía y dinámica de emplazamiento de las volcanitas del aréa de Guadalupe. Mission ORSTOM en Bolivie, La Paz, Rapport n°19, 28 p.

FORNARI, M., POZZO, L., SOLER, P., BAILLY, L., LEROY, J., & BONHOMME, M.G., 1993 - Miocene volcanic centers in the Southern Altiplano of Bolivia. The Cerro Morokho-Cerro Bonete area (Sur Lipez), this volume.

HÉRAIL, G., OLLER, J., BABY, P., BLANCO, J., BONHOMME, M. G., & SOLER, P., 1993 - The Tupiza, Nazareño, Estarca basins (Bolivia): strike-slip faulting and thrusting during the Cenozoic evolution of the southern branch of the Bolivian Orocline. This volume.

IGE(UMSA)-JICA, 1986 - Edades Radiométricas de Bolivia. Publ. especial de la Facultad de Ciencias Geológicas de la UMSA, La Paz, 53 p.

JIMENEZ CH., N., BARRERA I., L., FLORES B., O., LIZECA B., J.L., MURILLO S., F., HARDYMAN, R. F., TOSDAL, R. M., & WALLACE, A. R., 1993 - Marco geológico de la región de Berenguela. *In:* Investigación de metales preciosos en los Andes Centrales, Proyecto BID/TC-88-02-32-5, GEOBOL (La Paz), p. 63-74.

KUSSMAUL, S., JORDAN, L., & PLOSKONKA, E., 1975 - Isotopic ages of Tertiary volcanic rocks of SW-Bolivia. Geol. Jb. (Hannover), B14, p. 111-120.

LAVENU, A., BONHOMME, M. G., VATIN-PERIGNON, N., & PACHTERE de, P., 1989 - Neogene magmatism in the Bolivian Andes between 16° and 18° S. Stratigraphy and K-Ar geochronology. J. South Amer. Earth Sci., 2, 1, p. 35-47.

LAVENU A., NOBLET, C., BONHOMME, M.G., EGUEZ, A., F. DUGAS, & VIVIER, G., 1992 - New K/Ar age dates of Neogene and Quaternary volcanic rocks fro the Ecuatorian Andes: implications for

the relationships between sedimentation, volcanism, and tectonics, J. South Amer. Earth Sci., 5, 1, p. 1-19.

ROGERS, G.R., 1985 - A geochemical traverse across the north Chilean Andes. Unpub. Ph. D. thesis, The Open University, Milton Keynes

ROGERS, G.R. & HAWKESWORTH, C.J., 1989 - A geochemical traverse across the north Chilean Andes: evidence for crust generation from the mantle wedge. Earth Planet. Sci. Lett., 91, p. 271-285.

SOLER, P., CARLIER, G., FORNARI, M., & HÉRAIL, G., 1992 - An alternative model for the origin and the tectonic significance of the Neogene and Quaternary shoshonitic volcanism of the Andes. EOS Trans. AGU, Spring Meeting Suppl., 73, 14, p. 341.

SOLER, P., & JIMENEZ CH., N., 1993 - Magmatic constraints upon the evolution of the Bolivian Andes since Late Oligocene times, this volume.

SOLER, P., CARLIER, G., AITCHESON, S. J., & FORNARI, M., 1993 - Sr, Nd and Pb isotopic constraints upon the origin of the Quaternary shoshonitic lavas and the deep structure of the central Altiplano of Bolivia. EUG VII, Strasbourg (France), TERRA Absrtracts, Abstract Suppl. n°1 to TERRA nova, vol. 5, p. 584-585.

SOLER, P., CARLIER, G., & FORNARI, M., in prep. - The shoshonitic province of the southern Altiplano of Bolivia

THORPE, R.S. & FRANCIS, P.W., 1979 - Variations in Andean andesites compositions and their petrogenetic significance. Tectonophysics, 57, p. 53-70.

THORPE, R.S., FRANCIS, P.W., HAMMILL, M. & BAKER, C.W., 1982 - The Andes. In : Andesites : Orogenic andesites and related rocks, R.S. Thorpe, ed., John Wiley & sons, p. 187-205.

THORPE, R.S., FRANCIS, P.W. & O'CALLAGHAN, L., 1984 - Relative roles of source composition, fractionnal crystallization and crustal contamination in the petrogenesis of Andean volcanic rocks. Phil. Trans. Roy. Astron. Soc., A310, p. 675-692.

MAGMATIC CONSTRAINTS UPON THE EVOLUTION OF THE BOLIVIAN ANDES SINCE LATE OLIGOCENE TIMES

Pierre SOLER (1), and Nestor JIMENEZ CH. (2)

(1) ORSTOM, UR1H, 213 rue Lafayette, 75480 Paris Cedex 10, France, Mission ORSTOM, Casilla 9214, La Paz, Bolivia, and CNRS, URA 736, Université Paris 6, Tour 26, 3ème étage, 4 Place Jussieu, 75005 Paris, France
(2) GEOBOL, Servicio Geológico de Bolivia, Casilla 2729, La Paz, Bolivia

RESUMEN : Se presenta una síntesis de la distribución espacial y temporal de las rocas igneas (ácidas peraluminosas, alcalinas, shoshoníticas / peralcalinas) de tras-arco del Altiplano y de la Cordillera Oriental de Bolivia y se discuten las relaciones entre este magmatismo y los diferentes episodios de estructuración orogénica de los Andes Bolivianos.

KEY WORDS : Bolivia, Oligocene, Neogene, Magmatism, Arc, Back-arc

INTRODUCTION

In addition to their peculiar tectonic and morphological features, the central Andes of southern Peru, Bolivia and northwesternmost Argentina (i.e. the "Bolivian Orocline") display quite specific Oligocene to Present magmatic and metallogenic (the tin province) features when compared with adjacent segments of the Andes. We present a synthesis of available data relevant to the distribution in time and space of the different types of back-arc magmatic rocks in the Altiplano and Cordillera Oriental of Bolivia and discuss the relationships between this back-arc magmatism and the orogenic evolution of the Bolivian Andes.

THE DIFFERENT MAGMATIC EPISODES

In the Altiplano and Cordillera Oriental of Bolivia, East of the Oligocene to Present subduction -related volcanic arc of the Central Volcanic Zone of the Andes, three types of magmatic rocks are known since late Oligocene times : (1) acidic, often peraluminous, effusive and intrusive rocks; (2) alkaline volcanic rocks; and (3) shoshonitic and ultrapotassic volcanic and subvolcanic rocks. Available radiochronological data show that this back-arc magmatic activity is distributed into discrete episodes, each one displaying a specific position within the orocline.

Felsic magmatism

Four pulses of felsic, more or less peraluminous, magmatism have been documented within the Altiplano and the Cordillera Oriental of Bolivia and southern Peru.

1) The first one, with ages between 28 and 23.5 Ma, defines a belt restricted to the northern NW-trending branch of the Cordillera Oriental in southern Peru (data and references in Clark et al., 1990) and Bolivia. In Bolivia, the most conspicuous features of this belt are the granodioritic to granitic, metaluminous to slightly peraluminous massifs of the Cordillera Real southeast of La Paz (Illimani, Quimsa Cruz, Santa Vera Cruz - Evernden et al., 1977; McBride et al., 1983) and metaluminous stocks (Kumurana, Coriviri, San Pablo-Morococala - Evernden et al., 1977; Grant el al., 1979; Schneider and Halls, 1985) of the Potosi-Morococala area. This episode is characterized by a northwestward increasing peraluminosity and increasing initial Sr isotopic ratios (0.707 to 0.719) of the magmas.

2) A second episode (22 to 19 Ma) is documented only in the southeastern part of NW-trending branch of the Cordillera Oriental of Bolivia from Santa Vera Cruz to Kari Kari (Potosi). The

most striking features of this episode are subvolcanic stocks and extrusive rocks (Llallagua, Colquechaca, Tinquipaya,, ...) and the Kari Kari caldera (peraluminous, garnet and cordierite-bearing high-K andesite to high-K rhyolite with initial Sr isotopic ratio at 0.7105 - e.g. Francis et al., 1981; Schneider, 1985) and associated effusive rocks (Agua Dulce and Mondragon volcanics).

3) After a period of apparent magmatic quiescence, the belt corresponding to the third episode (17 to 13 Ma) has a greater longitudinal extension and is shifted towards the West with respect to the first two belts. It is documented in the Altiplano and Cordillera Oriental of southern Peru (see Clark et al., 1990). In the Altiplano and the western part of the Cordillera Oriental of northern Bolivia many small extrusive and shallow intrusive, mainly dacitic, bodies belong to this episode (Evernden et al., 1977; Grant et al., 1979; McBride et al., 1983; Redwood and Macintyre, 1989). In the Potosi area, the Cerro Rico, and the Cebadillas extrusive (slightly peraluminous dacites, with initial Sr isotopic ratio in the range 0.707-0.712 - Schneider, 1985) belong to this episode. This third belt extends southwards down to the Bolivia-Argentina border [volcanic centers of Tasna, Chocaya, Chorolque, Tatasi (Grant et al., 1978), San Vicente, Bonete and Morokho (Fornari et al., 1991, this volume)].

4) The fourth episode (10.5 and 2 Ma, main activity between 8,5 and 5 Ma) is the most important in volume. The main feature of this episode is the emission of enormous quantities of peraluminous quartz-latitic to rhyolitic ignimbrites with some resurgent domes in three centers within the Cordillera Oriental: Macusani (see Clark et al., 1990) in southern Peru, Morococala (Koeppen et al., 1987; Lavenu et al., 1989; Ericksen et al., 1990) and Los Frailes (Schneider, 1985; Schneider and Halls, 1985) in Bolivia. In Los Frailes the compositions and isotopic ratios of these tuffs are quite similar to those of the previous Cebadillas episode. In this area post-meseta domes of Pliocene age (4-2 Ma) are known. The partly eroded and undated stratovolcanoes (Cuzco, Cosuña, ...) immediatly to the south of Los Frailes would belong to this last Pliocene pulse. This episode also comprises various stocks and volcanic complexes in the Cordillera Oriental of southern Peru (see Clark et al., 1990), and in both the northern (Redwood and Macintyre, 1989) and southern (Orstom, unpub. data) Altiplano of Bolivia.

Alkaline volcanism

One of the more peculiar feature of the Bolivian Altiplano is the presence of a voluminous alkaline volcanism of late Oligocene - early Miocene age (28-21 Ma). This episode gathers various previously described volcanic formations, the kinship of which has been recognized only recently (see Jimenez et al., this volume; Soler et al., this volume.).

In the northern and central Altiplano of Bolivia, this volcanism — Abaroa Fm. towards the NW (Lavenu et al., 1989; Jimenez et al, 1993 and this volume), Tambo Tambillo lavas towards the SE (Evernden et al., 1977; Soler et al., this volume and unpub. data), and unnamed equivalents in the intermediate Andamarca-Corque region — define a NNW-trending, 400 km long, *en échelon* belt, which is quite oblique with respect to the mid-Miocene to modern calc-alkaline arc. In its northwesternmost part this belt is presently partly covered by the subduction-related arc, while southeastwards it is well apart from the arc. This belt seems to have a northern prolongation in the Altiplano of southern Peru where the presence of monzogabbros, and trachytic to phonolitic flows has been documented (Ayaviri area - ages between 28 and 23 Ma, Bonhomme et al., 1985).

In the southern Altiplano outcrops of alkaline volcanism [e.g. Julaca Fm., Rondal Fm. (Kussmaul et al., 1975; Fornari et al., 1991, this volume), Tupiza volcanics (Hérail et al., 1992, this volume) are less continuous and are mostly known along documented N-S and SW-NE trending strike-slip faults (Sempere et al., 1988, 1990a; Hérail et al., 1992, this volume).

Shoshonitic and ultrapotassic volcanism

Four short-lived episodes of shoshonitic / ultrapotassic volcanism have been documented along the Bolivian Orocline since late Oligocene times.

The first one (28-24 Ma) is mostly known in the Cordillera Oriental of southeastern Peru (Moromoroni, Crucero basin) (data and references in Clark et al., 1990). In the Cordillera Real southeast of La Paz some lamprophyric dykes of the Illimani massif and surrounding area (27.3 Ma - McBride et al., 1983) belong to this episode.

A second short-lived episode of shoshonitic volcanism (13-11 Ma) has been documented in Bolivia (Redwood and Macintyre, 1989; Soler et al., 1992a; Hérail et al., in press) within the Huarina Thrust and Fold Belt (Sempere et al., 1988, 1990a) at the transition Cordillera Oriental-northern Altiplano.

A third episode of shoshonitic volcanism of Pliocene age has been reported by Lefèvre (1979) in the Altiplano of southeasternmost Peru. This episode has not been documented so far in the Bolivian Altiplano.

A fourth episode of shoshonitic volcanism, Quaternary in age (less than 1 Ma), has been documented in the central Altiplano of Bolivia (Davidson et al., 1991; Carlier et al., 1992; Soler et al., 1992, 1993 and in prep.). It was already well known in southeastern Peru and northwesternmost Argentina.

The first episode of shoshonitic volcanism is coeval with the first episode of felsic magmatism to the northern NW-trending branch of the Cordillera Oriental, while the subsequent episodes of shoshonites seem to have occurred (although some overlapping may be observed) in periods during which no peraluminous, felsic magmatism is documented.

Magmatic episodes and tectonics in the Bolivian Andes since Late Oligocene times

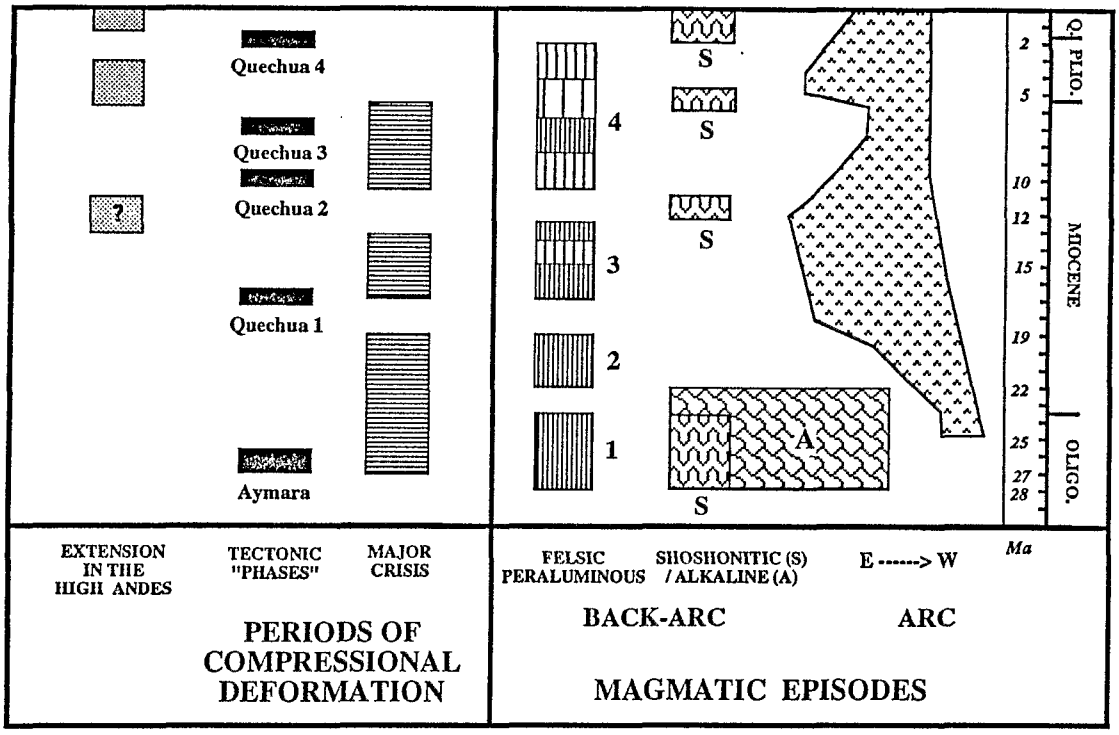

RELATIONS WITH THE TECTONIC EVOLUTION AND THE GEODYNAMIC SETTING

The long-lived episodes of felsic, more or less peraluminous magmatism seem to be coeval with long periods of compressional deformation (e.g. Sempere et al., 1988, 1990ab; Sempere, 1991; Gubbels et al., 1993; Hérail et al., 1993) which would include some climax of deformation corresponding to the so-called (and challenged; see Sempere, 1991) compressional phases or events (e.g. Lavenu, 1986; Sébrier and Soler, 1991).

The mid-Miocene to Quaternary short-lived episodes of shoshonitic/ultrapotassic volcanism seem be restricted to the periods during which extensional or trans-tensional conditions prevailed in the high Andes (Lavenu, 1986; Sébrier and Soler, 1991; Carlier et al., 1992b; Soler et al., 1992b, in prep.).

The shoshonites and the peraluminous rocks are restricted to the segment of the Andes and the time span in which a lithospheric scale underthrusting of the Brazilian shield beneath the Andes is documented. We consider (Carlier et al., 1992ab; Soler et al., 1992b, in prep.) that the source of the shoshohitic volcanism of the Central Andes is the subcontinental lithospheric mantle in which the low percentage of melting which produces primary peralkaline magmas is triggered by the "continental subduction" of the Brazilian Shield under the Andes. These magmas undergo complex processes of contamination (by difusion, partial melting of the country rocks and mingling, ...) in the lower and middle crust. They reach the surface only when extensional or trans-tensional conditions prevail. During the long-lived periods of compressionnal structuration no shoshonitic volcanism is observed and the peralkaline and shoshonitic magmas evolve through magmatic differentiation and crustal

contamination towards felsic (mostly dacitic), often peraluminous, magmas, the crustal origin of which (following the standard viewpoint) should be challenged. In this view, neither the shoshonitic volcanism nor the felsic, peraluminous magmatism are directly linked to the subduction of the Nazca plate under the South American continent.

This absence of direct relation with the subduction process is very clear for the late Oligocene - early Miocene period during which the documented alkaline "belt" is located between the western calc-alkaline arc and the eastern belt of felsic and shoshonitic/peralkaline magmatism. The beginning of this alkaline episode (and of episodes 1 of felsic magmatism and shoshonitic volcanism) corresponds to a period (30-25 Ma) during which no subduction-related calc-alkaline arc is documented — probably because the rate of convergence between the Nazca plate and South America was very low (e.g. Soler, 1991) —, and to the onset of orogenic deformation in the eastern part of the Altiplano, the Cordillera Oriental and Subandean zone of Bolivia (Sempere et al., 1990ab; Sempere, 1991). Although still poorly understood, this very primitive alkaline magmatism would be derived from the subcontinental lithospheric mantle in trans-tensional conditions.

REFERENCES

BONHOMME. M.G., AUDEBAUD, E., & VIVIER, G., 1985 - K-Ar ages of Hercynian to Neogene rocks along an East-West cross section in Southern Peru. Comunicaciones (Santiago), 35, p. 27-30.

CARLIER, G., SOLER, P., & CARLOTTO, V., 1992a - Mineralogical, geochemical, isotopic and geotectonic constraints upon the origin of Quaternaruy shoshonitic lavas in the Andes of Southeastern Peru. EOS Trans. AGU, Spring Meeting Suppl., 73, 14, p. 341-342.

CARLIER, G., SOLER, P., FORNARI, M., & HÉRAIL, G., 1992b - Orígen y significado tectónico del volcanismo shoshonítico neógeno a cuaternario en los Andes. Bol. Soc. Geol. Bol., 27, p. 173-175.

CLARK, A. H., FARRAR, E., KONTAK, D. J., LANGRIDGE, R. J., ARENAS F., M. J., FRANCE, L. J., MCBRIDE, S. L., WOODMAN, P. L., WASTENEYS, H. A., SANDEMAN, H. A., & ARCHIBALD, D. A., 1990 - Geologic and geochronologic constraints on the metallogenic evolution of the Andes of Southeastern Peru. Economic Geology, 85, p. 1520-1583.

DAVIDSON, J.P., DE SILVA, S.L., ESCOBAR, A., FEELEY, T. & BOHRSON, W. 1991 - Evaluation of magma sources for central Andean volcanics. 6to Congreso Geológico Chileno, Resumenes Expandidos, p. 347-349.

ERICKSEN, G.E., LUEDKE, R.G., SMITH, R.L., KOEPPEN, R.P., & URQUIDI B., F., 1990 - Peraluminous igneous rocks of the Bolivian tin belt. Episodes, 13, 1, p. 1-7.

EVERNDEN, J. F., KRIZ, S. J., & CHERRONI M., C., 1977 - Potassium-Argon ages of some Bolivian rocks. Economic Geology, 72, p. 1042-1061.

FORNARI, N., HÉRAIL, G., POZZO, L., & VISCARRA, G., 1991 - Los yacimientos de oro de los Lipez (Bolivia). Tomo I: Estratigraffía y dinámica de emplazamiento de las volcanitas del aréa de Guadalupe. Mission ORSTOM en Bolivie, La Paz, Rapport n°19, 28 p.

FORNARI, M., POZZO, L., SOLER, P., BAILLY, L., LEROY, J., & BONHOMME, M.G., 1993 - Miocene volcanic centers in the Southern Altiplano of Bolivia. The Cerro Morokho-Cerro Bonete area (Sur Lipez). This volume.

FRANCIS, P.W., BAKER, C.M.W., & HALLS, C., 1981 - The Kari Kari Caldera, Bolivia and the Cerro Rico stock. J. Volc. Geotherm. Res., 10, p. 113-124.

GRANT, J. N., HALLS, C., AVILA SALINAS, W., & SNELLING, N., 1979 - K-Ar ages of igneous rocks and mineralization in part of the Bolivian tin belt. Economic Geology, 74, p. 838-851.

GUBBELS, T. L., ISACKS, B. L., & FARRAR, E., 1993 - High-level surfaces, plateau uplift, and foreland development, Bolivian Central Andes. Geology, in press.

HÉRAIL, G., OLLER, J., BABY, P., SEMPERE, T., BLANCO, J., BONHOMME, M. G., & SOLER, P., 1992 - Las cuencas de Tupiza, Nazareño, Estarca: sucesión de tectónica de transcurrencia y de cabalgamiento en la estructuracion de los Andes de Bolivia. Bol. Soc. Geol. Boliviana, 27, p. 81-83.

HÉRAIL, G., OLLER, J., BABY, P., BLANCO, J., BONHOMME, M. G., & SOLER, P., 1993 - The Tupiza, Nazareño, Estarca basins (Bolivia): strike-slip faulting and thrusting during the Cenozoic evolution of the southern branch of the Bolivian Orocline. This volume.

HÉRAIL, G., SOLER, P., BONHOMME, M. G., & LIZECA, J. L., 1993 - Evolution géodynamique de la transition Altiplano - Cordillère Orientale au Nord d'Oruro (Bolivie) - Implications sur le déroulement de l'orogénèse andine. C. R. Acad. Sci. Paris, in press.

JIMENEZ CH., N., BARRERA I., L., FLORES B., O., LIZECA B., J. L., MURILLO S., F., HARDYMAN, R. F., TOSDAL, R. M., & WALLACE, A. R., 1993 - Marco geológico de la región de Berenguela. *In:* Investigación de metales preciosos en los Andes Centrales, Proyecto BID/TC-88-02-32-5, p. 63-74.

JIMENEZ CH., N., BARRERA I., L., FLORES B., O., LIZECA B., J. L., HARDYMAN, R. F., TOSDAL, R. M., & WALLACE, A. R., 1993 - Magmatic evolution of the Berenguele-Charaña region, northwestern Altiplano, Bolivia. This volume

KOEPPEN, R. P., SMITH, R. L., KUNK, M. J., FLORES, M., LUEDKE, R. G., & SUTTER, J. F., 1987 - The Morococala volcanics: highly peraluminous rhyolite ash flow magmatism in the Cordillera Oriental, Bolivia. GSA Annual Meeting, Phoenix, Arizona, Abstracts with Programs.

KUSSMAUL, S., JORDAN, L., & PLOSKONKA, E., 1975 - Isotopic ages of Tertiary volcanic rocks of SW-Bolivia. Geol. Jb. (Hannover), B14, p. 111-120.

LAVENU, A., 1986 - Etude néotectonique de l'Altiplano et de la Cordillère Orientale de Bolivie. Thèse de Doctorat d'Etat ès-Sciences, 434 p., Université Paris Sud - Orsay.

LAVENU, A., BONHOMME, M. G., VATIN-PERIGNON, N., & PACHTERE de, P., 1989 - Neogene magmatism in the Bolivian Andes between 16° and 18° S. Stratigraphy and K-Ar geochronology. J. South Amer. Earth Sci., 2, 1, p. 35-47.

LEFÈVRE, Ch., 1979 - Un exemple de volcanisme de marge active dans les Andes du Pérou (Sud) du Miocène à l'actuel (zonation et pétrogénèse des andésites et shoshonites). Thèse de doctorat d'Etat-ès-Sciences, Univ. Montpellier, 555 p.

MCBRIDE, S. L., ROBERTSON, C. R., CLARK, A. H., & FARRAR, E., 1983 - Magmatic and metallogenetic episodes in the northern tin belt, Cordillera Real, Bolivia. Geol. Rdsch., 72, p. 685-713.

REDWOOD, S. D., & MACINTYRE, R. M., 1989 - K-Ar dating of Miocene magmatism and related epithermal mineralization of the northeastern Altiplano of Bolivia. Econ. Geol., 84, p. 618-630.

SCHNEIDER, A., 1985 - Eruptive processes, mineralization and isotopic evolution of the Los Frailes Karikari volcanic field/Bolivia. Unpub. Ph D thesis, Imperial College, University of London.

SCHNEIDER, A., & HALLS, C., 1985 - Cronología de los procesos eruptivos y de mineralización el el campo volcánico de Los Frailes Kari Kari, Cordillera Oriental, Bolivia. Comunicaciones (Santiago), 35, p. 217-224.

SEBRIER, M., & SOLER, P., 1991 - Tectonics and magmatism in the Peruvian Andes from upper Oligocene to present. Geological Society of America, Special Paper 265 "Andean magmatism and its tectonic setting", R. Harmon & C. Rapela, eds., p. 259-278.

SEMPERE, T., HÉRAIL, G., & OLLER, J., 1988 - Los aspectos estructurales del oroclino boliviano. V Cong. Geol. Chileno, Santiago, Actas, t. 3, p. A127-A142.

SEMPERE, T., HÉRAIL, G., OLLER, J., & BONHOMME, M., 1990a - Late Oligocene-early Miocene major tectonic crisis and related basins in Bolivia. Geology, 18, p. 946-949.

SEMPERE, T., HÉRAIL, G., OLLER, J., BABY, P., BARRIOS, L., & MAROCCO, R., 1990b - The Altiplano : a province of intermontane foreland basins related to crustal shortening in the Bolivian Orocline area. Intern. Symp. Andean Geodynamics, Grenoble (France), Extended abstracts, ORSTOM, Série "Colloques et Séminaires", p. 167-170.

SEMPERE, T., 1991 - Cenozoic tectonic "phases" in Bolivia : some needed clarifications. 6to Cong. Geol. Chileno, Viña del Mar, Actas, 1, p. 877-881.

SOLER, P., 1991 - Contribution à l'étude du magmatisme associé aux marges actives. Pétrographie, géochimie et géochimie isotopique du magmatisme crétacé à pliocène le long d'une transversale des Andes du Pérou central. Implications géodynamiques et métallogéniques. Thèse de Doctorat d'Etat ès-Sciences, 857 p., Université Pierre et Marie Curie - Paris 6.

SOLER, P., HÉRAIL, G., LIZECA, J. L., & BONHOMME, M. G., 1992a - Tectónica, magmatismo y erosión al contacto entre el Altiplano y la Cordillera Oriental al Norte de Oruro - Implicaciones sobre la orogénesis andina en Bolivia. Bol. Soc. Geol. Boliviana, n° 27, p. 168-172.

SOLER, P., CARLIER, G., FORNARI, M., & HÉRAIL, G., 1992b - An alternative model for the origin and the tectonic significance of the Neogene and Quaternary shoshonitic volcanism of the Andes. EOS Trans. AGU, Spring Meeting Suppl., 73, 14, p. 341.

SOLER, P., CARLIER, G., AITCHESON, S. J., & FORNARI, M., 1993 - Sr, Nd and Pb isotopic constraints upon the origin of the Quaternary shoshonitic lavas and the deep structure of the central Altiplano of Bolivia. EUG VII, Strasbourg (France), TERRA Abstracts, Abstract Suppl. n°1 to TERRA nova, vol. 5, p. 584-585.

SOLER, P., CARLIER, G., BONHOMME, M.G., & FORNARI, M., 1993 - Field observations and K-Ar dating of Cerro Chiar Kkollu (Southern Altiplano, Bolivia). This volume.

SOLER, P., CARLIER, G., & FORNARI, M., in prep. - The shoshonitic province of the south-central Altiplano of Bolivia.

PETROLOGICAL MULTIPLICITY OF THE COLOMBIAN ANDES OPHIOLITES

Piera SPADEA (1) and Armando ESPINOSA (2)

(1) Department Georisorse Territorio, University of Udine, Italy
(2) INGEOMINAS, Cali, Colombia

RESUMEN. En los Andes del suroeste de Colombia, terrenos oceanicos de edad Cretacica-Terciaria temprana componen el basamento del la Cordillera Occidental y la Zona de Romeral hasta el flanco occidental de la Cordillera Central. Las rocas volcanicas mostran caracteristicas petrologicas y geoquimicas de T-MORB, IAT y de sequencia calco-alcalina de arco intraoceanico de islas. Las rocas ofioliticas de origen plutonica que se encuentran en la Zona de Romeral son similares a las sequencias generadas en zonas supra-subduccion.

KEY WORDS: ophiolites, Mesozoic, petrology, geochemistry, Colombian Andes.

INTRODUCTION

The Andean belt of Colombia is characterized by accreted oceanic terranes whose age of formation is referred to the early Cretaceous (or late Jurassic)-early Tertiary interval. Their emplacement is debated with respect to timing and mechanism. Petrological data on the primary features of the magmatic rocks are here presented and addressed mainly to the geodynamic setting of the magmatism and the reconstruction of the pre-collision history.

GEOLOGIC SETTING

In southwestern Colombia, Mesozoic oceanic sequences are present in the Serrania de Baudo along the Pacific coastal range (Goossens et al. 1977) and the Western Cordillera (Millward et al. 1984). To the east the oceanic sequences are bounded by the NNE trending Romeral fault system exposing fragments of mafic-ultramafic plutonics and mafic and ultramafic extrusives (Barrero 1979, Espinosa 1980, Spadea et al. 1987, 1989) and high-pressure metabasic rocks (Orrego et al. 1980). The Romeral Zone, extending from the Cauca-Patia graben to the western flank of Central Cordillera, is thought to represent a suture marking a Cretaceous ocean/continent boundary.

The Romeral Zone ophiolites and the volcanic sequences from Central Cordillera are interpreted as an oceanic terrane accreted onto the continental

margin before approximately 110 Ma (Bourgois et al. 1985) or 120 Ma ago (Aspden and McCourt 1986), while the Western Cordillera volcanic sequences are considered as an allochtonous terrane accreted onto the continental edge about 80-75 Ma (Bourgois et al. 1985) or 65-60 Ma ago (McCourt et al. 1984).

PETROCHEMICAL FEATURES

Some typical magmatic sequences occurring in the area between Buga to the north and the Colombia-Ecuador border to the south have been studied.

In Western Cordillera, the volcanic rocks known as Diabase Group (Volcanic Formation of the official geological map at the scale 1:100.000) include petrologically distinct magmatic asemblages, that are:

1. tholeiitic basalts, mostly aphyric or containing sparse olivine and pyroxene phenocrysts, moderately fractionated (mg number 63-45), relatively rich in Nb and similar in REE contents to mid-ocean ridge basalts, slightly light REEs-depleted. Their chemical features indicate affinities with T-MORB, as recognized by Millward et al. (1984);
2. basalts, aphyric or plagioclase-clinopyroxene phyric, basaltic andesites and andesites, mostly highly plagioclase- and clinopyroxene- or amphibole-phyric similar in chemistry to tholeiitic and calc-alkaline lavas from island-arcs. Evidences for these affinities are a low values of high field-strenght elements, a strong enrichment of LREEs, and lack of heavy REEs fractionation as shown in figure 1.

Plutonic rocks primarily associated and cogenetic with the two assemblages include ferrogabbro and plagiogranite (assemblage 1), and diorite-quartz diorite (assemblage 2).

In the Cauca trough and western Central Cordillera (Romeral Zone), basaltic to picritic extrusives and mafic-ultramafic plutonic sequences, interpreted as dismembered ophiolites, occur.

The volcanic sequences, previously referred to the Diabase Group (partly identified as Amaime Formation in the official geological map), include:

3. tholeiitic basalts sparsely olivine- and/or plagioclase phyric, with chemical characteristics of T-MORB. Lavas composed of highly olivine phyric picrites (atr Rio Boloblanco: Spadea et al. 1989) are associated with these basalts;
4. picritic basalts and picrites, mostly highly olivine phyric, characterized by relatively high contents of Ti and transition elements (at El Encenillo: Spadea et al. 1989) and strongly LREEs enrichments;
5. tholeiitic basalts, aphyric or sparsely augite phyric, low in Ti and high field--strenght elements, with IAT affinities.

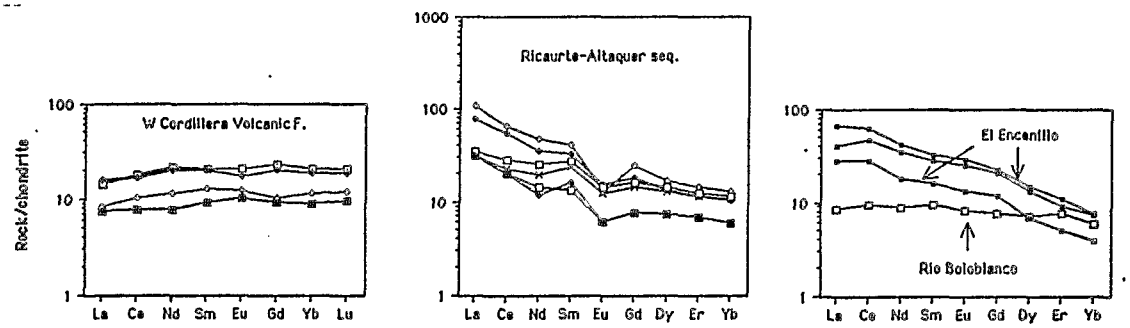

Figure 1. Typical REE patterns of Colombian Andes volcanics (assemblages 1-4).

The most conspicuous fragments of mafic-ultramafic plutonics occur in the Cauca trough near Bolivar, Ginebra and at Los Azules. The rocks show generally

well preserved magmatic features and allow to recognize different lithological assemblages characterizing petrologically each complex.

The Bolivar complex shows an about 800 meters thick sequence consisting upwards of mafic-ultramafic cumulates (interlayered dunite, websterite, wehrlite, olivine gabbronorite, gabbronorite), layered hornblende gabbronorite, metagabbro and metadiabase (now amphibolites). Remnants of mantle rocks (dunite and lherzolite: Benciolini and Spadea, in preparation) occur in the lower part. The whole sequence is intruded by pegmatitic quartz-diorite.

The Ginebra complex shows of an about 500 meters thick sequence of interlayered dunite, websterite, wehrlite and gabbronorite overlain by layered clinopyroxene metagabbro and massive metagabbro and metadiabase (now amphibolite). Metamorphosed basaltic pillow-lavas capped with volcanic siltstone occur on top of the sequence.

At Los Azules the plutonic sequence consists upwards of dunite-wehrlite cumulates, layered clinopyroxene-hornblende gabbro and massive pegmatitic gabbro. A well developed extrusive section consisting of dike swarm and lavas of basaltic to picritic composition occurs (Spadea et al. 1989).

Regarding the Bolivar and Ginebra plutonic sequences, most petrographical and mineralogical feature, particularly: a) lithological assemblage (occurrence of abundant websterite and gabbronorite in the lower cumulates), b) inferred crystallization order (olivine, clinopyroxene/orthopyroxene, plagioclase), c) mineral chemistry (particularly plagioclase up to 98% An in the gabbros), indicate a similarity with supra-subduction zone sequences. Further chemical studies will clarify if comagmatic sequences occur in the two complexes and the nature of the parental magma or magmas.

The Los Azules complex also displays some petrological features suggesting a supra-subduction zone setting. Its comagmatic origin is however suspect, and the widespread high-Mg rocks represent a distinctive features with respect to the other complexes from the Romeral Zone.

CONCLUSIONS

The volcanic sequences and the ophiolitic fragments from the Western and Central Cordillera of the southwestern Colombian Andes consist of different rock suites. Those emplaced during a younger, i. e., latest Cretaceous accretionary event, include tholeiites with T-MORB affinities and calc-alkaline and tholeiitic island-arc rocks. The volcanic rocks related to a older, i. e., early Cretaceous, accretionary event include a MORB-like, variably enriched tholeiitic suite and a island-arc tholeiitic suite. The ophiolitic fragments emplaced during the same event include plutonic sequences with characteristics of tholeiitic suites generated in supra-subduction zone.

The magmatic characteristics are consistent with some of the different settings proposed in the literature (subduction zone; oceanic plateau, as recently suggested by Storey et al , 1991). A geodynamic model, however, is difficult to infer only from the petrological data.

REFERENCES

ASPDEN, J. A., and McCOURT, W. M., 1986. Mesozoic oceanic terranes in the central Andes of Colombia. Geology, 14: 415-418.

BARRERO, D., 1979. Geology of the Central-Western Cordillera, west of Buga and Roldanillo, Colombia. INGEOMINAS, Popayan, Spec. Publ. 4, 75 p.

BENCIOLINI, L., and SPADEA, P. (in preparation). Mantle rocks from the Bolivar mafic-ultramafic sequence (Colombian Andes).
BOURGOIS, J., TOUSSAINT, J.-F., GONZALES, H., ORREGO, A., AZEMA, J., CALLE, B., DESMET, A., MURCIA, L.A., PABLO, A., PARRA, E., and TOURNON, J., 1985. Les ophiolites des Andes de Colombie: évolution structurale et signification géodynamique. In: Mascle, A. (ed). Geodynamique des Caraibes, Technips, Paris, 475-493.
ESPINOSA, A., 1980. Sur les roches basiques et ultrabasiques du bassin du Patia. Ph. D. thesis, University of Geneva, 147 p.
GOOSSENS, P.J., ROSE Jr., W.I., and FLORES, D., 1977. Geochemistry of tholeiites of the Basic Igneous Complex of northwestern South America. Geol. Soc. America Bull., 88: 1711-1720.
McCOURT, W. J., ASPDEN, J. A., and BROOK, M., 1984. New geological and geochronological data from the Colombian Andes: Continental growth by multiple accretion. Geol. Soc. London J. 141: 831-845.
MILLWARD, D., MARRINER, G.F., and SAUNDER, A.D., 1984. Cretaceous tholeiitic volcanic rocks from the Western Cordillera of Colombia. Geol. Soc. London J., 141: 847-860.
ORREGO, A., CEPEDA, H., and RODRIGUEZ, G., 1980; Esquistos glaucofanicos en el area de Jambalò, Cauca, Colombia. Geologia Norandina, 1: 5-10.
SPADEA, P., DELALOYE, M., ESPINOSA, A., ORREGO, A., and WAGNER, J.-J., 1987. Ophiolite complex from La Tetilla, Southwestern Colombia, South America. J. Geol., 95: 377-395.
SPADEA, P., ESPINOSA, A., and ORREGO, A., 1989. High-Mg extrusive rocks from the Romeral Zone ophiolites in the southwestern Colombian Andes. Chem. Geol., 77: 303-321.
STOREY, M., MAHONEY, J.J., KROENKE, L.W., and SAUNDERS, A.D., 1991. Are oceanic plateus sites of komatiite formation? Geology, 19: 376-379.

THE 1990-92 ERUPTIVE ACTIVITY OF THE NEVADO SABANCAYA STRATOVOLCANO (SOUTH PERU).

J.-C. Thouret*, A. Gourgaud*, G.Salas, D. Huaman** & R. Guillande*****
* URA 10 CNRS et Centre de Recherches Volcanologiques, Université Blaise Pascal, 5 rue Kessler, 63000 Clermont-Fd, France.
** Universidad Nacional San Agustin et Institutto Geofisico del Peru, Arequipa, Peru.
*** Geosciences Consultants, Paris.

The May 28, 1990, eruption of the Nevado Sabancaya volcano (south volcanic zone of Peru, Western Cordillera) ended an apparent dormant stage of about 200 years in duration. This ice-clad stratovolcano threatens about 35,000 people living in the Rio Colca and Siguas valleys. This study based on remote sensing and limited fieldwork aims to portray the geological and geomorphic features of the summit volcano, to follow the evolution of the explosive activity and the tephra-fall deposits that were expelled in October 1990 and December 1992, as well as to map hazard-zones at and around Nevado Sabancaya.

A remote sensing study based on SPOT images have been used to map the block-lava flows of Holocene age and the young twin domes of the summit volcano. Five SPOT images over the year 1990 have enabled us to follow-up how much the explosive activity has disrupted the summit and crater morphology. They were also used to evaluate how the ice cap has been fractured, carved, and covered by repeated thin tephra-fall, and how runout mudflows have been triggered (fig.1)

The tephra (ca. 0.025 km^3 in 1990) related to the vulcanian activity of Nevado Sabancaya are compositionally variable, from andesite (58% SiO_2) to dacite (63% SiO_2), in a K-rich calk-alkaline suite. The mineral assemblage of 1990-92 juvenile magma consists of plagioclase, green pyroxene, brown amphibole, biotite, destabilized olivine, and oxydes. From October 1990 to December 1992, the juvenile component increased from 15% to ca. 50 % by volume : there are black, glassy, slightly vesicular fragments, andesitic in composition, and grey fragments, dacitic in composition. In addition, a few mafic inclusions and banding are related to a weak geochemical contrast. Moreover, mineralogical desequilibrium also suggests an interaction between two contrasted magmas : a felsic one, dacitic, including oligoclase and hypersthene and a mafic one, andesitic or basaltic, including labrador, bronzite and olivine phenocrysts. Such preliminary data suggest the mingling of two contrasted magmas, a process that may be evolving during present-day eruptive activity.

Hazards posed by the the Nevado Sabancaya volcano are bound to the recent behaviour of similar volcanoes in that area, which have had Plinian eruptions over the past 500 years. In addition, Nevado Sabancaya has been active over the past 200 years, and is still ice-clad (3.5 km^2 of glacier ice) despite its two-year-long activity. Block-lava flows Holocene in age cover as much as 40 km^2 around the summit domes. Historical, thin plinian tephra-fall deposits are found as far as 11 km from the crater and block-and-ash pyroclastic-flow deposits as far as 7 km away from the source. Recent lahars have travelled ca. 25 km downvalley towards NE and SW.

Hazard appraisal and hazard-zone mapping are based on geological and geomorphological data, photo-interpretation, remote sensing, as well as on models of tephra dispersion and pyroclastic flowage. One map shows hazard zones for tephra fall, pyroclastic flows, lahars, and also for uncommon but catastrophic potential events (fig.2). These hazard zones are portrayed according to three types of eruptive behaviour : the 1990-92 moderate vulcanian activity, a possible increase of this vulcanian activity, and a potential Plinian large-scale event.

Figure 1. Geological and geomorphic evolution of the Nevado Sabancaya summit volcano over the year 1990.
1. preexisting vent before May 28, 1990 ; 2. crater and fractures as of July 1, 1990 ; 3. south dome ; 4. ice cap ; 5. wet ashfall deposits carried by slope runoff ; 6. fans of ash and debris deposited by rapid snow- and ice-melt ; 7. gully scouring the ice cap as of October 1990 ; 8. scarps or fractures detected by remote sensing (SPOT) and in the field as of July 1990 ; 9. scarps or fractures detected by remote sensing (SPOT) as of December 1990 ; 10. Nevado Ampato and Hualca Hualca ice caps slightly covered by ash and dust from Nevado Sabancaya.

Figure.2. Map showing the eruptive products and the areas likely to be affected by the present-day (1990-92) vulcanian activity or by a potentially increasing explosive activity at Nevado Sabancaya.
I. Areas affected by fallout : 1) present-day ballistic ejecta ; 2) ashfall towards east and 1-cm-thick isopach ; 3) potential ashfall towards west and 1-cm-thick isopach. *II. Areas affected by tephra-laden snow-and-ice avalanches* : 4) present-day area of gullies and avalanches; 5) ice cap covered by tephra and likely to be affected. *III. Areas likely to be affected by pyroclastic flows* : 6) circle line where the energy line of potential pyroclastic flows would intersect the topography of the summit volcano ; 7) presumed paths of potential channeled pyroclastic flows. *IV. Areas likely to be affected by lahars or debris flows* : 8) probable paths of potential lahars that would be triggered by pyroclastic flowage on the ice cap ; 9) possible paths of potential lahars that would be induced by surficial melt of the neighbour volcanoes ice caps ; 10) Nevado Sabancaya ice cap ; 11) seasonal snow cover (December-March) *V. Areas likely to be affected by lava flows* : 12) probable block-lava flows ; 13) possible lava flows. *VI. Other elements prone to risk* : 14) irrigation canals ; 15) unpaved roads ; 16) peat-bogs and pasture grounds.

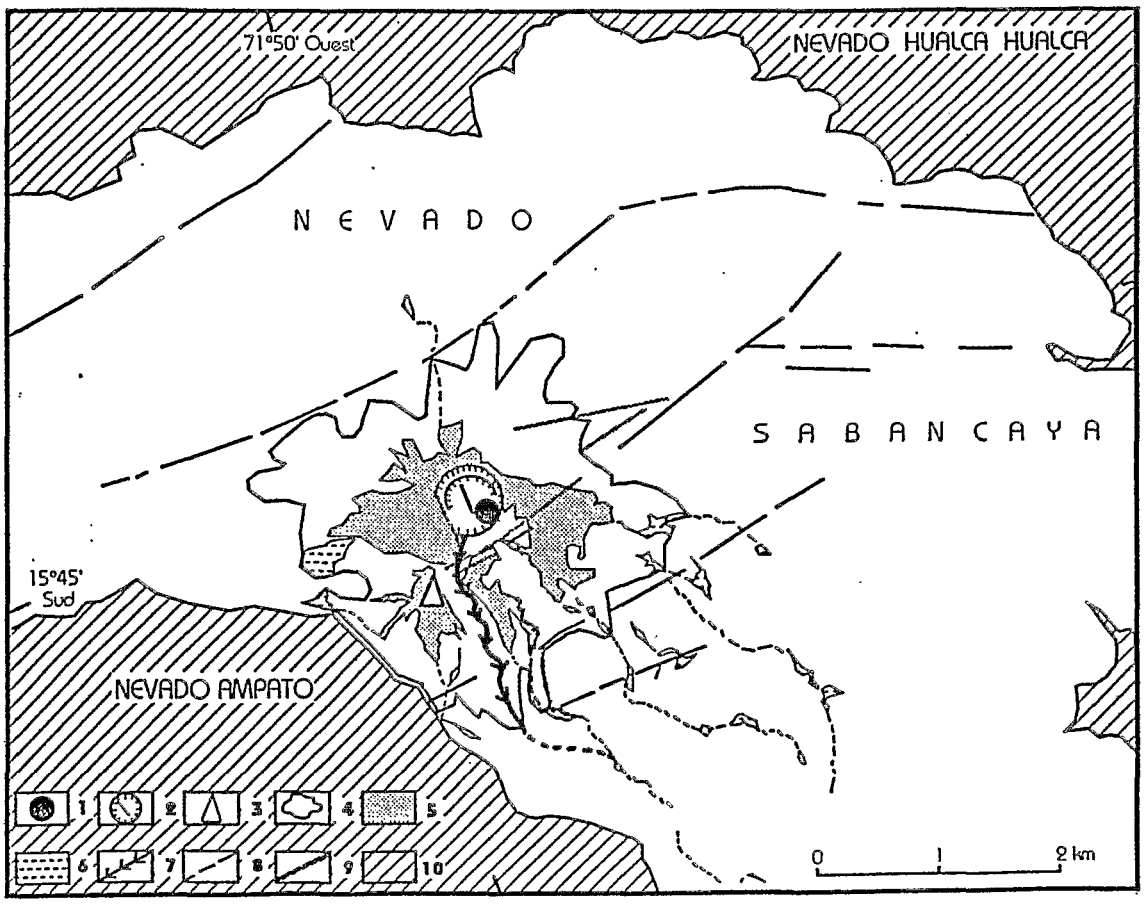

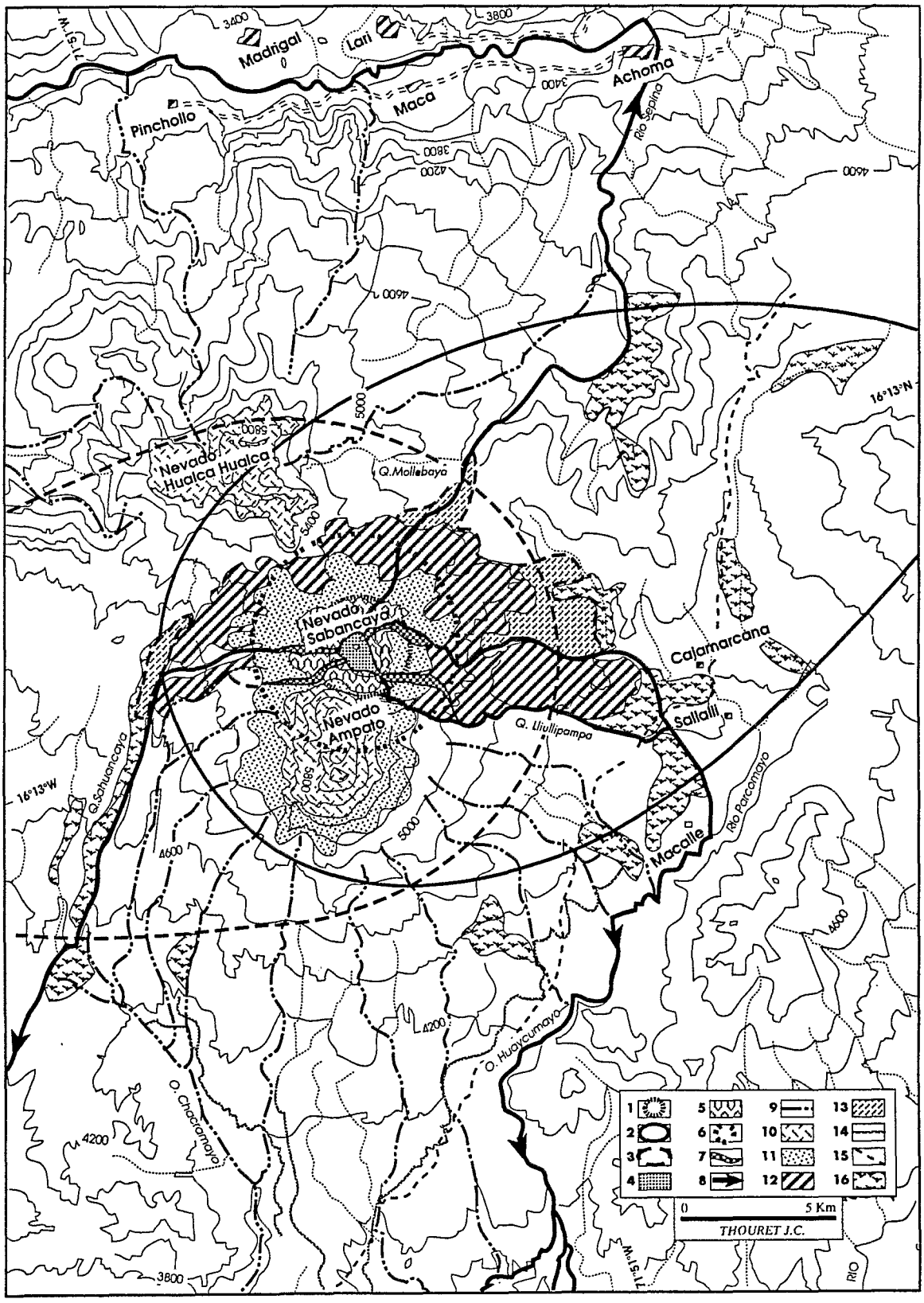
Madrigal
Lari
Achoma
Pinchollo
Maca
Río Colca
Nevado Hualca Hualca
Q.Mollebaya
Nevado Sabancaya
Nevado Ampato
Q. Lliullipampa
Q.Sahuancaya
Calamarcana
Sallalli
Macalle
Río Parcamayo
Q. Huaycumayo
Q. Chacamayo
16°13'W
16°13'N
3400
3800
4200
4600
5000
5400
5800
6000
1
2
3
4
5
6
7
8
9
10
11
12
13
14
15
16
0
5 Km
THOURET J.C.
N.I.S.I.T.
RIO

GEOCHEMICAL CHARACTERIZATION AND FISSION TRACK AGES OF HISTORICAL IGNIMBRITE FLOWS: THE SILLAR OF AREQUIPA (WESTERN CORDILLERA, SOUTHERN PERU)

Nicole VATIN-PERIGNON[1], Gérard POUPEAU[1], Richard A. OLIVER[2], Ludovic BELLOT-GURLET[1,2], Erika LABRIN[1], Francine KELLER[1] & Guido SALAS A[3].

(1) Laboratoire de Géologie, UA 69 CNRS, Université Joseph-Fourier, 15, rue Maurice Gignoux, 38031 Grenoble Cedex, France
(2) Institut Laüe-Langevin, B.P.156X, Avenue des Martyrs, 38042 Grenoble Cedex, France
(3) Universidad Nacional San Agustín, Casilla 1203, Arequipa, Perú

RESUMEN
El SA tufo corresponde a una única venida volcánica de enfriamiento con dos unidades. Las REE de sus obsidianas dan espectros característicos de alto-K riolitas y se distinguen de los demás tufos por su alto contenído en MREE. Su edad de 2.41 Ma (huellas de fisíon) es compatible con un período de alta convergencia y de espesamiento de la cortesa.

KEY WORDS: pyroclastic flow - volcanic glass - sillar of Arequipa - macusanites - fission track dating - rare earth elements

INTRODUCTION

The reputation of the tuff, the so-called Sillar of Arequipa (SA) as the best building stone in the Arequipa Province, is well-established in southern Peru.
The SA tuff is a white, welded, crystal-poor and pumice-rich rhyolitic tuff. It is extremely well exposed near the airport of Arequipa where it has infilled a pre-existing canyon, the Quebrada Añas Huayco (71°35'13"W - 16°20'14"S - 2525 m), and across which passes the main road to Yura and the railway to Puno.
This paper presents new petrological, major and trace element data on glass clasts and pumices from the SA tuff as well as FT ages on obsidian clasts from the SA tuff and the Macusani field (Eastern Cordillera). It examines the correlations between these two centres of ignimbritic volcanism and the timing of Pliocene to Recent deformations in southern Peru.

GEOLOGICAL SETTING

Previous reconnaissance studies and details of stratigraphy of the SA tuff are summarized by Salas et al. (1990). The SA tuff forms a single cooling sheet which consists of two distinct flow units. The base of the tuff has not been observed and although the overall thickness of the tuff is not known, it probably exceeds 25m (information from the quarriers) with 10m visible in the quarry situated to the south of the airport. The top of the SA tuff is separated from an overlying salmon-pink ash flow tuff by an irregular erosion surface. This tuff in turn is overlain by glacial conglomerates, coarse fluvial gravels and lahars which cap the mesa in the Arequipa area.

The outcrop within the quarry consists of 1) ***a lower flow unit*** (3-4m thick). This is a lithic-rich and well indurated tuff. At the base both white and oxidized fibreous and vesicular glassy pumices and glass shards tend to be small, rarely exceeding 1-2cm. Towards the top of this unit the pumices increase in size (~10-15cm) and relative abundance. It also contains about 30-35% of plagioclase, biotite, quartz and magnetite crystals, indicating a concentration by elutriation of ashes, and that up to 30% of the SA tuff may have been dispersed. Lithic clasts (up to 25%) are concentrated particularly at the base of the unit and consist mainly of subrounded oxidized andesite fragments (~5 cm). Isolated crystals are abundant in the fine- to medium-grained matrix of pumice shards and ashes. This lower unit shows facies variations from its base to the top. 2) ***The upper flow unit*** is a welded, homogeneous, pumice-rich (30%) rhyolitic tuff which shows large columnar joints indicating emplacement at a high temperature. Its exposure within the quarry is about 6m. The matrix is fine-grained, crystal-poor (~10%), with a mineralogy identical to the underlying unit. Lithic clasts are rare and small (0.5-3cm) and typical of the basement rocks (andesites). Grey to yellow glassy pumices are fragile, highly vesiculated and their phenocryst content is low (~5%). Coarse pumices occur at the top of this unit. Continuous layers or lenses several meters long are observed with coarse pumices (>5cm). The dense component concentrations and fines-depleted nature suggests a nearby source for the SA tuff.

Further to the west the Vitor tuffs which are crossed by the Panamerican South highway, has been dated by K/Ar spectrometry at 2.76±0.1 Ma (Vatin-Pérignon et al., 1982) and show some differences with the SA tuffs notably the nature of the clastic material which is made up of plutonic and metamorphic rocks as well as volcanic rocks.

PETROGRAPHY AND GEOCHEMISTRY

Dense obsidian glass clasts of the SA tuff are black and exhibit a pale brown color in thin section. Plagioclase microlites and cristallites have compositions ranging from

$Ab_{68}An_{17}Or_{15}$ to $Ab_{74}An_{20}Or_6$ which are close to albitic compositions. Biotite phenocrysts are similar in composition and size to those in the groundmass of the SA tuff. Accessory minerals of magnetite, containing 0.5 to 4% TiO_2, and apatite are present within the glasses. Several crystals of feldspar show out of equilibrium textures with the coexisting glass. Observations show that the alkali content is important, especially K and Na in glass clasts, biotite and plagioclase crystals.

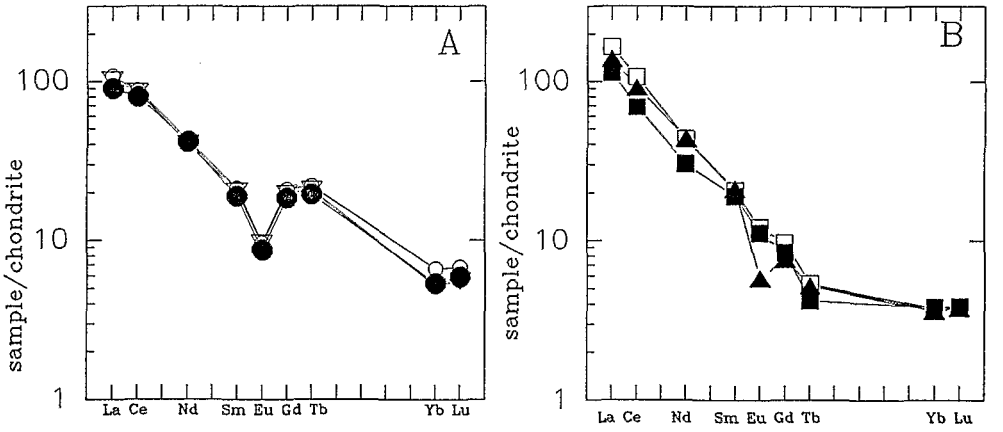

Chondrite-normalised REE profiles for (A) obsidian glasses from the SA tuff (2.4 Ma) and (B) pumices and glass shards from the Vitor tuff (2.76 Ma, Arequipa Province, Peru, filled triangle) and the Perez tuff (2.5 Ma, hollow square) and the Toba 76 (5.4 Ma, filled square), Bolivia.

The REE patterns of the 3 obsidian glass clasts analysed are all remarkably similar but the patterns are quite singular in apparence, having fairly high LREE values (La/Yb from 24 to 29) and a marked negative Eu anomaly; the HREE being depleted with respect to the LREE or MREE. In comparison with REE patterns from other similar types from the CVZ, the SA tuffis less enriched in LREE but more enriched for the MREE.

FISSION TRACK DATING

Three glass spherules from the SA tuff have been dated by fission-tracks. As the fossil tracks were, on the average, shorter than the nuclear reactor-induced fission-tracks, the samples were treated by the plateau method of Storzer & Poupeau (1973). Unannealed glass fragments from each sample were irradiated in the Orphée reactor and the neutron fluences monitored with NIST glass standards 962. The analytical procedures were the same as described in Poupeau et al. (1992) for the dating of macusanites. Fission-track ages were determined by the "difference" technique (Gleadow, 1981), without thermal treatment and after a heating step at 205°C for 2 hours and the size of tracks measured. It appears that the mean fossil track diameters are about 20% smaller that induced tracks. Therefore, the apparent ages of

the samples, in the range from 1.19±0.10 Ma (SA2-90) to 1.42±0.11 Ma (SA3-90), are only lower estimates of their formation ages. After thermal treatment at 205°C, the fossil and induced track diameter distribution have similar shapand mean values. The three samples analysed, SA1-90, SA2-90 and SA3-90 present then concordant formation ages, at respectively 2.32±0.21 Ma, 2.43±0.24 Ma and 2.48±0.17 Ma (1σ).

CONCLUSIONS

Because tuff ages have such important implications for regional geotectonic interpretation, we have determined TF ages of ignimbritic glasses from two different contexts in southern Peru. Macusanites from the ignimbritic field of the Puno district, present plateau ages distributed between 7.9 and 4.8 Ma in good agreement with ages reported independently by Cheilletz et al. (1992) on mineral separates. The 3 separate FT analyses of the SA tuff obsidian glass clasts yield an average age of 2.41±0.08 Ma which is significantly younger and must be related to a more recent compressional phase. The Macusani ignimbrite field may be related to an important phase of magmatism in the Eastern Cordillera arc system and belongs to the same volcanic cycle as the Bolivian Soledad tuffs (Redwood & Macintyre, 1989). Data on the SA tuff place the establishment and the evolution of the ignimbritic magma system in the Arequipa area within a precise temporal framework beginning with the eruption of the Vitor tuff at 2.76 Ma. The timing of the SA tuff correlates well with the F6 phase of deformation (Sébrier et al., 1988), contemporaneous with the early Quaternary period of high convergence rate during which the crust was thickned.

REFERENCES

CHEILLETZ, A., CLARK, A.H., FARRAR, E., ARROYO PAUCA, G., PICHAVANT, M. & SANDEMAN, H.A., 1992. **Tectonophysics** 205, 307-327.

GLEADOW, A.J.W., 1981. **Nuclear Tracks** 5, 3-14.

POUPEAU, G., LABRIN, E., SABIL, N., BIGAZZI, G., VATIN-PERIGNON, N. & ARROYO, G., **Nucl. Tr. Rad. Meas.**, submitted.

POUPEAU, G., SABIL, N., VILLA, I.M., BIGAZZI, G., VATIN-PERIGNON, N., FLORES, P., PEREYRA, P., SALAS, G. & ARROYO, G. 1992. **Tectonophysics** 205, 295-305.

SALAS ALVAREZ, G., VATIN-PERIGNON, N. & POUPEAU, G., 1990 *in* Géodynamique Andine, ORSTOM, Paris, 333-335.

REDWOOD, S.D.& MACINTYRE, R.M., 1989. **Economic Geology**, 54, 648-630.

SEBRIER, M., LAVENU, A., FORNARI, M. & SOULAS, J.-P., 1988. **Géodynamique** 3 (1-2), 85-106.

STORZER, D. & POUPEAU, G., 1973. **C. R. Acad. Sci. Paris**, 276D, 137-139.

VATIN-PERIGNON, N., VIVIER, G., SEBRIER, M. & FORNARI, M., 1982. **Bull. Soc. géol. France** 7, 24 (3), 649-650.

GRANITIC AND DIORITIC MAGMATISM DURING COMPRESSIONAL DEFORMATION WITHIN THE ANTARCTIC PENINSULA MAGMATIC ARC

Alan Vaughan[1] and Ian Millar[2].

(1) British Antarctic Survey, Madingley Rd. Cambridge CB3 0ET.
(2) NIGL, Keyworth, Nottingham, NG12 5GG.

RESUMEN: Granodioritas y dioritas del Peninsulo Antarctico de edad Jurásico Superior, emplazado en una sequencia de neises Triásico Superiores y gabbro posiblemente de edad Jurásico Superior, muestran estructuras de deformación que sugieran emplazamiento de rocas granodioriticas/dioriticas y movemiento syn-magmatico en zonas de cizalla. Estes zonas de cizalla se inclinan al norte-este con angulos a eso de 40° y marcadores cinemáticos indican una sensa de cizalla reverso-sinistral hacia el óceano.

KEY WORDS: Magmatism, shear zones, thrusting, Antarctic Peninsula

INTRODUCTION

Magmatism which is synchronous with thrust deformation has only recently been described, mainly from the north western Pacific margin of North America (Davidson *et al.* 1992, Ingram 1991, Karlstrom *et al.* 1993) and the Variscan of France (Blumenfeld and Bouchez 1988). New combined structural and magmatic studies of the Mesozoic magmatic arc in the Antarctic Peninsula, a former continuation of the southern Andes, have identified granitic magmatism during a period of thrusting within the arc.

GEOLOGICAL SETTING

Granodiorites dated as Upper Jurassic (141±3 Ma U-Pb zircon age) and co-eval diorites, emplaced in both gneissic basement of at least Upper Triassic age (227±1 Ma U-Pb zircon age) and gabbro of Upper Jurassic age or older from Palmer Land in the Antarctic Peninsula, record possible syn-emplacement ductile deformation with a reverse sense of shear. Gneiss, gabbro, and cross-cutting aplites (140±5 Ma Rb-Sr whole rock age, Harrison 1989) are also ductilely deformed in these reverse shear zones which are up to 150m wide. On a mesoscopic scale granodioritic and dioritic sheets parallel shear zone margins and exhibit a strong ductile foliation which dips shallowly eastward. Amphibole crystals within diorite sheets have a well developed preferred orientation and these, and the hinges of ductile folds developed within granodiorite sheets, plunge steeply ENE. S-C fabrics, also

within granodiorite sheets, indicate reverse shear with oceanward overthrusting to the WSW. Deformed granodiorite and diorite sheets are cut by steep thin granite dykes which are themselves sheared, suggesting that shear zone activity was episodic. The timing of magmatic and solid state deformation overlaps within the shear zone and structural evidence indicates lithological, spatial and temporal partitioning of deformation. Away from the shear zone intermixed gabbro, diorite and granodiorite suggest simultaneous emplacement of basic and felsic magmas and this is reflected in the presence of a high proportion of net-veined diorite within the shear zone. Also, ductile extensional syn-magmatic shear zones are evident in granodiorite and gabbro bodies away from the compressional shear zones.

CONCLUSIONS

The structural and igneous evidence suggests heterogeneous evolution of a zone of simple shear within the Antarctic Peninsula magmatic arc. The present zone of deformed rocks represents the end product of multiple pulses of reverse movement, with possible synchronous intrusion of granodiorite and diorite and further magmatic emplacement in tensional lulls, during overall compressional deformation. Comparison with areas of late Triassic to Middle Jurassic granitic magmatism synchronous with ductile shear within the southern Andes (Rapela et al. 1991) is currently being undertaken.

REFERENCES

Blumenfeld, P. and Bouchez, J.-L. 1988. Shear criteria in granite and migmatite deformed in the magmatic and solid states. *Journal of Structural Geology,* **10,** 361-372.

Davidson, C., Hollister, L.S. and Schmid, S.M. 1992. Rôle of melt in the formation of a deep-crustal compressive shear zone: the Maclaren Glacier metamorphic belt, south central Alaska. *Tectonics,* **11,** 348-359.

Harrison, S.M. 1989. Aspects of magmatism and metamorphism within a magmatic arc: evidence from north-western Palmer Land. *Unpublished PhD. Thesis,* NERC.

Ingram, G.M. 1991. The Great Tonalite Sill, S.E. Alaska: a record of late Cretaceous to early Tertiary orthogonal convergence and terrane accretion. Abstract, Tectonic Studies Group Conference 1991.

Karlstrom, K.E., Miller, C.F., Kingsbury, J.A. and Wooden, J.L. 1993. Pluton emplacement along an active ductile thrust zone, Piute Mountains, southeastern California: interaction between deformational and solidification processes. *Geological Society of America Bulletin,* **105,** 213-230.

Rapela, C.W., Dias, G.F., Franzese, J.R., Alonso, G. and Benvenuto, A.R. 1991. El Batolito de la Patagonia Central: evidencias de un magmatismo Triásico-Jurásico asociado a fallas transcurrentes. *Revista Geológica de Chile,* **18,** 121-138.

GITES MINÉRAUX
ORE DEPOSITS
YACIMIENTOS MINERALES

VOLCANISM AND POLYMETALLIC ORE DEPOSITS FROM SOUTHERN BOLIVIA
THE CERRO BONETE MINERALIZATIONS

Laurent BAILLY (1), Jacques L. LEROY (1) and Michel FORNARI (2)

(1) Université de Nancy 1, BP 239, 54506 Vandoeuvre-lès-Nancy cedex, France
(2) ORSTOM , CP 9214, La Paz, Bolivia

RÉSUMÉ : Le Cerro Bonete, dans le district minier du Sud Lipez, contient de nombreuses minéralisations à Bi-Ag-Pb-Zn exprimées sous la forme de filons à l'intérieur de domes dacitiques à rhyodacitiques. A partir de l'étude de la mine Bolivar, il est montré que le dépôt des minéralisations et le développement d'altérations zonaires à chlorite-illite sont liés à la circulation de fluides aqueux chauds entre 350 et 200°C. Le modèle "type épithermal" n'est pas retenu.

KEY WORDS : volcanic rocks, Pb - Zn - Ag - Bi mineralizations, hydrothermal alterations, Bolivian Andes.

INTRODUCTION

Bolivia is characterized by numerous mining districts which define a roughly East-West zoning. The Western Cordillera, the Altiplano and the Eastern Cordillera can respectively be characterized by Cu - Mo - Au - Fe, Cu - Pb - Zn - Ag - Au and Sn - W - Bi - Ag - Au mineralizations. Five districts are usually distinguished in the Eastern Cordillera (Sugaki et al, 1986), with from north to south, the La Paz (Sn - W), the Oruro (Sn), the Potosi (Sn - Ag), the Quechisla (Sn - Ag) and the Lipez (Pb - Zn - Ag - Bi) districts.

The Cerro Bonete mineralizations belong to the Lipez district, at the southernmost part of the Altiplano, near the Argentinian border. In this area, numerous small deposits and showers are known since the Spanish times, and sometimes mined. They are hosted by volcanic formations and wall-rock alteration is observed. Accurate mineralogical, geochemical and fluid inclusion studies were performed on three small mines and showers, among them the Bolivar mine, in order to know the nature of the mineralizations, the alterations products and the mechanisms of ore deposition ("epithermal type" or not).

GEOLOGICAL SETTING

In the sudied area (fig.1), the oldest formation, the Potoco formation, consists of continental conglomerates of Eocene to lower Oligocene age, with interbedded gypsum. It is unconformably overlain by the fine-grained sandstones of the San Vicente formation (Middle to Upper Oligocene). The Rondal formation corresponds to the first volcanic stage. It appears in the field as flows, sills and dykes of mafic rocks, emitted between 23.5 and 21 Ma (Kussmaul et al, 1975 ; Fornari et al, 1989). There are unconformably covered by the Quehua tuffs of Middle to Upper age, which are thick aerial explosive products emitted from various vents, with an interbedded conglomerate level.

They are intruded by several dacite domes, the Cerro Bonete, the Cerro Colorado or the Cerro Morokho towards the west, for example, which, in the area, host numerous Pb - Zn - Ag - Bi mineralizations such as the Bolivar mine. According to Kussmaul et al (1977) data, these domes would have a Miocene age.

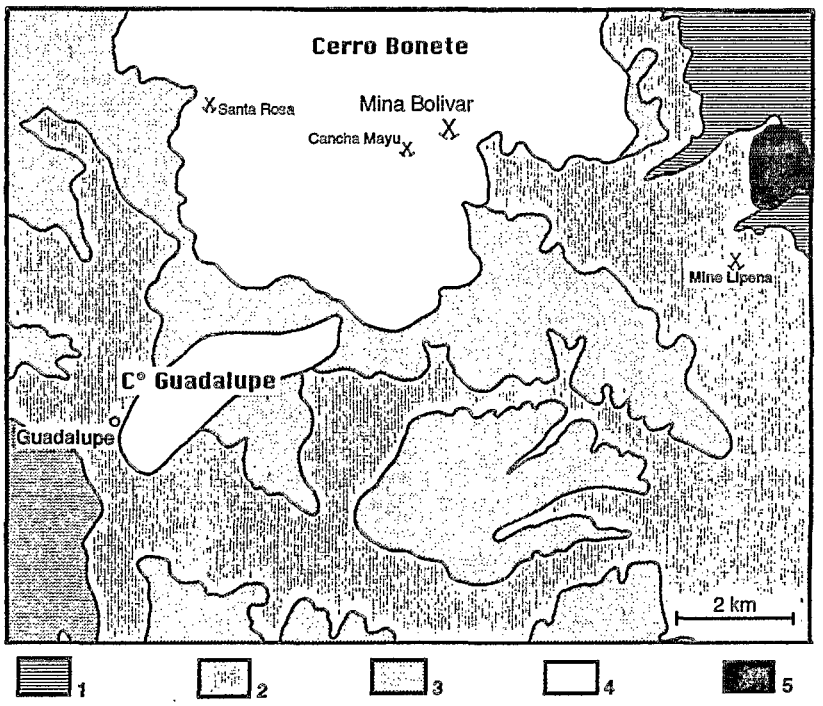

Fig.1 - Simplified geological map of the Cerro Bonete area (from unpublished Orstom La Paz report, 1989)
1 - San Vicente formation ; 2 - Rondal lavas ; 3 - Quehua tuffs ; 4 - intrusive domes ; 5 quaternary

PETROLOGY OF THE HOST FORMATIONS

The host rock of the mineralization in Bolivar mine is a rhyodacite (fig.2) with 36 vol% phenocrysts, plagioclases (8-19 vol% ; An40-55), biotite (> 9 vol% ; X_{Fe} between 0.3 and 0.4 ; $Al^{(IV)}$ = 0.25), quartz (1.5-6.5 vol%) and chloritized amphiboles. Microlites are observed in the matrix. They consist of quartz, Ca rich plagioclases (An55-66) and accessory minerals (Fe-Ti oxides and Fe sulfides). These rocks are peraluminous and characterized by medium SiO_2 (62.1-65.4 wt%) and alkalis ($Na_2O + K_2O$ = 5.4 - 7.1 wt% with Na / Na+K = 0.43-0.51).

MINERALIZATION

The ore deposit corresponds to a 10-25 cm thick main vein (N86°W), mined by COMIBOL up to 1979. It is hosted by one of the various domes which compose the Cerro Bonete complex. The main ore mineralization consists of pavonite ($AgBi_3S_5$), bismuthinite with pyrite and chalcopyrite with an average grade of 0.3% Bi, 0.2% Pb and 300g/t Ag (Richter et al, 1992).

The mineralization sequence (fig.3) can be divided into three stages characterized by the main following associations :

- stage 1 : arsenopyrite - pyrite 1
- stage 2 : pyrite 2 - chalcopyrite - Bi-Ag minerals (pavonite, bismuthinite, emplectite, aikinite)
- stage 3 : pyrite 3 - galena - sphalerite - grey coppers - marcasite - carbonates

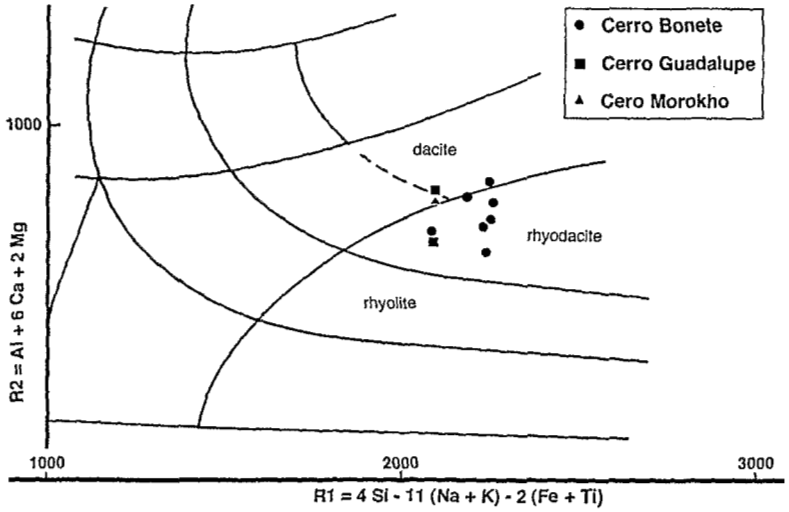

Fig. 2 - Cerro Bonete rhyodacite in a R1-R2 diagram (La Roche et al, 1980).

The R1-R2 diagram combines the chemical composition of the whole rocks and the chemical data on their minerals. It includes all the major elements as millications, a mineralogical network, the degree of silica saturation and the combined changes in the Fe / (Fe + Mg) and (Ab + Or) / An ratios in igneous rocks.

	Stade 1	Stade 2	Stade 3
Arsenopyrite	—	—	
Pyrite	—	—	—
Pavonite		—	
Aïkinite		—	
Emplectite		—	
Bismuthinite		—	
Chalcopyrite		—	
Galena		—	—
Sphalerite			—
Grey copper			—
Marcasite			—
Carbonates			—

Fig.3 - Mineralogical sequence observed at Bolivar mine

WALL - ROCK ALTERATION

The surrounding rhyodacite is altered in relation with the ore deposition. It was sampled up to 30 m from the mineralized vein in order to determine the nature of the alteration minerals and their space - time evolution. In contact to the vein, the primary plagioclase - biotite association is replaced by a dominant illite - subordinated chlorite association. Two chlorite crystallization stages separated by the illite development are observed. In getting farther away from the vein, the chlorite content increases and the illite one decreases. Few smectites appear. Simultaneously, the X_{Fe} for both chlorites and illites decreases, respectively 0.3 - 0.4 instead of 0.9 - 1.0 and 0.3 - 0.4 instead of 0.67, and the phengitic substitution of illites tends to increase. Such time - space zoning is observed in the three studied places (Bolivar mine, Cancha Mayu and Santa Rosa showers).

TEMPERATURE CONDITIONS

The temperature of the alteration was determined using the chlorite thermometer (Cathelineau, 1988) and fluid inclusion studies. Chlorite crystallization temperatures vary from 280 - 350°C, near the vein, to 210 - 260°C, 30 m away from the vein. The related fluids are aqueous and the fluid inclusion studies confirm these temperatures with T ranging from 360°C to 180°C according to the fluid stage.

CONCLUSIONS

In conclusion, all the mineralized zones hosted by the various rhyodacite domes which compose the Cerro Bonete are rather similar. This indicates similar conditions for alteration development and ore deposition. The temperatures (350°C to 200°C) indicate medium to low temperature hydrothermal systems. The alteration minerals are the same (nature, composition, space and time zoning) as the ore minerals (Bi - Ag - Pb - Zn paragenesis). According to the nature of the newly-formed minerals, these mineralized zones cannot be related to a typical "epithermal type" deposit.

REFERENCES

CATHELINEAU, M., 1988, Cation site occupancy in chlorites and illites as a function of temperature. Clay Minerals, 23, 471-485.

FORNARI, M., HERAIL, G., POZZO, I.L. y VISCARRA, G.,1989, Los yacimientos de oro de Los Lipez (Bolivia) tomo 1 : Estratigrafia y dinamica de emplazamiento de los volcanitas del area de Guadalupe. ORSTOM en Bolivia, n°19, La Paz.

KUSSMAUL, S., JORDAN, L. and PLOSKONKA, E., 1975, Isotopic ages of Tertiary volcanic rocks of SW Bolivia. Geol. Jahrb., 14, 111-120.

KUSSMAUL, S., HORMANN, P.K., PLOSKONKA, E. and SUBIETA, P.,1977, Volcanism and structure of southwestern Bolivia. J. Volcan. Geotherm. Research, 2, 73-111.

LA ROCHE, H. de, LETERRIER, J., GRANDCLAUDE, Ph. and MARCHAL, M., 1980, A classification of volcanic and plutonic rocks using a R1-R2 diagram and major elements analyses. Its relationships with current nomenclatures. Chem. Geol., 29, 183-210.

RICHTER, H.D., LUDINGTON, S., BROOKS, W.E., BRAY, E.A. (du), ENRIQUEZ-ROMERO, R., BAILEY, E.A., HINIJOSA-VELASCO, A. SORIA-ESCALANTE, E. and ESCOBAR-DIAZ, A., 1992, The Cerro Bonete area. U.S.G.S., Bull.,1975, 166-174.

SUGAKI, A., UENO, H., SHIMADA, N., KITAKAZA, A. HAYASHI, K., SANJINES, O.V. and VELARDE, O.V., 1986, Geological study on the ore in the Sur Lipez district, Bolivia. Sci. Rept. Tohoku Univ., 3, 16, 327-352.

LATE EOCENE-OLIGOCENE SHORTENING EPISODE IN EASTERN CORDILLERA OF COLOMBIA VIEWED BY EMERALD DATING

Alain CHEILLETZ(1), Gaston GIULIANI(1,2), and Thierry ARHAN(1)

(1) ENSG and CRPG-CNRS, BP 20, 54501, Vandoeuvre, France
(2) ORSTOM, Département TOA-UR 1H, 213 rue La Fayette, 75480 Paris, France

RESUMÉ: L'étude métallogénique des gisements d'émeraude de Colombie encaissés dans les shales noirs du Crétacé inférieur, conduit à d'intéressantes applications concernant l'évolution tectonique de la Cordillère Orientale et notamment la phase de déformation fini Eocène-Oligocène à laquelle sont attribués les mouvements ascendants de saumures hydrothermales associées à la formation des émeraudes.

KEY WORDS: Eastern Cordillera, Colombia, Emerald, Lower Cretaceous black shale, Eocene-Oligocene, Petroleum exploration.

INTRODUCTION

Recent progress in metallogenetic studies of Colombian emerald deposits (Giuliani et al., 1990a; Cheilletz et al., 1991) have issued important tectonic implications interesting the Eastern Cordillera of Colombian Andes. As suggested by Mégard (1987), the Eastern Cordillera constitutes an inverted sedimentary back-arc basin of Jurassic-Late Cretaceous age filled with thick accumulations of marine sediments. Eocene-Late Oligocene synorogenic non-marine molasse sequences buried the basin as a response to uplift of the Central Cordillera. Inversion of the Eastern Cordillera basin occurred during the Andean compressional episode at Late Miocene-Pliocene time.

The Colombian emerald deposits are grouped within two belts (Fig. 1) situated along the two major polyphased thrust zones that correspond approximatively to the original limits of the Cretaceous basin (Mégard, 1987; Schamel, 1991). The emerald mineralization consists of carbonate-pyrite veins and breccia hosted by Lower Cretaceous black-shales corresponding to Macanal (Berriasian-Valanginian; Eastern belt) and Paja (Hauterivian-Barremian; Western belt) formations. The genesis of the emerald mineralization is undoubtly attributed to epigenetic hydrothermal fluid circulations (Beus and Mineev, 1972.); however, the age of the tectonic phase responsible for the extension-vein network and hydraulic breccia trapping the mineralization has only recently been obtained by $^{40}Ar/^{39}Ar$ dating of cogenetic muscovite (Cheilletz et al., 1993). Two distinct Upper Eocene-Lower Oligocene ages have been determined for the deposits of Coscuez (35-38 Ma) and Muzo-Quipama (31.5-32.6) in the western belt.

In this paper, we attempt to briefly examine the consequences of the age of emerald formation on the regional tectonic-geologic framework.

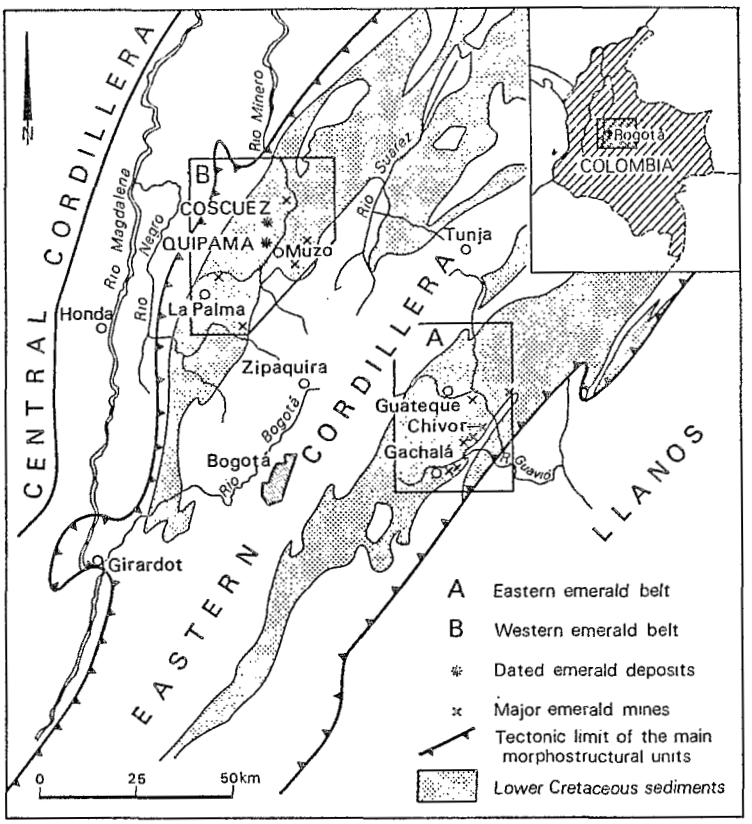

Figure 1: Tectonic provinces of the Colombian Andes and location of emerald deposits belts.

ORIGIN OF THE EMERALD DEPOSITS OF COLOMBIA

Petrographic observations and mass balance calculation in black-shale hosting the emerald vein network demonstrate that the hydrothermal fluid infiltration process is accompanied by a strong fluid-rock interaction leading to sodium and carbonate metasomatism; as a consequence, the enclosing black-shales are conversely leached in major, trace and REE elements (Giuliani et al., 1990b; 1993a). These chemical exchanges involve a local sedimentary origin for most of the elements constituting the vein-infilling minerals and particularly emerald (Be, Cr, V, Si, Al). The origin of the hydrothermal fluid responsible for chemical transfers has been approached by oxygen isotopic measurements (Giuliani et al., 1992); calculated $\delta\,^{18}O\ H_2O$ for carbonate and quartz indicate values of basinal formation waters. Sulfur isotopic data on pyrite and fluid inclusion studies of trapped brines within emerald crystals indicate an evaporitic source for the chlorine and sulfate components of the hydrothermal fluids (Giuliani et al., 1993b). Indeed, evaporitic plugs are known within the Cretaceous formations (Campbell and Bürgl, 1965) and thus might have been in contact with or percolated by the hydrothermal brines. Constrained by (1) the $^{40}Ar/^{39}Ar$ age determination, (2) an Eastern Cordillera subsiding model (Hébrard, 1985), and (3) lithostatic pressure equilibration assumption, isochoric

extrapolation of these complex brines in the NaCl-H_2O system lead to a pressure-temperature estimate of 1 Kb and 290-360°C for the emerald deposition (Cheilletz et al., 1993).

TECTONIC CONSEQUENCES

The location of the emerald deposits along the original limits of the Cretaceous basin suggests that these limits might constitute deep-seated rejuvenated faults allowing hot-fluid circulations up through the sedimentary pile. Hydro-fracturing and strongly reducing environment conditions highly favoured by the black shale lower Cretaceous horizons, provoked the emerald-pyrite-calcite precipitation. Comparison between thermo-barometric data for emerald generation (290-360° C, 1Kb; Cheilletz et al., 1993) and burial temperature estimations (135° C at 4500 m depth; Hébrard, 1985) requires a 165 to 225° C additional input within the Lower Cretaceous formations at the Eocene-Oligocene boundary. This can be obtained either by correlative intrusive emplacement as suggested earlier by Campbell and Burgl (1965) and Escovar (1979), but already not found in that area, or by heat conduction implemented during halokinetic ascent. Both mechanisms might be related to extensional or transtensional tectonic regime as evidenced at that period in the northernmost portion of the Andean chain (Stephan, 1985; Beck, 1986). However, detailed structural data are lacking in the emeraldiferous area to support that hypothesis.

CONLUSIONS

The tectonic evolution of the Eastern Cordillera is characterized by a strong shortening episode starting during the Eocene and corresponding to an acceleration of the convergence rate between Nazca and South American plates (Daly, 1989). At that time, sedimentation in the Eastern Cordillera basin is changing to non-marine clastic deposition, whereas the underlying mesozoic series are affected by alternating compressive and extensive-transpressive episodes in response to general crustal shortening. The emerald formation at 38-31 Ma appears as a good clock of this strong change in the tectonic regime of the Colombian Andes. Following that period, major crustal deformation involves collisional regime between the Caribbean arc system and South America, leading to thrusting and uplift of Eastern Cordillera during Late Miocene-Pliocene time particularly through rejuvenation of the older faulted limits of the Cretaceous basin (Fig.1). Considering the depth of formation of emerald (4250-4500m; Cheilletz et al., 1993), a minimum of 6000 m (excluding erosion) of vertical transfer can be deduced which is responsible for the inversion of the Cretaceous back-arc basin and emerald outcropping.

Considering petroleum exploration in the Magdalena Valley-Eastern Cordillera system, the study of emerald genesis within the Lower Cretaceous black-shales shows that temperatures of 360°C were reached at least in two large belts of these petroleum source rocks at Upper Eocene-Lower Oligocene time, implying that after an earlier maturation phase, some remobilization of trapped oil might have occurred in response to hydrothermal activity, as suggested by Fabre (1987).

REFERENCES

BECK C. (1986) - Collision caraïbe, dérive andine, et évolution géodynamique mésozoïque-cénozoïque des Caraïbes. *Rev. Géogr. Phys. et Géol. Dyn. Fr.*, 27/3-4, 163-182.

BEUS A.A. & MINEEV D.A. (1972) - Some geological and geochemical features of the Muzo-Coscuez emerald zone. Cordillera oriental: Colombia. *Inf. Ingeomin.*, 1-50, unpubl. rep.

CAMPBELL C.J. & BÜRGL H. (1965) - Section through the Eastern Cordillera of Colombia. South Amer., *Geol. Soc. Amer. Bull.*, U.S.A., 76/5, 567-589.

CHEILLETZ A., FÉRAUD G., GIULIANI G. & RODRIGUEZ C.T. (1991) - $^{40}Ar/^{39}Ar$ laser-probe dating of the Colombian emerald deposits: metallogenic implications. *S.G.A. Meeting, 25 Years Anniversary*, Nancy, 373-376.

CHEILLETZ A., FÉRAUD G., GIULIANI G. & RODRIGUEZ C.T. (1993)- Time-pressure-temperature constraints on the formation of Colombian emeralds: an $^{40}Ar/^{39}Ar$ laser-probe and fluid inclusion study. Accepted to *Economic Geology*.

DALY, M.D.(1989) - Correlations between Nazca/Farallon plate kinematics and forearc basin evolution in Ecuador. *Tectonics*, V.8, N°4, 769-790.

ESCOVAR R. (1979) - Geologia y geoquimica de las minas de esmeraldas de Gachalà, Cundinamaraca. *Bol. Geol.*, Republica Colombia, Minist. Minas y Petroleos, Inst. Nac. Invest. Geol.-Min., 22/3, 116-153.

FABRE, A. (1987) - Tectonique et génération d'hydrocarbures: un modèle de l'évolution de la Cordillère Orientale de Colombie et du bassin des Llanos pendant le Crétacé et le Tertiaire. *Arch. Sc. Genève*, V.40, 145-190.

GIULIANI G., RODRIGUEZ C.T. & RUEDA F. (1990a) - Les gisements d'émeraude de la Cordillère orientale de la Colombie: nouvelles données métallogéniques. *Mineralium Deposita*, 25, 105-111.

GIULIANI G., CHEILLETZ A. & RODRIGUEZ C.T. (1990b) - New metallogenic data on the emerald deposits of Colombia. *8th IAGOD Symposium*, Ottawa, 12-18 August 1990, Abstracts, 185-186.

GIULIANI G., SHEPPARD S.M.F. & CHEILLETZ A. (1992) - Fluid inclusions and $^{18}O/^{16}O$, $^{13}C/^{12}C$ isotope geochemistry contribution to the genesis of emerald deposits from the Oriental Cordillera of Colombia. *C. R. Acad. Sci. Paris*, t. 314, II: 269-274.

GIULIANI G., CHEILLETZ A., SHEPPARD S.M.F. & ARBOLEDA C. (1993a) - Geochemistry and origin of the emerald deposits of Colombia. *2nd SGA Meeting*, Granada, Spain, Extended Abstract, 4 p.

GIULIANI G., CHEILLETZ A., BAKER J. & ARHAN T. (1993b) - Evaporitic origin of the parent brines-bearing Colombian emeralds: fluid inclusion and sulfur isotopic evidences. *ECROFI Symposium*, Warsaw, Poland, Abstract, 2p.

HEBRARD F. (1985) - Les Foot-hills de la Cordillère Orientale de la Colombie entre les rios Casanare et Cusiana. Evolution géodynamique depuis l'Eo-Crétacé. *Thèse Doct. 3è Cycle Univ. P. et M. Curie, Paris VI*, Sci. Nat. Géol., 29 janv., 162 p.

MEGARD F. (1987) - Cordilleran Andes and Marginal Andes: A review of Andean Geology North of the Arica Elbow (18 deg.S) in Monger, J.W.H. and J. Francheteau, eds., Circum-Pacific orogenic belts and evolution of the Pacific ocean. *Am. Geophys. Union, Geodynamics Series*, V.18, 71-95.

SCHAMEL, S. (1991). Middle and Upper Magdalena basins, in Biddle, K.T. ed., Active Margin Basins, *AAPG memoir* 52, 283-303.

STEPHAN, J.F. (1985) - Andes et chaîne Caraïbe sur la transversale de Barquisimeto (Venezuela). Evolution Géodynamique: *Symposium Géodyn. Caraïbes*, Paris 5-8 Février 1985, ed. technip Paris, 505-529

LEAD ISOTOPIC PROVINCES IN PERU, BOLIVIA, AND NORTHERN CHILE

Ulrich PETERSEN[1], Andrew W. MACFARLANE[2], Antje DANIELSON[1]

(1) Department of Earth and Planetary Sciences, Harvard University, 20 Oxford Street, Cambridge, MA 02138, USA
(2) Department of Geology, Florida International Universty, Tamiami Trail, Miami, FL 33199, USA

En el Perú, Bolivia y el norte de Argentina y Chile definimos cuatro provincias isotópicas principales: en dos de ellas las menas epigenéticas y singenéticas derivan su Pb de los intrusivos; en las otras dos el Pb proviene de los sedimentos.

Pb isotopes, isotopic provinces, metallogeny, magma and ore sources.

Previous studies of ores and their igneous, sedimentary and metamorphic host rocks in the Andes of Perú, Bolivia, Argentina and Chile have revealed a number of lead isotope provinces (Macfarlane et al., 1990; Tilton et al., 1981; Gunnesch and Baumann, 1984; Puig, 1988, 1990; Kontak et al., 1990). In two of the three main provinces the lead isotope signatures of the ores resemble mainly those of the intrusive igneous rocks with which they are associated. This appears to be true for both epigenetic and syngenetic (or stratabound) hydrothermal ore deposits. It also seems to apply to all the ore minerals, even if they belong to different mineralization stages, and to most of the few gangue minerals analyzed. This suggests very strongly that the ore forming fluids either emanated directly from a magma or that meteoric fluids (including seawater) percolated deeply into the crust, leaching the ore metals from hot intrusives. In the third main lead isotope province the ore lead was probably derived from regionally abundant carbonaceous shales, but it is not clear if directly or as a result of melting the shales. Although some ore deposit types predominate in certain provinces, each province has an assortment of different ore deposit types that formed at various times.

New unpublished data and further examination of the evidence requires some modifications, so that our current nomenclature comprises:

I. The coast of Perú and northern Chile;
II. The high Andes;
III. The eastern Andes;
IV. The eastern foothills of the Andes.

The lead isotope values of Province I lie close to the Stacey-Kramers growth curve for the Mesozoic and Tertiary, but there are insufficient independent age determinations to decide if the progression of lead isotope values correlates with age. The lead isotope values of ores and igneous rocks in the coast of southern Perú, which is in the middle of province I, deviate considerably from the aforementioned values and reflect the very low 206/204 lead isotope composition of the Precambrian Arequipa massif. Throughout province I the lead isotope values of the ores are similar to those of the uncontaminated intrusive rocks (in contrast to the volcanic rocks in the southern coast of Perú and to the felsic units of the batholith in the central coast of Perú).

Our lead isotope province II extends along the high Andes of Perú, Bolivia and Argentina. On a 207/204 vs 206/204 lead isotope diagram the few available values for intrusive igneous rocks in central and northern Perú have a surprisingly small range of 207/204 ratios, whereas the ores of this region define an elongate field with its long axis at a significant angle to the Stacey-Kramers growth curve. On 208/204 vs 206/204 lead isotope diagrams the values for the intrusive igneous rocks and ore deposits of this region define even more elongate fields with their long axes at an angle with the Stacey-Kramers curve. Only two analyses of small basalt flows or sills do not fit these generalizations. On 207/204 vs 206/204 diagrams the aforementioned elongated ore field appears unrelated to the composition of the Paleozoic, Mesozoic and Tertiary metamorphic and sedimentary rocks in the region, although on 208/204 vs 206/204 diagrams one could invoke a relation to the Olmos and Pataz metamorphic basement rocks. However, the elongated ore fields may be more convincingly related to the lead isotope composition of pelagic sediments (Chow and Patterson, 1962) and manganese nodules (Reynolds and Dasch, 1971) on the Nazca plate. Toward lower values their axes point to the lead isotope composition of mid-ocean ridge basalt (Unruh and Tatsumoto, 1976).

NW of Lake Titicaca the Cretaceous and Tertiary ore deposits (formerly assigned to province IIIb but now included in province II as "SE Andes A") define a trend for lead 208/204 vs 206/204 that is similar to the one for ores and igneous rocks in the high Andes of central and northern Perú, but pointing more toward the composition of metalliferous sediments (Dasch, 1981) on the Nazca plate. However, in contrast to the high Andes ore deposits in northern and central Perú, but similar to the igneous rocks in that region, the SE Andes A ores have a very narrow range of 207/204 values.

Some western Bolivian ore deposits formerly assigned to province IIIa are now recognized to belong to province II. The Capillitas deposit in northern Argentina is assigned to province II because it is an enargite deposit like those in Perú and Bolivia that belong to this province and because its 206/204 lead isotope values correspond to this province. Some of the ore deposits in the high Andes of Chile also appear to belong to province II, as suggested by our unpublished lead isotope analyses for El Indio and Tambo and by some results of Tosdal et al. (1992) for Esperanza and Cancan. Hence, province II can now be traced, with minor variations in lead isotope fields, from Hualgayoc in northern Perú ($6^{o}46'S$) to somewhat south of $27^{o}S$ in nothern Argentina and Chile.

There are no obvious endmembers for the extensions of the longitudinal axes of the high Andes lead isotope fields toward greater 206/204, 207/204 and 208/204 values, unless one chooses to invoke crustal contamination with a Precambrian basement terrane that is isotopically like the Imataca Series of Venezuela (Montgomery and Hurley, 1978). Alternatively, one may infer that the high Andes intrusives and ores reflect the lead isotopic composition of varying mixtures of MORB, metalliferous sediments, manganese nodules, pelagic sediments and, perhaps, metamorphic basement complexes.

The eastern Andes ore deposits of Perú, Bolivia and Argentina which constitute province III are often located in Paleozoic carbonaceous marine shales. Their lead isotope values lie in an elongated field parallel to the Stacey-Kramers growth curve and to the field for province I ores and intrusives uninfluenced by the Arequipa massif, but at generally higher 207/204 and 208/204 values (for given 206/204 values). The progression of their lead isotope values (mainly 206/204) correlates with their ages. Given the known Ordovician age and current lead isotope composition of their predominant host rocks, this suggests that these ore leads were mostly derived from these sediments (Macfarlane et al., 1990).

In the region NW of Lake Titicaca the Carboniferous and Permo-Triassic ore deposits have very high 206/204 values (Kontak et al., 1990), indicating an important contribution of lead from metamorphic, sedimentary or volcanic country rocks. They correspond to a separate Fe-Mn-W-Sn-Cu metallogenic province IIIb ("SE Andes B") that predated the Andean orogen.

The only lead isotope information available for the eastern foothills of the Andes pertains to the San Vicente ore deposit, which is generally considered to be of the Mississippi Valley type. Its 206/204 and 208/204 lead isotope ratios are generally higher than those for provinces I, II and III. Presumably San Vicente inherited its lead from weathering products derived from Precambrian rocks in the Brasilian craton.

References:

Chow, T. J., Patterson, C.C., 1962: The occurrence and significance of lead isotopes in pelagic sediments. Geochim. et. Cosmochim. v.26, p.163-308.

Dash, E.J., 1981: Lead isotopic composition of metalliferous sediments from the Nazca plate. Geol. Soc. Am. Mem., 154, 199-210.

Gunnesch, K.A., and Baumann, A., 1984: The Atacocha district, central Perú: some metallogenic aspects. In: Syngenesis and Epigenesis in the Formation of Ore Deposits, Wauschkuhn, E.A., ed., Springer-Verlag, Berlin, p.448-456.

Kontak, D.J., Cumming,G.L., Krstic, D., Clark, A.H., and Farrar, E., 1990: Isotopic composition of lead in ore deposits of the Cordillera Oriental, southeastern Perú. Econ. Geol., 85, 1584-1604.

Macfarlane, A.W., Marcet, P., LeHuray, A.P., and Petersen, U., 1990: Lead isotope provinces of the Central Andes inferred from ores and crustal rocks. Econ. Geol., v.85, Nr.8, 85, 1857-1880.

Montgomery, C.W., and Hurley, P.M., 1978: Total rock U-Pb and Rb-Sr systematics in the Imataca Series, Guyana Shield, Venezuela. Earth Planet. Sci. Lett., v.39, p.281-290.

Puig, A., 1988: Geologic and metallogenic significance of the isotopic composition of lead in galenas of the Chilean Andes. Econ. Geol., v.83, p.843-858.

Puig, A., 1990: Lead isotopes in the Chilean ores. In: L.Fontbote, G.C. Amstutz, M. Cardozo, E. Cedillo, J. Frutos (eds.): Stratabound ore deposits in the Andes. Springer-Verlag Berlin Heidelberg. 749-758.

Reynolds, P.H. and Dash, E.J., 1971: Lead isotopes in marine manganese nodules and the ore-lead growth curve. Jour. Geophys. Research, 76, 5124-5129.

Tilton, G.R., Pollak, R.J., Clark, A.H., and Robertson, R.C.R., 1981: Isotopic composition of Pb in central Andean ore deposits. G.S.A. Mem., v.154, p.791-816.

Tosdal, R.M., Bouse, R.M., Gibson, P.C., Wallace, A.R., Moscoso, D.R., Cuitiffo, G.L., Maksacv, J.V., Vilca, N.C., Quispesivana, Q.L., Tejada, R.G., Jiminez, C.N., Lizeca, J.L., Murillo, F., Hardyman, R.F., Koeppen, R.P., 1992: Lead isotopic compositions as tracers in ore deposits in the central Andes of Peru, Bolivia and Chile. Workshop on: Ore forming processes of precious metal epithermal deposits, Santiago de Chile, May 12 to 16, 1992, 27-36.

Unruh, D.M., and Tatsumoto, M., 1976: Lead isotopic composition and uranium, thorium, and lead concentrations in sediments and basalts from the Nazca Plate. Scripps Inst. of Ocean. Initial Reports of the Deep Sea Drilling Project. p.341-347.

MINERALISATION RELATED TO CRUSTAL SHORTENING: THE MANTO-VEIN, GOLD-POLYMETALLIC UBINA DEPOSIT, BOLIVIA

Stewart D. REDWOOD(1), Stephen C. NANO(2), and Mario FLORES A.(3)

(1) Mintec, Casilla 13790, La Paz, Bolivia
(2) Minera Newcrest Chile Ltda., Ave. Providencia 1979, 3er Piso B, Providencia, Santiago, Chile.
(3) Calle Sucre 741, 3er Piso, La Paz, Bolivia.

RESUMEN: La mineralización de oro - polimetalico en Ubina (SW Bolivia) se presenta en un sistema hidrotermal grande relacionado a un intrusivo. Las estructuras forman vetas y han canalizado los fluidos para formar mantos que reemplazan rocas calcáreas. La intrusión y la mineralización han side controladas por una zona de cizallamiento siniestral que tiene un rumbo de 135° y que está relacionada con la compresión hacia el Este (antepais) durante el acortamiento de la corteza de los Andes centrales.

KEY WORDS: Andes, Mineralization, Crustal Shortening, Shear Zone, Ubina

INTRODUCTION

This paper describes the relationship between hydrothermal mineralisation and crustal shortening in the Central Andes, using the Ubina gold - polymetallic deposit as an example. Ubina is a large diameter, intrusion centred hydrothermal system located in SW Bolivia on the western edge of the Eastern Cordillera (Fig. 1). It has been mined on a small scale since Spanish colonial times for Sn, W, Ag, Au, Pb, Zn, Cu and Bi in veins and carbonate replacement mantos. Intrusion, flow dome extrusion and mineralisation are controlled by dilational zones within a 135° trending sinistral shear zone related to regional E-W compression and crustal shortening.

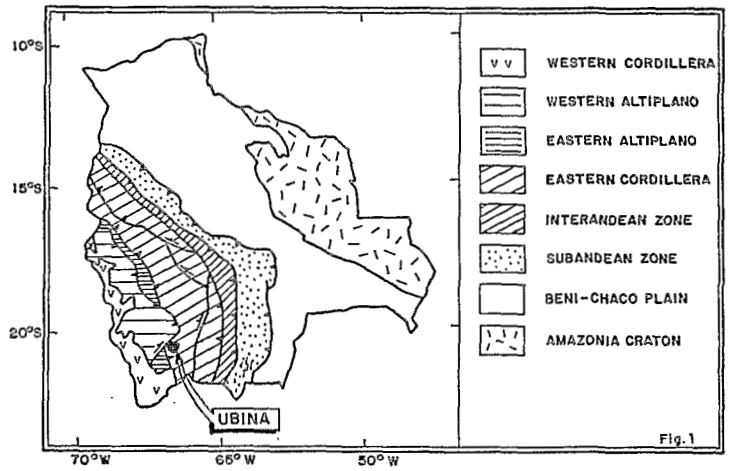

Figure 1: Tectonic map of Bolivia (ORSTOM) and location of Ubina.

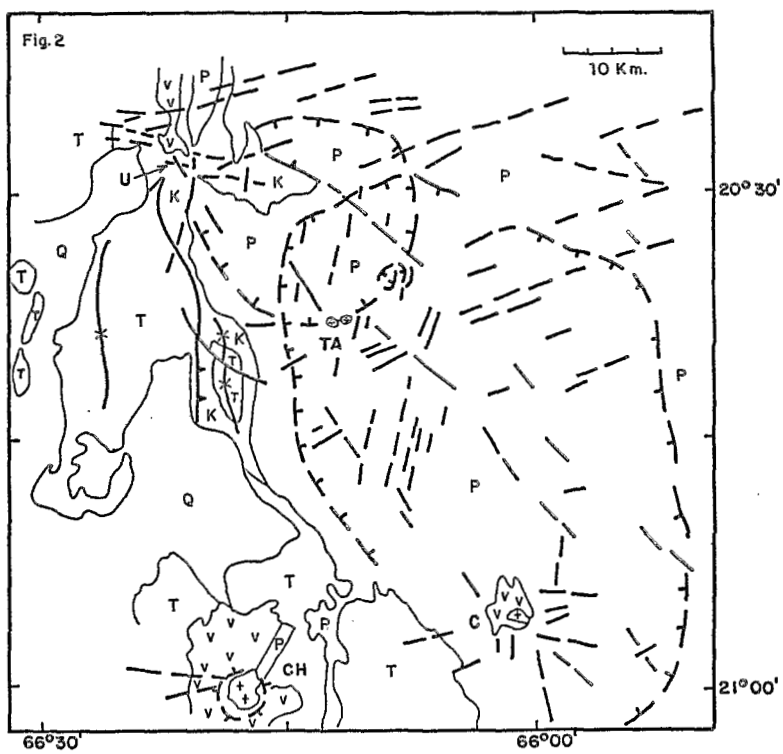

Figure 2: The structure and geology of the Ubina - Chorolque region. Mines: U - Ubina, TA - Tasna, C - Chorolque, CH - Chocaya (Animas, Siete Suyos, Gran Chocaya). Geology: P - Paleozoic, K - Cretaceous, T - Lower Tertiary, Q - Quaternary, V - volcanic rocks, + - intrusions.

GEOLOGICAL SETTING

Ubina is located in the autochthon just east of the Calazaya nappe at the junction of the Khenayani Fault System and the Main Altiplano Thrust (Fig. 1) which has at least 40 km of eastward (foreland) displacement (Baby *et al.*, 1992). This crustal shortening took place in the Late Oligocene - Early Miocene during the major tectonic crisis in the Bolivian Andes (Sempere *et al.*, 1990).

The Ubina deposit lies within a 10 - 15 km wide 135° trending structurally controlled belt of igneous related polymetallic systems of Middle Miocene age (16.2 - 16.4 Ma; Grant *et al.*, 1979), which include the Tasna and Chorolque Sn-W-Bi-Cu-Au-Ag-Pb-Zn-As-Sb deposits (Fig. 2). They have the same metallogenic signature as Ubina and are considered to be cogenetic. The three deposits are localised at the intersection of the 135° trending structural corridor with 060° and 080° structures (Fig. 2). Two large elliptical features evident on satellite images appear to have influenced the emplacement of these igneous centres, with Ubina and Tasna lying on the margin of the same circular structure (Fig. 2). These features may represent collapse above deep seated intrusive bodies but are not collapse calderas in the classic sense as they are not accompanied by voluminous volcanic outpourings.

DEPOSIT GEOLOGY AND MODEL

The Ubina district comprises Ordovician sediments overlain unconformably by Late Cretaceous - Paleocene red-bed sediments with marine carbonates, with Eocene - Middle Oligocene red bed sediments to the west (Fig. 3). These are cut by the mushroom shaped Ubina flow-dome of plagioclase-biotite-quartz phyric dacite. Minor porphyritic dacite stocks and dykes intrude the Cretaceous to the SE (Fig. 3).

Ubina belongs to the Bolivian Polymetallic Vein Deposit type (Ludington *et al.*, 1992) and is unusual in carrying significant gold. Fault structures form vein and stockwork mineralisation in all lithologies and have acted as feeders for stratabound, carbonate replacement, manto style mineralisation in the calcareous sediments of the Late Cretaceous Chaunaca and El Molino Formations. These have a combined thickness of about 530 metres of red marls with limestone beds and calcareous shales, siltstones and sandstones.

Mineralisation is zoned with an inner Sn-W-Au zone, a middle Au-Ag-Bi-Cu zone and an outer Ag-Sb-Hg-Ba-Pb zone. Arsenic and zinc are present in all zones. Zonation occurs over a vertical interval about 450 meters and has a radius of 4 km. The system is centred on the Manta Dorada plateau SE of the flow-dome. The minor dacitic intrusives are interpreted as apophyses of a stock beneath this area which has driven the hydrothermal system, with the Ubina flow-dome as a marginal volcanic offshoot (Fig. 3). The dome and flows are pervasively altered but have weak mineralisation due to lack of fracturing. Hydrothermal fluids may have ponded beneath the relatively impermeable flows to give telescoped mineralisation adjacent to the dome. The coincidence of the middle gold zone with the reactive carbonate formations on the Manta Dorada plateau is favorable for the development of large, replacement style deposits of gold, as supported by extensive rock and soil gold anomalies.

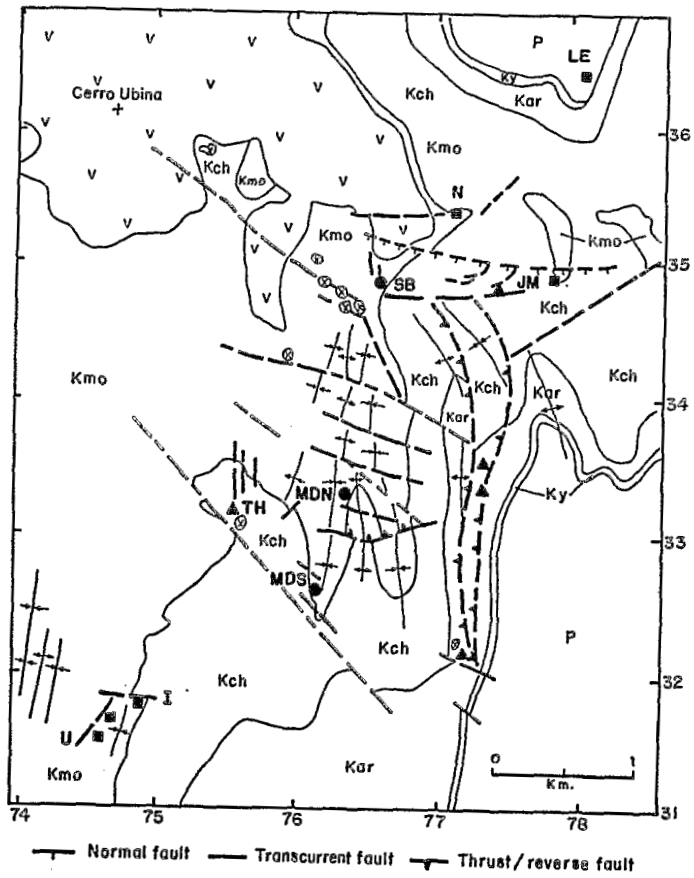

Figure 3: The geology and structure of the Ubina deposit. Stratigraphy: P - Paleozoic, K - Cretaceous, Ky - Yura Formation, Kar - Aroifilla Formation, Kch - Chaunaca Formation, Kmo - El Molino Formation, X - intrusions, V - volcanic/subvolcanic dacite.
Mines: ▲ - Sn-W-Au; ● - Au-Ag-Cu-Bi; ■ - Ag-Sb-Hg-Ba-Pb. Mine names: U - Ubina, I - Irma, TH - Tres Hugos, MDS - Manta Dorada South, MDN - Manta Dorada North, SB - Santa Barbara, JM - Jayaj Mayu, N - Normandia, LE - La Esperanza. UTM grid coordinates (Zone 19K GT).

STRUCTURAL CONTROL

Regional compression produced open N-S trending folds in the Cretaceous and Lower Tertiary sediments which overprint earlier, tight NW-SE trending folds in the Ordovician. The 135° trending shear zone postdates N-S folding and controlled the emplacement of the intrusions, flow-dome and hydrothermal activity at Ubina. The structural pattern at the deposit scale (Fig. 3) is interpreted to represent a brittle, simple (Riedel) shear zone with the main shear faults parallel to the regional 135° trend, with left lateral displacements of tens of meters.

The orientation and sinistral sense of displacement of the shear zone indicate E-W compression which is consistent with the crustal scale, eastward (foreland) directed compression that produced the large scale folding and thrusting in the Bolivian Andes. The Middle Miocene age inferred for igneous and hydrothermal activity at Ubina indicates continuation or reactivation of the regional compression following the main tectonic crisis in the Late Oligocene - Early Miocene.

CONCLUSIONS

1. Intrusion, flow-dome extrusion and hydrothermal gold - polymetallic mineralisation at Ubina are controlled by a sinistral 135° trending shear zone contemporaneous with, or immediately following crustal scale, eastward (foreland) directed compression.

2. Structures form veins in all lithologies at Ubina and acted as feeders for carbonate replacement, manto style mineralisation in calcareous lithologies.

2. A direct relationship between crustal shortening and hydrothermal mineralisation in the Central Andean margin is indicated.

REFERENCES

Baby, P., Sempere, T. Oller, J. and Herail, G., 1992, Evidence for major shortening on the eastern edge of the Bolivian Altiplano: the Calazaya nappe. *Tectonophysics*, **205**, 155 - 169.

Grant, J. N., Halls, C., Avila, W. and Snelling, N. J., 1979, K-Ar ages of igneous rocks and mineralization in part of the Bolivian tin belt. *Economic Geology*, **74**, 838 - 851.

Ludington, S., Orris, G. J., Cox, D. P., Long, K. R. and Asher-Bolinder, S., 1992, Mineral Deposit Models. In: United States Geological Survey and Servicio Geologico de Bolivia, *Geology and Mineral Resources of the Altiplano and Cordillera Occidental, Bolivia. USGS Bulletin*, **1975**, 63 - 89.

Sempere, T., Herail, G., Oller, J. and Bonhomme, M. G., 1990, Late Oligocene - Early Miocene major tectonic crisis and related basins in Bolivia. *Geology*, **18**, 946 - 949.

MAGNETITE-APATITE ORES IN THE ATACAMA FAULT ZONE, EL SALVADOR REGION, NORTHERN CHILE.

Peter J. TRELOAR[1], and Howard COLLEY[2]

[1] School of Geological Sciences, Kingston University, Penrhyn Road, Kingston-upon-Thames, KT1 2EE, UK.
[2] School of Construction and Earth Sciences, Oxford Brookes University, Gypsy Lane, Oxford, OX3 0BP, UK.

RESUME. Les gisements de magnetite-apatite de la faille d'Atacama sont situes dans des fentes au domino. Les apatites y presentent de fortes zonations en F, Cl et OH. Les variations des fugacities en F, Cl et OH refletent les changements de fugacite des halogenes au cours de l'evolution des magmas qui sont a l'origine des fluids hydrothermaux de la mineralisation.

KEY WORDS: Apatite, Halogens, Atacama Fault, Chile.

INTRODUCTION.

Iron ore deposits, with or without apatite, are characteristic of the westernmost part of the Chilean ore province (Sillitoe 1976; Brookstrom 1977). However, magnetite-apatite deposits are globally unusual and poorly understood. Once considered to represent ore deposits directly crystallised from a magma, a hydrothermal origin is now more generally accepted. However, questions about the origin of such deposits still remain, especially: how far removed are they from the magmatic/hydrothermal interface?; do they reflect a particularly high halogen concentration or oxygen fugacity within the parent magma from which the hydrothermal fluids are derived?; and why are they not widespread? Some small, well exposed, magnetite-apatite deposits within theAtacama Fault Zone of northern Chile present the opportunity to answer some of these questions.

GEOLOGICAL SETTING.

The Atacama Fault Zone is a trench parallel strike slip fault zone (Brown et al. in press) that runs N-S through northern Chile for over 1000km. Although displacement is dominantly left lateral, the fault zone has a complicated movement history. Within the El Salado sector, between 26 and 27°S, two distinct displacement trajectories are determined. An early phase of ductile dip slip movement with E-side down (Colley et al. 1989), was succeeded by a phase of sinistral strike slip movement which commenced within the ductile field but continued throughout a falling temperature regime into the brittle field (Brown et al. in press). Faulting, especially the more ductile faulting, was synchronous with granite emplacement (Grocott et al. 1993). The deformation history, kinematics and chronology of granite emplcement are all consistent with granite emplacement into a transtensional left lateral fault system,

ductility contrasts being driven by the thermal effects of granite emplacement.

The later, brittle, stages of this movement were accompanied by widespread iron mineralisation. Brittle faults are all coated with a magnetite ore, large areas of weakly fractured basic volcanics are iron stained on surface, and large, barely to viably economic, Fe deposits located within dilational fault jogs, are currently being evaluated and/or exploited. The strong structural control localising iron mineralisation into fault planes, together with extensive propylitic alteration suggest a fault controlled hydrothermal origin for the iron. In a small number of deposits magnetite, which is the dominant mineral within this part of the fault system, occurs in association with apatite and actinolite.

MAGNETITE-APATITE DEPOSITS.

The Fresia deposit is one of three magnetite-apatite deposits located within the Atacama fault system, north of El Salado. This deposit has a sinuous shape which is controlled by two sets of faults trending at 080° and 065°. Slickensides on both fault sets are shallow plunging, indicating localised dilation within the overall N-S trending Atacama fault system.

Carmen Mine lies 20km E of the Atacama fault system. This large open pit is located in Cretaceous volcanics of the La Cerro Florida formation. The deposit is marked by the intersection of two fault systems: an E-W trending set of steep faults with subhorizontal slickensides, and a N-trending array of conjugate dip slip faults, a geometry also consistent with localised dilation.

TEXTURES.

All the deposits are characterised by massive Fe-ore, dominantly magnetite although locally haematised. Apatite crystals vary in length. At Carmen Mine, they are up to 50 cm long, and are spectacularly zoned with rose pink cores grading to white rims. Apatite commonly occurs as individual coarse crystals floating within a matrix of magnetite, although it also occurs as acicular needles located within apatite-rich veins within which the apatites grew perpendicular to walls of opening fractures. Such fractures are often located within homogenous magnetite zones, the apatite crystals nucleating on a magnetite substrate. At Carmen the country rock has been clearly brecciated. Each block of country rock has a selvedge of magnetite on which needles of apatite and actinolite have nucleated. While both apatite and actinolite grew perpendicular to block faces and vein walls at the vein margins, they are randomly oriented within vein cavities. Large ragged apatites contain incusions of both actinolite and magnetite, but are frequently fractured with the fractures infilled by magnetite ore.

Country rocks are intensely epidotised and chloritised. The textures are characteristic of country rock hydrothermal brecciation of country rock sequences, with fractures and brecciated voids having been infilled initially by magnetite ore with growth of apatite and actinolite postdating the earliest precipitation of Fe-ore. Apatite, actinolite and magnetite must all have formed a stable paragenetic assemblage within the hydrothermal environment over a period of time, although the late stage fracturing of apatite with fracture infilling by magnetite implies that towards the end of the mineralisation period apatite was no longer stable.

APATITE CHEMISTRY.

Apatite crystals are strongly zoned. Light rare earth elements are enriched in cores with respect to rims. More significantly, apatite chemistries show extensive solid solution between hydroxy-, flour- and chlor-apatite end members. Up to 6.82%Cl and 3.09%F have been recorded. The former represents 100% of the end-member chlor-apatite and the latter 82% of the end-member flour-apatite. No carbonate end member is recorded within

the apatites and concentration of the hydroxy-end member is calculated by difference. Apatites are commonly zoned. F-poor crystals have higher Cl, and hence lower OH, contents in cores than rims, whereas F-rich crystals have F-rich and Cl- and OH-poor cores with F-poor and Cl- and OH-rich rims. The data sets and methodology of Korzhinskiy (1981) and Yardley (1985) can be used to calculate fugacity ratios between the halogens (F and Cl) within a hydrous fluid. If apatite chemistry is a reflection of halogen and water fugacities within the hydrothermal fluid, there is a clear trend from fluids with high f_F/f_{Cl} and f_F/f_{OH} ratios, through fluids with low f_F/f_{Cl} and high f_F/f_{OH} ratios to fluids with low f_{Cl}/f_{OH} and f_F/f_{OH} ratios. Although these trends are apparently incompatible with those described by Candela (1986), the initially high ratios of halogen to hydroxyl fugacities must reflect fundamentally halogen enriched magmas parenting the hydrothermal fluids.

DISCUSSION.

Two questions need to be answered. Firstly, what controls the widespread magnetite rich mineralisation? Secondly, what causes the occurrence and localisation of small numbers of magnetite-apatite deposits within an area dominated by Fe-rich and Fe-Cu bearing hydrothermal deposits?

Granite margins, originally ductilely deformed during transtensional emplacement, are frequently brittlely deformed within Fe-mineralised fault zones. Thus, mineralisation is a post-magmatic feature that affects a region in which the localised thermal softening due to granite emplacement has been largely dissipated. The hydrothermal fluids were likely to represent a mixing of magmatic and meteoric fluids within a regionally developed hydrothermal convective system. The concentration of iron suggests that the fluids were both acidic and highly reduced, compositional features probably influenced more by the magmatic than the meteoric contribution. Mineralisation, however, must represent interaction between oxidised near surface fluids and deeper level reduced fluids, at a particular, although as yet unspecified, crustal level. The dominant influence of the magmatic contribution may imply that the fluid chemistry reflects processes along the subduction interface, a supposition supported by the trench parallel position of Fe-rich deposits within the well defined pattern of metallogenic zonation within the Andean region (Sillitoe 1976).

Although these observations go some way to resolving the first question, they do not significantly relate to the problem as to why apatite bearing deposits are present at all, let alone as a small number of discrete bodies. The rapid changes in relative values of the halogen and hydroxyl fugacities are significant. Either these have to reflect extremely localised variations in halogen content in rocks being scavenged for iron by the circulating acid and reduced hydrothermal fluids, or they represent discrete short lived pulsed additions of halogens to the hydrothermal environment. Such additions should be through continued magmatism and magma degassing. Geochronological data show that magmatism and associated thermal softening, as evidenced by the ductile-brittle transition, migrated slowly west to east across the Atacama Fault system from 153Ma to 127Ma (Grocott et al, 1993). As the fault system was active throughout, it is likely that episodic release of halogen rich fluids from newly emplaced magmas occurred through the magmatic episode. Once these halogen rich fluids reached the cooled brittle environment and there mixed with the circulating hydrothermal fluids, they would generate localised halogen rich deposits.

REFERENCES.

Brookstrom A.A. 1977. Econ geol. 72. 1101-1130.
Brown M., Diaz F. & Grocott J. In press. Geol Soc Amer Bull.
Candela P.A. 1986. Chem Geol. 57. 289-301
Colley H., Treloar P.J. & Diaz F. 1989. Econ geol Monograph. 7. 208-217

Grocott J., Treloar P.J., Brown M., Dallmeyer R.D. & Taylor G.K. 1993. EUG VII. Terra Abstracts. 5. 204-205.
Korzhinskiy M.A. 1981. Geochem Internat. 18. 44-60
Sillitoe R.H. 1976. Geol. Ass. Canada. Sp. paper. 14. 59-100
Yardley B.W.D. 1985. Min Mag. 350. 77-80

HYDROTHERMAL ORE-DEPOSITS CONTROLLED BY STRUCTURE AND MAGMATISM IN CENTRAL PERU

César E. Vidal (1) and Donald C. Noble (2)

(1) Av. Paseo La Castellana 827, Surco, Lima-33, PERU
(2) Mackay School of Mines, Univ. of Nevada, Reno-USA

RESUMEN: Fallas regionales de rumbo Noreste con movimientos recurrentes y alternados entre desgarre dextral y basculamiento gravitacional al Sur, controlan la distribución de importantes distritos mineros caracterizados por yacimientos hidrotermales en la costa y sierra del Perú central.

KEY WORDS: Central Peru, faults, hydrothermal ore deposits.

The structural and magmatic evolution of Central Peru is best pictured by Megard (1978) and Pitcher et al. (1985). Their studies were based on regional mapping of mutually exclusive zones: the Western Cordillera and the Altiplano as opposed to the coastal areas, respectively. Topical correlation of tectonic events, magmatic pulses and geochemical fingerprinting has been elaborated for coastal and cordilleran domains (Noble et al., 1974, 1979; Cobbing, 1978; Atherton, 1989, 1992). The structural grain of this Andean transect depicts a plate edge with linear batholiths roughly parallel to paleo-basins, fold belts, volcanic arcs and metallogenetic provinces (Petersen, 1965; Ponzoni, 1980; Petersen and Vidal, 1983). Transverse features such as batholithic and metallogenetic segmentation have been described in a broad sense with little supporting evidence to make their application economically successful (Sillitoe, 1974b, Vidal, 1980). This contribution intends to correlate transverse fault movement with magmatism and hydrothermal activity, both on a regional scale and on a mining district scale.

Major transverse faults across the Andes in Central Peru control the location of Mesozoic and Cenozoic hydrothermal systems, which were driven in relation to subvolcanic and volcanic ediffices. Northeast-trending fault systems such as

exposed at Huaura, Chancay, and Agua Salada, north and east of Lima, are traced continuously over 50 to 70 km in fully exposed mountainous desert. Their movement was long-lived, recurrent and variable; dextral-wrench or strike-slip movements alternate mainly with gravitational downthrows to the southeast. Offsets in the order of several kilometers have been described by Bussell (1983) and by Vidal (1987). Variable nature of fault movement indicates variable stress regimes. Transient compressional periods during relatively rapid plate-convergence induced strike-slip. Tensional periods during slow-down or hault of subduction produced gravitational tectonics.
In the Western Cordillera and Altiplano region the Northeast-trending fault system is continuous although sparsely recognized. Conjugate Northwest-trending sinestral wrench faults with kilometric displacements are exposed in the Atacocha region, east of Cerro de Pasco. Indirect evidence of underlying Northeast faults such as fold deflections, graben- and horst-topography and location of stocks, volcanoes and vein swarms are present. Mining districts characterized by hydrothermal ore deposits which are controlled by structures related to Northeast-trending faults are: the Uchucchacua Ag+Mn skarns, the Río Pallanga, Huámpar, Caridad, Huarón and Casapalca Ag+Pb+Zn veins, the San Cristóbal W+Zn veins, the Santa Cruz de Cocachacra Ba+Zn massive sulfides and some of the Iscaycruz Zn skarns. The structural trend defined by the mining districts of Cerro de Pasco and Colquijirca may also be related to fundamental Northeast-trending basement faulting. Structural controls coincide to locate the newly-discovered ore bodies at the Santa Cruz de Cocachacra and Colquijirca districts to be presented as case studies.

Massive sulfide and barite deposits of middle Cretaceous age are actively mined from the Santa Cruz de Cocachacra mining district, 50 km east of Lima (Vidal, 1987). Estimated production plus reserves add up to 5 million tons of direct-shipping barite ores and 3 million tons of sphalerite ore at plus 8 per cent Zn cut-off. Detailed geological mapping and core-logging have revealed a localized succession of submarine pyroclastic flows, felsic lava domes and hydrothermal vents that overlapped in time with widespread calcareous sedimentation. Volcanism and ore deposition were structurally favored along an Andean trending, rift-like depression or second-order basin. Paleogeographic readjustments across Northeast-trending transverse growth-faults produced clastic reworking of exhalative-sedimentary ores and country rocks into deeper third-order basins. Tectonically-induced slope breccias accumulated adjacent to syn-sedimentary fault-scarps; rock and ore debrii were transported over distances up to 200 m. Redeposited ore material classified by size- and gravity-sorting, formed graded beds and unusually rich pyrite, sphalerite or barite deposits in the deepest parts of the basin. Subsequent erosion of the volcanic ediffice gave rise to proximal volcaniclastic breccias with distal sandstone and mudstone deposits, all of which overlie and preserve the ore-bearing

horizon.

Circa 20 million tons of Cu+Ag ores and 35 million tons of Zn+Pb+Ag ores had been mined from the world-class Cerro de Pasco mining district. Only 10 km to the south, the Colquijirca district has produced at least 100 million ounces of Ag from supergene enrichment zones and more recently 8 million tons of Zn+Pb+Ag ores. Mineral deposits in both districts are of complex hydrothermal nature; their association to the wanning stages of Miocene subaerial volcanism is clear (Silbermann and Noble, 1977; Vidal et al., 1984). The near Northsouth trend defined by the Cerro de Pasco and Colquijirca mining districts is characterized by a red-bed and lacustrine sequence of Eocene-Oligocene age, which unconformably overlies Jurassic limestone, Permian red beds and pre-Ordovician filites. Such a structural corridor is bound by Miocene volcanoes on both ends and longitudinal faulting along the edges. Recurrent fault movement is evidenced by cataclastic and mylonitic Zn+Pb ores in Cerro de Pasco's Cayac Noruega deposit. Evidence of underlying longitudinal faults such as Miocene dykes, intense dolomitization of Pucará limestones and strong East-West fracturing appear west of the Colquijirca district. Structural level as indicated by comparison of volcanic facies, volcanic geomorphology and ore textures appears higher at Colquijirca compared to Cerro de Pasco. Reconstruction of the Miocene configuration is interpreted as a volcano-tectonic depression or graben. Sigmoidal deflection of the graben from regional structure and predominance of east-west tensile features are interpreted as high level structures produced by basement rupture along Northeast-trending dextral-wrench faults.

REFERENCES

Atherton, M.P., 1989, "Volcanic facies, structure and geochemistry of the marginal basin rocks of central Peru". J. South Am. Earth Sci., vol. 2 No. 3, pp. 241-261.

Atherton, M.P., 1992, "Thermal and geotectonic setting of Cretaceous volcanic rocks near Ica, Peru, in relation to Andean crustal thinning". J. South Am. Earth Sci., vol. 5 No. 1, pp. 47-69.

Bussell, M.A., 1983, "Timing of tectonic and magmatic events in the Central Andes of Peru". J. Geol. Soc. London, vol. 140, pp. 279-285.

Cobbing, E.J., 1978, "The Andean geosyncline in Peru and its distinction from Alpine geosynclines". J. Geol. Soc. London, vol. 135, pp. 207-218.

Megard, F., 1978, "Etude géologique des Andes du Pérou central". ORSTOM, Mem. 86, 310 p.

Noble, D.C.; McKee, E.H.; Farrar, E. and Petersen, U., 1974, "Episodic Cenozoic volcanism and tectonism in the Andes of Peru". Earth Plan. Sci. Let., vol. 21, pp. 213-220.

Noble, D.C., McKee, E.H. and Megard, F., 1979, "Early Tertiary Incaic tectonism, uplift and volcanic activity, Andes of central Peru". Bull. Geol. Soc. Am., vol. 90, pp. 903-907.

Petersen, U., 1965, "Regional geology and major ore deposits of central Peru", Econ. Geol., vol. 60, pp. 407-476.

Petersen, G. and Vidal, C., 1983, "Tres épocas metalogenéticas evidenciadas en el Cenozoico del Perú". Soc. Geol. Perú, Bol. 71, pp. 107-116.

Pitcher, W.S.; Atherton, M.P.; Cobbing, E.J. and Beckinsale, R.D., 1985, "Magmatism at a plate edge. The Peruvian Andes." Blackie & Son Ltd., Glasgow, 328 pp.

Ponzoni, E., 1980, "Metalogenia del Perú". In: Metalogénesis en Latinoamérica, IUGS No. 5, pp. 101-140.

Silbermann, M.L. and Noble, D.C., 1977, "Age of igneous activity and mineralization, Cerro de Pasco, Peru". Econ. Geol., vol. 72, pp. 925-930.

Sillitoe, R.H., 1974b, "Tectonic segmentation of the Andes: implications for magmatism and metallogeny". Nature, London, vol. 250, pp. 542-545.

Vidal, C.E., 1980, "Mineral deposits associated with the Peruvian Coastal Batholith". Ph.D. thesis, Univ. Liverpool, 239 pp.

Vidal, C.E.; Mayta, O.; Noble, D.C. and McKee, E.H., 1984, "Sobre la evolución de soluciones hidrotermales desde el centro volcánico Marcapunta en Colquijirca-Pasco". Soc. Geol. Perú, Vol. Jubilar, 10, 14 p.

Vidal, C.E., 1987, "Kuroko-type deposits in the middle Cretaceous marginal basin of Central Peru". Econ. Geol., vol. 82, pp. 1409-1430.

EVOLUTION PRÉ-ANDINE
PRE-ANDEAN EVOLUTION
EVOLUCION PRE-ANDINA

LITHOSPHERIC MODELING OF THE ORDOVICIAN FORELAND BASIN IN THE PUNA OF NW ARGENTINA: IMPLICATIONS FOR THE INTERPRETATION OF EARLY PALEOZOIC TERRANES

Heinrich Bahlburg

Geologisch-Paläontologisches Institut, Universität Heidelberg, Im Neuenheimer Feld 234, 6900 Heidelberg, Germany.

Resumen

La cuenca Ordovícica de la Puna septentrional argentina se desarrollo de una posición de tras-arco a una de antepais. Modelos litosfericos demuestran que la interpretación original basada en datos sedimentológicos, volcanológicos y el cálculo de tazas de subsidencia tectónica corresponde a procesos fisicos vigentes en la evolución de cuencas de antepais. Sin embargo, los resultados de la modelación soportan dos procesos e interpretaciones distintos: (i) La evolución de la cuenca controlada por compresión asociada a un aumento del espesor de la litósfera, o (ii) la construcción de un arco sobre corteza continental de un margen pasivo anterior. Las dos alternativas tienen consecuencias geológicas distintas referiendose al mosáico de los terranes del Paleozoico temprano.

Key Words

Argentina, Ordovician, basin modeling, terranes

Introduction

Most studies of Early Paleozoic sedimentary basins in NW Argentina and N Chile led to qualitative reconstructions of their geotectonic evolution. Here I present the results of a lithospheric modeling approach towards a quantitative interpretation of the Ordovician basin in the Puna of NW Argentina which combines theoretical considerations with data obatined in the field.

The Early Palaeozoic Basin of NW Argentina

After the Pampean Orogeny in the early Cambrian, the Early Paleozoic evolution of marine basins starts in the Late Cambrian. The Late Cambrian Mesón Group overlies the Pampean Orogen with an erosional unconformity. It is c. 3000 m thick and consists predominantly of shallow marine, partly tidally influenced quartz-sandstones and shales. They were deposited on a west-facing marine platform (Kumpa and Sanchez, 1988). With a further erosional unconformity, the Mesón Group is overstepped to the E and W by the quartz-rich sandstones and shales of the Santa Victoria Group (Latest Cambrian to Early Llanvirn).

Restricted to the Arenig, a magmatic arc became active farther W in the western Puna region and in N Chile. It is mainly evidenced by basaltic to andesitic lavas of geochemical volcanic arc affinity, and associated volcanoclastic apron deposits of c. 3500 m thickness (Koukharsky et al., 1988; Breitkreuz et al., 1989; Bahlburg, 1990). At this time, the Puna basin and the siliciclastic platform of the Santa Victoria Group were in a back-arc position. Tectonic subsidence analysis indicates a major loading event in the western Puna during the Arenig which transformed the Puna basin into a foreland basin (Bahlburg, 1990). This was accompanied by the emergence of the Cordillera Oriental in the Early Llanvirn. In the Middle Ordovician, a c. 3500 m thick volcanoclastic turbidite complex was deposited in the Puna basin. Presently available data suggest that the Arenig arc had been extinct by this time.

In modification of earlier subduction models for the Andean margin in the Ordovician (Coira et al., 1982; Hervé et al., 1987), the evolution of the Ordovician basin in the puna and Cordillera Oriental was interpreted as connected to the collision of the Arequipa Terrane (Ramos, 1988; Forsythe et al., 1993), leading to the Early Ordovician arc being thrust eastward over its back-arc basin (Bahlburg, 1990). This interpretation was able to explain tectonic subsidence rates of up to 600 m/Ma associated with high sedimentation rates in the developing foreland basin. However, there is no positive evidence of the respective thrust fault, and alternative interpretations have to be tested.

According to the recently revived hypothesis of the Late Proterozoic supercontinent in the Cambrian (Bond et al., 1984; Dalziel, 1991; Dalla Salda et al., 1992), eastern North America rifted away from western South America during the Cambrian. This may be reflected in NW Argentina by the Late Cambrian-Early Ordovician potential rift-to-drift succession in the Argentinian Cordillera Oriental represented by the Mesón and Santa Victoria Groups (see above). Consequently it would be likely that a passive margin stage in the Late Cambrian and possibly Tremadoc preceded the development of the Arenig arc as part of an active margin.

In order to test both interpretations, an infinite beam elastic plate lithospheric loading model was applied which is able to take account of 1st order features observed in the evolution of the Ordovician Puna basin in NW Argentina. Two scenarios were testet: (i) that of lithospheric thickening through thrusting of the existing arc over its back-arc basin (Tectonic Scenario), and (ii) that of arc construction on a previously passive margin (Arc Scenario). Numerical details of the model will be discussed elsewhere (Bahlburg and Furlong, in prep.).

Model Scenarios

Arc Scenario: The first loading event in the Arenig (max. 6000 m load thickness) is taken to be dominated by early volcanic products of basic chemistry with a density of 2900 kg/m^3. The sediment shed from this evolving source is taken to be of corresponding increased density, i.e 2700 kg/m^3. On the far side of the basin, sediment input reflects metamorphic and plutonic sources, the sedimentary rocks of the eastern Puna basin are quartz-rich, and their density is assumed as 2500 kg/m^3. At the time of the second loading event in the Llanvirn (max. 2000 m load thickness), the arc is assumed to have evolved to upper crustal compositions with a density of 2800 kg/m^3, with a corresponding density of the eroded sediment of 2600 kg/m^3. For the third timestep in the Llandeilo no additional loading event is assumed as there is no record of active volcanism. The sediment is taken to reflect erosion to deeper levels of the arc, cutting into granitoids, and a density of 2500 kg/m^3 is used.

Tectonic Scenario: Throughout this scenario, an upper crustal density of 2800 kg/m^3 is assigned to the tectonic loads. Eroded sediment in all timesteps has a density of 2500 kg/m^3. No tectonic loads were added in the Llandeilo time step as tectonic subsidence data indicate a decrease in the subsidence rate at this time (Bahlburg, 1990).

Results And Discussion

The results obtained in the two different scenarios show only very minor differences between them. This is not surprising as the two runs differ only in the small density differences assigned to the various loads. These differences play only an insignificant role in comparison to the overriding interplay between the size of the loads and the flexural properties of the loaded lithosphere. Therefore it appears to be justified to ignore these minor discrepancies in the following discussion.

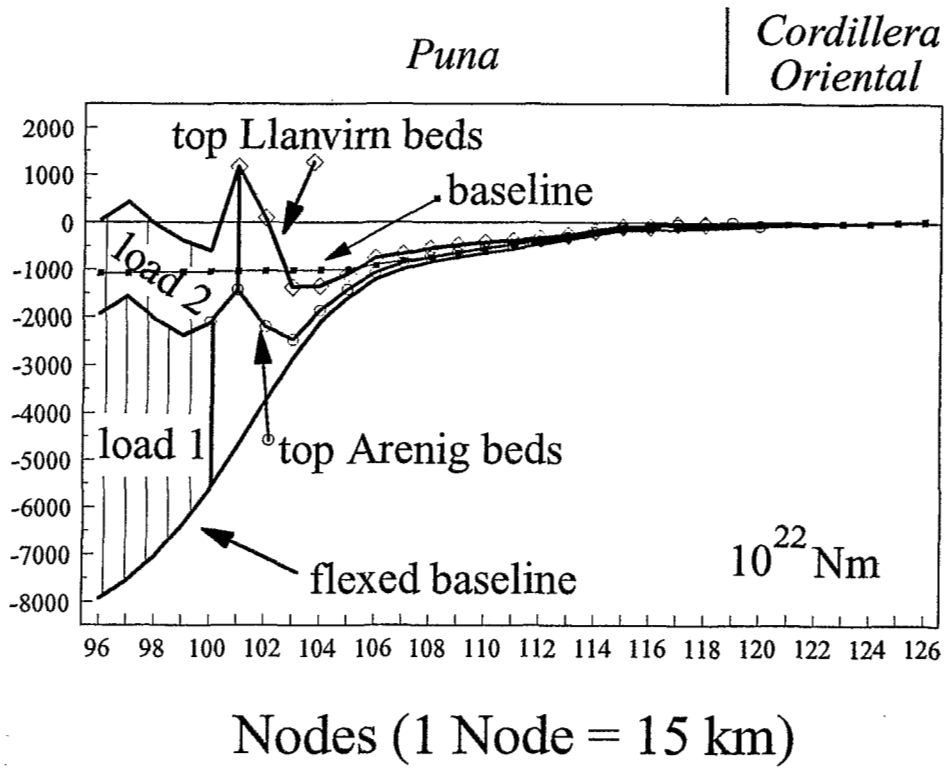

Fig. 1: Arc Scenario, results of timestep 2 (Llanvirn), assuming a flexural rigidity of the lithosphere of 10^{22} Nm. baseline: top of the lithosphere before loading; flexed baseline: top of the lithosphere after loading.

As the main conclusion from the model scenarios it can be stated that under both assumptions the geometry and facies patterns of the Ordovician Puna basin were reproduced well for a total load thickness of max. 8000 m, loading a lithosphere with a flexural rigidity of 10^{22} Nm, representing an equivalent elastic thickness of 13 km. This is a fitting value either for a thinned back-arc crust or a young leading edge at a previously passive margin (Karner and Watts, 1983; Erickson, 1993). The results are inconsequential in so far as no preference for either of the scenarios can be derived. However, they have distinctly different implications for interpretations of the geotectonic evolution of NW Argentina and N Chile.

According to Ramos (1988), the Arequipa Terrane docked to the Pampeanas Terrane in the Oclóyic Orogeny at the end of the Ordovician. Although there is no positive evidence of a major Ordovician suture in this region, the terrane boundary between the Pampeanas Terrane in the E, and the Arequipa Terrane in the W is assumed to be located along the border between the Cordillera Oriental and the Puna, or within the Puna. In either case, the Arenig arc would reside on the Arequipa Terrane. This interpretation corresponds to the Tectonic Scenario presented above. If, however, the Arenig arc was constructed on the previously passive margin of the Pampeanas Terrane, as is inherent to the Arc Scenario, the arc would reside on the former trailing edge of this terrane. The suture with the Arequipa Terrane would accordingly coincide with the position of the Ordovician subduction zone W of the Cordón de Lila in N Chile (Niemeyer, 1989). This interpretation is supported by the facies patterns and geometries of the Ordovician sedimentary rocks in the Cordillera Oriental which represent, from E to W, an uninterrupted shelf-slope-basin section (Bahlburg, 1991). Further field studies should be directed towards identifying the actual position of the suture between the Pampeanas and Arequipa Terranes.

References

BAHLBURG, H., 1990, The Ordovician basin in the Puna of NW Argentina and N Chile: geodynamic evolution from back-arc to foreland basin. *Geotektonische Forschungen* **75**, 1-107.

BAHLBURG, H., 1991, The Ordovician back-arc to foreland successor basin in the Argentinian-Chilean Puna: tectonosedimentary trends and sea-level changes. In: *Sedimentation, Tectonics, and Eustasy* (Edited by Macdonald, D.I.W.) . *Special Publications of the international Association of Sedimentologists* 12, 465-484 .

BOND, G.C., NICKESON, P.A. and KOMINZ, M.A., 1984, Breakup of a supercontinent between 625 and 555 Ma: new evidence and implications for continental histories. *Earth and Planetary Science Letters* **70**, 325-345.

BREITKREUZ, C., BAHLBURG, H., DELAKOWITZ, B. and PICHOWIAK, S., 1989, Volcanic events in the Paleozoic central Andes. *Journal of South American Earth Sciences* **2**, 171-189.

COIRA, B., DAVIDSON, J., MPODOZIS, C. and RAMOS, V., 1982, Tectonic and magmatic evolution of the Andes of northern Argentina and Chile. *Earth Science Reviews* **18**, 303-332.

DALLA SALDA, L., DALZIEL, I.W.D., CINGOLANI, C. and VARELA, R., 1992, Did the Taconic Appalachians continue into southern South America? *Geology* **20**, 1059-1062.

DALZIEL, I.W.D., 1991, Pacific margins of Laurentia and East Antarctica-Australia as a conjugate rift pair: evidence and implications for an Eocambrian supercontinent. *Geology* **19**, 598-601.

ERICKSON, S.G., 1993, Sediment loading, lithospheric flexure, and subduction initiation at passive margins. *Geology* **21**, 125-128.

FORSYTHE, R.D., DAVIDSON, J., MPODOZIS, C., and JESINKEY, C., 1993, Lower Paleozoic relative motion of the Arequipa block and Gondwana: paleomagnetic evidence from Sierra de Almeida of northern Chile. *Tectonics* **12**, 219-236.

HERVÉ, F., GODOY, E., PARADA, M.A., RAMOS, V. RAPELA, C., MPODOZIS, C. and DAVIDSON, J., 1987, A general view on the Chilean-Argentine Andes, with emphasis on their early history. *American Geophysical Union Geodynamic Series* **18**, 97-113.

KOUKHARSKY, M., COIRA, B., BARBER, E. and HANNING, M., 1988, Geoquímica de vulcanitas ordovícicas de la Puna (Argentina) y sus implicancias tectónicas. *V. Congreso Geológico Chileno* **3**, I137-158.

Karner, G.D. and Watts, A.B., 1983, Gravity anomalies and flexure of the lithosphere at mountain ranges. *Journal of Geophysical Research* **88**, B4, 449-477.

KUMPA, M. and SANCHEZ, M.C., 1988, Geology and sedimentology of the Cambrian Grupo Mesón (NW Argentina). In: *The southern Central Andes: contributions to structure and evolution of an active continental margin* (Edited by H. Bahlburg, C. Breitkreuz, and P. Giese). *Lecture Notes in Earth Sciences* **17**, 39-54.

NIEMEYER, H., 1989, El complejo igneo-sedimentario del Cordón de Lila, región de Antofagasta: Significado tectónico. *Revista Geológica de Chile* **16**, 163-181.

RAMOS, V.A., 1988. Late Proterozoic-Early Paleozoic of South America - a collisional history. *Episodes* **11**, 168-174.

A COLLISIONAL MODEL FOR THE STRATIGRAPHIC EVOLUTION OF THE ARGENTINE PRECORDILLERA DURING THE EARLY PALEOZOIC

Juan L. Benedetto (1) and Ricardo A. Astini (1)

(1) CONICET. Cátedra de Estratigrafía y Geología Histórica. Universidad Nacional de Córdoba. Av. Velez Sarsfield 299, 5000 Córdoba, Argentina.

RESUMEN. Se analiza la posible relación existente entre la historia sedimentaria y la evolución geodinámica de la Precordillera a la luz de la hipótesis de su origen como un microcontinente fragmentado de Laurentia y posteriormente acrecionado a Gondwana durante el Paleozoico temprano.

KEY WORDS: Argentina, Precordillera, Early Paleozoic, geodynamics.

On the basis of Dalziel's model (1991), Dalla Salda *et al.* 1992a; 1992b) suggested a Late Ordovician collision between South America and Laurentia in order to explain both, the Taconic orogeny in the Appalachians and the Famatinian orogeny in Western Argentina. According to this model, the carbonate platform of the Precordillera repr e sents the southward continuation of the Appalachian margin. However, several lines of evidence suggest that the precordilleran and eastern North America margins represent a conjugate rift pair, as was proposed by Bond *et al.*(1984). Herrera & Benedetto (1991) demonstrated that the brachiopod faunas of the San Juan Limestone (Early Ordovician) contain a significant proportion of Toquima-Table Head genera associated with several Celtic and Baltic elements. Because the Celtic genera have never been recorded from the North American Ordovician sequences, paleontological evidence do not supports continuity of South America and Laurentian margins. Nevertheless, the faunal affinities of trilobites suggest that both margins were very close during the Cambrian. The increasing amount of Celtic genera from Early Arenig to Early Llanvirn may reflect a gradual expansion of the Southern Iapetus Ocean. Petrologic evidence from the Famatina Range (Aceñolaza & Toselli, 1988; Mainheim & Miller, 1992) are particularly significant in demonstrating the existence of an Ordovician volcanic arc between the Gondwana basement and the Precordillera belt. Deep seismic reflection data across the Sierras Pampeanas and Precordillera boundary seem to be consistent with an allochtonous origin of the Precordillera (Cominguez & Ramos, 1991).

Recently, Benedetto (1993) proposed alternative paleogeographic models consistent with the biogeographic evidence. The hypothesis of Precordillera being a microcontinent which rifted from Laurentia in the Late Proterozoic or Early Cambrian, drifting from low to high latitudes is examined in detail in this paper and summarized in figure 1.

Late Proterozoic-Early Cambrian. The rifting and opening of the Southern Iapetus Ocean, at about 550-570 Ma produced the passive continental margin of Precordillera. A succession of red beds and evaporites which seems to underlie the Early Cambrian limestones in the northern Precordillera may represent a rift related sequence. Paleontological data indicate that a narrow ocean separated both margins. At the Precordillera latitude, the Late Precambrian-Early Cambrian Caucete Group was deposited on the Gondwana margin. This sequence, which could represent passive margin sedimentation, was folded and metamorphosed probably as a result of the development of an east-dipping subduction zone.

Middle-Late Cambrian. Carbonate deposition was continuous throughout the Precordillera platform. The Middle Cambrian successions are mainly subtidal, while the Late Cambrian is composed by intertidal dolostones. A coeval thick succession of rift-related shallow water sandstones and shales (Meson Group) was deposited on the Gondwana margin in northwestern Argentina.

Tremadoc. The Late Cambrian tidal flat carbonates (La Flecha Formation) are followed by a predominantly calcareous mid-shelf sequence (La Silla Formation). The deepening correlates with a global sea level rise which is reflected on the Gondwana margin by a widespread transgressive clastic sequence (Santa Victoria Group). In the Famatina basin, the black shales of the Volcancito Formation were deposited in an ensialic back-arc basin related to the Cambrian east-dipping subduction zone. A similar geodynamic scenary was proposed by Bahlburg and Breitkreuz (1991) to explain the origin of the Puna and Cordillera Oriental basins of northwestern Argentina.

Arenig. 90 Ma after the break-up, the Precordillera was placed approximately 2500 Km to the SE of Laurentia and a narrowing ocean separates it from Gondwana. To the east of the subduction zone an extensive volcanic arc system was active. Shallow marine fossiliferous shales, sandstones and layers of volcaniclastic materials (Suri Formation) filled the Famatina back-arc basin. The presence of brachiopods of Celtic affinities indicates for the first time a faunal connection with the Precordillera carbonate platform. Similar thick successions related to prograding shorelines and storm dominated deltaic complexes (Acoite and Sepulturas formations) were deposited in the Cordillera Oriental in northwest Argentina (Astini & Waisfeld, 1993).

Llanvirn-Llandeilo. Continued eastward subduction resulted in the closure and deformation of the Famatina back-arc basin (early stage of collision) giving rise to the Guandacol orogenic event. The Early Llanvirn is marked by extensive black shale deposition covering the carbonate platform (Astini *et al.*, 1988) in a starved peripheral foreland and accumulation of thick turbidites and olistostromes (i.e.Rinconada Formation) adjacent to the Gondwana basement. The major subsidence to the east could be interpreted as a response of active thrust loading along the eastern border of the Precordillera. The facies changes suggest that a block-faulted structure

accompanied the subsidence of the Precordillera collisional foredeep. Prominent diachronous conglomerates (i.e.La Cantera and Las Vacas Formations) suggest active motion of normal faults during the Llandeilo-Early Caradoc, but these coarse grained sediments also could have been derived from sinistral wrench faulting related to the collision. Along the open sea-faced margin a thick slope-to-basin clastic wedge was being built (Astini, 1988).

Caradoc-Ashgill. Upwarping and erosion of the distal portion of the peripheral foreland gave origin to a regional unconformity developed diachronically during the Late Ordovician in Precordillera (Astini, 1992). Thick carbonate megabreccias (Trapiche and Empozada formations) were shifted from the structural high into local strongly subsident depocenters evidencing active cannibalization of exposed older Ordovician strata. To the western belt, the clastic wedge interfingered with pillow lavas during the Caradoc (i.e.Yerba Loca and Alcaparrosa formations) (Astini, 1988). During the Hirnantian, eastern derived glacial sediments were deposited in the Precordillera.

Silurian-Devonian. Siliciclastic sequences are composed mainly by fine-grained shelf deposits, mostly confined to the east side of the forebuldge. The Early Silurian successions onlap the structural high to the west. On the easternmost border of the Precordillera basin, the influx of flysch-like sediments and olistostromes during the Llandovery and Wenlock (Mogotes Negros Formation) points out the final stages of the collision, although they might be related to a shear zone which displaced the Precordillera with a north-south trend (Ramos *et al.*,1986). The general stacking pattern and the cyclical facies arrange of Silurian and Devonian succcessions was controlled by eustacy or by the lithosphere rheology of the foreland.

REFERENCES

ACEÑOLAZA,G.F. & A.J.TOSELLI,1988. V Congr.Geol.Chileno,I:55-67

ASTINI,R.A.,1988. V Intern.Symp.Ordovician System, Abst.:2

ASTINI,R.A., F.L.CAÑAS & J.L.BENEDETTO, 1988. V Intern. Symp. Ordovician System, Abst.: 3.

ASTINI,R.A., 1992. Paleowathering records and paleosurfaces, 2nd Meeting.Abst.:6-7.

ASTINI,R.A. & B.G.WAISFELD, 1993. XII Congr.Argentino Geología.

BAHLBURG,H. & C.BREITKREUZ, 1991. J. South American Earth Sci., 4:171-188.

BENEDETTO,J.L., 1993. XII Congr. Geológico Argentino, Mendoza.

BOND,G.C., P.A.NICKESON & M.KOMINZ, 1984. Earth & Planet. Sci Letters, 70: 325-345.

COMINGUEZ,A.H. & V.A.RAMOS, 1991. Rev. Geol. Chile, 18: 3-14.

DALLA SALDA,L., C.A.CINGOLANI & R.VARELA, 1992a. Geology, 20: 617-620.

DALLA SALDA,L., I.W.D.DALZIEL, C.A.CINGOLANI & R.VARELA, 1992b. Geology, 20:1059-1062.

DALZIEL,I.W.D.,1991. Geology, 19:598- 601.

HERRERA,Z. & J.L.BENEDETTO, 1991. In:McKinnon,D.I. et al (Eds.), Brachiopods through time. Balkema.pp.283-301.

MANNHEIM,R. & H.MILLER, 1992. Conferencia Intern. Paleozoico Inferior de Ibero-América. Abst.:102.

RAMOS,V.A., T.E.JORDAN, R.W.ALLMENDINGER, C.MPODOZIS, S.M.KAY, J.M. CORTES & M.A.PALMA, 1986. Tectonics, 5:855-880.

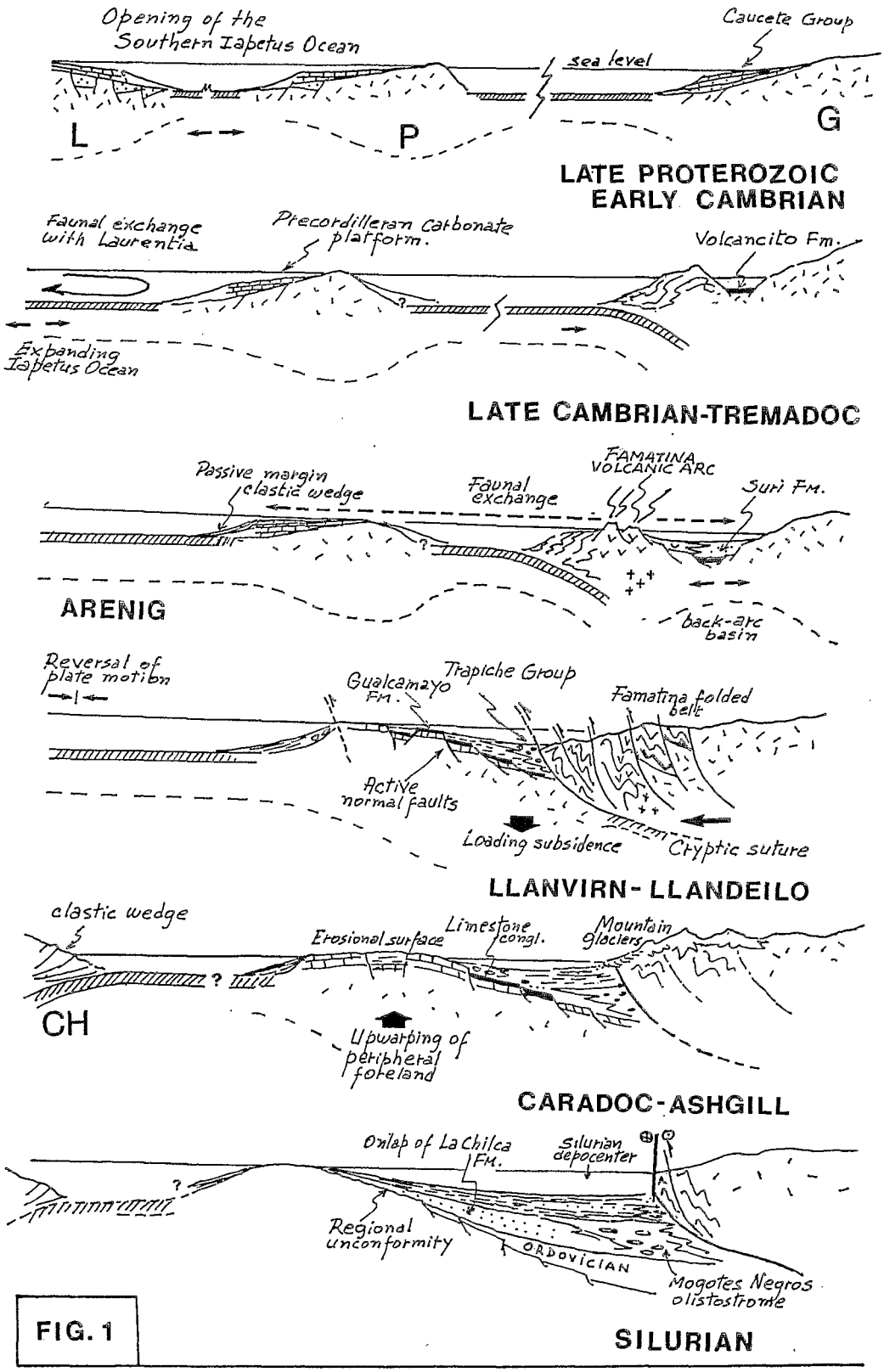

FIG. 1

CH: CHILENIA G: GONDWANA L: LAURENTIA P: PRECORDILLERA

THE ORIGIN AND EARLY HISTORY OF THE PACIFIC MARGIN OF SOUTH AMERICA: THEIR INFLUENCE ON THE DEVELOPMENT OF THE ANDEAN CORDILLERA

Ian W. D. DALZIEL

Institute for Geophysics
8701 Mopac Boulevard
Austin, Texas 78759-8397 USA

For nearly a century, various aspects of the foundation of the Andean Cordillera have led geologists (e.g. Burckhart, 1902; Steinmann, 1923; Dalmayrac et al., 1980) to speculate on the existence of a major continent to the west (present coordinates) of South America during the Paleozoic. Recently Moores (1991) and Dalziel (1991) have revived earlier ideas (Eisbacher, 1985; Bell and Jefferson, 1987) that the Pacific margins of North America and East Antarctica-Australia may have been juxtaposed in the late Precambrian. This has led to the idea that Laurentia, the Precambrian core of North America, may have "broken out" from between East Antarctica-Australia and South America during the Neoproterozoic to Cambrian amalgamation of Gondwanaland (Dalziel, 1991; Hoffman, 1991). According to this hypothesis the Neoproterozoic opening of the Pacific Ocean basin was balanced on a globe of constant radius by the closure of several ocean basins between the cratons that amalgamated to form Gondwana, and "southern Iapetus" opened at the end of the Neoproterozoic between Laurentia and the coalescing cratons of West Gondwana (Dalziel, 1992a,b).

Paleomagnetic data are compatible with clockwise rotation of Laurentia around the Pacific margin of Gondwana during the Paleozoic *en route* to final "docking" with northwestern Africa (present coordinates) to form Pangea (Dalziel, 1991, Fig. 2). Indeed several lines of evidence suggest that, following initial separation in the latest Neoproterozoic to Early Cambrian, Laurentia may have tectonically interacted with the Pacific margin of South America in the course of this motion (Dalla Salda et al., 1992a,b; Dalziel et al., 1992 and in press). The accompanying figure shows hypothetical, but paleomagnetically acceptable, relations of Laurentia and South America at specific times from the end of the Precambrian to the assembly of Pangea in the latest Paleozoic. The reconstructions may explain several long-standing tectonic problems, yet they do not appear to conflict with well-established interaction between Laurentia, Baltica, and other tectonic units of the present-day North Atlantic region. Critical elements of the overall hypothesis are outlined below. The suggestion of specific times of continent - continent collision is not meant to imply simple tectonic settings. The zone between the continents would have been as complex as the Tethys or present-day Mediterranean.

Latest Precambrian (570 Ma): The Labrador-Greenland promontory of Laurentia rifts from the Arica reentrant in the Gondwana margin, possibly while some Brazilide basins are still closing. The Arequipa massif is a fragment of the Ketilidian-Makkovik provinces of Greenland and Labrador. The Paleozoic intracratonic basin between the Arequipa and the Amazonian shield may mark a failed arm of the rift system.
Cambrian-Early Ordovician (500 Ma): Laurentia rifts from the proto-Andean margin, isolating the benthic trilobite fauna of the continent. The "southern cone" (from Georgia in the east to Trans-Pecos Texas in the west) may have remained attached to Gondwana in the vicinity of the present-day Weddell Sea.
Mid-Ordovician (487 Ma): Laurentia and Gondwana collide to form the Taconic-Famatinian (Ocloyic) orogen, possibly continuing into the Shackleton Range of Antarctica. Upon subsequent rifting (possibly pre-Ashgillian), the Precordilleran terrane of northwestern Argentina is detached from the Ouachita

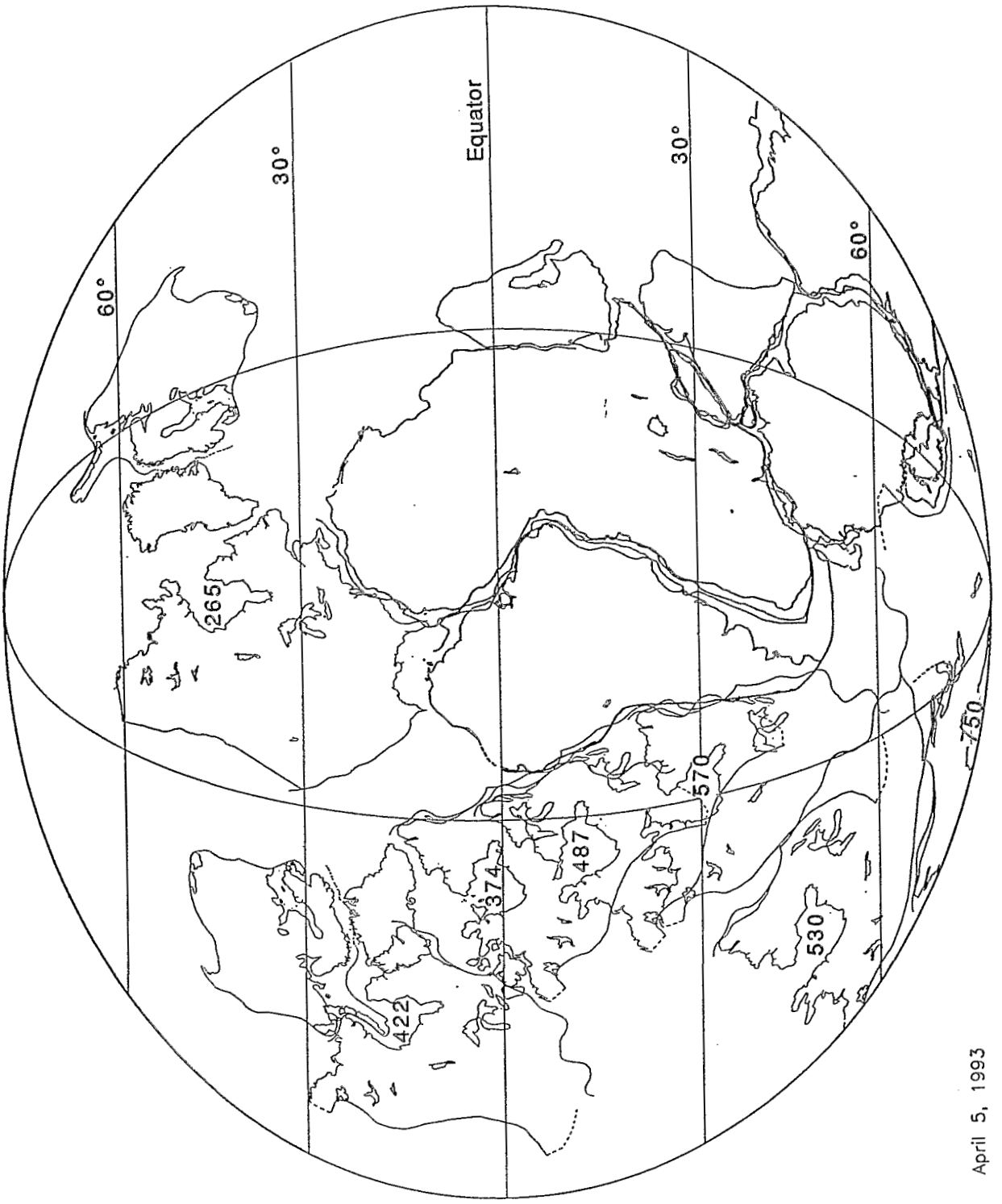
60°
30°
Equator
30°
60°
265
422
374
487
570
530
750
April 5, 1993

embayment of Laurentia, and the Oaxaca terrane of Mexico is detached from the area of the Arica reentrant of South America.
Late Ordovician and Silurian (422 Ma): Laurentia and Gondwana separate. Laurentia occupies temperate to tropical latitudes while the Pacific margin of Gondwana undergoes glaciation.
Devonian (374 Ma): Following the Laurentia-Baltica collision that ended the Caledonian orogeny, Laurentia and Gondwana collide once again in a dominantly right-lateral transpressive mode. Much of what is known as the Acadian orogeny in North America may reflect this interaction. Distribution of the Malvinokaffric and Cosmopolitan faunas would have been strongly influenced by the changing paleogeography over this time interval. Subduction of Pacific Ocean floor commences beneath the central Chilean margin.
Latest Paleozoic (265 Ma): Laurentia finally docks with present-day northwestern Africa in the Ouachita-Alleghanian orogenesis to terminate the Appalachian revolution and complete the amalgamation of Pangea. Pacific Ocean floor is subducted beneath the entire proto-Andean margin.

The hypothesis, if basically correct, has several major implications for the development of the Andean Cordillera in the Mesozoic and Cenozoic. For example: 1. As suggested by others (e.g. Dewey and Lamb, 1992) from a purely South American standpoint, the Arica reentrant may be an original feature and may have exerted control over the tectonic development of the Pacific margin throughout the Phanerozoic. The Patagonian and Colombian oroclines may also date from initial rifting. 2. The crust beneath the Altiplano may have been thickened initially in Grenvillian collision of the Laurentian craton with Amazonia. 3. Laurentia may have played a critical role in the diachronous initiation of subduction of Pacific Ocean floor beneath South America. 4. Subduction erosion along the Pacific margin of South America may have been limited to material accreted during the Phanerozoic.

References:

BELL, R. and JEFFERSON, C. W., 1987, An hypothesis for an Australia-Canadian connection in the Late Proterozoic and the birth of the Pacific Ocean: PacRim Congress 1987, Parkville, Australia, p. 39-50.
BURCKHARDT, C., 1902, Traces géologique d'un ancient continente Pacifique: Revista del Museo La Plata, v. 10, p. 179-192.
DALLA SALDA, L.H, CINGOLANI, C.A., and VARELA, R., 1992a, Early Paleozoic orogenic belt of the Andes in southwestern South America: Result of Laurentia-Gondwana collision?: Geology, v. 20, p. 617-620.
DALLA SALDA, L. H., DALZIEL, I.W.D., CINGOLANI, C.A., VARELA, R., 1992b, Did the Taconic Appalachians continue into southern South America?: Geology, v. 20: 1059-1062.
DALMAYRAC, B., Laubscher, G., Marocco, R., Martinez, C., and Tomasi, P., 1980, La chaîne hercynienne d'Amérique du sud; structure et evolution d'un orogène intracratonique: Geologische Rundschau, v. 69, p. 1-21.
DALZIEL, I.W.D., 1991, Pacific margins of Laurentia and East Antarctica-Australia as a conjugate rift pair: Evidence and implications for an Eocambrian supercontinent: Geology, v. 9, p. 598-601.
DALZIEL, I.W.D., 1992a, Antarctica; A tale of two supercontinents?: Annual Review of Earth and Planetary Sciences, v. 20, p. 501-526.
DALZIEL, I.W.D., 1992b, On the organization of American plates in the Neoproterozoic and the breakout of Laurentia: GSA Today, v. 2, p. 237-241.
DALZIEL, I.W.D., DALLA SALDA, L. H., and GAHAGAN, L.M., 1992, North America as an "exotic terrane" and the origin of the Appalachian-Andean mountain system: Geological Society of America Abstracts with Programs, v. 24, p. 288.
DALZIEL, I.W.D., DALLA SALDA, L. H., and GAHAGAN, L.M., 1993, Paleozoic Laurentia-Gondwana interaction and the origin of the Appalachian-Andean mountain system: Geological Society of America Bulletin (in press).
DEWEY, J.F., and LAMB, S.H., 1992, Active tectonics of the Andes: Tectonophysics, v. 205, p. 79-96.

EISBACHER, G.H., 1985, Late Proterozoic rifting, glacial sedimentation, and sedimentary cycles in the light of Windermere deposition, Western Canada: Paleogeography, Paleoclimatology, Paleoecology: v. 51, p. 231-254.
HOFFMAN, P.F., 1991, Did the breakout of Laurentia turn Gondwanaland inside out?: Science, v. 252, p. 1409-1412.
MOORES, E.M., 1991, Southwest U.S.-East Antarctic (SWEAT) connection: A hypothesis: Geology, v. 19, p. 425-428.
STEINMANN, G., 1923, Umfang, Beziehungen und Besonderheiten der andinen Geosynklinale: Geologische Rundschau, v. 14, p. 69-82.
VAN DER VOO, R., 1988, Paleozoic paleogeography of North America, Gondwana, and intervening displaced teranes: Comparisons of paleomagntism with paleoclimatology and biogeographical patterns: Geological Society of America Bulletin, v. 100, p. 311-324.

Figure Caption

Molleweide projection showing hypothetical, but paleomagnetically acceptable, positions of Laurentia with respect to South America during the Paleozoic. The figure is modified from an earlier diagram (Dalziel, 1991, Figure 2) that was constructed to show that Laurentia could have "broken out" from between East Antarctica-Australia and South America at the end of the Precambrian. In the present figure, Gondwana is reconstructed using marine geophysical data as before, with South America kept in its present-day coordinates. Paleomagnetic controls are mainly from Van Der Voo (1988).

Early Neoproterozoic Laurentia (ca. 750 Ma) is shown against East Antarctica-Australia as it may have been prior to opening of the Pacific Ocean basin and amalgamation of Gondwana (Moores, 1991; Dalziel 1991; Hoffman, 1991). Laurentia is shown in the late Neoproterozoic (ca. 570 Ma) with the Labrador-Greenland promontory located within the Arica reentrant (Dalziel, 1992b). The position for the Early Ordovician (500 Ma) is as in Dalziel (1991 and 1992a). The Laurentia-Gondwana collision suggested by Dalla Salda (1992a, b) to have resulted in the Taconic-Famatinian (-Shackleton?) orogen is shown at 487 Ma; this is perhaps about 25 million years too early for the main deformation and metamorphism, but the paleomagnetic control is better. The position for Laurentia at 422 Ma is that of Dalziel (1991). Right-lateral transpression between Laurentia and Gondwana suggested to account for the main effects of the Acadian orogeny is indicated at 374 Ma (Dalziel et al., 1992 and in press); this is rather late for the Acadian, but again the paleomagnetic control is better. The reconstruction of Pangea by ca. 265 Ma is based on marine geophysical data.

THE ACHALA BATHOLITH (CORDOBA, ARGENTINA) A COMPOSITE INTRUSION MADE OF INDEPENDANT MAGMATIC SUITES

Michel DEMANGE(1), Juan O. ALVAREZ(2), Luiz LOPEZ(2) and Juan J. ZARCO(2)

(1) Centre de Géologie Générale et Minière, Ecole des Mines, 35 rue Saint-Honoré, 77305 Fontainebleau, FRANCE
(2) Comisión Nacional de Energía Atómica, Avenidad del Libertador, 1871, Buenos Aires, ARGENTINA

ABSTRACT : In the Sierra de Cordoba (Argentina), the Achala batholith consists in four independent peraluminous magmatic suites which shows contrasted major and trace elements spectra and variable metallogenic specialisation.

KEY WORDS : Sierras pampeanas, S-type granites, differenciation , melallogenic specialisation

INTRODUCTION

The Achala batholith which outcrops over a surface of about 2500 km^2, is a major element of the Sierra Grande de Cordoba, the most oriental of the Pampean ranges. Several deposits and showings of W, Cu, U, F, Li, Be, Nb and Ta, are spacially associated with the batholith.

The recent papers dealing with its petrology and geochemistry consider only transversal cross-sections or limited sectors. The present study intends to take into account the whole batholith, since it is based on 84 reliable samples, carefuly selected out of the 450 available analyses, in order to to represent the different facies and the different sectors of the intrusion.

The Achala batholith is a post-tectonic intrusion emplaced in high grade metamorphic rocks of the pampean cycle (Upper Proterozoic). It is composite ; its main facies are synchronically emplaced in an environment of submeridian crustal shearing during a local extensional stage. An horizontal shortening induces the formation of NW to NNW trending magmatic shear zones which host synkinematic intrusions. After its emplacement, the batholith was affected by large dextral wrench faults associated with mylonites, which are anterior to the Upper Carboniferous, and by inverse faults related to the Andean cycle .

FOUR MAGMATIC SUITES

Structural, petrological and geochemical data allow one to divide the Achala batholith into homogoneus sectors and to recognise at least four magmatic suites ; the limits between the different domains, are not always obvious in the field, but are marked by strong geochemical discontinuities, particularly emphasized by the radiometric data.

Each suite regroups various petrographic facies : equigranular biotite granodiorites, porphyritic granodiorites and granites, coarse grained granites, equigranular muscovite granites, aplite and pegmatites.

All these different suites present a peraluminous character (S-type granites) but distinctions can be made using both trace and major elements : the Achala suite is richer in K, Rb, Sr, Zr, Th and U , the Champaqui suite richer in Na, Ba and Mg ; the Characato and Cumbrecita

suites are intermediate between the former.The Characato suite is particularly rich in REE ; Y and Nb present here a different behaviour.

Each suite seems to have its proper metallogenic specialization.: the uranium and fluorite deposits and showings appear related to the Achala suite , the W deposits and showings to the Characato suite and the pegmatites of metallogenic interest (Li, Be, Nb, Ta, P) to the Champaqui suite.

CONCLUSION

These difference that have been just mentionned, are observed even in the less differenciated members of the various suites ; the parental magmas must thus have been independent and these suites may be of very different ages.The published geochronological studies carried out without taking care of the composite character of the batholith, assing to the Achala batholith an age varying from Silurian to Carboniferous. : 399 ±25 Ma for the Achala suite (probably errorchron) (Rapela & al. 1982); 337±30 / 358±9 Ma for the Characato suite (Rapela & al. 1991). As long as new data are not available, one must thus be very cautious about any geotectonical interpretation of the Achala batholith.

REFERENCES

ALVAREZ, J. O., 1992. Determinación petrológica de facies ígneas regionales en el batolito de Achala y su posible evolución. *C.N.E.A. unpubl. report.*

BALDO, E. G. A., 1992. Estudio petrológico y geoquímico de las rocas ígneas y metamórficas entre Pampa de Olaen y Characato, extremo norte de la Sierra Grande de Córdoba. Córdoba, República Argentina. *Thesis, Fac. Cs. Ex., Fis. y Nat., Univ. Nac. de Córdoba.*

CUNEY, M., LEROY, J., VALDIVIEZO, A., DAZIANO, O., GAMBA, M., ZARCO, J, MORELLO, O., NINCI, C. and MOLINA, P., 1987. Geochemistry of uranium mineralised Achala granitic complex, Argentina : comparison with hercynian peraluminous leucogranites of Western Europe. In Metallogenesis of Uranium deposits. *Inter. Atom. Ener. Agency, Vienne, p. 211-232.*

GAMBA, M., 1981. Diferenciaciones petrográficas y geoquímicas en el área de Copina, sector sudeste del batolito de Achala, Sierra Grande de Córdoba. Distribución del uranio en las distintas facies graniticas. *C.N.E.A. unpubl. report.*

GORDILLO, C. E. and LENCINAS, A. N., 1979. Sierras Pampeanas de Córdoba y San Luis. *Seg. Simp. Geol. Reg. Arg., Acad. Nac. Cienc. Córdoba, 1, p. 577-650.*

LIRA, R. , 1985. Tipología y evolución de rocas graníticas en su relación con el hemiciclo endógeno de la geoquímica del uranio. Aspectos metalogenéticos. Sector septentrional del batolito de Achala, prov. de Córdoba. *Thesis, Fac. Cs. Ex., Fis. y Nat., Univ. Nac. de Córdoba.*

LIRA, R. and KIRSHBAUM, A., 1990. Geochemical evolutions of the granites from the Achala batholith of the Sierras Pampeanas. *Geological Society of America Special Paper, 241, p. 67-76.*

LOPEZ, L., 1991. Base de datos de litogeoquímica. Batolito de Achala. *C.N.E.A. unpubl. report.*

MONSBERGER, G., 1990. Estudio geológico y petrológico del granito de la Mesa de la Mula Muerta y su entorno encajonante. Pampa de Olaen, Depto. Punilla, Córdoba. *Fac. Cs. Ex., Fis. y Nat., Univ. Nac. de Córdoba unpubl. report.*

PATIÑO, M. G. de and PATIÑO DOUCE, A. E., 19087. Petrología y petrogénesis del batolito de Achala, provincia de Córdoba, a la luz de la evidencia de campo. *Asociación Geológica Argentina, XLII (1/2), p. 201-205.*

RAPELA, C. W., 1982. Aspectos geoquímicos y petrológicos del batolito de Achala, provincia de Córdoba. *Asociación Geológica Argentina, XXXVII (3), p. 313-330.*

RAPELA, C. W., HEAMAN, L. M. and Mc NUTT, R.J., 1982. Rb-Sr geochronology of granitoids rocks from the Pampean Ranges, Argentina. *J. Geol., 90, p. 574-582.*

RAPELA, C. W., TOSELLI, A., HEAMAN, L. and SAAVEDRA, J., 1990. Granite plutonism of the Sierras Pampeanas. An inner cordilleran paleozoic arc in the southern Andes. *Geological Society of America Special Paper, 241, p. 101-126.*

RAPELA, C. W., PANKHURST, R.J., KIRSCHBAUM, A. and BALDO, E. G. A., 1991.Facies intrusivas de edad carbonifera en el batolito de Achala : Evidencia de una anatexis regional en las Sierras pamapeanas? *Actas Congr. Geol. Chileno, p. 40-43.*

ZARCO, J. J., 1992. Prioritad de indicios unraníferos, modelo genético basado en el cisallamiento magmatico ocurrido durante el emplazamiento del batolito de Achala. *C.N.E.A. unpubl. report.*

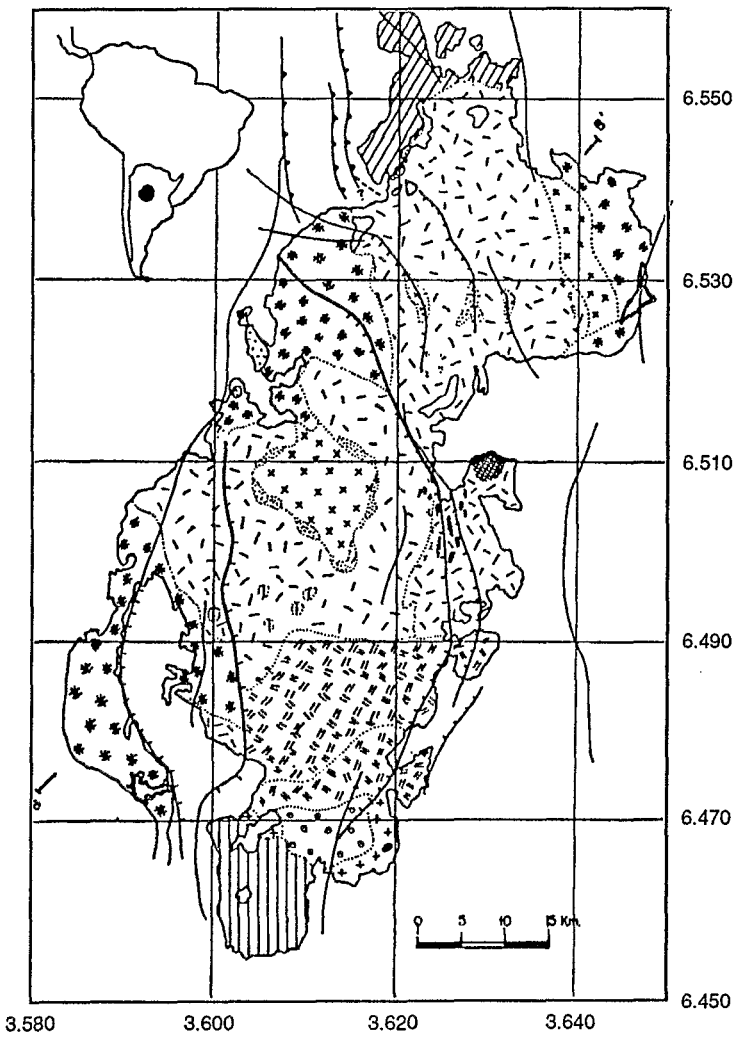

SUITE ACHALA

- Granodioritas I - E - IV - Dg
- Granitos - granodioritas porfiroides III A - B - C
- Granitos de grano grueso IV - A
- Granitos de grano grueso IV - B - C
- Granitos isogranulares de dos micas II - A
- Granitos - granodioritas de grano fino I - D - C/ I - A

SUITE CUMBRECITA

- Granitos porfiroides III A - B
- Granitos de grano grueso IV - A
- Granitos equigranulares II - C
- Granitos de grano fino I - B

SUITE CHAMPAQUI

- Granitos con dos micas o con muscovite granate

SUITE CHARACATO

- Granitos porfiroides y equigranulares con dos micas

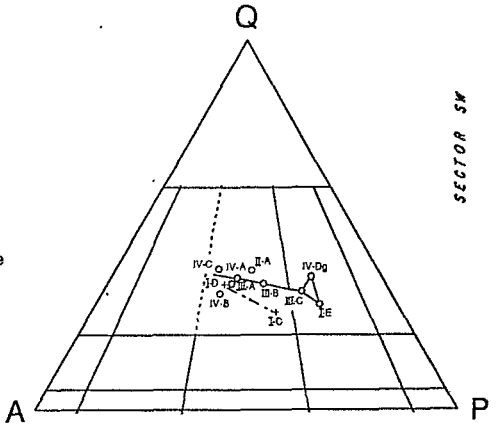

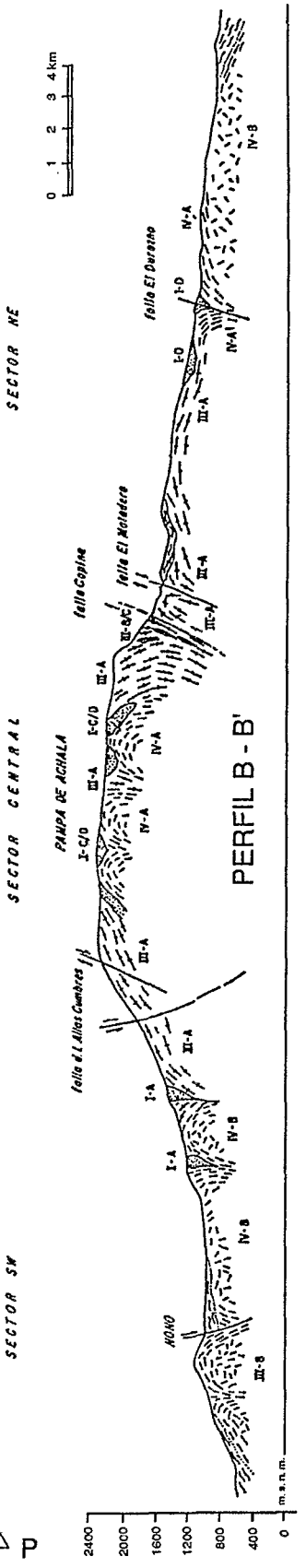

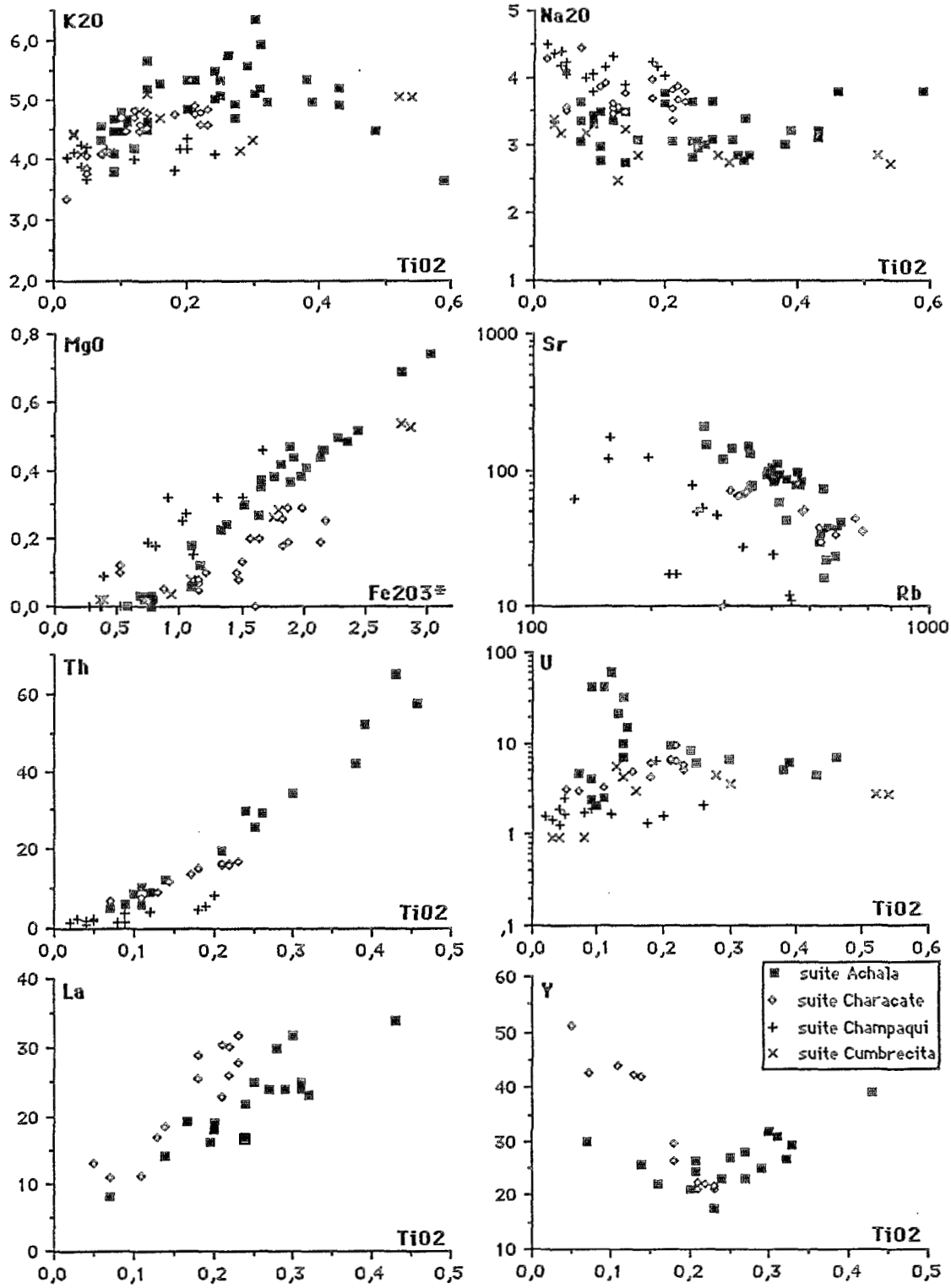
K2O
TiO2
Na2O
TiO2
MgO
Fe2O3*
Sr
Rb
Th
TiO2
U
TiO2
La
TiO2
Y
TiO2
suite Achala
suite Characate
suite Champaqui
suite Cumbrecita

STRUCTURAL EVOLUTION OF THE SIERRAS DE CORDOBA (ARGENTINA)

Michel DEMANGE[1], Edgardo G. BALDO[2] and Roberto D. MARTINO[2]

(1) Centre de Géologie Générale et Minière, Ecole des Mines, 35 rue Saint-Honoré, 77305 Fontainebleau, FRANCE
(2) CONICET & Departamento de Geología Basica, Universitad Nacional de Cordoba, Facultad de Ciencias Exactes, Fisicas y Naturales, Velez Sarsfield 299 , 5000 Cordoba, ARGENTINA

ABSTRACT : The Sierras de Cordoba (Argentina) shows the evolution of the western margin of the Rio de la Plata craton during the panamerican (=pampean) orogeny.from the extensional to the compressive stages This domains remained later on the internal (cratonic) side of the subsequent caledonian, variscan and andean orogenies.

KEY WORDS : Sierras pampeanas, Panamerican, Caledonian and Andean orogens

INTRODUCTION

The Sierras de Cordoba (Argentina), which corresponds to the easternmost Sierras Pampeanas, appear as a horst of metamorphic and magmatic terranes of precambrian and paleozoic age, uplifted by the andean movements. In spite of the synthesis proposed by Gordillo & Lencinas (1979), local structural observations (Dalla Salda 1984, Martino 1988) and of various geotectonical models (Ramos 1991), little is known on its orogenic evolution. The purpose of this paper in to present a first synthesis of this evolution based on a cross section on the central part of the Sierras (approximately at latitude 31°15' S) including cartography, structural analysis, geochemistry and study of the metamorphism.

PRE-OROGENIC EVOLUTION

Five main lithostratigraphic units have been recognised :

-- the **Sierra Chica Este** group, subdivided by the major La Estanzuela fault into the La Calera sub-group (kinzigites, calc-silicate-gneiss, marbles) of upper amphibolite facies and the El Diquecito subgroup (metagrauwackes, metabasic rocks) of granulite facies. This group which provided K/Ar ages of 1390-1516 My, is considered to be the western margin of the Rio de la Plata craton ;

- the **San Carlos group**, of amphibolite grade, is made of a very thick and monotoneous sequence of metagrauwackes with minor intercalations of metapelites and calc-silicate gneisses ; ortho-amphibolites, mafic and ultramafic (serpentine, harzburgite) rocks of MORB afinities (Mutti, Baldo 1992), dated by the K/Ar method between 850 and 1200 My, appear interbeded or constitute tectonic scales within the San Carlos group ; this group represent a deep seated sedimentation developped at the western margin of the Rio de la Plata craton, possibly in part on an oceanic crust ;

- the **orthogneissic group** represents pre-orogenic intrusives of granodioritic - granitic composition forming a calcalcaline trend, emplaced within the San Carlos group ;

- the **Igam group**, of amphibolite facies, comformably rests on the San Carlos group ; its lithologic association (calcitic and dolomitic marbles, calc-silicates gneiss, meta-quartzites, meta-litharenites, metapelites) represents a plateform sedimentation ;

The sedimentary environment contrast between the San Carlos and the Igam groups as well as the presence of orthogneisses in the sole San Carlos group sets the problem of possible orogenic movements prior to the Igam group deposition ;

- the **Mermela group**) appears only in the western part of the Sierra where it is limited by andean faults ; it is made of green pelites with minor levels of red pelites ans arenites ; its metamorphism and deformation are very weak ; in the Sierra de San Luis, the equivalent "filitas verde y esquistos" group contains moreover conglomerates and acidic vulcanites ; this group may represent the molasses of the panamerican orogeny (upper-proterozoic).

OROGENIC EVOLUTION

Early phases of deformation and metamorphism

The first recorded events are two phases of syn-metamorphic recumbent folds : the D1 folds, of centimetric to plurimetric scale, are accompagnied by a strong transposition and by migmatisation ; the D2 folds which are the most obvious, form pluri-kilometric structures with a westwards vergence.

The prograde metamorphism M1, of medium pressure type, is contemporaneous of these first tectonic events. Remnants of kyanite and staurolite are known, but the most common association observed in the metapelites is garnet + biotite1 + sillimanite + K feldspar + plagioclase + quartz. + ilmenite The major part of the Sierra de Cordoba presents a metamorphism of high amphibolite facies. There is no recorded isograde neither in the metapelites nor in the metabasites ; but variations of the metamorphic grade may be estimated using the variations of the compositions of the mineralswith in the metapelites : for instance the titanium content of the biotites may be a revelant parameter.

Magmatic rocks of tonalitic composition which often contain cordierite, are emplaced in the deepest part of the Sierra after this M1 event ; the bodies of this "San Carlos tonalite" present many migmatitic characters : numerous inclusions of the host rocks, progressives contacts with their surroundings. The metamorphic event M2 is linked with the emplacement of those migmatitic tonalites : the earlier M1 parageneses are reequilibrated into biotite2 + cordierite ± garnet + K feldspar + plagioclase + quartz + ilmenite. The conditions during this M2 event appears to be rather uniform : the estimated temperatures are of 650-700°C and the estimated pressures to 4,5 - 5 kb.

The D3 tectonic event forms north - south trending folds with a vertical axial plane marked by a fracture cleavage ; the emplacement of belts of pegmatites and of some granites appears to be controlled by these structures.

Ductile shearing and thrusting

Eastwards dipping, north - south trending mylonitic belts rework the earlier structures ; theses mylonites are often located in correspondance of the axial plane zones of the majors D2 folds ; their thickness ranges from a few 10 meters to more than a kilometer ; the streching lineations indicate a displacement towards north-west with a sinistral wrench fault component. These mylonites.have been initiated in a medium to high grade metamorphic surrounding (biotite + muscovite + sillimanite) which later evolved into greenschist facies. Mafic and ultramafic rocks often mark out theses mylonitic belts. In the eastern part of the Sierra, dykes of biotite-hornblende tonalites, dated at 570 My (K/Ar method) cut, and thus postdate, the mylonites.

These mylonitic belts carve the Sierra de Cordoba into several major blocks. Each block is thrusted westward over its neighbour and present a metamorphism wich increases towards the west. Thus, since blocks of higher metamorphic grade are trusted over blocks of lower grade, the metamorphic grade globally increases eastwards. The whole pattern shows how the Rio de la Plata craton was thrusted over its margin

The late panamerican and the youngest events

Several late phases of gentle folding, which locally interfere to form basin and dome structures, represent the latest manifestations of the panamerican orogeny.

In the Sierras de Cordoba, there is no obvious tectonic structure which may be related to the famatinian (=caledonian) orogeny. But, further west, in the Sierra de San Luis, this orogeny clearly affects the "filitas verde y esquistos" group. The Achala batholith, which is a very large (2500 km^2) composite intrusion of potassic peraluminous character, with an important crustal contribution, is dated of upper devonian to basal carboniferous (Rapella & al. 1991). It would thus represent the most intern magmatism of this orogeny.

The whole Sierras including the Achala batholith, are crosscut by large dextral wrench faults, which reactivate earlier structures. The small basins of Chancani and Tasa Cuna, of upper carboniferous to permian age, appear as pull-apart basins developed along these wrench faults.

The youngest structures are the andean inverse faults which induce the stricking horst and graben structure of the Sierras de Cordoba. Those andean faults frequently, but not always, rework the earlier accidents.

CONCLUSION

The Sierras de Cordoba show the evolution of the western margin of the Rio de la Plata craton, from the extensional stage (deposition of the San Carlos group) to the compressive stage during the panamerican (= pampean) orogeny. Later, this domain remained practically undeformed during the caledonian (=famatinianan) orogeny (as well as the subsequent variscan and andean orogenies) and was permanently located on the cratonic side. The main event of that caledonian orogeny is the emplacement of the Achala batholith in a very internal position.

REFERENCES

BALDO, E. G. A., 1992. Estudio petrológico y geoquímico de las rocas ígneas y metamórficas entre Pampa de Olaen y Characato, extremo norte de la Sierra Grande de Córdoba. Córdoba, República Argentina. *Thesis, Fac. Cs. Ex., Fis. y Nat., Univ. Nac. de Córdoba.*

DALLA SALDA, L., 1984. La estructura interna de las Sieras de Cordoba. Rev. Asoc. Arg. Tomo XXXIX, n° 1-2, 38-51.

GORDILLO, C. E. & LENCINAS, A. N., 1979. Sierras Pampeanas de Córdoba y San Luis. *Seg. Simp. Geol. Reg. Arg., Acad. Nac. Cienc. Córdoba, 1, p. 577-650.*

MARTINO, R., 1988. Geologia y Petrologia del basamento metamorfico de la region situada al norte de Cuchilla Nevada, Sierra Grande de Cordoba. *Thesis, Fac. Cs. Ex., Fis. y Nat., Univ. Nac. de Córdoba.*

MUTTI, D. I., 1989. Geologia del complexo gabbro - lherzolitico del Cerro de santa Cruz, Alta Garcia, Prov de Cordoba. *Rev. Asoc. Arg.min;, Metr. y Sed. (AMPS), tomo 20, n° 1/4, 53-58*

RAMOS, V., 1991. Late Proterozoic - Early Paleozoic of South America - a collisional history. *Episodes, vol. 11, n°3, 168-174.*

RAPELA, C. W., PANKHURST, R.J., KIRSCHBAUM, A. and BALDO, E. G. A., 1991.Facies intrusivas de edad carbonifera en el batolito de Achala : Evidencia de una anatexis regional en las Sierras pampeanas? *Actas Congr. Geol. Chileno, p. 40-43.*

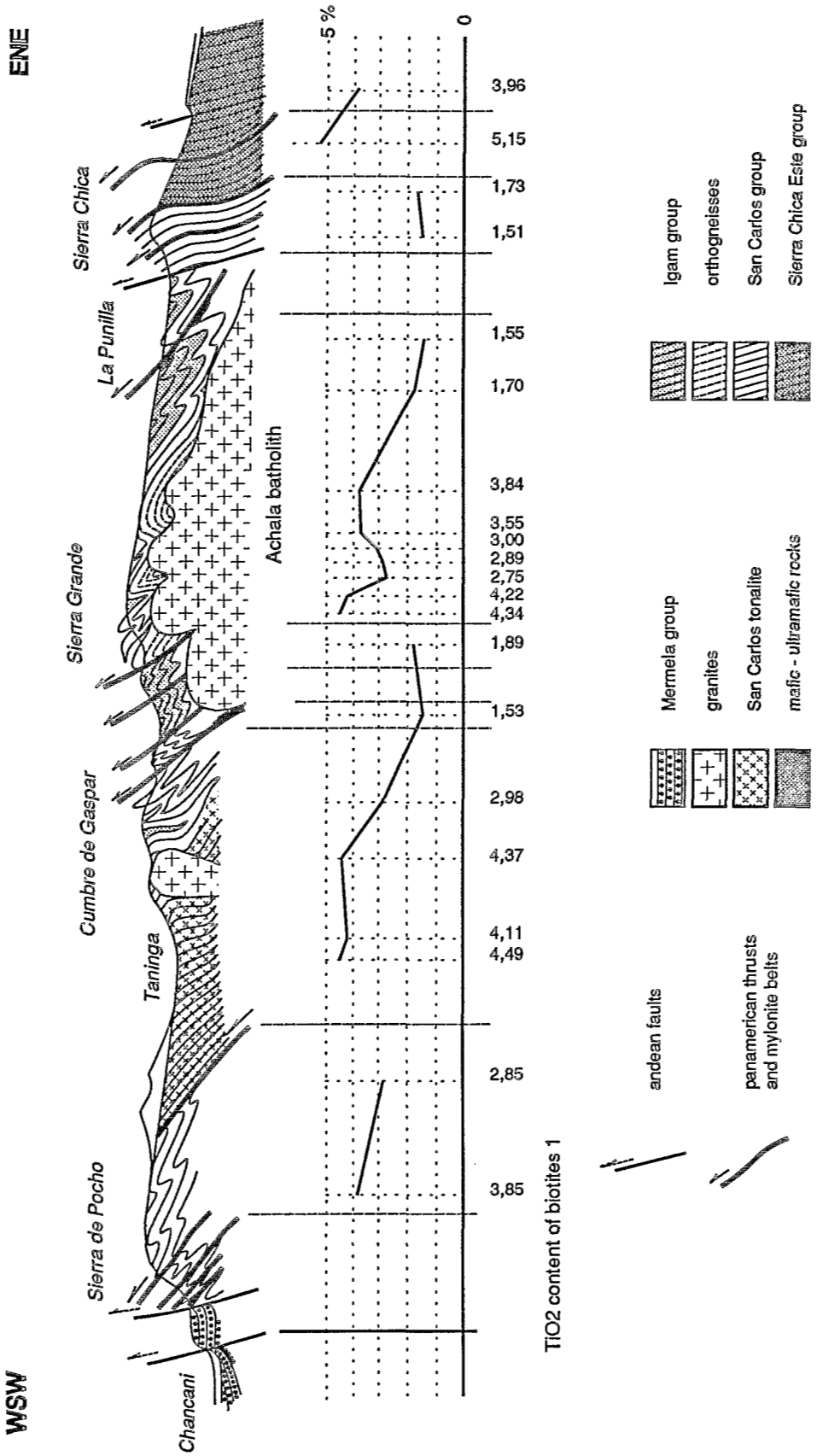
WSW
ENE
Chancani
Sierra de Pocho
Taninga
Cumbre de Gaspar
Sierra Grande
Achala batholith
La Punilla
Sierra Chica
-5 %
0
3,96
5,15
1,73
1,51
1,55
1,70
3,84
3,55
3,00
2,89
2,75
4,22
4,34
1,89
1,53
2,98
4,37
4,11
4,49
2,85
3,85
TiO2 content of biotites 1
andean faults
panamerican thrusts and mylonite belts
Mermela group
granites
San Carlos tonalite
mafic - ultramafic rocks
Igam group
orthogneisses
San Carlos group
Sierra Chica Este group

GEOCHEMISTRY OF UPPER PALEOZOIC-LOWER TRIASSIC GRANITOIDS OF CENTRAL FRONTAL CORDILLERA, ARGENTINA

Daniel A. Gregori[1-2], José L. Fernández-Turiel[2] and Angel López-Soler[2]

(1) Departamento de Geología, Universidad Nacional del Sur-CONICET, San Juan 670, 8000 Bahía Blanca, Argentina.
(2) Instituto de Ciencias de la Tierra "Jaume Almera", CSIC, Martí i Franqès s/n. 08028 Barcelona, Spain.

RESUMEN: Nuevos análisis químicos de granitoides del Paleozoico superior-Triásico inferior del sector central de la Cordillera Frontal de Argentina, muestra que se trata de rocas metalumínicas a levemente peralumínicas, con diópsido normativo. El alto valor promedio de Na_2O (4.3 %), la presencia de hornblenda y esfena modal asi como una relación A/CNK < 1 indican que pertenecen a los granitoides de tipo I. La abundancia y las relaciones entre los elementos mayoritarios y minoritarios permiten señalar que estas rocas integraron un arco magmático sobre corteza continental en el margen Pacífico del sector central de Chile y Argentina, generado por la implantación de un sistema de subducción activo durante el Paleozoico superior-Triásico inferior.

KEY WORDS: Geochemistry, granite, Frontal Cordillera, Argentina.

INTRODUCTION

Upper Paleozoic-Lower Triassic intrusive rocks crop out in the Frontal Cordillera of Argentina and Chile, between 27°S and 34°S. Although detailed field, petrological, geochemical and geochronological studies of granitoids have been carried out in the northern portion (29°S to 32°S) of Frontal Cordillera (Llambías et al., 1987; Nasi et al., 1985; Parada, 1988; Parada et al., 1991) relatively scarce geochemical and petrological data are available in the southern sector to 33°S. (cf. Caminos, 1979; Llambías and Caminos, 1987). In this paper we present new geochemical data, a brief description on the petrology and the possible tectonic setting of granitoids outcropping from 33° 10'S to 33° 45'S, in the Frontal Cordillera of Argentina.

GEOLOGICAL SETTING

Igneous activity during Late Paleozoic in Frontal Range of Argentina and Chile was described by Hervé et al. (1987) as Frontal Range Magmatic Belt (FRMB). Upper Paleozoic-Lower Triassic intrusive rocks at Frontal Cordillera of Mendoza province form the so-called "Frontal Cordillera Composite Batholith" (Polanski, 1958). It extends for 130 km south to Mendoza River and its width vary from 20 km at the Cordón del Plata to 40 km in the Cordón del Portillo. Several important plutonic bodies were mapped and described by Polanski (1972) in the Cordón del Plata area: Guevara Stock, Carrera Stock, Yesera Stock and Santa Clara Stock. In the Cordón del

Portillo area, the Las Cuevas Stock, Las Delicias Stock and the Cordón del Portillo Batholith were recognized, as is showed in the figure.

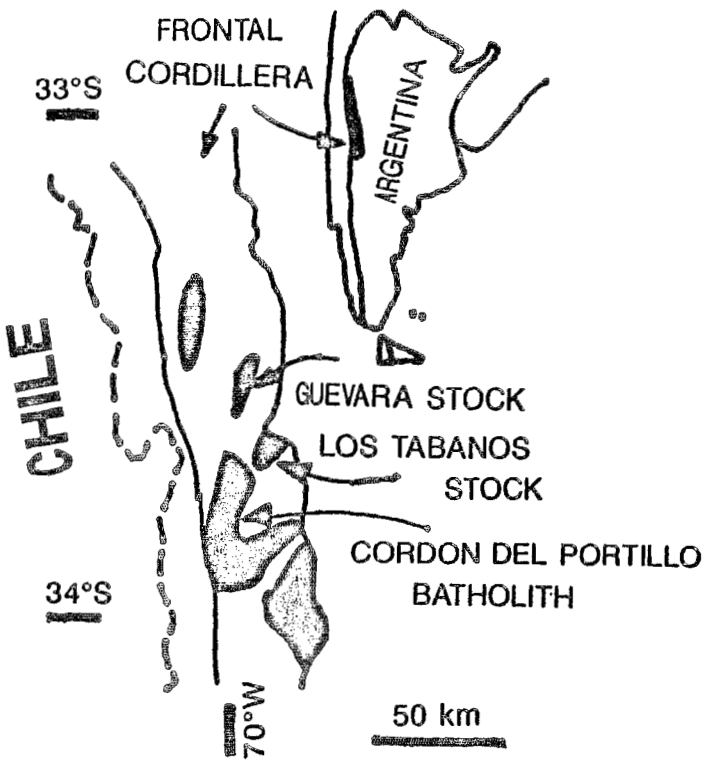

The host rocks where the Upper Paleozoic magmas were emplaced consist of metamorphic and sedimentary rocks. The metamorphic rocks comprise phyllites, schists, marbles, quartzites and serpentinized ultrabasic rocks, which show several deformations and the thermal effect of the granite intrusion. Radiometric age determinations presented by Caminos et al. (1979) confirm that the episode of regional metamorphism have a minimun age of 500±50 Ma. The sedimentary rocks are represented by shallow water marine sequences composed by conglomerates, sandstones and pelites outcropping in the eastern side of Cordón del Plata. Finally, Permian to Triassic andesitic and rhyolitic lavas (Choiyoi Group) overlies and are intruded by the granitic rocks under study.
The Guevara and Los Tábanos Stocks and Cordón del Portillo Batholith (Cerro Punta Blanca, Cerro Punta Negra, Quebrada del Portillo Argentino), were included in this study because radiometric ages were obtained by Caminos et al. (1979) in the Cordón del Portillo Batholith (Cerro Punta Blanca: K/Ar 337±15 Ma; Rb/Sr 348±35 Ma., Quebrada del Portillo: K/Ar 291±10 Ma. Rb-Sr 264±8 Ma.; Cerro Punta Negra: K/Ar 234±10 Ma.) and in the Guevara Stock (K/Ar 209±10 Ma.).

PETROGRAPHY

The granitoid rocks consists of medium (1-4 mm) to coarse (5-8 mm) grained biotite and hornblende granodiorites with equigranular to porphyritic textures. The mineralogy is composed mainly of plagioclase (An_{10}-An_{20}), quartz, microcline, biotite and ± Fe-hornblende. Common accesory minerals are zircon, apatite and sphene. Chlorite partially replaces biotite and sericite ± calcite is commonly found within plagioclase grains. Zoned plagioclase exhibiting altered cores and corroded quartz possibly represent an early stage of crystallization, whereas the later is characterized by unaltered euhedral grains of plagioclase, perthitic K-feldspar and granophyric intergrowth of K-feldspar and quartz.

GEOCHEMISTRY

Twenty seven samples of Guevara and Los Tábanos Stocks and Cordón del Portillo Batholith (Cerro Punta Blanca, Cerro Punta Negra, Quebrada del Portillo), collected mainly through east-west traverses along rivers, were analyzed for major and trace elements concentrations. The rocks have typical compositions of calc-alkaline magmatic suites, ranging from metaluminous quartz-monzonite to moderately peraluminous granites. The co-variation of element oxides with SiO_2 of different stocks shows that decreasing trends exist for nearly all the major and trace elements, except for K_2O, Na_2O and FeO* where a considerable scatter occurrs. This fact may partly be due to incipient post-magmatic alteration processes (e.g. albitization). Harker variation diagrams show decreasing trends with two clusters of samples in the range 61 to 70 % SiO_2, and 73 to 76 % SiO_2.

The co-variation of Rb vs. K/Rb supports the idea that all samples are part of a cogenetic suite, where a general differentiation trend from quartz-syenite and quartz-monzonite to granodiorite, granite and alkali-feldspar granite seems to exist. Chemical and mineralogical properties such as the relatively high Na_2O content (4.3 % averange), A/CNK ratio < 1.1, normative diopside, modal hornblende and sphene and a broad spectrum of composition, show as these rocks may be interpreted as I-type granitoids (Chappell and White, 1974).

According their Rb-Ba-Sr relationships, the 80 percent of them are granodiorites and quartz-diorites whereas the rest are granites. A late-orogenic trend with R2 approximately constant and a broad range of R1, as result of major variation of total alkalis, was identified using the R1-R2 diagram.

Tectonic discrimination diagrams after Maniar and Piccoli (1989) classify the rocks studied as IAG+CAG, whereas that ocean ridge granite (ORG) normalized multi-element variation diagrams (Pearce et al., 1984) display typical patterns of volcanic arc granites, with relative enrichments in K, Rb, Ba and Th to Nb, Zr and Y. Nb-Y and Rb-Nb+Y discrimination diagrams apparently confirm overall volcanic arc affinities for these rocks. Normal continental arc is reflected in the Rb/Zr versus Nb diagram (Brown et al., 1984) .

CONCLUSIONS

Pre-Andean Upper Paleozoic-Lower Triassic plutonic activity in the Pacific margin of central Argentina and Chile were interpreted as a magmatic arc generated by the existence of an eastward-dipping subduction regime (Ramos et al., 1984; Nasi et al., 1985). The new geochemical and mineralogical data of granitoid rocks from the central area of the Frontal Cordillera presented in this paper show that the intrusive bodies have similar features to the I type granites. They were possibly related with a continental arc generated by the subduction of oceanic plate underneath the continental plate.

REFERENCES

BROWN, G.C., THORPE, R.S. and WEBB, P.C., 1984, The geochemical characteristics of granitoids in contrasting arcs and comments on magma sources: J. geol. Soc. London, **141**, 413-426.

CAMINOS, R., 1979, Cordillera Frontal: *in* Turner, J.C.M., ed., Geología Regional Argentina, Academia Nacional de Ciencias, **I**, 397-453.

CAMINOS, R., CORDANI, U.J. and LINARES, E., 1979, Geocronología y geología de las rocas metamórficas y eruptivas de la Precordillera y Cordillera Frontal de Mendoza: II Congr. Geol. Chileno, Actas, **1**, F43-F61.

CHAPPELL, B.W. and WHITE, A.J.R., 1974, Two contrasting granite types: Pacific Geol., **8**, 173-174.

HERVE, F., GODOY, E., PARADA, M.A. RAMOS, V. A., RAPELA, C.W., MPODOZIS, C and DAVIDSON, J., 1987, A general view on the Chilean-Argentine Andes: *in* Monger, J.W.H., ed., Circum-Pacific orogenic belts on the evolution of the Pacific Ocean Basin: American Geophysical Union Geodynamic Series **18**, 97-113.

LLAMBIAS, E.J., SATO, A.M., PUIGDOMENECH, H.H. and CASTRO, C.E., 1987, Neopaleozoic batholiths and their tectonic setting. Frontal Range of Argentina between 29° and 31°S: X Congr. Geol. Argentino, Actas **IV**, 92-95.

LLAMBIAS, E.J. and CAMINOS, R., 1987, El magmatismo Neopaleozoico de Argentina: *in* Archangelsky, S. ed., El Sistema Carbonífero en la República Argentina, Academina Nacional de Ciencias, 253-279.

MANIAR, P.D and PICCOLI, P.M., 1989, Tectonic discrimination of granitoids: Geological Soc. of America Bull, **101**, 635-643.

NASI, C, MPODOZIS, C., CORNEJO, P., MOSCOSO, R. and MAKSAEV, V., 1985, El Batolito Elqui-Limarí Paleozoico superior-Triásico): características petrográficas, geoquímicas y significado tectónico: Rev. Geológica de Chile,
25-26, 77-111.

PARADA, M.A., 1988, Pre-Andean peraluminous and metaluminous leucogranites suites in the High Andes of central Chile: J S Amer Earth Sci, **1**, 211-221.

PARADA, M.A., LEVI, B. and NYSTROM, J.O., 1991, Geochemistry of the Triassic to Jurassic plutonism of central Chile (30 to 33 S); Petrogenetic implications and a tectonic discussion: *in* Harmon, R.S and Rapela, C.W., eds., Andean magmatism and its tectonic setting, Geological Soc. of America, Special Paper **265**, 99-112.

PEARCE, J.A., HARRIS, N.B.W. and TINDLE, A.G., 1984, Trace element discrimination diagrams for the tectonic interpretation of granitic rocks: J Petrol, **25**, 956-983.

POLANSKI, J., 1958, El bloque Varíscico de la Cordillera Frontal: Rev. Asoc. Geol. Argentina, **XII**, 165-196.

POLANSKI, J., 1972, Descripción Geológica de la Hoja 24 a-b, Cerro Tupungato, provincia de Mendoza. Servicio Geológico Nacional, Secretaría de Estado de Minería, Boletín 165, 117 p.

RAMOS, V.A., JORDAN, T.E., ALLMENDINGER, R.W., KAY, S.M., CORTES, J.M. and PALMA, M.A., 1984, Chilenia: un terreno alóctono en la evolución paleozoica de los Andes centrales: IX Congr. Geol. Argentino, Actas, **2**, 84-106.

ZIRCON FISSION TRACK DATING OF THE HUACHON GRANITE FROM THE EASTERN CORDILLERA OF CENTRAL PERU : EVIDENCE FOR LATE PALAEOZOIC AND LATE JURASSIC COOLING EVENTS.

by Gérard Laubacher[1], and Charles W. Naeser[2]

[1]*Institut Français de Recherche Scientifique pour le Développement en Coopération (ORSTOM), B.P. 5045, 34032 - Montpellier cedex1, France and Convenio ESPOL-ORSTOM , P.O.Box 5863 - Guayaquil, Ecuador*
[2]*U.S. Geological Survey, MS-424, P.O. Box 25026, Denver, Colorado 80225, USA.*

Abstract : Des datations sur zircons, par traces de fission, du granite de Huachon (Cordillère orientale du Pérou central) indiquent deux périodes de refroidissement, vers 270 Ma et 160 Ma. Le refroidissement à 270 Ma est interprêté comme l'âge de mise en place du granite. Dans le Pérou central, le refroissement a 160 Ma se corrèle avec un soulèvement et une forte érosion dans la Cordillère orientale, et d' épais conglomérats dans la zone subandine.

Key words : *zircon F-T dating, Late Jurassic cooling and uplift event, Eastern Cordillera, Andes of central Peru.*

Zircon fission track ages of three samples from the Huachon granite (75° 55'W and 10° 40'S) which lies in the eastern Andes of central Peru, approximately 200 km NE of Lima (Fig.1) are presented. The purpose is to constrain the age of emplacement of the pluton and to improve the knowledge of the uplift history of the Eastern Cordillera of central Peru where no F-T studies of uplift have been made. Apatite dating has also be made in this study, but it is not considered in this paper (*). The time scale of Odin & Odin (1990) is used here and all calculations and discussions assume a geothermal gradient of 30 ° C/km.

Fig. 1 : Location of the study zone

GEOLOGICAL SETTING

The Andes of central Peru are made up of the Western and Eastern Cordilleras that reach elevations of more than 6000 m and 5000m, respectively (Fig.1). In the study area, the two ranges are separated by the 50 to 100 km wide Altiplano which attains a height of approximately 4000m.

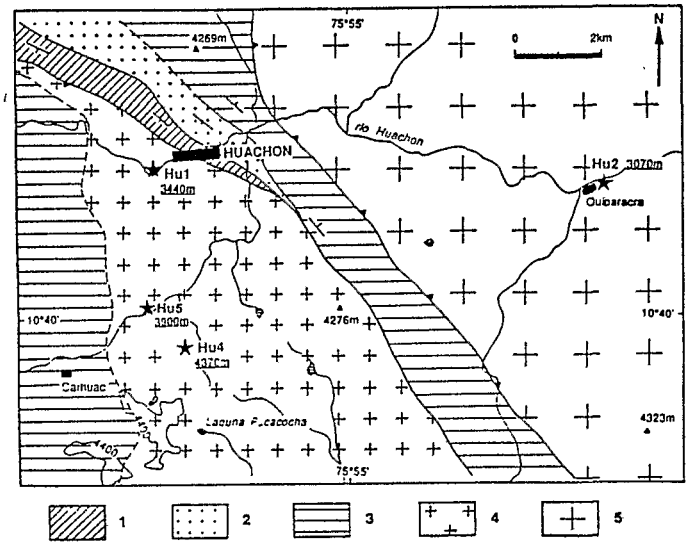

Fig. 2 : Geological sketch map of the Huachon area and location of the samples (stars). 1 : Pucara Group (Triassic and Liassic limestones); 2: Mitu Group (Permian and Triassic red beds); 3: undifferenciated low to intermediate metamorfic rocks of Lower Palaeozoic and Precambrian age; 4 : composite batholith including Precambrian to Andean granites.

The Eastern Cordillera is predominately made up of basement rocks of Precambrian and Palaeozoic age which have undergone a complexe pre-Andean orogenic history: Intense deformation and metamorfism asociated with magmatism occured during Late Precambrian and Late Paleozoic (Mégard *et al.* 1971; Dalmayrac *et al.* 1980). Upper Permian to Middle Triassic coarse continental red beds (Mitu group) were deposited during a period of intense volcanism and plutonism (Mégard 1978; Dalmayrac *et al.* 1980; Soler & Bonhomme 1987). The Andean deposits of the Eastern Cordillera consist of Upper Triassic to Upper Cretaceous marine and continental deposits. After Santonian time, the central Peruvian Andes emerged and from Late Eocene to the Present, the Eastern Cordillera has undergone deformation, strong uplift and deep erosion (Mégard *et al.* 1984).

The samples dated in this study were collected in the Huachon valley (Fig.2) that drains eastward to the Amazon lowlands. Three samples of the Huachon granite Hu-1, Hu-5 and Hu-4 were collected at 3440m, 3900m and 4370m of altitude respectively (Fig.2). The Huachon granite is a coarse-grained and porphyritic homogeneous batholith, intruded into Precambrian metasedimentary and igneous rocks. Two conventional K/Ar ages of 202 ± 9 Ma and 151 ± 7 Ma, have been obtained on potassic feldspars of two samples of the Huachon granite by Bonhomme, in Soler (1991).

METHODS

Zircon grains were recovered using heavy liquids and magnetic separation. F-T ages of zircons were determined using the external detector method (Naeser 1976, 1979). Zircons were prepared (Gleadow *et al.* 1976) and irradiated along with neutron dose monitors (U-doped glass SRM 962 for zircon and sphene) (Carpenter & Reimer 1974) in the U.S.Geological Survey reactor in Denver, Colorado. Thermal neutron dose was determined from the track density in calibrated muscovite detectors that covered the glass standards during the irradiations. Ages were calculated using the zeta method of calibration and calculation (Hurford & Green 1983) and the following age standarts : Fish Canyon Tuff, Tardree Rhyolite, and Buluk Tuff. Uncertainty in the age was calculated by combining the Poisson errors on the spontaneous and induced track counts, and the track counts in the detector covering the dosimeter (McGee *et al.* 1985).

RESULTS

The F-T data and ages for the three zircon concentrates dated are shown in table 1 below.

									DOSIMETER			
				ρ_s	FOSSIL	ρ_i	INDUCED		DENSITY			
			NUMBER	x 10^6	TRACKS	x 10^6	TRACKS		x 10^5	TRACKS		±2σ
SAMPLE	DF-	MINERAL	GRAINS	t/cm^2	COUNTED	t/cm^2	COUNTED	X^2	t/cm^2	COUNTED	Ma	(Ma)
HU-1	6037	zircon	7	24.7	3490	7.83	553	F	1.915	2694	190	19
HU-4	6038	zircon	6	21.5	994	6.83	158	F	1.915	2694	189	33
HU-51	6040	zircon	5	30.7	2420	5.82	229	F	1.915	2694	314	45
HU-52	6040	zircon	4	27.6	1534	6.62	184	F	1.915	2694	249	40

[1] with 587 Ma grain; [2] without 587 Ma grain; ZETAS Zircon (SRM 962) ; t/cm^2 = Tracks/centimeter^2 ; DF = Laboratory Number ; X^2(Chisquare probability) = Pass (P) or Fail (F) Chisquare test at 5%

The zircon ages show a significant spread and a complex cooling history. Of the 18 grains counted from the three samples, 17 have ages between 104 Ma and 358 Ma. One zircon crystal from sample Hu-5 has an age of 573 ± 175 Ma. At this time, we consider this older age to be unreliable, because no other ages come close to supporting

this result. It will not be included in any of the discussion. The probability density and histogram plot (Fig.3) show two peaks of ages, one at ≈270 Ma, and the other at ≈160 Ma.

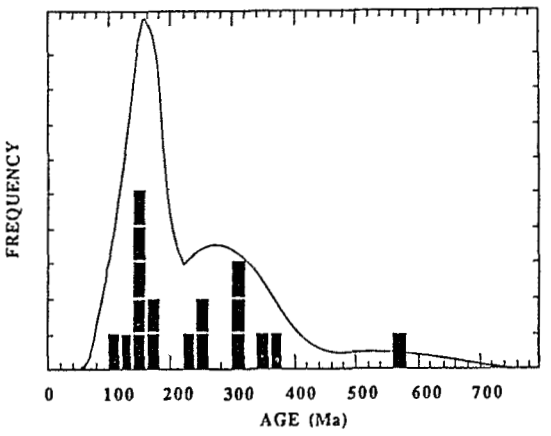

Fig. 3 : Probability density distribution for all zircons dated from the three samples of the Huachon granite. The solid rectangles represent each individual grain analysed.

CONCLUSIONS

The "**maximum" age at about 270 Ma** (Fig.3) suggest an important late Lower Permian cooling stage that we interpret as the emplacement age of the **Huachon granite**. The F-T ages of the zircons are compatible with the minimum ages of 202 and 151 Ma obtained by Bonhomme (in Soler 1991). The F-T ages suggest that it was emplaced at a depth where the temperature was between ≈150°C and ≈250°C during the Permian and remained at that depth (temperature) until a cooling (uplift/erosion) episode ≈160Ma. Residence of the samples in this temperature range would permit the annealing of the high uranium grains, while the tracks remained stable in the lower uranium grains.

The zircon data indicate that approximately 50°C-100°C cooling took place at ≈160Ma. This event cooled the rocks to a temperature where tracks were retained in the zircons (<175°C). This temperature was between ≈120°C and ≈200°C. Assuming a closure temperature of 200° ± 50°C for zircon and a geothermal gradient of 30°C/km, this indicates a period of exhumation and up to 3 km of materiel were removed from the roof of the Eastern Cordillera at this time.

Geological evidence of this Jurassic uplift event is recorded in several regions of Peru. In the eastern Andes and the Altiplano of central Peru, an important late-Middle to Late Jurassic uplift event is recognized by a lack of sedimentation during the Bathonian and Malm and strong erosion after deposition of the Chaucha formation of Bajocian age prior to the deposition of the Goyllarisquizga formation, whose base is thought to be Tithonian to Berriasian in age (Mégard 1978; Moulin 1989). This event has been assigned to extensional faulting related to Nevadian movements by Mégard (1978). The total thickness of post-Hercynian to Bajocian continental and marine sediments covering the Eastern Cordillera was over 2-3 km. Evidence of this Jurassic uplift event is also recorded in the Upper Sarayaquillo formation which outcrop approximately 100km east of the study area, in the Subandes. The Sarayaquillo formation, thought to be Bathonian to Malm in age (Koch 1962; Mégard 1978), consists of several hundred meters of thick red sandstones that grade upward into very coarse conglomerates (10 to 40cm clasts). These conglomerates become progressively finer and thinner to the east. Field observations (Laubacher, unpublished data) show that the lower strata of the conglomerates contain a few limestone clasts from the Pucara Group (Late Triassic and Early Jurassic) and abundant volcanic clasts of the Mitu Group (Late Permian to Early Triassic). The clasts in the conglomerates grade upward into significant percentages of quartzite and limestone derived from the Tarma and Copacabana Groups (Carboniferous to Lower Permian). The uppermost

conglomeratic strata contain only a few limestone clasts but large amounts of metamorphic and igneous clasts derived from Lower Palaeozoic and Precambrian rocks. Stream directions and petrogaphy of the conglomerates in the Sarayaquillo formation indicate a western source which was approximately at the location of the present Eastern Cordillera area. The clasts in the Sarayaquillo formation record progressively deeper erosion of the pre-Andean basement. This provides evidence for a progressive and plurikilometric uplift of the Eastern Cordillera which was probably related either to a strong normal faulting or to a left-lateral transform offset of the Peruvian margin (Jaillard *et al.* 1990) reactivating old, possibly Hercynian, structures.

In summary, the zircon data indicate that the Huachon granite emplaced at approximately 270Ma and that 50°C-100°C cooling took place in the Eastern Cordillera at about 160 Ma. This latter event cooled the Huachon granite to a temperature where tracks were retained in the zircons (<175°C). The cooling indicate up to 3 km erosion of the roof of the Eastern Cordillera in central Peru at about 160 Ma. This exhumation event correlates with uplift and tectonism in the Eastern Cordillera and deposition of coarse conglomerates in the Subandes of central Peru during Bathonian to Malm times.

References

Carpenter, B.S., & Reimer, G.M. 1974. Standard reference materials : calibrated glass standards for fission-track use. National Bureau of Standards, Special Publication 260-49, 16 p.

Dalmayrac, B., Laubacher, G., & Marocco R. 1980. Caractères généraux de l'évolution géologique des Andes Péruviennes. *Travaux et Documents*, **122**, ORSTOM, 501p.

Gleadow, A. J. W., Hurford, A. J., & Quaife, R. D. 1976. Fission-track dating of zircon: Improved etching techniques: *Earth and Planetary Science Letters* , **33**, 273-276.

Hurford, A.J., & Green, P.F. 1983. The zeta age calibration of fission-track dating. *Chemical Geology* (Isotope Geoscience Section), **1**, 285-317.

Jaillard, E., Soler, P., Carlier, G., & Mourier, T. 1990. Geodynamic evolution of the northern and central Andes during early to middle Mesozoic times : a Tethyan model. *Journal of the Geological Society, London*, **147**, 1009-1022.

Koch, E. 1962. Die Tektonik im Subandin des Mittel-Ucayali Gebietes, Ost-Peru. *Geotektonische Forschungen*, **15**, Stuttgart, 67p.

Mégard, F. 1978. Etude géologique des Andes du Pérou central. *Mémoire* **86**, ORSTOM, Paris, 310p.

Mégard, F., Dalmayrac, B., Laubacher, G., Marocco, R., Martinez, C., Paredes, J., Tomasi, P. 1971. La chaîne hercynienne au Pérou et en Bolivie, premiers résultats. *Cahier ORSTOM, série Géologie*, **III** (1), 5 - 44.

Mégard, F., Noble, D.C., McKee, E.H., & Bellon, H. 1984. Multiple pulses of Neogene compressive deformation in the Ayacucho intermontane basin, Andes of central Peru. **95**, 1108-1117.

McGee, V.E., Johnson, N.M. & Naeser, C.W. 1985. Simulated fissioning of uranium and testing of the fission-track dating method. *Nuclear Tracks and Radiation Measurements*, **10**, 365-379.

Moulin, N. 1989 .Facies et séquence de dépot de la plateforme du Jurassique moyen à l'Albien, et une coupe structurale des Andes du Pérou central. USTL, Montpellier. Thèse Doctorat, 287p.

Naeser, C.W. 1976. Fission-track dating. U.S. Geological Survey Open-File Report **76-190**, 65 p.

Naeser, C.W. 1979. Fission-track dating and geologic annealing of fission tracks. *In*: Jäger, E. & Hunziker, J.C. (eds), *Lectures in Isotope Geology*. Springer-Verlag, Berlin, 154-168.

Odin, G.S. & Odin, C. 1990. Echelle numérique des temps géologiques. *Géochronique* , **35**, 12-21.

Soler, P. 1991. Contribution à l'étude du magmatisme associé aux marges actives. Pétrographie, géochimie et géochimie isotopique du magmatisme Crétacé à Pliocène le long d'une transversale des Andes du Pérou central. Implications géodynamiques et métallogénétiques. Thèse Dr Univ. Paris VI, P. & M. Curie, 815 p..

Soler, P. & Bonhomme,M. 1987 . Données radiologiques K-Ar sur les granitoides de la Cordillère orientale des Andes du Pérou central. Implications tectoniques. Comptes rendus hebdomadaires de l'Académie des Sciences de Paris, (II), **304**, 841-845.

(*) The zircon F-T data of this abstract and additional apatite F-T data have been included in a paper submitted to the Journal of the Geological Society, London .

THE WEST-ARGENTINE PRECORDILLERA: A PALAEOZOIC BACK ARC BASIN

Werner P. LOSKE

Institut für Allgemeine und Angewandte Geologie
Luisenstr. 37, 80333 München 2, Germany

RESUMEN

Los sedimentos cambro - devónicos de la Precordillera exponen la evolución de parte del margen occidental del Gondwana en el Paleozoico. Las modas detríticas, características geoquímicas y el patrón de tierras raras de las psamitas ponen de manifiesto la evolución de un sistema de margen continental supuestamente pasivo a uno activo. El análisis de minerales pesados señalan un significante cambio gradual en la litología del área de aporte desde un origen cratónico reciclado hasta la exhumación del basamento cristalino. Nuevos datos geoquímicos de lavas sinsedimentarias (almohadilladas), permiten su identificación como basaltos originados en un rift de back arc. Todos los datos presentados conducen a la descripción de un modelo geotectónico que explica la secuencia sedimentaria de la Precordillera como correspondiente a una cuenca tipo back arc.

KEY WORDS: Argentine Precordillera, back arc, detrital modes, REE, heavy minerals

BACKGROUND

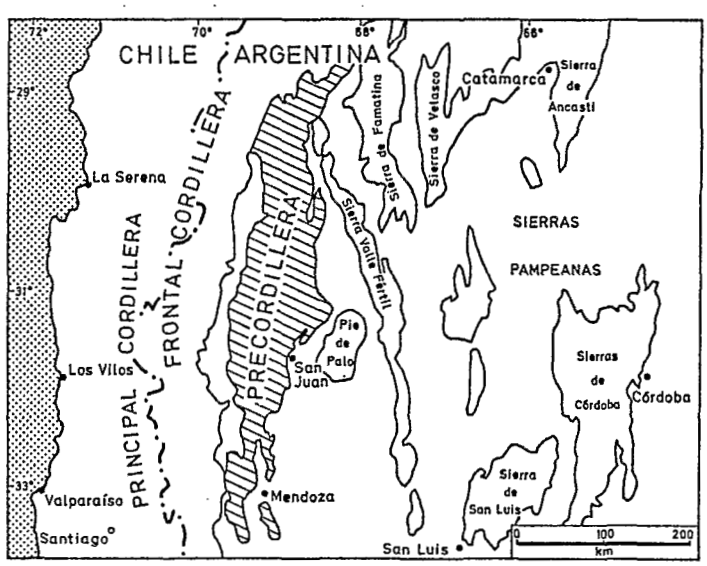

Fig. 1
Geographical location of the Argentine Precordillera

The Precordillera delineates an elongate, some 600 km long N-S striking orogenic belt north of the city of Mendoza (fig. 1). During Cambrian and Early Ordovician times a carbonate platform developed at the eastern margin of the basin, whereas the sediments further west are represented by marine siliciclastics. Non-carbonate sediments of regionally variable thickness were deposited in the whole basin beginning in the Mid-Ordovician.

The geotectonic evolution of the Precordillera has been discussed controversial by many authors. Baldis et al. (1984) believe that the Precordillera developed along a

passive continental margin on continental crust. A similar model emphazising the autochthony of the Precordillera is discussed by González Bonorino and González Bonorino (1991). Ramos et al. (1986) and Ramos (1988) described the Precordillera as a separate Palaeozoic terrane, that developed between the Pampeanas terrane in the east and a Chilenia terrane to the west along an active continental margin. Due to the magmatic arc of the Pampean Ranges in the east of the Precordillera basin, at least the Devonian sediments are interpreted by Ramos (1988) as a fore arc sequence. The inferred Devonian collision of the Chilenia terrane with the Pampean ranges allows for ceasing subduction. Dalla Salda et al. (1992 a, b) describe for the entire western margin of Gondwana a series of microcontinent collisions (slivers from eastern Laurentia) with the South American Continent.

THE PRECORDILLERA's EVOLUTION: ARGUMENTS

Detrital mode analysis sensu Dickinson and Suczek (1979) indicates for nearly all Ordovician-Devonian sandstone samples a passive continental margin environment. Only some of the Devonian sandstones display a "dissected arc" provenance, indicative for an active continental margin environment.

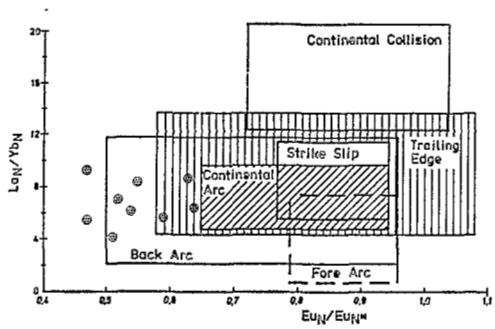

Fig. 2
REE fractionation (La_N/Yb_N) versus Eu-anomaly of the Precordillera sandstones (discrimination fields after McLennan et al. (1990))

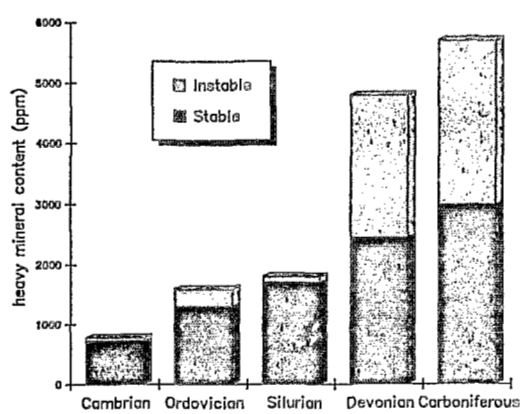

Fig. 3
Mean heavy mineral content of the stratigraphic units
stable minerals: zircon, tourmaline, rutile
"instable" minerals: apatite, epidote, garnet, titanite, zoisite

Environment normalized multielement pattern of the Precordillera sandstones show the flattest pattern if normalized to the mean element concentrations recommended by Bhatia (1983) for a continental island arc.

The rare earth element fractionation (La_N/Yb_N) and the Eu-anomaly show the typical pattern of "trailing edge" or "back arc" regions (fig. 2) if compared with the recommended values of McLennan et al. (1990).

The heavy mineral content of the Cambrian-Silurian sediments is reduced to the stable minerals zircon, tourmaline and rutile (fig. 3). Within the Devonian sediments a remarkable increase of quantity and variability of heavy minerals can be detected (e.g. apatite, epidote, garnet, titanite and zoisite).

Deducing from zircon morphologies, part of the Devonian heavy mineral spectra derived from granitoid source rocks. U-Pb dating of these zircons revealed a crystallization age of about 1100 Ma (Loske 1992 a, b).

Geochemical analyses of synsedimentary pillow basalts (Loske 1992 a) show a typical MORB pattern with an increase of Ba, Th and Nb, due to greywacke contamination of the lavas (Pearce 1983). Deducing from the low $^{87}Sr/^{86}Sr$ initial ratio of approx. 0.705, these rocks are typical nearly uncontaminated back arc rift basalts.

THE PRECORDILLERA's EVOLUTION: MODEL

The oldest sediments reported from the Precordillera region are by Lower/Early Middle Cambrian calcareous and siliciclastic strata (fig. 4 a). Because of the Cambrian magmatism and metamorphism in the Pampean Ranges (Bachmann et al. 1985, 1987) an active continental margin system which evolved during the earliest Cambrian/Precambrian due to subsidence of cold and heavy oceanic crust is the assumed starting condition for the proposed evolution of the Precordillera.

The siliciclastic slope facies documented in Mid-Cambrian/Lower Ordovician sediments in the western parts of the Precordillera basin and the easterly carbonate platform (fig. 4 b) demonstrate stable, continuous subsidence of the basin.

A severe cut in the sedimentation history of the Precordillera is observed in the Middle/Late Ordovician. Firstly the carbonate platform drowned, and secondly synsedimentary pillow lavas were extruded, signalizing the opening process of the back arc basin (fig. 4 c). Because there are no synsedimentary basalts known at least in the Silurian sediments, the opening phase of the back arc basin with formation of oceanic crust can be reduced to some 15-30 Ma. The volcanic arc which should have bordered the western margin of the Precordillera basin is not documented in the Precordillera region due to the problem of outcrop depth. Within the Famatina System, representing the northward prolongation of the Precordillera, the volcanic arc is today already exhumed (Clemens et al. 1992, Mannheim and Miller 1992). Contemporaneously to the rapid extension tectonics in the Precordillera, metamorphism in the Pampean Ranges shows retrograde characteristics and the magmatism is no longer subduction related (Rapela et al. 1990).

The Silurian is still documented by a "crustal stretching" regime (fig. 4 d). Graben and half graben structures (e.g. Villicum Graben) formed along the eastern and probably at the western margin of the Precordillera basin, whereas the central part of the basin remained rather stable and morphologically high, documented by omissions, condensed sedimentation and fine grained sediments. Tectonic activity in the hinterland and beginning erosion of granitoid provenance lithologies is documented by conglomerates containing many granitoid cobbles (Loske 1992 a). Sediments assigned to the Silurian on the western side of the basin are mostly fine grained because of the protection effect of the central Precordillera high.

The Devonian sediments display a flysch-like character indicating orogenic activity (folding) in the hinterland and the Precordillera itself (fig. 4 e). This deformation, accompanied by slight metamorphism, mainly in the western Precordillera, seems to be related to crustal compression processes produced by an eastwards dipping subduction zone to the west of the Precordillera basin (v. Gosen 1992). After closure of the whole basin Permocarboniferous sediments of mostly continental character covered many parts of the early Precordillera.

ACKNOWLEDGEMENTS

I like to express my thanks to Dr. Osvaldo Bordonaro (now Mendoza) and Dr. Silvio Peralta (San Juan) for their kindly help during fieldwork in September 1988. The Deutsche Forschungsgemeinschaft (DFG) supported field and lab work by a grant (Lo 373/2-1,2).

Fig. 4

Cartoons displaying the geological evolution of the Precordillera

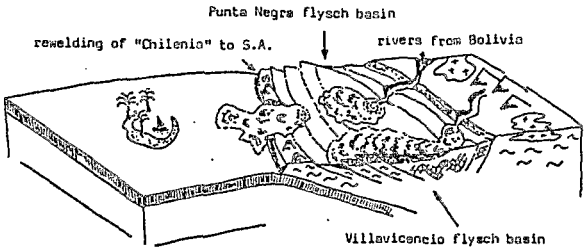

a. Early Cambrian:
initial crustal stretching along the (?) passive continental margin of Gondwana, a continental basement sliver ("Chilenia") is rifting off (see text for further discussion)

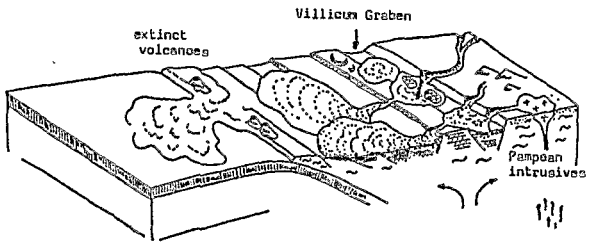

b. Mid Cambrian - Early Ordovican:
formation of a geosynclinal basin with a carbonate platform along the eastern margin an a siliciclastic submarine fan facies to the west; definite indications of subduction in the Pampean Ranges east of the Precordillera

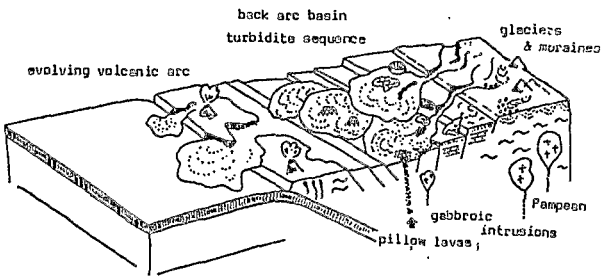

c. Mid Ordovican - Late Ordovician
formation of "oceanic crust" (pillow basalts) in the central Precordillera; drowning of the carbonate platform; overall siliciclastic, partly glacigenic sedimentation; possible formation of an active island arc at the western margin of the Precordillera back arc basin

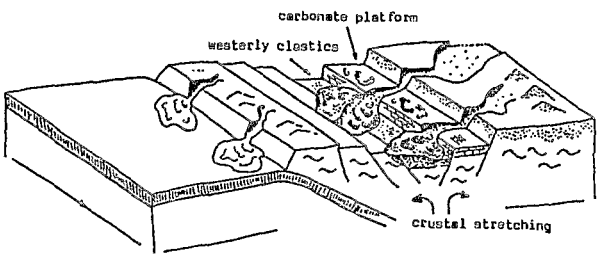

d. Silurian
submarine fan sedimentation in the western Precordillera basin; formation of graben-like structures along the eastern margin (e.g. Villicum Graben) due to continuous crustal extension

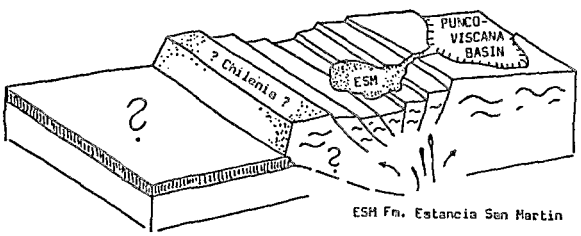

e. Devonian
flysch-like sedimentation related to orogenic closure of the Precordillera back arc basin forced by the rewelding of "Chilenia" to South America

REFERENCES

BACHMANN, G., GRAUERT, B. AND MILLER, H., 1985, Isotopic dating of polymetamorphic metasediments from Northwest Argentina: Zbl. Geol. Paläont. Teil I, 1985 H.9/10, p. 1257-1268.

BACHMANN, G., GRAUERT, B., KRAMM, U., LORK, A. AND MILLER, H., 1987, El magmatismo del cambrico medio/cambrico superior en el basamento del noroeste Argentino: investigaciónes isotópicas y geochronológicas sobre los granitóides de los complechos intrusivos de Santa Rosa de Tastil y Cañani: X Congreso Geologico Argentino, Tucumán 1987, Actas Tomo IV, p. 125-127.

BALDIS, B., BERESI, M., BORDONARO, O. AND VACA, A., 1984, The Argentine Precordillera as a key to Andean Structure: Episodes, 7(3), p. 14-19.

Bhatia, M.R., 1983, Plate tectonics and geochemical composition of sandstones: Journal of Geology, 91, p. 611-627.

CLEMENS, K., KURY, W., LOSKE, W., MANNHEIM, R., NEUGEBAUER, H., MILLER, H. AND TOSELLI, A., 1992, Geodynamische Entwicklung des paläozoischen Gondwana-Randes in West-Argentinien (Präkordillere, Famatina-System): 13. Geowissenschaftliches Lateinamerika-Kolloquium Münster 1992, abstr.

DALLA SALDA, L., CINGOLANI, C. AND VARELA, R., 1992 a, Early Paleozoic orogenic belt of the Andes in southwestern South America: Results of Laurentia-Gondwana collision ?: Geology, 20, p. 617-620.

DALLA SALDA, L.H., DALZIEL, I.W.D., CINGOLANI, C.A. AND VARELA, R., 1992 b, Did the Taconic Appalachians continue into southern South America ?: Geology 1992, Vol. 20/12, p. 1059-1062.

DICKINSON, W.R. AND SUCZEK, C.R., 1979, Plate tectonics and sandstone composition: AAPG, 63(12), p. 2164-2182.

GONZALEZ BONORINO, G. AND GONZALEZ BONORINO, F., 1991, Precordillera de Cuyo y Cordillera Frontal en el Paleozoico temprano: terrenos 'bajo sospecha' de ser autóctonos: Revista Geológica de Chile, Vol. 18/2, p. 97-107.

GOSEN, W. VON, 1992, Paleozoic tectonics in the Precordillera (Argentina): 13. Geowissenschaftliches Lateinamerika-Kolloquium Münster 1992, abstr.

LOSKE, W.P., 1992 a, The West-Argentine Precordillera: a lower Palaeozoic back arc basin ?: in: Conferencia Internacional Paleozico inferior de Ibero-America, Mérida, Abstracts, p. 96-97.

LOSKE, W.P., 1992 b, Sedimentologie, Herkunft und geotektonische Entwicklung paläozoischer Gesteine der Präkordillere West-Argentiniens: Münchner Geol. Hefte, 7, pp. 155.

MANNHEIM, R. AND MILLER, H., 1992, Sistema de Famatina, NW-Argentina: acreción de un arco volcánico en el borde occidental del Gondwana en el paleozoico inferior: in: Conferencia Internacional Paleozoico inferior de Ibero-America, Mérida, Abstracts, p. 102-103.

MCLENNAN, S.M., TAYLOR, S.R., MCCULLOCH, M.T. AND MAYNARD, J.B., 1990, Geochemical and Nd-Sr isotopic composition of deep-sea turbidites: Crustal evolution and plate tectonic associations: Geochim. Cosmochim. Acta, 54, p. 2015-2050.

PEARCE, J.A., 1983, Role of the sub-continental lithosphere in magma genesis at active continental margins, in: Pearce, J.A. and Norry, M.J. eds., Continental basalts and mantle xenoliths, p. 231-249.

RAMOS, V.A., 1988, The tectonics of the Central Andes; 30^0 to 33^0 S latitude: Geological Society of America Special Paper, 218, p. 31-54.

RAMOS, V.A., JORDAN, T.E., ALLMENDINGER, R.W., MPODOZIS, C., KAY, S.M., CORTES, J.M. AND PALMA, M., 1986, Paleozoic terranes of the Central Argentine - Chilean Andes: Tectonics, 5(6), p. 855-880.

RAPELA, C.W., TOSELLI, A., HEAMAN, L. AND SAAVEDRA, J., 1990, Granite plutonism of the Sierras Pampeanas; An inner cordilleran Paleozoic arc in the southern Andes, in Kay, S.M. and Rapela, C.W., eds., Plutonism from Antarctica to Alaska: Geological Society of America Special Paper 241, p. 77-90.

GEODYNAMIC EVOLUTION OF THE PALAEOZOIC GONDWANA MARGIN IN WESTERN ARGENTINA (FAMATINA-SYSTEM)

Rolf Mannheim

Institut für Allgemeine und Angewandte Geologie
Luisenstr. 37, 80333 München 2, Germany

RESUMEN

Los caracteres geoquímicos de los basaltos ordovicícos del Sistema de Famatina (SF) son comparables a los de basaltos calcoalcalinos modernos de arcos de islas oceánicos. Observaciones sedimentológicas prueban la existencia de una cuenca de retroarco entre el arco volcánico (SF) al oeste y el craton (Sierras Pampeanas) al este en el Ordovicíco (relacionado a coordenadas actuales). Durante la colisíon del arco con el continente se intruyeron granitoides anatécticos corticales en el SF (Orogénesis Famatiniana). Como indicadores de un estadio poscolisional aparecen leucogranitos peralcalinos (Devonico?). En el mismo ambiente geotectónico del SF se intruyeron basaltos de subducción. Los caracteres geoquímicos de estos basaltos corresponden a los de basaltos calcoalcalinos de un borde continental activo como del actual tipo Chile.

KEY WORDS: Famatina-System, island arc - back arc, collision, magmatism

INTRODUCTION

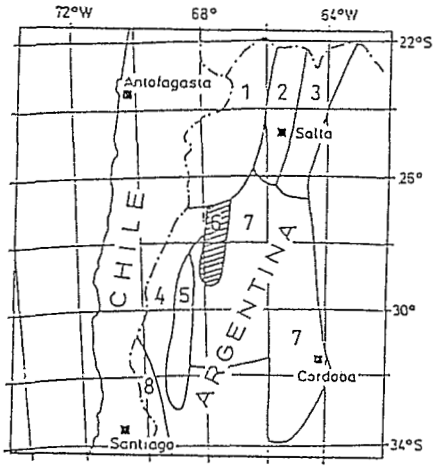

Fig.1: Morphostructural units in NW-Argentina. Puna (1), Cordillera Oriental (2), Sierras Subandinas (3), Cord. Frontal (4), Precordillera (5), Famatina-System (6), Sierras Pampeanas (7), Cord. Principal (8).

The Famatina System (FS) represents a lithostratigraphically and structurally independent unit within the NW-argentinian Sierras (fig.1). It is characterized by Lower to Middle Ordovician volcanosedimentary sequences, which are intruded by calcalkaline granitoids of Upper Ordovician to Devonian age and by syn- to postplutonic volcanic dykes. According to Aceñolaza and Toselli (1984) and Toselli et al. (1991) the magmatic characteristics of the FS advocate for a destructiv plate margin. In the concept of Willner et al. (1987) and Rapela et al. (1990) the Ordovician western Gondwana margin included a volcanic arc in the region of the FS and a several hundred km large zone of intrusion situated in the back of the arc. Dalla Salda et al. (1992 a,b) suggest an Ordovician collision between Laurentia and Gondwana, which lead to the Famatina Orogenesis.

GEOCHEMICAL AND SEDIMENTOLOGICAL ARGUMENTS

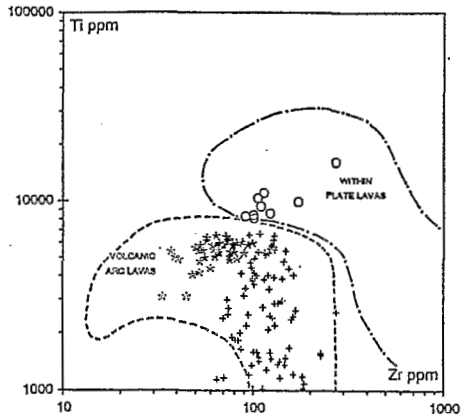

Fig.2: Intermediate to acid (+) and basic (o,*) volcanic rocks in the Ti vs. Zr diagram after Pearce (1982).

The Ordovician synsedimentary and discordant basic to acidic volcanics show congruent geochemical properties and are interpreted as calcalkaline magmas of a magmatic arc. In contrast, a younger generation (Devonian?) of discordant basic dykes reveals typical intraplate characteristics (fig.2).

The Ordovician basalts exhibit typical island arc patterns in MORB-normalized spider diagrams. Analogues patterns are known from modern oceanic island arcs (e.g. Mariana or Java arc, see Pearce 1983, fig.3).
The presence of a back arc basin located between the volcanic arc and the continent in the area of the FS is documented by the intimate association of olisthostromes, rich in volcaniclastic material, derived from the island arc, and distal cratonal turbidites. Intercalated calcareous turbidites are supposed to be introduced from a carbonate platform situated on the continent-ward side of the basin (Clemens 1992, Mannheim and Clemens 1992).

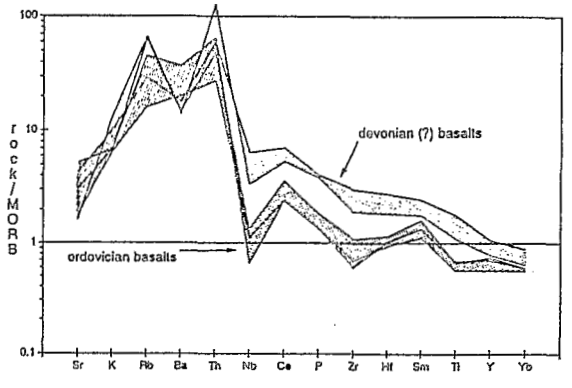

Fig.3: MORB-normalized spider diagrams of the famatinian basalts

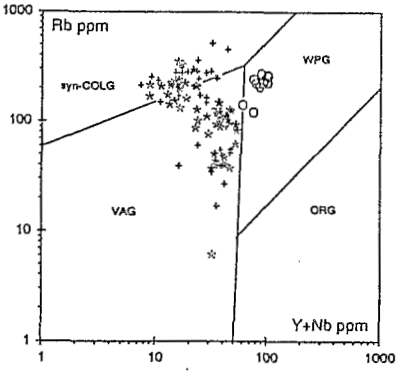

Fig.4: Intermediate and acid volcanic rocks in the Rb vs. (Y+Nb)-diagram after Pearce (1984).
Ordovician volc. (+,*), Devonian (?) leucogranites (o)

The intermediate to acid volcanics of the Ordovician show geochemical characteristics of an island arc in a compressional environment with clear syncollisional affinities (fig.4). They are not directly related by differentiation processes to the basic magmas, but are generated by crustal melting and magma mixing (Mannheim 1993).

Peralcaline A-type leucogranites (Devonian?) represent the late orogenic to postcollisional stage of the FS (fig.4). Subduction-related basalts generated by partial melting of a subcontinental mantle enriched by metasomatic processes intruded this geotectonic scenario. Calcalkaline basalts of the modern continental margin in central Chile exhibit similar patterns (fig.3, compare Pearce 1983).

CONCLUSONS

During the Cambrian the western edge of Gondwana changes from a passive to an active continental margin. This is reported by a subduction-related I-type magmatism in the Pampean Range, wich commenced in the Middle Cambrian (Lottner 1986, Willner et al. 1987, see fig.5 a).

In the Lower Ordovician a marginal basin opened due to mantle convection creating an extensional environment, and the initial arc developed to a rifted arc. In the Pampean Range (remnant arc) the I-type magmatism ceased as a result of the westward shift of the subduction zone. According to Rapela et al. (1990) the Lower Ordovician calcalkaline plutonic bodies intruded the "inner back arc" zone.
The FS represents the ocean-wards drifting part of the magmatic arc. Primary basic magmas were generated in a "depleted", purely oceanic mantle environment. From Tremadocian to Llanvirnian the basin received sediments from the continent and from the island arc (fig.5 b). In the FS the volcanic arc and the adjacent part of the back arc basin are actually exposed. The continent-ward part of the basin (carbonate platform?) has been probably overriden during the postordovician accretion of the island arc to the continent.

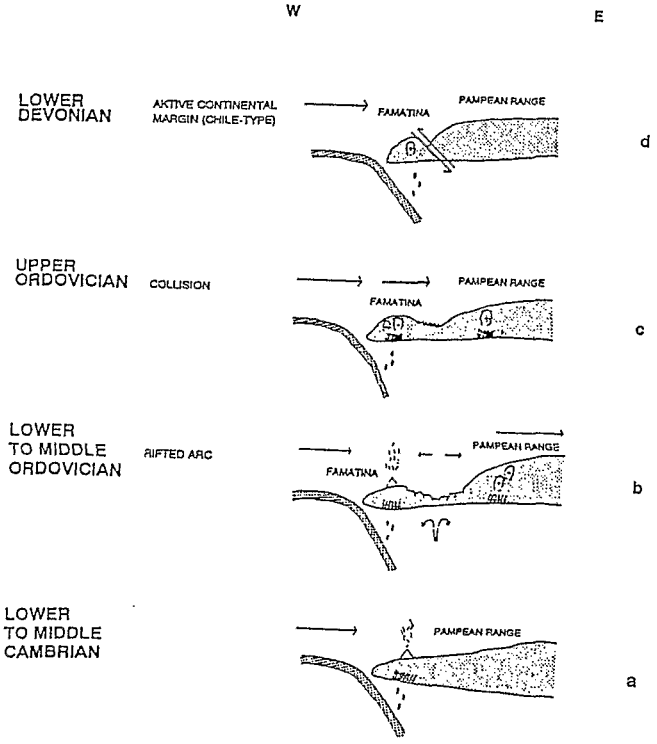

Fig.5: Geodynamic evolution of the Famatina-System in the Palaeozic

The closure of this short-lived marginal basin started in the Middle Ordovician. At the Ordovician/Silurian boundary large amounts of peraluminous collisional granitic melts intruded the FS (fig.5 c).

Probably in the Lower Devonian the island arc - continent collision was concluded, the FS was accreated to western Gondwana. The incessant subduction lead to the intrusion of basaltic magmas generated in a metasomatically enriched mantle. The "collision-thickened" active continental margin was intruded by late to postorogenic leucogranites indicating the extinction of the Famatinian Orogenesis (fig.5 d).

Similar Lower Palaeozoic back arc basins are described by Bahlburg (1990) for the Puna region situated north of the FS and by Loske (1992 a,b) for the Precordillera in the south (compare fig.1).

ACKNOWLEDGEMENTS

The autor wishes to acknowledge the scientific and logistic help of Dr. Hubert Miller (München) and Dr. Alejandro Toselli (Tucumán). The Deutsche Forschungsgemeinschaft (DFG) supported field and lab work (grants Mi 120/20-1,2).

REFERENCES

ACEÑOLAZA, F.G. AND TOSELLI, A.J., 1984, Lower Ordovician volcanism in NW Argentina. In: BRUTON, D.L., Aspects of the Ordovician system: 203-209; Paleont.Contrib.Univ.Oslo, N° 295.

BAHLBURG, H., 1990, The Ordovician basin in the Puna of NW Argentina and N Chile: geodynamic evolution from back arc to foreland basin. Geotekt.Forsch. 75: 107 pp.; Stuttgart (Schweizerbart).

CLEMENS, K., 1992, Sedimentologie, Herkunft und geotektonische Entwicklung präkambrischer und altpaläozoischer Gesteinsserien des Sistema de Famatina in NW-Argentinien. Diss.Uni.München, 164 pp.

DALLA SALDA, L.H., CINGOLANI, C.A. AND VARELA, R., 1992 a, Early Paleozoic orogenic belt of the Andes in southwestern South America; Results of Laurentia-Gondwna collision ?. Geology, 20: 617 - 620.

DALLA SALDA, L.H., DALZIEL, I.W.D., CINGOLANI, C.A. AND VARELA, R. (1992 b), Did the Taconic Appalachians continue into southern South America ?. Geology, 20/12: 1059 - 1062.

LOSKE, W.P., 1992 a, Sedimentologie, Herkunft und geotektonische Entwicklung paläozoischer Gesteine der Präkordillere West-Argentiniens. Münchner Geol. Hft. 7, 144 pp.

LOSKE, W.P., 1992 b, The West-Argentine Precordillera: a lower palaeozoic back-arc basin? Conf.Int.Paleoz.Inf.Ibero-America: 96; Mérida.

LOTTNER, U.S., 1986, Strukturgebundene Magmenentwicklung im altpaläozoischen Grundgebirge NW-Argentiniens am Beispiel der Sierra de Ancasti (Provinz Catamarca). Münster.Forsch.Geol.Paläont. 65: 180 pp.; Münster.

MANNHEIM, R., 1993, Genese der Vulkanite und Subvulkanite des altpaläozoischen Famatina-Systems, NW-Argentinien, und seine geodynamische Entwicklung. Münchner Geol. Hft. 9, 130 pp. (in press).

MANNHEIM, R. AND CLEMENS, K., 1992, Das Famatina-System: ein ordovizischer Inselbogen/Back-arc-Komplex. 13.Geowiss.Lateinam.Koll. (abstracts); Münster.

PEARCE, J.A., 1982, Trace element characteristics of lavas from destructive plate boundaries. In: THORPE, R.S. (ed.), Andesites: 525 - 548.

PEARCE, J.A., 1983, Role of the sub-continental lithosphere in magma genesis at active continental margins. In: HAWKESWORTH, C.J. AND NORRY, M-J. (eds.), Continental basalts and mantle xenoliths: 230-249; Nantwich (Shiva Publishing Ltd.).

PEARCE, J.A., HARRIS, N. AND TINDLE, A., 1984, Trace element discrimination diagrams for the tectonic interpretation of granitic rocks. Journ.Petrol. 25: 956-983.

RAPELA, C.W., TOSELLI, A., HEAMAN, L. AND SAAVEDRA, L., 1990, Granite plutonism of the Sierras Pampeanas; an inner cordilleran Palaeozoic arc in the southern Andes. In: KAY, S.M. AND C.W. RAPELA (eds.), Plutonism from Antartica to Alaska; Geol.Soc Am.Spec.Pap. 241: 77-99.

TOSELLI, A.J., ACEÑOLAZA, F.G., DURAND, F.R., ROSSI DE TOSELLI, J., INDRI, D., CISTERNA, C., LISIAK, H., LOPEZ, J., SAAL, A. AND ESTEBAN, S., 1991, El paleozoico inferior del Sistema de Famatina, Noroeste de Argentina. 6.Congr.Geol.Chil., Resum.expand.: 867-871.

WILLNER, A.P., LOTTNER, U.S. y MILLER, H., 1987, Early Palaeozoic structural development in the NW Argentine basement of the Andes and its implication for geodynamic reconstructions. In: McKENZIE, G.D. (ed.), Gondwana Six: structure, tectonics and geophysics. Geophys. Monograph 40: 229-239; Washington (Amer.Geophys.Union).

GEOTECTONIC DEVELOPMENT OF THE EARLY PALAEOZOIC GONDWANA MARGIN IN NORTHWESTERN ARGENTINA

Hubert MILLER

Institut für Allgemeine und Angewandte Geologie,
Luisenstr. 37, D-80333 München, Germany

RESUMEN: Durante el Paleozoico Inferior, el desarrollo magmático, sedimentario y tectonometamórfico del Noroeste Argentino dependía de la interacción entre el continente de Gondwana en el este y placas oceánicas Paleopacíficas en el oeste. Después de haber sido margen pasivo al límite Precámbrico/Cámbrico, este se transformó en un margen activo, temporalmente presentando un arco de islas con cuenca trasarco.

KEY WORDS: Argentina, Gondwana, Pacific Plates, Early Palaeozoic, Terranes

INTRODUCTION

The nature of the Early Palaezoic Gondwana margin in the southern Central Andes has been discussed controversially. On the one hand, a fairly monotonous development along a continuing ocean border was thought to be evident (MILLER 1984), and the collision of exotic terranes like "Chilenia" (RAMOS et al. 1986) were postulated; on the other hand, "Laurentia" (DALLA SALDA et al. 1992) while moving northward, alongside the coast of South America, should have left traces at the Gondwana margin.

Field work within the Pampean Ranges, the Famatina System and the Precordillera (Fig. 1) was done in cooperation with the University of Tucumán (F.G. ACEÑOLAZA, A. J. TOSELLI, J. ROSSI DE TOSELLI) and numerous co-workers who helped to a better understanding of the orogenic processes developed at this continental margin. Their cooperation is gratefully acknowledged. However, misinterpretations committed in the text below should be ascribed to the author alone.

GEOLOGICAL SETTING

The beginning of the Palaeozoic history of the southern Central Andes is characterized by the subsiding sedimentation and the beginning of deformation and metamorphism of the Puncoviscana Formation in Northwestern Argentina (Pampean Cycle; ACEÑOLAZA et al. 1990a). The southern exten-

sion of this orogen remains unclear; possibly it ends at lat. 30° S, while the southern Pampean Ranges, at least in parts may belong to an older orogenic cycle. In this case northern and southern Pampean Ranges would represent two different terranes, welded together before the Ordovician.

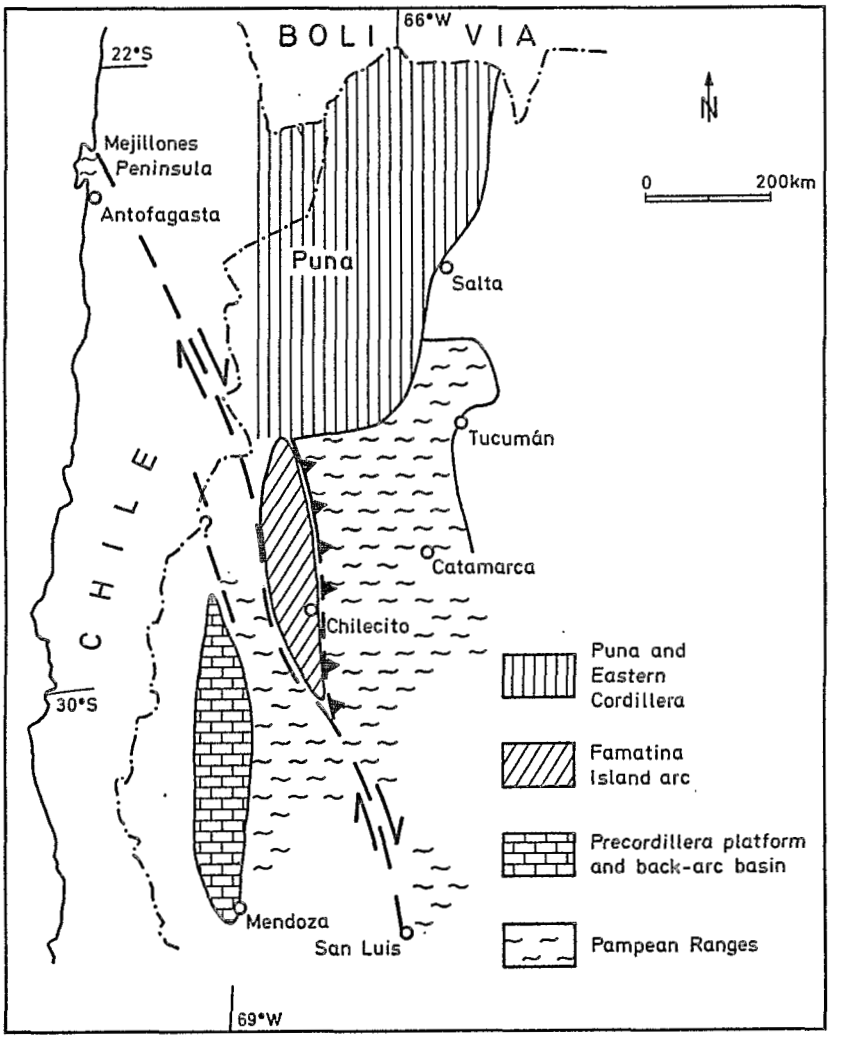

Fig. 1. Terranes in NW Argentina. The Precordillera/Eastern Pampean Sierra terrane is the most allochthonous; it moved dextrally up to 800 km to the north, if Mejillones Peninsula is included within this block.

Ordovician granitoids are widespread within the Pampean Ranges (RAPELA et al. 1992), while Precambrian magmatism is, up to now, poorly known, and Cambrian intrusives are documented only from two localities (BACHMANN et al. 1987).

On the other hand, Ordovician volcanism played an important role in the Precordillera, the Famatina Range, in the Puna and in the Eastern Cordillera. In these areas, a Cambro-Ordovician island arc - back-arc basin

evolution was accomplished by the closure of the basin in mid Palaeozoic times. In the area east of the Famatina Range the back-arc basin was to a large extent overthrusted by the Fiambalá Range and other Pampean Ranges after the Ordovician.

Within this puzzling frame, the Famatina System is a foreign element. The eastern and western borderlines of the Famatina system that apparently represents an exotic Ordovician island arc, placed between typical Pampean Range terranes at both sides, and a carbonate platform further to the west, were formed in a different way. To the east, a former back-arc basin is only preserved as remnants, including basic magmatics, marbles and calc-silicate rocks in the eastern slope of the Sierra de Fiambalá. Mostly it has disappeared underneath the westward driving Pampean Ranges. To the west, a thin slice of Pampean Range-type rocks slid along the Island arc, together with the carbonate platform of the Precordilleran system. ACEÑOLAZA & TOSELLI (1988) explained its present position assuming a large dextral transcurrent fault to the west of the Famatina system. This model was later extended to the north, including the Mejillones Peninsula within the slice of Western Pampean Sierras (ACEÑOLAZA et al. 1990b).

Thus, the Precordillera of Mendoza, San Juan and La Rioja and the Famatina System are defined as fragments of the same island arc - back-arc basin system which developed at the western edge of Gondwana. West of the Precordillera the island arc has been covered by younger rocks or may partly be present in metamorphic metabasalt-metasediment series of the Chilean High and Coastal Cordillera. East of the Famatina system, only small remnants of the back-arc basin remained at the western slope of the Fiambalá Range as slices of early Palaeozoic oceanic magmatic rocks, calc-silicates and mica-schists.

The composition of syn- and postsedimentary magmas changed from magmatic arc to syn-collisional in character with time (SCHÖN 1991, MANNHEIM 1992). The diversity of the western border of Gondwana can neither be explained only by assuming a micro-continent collision nor only by continent-parallel gliding of slices of continental crust, nor only by persistent and homogeneous subduction processes. In fact, this complexity results from a variable stress field, controlled by various Palaeopacific oceanic plates which collided with the continent at variable angles, producing transpressional and transtensional tectonics as well as right-angle collisions of parautochthonous island arcs with their continental hinterland.

CONCLUSIONS

In the Eastern Cordillera as well as in the Famatina Range a continuous development from island arc to collision type magmatism has been found. Repeated extension and collision seem to be typical features of the Gondwana margin in the Palaeozoic. The northward movement of a small slice of crust, comprising the Precordillera and parts of the Pampean Ranges, destroyed an Ordovician island arc; this transcurrent fault must therefore be younger than the island arc itself. The all over present Ordovician magmatism belongs geotectonically to the subduction episode that produced the island arc. Magmatism diminished in the Devonian, and revived once more in the Carboniferous. This probably gives a hint to the

time of dextral shearing in the Devonian, and to a revival of subduction in the Carboniferous.

For all these processes, subduction of oceanic Palaeopacific plates is needed which were moving continentwards under varying angles. In this scenario there is no room for a continuously northward gliding Laurentia continent alongside South America during the Early Palaeozic.

REFERENCES:

ACEÑOLAZA, F.G. & TOSELLI, A.J, 1988, El sistema de Famatina, Argentina: su interpretación como orógeno de margen continental activo. 5° Congr. geol. Chil. Santiago de Chile, acta 1: 55-67.

ACEÑOLAZA, F.G., MILLER, H. & TOSELLI, A.J., eds., 1990a, El ciclo Pampeano en el Noroeste Argentino, 227 pp., Ser. Correlación Geológica 4, S.M.de Tucumán.

ACEÑOLAZA, F.G., MILLER, H. & TOSELLI, A.J., 1990b, Interpretación tectónica de los límites del terrane del Famatina, Argentina. Comunicaciones 41: 41-46, Santiago de Chile.

BACHMANN, G., GRAUERT, B., KRAMM, U., LORK, A. & MILLER, H., 1987, El magmatismo del Cámbrico Medio/Cámbrico Superior en el basamento del noroeste de Argentina: Investigaciones isotópicas y geocronológicas sobre los granitoides de los complejos intrusivos de Santa Rosa de Tastil y Cañaní. 10° Congr. geol. Argent. Tucumán 6: 125-127.

DALLA SALDA, L.H., DALZIEL, I.W.D., CINGOLANI, C.A. & VARELA, R., 1992: Did the Taconic Appalachians continue into southern South America?. Geology 20(12): 1059-1062.

MANNHEIM, R., 1992, Genese der Vulkanite und Subvulkanite des alt-paläozoischen Famatina-Systems, NW-Argentinien, und seine geodynamische Entwicklung. 130 pp., Dr.rer.nat. thesis, Univ. München.

MILLER, H., 1984, Orogenic development of the Argentinian/Chilean Andes during the Palaeozoic. J. geol. Soc. London 141: 885-892.

RAMOS, V.A., JORDAN, T.E., ALLMENDINGER, R.W., MPODOZIS, C., KAY, S.M., CORTES, J.M. & PALMA, M., 1986, Paleozoic terranes of the central Argentine-Chilean Andes. Tectonics 5: 855-880.

RAPELA, C.W., COIRA, B. TOSELLI, A. & SAAVEDRA, J., 1992, El magmatismo del Paleozoico Inferior en el Sudoeste de Gondwana. <in> GUTIERREZ MARCO, J.G., SAAVEDRA, J. & RABANO, I. eds.: Paleozoico Inferior de Ibero-América; Univ. de Extremadura.

SCHÖN, Ch., 1991, Magmenentwicklung und Intrusionsgeschichte im Süd-teil der Sierra de Cachi, NW-Argentinien. 142 pp., Dr.rer.nat. thesis, Univ. München.

PALEOZOIC TECTONIC EVOLUTION OF THE CENTRAL ANDES IN NORTHERN ARGENTINA AND CHILE

Ricardo MON

Facultad Ciencias Naturales, UNT.
Miguel Lillo 205, 4000 Tucumán, Argentina.

RESUMEN: En este sector andino se presentan dos cinturones colisionales, intracratónicos, vergentes hacia el oeste: el Oclóyico (Ordovócico superior) y el Chánico (Carbónico superior). Evolucionaron entre las Sierras Pampeanas y masas continentales Pacíficas separadas o erosionadas tectónicamente.

KEY WORDS: intracratonic, continental subduction, collision, decollement.

INTRODUCTION

This part of the Central Andes shows two collision belts of different age, situated between the Pampean Ranges Craton to the east and continental "pacific" masses to the west. The Arequipa Massif would be a part of them. Their tectonic relationships, observed in the eastern slope of the Andes, allow to reinterprete some of the modells proposed till now.

THE PALEOZOIC BELTS

The Ocloyic belt, situated against the Pampean Ranges (Fig.1), is developed in a 5 Km sequence of turbidites interbedded with volcanics. It shows NNE-SSW folds associated with cleavage dipping to ESE (Puna). To the east the ductile deformation decreases gradually and the Ocloyic belt passes to a west –verging fault belt (Eastern Cordillera). The ordovician sequences with cleavage development are intruded by post-tectonic granitoides. The whole complex is covered unconformably by Silurian and Devonian shelf beds.

The Chanic belt consists in a 3500 m thick sequence of Devonian and Carboniferous turbidites, interbedded with basic and ultrabasic volcanics, grading to the east to shelf sediments (Bahlburg et al 1987). The turbidites are affected by WSW verging folding associated with ENE dipping cleavage (Bell, 1984). They are intruded by Upper Carboniferous granitoides and covered unconformably by Lower Permian beds. The Chanic belt shows a remarkable resemblance with the eastward –situated Ocloyic one, the difference being that its sedimentary, magmatic and tectonic evolution is much younger.

These belts are separated by a crystalline basement ridge (Fig. 1 and 2). They developed from intracontinental extensional basins (Bahlburg et al op cit.). They do

not show any participation of oceanic crust.

The closure of both collision belts is related to continental subduction along two parallel sutures. This mechanism was recognized by Matte & Xu Zhi, (1988) in other continents. The folding of the Ocloyic and Chanic belts could be related to basal decollements, which do not attain the surface, allowing the sliding of the Paleozoic sequences over the crystalline basement. Only the thrust of the crystalline basement over the Ocloyic belt is exposed. (Fig.2).

THE PRECAMBRIAN BASEMENT

The basement underlying the Paleozoic belts described above crops out in the Sierras Pampeanas Craton, Arequipa Massif and some intermediate small exposures. It is constituted by several accreted belts separated by transitional contacts, faults and ductile shear zones (Mon & Hongn, 1991). It is intruded by magmatic arcs containing plutonic bodies of different ages and origins. There are basic and ultrabasic belts too. The metamorphic belts show polyphase deformation due to the overprinting of distinct folding episodes. Part of the plutons are polydeformed too and affected by ductile shear zones.

Middle Cambrian and Ordovician sequences cover unconformably the north part and some sectors of the west border of the Pampean Ranges Craton. To the east it is covered by the Eopaleozoic sequences filling the Chaco- Paraná Basin. The age of the its components, according stratigraphic and reliable isotopic data, goes from the Precambrian-Cambrian border (600 Ma) till at least 1200 Ma (Villar & Coleman, 1986). Moreover there is a significant number of isotopic data yielding younger ages up until the Upper Paleozoic. These show a great dispersion and do not allow one to get a coherent geological picture, being that they are incompatible with the stratigraphic relationships exposed above. (Mon & Hongn, op cit.)

The connections between the Pampean Ranges Craton and the Arequipa Massif are not visible. According to the paleomagnetic studies of Shackleton et al. 1979, the last one has remained together with South American plate at least after 850 Ma.

RELATIONSHIPS BETWEEN THE PRECAMBRIAN BASEMENT AND THE PALEOZOIC FOLD BELTS

Between 22° and 24° S the Cambrian and Ordovician sequences of the Ocloyic belt are covering unconformably the basement. South of 24° S, the basement is thrust over the ordovician sequences of this belt along more than 300 Km (see Fig. 1 and 2). The Chanic belt north of 25° S is lying over Precambrian Arequipa Basement and to the south over the west extension of the Precordillera Ocloyic belt (Fig. 3).

GEOTECTONIC HYPOTHESES AND DISCUSSION

During Paleozoic time the deformation migrated to the west with the generation of the Eopaleozoic Ocloyic belt (Upper Ordovician-Silurian) and then the Upper Carboniferous Chanic belt. Both show intracratonic evolution and they were closed by continental subduction. This scheme is in agreement with most of the observed facts and available information. It remains as a problematic question the destiny of the continental masses situated to the west of the paleozoic fold belts. Dalla Salda et al.

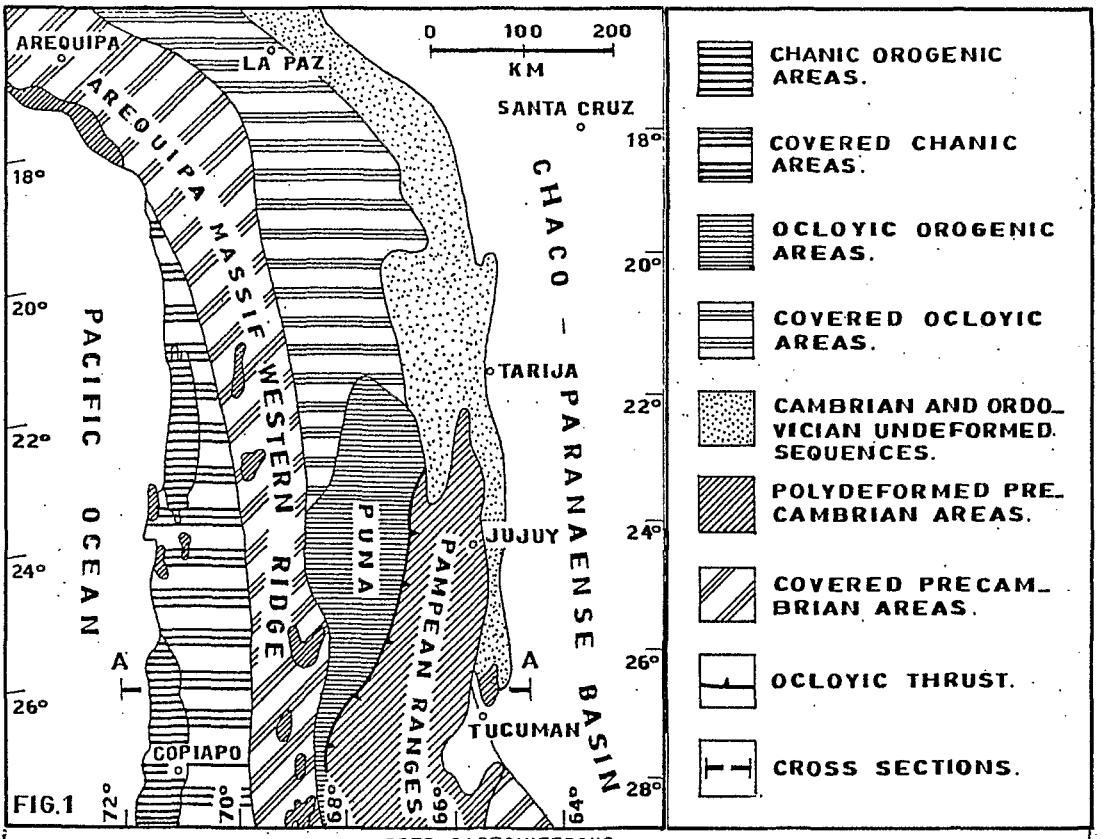
AREQUIPA
LA PAZ
SANTA CRUZ
TARIJA
JUJUY
TUCUMAN
COPIAPO
AREQUIPA MASSIF
WESTERN RIDGE
PACIFIC OCEAN
PUNA
PAMPEAN RANGES
CHACO - PARANAENSE BASIN
0 100 200
KM
18°
20°
22°
24°
26°
28°
72°
70°
68°
66°
64°
A
A
CHANIC OROGENIC AREAS.
COVERED CHANIC AREAS.
OCLOYIC OROGENIC AREAS.
COVERED OCLOYIC AREAS.
CAMBRIAN AND ORDOVICIAN UNDEFORMED SEQUENCES.
POLYDEFORMED PRECAMBRIAN AREAS.
COVERED PRECAMBRIAN AREAS.
OCLOYIC THRUST.
CROSS SECTIONS.
FIG.1

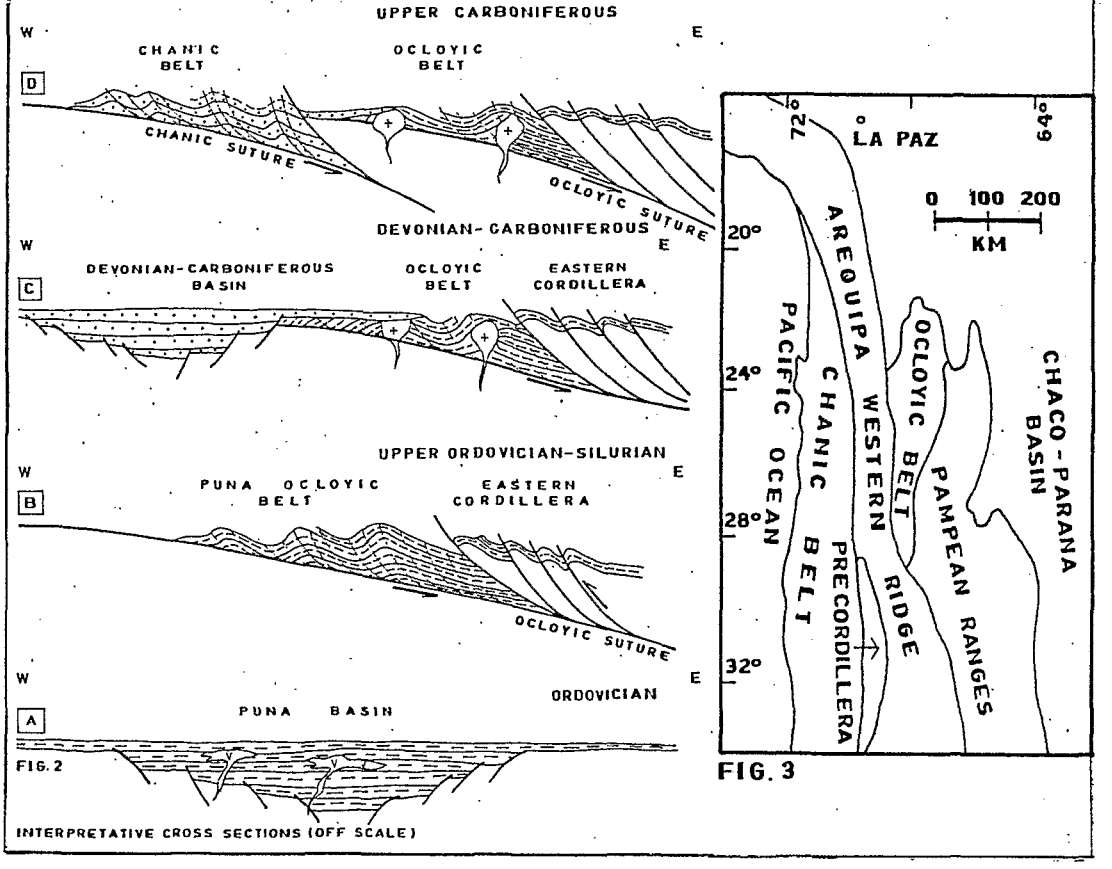
UPPER CARBONIFEROUS
W
E
D
CHANIC BELT
OCLOYIC BELT
CHANIC SUTURE
OCLOYIC SUTURE
DEVONIAN-CARBONIFEROUS
C
DEVONIAN-CARBONIFEROUS BASIN
OCLOYIC BELT
EASTERN CORDILLERA
UPPER ORDOVICIAN-SILURIAN
B
PUNA OCLOYIC BELT
EASTERN CORDILLERA
OCLOYIC SUTURE
ORDOVICIAN
A
PUNA BASIN
FIG. 2
INTERPRETATIVE CROSS SECTIONS (OFF SCALE)

LA PAZ
0 100 200
KM
20°
24°
28°
32°
72°
64°
AREQUIPA
WESTERN
CHANIC BELT
PRECORDILLERA
RIDGE
OCLOYIC BELT
PAMPEAN RANGES
PACIFIC OCEAN
CHACO-PARANA BASIN
FIG. 3

1992 postulate that they were displaced to the north and that they could be incorporated to the Appalachian Orogenic belt. The erosive subduction is other possible mechanisme, Stern & Mpodozis, 1991 postulate that, at least, 200 Km of Prejurassic basement was eliminated after Mesozoic in the west border of South America.

Other geotectonic hypotheses for instance Coira et al, 1982, attribute the evolution of the Paleozoic fold belts to fore arc basins, incorporating to the modell the granitoides of the west border of the Sierras Pampeanas Craton as an Ordovician-Silurian magmatic arc. According the observations of Mon & Hongn, (1991) the greater part of this border is constituted by multiply –deformed precambrian granitic and metamorphic rocks thrust over the Ordovician sequences. The presence of a simple Ordovician-Silurian magmatic arc in this domain could not be confirmed.

REFERENCES

BAHLBURG, H., C. BREITKREUZ & W. ZEIL. 1987. Paleozoic basement developing in Northern Chile (21° -27°). Geologische Rundschau 76: 633-646.

BELL, C. 1984. Deformation produced by subduction of a paleozoic turbidite sequence in Northern Chile. Journal Geological Society of London 141: 339-347.

COIRA, B., J. DAVIDSON, C. MPODOZIS & V. RAMOS. 1982. Tectonic and magmatic evolution of the Andes in Northern Argentina and Chile. Earth Sciences Review 18: 303-332.

DALLA SALDA, L., W.D. DALZIEL, C. CINGOLANI & R. VARELA.1992. Did the Taconic Appalachians continue into southern South America?
Geology 20: n.12. In press.

MATTE, P. & XU ZHI, Q. 1988. Decollements in slate belts, examples from European Variscides and the Qin Ling belt of Central China. Geologische Rundschau 77: 227-238.

MON, R. & F.D. HONGN. 1991. The structure of the Precambrian and Lower Paleozoic basement of the Central Andes between 22° and 32°S. Lat. Geologische Rundschau 80: 745- 758.

SHACKLETON, R.M., A.C. RIES, M.P. COWARD & P.R. COBBOLD, 1979. Structure, Metamorphism and Geochronology of the Arequipa Massif.
Journal Geological Society of London. 136: 298-318. STERN, C.R. & C. MPODOZIS 1991. Geologic evidence for subduction erosion along the west coast of Central and Northern Chile. Sexto Congreso Geol_ gico Chileno 1: 205- 207.

VILLAR, L & R. COLEMAN, 1986. Reinterpretación geológica de la faja ultrabásica de alto grado de metamorfismo, Fiambalá , Catamarca. Asociación Geológica Argentina, Revista. 41: 410-413.

STRUCTURE AND EVOLUTION OF THE CALINGASTA-PUCHUZUN AREA IN THE WESTERN MARGIN OF THE PRECORDILLERA OF ARGENTINA

Jose SELLES-MARTINEZ

Departamento de Geologia - Universidad de Buenos Aires. Ciudad Universitaria. 1428 Buenos Aires. Argentina.

RESUMEN: Bloques limitados por fallas Norte-Sur, inversas de alto angulo que inclinan al Este y sobrecorrimientos que inclinan al Oeste. presentan distintas estructuras y secuencias como resultado de su historia pre-terciaria. Sobre las Formaciones ordovicicas, plegadas en zig zag, con ejes de RAz 315°, yacen discordantemente unidades devonicas y mas jovenes con plegamiento suave y ejes Norte-Sur. El Triasico cubre al conjunto con inclinacion al poniente.

KEY WORDS: Precordillera-Paleozoic-Structure-Tectonics

INTRODUCTION

The western margin of the Argentine Precordillera at the Rio San Juan section is composed of several elongated blocks of North-South trend. Sedimentary sequences show different structural styles due to their different pre-Tertiary evolution. Andean trends mask a late Devonian compressive episode and possibly a late Ordovician transpressional one. The stratigraphy and main structural characteristics of the Precordillera have been summarized in Ramos et al., 1986, and will not be described here. Quartino et al., 1973 carried out a regional survey and revised and reorganized the stratigraphic nomenclature. Sessarego, 1988 and Selles-Martinez 1992 have studied the stratigraphy and structure of the area north of the Rio San Juan. Evidences from sedimentary and paleontological records lead the author (Selles-Martinez, 1988) to the idea that a common history linked the Precordillera of Argentina and the Appalachians of North American during Cambrian to late Ordovician times. Paleomagnetic information is still scarce and a definitive position can not still be taken, (Mena y Selles-Martinez,

1989). The understanding of pre-Andean, and most important, pre-Gondwanide structures is an important key for testing whether or not the Precordillera is a displaced, accreted or autochthonous terrane. This paper is a contribution to the analysis of structural features of outcropping units and a first approach to discriminate deformational episodes in the area. Petrological, isotopic and paleomagnetic studies are still been carried to clarify this scenario.

GEOLOGICAL SETTING

Five principal blocks (Tontal, Del Salto-Rio Seco, Del Alto de los Pajaritos and El Carrizal ones) are limited by faults running N-S, dipping to the east as Eastern and Western Tontal Fault (high angle, reverse) and overthrusts dipping about 30° to the East. Most of the contacts between formations are of tectonic origin and it is very difficult to determine their relationships, even in the same block. Figure 1 is a geologic sketch of the area.

CONCLUSIONS

The Eastern Tontal Fault bounds the Tontal Block (composed by Ordovician silts and sandstones and gabbroic intrusives) to the west. Tight folds with axis trending N-NE are representative of the structure in the area. The Tontal Fault Zone includes Western Tontal Fault showing horses and splays of different scales, mixing Ordovician and Permo-Triassic units. The Del Salto-Rio Seco Tectonic Window is one of the most interesting structures in the area, and its internal structure and evolution is far of being completely understood. North-South and transverse faults define minor blocks. The structure of El Planchon and El Salto Fms. is a broad anticline with minor refolding. Pencil structure in the former evidences that deformation in the area never reached cleavage stage at least after Devonian times. Codo Fm. forms a broad anticline in both margins of the river, bounded to the East by the conglomerates of El Raton Fm. The contact is clearly an unconformity in the vicinity of km 117 Creek, but becomes tectonic to the north due to a more intense deformation associated with the proximity of a blind thrust in the anticline core. Homoclinal sequences of Uspallata Group outcrop in the center of Rio Seco Creek, and are tectonically linked to El Planchon Fm. to the E, which is in turn separated by another fault from Carbonic clastics of El Raton Fm. Western and Eastern Tontal Faults rise Alcaparrosa Fm. at Sierra del Tigre. In the Alto de los Pajaritos Block the outcropping of the angular unconformity between Don Polo and Codo Fm. is outstanding. Don Polo clastics are folded in a tight to chevron style. Bulbous hinges, saddle reefs, en echelon quarts veins and cleavage crenulation are common features, but delicate ichnofossils have been preserved. Milonitic textures in the same Fm. shows that at least some horizons have undergone intense shearing (decollement

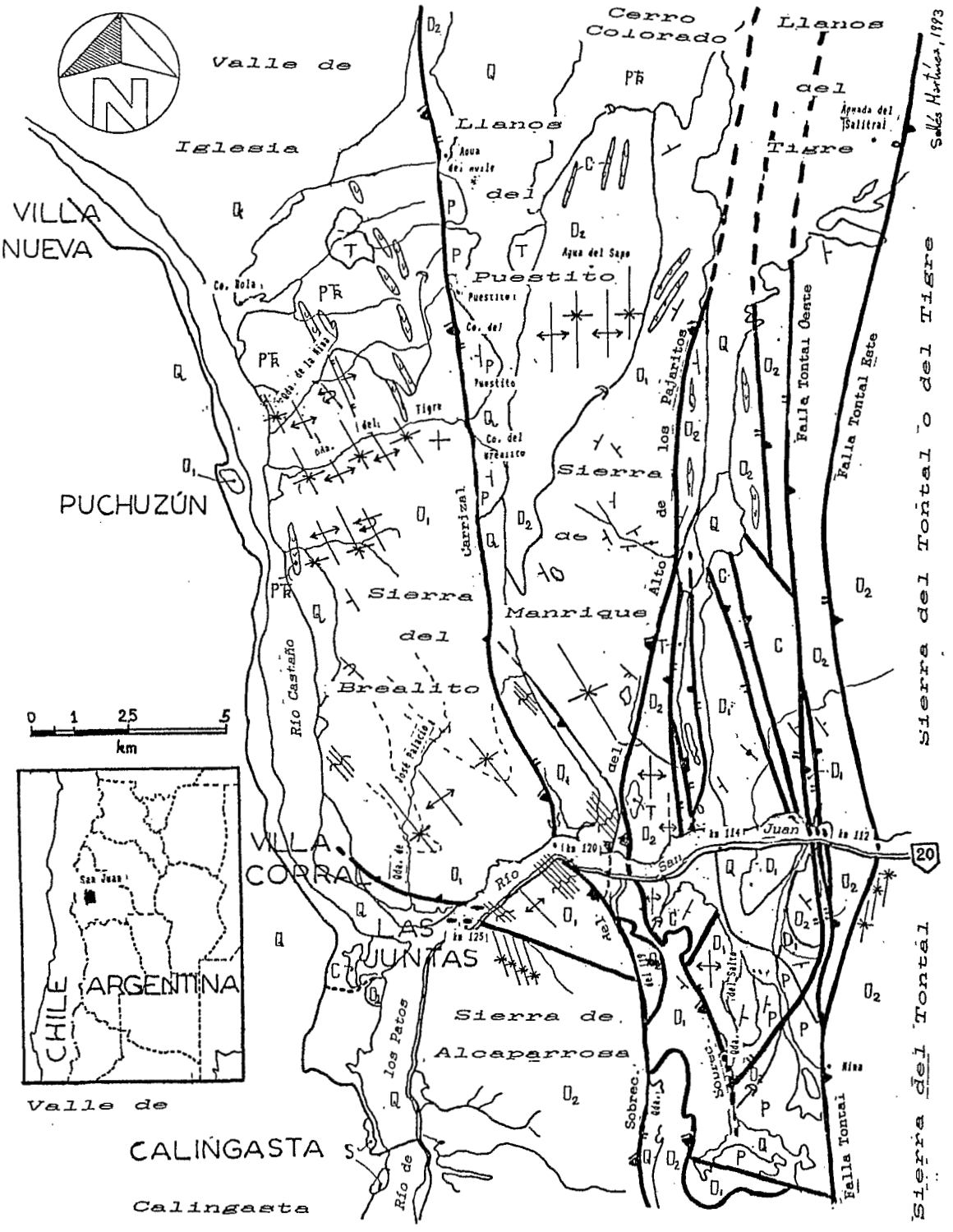

Figure 1: Geological and structural sketch of the Rio San Juan area (westernmost Precordillera of Argentina).
O_1= Don Polo Fm; O_2= Alcaparrosa Fm; S= Calingasta Fm; D_1= El Planchon Fm; D_2= Codo Fm; C= El Raton and La Capilla Fm; P= El Salto Fm; PTr= Choiyoi Fm; Tr= Uspallata G; T= Tertiary; Q= Quaternary.

surfaces?) possibly in ordovician times. Fold axes in Don Polo Fm. trend Az 315 and NE flanks are frequently overturned. Well developed kink bands in this and next Block show coherent with a folding episode with main compressional stress directed SW-NE followed by vertical shearing to the NE. Folds in Codo Fm. are opened with N-S trending axes. Younger units in this Block show homoclinal to the west. In the westernmost block, the El Carrizal one, Alcaparrosa Fm. is tightly folded with axes running to Az 340, a fault, trending Az 315 (50m wide fault zone) is the western limit of the outcrops of Don Polo Fm. in the southern margin of the San Juan River (km 125 Creek). The structure follows the same structural pattern in the northern portion of the block where Ordovician clastics are umcomformably covered by Choiyoi ignimbrites (Qda. de la Mina area). This Triassic volcanics deep gently to the west. The region shows thin-skinned style for Andean structures, which are in part reactivation of ancient ones, (like Tontal Fault). The sinistral displacement shown by the El Carrizal Thrust at the Rio San Juan valley is interpreted as a lateral ramp, cutting upsequence and has acted as a discontinuity during more recent deformation leading to a small amount of sinistral displacement on this surface and probably on a hidden fault along the river valley resulting in a counterclockwise rotation of fold axis in the vicinity of the river, and also helpd for the displacements of El Raton Fm. outcrops north of km 117. This sinistral shear has not affected Tontal Faults.

REFERENCES

MENA, M. and SELLES-MARTINEZ J., 1989. Aloctonia de la Precordillera durante el Paleozoico Inferior: evidencias paleomagneticas. Reunion sobre geotransectas de America del Sur. Actas 190/194.

QUARTINO, B.J., R. ZARDINI and A.J. AMOS, 1973. Estudio y exploracion geologica de la region Barreal-Calingasta. Asociacion Geologica Argentina. Monografia. 176 pp.

RAMOS, V.A., T.M. JORDAN, R.W. ALLMENDINGER, C. MPODOZIS, E.M. KAY, J.M. CORTES and M.A. PALMA, 1986. Paleozoic Terranes of the Central Argentine-Chilean Andes. Tectonics V5 (6) 855/880.

SELLES-MARTINEZ, J., 1988. Were the Precordilleran and Appalachian Shelves opposite margins of the Iapetus? Symposium: Lithospheric processes in Andean Type tectonics. VII Congreso Latinoamericano. Belem do Para. Abstracts.

SELLES-MARTINEZ, J. 1992. Estructura del borde occidental de la Precordillera, entre la Sierra del Tontal y el rio Castano, desde el rio San Juan hasta la base del Co. Colorado. Thesis. Universidad de Buenos Aires. Umpublished.

SESSAREGO, H., 1988. Estratigrafia de las secuencias devonicas a triasicas aflorantes al norte del Rio San Juan y al oeste de la Sierra del Tigre. Tesis Doctoral. Universidad de Buenos Aires. Umpublished.

PALEOZOIC TO JURASSIC EVOLUTION OF BOLIVIA

Thierry SEMPERE

Convenio YPFB - Orstom (UR 1H), Santa Cruz, Bolivia; and LGTE, Département de Géologie Sédimentaire, Université Paris-VI, Paris, France. Present address: consulting geologist, 13 rue Geoffroy l'Angevin, 75004 Paris, France.

RESUMEN: El registro Cámbrico superior a Jurásico de Bolivia, principalmente marino, ilustra la evolución del Gondwana sudoccidental desde la finalización de la fragmentación de la Protopangea hasta la dislocación de la Pangea. Una crisis compresional durante el Ordovícico medio inició el funcionamiento activo del margen, marcado por una fuerte subsidencia del Ashgill al Mississipiano. Depósitos someros a continentales, menos espesos, caracterizan la época de la Pangea (Pennsylvaniano-Jurásico).

KEY WORDS: Gondwanaland, Bolivia, Paleozoic, Mesozoic, sedimentary record, geotectonics

INTRODUCTION AND REGIONAL SETTING

The late Cambrian to Jurassic record of Bolivia illustrates the evolution of the southwestern margin of Gondwanaland from the definitive break-up of the late Proterozoic Protopangea to the dislocation of Pangea.

Present state of knowledge of the Bolivian Phanerozoic stratigraphy distinguishes eight main periods (Sempere, in press). The stratigraphic units dealt with in this paper belong to the Tacsara (late Cambrian - middle? Caradoc, ≈80 Myr or more), Chuquisaca (late Caradoc? - middle Famennian, ≈85 Myr), Villamontes (late Famennian - Mississipian, ≈40 Myr), Cuevo (Pennsylvanian - early Triassic, ≈85 Myr), and Serere (middle Triassic - middle? Jurassic, ≈95 Myr) supersequences. Boundaries between these supersequences are generally sharp. The late Cambrian to Permian record is mostly of marine origin, whereas the Triassic-Jurassic record is exclusively continental. The Silurian to Jurassic record of Bolivia resembles the coeval record of the Paraná basin (Sempere, 1990, in press).

From late Ordovician to Mesozoic times, Bolivia laid in the southern part of the subsident Bolivia-Peru basin, which ran parallel to the southwestern margin of Gondwanaland and remained bounded southwards by the Sierras Pampeanas area in Argentina. The marine transgressions thus reached Bolivia from the northwest during this interval.

The known basement of the "Phanerozoic" series in Andean Bolivia generally consists of late Proterozoic-early Cambrian rocks, but crops out only in a few spots. In most of the Cordillera Oriental and Subandean belt, the basal décollements of the Andean thrusts are located in shales of Ordovician, Silurian or Devonian age, and, in each case, no older strata are exposed. Some ancient structural elements have largely controlled both Phanerozoic sedimentation and deformations in southwestern Bolivia (Sempere et al., 1991).

LATE CAMBRIAN TO MIDDLE ORDOVICIAN (TACSARA SUPERSEQUENCE)

When Protopangea dislocated in latest Proterozoic and Cambrian time (Bond et al., 1984), North America drifted from South America northwestwards, and the western margin of Gondwanaland (also southeastern margin of the Iapetus ocean) evolved as a passive margin submitted to a large-scale dextral shear. These tensional conditions initiated the Puna aulacogen in middle to late Cambrian time, and favored the installation of a wide marine epicontinental basin along the proto-Andean domain, which was the locus of thick sedimentation (Sempere, 1992, in press).

An important geodynamic upheaval occurred in middle Ordovician time and the Gondwanaland-southern Iapetus margin became active. A magmatic arc appeared, separating a fore-arc from the wide marine back-arc basin, inside which most part of Andean Bolivia is presently located. Closure and deformation of the Puna aulacogen propagated from the west, starting near the Arenig-Llanvirn boundary (according to data displayed by Bahlburg, 1990), and produced the Ocloyic belt of the Argentine-Chilean Puna and southwestern Bolivia. The rest of the previous depositional area evolved as the marine foreland basin of this deformation, which apparently continued well into Caradoc time. The development of the Ocloyic deformation was apparently

coeval with the Taconic deformation of the northern Andes and of the symmetrical margin of eastern North America. Development of roughly synchronous major compressional deformations on both sides of the southern Iapetus ocean suggests that a major global plate reorganization occurred in middle Ordovician time (Sempere, 1992, in press).

In southwestern Bolivia (Tarija area), the sequence begins with shallow-marine clastics, which grade to open-marine, thick graptolite shales intercalated with subordinate turbidites and slumps (late Cambrian-Llanvirn). These strata are affected in this area by the Ocloyic deformation, which is post-dated in northernmost Argentina by beds of Ashgill and Llandovery age (Isaacson et al., 1976; Benedetto et al., 1992). The Ocloyic deformation shows an decrease in intensity from west to east and southwest to northeast. It is unknown north of lat 20°S, where a thick (≈ 4000 m) shallowing-upward siliciclastic sequence of Llanvirn to Caradoc age, conformably overlain by the Chuquisaca supersequence, was deposited during the development of the Ocloyic deformation in the south. These thick and monotonous shallow-marine sandstone-siltstone intercalations are therefore interpreted as the fill of the marine foreland basin related to this deformation (Sempere, 1989, 1992, in press).

LATE ORDOVICIAN TO MIDDLE FAMENNIAN (CHUQUISACA SUPERSEQUENCE)

This interval consists of two stratigraphic sets (late Caradoc?-early? Llandovery, and late Llandovery-middle Famennian). The first set begins with black shales (Tokochi Fm; Sempere et al., 1991) which overlie shallow-marine Caradoc strata and were deposited in a relatively deep, anoxic environment during a maximum flooding episode. They are overlain by resedimented glacial-marine diamictites (Cancañiri Fm, Ashgill), which are in turn sharply overlain by the thinning-upward Llallagua Fm (thickly-bedded turbidites) and/or by the late Llandovery to Ludlow age Uncía/Kirusillas Fm (dark shales, with minor turbidites). The first 3 units reach their maximum thickness in the eastern UCU domain, whereas they rapidly thin out to the southeast and east. Some rare limestone beds are known at Ashgill (Toro et al., 1992) and early Wenlock levels (Merino, 1991). Deposition of the late Caradoc? to early? Llandovery strata occurred in a basin controlled by active normal faulting, but facies succession was induced by a major glacio-eustatic sea-level low (Ashgill ice age) which developed between two maximum flooding episodes (Tokochi and Uncía/Kirusillas Fms). The mostly resedimented Cancañiri and Llallagua Fms are interpreted to represent lower and upper lowstand deposits, respectively.

The late Llandovery-middle Famennian set includes several units in the Bolivian Andes, Subandean belt and Chaco-Beni plains. This interval was a time of onlap toward the northeast, and of deposition of major source rocks in Bolivia. The units are generally thick and form three main shallowing-upward megasequences, beginning with thick dark shales and ending with sandstone-dominated units, respectively of late Llandovery-Lochkovian, Pragian-early Givetian, and late Givetian-middle Famennian ages (Racheboeuf et al., 1992). Decrease and geographic homogeneization of subsidence in ≈Llandovery time are interpreted to mark a change in tectonic regime (also reflected by the northeasterly onlap): whereas the late Caradoc?-early? Llandovery set was deposited through activity of a wide tectonic trough in the UCU domain, the late Llandovery-middle Famennian set was deposited in a large, subsident, marine "foreland" basin related to sinistral transpressional activity of the Gondwanaland margin (Sempere, 1992, in press).

LATE FAMENNIAN-MISSISSIPIAN (VILLAMONTES SUPERSEQUENCE)

The conflictive stratigraphy of the Villamontes (≈Ambo Group; ≈Machareti + Mandiyuti groups) and Cuevo (≈Tarma and/or Copacabana groups) supersequences is currently undergoing major revisions, through integration of new biostratigraphic data and analysis of stratigraphic and seismic sections. In much contrast with the underlying series, facies vary rapidly at all scales, and correlations are difficult. Tectonic, eustatic and climatic controls on sedimentation are taken into account to favor first-order correlation tools such as major climatic changes and eustatic events. Resedimented deposits, where predominant, are interpreted to mark local tectonic activity and lead to define active slopes and highs.

The Villamontes-Cuevo contact marks a noteworthy paleoclimatic change in northwestern Bolivia, from cool or temperate and rainy, to relatively warm and arid conditions. This climatic change, marked in other parts of Bolivia, is consistent with what is known of the coeval South pole southeastwards migration (Veevers and Powell, 1987). It provides a correlation horizon, as a first approximation because it is likely to have been slightly diachronous. On the basis of conodont biostratigraphy, its age would lie within the Serpukhovian or approximately coincide with the Mississipian-Pennsylvanian boundary (D. Merino, in prep.). Furthermore, the major global regression-transgression event which occurred in Serpukhovian and earliest Pennsylvanian time (Saunders and Ramsbottom, 1986; Veevers and Powell, 1987) is apparently recorded by the upper Villamontes and lower Cuevo facies. A paleosol may occur at this contact.

The mainly marine Villamontes supersequence overlies Devonian strata with a sharp or rapidly transitional contact. Mudstones are black to grey, with some purple shade in the south. Plant fossils are locally common. In the northern Subandean belt, facies include thick mud-dominated slumps, sandstone olistoliths, shallow-

marine black laminated shales, sandstones and coal, whereas in the related Lake Titicaca area they display a basal glacial-marine horizon, dark shales, cross-bedded sandstones, diamictites, and coal.

In the Chaco basin and adjacent Subandean belt, the Villamontes supersequence roughly equates with the Machareti and Mandiyuti subgroups. Basal facies commonly document a brutal increase in paleodepth. Machareti and Mandiyuti facies are dominated by clast-bearing resedimented deposits, proceed from the Chaco high, and include rarely stratified "diamictites", debris flows, muddy to sandy mass flows and slumps, stratified olistoliths, cross-bedded sandstones, thick and thin regularly-bedded turbidites, regularly-bedded fine-grained sandstones and mudstones, and rarer laminated mudstones. Convincing glacial-marine features are only observed in the Machareti, although reworked glacial clasts exist in the Mandiyuti. Many resedimented facies were deposited in submarine channels and valleys, which locally display vertical coalescence. Amplitude of scouring at their base apparently increases upsection. The Machareti shows marked lithologic contrasts between mud-dominated and sand-dominated facies, whereas the Mandiyuti is predominantly sandy and shows near-shore to continental facies in its uppermost part, which indicates a major and rapid shallowing of depositional environments and is interpreted to represent the Serpukhovian global-scale regression (Veevers and Powell, 1987) in Bolivia. Mudstones in the Machareti are dark grey to purplish, locally with plant debris, whereas they are bright brownish red in the uppermost Machareti and the whole Mandiyuti, indicating a roughly coeval climatic change (see above).

Some Mississipian strata post-date uplifts of late Devonian or earliest Mississipian age, and Pennsylvanian to early Permian limestones locally onlap upon paleoreliefs formed in late Devonian and/or Mississipian time. Although these limestones may overlie strata as old as Ordovician in age, no angular unconformities are known, which stands against a "Hercynian" major deformation. Furthermore, the "Hercynian" metamorphism and deformation of Bard et al. (1974) has been proved to be of late Triassic age (Farrar et al., 1990) and is only of local importance. But, because of the late Devonian to early Mississipian deformations known in Peru, of the coeval inferred uplifts in several parts of Bolivia, and other evidences for synsedimentary tectonic instablility, it seems clear that the late Devonian and especially the Mississipian were times of high epeirogenic activity in the Bolivia-Peru basin. The Mississipian sedimentation may thus be considered as the culmination of the Silurian-Devonian evolution (see Sempere, in press).

PENNSYLVANIAN TO EARLY TRIASSIC (CUEVO SUPERSEQUENCE)

Controlled by a low subsidence and subtropical climatic conditions, a shallow carbonate platform extended in western Bolivia (Copacabana Fm), while littoral to continental sands were deposited in southeastern Bolivia (Cangapi Fm). Occurrences of eolian deposits and evaporites in the Pennsylvanian and early Permian may be noted, as well as similarities with the Amazon basin. Tuffaceous beds document contemporaneous explosive magmatism in the west. An extensive restricted-marine carbonate transgression developed in the middle to late Permian (Vitiacua/Chutani Fm; Sempere et al., 1992), as in the Paraná and Karoo basins, and was followed by a general regression.

Deposition of the Cuevo supersequence was coeval with an important compressional or transpressional intracratonic deformation mainly known in the Cordillera Oriental of central and southern Peru. This widespread "Gondwanian"-age deformation is postdated by a post-orogenic calc-alkaline magmatism of early to middle Triassic age, which evolved in the late middle Triassic toward continental tholeiitic compositions indicating regional extension or transtension (see Soler and Sempere, 1993), which in Bolivia initiated the Serere supersequence.

MIDDLE TRIASSIC TO MIDDLE? JURASSIC (SERERE SUPERSEQUENCE)

The stratigraphy of this time interval in Bolivia was recently updated (Oller and Sempere, 1990). An initial rifting process of late middle Triassic age developed in several areas, probably within an extensive and complex extensional to transtensional setting related to the coeval fracturation of Pangea. Numerous small grabens were filled by fluvio-lacustrine red beds and evaporites, while alkaline and tholeiitic magmatisms developed, as in other parts of western South America (see Soler and Sempere, 1993).

Abortion of rifting in Bolivia was probably a consequence of a regional tectonic reorganization at ≈220 Ma, which produced local intracratonic transpressional conditions, as evidenced by the pervasive cataclasis of the Zongo-Yani (Bolivia) and Abancay (southern Peru) Triassic intrusions and the deformation of their enclosing strata (Bard et al., 1974; Dalmayrac et al., 1980; Farrar et al., 1990). Some grabens or transtensional structures were inverted during this event, which probably marked the regional resumption of subduction along the Pacific margin. The subsequent, late Triassic-middle? Jurassic, onlapping sedimentation (mainly fluvial and eolian sands, as in the Paraná basin) was controlled by the thermal subsidence which developed after rifting became inactive (Oller and Sempere, 1990).

This evolution ended with a late Jurassic large-scale rifting event, apparently related to the initiation of the southern Atlantic rift system. Bolivia, which until then had somehow behaved in a cratonic way, was then captured by the Andean-Pacific system.

CONCLUSIONS

The Bolivian Phanerozoic record illustrates the dislocation of the late Proterozoic Protopangea, the initiation and evolution of the western Gondwanaland margin, the aggregation and consolidation of Pangea, its subsequent fracturation and dislocation, and the convergence effects of the motion of South America.

The late Cambrian to Mississipian record (≥ 205 Myr) highlights the regional evolution from the break-up of Protopangea to the assemblage of Pangea. The source rocks of the Bolivian hydrocarbons presently under production were deposited during this period of high subsidence.

The Pennsylvanian to mid-Jurassic record (≈165 Myr) illustrates the epoch of Pangea. Final coalescence, consolidation and subsequent fracturation of Pangea occurred during this time interval. Active subduction probably ceased in the Permian in relation to the coalescence of Pangea (Kay et al., 1989), but resumed in the late Triassic. In the central Andean region, the coeval geological evolution includes a complex set of tectonic, magmatic and sedimentary events.

Much Bolivian oil and gas occurs in Devonian and Carboniferous reservoirs, and is derived from source rocks deposited during epochs of major marine inundation (Ordovician-early Mississipian: thick dark shale units, major subsidence; middle Pennsylvanian-late Permian: thinner shallow-marine carbonates and dark mudstones). Propagation of Andean thrust deformation, and sedimentary and tectonic burying of Paleozoic organic-rich units, have had a major control on hydrocarbon migration and present-day distribution. The geometry of the Paleozoic basin and sedimentary pile closely controls the geometry of Andean deformations.

REFERENCES

Bahlburg, H., 1990. The Ordovician basin in the Puna of NW Argentina and N Chile: geodynamic evolution from back-arc to foreland basin. Geotekt. Forsch., 75, 107 p.

Bard, J.P., R. Botello, C. Martinez, and T. Subieta, 1974. Relations entre tectonique, métamorphisme et mise en place d'un granite éohercynien à deux micas dans la Cordillère Real de Bolivie (massif de Zongo-Yani). Cah. ORSTOM (Géol.), 6: 3-18.

Benedetto, J.L., T.M. Sánchez, and E.D. Brussa, 1992. Las cuencas silúricas de América Latina: In "Paleozoico inferior de Ibero-América", J.G. Gutiérrez Marco, J. Saavedra and I. Rábano (eds.), Universidad de Extremadura, 119-148.

Bond, G.C., P.A. Nickeson, and M.A. Kominz, 1984. Breakup of a supercontinent between 625 Ma and 555 Ma: new evidence and implications for continental histories. Earth Plan. Sci. Lett., 70,: 325-345.

Dalmayrac, B., G. Laubacher, and R. Marocco, 1980. Caractères généraux de l'évolution géologique des Andes péruviennes. Trav. Doc. ORSTOM, 122, 501 p.

Farrar, E., A.H. Clark and S.M. Heinrich, 1990. The age of the Zongo pluton and the tectonothermal evolution of the Zongo-San Gabán Zone in the Cordillera Real, Bolivia. I Int. Symp. And. Geod., Grenoble, 171-174.

Isaacson, P.E., B. Antelo, and A.J. Boucot, 1976. Implications of a Llandovery (early Silurian) brachiopod fauna from Salta Province, Argentina. J. Paleont., 50: 1103-1112.

Kay, S. M., V.A. Ramos, C. Mpodozis, and P. Sruoga, 1989. Late Paleozoic to Jurassic silicic magmatism at the Gondwana margin: analogy to the Middle Proterozoic in North America?. Geology, 17: 324-328.

Merino, D., 1991. Primer registro de conodontos silúricos en Bolivia. Rev. Técn. YPFB, Santa Cruz, 12: 271-274.

Oller, J., and T. Sempere, 1990. A fluvio-eolian sequence of probable middle Triassic-Jurassic age in both Andean and Subandean Bolivia. I Int. Symp. And. Geod., Grenoble, 237-240.

Racheboeuf, P.R., A. Le Hérissé, C. Babin, F. Guillocheau, and M. Truyols-Massoni, 1992. Le Dévonien de Bolivie: le cadre stratigraphique revu à la lumière des corrélations intercontinentales. Eur. Conf. Paleont. Stratig. Latin-Am., Lyon, 43.

Sempere, T., 1989. Paleozoic evolution of the central Andes (10°-26°S). Int. Geol. Cong., 28th, Washington, 3: 73.

Sempere, T., 1990. Cuadros estratigráficos de Bolivia: propuestas nuevas. Rev. Técn. YPFB, 11: 215-227.

Sempere, T., 1992, The early Paleozoic of Bolivia and the central Andes: sequence stratigraphy, paleogeography, and control on Andean deformation and hydrocarbon generation. Int. Conf. Low. Pal. Ibero-Am., Mérida, 136-137.

Sempere, T., in press. Phanerozoic evolution of Bolivia and adjacent regions. In: A.J. Tankard (ed.), Am. Ass. Petr. Geol. Mem.

Sempere, T., P. Baby, J. Oller, and G. Hérail, 1991. La nappe de Calazaya: une preuve de raccourcissements majeurs gouvernés par des éléménts paléostructuraux dans les Andes boliviennes. C. R. Acad. Sci., II, 312: 77-83.

Sempere, T., E. Aguilera, J. Doubinger, P. Janvier, J. Lobo, J. Oller, and S. Wenz, 1992. La Formation de Vitiacua (*Permien moyen à supérieur - Trias ?inférieur, Bolivie du Sud*): stratigraphie, palynologie et paléontologie. N. Jb. Geol. Pal., Abh., 185: 239-253.

Soler, P., and T. Sempere, 1993. Stratigraphie, géochimie et signification paléotectonique des roches volcaniques basiques mésozoïques des Andes boliviennes. C. R. Acad. Sci., II, 316: 777-784.

Toro, M., Vargas, C., and Birhuet, R., 1992. Los trilobites ashgillianos de la Formación Cancañiri (región de Milluni, Cordillera Real, departamento de La Paz). X Cong. Geol. Bol., La Paz, 188-190.

Veevers, J.J., and C. McA. Powell, 1987. Late Paleozoic glacial episodes in Gondwanaland reflected in transgressive-regressive depositional sequences in Euramerica. Geol. Soc. Am. Bull., 98: 475-487.

TECTONIC CONTROLS ON GONDWANA BREAK-UP MODELS: EVIDENCE FROM THE PROTO-PACIFIC MARGIN OF ANTARCTICA AND THE SOUTHERN ANDES

Bryan C. Storey

British Antarctic Survey, High Cross, Madingley Road, Cambridge, CB3 0ET, U.K.

RESUMEN: Se presenta un modelo placa interacción para las primeras etapas del desmembramiento de Gondwana el que vincula una zona ancha de fusión de la astenósfera a un cambio en fuerzas de la subducción placa límite. La presencia de uno plumo astenósferico haya debilado termalmente la litósfera y haya inducido hendeduramiento local contribuir para sino causar la separación final del este y oeste de Gondwana.

KEY WORDS: Gondwana break-up, rifting, magmatism, subduction

INTRODUCTION

Although the association between continental extension, supercontinent break-up, mantle plumes and massive bursts of igneous activity is well recognized, their causal relationship remains a matter of conjecture [Sengor and Burke, 1978]. According to active mantle hypotheses, rifting and associated magmatism are initiated by doming above a mantle plume (Richards et al. 1989) whereas alternative hypotheses consider the presence of a plume enhances break-up only if the stress field is such that initial rifting is likely to occur (White and McKenzie, 1989). In the West Antarctic and Andean sector of Gondwana, initial stages of Gondwana break-up are associated with the large Antarctic-Karoo-Tasman basalt province. Formation of this within-plate province was synchronous with active margin tectonics and development of both a proto-Pacific margin magmatic suite along the Antarctic margin and the extensive Tobífera volcanic suite associated with the Rocas Verdes marginal basin system of southern South America and South Georgia. Consequently the West Antarctic and Andean sector of Gondwana affords an excellent location in which to investigate possible relationships between tectonism, magmatism and the onset of seafloor spreading in continental extension zones (Storey and Alabaster, 1991).

BREAK-UP MODEL

The magmatic record along the proto-Pacific margin of Gondwana records important changes in subduction zone parameters during the initial stages of Gondwana break-up consistent with extension in the overriding plate (Storey et al. 1992). This, together with the

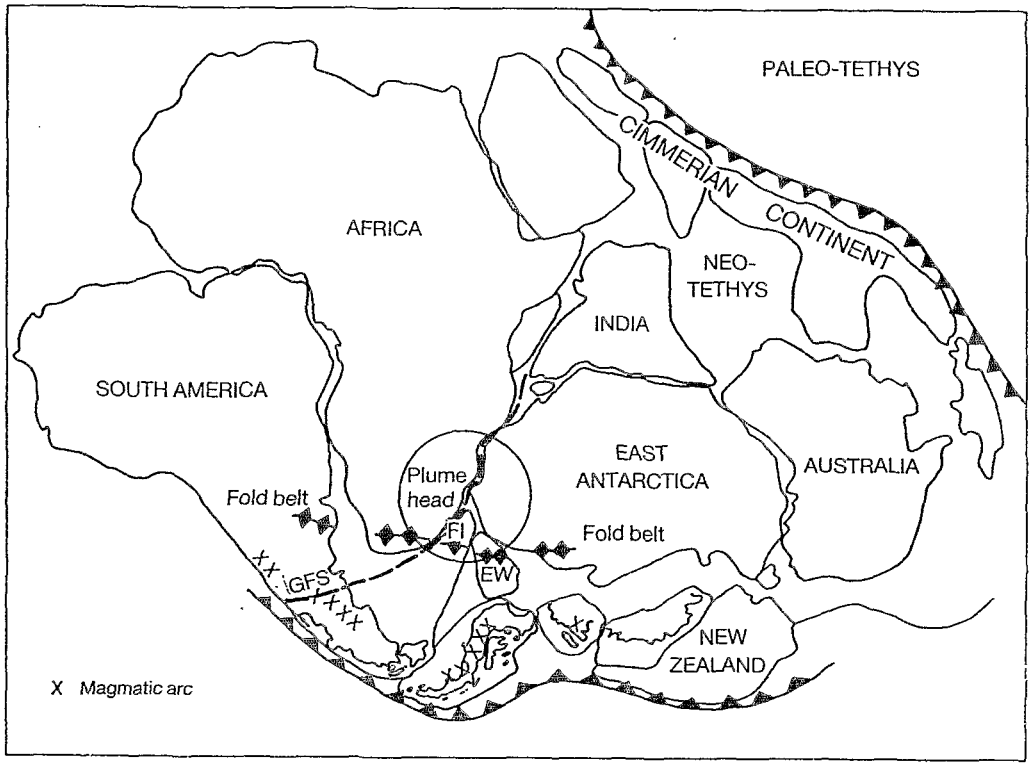

Figure 1. Pre-break-up (early Mesozoic) Gondwana reconstruction illustrating subduction on both sides of the continent, the Gondwanian fold belt and the plume head of White and McKenzie (1989). GFS, Gastre Fault System; FI, Falkland Islands.

record of subduction along the Tethyan margin, suggests that subduction pull on the opposite sides of the supercontinent (Fig. 1) may have given rise to tension within the Gondwana plate leading eventually to break-up. The gravitational potential of crust overthickened during the Permo-Triassic compressional event may have been a contributing factor also. A mantle plume beneath the Karoo province, although not essential to the model, may have thermally weakened the lithosphere, increased magma production rates and induced local rifting, contributing to, but not causing, the eventual separation of East and West Gondwana. Regional tensional forces may have been weak at this time such that sea-floor spreading and continental break-up did not, as far as we know, commence until approximately 155 Ma, 40 Ma after the main plume-related volcanic event of the Karoo (195±4 Ma).

The change from Gondwanide compression to lithospheric extension maybe linked in Early Jurassic times to a reduction in plate boundary forces and a change from a shallow to a steeply dipping subduction zone. During the initial rifting stage a broad extensional province developed in southern South America and West Antarctica (Fig. 2) behind an oceanward migrating magmatic arc. Initial rifting magmas were formed by decompression

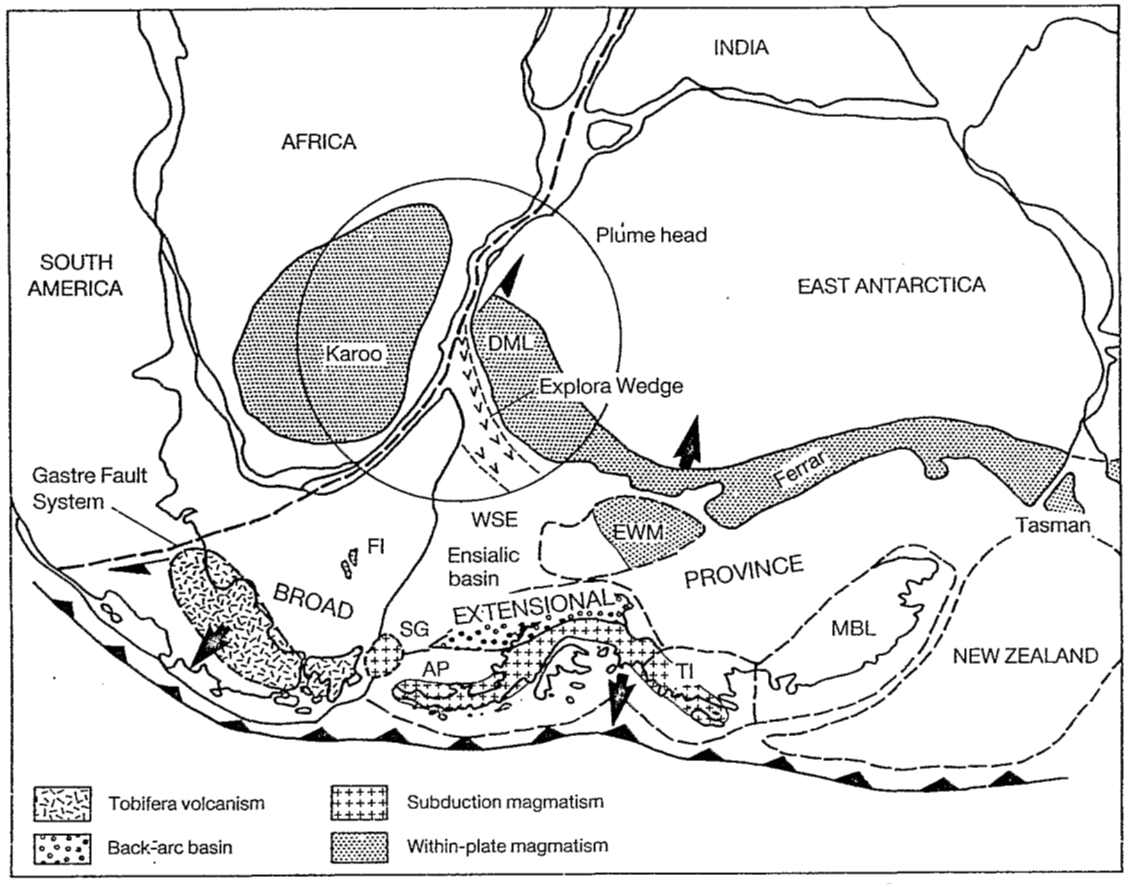

Figure 2. Initial rifting stage of Gondwana break-up illustrating a subduction related magmatic belt, a within-plate magmatic province and a broad extensional province in a back-arc setting.

melting of a mantle source previously enriched (as in the case of the Ferrar magma) or enriched by contemporaneous subduction-induced processes. The mantle may have risen passively in response to crustal extension associated with changing plate boundary forces or possibly by subduction induced convective flow. Anatectic melting at the base of the crust and fractionation of the mafic magmas formed silicic magmas on the margin of the extending basin. A plume beneath the Karoo provinces may have increased magma production rates, formed dipping reflector sequences and induced local rifting.

The broad extensional province is separated from the stable cratonic areas by a major transfer fault zone represented in southern South America by the Gastre Fault System (Rapela & Pankhurst, 1992). Its easterly continuation cuts across the axis of the plume head and may have been controlled by the plumes position. Movement (possibly transtensional) along this zone may have resulted in translation and rotation of the Falkland Islands and the Ellsworth-Whitmore mountains crustal block of West Antarctica during the early break-up stages, and NE movement of East Antarctica relative to Africa (Fig. 2).

The coincidence of break-up with emplacement of high magnesian andesites (155-160 Ma) indicative of atypical thermal conditions during subduction, suggest that geothermal gradients may have been high at this stage and influenced break-up.

CONCLUSIONS

Although the true causes of Gondwana break-up may never be firmly established the data indicate the importance of a plate interaction model encompassing a reduction in subduction plate boundary forces. The combination of subduction pull on the opposite sides of Gondwana combined with the more local tensional effects of a mantle plume and collapse of overthickened lithosphere may have been sufficient to cause break-up and the final separation of east and west Gondwana. The delay of ca. 30 Ma between the Karoo magmatism and final separation suggests the mantle plume did not provide the essential trigger for Gondwana break-up but it may have controlled the ultimate position of break-up and of major fault systems.

REFERENCES

RAPELA, C.W. & PANKHURST, R.J. 1992. The granites of northern Patagonia and the Gastre Fault System in relation to the break-up of Gondwana. In: STOREY, B.C., ALABASTER, T. & PANKHURST, R.J. (eds) Magmatism and the causes of continental break-up, Geological Society Special Publication No. 68, pp. 209-220.

RICHARDS, M.A. DUNCAN, R.A. & COURTILLOT, V.E. 1989. Flood basalts and hotspot tracks: Plume heads and tails. Science, 246, 103-107.

SENGOR, A.M.C. & BURKE, K. 1978. Relative timing of rifting and volcanism on earth and its tectonic implications. Geophysical Research Letters, 5, 419-421.

STOREY, B.C. & ALABASTER, T. 1991. Tectonomagmatic controls on Gondwana break-up models: evidence from the proto-Pacific margin of Antarctica. Tectonics, 10, 1274-1288.

STOREY, B.C., ALABASTER, T., HOLE, M.J., PANKHURST, R.J. & WEVER, H.E. Role of subduction-plate boundary forces during the initial stages of Gondwana break-up: evidence from the proto-Pacific margin of Antarctica. In: STOREY, B.C., ALABASTER, T. & PANKHURST, R.J. (eds) Magmatism and the causes of continental break-up, Geological Society Special Publication No. 68, pp. 149-163.

WHITE, R. & MCKENZIE, D. 1989. Magmatism at rift zones: the generation of volcanic continental margins and flood basalts. Journal of Geophysical Research, 94, 7685-7729.

LA INFLUENCIA DE UNA PALEOCORDILLERA EN EL DESARROLLO DEL CICLO CORDILLERANO

David Zubieta Rossetti
YPFB-GXG,CC1659,Santa Cruz,Bolivia

RESUMEN

The main purpose of this paper is to present an evolutive model for the Cordilleran Cycle in the central part of Bolivia,in this region before the development of paleozoic basin, a mountain range was build during the movements of the Ocloyic Phase,this tectonic event represent the principal control for deposition of marine sediments.

PALABRAS CLAVE: Tectónica, Paleocordillera, CicloCordillerano,Llanura Central, Bolivia.

INTRODUCCION

El desarrollo evolutivo del Ciclo Cordillerano [Suarez S. 1989] en el sector Oeste del continente de Gondwana, se extendió en el territorio de Sudamerica, incluyendo gran parte de la geografía de Bolivia.

Altiplano, Cordillera Oriental, Sierras Subandinas y el subsuelo de las Llanuras de Madre de Dios y Chaco-Beniana, representan unidades geomorfológicas, donde las rocas del Ciclo Cordillerano estan ampliamente representadas.

El área de estudio esta ubicada entre los 63º 50′ y 64 º50′ de longitud y entre los 17º y 17º 30′ de latitud Sud (Fig. 1).El sector Sur presenta afloramientos de rocas paleozoicas expuestas en las serranias que conforman la faja Subandina Central y se extienden hacia el oriente , en el subsuelo de la llanura adyacente, conformando estructuras anticlinales de gran interes petrolero como consecuencia de los descubrimientos alcanzados en los últimos años.

La presencia de un nuevo elemento tectónico identificado en base a la interpretación de líneas sísmicas conjuntamente con la información obtenida de varios pozos exploratorios perforados en el area, ha permitido ampliar el conocimiento sobre la distribución de las secuencias del Ciclo Cordillerano en el subsuelo de la Llanura Central y su prolongación hacia la zona del Boomerang .

MARCO GEOLOGICO

El carácter regional de la cuenca para el Ciclo Cordillerano es considerada intracratónica para algunos investigadores y pericratónica para otros,su desarrollo tuvo lugar en un ambiente marino, con sedimentación predominante silicoclástica Kozlowky, 1923]. Las fuentes de detritos para esta amplia cuenca ,provenian de diferentes partes: Para el sector Sur de la Cordillera Oriental y Sierras Subandinas, los aportes se movilizaron desde el macizo Pampeano-Púnico, [Borelli,1921, Padula et al. 1967] mientras que las tierras altas del Escudo Brasileño, suministraron sedimentos al sector de Chiquitos [Chamot, 1969, Ahlfeld y Branisa, 1960]. El macizo de Arequípa localizado al Oeste representó también una importante área de aporte para la cuenca Paleozoica [Isaacson, 1975 a, 1977, Laubacher et al, 1982, Dalmayrac et al 1980, Isaacson y Sabloc, 1989, 1990].

En el área de estudio,la sedimentación del Ciclo Cordillerano está directamente vinculada al levantamiento de una paleocordillera ,conformada por sedimentitas cambro-ordovicicas.Los mecanismos de esta deformación es producida como consecuencia de una tectónica compresiva de significativa intensidad, que dio lugar a un sistema de duplexes originado durante la fase Ocloyica [Zubieta et al. 1993]

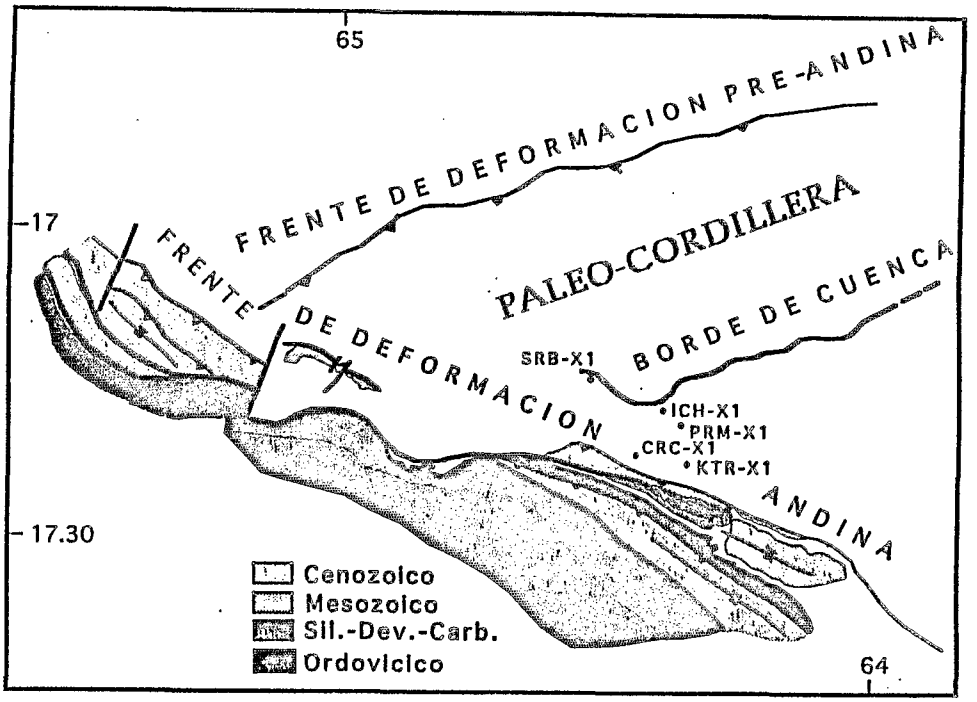

Fig. No.1 Mapa de ubicación d el área de Estudio.

DISCUSION

La estructuracion de esta "paleocordillera,emplazada en el subsuelo de la Llanura Central,representa el registro de una crisis tectónica ,que se prolongó durante la iniciación del Ciclo Cordillerano.Sedimentos compuestos por diamigtitas de textura gruesa,constituyen evidencias de la inestabilidad de la cuenca,de la misma manera que las rocas calcareos reflejan variaciones de las condiciones climáticas.

Los pozos exploratorios perforados en el area del Chapare,ocupan diferentes posiciones dentro la cuenca,un block diagrama elaborado en base a la informacion sismica,muestra la morfologia de la cuenca referida a la base de ciclo sedimentario (Fig. 2).Los pozos Ichoa y Surubi se encuentran muy cerca del borde,mientras que Puerto Ramos,Carrasco y Bulo Bulo,avanzan progresivamente hacia la parte mas profunda de la cuenca.

El registro litologico de los pozos Ichoa y Surubi ,en los tramos inferiores,muestran caracteristicas que confirman la sedimentacion en un borde de cuenca,en efecto varias lineas sismicas,en su prolongación hacia la zona del Boomerang, reflejan el acuñamiento de las unidades inferiores.este evento sin embartgo no siempre puede ser observado debido a la intensa erosión a la que fueron sometidas las secuencias siluro-devonicas durante el Mesozoico .

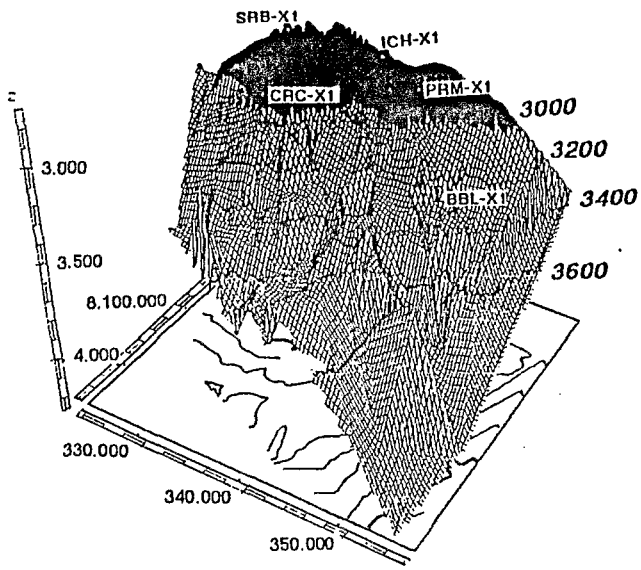

Fig. No.2 Block diagrama sísmico de la base del ciclo Cordillerano. Escala vertical en mili segundos.

CONCLUSION

La fase compresiva Ocloyica dejo impresa su deformación en rocas ordovicicas que afloran al Sur de Bolivia pero tambien esta presente en latitudes mas septentrionales;su efecto determinó el surgimiento de la paleocordillera,conformada por rocas cambro-ordovicicas, que posteriormente fueron erodadas y proveyeron de sedimentos a la cuenca que se instauraba .En consecuencia este elemento tectónico no solamente representó un importante area de aporte,sino tambien controlo la sedimentación del Ciclo Cordillerano .

BIBLIOGRAFIA

Ahlfeld,F., Branisa,L.,1960,Geología de Bolivia, La Paz. Edit. Don Bosco,245 p.

Bonnarelli, G.,1921, Tercera Contribución al conocimiento de las Registiones Petrolíferas Subandinas del norte (Provincias Salta y Jujuy):Buenos Aires,Anales del Ministerio de Agric. Sec. Geol. Mineral y Min., v:15, No.1 Buenos Aires, 96 p.

Chamot,G.,1969, Devonian of the clasical Icla area,Bolivia , manuscrito inedito.

Dalmayrac,B.,Laubacher,G.,Marocco,R.,Martinea,C. y Tomasi,P.,1980 , La chaine hercinienne d'amerique du Sud.Structure et evolutiond'un orogene intracratonique.Geologische Rundschau,69, 1. 21.

Isaacson,P.E.,1975a.Evidence of a Western extra continental land source during the Devonian Period in the Central Andes. Geological Society of America,Bulletin v.86,n 1 ,p.39-46 .

------- 1977 Devonian Estratigraphy and brachiopod paleontology of Bolivia.Part A Orthida and strophomenida,Paleogeographyca,abteinlung A,155,133-192

------- y Sablock,P.E.,1989,Devonian System in Bolivia,Peru and North Chile. Canadian Society of Petroleoum Geologist,Memoir,14,vol.1

Isaacson,PE. y Sablock,P.E.,1990,Devonian paleogeographyand paleogeoreaphy of the central Andes,Paleozoic Paleogeography and Biogeography,Geological Society Memori,n 12

Kozlowski,R.,1923, Faune Devonienne de Bolivie.Paris,Annales de Paleontology,v. XII.

Laubacher ,G.,Boucot,A.J.,and Gray, J., 1982, Additions to Silurian Stratigraphy,litofacies,biogeography and paleontology of Bolivia and South Peru. Journal of Paleontology, v.56, n 5, p.1138-1170.

Suárez,Soruco,R., 1989, El Ciclo Cordillerano en Bolivia y sus relaciones con paises limitrofes. Revista tecnica YPFB, 10 (3-4)

Zubieta Rosetti, D.,Huyghe,P.,Mascle,G.,Mugnier,J.L.,Baby,P.,1993,Influence de l'heritage anté-devonien au front de la chaine andine,C.R.Acad. Sci.Paris,t.316,SerieII,p.951-957

INDEX DES AUTEURS
AUTHORS'INDEX
INDICE DE LOS AUTORES

ORSTOM Éditeur
Dépôt légal : septembre 1993

ORSTOM Éditions
213, rue La Fayette
F-75480 Paris Cedex 10
Diffusion
72, route d'Aulnay
F-93143 Bondy Cedex
ISSN : 0767-2896
ISBN : 2-7099-1154-X

Photographie de couverture : Le village de Tomarapi au pied du volcan Sajama qui culmine à 6542 m (Bolivie). Cliché : Thierry Sempere